Handbook of Copper Pharmacology and Toxicology

Edited by

Edward J. Massaro

HUMANA PRESS

Handbook of Copper Pharmacology and Toxicology

Handbook of Copper Pharmacology and Toxicology

Edited by

Edward J. Massaro

The National Health and Environmental Effects Research Laboratory, Research Triangle Park, NC

Humana Press

Totowa, New Jersey

999 Riverview Drive, Suite 208
Totowa, New Jersey 07512

www.humanapress.com

Production Editor: Jessica Jannicelli.
Cover design by Patricia F. Cleary.

For additional copies, pricing for bulk purchases, and/or information about other Humana titles, contact Humana at the above address or at any of the following numbers: Tel.: 973-256-1699; Fax: 973-256-8341; E-mail: humana@humanapr.com or visit our website: http://humanapress.com

This publication is printed on acid-free paper. ∞
ANSI Z39.48-1984 (American National Standards Institute) Permanence of Paper for Printed Library Materials.

Printed in the United States of America. 10 9 8 7 6 5 4 3 2 1

Library of Congress Cataloging-in-Publication Data

Handbook of copper pharmacology and toxicology / edited by Edward J. Massaro.
p. ; cm.
Includes bibliographical references and index.
ISBN 0-89603-943-9 (alk. paper)
1. Copper--Toxicology--Handbooks, manuals, etc. 2. Copper--Metabolism--Disorders--Handbooks, manuals, etc. 3. Copper--Metabolism--Handbooks, manuals, etc. I. Massaro, Edward J.
[DNLM: 1. Copper--metabolism. 2. Copper--adverse effects. 3. Copper--therapeutic use. 4. Metalloproteins--physiology. QU 130.5 H2356 2003]
RA1231.C7 H36 2003
615.9'25652--dc21

2002067890

PREFACE

Copper (Cu), an essential trace element, is required for the survival of organisms ranging from bacteria to mammals. Because Cu ions can adopt distinct redox states (oxidized Cu[II] or reduced Cu[I]), they play a pivotal role in cell physiology as catalytic cofactors in the redox chemistry of enzymes involved in a broad spectrum of biological activities. For example, copper is an important cofactor in mitochondrial respiration, iron absorption, collagen and elastin crosslinking, and free radical scavenging.

Copper balance studies in volunteer human subjects have indicated a minimum requirement of 1.5 –2.0 mg per diem. Therefore, the RDA (Recommended Dietary Allowances) has been set at 2–3 mg per diem. In the United States, the average daily intake of Cu is approx 1 mg and diet is the primary source. The bioavailability of Cu from the diet is about 65–70% depending on a variety of factors including its chemical form and interaction with other metals and dietary components. Although ingested Cu is readily absorbed, little excess is stored. Therefore, it is both noteworthy and puzzling that symptoms of Cu deficiency have not been identified in the general population. However, the biological half-life of dietary Cu is 13–33 d with biliary excretion being the major route of elimination. In healthy persons, serum Cu concentrations range up to approx 1.5 mg/L. Gastrointestinal symptoms occur at whole blood concentrations near 3.0 mg Cu/L.

It is well known that Cu plays a fundamental role in the biochemistry of the human nervous system. The dramatic neurodegenerative phenotypes of Menkes and Wilson diseases underscore the essential nature of this metal in nervous system development and the consequences of perturbation of neuronal Cu homeostasis. In addition, inherited loss of ceruloplasmin, an essential ferroxidase contains 95% of the Cu found in human plasma, is associated with progressive neurodegeneration of the retina and basal ganglia. Recent studies also have implicated Cu in the pathogenesis of neuronal injury in Alzheimer's disease and the prion-mediated encephalopathies, suggesting that further elucidation of the mechanisms of Cu trafficking and metabolism within the nervous system will be of direct relevance to understanding the pathophysiology and treatment of some neurodegenerative diseases.

Free radical damage has been implicated in several pathological conditions of the central nervous system (CNS) and multiple lines of evidence implicate redox-active transition metals as the mediators of the oxidative stress associated with these disorders. Free radicals produce tissue damage through a variety of mechanisms, including excitotoxicity, metabolic dysfunction, and disturbance of intracellular calcium homeostasis. Considerable research data implicate oxidative stress in ischemia/reperfusion injury and chronic neurodegenerative disorders such as familial amyotrophic lateral sclerosis (ALS) and Parkinson's disease. Gain-of-function missense mutations in the cytosolic Cu/Zn enzyme, superoxide dismutase, are associated with the motor neuron degeneration of ALS and current evidence suggests a direct pathogenic role for Cu in this process. It would appear then that therapeutic approaches focused on limiting oxidative stress may be useful in ameliorating such conditions.

The precise distribution of Cu in the cell occurs through diverse pathways. For example, the delivery of Cu to Cu/Zn superoxide dismutase (SOD1) is mediated through a soluble factor identified as *Saccharomyces cerevisiae* LYS7 and human CCS (Cu chaperone

for SOD). This factor is specific for SOD1 and does not deliver Cu to proteins in the mitochondria, nucleus, or secretory pathway. Yeast cells containing a lys7Delta null mutation have normal levels of SOD1 protein but fail to incorporate Cu into this enzyme which is, therefore, devoid of superoxide scavenging activity. LYS7 and CCS specifically restore the biosynthesis of holoSOD1 in vivo. Elucidation of the CCS Cu delivery pathway may aid development of novel therapeutic approaches to human diseases that involve SOD1 such as ALS.

Recently, components of the Cu homeostasis system of humans have been characterized at the molecular level. These include Cu-transporting P-type ATPases, Menkes and Wilson proteins, and Cu chaperones. The findings have contributed to a better understanding of the physiology of both Cu deficiency and toxicity. For example, because Cu is highly toxic, cellular uptake and intracellular distribution must be precisely orchestrated processes. Thus, Cu homeostasis is maintained by the coordinated activity of a number of proteins that results in its delivery to specific subcellular compartments and, subsequently, Cu-requiring proteins without release of free Cu ions that could damage cellular components. Genetic studies in prokaryotic organisms and yeast have identified membrane-associated proteins that mediate the uptake or export of Cu from cells. Within cells, small cytosolic proteins, the Cu chaperones, bind Cu ions and deliver them to specific compartments and Cu-requiring proteins. The identification of mammalian homologs of these proteins supports a structural and functional conservation of Cu utilization across the evolutionary spectrum from bacteria to yeast to mammals. Furthermore, studies of the function and localization of the products of the Menkes and Wilson's disease genes, which are defective in patients afflicted with these diseases, have provided valuable insight into the mechanisms of Cu balance and their role in maintaining appropriate Cu distribution in mammalian cells and tissues.

In Wilson's disease, a Cu toxicosis condition, and Menkes disease (including mild Menkes disease and occipital horn syndrome [OHS]), a Cu deficiency disorder, Cu homeostasis is perturbed by genetic mutation. Wilson's disease is an autosomal recessive inherited disorder of Cu metabolism resulting in pathological accumulation of Cu in many tissues and organs. The Menkes disease complex of related disorders of Cu transport are responsible for abnormal neurodevelopment and connective tissue pathology that can precipitate premature death. In addition, excessive intake of Cu can result in early childhood cirrhosis (ECC, Indian Childhood Cirrhosis [ICC] or, when found outside India, Idiopathic Cu Toxicosis [ICT]).

Menkes disease is a recessive, X-linked neurodegenerative disease that occurs in approx 1 in 200,000 live births. The affected males manifest a systemic Cu deficiency due to malabsorption caused by a defect in the Menkes (*ATP7A*) gene, designated MNK, which encodes a transmembrane Cu-transporting P-type ATPase that functions to export dietary Cu from the gastrointestinal tract. Based on homology to known P-type ATPases, the MNK gene product is highly evolutionarily conserved. Copper export from the gastrointestinal tract is activated upon the binding of Cu(I) to the six metal-binding repeats in the amino-terminal domain of the Menkes protein. Each of the Menkes protein amino-terminal repeats contains a conserved -X-Met-X-Cys-X-X-Cys- motif (where X is any amino acid). Such metal-binding repeats are conserved in other cation-exporting ATPases involved in metal metabolism and in proteins, such as metallothionein, involved in cellular defense against heavy metals intoxication. Owing to reduction/loss of Menkes protein activity and dietary intake, Cu accumulates in the cytoplasm of cells of the intestine bound to metallothionein resulting, ultimately in the Cu deficiency syndrome pathogno-

monic of Menkes disease. In addition to neurological perturbation, characteristic features of the disease include arterial degeneration and hair abnormalities that can be explained by the decrease in the activity of cuproenzymes.

Mild Menkes disease and OHS (a mild Menkes disease variant) also have been identified as genetic disorders resulting from mutations within the Menkes disease gene. Because the clinical spectrum of Menkes disease is broad, males with mental retardation and connective tissue abnormalities should be screened for biochemical evidence of defective Cu transport. The Menkes/OHS gene normally is expressed in nearly all human tissues and its Cu-transporting P-type ATPase product localizes to the trans-Golgi network. Mutations of the Menkes gene show great variety, including missense, nonsense, deletion, and insertion mutations. In over 70% of the Menkes and OHS patients studied, expression of the gene is abnormal. Major gene deletions, detectable by Southern blotting, account for 15–20% of Menkes/OHS patients. The central region of the gene appears particularly prone to mutation and mutations affecting RNA processing appear to be relatively common. Mutations in the Menkes gene in patients with mild Menkes disease or OHS indicate these diseases to be allelic variants of Menkes disease. Improved understanding of the molecular and cell biological mechanisms involved in normal Cu transport ultimately may yield new and better approaches to the management of these disorders. Of interest in this regard are mutations in the mottled gene, the murine homolog of the Menkes gene. Mutations of this gene have been demonstrated in mottled mutant mice that display biochemical and phenotypic abnormalities similar to those observed in patients with Menkes disease.

The objective in treatment of Menkes disease and OHS is to deliver Cu to the intracellular compartments where cuproenzymes are synthesized. Currently, the treatment of choice is parenteral Cu administration. Unfortunately, in patients with classical Menkes disease, treatment started after the age of 2 mo does not prevent the characteristic neurological degeneration. Even when treatment is initiated in newborns, neurological degeneration is prevented only in some cases. Moreover, early treatment cannot improve non-neurological problems such as perturbed connective tissue development.

The Wilson's disease gene encodes a Cu-transporting P-type ATPase, *ATP7B*. In humans, it is localized on chromosome 13. Approximately 100 mutations of the gene have been documented. They occur throughout the gene. The most common is the His1069Gln point mutation. Wilson's disease includes a variety of clinical conditions, the most common of which are liver disease (ranging from acute hepatitis to fulminant hepatic failure and chronic hepatitis to cirrhosis), hemolytic anemia and neuropsychiatric disturbances. The diagnosis of Wilson's disease usually is made on the basis of clinical findings (Kayser–Fleischer rings, typical neurologic symptoms) and abnormal clinical laboratory values (e.g., low serum ceruloplasmin, increased hepatic Cu content). Lifelong treatment with chelating agents (D-penicillamine, trientine) or zinc usually is sufficient to stabilize the patient and to achieve clinical remission in most.

Liver diseases of infancy and childhood generally are rare and, within the spectrum of these disorders, only a few subtypes are related to abnormal hepatic Cu accumulation. Idiopathic Cu toxicosis has been defined as such a subtype. Although this disease is characterized by distinct clinical and pathologic features, its exact etiology is controversial. It has been hypothesized that idiopathic Cu toxicosis is caused by synergistic interaction between an autosomal recessive inherited defect in Cu metabolism and excess dietary Cu. In this regard, numerous cases of infantile cirrhosis originating in several families in the

Austrian province of the Tyrol have been investigated. Although termed Endemic Tyrolean Infantile Cirrhosis (ETIC), this disorder is indistinguishable from Indian Childhood Cirrhosis (ICC) and Idiopathic Cu Toxicosis (ICT) and resembles the early form of Wilson's disease (WND). It was suggested that ETIC might be the manifestation of an allelic variant of the WND gene, which codes for the ATP7B Cu-transporting P-type ATPase. Assuming that the incidence of ETIC is the result of a founder effect, the possible role for *ATP7B* in ETIC was investigated by association studies and haplotype sharing. Because of its lethality, the mapping of ETIC had to focus on obligate gene carriers, the parents of the patients. The data obtained indicated that ETIC is a genetic entity separate and distinct from WND. Cases of Cu-associated Early Childhood Cirrhosis (ECC) have been reported from Austria, Australia, Germany, Ireland, and the United States. Cases occurring in India are designated Indian Childhood Cirrhosis (ICC) while cases occurring outside of India are designated Non-Indian Childhood Cirrhosis (NICC) or Idiopathic Cu Toxicosis (ICT). It is of interest to note that eight cases of infantile liver cirrhosis, classified as ICT, were reported in five families in Emsland, a predominantly rural area in Northern Germany. In two of these cases, although the children had been exposed to increased levels of dietary Cu, a diagnosis of ICT could not be confirmed. However, in the remaining six cases, clinical presentation and liver pathology were consistent with a diagnosis of ICT. Analysis of the pedigrees of the affected families revealed complex relationships and occasional consanguinity among the parents suggestive of an autosomal recessive mode of inheritance. Furthermore, the households were served by private wells delivering water of low pH through Cu pipes. Thus, chronic alimentary exposure to increased levels of Cu may have precipitated the condition. The findings of this investigation support the hypothesis that ICT develops in genetically predisposed infants who are exposed to increased levels of dietary Cu. It should be emphasized that, although reducing dietary Cu intake cannot prevent the development of Wilson's disease, it can alleviate the symptoms of ICT.

The gene associated with Wilson's disease (*ATP7B*) as well as the Cu-transport genes *hCTR1*, *hCTR2,* and *ATOX1* have been excluded as etiologic agents both in NICC and Cu toxicosis in Bedlington terriers (which is phenotypically similar to Wilson's disease and ICC). A genome-wide screen is being carried out to localize the NICC gene. If the NICC and Bedlington terrier Cu toxicosis genes are homologous, the canine mutation should be of great utility in defining the molecular pathology of NICC. If there is no homology, the genes will still represent an important addition to the list of genes associated with mammalian diseases of Cu metabolism.

It has been suggested that elevated Cu concentrations in wheat and maize from an area of China (Linzhou) at high risk area of esophageal cancer may be related to the etiology of this cancer. Unfortunately, there is little information on the possible association of excess dietary Cu and cancer. Indeed, there is little information on the relation (if any) of Cu status and most diseases afflicting humans in particular and animals in general. This situation is even less clear with regard to the plant kingdom and the so-called "lower organisms." Obviously, there is much work to be done. With this in mind, the *Handbook of Copper Pharmacology and Toxicology* has been developed to provide researchers and students with a view of the current status of research in selected areas of Cu pharmacology and toxicology and to stimulate research in these areas. If the *Handbook* proves useful, updated versions will be forthcoming. Therefore, we invite your comments and suggestions.

Edward J. Massaro

Contents

Contributors

Magdalena Araya • *Instituto de Nutrición y Tecnologia de los Alimentos, Universidad de Chile, Santiago, Chile*

Hans-Peter Bächinger • *Shriner's Hospital, Oregon Health Sciences University, Portland, OR*

Thomas A. Bayer • *Laboratory for Psychiatric Brain Disease, Department of Psychiatry, University of Bonn Medical Center, Bonn, Germany*

Jude Beaudoin • *Department of Biochemistry, University of Sherbrooke Faculty of Medicine (CHUS), Sherbrooke, Canada*

Daniel R. Bellemare • *Department of Biochemistry, University of Sherbrooke Faculty of Medicine (CHUS), Sherbrooke, Canada*

Konrad Beyreuther • *ZMBH-Center for Molecular Biology, University of Heidelberg, Heidelberg, Germany*

Claudia Bolognesi • *Toxicological Evaluation Unit, National Cancer Institute, Genova, Italy*

Jimo Borjigin • *Department of Embryology, Carnegie Institution of Washington, Baltimore, MD*

George J. Brewer • *Department of Human Genetics, University of Michigan, Ann Arbor, MI*

David R. Brown • *Department of Biology and Biochemistry, University of Bath, Bath, UK*

Lesley R. Brown • *Department of Chemistry, Goucher College, Baltimore, MD*

Bruno Burlando • *Department of Science and Advanced Technologies, University of Eastern Piedmont at Alessandria, Alessandria, Italy*

James Camakaris • *Department of Genetics, University of Melbourne, Victoria, Australia*

Maria Teresa Carrì • *Centro di Neurobiologia Sperimentale "Mondino-Tor Vergata-S. Lucia," Rome, Italy*

Maria Rosa Ciriolo • *Department of Biomedical Sciences, University "G. D'Annunzio," Chieti, Italy*

Paul A. Cobine • *National Research Centre for Environmental Toxicology, University of Queensland, Brisbane, Australia*

Matthew J. Cooper • *Department of Biochemistry and Molecular Biology, Oregon Health Sciences University, Portland, OR*

Charles T. Dameron • *Department of Chemistry and Biochemistry, Duquesne University, Pittsburgh, PA*

Francesca De Rienzo • *INFM and Physics Department, University of Modena and Reggio Emilia, Modena, Italy*

Alessandro Desideri • *National Institute for the Physics of Matter (INFM) and Department of Biology, University of Rome "Tor Vergata," Rome, Italy*

Hermann H. Dieter • *Federal Environmental Agency, Berlin, Germany*

Mattia Falconi • *National Institute for the Physics of Matter (INFM) and Department of Biology, University of Rome "Tor Vergata," Rome, Italy*

Simonetta Ferruzza • *Istituto Nazionale di Ricerca per gli Alimenti e la Nutrizione (INRAN), Rome, Italy*

Michael J. Francis • *Wellcome Trust Centre for Human Genetics, University of Oxford, Oxford, UK*
R. Razif Gabdoulline • *European Media Laboratory, Heidelberg, Germany*
Mauricio González • *Instituto de Nutrición y Tecnologia de los Alimentos, Universidad de Chile, Santiago, Chile*
David A. Harris • *Department of Cell Biology and Physiology, Washington University School of Medicine, St. Louis, MO*
Edward D. Harris • *Department of Biochemistry and Biophysics, Texas A&M University, College Station, TX*
Jose Heredia • *Department of Environmental Toxicology, University of California, Santa Cruz, CA*
Nina Horn • *Department of Biochemistry, John F. Kennedy Institute, Glostrup, Denmark*
Lars Riff Jensen • *Department of Medical Genetics, The Panum Institute, University of Copenhagen, Copenhagen, Denmark*
Christopher E. Jones • *National Research Centre for Environmental Toxicology, University of Queensland, Brisbane, Australia*
Jerry Kaplan • *Department of Pathology, University of Utah School of Medicine, Salt Lake City, UT*
Bart Keijser • *Leiden Institute of Chemistry, Leiden University, Leiden, The Netherlands*
Dominik Klein • *Institute of Toxicology and Environmental Hygiene, Technical University Munich, München, Germany*
Hiroko Kodama • *Department of Pediatrics, Teikyo University School of Medicine, Tokyo, Japan*
Daniel J. Kosman • *Department of Biochemistry, School of Medicine and Biomedical Sciences, SUNY Buffalo, Buffalo, NY*
David Kramer • *Centre for Cellular and Molecular Biology, School of Biological and Chemical Sciences, Deakin University, Victoria, Australia*
Simon Labbé • *Department of Biochemistry, University of Sherbrooke Faculty of Medicine (CHUS), Sherbrooke, Canada*
Sharon La Fontaine • *Centre for Cellular and Molecular Biology, School of Biological and Chemical Sciences, Deakin University, Victoria, Australia*
Arturo Leone • *Dipartimento di Scienze Farmaceutiche, Università di Salerno, Salerno, Italy*
Rosa Lerose • *Dipartimento di Scienze Farmaceutiche, Università di Salerno, Salerno, Italy*
Josef Lichtmannegger • *Institute of Toxicology, GSF National Research Center for Environment and Health, Neuherberg, Germany*
Maria C. Linder • *Department of Chemistry and Biochemistry, and Institute for Molecular Biology and Nutrition, California State University, Fullerton, CA*
Svetlana Lutsenko • *Department of Biochemistry and Molecular Biology, Oregon Health Sciences University, Portland, OR*
Brian C. MacArthur • *Department of Biochemistry and Molecular Biology, Oregon Health Sciences University, Portland, OR*
Sudeep Majumdar • *Department of Biochemistry and Biophysics, Texas A&M University, College Station, TX*

Edward J. Massaro • *The National Health and Environmental Effects Research Laboratory, Research Triangle Park, NC*
Ian R. McDonald • *Department of Biological Sciences, University of Warwick, Coventry, UK*
Maria Cristina Menziani • *Department of Chemistry, University of Modena and Reggio Emilia, Modena, Italy*
Julian F. B. Mercer • *Centre for Cellular and Molecular Biology, School of Biological and Chemical Sciences, Deakin University, Victoria, Australia*
Sabeeha Merchant • *Department of Chemistry and Biochemistry, University of California at Los Angeles, Los Angeles, CA*
Helena Mira • *Department of Biochemistry and Molecular Biology, Universidad de Valencia, Valencia, Spain*
Lisbeth B. Møller • *Department of Biochemistry, John F. Kennedy Institute, Glostrup, Denmark*
Anthony P. Monaco • *Wellcome Trust Centre for Human Genetics, University of Oxford, Oxford, UK*
Gerd Multhaup • *ZMBH-Center for Molecular Biology, University of Heidelberg, Heidelberg, Germany*
J. Colin Murrell • *Department of Biological Sciences, University of Warwick, Coventry, UK*
Fabio Nobili • *Istituto Nazionale di Ricerca per gli Alimenti e la Nutrizione (INRAN), Rome, Italy*
Yasumitsu Ogra • *Graduate School of Pharmaceutical Sciences, Chiba University, Chiba, Japan*
Manuel Olivares • *Instituto de Nutrición y Tecnologia de los Alimentos, Universidad de Chile, Santiago, Chile*
Andrea Onetti-Muda • *Dipartimento di Medicina Sperimentale e Patologia, Universitá di Roma "La Sapienza," Rome, Italy*
Maria Gabriella Pagliuca • *Dipartimento di Scienze Farmaceutiche, Universitá di Salerno, Salerno, Italy*
Benoit Pelletier • *Department of Biochemistry, University of Sherbrooke Faculty of Medicine (CHUS), Sherbrooke, Canada*
Lola Peñarrubia • *Department of Biochemistry and Molecular Biology, Universidad de Valencia, Valencia, Spain*
Jeanette Quinn • *Department of Chemistry and Biochemistry, University of California at Los Angeles, Los Angeles, CA*
Manchi C. M. Reddy • *Department of Biochemistry and Biophysics, Texas A&M University, College Station, TX*
Luisa Rossi • *Centro di Neurobiologia Sperimentale "Mondino-Tor Vergata-S. Lucia," Rome, Italy*
Giuseppe Rotilio • *Department of Biology, University of Rome "Tor Vergata," Rome, Italy*
Yula Sambuy • *Istituto Nazionale di Ricerca per gli Alimenti e la Nutrizione (INRAN), Rome, Italy*
Vicente Sancenón • *Department of Biochemistry and Molecular Biology, Universidad de Valencia, Valencia, Spain*

Maria Laura Scarino • *Istituto Nazionale di Ricerca per gli Alimenti e la Nutrizione (INRAN), Rome, Italy*
Marc Solioz • *Department of Clinical Pharmacology, University of Berne, Berne, Switzerland*
Graham Stafford • *Department of Biological Sciences, University of Warwick, Coventry, UK*
Toshihiro Sugiyama • *Department of Biochemistry, Akita University School of Medicine, Akita, Japan*
Karl H. Summer • *Institute of Toxicology, GSF National Research Center for Environment and Health, Neuherberg, Germany*
Xing Sun • *Department of Embryology, Carnegie Institution of Washington, Baltimore, MD*
Kazuo T. Suzuki • *Graduate School of Pharmaceutical Sciences, Chiba University, Chiba, Japan*
Kunihiko Terada • *Department of Biochemistry, Akita University School of Medicine, Akita, Japan*
Ryan Teves • *Department of Environmental Toxicology, University of California, Santa Cruz, CA*
Ruslan Tsivkovskii • *Department of Biochemistry and Molecular Biology, Oregon Health Sciences University, Portland, OR*
Zeynep Tümer • *Department of Medical Genetics, The Panum Institute, University of Copenhagen, Copenhagen, Denmark*
Ricardo Uauy • *Instituto de Nutrición y Tecnologia de los Alimentos, Universidad de Chile, Santiago, Chile*
Aldo Viarengo • *Department of Science and Advanced Technologies, University of Eastern Piedmont at Alessandria, Alessandria, Italy*
Erik Vijgenboom • *Leiden Institute of Chemistry, Leiden University, Leiden, The Netherlands*
Rebecca C. Wade • *European Media Laboratory, Heidelberg, Germany*
Michael M. Wang • *Department of Neurology, The Johns Hopkins University School of Medicine, Baltimore, MD*
Wasantha A. Wickramasinghe • *National Research Centre for Environmental Toxicology, University of Queensland, Brisbane, Australia*
Cisca Wijmenga • *Department of Medical Genetics, Wilhelmina Children's Hospital, University Medical Centre, Utrecht, The Netherlands*
Reinhard Wimmer • *Department of Life Sciences, Aalborg University, Aalborg, Denmark*
Shinya Yoshikawa • *Department of Life Science, Himeji Institute of Technology, Hyogo, Japan*
Zhiwu Zhu • *Department of Environmental Toxicology, University of California, Santa Cruz, CA*

I
Copper in Mammals

1

Biochemistry and Molecular Biology of Copper in Mammals

Maria C. Linder

1. NUTRITIONAL BIOCHEMISTRY AND METABOLISM

In this chapter, we review what we know about the availability of copper in foodstuffs, its intestinal absorption, transport to cells and tissues, uptake by and distribution within cells, and its metabolism, release, and excretion from the body. The emphasis is on the adult human being. More detailed information may be found in books edited by Linder *(1,2)*, Sarkar *(3)*, and Leone and Mercer *(4)*, 1996 reviews by Linder *(5)* and Linder and Hazegh-Azam *(6)*, and more specialized reviews by Harris *(7)*, Pena et al. *(8)*, Linder et al. *(9,10)*, and others *(11,12)*.

1.1. Dietary Copper Intake

Copper is an essential trace metal found in the Cu(II) and Cu(I) states in all living organisms. Table 1 presents average values for concentrations of copper in water, soil, and different kinds of foodstuffs. For humans and other mammals, the best plant food sources are seeds, including whole grains, nuts, and beans, where (like most trace elements and vitamins) it is concentrated in the germ and bran. The best animal food sources are shellfish and liver. Even with copper piping, drinking water does not normally contribute significantly to intake *(13)*.

In mammals, virtually all copper is taken in through the diet and absorbed from the gastrointestinal tract, although small amounts can penetrate the skin when applied in specific ointments and even by leaching into the sweat from copper bracelets *(14,15)*. Average intakes of copper by human adults, at least in the United States and Western Europe, are about 1 mg/d, although they vary in the range from 0.6 to 1.6 mg *(1,16,17)*. Very recently, a US Recommended Daily Allowance (RDA) of 0.9 mg for normal adult women and men (with higher levels for pregnant women) was hammered out by a committee of the National Academy of Sciences *(18)*, replacing the earlier "safe and adequate intake" range of 1.5–3.0 mg/d. This considerably lower recommended value is based in part on data obtained from copper balance studies in young men maintained for 2.5–6 wk on diets delivering specific levels of copper (from 0.66 to 0.38 and then 2.49 mg/d) *(16–19)*. These studies showed that, at least acutely, humans could adapt considerably to changes in copper intake, retaining more and excreting less when intake was low, and vice versa. Even those on the lowest intake (0.38 mg/d) for 6 wk only, lowered their plasma ceruloplasmin–copper concentrations about 10% (still among the most sensitive indices of copper status). At higher intakes, the percentage of copper absorbed was less and body turnover (excretion) was enhanced *(19)*. Excretion was the main factor controlling homeostasis. Although an

From: Handbook of Copper Pharmacology and Toxicology
Edited by: E. J. Massaro © Humana Press Inc., Totowa, NJ

Table 1
Copper Content of Water, Soil, Foods, and Mammalian Organs (Range of Average Values)

Item	*Copper content (μg/mL or g wet weight)*
Uncontaminated fresh water	0.0001–0.001 (proposed WHO limit 2 μg/mL)
Uncontaminated seawater	
Surface	0.001
1000 m below	0.1
Soils (other than rocks, where most Cu is)	
Inorganic	≥4
Organic	20–30
Vegetables	0.3–3
Fruits	0.4–1.5
Seeds and grains (whole)	3–8
Nuts (whole)	6–37
Potatoes	2.1
Maize	1.4
Yeast	8
Shellfish	12–37
Fish	
Freshwater	0.3–3
Seawater	2–3
Liver and kidney	4–12
Heart	4.5–4.8
Brain	3.1–5.2
Muscle	0.9–1.0
Hair and nails	8–20

Note: Range of average values is from ref. *1*.

adaptability to copper intake is supported, at least indirectly by other research, not everyone will agree that the recommended intake might not have some negative consequences, long term. It is true that actual intakes of copper by Americans and Europeans are mostly within the recommended range and that overt copper deficiency is rare. Overt deficiency (with severe developmental consequences) occurs when there is a genetic defect in the functioning of a copper transporter (ATP7A), resulting in Menkes disease or the milder Occipital Horn Syndrome (*see* Sections 1.2. and 1.5.). Marginal deficiency is another question, and until we know how to define this better, some concerns about adequacy of intake will continue.

1.2. Copper Absorption

In humans and other mammals where it has been tested, copper is absorbed primarily or exclusively by the small intestine. (There may be some absorption in the stomach, but the available data are contradictory *[1]*.) The percentage of copper absorbed is inversely related to dose *(1,5)*, particularly in the extremes; at low doses, most of the copper in the diet is absorbed; at high doses the percentage is much lower (only 10% in the case of rats given 10 times the normal intake *[1]*). In humans with normal intakes, 55–75% is absorbed; in rats, the average percentage is somewhat less (30–50%). These values are based on the appearance of radioactive or heavy isotopes of copper in blood and tissues. It should, however, be pointed out that in addition to the approx 1 mg of copper received daily in the diet, a great deal more copper enters the digestive tract daily from endogenous organs and tissues, and most of that is reabsorbed as well *(1,5)*. In humans, saliva (0.33–0.45 mg), gastric juices (1 mg), the bile (2.4 mg), as well as pancreatic

(0.4–1.3 mg) and duodenal fluids (0.4–2.2 mg) daily contribute an average of between 4 and 7.5 mg of additional copper to the contents of the digestive tract, and all but about 1 mg of that copper is reabsorbed. The 1 mg or so not reabsorbed represents most of copper excreted daily by human adults. Very little copper exits the body by other routes (only 30–60 µg/d in the urine of adult humans) *(1,5)*. This means that copper is very actively recycled between the digestive tract and body fluids and tissues (particularly the liver) and that dietary copper is only a small proportion of the total absorbed daily. Copper secreted via the bile is the least readily reabsorbed, thus, the bile is the main route for copper excretion for the mammal (*see* Section 1.5.).

As concerns the details of intestinal copper absorption, the mechanisms by which it enters the cells of the intestinal mucosa and crosses into the interstitial fluid and blood are still not well understood. However, important recent progress has been made in identifying transporters and some other proteins that are likely to be involved. Earlier studies, mainly with rodents, indicated that the uptake of Cu(II) across the brush border involved both a nonenergy-dependent saturable carrier, active at lower copper concentrations, and diffusion—at higher concentrations *(1)*. At the basolateral membrane of the cell, it was surmised that transfer into the blood and interstitial fluid was energy dependent and more rate limiting for overall absorption, there being conditions in which much copper enters the enterocyte but does not necessarily go further (and accumulates). However, at high concentrations, there is increased uptake as well as overall absorption. For this, additional carrier systems and/or diffusion may come into play, mediating additional transfer of copper across the basolateral/serosal membrane. Thus, even though a decreased percentage of copper is absorbed at high doses, actual absorption is greater at higher than at lower doses. It may be that some of the carriers (or transport mechanisms) recruited at higher copper doses are those that specialize in the transport of other transition metals, such as Zn(II) and Fe(II/III): High doses of the latter metal ions can inhibit copper absorption, and vice versa *(1,20,21)*, particularly at the basolateral end of the enterocyte. Rates of basolateral copper transport also vary with physiological condition, increasing with pregnancy and in cancer *(1,22)*, and decreasing (at least in female rats) upon repeated treatment with estrogen *(22)*. This implies that expression and/or deployment of copper transporters/transport systems can vary and is regulated. In the conditions cited, retention of copper by the enterocyte varies inversely with overall transport, accumulating when the serosal transfer system is less active, and not accumulating when it is. Copper retained in the mucosal cells will be released back into the digestive tract when these cells migrate to the tips of the villi and are sloughed off, thus contributing further to the pool of copper available for reabsorption and excretion.

Whether and how nutritional copper status regulates copper absorption by the enterocyte has not been examined much at the cellular level. The existing data suggest the possibility of a biphasic response to copper dose. With the polarized Caco2 cell monolayer model, it was found that pretreatment with excess copper *enhanced* uptake and overall transport of 1 µM ^{64}Cu *(23)*, a response that is opposite to what would be expected for homeostasis. We have recently confirmed these results (Zerounian and Linder, unpublished) and examined, as well, the effects of copper deprivation. Cells depleted of copper by three different chelators responded by markedly increasing their uptake and overall transport of copper *(24)*. Others have reported that copper deficiency or excess did not influence the expression of CTR1 *(25)*, a transporter thought to be involved at least in some aspect of copper absorption (*see* later in this section).

Within the mucosal cell, most newly absorbed copper (about 80%) is retained in the cytosol, and most of that is bound to metallothioneins and/or proteins of similar size *(1)*. Metallothioneins are small cysteine-rich proteins that store copper and other divalent metal ions (notably those of Zn, Mn, and Cd) (*see* refs. *1–3*). As the affinity of these proteins for Cu(II) is higher than for most other abundant metal ions [notably Zn(II)], the incoming copper will displace these ions. If metallothionein concentrations in the mucosal cells are high (as when induced with high intakes of zinc), the binding of copper to metallothionein will interfere with its transfer across the serosal surface. Thus, high

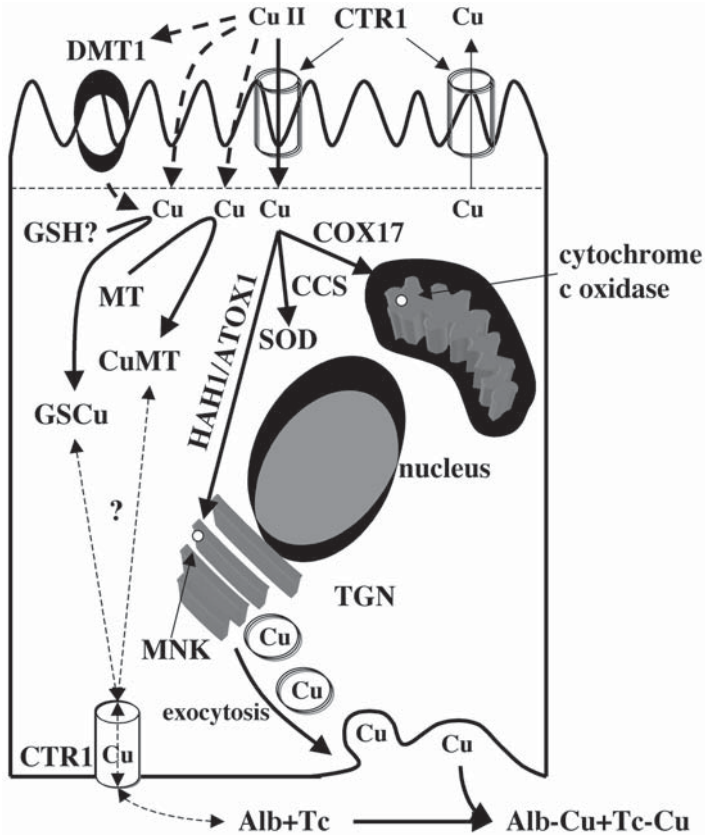

Fig. 1. Possible mechanisms of copper uptake and transport in the intestinal cell (*see* text for details). Starting at the brush border (top of the cell model), copper may enter through CTR1 and DMT1. Copper is picked up on the inside of the brush-border membrane by several chaperone carriers that deliver the metal ion to specific sites: HAH1/ATOX1 to MNK in the trans-Golgi network (TGN); COX17 to the mitochondria; CCS to superoxide dismutase (SOD). Glutathione (GSH) and metallothionein (MT) may also pick up the copper directly, possibly to shuttle it to the basolateral end of the enterocyte. There, it might be released to albumin and transcuprein in the circulation (perhaps via CTR1). Alternatively, copper arriving at the ATP7A (MNK protein in the TGN) may be pumped into developing vesicles for exocytic release.

doses of zinc are used to inhibit intestinal copper absorption in Wilson disease, where accumulation of excess copper is a problem (*see* Section 1.5.).

With regard to the potential transporters and carrier systems for intestinal absorption, several genes and gene products have emerged in the last several years that are likely to participate, although many functional details still need to be verified or established. Most of these mammalian copper transport genes and their products were identified by using sequence information from analogous genes in yeasts *(8,12,26–28)*. CTR1, cloned in humans *(29)* and more recently in mice *(25,30)*, is homologous to (and can substitute for) yeast ctr1 in complementation experiments *(29)*. The corresponding ubiquitously expressed 190-amino-acid human transmembrane protein (about 22 kDa, with 3 transmembrane regions, and a hydrophilic, histidine and methionine-rich N-terminal domain external to the cell) is a candidate for the copper transporter in the brush border of intestinal cells. However, it seems likely that it is also in the basolateral membrane, because copper can and will enter the enterocyte from the blood. Transfection experiments have confirmed that hCTR1 promotes copper uptake into

mammalian cells *(30–32)* [in addition to yeast *(29)*]. In yeast, it appears that uptake is coupled with efflux of two K^+ ions *(8,33)* and that the reduced form [Cu(I)] is transported. CTR1 might thus provide for the facilitated diffusion of copper across the brush border, even at low copper concentrations. (It might even work in both directions, also facilitating release of excess copper into the gastrointestinal tract. We know that copper can flow through the intestinal wall in both directions, although, normally. the net direction is toward the blood *[1]*.) There are two major mRNA transcripts (2 and 5.5 kb) expressed in human and mouse intestine (and most other tissues), which might target the transporter to different parts of the cell. In rats, however, one of the forms greatly predominates, the other predominating in the liver and hypothalamus *(25)*. Expression of the mammalian homolog (hCTR2) of another (low-affinity) yeast transporter (ctr2) has also been detected at the mRNA level in most tissues, although its greatest expression was in placenta, and there was very little in liver and intestine *(8,29)*. However, it was ineffective in complementing copper transport-deficient yeasts.

Another candidate transporter in the brush border that must be considered is DMT1/Nramp2, a divalent metal transporter that clearly carries Fe(II), Zn(II) and Mn(II) *(34–36)*. Ubiquitously expressed in tissues and present in the intestinal brush border, its transport of metal ions is proton coupled and dependent on the membrane potential, as shown by the large inward current evoked in DMT1/DCT1-transfected oocytes upon their exposure to Fe(II), at pH 5.5, and loss of most of this current at pH 7.5 *(34)*. Cu(II) and the ions of Zn, Mn, Cd, and Co were also effective in evoking current. Whether and/or when this large (561 amino acid) protein, with 12 transmembrane segments, is actually involved in normal copper transport has not yet been fully established. A role in iron absorption, as well as homeostatic regulation of its expression by iron within the intestine, has been well established *(37,38)*; although the 3'UTR of two forms of the mRNA *(39)* contain an iron-responsive element (IRE), regulation by iron is mainly through changes in rates of transcription *(39,40)*. In the Caco2 cell intestinal model system, we found no competition between Cu(II) and Fe(II) or Zn(II) for uptake of either ^{64}Cu(II) or ^{59}Fe(II) at equimolar concentrations *(41)*. However, preliminary evidence indicates that iron deficiency enhances not just iron but also copper uptake (N.R. Zerounian and M.C. Linder, unpublished) and that inactivation of DMT1 mRNA by antisense oligomers reduces uptake of both metal ions in polarized Caco2 cells *(42)*. The results suggest that DMT1 can mediate copper uptake when the metal ion is present in sufficient concentrations and/or when other metal ions are absent.

Several other genes and gene products involved in copper transport within mammalian cells and across their cell membranes have been identified, most of which are ubiquitously expressed, including by intestinal enterocytes. Assuming that these proteins have the same kinds of function in intestinal cells as they do in other cell types, one can imagine one or more pathways by which copper can travel from the brush border to the basolateral membrane and across into the blood, during intestinal absorption. This is summarized in Fig. 1. Along with the putative membrane transporters already described (CTR1, DMT1), one of the major discoveries initially made in yeast and then verified for mammalian cells is that there is a battery of what are now called "copper chaperone proteins" that carry copper to specific intracellular sites and enzymes. This fits with (and further substantiates) the concept that copper ions are prevented from being free in solution by being bound tightly to specific proteins and handed directly from one protein to another. (The same concept has emerged from studies of copper transport proteins in the blood plasma [*see* Section 1.3.].) Thus, copper entering cells will be carried by HAH1/ATOX1 (corresponding to yeast Atx1) to the trans-Golgi network (TGN) (or related vesicles), delivering copper to the P-type ATPases located there *(8,43,44)*. In the case of the enterocyte, it would be ATP7A or MNK (the protein defective in Menkes disease); in the liver, it would be ATP7B or WND (the protein defective in Wilson disease). MNK and WND are thought to then transfer the copper into the TGN, for insertion into copper-dependent proteins that are secreted and for release of other forms of copper from specific cells. In the case of the enterocyte, we can imagine this exocytotic, energy-dependent system to be important for release of copper to the blood

via exocytosis (Fig. 1). (In the case of the hepatocyte, WND is involved in the release of copper into bile canaliculi [*see* Sections 1.4. and 1.5.].)

Another chaperone, CCS (Fig. 1), delivers copper to the Cu/Zn superoxide dismutase (SOD) in the cytoplasm *(8,45,46)*, which protects cells against superoxide radicals (*see* Section 2.1.2.). A third, COX17, takes copper to the mitochondria *(8,47,48)*, where it is required for cytochrome-*c* oxidase, the terminal enzyme in respiration. Mediating insertion of copper into the latter enzyme may be the mammalian homologs of Sco1 and Sco2, which, in yeast, are necessary for assembly of this complex molecule *(8)*. Some of the entering copper will also associate with cytosolic metallothionein(s) (MTs) (Fig. 1). As already related, radioisotope studies have shown that as it enters the enterocyte, most of the copper is in the cytoplasm. Most of that is with protein(s) of the size of MT (apparent molecular weight [M_r] about 10,000, actual molecular weight about 6000), and traces with something of the size of SOD (about 35 kDa) *(1,49,50)*. [Little or none of the radioactive copper (or of copper measured directly) has been found to elute with components of the size of amino acids *(1,49–52)*.] Because the chaperones Atx1 and Cox17 (at least in yeast) are almost the same size as MT (73 and 69 amino acids, respectively, vs 61 for MT), it seems likely that some of the radioactive copper that was thought to be with MT is actually attached to these chaperones. A portion of the newly entered radioactivity in the enterocytes is also associated with larger organelles and vesicles.

Based on this system of copper transporters/chaperones, one might postulate that (Fig. 1), after crossing the brush border of the enterocyte, most of copper is normally shuttled to the TGN and into its channels through delivery of the copper by ATOX1/HAH1 to the MNK protein (ATP7A). Energy is required for pumping the copper into the TGN channels, from where it may be packaged into vesicles and migrate to the basolateral membrane, for exocytosis. (The form of copper that would be delivered is unknown.) This could be the major pathway for overall intestinal absorption in the normal state. However, one can also speculate that alternative pathways exist involving cytosolic chaperones (perhaps still to be identified) that might carry copper to CTR1 in the basolateral membrane, for transfer to the blood along a chemical gradient. In addition, the delivery of copper to specific enzymes and organelles is not a "one-way street." Thus, either the same or as yet unknown chaperones must carry intracellular copper back to plasma membrane transporters, for exit from both ends of the enterocyte. (Turnover of intracellular, copper-dependent proteins is also occurring and will free copper that must be either reincorporated or released from the cells.)

Still another possibility to be considered (Fig. 1) is that glutathione (GSH) plays the role of a general chaperone for copper ions *(7)* and delivers it to CTR1 in the plasma membranes, but this has been difficult to document and remains to be further explored. Clearly, in vitro, GSH will reduce and bind Cu(I) as well as deliver it to MT and some copper-dependent apoenzymes, like SOD and hemocyanin *(7)*. Cellular GSH levels are high (in the millimolar range) and inversely related to cellular copper concentrations. In a particular line of hepatoma cells (HAC) *(53,54)*, fractionation (by size-exclusion chromatography on Superose 12B) of cytosol after ^{67}Cu treatment showed that, initially, radioactivity associated with a M_r 4200 peak that eluted in the same position as a mixture of Cu(II) and GSH. Moreover, labeling of this component declined fairly rapidly and coincided with the increased labeling of a component of the M_r of metallothionein *(54)*. (SOD labeling occurred later.) The inverse relationship between Cu and GSH levels in cells could reflect a propensity for Cu(II) to oxidize GSH, and indeed, excess copper promotes an increase in Se-dependent GSH peroxidase. However, as already described, most previous fractionations of intestinal cytoplasm did not find newly absorbed radiocopper with components in the size range of GSH–Cu (a tripeptide complex) or with a component of M_r of 4200 (using Sephadex G75). Also, Superose 12B is not a very good medium for separating components unless they are very different in shape and size. The column itself was equilibrated with buffer purged of air, but no evidence was provided that anaerobic fractionation made a difference, and the cell extract was certainly not anaerobic prior to its application. The radiocopper in the proposed GSH complex was most highly labeled 1 h after ^{67}Cu administration and remained at that level for several hours thereafter, suggesting considerable stability. Clearly, this

needs to be explored further. Most recently, observations that copper binds to chaperones after it has entered by a variety of means (that might involve different transporters) points to the possibility that recognition (and thus direct binding) of the chaperone to the membrane transporter might not be required *(55)*. If so, perhaps GSH mediation is involved in that step; if not, one would expect that the copper transporters would have sites for chaperone binding (perhaps different ones for different chaperones); this remains to be examined. In any event, because there are specific chaperones, GSH may not normally be needed directly for copper distribution within the cell. However, it might be needed to restore the abilities of copper binding proteins (with thiol groups) to bind their copper; if the chaperones are not available for some reason, it might play a backup role. It might also provide electrons for reduction of copper during transport; in addition, it might even play the role of a generalized copper chaperone, for proteins that have no specific chaperone to provide them with the element.

Either way, another of the emerging themes in copper physiology (and also other areas of metabolism) is redundancy of function. Thus, the absence of a particular (and seemingly critical) transport protein or transporter is usually not lethal, and the phenotype can even be mild. For example, the knockout of ATOX1 *(56)* resulted in growth retardation and failure to thrive after birth, but development continued to some degree (intestinal absorption was probably not completely absent). (ATOX1 was particularly important to placental transfer *[56]*.) Similarly, although intestinal copper absorption is greatly diminished in Menkes disease, it is not zero, and the difficulty in postnatal survival with Menkes is, in part, the result of gestational/developmental abnormalities arising from defective copper transport in other tissues *(57)*.

1.3. Transport of Copper to Tissues and Its Uptake

After copper emerges on the "blood" side of the enterocyte, it immediately binds to proteins of the interstitial fluid and portal blood plasma. Two proteins with specific, high-affinity copper binding sites have been identified. One of these is albumin, which binds copper with the help of the the three amino acids at its N-terminus (including a histidine in the third position). High-affinity copper binding has been demonstrated for human *(58,59)* and bovine *(58,60)* albumin. The histidine near the N-terminus is missing in the albumins of some other vertebrates, including the dog and pig *(1)*. This does not eliminate binding but lowers copper affinity about 10-fold *(60)*. Albumin is, by far, the most abundant plasma protein and it can be calculated that there is sufficient albumin in 1 mL of plasma to bind 30 μg of Cu! In actuality, only about 100–150 ng/mL (or 10–12% of the total plasma copper) are bound to this protein at any time *(10,61,62)*. At least in rats and humans, most of the rest is associated with two other proteins, ceruloplasmin, and a macroglobulin, transcuprein, first identified in rats *(10,63,64)*. Together, transcuprein and albumin represent the bulk of the exchangeable copper pool in blood plasma (and presumably interstitial) fluid *(1,5,9,10)*. Ceruloplasmin is not part of this pool, as its copper is not exchangeable or dialyzable. It also seems unlikely that histidine (or other amino acids) participate as Cu–amino acid complexes. There is no firm evidence that copper is bound to histidine or other amino acids in vivo, although it may exist as a trinuclear complex with albumin–copper *(59)*. Histidine (100 μ*M*) does accelarate the rate at which copper comes off albumin and transcuprein *(1,9)*, but release is still very slow. Minutes after ingestion or injection of radioactive copper, virtually all of it is associated with macroglobulin and albumin in the plasma (Fig. 2A), and none is detected in the low-molecular-weight fractions where amino acids and small peptides elute in size-exclusion chromatography. (The same is true when plasma is labeled by direct addition of radioactive copper ions *[63]*.) So soon after administration, none of the radioactive copper is with ceruloplasmin (Fig. 2A). This contrasts with the distribution of nonradioactive copper, the bulk of which, at any time, is with ceruloplasmin (about 70%) *(61,62)*. Thus, about 12% each of the total copper is with albumin and transcuprein, and traces are with a variety of other enzymes, clotting factors, and some low-molecular-weight peptides (Table 2). As already indicated, off-rates for copper from transcuprein

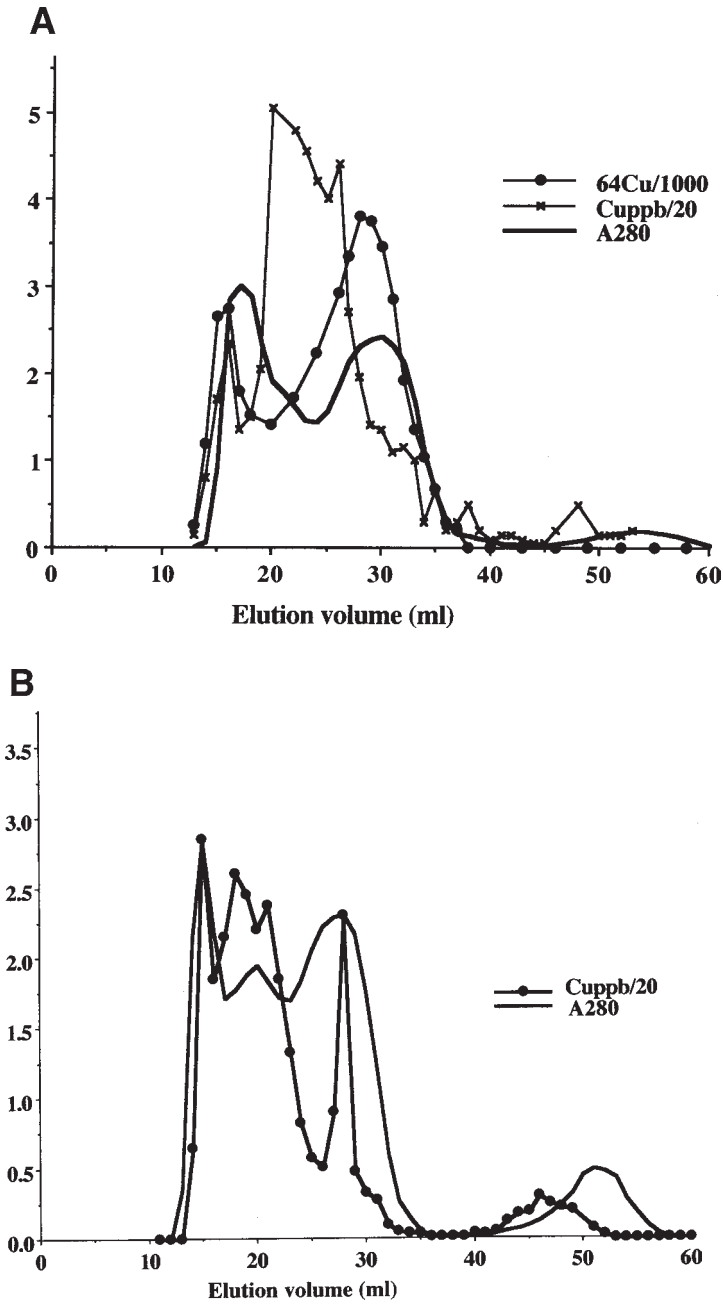

Fig. 2. Distribution of radioactive copper and total copper among plasma membrane components fractionated by size-exclusion chromatography. **(A)** Copper-64 radioactivity (closed circles), actual copper (ppb, divided by 20; determined by furnace atomic absorption) (x), and proteins (absorbance at 280 nm) (solid line) in fractions eluted from Sephadex G150 after application of plasma from a rat 15 min after injection of ^{64}Cu(II)-nitrilotriacetate (about 10 ng Cu). **(B)** Copper concentrations (determined by furnace atomic absorption) (closed circles) and proteins (absorbance at 280 nm) (solid line) in fractions eluted from Sephadex G150 after application of serum from a patient with hemochromatosis. (In such patients, there is somewhat less ceruloplasmin.)

or albumin are very slow, but the two proteins rapidly exchange copper with each other *(1,10,64)*. This mimics the pattern of events in the cell, where intracellular copper chaperones directly exchange copper with their specific protein targets *(44,66,67)*. The ability of copper to bind to transcuprein in the face of abundant albumin (with its high-affinity copper sites) speaks to its own high affinity for copper.

Rodents express a different spectrum of macroglobulins in their blood plasma than do humans and most other mammals. Rat transcuprein appears to be α_1-inhibitor3, a monomeric macroglobulin with a total molecular weight of about 200,000 *(64)*. Macroglobulins are known to bind other proteins (including, but not confined to, proteases). As the apparent molecular weight of the ^{67}Cu-labeled rat transcuprein is 270,000, and as another polypeptide of M_r 70,000 is found with radiocopper-labeled transcuprein, the copper carrier may be in the form of a complex. The identity of this 70,000 subunit and the question of whether it is required for copper transport are still being explored. α_1-Inhibitor3 and the main human macroglobulin (α_2-macroglobulin) both have a highly homologous, histidine-rich region that seems like a good prospect for copper binding. Because human plasma, like rat plasma, shows binding of radioactive copper to a macroglobulin (in this case, α_2-macroglobulin, as determined by immunoprecipitation; Goforth and Linder, unpublished), and analysis of actual copper in human serum confirms that 10–15% is bound to a large protein *(61,62)* (Fig. 2B), it seems likely that α_2-macroglobulin plays the same role in nonrodent mammals as α_1-inhibitor3 does in rodents (i.e., that the "transcuprein" of nonrodents is α_2-macroglobulin). Copper appears to bind to α_2-macroglobulin *(1)* and may do so with equal affinity to rat transcuprein *(68)*. α_2-Macroglobulin has also been identified as the main plasma carrier of Zn(II), although the two metal ions do not compete in their binding *(63)*.

Upon binding to these two proteins in the portal blood, most of the incoming copper goes directly into the cells of the liver and some also to the kidney. (Very little of it initially goes to other tissues and organs.) The liver is the most important organ for copper homeostasis. Not only is it the main initial repository of incoming copper, but it also releases a good portion of that copper back into the plasma, bound to newly synthesized ceruloplasmin. In addition, it is the source of copper excreted in the bile. Once back in the blood plasma, the copper on ceruloplasmin is available for uptake by tissues throughout the rest of the organism *(9,63)*. Just as most of the copper on albumin and transcuprein (and thus in the exchangeable blood plasma pool) appears to be targeted to the liver and kidney, so ceruloplasmin is probably the main source of copper for other tissues, under normal circumstances. This conclusion derives from studies in which (1) tissue uptake of copper given intravenously as ceruloplasmin, or ionic copper was compared *(9,69,70)*; (2) uptake of ionic ^{64}Cu/^{67}Cu was followed over time and it was found that uptake by nonhepatic tissues only occurred after the appearance of radioactive copper in plasma ceruloplasmin *(63)*; and (3) uptake of ^{67}Cu from ceruloplasmin and turnover of ceruloplasmin–copper were followed and found to be enhanced by copper deficiency *(10)*. Data from heavy isotope studies in humans are consistent with the concept that plasma ceruloplasmin distributes copper to tissues *(16)*. Two phases in the distribution of newly absorbed copper to tissues can thus be distinguished—the first being distribution to the liver (and kidney) in the period when transcuprein and albumin are carrying the radioisotope, and the second being distribution to other tissues after radiocopper is released from the liver on plasma ceruloplasmin and the radioisotope is no longer bound to transcuprein and albumin.

This scenario does not prove that, in the absence of albumin or transcuprein, for example, copper will not still first enter the liver or that, in the absence of ceruloplasmin, tissues will be generally deprived of copper. From "natural" genetic knockouts of albumin (Nagase analbuminemic rats) and ceruloplasmin (human aceruloplasminemia), it is clear that albumin is not required for copper uptake by the liver and kidney *(71)* and that ceruloplasmin copper is not the only form of copper available to most nonhepatic tissues *(72–74)*. Using various cell lines, we and others have shown that copper can be taken up from ceruloplasmin as well as from albumin, transcuprein, or Cu-dihistidine *(72,75–77)*.

Table 2
Copper-Binding Components in Human Blood Plasma

Component	Estimated contribution to total copper content (μg/L)	(μM)	(%)
Ceruloplasmin	650–700	10–11	65–70
Albumin	120–180	2–3	12–18
Transcuprein (macroglobulin)	90	1.4	9
Ferroxidase II	10	0.16	1
Extracellular SOD and histidine-rich glycoprotein	<10	<0.16	<1
Blood clotting factors V and VIII	<5?	<0.08	<0.5?
Extracellular metallothionein and amine oxidase	<1?	<0.02	<0.1?
15–60 kDa components	40	0.63	4
Small peptides and amino acids	35	0.55	4
"Free" copper ions	0.0001	0.0000002	~0

Source: Modified from refs. *1* and *65*.

Thus, again, it seems that there is more than one way in which copper can be carried to cells for uptake and that more than one protein can serve the same function. (Redundancy of function supports survival.) There appear to be differences in uptake efficiency, but this may not matter normally. Data obtained in several rat studies, in which uptakes of iv administered ^{67}Cu from ceruloplasmin and exchangeable plasma copper were compared, indicated consistent differences in the avidity of given tissues for a particular copper form *(10,69–71)*. Most nonhepatic tissues (and particularly the heart and placenta) show a preference for ceruloplasmin–copper. As ceruloplasmin copper is buried in its structure and not exchangeable in solution at physiological pH, the uptake of copper from ceruloplasmin must involve interaction with specific receptors on the cell surface. Specific receptors for ceruloplasmin in the plasma membranes of many different tissues have been detected by several research groups *(1,72,78–80)*. Similarly, because the copper on transcuprein and albumin is targeted more specifically to liver and kidney, it seems likely that specific receptors mediate uptake also from these carriers (or at least from transcuprein). Because transcupreins appear to be macroglobulins, the macroglobulin receptor could be involved, although this remains to be examined.

Actual uptake of the copper delivered by transcuprein, albumin, and ceruloplasmin to specific receptors (or by other means, such as a dihistidine complex given in vitro) might occur via the ubiquitously expressed transporter, CTR1, already described in connection with intestinal copper absorption. Earlier studies with cultured hepatocytes as well as fibroblasts, principally by Ettinger et al. *(81)* and McArdle et al. *(82),* had identified a single saturable, nonenergy-dependent transporter, with a K_m for Cu(II/I) in the range of 11–15 μ*M* for rat and mouse hepatocytes, and V_{max} of 0.2–3 nmol/min/mg cell protein *(1)*. Transport was inhibited by several other divalent metal ions, notably those of Zn, Mn, and Cd, which may distinguish it from ctr1 and hCTR1. A fivefold higher concentration than that of Cu(II) inhibited absorption 40%, 65%, and 75%, respectively, over 20 min *(83)*. Another potential difference between these transporters is that (at least in yeast) ctr1 transport appears to involved reduction to Cu(I) *(84)*. This suggests either that the "copper" transporter previously identified is not CTR1 but rather a transporter that favors the uptake of other divalent metal ions, or that the characteristics of mammalian CTR1 are such that it transports not just copper ions but also other metal ions. These matters remain to be explored, but the apparent differences suggest that a still undiscovered copper transporter could be involved, at least in normal copper uptake by the hepatocyte. [Other human homologs of yeast ctrs are being identified and characterized *(8,84)*.]

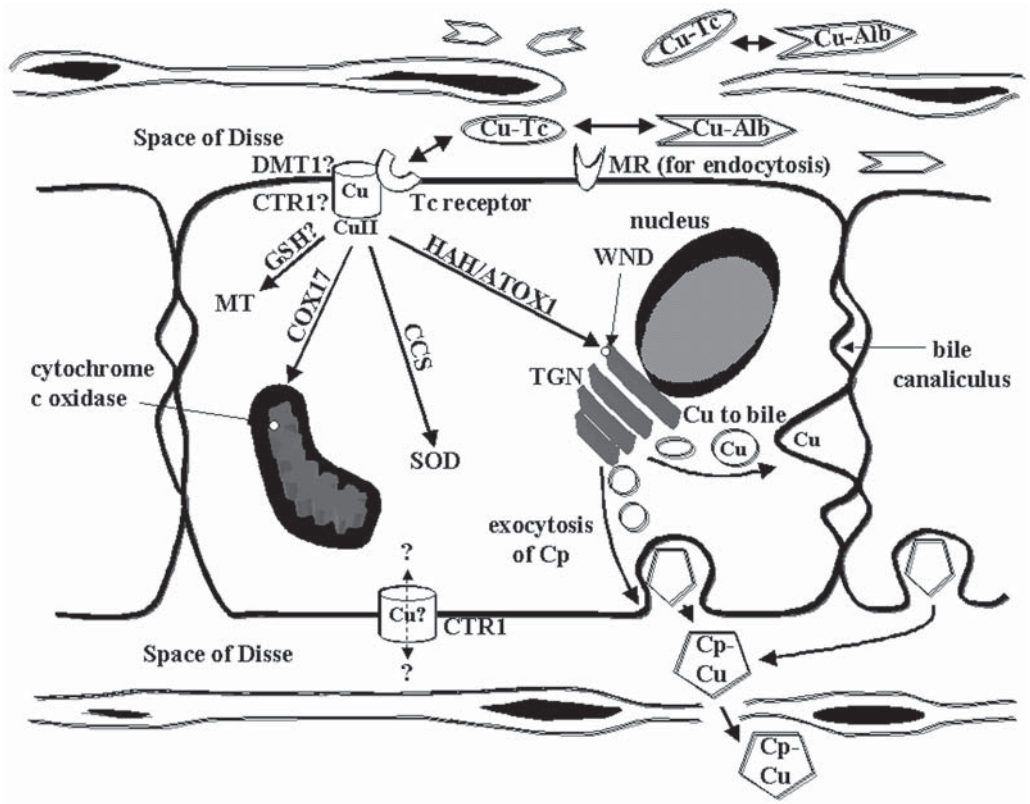

Fig. 3. Model of copper uptake and transport in the liver and hepatocytes. The central cells depicted are the parenchymal hepatocytes, separated from the blood circulation by endothelial cells and the Space of Disse. Copper may enter the hepatocyte via CTR1, DMT1, or some as yet undiscovered transporter. Receptors for macroglobulin/transcuprein (Tc) may be involved, as may receptor-mediated endocytosis mediated by the macroglobulin receptor (MR). Copper is most probably delivered by transcuprein (Tc) which exchanges copper with albumin (Cu–Alb). Copper entering from the membrane transporter is picked up by chaperones and carried to specific sites (as in the case of the intestinal cell; *see* Fig. 1 and text) and/or perhaps by glutathione (GSH) and metallothionein (MT). HAH1/ATOX1 carries copper to the ATP7B (WND) transporter in the trans-Golgi network (TGN), from where it is either pumped into vesicles destined for to the bile or into vesicles making ceruloplasmin (Cp) for secretion into the blood plasma. More recent evidence indicates that the WND protein can cycle to the canalicular membrane, for enhanced excretion of copper via the bile (*see* text).

Another possibility is that the transporter is DMT1/Nramp2, the proton-dependent divalent metal transporter already described in connection with intestinal copper (and iron) absorption. There are multiple isoforms of the mRNA for this transporter, it is abundantly expressed by hepatocytes, and there is at least indirect evidence DMT1 can transport copper (*see* Section 1.2.). The original studies of Ettinger and colleagues, however, did not report that Fe(II) used the same uptake mechanism or that proton coupling was involved. They also found that Ni(II) was not competitive. In contrast, transport by DMT1 is proton coupled and Ni(II) is probably a substrate *(34)*.

The first phase of distribution, in which copper enters liver and kidney and is released from there into the bile and with ceruloplasmin, is illustrated in Fig. 3. Here, it is postulated that copper enters the *hepatocyte* from transcuprein either via receptor-mediated endocytosis (through the macroglobulin receptor) and/or via transfer to a transporter that remains to be identified (CTR1? DMT1?). Upon crossing the cell surface, it is carried to essential enzymes in the cytoplasm and subcellular compartments via specific chaperones already described and/or is picked up by metallothionein and/or

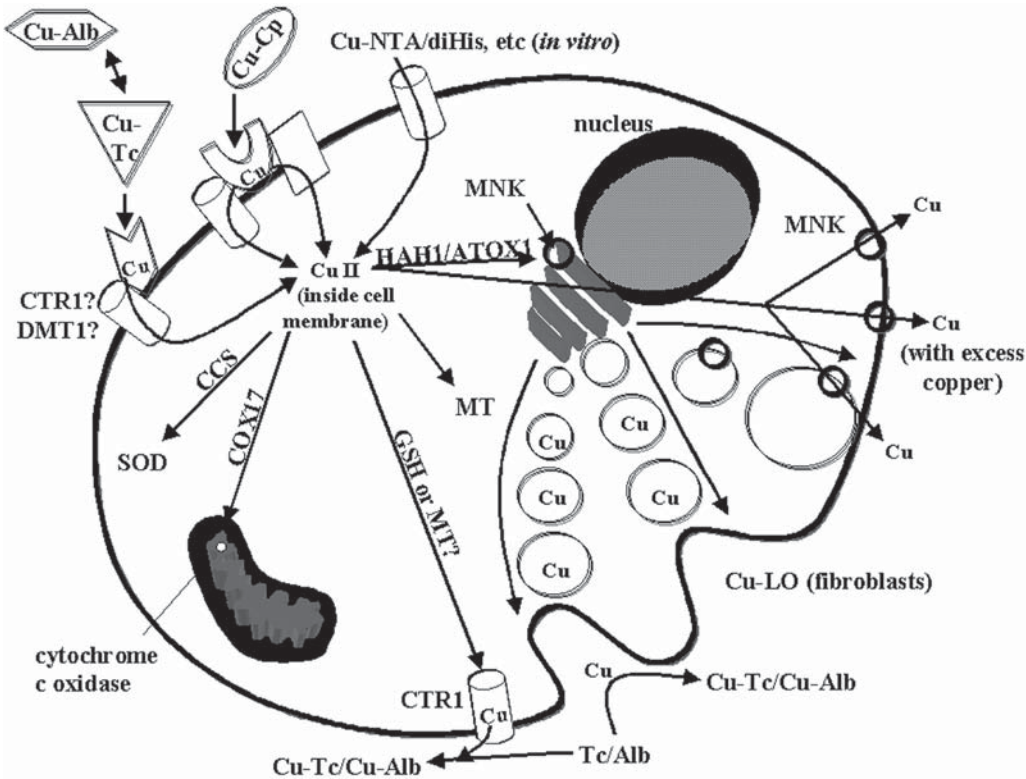

Fig. 4. Model of copper uptake and transport in nonhepatic cells. Most cells probably gain copper through CTR1 and/or DMT1 in the plasma membrane, which is associated with specific receptors for the plasma protein carriers of copper, particularly ceruloplasmin (Cp) and probably also transcuprein/macroglobulin (Tc)—which exchanges copper with albumin (Cu–Alb). As in other cells (*see* Figs. 1 and 3 and text), copper chaperones transfer the metal ion to various intracellular sites, including the ATP7A protein (MNK) in the TGN. Exit of copper from the cell may involve facilitated diffusion (perhaps using CTR1) down a concentration gradient, and exocytosis of two kinds (1) attached to specific secreted proteins/enzymes (like lysyl oxidases) or (2) for attachment to plasma albumin and transcuprein/macroglobulin in the blood plasma. The MNK also cycles between the TGN and the plasma membrane, and when attached to the latter, it is able to pump the ions directly into the plasma. This is particularly the case when excess copper enters the cell and must be deported.

glutathione. A good portion of it flows via HAH1/ATOX1 to the WND protein (ATPase7B) in the TGN, from where it is transferred to the secretory pathway, becoming incorporated into plasma ceruloplasmin as well as into the bile.

The phase of distribution in which copper enters nonhepatic cells from ceruloplasmin or other copper carriers is illustrated in Fig. 4. Certainly, CTR1 seems likely to be involved in copper uptake in most of these tissues. (It might also function in copper release.) DMT1 is also a candidate for mediating copper uptake. As postulated for hepatocytes, CTR1 and DMT1 (or another transporter) might receive copper from transcuprein (and/or albumin), perhaps with the mediation of a specific receptor. Donation of copper from ceruloplasmin would also involve specific receptors, the presence of which on many cell membranes has already been mentioned *(72,78–80)*. Ceruloplasmin receptors most likely are linked to the same copper transporters. Thus, with vesicles isolated from the placenta, it was shown that copper on ceruloplasmin and with copper–histidine competed for the same uptake mechanism *(75)*. This is consistent with earlier findings that specific binding of ^{67}Cu-ceruloplasmin

to plasma membrane preparations from several mammalian tissues was blocked by an excess of ionic copper *(72)*. All in all, the details of how copper crosses into cells are still far from clear and as already mentioned, reduction/reoxidation might be involved.

1.4. Distribution and Metabolism of Copper Intracellularly

As already described in some detail for the enterocyte and hepatocyte, copper that has entered the cell through one or more membrane transporters is distributed intracellularly by specific copper chaperones. These chaperones (with the possible assistance of glutathione or metallothionein) deliver the trace element to a variety of copper-dependent proteins and/or organelles (Fig. 4). Each cell has its own pattern of copper protein expression, although virtually all express cytochrome oxidase, Cu/Zn superoxide dismutase, and metallothionein. Most tissues also express MNK rather than WND, although some tissues (like placenta and mammary gland) express both (*see* Section 2.2.). Additional copper enzymes are crucial for various organs, including several enzymes in the central nervous system and adrenal for the production of catecholamines and peptide hormones, the production of melanin by melanocytes, the crosslinking of collagen and elastic fibers by enzymes from fibroblasts, and so on (*see* Section 2.1.). It is clear that virtually no copper is present in cells (or in body fluids) as the free ion *(85)*. The rates at which copper becomes incorporated into the various copper-dependent enzymes or other proteins will vary, probably depending on several factors, including the availability of chaperones, how far (or deeply) into cellular compartments it must travel, and whether it can bind directly or only during folding of a protein. Again depending on cell type, entering copper may or may not equilibrate rapidly with intracellular copper pools. These pools will, in turn, be replenished not just from uptake of new copper by the cell but from copper released during continuous degradation of copper proteins. Indeed, evidence from human studies with stable copper isotopes indicates that relatively little copper enters and leaves the cells of most tissues on a daily basis *(16,19)*. Most is recycled. This contrasts with what happens in the liver, intestine, and other tissues responsible for formation of digestive secretions—which put out (and must replenish) more than 5 mg Cu every day (*see* Section 1.2.).

1.5. Release of Copper from Cells and Copper Excretion

Except in the case of the hepatocyte, how copper is released from cells under normal circumstances is hardly understood. Clearly, except for the tissues producing secretions for the gastrointestinal tract (including salivary glands, the pancreas, and epithelia in the stomach and intestine), most copper must return to the liver for excretion. Here, it can be brought by all three of the plasma carriers (Fig. 3), not only by transcuprein and albumin (which particularly target the liver) but also by ceruloplasmin, which is taken up as well *(10,69,70,73,76,77)*. In the latter case, most of the ceruloplasmin enters hepatocytes after desialylation, via the galactose receptor and receptor-mediated endocytosis (used for uptake of asiologlycoproteins as a whole) *(1,80)*. The epithelial cells lining the sinusoids have specific ceruloplasmin receptors, whereas hepatocytes do not. The endothelial cells can desialylate ceruloplasmin *(1,80)*.

Although (as already mentioned) most copper is recycled within given cells and tissues, some is, no doubt, regularly released back into the blood. CTR1 might be involved in this release, although this is pure speculation. An important and known means for exit of copper from nonhepatic cell is through MNK. There is evidence that release can occur in two different ways—one being through exocytosis (Fig. 4) (as postulated for the enterocyte; Fig. 1); and the other by trafficking to the plasma membrane (Fig. 4). The latter process would appear to come into play particularly when large amounts of copper need to be deported. Camakaris, Mercer, Petris and their co-workers have uncovered a remarkable mechanism present in normal cells but stimulated by the influx of excess copper *(86–89)*. This mechanism involves the cycling of MNK between the TGN and the plasma membrane, so that more is present on the cell surface when excess copper needs to be exported. This was first demonstrated in CHO cells that developed resistance to copper toxicosis *(86,87)*. In cells that became

resistant, treatment with high doses of copper resulted in deployment of MNK to the plasma membrane, promoting efflux of copper and preventing over accumulation. Cells that were not resistant were unable to do this and so suffered the effects of copper toxicosis (*see* Section 4.). Whether this mechanism is widely employed by different types of mammalian cell and/or whether it also functions under normal conditions of copper entry and efflux in mammals remain to be determined. Even in normal conditions, however, MNK is likely to be involved in copper leaving some cells by exocytosis (Fig. 4), as suggested for the enterocyte (Fig. 1). (In this case, the MNK transporter would pump copper into vesicles destined for coalescence with the plasma membrane.) In Menkes disease (where MNK is defective), certain cells (like fibroblasts) accumulate copper (*see* Section 3.2.1.).

In hepatocytes, WND plays the same kind of role. The primary pathway for excretion of copper from the body is from hepatocytes, via the bile, and WND is crucial to that process (Fig. 3). Although (as for MNK) the WND ATPase (7B) has mainly been located in the trans-Golgi network, recent studies indicate that these vesicles are close to the canalicular membrane, where the bile is released *(89)*. Moreover, using polarized cultured hepatoma cells, it was demonstrated that treatment with copper caused a migration of WND to the apical membrane, forming the bile canaliculi *(90)*. This is identical to the response of MNK in other cell lines and points to a general pattern of cell and organ response. Increased trafficking of WND from the TGN to the plasma membrane also fits with long-standing observations that excess copper entering the blood will stimulate its immediate biliary excretion *(1,5,9)*. WND may also play a role in copper exit from cells in the brain, kidney, cornea, and spleen, because in Wilson disease (where this protein is defective) copper accumulates in these tissues (as well as in the liver).

Because the bile is the main route for net excretion of copper from the mammal, it would seem that most copper from peripheral tissues must return to the liver to exit from the body. Alternatively or in addition, because of the relatively large amounts of copper cycling between the digestive tract and liver (*see* Section 1.2.), copper could come to the liver more indirectly, first entering cells of other tissues/glands/organs involved in production of digestive tract secretions, entering the digestive tract from there and then being reabsorbed, coming to the liver via the portal circulation.

Once in the hepatocyte, copper destined for permanent excretion would be directed to the bile. How bile is formed is still being elucidated; however, substituents of the bile must cross specialized portions of the hepatocyte's plasma membrane that have a brush border and form the bile canaliculi. The route taken by copper to the bile is at least partly the same as that already described in connection with the disposition of copper in hepatocytes in the first phase of dietary copper distribution (Fig. 3). This would involve HAH1/ATOX1, WND, and exocytosis [or trafficking of WND to the brush border of the bile canaliculus, as already described *(91)*]. In addition, at least some of the copper entering on asioloceruloplasmin may be carried there on that protein (or portions thereof). The appearance of ceruloplasmin protein and copper coming from plasma in the bile has been traced *(5,92,93)*, although its quantitative contribution to biliary copper excretion is unclear. Indeed, it has been proposed that a large fragment of ceruloplasmin, high in copper and resistant to proteolysis, may furnish a means of excreting copper without intestinal reabsorption *(94)*. As concerns the other forms in which copper is found in the bile, the available data from different laboratories are not in agreement *(1)*, so this needs further examination.

As already mentioned, copper in bile is less reabsorbable than that in other gastrointestinal juices. However, reabsorbability varies in relation to the amounts of copper flowing into hepatocytes from the intestine (or with injection). Thus, when more copper is to be excreted, a larger proportion will not be reabsorbable, and vice versa *(1)*. Similarly, a larger proportion of copper entering the hepatocytes is relegated to the bile when excess copper enters, and vice versa. Thus, much of copper homeostasis is controlled by the level and form in which it is excreted through the bile. In addition, it should be noted that copper can be lost from the organism as a consequence of entering the gastrointestinal tract through other secretions. Although these secretions contain copper in a more absorbable form

(1), they would provide a means of losing copper, at least when the biliary route is blocked. (As shown some years ago in rats, the rate of loss of whole-body copper was halved when the common bile duct was ligated *[94]*.) Clearly, this is not sufficient to prevent a gradual toxic accumulation of copper in Wilson disease (or the corresponding disease in LEC rats). However, this toxic accumulation takes some years and is thus not as rapid as one would anticipate if the bile (and WND) were the only route. (Assuming that at least 0.3 mg of new copper is absorbed every day and the bile is the only excretory route, the total copper in a teenagers and young adults might double in a year. Most of this extra copper would end up in the liver, increasing its already high concentration many times, in just one year, which is not what occurs *[15]*.) This demonstrates again that there are backup mechanisms by which copper can be transported when the main one fails. Some of these will be less effective than others and cause pathology more rapidly, but there is usually this kind of redundancy. In any event, the regulation of copper excretion appears to be the main mechanism for homeostasis. Copper excretion is greater when absorption and intake are greater, and when intakes and absorption are low, copper is conserved by lowering excretion *(16,19)*.

2. FUNCTIONS OF COPPER AND REGULATION OF COPPER METABOLISM

2.1. Functions of Individual Copper Enzymes/Proteins and Their Regulation

Most of the copper transporters and chaperones already described, that have been cloned and investigated so far, are listed in Table 3, along with a brief summary of what occurs when they are defective or "knocked out" (if this is known). For most of these, more detailed descriptions of their functions have already been provided. The fact that copper is an essential element, however, is not because of its carriers and transporters but because of specific copper-dependent enzymes (and perhaps also other factors) that are crucial for life and for human metabolism and function. A list of the known copper-containing enzymes/proteins in humans and mammals is given in Table 4, along with brief descriptions of their functions. This is in addition to the list of plasma copper constituents given in Table 2. Ceruloplasmin is included in Tables 2–4, because it plays a variety of roles in addition to that of delivering copper via the blood. Further descriptions of the most interesting aspects of the functions of these copper enzymes and how their expression and functionality are regulated follow.

2.1.1. Cytochrome-c Oxidase

This terminal enzyme for mitochondrial (and thus cellular) respiration is fundamental to oxidative phosphorylation and thus for the production of usable energy in the form of ATP for almost all living organisms. It is the site for binding of most of the oxygen utilized by cells (via heme), where copper aids in the transfer of electrons (coming electron transport through cytochrome-*c*) for reduction of oxygen to water. A complex enzyme that sits within the inner mitochondrial membrane, it has 2 heme groups and 3 copper atoms, as well as 13 subunits (in humans), three of which are encoded by mitochondrial DNA. (Further details are available from previous reviews *[1,5]*.) How the assembly of this molecule, with subunits from the cytoplasm as well as from the mitochondrial matrix (and copper delivered by COX17), is coordinated is sure to be quite a tale when it is elucidated. Studies with yeast cytochrome-*c* oxidase indicate that two other proteins (Sco1 and Sco2) are necessary for structural assembly and insertion of the copper *(8)*.

2.1.2. Cu/Zn Superoxide Dismutase

This similarly ubiquitous protein, consisting of two subunits of about 16 kDa and two histidine-bridged atoms of Cu and Zn, is part of the core system in most living organisms for controlling and preventing destructive effects of reactive oxygen species. It converts superoxide anions to peroxide, for further disposal (by catalase, glutathione peroxidase, and similar enzymes). Drosophila and microorganisms lacking the enzyme have been shown to be more vulnerable to damage by reactive oxygen species *(65)*. In mice where the gene has been knocked out, there is gradual damage to (and

Table 3
Transporters and Chaperones of Copper Found in Mammalian Cells and Their Potential Functions

Protein	*Probable potential functions*	*Genetic disease model*	*Knockout symptoms*
MNK	Cu transport into TGN (most cells) Cellular copper release Incorp. of Cu into lysyl oxidase Role in mammary gland/placenta	Menkes Brindled mouse Occipital Hom Synd.	Cu deficiency; decreased intestinal transfer; death Excess copper accumulation in some cells Connective tissue defects
WND	Cu transport into TGN (hepatic) Role in placenta/mammary gland Incorp. of Cu into ceruloplasmin Biliary copper excretion	Wilson LEC rat Toxic milk mouse	Accumulation of excess copper in liver and other organs, leading to tissue damage and death if untreated
CTRI	Cu transport (plasma membrane)	Knockout	Homozygote dies in utero in early–mid embryogenesis Heterozygote is copper deficient (also brain)
DMT1	Divalent metal transport across plasma membrane	Microcytic anemia mice Belgrade rat	Fe deficiency, because of decreased intestinal absorption Immune defect? (Nramp2)
Hephaestin	Oxidation of Fe during Fe transport (ceruloplasmin homolog; in TGN?)	sla mouse	Sex-linked anemia
Ceruloplasmin	Oxidation of Fe during cell release Delivery of Cu to many cells GPI linked to brain astrocytes and glia Scavenger of reactive oxygen species	Aceruloplasminemia	Accumulation of excess Fe in several tissues
ATOXI/HAHI	Delivery of Cu to WND/MNK	(Yeast; murine knockout)	Decreased placental Cu transfer; failure to thrive after birth (Cu deficiency?)
CCS	Delivery of Cu to SOD	(Yeast)	Decreased SOD activity
COX17	Delivery of Cu to mitochondria	(Yeast)	Decreased cytochrome oxidase activity

Table 4
Copper-Dependent Enzymes in Mammals

Enzyme	*Function*
Cytochrome-*c* oxidase	Cell respiration/formation of ATP/reduction (utilization) of O_2
Cu/Zn superoxide dismutase	Antioxidant defense in cytoplasm
Metallothionein	Storage of excess Cu and other divalent metal ions [not Fe(II)] Possible donor of Cu to certain apoproteins Possible superoxide dismutase when copper loaded
Ceruloplasmin (extracellular)	Ferroxidase/promotes flow of Fe from liver to blood Scavenger of reactive oxygen species/acute phase reactant Source of copper for tissues (130 kDa)
Protein-lysine-6-oxidase (lysyl oxidase) (extracellular)	Crosslinking of collagen and elastin fibers for maturation/ stabilization of extracellular matrix
Tyrosinase (catechol oxidase)	Formation of melanin through crosslinking and modification of tyrosines (in melanocytes)
Dopamine-β-monooxygenase	Formation of catecholamines and related neurotransmitters and hormones (chromaffin granules)
α-Amidating enzyme	Modifies C-terminal ends of hypothalamic peptide hormones ending in glycine, leaving the COOH of the next to last AA amidated (necessary for hormone maturation)
Diamine oxidase (cellular and extracellular)	Inactivation of histamine and polyamines?
Amine oxidase (extracellular)	Inactivation of histamine, tyramine, dopamine, serotonin?
Hephaestin	Ferroxidase, in trans-Golgi of enterocytes; aids iron absorption homology to ceruloplasmin (134 kDa)
Cartilage matrix glycoprotein	Ferroxidase/amine oxidase, homologous to ceruloplasmin (chondrocytes and eye ciliary epithelia) (550-kDa tetramer)
Prion protein (PrP^C)	May protect against reactive oxygen species; has SOD-like activity; may return copper to neurons at synapses (many cells)
S-Adenosylhomocysteine hydrolase[a]	Sulfur amino acid metabolism
Blood clotting factors V and VIII	Blood clotting

[a]Bethin et al. *(96)*.

associated peripheral neuropathy of) neuromuscular junctions in the hindlimbs *(97)*. Most probably, phenotypic responses are not more dramatic because of a redundancy of function in the antioxidant system of mammals. Mutations of Cu/Zn SOD have also been of interest in connection with amyotropic lateral sclerosis (ALS), where a gain of function (rather than loss of activity) may be responsible for the underlying neurological symptomology *(98–100)*. Normally, expression of Cu/Zn SOD appears to be fairly constitutive. However, and at least in certain cells, it is one of the first enzymes to reduce its activity (which depends on copper) when copper becomes less available *(1,18)*, and hyperoxia induces expression of SOD in the lung (along with metallothionein) *(101)*.

2.1.3. Metallothioneins

These 61 amino acid proteins (with 20 cysteines) come in at least 2 isoforms encoded by several genes and are adept at tightly binding divalent metal ions (except Fe). They appear to function as an adaptive mechanism for holding/storing metal ions not needed for metabolism at that moment and for sequestering them in innocuous form when they are present in excess amounts *(1)*. (Thus, for example, cadmium accumulates in metallothionein (particularly in the kidney) throughout life, as it is difficult to excrete *[2]*. Excess copper accumulates in MT in Wilson-disease-affected tissues.) Production

(synthesis) of the protein is responsive to metal-ion influx, so that more is made when needed. Zinc and cadmium are particularly good inducers, although copper can also be effective in some tissues *(1)*. Some other factors, notably the hormones glucagon and cortisol as well as agents that induce inflammation and the acute-phase response, also enhance expression. Glucagon and cortisol are released in fasting, when enhanced protein degradation for gluconeogenesis might release extra amounts of metal ions for sequestration. Although MTs can bind exotic metal ions, such as those of Hg, Ag, and Ni, in actuality the proteins mainly bind Zn, Cu, and Cd ions. Of the latter ions, Cu is bound most tightly and can displace the other ions. Because Zn and Cd ions are not as reactive as Cu with regard to oxygen radical formation, binding of copper to MT is protective for the cell. In addition, Cu–thionein (Cu–MT) appears to have some superoxide dismutase activity *(102)*. In the absence of SOD, oxidative stress induces expression of MT *(101,103)*.

2.1.4. Ceruloplasmin

The potential roles of this protein, which is mainly found in extracellular fluids and blood plasma, have already been described in connection with copper delivery to cells and excretion of copper from the body (*see* Sections 1.3. and 1.5.). It consists of a single polypeptide chain (about 120 kDa with 12 kDa carbohydrate), with internal threefold homology, and six plastocyanin-like domains, into which six nondialyzable copper atoms (supplied by WND) are incorporated, presumably during its folding in the TGN. Recent interest has focused primarily on another of its functions (evident for some time), namely its role in iron transport. Ceruloplasmin is a ferroxidase, and it is thought that the ability to oxidize Fe(II) to Fe(III) is helpful in providing iron in the form needed to bind to its plasma carrier, transferrin, as it emerges from cells for further transport (as to the bone marrow for incorporation into red blood cells, where most iron resides). In severe copper deficiency, where there is little or no copper-containing (and thus ferroxidase-active) ceruloplasmin in the plasma (or elsewhere), iron accumulates in the liver and some other tissues. In this condition, iv infusion of ceruloplasmin (and not copper–albumin) results in immediate release of liver iron into the blood plasma *(1,104,105)*. Recent observations made in some families with genetic apoceruloplasminemia *(73)* and with the mouse knockout *(107,108)* lend further support to this concept. Nevertheless, only 1–2% of the normal plasma level of ferroxidase-active ceruloplasmin is sufficient to support its role in iron efflux *(109)*, and it, alone, cannot be responsible for this process. (About 22 mg or about 0.7% of the iron in the adult human body fluxes in and out of red blood cells alone, every day, and a major portion of that enters and leaves liver cells [including hepatocytes]). If even 1% of that iron did not leave hepatocytes because of lack of ceruloplasmin, this would cause a rapid and massive accumulation of iron in liver. Instead, accumulation is gradual and takes many years in humans.] Of additional recent interest is the finding of glycosylphosphatidylinositol-linked (GPI-linked) ceruloplasmin on astrocytes *(110)* and glia *(111)* in the brain. A product of alternative splicing of the ceruloplasmin transcript *(112)*, this form of ceruloplasmin may also be involved in iron transport *(112,113)*. However, it appears unlikely that ceruloplasmin plays a role in releasing iron from enterocytes during iron absorption *(41)*.

Ceruloplasmin is also an acute-phase reactant, which means that its concentrations in plasma increase during inflammation or infection. During inflammation and infection, transport of iron is diminished. Thus, when the body limits iron transport through the blood (which protects it against the virulence of infections) *(1,2,5,6)*, there is an *increase* in the synthesis and secretion of copper-containing ceruloplasmin from the liver (the opposite of what one would expect if ceruloplasmin were only concerned with releasing iron into the plasma). It seems likely that this reflects a need for protection (by ceruloplasmin) against the endogenous production of reactive oxygen species used against invading organisms or antigens. (Ceruloplasmin is a scavenger of a variety of such radicals *[1,5,65]*.) It appears that the regulation of ceruloplasmin expression is controlled not just by inflammatory cytokines but also through hypoxia-inducible factor (HIF1) *(114)* and even insulin *(115)*. (HIF regulation also links it to iron metabolism.)

As already indicated in the earlier copper transport sections (Sections 1.3. and 1.5.), ceruloplasmin supplies copper to cells all over the body and appears to be the preferred source of plasma copper for certain tissues, like the heart and placenta. The abundant evidence for this function of ceruloplasmin is detailed in several reviews *(5,9,10)*.

2.1.5. Hephaestin

This is another protein with some of the characteristics of ceruloplasmin and a link to iron metabolism. It was identified as responsible for a sex-linked anemia in mice *(116)* and is thought to be involved in intestinal iron absorption. A transmembrane protein of about 134 kDa, with ferroxidase activity *(117)*, it appears to be located primarily in trans-Golgi vesicles (*see* Fig. 1). Here, it may oxidase Fe for binding to apotransferrin, allowing its release into the blood as holotransferrin (through exocytosis). Its expression (as mRNA) is highest in the small intestine. Smaller amounts of its mRNA are expressed in skin, lung, and kidney.

2.1.6. Cartilage Matrix Glycoprotein (CMGP)

This is another intracellular ceruloplasmin homolog, composed of four disulfide-bonded subunits (each of 116 kDa) and with ferroxidase and oxidase activities *(118)*. Located in the vesicular portions of chondrocytes, as well as in the epithelial cells of the eye *(119,120)*, it may play a role in the formation of the extracellular matrix.

2.1.7. Lysyl Oxidase (Protein-6-Lysine Oxidase)

This enzyme is integral to the formation, maturation, and stabilization of connective tissue, which is part of the extracellular matrix of organs and tissues (including cartilage and bone) throughout the body. Secreted by fibroblasts (most likely after copper is incorporated in the trans-Golgi by MNK), it catalyzes the crosslinking of elastic and collagen fibers. Copper is important for lysyl oxidase activity, in that failure of the development of normal connective tissue is symptomatic of copper deficiency, Menkes disease, and its milder cousin, Occipital Horn Syndrome. A multimeric protein composed of 32 kDa subunits, it requires copper for (or for development of) its activity. The first gene for lysyl oxidase was cloned from rat aorta *(121)* and human placenta *(122)* and codes for a polypeptide of about 400 amino acids, although several mRNA transcripts (ranging from 2 to 5.5 kb) can be expressed. The cofactor, lysine tyrosyl quinone (LTQ), is part of the enzyme's active site. Recent evidence suggests that the role of copper may not be catalytic as much as supportive of cofactor formation and structure and/or enzyme integrity *(123,124)*. Although copper availability determines how active the enzyme can be, nutritional copper status does not alter expression of the protein or its mRNA *(125)*. Recently, several lysyl oxidase-like genes have been identified and cloned. Some of these are particularly expressed by placenta and other reproductive tissues *(126,127)*, and their functions will need to be elucidated.

2.1.8. Prion Protein (PrP^C)

Of great potential interest is the recent discovery that the normal prion protein, which goes awry in bovine spongiform encephalopathy (mad cow disease) or Creutzfeldt–Jakob disease, is another copper-dependent antioxidant enzyme, important for maintaining a healthy central nervous system. The normal prion protein (33–35 kDa, varying in glycosylation) is expressed not only in neurons but in other cells, including skeletal muscle. GPI-anchored to the outside of the plasma membrane, there appear to be at least two forms (synaptic and nonsynaptic) associated with neurons, and concentrations of the protein are particularly high in the areas of the synapse *(128)*. Although knockout mice did not exhibit gross disturbances in behavior or development, they displayed changes in electrophysiology and circadian rhythms and, particularly, an increased sensitivity to various kinds of stress *(128)*. Copper binds to four identical sequences of eight amino acids ("octarepeats"; PHGGGWGQ) in the N-terminal region of the protein, probably via the imidazole and glycine N's *(129)*. (However, up to five copper atoms can be bound.) There is evidence that copper lends structural stability not

only to the N-terminal region of the protein but also to other parts of the molecule *(130,131)*. The normal protein is reported to have superoxide dismutase-like activity *(132–134)*. Exposure to reactive oxygen species results in copper dependent, fragmentation of the N-terminal part of the protein *(131)*. Cleavage of the copper-containing N-terminal region is also associated with turnover of the protein and cellular uptake of its copper *(128)*, and this turnover is quite rapid. Apparently, there can be synaptic release of high concentrations of copper *(128)*, and the prion protein might be a means of reabsorbing it locally (*see* next paragraph).

Disturbance of normal prion protein metabolism, through infection with the protease-resistant form that accumulates in the spongiform encephalopathies (PrP^{SC}), impairs the ability of neurons to respond to oxidative insults *(135)*. PrP^{C} knockout mice have increased levels of oxidized lipids and proteins in their brains and other tissues *(136)*. The thiobarbituric acid-reactive substances (TBARS) contents of the parietal cortex, hippocampus, cerebellum, and entorhinal cortex of the brain were all significantly elevated (46–175%), the greatest change being in the hippocampus. Increases in the carbonyl contents of brain proteins were 44–50% in the hippocampus and parietal cortex and 143% in the cerebellum. Evidence of similar elevations in oxidized lipids and proteins was obtained for the skeletal muscle, liver and heart of the knockout mice. Cu/Zn SOD levels in the tissues of these animals were markedly lower, particularly in the hippocampus and parietal cortex (where they were down more than 90%). This in itself might explain the increased oxidative damage observed and offers the possibility that the normal prion protein is somehow involved in making copper available to SOD in certain cells. Indeed, it has been reported that enhanced expression of PrP^{C} increases a cell's ability to take up copper *(137)*. It also appears to increase its resistance to copper toxicity and oxidative stress *(138)*, again implying a dual function—as means of copper uptake and radical inactivation. Exposure to large (100 μ*M*) and perhaps nonphysiological concentrations of Cu(II) or Zn(II) [but not Mn(II)] induced endocytosis of the protein *(139)*, which would bring its copper (or zinc) into the cell. (The binding of Zn is not as firm as that of Cu.) The addition of octarepeats to the prion protein (as occurs in some forms of spongiform encephalopathy) prevented copper-induced endocytosis, consistent with other evidence that the lack of removal/turnover of the prion protein results in (or contributes to) the brain damage seen in these diseases. Additional views on this protein are available *(140)*.

2.2. *Copper in Embryogenesis, Pregnancy, and Lactation*

2.2.1. Embryogenesis

From the description of copper enzyme functions alone it is obvious that copper is critical for embryogenesis, as well as the growth and development of mammals. Several documented aspects highlighting this point are as follows: (1) During embryogenesis and its underlying massive cell proliferation, respiration and cytochrome oxidase activity are fundamental; (2) during gestation, the placenta is very active in transferring copper to the fetus *(1,141)*; (3) "knocking out" expression of CTR1 is lethal *(30,31)*; (4) "knocking out" the copper chaperone ATOX1 results in serious complications (in this case more after birth) *(56)*; and (5) the fetus accumulates a store of copper in the liver in the last part of gestation, which is rapidly used up during the initial phases of postpartum growth *(141)*. Based on RNA studies in mice, it is surmised that the MNK protein is expressed in all tissues—including developing liver hepatocytes—and particularly in the brain choroid plexus, during embryogenesis *(142)*. In contrast, WND mRNA expression is initially confined to the central nervous system (CNS), liver, and heart, but also occurs in the intestine, thymus, and lung epithelia in later gestation. As demonstrated by the symptoms of Menkes disease at birth, there are important functions of MNK in prenatal brain development. Most details of copper metabolism during embryogenesis (just as the process itself) are still unknown. What we know more about is what happens to maternal copper metabolism and transport of copper to the fetus during gestation.

2.2.2. Copper Metabolism in Gestation

Particularly during the last third of gestation, considerable copper is transferred to the fetus from the maternal circulation. This is utilized not only for the activation of the copper-dependent enzymes described in previous sections, but also allows the accumulation of what would appear to be a store of excess copper in liver hepatocyte nuclei *(1,2,141)*. Here, it is bound to metallothionein. Along with similar prebirth liver stores of iron and zinc, this excess copper is used up during the suckling period, presumably in support of the rapid cell proliferation and tissue growth occurring after birth. Some things are known about how the copper is delivered from mother to fetus. Most of it traverses the placenta, although some of it may be absorbed by ingestion of amniotic fluid *(70).* In vitro, placental cells can take up copper administered in several different forms, including Cu–dihistidine and ceruloplasmin *(75,76,141–145)*. In vivo, it was shown in rats that maternal plasma ceruloplasmin is the preferred source, as the copper from iv infused ^{67}Cu–ceruloplasmin entered the placenta much more rapidly than ionic ^{67}Cu, and treatment of the dam with cycloheximide, to inhibit synthesis and secretion of ^{67}Cu–ceruloplasmin by the liver (after administration of ionic ^{67}Cu), reduced uptake by the placenta *(70,141)*. Evidently because other carriers can also deliver copper (although perhaps at a slower rate), copper transfer to the fetus is not severely compromised in aceruloplasminemia *(146)*. Even when delivered as ^{67}Cu–ceruloplasmin, copper entering the fetal circulation in the last part of gestation appears to be in ionic form, allowing it to bind to fetal plasma proteins of the sizes of albumin and transcuprein *(70)*. The placenta expresses both WND and MNK, but probably not ceruloplasmin. (There are reports of placental expression of ceruloplasmin mRNA, but in those studies the yolk sac was not separated and it might be the actual expression site.) The placenta probably also expresses CTR1 and DMT1 (as well as the copper chaperones), because most cells do. Thus, copper uptake by the placenta and its distribution and transfer to the fetal circulation may follow aspects of the patterns described for nonhepatic as well as hepatic cells (Figs. 3 and 4). Evidence suggests that WND is involved in copper transport at the maternal side of the placenta. This is supported by mRNA expression and copper accumulation studies *(147)*, the latter in the LEC rat model of Wilson disease (where WND is defective). Also, the fetuses in the toxic milk and LEC rat Wilson disease models are copper deficient at birth. (In addition, there is a report of copper accumulation in the placenta of a Wilson disease patient *[148]*.) In contrast, the MNK protein seems to be active on the fetal side of the placenta *(149)*, and a defect in it also produces fetal copper deficiency. Successive pumping of incoming copper into vesicles, first by WND and then MNK, as well as intermediary transfer by ATOX1/HAH1, leading to transcytosis and/or trafficking of MNK to the fetal plasma membrane, must result in release of copper into the fetal circulation.

2.2.3. Copper Metabolism and Transport During Suckling and Lactation

Although a store of copper is deposited in the liver before birth, that copper is not nearly sufficient to support the needs of the newborn during suckling *(141)*. Thus, much copper is delivered to offspring after birth, via the milk. The components of the milk that carry copper have not been fully identified but include citrate and ceruloplasmin. Recent fractionation studies of human milk *(150)* indicate that copper is present in components of all sizes (from >2000 to <2 kDa), but that the largest percentages were with the smallest (35%) and largest (24%) components. We found that in the milk of the human *(9,151)*, pig *(9,141,152)* and rat *(10,153)* ceruloplasmin contributes 20–25% of the copper. We also found that feeding rat pups (but not weanling rats) ^{67}Cu–ceruloplasmin (synthesized in vivo) resulted in a much faster absorption of ^{67}Cu than when ionic ^{67}Cu(II) was administered with the milk *(151)*, indicating that the ceruloplasmin in milk has a nutritional value. Most of the ceruloplasmin in milk is produced by the lactating mammary gland and not transferred from the maternal plasma. There is a dramatically increased expression of ceruloplasmin mRNA (and total RNA) in the mammary gland, along with growth of mammary tissue, in conjunction with lactation *(10,152,153)*. Uptake of ^{67}Cu from the blood plasma by the mammary gland is greatly accelarated by lactation

(10,153), and incorporation of ^{67}Cu into milk ceruloplasmin precedes incorporation of the isotope into plasma ceruloplasmin. Transfer of ^{125}I–albumin from maternal plasma to milk is very much slower than the appearance of ^{67}Cu in milk ceruloplasmin [after administration of $^{67}Cu(II)$ as the metal ion to the dam] (Ilagan and Linder, unpublished). In the toxic milk mouse, there appears to be mislocalization of the WND protein in mammary epithelial cells *(154)* and this may be responsible for the copper-deficient milk produced in these mutants. However, in this model *(154,155)* and in Wilson disease *(156)*, some copper still enters the milk. So MNK may also be involved. These results indicate how important copper is for the rapidly growing newborn mammal in the suckling period. Further aspects of human copper metabolism and nutrition in the perinatal period are described in several reviews *(157–159)*.

3. COPPER IN DISEASES AND GENETIC DISEASES OF COPPER METABOLISM

3.1. Inflammation, Infection, and Cancer

Copper metabolism is altered in inflammation, infection, and cancer. As already mentioned, plasma ceruloplasmin is an acute-phase reactant, and synthesis and secretion of the protein by hepatocytes is stimulated by inflammatory cytokines (particularly interleukin-1 [IL-1] and IL-6) *(1,5)*. The increase in ceruloplasmin may protect cells from radicals released to combat the influx of foreign organisms or antigens, because it is a general radical scavenger, and most cells (including erythrocytes) have specific receptors on their surface that are likely to be saturated with ceruloplasmin at normal plasma concentrations. (These receptors may have dual roles, depending on cell type, providing a means for delivering copper to some and protecting the vulnerable cell membrane fatty acids in others.) Copper itself is important for many aspects of the immune response, including production of IL-2 by activated lymphocytic cells *(160)*, and supports the activity and effectiveness of cellular and humoral immunity *(1,161–163)*.

Whereas levels of iron in serum decline in infection and inflammation, copper concentrations and ceruloplasmin rise. The same is true in cancer *(164,165)*. Indeed, levels of plasma ceruloplasmin antigen or oxidase activity are positively correlated with disease stage, as shown particularly for lung and colon cancer *(165)*. Cytokines may again be involved in the response to the presence of a tumor, although this has not been adequately examined. Malignant tumors absorb copper with considerable avidity and have concentrations of copper that are often higher than those of their tissue of origin. Copper is absorbed by the tumors both from ceruloplasmin and from nonceruloplasmin sources in the blood *(69)*.

Copper may also have a role in angiogenesis *(1,166)*, which is vital to continued tumor growth. Earlier studies had implicated copper in the stimulation of new blood vessel formation *(1)*. This was recently confirmed with cultured endothelial cells *(167)*, although the doses used were very high and unphysiological (500 μM $CuSO_4$). Angeogenin, a potent stimulator of angiogenesis, appears to bind to endothelial cells more tightly when copper (at physiological concentrations) is added *(168)*. Specific small peptides generated by the proteolysis of SPARC, an extracellular matrix protein that is expressed by endothelial cells during remodeling of blood vessels, specifically bind copper and markedly stimulate angiogenesis *(169)*. In addition, recent studies provide evidence that limiting the biological availability of copper, by administration of penicillamine *(170)* or tetrathiomolybdate *(171)*, slows tumor growth and that this is the result of the inhibition of angiogenesis *(170)*. On the other side of the coin, it has long been known that certain complexes of copper can inhibit tumor growth in experimental animal models *(164)*. Such an effect of copper on tumors might involve the stimulation of apoptosis, as has been demonstrated for several unnatural complexes of copper (including Cu–nitrilotriacetate and orthophenanthroline) in certain cancer cell lines, in vitro *(65)*.

The presence of cancer (at least in rat models) enhances intestinal copper absorption *(172)* and increases plasma copper and ceruloplasmin concentrations *(1,15)*. It is still unclear whether this reflects needs of the cancer cell and/or that of the host.

3.2. Genetic Diseases of Copper Transport and Metabolism

3.2.1. Menkes and Wilson Diseases

The genetic bases of these two major diseases of copper transport were uncovered by several research groups in the early 1990s. First, the gene responsible for Menkes disease (and the less severe occipital horn syndrome) was cloned *(173–175)* in 1993, then that for Wilson disease *(176,177)*. As already described in some detail in earlier sections of this review, the corresponding normal proteins encoded by these genes are both P-type ATPases (ATP7B and 7A, for WND and MNK, respectively). They are usually expressed in different cell types (MNK quite widely, and WND primarily in hepatocytes and certain areas of the brain); located in the trans-Golgi network and vesicular compartments (Figs. 1, 3, and 4), they can be translocated to the plasma membrane under conditions when copper secretion or efflux needs to be promoted. Menkes disease results in abnormal gestational development and a copper-deficient phenotype, because of reduced copper transport to the fetus (via the placenta) as well as to the newborn after birth (via the milk). This reflects functions of MNK in placental copper transfer and intestinal absorption (*see* Sections 2.2.2. and 2.2.3.). Of special recent interest are findings that several translation products from alternatively spliced MNK gene transcripts travel to other parts of cells and even into the nucleus *(178–180)*. This indicates that the MNK gene product is not only an ATPase that pumps copper into TGN channels (or out of the cell at the plasma membrane) but that it has other, as yet undiscovered functions. Expression of alternative splicing products would, of course, also be affected by certain kinds of MNK mutations, and their malfunction might explain additional symptomology associated with Menkes disease or Occipital Horn Syndrome.

In contrast to Menkes disease, Wilson disease occurs more gradually, and after birth. It results in the accumulation of excess copper in liver and some other tissues and oxidative damage *(65)*. In this case the problem is excretion, because in the absence of the normal WND/ATP7B protein, it is difficult for copper to enter the bile (*see* Section 1.5.). Accumulation of excess copper in tissues (although mitigated by binding to metallothionein) promotes formation of reactive oxygen species, eventually resulting in liver cirrhosis *(65,181–184)*. The brain and some endocrine organs are also affected. Further details may be found in more recent reviews of these diseases *(57,185–189)*.

3.2.2. Aceruloplasminemia

A genetic absence of the production of active ceruloplasmin has been detected in a few families and has been mimicked by knocking out the gene in mice. As already described in considerable detail in most of the earlier sections of this review, ceruloplasmin has many functions, including antioxidant defense, copper transport, and iron transport. Presumably because of redundancy of function, so that other proteins and enzyme take up the slack when ceruloplasmin is missing, the absence of ceruloplasmin does not produce marked changes in copper metabolism and may not have a great effect on the redox state (although the latter has not as yet been thoroughly examined). It does, however, produce a gradual accumulation of iron in liver and some other tissues *(108,190)*. As already described, this would be much faster and more severe if ceruloplasmin were the only way in which iron destined for transferrin could be oxidized; even very low levels of ceruloplasmin (1–2% of normal) are sufficient to prevent liver accumulation and promote iron release into the blood *(109)*.

3.2.3. Spongiform Encephalopathies and Alzheimer's Disease

As already partly described, changes in copper metabolism are implicated in generation of the neurological damage that underlies "mad cow disease" and similar prion protein diseases (*see* Section 2.1.8.). The abnormal form of the prion protein implicated in this disease (PrP^{SC}), which accu-

mulates and is resistant to proteolysis, probably normally functions in transport of copper at synapses and perhaps also (directly and/or indirectly) in the scavenging of radicals. Lack of these normal activities appears to underlie some of the damage sustained by the brain in these diseases (*see* Section 2.1.8. for further details of PrP^C function). The β-amyloid protein, which forms the damaging brain "tangles" in Alzheimer's disease, also has some connection to copper *(185)*, although what this might be in the normal state is still far from clear. Copper (and zinc) are associated with the amyloid deposits of the disease *(191)*. However, at least in vitro, zinc precipitates aggregation of the amyloid protein, and copper works against the effect of zinc (except at high concentrations) *(192)*.

4. COPPER TOXICITY

Although copper is redox active as the free ion and in the form of certain complexes *(65)*, the amounts of copper that are normally ingested, and even intakes that are considerably higher, are usually not problematic for humans and rodents. This conclusion is echoed by the recent intake guidelines for copper released by the National Academy of Sciences, in which daily intakes of copper as high as 3 mg/d for children 4–8 yr of age and 8–10 mg/d for adults are considered tolerable *(18)*. (These intakes are 7–11 times higher than recommended daily intakes.)

A review of potentially toxic effects of excess copper (and/or exposure to copper complexes) *(65)* leads to the conclusion that for most mammals, copper is a relatively benign trace element, there being excellent mechanisms for excreting excess amounts absorbed, particularly through the bile (*see* Section 1.5.). Except unusual in and some genetically-based special circumstances, copper is not implicated in pathologies, including genomic instability—such as mutations or other alterations to DNA: apoptosis or necrosis. Moreover, copper-containing enzymes (and even many copper complexes like copper-aspirinate) are capable of (and/or integral to) the defense of the organism against reactive oxygen species, the effects of which are implicated in many chronic diseases (including Alzheimer's, Parkinson's, and even atherosclerosis). Nevertheless, certain individuals, presumably with inherited propensities to accumulate more copper, have been vulnerable to toxicity from ingestion of high copper doses. These include certain infants in India who developed Indian Childhood Cirrhosis from drinking formula heated in brass vessels *(193)*, and the equivalent in certain families in the Tyrol *(193)*. Some specific mammals are also vulnerable, namely dogs and sheep. Both of these species appear to have a limited ability to excrete excess copper in the bile *(194,195)*, but this is not because of a defect in WND *(196,197)*. Dogs tend to accumulate copper in their livers throughout their life-span, and many die of copper toxicosis. Reductions in intake can prevent this from happening.

REFERENCES

1. Linder, M. C. (ed.) (1991) *Biochemistry of Copper.* Plenum, New York.
2. Linder, M. C. (ed.) (1991) *Nutritional Biochemistry and Metabolism*, 2nd ed. Appleton & Lange, Norwalk, CT.
3. Sarkar, B. (ed.) (1999) *Metals and Genetics*. Kluwer Academic/Plenum, New York.
4. Leone, A. and Mercer, J. F. B. (eds.) (1999) *Copper Transport and its Disorders*, Advances in Experimental Medicine and Biology, Vol. 448. Kluwer Academic/Plenum, New York.
5. Linder, M. C. and Hazegh-Azam, M. (1996) Copper biochemistry and molecular biology. *Am. J. Clin. Nutr.* **63**, 797S–811S.
6. Linder, M. C. (1996) Copper, in *Present Knowledge in Nutrition*, 7th ed. (Ziegler, E. E. and Filer, L. J., Jr., eds.), ILSI, Washington, DC, pp. 307–319.
7. Harris, E. D. (2000) Cellular copper transport and metabolism. *Annu. Rev. Nutr.* **20**, 291–310.
8. Pena, M. M. O., Lee, J., and Thiele, D. J. (1999) A delicate balance: homeostatic control of copper uptake and distribution. *J. Nutr.* **129**, 1251–1260.
9. Linder, M. C., Wooten, L., Cerveza, P., Cotton, S., Shulze, R., and Lomeli, N. (1998) Copper transport. *Am. J. Clin. Nutr.* **67 (Suppl.)**, 965S–971S.
10. Linder, M. C., Lomeli, N. A., Donley, S., Mehrbod, F., Cerveza, P., Cotton, S., et al. (1999) Copper transport in mammals, in *Copper Transport and its Disorders* (Leone, A. and Mercer, J. F. B., eds.), Kluwer Academic/Plenum, New York, pp. 1–16.
11. Vulpe, C. and Packman, S. (1995) Cellular copper transport, *Annu. Rev. Nutr.* **15**, 293–322.

12. Eide, D. J. (1998) Molecular biology of metal ion transport in Saccharomyces cerevisiae. *Annu. Rev. Nutr.* **18**, 441–469.
13. Dunham, R. and Smith, H. E. (1992) Lead and copper—a model home approach. *Proceedings of the Water Quality Technology Conference*, pp. 341–352.
14. Walker, W. R. (1982) The results of a copper bracelet clinical trial and subsequent studies, in *Inflammatory Diseases and Copper* (Sorenson, J. R. J., ed.), Humana, Totowa, NJ, pp. 469–478.
15. Goode, C. A. (1991) Copper and disease, in *Biochemistry of Copper* (Linder, M. C., ed.), Plenum, New York, pp. 331–366.
16. Scott, K. C. and Turnlund, J. R. (1994) Compartment model of copper metablism in adult men. *J. Nutr. Biochem.* **5**, 342–350.
17. Turnlund, J. R., Keyes, W. R., Anderson, H. L., and Acord, L. L. (1989) Copper absorption and retention in young men at three levels of dietary copper using the stable isotope ^{65}Cu. *Am. J. Clin. Nutr.* **49**, 870–878.
18. Trumbo, P., Yates, A. A., Schlicker, S., and Poos, M. (2001) Dietary reference intakes: Vitamin A, vitamin K, arsenic, boron, chromium, copper, iodine, iron, manganese, molybdenum, nickel, silicon, vanadium and zinc. *J. Am. Diet. Assoc.* **101**, 294–301.
19. Turnlund, J. R., Keyes, W. R., Peiffer, G. L., and Scott, K. C. (1998) Copper absorption, excretion, and retention by young men consuming low dietary copper determined by using the stable isotope ^{65}Cu. *Am. J. Clin. Nutr.* **67(Suppl.)**, 1219–1225.
20. Wapnir, R. A. and Lee, S. Y. (1993) Dietary regulation of copper absorption and storage in rats: effects of sodium, zinc and histidine-zinc. *J. Am. Coll. Nutr.* **12**, 714–719.
21. Yu, S., West, C. E., and Beynen, A.C. (1994) Increasing intakes of iron reduce status, absorption and biliary excretion of copper in rats. *Br. J. Nutr.* **71**, 887–895.
22. Cohen, N. L., Illowsky, B. and Linder, M. C. (1979) Altered copper absorption in tumor bearing and estrogen treated rats. *Am. J. Physiol.* **236**, E309–E315.
23. Arredondo, M., Uauy, R., and Gonzalez, M. (2000) Regulation of copper uptake and transport in intestinal cell monolayers by acute and chronic copper exposure. *Biochim. Biophys. Acta* **1474**, 169–176.
24. Zerounian, N., Mohammadi, G., and Linder, M. C. (2001) Effects of copper and iron availability on copper absorption in the Caco2 cell intestinal model. *J. Trace Elents Exp. Biol.* **14**, 322 [Abstract].
25. Lee, J., Prohaska, J. R., Dagenais, S. L., Glover, T. W., and Thiele, D. J. (2000) Isolation of a murine copper transporter gene, tissue specific expression and functional complementation of a yeast copper transport mutant. *Gene* **254**, 87–96.
26. Dancis, A., Yuan, D. S., Haile, D. Askwith, D., Eide, D., Moehle, C., et al. (1994) Molecular characterization of a copper transport protein in S. cerevisiae: an unexpected role for copper in iron transport. *Cell* **76**, 393–402.
27. Dancis, A., Haile, D., Yuan, D. S., and Klausner, R. D. (1994) The *Saccharomyces cerevisiae* transport protein (ctr1p). Biochemical characterization, regulation by copper, and physiological role in copper uptake. *J. Biol. Chem.* **269**, 25,660–25,667.
28. Labbe, S. and Thiele, D. J. (1999) Pipes and wiring: the regulation of copper uptake and distribution in yeast. *Trends Microbiol.* **7**, 500–505.
29. Zhou, B. and Gitschier, J. (1997) hCTR1: a human gene for copper uptake identified by complementation in yeast. *Proc. Natl. Acad. Sci. USA* **94**, 7481–7486.
30. Kuo, Y.-M., Zhou, B., Cosco D., and Gitschier, J. (2001) The copper transporter CTR1 provides an essential function in mammalian embryonic development. *Proc. Natl. Acad. Sci. USA* **98**, 6836–6841.
31. Moller, L. B., Petersen, C., Lund, C., and Horn, N. (2000) Characterization of the hCTR1 gene: genomic organization, function, expression and identification of a highly homologous processed gene. *Gene* **257**, 13–22.
32. Lee, J., Prohaska, J. R. and Thiele, D. J. (2001) Essential role for mammalian copper transporter Ctr1 in copper homeostasis and embryonic development. *Proc. Natl. Acad. Sci. USA* **98**, 6842–6847.
33. DeRome, L. and Gadd, G. M. (1987) Measurement of copper uptake in Saccharomyces cerevisiae using a Cu^{2+}-selective electrode. *FEMS Microbiol. Lett.* **43**, 283–287.
34. Gunshin, H., Mackenzie, B., Berger, U. V., Gunshin, Y., Romero, M. F., Boron, W. F., et al. (1997) Cloning and characterization of a mammalian proton-coupled metal-ion transporter. *Nature* **388**, 482–488.
35. Fleming, M. D., Trenor, C. C. III, Su, M. A., Foernsler, D., Beier, D. R., Dietrick, W. F. et al. (1997) Microcytic anaemia mice have a mutation in Nramp2, a candidate iron transporter gene. *Nature Genet.* **16**, 383–386.
36. Fleming, M. D., Romano, M. A., Su, M. A., Garrick, L. M., Garrick, M. D., and Andrews, N. C. (1998) Nramp2 is mutated in the anemic Belgrade (b) rat: evidence of a role for Nramp2 in endosomal iron transport. *Proc. Natl. Acad. Sci. USA* **95**, 1148–1153.
37. Roy, C. N. and Enns, C. A. (2000) Iron homeostasis: new tales from the crypt. *Blood* **96**, 4020–4027.
38. Andrews, N. C. (2000) Intestinal iron absorption: current concepts circa 2000. *Dig. Liver Dis.* **32**, 56–61.
39. Hentze, M. W., Muckenthaler, M., Brennan, K., Galy, B., Hubert, N., and Hentze, S. (2001) Genome-wide analysis of iron metabolism. *BioIron 2001.*
40. Zoller, H., Theurl, I., Vogel, W., and Weiss, G. (2001) Pathways for iron dependent regulation of divalent metal transporter1 and ferroportin 1. *BioIron 2001.*
41. Zerounian, N.R. and Linder, M.C. (2001) Effects of copper and ceruloplasmin on iron transport in the Caco2 cell intestinal model. *J. Nutr. Biochem.* **13**, 138–148.
42. Arredondo, M., Mazariegos, D., and Nunez, M. T. (2001) The activity of the iron transporter DMT1 is inhibited by the hereditary hemochromatosis gene product. *BioIron 2001.*
43. Klomp, L. W., Lin, S. J., Yuan, D. S., Klausner, R. D., Culotta, V. C., and Gitlin, J. D. (1997) Identification and functional expression of HAH1: a novel human gene involved in copper homeostasis. *J. Biol. Chem.* **272**, 9221–9226.

44. Larin, D., Mekios, C., Das, K., Ross, B., Yang, A. S., and Gilliam, T. C. (1999) Characterization of the interaction between the Wilson and Menkes disease proteins and the cytoplasmic chaperone, HAH1. *J. Biol. Chem.* **274**, 28,497–28,504.
45. Culotta, V. C., Klomp, L. W., Strain, J., Casareno, R. L., Krems, B., and Gitlin, J. D. (1997) The copper chaperone for superoxide dismutase. *J. Biol. Chem.* **272**, 23,469–23,472.
46. Casareno, R. L., Waggoner, D., and Gitlin, J. D. (1998) The copper chaperone CCS directly interacts with copper/zinc superoxide dismutase. *J. Biol. Chem.* **273**, 23,625–23,628.
47. Glerum, D.M., Shtanko, A. and Tzagoloff, A. (1996) Characterization of COX17: a yeast gene involved in copper metabolism and assembly of cytochrome oxidase. *J. Biol. Chem.* **271**, 14,504–14,509.
48. Amaravadi, R., Glerum, D. M., and Tzagoloff, A. (1997) Isolation of a cDNA encoding the human homolog of COX17, a yeast gene essential for mitochondrial copper recruitment. *Hum. Genet.* **99**, 329–333.
49. Sonsma, T. Hixon, P., McWilliams, K., and Linder, M. C. (1981) Mechanism and regulation of intestinal copper absorption, in *Trace Element Metabolism in Man and Animals* (Howell, J. M., Gawthorne, J. M., and White, C. L., eds.), Australian Academy of Science, Canberra, pp. 145–147.
50. Fischer, P. W. F., Giroux, A., and Labbe, M. R. (1983) Effects of zinc on mucosal copper binding and on the kinetics of copper absorption. *J. Nutr.* **113**, 462–469.
51. Bremner, I. (1980) Absorption, transport and distribution of copper. *Ciba Found. Symp. (1979) Exerpta Med.* **79**, 23–48.
52. Ogiso, T., Ogawa, N., and Miura, T. (1979) Inhibitory effect of high dietary zinc on copper absorption in rats. II. Binding of copper and zinc to cytosol proteins in the intestinal mucosa. *Chem. Pharm. Bull.* **27**, 515–521.
53. Freedman, J. H. and Peisach, J. (1989) Intracellular copper transport in cultured hepatoma cells. *Biochem. Biophys. Res. Commun.* **164**, 134–140.
54. Freedman, J. H., Ciriolo, M. R., and Peisach, J. (1989) The role of glutathione in copper metabolism and toxicity. *J. Biol. Chem.* **264**, 5598–5605.
55. Portnoy, M. E., Schmidt, P. J., Rogers, R. S., and Culotta, V. C. (2001) Metal transporters that contribute copper to metallochaperones in *Saccharomyces cerevisiae*. *Mol. Genet. Genom.* **265**, 873–882.
56. Hamsa, I., Faisst, A., Prohaska, J., Chen, J., Gruss, P. and Gitlin, J. D. (2001) The metallochaperone Atox1 plays a critical role in perinatal copper homeostasis. *Proc. Natl. Acad. Sci. USA* **98**, 6848–6852.
57. Kaler, S. G. (1998) Metabolic and molecular bases of Menkes disease and occipital horn syndrome. *Pediatr. Dev. Pathol.* **1**, 85–99.
58. Masuoka, J., Hegenauer, J., Van Dyke, B. R., and Saltman, P. (1993) Intrinsic stoichiometric equilibrium constants for the binding of zinc(II) and copper(II) to the high affinity site of serum albumin. *J. Biol. Chem.* **268**, 21,533–21,537.
59. Lau, S. and Sarkar, B. (1971) Ternary coordination complex between human serum albumin, copper(II) and L-histidine. *J. Biol. Chem.* **246**, 5938–5943.
60. Masuoka, J. and Saltman, P. (1994) Zinc(II) and copper (II) binding to serum albumin. A comparative study of dog, bovine, and human albumin. *J. Biol. Chem.* **269**, 25,557–25,561.
61. Wirth, P. L. and Linder, M. C. (1985) Distribution of copper among multiple components of human serum. *J. Natl. Cancer Inst.* **75**, 277–284.
62. Barrow, L. and Tanner, M. S. (1988) Copper distribution among serum proteins in paediatric liver disorder and malignancies. *Eur. J. Clin. Invest.* **18**, 555–560.
63. Weiss, K. C. and Linder, M. C. (1985) Copper transport in rats involving a new plasma protein. *Am. J. Physiol.* **249**, E77–E88.
64. Liu, N. M., Lo, L. S. L., Askary, S. H., Goforth, J., Vivas, E., Tsai, M., et al. (2002) Transcuprein is a macroglobulin regulated by copper and iron, in press.
65. Linder, M. C. (2001) Copper and genomic stability in mammals. *Mutat. Res.* **475**, 151–152.
66. Huffman, D. L. and O'Halloran, T. V. (2001) Function, structure, and mechanism of intracellular copper trafficking proteins. *Annu. Rev. Biochem.* **70**, 677–701.
67. Wernimont, A. K., Huffman, D. L., Lamb, A. L., O'Halloran, T. V., and Rosenzweig, A. C. (2000) Structural basis for copper transfer by the metallochaperone for the Menkes/Wilson disease proteins. *Nat. Struct. Biol.* **7**, 766–771.
68. Goforth, J., Vivas, E., Liu, N., Askary, H. S., Lo, L. S. L., and Linder, M. C. (2001) Correspondence between rat transcuprein and human alpha-2-macoglobulin in copper binding. *FASEB J.* **15** [Abstract A271.].
69. Campbell, C. H., Brown, R., and Linder, M. C. (1981) Circulating ceruloplasmin is an important source of copper for normal and malignant cells. *Biochim. Biophys. Acta* **678**, 27–38.
70. Lee, S. H., Lancey, R., Montaser, A., Madani, N. and Linder, M. C. (1993) Ceruloplasmin and copper transport during the latter part of gestation in the rat. *Proc. Soc. Exp. Biol. Med.* **203**, 428–439.
71. Vargas, E. J., Shoho, A. R., and Linder, M. C. (1994) Copper transport in the Nagase analbuminemic rat. *Am. J. Physiol.* **267**, G259–G269.
72. Orena, S. J., Goode, C. A., and Linder, M. C. (1986) Binding and uptake of copper from ceruloplasmin. *Biochem. Biophys. Res. Commun.* **139**, 822–825.
73. Harris, Z. L., Takahashi, Y. Miyajima, H., Serizawa, M., MacGillivray, R. T. A., and Gitlin, J. D. (1995) Aceruloplasminemia: molecular characterization of this disorder of iron metabolism. *Proc. Natl. Acad. Sci USA* **92**, 2539–2543.
74. Meyer, L. A., Durley, A. P., Prohaska, J. R., and Harris, Z. L. (2001) Copper transport and metabolism are normal in Aceruloplasminemic mice. *J. Biol. Chem.*, **276**, 36,857–36,861.

75. Hilton, M., Spenser, D. C., Ross, P. Ramsey, A., and McArdle, H. J. (1995) Characterisation of the copper uptake mechanism and isolation of the ceruloplasmin receptor/copper transporter in human placental vesicles. *Biochim. Biophys. Acta* **1245**, 153–160.
76. Mas, A. and Sarkar, B. (1992) Uptake by ^{67}Cu by isolated human trophoblast cells. *Biochim. Biophys. Acta* **1135**, 123–128.
77. Percival, S. S. and Harris, E. D. (1990) Copper transport from ceruloplasmin: characterization of the cellular uptake mechanism. *Am. J. Physiol.* **258**, C140–C146.
78. Stevens, M. D., DiSilvestro, R. A., and Harris, E. D. (1984) Specific receptors for ceruloplasmin in membrane fragments from aortic and heart tissues. *Biochemistry* **23**, 261–266.
79. Kataoka, M. and Tavassoli, M. (1985) Identification of ceruloplasmin receptors on the surface of human blood monocytes, granulocytes, and lymphocytes. *Exp. Hematol.* **13**, 806–810.
80. Tavassoli, M., Kishimoto, T., and Kataoka, M. (1986) Liver endothelium mediates the hepatocyte's uptake of ceruloplasmin. *J. Cell Biol.* **102**, 1298–1303.
81. Ettinger, M. J., Darwish, H. M., and Schmitt, R. C. (1986) Mechanisms of copper transport from plasma to hepatocytes. *Fed. Proc.* **45**, 2800–2804.
82. McArdle, H. J., Guthrie, J. R., Ackland, M. L., and Danks, D. M. (1987) Albumin has no role in the uptake of copper by human fibroblasts. *J. Inorg. Biochem*. **31**, 123–131.
83. Schmitt, R. C., Darwish, H. M., Cheney, J. C., and Ettinger, M. J. (1983) Copper transport kinetics by isolated rat hepatocytes. *Am. J. Physiol.* **244**, G183–G191.
84. Zhou, H. and Thiele, D. J. (2001) Identification of a novel high affinity copper transport complex in the fission yeast *Schizosaccharomyces pombe*. *J. Biol. Chem.* **276**, 20,529–20,535.
85. Rae, T. D. , Schmidt, P. J., Pufahl, R. A., Culotta, V. C., and O'Halloran, T. V. (1999) Undetectable intracellular free copper: the requirement of a copper chaperone for superoxide dismutase. *Science* **284**, 805–808.
86. Petris,M. J., Mercer, J. F. B., Culvenor, J. G., Lockhart, P., Gleeson, P. A. and Camakaris, J. (1996) Ligand-regulated transport of the Menkes copper P-type ATPase efflux pump from the Golgi apparatus to the plasma membrane: a novel mechanism of regulated trafficking. *EMBO J.* **15**, 6084–6095.
87. Camakaris, J., Petris, M. J., Bailey, L., Shen, P., Lockhart, P., Glover, T. W., et al. (1995) Gene amplification of the Menkes (MNK; ATP7A) P-type ATPase gene of CHO cells is associated with copper resistance and enhanced copper efflux. *Hum. Mol. Genet.* **4**, 2117–2123.
88. Petris, M. J. and Mercer, J. F. B. (1999) The Menkes protein (ATP7A; MNK) cycles via the plasma membrane both in basal and elevated extracellular copper using a C-terminal di-leucine endocytic signal. *Hum. Mol. Genet*. **8**, 2107–2115.
89. Camakaris, J., Voskoboinik, I., and Mercer, J. F. B. (1999) Molecular mechanisms of copper homeostasis. *Biochem. Biophys. Res. Comm.* **261**, 225–232.
90. Schaefer, M., Roelofsen, J., Wolters, H., Hofmann, W. J., Muller, M., Kuipers, F., et al. (1999) Localization of the Wilson's disease protein in human liver. *Gastroenterology* **117**, 1380–1385.
91. Roelofsen, J., Wolters, H., Van Luyn, J. A., Miura, N., Kuipers, F., and Vonk, R. J. (2000) Copper-induced apical trafficking of ATP7B in polarized hepatoma cells provides a mechanism for biliary copper excretion. *Gastroenterology* **119**, 782–793.
92. Kressner, M. S., Stockert, R. J., Morell, A. G., and Sternlieb, I. (1984) Origins of biliary copper. *Hepatology* **4**, 867–870.
93. Chowrimootoo, G. F. E. and Seymour, C. A. (1994) The role of ceruloplasmin in copper excretion. *Biochem. Soc. Trans*. **22**, 190S [Abstract].
94. Iyengar, V., Brewer, G. J., Dick, R. D., and Owyang, C. (1988) Studies of cholecystokinin-stimulated biliary secretions reveal a high molecular weight copper binding substance in normal subjects that is absent in patients with Wilson's disease. *J. Lab. Clin. Med.* **111**, 267–274.
95. Linder, M. C. and Roboz, M. (1986) Turnover and excretion of copper in rats as measured with ^{67}Cu. *Am. J. Physiol.* **251**, E551–E555.
96. Bethin, K. E., Cimato, T. R., and Ettinger, M. J. (1995) Copper binding to mouse liver *S*-adenosyl homocysteine hydrolase and the effects of copper on its levels. *J. Biol. Chem.* **270**, 20,702–20,711.
97. Flood, D. G., Reaume, A. G., Gruner, J. A., Hoffmann, E. K., Hirsch, J. D., Lin, Y.-G., et al. (1999) Hindlimb motor neurons require Cu/Zn superoxide dismutase for maintenance of neuromuscular junctions. *Am. J. Pathol*. **155**, 663–672.
98. Valentine, J. S., Hart, P. J., and Gralla, E. B. (1999) Copper-zinc superoxide dismutase and ALS, in *Copper Transport and its Disorders* (Leone, A. and Mercer, J. F. B., eds.), Kluwer Academic/Plenum, New York, pp. 193–203.
99. Carri, M. T., Battistoni, A., Ferri, A., Gabbianelli, R. and Rotilio, G. (1999) A study of the dual role of copper in superoxide dismutase as antioxidant and pro-oxidant in cellular models of amyotropic lateral sclerosis, in *Copper Transport and its Disorders* (Leone, A. and Mercer, J. F. B., eds.), Kluwer Academic/Plenum, New York, pp. 205–213.
100. Johnson, M. A., Macdonald, T. L., Mannick, J. B., Conaway, M. R., and Gaston, B. (2001) Accelarated S-nitrosothiol breakdown by amyotropic lateral sclerosis mutant copper, zinc-superoxide dismutase. *J. Biol. Chem.*, **276**, 39,872–39,878.
101. Levy, M. A., Tsai, Y. H., Reaume, A., and Bray, T. M. (2001) Cellular response of antioxidant metalloproteins in Cu/Zn SOD transgenic mice exposed to hyperoxia. *Am. J. Physiol.* **281**, L172–L182.
102. Kang, Y. J. (1999) The antioxidant function of metallothionein in the heart. *Proc. Soc. Exp. Biol. Med.* **222**, 263–273.
103. Ghoshal, K., Majumder, S., Li, Z., Bray, T. M., and Jacob, S. T. (1999) Transcriptional induction of MT-I and II genes in the livers of Cu/Zn-SOD knockout mice. *Biochem. Biophys. Res. Commun.* **264**, 735–742.
104. Ragan, H. A., Nacht, S., Lee, G. R., Bishop, C. R., and Cartwright, G. E. (1969) Effect of ceruloplasmin on plasma iron in copper deficient swine. *Am. J. Physiol.* **217**, 1320–1323.

105. Osaki, S. and Johnson, D. A. (1969) Mobilization of liver iron by ferroxidase (ceruloplasmin). *J. Biol. Chem.* **244**, 5757–5761.
106. Tran, T., Ashraf, M., Jones, L. T., Westbrook, T., Hazegh-Azam, M., and Linder, M. C. (2001) Dietary iron status has little effect on expression of ceruloplasmin but alters that of ferritin in rats. *J. Nutr.* **132**, 351–356.
107. Harris, Z. L., Durley, A. P., Man, T. M., and Gitlin, J. D. (1999) Targeted gene disruption reveals an essential role for ceruloplasmin in cellular iron efflux. *Proc. Natl. Acad. Sci. USA* **96**, 10,812–10,817.
108. Yoshida, K., Furihata, K., Takeda, S., Nakamura, A., Yamamoto, K., Hiyamuta, S., et al. (1995) A mutation in the ceruloplasmin gene is associated with systemic hemosiderosis in humans. *Nature Genet.* **9**, 267–272.
109. Roeser, H. P., Lee, G. R., Nacht, S., and Cartwright, G. E. (1980) A role of ceruloplasmin in iron metabolism. *J. Clin. Invest.* **49**, 2408–2417.
110. Patel, B. N. and David, S. (1997) A novel glcosylphosphatidylinositol-anchored form of ceruloplasmin is expressed by mammalian astrocytes. *J. Biol. Chem.* **272**, 20,185–20,190.
111. Salzer, J. L., Lovejoy, L., Linder, M. C., and Rosen, C. (1998) Ran-2, a glial lineage marker, is a GPI-anchored form of ceruloplasmin. *J. Neurosci.* **54**, 147–157.
112. Patel, B. N., Dunn, R. J., and David, S. (2000) Alternative RNA splicing generates a glycosylphosphatidylinositol-anchored form of ceruloplasmin in mammalian brain. *J. Biol. Chem.* **275**, 4305–4310.
113. Harris, Z. L., Klomp, L. W., and Gitlin, J. D. (1998) Aceruloplasminemia: an inherited neurodegenerative disease with impairment of iron homeostasis. *Am. J. Clin, Nutr.* **67(Suppl.)**, 972S–977S.
114. Mukhopadhyay, C. K., Mazumder, B., and Fox, P. L. (1999) Role of hypoxia inducible factor-1 in transcription activation of ceruloplasmin by iron deficiency. *J. Biol. Chem.* **275**, 21,048–21,054.
115. Mukhopadhyay, C. K. and Fox, P. L. (2001) Dual regulation of ceruloplasmin transcription by insulin in HepG2 cells. *Bioiron 2001*.
116. Vulpe, C. D., Kuo, Y.-M., Murphy, T. L., Cowley, L., Askwith, C., Libina, N., et al. (1999) Hephaestin, a ceruloplasmin homolog implicated in intestinal iron transport, is defective in the sla mouse. *Nature Genet.* **21**, 195–199.
117. Vulpe, C. D., Attieh, Z. K., Allaeddine, R. M., and Su, T. (2001) Identification of a ferroxidase activity for hephaestin. *FASEB J.* **15** [Abstract] A800.
118. Fife, R. S. Moody, S., Houser, D., and Proctor, C. (1994) Studies of copper transport in cultured bovine chondrocytes. *Biochim. Biophys. Acta* **1201**, 19-22.
119. Fife, R. S. Palmoski, M. J., and Brandt, K. D. (1986) Metabolism of cartilage matrix glycoprotein in normal and osteoarthritic canine articular cartilage. *Arthritis Rheum.* **29**, 1256–1262.
120. Haddad, A. De Almedia, J. C., Laicine, E. M., Fife, R. S., and Pelletier, G. (1990) The origin of the intrinsic glycoproteins of the rabbit vitreous body: an immunohistochemical and autoradiographic study. *Exp. Eye Res.* **50**, 555–561.
121. Trackman, P. C., Pratt, A. M., Wolanski, A., Tang, S. S., Offner, G. D., Troxler, R. F., et al. (1990) Cloning of rat aorta lysyl oxidase cDNA: complete codons and predicted amino acid sequence. *Biochemistry* **29**, 4863–4870.
122. Hamalainen, E. R., Jones, T. A., Sheer, D., Taskinen, K., Pihlajaniemi, T., and Kivirikko, K. I. (1991) Molecular cloning of human lysyl oxidase and assignment of the gene to chromosome 5q23.2-31.2. *Genomics* **11**, 508–516.
123. Tang, C. and Klinman, J. P. (2001) The catalytic function of bovine lysyl oxidase in the absence of copper. *J. Biol. Chem.* **276**, 30,575–30,578.
124. Wang, S. X., Mure, M., Medzihradszky, K. F., Burlingame, A. L., Brown, D. E., Dooley, D. M., et al. (1996) A crosslinked cofactor in lysyl oxidase: redox function for amino acid side chains. *Science* **273**, 1078–1084.
125. Rucker, R. B., Kosonen, T., Clegg, M. S., Mitchell, A. E., Rucker, B. R., Uriu-Hare, J. Y., et al. (1998) Copper, lysyl oxidase, and extracellular matrix protein cross-linking. *Am. J. Clin. Nutr.* **67(Suppl.)**, 996S–1002S.
126. Jourdan-Le Saux, C., Tronecker, H., Bogic, L., Bryant-Greenwood, G. D., Boyd, C. D., and Csiszar, K. (1999) The LOXL2 gene encodes a new lysyl oxidase-like protein and is expressed at high levels in reproductive tissues. *J. Biol. Chem.* **274**, 12,939–12,944.
127. Maki, J. M. and Kivirikko, K. I. (2001) Cloning and characterization of a fourth human lysyl oxidase isoenzyme. *Biochem. J.* **355**, 381–387.
128. Brown, D. R. (2001) Prion or prejudice: normal protein and the synapse. *Trends Neurosci.* **24**, 85–90.
129. Aronoff-Spencer, E., Burns, C. S., Avdievich, N. I., Gerfen, G. J., Peisach, J., Antholine, W. E., et al. (2000) Identification of the Cu2+/– binding sites in the N-terminal domain of the prion protein by EPR and CD spectroscopy. *Biochemistry* **39**, 12,760–13,771.
130. Miura, T., Hori-I, A., and Takeuchi, H. (1996) Raman spectroscopy study on the copper(II) binding mode of prion octapeptide and its pH dependence. *FEBS Lett.* **396**, 248–252.
131. McMahon, H. E. M., Mange, A., Nishida, N., Cerminon, C., Casanova, D., and Lehmann, S. (2001) Cleavage of the amino terminus of the prion protein by reactive oxygen species. *J. Biol. Chem.* **276**, 2286–2291.
132. Brown, D. R., Clive, C., and Haswell, S. J. (2001) Antioxidant activity related to copper binding of native prion protein. *J. Neurochem.* **76**, 69–76.
133. Brown, D. R., Wong, B.-S., Hafiz, F., Clive, C., Haswell, S. J., and Jones, I. M. (1999) Normal prion protein has an activity like that of superoxide dismutase. *Biochem. J.* **344**, 1–5.
134. Brown, D. R., Hafiz, F., Glasssmith, L. L., Wong, B.-S., Jones, I. M., Clive, C., et al. (2000) Consequences of manganese replacement of copper for prion protein function and proteinase resistance. *EMBO J.* **19**, 1180–1186.
135. Milhavet, O., McMahon, H. E. M., Rachidi, W., Nishida, N., Katamine, S., Mange, A., et al. (2000) Prion infection impairs the cellular response to oxidative stress. *Proc. Natl. Acad. Sci. USA* **97**, 13,937–13,942.
136. Klamt, F., Dal-Pizzol, F., Conte da Frota M. L., Jr., Walz, R., Andrades, M. E., Gomes da Silva, E., et al. (2001) Imbalance of antioxidant defense in mice lacking cellular prion protein. *Free Radical Biol. Med.* **30**, 1137–1144.

137. Brown, D. R. (1999) Prion protein expression aids cellular uptake and veratidine-induced release of copper. *J. Neurosci. Res.* **58**, 717–725.
138. Brown, D. R., Schmidt, B., and Kretzschmar, H. A. (1997) Expression of prion protein in PC12 is enhanced by exposure to oxidative stress. *Int. J. Dev. Neurosci.* **15**, 961–972.
139. Sumudhu, W., Perera, S., and Hooper, N. M. (2001) Ablation of the metal ion-induced endocytosis of the prion protein by disease-associated mutation of the octarepeat. *Curr. Biol.* **11**, 519–523.
140. Brockes, J. P. (1999) Topics in prion cell biology. *Curr. Opin. Neurobiol.* **9**, 571–577.
141. Linder, M. C., Donley, S., Dominguez, D., Wooten, L., Mehrbod, F., Cerveza, P., et al. (1999) Copper transport and ceruloplasmin during lactation and pregnancy, in *Metals and Genetics* (Sarkar, B., ed.), Kluwer Academic/ Plenum, New York, pp. 117–129.
142. Kuo, Y.-M., Gitschier, J., and Packman, S. (1997) Developmental expression of the mouse mottled and toxic milk genes suggests distinct functions for the Menkes and Wilson disease copper transporters. *Hum. Mol. Genet.* **6**, 1043–1049.
143. McArdle, H. J. and Erlich, R. (1989) Copper uptake and transfer to the mouse fetus during pregnancy. *J. Nutr.* **121**, 208–214.
144. McArdle, H. J. and van den Berg, G. J. (1992) The accumulation of copper by microvilli isolated from human term placenta. *J. Nutr.* **122**, 1260–1265.
145. Tong, K. K. and McArdle, H. J. (1995) Copper uptake by cultured trophoblast cells isolated from human term placenta. *Biochim. Biophys. Acta* **1269**, 233–246.
146. Meyer, L. A., Durley, A. P., Prohaska, J. R., and Harris, Z. L. (2001) Copper transport and metabolism are normal in aceruloplasminemia. *J. Biol. Chem.* **276**, 36,857–36,861.
147. Muramatsu, Y., Tamada, T., Moralejo, D. H., Suzuki, Y., and Matsumoto, K. (1998) Fetal copper uptake and a homolog (Atp7b) of the Wilson's disease gene in rats. *Res. Commun. Mol. Pathol. Pharmacol.* **101**, 225–231.
148. Oga, M., Matsui, N., Anai, T., Yoshimatsu, J., Inoue, I., and Miyakawa, I. (1993) Copper disposition of the fetus and placenta in a patient with untreated Wilson's disease. *Am. J. Obstet. Gynecol.* **169**, 196–198.
149. Mann, J., Camakaris, J., and Danks, D. M. (1980) Copper metabolism in mottled mouse mutants. Defective placental transfer of 64Cu to foetal brindled (Mobr) mice. *Biochem. J.* **186**, 629–631.
150. Coni, E., Bocca, B., Galoppi, B., Alimonti, A., and Caroli, S. (2000) Identification of chemical species of some trace and mnor elements in mature breast milk. *Microchem. J.* **67**, 187–194.
151. Wooten, L., Shulze, R. A., Lancey, R. W., Lietzow, M., and Linder, M. C. (1996) Ceruloplasmin is found in milk and amniotic fluid and may have a nutritional role. *J. Nutr. Biochem.* **7**, 632–639.
152. Cerveza, P. J., Mehrbod, F., Cotton, S. J., Lomeli, N., Linder, M. C., Fonda, E. G., et al. (2000) Milk ceruloplasmin and its expression by mammary gland and liver in pigs. *Arch. Bioch. Biophys.* **373**, 451–461.
153. Donley, S. A., Ilagan, B. J., Rim, H., and Linder, M. C. (2002) Copper transport to mammary gland and milk during lactation in rats, submitted.
154. Michalczyk, A. Rieger, J., Allen, K., Mercer, J., and Ackland, M. (2000) Defective trafficking of the Wilson disease protein ATP7B in the mammary gland of the toxic milk mouse. *Biochem. J.* **352**, 565–571.
155. Rauch, H. (1983) Toxic mik, a new mutation affecting copper metabolism in the mouse. *J. Heredity* **74**, 141–144.
156. Dorea, J. G. (2000) Iron and copper in human milk. *Nutrition* **16**, 209–220.
157. Olivares, M., Pizarro, F., Speisky, H., Lonnerdal, B., and Uauy, R. (1998) Copper in infant nutrition: safety of World Health Organization provisional guideline value for copper content of drinking water. *J. Pediat. Gastroenterol. Nutr.* **26**, 251–257.
158. Olivares, M., Araya, M., and Uauy, R. (2000) Copper homeostasis in infant nutrition: deficit and excess. *J. Pediatr. Gastroenterol.* **31**, 102–111.
159. Chierici, R., Saccomandi, D., and Vigi, V. (1999) Dietary supplements for the lactating mother: influence on the trace element content of milk. *Acta Paediatr.* **88(Suppl.)**, 7–13.
160. Hopkins, R. G. and Failla, M. L. (1999) Transcriptional regulation of interleukin-2 gene expression is impaired by copper deficiency in Jurkat human T lymphocytes. *J. Nutr.* **129**, 596–601.
161. Percival, S. S. (1998) Copper and immunity. *Am. J. Clin, Nutr.* **67(Suppl.)**, 1064S–1068S.
162. Huang, Z. L. and Failla, M. L. (2000) Copper deficiency suppresses effector activities of differentiated U937 cells. *J. Nutr.* **130**, 1536–1542.
163. Gengelbach, G. P. and Spears, J. W. (1998) Effects of dietary copper and molybdenum on copper status, cytokine production, and humoral immune response of calves. *J. Dairy Sci.* **81**, 3286–3292.
164. Linder, M. C., Morris, H. P., and Criss, W. (1977) Iron and copper metabolism in cancer as exemplified by ferritin and ceruloplasmin in rats with transplantable tumors, in *Morris Hepatomas: Mechanisms of Regulation* (Criss, W. ed.), Plenum, New York, pp. 643–664.
165. Linder, M. C., Moor, J. R., and Wright, K. (1981) Ceruloplasmin assays in diagnosis and treatment of human lung, breast and gastrointestinal cancer. *J. Natl. Cancer Inst.* **67**, 263–275.
166. Gullino, P. M., Ziche, M., and Alessandri, G. (1990) Ganglioside, copper ions and angiogenic capacity of adult tissues. *Cancer Metastasis Rev.* **8**, 239–251.
167. Hu, G. F. (1998) Copper stimulates proliferation of human endothelial cells under culture. *J. Cell Biochem.* **69**, 326–335.
168. Soncin, F., Guitton, J. D., Cartwright, T., and Badet, J. (1997) Interaction of human angiogenin with copper modulates angiogenin binding to endothelial cells. *Biochem. Biophys. Res. Commun.* **236**, 604–610.
169. Lane, T. F., Iruela-Arispe, M. L., Johnson, R. S., and Sage, E. H. (1994) SPARC is a source of copper-binding peptides that stimulate angiogenesis. *J. Cell Biol.* **125**, 929–943.

170. Yoshida, D., Ikeda, Y. and Nakazawa, S. (1995) Copper chelation inhibits tumor angiogenesis in the experimental 9L gliosarcoma model. *Neurosurgery* **37**, 287–292.
171. Brewer, G. J. (2001) Copper control as an antiangiogenic anticancer therapy: lessons from treating Wilson's disease. *Exp. Biol. Med.* **226**, 665–673.
172. Goode, C. A. (1991) Copper and disease, in *Biochemistry of Copper* (Linder, M. C., ed.), Plenum, New York, pp. 331–366.
173. Mercer, J.F.B., Livingston, J., Hall, B., Paynter, J.A., Begy, C., Chandrasekharappa, S., et al. (1993) Isolation of a partial candidate gene for Menkes disease by positional cloning. *Nature Genet.* **3**, 20–25.
174. Vulpe, C., Levinson, B., Whitney, S., Packman, S., and Gitschier, J. (1993) Isolation of a candidate gene for Menkes disease and evidence that it encodes a copper-transporting ATPase. *Nature Genet.* **3**, 7–13.
175. Chelly, J., Tumer, Z., Tonnesen, T., Petterson, A., Ishikawa-Brush, Y., Tommerup, N., et al. (1993) Isolation of a candidate gene for Menkes disease that encodes a potential heavy metal binding protein. *Nature Genet.* **3**, 14–9.
176. Bull, P. C., Thomas, G. R., Rommens, J. M., Forbes, J. R., and Cox, D. W. (1993) The Wilson disease gene is a putative copper transporting P-type ATPase similar to the Menkes gene. *Nature Genet.* **5**, 327–337.
177. Tanzi, R. E., Petrukhin, K., Chernov, I., Pellequer, J. L., Wasco, W., Toss, B., et al. (1993) The Wilson disease gene is a copper-transporting ATPase with homology to the Menkes disease gene. *Nature Genet.* **5,** 344–350.
178. Harris, E. D., Reddy, M. C., Qian, Y., Tiffany-Castingliano, E., Majumdar, S., and Nelson, J. (1999) Multiple forms of the Menkes CuATPase. *Adv. Exp. Med. Biol.* **448**, 39–51.
179. Harris, E. D., Reddy, M. C., and Majumdar, S. (2001) Evidence for two promoters in the Menkes disease gene. *FASEB J.* **15** [Abstract A271].
180. Majumdar, S., Reddy, M. C., and Harris, E. D. (2001) Indication of a nuclear copper transporter in human cells. *FASEB J.* **15** [Abstract A775].
181. Wu, J., Forbes, J. R., Chen, H. S., and Cox, D. W. (1994) The LEC rat has a deletion in the copper transporting ATPase gene homologous to the Wilson disease gene. *Nature Genet.* **7**, 6541–6545.
182. Theophilos, M. B., Cox, D., and Mercer, J. F. B. (1996) The toxic milk mouse is a murine model of Wilson disease. *Hum. Mol. Genet.* **5**, 1619–1624.
183. Okayasu, T., Tochimaru, H., Takahashi, T., Takekoshi, Y., Li, Y., Togashi, Y., et al. (1992) Inherited copper toxicity in Long–Evans Cinnamon rats exhibiting spontaneous hepatitis: a model of Wilson's disease. *Pediatr. Res.* **31**, 253–257.
184. Buiakova, O. I., Xu, J., Lutsenko, S., Zeitlin, S., Das, K., Das, S., et al. (1999) Null mutation of the murine ATP7B (Wilson disease) gene results in intracellular copper accumulation and late-onset hepatic nodular transformation. *Hum. Mol. Genet.* **9**, 1665–1671.
185. Strausak, D., Mercer, J. F., Dieter, H. H., Stremmel, W., and Multhaup, G. (2001) Copper in disorders with neurological symptoms: Alzheimer's, Menkes, and Wilson diseases. *Brain Res. Bull.* **55**, 175–185.
186. Mercer, J. F. (2001) The molecular basis of copper-transport diseases. *Trends Mol. Med.* **7**, 64–69.
187. Cox, D. W. (1999) Disorders of copper transport. *Br. Med. Bull.* **55**, 544–555.
188. Menkes, J. H. (1999) Menkes disease and Wilson disease: two sides of the same copper coin. Part I. Menkes disease. *Eur. J. Paediatr. Neurol.* **3**, 147–158.
189. Menkes, J. H. (1999) Menkes disease and Wilson disease: two sides of the same copper coin. Part II. Wilson disease. *Eur. J. Paediatr. Neurol.* **3**, 245–253.
190. Gitlin, J. D. (1998) Aceruloplasminemia. *Pediatr. Res.* **44**, 271–276.
191. Cherny, R. A., Atwood, C. S. A., Xilinas, M. E., Gray, D. N., Jones, W. D., McLean, C. A., et al. (2001) Treatment with a copper–zinc chelator inhibits beta-amyloid accumulation in Alzheimer's disease transgenic mice. *Neuron* **30**, 665–676.
192. Suzuki, K., Miura, T. and Takeuchi, H. (2001) Inhibitory effect of copper(II) on zinc(II)-induced aggregation of amyloid beta-peptide. *Biochem. Biophys. Res. Commun.* **285**, 991–996.
193. Tanner, M. S. (1999) Indian childhood cirrhosis and Tyrolean childhood cirrhosis, in *Copper Transport and Its Disorders* (Leone, A. and Mercer, J. F. B., eds.), Kluwer Academic/Plenum, New York, pp. 127–137.
194. Lockhart, P. J. (1999) Molecular analysis of copper transport in sheep, doctoral thesis, University of Melbourne, Melbourne, Victoria, Australia.
195. Montaser, A., Tetreault, C., and Linder, M. C. (1992) Comparison of copper binding proteins in dog serum with those in other species. *Proc. Soc. Exp. Biol. Med.* **200**, 321–329.
196. Dagenais, S. L., Guevara-Fujita, M., Loechel, R., Burgess, A. C., Miller, D. E., Yusbasiyan-Gurkan, V., et al. (1999) The canine copper toxicosis locus is not syntenic with ATP7B or ATX1 and maps to a region showing homology to human 2p21. *Mamm. Genome* **10**, 753–756.
197. van der Sluis, B. J. A., Breen, M., Nanji, M., van Wolferen, M., de Jong, P., Binns, M. M., et al. (1999) Genetic mapping of the copper toxicosis locus in Bedlington terriers to dog chromosome 10, in a region syntenic to human chromosome region 2p13–p16. *Hum. Mol. Genet.* **8**, 501–507.

II
Copper Proteins

2

Biochemistry of the Wilson's Disease Protein

Svetlana Lutsenko, Ruslan Tsivkovskii, Matthew J. Cooper, Brian C. MacArthur, and Hans-Peter Bächinger

1. INTRODUCTION

Copper is an essential metal, utilized as a cofactor by numerous enzymes regulating vital cellular functions, including oxidative phosphorylation, neurotransmitter biosynthesis, radical detoxification, iron uptake, and many others (for review, *see* refs. *1* and *2*). The importance of copper for normal cell metabolism is best illustrated by the existence of severe genetic disorders, in which the normal distribution of copper is disrupted *(3–5)*. Menkes disease (MNK) is an inborn copper deficiency associated with severe developmental delays, mental retardation, poor temperature control, and connective tissue abnormalities. All of these symptoms can be ascribed to the malfunction of various enzymes, which require copper as a cofactor. Such enzymes include cytochrome-*c* oxidase, tyrosinase, lysyl oxidase, peptidyl-ß-amidase, and many others. Recent identification of the Menkes disease gene (*ATP7A*) revealed that it encoded a copper-transporting ATPase or the Menkes disease protein *(6–8)*, which has a dual function: to transport copper from the cytosol to copper-dependent enzymes located within the secretory pathway and to export excess copper out of the cell.

Although the Menkes disease protein is indispensable for copper distribution from the intestine to various tissues, by itself it is insufficient for normal copper homeostasis. The product of another gene, *ATP7B*, plays a key role in removing excess copper from human body by transporting copper from the liver to the bile *(9–11)*. Mutations in *ATP7B* lead to vast accumulation of copper in the liver, brain, and kidneys, causing a set of pathological symptoms, known as Wilson's disease (WND). Severe liver lesions, neurological problems, and a wide spectrum of psychiatric abnormalities are common symptoms of WND *(12)*. The Wilson's disease gene, *ATP7B*, was isolated and fully characterized in 1993–1994; these studies revealed that it encodes a copper-transporting ATPase with over 50% sequence homology to the Menkes disease protein *(9–11,13,14)*.

Although the Menkes disease protein (MNKP) and Wilson's disease protein (WNDP) have significant structural identity and also function similarly in the in vitro systems *(15–17)*, their distinct tissue distribution and alterations in their expression during development *(18)* suggest that the relative abundance and activity of these proteins are controlled by a specific set of environmental cues. Understanding the regulatory mechanisms acting on these proteins represents one of the most unexplored and exciting area of copper homeostasis.

The detailed biochemical characterization of the Menkes and Wilson's disease proteins is the first step toward elucidation of their specific physiological roles in a cell. Such studies can be aided

From: Handbook of Copper Pharmacology and Toxicology
Edited by: E. J. Massaro © Humana Press Inc., Totowa, NJ

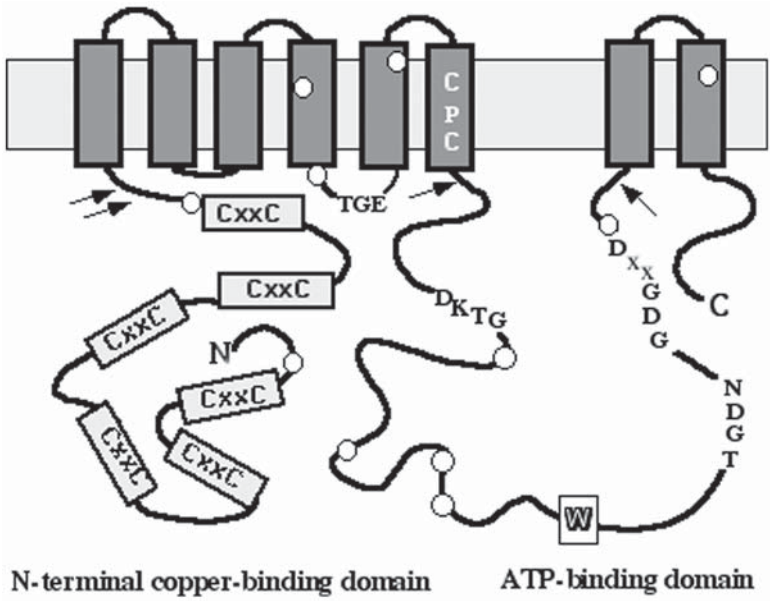

Fig. 1. Schematic representation of the transmembrane organization of WNDP. The blocks in the N-terminal portion indicate the position of copper-binding sites with a conserved sequence motif GMTCxxC. The single arrows indicate the beginning and the end of the ATP-binding domain; the double arrow indicates the end of the N-terminal domain. Open circles mark the location of some of the Wilson's disease mutations and TGE, DKTG, TGDN, and GDGxxD are the sequence motifs conserved in all P-type ATPases; W in a block shows the position of a single tryptophan residue in the ATP-binding domain. CPC is a sequence motif that is specific for copper-transporting ATPases.

considerably by comparative analysis of WNDP or MNKP with much better characterized cation-transporting ATPases, such as Ca^{2+}-ATPase or Na^{+},K^{+}-ATPase, which belong to the same protein family as WNDP and MNKP.

2. HUMAN COPPER–TRANSPORTING ATPASES AS MEMBERS OF THE P-TYPE ATPASE FAMILY

Analysis of the primary sequence of the *ATP7A* and *ATP7B* gene products revealed that the corresponding proteins, MNKP and WNDP, belong to a family of cation-transporting P-type ATPases. The P-type ATPases are a large group of membrane proteins that utilize energy of ATP hydrolysis to transport various ions across cell membranes. During the catalytic cycle the γ-phosphate of ATP is transferred to the invariant Asp residue within the nucleotide-binding site of ATPase with the formation of acylphosphate intermediate; this property distinguish the P-type ATPases from other cation-transporting pumps. Because both Wilson's disease and Menkes disease are associated with defects in copper distribution, it was proposed that WNDP and MNKP function in a cell as copper-transporting P-type ATPases. In agreement with this proposal, recent studies by Voskoboinik et al. have shown that MNKP and WNDP transport copper across cell membranes and ATP stimulates the MNKP- and WNDP-dependent transport *(19,20)*.

Today, over 100 members of the P-type ATPase family has been described and a wealth of information has been accumulated regarding the structure and function of some of these proteins (for review, *see* refs. *21* and *22*). The first crystal structure of a P-type ATPase, the Ca^{2+}-ATPase from sarcoplasmic reticulum, has been recently solved, providing an important framework for studies on

molecular mechanisms of the ATP-driven ion transport *(23)*. To understand how this information can be utilized for analysis of WNDP and MNKP, it could be beneficial to dissect features that are common for the human copper-transporting ATPases and other P-type ATPases, as well as to identify the unique structural and functional characteristics of MNKP and WNDP.

Like all P-type ATPases, WNDP and MNKP have several highly conserved sequence motifs, such as DKTG, TGDN, GDGxxD, and TGEA/S (Fig. 1). The invariant residues in these motifs are known to play key roles in catalysis and accompanying conformational transitions, indicating that the basic mechanisms of ATP hydrolysis and coupling between the hydrolytic and ion-transport steps are likely to be the same for human copper-transporting ATPases and other P-type pumps.

At the same time, human copper-transporting ATPases have several unique structural and functional characteristics (*see* Sections 2.2. and 2.4.), indicating that specific details of their molecular mechanism and their intracellular behavior differ from those of well-characterized P-type ATPases. For this reason, in our early attempt to classify the P-type ATPases, we placed the copper-transporting and other structurally similar transient metal-transporting ATPases into a separate subgroup (P_1-type ATPases), in contrast to P_2-ATPases, such as Ca^{2+}-ATPase and Na^+,K^+-ATPase, which transport alkali and alkali-earth ions *(24)*. Solioz and Vulpe later suggested an alternative name for the P_1-ATPases, CPx-ATPases, based on the presence of characteristic motif CPx in the transmembrane portion of these proteins *(25)*. In a recent and more complete classification scheme, Axelson and Palmgren also placed the P_1-ATPases in a separate group (type IB), distinct from four other P-type ATPase subfamilies *(26)*.

The comparison of structural and functional properties of mammalian copper-transporting ATPases (P_1-ATPases) and P_2-type ATPases reveals the following interesting differences between these two groups of pumps.

2.1. Physiological Role

The major function of all well-characterized P_2-type ATPases is to maintain the concentration gradient of the transported cations across cell membranes; the generated gradients then serve as a driving force for such physiological processes as muscle contraction, nutrients uptake, or electrical activity of neurons. Whether human copper-ATPases have a similar role and maintain a concentration gradient of copper across cell membranes remains to be elucidated. In the cytosol, essentially all copper apparently exists in a protein-bound form *(27)*, but its status in the intracellular compartments is less clear. If, in organelles, copper is present in a free form and therefore the transmembrane copper gradient is generated, it remains unknown whether such gradient drives any secondary process. However, it is now well established that the eucaryotic copper-transporting ATPases represent key components of a biosynthetic, cofactor-delivery pathway, transporting copper to copper-dependent enzymes. Incorporation of copper into proteins in the secretory pathway is essential for numerous physiological functions, including respiration, neurotransmitter biosynthesis, and high-affinity iron uptake; however, the role of copper in these processes is indirect.

In addition to their important role in delivering copper to the copper-dependent enzymes, human copper-transporting ATPases regulate the intracellular concentration of copper by removing excess copper from the cell. This "detoxification" function of copper-transporting ATPases is very similar to the functional role of bacterial Cd^{2+}-ATPase and Pb^{2+}-ATPases and likely appeared first during evolution. It was later extended to accommodate eucaryotic cell needs in having copper inside various cell organelles. To carry out this dual function, WNDP and MNKP have to be located, at least temporarily, in different cell compartments.

In agreement with this prediction, MNKP was shown to cycle between the trans-Golgi network (TGN) and the plasma membrane: Under basal conditions, MNKP was detected predominantly in TGN, whereas increase in copper concentration led to the redistribution of MNKP from TGN to the plasma membrane *(28,29)*. Similarly, the intracellular localization of WNDP depends on copper

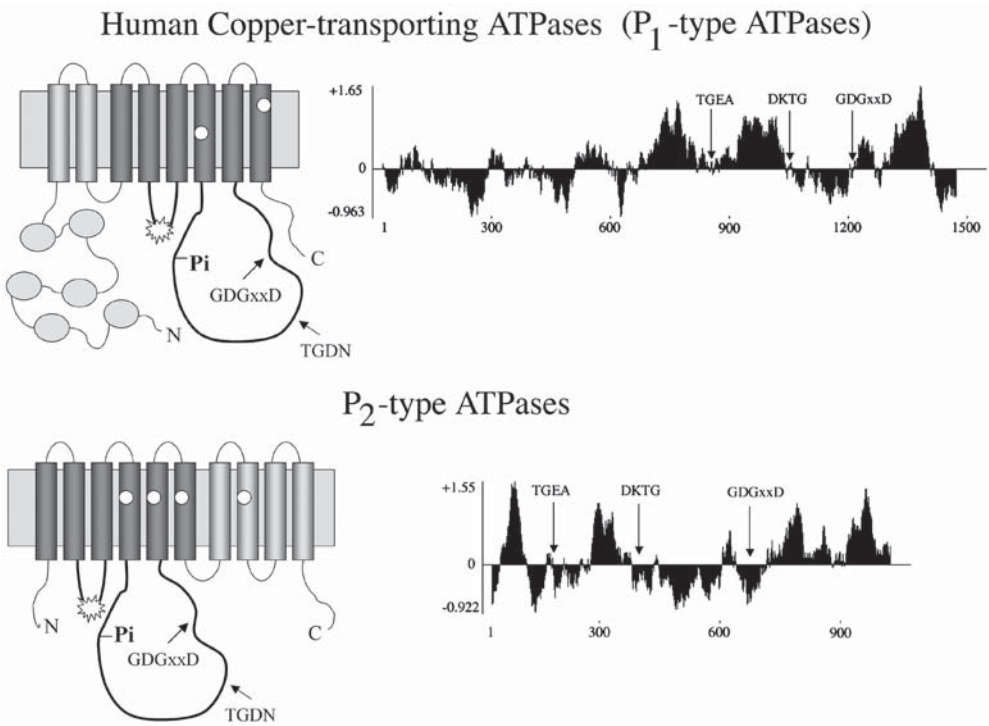

Fig. 2. Comparison of the transmembrane topology and organization of the cation-translocation pathway in human copper-transporting ATPases (P_1-type ATPases) and P_2-type ATPases. The letters and the arrows/vertical lines mark the positions of the conserved sequence motifs; Pi indicates the Asp residue in the DKTG motif that is phosphorylated during the catalytic cycle and the asterisk shows the position of the TGEA/S sequence in the transmembrane model of ATPases. The transmembrane segments that are common for the P_1- and P_2-ATPases are dark colored, the membrane segments unique for each group of ATPases are light gray; the open circles indicate the transmembrane segments known to be important for cation coordination and transport activity in both groups of pumps.

concentration *(30,31)*. In response to increased copper, WNDP redistributes from its primary localization site, TGN, to a vesicular compartment (probably endosomes). Thus, changes in copper concentration seem to regulate copper transport across various cell membranes by altering the number of copper transporters present at these membranes. So far, the dependence of intracellular localization on concentration of the transported ion seems to be a unique property of human copper-transporting ATPases. Whether this mode of regulation is the only way of altering copper transport across the membranes or whether the changes in copper concentrations also control the activity of MNKP and WNDP remains to be elucidated.

2.2. *Transport Characteristics*

Copper can bind to proteins in either reduced, Cu^{1+}, or in the oxidized, Cu^{2+}, form. The ability of copper to exist in different oxidation states raises an interesting possibility that copper oxidation may occur in the secretory pathway or in another intracellular organelle as the last step of the copper-transport process. Copper binds to WNDP and MNKP in the reduced form (*see* Section 3.) and is likely to be transported in the same form *(32)*. Copper is then released from the transporters, possibly with a change in oxidation state, and becomes incorporated into copper-dependent enzymes. [Inter-

estingly, chloride ions seems to play an important role in this process, at least in yeast *(33)*]. The alternative possibility is that copper is picked up from the ATPases through direct intermolecule interactions either by target proteins or by low-molecular-weight copper carriers. If this last scenario is correct, then the intracellular transport of copper is unique, because the entire ion-transport process would be mediated through a chain of specific protein–protein interactions.

2.3. Cation Recognition

The extremely low concentrations of free copper in a cell *(27)* results in another interesting property of WNDP and MNKP. Unlike many P-type ATPases, which recognize free cations present in the cytosol, eucaryotic copper-transporting ATPases receive copper from so-called copper chaperones, small cytosolic proteins that presumably work as shuttles between the copper uptake system and other components of the copper distribution pathway *(34–36)*. Thus, specificity of MNKP and WNDP for the transported ion is defined not only by the stereochemistry of copper binding sites, but also by specific recognition of the copper-carrier protein, HAH1.

2.4. The Structural Differences Between the P_1- and P_2-ATPases

It is probably not a coincidence that in addition to the functional differences described earlier, copper-transporting ATPases have structural features that make them quite distinct from the P_2-ATPases. The most obvious difference is the organization of the cation-translocation pathway (Fig. 2). In their membrane portion, P_2-ATPases have 10 transmembrane segments: 4 segments before the ATP-binding domain and 6 segments in the C-terminal portion after the ATP-binding domain. The transmembrane segments involved in cation coordination and transport in the P_2-ATPases contain a large number of hydrophilic and helix-breaking amino acid residues, which are essential for binding of the positively charged ions in the membrane *(37–39)*.

In contrast, the P_1-ATPases have a total of eight membrane-spanning regions: six before the ATP-binding domain, and only one pair after the ATP-binding domain. The membrane portion of the P_1-ATPases has fewer hydrophilic and helix-breaking residues, and the segments, corresponding to the last four C-terminal transmembrane helixes of P_2-ATPases, are absent in the structure of copper pumps (Fig. 2). Interestingly, these last four transmembrane segments play an important role in the insertion and maintenance of the ion-binding segments in P_2-ATPases and may even contribute to cation coordination *(40,41)*. The absence of these fragments in the copper-ATPases suggests that the P_1- and P_2-ATPases likely to have different mechanisms for insertion of some transmembrane hairpins and for overall assembly of the cation-translocation pathway.

It is also interesting that the transmembrane segments immediately after the ATP-binding domain, which play a central role in ion coordination in the P_2-type ATPases, do not contain any obvious ligands for copper binding in WNDP and MNKP. Currently, the only candidate for copper binding in the membrane is the CPC motif in the sixth transmembrane helix (*see* Fig. 1). This suggests that additional coordination of copper could be provided either by side chains of Ser/Thr and Tyr residues or by the backbone carbonyls of other transmembrane segments. Alternatively, it is possible that two additional transmembrane segments present at the N-terminal part of the protein are required to form the copper-translocation pathway. If the first membrane hairpin, which is absent in the structure of the P_2-ATPases, is directly involved in copper transport, then the mechanism of coupling between the ATP hydrolysis and cation transport could be quite different for the P_1-type and P_2-type pumps.

Another obvious difference between the P_1- and P_2-type ATPases is the role of the N-terminal domain in cation binding and selectivity. Mutations in the N-terminal domain do not have a dramatic effect on the cation affinity of the characterized P_2-ATPases, which is defined mainly by the residues located in the transmembrane portion of these proteins (*[22,42]* and Fig. 2). What specific role the N-terminus of the P_2-ATPases plays in the transport process, if any, is still not clear. In contrast, the N-terminal domain of the copper-transporting ATPases contains multiple copper-binding sites (*see* Fig.

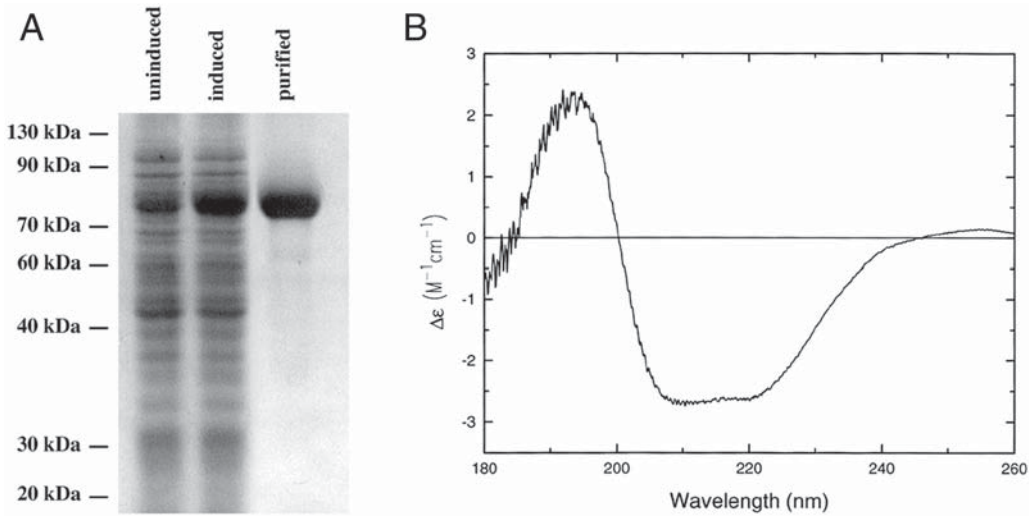

Fig. 3. **(A)** Expression of N-WNDP-HT in *Escherichia coli* and purified soluble protein used for further analysis of the secondary structure. **(B)** Circular dichroism spectroscopy of N-WND-HT reveals the following secondary structure elements for this domain: 19.5% α-helix, 26% β-sheet, 21% β-turn, and 33.5% random coil.

1 and text below), and the presence of at least one or more of these repeats is essential for copper transport by MNKP and WNDP *(34,43–45)*. This interesting difference between the P_1- and P_2-ATPases seemed critical for dissecting the molecular mechanism of copper transport and prompted us and other investigators to focus our attention on biochemical characterization of the N-terminal domain of WNDP and MNKP.

3. N-TERMINAL DOMAIN AND COPPER-BINDING PROPERTIES OF WNDP

The N-terminal domain of WNDP and MNKP is an unique and intriguing feature in the structure of these proteins. It is composed of 6 repetitive sequences, each of which is about 70 amino acid residues long (Fig. 1). Each repeat contains a highly conserved motif GMTCxxCxxxIE, which is also present in the bacterial mercury-binding protein MerP and in bacterial Cd^{2+}-transporting ATPase. Based on this sequence homology with bacterial metal-binding proteins, it was proposed that the sequence repeats in the N-terminus of WNDP and MNKP play a role in copper binding *(6–11)*. Later studies from Gitschier et al. *(46)* and Steele and Opella *(47)* revealed that the overall fold of the single sequence repeat from Menkes disease protein and MerP are the same, highlighting the remarkable conservation of this particular metal-binding motif through evolution.

The involvement of the N-terminal domain in copper binding was directly demonstrated by us and other groups following heterologous expression of this domain and biochemical characterization of purified proteins *(48–51)*. We found that the N-terminal domains of WNDP and MNKP (N-WNDP and N-MNKP, respectively) bind copper with stoichiometry close to six coppers per domain or one copper per metal-binding repeat *(48)*. Copper binds to these proteins in vivo and in vitro, however, efficient in vitro binding is only achieved in the presence of reducing agents *(48)*, suggesting that copper binds to the protein in the reduced copper(I) form. These studies also demonstrated that Cys residues play an important role in copper coordination. Recent X-ray absorption spectroscopy analysis directly demonstrate that copper is bound to N-MNKP and N-WNDP in the reduced Cu(I) form and is coordinated primarily by two Cys residues *(52,53)*. Different copper stoicheometry (eight or

four coppers bound per domain) with alternative stereochemistry was reported by the Dameron group *(50,54)*. These studies utilized the refolded protein, and discrepancies between these results and our data are likely to reflect the difference between the in vitro and in vivo loading of the N-terminal domains with copper.

Although it is clear that in the isolated metal-binding repeat, copper is coordinated by Cys residues in a flexible and fairly exposed loop *(46)*, the arrangement of the multiple copper sites in the fully loaded N-terminal domain remain unknown. We expressed N-WNDP with a short histidine tag (N-WNDP-HT) in a soluble form and characterized the secondary structure of the purified N-WNDP-HT using circular dichroism spectroscopy (Fig. 3). These experiments revealed that the composition of the secondary-structure elements of N-WNDP (*see* Fig. 3 legend) closely resembles those of the single metal-binding repeat, suggesting that when all six domains come together there is no marked alterations in the overall fold of these repeats.

Recent studies by Sarkar and colleagues demonstrated that copper binding to N-WNDP is accompanied by conformational changes and by changes in the tertiary structure of the protein *(53)*. These results are very interesting, but it remains uncertain how closely the reported structural rearrangements resemble the changes taking place under more physiological conditions. Our studies using limited proteolytic digestion of soluble copper-free and copper-bound N-WNDP maltose-binding fusion (N-WNDP-MBP) demonstrate that, although some protein regions slightly change their exposure to protease as a result of copper binding, the overall proteolytic pattern of copper-free and copper-bound N-WNDP remain the same. This result suggests that there is no dramatic alterations in the overall fold of these proteins upon in vivo copper binding (unpublished observation).

It seems most likely that the copper-induced conformational changes affect the configuration of loops connecting the metal-binding repeats and/or the distance between various metal-binding repeats. This is not to say that the small changes in the conformation of the N-terminal domain do not have a major impact on the WNDP function. In fact, as we have shown recently, copper binding to the N-terminal domain has a marked effect on domain–domain interactions within WNDP, which, in turn, may lead to changes in the enzyme activity and intracellular trafficking (*see* Section 4.).

4. ATP-BINDING DOMAIN AND THE NUCLEOTIDE-BINDING PROPERTIES OF WNDP

The energy-driven translocation of copper across cell membranes is likely to require coordination and interaction among three major domains of copper-transporting P-type ATPases; the copper-binding domain, the ATP-hydrolyzing domain, and the membrane portion of the protein, containing the ion-translocation pathway. In our earlier work, we hypothesized that the N-terminal domain can play a regulatory role modulating the catalytic properties of WNDP and MNKP in response to copper binding *(13)*. We also suggested that the regulatory function can be carried out via specific protein–protein interactions of the N-terminal domain with the second large cytosolic loop, containing the ATP-binding domain *(13)*. To test this hypothesis, we have recently expressed, purified, and characterized the ATP-binding domain of WNDP (ATP-BD) and analyzed the domain–domain interactions within WNDP *(55)*. The results of these studies are discussed next.

Current expression systems do not permit direct measurements of the nucleotide-binding properties of human copper-transporting ATPases. However, one can get important and reliable information about the nucleotide specificity and relative nucleotide-binding affinities of proteins by using their isolated nucleotide binding domains *(56–58)*. In determining the borders of the putative ATP-binding domain of WNDP, we were aided by studies on other members of the P-type ATPase family, such as Ca^{2+}-ATPase and Na^{+},K^{+}-ATPase. In these proteins, the major cytosolic loop that contains the highly conserved motifs DKTG, TDGN, and GDGxxD (*see* Fig. 1) was shown to be sufficient for selective binding of nucleotides *(56–58)*. Although the overall homology between Ca^{2+}-ATPase and copper-ATPases is just 5%, the similarity between regions corresponding to the ATP-binding domain

Table 1
Apparent Affinities of the Purified ATP-BD for Various Nucleotides in the Absence or Presence of the Copper-Free and Copper-Bound N-Terminal Domain (N-WNDP-Cu and N-WNDP+Cu, Respectively)

	ATP-BD + (μM)	*ATP-BD N-WNDP(-Cu) (μM)*	*ATP-BD + N-WNDP(+Cu) (μM)*
K_a for TNP-ATP	1.89 ± 0.72	10.36 ± 0.46	6.72 ± 1.45
K_a for ATP	268 ± 23	1137 ± 238	339 ± 80
K_a for ADP	85 ± 5	n.d.	n.d.
K_a for AMP	79 ± 18	52 ± 31	168 ± 37

is higher (18–23%), suggesting that the overall fold and some nucleotide-binding properties could be well preserved among all members of the P-type ATPase family.

We expressed the fragment K^{1010}–K^{1325} of WNDP (Fig. 1) as a histidine tag (HT) fusion in *E. coli*, purified it from the soluble fraction, and demonstrated that it formed an independently folded domain (ATP-binding domain, or ATP-BD) *(55)*. ATP-BD has both the nucleotide-binding and ATP-hydrolyzing activities *(55)*; the affinities of the purified ATP-BD for nucleotides are summarized in Table 1.

Analysis of the nucleotide-binding properties of ATP-BD yielded several interesting results. First, the ATP-binding domain of WNDP was found to bind ADP and AMP equally well and with significant affinity (*see* Table 1), in contrast to previously characterized domains of P_2-type ATPases, which show fairly low affinity for these nucleotides and a large difference in the affinity for ADP and AMP *(56,57)*. The lower selectivity of ATP-BD toward nucleotides resembles the property of the P-type ATPase from *Methanococcus jannaschii (59)*, a soluble protein structurally equivalent to the isolated ATP-binding domain, and probably reflects the early evolutionary origin of copper-transporting ATPases.

Interestingly, both ATP-BD and the *Methannococcus* P-type ATPase have a low but measurable ATPase activity *(55,59)*, a property that has not been observed in the isolated ATP-binding domains of the P_2-ATPases. This interesting difference likely reflects a more compact folding of the ATP-binding domain of WNDP and the bacterial P-type ATPases; ATP-BD is 70–80 amino acid residues shorter than the corresponding domain of the P_2-type ATPases and lacks several loops, which could be important for precise nucleotide selection in Ca^{2+}-or Na^+,K^+-ATPase. The molecular modeling of the WNDP ATP-binding domain using the published crystal structure of Ca^{2+}-ATPase further illustrates these points (Fig. 4).

As shown in Fig. 4, the ATP-binding domain of P-type ATPases consists of two distinct parts, the phosphorylation domain (P-domain), which includes the highly conserved residues DKTG, TGDN, and GDGxxD, and the N domain, which contains residues important for binding of the adenosine moiety of nucleotides *(23)*. The P domains of WNDP and Ca^{2+}-ATPase are structurally very similar (i.e., consistent with the common role these regions play in catalytic cycle of ATPases). In contrast, the N domains involved in the nucleotide binding are quite different. The differences in the number, length, and position of several loops in the N domain of P_1-type and P_2-type ATPases (*see* Fig. 4) are likely to be responsible for the differences in their nucleotide selectivity (*see* above).

Another novel and interesting property of the WNDP ATP-binding domain is its ability to bind ATP (the substrate of ATP hydrolysis) and ADP (the product of the reaction) simultaneously *(55)*. Given the distinct subdomain organization of ATP-BD (Figs. 4 and 5), it is tempting to speculate that ATP binds in close proximity to the Asp residue in the DKTG motif (the residue, which in P-type ATPases accepts γ-phosphate from ATP, forming phosphorylated intermediate) while ADP is bound in the adenosine-binding pocket of the N domain. During the catalytic cycle, two subdomains would

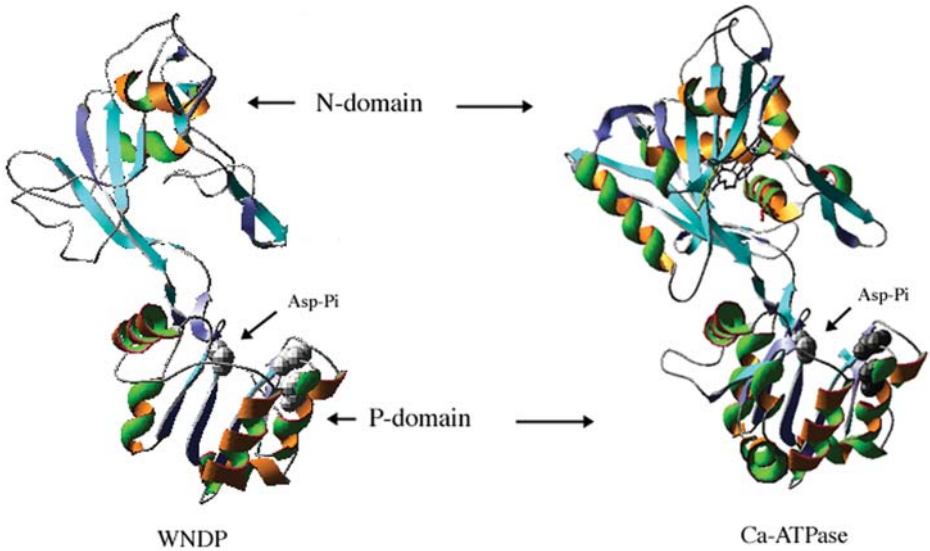

Fig. 4. Comparison of three-dimensional fold of the ATP-binding domains of WNDP and Ca-ATPase. The homology modeling was carried out using published coordinates for Ca^{2+}-ATPase (accession N. 1EUL) and SwissPdbViewer software. The balls in the lower P-domain indicate the positions for invariant Asp in the DKTG motif, two Asp residues in the GDGxxD sequence, and the location of the TGDN motif. The chain of balls in the upper N domain marks the site of the TNP-AMP (the AMP analog) binding in the crystal structure of Ca^{2+}-ATPase and the equivalent region in the structure of ATP-BD.

come together [as described for Ca^{2+}-ATPase in *(23)*], forming a "closed state." The hydrolysis of ATP would then be accompanied by transfer of the adenosine moiety from the P domain to the N domain as shown in Fig. 5 with formation of an "open state" in which both ATP- and ADP-binding sites are ascessible.

It is significant that the nucleotide-binding properties of ATP-BD are modified in the presence of the N-terminal domain (*see* Table 1 and Section 5.). This change reflects the interaction between two functional domains of WNDP and suggests that domain–domain interactions play an important role in the functional activity of WNDP and homologous MNKP. The ability of ATP-BD to fold independently, to bind and hydrolyze ATP, and to interact with the N-WNDP specifically makes this isolated nucleotide-binding domain a convenient tool for analysis of numerous disease-causing mutations located in this region of WNDP *(60,61)* (*see* Fig. 1).

5. COPPER-DEPENDENT DOMAIN–DOMAIN INTERACTIONS AND THE REGULATORY ROLE OF THE N-TERMINAL DOMAIN

The N-terminal domain of human copper-transporting ATPases is essential for the copper-dependent functions of these proteins. Mutations of Cys residues in the metal-binding motifs inactivate the copper-transporting activity of WNDP and prevent copper-dependent trafficking of WNDP in a cell *(34,45)*. At the same time, recent studies conducted in several laboratories convincingly demonstrated that the entire N-terminal domain was not essential for the transport function of copper-ATPases: the large portion of this domain could be deleted or mutagenized without significant loss of the copper-transport activity *(34,43,44)*. These results are consistent with the fact that the bacterial, yeast, and plant copper-ATPase can carry out their functions with fewer than six (one to three) metal-binding repeats (e.g., *see* ref. *62*). Because extra metal-binding repeats are not important for function, it seems likely that they play a role in regulation of WNDP and MNKP.

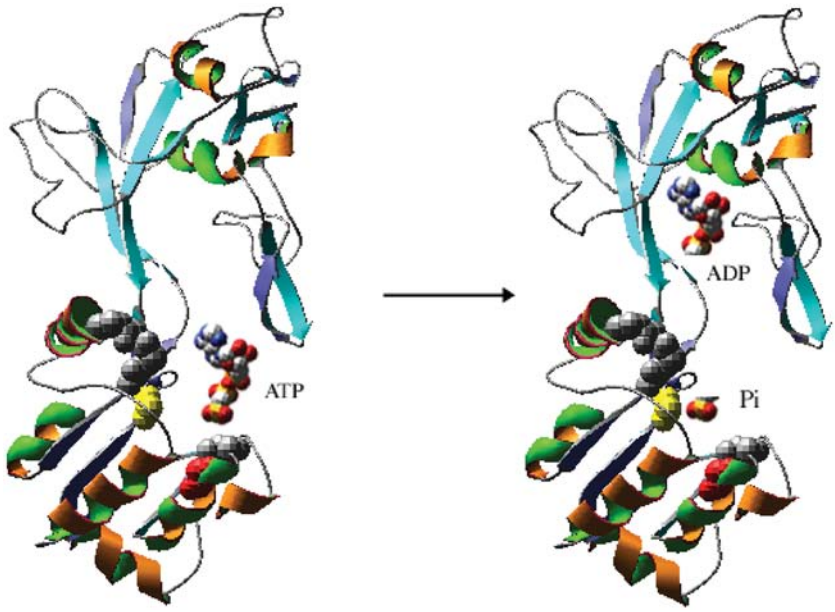

Fig. 5. Hypothetical model showing how ATP and ADP could bind to ATP-BD simultaneously *(55)* in the isolated ATP-BD (*see* text for details).

The regulatory role for the N-terminal domain has been suggested by several authors *(20,44,48,53)*, and recent studies indicate that copper binding to the N-terminal domain triggers the intracellular relocalization of MNKP and WNDP *(44,45)*. However, only one or two metal-binding repeats, which are important for transport function, seem to be necessary and sufficient for copper-induced trafficking *(44,63,64)*. Therefore, the first four metal-binding repeats were proposed to function by preventing protein trafficking before they are filled up with copper (*see* the model in ref. *53*).

Our recent studies shed some light on how the N-terminal domain may regulate the copper-dependent functions of WNDP. We found that N-WNDP interacts specifically with the ATP-binding domain of WNDP and that the interactions between these two domains are copper dependent: In the absence of copper, two domains interact tightly, whereas copper-bound N-WNDP does not bind to ATP-BD very well *(55)*. How many bound copper atoms are sufficient to induce the change in intradomain interactions is a subject of future investigations.

Importantly, the domain–domain interactions have a clear effect on the conformational state of the ATP-binding domain: when N-WNDP is bound to ATP-BD, the affinity of the latter to nucleotide is decreased several-fold (*see* Table 1). Therefore it is tempting to speculate that binding of copper to the N-terminal domain is accompanied by conformational changes that alter the interaction between N-WNDP and the ATP-binding domain (Fig. 6). This change, in turn, may modify the nucleotide-binding properties of WNDP and possibly the rate of ATP-hydrolysis.

It is also quite possible that copper-induced changes in domain–domain interactions and the subsequent conformational transitions lead to exposure of sites for the intracellular trafficking machinery, resulting in copper-dependent relocalization of WNDP in a cell. The mutagenesis studies and analysis of the naturally occurring mutants *(63,65)* revealed that the copper-dependent trafficking of MNKP and WNDP can be disrupted by amino acid substitutions in various regions of these proteins. These results suggest that a certain conformation of a functionally active protein rather than its mere ability to bind copper is important for trafficking of copper-ATPase. Although the precise molecular mecha-

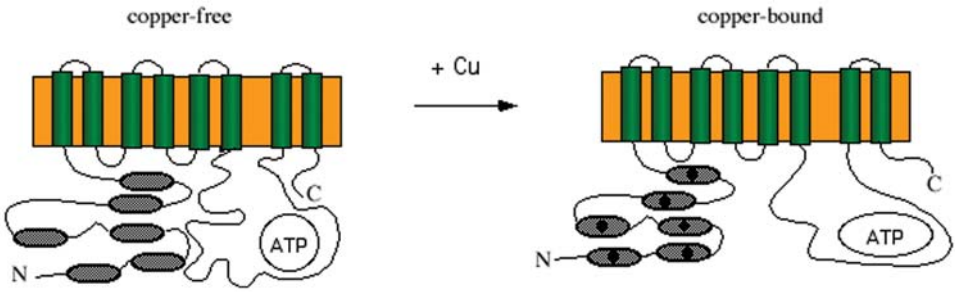

Fig. 6. Copper binding to N-WNDP decreases the interactions of N-terminal domain with ATP-BD, which in turn, changes the ATP-BD conformation.

nism of the WNDP trafficking and targeting is still unclear, it is likely to involve series of copper-dependent posttranslational events, based on changes in domains conformation induced by copper.

6. PRACTICAL ASPECTS OF EXPRESSION, PURIFICATION, AND BIOCHEMICAL ANALYSIS OF THE WNDP FUNCTIONAL DOMAINS

6.1. Expression of the N-Terminal Domain

Most of the biochemical studies described earlier utilized the heterologous expression, purification, and analysis of isolated functional domains of WNDP. Although, in general, this approach has certain limitations, it proved to be very fruitful and informative for WNDP. The key to successful biochemical characterization of isolated domains is the ability to obtain them in a soluble and well-folded form. The N-terminal domains of WNDP and MNKP contain over 600 amino acid resides and a large number of cysteines, which makes their expression in a soluble form a challenging task. In fact, in our first experiments the expression of N-MNKP and N-WNDP as fusions with maltose-binding protein (N-MNKP-MBP and N-WNDP-MBP, respectively) led to largely insoluble proteins deposited in inclusion bodies. Using the fluorescent Cys-directed probe (*see* Section 6.2. for details), we determined that most of the Cys residues in these proteins were unavailable for modification without prior reduction with dithiotreitol or ß-mercaptoethanol, suggesting that Cys residues were involved in the formation of disulfide bridges (unpublished observation). It also suggested that incorrect S–S bridge formation could have lead to protein misfolding and insolubility.

To overcome this problem, we utilized the innovative approach proposed by Yasukawa et al. *(66)*. In this work, the solubility of eucaryotic proteins expressed in *E. coli* was shown to be markedly enhanced by presence of thioredoxin expressed from a separate plasmid. Indeed, in our experiments, coexpression of N-WNDP-MBP and N-MNKP-MBP with thioredoxin led to a dramatic increase in protein solubility (up to 60% of expressed protein was found in the soluble portion). Analysis of soluble N-WNDP-MBP and N-MNKP-MBP using Cys-directed probe revealed that the soluble domains have their Cys in the reduced form, not in S-S bridges (Fig. 7).

6.2. Copper Loading and Analysis of Copper Binding

The ability to keep Cys residues in the reduced form in a cell was extremely important, because it allowed us to develop a procedure for the in vivo loading of N-WNDP and N-MNKP with copper *(48)* (*see* Fig. 7). N-WBDP and N-MNKP in a copper-bound form can then be purified from cells using affinity chromatography and the amount of bound copper can be determined using a spectrophotometric assay *(67)* based on complexation of Cu(I) with bicinchoninic acid (BCA), as shown in

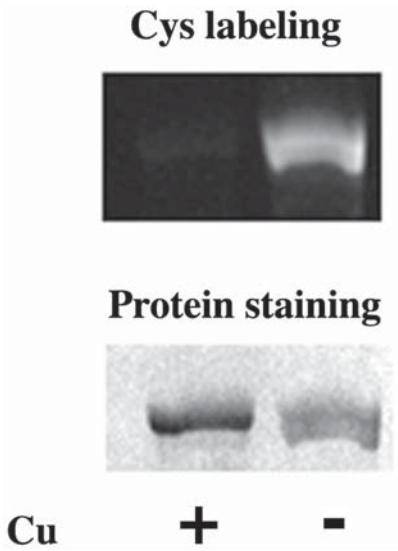

Fig. 7. Expression of N-MNKP-MBP in the presence of thioredoxin and in vivo loading with copper. *E. coli* cells transformed with N-MNKP-MBP and thioredoxin-containing plasmids were grown under standard conditions. Copper was added up to 500 μ*M* (+) to one of the cultures and the protein expression in control and copper-treated sample was induced with IPTG as described *(48)*. Following affinity purification, the availability of Cys residues for labeling with fluorescent coumarin maleimide (CPM) and the amount of copper bound to the protein were determined. In this experiment, the (+) copper sample contained 5.19 mol Cu/mol protein. Similar results were obtained with N-WNDP-MBP fusion.

Fig. 8, or by atom absorption spectroscopy. The two procedures yield similar results, although care should be taken using the BCA assay, because the accuracy of this procedure may be affected by buffer composition, (e.g., by presence of imidazole (*67*; and our unpublished data).

Binding of copper to N-WNDP, N-MNKP, or to copper chaperones, such as HAH1, all of which contain the same CxxC motif for copper coordination, can be monitored by decrease of the Cys residues reactivity toward fluorescent reagents following copper binding to the protein, as shown in Fig. 7. Although this assay is indirect and has to be confirmed by the BCA-based analysis or by atom absorption spectroscopy, it could be very valuable when comparing multiple samples. The labeling assay is fairly independent on buffer composition and requires significantly less protein than the BCA-based procedure and atom absorption spectroscopy. We observed good agreement in copper stoicheometry values comparing the BCA procedure with the fluorescent probe-based assay, and we routinely used both protocols for the copper-binding measurements.

6.3. Choosing a Tag for Affinity Purification of the Copper-Binding Domain

For the characterization of the copper-binding domain of WNDP, we utilized the MBP fusion and a histidine tag. The advantage of the MBP fusion is that MBP does not bind copper and therefore does not appear to interfere with copper-binding properties of WNDP, in contrast to HisTag, which binds copper (Cu^{2+}). The disadvantage of MBP fusion is its large size (42 kDa), which complicates structural analysis of the fusion protein. For the characterization of MerP, expressed as a MBP fusion, MBP was cleaved prior to spectroscopic analysis *(47)*; however, trombin cleavage of N-WNDP-MBP, which is significantly larger than MerP-MBP, was fairly inefficient (our data). Therefore, for characterization of the N-WNDP secondary structure, we utilized a HisTagged version of this protein (Fig. 3).

Interestingly, N-WNDP-HT can be expressed in a soluble form in *E. coli* in the absence of thioredoxin, but it has to be reduced in vitro in order to get copper bound (Fig. 9).

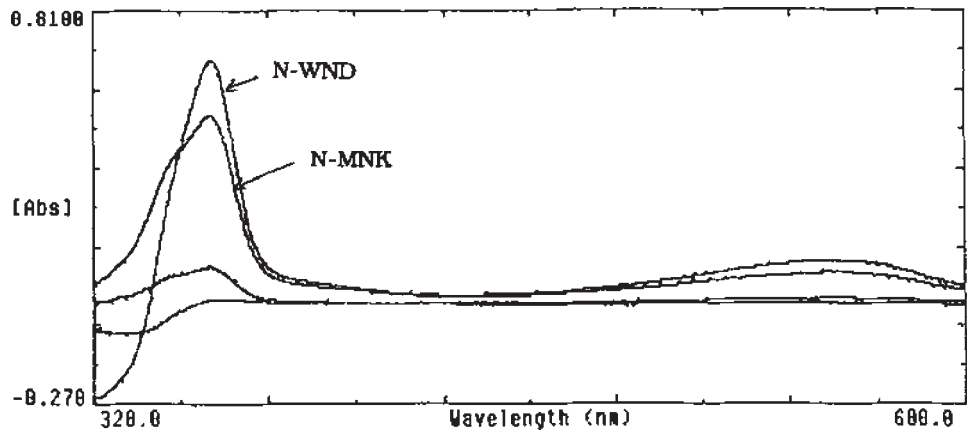

Fig. 8. Measurements of copper-binding to N-WNDP (N-WND) and N-MNKP (N-MNK) using bicinchoninic acid. Proteins loaded with copper in vivo as in Fig. 7 were used to estimate the amount of bound copper.

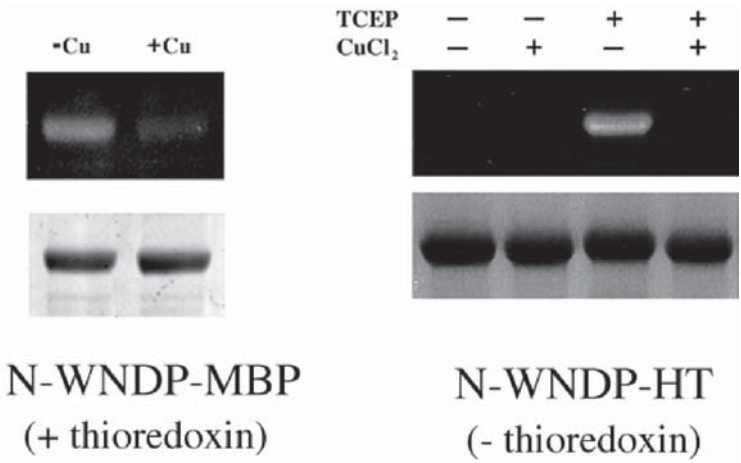

Fig. 9. Comparative analysis of the in vitro copper-binding properties of N-WNDP-MBP and N-WNDP-HT. Left panel: N-WNDP-MBP was expressed in the presence of thioredoxin, purified using amylose resin, and loaded with copper in vitro in the presence of ascorbate as described in ref. *48*. Copper-binding was monitored by labeling of Cys residues with fluorescent coumarin maleimide and confirmed with BCA assay. Right panel: N-WNDP-HT was expressed without thioredoxin, purified on NTA resin and was either eluted with Imidazole (first two lanes) or was incubated with or without copper in the presence of reducing reagent [tris-(2-carboxyethyl)phosphine hydrochloride, TCEP] while it is was bound to the resin. Note that without reduction, Cys residues are unavailable for labeling with the fluorescent probe. Following washes and elution with imidazole, the amount of copper bound to N-WNDP-HT was determined as above.

Although the N-WNDP-HT is useful for analysis of copper-independent properties of this domain, such as overall folding, and structure, its usefulness for analysis of copper binding is somewhat ambiguous because of the ability of HisTag to bind copper. In fact, our initial attempts to load N-WNDP with copper either in vivo or in vitro led to protein precipitation. The precipitation problem can be avoided if copper is added to N-WNDP-HT during purification while protein is still bound to the NTA resin and the His tails are sequestered by interactions with Ni. This protocol allowed copper to bind to Cys residues, as shown in Fig. 9.

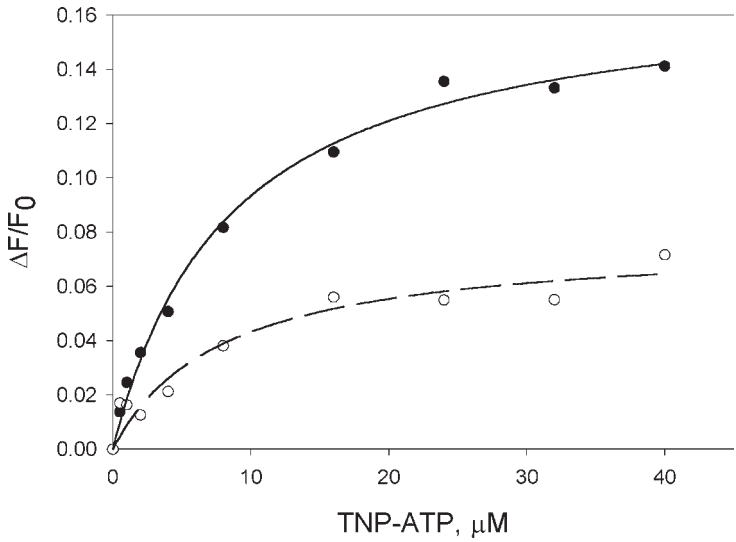

Fig. 10. The comparison of the nucleotide-binding properties for the ATP-binding domains of WNDP (filled circles) and Na^+,K^+-ATPase (the typical representative of the P_2-type ATPases, empty circles). The identical amounts of purified nucleotide-binding domains were mixed with increasing concentrations of TNP-ATP and the nucleotide-binding was monitored by the increase in TNP-ATP fluorescence.

The column-based procedure yields a copper-bound N-WNDP with stoichiometry close to what was found for in vitro-loaded N-WNDP-MBP; however, there is a marked difference between N-WNDP-HT and N-WNDP-MBP in the stability of the copper–protein complex. Although copper is bound tightly to N-WNDP-MBP, such that copper-bound protein can be dialyzed or concentrated significantly without losing copper, the HisTag fusion of WNDP quickly loses its copper upon concentration and then begins to aggregate when protein concentration exceeds 1–2 mg/mL. We conclude that the MBP fusion expressed in the presence of thioredoxin and loaded with copper in vivo currently represents a much better system for characterization of N-WNDP and N-MNKP properties.

6.4. ATP-Binding Domain

The problems associated with the HisTag, which we discussed earlier, could be the result of the fact that both the HisTag and the N-terminal domain can bind copper, and the presence of two copper-binding motifs generates protein with completely new properties. Using the HisTag, however, works fairly well for expression and purification of the ATP-binding domain of WNDP (ATP-BD). Although solubility of this domain is rather limited, and is not improved by coexpression with thioredoxin, it is possible to obtain up to 500 μg of purified protein from 2 L of cell culture following induction with 0.1 m*M* isopropyl-l-thio-β-D-galactopyranoside (IPTG) at room temperature *(55)*.

The ability of the ATP-binding domain to bind the nucleotides can be quickly assessed using the fluorescent analog ATP (thrinitrophenyl-ATP, TNP-ATP). In solution, this reagent has low fluorescence; binding of TNP-ATP to proteins is accompanied by an increase in fluorescence, as shown in Fig. 10.

The specificity of TNP-ATP binding and relative affinities toward various nucleotides can then be determined by competition studies as in refs. *55–58*. The disadvantage of TNP-ATP as a probe for the nucleotide-binding site is a relatively high nonspecific binding because of protein interaction with TNP moiety. However, there are also certain advantages. The TNP-ATP-based assay not only estimates the ability of the isolated domain to binds nucleotides, it also can be used to monitor the

changes in the microenviroment of the probe. As shown in Fig. 10, whereas the affinities of ATP-BD and the ATP-binding domain of the Na pump for TNP-ATP are comparable, the increase in the TNP-ATP fluorescence is larger when it binds to ATP-BD, indicating that the microenvironment of TNP-ATP differs in ATP-BD and Na^+,K^+-ATPase ATP-binding domain. Therefore, one can utilize this protocol to estimate whether mutations in ATP-BD alter the surrounding environment of the nucleotide-binding site.

7. CONCLUSION

WNDP and MNKP represent a novel group of ion transporters with fascinating structural and functional properties. The first important steps in biochemical analysis of these proteins have been made and further studies will undoubtedly uncover new and exciting information about molecular mechanisms of copper distribution in human cells.

ACKNOWLEDGMENTS

The authors thank Joel Walker, Scott Vanderwerf, and Gloria Ellis for help with the manuscript preparation and Dr. Martina Ralle for helpful discussions. This work was supported by the National Institute of Health Grant DK-55719 (to SL).

REFERENCES

1. Pena M. M., Lee J., and Thiele D. J. (1999) A delicate balance: homeostatic control of copper uptake and distribution. *J. Nutr.* **129(7)**, 1251–1260.
2. Vulpe, C. D. and Packman, S. (1995) Cellular copper transport. *Annu. Rev. Nutr.* **15**, 293–322.
3. Waggoner, D. J., Bartnikas, T. B., and Gitlin, J. D. (1999) *Neurobiol. Dis.* **6**, 221–230.
4. Cox, D. W. (1999) Disorders of copper transport. *Br. Med. Bull.* **55(3)**, 544–555.
5. Danks, D. M. (1989) Disorders of copper transport, in *Metabolic Basis of Inherited Disease*, McGraw-Hill, New York, pp. 1411–1432.
6. Vulpe, C., Levinson, B., Whitney, S., et al. (1993) Isolation of a candidate gene for Menkes disease and evidence that it encodes a copper-transporting ATPase. *Nature Genet.* **3**, 7–13.
7. Chelly, J., Tumer, Z., Tonnesen, T., Petterson, A., Ishikawa-Brush, Y., Tommerup, N., et al. (1993) Isolation of a candidate gene for Menkes disease that encodes a potential heavy metal binding protein. *Nature Genet.* **3(1)**, 14–19.
8. Dierick, H. A., Ambrosini, L., Spencer, J., et al. (1995) Molecular structure of the Menkes disease gene (ATP7A). *Genomics* **28**, 462–469.
9. Tanzi, R. E., Petrukhin, K., Chernov, I., et al. (1993) The Wilson disease gene is a copper transporting ATPase with homology to the Menkes disease gene. *Nature Genet.* **5**, 344–350.
10. Bull, P. C., Thomas, G. R., Rommens, J. M., et al. (1993) The Wilson disease gene is a putative copper transporting P-type ATPase similar to the Menkes gene [published erratum appears in *Nature Genet.* 1994 Feb;**6(2)**:214]. *Nature Genet.* **5**, 327–337.
11. Yamaguchi, Y., Heiny, M. E., and Gitlin, J. D. (1993) Isolation and characterization of a human liver cDNA as a candidate gene for Wilson disease. *Biochem. Biophys. Res. Commun.* **197**, 271–277.
12. Scheinberg, L. H. and Sternlieb, I. (1984) Wilson's disease, in *Major Problems in Internal Medicine* (Smith, L. H., Jr., ed.) WB Saunders, Philadelphia.
13. Petrukhin, K., Lutsenko, S., Chernov, I., et al. (1994) Characterization of the Wilson disease gene encoding a P-type copper transporting ATPase: genomic organization, alternative splicing, and structure/function predictions. *Hum. Mol. Genet.* **3**, 1647–1656.
14. Thomas, G. R., Forbes, J. R., Roberts, E. A., et al. (1995) The Wilson disease gene: spectrum of mutations and their consequences [published erratum appears in *Nature Genet.* 1995 Apr;**9(4)**:451]. *Nature Genet.* **9**, 210–217.
15. Yamaguchi, Y., Heiny, M. E., Suzuki, M., and Gitlin, J. D. (1996) Biochemical characterization and intracellular localization of the Menkes disease protein. *Proc. Natl. Acad. Sci. USA* **93**, 14,030–14,035.
16. Hung, I. H., Suzuki, M., Yamaguchi, Y., et al. (1997) Biochemical characterization of the Wilson disease protein and functional expression in the yeast *Saccharomyces cerevisiae*. *J. Biol. Chem.* **272**, 21,461–21,466.
17. La Fontaine, S., Firth, S. D., Camakaris, J., Englezou, A., Theophilos, M. B., Petris, M. J., et al. (1998) Correction of the copper transport defect of Menkes patient fibroblasts by expression of the Menkes and Wilson ATPases. *J. Biol. Chem.* **273**, 1375–1380.
18. Kuo, Y. M., Gitschier, J., and Packman, S. (1997) Developmental expression of the mouse mottled and toxic milk genes suggests distinct functions for the Menkes and Wilson disease copper transporters. *Hum. Mol. Genet.* **6**, 1043–1049.
19. Voskoboinik, I., Brooks, H., Smith, S., et al. (1998) ATP-dependent copper transport by the Menkes protein in membrane vesicles isolated from cultured Chinese hamster ovary cells. *FEBS Lett.* **435**, 178–182.

20. Voskoboinik, I., Strausak, D., Greenough, M., Brooks, H., Petris, M., Smith, S., et al. (1999) Functional analysis of the N-terminal CXXC metal-binding motifs in the human menkes copper-transporting P-type ATPase expressed in cultured mammalian cells. *J. Biol. Chem.* **274(31)**, 22,008–22,012.
21. Carafoli, E. and Brini, M. (2000) Calcium pumps: structural basis for and mechanism of calcium transmembrane transport *Curr. Opin. Chem. Biol.* **4**, 152–161.
22. Andersen, J. P. and Vilsen, B. (1995) Structure-function relationships of cation translocation by Ca(2+)- and Na+, K(+)-ATPases studied by site-directed mutagenesis. *FEBS Lett.* **359**, 101–106.
23. Toyoshima, C., Nakasako, M., Nomura, H., and Ogawa, H. (2000) Crystal structure of the calcium pump of sarcoplasmic reticulum at 2.6 A resolution [see comments]. *Nature* **405**, 647–655.
24. Lutsenko, S. and Kaplan, J. H. (1995) Organization of P-type ATPases: significance of structural diversity. *Biochemistry* **34**, 15,607–15,613.
25. Solioz, M. and Vulpe, C. (1996) CPx-type ATPases: a class of P-type ATPases that pump heavy metals [see comments]. *Trends Biochem. Sci.* **21**, 237–241.
26. Axelson, K. B. and Palmgren, M. G. (1998) Evolution of substrate specificities in the P-type ATPase superfamily. *Mol. Evol.* **46**, 84–101.
27. Rae, T. D., Schmidt, P. J., Pufahl, R. A., et al. (1999) Undetectable intracellular free copper: the requirement of a copper chaperone for superoxide dismutase [see comments]. *Science* **284**, 805–808.
28. Petris, M. J., Mercer, J. F., Culvenor, J. G., et al. (1996) Ligand-regulated transport of the Menkes copper P-type ATPase efflux pump from the Golgi apparatus to the plasma membrane: a novel mechanism of regulated trafficking. *EMBO J.* **15**, 6084–6095.
29. Petris, M. J. and Mercer, J. F. (1999) The Menkes protein (ATP7A; MNK) cycles via the plasma membrane both in basal and elevated extracellular copper using a C-terminal di-leucine endocytic signal. *Hum. Mol. Genet.* **8**, 2107–2115.
30. Schaefer, M., Hopkins, R. G., Failla, M. L., and Gitlin, J. D. (1999) Hepatocyte-specific localization and copper-dependent trafficking of the Wilson's disease protein in the liver. *Am. J. Physiol.* **276**, G639–G646.
31. Roelofsen, H., Wolters, H., Van Luyn, M. J., et al. (2000) Copper-induced apical trafficking of ATP7B in polarized hepatoma cells provides a mechanism for biliary copper excretion [in process citation]. *Gastroenterology* **119**, 782–793.
32. Camakaris, J., Petris, M. J., Bailey, L., et al. (1995) Gene amplification of the Menkes (MNK; ATP7A) P-type ATPase gene of CHO cells is associated with copper resistance and enhanced copper efflux. *Hum. Mol. Genet.* **4**, 2117–2123
33. Davis-Kaplan, S. R., Askwith, C. C., Bengtzen, A. C., Radisky, D., and Kaplan, J. (1998) Chloride is an allosteric effector of copper assembly for the yeast multicopper oxidase Fet3p: an unexpected role for intracellular chloride channels *Proc. Natl. Acad. Sci. USA* **95**, 13,641–13,645.
34. Hung, I. H., Suzuki, M., Yamaguchi, Y., et al. (1997) Biochemical characterization of the Wilson disease protein and functional expression in the yeast *Saccharomyces cerevisiae*. *J. Biol. Chem.* **272**, 21,461–21,466.
35. Klomp, L. W., Lin, S. J., Yuan, D. S., et al. (1997) Identification and functional expression of HAH1, a novel human gene involved in copper homeostasis. *J. Biol. Chem.* **272**, 9221–9226.
36. Pufahl, R. A., Singer, C. P., Peariso, K. L., et al. (1997) Metal ion chaperone function of the soluble Cu(I) receptor Atx1 [see comments]. *Science* **278**, 853–856.
37. Clarke, D. M., Loo, T. W., Inesi, G., and MacLennan, D. H. (1989) Location of high affinity Ca2+-binding sites within the predicted transmembrane domain of the sarcoplasmic reticulum Ca2+-ATPase. *Nature* **339**, 476–478.
38. Lingrel, J. B., Croyle, M. L., Woo, A. L., and Arguello, J. M. (1998) Ligand binding sites of Na,K-ATPase. *Acta Physiol. Scand.* **643**, 69–77.
39. Asano, S., Tega, Y., Konishi, K., et al. (1996) Functional expression of gastric H+,K(+)-ATPase and site-directed mutagenesis of the putative cation binding site and catalytic center. *J. Biol. Chem.* **271**, 2740–2745.
40. Bamberg, K. and Sachs, G. (1994) Topological analysis of H+,K(+)-ATPase using in vitro translation. *J. Biol. Chem.* **269**, 16,909–16,919.
41. Lutsenko, S., Daoud, S., and Kaplan, J. H. (1997) Identification of two conformationally sensitive cysteine residues at the extracellular surface of the Na,K-ATPase alpha-subunit. *J. Biol. Chem.* **272**, 5249–5255.
42. Karlish, S. J., Goldshleger, R., and Stein, W. D. (1990) A 19-kDa C-terminal tryptic fragment of the alpha chain of Na/K-ATPase is essential for occlusion and transport of cations. *Proc. Natl. Acad. Sci. USA* **87**, 4566–4570.
43. Iida, M., Terada, K., Sambongi, Y., et al. (1998) Analysis of functional domains of Wilson disease protein (ATP7B) in *Saccharomyces cerevisiae*. *FEBS Lett.* **428**, 281–285.
44. Strausak, D., La Fontaine, S., Hill, J., et al. (1999) The role of GMXCXXC metal binding sites in the copper-induced redistribution of the Menkes protein. *J. Biol. Chem.* **274**, 11,170–11,177.
45. Forbes, J. R., Hsi, G., and Cox, D. W. (1999) Role of the copper-binding domain in the copper transport function of ATP7B, the P-type ATPase defective in Wilson disease. *J. Biol. Chem.* **274**, 12,408–12,413.
46. Gitschier, J., Moffat, B., Reilly, D., et al. (1998) Solution structure of the fourth metal-binding domain from the Menkes copper-transporting ATPase [see comments]. *Nat. Struct. Biol.* **5**, 47–54.
47. Steele, R. A. and Opella, S. J. (1997) Structures of the reduced and mercury-bound forms of MerP, the periplasmic protein from the bacterial mercury detoxification system. *Biochemistry* **36**, 6885–6895.
48. Lutsenko, S., Petrukhin, K., Cooper, M. J., et al. (1997) N-Terminal domains of human copper-transporting adenosine triphosphatases (the Wilson's and Menkes disease proteins) bind copper selectively in vivo and in vitro with stoichiometry of one copper per metal-binding repeat. *J. Biol. Chem.* **272**, 18,939–18,944.

49. DiDonato, M., Narindrasorasak, S., Forbes, J. R., et al. (1997) Expression, purification, and metal binding properties of the N-terminal domain from the wilson disease putative copper-transporting ATPase (ATP7B). *J. Biol. Chem.* **272**, 33,279–33,282.
50. Cobine, P. A., George, G. N., Winzor, D. J., et al. (2000) Stoichiometry of complex formation between copper(I) and the N-terminal domain of the Menkes protein. *Biochemistry* **39**, 6857–6863.
51. Jensen, P. Y., Bonander, N., Moller, L. B., and Farver, O. (1999) Cooperative binding of copper(I) to the metal binding domains in Menkes disease protein. *Biochim. Biophys. Acta* **1434**, 103–113.
52. Ralle, M., Cooper, M. J., Lutsenko, S., and Blackburn, N. J. (1998) X-ray absorption studies on the soluble N-terminal domain of the Menkes disease protein (N-MNK-P) with multiple copper site occupancy. Evidence for a two-coordinate copper-cysteinate coordination environment. *J. Am. Chem. Soc.* **120**, 13,525–13,526.
53. DiDonato, M., Hsu, H. F., Narindrasorasak, S., et al. (2000) Copper-induced conformational changes in the N-terminal domain of the Wilson disease copper-transporting ATPase. *Biochemistry* **39**, 1890–1896.
54. Harrison, M. D., Meier, S., and Dameron, C. T. (1999) Characterisation of copper-binding to the second sub-domain of the Menkes protein ATPase (MNKr2). *Biochim. Biophys. Acta* **1453**, 254–260.
55. Tsivkovskii, R., MacArthur, B. C., and Lutsenko, S. (2001) The K^{1010}-K^{1325} fragment of the Wilson's disease protein binds nucleotides and interacts with the N-terminal domain of this protein in a copper-dependent manner. *J. Biol. Chem.* **276**, 2234–2242.
56. Gatto, C., Wang, A. X., and Kaplan, J. H. (1998) The M4M5 cytoplasmic loop of the Na,K-ATPase, overexpressed in *E. coli*, binds nucleoside triphosphates with the same selectivity as the intact native protein. *J. Biol. Chem.* **273**, 10,578–10,585.
57. Capieaux, E., Rapin, C., Thines, D., et al. (1993) Overexpression in *Escherichia coli* and purification of an ATP-binding peptide from the yeast plasma membrane H(+)-ATPase. *J. Biol. Chem.* **268**, 21,895–21,900.
58. Moutin, M. J., Cuillel, M., Rapin, C., et al. (1994) Measurements of ATP binding on the large cytoplasmic loop of the sarcoplasmic reticulum Ca(2+)-ATPase overexpressed in *Escherichia coli*. *J. Biol. Chem.* **269**, 11,147–11,154.
59. Ogawa, H., Haga, T., and Toyoshima, C. (2000) Soluble P-type ATPase from an archaeon, *Methanococcus jannaschii*. *FEBS Lett.* **471**, 99–102.
60. Shah, A. B., Chernov, I., Zhang, H. T., et al. (1997) Identification and analysis of mutations in the Wilson disease gene (ATP7B): population frequencies, genotype-phenotype correlation, and functional analyses. *Am. J. Hum. Genet.* **61**, 317–328.
61. Thomas, G. R., Forbes, J. R., Roberts, E. A., et al. (1995) The Wilson disease gene: spectrum of mutations and their consequences [published erratum appears in *Nature Genet.* 1995 Apr;**9(4)**:451]. *Nature Genet.* **9**, 210–217.
62. Solioz, M., Odermatt, A., and Krapf, R. (1994) Copper pumping ATPases: common concepts in bacteria and man. *FEBS Lett.* **346**, 44–47.
63. Forbes, J. R. and Cox, D. W. (2000) Copper-dependent trafficking of wilson disease mutant ATP7B proteins [in process citation]. *Hum. Mol. Genet.* **9**, 1927–1935.
64. Goodyer, I. D., Jones, E. E., Monaco, A. P., and Francis, M. J. (1999) Characterization of the Menkes protein copper-binding domains and their role in copper-induced protein relocalization. *Hum. Mol. Genet.* **8**, 1473–1478.
65. Ambrosini, L. and Mercer, J. F. (1999) Defective copper-induced trafficking and localization of the Menkes protein in patients with mild and copper-treated classical Menkes disease. *Hum. Mol. Genet.* **8**, 1547–1555.
66. Yasukawa, T., Kanei-Ishii, C., Maekawa, T., et al. (1995) Increase of solubility of foreign proteins in *Escherichia coli* by coproduction of the bacterial thioredoxin. *J. Biol. Chem.* **270**, 25,328–25,331.
67. Brenner, A. J. and Harris, E. D. (1995) A quantitative test for copper using bicinchoninic acid [published erratum appears in *Anal. Biochem.* 1995 Sep 20;**230(2)**:360]. *Anal. Biochem.* **226**, 80–84.

3

Biologically Relevant Properties of Copper-Containing Proteins Analyzed by Means of Semiquantitative and Quantitative Theoretical Descriptors

Francesca De Rienzo, R. Razif Gabdoulline, Rebecca C. Wade, and M. Cristina Menziani

1. INTRODUCTION

1.1. Mutual Relation Between Molecular Structure and Functional Properties

Acquiring insights into the mechanisms governing biological activity and, in general, molecular recognition has important consequences because it can result in improved techniques for designing new drugs and engineering proteins with desired properties and functions in a specific environment.

Much effort has been directed toward the design of small molecules with potential drug properties. The most widespread approach to drug design relies on the search for meaningful qualitative (SAR) and quantitative (QSAR) structure–activity relationships within series of organic compounds *(1,2)*. Theoretical descriptors of the structural and electronic features of the series of molecules at hand are used to rationalize the biological activity or other biochemical or pharmacological properties observed in different biological contexts and to understand the mutual influence of structure and property.

Notwithstanding the overwhelming growth of information about protein function, provided by protein biochemistry and DNA cloning techniques, applications of QSAR techniques to peptides and proteins are less developed. Statistical models with good predictive ability have indeed been reported in the literature. They make use of amino acid scores derived from the application of principal-components analysis (PCA) to descriptor matrices of various amino acid properties such as empirical scales, three-dimensional (3D) descriptors, interaction properties descriptors, and so forth *(3)*. However, the descriptors utilized in all of these approaches are computed for isolated amino acids or for simplified model systems, and the physical interpretation of the correlations obtained is often difficult.

To our knowledge, very little attention has been devoted to date to the use of descriptors related to the 3D structure of proteins.

This work presents an analysis of the structural determinants of association and redox properties in biological systems assisted by advanced computational techniques. Several theoretical descriptors, originally developed to rationalize the reactivity determinants of small organic molecules, are used to produce quantitative and/or semiquantitative models, which can pinpoint the causes that deter-

From: Handbook of Copper Pharmacology and Toxicology
Edited by: E. J. Massaro © Humana Press Inc., Totowa, NJ

mine variations in molecular recognition and redox properties in protein systems. In particular, the attention is focused on those modifications of the protein structure that affect the functional properties of the protein itself. Development of theoretical models for the analysis of the thermodynamic and kinetic aspects of electron-transfer processes can, in addition, contribute to achieving detailed interpretations of experimental data and performing protein structure-based design.

1.2. The Blue Copper Proteins

The blue copper proteins are redox proteins containing at least one copper site *(4)*. Their name derives from the intense blue color characteristic of their oxidized [Cu(II)] state, which results from a strong visible absorption in the region of 600 nm. This, together with other distinctive physicochemical properties (i.e., a very small hyperfine coupling constant in the electron paramagnetic resonance (EPR) spectrum and a relatively high but variable redox potential), has fascinated chemists for many years. The "blue copper proteins" include different groups of protein with different structural features. Here, however, the focus will be on the small and soluble electron-carrier proteins with a single copper site, which are also referred to as "cupredoxins" or "type I copper proteins," because of the specific structural features of their Cu site.

The cupredoxins have been isolated from a variety of bacterial, algal, and plant sources, where they participate in biochemical processes important for the organism's life, by shuttling electrons from a protein acting as an electron donor to another acting as an electron acceptor *(4)*.

Many experimental data on this protein family are available from mutagenesis studies, kinetic analysis, and biochemical assays *(4–18)*. The most extensive studies have been performed on cupredoxins belonging to seven different subfamilies named plastocyanins, azurins, pseudoazurins, amicyanins, rustiyanins, basic proteins (BP), and stellacyanins. These proteins differ slightly in their spectroscopic, thermodynamic and structural properties *(4)* and in the role they play inside the hosting organisms *(19)*. High-resolution X-ray and nuclear magnetic resonance (NMR) structures are known for members of the plastocyanin, azurin, and pseudoazurin subfamilies and a few others are available for the amicyanin, rusticyanin, stellacyanin, and BP proteins (Table 1). In addition, two experimental structures of cupredoxins in complex with their redox partners are known: a crystal structure of the amicyanin from *Paracoccus denitrificans* bound to its electron donor, methylamine dehydrogenase (MADH), and the electron acceptor cytochrome c551i *(20)*, and an NMR-based structure of spinach plastocyanin interacting with its electron donor, cytochrome-f from turnip *(21,22)*. These two structures, together with all of the other experimental data, provide important information about the functional role and the binding properties of the cupredoxins, which have not yet been fully elucidated.

Analysis of the known 3D structures has shown that, in each cupredoxin, the polypeptide chain folds back on itself to give eight parallel or antiparallel β-strands arranged in a Greek key motif and constituting a single globular domain identified as a β-barrel or β-sandwich. However, features such as the relative positions of the strands, the length of loops, and the extent of hydrogen-bonding differentiate them *(4)*.

The copper-binding site is invariably located at one end of the β-barrel, the so-called "northern" end in the most popular viewing perspective of the plastocyanin proteins (Fig. 1). The copper occupies a cleft formed by the loops that also provide the ligand residues to the metal atom. In almost all of the cupredoxins, with a few exceptions, there are four copper ligands, a cysteine, two histidines, and a methionine, generally arranged to form a distorted tetrahedron *(4)*. The copper-site region is overall hydrophobic, as a result of the presence of nonpolar amino acids that surround the exposed edge of one histidine ligand. This is the only surface feature that appears to be common to all of the blue copper proteins and is, therefore, a clear requirement for an electron-transfer and redox-partner-binding site. This hypothesis is also supported by the two known structures of cupredoxin complexes. The rest of the surface varies considerably from one cupredoxin subfamily to another, thus other electron-transfer and redox-protein-binding sites are also likely to exist among the proteins. Indeed,

Table 1
Structural and Physiological Information About the Blue Copper Protein Subfamilies

		Structural information				Charge			
Subfamily	*Organism*	*Protein data bank pdb code*	*State*	*Resolution(Å)*	*Residue range*	*Ox*	*Red*	*Electron donor*	*Electron acceptor*
Plastocyanin	Seed plant: *Spinacia oleracea*	1ag6	Ox	1.70	1–99	–7	–8		
	Seed plant: *Petroselinum crispum*	1plb	Ox	*nmr*	1–97	–6	–7		
	Seed plant: *Populus nigra*	1pnd	Ox	1.60	1–99	–7			
		5pcy	Red	1.80	1–99		–8		
	Seed plant: *Phaseolus vulgaris*	9pcy	Red	*nmr*	1–99	–7	–8		
	Fern: *Dryopteris crassirhizoma*	1kdj	Ox	1.70	1–102	–5			
		lkdi	Red	1.80	1–102		–6		
	Green alga: *Ulva pertusa*	1iuz	Ox	1.60	1–100	–5	–6	Cyt f[a]	P700+ in PSI[a]
	Green alga: *Chlamydomonas reinhardtii*	2plt	Ox	1.50	1–100	–5	–6		
	Green alga: *Enteromorpha prolifera*	7pcy	Ox	1.80	1–100	–5	–6		
	Photosynthetic prokaryote: *Prochlorotrix hollandica*	1b3i	Ox	*nmr*	1–97	+3	+2		
	Cyanobacterium: *Phormidium laminosum*	1baw	Ox	2.80	1–105	–2	–3		
	Cyanobacterium: *Anabaena variabilis*	1nin	Ox	*nmr*	1–105	+2	+1		
	Cyanobacterium: *Synechocystis sp.*	1pcs	Ox	2.15	1–101	–1	–2		
Azurin	*Achromobacter xylosioxidans I*	1rkr	Ox	2.45	1–129	+3	+2		
	Achromobacter xylosioxidans II	1arn	Ox	2.60	1–129	+2	+1	Cyt c55l[b]	Nitrite reductase[b,c]
	Alcaligenes denitrificans	2aza	Ox	1.80	1–129	+1	0		
	Psuedomonas aeruginosa	4azu	Ox	1.90	1–128	0	–1		
	Psuedomonas fluorescens (*Biotype A*)	1joi	Ox	2.05	1–128	+1	0	or	
	Psuedomonas putida	1nwo	Ox	1.92	1–128	+2	+1	AADH[b]	or Cyt oxidase[b]
Pseudoazurin	*Alcaligenes faecalis*	8paz	Ox	1.60	1–123	+1		n.d.[d]	Cu-NIR (green)[e]
		3paz	Red	1.73	1–123		0		
	Achromobacter cycloclastes	1zia	Ox	1.54	1–124	+2		n.d.[d]	Cu-NIR (green)[e]
		1zib	Red	2.00	1–124		+1		
	Paracoccus denitrificans (*subsp. Thiosphaera pantotropha*)	1adw	Ox	2.50	1–123	–3	–4	n.d.[d]	Cyt cd1[e]
	Methylobacterium extorquens	1pmy	Ox	1.50	1–123	+3	+2	MADH[e] or Methanol	Cyt c-type[e] DH
Amicyanin	*Paracoccus denitrificans*	1aac	Ox	1.31	1–105	–1			Cyt c551I
		2rac	Red	1.30	1–105		–2	MADH	
	Paracoccus versutus	aminmr[f]		*nmr*	1–106	–2	–3		or Cyt c-type
Rusticyanin	*Thiobacillus ferrooxidans*	1rcy	Ox	1.90	4–155	+2		Cyt c552	Cyt Oxidase
		1a3z	Red	1.90	4–155		+1		
CBP	*Cucumis sativus*	2chp	Ox	1.80	1–96	+8	+7	n.d.[e]	n.d.[e]
Stellacyanin	*Cucumis sativus*	1jer	Ox	1.60	1–109	–2	–3	n.d.[e]	n.d.[e]

[a]cyt f and P700+ are redox partners for all the plastocyanins. Plastocyanins from bacteria are also able to bind cytochrome oxidase.
[B]When cytochrome c551 is the donor, a nitrite reductase is the acceptor, whereas cytochrome oxidase is the acceptor when AADH is the donor.
[c]Cu-NIR (blue) is the nitrite reductase interacting with azurins in *Achromobacter xylosoxidans*, whereas the heme-containing cytochrome cd1 binds to all the other azurins listed.
[d]Not determined.
[e]Pseudoazurins bind to Cu- and heme-containing NIRs and probably also to deaminases and c-type cytochromes in methylotrophic bacteria.
[f]This structure was kindly provided by Dr. M. Ubbink.

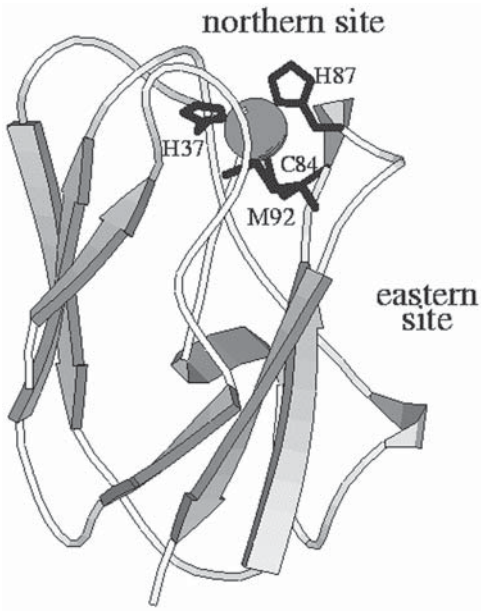

Fig. 1. Ribbon structure representation of a blue copper protein (spinach plastocyanin) showing the location of the Cu site, also known as the "northern" site, and the "eastern" site. The Cu atom and the side chains of the Cu-ligand residues are shown in sphere and stick representations, respectively.

experimental evidence shows that the type I copper proteins can participate in electron-transfer reactions with different redox proteins *(23)*.

The overall electron-transfer process between a cupredoxin and one of its partners can be written simply as follows:

$$A_{ox} + B_{red} \underset{k_{-2}}{\overset{k_2}{\leftrightarrow}} A_{red} + B_{ox} \tag{1}$$

where the cupredoxin can be either A or B, depending on its redox state and the protein with which it is interacting, and k_2 is the kinetic constant for the overall electron transfer reaction *(24)*. However, the molecular mechanism of this reaction is quite complex and the details have not yet been elucidated exhaustively. The overall process is commonly thought to consist of different successive steps: (1) the formation of the complex between the two redox partners, which is necessary to bring the proteins into contact, (2) the electron transfer itself, and (3) the dissociation of the complex after the redox reaction has taken place. These steps can be summarized as follows:

$$A_{ox} + B_{red} \underset{k_{off'}}{\overset{k_{on'}}{\leftrightarrow}} A_{red}/B_{ox} \underset{k_{-et}}{\overset{k_{et}}{\leftrightarrow}} A_{ox}/B_{red} \underset{k_{on''}}{\overset{k_{off''}}{\leftrightarrow}} A_{ox} + B_{red} \tag{2}$$

where $k_{on'}$ and $k_{off'}$ are the rate constants for the association process, k_{et} and k_{-et} are the rate constants for the direct and reverse electron-transfer reaction, respectively, and $k_{off''}$ and $k_{on''}$ are the rate constants for the complex dissociation reactions (which are not necessarily the same as $k_{off'}$ and $k_{on'}$).

Long-range molecular recognition properties and electrostatic effects are thought to play important roles in the association process that leads to complex formation and to the interaction of specific binding surfaces of the two proteins (thus affecting $k_{on'}$ and $k_{off'}$ values). Redox properties are, on the other hand, important for the real electron-transfer step and, therefore, affect the rate constants k_{et} and k_{-et}. Therefore, both the molecular recognition and redox properties of the cupredoxins influence the

kinetics of the overall electron-transfer reaction *(25)*. One of the most discussed issues is whether specificity of interaction of the blue copper proteins with their partners is a requirement for a high electron-transfer rate. This question acquires importance if it is considered that one electron-transfer protein is often able to interact with several different donor and acceptor proteins and, similarly, more than one species of redox protein may be able to mediate electron-transfer between two particular proteins *(23)*.

In this work, the structural features of the cupredoxins that appear to be the main determinants of molecular recognition and redox properties of the cupredoxins are highlighted and rationalized by means of theoretical descriptors of different complexity.

Two different approaches have been tested:

1. A similarity analysis, where descriptors determined from the protein 3D structures are used as indices of the binding features of proteins, in order to provide a classification of the blue copper protein subfamilies with respect to their recognition properties
2. A QSAR analysis, where descriptors are used to relate quantitatively variations in the kinetic rate constants, or thermodynamic properties crucial for function, of a particular cupredoxin species (namely the plastocyanin from spinach) to perturbation of the structure properties of the protein itself

These two approaches and their applications are drawn in Scheme 1.

2. SIMILARITY ANALYSIS OF THE BLUE COPPER PROTEIN SUBFAMILIES WITH RESPECT TO THEIR MOLECULAR INTERACTION PROPERTIES

The molecular requirements necessary for the blue copper proteins to interact with their redox partners are analyzed. As highlighted in Section 1.2., the blue copper proteins are divided into subfamilies depending on their physicochemical, biological, and functional properties. What has not yet been assessed about these proteins is whether and to what extent they bind specifically to their redox partners and whether cupredoxins belonging to different subfamilies can substitute one for the other in binding to the same partners *(23)*. Recognition of and interaction with a specific protein partner is commonly mediated by protein surface features, such as charge distribution. Therefore, comparison of the surface features of the different cupredoxins can be helpful in pinpointing the similarity and/or dissimilarity in their recognition properties and preferential binding mechanisms *(26–28)*. The properties considered are the molecular electrostatic potential, which is important in biomolecular recognition at medium- and long-range distances, and hydrophobic potential, which is involved in short-range recognition, docking, and electron transfer. The analysis of these interaction properties was performed for a representative set of different cupredoxins selected from the available experimentally-determined structures (*see* Table 1).

2.1. Sequence and Structure Analyses

The first step for comparing different proteins belonging to the same superfamily is the analysis their primary structure (i.e., the amino acid sequence).

Preliminary hints for the analysis of the protein sequences were given by the alignment of all the selected cupredoxin sequences. This alignment was obtained with the CLUSTALX program *(29)* and is reported in Fig. 2. It shows clearly that the most conserved region among the different protein subfamilies is the Cu site (i.e., the residues liganding to the Cu atom).

A structure-based pairwise sequence alignment was then performed by the program MODELLER *(30)*.

The alignment obtained for eight selected cupredoxins, which are representative of the different protein subfamilies studied, is reported in Fig. 3. The rational behind the use of structure-based sequence alignments rests in the fact that proteins belonging to different cupredoxin subfamilies often have very low sequence similarity (<20%) although they share the same fold and global archi-

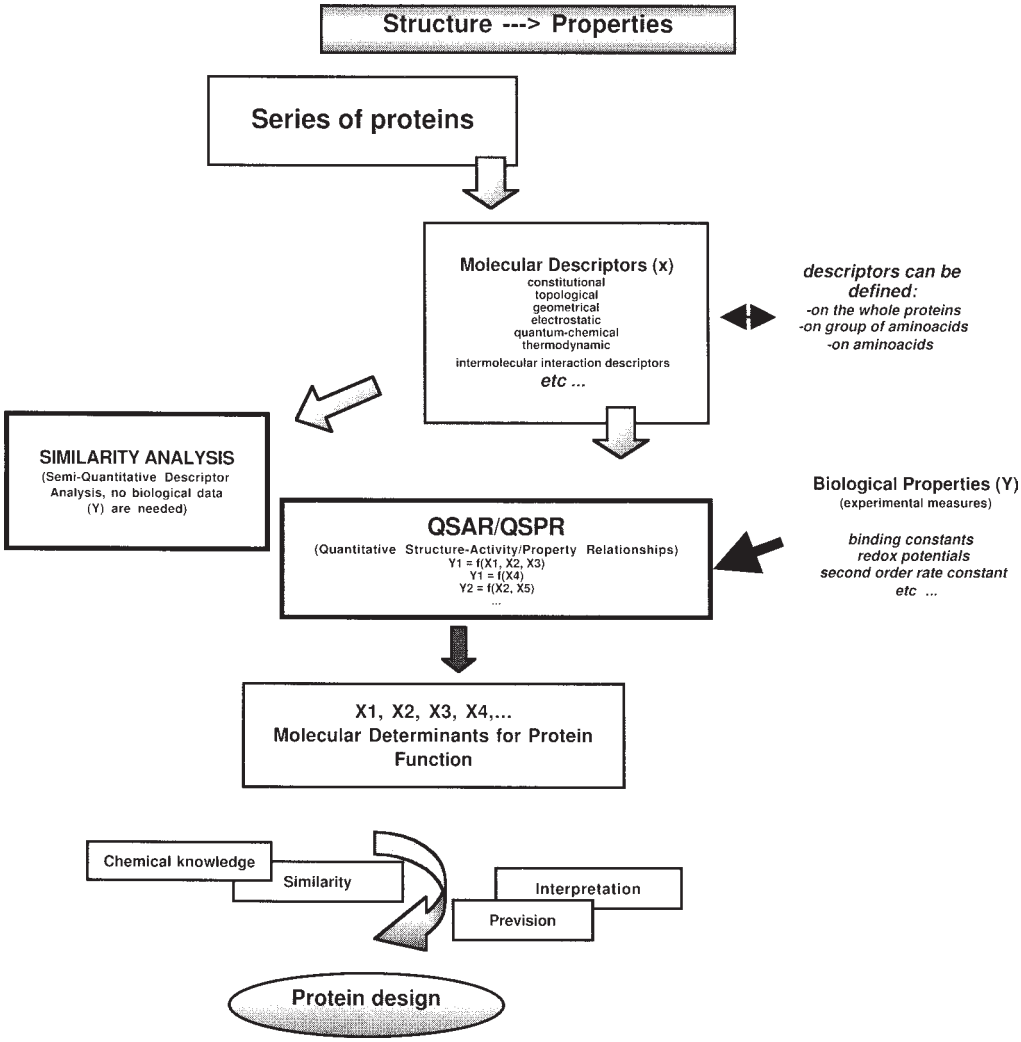
Structure ---> Properties
Series of proteins
Molecular Descriptors (x)
constitutional
topological
geometrical
electrostatic
quantum-chemical
thermodynamic
intermolecular interaction descriptors
etc ...
descriptors can be defined:
-on the whole proteins
-on group of aminoacids
-on aminoacids
SIMILARITY ANALYSIS
(Semi-Quantitative Descriptor Analysis, no biological data (Y) are needed)
QSAR/QSPR
(Quantitative Structure-Activity/Property Relationships)
Y1 = f(X1, X2, X3)
Y1 = f(X4)
Y2 = f(X2, X5)
...
Biological Properties (Y)
(experimental measures)
binding constants
redox potentials
second order rate constant
etc ...
X1, X2, X3, X4,...
Molecular Determinants for Protein Function
Chemical knowledge
Similarity
Interpretation
Prevision
Protein design

Scheme 1.

Fig. 2. Multiple sequence alignments of the blue copper proteins listed in Table 1. The asterisk points to the most conserved residues, which are the Cu ligands.

Fig. 3. Structure-based pairwise sequence alignment for eight proteins representative of the different blue copper protein subfamilies. Black underlining indicates residues found in β-strands, while boxes indicate residues found in α-helices.

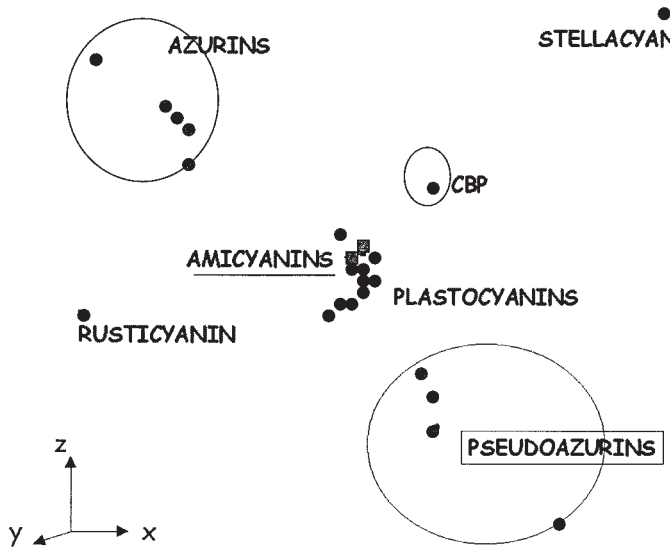

Fig. 4. Clusterization of the proteins listed in Table 1 in the sequence identity space. Each point represents a protein.

tecture. Therefore, the use of structural information is particularly relevant for the correct analysis of the differences that have arisen among these proteins during evolution.

Computed pairwise sequence identity percentages (reported in Table 2) as ID(a,b) were derived from the structure-based sequence alignments as follows:

$$\mathrm{ID(a,b)} = (n/N)100 \tag{3}$$

where n is the number of identical residues in the same alignment position of proteins a and b and N is the total number of aminoacids in the shortest of the two sequences compared.

ID(a, b) values were used as sequence similarity descriptors. A distance matrix, obtained by computing distances between any two proteins a and b [D(a,b)] in sequence space, as

$$D\mathrm{(a,b)} = \mathrm{sqrt}(1–\mathrm{ID(a,b)}/100) \tag{4}$$

was then used for a cluster analysis as described in detail in De Rienzo et al. *(19)*. The resulting distribution, shown in Fig. 4, clearly highlights how the different subfamilies are clustered in different regions of sequence space and how every member of a subfamily is closer to its own cluster than to any other one.

From the sequence analyses, we can state that all the plastocyanins (both eukaryotic and cyanobacterial) and the amicyanins belong to the same cluster, in agreement with previous spectroscopic studies results *(31)*. Azurins and pseudoazurins define two well-separated families and the same can also be hypothesized for rusticyanin, stellacyanin, and BCP, although only one structure is known for each of these protein families, at present.

2.2. *Protein Interaction Property Similarity Analysis (PIPSA)*

Many problems complicate the study of the interaction properties of cupredoxins. First, different surface properties can influence the recognition and diffusion of the proteins toward their partners at different stages of the binding process. For example, whereas hydrophobic properties are important for short-range docking interactions, electrostatics are a determinant for long-range recognition and protein steering. The extent to which these properties, in particular the electrostatic interactions, are

Table 2
Pairwise Structure-Based Sequence Identity Percentages [ID(a,b)] Computed for the Oxidized Form of the Proteins in Table 1

	1aac	*1adw*	*1ag6*	*1arn*	*1b3i*	*1baw*	*1iuz*	*1jer*	*1joi*	*1kdj*	*1nin*	*1nwo*	*1pcs*	*1plb*	*1pmy*	*1pnd*	*1rcy*	*1rkr*	*1zia*	*2aza*	*2cbp*	*2plt*	*4azu*	*7pcy*	*8paz*	*9pcy*	*aminmr*
1aac	100	22	25	14	28	30	17	9	13	17	29	18	32	25	19	20	9	16	29	13	14	27	15	21	25	24	54
1adw	22	100	29	1	33	28	24	14	9	19	24	9	34	30	46	24	4	0	67	7	16	27	2	24	59	29	21
1ag6	25	29	100	16	43	42	58	15	17	35	41	17	46	70	26	78	16	14	32	12	10	60	11	57	24	84	26
1arn	14	1	16	100	1	10	15	3	60	20	18	62	10	19	12	13	16	67	10	87	4	16	60	15	12	16	15
1b3i	28	33	43	1	100	49	41	16	15	32	49	17	45	40	23	39	24	15	34	19	16	45	0	39	28	42	28
1baw	30	28	42	10	49	100	41	11	8	29	57	16	60	44	25	42	10	20	30	13	8	50	11	42	26	41	29
1iuz	17	24	58	15	41	41	100	17	6	42	42	17	41	64	25	61	18	14	26	13	17	63	7	86	23	59	18
1jer	9	14	15	3	16	11	17	100	1	14	12	1	9	6	0	13	8	2	1	2	33	15	2	11	1	2	9
1joi	13	9	17	60	15	8	6	1	100	20	14	84	19	15	8	19	18	63	13	59	14	20	70	13	11	18	12
1kdj	17	19	35	20	32	29	42	14	20	100	32	20	34	36	16	36	16	20	22	21	11	35	25	44	23	35	18
1nin	29	24	41	18	49	57	42	12	14	32	100	16	55	44	26	44	20	14	29	17	14	51	13	42	23	43	27
1nwo	18	9	17	62	17	16	17	1	84	20	16	100	19	15	13	15	18	62	9	58	14	16	66	14	10	16	17
1pcs	32	34	46	10	45	60	41	9	19	34	55	19	100	49	26	44	20	16	30	19	10	52	15	41	23	45	34
1plb	25	30	70	19	40	44	64	6	15	36	44	15	49	100	24	65	19	15	34	18	10	60	10	63	26	73	24
1pmy	19	46	26	12	23	25	25	0	8	16	26	13	26	24	10	0 23	3	3	52	3	18	24	11	26	44	28	19
1pnd	20	24	78	13	39	42	61	13	19	36	44	15	44	65	23	100	15	14	25	12	9	62	14	57	22	79	22
1rcy	9	4	16	16	24	10	18	8	18	16	20	18	20	19	3	15	100	16	4	14	10	21	14	18	2	19	13
1rkr	16	0	14	67	15	20	14	2	63	20	14	62	16	15	3	14	16	10	0 13	69	10	11	73	6	11	17	16
1zia	29	67	32	10	34	30	26	1	13	22	29	9	30	34	52	25	4	13	100	1	15	32	12	26	67	31	22
2aza	13	7	12	87	19	13	13	2	59	21	17	58	19	18	3	12	14	69	1	100	10	16	62	14	11	15	15
2cbp	14	16	10	4	16	8	17	33	14	11	14	14	10	10	18	9	10	10	15	10	100	14	11	15	12	11	12
2plt	27	27	60	16	45	50	63	15	20	35	51	16	52	60	24	62	21	11	32	16	14	100	9	62	24	58	30
4azu	15	2	11	60	0	11	7	2	70	25	13	66	15	10	11	14	14	73	12	62	11	9	100	21	0	11	16
7pcy	21	24	57	15	39	42	86	11	13	44	42	14	41	63	26	57	18	6	26	14	15	62	21	100	26	57	19
8paz	25	59	24	12	28	26	23	1	11	23	23	10	23	26	44	22	2	11	67	11	12	24	0	26	100	26	19
9pcy[a]	24	29	84	16	42	41	59	2	18	35	43	16	45	73	28	79	19	17	31	15	11	58	11	57	26	100	24
aminmr	54	21	26	15	28	29	18	9	12	18	27	17	34	24	19	22	13	16	22	15	12	30	16	19	19	24	100

[a] Reduced form of *P. vulgaris* pc.

effective depends on environmental conditions, such as ionic strength and pH. A further complication is introduced by the functional features of the cupredoxins themselves. Because the cupredoxins are redox proteins, both their oxidized and reduced states need to be taken into account: Different interaction properties should, in fact, characterize the two redox states for the proteins to be able to interact with both the electron-donor and electron-acceptor protein partners.

All of these variables were carefully taken into account while computing the hydrophobic and the electrostatic potentials of the representative structures selected for the analysis. Thus, for example, the electrostatic potential was computed at two different values of the ionic strength, 0 m*M* and 150 m*M*, the physiological ionic strength of many biological systems, and this analysis was performed for both the reduced [Cu(I)] and oxidized [Cu(II)] states of the proteins.

A qualitative comparison of the computed interaction properties highlighted differences in these properties among different blue copper protein subfamilies. This observation becomes immediately clear from Fig. 5 (top), where the molecular electrostatic potentials (MEPs) are plotted for eight proteins representative of the different subfamilies. These plots show that whereas some proteins are actually characterized by similar monopolar or dipolar molecular electrostatic potential (MEP) distributions (such as CPB, plastocyanins, pseudoazurins and amicyanins), others present different, heterogeneous, distributions (azurins, stellacyanin, and rusticyanin).

The question is now how to translate these qualitative observations into a quantitative measure of the similarities and differences in distribution and magnitude of the protein molecular interaction fields (MIFs). This problem might appear fictitious, but it is not. When dealing with large-scale analysis of hundreds of proteins, a quantitative and automated method, is, in fact, necessary.

To solve this problem, the PIPSA (Protein Interaction Property Similarity Analysis) program, was developed *(19,28)*. PIPSA provides a useful method for automated pairwise comparison of the protein MIFs, using similarity indices as semiquantitative descriptors.

For this work, MEPs were computed by solving the linearised Poisson-Boltzmann equation as implemented in the UHBD program *(32)*. Hydrophobic potentials were computed with the GRID program (version 17, Molecular Discovery Ltd., Oxford, UK) (using a "dry" probe). Details of the calculations are given in ref. *19*.

Molecular interaction fields of any two proteins a and b, ϕa and ϕb, were then compared by means of the Hodgkin similarity index SI(a,b) *(33)*.

$$SI(a,b) = 2(Ma,Mb)/(Ma^2 + Mb^2) \tag{5}$$

with

$$(Ma, Mb) = \sum_{i,j,k} \phi a(i, j, k)\phi b(i, j, k) \tag{6}$$

where i, j, and k are the grid points where the potentials are compared.

This index was chosen for implementation in the PIPSA procedure among the other indices developed for small molecules *(34)* because it takes into account both the distribution and the magnitude of the compared molecular potentials.

In order to take into account the different range in which the electrostatic and hydrophobic interactions are effective, a region of interest for the comparison of the MIFs (called skin of the protein) was selected in relation to the type of MIF calculated. Therefore, MEPs were compared in a region extending from a 3 Å distance from the van der Waals surface of the proteins and having a thickness of 4 Å, while the interesting region for the hydrophobic properties was chosen to have the same thickness but to be 2 Å from the protein surface.

In addition, we were interested in analyzing those protein regions that are expected to be particularly relevant either for the association and interaction of the proteins with their partners or for electron transfer. Therefore, the comparison of protein MIFs was performed for particular regions of the surface: (1) the northern site, which is the putative region mediating electron transfer and redox partner binding for all the cupredoxins, (2) the eastern site, which is a highly acidic region in eukary-

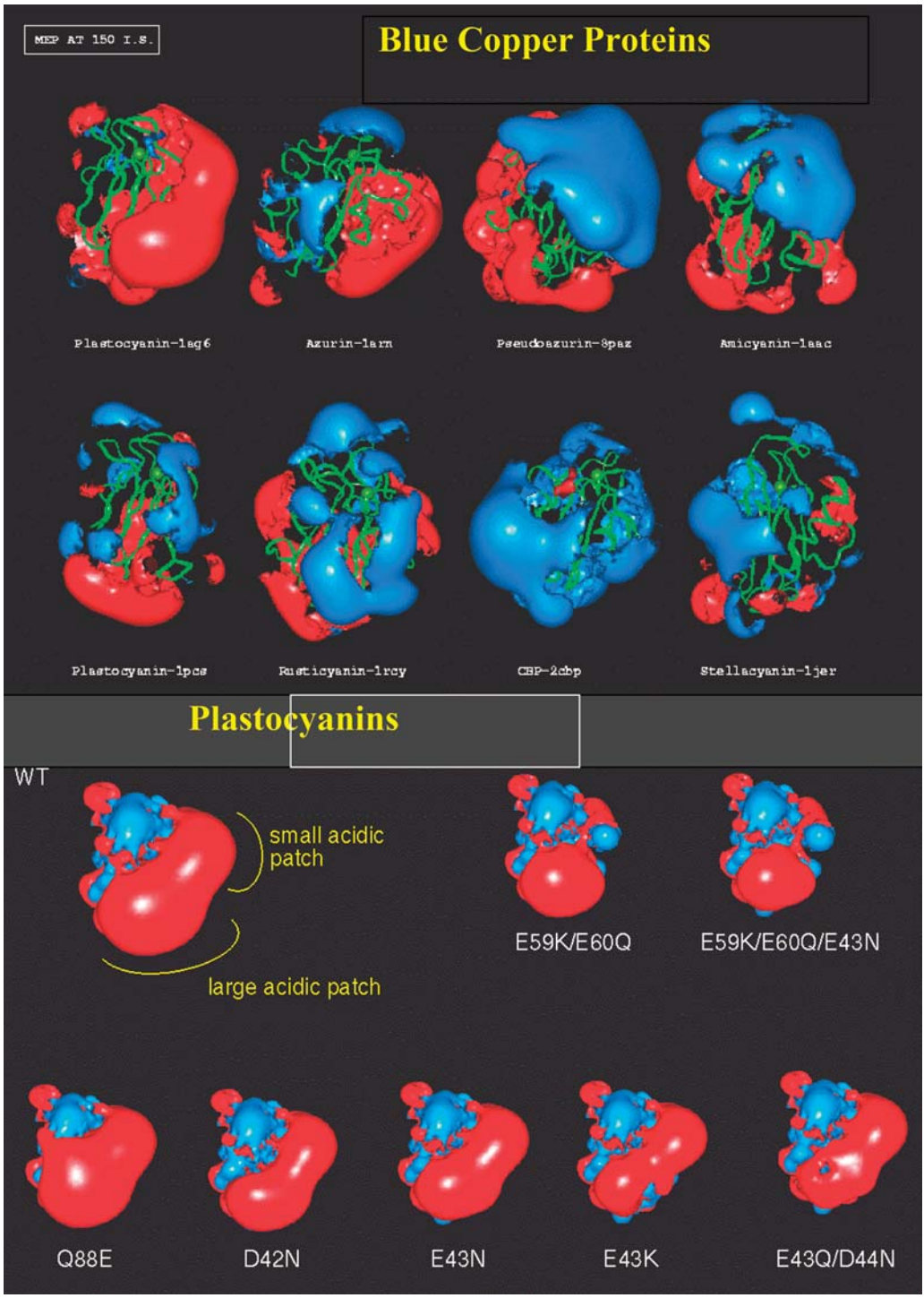

Fig. 5. Molecular electrostatic potentials for eight proteins representative of the different blue copper protein subfamilies (top) and for the wt plastocyanin and its mutants in the eastern site at 150 m*M* (bottom). Isopotential contours are at –0.5 (red) and +0.5 (blue) kcal/mol/*e* are displayed.

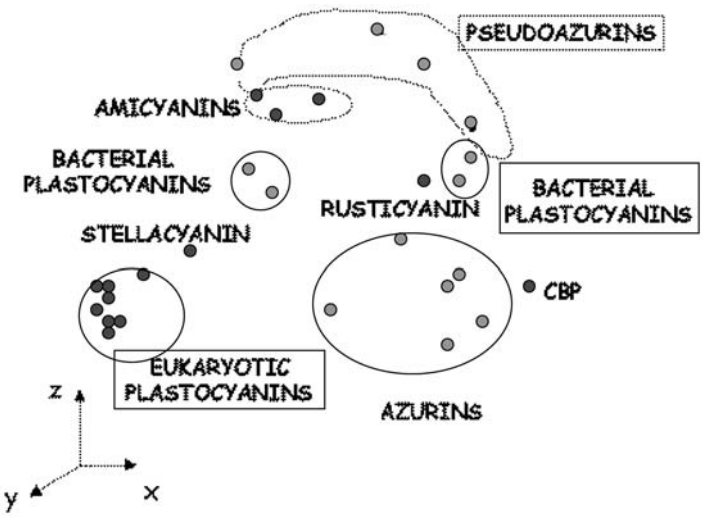

Fig. 6. Clusterization of the oxidized forms of the proteins listed in Table 1 in the MEP SI space. The picture is obtained by 3D projection of d(a,b) for MEPs computed at an ionic strength of 150 m*M*. Each point represents a protein.

otic plastocyanins and is probably important for protein binding, as indicated by the interaction of plastocyanin with cytochrome-f in the pc/cyt f complex structure *(21)*, and (3) the region at the interface between amicyanin and its partner MADH in the X-ray ternary complex determined by Chen et al. *(20)*. Investigation of the MIFs at these regions may reveal whether they are commonly involved in molecular recognition processes in the cupredoxin subfamilies.

2.3. Classification of the Descriptors

The different pairwise indices obtained for the MIFs were analyzed in a manner similar to the sequence identity indices. Distance matrices were computed from distances given by

$$d(a,b) = \mathrm{sqrt}(1-\mathrm{MIFSI}) \tag{7}$$

where MIFSI is either the molecular electrostatic potential similarity index (MEP SI) or the hydrophobic potential similarity index (HYD SI). d(a,b) can be considered as the distance between any two proteins a and b in the molecular interaction field similarity space. Cluster analyses were then performed with these derived descriptors.

Among the different MIF similarity descriptors obtained for the protein systems, MEP SIs computed at an ionic strength of 150 m*M* are collected in Table 3. These values are reported here by way of an example, as they proved to be particularly informative and revealing. A complete analysis of all the collected indices is described in De Rienzo et al. *(19)*. The results of the cluster analysis of the computed data in Table 3 are displayed in Fig. 6. This figure shows how the different proteins (in their oxidized state) cluster with respect to their molecular electrostatic properties. It is evident that the selected proteins cluster quite differently in MEP space (Fig. 6) and in sequence space (Fig. 4).

The correlations between the pairwise sequence identity percentages [ID(a,b)] and the pairwise MIF SI descriptors (both MEP SI and HYD SI) are shown in Fig. 7. From these plots, we can immediately see that HYD SIs can be approximately deduced from ID(a,b). That is to say, that hydrophobic properties seem to be strictly connected with sequence features. This might be the result of the fact that hydrophobic effects are effective at a closer distance to the protein surface than electrostatic effects. Nevertheless, analysis of the HYD SIs clearly showed the presence of a conserved hydropho-

Table 3
Molecular Electrostatic Potential Pairwise Similarity Index [SI(a,b)] Values Computed at 150 m*M* on the Whole Skin of the Oxidized Form of the Proteins in Table 1

	1aac	*1adw*	*1ag6*	*1arn*	*1b3i*	*1baw*	*1iuz*	*1jer*	*1joi*	*1kdj*	*1nin*	*1nwo*	*1pcs*	*1plb*	*1pmy*	*1pnd*	*1rcy*	*1rkr*	*1zia*	*2aza*	*2cbp*	*2plt*	*4azu*	*7pcy*	*8paz*	*9pcy*	*aminmr*
1aac	1	0.693	−0.057	0.077	0.636	0.542	−0.014	0.367	0.158	−0.207	0.509	0.116	0.564	−0.022	0.611	−0.136	0.301	0.374	0.811	0.115	−0.114	−0.186	0.264	−0.036	0.736	−0.2	0.531
1adw	0.693	1	0.051	−0.057	0.421	0.441	−0.02	0.219	0.221	0.039	0.313	0.11	0.395	0.051	0.55	−0.044	0.224	0.05	0.778	−0.059	−0.399	−0.18	−0.035	−0.048	0.853	−0.113	0.685
1ag6	−0.057	0.051	1	−0.062	−0.215	0.173	0.801	0.516	0.042	0.372	−.244	−0.107	0.245	0.876	−0.395	0.828	−0.087	−0.028	−0.219	0.001	−0.491	0.786	0.246	0.79	−0.212	0.877	−0.131
1arn	0.077	−0.057	−0.062	1	0.398	0.343	0.186	0.184	0.418	−0.142	0.448	0.466	0.318	−0.066	0.094	−0.171	0.321	0.592	−0.035	0.564	0.339	0.137	0.446	0.092	−0.086	−0.026	−0.057
1b3i	0.636	0.421	−0.215	0.398	1	0.447	−0.115	0.171	0.474	−0.385	0.616	0.353	0.45	−0.111	0.625	−0.183	0.565	0.502	0.59	0.18	0.037	−0.171	0.173	−0.075	0.499	−0.173	0.252
1baw	0.542	0.441	0.173	0.343	0.447	1	0.202	0.31	0.206	0.026	0.466	0.062	0.625	0.168	0.315	0.024	0.558	0.33	0.376	0.314	−0.332	0.004	0.364	0.053	0.374	0.001	0.35
1iuz	−0.014	−0.02	0.801	0.186	−0.115	0.202	1	0.642	0.25	0.316	0.017	0.152	0.11	0.799	−0.266	0.74	0.018	0.028	−0.198	0.085	−0.306	0.883	0.427	0.936	−0.291	0.734	−0.189
1jer	0.367	0.219	0.516	0.184	0.171	0.31	0.642	1	0.142	0.262	0.047	0.159	0.445	0.556	0.163	0.495	0.244	0.235	0.149	−0.097	−0.219	0.638	0.509	0.66	0.08	0.514	−0.056
1joi	0.158	0.221	0.042	0.418	0.474	0.206	0.25	0.142	1	0.053	0.325	0.684	0.124	0.132	0.292	0.033	−0.027	0.23	0.125	0.201	−0.009	0.171	0.277	0.247	0.27	0.093	0.245
1kdj	−0.207	0.039	0.372	−0.142	−0.385	0.026	0.316	0.262	0.053	1	−0.14	−0.021	−0.011	0.27	−0.136	0.175	−0.263	−0.201	−0.124	−0.076	−0.281	0.278	−0.033	0.213	−0.035	0.212	0.114
1nin	0.509	0.313	−0.244	0.448	0.616	0.466	0.017	0.047	0.325	−0.14	1	0.316	0.42	−0.225	0.445	−0.378	0.361	0.405	0.455	0.252	0.178	−0.155	0.256	−0.05	0.386	−0.332	0.386
1nwo	0.116	0.11	−0.107	0.466	0.353	0.062	0.152	0.159	0.684	−0.021	0.316	1	−0.023	−0.021	0.363	−0.136	0.084	0.243	0.158	0.169	0.306	0.089	0.28	0.114	0.191	−0.077	0.168
1pcs	0.564	0.395	0.245	0.318	0.45	0.625	0.11	0.445	0.124	−0.011	0.42	−0.023	1	0.174	0.246	−0.02	0.361	0.458	0.39	0.264	−0.189	0.037	0.454	0.104	0.308	0.046	0.274
1plb	−0.022	0.051	0.876	−0.066	−0.111	0.168	0.799	0.556	0.132	0.27	−.225	−0.021	0.174	1	−0.276	0.841	−0.056	0.053	−0.21	−0.007	−0.441	0.814	0.275	0.809	−0.198	0.85	−0.132
1pmy	0.611	0.55	−0.395	0.094	0.625	0.315	−0.266	0.163	0.292	−0.136	0.445	0.363	0.246	−0.276	1	−0.357	0.365	0.223	0.729	−0.097	0.099	−0.396	−0.092	−0.312	0.678	−0.463	0.511
1pnd	−0.136	−0.044	0.828	−0.171	−0.183	0.024	0.74	0.495	0.033	0.175	−.378	−0.136	−0.02	0.841	−0.357	1	−0.057	−0.132	−0.286	−0.008	−0.432	0.768	0.073	0.779	−0.269	0.904	−0.209
1rcy	0.301	0.224	−0.087	0.321	0.565	0.558	0.018	0.244	−0.027	−0.263	0.361	0.084	0.361	−0.056	0.365	−0.057	1	0.428	0.299	0.107	−0.113	−0.013	0.252	−0.023	0.241	−0.111	0.064
1rkr	0.374	0.05	−0.028	0.592	0.502	0.33	0.028	0.235	0.23	−0.201	0.405	0.243	0.458	0.053	0.223	−0.132	0.428	1	0.244	0.395	0.025	0.143	0.53	−0.02	0.062	−0.132	0.037
1zia	0.811	0.778	−0.219	−0.035	0.59	0.376	−0.198	0.149	0.125	−0.124	0.455	0.158	0.39	−0.21	0.729	−0.286	0.299	0.244	1	−0.044	−0.083	−0.372	−0.001	−0.234	0.87	−0.385	0.641
2aza	0.115	−0.059	0.001	0.564	0.18	0.314	0.085	−0.097	0.201	−0.076	0.252	0.169	0.264	−0.007	−0.097	−0.008	0.107	0.395	−0.044	1	0.124	−0.028	0.192	−0.005	−0.036	0.079	0.039
2cbp	−0.114	−0.399	−0.491	0.339	0.037	−0.332	−0.306	−0.219	−0.009	−0.281	0.178	0.306	−0.189	−0.441	0.099	−0.432	−0.113	0.025	−0.083	0.124	1	−0.349	0.102	−0.396	−0.171	−0.501	−0.255
2plt	−0.186	−0.18	0.786	0.137	−0.171	0.004	0.883	0.638	0.171	0.278	−.155	0.089	0.037	0.814	−0.396	0.768	−0.013	0.143	−0.372	−0.028	−0.349	1	0.41	0.902	−0.455	0.81	−0.23
4azu	0.264	−0.035	0.246	0.446	0.173	0.364	0.427	0.509	0.277	−0.033	0.256	0.28	0.454	0.275	−0.092	0.073	0.252	0.53	−0.001	0.192	0.102	0.41	1	0.317	−0.151	0.143	−0.041
7pcy	−0.036	−0.048	0.79	0.092	−0.075	0.053	0.936	0.66	0.247	0.213	−0.05	0.114	0.104	0.809	−0.312	0.779	−0.023	−0.02	−0.234	−0.005	−0.396	0.902	0.317	1	−0.33	0.812	−0.222
8paz	0.736	0.853	−0.212	−0.086	0.499	0.374	−0.291	0.08	0.27	−0.035	0.386	0.191	0.308	−0.198	0.678	−0.269	0.241	0.062	0.87	−0.036	−0.171	−0.455	−0.151	−0.33	1	−0.389	0.735
9pcy [a]	−0.2	−0.113	0.877	−0.026	−0.173	0.001	0.734	0.514	0.093	0.212	−.332	−0.077	0.046	0.85	−0.463	0.904	−0.111	−0.132	−0.385	0.079	−0.501	0.81	0.143	0.812	−0.389	1	−0.275
aminmr	0.531	0.685	−0.131	−0.057	0.252	0.35	−0.189	−0.056	0.245	0.114	0.386	0.168	0.274	−0.132	0.511	−0.209	0.064	0.037	0.641	0.039	−0.255	−0.23	−0.041	−0.222	0.735	−0.275	1

[a] Reduced form of the plastocyanin from *P. Vulgaris*.

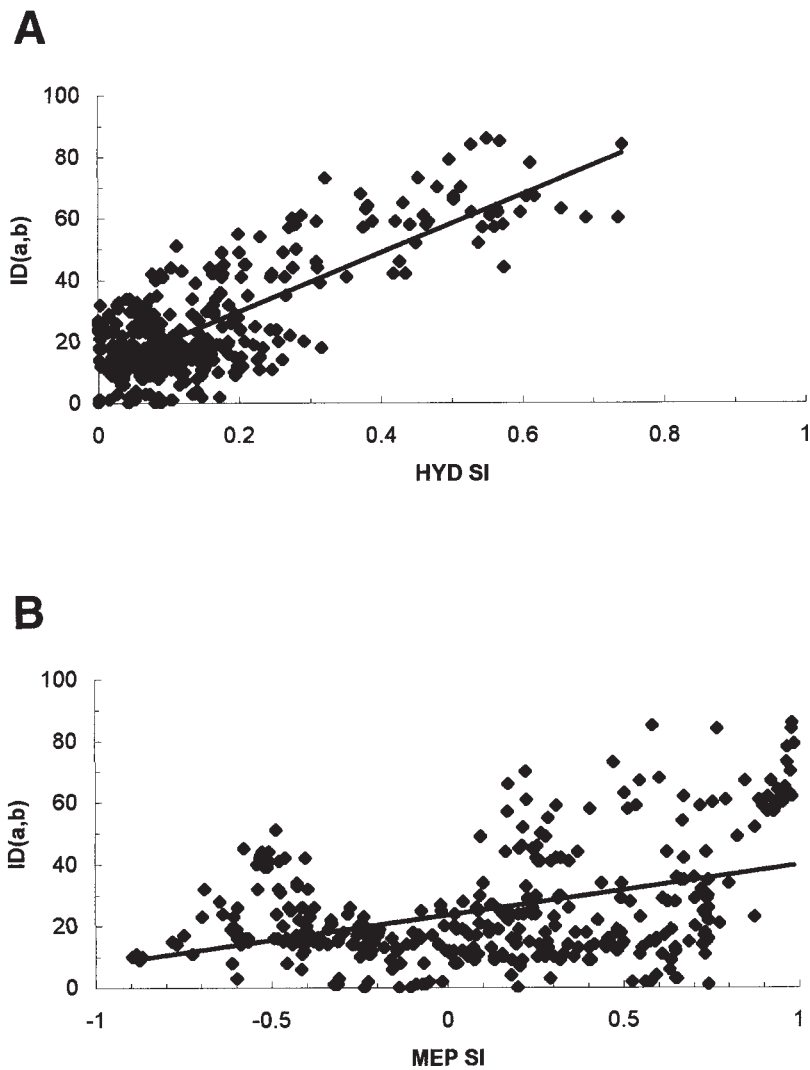

Fig. 7. **(A)** Comparison between the cupredoxin pairwise sequence identity percentages [ID(a,b)] and the hydrophobic potential similarity indices (HYD SI). The linear regression is $ID(a,b) = 94.93SI_{HYD} + 10.90$; $n = \sum_{i=1}^{26} i$; $r^2 = 0.61$; $r = 0.78$. **(B)** Comparison between the cupredoxin pairwise sequence identity percentages [ID(a,b)] and the electrostatic potential similarity indices (MEP SI). The linear regression is $ID(a,b) = 16.24SI_{MEP} + 23.58$; $n = \sum_{i=1}^{26} i$; $r^2 = 0.17$; $r = 0.41$.

bic patch in the Cu-site region, which is common to all of the cupredoxins (consistent with prior literature). Given the possible importance of hydrophobic features for the electron-transfer process, it might be suggested that all of the cupredoxins should show similarity in electron-transfer properties.

On the other hand, the analysis of MEPs proved to be more interesting and to provide additional information, complementary to that of sequence and structure analyses.

2.4. MIF Similarity Analysis Results

The results showed how the members of the subfamilies can be classified according to their recognition properties, providing clues for experiments to identify redox partners for some of the blue copper proteins.

A conserved hydrophobic region around the Cu site probably plays a functional role in all of the cupredoxins independently from their redox partners. Considering that the Cu is the redox center and is responsible for the transfer of the electrons, it is highly probable that the reason why the northern site is conserved is that it mediates electron transfer.

The other two regions analyzed, the eastern and the MADH/amicyanin site, do not appear to be recognition sites common to all the cupredoxins. The eastern site is probably important only for the plastocyanins, whereas the other is only for the amicyanins.

The low specificity of binding displayed by many of the blue copper proteins is also highlighted by analysis of MEPs. Briefly, the most noteworthy results are as follows:

1. Plastocyanins can be divided, according to their interaction properties, into three subclusters: the *eukaryotic plastocyanins* that have a highly negative potential becauseof two conserved acidic regions (res. 42–45 and 59–61) in the eastern site (Figs. 1 and 5 [top]); the *cyanobacterial plastocyanins* that, because of their less negative potential (Fig. 5 [top]) and the presence of a unique conserved patch of acidic amino acids (res. 59–61), seem to be more similar to azurins and pseudoazurins; and the *fern plastocyanin* that shows unique recognition features that are roughly intermediate between those of cyanobacterial and plant plastocyanins.
2. *Azurins* (from *A. xylosoxydans*) and *pseudoazurins* (from *A. cycloclastes* and *A. faecalis*), which interact with redox partners belonging to the same family (Cu-containing NIRs) in their reduced form *(8,35)*, show very similar interaction properties in the region around their Cu site. This supports the idea that the binding of these proteins to their partners involves their Cu sites.
3. *Amicyanins* cluster together with *pseudoazurins* in MIF similarity space (Fig. 6) rather than with plastocyanins as seen in sequence and structure classifications (Fig. 4). These findings provide new support to the hypothesis *(36)* that these two proteins (amicyanin and pseudoazurin) can operate as isofunctional proteins under particular environmental conditions.

Finally, it is important to stress that the experimental data available on the binding specificities and the redox partners of the cupredoxins, which are few and often controversial, often do not point to unequivocal functions for these proteins. Therefore, comparative analysis based on similarity indices is a useful aid to unraveling the experimental information, and explaining, on a structural basis, the complex behavior of the cupredoxins.

Automated and reliable techniques, such as the method presented here based on the use of descriptors, are particularly suited for large-scale analysis. This is becoming more and more important in the postgenomic era for structural and functional proteomics, because analyses and comparisons of hundreds of proteins (either structurally determined or modeled) will be required.

3. QUANTITATIVE ANALYSIS OF THERMODYNAMIC AND KINETIC PROPERTIES OF THE ELECTRON-TRANSFER PROCESS MEDIATED BY SPINACH PLASTOCYANIN

We now shift focus from the classification of the different cupredoxin subfamilies to the study of a particular blue copper protein, the plastocyanin from spinach. This protein is selected as it has been subjected to extensive experimental characterization; a similar computational analysis could be applied to other Cu proteins.

Plastocyanins consist of approx 100 amino acid residues *(4)*. They are found in the chloroplasts of higher plants, blue-green algae, and photosynthetic cyanobacteria, where they take part in the photosynthetic process by transporting electrons from the membrane-bound heme protein cytochrome-f (cyt f) to the chlorophyll-containing pigment P700 of Photosystem I (PSI).

Photosynthesis allows organisms to transform light energy into the chemical energy they need to survive, through a complex series of interrelated molecular processes and physicochemical reactions. Discovering the secrets of the photosynthetic process is an intriguing and important challenge for the

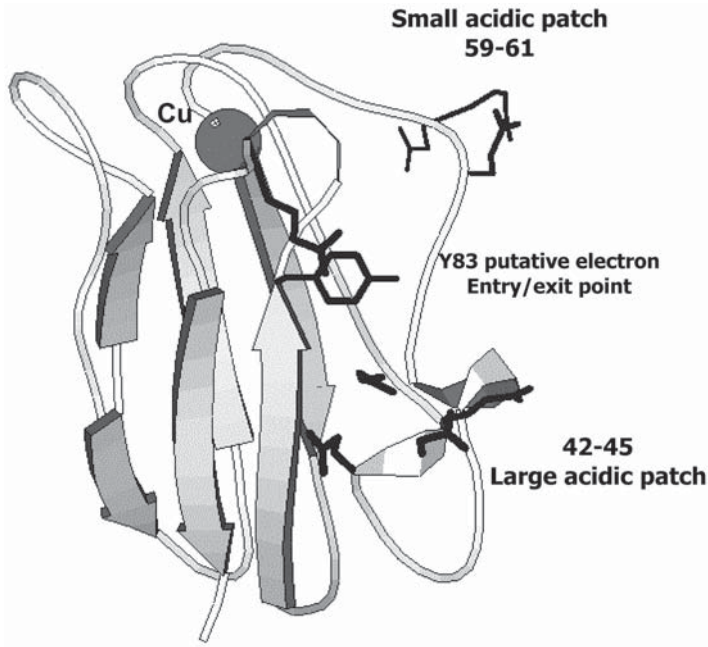

Fig. 8. Three-dimensional structure of spinach plastocyanin, the amino acids constituting the small and large acidic patch at the eastern site of the protein are highlighted.

research community, especially in view of the fact that it can provide virtually all of the energy for all living organisms on our planet to survive.

The plastocyanins are the best studied and structurally characterized cupredoxins. In addition, many experimental thermodynamic and kinetic studies have been performed on the overall electron-transfer reactions between plastocyanin and its electron donor, cytochrome-f. All of the data collected *(5,6,9,11,25)* indicate that the overall reaction between plastocyanin and cytochrome-f,

$$PC_{ox} + CYT_{red} \underset{k_{-2}}{\overset{k_2}{\leftrightarrow}} PC_{red} + CYT_{ox} \tag{8}$$

can be described, to a first approximation, as a three-step process:

$$PC_{ox} + CYT_{red} \underset{k_{off}}{\overset{k_{on}}{\leftrightarrow}} (PC_{ox}/CYT_{red})_a \underset{k_{der}}{\overset{k_{rearr}}{\leftrightarrow}} (PC_{ox}/CYT_{red})_b \underset{k_{ret}}{\overset{k_{et}}{\leftrightarrow}} (PC_{red}/CYT_{ox}) \underset{k'_{on}}{\overset{k'_{off}}{\leftrightarrow}} PC_{red} + CYT_{ox} \tag{9}$$

where k_{on} and k_{off} are respectively the on and off rate constants for association of the oxidized plastocyanin (PC_{ox}) and reduced cytochrome-f (CYT_{red}), which might be different from those (k'_{on} and k'_{off}) for dissociation of the PC_{red}/CYT_{ox} complex; k_{rearr} and k_{der} are the forward and reverse rate constants, respectively, for the rearrangement of the complex; and k_{et} and k_{ret} are the forward and reverse electron-transfer rate constants, respectively.

Two different regions on the plastocyanin surface are thought to be involved in different steps of the overall reaction: the so-called "eastern" site and "northern" site, which are highlighted in Fig. 1.

The eastern site is the large negatively charged surface area that is a distinctive feature of the higher plant plastocyanins and consists of two negatively charged patches (the "acidic patches") that surround the solvent-exposed Tyr83. The large acidic patch includes residues Asp42, Glu43, Asp44, and Glu45, and the small acidic patch includes residues Glu59, Glu60 and Asp61 (Figs. 1 and 8). Evidence

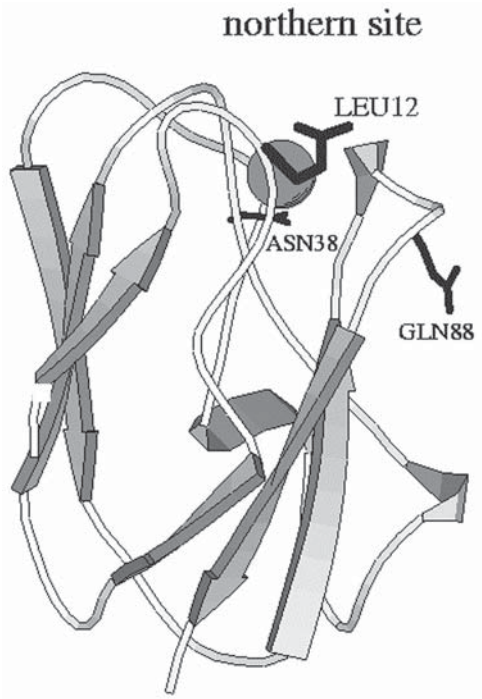

Fig. 9. Three-dimensional structure of spinach plastocyanin with the aminoacids mutated at the northern site highlighted.

has been found for this site to be involved in the association process of plastocyanin and cytochrome-f *(4)*. The hypothesis that the eukaryotic plastocyanin eastern site is likely to be necessary for recognition of the basic patch in cytochrome-f and assembling of an electrostatic complex is supported by the NMR-based structures of the spinach plastocyanin/turnip cytochrome-f complex *(21,22)*.

The northern site is the hydrophobic region that contains the Cu and is, as discussed previously, almost conserved in all of the cupredoxin subfamilies and therefore commonly thought to be involved in the electron-transfer process. The electron-transfer properties of plastocyanin are largely determined by its redox potential and thermodynamic parameters for the oxidation/reduction of Cu(I)/Cu(II). In fact, the reduction potential (E°) determines the ability of the redox protein to oxidize its electron-donor partner and reduce its electron-acceptor partner, therefore influencing the overall process of electron transfer mediated by the protein. Variations of the reduction potential and the thermodynamic properties of the copper center are interesting factors to be analyzed, especially in view of the fact that they depend, in addition to Cu-ligand interactions, on the charge distribution of the protein surface and on the electrostatic properties and ionic strength of the environment, which are all factors also influencing the recognition and association events prior to electron transfer (Eq. 9). For example, the perturbation of the surface charge distribution due to mutations can, on one hand, influence the ability of the protein to attract its partner, thus influencing their association, and, on the other hand, modify the hydrogen-bonding network to varying extents in the two redox states, thus promoting a selective stabilisation of one with respect to the other and affecting the redox properties.

Here, two different subsets of plastocyanin mutants, located in the northern and in the eastern site regions, are analyzed. For this study, the plastocyanin from spinach was chosen, because the structure of this plastocyanin variant is known both in its isolated form and in a complex with a cytochrome-f from turnip *(21,22,37)*. The aim is to investigate whether and to what extent it is possible to rationalize variations in kinetic properties and redox thermodynamic parameters observed experi-

mentally for the spinach plastocyanin on the basis of structural and electrostatic modifications of the protein. This is done by applying a QSPR/QSAR approach, where descriptors of different types were tested. The technique used allows the prediction of protein functionality and the design of new protein variants (in particular, mutant proteins) with desired activities.

3.1. QSPR Analysis: The Structural Molecular Determinants of the Spinach Plastocyanin Reduction Thermodynamics

A debated issue in biological redox chemistry is how the two oxidation states of the copper atom in cupredoxins [Cu(I)/Cu(II)] are stabilized by the protein matrix and the solvent and, consequently, which relationship can be established between the observed reduction potential ($E^{\circ\prime}$) and the protein structure/sequence features. Understanding the interconnection of these effects would allow, on one hand, the prediction of the functional properties of cupredoxin mutants and, on the other hand, the engineering of new proteins with desired redox activity and thermodynamic properties.

With this aim, it is particularly interesting to study the effects of point mutations altering the electrostatic potential in the region of the copper on the thermodynamics of Cu(II) reduction. The variation in the reduction enthalpy and entropy is analyzed by a QSPR approach, in order to derive quantitative models for the rationalization and interpretation of the observed behaviors *(38)*.

The functionally important residues Leu12 and Gln88 are replaced with charged and polar residues (L12E, L12K, L12H, L12Q, L12G, Q88E, and Q88K) and Asn38 is substituted with Asp (N38D). The location of these three residues is highlighted in Fig. 9. Both Leu12 and Gln88 are surface residues. The former contributes to the hydrophobic patch at the northern site of plastocyanin and seems to be involved in the interaction with photosystem I (PSI) *(39)*, whereas the latter protrudes through the acidic eastern site of the protein, which is involved in the interaction with cytochrome-f *(21)*. Although Asn38 does not contribute to the protein surface, it has been shown to occupy a strategic position for the stabilization of the architecture of the copper site *(40)*. In addition, both Gln88 and Asn38 are adjacent to a Cu-ligand histidine: His 87 and His37, respectively. Therefore, investigating whether mutations of these residues might alter the structure of the copper coordination region and, as a consequence, its functional properties would be a first step toward comprehension of the structural mechanisms that regulate the protein redox capabilities.

3.1.1. Selected Descriptors

The experimental data to be rationalized are obtained with cyclic voltammetry and relate to the Cu(II) to Cu(I) reduction thermodynamics of plastocyanin mutants *(38)*. The entropic ($\Delta S^{\circ\prime}$) and enthalpic ($\Delta H^{\circ\prime}$) contributions to the redox potential $E^{\circ\prime}$ are reported in Table 4, together with the values of the most representative computed descriptors. All descriptors are computed on the minimized molecular dynamics average structure of the proteins, as described in detail in ref. *38*. Among the many computed descriptor, the most interesting and explanatory descriptors are as follows:

1. D_z. The component of the dipole moment of the proteins along the *z* axis, which has its origin at the center of mass of the protein and points toward the copper site. This property was computed with the UHBD program *(32)*.
2. BIC. The bonding information content defined by Shannon information theory *(41)*. According to its definition, the BIC index encodes the branching ratio, unsaturation, and constitutional diversity of a molecule.
3. SI. The similarity index computed by comparing, in a pairwise fashion, the magnitude and the distributions of MEPs of the wt plastocyanin and its mutants. This comparison is performed in a restricted region close to the protein "northern" site.
4. DPSA. The difference in the charged partial surface areas of the proteins *(42)*, which are computed on the minimized average structures: DPSA = PPSA – PNSA, where PPSA is the partial positive [$(\sum(+SA_i)$] and PNSA is the partial negative [$\sum(-SA_i)$] surface area of the proteins. $+SA_i$ and $-SA_i$ are the surface area contributions of the ith positive and negative atom, respectively.

Table 4
Experimental Thermodynamic Parameters and Theoretical Molecular Descriptors Computed on the Minimized Average Structure of Plasocyanin and Its Mutants and Used for QSAR Modeling

	$E^{o\prime}$ (mV)	$\Delta H^{o\prime}_{rc}$ (kJ/mol)	$\Delta S^{o\prime}_{rc}$ (J/mol K)	D_Z (D)	BIC	SI	DPSA $(A)^2$	IE_{HB} (kcal/mol)
WT	411	–52	–41	28.00	85.06	1.000	6498.1	–2.23
L12E	394	–45	–23	–91.15	84.89	–0.170	6314.6	–2.19
L12K	424	–55	–49	36.85	86.51	0.270	6772.4	–5.61
Q88E	372	–47	–39	–44.54	84.42	—	6507.4	—
Q88K	392	–53	–50	28.82	86.09	—	6847.4	—
L12H	372	–48	–39	–54.19	85.40	0.160	6648.4	0.00
L12H (pH 6.2)	408	–55	–54	4.12	85.70	0.430	6795.4	–3.03
L12Q (pH 7.4)	372	–49	–45	–47.45	85.51	0.128	6691.6	0.00
L12G	398	–46	–28	–96.03	83.85	0.014	6440.6	–3.29
N38D	415	–54	–48	–124.93	84.42	—	6618.7	–3.86

5. IE_{HB} (kcal/mol). The hydrogen-bonding contribution of the mutated residue to the total energy of the protein. This index was computed using the CHARMM program *(43)* and setting a dielectric constant $\varepsilon = 4r$

The descriptors BIC and DPSA were computed by including in the calculations only the amino acids S11-F14, G34-V39, M57-L63, Y83, C84, S85–V93, and Cu100, which define the solvent accessible surface of the proteins in the region of the Cu site where the mutated residues L12, N38, and Q88 are located.

3.1.2. QSAR /QSPR Models

The results of the QSAR analyses performed are reported in Figs. 10 and 11. A meaningful descriptor is the *z* component of the protein dipole moment (D_z), which can explain the 86% of the variation in reduction enthalpy for the series of mutants considered (Fig. 10):

$$\Delta H^{\circ\prime}_{rc} = -0.0686\, D_z - 51.795,\ n = 9,\ R^2 = 0.858\ \ s^2 = 2.38 \quad (10)$$

omitted: N38D

where *n* is the number of compounds, *R* is the correlation coefficient, *s* is the standard deviation, and *F* is the value of the Fisher ratio. This correlation implies that if we introduce a positively charged residue in the region of the Cu site, the dipole moment vector (*D*) moves toward the copper site, so that its projection on the *z* axis (D_z) increases. In this case, the *z* axis coincides with the main axis of the cylinder-shaped protein, as clearly shown in Fig. 10.

Additional insights are provided by the BIC (Fig. 11A), which explains the salient structural features of the mutated protein (branching ratio, unsaturation degree, and constitutional diversity of the mutated residues) that are responsible for the interprotein nonspecific interactions established among nonpolar moieties. It can be deduced that an increased amount of dispersion interactions within the protein induces a stabilization of the reduced state (more negative $\Delta H^{\circ\prime}_{rc}$ values). Again, the variant N38D is an outlier:

$$\Delta H^{\circ\prime}_{rc} = -3.71\mathrm{BIC} + 266.318,\ n = 9,\ R^2 = 0.629,\ s^2 = 6.245 \quad (11)$$

which is related to the protein *s* ability.

The variation of the reduction entropy turns out to be connected with the charge redistribution at the northern site of the protein. In fact, $\Delta S^{\circ\prime}_{rc}$ correlates with the difference in partial positive and negative surface area of the proteins (DPSA), which is related to the protein$\prod\sigma$ ability to establish intermolecular hydrogen-bonding interactions (Fig. 11B):

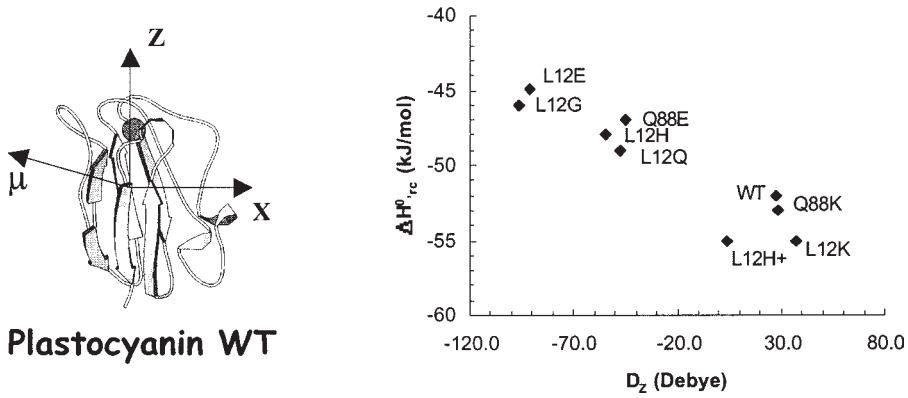

Fig. 10. Experimental $\Delta H°$ values versus D_z (the z component of the dipole moment). The linear regression obtained is $\Delta H° = -0.0686 D_z - 51.795$, $n = 9$, $R^2 = 0.858$, $s^2 = 2.38$, $F = 42.45$, omitted: N38D. The position and orientation of μ, the total dipole moment of the wild type plastocyanin, is shown with respect to the protein structure.

$$\Delta S°'_{rc} = -0.053\text{DPSA} - 309.18,\ n = 10,\ R^2 = 0.853,\ s^2 = 18.14 \quad (12)$$

More precisely, an increase in the negative surface area in the northern part of the protein (described by the PNSA component of DPSA) seems to be responsible for less negative $\Delta S°'_{rc}$ data values.

Less negative $\Delta S°'_{rc}$ are also the result of increasing dissimilarity between the mutants and the wild type in the Cu-site region, as indicated by the similarity index (SI). The SI computed around the Cu site describes 90% of the variation in $\Delta S°'_{rc}$ of the complete L12 series of mutants (Fig. 11C):

$$\Delta S°'_{rc} = -55.87\text{SI} - 31.92,\ n = 6,\ R^2 = 0.906,\ s^2 = 16.22 \quad (13)$$

Finally, the redox potential appears to be correlated with the hydrogen-bonding network established by the residue in position 12. This is shown in Fig. 11D, where $E°'$ is plotted vs IE_{HB}, the energy resulting from hydrogen-bonding interactions between residue 12 and the rest of the protein in each mutant. This residue is the mutated aminoacid closest to the Cu site and therefore its mutations are useful to test the influence on the reduction potential of different metal site rigidity resulting from different hydrogen-bonding networks.

$$E°' = -9.44\text{IE}_{HB} + 375.41,\ n = 8,\ R^2 = 0.864,\ s^2 = 59.26 \quad (14)$$

Q88 mutants are not included in this correlation because they are located too far away from the Cu-site to be effective.

On the contrary, the mutant N38D has been included because N38 plays an important role in the copper-site architecture. In this respect, it is interesting to stress that the observation that N38D is an outlier in almost all of the correlations (with the exception of that in Fig. 11D) is consistent with the experimental information available from the literature. In fact, experiments *(40)* show that the protein structure becomes unstable and often releases the copper atom when this mutation is introduced.

In summary, the correlations obtained proved to be informative on how electrostatic and solvation effects control the $E°'$ values of spinach plastocyanin through compensating variations of the reduction enthalpy and reduction entropy. The variation of the reduction enthalpy for the series of mutants considered is well explained on the basis of electrostatic considerations. Stabilization of the reduced state, which implies a more negative $\Delta H°'_{rc}$ value, is associated with increasing values of the component of the dipole moment along the z axis and with an increased

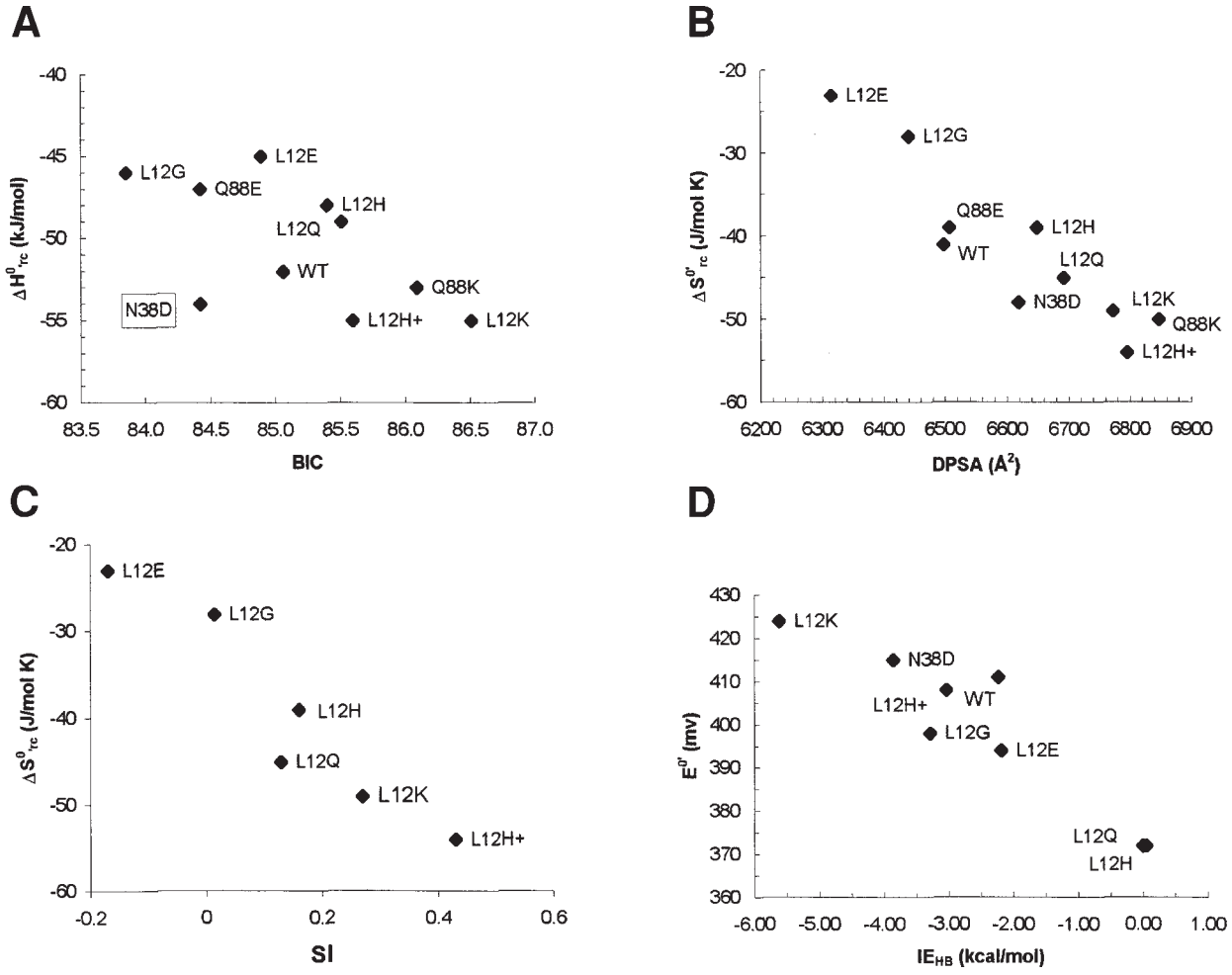

Fig. 11. Correlations between experimental thermodynamic parameters $\Delta H^{\circ'}_{rc}$ **(A)**, $\Delta S^{\circ'}_{rc}$ (**B** and **C**), $E^{\circ'}$ **(D)**, and protein structure descriptors.

amount of dispersion interactions within the protein. The variation in the reduction entropy resulting from mutations appears to be linked to the hydrogen-bonding donor/acceptor character of the northern part of the protein, above the metal site, and to the perturbation of the structure and the electrostatic potential distribution around the copper site with respect to the wild-type plastocyanin. These properties influence the reduction-induced reorganization of the water molecules on the protein surface in the same region.

3.2. QSAR Analysis: The Structural Molecular Determinants of the Spinach Plastocyanin/Cytochrome-f Association Kinetics

The main goal is to establish relationships between structural and kinetic parameters determined for the overall electron-transfer process between cytchrome-f and plastocyanin [Eq. (8)]. In particular, we will investigate the role of the negative patch on the eukaryotic plastocyanin eastern site in the recognition process, first step of Eq. (9), and, as a consequence, in the overall electron-transfer processes with cytochrome-f. The availability of experimental values of the overall kinetic constants k_2 [Eq. (8)], which were determined by Kannt et al. *(24)* for the in vitro electron-transfer reaction between wild-type and mutant spinach plastocyanins (D42N, E43N, E43K, E43Q/D44N, E59K/E60Q, E59K/E60Q/E43N, and Q88E) and the soluble part of turnip cytochrome-f, allows comparisons and QSAR analyses.

The relevance of the negative patch for the interaction between pc and cyt f is highlighted by the structure of the complex obtained from NMR data, which is shown in Fig. 12. The mutated residues in the eastern site (D42N, E43N, E43K, E43Q/D44N, E59K/E60Q, E59K/E60Q/E43N, and Q88E) are shown in Fig. 8. Residues D42, E43, and D44 are in the large acidic patch, whereas residues E59 and E60 are in the small acidic patch. Residue Q88 is not part of the acidic area, although it makes interactions with Y83, which lies almost in the middle of the eastern site and is thought to be a possible entry/exit point for electrons. Furthermore, as previously stated, Q88 is covalently bound to the Cu ligand H87.

The experimental data available from Kannt et al. *(24)* relative to mutations in the eastern site are collected in Table 5, together with the indices used for QSAR analysis.

3.2.1. Selected Descriptors

The X-ray structure deposited in the pdb (1ag6) was used for the QSAR analysis. The protein was mutated (D8G) to the spinach plastocyanin wt sequence (according to the SWISSPROT protein sequence database). Afterward, mutants (D42N, E43K, E43N, Q88E, E43Q/D44N, E59K/E60Q, E59K/E60Q/E43N) were produced by substituting the appropriate residues.

The molecular electrostatic potentials of the proteins were computed with the UHBD program *(32)* in a way similar to that described in Section 2.2. The Hodgkin similarity index [SI, Eq. (5)] *(33)*, computed between the molecular electrostatic potential of each mutant and the wt protein, and the derived index sqrt(2–2SI) were used as quantitative descriptors of the perturbation of the molecular electrostatic potential of wt plastocyanin caused by the introduction of mutations at the eastern site of the protein. The SI provides a measure of the similarity between the magnitudes and distributions of the molecular electrostatic potentials of the considered mutant and the wild type. The sqrt(2–2SI) index is instead a measure of the difference only in the magnitude of the MEPs of the two proteins compared, assuming that these MEPs are not highly different. This assumption is reasonable because only a few residues (either one, two, or three) are mutated at the same time.

Assuming that all the wild-type and mutant forms under study interact with cytochrome-f with overall similar features, the SI and sqrt(2-2SI) values relate to the electrostatic enhancement of association rates of pc mutants with cyt f. Therefore, these indices can be employed in QSAR analyses, in correlation with the experimental overall rate constants to estimate whether and to what extent mutations in the eastern acidic area influence the overall electron-transfer reaction by affecting the association step and/or the electron-transfer step (Eq. 9).

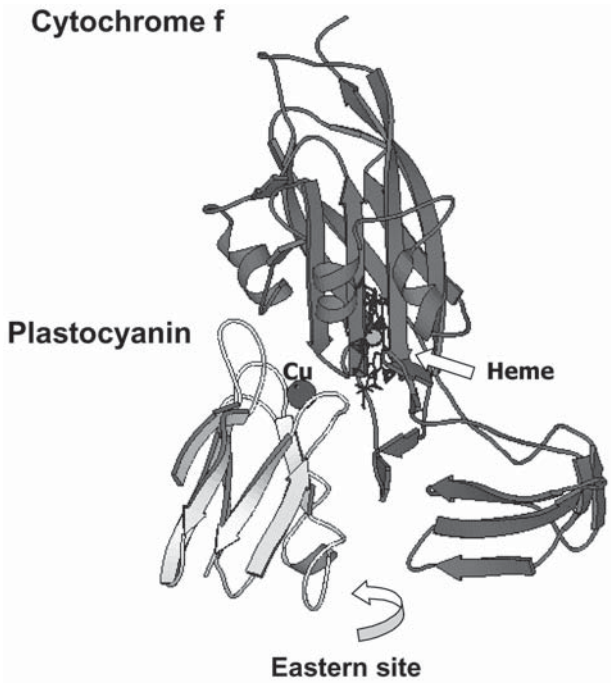

Fig. 12. NMR-based 3D structure of the spinach plastocyanin/turnip cytochrome-f complex *(21)*. The metal ion (which defines the Cu site or northern site) in the plastocyanin and the heme cofactor in the cytochrome-f structure are indicated. The eastern site in plastocyanin is also highlighted.

Table 5
Experimental k_2 Values for the Reaction of wt and Mutant Plastocyanins with Cytochrome-f *(25)* and $1n(k_2/k_{2\_WT})$ Values at pH 7.5 and 6.0; SI Values Computed by Comparing the MEPs of the Mutants Relative to the wt Plastocyanin on the Complete Skin [SI and sqrt(2–2SI)] and on the Protein Eastern Site [SIes and sqrt (2–2SIes)]

	$10^{-6}\,k_{2\_7.5}\,(M^{-1}s^{-1})$	$log(k_2/k_{2\_wt\_7.5})$	$10^{-6}k_{2\_6.0}\,(M^{-1}s^{-1})$	$log(k_2/k_{2\_wt\_6.0})$	*SI*	*sqrt(2–2SI)*	*SI–es*	*sqrt(2–2SI–es)*
WT	180(±20)	0.000	185(±20)	0.000	1.0000	0.000	1.000	0.000
Q88E	170(±20)	–0.062	220(±30)	0.173	0.9780	0.210	0.974	0.228
D42N	58.6(±4)	–1.121	76.5(±1.5)	–0.830	0.9780	0.210	0.973	0.232
E43N	40.0(±1.5)	–1.505	56.1(±1)	–1.193	0.9750	0.224	0.968	0.253
E43K	22.4(±0.8)	–2.087	29.3(±0.7)	–1.843	0.8850	0.480	0.854	0.540
E43QD44N	23.0(±0.8)	–2.056	26.9(±0.6)	–1.928	0.9020	0.443	0.873	0.504
E59KE60Q	12.2(±0.3)	–2.688	13.8(±0.2)	–2.596	0.7920	0.645	0.752	0.704
E59KE60QE43N	5.31(±0.01)	–3.523	5.56(±0.01)	–3.505	0.6570	0.828	0.576	0.921

3.2.2. MEP Analysis

Important differences in MEPs are found between the wild type and mutant plastocyanins and between different mutants, as shown in Fig. 5 (bottom). Perturbation of the eastern-site acidic MEP is particularly relevant when mutations are introduced in the small patch, such as in the case of the mutants E59K/E60Q and E59K/E60Q/E43N.

The extent to which the MEP of wild-type spinach plastocyanin is modified in the different mutant proteins has been quantified by the similarity indices SI and sqrt(2–2SI). The QSAR analyses performed using these indices proved to be useful for interpretation of the kinetic data available on structural and electrostatic bases.

The best correlations obtained are reported in Fig. 13:

$$\ln(k_{2\_WT\_pH7.5}/k_2) = -4.29\ \mathrm{sqrt}(2\text{-}2SI),\ n = 8,\ R^2 = 0.897,\ s^2 = 0.180 \quad (15)$$

and at pH = 6.0:

$$\ln(k_{2\_WT\_pH6.0}/k_2) = -4.41\ \mathrm{sqrt}(2\text{–}2SI) + 0.20,\ n = 8,\ R^2 = 0.902,\ s^2 = 0.179 \quad (16)$$

The same relative rates are plotted against values of sqrt(2–2SIes) computed between the wild-type and mutant plastocyanins on the eastern site at pH = 7.5:

$$\ln(k_{2\_WT\_pH7.5}/k_2) = -3.88\ \mathrm{sqrt}(2\text{–}2SIes) + 0.01,\ n = 8,\ R^2 = 0.903,\ s^2 = 0.169 \quad (17)$$

and at pH 6.0:

$$\ln(k_2/k_{2\_WT\_pH6.0}) = -3.99\ \mathrm{sqrt}(2\text{–}2SIes) + 0.22,\ n = 8,\ R^2 = 0.908,\ s^2 = 0.170 \quad (18)$$

The k_2 values highlight that the more the MEP of the wt protein is perturbed, the more the overall reaction with cyt f is hampered. This implies that the overall rate constants for the studied reaction of wild-type and mutant plastocyanins with cytochrome-f are mainly affected by modifications of the electrostatics at the eastern site. When one or more negatively charged residues in the plastocyanin eastern site are mutated into positively charged or polar residues, the electrostatic properties of the eastern face change, reducing its ability to attract the cytochrome-f basic patch and consequently influencing the overall reaction rate.

Furthermore, association rates between the two proteins computed by Brownian dynamics simulation also show a correlation with the experimental electron-transfer rates (data not published). This gives additional support to the suggestion that the descriptors used provide an estimate of the effects of mutations on electrostatically influenced protein–protein association rates and, as a consequence, of the electron-transfer rate.

However, the application of these SI descriptors is not general. In fact, mutants far from the binding site will affect the SI indices but will have little effect on association rate. This problem can be partially overcome by computing SIs over a region around the protein–protein interface in the bound complex.

As a whole, the regression models in Fig. 13 prove that computation of MEP SIs provides an efficient way to estimate approximately relative reaction rates when these are dominated by changes in the electrostatic potential of the mutated protein.

4. FINAL REMARKS

The most innovative aspect of the similarity analysis and the QSPR and QSAR approaches presented here is the result of the fact that theoretical descriptors are not computed on isolated amino acids or on very simple model systems but on the three-dimensional structures of the proteins of interest.

Comparative analysis of the 3D molecular interaction fields of a family of proteins by similiarity indices is a useful tool to gain insight into the recognition features of the proteins and into the changes caused by evolution. This method is particularly suited for large-scale analyses, which will become increasingly important in structural and functional genomics projects. For these, rapid automated and reliable techniques are required to perform comparisons of large numbers of experimentally determined and modeled protein structures.

In the study of spinach plastocyanin, in addition to global descriptors, local descriptors were derived by focusing on the northern part of the protein, where the Cu atom and its ligands are situated and where the electron transfer is likely to take place, and on the eastern site, where a large acidic area that is probably important for recognition is found.

The correlations obtained allow one to distinguish whether variation in functions and kinetics observed among the mutants are the result of structural modifications of the restricted area around the redox center and the acidic patch or to more extended perturbation involving the whole protein.

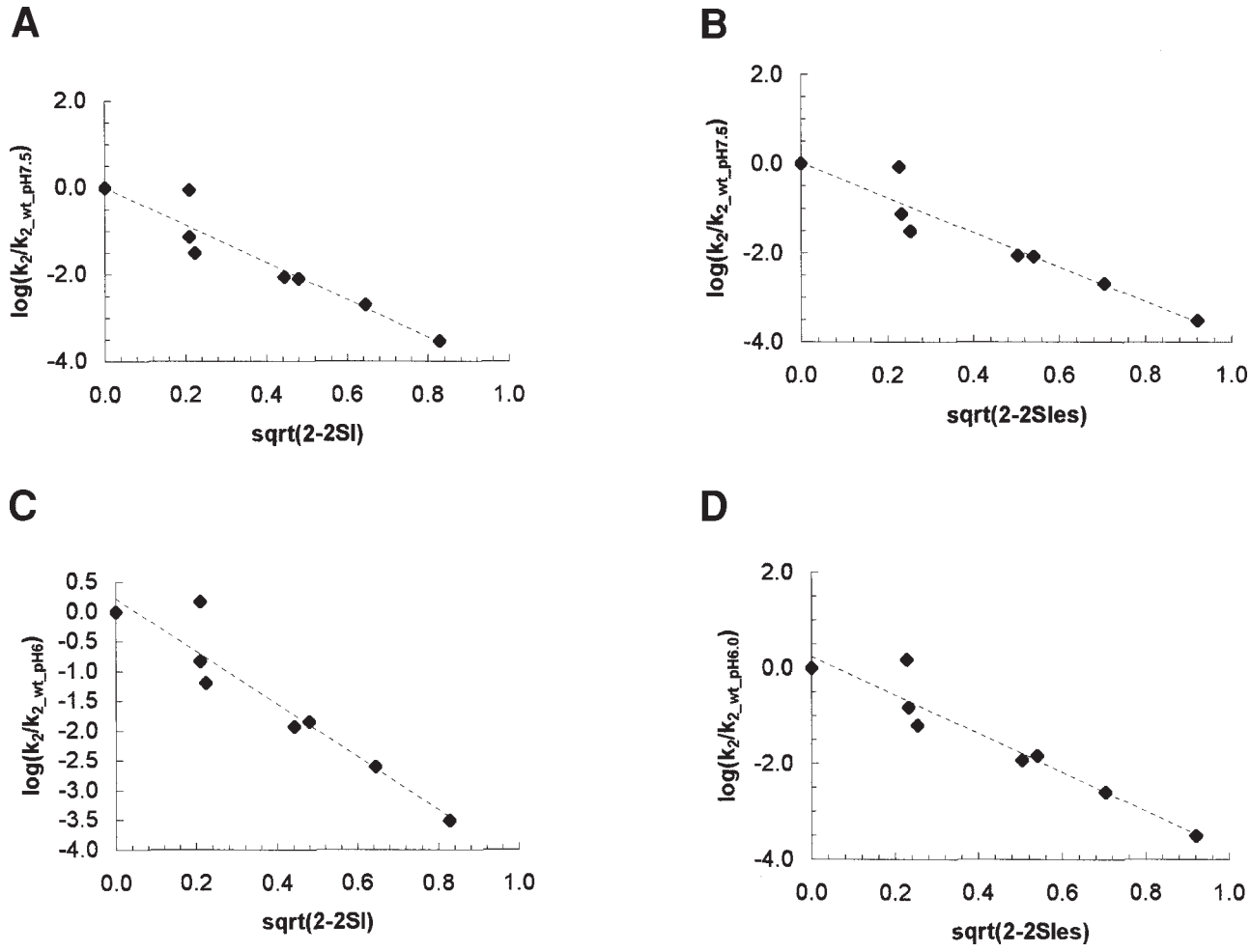

Fig. 13. The experimental k_2 values *(24)* measured at pH 7.5 and 6 for the mutants relative to the wt plastocyanin [$\ln(k_2/k_{2\_WT})$] are plotted against the electrostatic potential similarity index, expressed as sqrt(2–2SI) and computed by comparing the wild-type and mutant plastocyanins on the whole proteins (**A** and **B**) and on the eastern site (**C** and **D**).

Site-directed mutagenesis is a valuable techniques for assessing the importance of specific amino acid residues for protein activity. However, the results of these experiments are usually interpreted qualitatively or empirically.

The quantitative approach applied to plastocyanin has been shown to be helpful in providing a physical interpretation of the available experimental data and constitute a promising predictive tool for protein engineering.

REFERENCES

1. Livingstone, D. J. (2000) The characterization of chemical structures using molecular properties. A survey. *J. Chem. Inform. Comput. Sci.* **40**, 195–209.
2. Karelson, M., Lobanov, V. S., and Katritzky, A. R. (1996) Quantum-Chemical Descriptors in QSAR/QSPR. *Chem. Rev.* **96**, 1027–1043.
3. Sandberg, M., Eriksson, L., Jonsson, J., Sjostrom, M., and Wold, S. (1998) New chemical descriptors relevant for the design of biologically active peptides. A multivariate characterization of 87 amino acids *J. Med. Chem.* **41**, 2481–2491.
4. Baker, E. N. (1994) Copper proteins with type 1 sites, in *Encyclopedia of Inorganic Chemistry* (King, R. B., ed.), Wiley–Interscience, Chichester, p. 883, and references therein.
5. Gross, E. L., Curtiss, A., Durell, S. R., and White, D. (1990) Chemical modification of spinach plastocyanin using 4-chloro-3,5-dinitrobenzoic acid: characterization of four singly-modified forms. *Biochim. Biophys. Acta* **1016**, 107–114.
6. Hibino, T., Lee, B. H., Yajima, T., Odani, A., Yamauchi, O., and Takabe, T. (1996) Kinetic and cross-linking studies on the interactions of negative patch mutant plastocyanin from *Silene pratensis* with photosystem I complexes from cyanobacteria, green algae, and plants. *J. Biochem.* **120**, 556–563.
7. Kukimoto, M., Nishiyama, M., Ohnuki, T., Turicy S., Adman, E. T., Horinouchi, S., et al. (1995) Identification of interaction site of pseudoazurin with its redox partner, copper-containing nitrite reductase from *Alcaligenes faecalis* S-6. *Protein Eng.* **8**, 153–158.
8. Kukimoto, M., Nishiyama, M., Tanokura, M., Adman, E. T., and Horinouchi, S. (1996) Studies on protein-protein interaction between copper-containing nitrite reductase and pseudoazurin from *Alcaligenes faecalis* S6. *J. Biol. Chem.* **271**, 13,680–13,683.
9. Lee, B. H., Hibino, T., Takabe, T., Weisbeek, P. J., and Takabe, T. (1995) Site-directed mutagenesis study on the role of negative patches on *silene* plastocyanin in the interactions with cytochrome f and photosystem I. *J. Biochem.* **117**, 1209–1217.
10. Libeu, C. A. P., Kukimoto, M., Nishiyama, M., Horinouchi, S., and Adman, E. T. (1997) Site-directed mutants of pseudoazurin: explanation of increased redox potentials from X-ray structures and from calculation of redox potential differences. *Biochemistry* **36**, 13,160–13,179.
11. Qin, L. and Kostic, N. M. (1993) Importance of protein rearrangement in the electron-transfer reaction between the physiological partners cytochrome f and plastocyanin. *Biochemistry* **72**, 6073–6080.
12. Sigfridsson, K., Young S., and Hansson O. (1997) Electron transfer between spinach plastocyanin mutants and photosystem I. *Eur. J. Biochem.* **245**, 805–812.
13. Sykes, A. G. (1994) Active-site properties of the blue copper proteins. *Adv. Inorg. Chem.* **36**, 377–408.
14. Ubbink, M., Hunt, N. I., Hill, H. A., and Canters, G. W. (1994) Kinetics of the reduction of wild-type and mutant cytochrome c-550 by methylamine dehydrogenase and amicyanin from *Thiobacillus versutus*. *Eur. J. Biochem.* **222**, 561–571.
15. van de Kamp, M., Silvestrini, M. C., Brunori, M., Van Beeumen, J., Hali, F. C., and Canters, G. W. (1990) Involvement of the hydrophobic patch of azurin in the electron-transfer reactions with cytochrome c551 and nitrite reductase. *Eur. J. Biochem.* **194**, 109–118.
16. Van Pouderoyen, G., Mazumdar, S., Hunt, N. I., Hill, A. O., and Canters, G. W. (1994) The introduction of a negative charge into the hydrophobic patch of *Pseudomonas aeruginosa* azurin affects the electron self-exchange rate and the electrochemistry. *Eur. J. Biochem.* **222**, 583–588.
17. Yamanaka, T. and Fukumori, Y. (1995) Molecular aspects of the electron transfer system which participates in the oxidation of ferrous ion by *Thiobacillus ferrooxidans*. *FEMS Microbiol. Rev.* **17**, 401–413.
18. Young, S., Sigfridsson, K., Olesen, K., and Hansson, O. (1997) The involvement of the two acidic patches of spinach plastocyanin in the reaction with photosystem I. *Biochim. Biophys. Acta* **1322**, 106–114.
19. De Rienzo, F., Gabdoulline, R. R, Menziani, M. C., and Wade, R. C. (2000) Blue copper proteins: a comparative analysis of their molecular interaction properties. *Protein Sci.* **9**, 1439–1454.
20. Chen, L., Durley, R. C. E., Mathews, F. S., and Davidson, V. L. (1994) Structure of an electron transfer complex: methylamine dehydrogenase, amicyanin and cytochrome c551i. *Science* **264**, 86–90.
21. Ubbink, M., Ejdebaeck, M., Karlsson, B. G., and Bendall, D. S. (1998) The structure of the complex of plastocyanin and cytochrome f, determined by paramagnetic NMR and restrained rigid-body molecular dynamics. *Structure* **6**, 323–335.
22. Ejdeback, M., Bergkvist, A., Karlsson, B. G., and Ubbink, M. (2000) Side-chain interactions in the plastocyanin-cytochrome f complex. *Biochemistry* **39**, 5022–5027.

23. Williams, P. A., Fuelop, V., Leung, Y.-C., Chan, C., Moir, J. B. W., Howlett, G., et al. (1995) Pseudospecific docking surfaces on electron transfer proteins as illustrated by pseudoazurin, cytochrome c550 and cytochrome cd1 nitrite reductase. *Nat. Struct. Biol.* **2**, 975–982.
24. Kannt, A., Young, S., and Bendall, D. S. (1996) The role of acidic residues of plastocyanin in its interaction with cytochrome f. *Biochim. Biophys. Acta* **1277**, 115–126.
25. Hope, A. B. (2000) Electron transfer amongst cytochrome f, plastocyanin and photosystem I: kinetics and mechanisms. *Biochim. Biophys. Acta* **1456**, 5–26.
26. Demchuk, E., Mueller, T., Oschkinat, H., Sebald, W., and Wade, R. C. (1994) Receptor binding properties of four-helix-bundle growth factors deduced from electrostatic analysis. *Protein Sci.* **3**, 920–935.
27. Wade, R. C., Gabdoulline, R. R., Luedemann, S. K., and Lounnas, V. (1998) Electrostatic steering and ionic tethering in enzyme-ligand binding: insights from simulations. *Proc. Natl. Acad. Sci. USA* **95**, 5942–5949.
28. Blomberg, N., Gabdoulline, R. R., Nilges, M., and Wade, R. C. (1999) Classification of protein sequences by homology modeling and quantitative analysis of electrostatic similarity. *Proteins* **37**, 379–387.
29. Jeanmougin, F., Thompson, J. D., Gouy, M., Higgins, D. G., and Gibson, T. J. (1998) Multiple sequence alignment with ClustalX. *Trends Biochem. Sci.* **23**, 403–405.
30. Sali, A. and Blundell, T. L. (1993) Comparative protein modeling by satisfaction of spatial restraints. *J. Mol. Biol.* **234**, 779–815.
31. Adman, E. T. (1991) Copper protein structures. *Adv. Protein Chem.* 42, 145–197.
32. Madura, J. D., Briggs, J. M., Wade, R. C., Davis, R., Luty, B. A., Ilin, A., et al. (1995) Electrostatic and diffusion of molecules in solution: simulation with the University of Huston Brownian dynamics program. *Compar. Phys. Commun.* **91**, 57–95.
33. Hodgkin, E. E. and Richards, W. G. (1987) Molecular similarity based on electrostatic potential and electric field. *Int. J. Quant. Chem. Quant. Biol. Symp.* **14**, 105–110.
34. Carbo, R., Leyda, L., and Arnau, M. (1980) An electron density measure of the similarity between two compounds. *Int. J. Quant. Chem.* **17**, 1185–1189.
35. Dodd, F. E., Hasnain, S. S., Hunter, W. N., Abraham, Z. H. L., Debenham, M., Kanzler, H., et al. (1995) Evidence for two distinct azurins in *Alcaligenes xylosoxidans* (NCIMB 11015): potential electron donors to nitrite reductase. *Biochemistry* **34**, 10,180–10,186.
36. Inoue, T., Kay, Y., Harada, S., Kasai, N., and Oshiro, Y. (1994) Refined crystal structure of pseudoazurin from *Methylobacterium extorquens* AM1 at 1.5 A resolution. *Acta Crystallogr.* **D50**, 317–328.
37. Xue, Y., Okvist, M., and Young, S. (1998) Crystal structure of spinach plastocyanin at 1.7 A resolution. *Protein Sci.* **7**, 2099–2150.
38. Battistuzzi, G., Borsari, M., Loschi, L., Menziani, M. C., De Rienzo, F., and Sola, M. (2001) Control of metalloprotein redox potentials: the role of electrostatic and solvation effects probed on plastocyanin mutants. *Biochemistry* **40**, 6422–6430.
39. Sigfridsson, K., Young, S., and Hansson, O. (1996) Structural dynamics in the plastocyanin–photosystem 1 electron-transfer complex as revealed by mutant studies. *Biochemistry* **35**, 1249–1257.
40. Dong, S., Ybe, J. A., Hecht, M. H., and Spiro, T. G. (1999) H-bonding maintains the active site of type 1 copper proteins: site-directed mutagenesis of Asn38 in poplar plastocyanin. *Biochemistry* **38**, 3379–3385.
41. Kier, L. B. (1980) Molecular structure influencing either a sweet or bitter taste among aldoximes. *J. Pharm. Sci.* **69**, 807–811, and references therein.
42. Stanton, D. T. and Jurs, P. C. (1990) Development and use of charged partial surface area structural descriptors in computer-assisted quantitative structure-property relationship studies. *Anal. Chem.* **62**, 2323–2329.
43. Brooks, B. R., Bruccoleri, R. E., Olafson, B. D., States, D. J., Swaminathan, S., and Karplus, M. (1983) CHARMM: a program for macromolecular energy, minimization and dynamics calculations. *J. Comput. Chem.* **4**, 187–217.

4

Molecular Modeling and Dynamics of Copper Proteins

Mattia Falconi and Alessandro Desideri

1. INTRODUCTION

1.1. The Importance of Copper Proteins

For many decades, it has been widely accepted that copper is an essential trace element required for survival by all organisms from bacterial cells to humans *(1)*. What is so special about this trace element that makes it essential in biology? Copper ions undergo unique chemistry because of their ability to adopt distinct redox states, either oxidized, Cu(II), or reduced, Cu(I). Consequently, Cu ions serve as important catalytic cofactors in redox chemistry for proteins that carry out fundamental biological functions required for growth and development (Table 1). Copper proteins show a variety of functions (Table 2) and can be classified by the kind and number of prosthetic centers (Table 3) and/or by the Cu center type found in the protein structure (Table 4). Copper-requiring proteins are involved in a variety of biological processes, and metal deficiency in these enzymes, or alteration in its activity, often causes disease states or pathophysiological conditions. Although it is clear that Cu is essential, it is also a potent cytotoxic agent when allowed to accumulate in excess with respect to cellular needs. In fact, because of its special redox chemistry, copper readily participates in reactions that result in the production of highly reactive oxygen species (ROS), including hydroxyl radicals *(2)*. Hydroxyl radicals are believed to be responsible for devastating cellular damage that includes lipid peroxidation in membranes, direct oxidation of proteins, and cleavage of DNA and RNA molecules. Indeed, the generation and action of ROS are thought to be major contributing factors to the development of cancer, disease of the nervous system, and aging *(3)*. In addition to the generation of ROS, Cu may manifest its toxicity by displacing other metals cofactors from their natural ligands in key cellular signaling proteins. It is highly likely that Cu is able to displace metal ions in a number of catalytic or structural motifs in many cellular proteins. Given that Cu is both essential and toxic, organisms must implement uptake mechanisms to extract Cu from nutrients, transport Cu across the biological membranes, and deliver it to Cu-requiring proteins. Furthermore, precise regulatory mechanisms must be in place to prevent the accumulation of Cu ions to toxic levels *(4)*. Details of the structure and dynamics behavior of copper proteins at atomic resolution are central to understanding mechanism of catalysis, ligand binding, allosteric modulation, and protein–protein interaction.

The methods of computational chemistry and molecular modeling allow us to study such processes with temporal details and space resolution that are difficult, or impossible, to obtain experimentally. Accurate modeling and simulation usually begin with known structures, obtained from the

From: Handbook of Copper Pharmacology and Toxicology
Edited by: E. J. Massaro © Humana Press Inc., Totowa, NJ

Table 1
Copper-Binding Proteins

Common name	*Biological function*
Cu,Zn superoxide dismutase	Free-radical detoxification
Cytochrome-*c* oxidase	Electron transport in the mitochondria
Lysyl oxidase	Crosslinking of collagen and elastin
Dopamine β-hydroxylase	Catecholamine production
Tyrosinase	Melanin production
Peptidylglycine monooxygenase	Bioactivation of peptide hormones
Ceruloplasmin	Ferroxidase, Cu transport
Clotting factors V and VIII	Blood clotting
Angiogenin	Induction of blood vessel formation
Metallothionein	Cu sequestration
Prion protein	Normal function currently unknown; copper-binding properties suggests potential role in Cu uptake
β-Amyloid precursor protein	Normal function currently unknown
Hephaestin	Iron egress from intestines

Table 2
Copper Proteins by Function

Function	*Protein class/family*
Catalysis	Oxidoreductases
	Amine oxidase
	Ammonia monooxygenase
	Ascorbate oxidase
	Ceruloplasmin
	Cu,Zn superoxide dismutase
	Cytochrome-*c* oxidase
	Diamine oxidase
	Dopamine β-hydroxylase
	Galactose oxidase
	Laccase
	Lysyl oxidase
	Methane monooxygenase
	N_2O reductase
	Nitrite reductase
	Peptidylglycine α-hydroxylating monooxygenase
	Phenylalanine hydroxylase
	Tyrosinase
	Ubiquinone oxidase
Electron transfer	Auracyanin
	Azurin
	Phytocyanin family
	Plastocyanin family
	Rusticyanin

Table 3
Copper Proteins by Cu Center Type

Copper center	*Protein class / family*
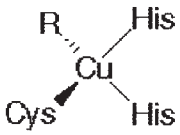 $Cu(N^{\delta}_{His})_2S^{\gamma}_{Cys}R$ $R = S^{\delta}_{Met}$ (azurin, plastocyanin, laccase) $R = O^{\varepsilon}Glu$ (phytocyanins) $R = H_2O$ (ceruloplasmin)	Type I (blue copper proteins) • Small blue proteins ° Auracyanin ° Azurin ° Phytocyanin family ° Plastocyanin family ° Rusticyanin • Blue oxidases ° Ascorbate oxidase ° Ceruloplasmin ° Laccase • Nitrite reductase
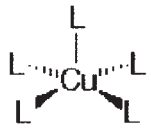 $Cu(N^{\varepsilon}His)mRn$ L = N, O or S ligands; R = O or S ligands m = 1 to 4; n = 0 to 3; m+n = 4 or 5	Type II • Cu,Zn superoxide dismutase • Dioxygenases • Monooxygenases ° Dopamine ß-hydroxylase ° Methane monooxygenase ° Peptidylglycine α-hydroxylating monooxygenase ° Phenylalanine hydroxylase • Nitrite reductase • Non-blue oxidases ° Amine oxidase ° Diamine oxidase ° Galactose oxidase ° Lysyl oxidase
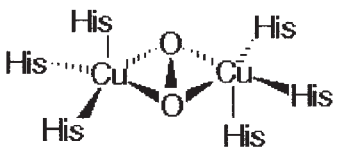 $\mu\text{-}O_2[Cu(N^{\varepsilon}_{His})_3]_2$	Type III • Catechol oxidase • Haemocyanins • Tyrosinase

Table 3 *(Continued)*
Copper Proteins by Cu Center Type

Copper center	*Protein class / family*
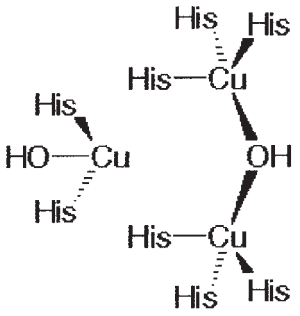 $Cu(N^{\varepsilon}_{His})_2OH{\cdot}\mu\text{-}OH[Cu(N^{\varepsilon}_{His})_3]_2$	Trinuclear centre (type II + type III) • Blue oxidases ◦ Ascorbate oxidase ◦ Ceruloplasmin ◦ Laccase
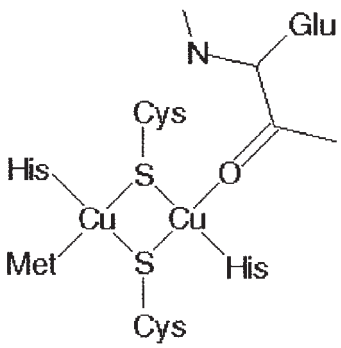 $Cu_2(N^{\delta}_{His})2O^{\alpha}_{Glu}S^{\delta}_{Met}(\mu\text{-}S^{\gamma}_{Cys})_2$	Cu_A • Cytochrome c oxidase • N_2O reductase
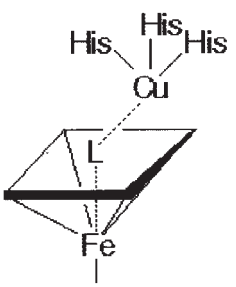 $CuN^{\delta}_{His}(N^{\varepsilon}_{His})_2L$ L = bridging ligand between Cu_B and Fe of heme a_3	Cu_B • Cytochrome c oxidase • Ubiquinone oxidase

Table 4
Copper Proteins by Type and Number of Prosthetic Centers[a]

Simple	*Complex*
Type I only	
• Small blue proteins	
° Auracyanin	
° Azurin	
° Phytocyanin family	
° Plastocyanin family	
° Rusticyanin	• Heme–copper proteins
	° Cytochrome-c oxidase
	° N_2O reductase
	° Ubiquinone oxidase
Type II only	
• Galactose oxidase	
• Peptidylglycine α-hydroxylating monooxygenase	• Cu–TPQ proteins
	° Amine oxidase
Type III only	° Diamine oxidase
• Catechol oxidase	° Lysyl oxidase
• Hemocyanins	
• Tyrosinase	• Cu–Zn proteins
	° Cu,Zn superoxide dismutase
Type I + type II	
• Nitrite reductase	
Type I + trinuclear	
• Multicopper oxidases	
° Ascorbate oxidase	
° Ceruloplasmin	
° Laccase	

[a]The solid circles represent a protein family, while the open circles represent a specific protein.

X-ray diffraction or from nuclear magnetic resonance (NMR) studies. Molecular dynamics (MD) simulation represents an excellent tool to explore the conformational space of proteins with known three-dimensional (3D) structures. In this review, we focus on recent advances in understanding copper proteins functionality through molecular modeling and molecular dynamics simulation.

2. COMPUTATIONAL METHODS

2.1. Molecular Modeling

Molecular modeling is a general term that covers a wide range of molecular graphics and computational chemistry techniques used to build, display, manipulate, simulate, and analyze molecular structures and to calculate properties of these structures. Molecular modeling is used in a number of different research areas and the criterion for a successful modeling experiment should not be how accurately the calculations are performed, but whether they are useful in rationalizing the behavior of the molecule or in enhancing the creativity of the chemist in the design of novel compounds. Useful information about these techniques can be also found on the Web *(5)*.

2.2. Molecular Graphics

A somewhat arbitrary distinction is to divide molecular modeling techniques into molecular graphics and computational chemistry. Molecular graphics is the core of a modeling system, providing for the visualization of molecular structures and their properties. Molecular graphics provides the ability to display structures in a variety of styles and color schemes, with visual aids such as depth cuing, and the ability to move the structures interactively in three dimensions. Simple tools for manipulating structures, such as modifying torsion angles and calculating geometry, are frequently included in the molecular graphics programs. The visualization of molecular properties is an extremely important aspect of molecular modeling. The properties might be calculated using a computational chemistry program and visualized, for instance as 3D contours, along with the associate structures. Although manipulation of structures is usually interactive, the calculation of properties in some cases may require a significant amount of computer time. The graphics part of the modeling system also provides the interface to the computational chemistry tools, allowing calculations to be defined and run and then analyzed when complete.

2.3. Building and Modifying Structures

Small molecule structures can be built in three dimensions by joining basic building blocks from a fragment library and then modifying atom and bond types. Macromolecule structures such as proteins and nucleic acids, consisting of large numbers of specific units, can be built by specifying the sequence of the units and the conformation in which the units should be joined. There are a number of sources of experimentally derived molecular structural data that can be visualized and modified. These include the RCSB Protein Data Bank (PDB) *(6)* (web address http://www.rcsb.org/pdb), which maintains a library of protein and nucleic acid structures, and the Cambridge Structural Database, with a database of small molecule structures (web address http://www.ccdc.cam.ac.uk/index.html).

2.4. Molecular Mechanics

When a structure is built, it usually needs to be refined to bring it to a stable, sterically acceptable, and chemically reasonable conformation. The refinement process is known as minimization (optimization) and is an iterative procedure in which the coordinates of the atoms are adjusted so that the energy of the structure is brought to a local minimum. The structure with the lowest energy is considered to have the most stable arrangement and, by definition, the optimum geometry at the given computational method. Molecular mechanics methods take a classical approach to calculating the energy of a structure. The molecule is treated essentially as a set of charged-point masses that are coupled together with springs. The total energy of a structure is calculated using an analytical function that sums a number of individual energy terms known as a force field. Molecular mechanics enables the energy of a structure to be evaluated quickly and can be applied to structures of large proteins. The methods can also be used to evaluate the energy of two or more interacting molecules, as when docking a substrate into an enzyme active site.

2.5. Comparative Protein Modeling

Insights into the 3D structure of a protein are of great assistance when planning experiments aimed at the understanding of protein function and during the drug design process. The experimental elucidation of the 3D structure of proteins is, however, often hampered by difficulties in obtaining sufficient protein, diffracting crystals, and many other technical aspects. Therefore, the number of solved 3D structures increases only slowly compared to the rate of sequencing of novel cDNAs, and no structural information is available for the vast majority of the protein sequences registered in the databases. In this context, it is not surprising that predictive methods have gained much interest.

Proteins from different sources and sometimes diverse biological functions can have similar sequences, and it is generally accepted that high sequence similarity is reflected by distinct structure similarity. Indeed, the root mean square deviation (RMSD) of the α-carbon (C_α) coordinates for

protein cores sharing 50% residue identity is expected to be around 1.0 Å. This fact served as the premise for the development of comparative protein modeling (also often called "modeling by homology" or "knowledge-based modeling"), which is presently the most reliable method. Comparative model building consist of the extrapolation of the structure for a new (target) sequence from the known 3D structure of related family members (templates). Although the high precision structures required for detailed studies of protein–ligand interaction can only be obtained experimentally, theoretical protein modeling provides the molecular biologists with "low-resolution" models that hold enough essential information about the spatial arrangement of important residues to guide the design of experiments. The rational design of many site-directed mutagenesis experiments could therefore be improved if more of these "low-resolution" theoretical model structures were available.

2.5.1. Preliminary Procedure

Comparative protein modeling requires at least one sequence of known 3D structure with significant similarity to the target sequence. In order to determine if a modeling request can be carried out, one compares the target sequence with a database of sequences derived from the PDB *(6)*. The choice of template structures can be further restricted to those that share at least 30% residue identity. This procedure might allow the selection of several suitable templates for a given target sequence, and up to 10 templates are generally used in the modeling process. The best template structure (i.e., the one with the highest sequence similarity to the target) will serve as the reference. All of the other selected templates will be superimposed onto it in 3D. The 3D match is carried out by superimposing corresponding $C_{Å}$ atom pairs selected automatically from the highest scoring local-sequence alignment. This superposition can then be optimized by maximizing the number of C_α pairs in the common core while minimizing their relative mean square deviation. Each residue of the reference structure is then aligned with a residue from every other available template structure if their C_α atoms are located within 3.0 Å. This generates a structurally corrected multiple-sequence alignment. The target sequence now needs to be aligned with the template sequence or, if several templates were selected, with the structurally corrected multiple-sequence alignment. Residues that should not be used for model building (e.g., those located in nonconserved loops) will be ignored during the modeling process. Thus, the common core of the target protein and the loops completely defined by at least one supplied template structure will be built.

2.5.2. Building the Model

The next step is the construction of a framework, which is computed by averaging the position of each atom in the target sequence, based on the location of the corresponding atoms in the template. When more than one template is available, the relative contribution, or weight, of each structure is determined by its local degree of sequence identity with the target sequence. Following framework generation, loops for which no structural information was available in the template structures are not defined and therefore must be constructed. Although most of the known 3D structures available share no overall similarity with the template, there may be similarities in the loop regions and these can be inserted as loop structure in the new protein model. Using a "spare part" algorithm *(7,8)*, one searches for fragments that could be accommodated onto the framework among the PDB entries determined with a resolution better than 2.5 Å. Each loop is defined by its length and its "stems," namely the C_α atom coordinates of the four residues preceding and following the loop. The fragments that correspond to the loop definition are extracted from the PDB entries and rejected if the relative mean square deviation computed for their "stems" is greater than a specified cutoff value. Furthermore, only fragments that do not overlap with neighboring segments should be retained. The accepted "spare parts" are sorted according to their RMSD, and a C_α framework based on the five best fragments can be added to the model. Because the loop building only adds C_α atoms, the backbone carbonyl and nitrogens must be completed in these regions. This step can be performed by using a library of pentapeptide backbone fragments derived from the PDB entries determined with a resolu-

tion better than 2.0 Å. These fragments are then fitted to overlapping runs of five C_α atoms of the target model. The coordinates of each central tripeptide are then averaged for each target backbone atom (N, C, O) and added to the model.

For many of the protein side chains, there is no structural information available in the templates. These cannot, therefore, be built during the framework generation and must be added later. The number of side chains that need to be built is dictated by the degree of sequence identity between target and template sequences. To this end, one uses a table of the most probable rotamers for each aminoacid side chain depending on their backbone conformation. All of the allowed rotamers of the residues missing from the structure are analyzed to see if they are acceptable by a van der Waals exclusion test. The most favored rotamer is added to the model.

2.5.3. Model Refinement and Quality

Idealization of bond geometry and removal of unfavorable nonbonded contacts can be performed by energy minimization algorithms using force fields such as CHARMM *(9)*, AMBER *(10)*, or GROMOS *(11)*. The refinement of a primary model should be performed by no more than 100 steps of steepest descent, followed by 200–300 steps of conjugate gradient energy minimization. It is necessary to keep the number of minimization steps to a minimum to avoid optimized models from being moved away from the control structure. Constraining the positions of selected atoms in each residue generally helps avoid excessive structural drift during force-field computations.

A model is considered wrong if at least part of its structural features is misplaced relatively to the rest of the model. Errors of that type can very easily slip into a model when erroneous sequence alignments are used during the building procedure. Another source of inaccuracy is the deviation from ideal stereochemical values for bond lengths and angles. It is crucial to realize that proper stereochemistry is not a criteria for model correctness. In other terms, it is possible to build models that would comply with such criteria and have no strictly biological meaning. The accuracy of a model is also limited by the deviation from the used template structure(s). Almost every protein model contains nonconserved loops, which are expected to be the least reliable portions of a protein model. Indeed, these loops often deviate markedly from experimentally determined control structures. In many cases, however, these loops also correspond to the most flexible parts of the structure, as evidenced by their high crystallographic temperature factors (or multiple solutions in NMR experiments). On the other hand, the core residues, the least variable in any given protein family, are usually found in essentially the same orientation as in experimental control structures, whereas far larger deviations are observed for surface aminoacids. This is expected because the core residues are generally well conserved and the conformation of their side chains are constrained by neighboring residues. In contrast, the more variable surface amino acids will tend to show more deviations because there are few steric constraints imposed upon them. Finally, when modeling metalloproteins, it is very important that the putative metal ligands of the new modeled structure maintain the geometry required to coordinate the metal.

2.6. Molecular Dynamics

Useful information can be gained from the study of minimum energy structures by molecular mechanics. However, these structures are static models, whereas molecules are flexible structures subject to thermal motion. The ability of proteins to operate as catalysts clearly depends on subtle details of their structure. The overall shape and disposition of functional groups within active site is what gives proteins some of their special properties: high substrate specificity, transition state stabilization, and the ability to transmit information to other units in a protein complex (allostery), to name but a few. As experimental and theoretical investigations have uncovered information about the structural component of proteins function, so too have they shown that proteins exhibit a rich variety of motions *(12–14)*. If one considers just a few of the tasks proteins must perform in a living organism, it becomes apparent that motion, as well as structure, is an essential component of protein

function. Receptor proteins lie partially buried in the cell membrane, and, on binding their target molecule, transmit this information into the cell by changing conformation, allowing the cell to respond to the external stimulus. Transport proteins bind ligands within their interior, releasing the ligand when conditions within the cell demand it. The allosteric effect involves motion of the subunits, whereas the entry and exit of the ligand often requires an environmentally induced local conformational change. Many proteins are synthesized in a part of the cell distant from where they will perform their function. Transport of the protein from its point of manufacture to its point of use may require crossing membranes inside the cell. The folded protein is often too large to cross the membrane, and so must first unfold, traverse the membrane as a linear sequence, and refold on the other side. Enzymes must often provide a very specific, nonaqueous environment for catalysis. Several known proteins completely engulf their substrate, perform the chemical reaction within the enclosed active site, then open to release the products. In considering just these few examples, we see that in addition to the importance of their structure, proteins exhibit a variety of motions as they operate within the cell.

New insights about the functional significance of protein motions are given by the technique of molecular dynamics *(15)* that is used to simulate the thermal motion of a structure, as a function of time, using the forces acting on the atoms to drive the motion. As the masses of the atoms are known, Newton's second law of motion ($F = ma$) may be used to compute the accelerations and thus the velocities of the atoms. The accelerations and velocities may then be used to calculate new positions for the atoms over a short time step (around 1.0 fs), thus moving each atom to a new position in space. This process iterates many thousands of times, generating a series of conformations of the structure known as a trajectory. The velocities of the atoms are related directly to the temperature at which the simulation is running. A simulation run at 300 K provides information on structural fluctuations that occur around the starting conformation, illustrating which parts of a molecule are most flexible, and can also provide informations on the pathways of conformational transitions. If the temperature of the simulation is increased, more energy is available to climb and cross energetic barriers. Thus, high-temperature (i.e., 1000 K) simulations are often used to search conformational space.

Using molecular dynamics simulations, a vast amount of data are generated. The problem is in analyzing these data. A simulation can be analyzed quantitatively by defining properties of interest and then graphing those properties against each other. For example, graphs that illustrate how the geometry or energy of the structure varies during the simulation can be created and compared. The simulation can be also analyzed in a qualitative way by replaying the simulation as a movie, a process known as animation.

2.6.1. Potential Function

In order to perform molecular dynamics simulations, one needs a mathematical function, or force field, to describe the system. The force fields are empirically derived and describe the potential energy of the system as a function of the positions of the atoms. The parameters for these equations are derived primarily from the results of *ab initio* quantum mechanics, spectroscopic data, and crystallographic data. The force field is calibrated by fine-tuning of these parameters to reproduce structures and energy trends for relevant model compounds. It is often possible to achieve good agreement with experiment because the functions are parameterized to reproduce the experimental data and therefore include the effects of any omitted terms that would make the approach more theoretically rigorous.

2.6.2. Physics of Molecular Dynamics Simulation

Molecular dynamics calculates the motion of a molecule by generating the changes of the atomic coordinates as a function of time. These sets of related coordinates define a trajectory in conformational space. A static structure is used as the starting point for these calculations, usually the minimized crystal structure. The velocities of the atoms are slowly increased from zero to values corresponding to a specified temperature in a process known as temperature equilibration, which is

part of a start-up procedure needed to ensure that the initial forces are reasonable. The atomic velocities, v_i, are related to the absolute temperature, T, through the total kinetic energy, by

$$\tfrac{1}{2}\sum m_i v_i^2 = \tfrac{3}{2} N k_b T$$

where m_i is mass of the atom, k_b is the Boltzmann constant, and the sum is over N atoms. New positions and velocities of all the atoms are determined by solving the equations of motion using the old positions, the old velocities, and the accelerations. Accelerations are related to forces via Newton's second law

$$F = ma$$

and the forces are related to the gradient of the first derivatives of the potential energy needed for energy minimization by

$$F = \frac{-\delta U}{\delta x_i}$$

so that

$$a_i = -\left(\frac{1}{m}\right)\frac{\delta U}{\delta x_i}$$

New atomic positions, $x_i(t + \Delta t)$, and velocities, $v_i(t + \Delta t)$, are derived from the elementary mechanics as

$$x_i(t+\Delta t) = x_i(t) + v_i(t)\Delta t + \tfrac{1}{2} a_i(t)\Delta t^2$$
$$v_i(t+\Delta t) = v_i(t) + a_i(t)\Delta_t$$

For this simple scheme to work, the time step, Δt, must be so small that positions (and forces) change very slightly with each step (less than 1/100 Å). Typical values of Δt range from 0.5 to 2.0 fs. In practice, the equations used to integrate the equations of motions in protein simulations are slightly more complicated than those given above, and because of the large amount of atoms, some methods are used for the simplification of calculations and the increase of computational speed *(16)*.

2.6.3. Force Field

As an example of a force field, we report on one of the more utilized in literature, the GROMOS force field *(11)*. The GROMOS force field is represented in terms of the potential energy function $U(r)$:

$$U(r) = U_{bond} + U_{angle} + U_{dihedral} + U_{improper} + U_{nb}$$

where the bond-stretching, angle-bending, dihedral torsional, and improper dihedral bending potentials, respectively, are

$$U_{bond} = \sum_{i=1}^{N_b} \tfrac{1}{2} K_{b_i} (d_i - d_i^\circ)^2$$

$$U_{angle} = \sum_{i=1}^{N_\theta} \tfrac{1}{2} K_{\theta_i} (\theta_i - \theta_i^\circ)^2$$

$$U_{dihedral} = \sum_{i=1}^{N_\varphi} \tfrac{1}{2} K_{\varphi_i} [1 + \cos(n_i \varphi_i - \delta_i)]$$

$$U_{improper} = \sum_{i=1}^{N_\xi} \tfrac{1}{2} K_{\xi_i} (\xi_i - \xi_i^\circ)^2$$

N_b, N_θ, N_φ, and N_ξ are the number of bond, angle, dihedral and improper dihedral terms, respectively. K_b, K_θ, K_φ, and K_ξ are the force constants and d_i°, θ_i°, and ξ_i° are the energy equilibrium values. n_i and δ_i are the dihedral angle multiplicity and phase, respectively. Whenever constraints are used to model the chemical bonds *(17)*, the corresponding bond-stretching potential term is not considered to be part of the Hamiltonian. The nonbonding potential term is described by the sum of a Lennard–Jones potential and a standard Coulombic term:

$$U_{nb} = \sum_{i<j}^{N} \left(\frac{C_{12}(i,j)}{r_{ij}^{12}} - \frac{C_6(i,j)}{r_{ij}^{6}} + \frac{q_i q_j}{4\pi\varepsilon_0 r_{ij}} \right)$$

where $\{C6(i,j), C12(i,j), q_i\}$ are a specific set of parameters and partial charges (i.e., the 37c and 37d sets of parameters for systems in water and in vacuum, respectively). Moreover, first and second neighbors (i.e., pairs of atoms separated by one and two covalent bonds, respectively) are not considered to be interacting through the nonbonding terms *(11)*.

3. APPLICATION OF COMPUTATIONAL METHODS TO COPPER PROTEINS

3.1. Study of Copper Proteins Through Molecular Modeling

The problem of modeling the interactions of metals in proteins is not easy because of their complex coordination chemistry, spin variability, and the polarizability of the outer-shell electrons *(18)*. Attempts to model bound metal using the potential functions, usually adopted for amino acids, gives often unrealistically strong nonbonding interactions and distorted metal center geometries. Notwithstanding a lot of modeling papers, intended to predict the structure of a whole copper protein or to test the copper center properties, in comparison with data derived from different experimental techniques, have been carried out by using various methods to handle the metal sites *(18)*.

Modeling articles on copper proteins have been divided in three different classes:

I. *Modeling of mutant proteins carried out to plan or verify a series of experimental data (19–22)*. In this kind of article, the modeling procedure is relatively simple and only requires substitution of the side chain that must be changed with the chain of the new selected amino acid, leaving the backbone unaltered. The side chains are then scanned looking for a rotamer that had no van der Waals contacts with the neighboring residues in its spatial environment.

In the article by Folcarelli et al. *(19)*, the modeling procedure permits the explanation of the difference in stability resulting from a series of Lys→Arg mutations carried out in *Xenopus laevis* Cu,Zn superoxide dismutase (SOD) protein. In particular, the decrease in stability was shown to originate from a perturbation of dimer association, whereas the increase in stability was the result of the presence of additional hydrogen bonds. The same kind of substitution was previously found to increase heat stability in human Cu,Zn SOD *(20)*. In this work, the stabilizing effect of Lys→Arg substitutions was rationalized on the basis of a detailed analysis of the modeled structures of wild-type and mutant Cu,Zn SOD (Lys9→Arg). In addition to demonstrating that every thermostable protein can be further stabilized, these works provide direct evidence, supported by molecular modeling, that arginine residues are important stabilizing elements in proteins.

In the paper of Dong and co-workers *(21)*, the effect of mutating an asparagine residue (Asn38) in poplar plastocyanin, adjacent to one of the histidines bound to the copper, was investigated. The mutant proteins having Asn38 mutated in Gln, Thr and Leu are capable of folding and binding Cu^{2+}, but the blue color fades and the rate of fading increases in the order Gln < Thr < Leu. The wild-type properties are slightly perturbed for Asn38→Gln, but Asn38→Thr shows remarkable similarity to another type-I Cu protein, azurin from *Pseudomonas aeruginosa*. The Cu–S(Cys) bond is longer in azurin than in poplar plastocyanin, and the NH hydrogen bond to the ligating S atom is shorter.

Molecular modeling has been used to suggests a similar effect for Asn38→Thr because the threonine residue shifts toward Ser85 in order to avoid a steric clash and to optimize hydrogen-bonding. The results demonstrate that hydrogen-bonding adjacent to the type-I site stabilizes an architecture that both modulates the electronic properties of the Cu and suppresses side reactions of the cysteine ligand.

In a recent work, Zhu and collaborators *(22)* studied the physiologic complex between the methylamine dehydrogenase (MADH) and amicyanin, which is required for interprotein electron transfer. Kinetic data and thermodynamic analysis are used to probe the molecular basis for stabilization of the protein complex by an interprotein salt bridge between Arg99 of amicyanin and Asp180 of the α-subunit of MADH. Asp180 of MADH was converted to arginine to examine the effect on complex formation with native and mutant amicyanins. This mutation had no effect on the methylamine oxidation carried out by MADH, but significantly affected its interaction with amicyanin. These results are explained by the authors through a molecular model able to describe the sequence of events that leads to stable complex formation between MADH and amicyanin.

II. *Homology modeling of copper proteins using one or more X-ray structures as a template*. The model building and the analysis of a structural domain, or of the whole molecule, is applied to get new insights about protein function or to build philogenetic trees through a comparative analysis *(23–33)*.

Villoutreix and Dahlback *(31)* have investigated the A domains of human blood coagulation factor V by molecular modeling. Factor V (FV) is a large (2196 amino acids) nonenzymatic cofactor in the coagulation cascade with a domain organization (A1–A2–B–A3–C1–C2), similar to the one of factor VIII (FVIII). FV is activated to factor Va (FVa) by thrombin, which cleaves away the B domain, leaving a heterodimeric structure composed of a heavy chain (A1–A2) and a light chain (A3–C1–C2). Activated protein C (APC), together with its cofactor protein S (PS), inhibits the coagulation cascade via limited proteolysis of FVa and FVIIIa (APC cleaves FVa at residues R306, R506, and R679). The A domains of FV and FVIII share important sequence identity with the plasma copper-binding protein ceruloplasmin (CP). The X-ray structure of CP and theoretical models for FVIII have been recently reported and these informations allowed the authors to build a theoretical model (994 residues) for the A domains of human FV/FVa (residues 1–656 and 1546–1883). Structural analysis of the FV model indicates the following: (1) the three A domains are arranged in a triangular fashion, as in the case of CP, and the organization of these domains should remain essentially the same before and after activation; (2) a type-II copper ion (*see* Table 3) is located at the A1–A3 interface; (3) residues R306 and R506 (cleavage sites for APC) are both solvent exposed; (4) residues 1667–1765 within the A3 domain, expected to interact with the membrane, are essentially buried; (5) APC does not bind to FVa residues 1865–1874.

A 3D model of Fet3, the multicopper oxidase of yeast involved in the oxidation of extracellular ferrous iron and in its transport into the cell through the permease Ftr1, has been built *(33)*. Fet3 consists of three cupredoxin domains, joined by a trinuclear copper cluster, which is connected to the blue copper site located in the third domain (Table 3). Close to this site, which is the primary electron acceptor from the substrate, residues for a potential iron-binding site have been identified. The surface distribution of negatively charged residues suggests that Fet3 can translocate Fe^{3+} to the permease Ftr1 through an electrostatic guide.

In a recent work, a model for the incorporation of metal from the copper chaperone CCS into Cu,Zn SOD has been proposed *(32)*. Previous studies have identified the human copper chaperone CCS as the presumed factor responsible for copper incorporation into SOD *(34,35)*. The 3D structure of CCS was homology modeled using the periplasmic protein from the bacterial mercury-detoxification system *(36)* and the structure of one subunit of the human SOD dimeric enzyme *(37)* as templates. On the basis of the 3D model, a mechanism for the transfer of copper from CCS to SOD is proposed that accounts for electrostatic acceptor recognition, copper storage, and copper-transfer properties. The proposed model identifies a path for copper transfer based on the presence of differ-

ent metal sites characterized by sulfur ligands. The modeled structure was found to be strictly close to the subsequently published X-ray structure of CCS *(38)*.

III. *Building of the copper active site based from data derived from spectroscopic studies in order to understand the chemistry of substrate catalysis and/or the inhibitory effect of specific molecules*. This analysis can be done on X-ray-determined PDB structures or on modeled structures, depending on the availability of the 3D structure of the investigated protein *(39–41)*.

In the article by Grossmann and collaborators *(39)*, the extended X-ray absorption fine structure technique (EXAFS [Extended X-ray Absorption Fine Structure]), and the homology modeling approach have been used to define the structural features that specify the nature of the copper site in rusticyanin. Rusticyanin, a blue copper protein possessing the highest redox potential among this class of proteins and a high stability at acidic pH, displays a good degree of homology with the C-terminal end of other single-copper-containing blue proteins and to the blue copper domain of the multicopper proteins such as the nitrite reductases *(39)*. EXAFS data at pH 2.0 indicate that Cu is ligated to two His and a Cys, similar to other blue copper centers (Table 3). Modeling studies suggest that His85 is the ligating histidine from the N-terminal end. Its neighboring residue is a serine rather than the asparagine found in all known blue Cu proteins *(39)*. The high stability of the copper site may arise in part because of this substitution. The Cu-binding site is surrounded by aromatic residues that may provide further protection for the metal in an acidic environment. In addition, the high number of solvent-exposed lysine residues is likely to be of functional relevance under low-pH conditions. EXAFS data show a very small change in the copper site upon reduction, consistent with a more constrained copper center in rusticyanin compared to azurin and a higher redox potential value.

In another work *(40)*, molecular modeling has been used to hypothesize the structure of diamine oxidase active site derived from the study of the possible conformations assumed by *O*-alkylhydroxylamine inhibitors. A new series of aliphatic and aromatic *O*-alkylhydroxylamines were synthesized to explore further the structure–activity relations. The authors found the following: (1) branched compounds are less active than their straight-chain counterparts; (2) the bulkness of the aliphatic substituent has an important role in decreasing the activity; (3) the presence of a double bond compared to a triple bond has no significant effect in reducing the activity; (4) compounds having a longer straight chain were less active than derivatives having a shorter chain; (5) benzylic compounds were less active than aliphatics compounds having straight chains. A current model for the action of diamine oxidase proposes a crucial role for a trihydroxyphenylalanine quinone cofactor as part of the active site together with a copper atom *(42,43)*. Using molecular modeling, the authors were able to define the region of space that is just beyond the reactive carbonyl of the trihydroxyphenylalanine residue at the active site of diamine oxidase. They suggest that a negatively charged species, such as an aspartate or a glutamate, resides in a trough about 7–8 Å from the trihydroxyphenylalanine carbonyl carbon and this species helps in a selective binding of substrates such as putrescine and histamine.

Stillman and co-workers applied circular dichroism (CD), kinetic and mass spectrometry, and molecular modeling (based on CD and EXAFS data), to study copper(I) and mercury(II) binding to metallothionein *(41)*. Metallothionein (MT) is remarkable in its metal-binding properties: For the mammalian protein, well-characterized species exist having various metal to sulfur ratios, such as M7S20, M12S20, and M18S20. where M = Cd(II), Zn(II), Hg(II), Ag(I), Au(I), and Cu(I). Optical spectra and CD and luminescence spectra provide rich detail of a complicated metal-binding chemistry when metals are added directly to the metal-free or zinc-containing protein. Three-dimensional modeling was carried out using the results of the CD and EXAFS studies and model calculations for Zn7–MT, Hg7–MT, and Cu12–MT are described in the article.

3.2. Study of Copper Proteins Through Molecular Dynamics Simulation

It is now recognized that the atoms of which a protein is composed are in a state of constant motion at ordinary temperatures. The presence of such motional freedom implies that a native protein at

room temperature samples a range of conformations. Most are usually close to the average structure, but, at any given moment, each protein molecule is likely to differ significantly from the average and these fluctuations are likely to play a role in protein function. Molecular dynamics simulation has been widely used to understand the functional properties of the copper proteins. MD has shown to be a valid tool for investigating the physical properties of the proteic matter, for the interpretation of the X-ray diffraction data in the process of structure determination, and in the analysis of the relationship between protein motion and protein function. Molecular dynamics articles on copper proteins have been divided in three classes:

I. *Use of restrained MD to refine structures obtained by X-ray diffraction (44–49), NMR spectroscopy (50–52), and molecular modeling (53).* Among the copper containing proteins we report the following examples.

Protein structures are now routinely refined using restrained molecular dynamics. In a work by Djinovic and collaborators *(44)*, the structure of yeast Cu,Zn SOD has been determined to 2.5 Å resolution. The enzyme crystallizes in the P2(1)2(1)2 space group with two dimeric enzyme molecules per asymmetric unit. The structure has been solved by a molecular replacement technique using the dimer of the bovine enzyme as the search model and has been refined by molecular dynamics with crystallographic pseudoenergy terms, followed by conventional crystallographic restrained refinement. The *R* factor for 32,088 unique reflections in the 10.0–2.5 Å resolution range (98.2% of all possible reflections) is 0.158 for a model comprising two protein dimers and 516 bound solvent molecules, with a root mean square deviation of 0.016 Å from the ideal bond lengths and an average *B* factor value of 29.9 $Å^2$.

In another work by Bond and co-workers *(45)*, the crystal structure of the "blue" copper protein plastocyanin from the cyanobacterium *Phormidium laminosum* has been solved at 2.8 Å resolution. *P. laminosum* plastocyanin crystallizes in space group *P43212* with unit-cell dimensions $a = 86.57$ and $c = 91.47$ Å and with three protein molecules per asymmetric unit. The final residual *R* is 19.9%. The structure was solved using molecular replacement and refined through MD. The molecule of *P. laminosum* plastocyanin has 105 amino acid residues. The single Cu atom is coordinated by the same residues, two histidines, a cysteine, and a methionine, as in other plastocyanins. In the crystal structure, the three molecules of the asymmetric unit are related by a noncrystallographic threefold axis. A Zn atom lies between each pair of neighboring molecules in this ensemble, being coordinated by a surface histidine residue of one molecule and by two aspartates of the other.

Recently, a novel type of catalytic copper cluster has been found in nitrous oxide reductase (N_2OR) *(47)*, which catalyses the two electron reduction of N_2O to N_2. Nitrous oxide reductase is a 1160-residue homodimer, whose structure has been solved at 2.4 Å upon refinement through MD. Each N_2OR monomer is composed of two distinct domains. The N-terminal domain (residues 10–443) adopts a seven-bladed β-propeller fold, with the Cu_Z center located at one end of the propeller on the pseudo-sevenfold axis. The C-terminal domain (residues 478–581) forms an antiparallel β-sandwich in the Greek key motif and adopts a cupredoxin fold already seen in bovine cytochrome-*c* oxidase, with the Cu_A center located in a loop region between strands β8 and β9. In the dimer, the C-terminal domain of one monomer faces the N-terminal domain of the second monomer. The Cu_Z center of N_2OR comprises 4 copper ions that adopt the shape of a distorted tetrahedron, and 10 ligands: 7 histidines residues and 3 hydroxide ions. Two histidine residues (His270 and His437) of the Cu_Z center belong to the loops located on the top of the propeller domain and the remaining five (His79, His80, His128, His325, and His376) belong to the innermost strand of the blades. The seven His ligands are not part of a consensus sequence. The Cu_A center of one monomer is in close proximity to the Cu_Z center of the second monomer. The structure of the Cu_Z center suggests that there is only one possible site for N_2O binding. The Cu_Z center could behave as an electron buffer, three copper ions being reduced by the Cu_A center prior to substrate processing. The catalytic copper would remain oxidized and, therefore, able to bind the substrate. This electron reservoir could favor a fast electron exchange and prevent the formation of a dead-end products. Recently, inorganic sulfur chemical

determination and the high-resolution structure of Pd–N_2OR identified, in the Cu_Z cluster, a bridging inorganic sulfur instead of an oxygen *(48)*, a result that reconciles the novel Cu_Z cluster with the hitherto puzzling spectroscopic data.

Ubbink and collaborators *(50)* have used the diamagnetic chemical shift and intermolecular pseudocontact shifts in the NMR spectrum of plastocyanin as input in restrained rigid-body molecular dynamics calculations to determine the structure of the transient complex between cytochrome-f and plastocyanin. An ensemble of 10 structures was obtained, in which the root mean square deviation of the plastocyanin position relative to cytochrome-f is 1.0 Å. Electrostatic interaction is maintained at the same time as the hydrophobic side of plastocyanin makes close contact with the heme area, thus providing a short electron-transfer pathway (Fe–Cu distance 10.9 Å) via residues Tyr1 or Phe4 (cytochrome-f) and the copper ligand His87 (plastocyanin). The combined use of diamagnetic and paramagnetic chemical shift changes has permitted one to obtain detailed information about the structure of a transient complex of redox proteins. The structure suggests that the electrostatic interactions "guide" the partners into a position optimal for electron transfer, which may be stabilized by short-range noncovalent interactions.

The three-dimensional solution structure of amicyanin from *Thiobacillus versutus* has been determined and refined by using distance geometry and restrained molecular dynamics *(51)*. A total of 984 experimentally derived constraints were used for the final refinement (881 distance constraints and 103 dihedral angle constraints). Stereospecific assignments were made for 17 prochiral β-methylene protons (33%) and the methyl groups of 8 valine residues. Fourteen structures were selected to represent the solution structure. They show an average pairwise backbone root mean square deviation of 1.19 Å. The overall structure can be described as a β-sandwich, built up of nine β-strands. The copper atom is located between three loops on one end of the molecule. Two of these loops contribute the copper ligands. His54 is on the loop between β-strands 4 and 5. The other three ligands, Cys93, His96, and Met99, are located evenly spaced on the loop between β-strands 8 and 9. This loop is folded in two consecutive type-I turns with His96 as the donor and acceptor of the NH_i–CO (i–3) hydrogen bonds. The folding is reminiscent of the general cupredoxin fold, however the region between β-strands 5 and 7 and the N-terminal extension, which forms an extra β-strand, seems to be unique to amicyanin. The partly surface-exposed copper ligand His96 is surrounded by a hydrophobic patch consisting of seven residues.

Single crystals of the reduced form of Cu,Zn SOD [space group *P2(1)2(1)2(1)*, one dimer per asymmetric unit] have been obtained and their X-ray structure refined at 1.9 Å resolution *(52)*. The structure shows that the imidazolate bridge is maintained in the present crystalline form. It is confirmed that in solution the bridge is broken and the involved histidine is protonated on the side of copper. Based on the Nuclear Overhauser Effect (NOE) constraints, and with the aid of molecular dynamics calculations, a structural model is proposed for the molecule in solution. Both structures are considered significant as far as the enzymatic mechanism is concerned.

Tsigelny and collaborators *(53)* have modeled the extracellular domains of individual subunits (amino acids 31–200) in the nicotinic acetylcholine receptor, using sequence homology with copper-binding proteins of known crystal structure, such as pseudoazurin *(54)* and plastocyanin *(55)*, and data from recent site-specific mutagenesis, antibody mapping, and site-directed labeling studies (*53* and references therein). These data permitted one to build an initial model that was refined using molecular dynamics and mechanics as well as electrostatic and solvation energy calculations. The sequences between residues 31 and 164 in the α_1-subunit and the corresponding residues in homologous receptor subunits show similarity with the core sequence of the cation-binding site in plastocyanin and pseudoazurin, a region in the template proteins characterized by multiple hairpin loops. Electrostatic factors also appear to distinguish the ligand-binding interfaces, α–γ and α–δ, from the other three interfaces on the pentameric receptor.

II. *Molecular dynamics simulation has been widely used to interpret functional and spectroscopic properties experimentally obtained on copper proteins (56–73).* As an example, we briefly

review the work carried out on the bovine Cu,Zn SOD, an ezyme that has been intensively studied through MD simulation.

Several molecular dynamics simulations have been carried out on the bovine Cu,Zn SOD. At the beginning, only one-half of the dimer (i.e., the orange subunit) has been taken into account because of the large dimensions of the whole molecule. In these first MD studies *(57,58,61)*, the motions of the active site and the corresponding path followed by the superoxide approaching the copper ion have been analyzed. Trajectory analysis revealed that the superoxide is directed toward the catalytic metal through the concomitant motions of several active-site invariant residues. The significant number of local minima and the small variations in free energy encountered by the superoxide confirm that this molecule does not follow a straightforward energy minimization path, rather suggesting a variety of copper-approaching walks. The significant role of protein fluctuations in the enzyme–substrate interactions has been confirmed by a study combining Brownian and molecular dynamics simulation in the presence of substrate *(60)* and by MD calculations carried out on homology models of human Cu,Zn SOD mutants *(59,62)*. A common aspect stems out from these dynamic simulations: the existence of a series of concerted motions that organize, sterically and energetically, the active site for the catalytic event. On the basis of these works, a preliminary 100-ps MD simulation of the Cu,Zn SOD in water, taking into account for the first time the entire dimer, has been carried out to study the behavior of the two active sites of this enzyme *(63)*. The active site of each subunit has been monitored during the entire simulation by calculating the distances between functional residues and the catalytic copper. The results indicated that the electrostatic residues orientation is maintained in each active site while the solvent accessibility is different. Analysis of the MD simulation, carried out by using the atomic displacement covariance matrix, has shown a different intrasubunit correlation pattern of the two monomers and the presence of intersubunit correlations. The simulation has indicated for the first time an asymmetry in the two active sites and the presence of different dynamic behavior of the two SOD subunits. In a subsequent work, a 300-ps MD simulation of the whole Cu,Zn SOD dimer has been carried out in water and the trajectory has been analyzed using the essential dynamics method *(64)*. The results indicated that the motion is defined by few preferred directions identified by the first four to six eigenvectors and that the motion of the two monomers at each instant is not symmetric. Large, intrasubunit and intersubunit motions involving different subdomains of the protein are observed. A mechanical coupling between the two subunits is also suggested because displacements of the loops surrounding the active site in one monomer are correlated with the motion of parts of the second toward the intersubunit interface.

In a more recent work, with longer trajectories (up to 1.0 ns), MD simulations of solvated dimeric Cu,Zn SOD have been carried out at four temperatures, namely 200, 225, 250, and 300 K *(70)*. Analysis of the backbone-to-backbone hydrogen bond number indicated that the symmetry observed in the two subunits at 200 K is gradually lost by heating the system. The C_α atoms displacement cross-correlation maps confirm that the asymmetric behavior of the two subunits increases as a function of temperature. The dynamic cross-correlation of the subunits volumes indicates a fast correlation between the two subunits at 300 K, which is delayed upon lowering the simulation temperature. These results indicated that temperature plays an essential role in injecting such an asymmetry, the two subunits being asymmetric and in rapid communication at 300 K, and almost symmetric and in slow communication at lower temperatures.

Molecular dynamics simulation at a different temperature has been also carried out to interpret the "glasslike" transition *(69)*, experimentally observed at approx 200 K by neutron-scattering experiments. The transition is well reproduced when the protein is simulated in the presence of water solvent, whereas the simulations without solvent are not able to reproduce the experimental results. Analysis of anharmonicity and anisotropy of the atomic motions indicates that these parameters are good indicators for the occurrence of the transition. Analysis of the atomic fluctuations of different protein shells, having different degrees of exposure to the solvent, shows that the transition is driven

by the protein atoms belonging to the external shell, whose Debye–Waller factors are found to be larger *in vacuo* than in the solvated system.

Molecular dynamics simulation was also comparatively applied to the wild-type Cu,Zn SOD from *Xenopus laevis* and to one of its mutants to explain the unusual catalytic enhancement introduced by a mutation *(68)*. Neutralization by site-directed mutagenesis of four charged and highly conserved residues of the electrostatic loop of *X. laevis* Cu,Zn SOD involved in the electrostatic attraction of the substrate (Lys120→Leu, Asp130→Gln, Glu131→Gln and Lys134→Thr) gives rise to a mutant enzyme that displays an affinity for monovalent inhibitor anions, such as N_3^-, higher than that of the wild type. Analysis of 300 ps of molecular dynamics simulation carried out on the wild-type and on the *X. laevis* Cu,Zn SOD mutant indicates that the two proteins display a distinct dynamical behavior. In particular, the root mean square deviation from the starting structure, the number of residues in random coil conformations, and the number of residues in unfavorable regions of the Ramachandran plot indicate that the mutant displays a rigidity higher than the native enzyme. This is also evidenced by the loss of dynamical cross-correlations in the simulation of the mutant, which, on the other hand, are present in the wild type. Moreover, the mutant protein shows a different organization of the backbone-to-backbone hydrogen-bond network that generates a rigid structure leading to an increase of the active-site accessibility when compared to the native enzyme. It is suggested that the rigid state in which the mutant is confined, accompanied by the increase of the solvent-accessible surface of the active site may explain the difference in reactivity toward the inhibitor anion. In the two proteins, time evolution analysis of the Voronoi volumes of the single subunits *(71)* indicated that one monomer shows higher volume fluctuations and a more variable behavior if compared to the other one. The dynamical structural asymmetry is higher in the mutant than in the wild-type enzyme. Dynamical correlation of the Voronoi volume of one subunit with that of the other shows that in the mutant changes in the volume of one subunit are transmitted to the other subunit more slowly than in the native enzyme. This result indicates that perturbation of the mechanical communication between the two subunits may be brought about by mutations located in the active sites, far from the intersubunit interface of the enzyme, suggesting a strict interrelation even between protein regions located far away.

The dynamical behavior of the dimer observed in these works suggests the presence of a mechanical coupling between the two subunits, a phenomenon that may help to suggest some conclusions about the evolutionarily constant dimericity of the eukariotic Cu,Zn SODs. At least four basic reasons underlie the presence of quaternary association in the eukariotic Cu,Zn SODs. The first is diffusion: The SOD subunit exposes a greater catalytic target if a great part of the monomer surface is covered by the dimer contact. In this way, the percentage of reacting surface, with respect to the total, is increased. The second is electrostatics: Because different dielectric properties encountered by the neighbor charges, the association between monomers allows one to generate the particular electrostatic field surrounding this protein. In the dimer, the potential field is composed of a dome-shaped positive potential attracting the superoxide located only in proximity of the catalytic ions *(26)*. The third is stability: The Cu,Zn SOD monomer structure is highly stabilized by the complex network of weak interactions that take place between the subunits, at the dimer interface. The fourth is protein motion. In the kinetic model proposed *(58,61)*, the channel-crossing rate constant, intermediate between a diffusion controlled and an electron-transfer rate constant, large enough to be neglected, is supposed to be reduced by frictional and perhaps by gating effects resulting from the motion of the protein. The asymmetric motions that have been observed in these works could be the result of concerted interactions between the subunits; they contribute to the reduction of free-energy barriers and allow the incoming superoxide to react with the copper.

Recently the backbone NMR assignment of reduced human dimeric Cu,Zn SOD, performed on isotopes enriched samples of both wild-type SOD and the monomeric F50E/G51E/E133Q mutant *(74)*, has confirmed these MD suggestions. The experiments indicate a larger mobility in the wild-

type form, with respect to the monomer, in the picosecond to nanosecond time-scale because of the fluctuations of structural elements which provides the correct electrostatic driving force, guiding the superoxide in the active channel and favoring the SOD activity.

III. *The use of MD simulations to understand the dynamics of protein–water interaction* has been carried out on two small copper-containing proteins such as plastocyanin *(75–77)*, and azurin *(78,79)*. Among these articles we report the following examples.

Molecular dynamics simulations of copper plastocyanin were carried out to study protein structure and dynamics as a function of hydration *(75)*. The simulation of plastocyanin were performed at 300 K in the presence of 44, 80, 228, 682, and 2516 water molecules, respectively. For each different hydrated system, the simulation covered 110 ps; the trajectories of the last 80 ps were used for the analysis. Structural and dynamical properties of the protein are considerably altered upon the addition of water. The gyration ratio value indicates that the most compact structure is obtained in the presence of 80 water molecules. Both the root mean square (RMS) deviations from the initial structure and the fluctuations of the protein atoms depends significantly on the number of hydration water molecules. The largest RMS deviations are obtained at intermediate hydration level, whereas the smallest value is recorded at full hydration. The RMS fluctuations are minimized in the presence of 80 water molecules and maximized at a high hydration level. The interplay among protein dynamics, hydration water, and the amino acid residue properties is discussed in the article.

In order to study the dynamical properties of the solvent–protein interface, a detailed analysis of the time relaxation behavior of the hydration shells around each atom of copper plastocyanin has been performed by means of a time-correlation function technique *(77)*. In computing the function, which allowed the authors to extract average water residence times and coordination numbers within atomic shells of a given radius, attention has been focused on the short and long time limits of the function itself, also in connection with a detailed analysis of the statistical uncertainty. Water residence times distribution around plastocyanin has been calculated for the first coordination shell. Water residence times near charged and polar atoms were found to be longer than those of nonpolar ones; moreover, side-chain oxygens and nitrogens, which form hydrogen bonds with solvent molecules, show water residence times larger than other atom types, and for negatively and positively charged residues, these times correlate to the hydrogen-bond average duration. The accessibility of the solvent to protein atoms, investigated in terms of coordination numbers, has been compared to the more standard solvent-accessible surface. The active site, including the copper atom and its ligands, has been studied in greater detail to better understand the connections between the water molecule dynamical properties and the protein biological functionality. In particular, the copper site, which was believed to be inaccessible to the solvent, was found to be accessible by at least one water molecule that does not exchange with bulk and that has a permanent contact with the metal.

A system containing the globular protein azurin and 3658 water molecules has been simulated to investigate the influence on water dynamics exerted by a protein surface *(79)*. Evaluation of water mean residence time for elements having different secondary structure did not show any correlation. Identically, comparison of solvent residence time for atoms having different charge and polarity did not show any clear trend. The main factor influencing water residence time in proximity to a specific site was found to be its solvent accessibility. For surfaces having high solvent accessibility, all atoms, independently of their character, are surrounded by water molecules that rapidly exchange with the bulk solvent. For atoms having a solvent-accessible surface lower than approx 16 $Å^2$, a relation is found for which charged and polar atoms are surrounded by water molecules characterized by residence times longer than the nonpolar ones, whereas solvent accessibility is not able to modulate the water residence time for apolar sites.

4. CONCLUDING REMARKS

In this review, we have shown that computer-simulation techniques represent a valid tool to support or validate experimental data. A large bibliography is available just focusing on copper protein applications, indicating that the computational approach is widely used in the study of proteins. At present, molecular modeling and molecular dynamics simulation methods are becoming increasingly more accessible to the experimental biochemists. A wide use of these tools is now possible because of the availability of fast and relatively inexpensive desktop computers. A large variety of reliable computer programs for the visualization and the analysis of the macromolecules are often free and available on the Internet, however, sometimes, the use of these programs may be still difficult because of the complexity and dimensions of biological macromolecules. Moreover, before using these programs, great attention must be given to their theoretical basis in order to be confident of the results obtained. The survey given in this review provides an introduction to the capabilities of the simulative tools applied to the study of copper proteins and to the potentiality of these methods in describing precious insights in the study of the macromolecules.

REFERENCES

1. Linder, M. C. (1991) *Biochemistry of Copper*. Plenum, New York.
2. Halliwell, B. and Gutteridge, J. M. C. (1984) Oxygen toxicity, oxygen radicals, transition metals and diseases. *Biochem. J.* **219**, 1–4.
3. Halliwell, B. and Gutteridge, J. M. C. (1990) Role of free radicals and catalytic metal ions in human disease: an overview. *Methods Enzymol.* **186**, 1–85.
4. Peña, M. M. O., Lee, J., and Thiele, D. J. (1999) A delicate balance: homeostatic control of copper uptake and distribution. *J. Nutr.* **129**, 1251–1260.
5. Guex, N. and Peitsch, M. C. (2000) Principles of protein structure, comparative protein modelling and visualisation. http://www.expasy.ch/swissmod/course/ course-index.htm.
6. Berman, H. M., Westbrook, J., Feng, Z., Gilliland, G., Bhat, T.N., Weissig, H., et al. (2000) The protein data bank. *Nucleic Acids Res.* **28**, 235–242.
7. Jones, T. J. and Thirup, S. (1986) Using known substructures in protein model building and crystallography. *EMBO J.* **5**, 819–822.
8. Claessens, M., Cutsem, E. V., Lasters, I., and Wodak, S. (1989) Modeling the polypeptide backbone with "spare parts" from known protein structures. *Protein Eng.* **2**, 335–345.
9. Brooks, B. R., Bruccoleri, R. E., Olafson, B. D., States, D. J., Swaminathan, S. and Karplus, M. (1983) CHARMM: a program for macromolecular energy, minimization, and dynamics calculations. *J. Compar. Chem.* **4**, 187–217.
10. Weiner, P. K. and Kolman, P. A. (1981) AMBER: assisted model building with energy refinement. A general program for modeling molecules and their interaction. *J. Compar. Chem.* **2**, 287–303.
11. van Gunsteren, W. F. and Berendsen, H. J. C. (1987) *Groningen Molecular Simulation (GROMOS) Library Manual*. Biomos, Groningen.
12. Gurd, F. R. N. and Rothgeb, M. T. (1979) Motions in proteins. *Adv. Protein Chem.* **33**, 73–165.
13. Huber, R. and Bennet, W. S. Jr. (1983) Functional significance of flexibility in proteins. *Biopolymers* **22**, 261–279.
14. Fraunfelder, H. and Gratton, E. (1986) Protein dynamics and hydration. *Methods Enzymol.* **127**, 207–217.
15. Daggett, V. and Levitt, M. (1993) Realistic simulations of native-protein dynamics in solution and beyond. *Annu. Rev. Biophys. Biomol. Struct.* **22**, 353–380.
16. Allen, M. P. and Tildesley, D. J. (1987) *Computer Simulation of Liquids*. Clarendon, Oxford.
17. Ryckaert, J. P., Ciccotti, G., and Berendsen. H. J. C. (1977) Numerical integration of the cartesian equations of motions of a system with constraints: molecular dynamics of N-alkanes. *J. Compar. Phys.* **23**, 327–341.
18. Wampler, J. E. (1994) Computational chemistry and molecular modeling of electron-transfer proteins. *Methods Enzymol.* **243**, 559–607.
19. Folcarelli, S., Battistoni, A., Carri, M. T., Polticelli, F., Falconi, M., Nicolini, L., et al. (1996) Effect of Lys-Arg mutation on the thermal stability of Cu,Zn superoxide dismutase. Influence on the monomer-dimer equilibrium. *Protein Eng.* **9**, 323–325.
20. Mrabet, N. T., Van den Broeck, A., Van den brande, I., Stanssens, P., Laroche, Y., Lambeir, A. M., et al. (1992) Arginine residues as stabilizing elements in proteins. *Biochemistry* **31**, 2239–2253.
21. Dong, S., Ybe, J. A., Hecht, M. H., and Spiro, T. G. (1999) H-Bonding maintains the active site of type 1 copper proteins: site-directed mutagenesis of Asn38 in poplar plastocyanin. *Biochemistry* **38**, 3379–3385.
22. Zhu, Z., Jones, L. H., Graichen, M. E., and Davidson, V. L. (2000) Molecular basis for complex formation between methylamine dehydrogenase and amicyanin revealed by inverse mutagenesis of an interprotein salt bridge. *Biochemistry* **39**, 8830–8836.
23. Frigerio, F., Falconi, M., Gatti, G., Bolognesi, M., Desideri, A., Marmocchi F., et al. (1989) Crystallographic characterization and three-dimensional model of yeast Cu,Zn superoxide dismutase. *Biochem. Biophys. Res. Commun.* **160**, 677–681.

24. Falconi, M., Rotilio, G., and Desideri, A. (1991) Modeling the three-dimensional structure and electrostatic potential field of the two Cu,Zn superoxide dismutase variants from *Xenopus laevis*. *Proteins* **10**, 149–155.
25. Fields, B. A., Guss, J. M., and Freeman, H. C. (1991) Three-dimensional model for stellacyanin, a "blue" copper-protein. *J. Mol. Biol.* **222**, 1053–1065.
26. Desideri, A., Falconi, M., Polticelli, F., Bolognesi, M., Djinovic, K., and Rotilio, G. (1992) Evolutionary conservativeness of electric field in the Cu,Zn superoxide dismutase active site. Evidence for coordinated mutations of charged aminoacid residues. *J. Mol. Biol.* **223**, 337–342.
27. Oetting, W. S. and King, R. A. (1992) Analysis of mutations in the copper B binding region associated with type I (tyrosinase-related) oculocutaneous albinism. *Pigment Cell Res.* **5**, 274–278.
28. Gane, P. J., Dunwell, J. M., and Warwicker, J. (1998) Modeling based on the structure of vicilins predicts a histidine cluster in the active site of oxalate oxidase. *J. Mol. Evol.* **46**, 488–493.
29. Polticelli, F., Falconi, M., O'Neill, P., Petruzzelli, R., Galtieri, A., Lania, A., et al. (1994) Molecular modeling and electrostatic potential calculations on chemically modified Cu,Zn superoxide dismutases from Bos taurus and shark Prionace glauca: role of Lys134 in electrostatically steering the substrate to the active site. *Arch. Biochem. Biophys.* **312**, 22–30.
30. Hung, I. H., Casareno, R. L., Labesse, G., Mathews, F. S., and Gitlin, J. D. (1998) HAH1 is a copper-binding protein with distinct aminoacid residues mediating copper homeostasis and antioxidant defense. *J. Biol. Chem.* **273**, 1749–1754.
31. Villoutreix, B. O. and Dahlback, B. (1998) Structural investigation of the A domains of human blood coagulation factor V by molecular modeling. *Protein Sci.* **7**, 1317–1325.
32. Falconi, M., Iovino, M., and Desideri, A. (1999) A model for the incorporation of the metal from the copper chaperone CCS to Cu,Zn superoxide dismutase. *Structure* **7**, 903–908.
33. Di Patti, M. C., Pascarella, S., Catalucci, D., and Calabrese, L. (1999) Homology modeling of the multicopper oxidase Fet3 gives new insights in the mechanism of iron transport in yeast. *Protein Eng.* **12**, 895–897.
34. Cizewski-Culotta, V., Klomp, L. W. J., Strain, J., Casareno, R. L. B., Krems, B., and Gitlin, J. D. (1997) The copper chaperone for superoxide dismutase. *J. Biol. Chem.* **272**, 23,469–23,472.
35. Casareno, R. L. B., Waggoner, D., and Gitlin, J. D. (1998) The copper chaperone CCS directly interacts with copper/zinc superoxide dismutase. *J. Biol. Chem.* **273**, 23,625–23,628.
36. Steele, R. A. and Opella, S. J. (1997) Structures of the reduced and mercury-bound form of MerP, the periplasmic protein from the bacterial mercury detoxification system. *Biochemistry* **36**, 6885–6895.
37. Parge, H. E., Hallewell, R. A., and Tainer, J. A. (1992) Atomic structures of wild-type and thermostable mutant recombinant human Cu,Zn superoxide dismutase. *Proc. Natl. Acad. Sci. USA* **89**, 6109–6113.
38. Lamb, A. L., Wernimont, A. K., Pufahl, R. A., Culotta, V. C., O'Halloran, T. V., and Rosenzweig, A.C. (1999) Crystal structure of the copper chaperone for superoxide dismutase. *Nat. Struct. Biol.* **8**, 724–729.
39. Grossmann, J. G., Ingledew, W. J., Harvey, I., Strange, R. W., and Hasnain, S. S. (1995) X-ray absorption studies and homology modeling define the structural features that specify the nature of the copper site in rusticyanin. *Biochemistry* **34**, 8406–8414.
40. High, A., Prior, T., Bell, R. A., and Rangachari, P. K. (1999) Probing the "active site" of diamine oxidase: structure-activity relations for histamine potentiation by *O*-alkylhydroxylamines on colonic epithelium. *J. Pharmacol. Exp. Ther.* **288**, 490–501.
41. Stillman, M. J., Thomas, D., Trevithick, C., Guo, X., and Siu, M. (2000) Circular dichroism, kinetic and mass spectrometric studies of copper(I) and mercury(II) binding to metallothionein. *J. Inorg. Biochem.* **79**, 11–19.
42. Hartman, C. and Klinman, J. P. (1991) Structure–function studies of substrate oxidation by bovine serum amine oxidase: relationship of cofactor structure and mechanism. *Biochemistry* **30**, 4605–4611.
43. Hartman, C., Brzovic, P., and Klinman, J. P. (1993) Spectroscopic detection of chemical intermediates in the reaction of para-substituted benzylamines with bovine serum amine oxidase. *Biochemistry* **32**, 2234–2241
44. Djinovic, K., Gatti, G., Coda, A., Antolini, L., Pelosi, G., Desideri, A., et al. (1992) Crystal structure of yeast Cu,Zn superoxide dismutase. Crystallographic refinement at 2.5 Å resolution. *J. Mol. Biol.* **225**, 791–809.
45. Bond, C. S., Bendall, D. S., Freeman, H. C., Guss, J. M., Howe, C. J., Wagner, M. J., et al. (1999) The structure of plastocyanin from the cyanobacterium *Phormidium laminosum*. *Acta Crystallogr. D. Biol. Crystallogr.* **55**, 414–421.
46. Bordo, D., Matak, D., Djinovic-Carugo, K., Rosano, C., Pesce, A., Bolognesi, M., et al. (1999) Evolutionary constraints for dimer formation in prokaryotic Cu,Zn superoxide dismutase. *J. Mol. Biol.* **285**, 283–296.
47. Brown, K., Tegoni, M., Prudencio, M., Pereira, A. S., Besson, S., Moura, J. J., et al. (2000) A novel type of catalytic copper cluster in nitrous oxide reductase. *Nat. Struct. Biol.* **7**,191–195.
48. Brown, K., Djinovic-Carugo, K., Haltia, T., Cabrito, I., Saraste, M., Moura, J. J., et al. (2000) Revisiting the catalytic CuZ cluster of N_2O reductase: evidence of a bridging inorganic sulphur. *J. Biol. Chem.* **275**, 41,133–41,136.
49. Pesce, A., Battistoni, A., Stroppolo, M. E., Polizio, F., Nardini, M., Kroll, J. S., et al. (2000) Functional and crystallographic characterization of *Salmonella typhimurium* Cu,Zn superoxide dismutase coded by the sodCI virulence gene. *J. Mol. Biol.* **302**, 465–478.
50. Ubbink, M., Ejdeback, M., Karlsson, B. G., and Bendall, D. S. (1998) The structure of the complex of plastocyanin and cytochrome f, determined by paramagnetic NMR and restrained rigid-body molecular dynamics. *Structure* **6**, 323–335.
51. Kalverda, A. P., Wymenga, S. S., Lommen, A., van de Ven, F. J., Hilbers C. W., and Canters G. W. (1994) Solution structure of the type 1 blue copper protein amicyanin from *Thiobacillus versutus*. *J. Mol. Biol.* **240**, 358–371.
52. Banci, L., Bertini, I., Bruni, B., Carloni, P., Luchinat, C., Mangani, S., et al. (1994) X-ray, NMR and molecular dynamics studies on reduced bovine superoxide dismutase: implications for the mechanism. *Biochem. Biophys. Res. Commun.* **202**, 1088–1095.

53. Tsigelny, I., Sugiyama, N., Sine, S. M., and Taylor, P. (1997) A model of the nicotinic receptor extracellular domain based on sequence identity and residue location. *Biophys. J.* **73**, 52–66.
54. Adman, E. T., Turley, S., Bramson, R., Petratos, K., Banner, D., Tsernoglou, D., et al. (1989) A 2.0 Å structure of the blue copper protein (cupredoxin) from *Alcaligenes faecalis* S-6. *J. Biol. Chem.* **264**, 87–99.
55. Guss, J. M. and Freeman, H. C. (1983) Structure of oxidized poplar plastocyanin at 1.6 Å resolution. *J. Mol. Biol.* **169**, 521–563.
56. Chen, L. X. Q., Engh, R. A., Brunger, A. T., Nguyen, D. T., Karplus, M., and Fleming, G. R. (1988) Dynamics simulation studies of apoazurin of *Alcaligenes denitrificans*. *Biochemistry* **27**, 6908–6921.
57. Shen, J., Subramaniam, S., Wong, C. F., and McCammon, A. J. (1989) Superoxide dismutase: fluctuations in the structure and solvation of the active site channel studied by molecular dynamics simulation. *Biopolymers* **28**, 2085–2096.
58. Shen, J. and McCammon, A. J. (1991) Molecular dynamics simulation of superoxide interacting with superoxide dismutase. *Chem. Phys.* **158**, 191–198.
59. Banci, L., Carloni, P., La Penna, G., and Orioli, P. L. (1992) Molecular dynamics studies on superoxide dismutase and its mutants: the structural and functional role of Arg143. *J. Am. Chem. Soc.* **114**, 6994–7001.
60. Luty, B. A., El Amrani, S., and McCammon, A. J. (1993) Simulation of the bimolecular reaction between superoxide and superoxide dismutase: synthesis of the encounter and reaction steps. *J. Am. Chem. Soc.* **115**, 11.874–11.877.
61. Wong, Y., Clark, T. W., Shen, J., and McCammon, A. J. (1993) Molecular dynamics simulation of substrate-enzyme interactions in the active site channel of superoxide dismutase. *Mol. Simul.* **10**, 277–289.
62. Banci, L., Carloni, P., and Orioli, P. L. (1994) Molecular dynamics studies on mutants of Cu,Zn superoxide dismutase: the functional role of charged residues in the electrostatic loop VII. *Proteins* **18**, 216–230.
63. Falconi, M., Paci, E., and Gallimbeni, R. (1996) Dimer asymmetry in superoxide dismutase studied by molecular dynamics simulation. *J Computer Aided Mol. Des.* **10**, 490–498.
64. Chillemi, G. , Falconi, M., Amadei, A., Zimatore, G., Desideri, A., and Di Nola, A. (1997) The essential dynamics of Cu,Zn superoxide dismutase: suggestion of intersubunit communication. *Biophys. J.* **73**, 1007–1018.
65. Ciocchetti, A., Bizzarri, R., and Cannistraro, S. (1997) Long-term molecular dynamics simulation of copper plastocyanin in water. *Biophys. Chem.* **69**, 185–198.
66. Daizadeh, I., Medvedev, E. S., and Stuchebrukhov, A. A. (1997) Effect of protein dynamics on biological electron transfer. *Proc. Natl. Acad. Sci. USA* **94**,3703–3708.
67. Ungar, L. W., Scherer, N. F., and Voth, G. A. (1997) Classical molecular dynamics simulation of the photoinduced electron transfer dynamics of plastocyanin. *Biophys. J.* **72**, 5–17.
68. Falconi M., Venerini, F., and Desideri, A. (1998) A spectroscopic and molecular dynamics study of native and of a mutant of *Xenopus laevis* Cu,Zn superoxide dismutase: mechanistic consequences of replacing four charged aminoacids on the "electrostatic" loop. *Biophys. Chem.* **75**, 235–248.
69. Melchionna, S., Falconi, M., and Desideri, A. (1998) Effect of temperature and hydration on protein fluctuations: molecular dynamics simulation of Cu,Zn superoxide dismutase at six different temperatures. *J. Chem. Phys.* **108**, 6033–6041.
70. Falconi, M., Melchionna, S., and Desideri, A. (1999) Molecular dynamics simulations of Cu,Zn superoxide dismuta se: effect of temperature on dimer asymmetry. *Biophys. Chem.* **81**, 197–205.
71. Falconi, M., Venerini, F., and Desideri, A. (1999) Dependence of the mechanical intersubunit communication of a dimeric protein to specific mutations as revealed by molecular dynamics simulation. *J. Mol. Liquids* **84**, 29–37.
72. Paciaroni, A., Stroppolo, M. E., Arcangeli, C., Bizzarri, A. R., Desideri, A., and Cannistraro, S. (1999) Incoherent neutron scattering of copper azurin: a comparison with moleculardynamics simulation results. *Eur. Biophys. J.* **28**, 447–456.
73. Backgren, C., Hummer, G., Wikstrom, M., and Puustinen, A. (2000) Proton translocation by cytochrome c oxidase can take place without the conserved glutamic acid in subunit I. *Biochemistry* **39**, 7863–7867.
74. Banci, L., Bertini, I., Cramaro, F., Del Conte, R., Rosato, A., and Viezzoli, M. S. (2000) Backbone dynamics of human Cu,Zn superoxide dismutase and of its monomeric F50E/G51E/E133Q mutant: the influence of dimerization on mobility and function. *Biochemistry* **39**, 9108–9118.
75. Wang, C. X., Bizzarri, A. R., Xu, Y. W., and Cannistraro, S. (1994) Molecular dynamics of copper plastocyanin: simulations of structure and dynamics as a function of hydration. *Chem. Phys.* **183**, 155–166.
76. Bizzarri, A. R. and Cannistraro, S. (1996) Molecular dynamics simulation evidence of anomalous diffusion of plastocyanin hydration water. *Phys. Rev. E* **53**, 3040–3043.
77. Rocchi, C., Bizzarri, A. R., and Cannistraro, S. (1997) Water residence times around copper plastocyanin: a molecular dynamics simulation approach. *Chem. Phys.* **214**, 261–276.
78. Arcangeli, C., Bizzarri, A. R., and Cannistraro, S. (1999) Long-term molecular dynamics simulation of copper azurin: structure, dynamics and functionality. *Biophys. Chem.* **78**, 247–257.
79. Luise, A., Falconi, M., and Desideri, A. (2000) Molecular dynamics simulation of solvated azurin: influence of surface solvent accessibility on water residence times. *Proteins* **39**, 56–67.

5

The Prion Protein and Copper

What Is the Connection?

Lesley R. Brown and David A. Harris

1. INTRODUCTION

Prion diseases are neurodegenerative disorders that result from changes in the conformation of a single, highly unusual membrane glycoprotein called PrP (prion protein). This molecular transition converts a normal version of the protein (PrP^{C}) into a pathogenic form (PrP^{Sc}) that constitutes the major component of an unprecedented type of infectious particle (prion) devoid of nucleic acid. Although there is a wealth of information now available about the role of PrP^{Sc} in the disease process, relatively little is known about the normal physiological function of PrP^{C}. Aside from its intrinsic biological interest, identifying the function of PrP^{C} is likely to be important in understanding the pathogenesis of prion diseases, as it has been suggested that impairment of this function as a result of conversion to PrP^{Sc} may explain some features of the disease phenotype.

Several lines of evidence have emerged recently suggesting that PrP^{C} may play an important role in the cellular metabolism of the essential trace metal, copper. Taken together, these data constitute the most substantial clues to the normal function of PrP^{C} to emerge in the 15 yr since the protein was discovered. They suggest the hypothesis that PrP^{C} may function in cellular pathways responsible for uptake, delivery, or excretion of copper ions. There is also some evidence for an interaction between PrP^{Sc} and copper, raising the possibility that copper metabolism may be altered during prion diseases and that manipulation of copper levels may be useful in treatment of these disorders. In this chapter, we will first provide a brief overview of prion diseases and the physiological function of PrP^{C}, and then go on to summarize and evaluate the evidence for a connection between copper and the two isoforms of PrP.

2. PRION DISEASES AND PrP

The prion disorders include Creutzfeldt–Jakob disease (CJD), kuru, Gerstmann–Sträussler syndrome, and fatal familial insomnia in man, as well as scrapie and bovine spongiform encephalopathy ("mad cow disease") in animals. In man, these diseases are characterized clinically by dementia and motor dysfunction and neuropathologically by neuronal loss, spongiosis, and amyloid deposition. Infectious, inherited, and sporadic forms of prion diseases have been described. Prion diseases are of now of enormous concern from a public health standpoint because of an epidemic of bovine spongiform encephalopathy in Britain and other European countries and recent evidence that this disease has already been transmitted to human beings by consumption of contaminated beef *(1,2)*.

From: Handbook of Copper Pharmacology and Toxicology
Edited by: E. J. Massaro © Humana Press Inc., Totowa, NJ

There is also great concern that these diseases could be acquired by blood transfusion or the administration of blood-derived products.

Prion diseases have been of great interest from a scientific standpoint because they exemplify a novel mechanism of biological information transfer. The central molecular event in these disorders is the conversion of PrP^{C}, a normal cell-surface glycoprotein, into PrP^{Sc}, a conformationally altered isoform that is infectious in the absence of nucleic acid (reviewed in refs. *3* and *4*). PrP^{Sc} propagates itself by impressing its altered conformation on PrP^{C}, thereby generating additional molecules of PrP^{Sc} in an autocatalytic reaction. This conversion process is initiated by exogenous PrP^{Sc} in cases of infectious origin and occurs spontaneously in PrP molecules carrying germline mutations that are linked to inherited prion disorders. Sporadic cases are thought to be the result of spontaneous conversion of wild-type PrP^{C} molecules to the PrP^{Sc} state at a low frequency or, alternatively, to rare somatic mutations in the PrP gene. The complete structures of PrP^{C} molecules from several species have been determined by NMR techniques and consist of a flexible N-terminal domain and a folded C-terminal domain containing three α-helices *(5,6)*. Because there is not yet an experimentally defined structure for PrP^{Sc}, the precise structural differences between the two PrP isoforms remain to be determined, although it is clear that PrP^{Sc} contains significantly more β-sheets and is more protease resistant than PrP^{C}. Because PrP^{C} and PrP^{Sc} are thought to have the same amino acid sequence and differ only in their conformation, prion diseases are sometimes referred to as disorders of protein folding. Self-propagating alterations in protein conformation have been described in yeast and fungi, underscoring the generality of the prion concept in nature *(7)*.

A great deal of evidence now supports the validity of the prion hypothesis. It is clear that PrP plays a key role in the disease process and it has become increasingly difficult to explain all of the existing data by a viral theory of pathogenesis. It is important to recognize, however, that what is perhaps the most definitive test of the protein-only model has yet to be successfully carried out, producing infectivity *de novo* in a test tube by experimental manipulation of recombinant or synthetic PrP. The absence of this evidence does not invalidate the prion hypothesis, but simply underscores the difficulty of reconstituting this remarkable molecular transformation outside the cellular environment.

3. THE FUNCTION OF PRP^{C}

Although we now have a detailed picture of how PrP^{Sc} figures in the disease process, the normal biological function of PrP^{C} remains a mystery. PrP^{C} is expressed in neurons and glia of the brain and spinal cord beginning early in embryogenesis, and it is found at lower levels in many peripheral tissues *(8–10)*. Its localization on the cell surface would be consistent with roles in cell adhesion and recognition, ligand uptake, or transmembrane signaling. In addition, because PrP^{C} has been reported to be concentrated at presynaptic sites, it is possible that the protein serves some function in synaptic transmission *(11)*. Identifying the normal function of PrP^{C} may be important in understanding the pathogenesis of prion diseases, as it is possible that loss of this function as a result of conversion to PrP^{Sc} may explain some features of these disorders.

In principle, *Prn-p*$^{0/0}$ mice, in which the PrP gene has been ablated by homologous recombination, might provide clues to the normal function of PrP^{C}. However, two different lines of these mice display no gross anatomical or developmental abnormalities *(12,13)*. Several subtle phenotypic defects have been reported in these lines, including alterations in synaptic transmission *(14,15)*, ionic currents *(16,17)*, nerve fiber organization *(18)*, and circadian rhythm *(19)*. How these abnormal phenotypes might relate to the normal function of PrP^{C} is unclear. It is possible that a compensatory effect of other proteins minimizes the phenotypic effect of PrP ablation, particularly when PrP is absent throughout development. However, there are no deleterious effects on adult mice when PrP synthesis has been reduced to about 10% of normal thorough the use of a tetracycline-regulated promoter *(20)*. Several lines of *Prn-p*$^{0/0}$ mice do show a dramatic neurodegenerative phenotype, but this is now know to be the result of artifactual upregulation of the adjacent gene encoding doppel, a PrP paralog, rather than to a loss of PrP itself *(21)*.

4. COPPER AND PRP^C

There are now several kinds of experimental evidence linking copper to PrP^C and suggesting possible physiological functions for the protein.

4.1. Copper Binding

A number of studies now make it clear that PrP^C can bind copper ions. At least one set of binding sites is comprised of a tandem series of four octapeptide repeats in the N-terminal half of the protein, which, in humans, have the sequence PHGGGWGQ (Fig. 1). (A fifth octapeptide repeat lacks histidine and is not likely to be involved in copper binding.) Synthetic peptides as well as bacterially synthesized PrP molecules that encompass the histidine-containing repeats have been shown to bind copper ions based on a variety of techniques, including equilibrium dialysis, mass spectrometry, fluorescence spectroscopy, circular dichroism, Raman spectroscopy, electron paramagnetic resonance, and nuclear magnetic resonance *(22–32)*. The measured affinity with respect to total copper has been found to be 2–10 μM in most studies, but it has been pointed out that because binding experiments are usually carried out in the presence of amino acids like histidine or glycine that can themselves chelate copper, the actual affinity with respect to free copper ions may be much higher, in the range of 10^{-14} *M (27)*. Most reports now suggest a stoichiometry of one copper ion per octapeptide repeat, with positive cooperativity in the binding of four successive copper ions. There has been some debate concerning the structure of the metal–protein-binding site, although it appears likely that nitrogen atoms in histidine side chains as well as in glycine backbone amides serve as coordination centers. Copper binding to the octapeptide repeats is specific for copper over other transition metals and is pH dependent, with affinity falling sharply below pH 6.0. Recent evidence suggests that there is likely to be a fifth copper binding site in PrP, probably involving histidine residues 96 and/or 111, although this site remains to be thoroughly characterized *(27,28)*. There are also reports that several additional binding sites may exist in more C-terminal regions of the protein *(24,33)*.

An important question is whether copper binds to PrP^C in vivo and whether the affinity, stoichiometry, and specificity are the same as for binding of the metal to recombinant PrP and synthetic peptides. It is possible, for example, that the presence of posttranslational modifications such as N-linked oligosaccharides and the C-terminal glycolipid anchor modify the copper binding properties of the protein. It has been claimed that PrP^C immunopurified from brain or cell lysates does, in fact, contain bound copper ions *(34)*, but these data must be viewed with caution, because a micromolar affinity is not likely to be sufficient to retain the metal during the immunopurification step.

4.2. Changes in Molecular and Biochemical Properties

Several spectroscopic studies suggest that binding of copper induces a conformational change in PrP^C, favoring the formation of β-sheets *(26,30,35–38)*. At least part of this effect is likely to involve structural changes in the normally flexible N-terminal part of the protein containing the copper-binding octapeptide repeats. These results are consistent with the hypothesis that binding of copper to PrP^C triggers a functional change in the molecule that is related to its physiological purpose.

Copper also causes alterations in the biochemical properties of PrP^C. We have found that the metal rapidly and reversibly causes PrP^C in lysates of brain tissue and transfected cells to become detergent insoluble and protease resistant, properties normally associated with PrP^{Sc} *(39)* (Fig. 2). However, the copper-treated form of PrP^C is distinct from PrP^{Sc}, because it still reacts in the native state with the monoclonal antibody 3F4, the epitope for which is buried in PrP^{Sc}. These effects of copper on the biochemical properties of PrP^C require the presence of at least one histidine-containing octapeptide repeat, consistent with direct binding of metal to the protein. Copper has also been reported to induce protease resistance in purified recombinant PrP, although this effect required deamidation of the protein, and the protease cleavage site observed was distinct from the one seen after metal treatment

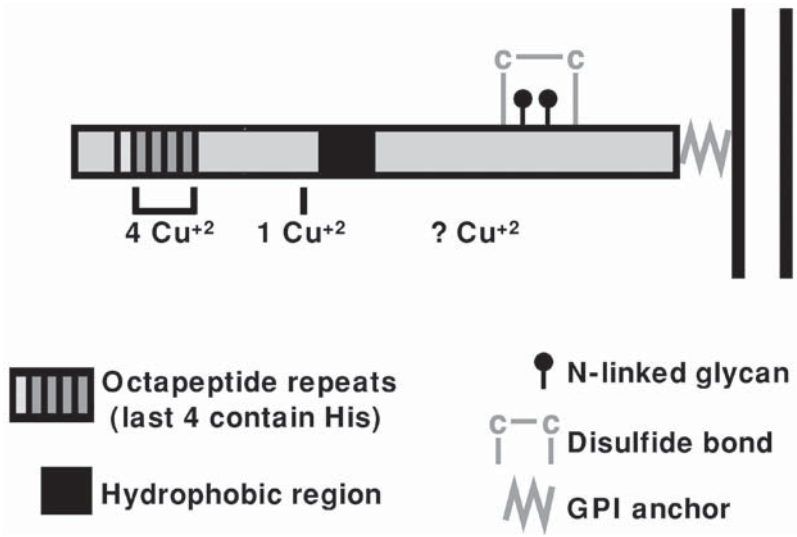

Fig. 1. Schematic structure of mammalian PrP^C. The likely positions of the copper binding sites are indicated.

of brain- and cell-derived protein (37). Copper also causes aggregation of a synthetic peptide derived from residues 106–126 of PrP, thereby enhancing its toxicity to cultured neurons *(40)*. Finally, copper has been found to produce covalent modifications of PrP^C. The metal causes oxidation of recombinant PrP, involving either methionine or histidine residues *(41,42)* and also induces a cleavage of the N-terminus of the protein in the presence of hydrogen peroxide *(43)*.

4.3. Enzymatic Activity

Several recent studies have suggested that PrP^C may function as a cuproenzyme. Recombinant PrP refolded in the presence of copper has been reported to exhibit a superoxide dismutase (SOD) activity, as did PrP^C immunoprecipitated from brain tissue *(34,44–47)*. This enzymatic activity depended on the presence of the octapeptide repeats as well as on bound copper ions and was not affected by KCN, thus distinguishing it from the activity of Cu–Zn SOD. In addition, immunodepletion of PrP^C from brain extracts was found to cause a reduction in SOD activity *(48)*.

Although it would be certainly intriguing if PrP^C functioned as an SOD-like enzyme, the biological significance of these results is uncertain for several reasons. First, the enzymatic activity measured for recombinant PrP depended on refolding the protein from a denatured state in the presence of 5 m*M* copper, which is a highly supraphysiological concentration and is inconsistent with the ability of micromolar concentrations of the metal to bind to the octapeptide repeats of the protein after it has already been folded. Second, even small organic molecules like amino acids can bind copper and exhibit weak dismutase activity, calling into question whether the protein moiety contributes at all to the SOD activity measured for PrP^C. Finally, copper binds much more weakly to PrP^C than to known cuproenzymes like Cu–Zn SOD, which must be denatured to remove bound metal, arguing against the possibility that the copper plays a specific catalytic role in PrP^C.

Whether PrP^C displays other copper-dependent enzymatic activities is unclear. There are two reports that the octapeptide repeat region of PrP can function as a copper reductase, an activity that depended on the presence of tryptophan residues *(49,50)*. In contrast, another study indicated that rather than being subject to reduction, Cu(II) bound to the octapeptide repeats is maintained in a redox-inactive state *(51)*. These reports have yet to be followed up.

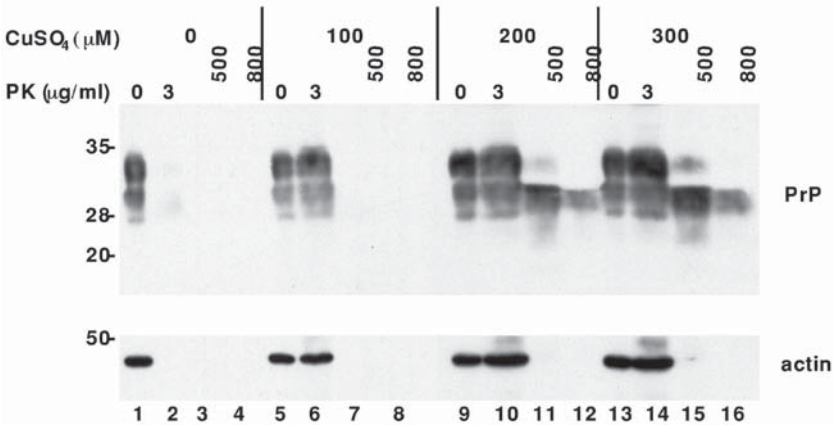

Fig. 2. Cu^{2+} causes PrP to become proteinase K resistant. Detergent extracts of mouse brain were incubated with the indicated concentrations of $CuSO_4$ for 30 min and then digested with different amounts of proteinase K (PK) for 30 min at 37°C. After termination of the digestion with PMSF, proteins were separated by sodium dodecyl sulfate-polyacrylamide gel electrophoresis and immunoblotted with either anti-PrP antibody or with anti-actin antibody. The lanes containing undigested samples (0 μg/mL PK) represent 8 μg of protein, and the other lanes represent 40 μg of protein. (Reprinted from ref. *39*.)

4.4. Cellular Trafficking

Our previous studies revealed that PrP^C constitutively cycles between the plasma membrane and an early endocytic compartment in neuronal cells, with clathrin-coated pits mediating endocytic uptake of the protein *(52,53)*. We have found that copper causes a dramatic alteration in this cellular trafficking pathway (*54*; L. R. Brown and D. A. Harris, unpublished). Initially, we observed that incubation of cells with Cu^{2+} concentrations above 100 μ*M* for 30–90 min caused a marked reduction in the total amount of PrP^C on the cell surface, as determined by biotinylation or by immunofluorescence staining. This effect was also seen with Zn^{2+}, but not with Co^{2+}, Mn^{2+}, Cd^{2+}, Ni^{2+}, or Fe^{2+}. The effect, which was observed for mammalian as well as chicken PrP^C expressed in neuroblastoma cells, was temperature dependent (it did not occur at 4°C) and was rapidly reversible (within minutes). Neither copper nor zinc had any effect on the distribution of the transferrin receptor, suggesting that the metals were not causing a generalized stimulation of endocytosis.

Several lines of evidence indicated that the primary effect of copper is to stimulate the endocytosis of PrP^C, with relatively little change in the rate of recycling. To measure endocytosis and recycling, we used biochemical methods to follow the internalization of surface PrP^C molecules that had been labeled by iodination or biotinylation *(54)*. Alternatively, we used immunocytochemical techniques to visualize the metal-induced redistribution of surface PrP^C molecules that had been prelabeled with anti-PrP antibodies (L. R. Brown and D. A. Harris, unpublished). We found that the antibody-tagged protein was translocated from the cell surface to punctate intracellular compartments in the presence of copper (Fig. 3). The internalized PrP^C partially colocalized with both fluorescent transferrin and fluorescent wheat germ agglutinin, but not with LysoTracker (a fluorescent lysosomotropic amine), implying that the protein was being delivered to early endosomes and the Golgi, but not to lysosomes.

Copper-induced endocytosis of PrP^C depends on the presence of the histidine-containing repeats, implying that the effect is the result of binding of the metal to PrP^C rather to some other cellular protein that indirectly modulates endocytosis. Chicken or mouse PrP^C molecules in which the repeats have been deleted or the critical histidine residues mutated are poorly endocytosed in response to copper *(54,55)*. Interestingly, an insertionally mutated form of PrP containing 14 octapeptide repeats

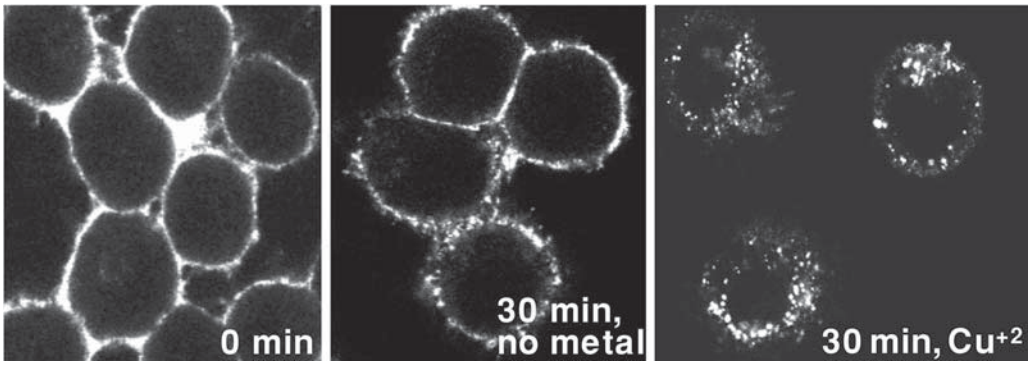

Fig. 3. Copper causes endocytosis of antibody-labeled PrP^C. N2a cells expressing chicken PrP were labeled with PrP antibody at 4°C (left panel) and were then warmed to 37°C for 30 min either in the absence of metal (middle panel) or in the presence of 250 μ*M* CuSO4 (right panel).

that is associated with familial Creutzfeldt–Jakob disease is also refractory to copper-induced endocytosis *(55)*, implying that the normal complement of five repeats is necessary for optimal copper binding or for whatever structural change the metal induces that triggers endocytosis. We have hypothesized that copper binding may enhance the affinity of PrP^C for a putative receptor on the cell surface that is required for targeting to clathrin-coated pits *(54)*.

4.5. Copper Content of Cells and Tissues

An initial report indicated that the content of copper, but not of several other transition metals, is only 10% of normal in crude membranes, synaptosomes, and endosomes derived from the brains of *Prn-p*$^{0/0}$ mice, which carry a disrupted PrP gene *(23)*. Moreover, removal of surface PrP^C from wild-type cerebellar neurons using a phospholipase dramatically reduced the membrane copper content. Copper content was determined in these experiments using X-ray fluorescence and atomic absorption spectroscopy. A subsequent study from the same authors *(11)* reported that synaptosomes from *Prn-p*$^{0/0}$ mice had a copper content that was 50% of the wild-type level, a considerably smaller difference than in the original report. Based on these results, the authors proposed that PrP^C may play a role in regulating copper release at the synapse *(56)*.

We have re-examined this subject, using mass spectrometry to measure the concentrations of several transition metals in brain tissue from wild-type and *Prn-p*$^{0/0}$ mice, as well as in Tga20 mice that overexpress PrP by 10-fold. We were unable to find any differences in metal content in either whole brain or of several subcellular fractions among mice of these three genotypes *(57)* and we believe that the results of Brown and colleagues *(11,23)* are likely to be in error.

4.6. Oxidative Stress

A number of pieces of evidence suggest that PrP^C may play a role in protecting cells from oxidative stress and this function has been proposed to involve the ability of the protein to bind copper (reviewed in ref. *56*). The most direct evidence for a protective role of PrP^C is the observation that neurons cultured from the brains of *Prn-p*$^{0/0}$ mice are more susceptible to oxidative stress induced by several different agents, including xanthine oxidase, copper, and hydrogen peroxide *(58–60)*. Conversely, PC12 cells selected for resistance to oxidative stress (or resistance to copper toxicity) have higher levels of PrP^C *(61)*. In addition, several studies suggest that protein and lipid markers of oxidative stress are increased in brain tissue from *Prn-p*$^{0/0}$ mice *(62,63)*.

How might PrP^C contribute to protection from oxidative stress? Certainly, one possible explanation would be that the protein itself possesses a copper-dependent SOD activity, which could protect

cells from superoxide radicals generated in the extracellular space, by analogy to the role of cytoplasmic Cu–Zn SOD. As discussed earlier, however, we feel that the reported SOD-like activity of copper-refolded PrP^C is unlikely to be physiologically significant. Another suggested hypothesis is that PrP^C is important for the delivery of copper ions to Cu–Zn SOD. It has been reported that the enzymatic activity and the ^{64}Cu loading of Cu–Zn SOD from the brains of *Prn-p*$^{0/0}$ mice is 10–50% of normal *(59,62,64)*. Conversely, it has been claimed that the activity and copper loading of Cu–Zn SOD are increased in PrP-overexpressing mice. However, as shown in Fig. 4, we have been unable to replicate these two sets of results *(57)*. The activities of other antioxidant enzymes such as catalase and glutathione reductase have been reported to be decreased in *Prn-p*$^{0/0}$ mice *(60,62)*, but whether PrP^C plays a direct role in regulating these molecules remains to be determined. At this point, then, the mechanism by which PrP^C protects cells from oxidative stress and whether this process involves binding of copper ions remain uncertain.

5. COPPER AND PrP^{Sc}

There are now several results that suggest a connection between copper and PrP^{Sc}, the pathogenic isoform of PrP. First, copper facilitates restoration of protease resistance and infectivity during refolding of guanidine-denatured PrP^{Sc} *(65)*. Second, the protease cleavage pattern of PrP^{Sc} derived from the brains of CJD patients is altered by addition of metal-chelating agents and by the readdition of copper and zinc in micromolar concentrations *(66)*. In fact, the cleavage patterns of two different PrP^{Sc} subtypes, corresponding to distinct prion strains, can be interconverted by manipulation of their bound metal. These effects of copper may not be the result of direct binding of the metal to PrP^{Sc}, because it has been reported that, in contrast to PrP^C, PrP^{Sc} does not bind to a copper-loaded affinity column (*67*). In fact, it is possible that loss of metal binding by PrP could play a role in prion-induced pathology. Finally, it was reported almost 25 yr ago that administration of the copper-chelating agent cuprizone to mice caused a spongiform degeneration of the brain similar to scrapie (*68*). Altogether, these results suggest that alterations in copper metabolism could play some role in the pathogenesis of prion diseases and even raise the possibility that manipulation of copper levels could represent a therapeutic modality.

6. CONCLUSIONS

A considerable body of data now indicates some connection between PrP and copper ions. How is one to evaluate this evidence, some of which has proven to be controversial, and what is its biological significance? First, we will address the possible role of copper in the physiological function of PrP^C. Probably the most compelling and widely agreed upon observation is that copper ions bind to PrP^C. It is clear that the histidine-containing octapeptide repeats represent one set of binding sites and that additional binding sites in more C-terminal locations also exist. Although there has been debate about the absolute value of the binding constants, it seems clear that PrP^C binds copper with an affinity that is considerably lower than that of *bona fide* cuproenzymes like Cu–Zn SOD and ceruloplasmin, which need to be denatured to remove their bound metal. Thus, it is unlikely that copper serves an enzymatic function in PrP^C, such as catalyzing the dismutation of superoxide anions. Rather, the affinity of PrP^C for copper is similar to that of amino acids, peptides, and proteins like albumin in the extracellular medium. Thus, it seems most likely that the role of PrP^C involves the reversible binding of copper ions that have been transferred from other extracellular ligands. Consistent with this idea, the total concentration of Cu^{2+} in plasma and cerebrospinal fluid (1–10 μM) is similar to the estimated K_d for copper binding to PrP^C and the concentration of the metal in brain tissue is estimated to be even higher (100 μM) *(69)*.

Our observation that copper stimulates the endocytosis of PrP^Csuggests the hypothesis that PrP^C functions as a recycling receptor for the cellular uptake or efflux of copper ions. In an uptake model, PrP^C on the plasma membrane binds Cu^{2+} via the peptide repeats and then delivers the metal by endocytosis to an acidic, endosomal compartment. Copper ions then dissociate from PrP^C by virtue of the

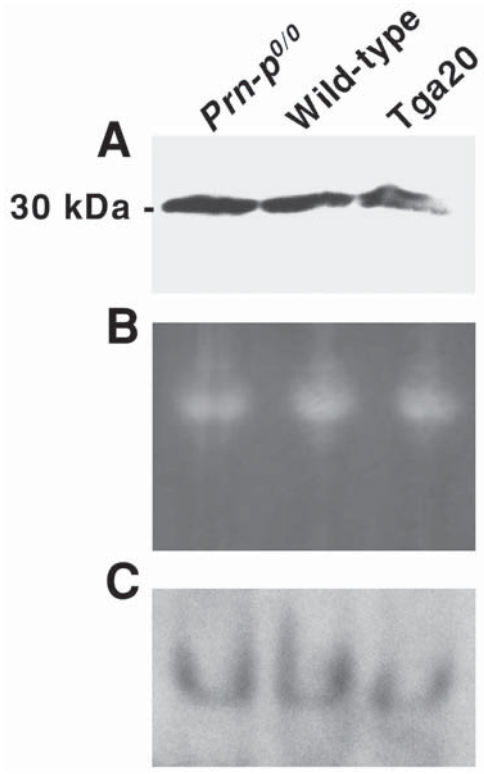

Fig. 4. Cu-Zn SOD protein, activity, and copper incorporation are similar in cultures of cerebellar neurons from *Prn-p*$^{0/0}$, wild-type, and Tga20 mice. Lysates of cerebellar cultures were subjected to electrophoresis on a 10% polyacrylamide gel under nondenaturing conditions. **(A)** Western blot analysis of lysates using an antiserum against Cu–Zn SOD; **(B)** gel-based assay for SOD activity was performed using nitro blue tetrazolium; **(C)** autoradiography of lysates from ^{64}Cu-labeled cultures. (Reprinted from ref. *57*.)

low endosomal pH and, after reduction to Cu^{1+}, are transported into the cytoplasm by a transmembrane transporter. PrP^C subsequently returns to the cell surface to bind additional copper, and the cycle is repeated. This proposed function for PrP^C is analogous to that of the transferrin receptor in uptake of iron, with the exception that metal ions bind directly to the receptor in the case of PrP^C rather than to a protein carrier comparable to transferrin. In a second model, PrP^C serves as a receptor that facilitates cellular efflux of copper via the secretory pathway. PrP^C is first delivered via endosomal vesicles to the trans-Golgi network or other post-Golgi compartments, and it then serves to bind copper ions that have been pumped into these compartments during transit to the cell surface in secretory vesicles. In addition to acting as a carrier for copper ions, PrP^C could also play a role in specifically transferring the metal from the Menkes or Wilson transporters to secreted cuproproteins such as ceruloplasmin by physically interacting with these molecules. Our immunocytochemical localization of copper-internalized PrP^C in both endosomes and the Golgi is consistent with either an uptake or efflux model.

It remains to be proven whether these models, or other ones, will turn out to be correct. The fact that, in our hands, the copper content of brain fractions from *Prn-p*$^{0/0}$ mice is normal *(57)* would seem to indicate that if PrP^C is involved in cellular uptake or efflux of copper, it is not likely to represent the primary or major pathway. Rather, PrP^C may be part of a more specialized copper trafficking pathway. This conclusion is also consistent with our observation (at variance with ref. *70*) that cells expressing different amounts of PrP^C do not show obvious differences in net uptake of ^{64}Cu (Pauly

and Harris, unpublished data). In addition, the fact that *Prn-p*$^{0/0}$ mice do not, in our experiments, have reduced Cu–Zn SOD or cytochrome oxidase levels *(57)* suggests that PrP^{C} is not involved in the specialized pathways involved in copper delivery to these two cuproenzymes. Because several pieces of evidence indicate that neurons from *Prn-p*$^{0/0}$ mice are more susceptible to oxidative stress, it is possible that PrP^{C}-mediated copper uptake plays a role in delivery of the metal to other enzymes capable of protecting cells from oxidative damage.

Finally, it is possible that copper plays some role in prion diseases. Alterations in metal metabolism are known to be involved in the pathogenesis of several other neurodegenerative disorders *(71)*. Although the primary pathology in prion diseases is likely to be the result of a toxic effect of PrP^{Sc} or some other abnormal form of PrP (*77*), it is possible that loss of a copper-related function of PrP^{C} contributes in an ancillary way to the disease phenotype (e.g., via oxidative damage or abnormalities in metal trafficking) *(72–74)*. In addition, copper may play a role in the conversion of PrP^{C} to PrP^{Sc}. The fact that copper-treated PrP is protease resistant but reactive with 3F4 monoclonal antibody raises the possibility that this form of the protein represents a physical state that is intermediate between that of PrP^{C} and PrP^{Sc}. Thus, some additional biochemical alteration might convert copper-bound PrP fully and irreversibly to the scrapie form. Intermediate states of PrP have been postulated on the basis of theoretical considerations *(75)*, and PrP species that are distinct from both PrP^{C} and PrP^{Sc} have been postulated to be the primary neurotoxic species in some prion diseases *(76,77)*. It is thus possible to envisage that copper either initiates or modulates the production of pathogenic PrP molecules in prion diseases and that manipulation of copper levels may represent a strategy for treating these disorders.

ACKNOWLEDGMENT

The authors were supported by a fellowship (L.R.B.) and a grant (D.A.H.) from the NIH.

REFERENCES

1. Collinge, J. (1999) Variant Creutzfeldt-Jakob disease. *Lancet* **354**, 317–323.
2. Weissmann, C. and Aguzzi, A. (1997) Bovine spongiform encephalopathy and early onset variant Creutzfeldt–Jakob disease. *Curr. Opin. Neurobiol.* **7**, 695–700.
3. Collinge, J. (2001) Prion diseases of humans and animals: their causes and molecular basis. *Annu. Rev. Neurosci.* **24**, 519–550.
4. Prusiner, S. B. (1998) Prions. *Proc. Natl. Acad. Sci. USA* **95**, 13,363–13,383.
5. Liu, H., Farr-Jones, S., Ulyanov, N. B., Llinas, M., Marqusee, S., Groth, et al. (1999) Solution structure of Syrian hamster prion protein rPrP(90-231). *Biochemistry* **38**, 5362–5377.
6. Riek, R., Hornemann, S., Wider, G., Glockshuber, R., and Wüthrich, K. (1997) NMR characterization of the full-length recombinant murine prion protein, mPrP(23-231). *FEBS Lett.* **413**, 282–288.
7. Wickner, R. B., Edskes, H. K., Maddelein, M. L., Taylor, K. L., and Moriyama, H. (1999) Prions of yeast and fungi: proteins as genetic material. *J. Biol. Chem.* **274**, 555–558.
8. Harris, D. A., Lele, P., and Snider, W. D. (1993) Localization of the mRNA for a chicken prion protein by in situ hybridization. *Proc. Natl. Acad. Sci. USA* **90**, 4309–4313.
9. Manson, J., West, J. D., Thomson, V., McBride, P., Kaufman, M. H., and Hope, J. (1992) The prion protein gene: a role in mouse embryogenesis? *Development* **115**, 117–122.
10. Moser, M., Colello, R. J., Pott, U., and Oesch, B. (1995) Developmental expression of the prion protein gene in glial cells. *Neuron* **14**, 509–517.
11. Herms, J., Tings, T., Gall, S., Madlung, A., Giese, A., Siebert, H., et al. (1999) Evidence of presynaptic location and function of the prion protein. *J. Neurosci.* **19**, 8866–8875.
12. Büeler, H., Fischer, M., Lang, Y., Fluethmann, H., Lipp, H.-P., DeArmond, S. J., et al. (1992) Normal development and behavior of mice lacking the neuronal cell-surface PrP protein. *Nature* **356**, 577–582.
13. Manson, J. C., Clarke, A. R., Hooper, M. L., Aitchison, L., McConnell, I., and Hope, J. (1994) 129/Ola mice carrying a null mutation in PrP that abolishes mRNA production are developmentally normal. *Mol. Neurobiol.* **8**, 121–127.
14. Collinge, J., Whittington, M. A., Sidle, K. C., Smith, C. J., Palmer, M. S., Clarke, A. R., et al. (1994) Prion protein is necessary for normal synaptic function. *Nature* **370**, 295–297.
15. Manson, J. C., Hope, J., Clarke, A. R., Johnston, A., Black, C., and MacLeod, N. (1995) PrP gene dosage and long term potentiation. *Neurodegeneration* **4**, 113–114.
16. Colling, S. B., Collinge, J., and Jefferys, J. G. R. (1996) Hippocampal slices from prion protein null mice: disrupted Ca^{2+}-activated K^{+} currents. *Neurosci. Lett.* **209**, 49–52.

17. Herms, J. W., Tings, T., Dunker, S., and Kretzschmar, H. A. (2001) Prion protein affects Ca^{2+}-activated K^+ currents in cerebellar Purkinje cells. *Neurobiol. Dis.* **8**, 324–330.
18. Colling, S. B., Khana, M., Collinge, J., and Jefferys, J. G. R. (1997) Mossy fibre reorganization in the hippocampus of prion protein null mice. *Brain Res.* **755**, 28–35.
19. Tobler, I., Gaus, S. E., Deboer, T., Achermann, P., Fischer, M., Rulicke, T., et al. (1996) Altered circadian activity rhythms and sleep in mice devoid of prion protein. *Nature* **380**, 639–642.
20. Tremblay, P., Meiner, Z., Galou, M., Heinrich, C., Petromilli, C., Lisse, T., et al. (1998) Doxycycline control of prion protein transgene expression modulates prion disease in mice. *Proc. Natl. Acad. Sci. USA* **95**, 12,580–12,585.
21. Weissmann, C. and Aguzzi, A. (1999) PrP's double causes trouble. *Science* **286**, 914–915.
22. Aronoff-Spencer, E., Burns, C. S., Avdievich, N. I., Gerfen, G. J., Peisach, J., Antholine, W. E., et al. (2000) Identification of the Cu^{2+} binding sites in the N-terminal domain of the prion protein by EPR and CD spectroscopy. *Biochemistry* **39**, 13,760–13,771.
23. Brown, D. R., Qin, K. F., Herms, J. W., Madlung, A., Manson, J., Strome, R., et al. (1997) The cellular prion protein binds copper in vivo. *Nature* **390**, 684–687.
24. Cereghetti, G. M., Schweiger, A., Glockshuber, R., and Van Doorslaer, S. (2001) Electron paramagnetic resonance evidence for binding of Cu^{2+} to the C-terminal domain of the murine prion protein. *Biophys. J.* **81**, 516–525.
25. Hornshaw, M. P., McDermott, J. R., and Candy, J. M. (1995) Copper binding to the N-terminal tandem repeat regions of mammalian and avian prion protein. *Biochem. Biophys. Res. Commun.* **207**, 621–629.
26. Hornshaw, M. P., McDermott, J. R., Candy, J. M., and Lakey, J. H. (1995) Copper binding to the N-terminal tandem repeat region of mammalian and avian prion protein: structural studies using synthetic peptides. *Biochem. Biophys. Res. Commun.* **214**, 993–999.
27. Jackson, G. S., Murray, I., Hosszu, L. L., Gibbs, N., Waltho, J. P., Clarke, A. R., and Collinge, J. (2001) Location and properties of metal-binding sites on the human prion protein. *Proc. Natl. Acad. Sci. USA* **98**, 8531–8535.
28. Kramer, M. L., Kratzin, H. D., Schmidt, B., Romer, A., Windl, O., Liemann, S., et al. (2001) Prion protein binds copper within the physiological concentration range. *J. Biol. Chem.* **276**, 16.711–16.719.
29. Miura, T., Hori-i, A., Mototani, H., and Takeuchi, H. (1999) Raman spectroscopic study on the copper(II) binding mode of prion octapeptide and its pH dependence. *Biochemistry* **38**, 11,560–11,569.
30. Stöckel, J., Safar, J., Wallace, A. C., Cohen, F. E., and Prusiner, S. B. (1998) Prion protein selectively binds copper(II) ions. *Biochemistry* **37**, 7185–7193.
31. Viles, J. H., Cohen, F. E., Prusiner, S. B., Goodin, D. B., Wright, P. E., and Dyson, H. J. (1999) Copper binding to the prion protein: structural implications of four identical copper binding sites. *Proc. Natl. Acad. Sci. USA* **96**, 2042–2047.
32. Whittal, R. M., Ball, H. L., Cohen, F. E., Burlingame, A. L., Prusiner, S. B., and Baldwin, M. A. (2000) Copper binding to octarepeat peptides of the prion protein monitored by mass spectrometry. *Protein Sci.* **9**, 332–343.
33. Van Doorslaer, S., Cereghetti, G. M., Glockshuber, R., and Schweiger, A. (2001) Unraveling the Cu^{+2} binding sites in the C-terminal domain of the murine prion protein: a pulse EPR and ENDOR study. *J. Phys. Chem. B* **105**, 1631–1639.
34. Brown, D. R., Clive, C., and Haswell, S. J. (2001) Antioxidant activity related to copper binding of native prion protein. *J. Neurochem.* **76**, 69–76.
35. Marcotte, E. M. and Eisenberg, D. (1999) Chicken prion tandem repeats form a stable, protease-resistant domain. *Biochemistry* **38**, 667–676.
36. Miura, T., Horii, A., and Takeuchi, H. (1996) Metal-dependent alpha-helix formation promoted by the glycine-rich octapeptide region of prion protein. *FEBS Lett.* **396**, 248–252.
37. Qin, K., Yang, D.-S., Yang, Y., Chishti, M. A., Meng, L.-J., Kretzschmar, H. A., et al. (2000) Copper(II)-induced conformational changes and protease resistance in recombinant and cellular PrP. Effect of protein age and deamidation. *J. Biol. Chem.* **275**, 19,121–19,131.
38. Wong, B. S., Venien-Bryan, C., Williamson, R. A., Burton, D. R., Gambetti, P., Sy, M.-S., et al. (2000) Copper refolding of prion protein. *Biochem. Biophys. Res. Commun.* **276**, 1217–1224.
39. Quaglio, E., Chiesa, R., and Harris, D. A. (2001) Copper converts the cellular prion protein into a protease-resistant species that is distinct from the scrapie isoform. *J. Biol. Chem.* **276**, 11,432–11,438.
40. Jobling, M. F., Huang, X., Stewart, L. R., Barnham, K. J., Curtain, C., Volitakis, I., et al. (2001) Copper and zinc binding modulates the aggregation and neurotoxic properties of the prion peptide PrP106–126. *Biochemistry* **40**, 8073–8084.
41. Requena, J. R., Groth, D., Legname, G., Stadtman, E. R., Prusiner, S. B., and Levine, R. L. (2001) Copper-catalyzed oxidation of the recombinant SHa(29–231) prion protein. *Proc. Natl. Acad. Sci. USA* **98**, 7170–7175.
42. Wong, B. S., Wang, H., Brown, D. R., and Jones, I. M. (1999) Selective oxidation of methionine residues in prion proteins. *Biochem. Biophys. Res. Commun.* **259**, 352–355.
43. McMahon, H. E. M., Mangé, A., Nishida, N., Créminon, C., Casanova, D., and Lehmann, S. (2001) Cleavage of the amino terminus of the prion protein by reactive oxygen species. *J. Biol. Chem.* **276**, 2286–2291.
44. Brown, D. R., Hafiz, F., Glasssmith, L. L., Wong, B. S., Jones, I. M., Clive, C., et al. (2000) Consequences of manganese replacement of copper for prion protein function and proteinase resistance. *EMBO J.* **19**, 1180–1186.
45. Brown, D. R., Iordanova, I. K., Wong, B. S., Venien-Bryan, C., Hafiz, F., Glasssmith, L. L., et al. (2000) Functional and structural differences between the prion protein from two alleles *prnp*^{a} and *prnp*^{b} of mouse. *Eur. J. Biochem.* **267**, 2452–2459.
46. Brown, D. R., Wong, B.-S., Hafiz, F., Clive, C., Haswell, S. J., and Jones, I. M. (1999) Normal prion protein has an activity like that of superoxide dismutase. *Biochem. J.* **344**, 1–5.

47. Wong, B. S., Clive, C., Haswell, S. J., Williamson, R. A., Burton, D. R., Gambetti, P., et al. (2000) Copper has differential effect on prion protein with polymorphism of position 129. *Biochem. Biophys. Res. Commun.* **269**, 726–731.
48. Wong, B. S., Pan, T., Liu, T., Li, R., Gambetti, P., and Sy, M. S. (2000) Differential contribution of superoxide dismutase activity by prion protein *in vivo*. *Biochem. Biophys. Res. Commun.* **273**, 136–139.
49. Huang, H., Hartshorn, M. A., Atwood, C. S., Farrag, Y. W., Multhaup, G., Tanzi, R. E., et al. (1999) Redox interactions between Cu(II) and prion protein fragments. *Soc. Neurosci. Abstr.* **25**, 41.
50. Ruiz, F. H., Silva, E., and Inestrosa, N. C. (2000) The N-terminal tandem repeat region of human prion protein reduces copper: role of tryptophan residues. *Biochem. Biophys. Res. Commun.* **269**, 491–495.
51. Shiraishi, N., Ohta, Y., and Nishikimi, M. (2000) The octapeptide repeat region of prion protein binds Cu(II) in the redox-inactive state. *Biochem. Biophys. Res. Commun.* **267**, 398–402.
52. Shyng, S. L., Heuser, J. E., and Harris, D. A. (1994) A glycolipid-anchored prion protein is endocytosed via clathrin-coated pits. *J. Cell Biol.* **125**, 1239–1250.
53. Shyng, S. L., Huber, M. T., and Harris, D. A. (1993) A prion protein cycles between the cell surface and an endocytic compartment in cultured neuroblastoma cells. *J. Biol. Chem.* **268**, 15,922–15,928.
54. Pauly, P. C. and Harris, D. A. (1998) Copper stimulates endocytosis of the prion protein. *J. Biol. Chem.* **273**, 33,107–33,110.
55. Perera, W. S. and Hooper, N. M. (2001) Ablation of the metal ion-induced endocytosis of the prion protein by disease-associated mutation of the octarepeat region. *Curr. Biol.* **11**, 519–523.
56. Brown, D. R. (2001) Prion and prejudice: normal protein and the synapse. *Trends Neurosci.* **24**, 85–90.
57. Waggoner, D. J., Drisaldi, B., Bartnikas, T. B., Casareno, R. L. B., Prohaska, J. R., Gitlin, J. D., et al. (2000) Brain copper content and cuproenzyme activity do not vary with prion protein expression level. *J. Biol. Chem.* **275**, 7455–7458.
58. Brown, D. R., Schmidt, B., and Kretzschmar, H. A. (1998) Effects of copper on survival of prion protein knockout neurons and glia. *J. Neurochem.* **70**, 1686–1693.
59. Brown, D. R., Schulzschaeffer, W. J., Schmidt, B., and Kretzschmar, H. A. (1997) Prion protein-deficient cells show altered response to oxidative stress due to decreased SOD-1 activity. *Exp. Neurol.* **146**, 104–112.
60. White, A. R., Collins, S. J., Maher, F., Jobling, M. F., Stewart, L. R., Thyer, J. M., et a;. (1999) Prion protein-deficient neurons reveal lower glutathione reductase activity and increased susceptibility to hydrogen peroxide toxicity. *Am. J. Pathol.* **155**, 1723–1730.
61. Brown, D. R., Schmidt, B., and Kretzschmar, H. A. (1997) Effects of oxidative stress on prion protein expression in PC12 cells. *Int. J. Dev. Neurosci.* **15**, 961–972.
62. Klamt, F., Dal-Pizzol, F., Conte da Frota, M. L., Walz, R., Andrades, M. E., da Silva, E. G., et al. (2001) Imbalance of antioxidant defense in mice lacking cellular prion protein. *Free Radical Biol. Med.* **30**, 1137–1144.
63. Wong, B. S., Liu, T., Li, R., Pan, T., Petersen, R. B., Smith, M. A., et al. (2001) Increased levels of oxidative stress markers detected in the brains of mice devoid of prion protein. *J. Neurochem.* **76**, 565–572.
64. Brown, D. R. and Besinger, A. (1998) Prion protein expression and superoxide dismutase activity. *Biochem. J.* **334**, 423–429.
65. McKenzie, D., Bartz, J., Mirwald, J., D., O., Marsh, R., and Aiken, J. (1998) Reversibility of scrapie inactivation is enhanced by copper. *J. Biol. Chem.* **273**, 25,545–25,547.
66. Wadsworth, J. D. F., Hill, A. F., Joiner, S., Jackson, G. S., Clarke, A. R., and Collinge, J. (1999) Strain-specific prion-protein conformation determined by metal ions. *Nature Cell Biol.* **1**, 55–59.
67. Shaked, Y., Rosenmann, H., Hijazi, N., Halimi, M., and Gabizon, R. (2001) Copper binding to the prp isoforms: a putative marker of their conformation and function. *J. Virol.* **75**, 7872–7874.
68. Pattison, I. H., and Jebbett, J. N. (1971) Histopathological similarities between scrapie and cuprizone toxicity in mice. *Nature* **230**, 115–117.
69. Smith, R. M. (1983) Copper in the developing brain, in *Neurobiology of the Trace Elements* (Dreosti, I. E. and Smith, R. M., eds.), Humana Press, Totowa, NJ, Vol. 1, pp. 1–40.
70. Brown, D. R. (1999) Prion protein expression aids cellular uptake and veratridine-induced release of copper. *J. Neurosci. Res.* **58**, 717–725.
71. Sayre, L. M., Perry, G., Atwood, C. S., and Smith, M. A. (2000) The role of metals in neurodegenerative diseases. *Cell. Mol. Biol.* **46**, 731–741.
72. Guentchev, M., Voigtlander, T., Haberler, C., Groschup, M. H., and Budka, H. (2000) Evidence for oxidative stress in experimental prion disease. *Neurobiol. Dis.* **7**, 270–273.
73. Milhavet, O., McMahon, H. E., Rachidi, W., Nishida, N., Katamine, S., Mange, A., et al. (2000) Prion infection impairs the cellular response to oxidative stress. *Proc. Natl. Acad. Sci. USA* **97**, 13,937–13,942.
74. Wong, B. S., Pan, T., Liu, T., Li, R., Petersen, R. B., Jones, I. M., Gambetti, P., et al. (2000) Prion disease: A loss of antioxidant function? *Biochem. Biophys. Res. Commun.* **275**, 249–252.
75. Cohen, F. E. and Prusiner, S. B. (1998) Pathologic conformations of prion proteins. *Annu. Rev. Biochem.* **67**, 793-819.
76. Hegde, R. S., Tremblay, P., Groth, D., DeArmond, S. J., Prusiner, S. B., and Lingappa, V. R. (1999) Transmissible and genetic prion diseases share a common pathway of neurodegeneration. *Nature* **402**, 822–826.
77. Chiesa, R. and Harris, D. A. (2001) Prion diseases: what is the neurotoxic molecule? *Neurobiol. Dis.* **8**, 743–763.

6

Prion Protein

A Synaptic Cuproprotein

David R. Brown

1. PRION DISEASES

The names bovine spongiform encephalopathy (BSE), Creutzfeldt–Jakob disease (CJD), and scrapie are now household names despite the fact that the human disease (CJD) remains a disease of very low incidence, accounting for 1 in 10^6 deaths per annum worldwide. BSE and CJD are examples of prion diseases, fatal neurodegenerative conditions *(1)*. Before the BSE epidemic, prion diseases were infamous because the cause could not be linked to a known pathogen such as a virus or bacterium but to a single protein termed the prion protein. Prusiner's protein-only hypothesis for the cause of prion diseases *(2)* has become quite famous in recent years and won him the Nobel Prize *(3)* despite the lack of decisive proof of the theory that the altered isoform is all that is need to induce prion diseases. There is continued support for the hypothesis that "transmissible spongiform encephalopathies" are not just the result of conformationally corrupted protein (PrP^{Sc}) passing from individual to individual. At the far end of this opposition are those who believe that there is a hidden virus that stimulates production of the abnormal prion protein but is the real culprit. At the other end are those who say that the "protein-only" cause is inadequate as tests show that recombinant prion protein forced to take on a similar conformation to that found in disease does not induce prion disease when injected into *(4,5)*. The evidence that confounds the idea that PrP^{Sc} is not sufficient to cause disease is growing. It is now possible to isolate PrP^{Sc} from mouse brain that has much lower infectivity than a standard PrP^{Sc} preparation *(6)*. However, infectivity can be restored to this protein by the addition of heparin sulfate *(6)*. Nevertheless, mice that cannot express the prion protein because of genetic ablation cannot be infected with the disease *(7)*. Thus, only those that express the prion protein can get prion disease. Despite the possibility that a virus might emerge as the cause of prion disease, the diseases themselves are inseparable from the prion protein. Therefore, understanding what the prion protein does and how it is important to cellular metabolism is central to the whole enigma of the prion diseases.

2. THE PRION PROTEIN

The genetic code of the prion protein was identified only after the isolation of the abnormal isoform (PrP^{Sc}) from infected brains. Discovery of the gene led to the realization that there was a normal brain protein involved in the disease *(1,3)*. However, what this protein actually does in the brain has

From: Handbook of Copper Pharmacology and Toxicology
Edited by: E. J. Massaro © Humana Press Inc., Totowa, NJ

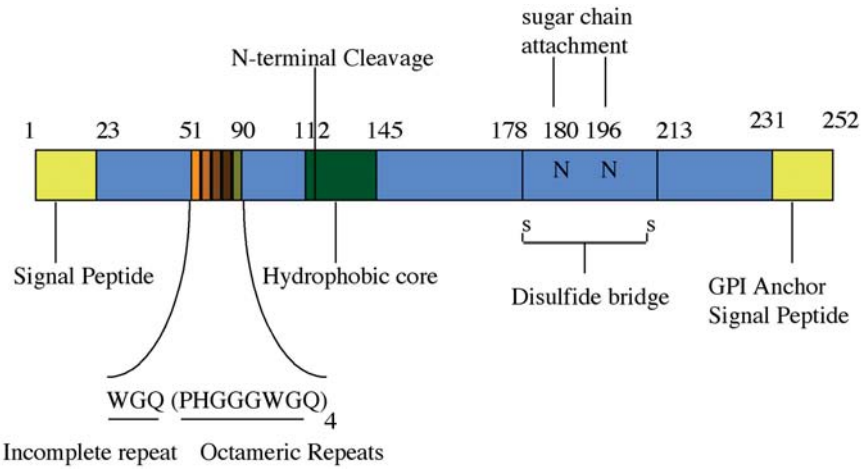

Fig. 1. The primary structure of the mouse prion protein. This protein is anchored to the cell membrane by a glycosylphospholipid (GPI) anchor. The signal peptide for entry into the endoplasmic reticulum and the GPI signal peptide are cleaved off before the protein reaches the cell surface. Glycosylation can occur at one two or none of the asparagine residues indicated. A hydrophobic region envelopes a cleavage point where the protein is cleaved during normal metabolic breakdown. A disulfide bond links two regions of the protein that form separate α-helices in the three-dimensional structure of the protein. The complete octarepeats can bind up to four copper atoms. Most mammals also have an incomplete repeat prior to this.

remained a mystery for the last 15 yr. The prion protein (PrP^C) is a glycoprotein expressed (Fig. 1) on the surface of many cell types *(8–12)*. The protein is linked to the cell membrane by a glycosal phosphatidyl insoitol anchor *(13)*. It has one or two sugar chains linked close to the C-terminus but may also exist in a nonglycosilated form. PrP^C is probably expressed by all vertebrates. Many mammalian and avian genes have been sequenced and, recently, the coding sequence for turtle prion protein has also been described *(14,15)*. One region of the protein that encapsulates a normal metabolic splice site is so precisely conserved and is so unique among protein sequences that it must represent a functional domain of the protein essential to normal activity of the protein. Two separately derived "strains" of mice in which protein expression has been knocked out (Zrch1, Npu) were examined for gross disturbances in behavior and development *(16,17)*. None were found, and on the basis of this, some experts suggested that the protein had a redundant function or no function at all. However, why would the sequence of the prion protein be so highly conserved from turtle to man? Possibly its function is so essential that, like many such proteins, normal metabolism has mechanisms to compensate for its loss.

Yet, even this picture has been blurred when other strains of prion-protein-deficient mice (Zrch2, Ngs, Rcm0) were found to develop late-onset motor disturbances and the loss of Purkinje cells in the cerebellum *(18–20)*. A recent article has suggested that these other strains of PrP^C-deficient mice become ill because another protein, termed doppel, with a small degree of homology (approx 25%) to the prion protein is highly expressed in these mice *(19)*. This expression is possibly driven by the prion protein promoter running directly into the doppel reading frame, which is directly in tandem with that of the prion protein. Whatever the role of doppel in causing the phenotype of these PrP^C-deficient mice, the late-onset pathology is abrogated by reintroducing prion protein expression *(20)*. It is possible that renewed prion protein expression has a negative feedback effect on the prion protein promoter, inhibiting doppel expression. Regardless of this, the implication is that prion protein expression has a positive function in preventing disease. A close study of the doppel protein with NMR has shown stronger homology to PrP^C at the secondary-structure level than the primary-

sequence homology would suggest *(21)*. These nuclear magnetic resonance (NMR) results show a similar globular domain containing three helical domains and a small amount of β-sheet structure. However, unlike PrP^C, doppel contains two disulfide bridges and is more heavily glycosilated *(22)*. There is also evidence from my group's own work that doppel, unlike PrP^C, is unable to bind Cu, which is not surprising because it lacks the octameric repeat region involved in Cu binding to PrP^C.

In Rcm0 mice and other PrP knockout mice with late-onset neurodegeneration, the increased doppel expression is ectopic *(19–22)*. In wild-type mice, doppel is expressed predominantly in other regions such as heart and testes. Cell death in mice overexpressing doppel in the brain is possibly related to increased production of nitric oxide. Rcm0 mice show increased levels of the enzymes that generate nitric oxide (iNOS and nNOS) and signs of oxidative and nitroxic damage to lipids *(23)*. Despite these interesting investigations there is little evidence that doppel plays any role in prion disease. Studies from the lab of Aguzzi suggest that mice that lack doppel expression are just as sensitive to infection by scrapie and show similar degrees of neurodegeration. These results came from transplantation studies in which tissue from the brains of doppel knockout mice were implanted into the brains of PrP knockout mice *(24)*. Thus, it remains to be determined what the normal function of the doppel protein is and whether doppel expression will affect disease progression in prion disease.

The initial suggestion that knocking out prion protein expression has no implication has also proven to be false for the two strains of PrP^C-deficient mice that do not develop late-onset disease. At the level of the whole animal, there are behavioral differences related to changes in circadian rhythms *(25)*. At the level of the nervous system, there are changes in electrophysiological parameters *(26,27)*. PrP^C-deficient mice are also more sensitive to kindling agents that cause fits *(28)*. Although there is contradictory evidence from some investigators working with slice preparations at room temperature *(29)*, there is evidence that parameters such as long-term potentiation and GABA-type inhibitory currents are abnormal in PrP^C-deficient slices at physiological temperatures *(26)*. Other parameters also differ, as do responses to stress-inducing agents such as exogenous copper and hydrogen peroxide *(30,31)*. Down at the level of single cells, PrP^C-deficient cells are less viable in culture than wild-type cells and are more susceptible to oxidative damage and toxicity from agents such as copper and cytosine arabinoside *(32–36)*. Astrocytes show changes in ability to take up glutamate *(37)* and microglia are less responsive to activating substances *(11)*. Therefore, at all levels, PrP^C-deficient mice show a clear phenotype, indicating that they are more sensitive to various kinds of stresses implying that PrP^C has an important function protecting cells from environment assaults. Furthermore, there is now evidence that prion protein expression increases when the brain is stressed by oxidative damage *(38)*. Brains of patients with Alzheimer's disease show a 10-fold increase in the level of prion protein expression.

3. THE PRION PROTEIN AT SYNAPSES

The prion protein is expressed by many cells. These include glia *(11,12)* and blood cells *(39)* as well as neurones. Therefore, a neurone-only function for the prion protein is not valid. However, the fact that the protein is expressed in neurones at higher levels than in any other cells suggests that the prion protein has special importance for neurones. Additionally, PrP^C is highly concentrated at the synapse *(40)*. There is evidence of intense localization not only at CNS synapses but also at end plates. There is little reason to think that the expression of PrP^C is limited either presynaptically or postsynaptically. Although expressed by neurones, PrP^C is expressed by muscle cells as well *(10)*. There is evidence for specific axonal transport of different PrP^C glycoforms, suggesting that perhaps one glycoform or another might be specifically presynaptic *(41)*. PrP^C can be isolated in detergent-insoluble rafts *(42)*. There is evidence that such rafts may represent specialized areas of synaptic membrane that might, in turn, give rise to cavaeolilike domains. PrP^C is associated with such specific regions of the membrane *(43)*. The full details of the specialized association with the synaptic membrane have not yet emerged, but it is likely that there are two forms of prion protein in neurones: synaptic and nonsynaptic.

As indicated earlier, PrP^C-deficient mice show a number of electrophysiological differences, suggesting that PrP^C expression somehow influences neurotransmission. There is no evidence to suggest that synaptic activity influences the level of expression of PrP^C. Furthermore, there is no knowledge on what causes clustering of PrP^C at synapses. As already stated, the expression of PrP^C in other cell types suggests that it has a function that is not limited to excitable cells. Therefore, it is likely that the function of PrP^C is related to protection of the synapse rather than direct augmentation of or involvement in neurotransmission. A better idea of the nature of the function of PrP^C has emerged since it has become established that the prion protein binds copper.

4. COPPER BINDING

Structural studies of the prion protein have concentrated on the globular domain of the C-terminus because of its solubility when prepared from bacterial inclusion bodies *(44)*. Further studies have found little structure in the N-terminus, a region of approx 90 amino-residues *(45)*. Such a suggestion that a large part of this protein has no structure is surprising, as it contains what appears to be a conserved functional domain of 32 amino residues formed from 4 repeats of an octomer, each of which contains histidine. In birds and turtles, this sequence is a hexameric repeat region, but it is found in a similar position. Analysis of peptides based on this region suggested that copper might bind to this region but with a surprising low K_d of 6.7 μM *(46,47)*. At the time of this finding, this low affinity suggested to many that this binding was nonspecific. However, further analysis of a larger N-terminal fragment (amino residues 23–98) using equilibrium dialysis provided more rigorous support for the idea that PrP^C binds copper *(30)*. These new data suggested that the N-terminal could be saturated by 5 atoms of copper, and 3.4 atoms showed cooperativity in binding even though the first atom of copper again appeared to bind at a low K_d of 5.9 μM. The interpretation of this is nevertheless that once one atom of copper has bound to PrP^C, further binding occurs at a higher K_d, implying that perhaps the low initial K_d's reflect the artificial nature of attempting to add copper to the protein in a nonphysiological manner.

More recently, studies have continued with new peptides based on the octameric repeat region *(48–53)*. These studies have focused on the interaction between the copper and the amino residues in the octameric repeat. Binding of copper to the repeat causes a change in conformation of amino residues outside of the repeat region itself *(49)*. Peptides based on the repeat region appear to bind the copper in the form of Cu(II) *(53)* and coordinate it between the four single histidine residues of the repeats *(48)*. The coordination of the two or four atoms of copper may require one or two histidines per atom. However, despite the suggestion that copper is bound as Cu(II), there is evidence that this copper can go through redox cycling; when this occurs, tryptophan residues within the repeats also interact with the Cu(I) *(51)*. Although in vitro studies of peptides provide interesting insights, they are not necessarily indicative of what occurs in cells.

A very recent study by Jackson et al. *(54)* using NMR to monitor the binding of the first atom of Cu to an octameric-repeat region peptide has suggested that the correct K_d for this interaction is in the low femtomolar range (8×10^{-14} M). Additionally, Jackson et al. *(54)* also suggest that a fifth copper atom can bind at another site (involving histidines at amino residue 96 and 111 in the human sequence). Evidence for this binding has been reported *(30,55,56)*. The K_d as reported by Jackson et al. *(54)* for this fifth site is also reported to be in the femtomolar region, but this was determined for a fragment of PrP in which the octameric repeat region had been deleted (PrP90–231). However, recent research from my own laboratory suggests that the K_d for the fifth site in full-length PrP is considerably less than this (27 μM), whereas that for the first atom of Cu to bind in the octameric repeat region of full-length PrP is much lower than any previously reported (8×10^{-17} M, determined by competition assay). Regardless of the exactitude of these measurements, the implication is that PrP^C is a true Cu-binding protein. The variability in the affinities determined would, however, sug-

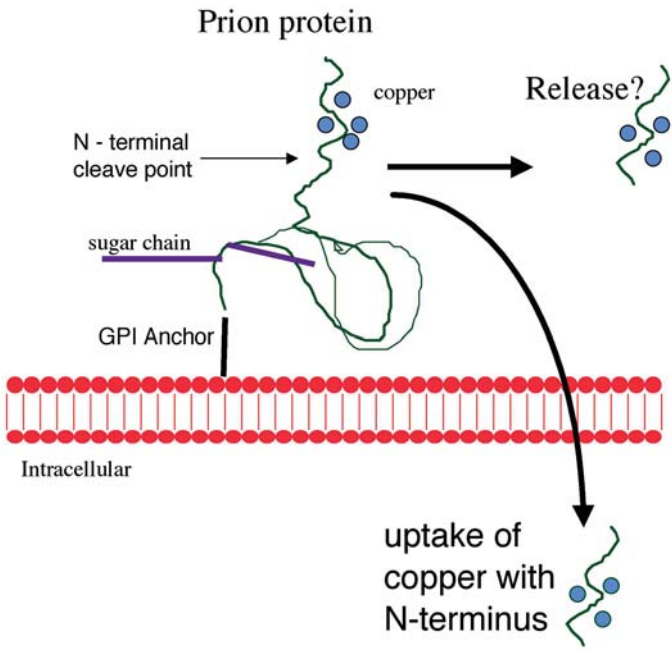

Fig. 2. The majority of the prion protein synthesized by cells is anchored to the outside of the cell membrane by a GPI anchor. The prion protein may come to the surface-binding copper or it might bind additional copper on reaching the cell surface. The turnover of the prion protein is very fast. The protein has a half-life of 1 h or less. It is not exactly known where N-terminal cleavage occurs. Cleavage at the cell surface would result in release of the copper-binding domain into the extracellular space separating it from the globular C-terminal domain. However, there is more evidence to suggest that cleavage occurs intracellularly, in which case the copper would be released inside the cell where it could be mobilized for other activities.

gest that Cu binding to PrP^C is very sensitive to the test conditions and PrP^C might show diminished Cu binding in unfavorable environments.

The case for PrP^C binding copper was strengthened by studies that looked at changes caused by depletion of PrP^C from cells. Mice lacking PrP^C expression were initially dismissed as lacking any phenotype after superficial behavior and developmental studies failed to see any difference between PrP^C knockout mice and wild-type mice *(16)*. However, analyses of these mice indicated a number of differences at the level of cells indicative of both a disturbance and a relation to copper *(30)*. Synaptosomes purified from the brains of PrP^C knockout mice contained substantially less copper than wild-type mice *(30)*. Synaptic release of copper has been documented since the 1960s, although the reason for it remains a mystery *(57)*. Imbalance in synaptic copper caused disturbance to activity of receptors such as GABA receptors and altered long-term potentiation *(58,59)*. PrP^C knockout mice have been studied electrophysiologically and found to have altered GABA-type inhibitory currents and also altered LTP *(26)*. Additionally, if copper is applied to cerebellar slices from PrP^C knockout mice, there is a decrease in both the frequency and amplitude of spontaneous currents measured on Purkinje cells *(30)*. This effect is not seen on patching Purkinje cells from wild-type mice. These results suggest that PrP^C knockout mouse synapses are intolerant to high copper concentrations.

Further evidence for differences in the way neurones lacking PrP^C deal with copper comes from culture studies using cerebellar cells derived from PrP^C knockout mice. Growing cerebellar cells in medium containing low amounts of copper reveals that wild-type cells retain higher amounts of copper than PrP^C knockout cerebellar cells *(30)*. This difference can be abolished if PrP^C is cleaved from the surface of the cells with an enzyme that cuts the glycosylphospholipid (GPI) anchor. Analysis of

uptake of radioactive copper by cerebellar cells overexpressing PrP^C or lacking PrP^C show differences to that of wild-type cells *(60)*. Both membrane retention and uptake into the cytosol of copper at nanomolar concentrations is greatly enhanced by prion protein expression by cerebellar cells (Fig. 2). Cells lacking PrP^C expression still take up copper but to a lower degree than wild-type cells *(60)*. Furthermore, my lab has new evidence suggesting that PrP knockout cells compensate by other copper uptake proteins such as the mCTR proteins.

Exposure of cells to copper increased the turnover rate of PrP^C *(61)*. This further supports the idea that PrP^C may take up copper and if new binding of copper occurs to PrP^C at the surface, this would lead to increase entry of copper into the cell. Evidence for this comes from a recent study *(62)* that shows that removal of either the whole octa-repeat region or mutation of the histidines in two of the repeats of PrP^C did not lead to increased turnover of PrP^C when cells transfected with these mutants were exposed to copper. Furthermore, a similar analysis of a mutant with an expanded number of repeats showed that the expansion mutant was not turned over faster when the expressing cells were when exposed to copper. These results show the importance of the interaction between copper and PrP^C for the normal function and metabolism of the protein.

Copper taken into cells via PrP^C appears to be utilized differently to copper taken up by the cell by alternative mechanisms. Veratridine-induced depolarization is known to cause increased release of copper at synapses *(63)*. The copper so released can be utilized from pools of copper taken up by high-affinity transporting protein only minutes earlier. Studies of cerebellar neurones loaded with radioactive copper have shown that PrP^C-expressing neurones release large amounts of radiolabeled copper on depolarization with veratridine and neurones expressing higher levels of PrP^C release considerably more *(60)*. However, veratridine-induced release of copper is virtually abolished if the cerebellar neurones lack PrP^C expression or if the cerebellar neurones are pretreated to cleave PrP^C from the cell surface before loading with radioactive copper. On the basis of these results, it is reasonable to conclude that prion protein expression regulates the amount of copper associated with the synapse.

5. ANTIOXIDANT ACTIVITY

Why would copper associated with the prion protein at the synapse be of any benefit? Since 1996, there has been increasing evidence that the prion protein increases cellular resistance to oxidative stress *(64)*. Cerebellar neurones and astrocytes from PrP^C knockout mice are more sensitive to superoxide toxicity *(32,34)*. Additionally, there is evidence from cell culture models that toxicity of PrP^{Sc} involves oxidative stress, as blocking toxicity of the neurotoxic peptide mimic of PrP^{Sc} can be achieved with antioxidants *(65)*. Cultured cells "infected" with PrP^{Sc} are also much more sensitive to oxidative assault than noninfected cells *(66)*. Our laboratory also has evidence that when N2A neuroblastoma cells are transfected to overexpress PrP^{Sc} they show increased resistance to the toxicity of superoxide. However, when those cells are infected so that they express large amounts of PrP^{Sc} instead they are more sensitive to superoxide toxicity (Fig. 3). More recently, there is evidence that PrP^C itself is upregulated in prion disease and possibly other diseases marked by the presence of oxidative damage *(38)*.

Not only are neurones lacking PrP^C expression more sensitive to oxidative stress, but the same PrP^C-deficient neurones are also more sensitive to copper toxicity *(33)*. PC12 cell lines developed to be more resistant to copper toxicity are more resistant to oxidative stress and show increased expression of PrP^C *(65)*. A peptide based on the octameric-repeat region of PrP^C can block both toxicity caused by either oxidative stress or exogenous copper *(33)*. Oxidative stress and copper toxicity are linked together by the complexity of Fenton chemistry in that copper can catalyze the interconversion of various reactive oxygen species or generate the hydoxyl radical directly from water. Thus, sequestering copper has immediate protective benefits for cells very sensitive to oxidative damage.

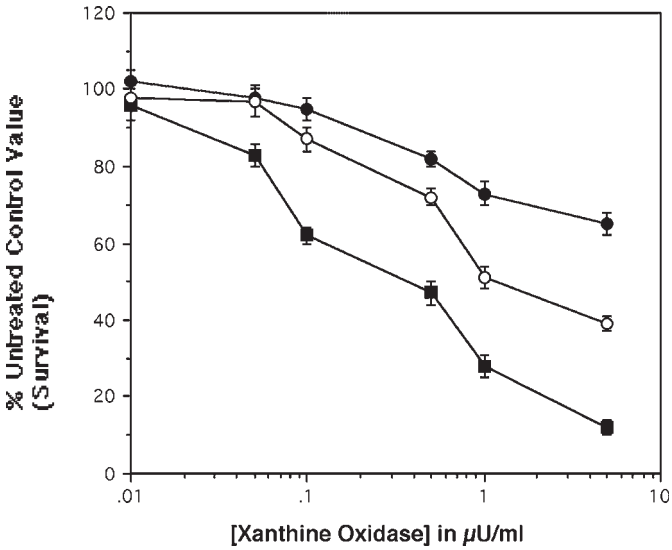

Fig. 3. N2A neuroblastoma cells were transfected with a construct (pCDNA3) expressing PrP^C. Cells expressing large amounts of PrP^C (●) are more resistant to the toxicity of superoxide as generated by xanthine oxidase (in the presence of 40 U/mL of catalase) than non transfected cells (O). However, infection of these cells with the ME7 strain of scrapie so that the cells generate PrP^{Sc} (■) renders them much more sensitive to superoxide toxicity. Survival was determined using an MTT based assay. Shown are the mean and SEM of four separate experiments.

Analysis of recombinant mouse and chicken prion protein has led to the discovery of an important gain of function once PrP^C binds copper *(55)*. Recombinant PrP^C with at least two atoms of copper bound specifically via the octameric-repeat region has an activity like that of superoxide dismutase (SOD), implying that the prion protein may act to detoxify superoxide, thus preventing oxidative stress from occurring *(67)*. PrP^C binding four atoms of copper has higher activity than that binding only two. However, the activity is enzymatic, because copper forced to bind to a mutant prion protein lacking the octameric region does not endow the protein with this antioxidant activity *(55)*. There is also evidence that SOD by the prion protein leads to specific oxidation of methionines that are clustered in the C-terminal of the protein *(68)*. Although many SOD remove the extra electron of superoxide by forming hydrogen peroxide, it is also possible that the electron can be removed by rapid oxidation of methionines. PrP^C is rapidly turned over and part of its metabolic breakdown involves cleavage of the N-terminal at a site that lies between the octameric repeat and the methionine-rich globular C-terminal domain. Thus, separating the copper from what is probably the active site of the protein in its catalytic form.

These results have also been confirmed with native PrP^C purified from either the brains of mice or from cultured neurones *(56)*. PrP^C purified from mouse brain has three atoms of Cu bound per molecule. This is sufficient to endow it with SOD activity. By growing neurones in culture under conditions of low copper, it is possible for cells to express PrP^C, which has very low Cu bound. It was not possible to isolate PrP^C from cells grown under low-Cu conditions with less than one atom of Cu bound per molecule. Such purified protein lacked SOD activity. Neurones grown under different copper conditions could be induced to express PrP^C with one, two, three, or four atoms of copper bound. Increasing Cu concentration in the cell culture medium to 25 μ*M* (which is toxic) did not

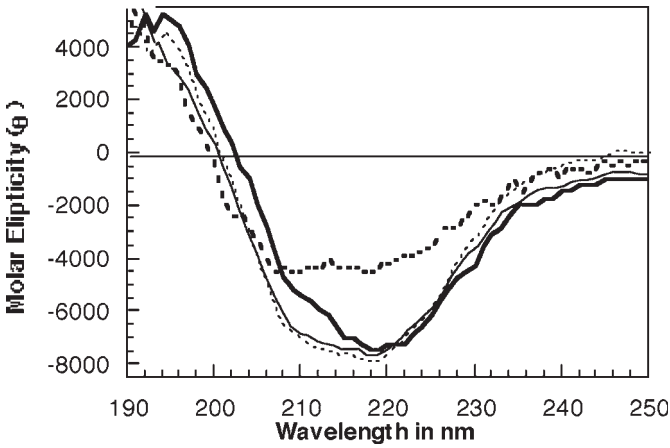

Fig. 4. Circular dichrosim spectra analysis of recombinant mouse PrP of different alleles. Recombinant protein was produced from *E. coli* based either on the a allele (PrPa) or the b allele (PrPb) The far UV spectra for PrP samples were analyzed using circular dichroism spectroscopy. Samples were refolded to bind copper and measured immediately or when aged for 4 wk. Shown are fresh PrPa (thin unbroken line), PrPb (thick dotted light) aged PrPa (thick unbroken line) and aged PrPb (thick dotted line). Values are expressed as molar ellipticity (θ) for 190–250 nm.

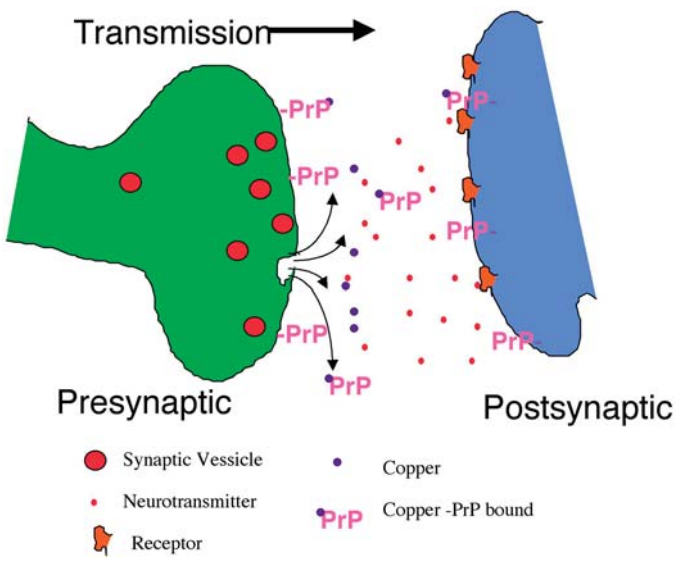

Fig. 5. The highest concentration of the prion protein is found at synapses. It has been found that expression of prion protein increases the amount of copper found at and released by synapses. It is possible that the prion protein could be released along with copper bound to it. Alternatively, copper could be captured by PrP on membranes on either side of the synpatic cleft. However, studies on the effects of copper on synapses suggest that the absence of prion protein expression makes synapse more susceptible to the deleterious effects of copper on neurotransmission implying that the prion protein is expressed there to have a protective role.

increase the amount of copper bound to PrP^C isolated from the neurones. PrP^C with two, three, or four copper atoms bound could protect neurones against the toxicity of superoxide, indicating that not only does the protein exhibit SOD activity in the test tube but it is also an effective antioxidant in culture.

Analysis of what happens when the PrP^C binds other cations has shown that manganese can substitute for copper and that manganese-binding PrP^C also has some SOD activity *(67)*. However, this activity is rapidly lost and the manganese-binding protein undergoes a folding transition resulting in protease-resistant protein. Such protein has similarities to the abnormal form of the protein PrP^{Sc}. Although this resistant protein might not be infectious, this insight provides the intriguing possibility that the disease-specific form of the protein might be generated in vivo by incorporation of the wrong metal either as a result of dietary imbalance in metal ions or some other abnormality in metabolism of metals.

Changes in the amino acid sequence also influence the SOD activity of PrP^C. Pure bread laboratory strains of mice usually express one of two alleles that differ only at two amino residues. A mouse strain that, as a general simplification, has a longer incubation time for the mouse form of scrapie prion disease expressed what is called the "b" allele of PrP^C *(69)*. Recombinant protein generated to have the sequence of the b allele has higher SOD activity than that of the normal allele *(70)*. Additionally, this protein is more labile and breaks down more rapidly and loses activity more rapidly than the more common form of the mouse prion protein. These changes are reflected in the differences in the circular dichroism spectra of the proteins measured after aging the two proteins for several weeks (Fig. 4).

These findings suggest that PrP^C is a copper-binding protein with antioxidant activity, expressed at the synapse (Fig. 5). A synaptic SOD may have benefits protecting synaptic termini from the damaging effects of superoxide and reactive oxygen species. Superoxide is known to inhibit some aspects of neurotransmission, and loss of synaptic spines is a common feature of diseases involving oxidative damage. Thus, as described earlier the reason for the high expression of the prion protein at the synapse may be the need to protect synaptic integrity.

6. BAD EFFECTS OF COPPER ON PRION PROTEIN

Several studies have now indicated that aberrant interaction between copper and PrP^C leads to misfolding of the protein and can also enhance the neurotoxicity of its potentially toxic domains. Experiments with recombinant PrP that had been left to age showed that exposure of this material to high (nonphysiological) concentrations of free copper led to a change in proteinase resistance of the protein *(71)*. Conformational transition in PrP is typical of the conversion process between PrP^C and PrP^{Sc}. However, not all conformational transitions leading to proteinase resistance and fibril formation are the same. Indeed, further analysis of this process using PrP^C derived from cells suggests the conformational changes induced by exposure to free copper are not the same as those that distinguish PrP^{Sc} from PrP^C *(72)*. The implication of this is that one has to be careful in the interpretation of experiments based on proteinase K resistance. Although such an assay is useful in distinguishing PrP^{Sc} from PrP^C, it does not imply that all proteinase-resistant PrP is PrP^{Sc}. Manganese can also induce proteinase resistance in recombinant PrP and PrP^C purified from cells grown in the presence of high manganese *(70)*. Proteinase resistant protein produced in this manner possesses a conformation more equivalent to that of PrP^{Sc}. Nevertheless, without increased infectivity there is still no evidence that proteinase-resistant PrP generated in this way is PrP^{Sc}.

Some experiments have looked at the ability of copper to increase the "infectivity" of PrP. In these experiments, an extract of brain high in PrP^{Sc} was produced and treated to reduce infectivity *(73)*. Incubating the resulting material with high copper resulted in a restoration of the infective titer of the protein. However, these manipulations are rather unsatisfactory, as the infectivity of the material was not abolished and, as stated earlier, it is not fully clear what other than PrP^{Sc} is necessary for infectivity in prion diseases. It is quite possible the effect was related to the oxidizing potential of copper rather than copper *per se*.

Other experiments have studied the effects of copper on the neurotoxicity of PrP^{Sc} or the peptide mimic PrP106–126. Chelation of copper in culture models of PrP106–126 neurotoxicity abolish the toxicity of the peptide, suggesting that copper is necessary for PrP106–126 toxicity *(74)*. Neurones grown in low concentrations of copper are also more resistant to the toxicity of PrP106–126. Transition metals have been shown to have a critical effect on the ability of the β-amyloid protein to induce fibril formation of that protein *(75)*. Another study has investigated whether this property is common to other prion protein peptides, by studying the effect of metals on PrP106–126 aggregation *(76)*. In that article, the authors show that fibrillization of PrP106–126 was completely inhibited in a transition-metal-depleted environment. Cu^{2+} and, to a lesser extent, Zn^{2+} could restore PrP106–126 aggregation. The metal-binding site was localized and found to comprise the N-terminal amino group: histidine 111 and methionine 112. Although our own studies have suggested that these residues are unnecessary for PrP106-126 toxicity *(77)*, the known ability of Cu to interact with β-sheet-rich structures could exacerbate fibrillization, even in the absence of the histidine.

The implication of these results is that interaction between PrP and copper can be of two forms. The first is appropriate and leads to protective effects such as correct delivery of copper or antioxidant activity. The second is aberrant and involves misfolded protein and can result in neuronal death. This second effect probably involves the interaction of copper with a site outside the octameric-repeat region.

7. THE RELEVANCE PRION PROTEIN FUNCTION AND COPPER BINDING TO PRION DISEASE

If loss of prion protein function has consequences for disease progression in prion diseases, then one would expect that the earliest changes in prion disease would be seen at the synapse. Recent studies of changes in neurones in experimental prion disease have identified loss of dendritic spines occurring before any other change in prion disease *(78)*. However, such changes, although fitting with the hypothesis that loss of prion protein function contributes to neurodegeneration in prion disease, do not prove the connection.

As already mentioned, PrP^{C} expression is necessary if not sufficient for prion disease *(7)*. However, animals lacking PrP^{C} expression do not develop a spontaneous form of prion disease. Nevertheless, these mice do have a phenotype indicative of a disturbance and neurones lacking PrP^{C} expression in particular are more sensitive to oxidative stress. PrP^{C}-deficient cells have diminished cellular activity of SOD and diminished copper content.

Studying neurodegeneration in vivo has been a problem in prion disease. Insights into the mechanism by which PrP^{Sc} is neurotoxic have come from cell culture studies using the peptide mimic of PrP^{Sc}, PrP106–126 *(32,33,60,64)*. This peptide has effects on cells that include reducing their resistance to oxidative stress and decreasing activity of SOD in cells *(32)*. Studies with similar peptides have suggested that PrP106-126 could bind directly to PrP^{C} in the vicinity of the palendromic repeat, which, as suggested earlier may be the active site of the protein *(79)*. This interaction directly inhibits the SOD activity of PrP^{C} *(56,74)*. Furthermore, PrP^{Sc} can also inhibit the activity of PrP^{C}. In a reactive environment such as the damaged brain, this would expose neurones to the toxicity of substance such as superoxide generated by microglia or excess neurotransmitters such as glutamate, which can activate intracellular production of superoxide.

PrP106–126 also inhibits copper uptake. This effect is seen only in cells expressing PrP^{C} *(74)*. This inhibition of copper uptake is thus probably a result of interaction between PrP106–126 and PrP^{C} at the cell surface. This interaction would have a similar effect to a PrP knockout phenotype, implying a loss of function of PrP^{C}. The consequences of this are decreased incorporation of copper into enzymes such as SOD *(80)*. This would further compromise cellular resistance to oxidantive stress. Although not conclusive, these observations are pointing in the direction that loss of PrP^{C} function is a disadvantage for a cell. In a healthy animal, this disadvantage might not lead to death,

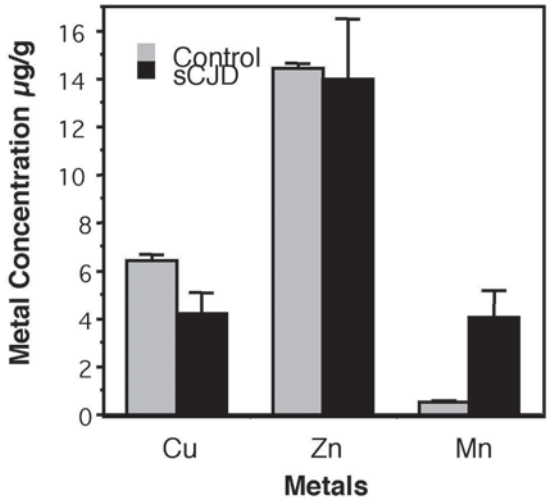

Fig. 6. Metals in the brains of patients with CJD were measured using mass spectroscopy. Changes in manganese and copper were observed suggesting that prion disease causes dramatic changes in the metal content of the brain. These changes may be a result of the disease but they suggest that prion diseases involve disturbances to the metabolism of trace elements. Shown are the mean and SEM of nine results for CJD patients (gray bars) and three for control patients (open bars).

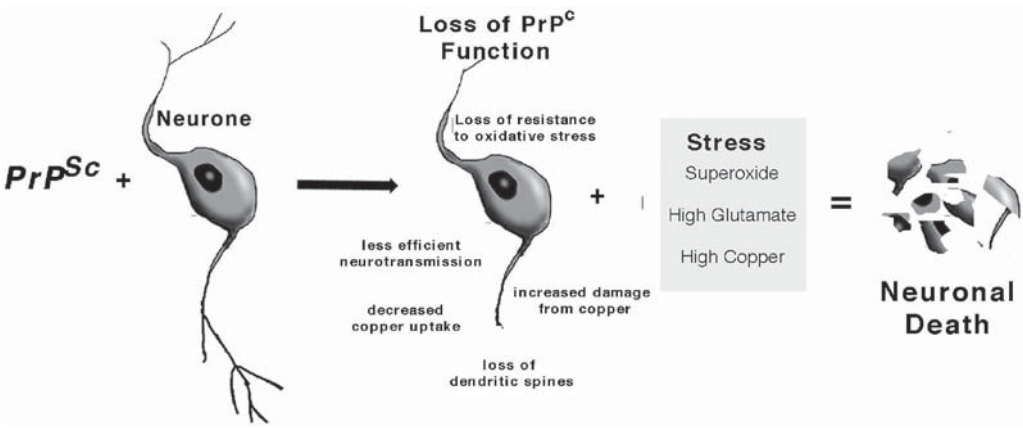

Fig. 7. The critical question as regards prion disease is how conversion of the normal cellular isoform (PrP^C) to the disease-specific isoform (PrP^{Sc}) causes neurones to die. It is likely that the conversion of PrP^C to PrP^{Sc} results in a loss of PrP^C function without upregulation of compensatory mechanisms. These upregulatory mechanisms would probably be active when there is no PrP^C expression detected by the cells. Although this loss of function might not induce cell death on its own, the neurone, having lost functional PrP^C, might be more susceptible to the toxicity of substances generated in the brain as a reaction to the presence of inflammatory PrP^{Sc}. This combination of effects might then lead to neuronal death.

but in an animal in which an inflammatory response has been initiated, loss of active PrP^C would be a clear disadvantage.

Recently studies of transition metals in prion diseases have begun to emerge. Studies of the brain of CJD patients have shown that the levels of copper in their brains are decreased *(81)* (Fig. 6). Similar studies with mice experimentally infected with the disease scrapie confirm this result. The changes in copper in this model precede neruonal death and follow the course of PrP^{Sc} generation in the brain. Furthermore, analysis of PrP^{Sc} isolated from the brain of CJD patients and mice with scrapie has shown that this protein lacks significant copper binding and the antioxidant activity associated with PrP^C has been lost completely. This implies that prion disease does cause a loss of PrP^C function that is directly related to the ability of the protein to bind copper. Maintaining functional PrP^C is clearly advantageous and there is evidence to suggest this can protect against prion disease (Fig. 7). PrP knockout mice that have been modified to express hamster PrP via a GFAP promoter express PrP^C only in astrocytes. These mice are susceptible to infection with hamster scrapie and develop prion disease *(82)*. Wild-type mice are highly resistant to hamster scrapie because of specific differences between the protein sequence of hamster and mouse PrP^C. However, if wild-type mice are made transgenic to express hamster PrP^C in astrocytes, they cannot be infected with hamster scrapie. The implication of this is that mouse PrP^C, which cannot be converted to mouse PrP^{Sc} by hamster PrP^{Sc}, protects against prion disease. This suggests that where there is sufficient functional PrP^C, neurones may be protected from neuronal death caused by prion disease. In years to come, strategies that protect or restore the normal copper-dependent functions of PrP^C might be useful therapeutics to treat or prevent prion disease.

In the future years, we may see a deeper understanding of the nature and cause of prion disease, but, in parallel, we are likely to see the prion protein become accepted as a cuproprotein essential to normal neuronal survival and function.

REFERENCES

1. Prusiner, S. B. (1991) Molecular biology of prion disease. *Science* **252**, 1515–1522.
2. Prusiner, S. B. (1982) Novel proteinaceous infectious particles cause scrapie. *Science* **216**, 136–144.
3. Prusiner, S. B. (1998) Prions. *Proc. Natl. Acad. Sci. USA* **95**, 13,363–13,383.
4. Post, K., Brown, D. R., Groschup, M., Kretzschmar H., and Riesner, D. (2000) Neurotoxicity but not infectivity of prion protein can be induced reversibly in vitro. *Arch. Virol.* **16(Suppl.)**, 265–273.
5. Hill, A. F., Antoniou, M., and Collinge, J. (1999) Protease-resistant prion protein produced *in vitro* lacks detectable infectivity. *J. Gen. Virol.* **80**, 11–14.
6. Shaked, G. M., Meiner, Z., Avraham, I., Taraboulos, A., and Gabizon, R. (2001) Reconstitution of prion infectivity from solubilized protease-resistant prp and nonprotein components of prion rods. *J Biol Chem.* **276**, 14,324–14,328.
7. Büeler, H., Aguzzi, A., Sailer, A., Greiner, R.-A., Autenried, P., Auget, M., et al. (1993) Mice devoid of PrP are resistant to scarpie. *Cell* **73**, 1339–1347.
8. Kretzschmar, H. A., Prusiner, S. B., Stowring, L. E., and DeArmond, S. J. (1986) Scrapie prion proteins are synthesized in neurons. *Am. J. Pathol.* **122**, 1–5.
9. Moser, M. Colello, R. J. Pott , U., and Oesch, B. (1995) Developmental expression of the prion protein in glial cells. *Neuron* **14**, 509–517.
10. Brown, D. R., Schmidt, B., Groschup, M. H., and Kretzschmar, H. A. (1998) Prion protein expression in muscle cells and toxicity of a prion protein fragment. *Eur. J. Cell Biol.* **7**, 29–37.
11. Brown, D. R., Besinger, A., Herms, J. W., and Kretzschmar, H. A. (1998) Microglial expression of the prion protein. *Neuroreport* **9**, 1425–1429.
12. Brown, D. R. (1999) Prion protein peptide neurotoxicity can be mediated by astrocytes. *J. Neurochem.* **73**, 1105–1113.
13. Stahl, N., Baldwin, M. A., Hecker, R., Pan, K-M., Burlingame, A. L., and Prusiner, S. B. (1992) Glycosylinositol phospholipid anchors of the scrapie and cellular prion proteins contain sialic acid. *Biochemistry* **31**, 5043–5053.
14. Wopfner, F., Wiedenhöfer, G., Schneider, R., von Bunn, A., Gilch, S., Schwarz, T. F., et al. (1999) Analysis of 27 mammalian and 9 avian PrPs reveals high conservation of flexible regions of the prion protein. *J. Mol. Biol.* **289**, 1163–1178.
15. Simonic, T. Duga, S., Strumbo, B., Asselta, R., Ceciliani, F., and Ronchi S. (2000) cDNA cloning of turtle prion protein. *FEBS Lett.* **469**, 33–38.
16. Büeler, H., Fischer, M., Lang, Y., Bluethmann, H., Lipp, H.-P., DeArmond, S.J., et al. (1992) Normal development and behaviour of mice lacking the neuronal cell-surface PrP protein. *Nature* **356**, 577–582.

17. Manson, J. C., Clarke, A. R., Hooper, M. L., Aitchison, L., McConnell, I., and Hope, J. (1994) 129/Ola mice carring a null mutation in PrP that abolishes mRNA production are developmentally normal. *Mol. Neurobiol.* **8**, 121–127.
18. Sakaguchi, S., Katamine, S., Nishida, N., Moriuchi ,R., Shigematsu, K., Sugimoto, T., et al. (1996) Loss of cerebellar Purkinje cells in aged mice homozygous for a disrupted PrP gene. *Nature* **380**, 528–531.
19. Moore, R. C., Lee, I. Y., Silverman, G. L., Harrison, P. M., Strome, R., Heinrich, C., et al. (1999) Ataxia in prion protein (PrP)-deficient mice is associated with upregulation of the novel PrP-like protein doppel. *J. Mol. Biol.*, **292,** 797–817.
20. Rossi, D., Cozzio, A., Flechsig, E., Klein, M. A. Rülicke, T., Aguzzi, A., et al. (2001) Onset of ataxia and Purkinje cell loss in PrP null mice inversely correlated with Dpl level in brain. *EMBO J.* **20**, 695–702.
21. Mo, H., Moore, R. C., Cohen, F. E., Westaway, D., Prusiner, S. B., and Wright, P. E. (2001) Two different neurodegenerative diseases caused by proteins with similar structures. *Proc. Natl. Acad. Sci. USA* **98,** 2352–2357.
22. Silverman, G. L., Qin, K., Moore, R. C., Yang, Y., Mastrangelo, P., Tremblay, P., et al. (2000) Doppel is an N-glycosylated , glycosylphosphatidylinositol-anchored protein. Expression in testis and ectopic production in the brains of Prnpo/o mice predisposed to Purkinje cell loss. *J. Biol. Chem.* **275**, 26,834–26,841.
23. Wong, B.-S., Liu, T., Paisley, D., Li, R., Pan, T. Chen, S. G., Perry, G., et al. (2001) Induction of HO-1 and NOS in doppel-expressing mice devoid of PrP: implications for Doppel function. *Mol. Cell Neurosci.* **17**, 768–775.
24. Behrens, A. Brandner, S., Genoud, N., and Aguzzi, A. (2001) Normal neurogenesis and scrapie pathogenesis in neural grafts lacking the prion protein homologue Doppel. *EMBO Rep.* **2**, 1–6.
25. Tobler I, Gaus S. E , Deboer T., Achermann P., Fischer M., Rülicke T., et al. (1996) Altered circadian rhythms and sleep in mice devoid of prion proteins *Nature* **380**, 639–642.
26. Collinge, J., Whittington, M. A., Sidle, K. C. L., Smith, C. J., Palmer, M. S., Clarke, A. R., et al. (1994) Prion protein is necessary for normal synaptic function. *Nature* **370,** 295–297.
27. Colling, S. B., Collinge, J., and Jefferys, J. G. R. (1996)Hippocampal slices from prion protein null mice: disruption of Ca^{2+}-activated K^+ currents. *Neurosci. Lett.* **209**, 49–52.
28. Walz, R., Amaral, O. B., Rockenbach, I. C., Roesler, R., Izquierdo, I., Cavalheiro, E. A., Martins, V. R., and Brentani, R. R. (1999) Increased sensitivity to seizures in mice lacking cellular prion protein. *Epilepsia* **40**, 1679–1682.
29. Lledo P. M., Tremblay P., DeArmond S. J., Prusiner S. B., and Nicoll, R.A. (1996) Mice deficient for prion protein exhibit normal neuronal excitability and synaptic transmission in the hippocampus. *Proc. Natl. Acad. Sci. USA* **93**, 2403–2407.
30. Brown, D. R., Qin, K., Herms, J. W., Madlung, A., Manson, J., Strome, R., et al. (1997) The cellular prion protein binds copper in vivo. *Nature* **390**, 684–687.
31. Herms, J. Tings T., Gall, S., Madlung, A., Giese, A., Siebert, H., et al. (1999) Evidence of presynaptic location and function of the prion protein. *J. Neurosci.* **19**, 8866–8875.
32. Brown, D. R., Schultz-Schaeffer, W. J., Schmidt, B., and Kretzschmar, H. A (1997) Prion protein-deficient cells show altered response to oxidative stress due to decreased SOD-1 activity. *Exp. Neurol.* **146**, 104–112.
33. Brown, D. R., Schmidt, B. and Kretzschmar, H. A. (1998)Effects of copper on survival of prion protein knockout neurones and glia. *J. Neurochem.* **70**, 1686–1693.
34. Brown, D. R., Schmidt, B., and Kretzschmar, H. A. (1998d) A prion protein fragment primes type 1 astrocytes to proliferation signals from microglia. *Neurobiol. Dis.* **4**, 410–422.
35. Kuwahara, C., Takeuchi, A. M., Nishimura, T., Haraguchi, K., Kubosaki, A., Matsumoto, Y., et al. (1999) Prions prevent neuronal cell line death. *Nature* **400**, 225–226.
36. White, A. R., Collins, S. J., Maher, F., Jobling, M. F., Stewart, L. R., Thyer, J. M., et al. (1999). Prion protein-deficient neurons reveal lower glutathione reductase activity and increased susceptibility to hydrogen peroxide toxicity. *Am. J. Pathol.* **155**, 1723–1730.
37. Brown, D. R. and Mohn, C. M. (1999) Astrocytic glutamate uptake and prion protein expression. *Glia* **25**, 282–292.
38. Guentchev, M., Voigtländer, T., Haberler, C., Groschup, M. H., and Budka, H. (2000) Evidence for oxidative stress in experimental prion disease. *Neurobiol. Dis.* **7**, 270–273.
39. Diomede, L., Sozzani, S., Luini, W., Algeri, M., De Gioio, L., Chiese, R., et al. (1996) Activation effects of a prion protein fragment [PrP-(106–126)] on human leucocytes. *Biochem. J.* **320**, 563–570.
40. Salès, N., Rodolfo, K., Hässig, R., Faucheux, B., Di Giamberdino, L., and Moya, K. L. (1998) Cellular prion protein localization in rodent and primate brain. *Eur. J. Neurosci.* **10**, 2464–2471.
41. Rodolfo, K., Hässig, R., Moya, K. L., Grassi, J., and Di Giamberardino, L. (1999) A novel cellular prion protein isoform present in anterograde but not in retrograde axonal transport. *Neuroreport* **10**, 3639–3644.
42. Naslavsky, N.,Stein, R.,Yanai, A.,Friedlander, G., and Taraboulos, A. (1997) Characterization of detergent-insoluble complexes containing the cellular prion protein and its scrapie isoform. *J. Biol. Chem.* **272**, 6324–6331.
43. Madore, N., Smith, K. L., Graham, C. H., Jen, A., Brady, K., Hall, S., et al. (1999) Functionally different GPI proteins are organized in different domains on the neuronal surface. *EMBO J.* **18**, 6917-6926.
44. Riek, R., Hornemann, S., Wider, G., Billeter, M., Glockshuber, R., and Wüthrich, K. (1996) NMR structure of the mouse prion rotein domain prp(121–231). *Nature* **382** 180–182.
45. Hornemann, S., Korth, C., Oesch, B., Riek, R., Wider, G., Wüthrich, K., and Glockshuber, R. (1997) Recombinant full-length murine prion protein mPrP(23–231): purification and spectroscopic characterization. *FEBS Lett.* **413**, 277–281.
46. Hornshaw, M. P., McDermott, J. R., and Candy, J. M. (1995a). Copper binding to the N-terminal tandem repeat regions of mammalian and avian prion protein. *Biochem. Biophys. Res. Commun.* **207,** 621–629.
47. Hornshaw, M. P., McDermott, J. R., Candy, J. M., and Lakey, J. H. (1995) Copper binding to the N-terminal repeat region of mammalian and avian prion protein: structural studies using synthetic peptides. *Biochem. Biophys. Res. Commun.* **214**, 993–999.

48. Viles, J. H., Cohen F. E., Prusiner, S. B., Goodin, D. B., Wright, P. E., and Dyson, H. J. (1999) Copper binding to the prion protein: structural implications of four identical cooperative binding sites. *Proc. Natl. Acad. Sci. USA* **96,** 2042–2047.
49. Miura, T., Hori-i, A., and Takeuchi, H. (1996) Metal dependent α-helical formation promoted by glycine rich octapeptide region of prion protein. *FEBS Lett.* **396**, 248–252.
50. Miura, T., Hori-i, A., Mototani, H., and Takeuchi, H. (1999) Raman spectroscopic study on the copper(II) binding mode of prion octapeptide and its pH dependence. *Biochemistry* **38,** 11,560–11,569.
51. Ruiz, F. H., Silva, E., and Inestrosa, N. C. (2000) The N-terminal tandem repeat region of human prion protein reduces copper: role of tryptophan residues. *Biochem. Biophys. Res. Commun.* **269**, 491–495.
52. Shiraishi, N., Ohta, Y., and Nishikimi, M. (2000) The octapeptide repeat region of prion protein binds Cu(II) in the redox inactive state. *Biochem. Biophys. Res. Commun.* **267,** 398–402.
53. Whittal, R. M., Ball, H. L., Cohen, F. E., Burlingame, A. L., Prusiner, S. B., and Baldwin, M. A. (2000) Copper binding to octarepeat peptides of the prion protein monitored by mass spectrometry. *Protein Sci.* **9**, 332–343.
54. Jackson, G. S., Murray, I., Hosszu, L. L. P., Gibbs, N., Waltho, J. P., Clarke, A. R., and Collinge, J. (2001) Location and properties of metal binding sites on the human prion protein. *Proc. Natl. Acad. Sci. USA* **98**, 8531–8535.
55. Brown, D.R., Wong, B.-S., Hafiz, F., Clive, C., Haswell, S. J., and Jones, I. M. (1999) Normal prion protein has an activity like that of superoxide dismutase. *Biochem. J.* **344**, 1–5.
56. Brown, D. R., Clive, C., and Haswell, S. J. (2001) Anti-oxidant activity related to copper binding of native prion protein. *J. Neurochem.* **76,** 69–76.
57. Colburn, R. W. and Maas, J. W. (1965) Adenosine triphosphate–metal–norepinephrine ternary complexes and catecholamine binding *Nature* **208**, 37–41.
58. Gabrielsson, B., Robson, T., Norris, D., and Chung, S. H. 1986. Effects of divalent metal ions on the uptake of glutamate and GABA from synaptosomal fractions. *Brain Res.* **384**, 218–223.
59. Vlachová, V., Zemkova, H., and Vyklickt Jr., L. (1996) Copper modulation of NMDA responses in mouse and rat cultured hippocampal neurons. *Eur. J. Neurosci.* **8**, 2257–2264.
60. Brown, D. R. (1999) Prion protein expression aids cellular uptake and veratridine-induced release of copper. *J. Neurosci. Res.* **58**, 717–725.
61. Pauly, P. C. and Harris, D. A. (1998) Copper stimulates endocytosis of the prion protein. *J. Biol. Chem.* **273**, 33,107–33,110.
62. Sumudhu, W., Perera, S., and Hooper, N. M. (2001) Ablation of the metal ion-induced endocytosis of the prion protein by disease-associated mutation of the octarepeat region. *Curr. Biol.* **11**, 519–523.
63. Barnea, A., Hartter, D. E., and Cho, G. (1989) High affinity uptake of ^{67}Cu into veratridine releasable pool in brain tissue. *Am. J. Physiol.* **257**, C315–C322.
64. Brown, D. R., Schmidt, B., and Kretzschmar, H. A (1996) Role of microglia and host prion protein in neurotoxicity of a prion protein fragment. *Nature* **380,** 345–347.
65. Brown, D. R., Schmidt, B., and Kretzschmar, H. A. (1997c) Expression of prion protein in PC12 is enhanced by exposure to oxidative stress. *Int. J. Dev. Neurosci.* **15**, 961–972.
66. Milhavet, O., McMahon, H. E., Rachidi, W., Nishida, N., Katamine, S., Mange, A., et al. (2000) Prion infection impairs the cellular response to oxidative stress. *Proc. Natl. Acad. Sci. USA* **97**,13,937–13.942.
67. Brown, D. R., Hafiz, F., Glasssmith, L. L., Wong, B.-S., Jones, I. M., Clive, C., et al. (2000) Consequences of manganese replacement of copper for prion protein function and proteinase resistance. *EMBO J.* **19,** 1180–1186.
68. Wong, B.-S., Wang, H., Brown, D. R., and Jones, I. M. (1999) Selective oxidation of methionine residues in prion proteins. *Biochem. Biophys. Res. Commun.* **279**, 352–355.
69. Carlson, G. A., Goodman, P. A., Lovett, M., Taylor, B. A., Marshall, S. T., Peterson-Torchia, M., et al. (1988) Genetics and polymorphism of the mouse prion gene complex: control of scrapie incubation time. *Mol. Cell Biol.* **8**, 5528–5539.
70. Brown, D. R. , Iordanova, I. M., Wong, B.-S., Vénien-Bryan, C., Hafiz, F., Glasssmith, L. L., et al. (2000) Functional and structural differences between the prion protein from two alleles *prnp*^{a} and *prnp*^{b} of mouse. *Eur. J. Biochem.* **267**, 2452–2459.
71. Qin, K., Yang, D.-S., Yang, Y., Christi, M. A., Meng, L.-J., Yip, C. M., et al. (2000) Copper(II)-induced conformational changes and protease resistance in recombinant and cellular PrP. *J. Biol. Chem.* **275**, 19,121–19,131.
72. Quaglio, E., Chiesa, R., and Harris, D. A. (2001) Copper converts the cellular prion protein into a protease-resistant species that is distinct from the scrapie isoform. *J. Biol. Chem.* **276**, 11,432–11,438.
73. McKenzie, D., Bartz, J., Mirwald, J., Olander, D., Marsh, R., and Aiken J. (1998) Reversibility of scrapie inactivation is enhanced by copper. *J. Biol. Chem.* **273**, 25,545–25,547.
74. Brown, D. R. (2000) PrPSc-like prion protein peptide inhibits the function of cellular prion protein. *Biochem. J.* **252,** 511–518.
75. Atwood, C. S., Moir, R. D., Huang, X., Scarpa, R. C., Bacarra, M. E., Romano, D. M., et al. (1998) Dramatic aggregation of Alzheimer Aβ by Cu(II) is induced by conditions representing physiological acidosis. *J. Biol. Chem.* **273**, 12,817–12,826.
76. Jobling, M. F., Huang, X., Stewart, L. R., Barnham, K. J., Curtain, C., Volitakis, I., et al. (2001) Copper and zinc binding modulates the aggregation and neurotoxic properties of the prion peptide PrP106–126. *Biochemistry* **40**, 8073–8084.
77. Brown, D. R. (2000) Prion protein peptides: optimal toxicity and peptide blockade of toxicity. *Mol. Cell Neurosci.* **15,** 66–78.
78. Belichenko, P. V., Brown, D., Jeffrey, M., and Fraser, J. R. (2000) Dendritic and synaptic alterations of hippocampal pyramidal neurones in scrapie-infected mice. *Neuropathol. Appl. Neurobiol.* **26,** 143–149.
79. Kaneko, K., Wille, H., Mehlhorn, I., Zhang, H., Ball, H., Cohen, F. E., et al. (1997) Molecular properties of complexes formed between the prion protein and synthetic peptides. *J. Mol. Biol.* **270**, 574–586.

80. Brown, D. R. and Besinger, A. (1998) Prion protein expression and superoxide dismutase activity. *Biochem. J.* **334**, 423–429.
81. Wong, B.-S., Chen, S. G., Colucci, M., Xie, Z., Pan, T., Liu, T., et al. (2001) Human prion diversity is associated with abnormal metal binding. *Neurosci. Soc. Abst.* **27**, 2523.
82. Raeber, A., Race, R. E., Brandner, S., Priola, S. A., Sailer, A., Bessen, R. A., et al. (1997) Astrocyte-specific expression of hamster prion protein (PrP) renders PrP knockout mice susceptible to hamster scrapie. *EMBO J.* **16**, 6057–6065.

7
Cytochrome-*c* Oxidase

Shinya Yoshikawa

1. INTRODUCTION

Cytochrome oxidase is the terminal oxidase of most of aerobic organisms and reduces molecular oxygen (O_2) to water *(1)*. The electrons and protons required for the formation of water molecules are transferred from both sides of the mitochondrial inner membranes in eukaryotic cells and of the cell membrane in prokaryotic cells *(1)*. The migration of positive and negative charges from the different sides of the membrane produces electric potential across the membrane. In addition to the O_2 reduction, this enzyme pumps protons from the inside to the outside of the membrane to produce a proton gradient across the membrane in addition to the membrane potential produced by the net migration of the positive charges *(1,2)*. This enzyme contains heme iron and copper ions in the catalytic center *(1)*. Because of the intriguing reaction of this copper-containing enzyme in addition to its physiological importance, many articles have been published on its structure and function, isolated from various organisms and tissues, in the last 75 yr or so *(1,3,4)* since its discovery by Warburg *(5)*. Progress in understanding of the reaction mechanism of cytochrome-*c* oxidase has been accelerated by X-ray structures of the enzyme isolated from mammalian tissue and bacterial cells, which began to appear as late as in 1995 *(6,7)*.

In this chapter, the mechanism of this enzyme will be discussed based mainly on the nonempirical structural information on this enzyme, including X-ray structures. Emphasis will be placed on the importance of careful experimental procedures involved in the process of structural determination.

2. PURIFICATION, CRYSTALLIZATION, AND CONSTITUENT DETERMINATION OF CYTOCHROME-*C* OXIDASE

2.1. Purification and Crystallization

Cytochrome-*c* oxidase was first isolated from bovine heart muscle as early as in 1941 by Yakushiji and Okunuki *(8)*. They used a natural detergent, sodium cholate, for solubilizing the enzyme. This enzyme is a multisubunit protein with two extramembrane moieties on both ends of the transmembrane core moiety. The most critical step for isolation of a membrane protein is to extract the protein from the biological membrane by replacing the membrane phospholipid bilayer with detergents. This

From: Handbook of Copper Pharmacology and Toxicology
Edited by: E. J. Massaro © Humana Press Inc., Totowa, NJ

step is called solubilization. The efficiency of the solubilization and the stability of the solubilized protein in mixed-micelle states is greatly dependent on the detergent species. It should be noted that no detergent better than sodium cholate, first used 60 yr ago *(8)*, has been found for solubilizing bovine heart cytochrome-*c* oxidase. The solubilized fraction usually contains various protein contaminants. However, if the solubilization is successful in (i.e., if the solubilized protein is integral), the removal of contaminant proteins is rather simple. A drawback of using sodium cholate for purification of bovine heart cytochrome-*c* oxidase is its deteriorative effects on protein conformation and its inhibitory effect of the enzyme activity. Thus, cholate must be replaced with nondeteriorative detergent as soon as possible after removal of the contaminant proteins. Many kinds of nonionic detergent with low critical micelle concentations are appropriate for this purpose. Crystals of bovine heart cytochrome-*c* oxidase solubilized with cholate and replaced with decylmaltoside diffracted X-rays up to 2.0 Å resolution, which is the highest resolution so far obtained for this enzyme *(9)*.

Crystallization conditions are also greatly influenced by the detergent species used for stabilizing a membrane protein in aqueous solution *(10,11)*. In fact, dodecylmaltoside also stabilizes the absorption spectrum and enzymic activity as effectively as decylmaltoside. However, no crystal has yet been obtained from preparations stabilized with dodecylmaltoside. At present, many kinds of synthetic detergent are commercially available. However, it is desirable to search for the best detergents for crystallization and for solubilization of each protein by synthesizing new detergents that are commercially unavailable. These strong effects of detergent structure on crystallization condition for each membrane protein provide a great advantage for crystallization of membrane protein, because completely different crystallization conditions for a membrane protein can be obtained by exchanging the detergent species.

2.2. Composition of Bovine Heart Cytochrome-c Oxidase

This enzyme has four redox active metal sites, two heme sites (hemes a and a_3), and two copper sites (Cu_A and Cu_B) *(1)*. The structure of heme A, which is involved in both heme sites, were determined by Caughey and co-workers in 1995 *(12)*. The heme is characterized by a hydroxyl farnesylethyl group at position 2 and a formyl group at position 8 of the porphyrin substitute groups. The formyl group provides a bright blue–green color when the heme is in the ferrous low-spin state. The absorption spectrum of heme is sensitive to the oxidation and spin states of the iron atom. Thus, absorption spectroscopy has been used in the investigation of heme function. Thus, accurate determinations of the extinction coefficients of these hemes are indispensable for extensive studies on the mechanism of electron-transfer reactions within the enzymes. The accuracy of a metal content analysis is limited by the purity of the purified sample. After the initial purification of the enzyme by Yakushiji and Okunuki *(8)*, many reports on iron analysis and extinction coefficients of the two hemes were published *(1,3,4,13,14)*. Unfortunately, a significant amount of contaminant iron binds to contaminating proteins. This was shown by a significant decrease in iron content by purification of the enzyme preparation with crystallization in the final step *(14)*. No other method is able to remove the contaminant iron. As given Table 1, the iron content decreases with repeated crystallization. Twofold crystallization is sufficient for complete removal of the contaminant iron. One of the advantages of crystallization for purification of multicomponent large proteins is that crystallization is unlikely to remove loosely bound enzyme components (overpurification). Thus, if a particular component is not influenced by repeated crystallization, it is highly likely to be an intrinsic constituent of the protein. Thus, the redox inactive metals, Mg^{2+} and Zn^{2+}, given in Table 1 *(14)*, are likely to be intrinsic although the physiological roles are still unknown. Furthermore, all three copper atoms must be intrinsic to this enzyme because the copper content is insensitive to repeated crystallization. The extinction coefficient of the enzyme determined by the iron content of the enzyme preparation purified with crystallization is 1.2–1.4 times greater than previous values determined for uncrystallized enzyme preparations *(14)*.

Table 1
Effect of Crystallization on the Metal Content of Bovine Heart Cytochrome-*c* Oxidase

Preparation	*Atoms/enzyme molecule*				ε^{red} *604–630 nm* (mM^{-1} cm^{-1})
	Fe	*Cu*	*Mg*	*Zn*	
Before crystallization[a]	2.90	2.90	1.04	0.97	32.2
Once crystallized[a]	2.21	3.04	1.07	1.01	42.2
Twice crystallized[a]	2.06	3.00	1.06	1.00	45.6
Three times crystallized[a]	2.00	2.95	1.04	1.04	46.6
Twice crystallized, averaged[b]	2.00 (0.07)	2.95 (0.12)	1.02 (0.08)	1.04 (0.04)	46.6 (1.16)

Note: All of the values were determined assuming that the three-times crystallized sample contains two iron atoms per molecule of enzyme.

[a]Enzyme stabilized with $CH_3(CH_2)_{11}(OCH_2CH_2)_8OH$ was used.

[b]Averaged values with standard deviation (in parentheses) for three and four enzyme preparations stabilized with $CH_3(CH_2)_{11}(OCH_2CH_2)_8OH$ and $CH_3(CH_2)_{11}(OCH_2CH_2)_{23}OH$, respectively.

The composition of protein subunits of a large multisubunit protein such as bovine heart cytochrome-*c* oxidase is not easily determined if it has not been crystallized. For example, the smallest subunit of bovine heart cytochrome-*c* oxidase is smaller than 5 kDa and does not have redox active metal. Its physiological role is still unknown. However, two groups proposed that the subunit was an intrinsic constituent, based only on the result that a band in sodium dodecyl sulfate–poliacrylamide gel electrophoresis (SDS-PAGE) corresponding to the subunit is detectable reproducibly in many purified preparations *(15,16)*. The proposal was not widely accepted because copurification of the small subunit had not been discounted. The debate ended when the X-ray structure of bovine heart cytochrome-*c* oxidase at 2.8 Å resolution reported in 1996 *(17)* showed the specific assembly of the smallest subunit with large-core subunits, which included redox active metal sites. The presence of the other 10 subunits, whose physiological roles are unknown, are also conclusively shown by the X-ray structure at 2.8 Å resolution *(17)*. Thus, X-ray structural determination is essential for the determination of the composition of a large multicomponent protein. Repeated crystsllization is extremely effective for removing contaminant proteins, which are readily detectable via SDS-PAGE. However, the accuracy of quantitative determination of each subunit content is much lower than that of metal content analysis.

Phospholipid content is also not easy to determine. Detergent treatment may remove intrinsic phospholipids because the phospholipid themselves are detergents. Furthermore, quantitative analysis of phospholipids is not as accurate as that of metals. For the complete determination of phospholipid content, X-ray structures at high resolution are required, as in the case of the determination of subunit composition. Eight phospholipids are identified in an X-ray structure at 2.8 Å resolution *(17)*. The total phosphorous content in the crystalline enzyme preparation (approx 20 per enzyme) is definitely higher than the total phosphorous in the phospholipids detectable in the X-ray structure in the enzyme molecule. Also, no caldiolipin, which is likely to be essential for the enzyme activity *(18,19,20)*, has been detected in the X-ray structure, indicating that X-ray structure at 2.8 Å resolution is not accurate enough for the determination of phospholipid composition.

3. FUNCTIONS OF REDOX ACTIVE METAL SITES OF CYTOCHROME-*C* OXIDASE

3.1. Spectral Properties

Keilin and Hartree discovered two types of cytochrome containing heme a: one of them oxidizes cytochrome-*c* and reduces another cytocrome, which is autoxidizable *(21)*. The former is named cytochrome a and the latter, cytochrome a_3 *(21)*. However, as shown in X-ray structure, two cytochromes are not independent proteins, but the two heme sites are located within the single polypeptide of subunit I. Thus, the two heme iron sites are called hemes a and a_3.

A respiratory inhibitor, cyanide, specifically binds to heme a_3 in the oxidized state and stabilizes the oxidized state strongly *(22)*. The cyanide-bound heme a_3 cannot be reduced even with an excess amount of dithionite, whereas heme a is unreactive to cyanide and is readily reduced by dithionite. Thus, a difference spectrum of the cyanide-treated enzyme reduced with dithionite versus the cyanide-treated enzyme without the addition of the reductant provides the redox difference spectrum of heme a, provided no interaction exists between the two hemes. On the other hand, a difference spectrum of the fully reduced enzyme against the fully oxidized enzyme gives the sum of the redox difference spectra of heme a and heme a_3. Thus, the redox difference spectrum of heme a_3 can be determined by subtracting the redox difference spectrum of heme a determined as earlier from the redox difference spectrum without addition of the inhibitor. As stated earlier, these procedures are appropriate for the spectral separation if the spectral changes in the two hemes are independent of each other. The proximity of the two hemes as shown in the X-ray structure of the enzyme *(17)* strongly suggests some interaction between the two hemes. Nevertheless, the spectral properties of the two hemes thus obtained are consistent with the expected structures of the two hemes. The difference spectrum of heme a shows a sharp intense band in the visible (α-band) region indicating that the reduced heme a is in a six-coordinated ferrous low-spin state. On the other hand, the weak α-band of the difference spectrum of heme a_3 indicates a five-coordinated ferrous high-spin state. Both hemes contribute to the Soret band region in almost equal amounts. These spectral analysis were first done extensively by Yonetani *(23)*, followed by Vanneste *(24)*. The extinction coefficients determined by the above procedure have been used for all kinetic investigations of the internal electron-transfer reactions as well as redox titration studies.

The strong absorption spectra of the two hemes mask the absorption spectrum of Cu_A. In fact, the Cu_A moiety of one of the subunits (obtained by recombinant methods) shows an absorption spectrum in the visible Soret region of heme, although much weaker than the heme spectra *(25)*. The contribution of Cu_A seems negligibly small in calculations of the redox difference spectra of the two hemes. On the other hand, Cu_A contributes significantly to the near-infrared band region *(26,27)*. The redox state of Cu_A has been monitored by the spectrum in this region. The magnitude of the redox difference absorption at 825 nm is approx 1/30 of those in the α-band peaks *(14)*. However, the contribution of the heme absorption to the near-infrared region should not be ignored (13). No absorption spectrum assignable to Cu_B has been reported, although reversible one-electron reduction has been established by redox titration studies (4,14,28). Perhaps, the electron paramagnetic resonance (EPR) signal detected under conditions similar to enzymic turnover is the only spectrum of this copper obtained thus far *(29)*.

Cu_A shows a strong EPR signal near $g = 2.0$. The signal was assigned to a mononuclear copper center similar to the structure of type-I copper *(30)*. However, about 10 yr ago, similarity between the EPR-detectable copper in nitrous oxide reductase (N_2OR) and Cu_A in cytochrome-*c* oxidase was reported *(31)*. The similarity between the two copper sites was proposed also by electron spin echo envelope modulation data *(32)* and magnetic circular dichroism (MCD) and extended X-ray absorption fine structure (EXAFS) spectroscopies *(33)*. The similarity suggests that the Cu_A site is a mixed-

valence dinuclear copper center in which an electron equivalent is delocalized between the two Cu^{2+} ions to provide a [Cu(1.5)···Cu(1.5)] center. The structure is confirmed by the multifrequency EPR spectrum of the Cu_A site in bovine heart cytocrome-*c* oxidase *(34)*.

The low-spin heme EPR signal is reasonably assigned to heme a in the fully oxidized state as prepared. However, quantitation of each of the two EPR signals indicates that the EPR-detectable component of each metal corresponds to roughly half of each metal contained in the enzyme. No other EPR signal assignable to that of intrinsic metals has been observed in the fully oxidized enzyme. These results suggest that only Cu_A and heme a in the fully oxidized state are EPR visible. It was proposed as early as in 1969 that Cu_B and heme a_3 in the fully oxidized state are antiferromagnetically coupled with each other to eliminate the EPR spectra of both metal sites *(30)*. The proposal was confirmed by several subsequent investigations *(35–37)*.

3.2. Redox Properties

Redox titrations of this enzyme have been done by various methods, including changing the potential of the enzyme solution and additions of reductants and oxidants *(14,28,38–43)*. In the potentiometric method, various electron-transfer mediators must be added for equilibration between the enzyme and the electrode, because the redox active sites of the enzyme are located inside the protein. For titrations with chemical reagents, NADH with a catalytic amount of phenazinemethosulfate, dithionite, ferricyanide, ferrocyanide, and O_2 have been used. The results so far obtained are not consistent with each other.

Redox titration experiments of cytochrome-*c* oxidase are influenced by many factors. Because of the extremely high reactivity with O_2, a trace amount of contaminant O_2 affects the titration results. On the other hand, complete removal of O_2 from cytochrome oxidase in a mixed-micelle state is very difficult and tedious. Attainment of the equilibrium state is usually assessed monitoring the spectrum to an asymptotic level. Slight damage to the conformation of the enzyme could influence the kinetic properties of the redox active metal sites to give no apparent spectral change with time without attaining the equilibrium state. Thus, both the stability and integrity of the enzyme preparation are critical for the redox titration of cytochrome-*c* oxidase. Another important point often neglected is the effect of electron-transfer mediator. This point is especially important for the redox titration of cytochrome-*c* oxidase because the electron-transfer mediators stimulate autoreduction (reduction of the active site metals by electrons from amino acids in the protein moiety) *(14)*. For example, it has been shown that phenazinemethosulfate under anaerobic conditions influences the reductive titration curve *(14)*. Furthermore, significant amounts of contaminant metals are included in the cytochrome-*c* oxidase preparation if the enzyme is not purified by crystallization *(14)*. The contaminant metals could influence the titration curve by redox interactions with the metal sites of cytocrome-*c* oxidase.

An anaerobic reductive titration using an anaerobic titration system designed for detergent-stabilized redox enzymes is given in Fig. 1, where bovine heart cytochrome oxidase purified by crystallization was used *(14)*. Dithionite was used as the reductant without additional electron-transfer mediators. The spectral changes in Soret, visible, and near-infrared regions proceed essentially in parallel, as shown in the absorption changes at fixed wavelengths given in the insets. The results indicate that the oxidation state of all four redox active metal sites are essentially identical at any overall oxidation state, indicating that the redox potentials of all four metal sites are essentially identical. The insets show that six electron equivalents are required for complete reduction of the fully oxidized enzyme.

The initial 1- to 2-electron equivalents provide the absorbance change with shallow slopes as shown in the inset of Fig. 1. The shallow slopes are not the result of incomplete anaerobiosis because increasing the number of evacuation–equilibration cycles for removing O_2 from 3–10 times did not remove the initial shallow portion of the titration curve. Incomplete anaerobiosis (one cycle of the evacuation–equilibration treatment) provided a two-phase curve similar to those given in the insets

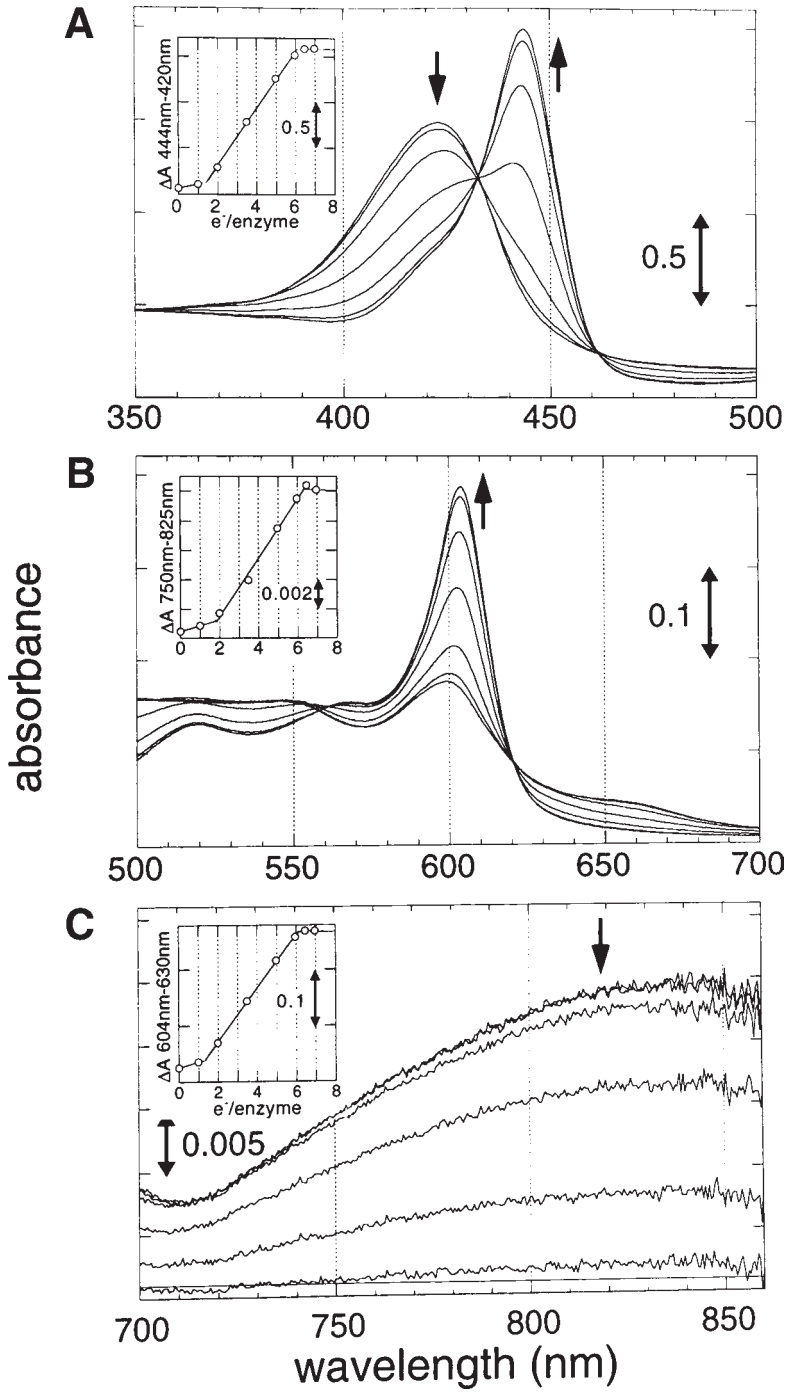

Fig. 1. A reductive titration of the crystalline bovine heart cytochrome-*c* oxidase with dithionite. Absolute spectra for each oxidation states are shown for Soret **(A)** and visible **(B)** regions. The difference spectra against that in the fully reduced state are given for the near-infrared region **(C)**. The insets show titration curves against the electron equivalent per enzyme. The reaction mixture contained 7.5 μ*M* bovine heart cytochrome-*c* oxidase in 0.1 *M* sodium phosphate buffer (pH 7.4). The enzyme preparation was stabilized with a synthetic nonionic detergent, $CH_3(CH_2)_{11}(OCH_2CH_2)_8OH$. The light path was 1 cm.

of Fig. 1, but both slopes were shallower than those given in the insets. The above results are consistent with the X-ray structure of fully oxidized bovine heart cytochrome-*c* oxidase in which peroxide is bridged between Fea_3^{3+} and Cu_B^{2+}. The initial two-electron equivalents are mainly used for cleavage of the O–O bond of the bridging peroxide to generate the fully oxidized form with no bridging ligand.

A discrepancy in the redox titration for the samples with and without purification by crystallization is detectable in the relative distribution of electron equivalents in the four redox active sites *(14,28,38–43)*. Various uneven distribution have been reported *(38–43)*. It should be noted that crystalline enzyme preparation shows an even distribution of electron equivalents added *(14,28)*. The integral enzyme in mitochondrial membrane is the most likely to show an even distribution. The structures of the four redox active metal centers are quite different from each other. However, it is not surprising that different structures of metal sites have an identical redox potential, because small structural changes in bond length or bond angles could induce large changes in the affinity of the metal for electrons. The equipotential property of the four redox active metal sites is expected to facilitate facile electron transfers among the four sites, as well as multiple-electron transfers to the bound O_2.

3.3. Electron Transfer Mechanism

The kinetics of internal electron transfer during the course of O_2 reduction have been extensively studied by following the absorption changes in visible, Soret, and near-infrared regions. At ambient temperature, O_2 reduction by this enzyme is complete within 0.1 ms or so. A conventional stopped-flow apparatus with a dead time of 1 ms or longer cannot be used for the kinetic investigation. Thus, a flow–flash method developed by Gibson and Greenwood *(44)* has long been used for kinetic investigations. This method is outlined as follows: The fully reduced enzyme solution saturated with CO is mixed with O_2-containing buffer using a stopped-flow apparatus to introduce the mixture into an observation cell designed for effective flash irradiation of the mixture. When the flow stops, the flash is turned on to photolysing CO from the enzyme and triggers the initiation of the reaction between the fully reduced enzyme with O_2. The affinity of CO to the enzyme is not high enough for complete protection of the enzyme from auto-oxidation (oxidation by O_2), although CO inhibits the reaction between the enzyme and O_2 for several milliseconds. Thus, the flash–photolysis system equipped with a stopped-flow apparatus is required to observe the O_2 reduction kinetics. Since the historical work by Gibson and Greenwood in 1963 *(44)*, the reaction was extensively studied with various instrumental improvements for about 30 yr. In 1994, the electron-transfer pathway from cytochrome-*c* to O_2 was determined as cytochrome-*c* to Cu_A to heme a to [heme a_3···Cu_B] *(45)*.

3.4. Chemistry of O_2 Reduction

As shown in Fig. 2, the one-electron reduction process of O_2 in the ground state has a negative oxidation–reduction potential; all the other steps have positive potential *(13)*. In other words, a one-electron reduction of O_2 is energetically unfavorable, but the other steps are strongly favorable. This unfavorable one-electron reduction of O_2 contributes greatly to the stability of oxygenated forms of hemoglobins and myoglobins because, in the oxygenated forms, Fe^{2+}–O_2 is isolated within the protein moiety so that a second electron for the two-electron reduction of O_2 is not available. On the other hand, ferrous heme in aqueous solution is readily auto-oxidizable, because the second electron is available from another ferrous heme iron. In the two-electron reduction, a μ-peroxo complex (a peroxide compound with two heme irons on both ends) is formed as an intermediate species. In fact such a μ-peroxo intermediate has been identified in an auto-oxidation reaction of an amine cobalt compound *(46)*. It was well known long before publication of the X-ray structure of the O_2 reduction site of cytochrome-*c* oxidase that, in contrast to hemoglobins and myoglobins, the penta-coordinated heme iron in the O_2-binding site is located near one of the copper sites, Cu_B *(4,47)*. The structure suggests an effective O_2 reduction process including the μ-peroxo intermediate between ferric heme

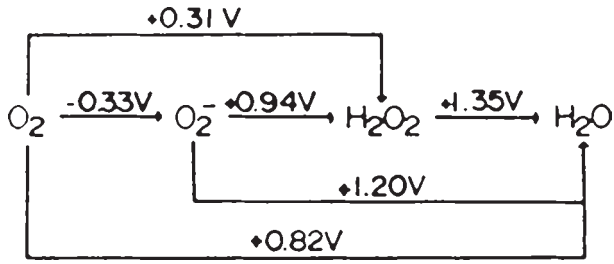

Fig. 2. Standard oxidation–reduction potentials for the steps involved in the conversion of O_2 to water at 25°C and pH 7.0.

a_3 iron and cupric Cu_B ion. The mechanism was proposed by Caughey et al. 25 yr ago *(47)*, and was widely accepted. An important corollary of this mechanism is a negligibly low level of the oxygenated intermediate (Fe_{a3}^{2+}–O_2) during the course of the O_2 reduction. The formation of the μ-peroxo intermediate (Fe_{a3}^{3+}–O–O–Cu_B^{2+}) from the oxygenated form (Fe_{a3}^{2+}–O_2···Cu_B^{1+}) is rate limited by an electron transfer from Cu_B^{1+} to the oxygen atom of the O_2 closest to Cu_B. The electron-transfer rate through such a short distance (approx 2 Å) could be on the order of 1 ps. On the other hand, formation of the oxygenated form is rate limited by migration of O_2 through an O_2 transfer pathway, which is limited by the protein dynamics. Thus, formation of the oxygenated form is likely to be much slower than the transition to the μ-peroxo form. The oxygenated form is therefore undetectable during the course of O_2 reduction.

3.5. Resonance Raman Studies on O_2 Reduction by Cytochrome-c Oxidase

As described in Section 3.3., the reaction of the fully reduced enzyme with O_2 has been investigated extensively for so many years by the flow–flash method by following the spectral changes in the visible–Soret and near-infrared regions *(4,45)*. The method is very effective for investigations of the kinetics of the redox reaction between the metal sites. However, the electronic spectra provide essentially no information about the chemical structure of the ligand on Fe_{a3}. An important approach for identification of the chemical structure of the intermediate species is the trial for trapping the oxygenated form at low temperature by Chance and co-workers *(48)*. They followed the reaction by visible spectroscopy. The oxygenated form was identified by the very weak photosensitivity of the intermediate in addition to the characteristic visible spectrum at 590 nm closely similar to that of the CO compound. Subsequently, a similar approach was done by Gibson's group in which they followed the disappearance of the oxygenated form by its photosensitivity to laser flashes *(49)*. These works have contributed significantly to improvements of our understanding of the mechanism of O_2 reduction by the emzyme. However, they have never succeeded in obtaining direct chemical structural evidence for the oxygenated form.

Vibrational spectroscopy is amenable to examination of the chemical structures of the ligands on heme a_3 in the intermediate species. Time-resolved resonance Raman spectroscopy was applied effectively for identification of the intermediate species during the course of O_2 reduction. Three research groups identified almost at once the initial intermediate as an oxygenated form (Fe^{2+}–O_2) decisively *(50–52)*. The identification of Fe^{2+}–O_2 is extremely astonishing considering the above discussion. Figure 3 shows the resonance Raman band of the initial intermediate during the course of the reaction between the fully reduced enzyme with O_2, determined by one of the three groups. The results were taken by using the extensively improved instrumentation given in the article by Ogura et al. *(53)*. Because of the weak intensity of the resonance Raman band, the bands were identified only in the difference spectrum between the spectrum obtained for the naturally abundant $^{16}O_2$ and that for an isotopically labeled $^{18}O_2$, as shown in Fig. 3. To examine the mode of binding of O_2 to Fe_{a3}^{2+}, a

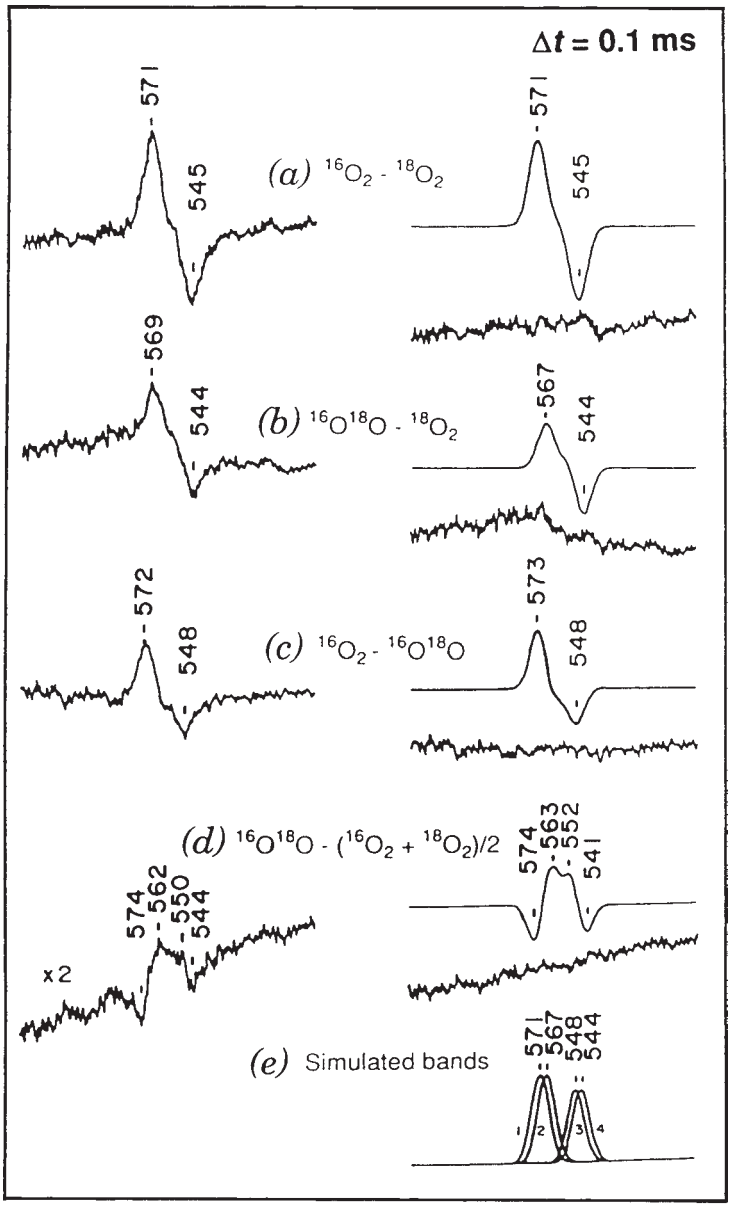

Fig. 3. Resonance Raman spectra of the Fe^{2+}-O_2 stretching frequency region of bovine heart cytochrome-*c* oxidase at 0.1 ms after initiation of the reaction of the fully reduced enzyme with O_2. Spectra on the left-hand and right-hand sides are the observed spectra and the calculated spectra with the differences of the observed vs calculated spectra, respectively. Spectrum d is obtained by the following calculation: (Spectrum b–Spectrum c)/2. (e) Simulated bands for Fe–$^{16}O_2$ (1), Fe–$^{16}O^{18}O$ (2), Fe–$^{18}O^{16}O$ (3), and Fe–$^{18}O_2$ (4). The peak intensity ratio is 6:6:5:5. All bands have the Gaussian band shape with a half-maximal bandwidth of 12.9 cm^{-1}.

terminally labeled $^{16}O^{18}O$ was used. If O_2 binds to Fe_{a3} in a bent end-on fashion, two bands with equal intensity are expected at a band position near but slightly lower than that of $^{16}O_2$ and at a position slightly higher than that of $^{18}O_2$. On the other hand, for a side-on fashion, a single band is expected at a position halfway between those of $^{16}O_2$ and $^{18}O_2$. If only an oxide binds to the heme iron to produce a ferryl oxide ($Fe^{4+}=O^{2-}$), the terminally labeled $^{16}O^{18}O$ provides two bands strictly at the positions obtained for $^{16}O_2$ or $^{18}O_2$. As shown in Fig. 3D, the spectrum obtained for $^{16}O^{18}O$ is not identical with the average of $^{16}O_2$ and $^{18}O_2$. The difference spectrum is able to be simulated by the four bands given in Fig. 3D, which indicates a bent end-on type coordination of O_2 to Fe_{a3}^{2+}. Furthermore, the band at 571 cm^{-1} is in the range of the Fe–O_2 stretch band of various hemoglobins and myoglobins. This is one of the most fundamental results for elucidation of the reaction mechanism of this enzyme, which is inconsistent with the conclusion given in Section 3.4.

The next intermediate exhibits resonance Raman band at 785 cm^{-1}, followed by the band at 804 cm^{-1}, which is the result of the third intermediate. Similar analysis of the second intermediate using $^{16}O_2$, $^{18}O_2$, and $^{16}O^{18}O$ showed, again, astonishingly that the 785-cm^{-1} intermediate is the ferryl oxide *(53)*. That was the case for the 804-cm^{-1} band *(53)*. The implication of these results will be discussed next in relation to the O_2 reduction mechanism.

4. X-RAY STRUCTURES OF THE REDOX ACTIVE METAL SITES

The electron density of the Cu_A site is spherical at 2.8 Å resolution, as shown in Fig. 4A *(6)*. However, location of amino acid side chains clearly shows that the Cu_A site includes two copper atoms. The arrangement of these amino acids suggests that two cysteine sulfur atoms bridge the two copper atoms and form a rhombic square planar coordination structure. Each copper atom has two other amino acid ligands arranged perpendicularly against the rhombic plane in tetrahedral arrangement. The two tetrahedral copper sites are symmetrically opposed at 2.8 Å resolution. However, at 2.3 Å resolution, some asymmetry is detectable (unpublished observation). In any case, the structure is fully consistent with the multifrequency EPR data *(34)*.

As expected, Fe_a is in a hexa-coordinated structure (Fig. 4B) *(6)*. The heme plane is perpendicular to the membrane surface plane, which is defined by both ends of the transmembrane helices. The long alkyl side chain at position 2 is close to fully extended. Two propionate groups point toward the membrane surface plane on the intermembrane side. It should be noted that no other method is able to determine these structures and orientation of the heme. On the other hand, an extremely high resolution of the X-ray structure is required for determination of the positions of the double bonds in the long alkyl chain. Nuclear magnetic resonance (NMR) *(12)* and mass spectrometry are better suited for these determination than X-ray structural analysis.

Figure 5 shows a stereoscopic drawing of the heme a_3 and Cu_B sites (the O_2 reduction site) in the fully oxidized state at 2.3 Å resolution *(9)*. Unexpectedly, this structure includes a peroxide (O_2^{2-}) between Cu_B and Fe_{a3}. The refined model for the residual electron density between Cu_B and Fe_{a3} indicates the presence of peroxide (O_2^{2-}) bridging between the two metal ions. The atomic distance between the two oxygen atoms (1.62 Å) is slightly longer than that of the O–O bond of hydrogen peroxide (H_2O_2) but definitely shorter than that of the two oxygen atoms in a hydrogen-bonded state. The bond lengths for Cu_B–O and Fe_{a3}–O are 2.16 Å and 2.52 Å, respectively, showing a fairly weak coordination of a peroxide oxygen atom to Fe_{a3}^{3+}. The weak coordination is consistent with the high-spin state of Fe_{a3} in the fully oxidized state as prepared *(35–37)*. The peroxide on the Fe_{a3}–Cu_B site is consistent with the titration results as described in Section 3.2. *(14)*.

The copper ion, Cu_B, has three imidazole ligands from His290, His291, and His240. Another unexpected finding is a direct covalent linkage between the nitrogen atom of the imidazole ring of His240 and the ortho carbon atom of the phenol ring of Tyr244 *(9)*. This covalent linkage is detectable conclusively and nonempirically at 2.3 Å resolution in the fully oxidized state and at 2.35 Å resolution in the fully reduced state *(9)*. The covalent linkage structure is consistent with the electron

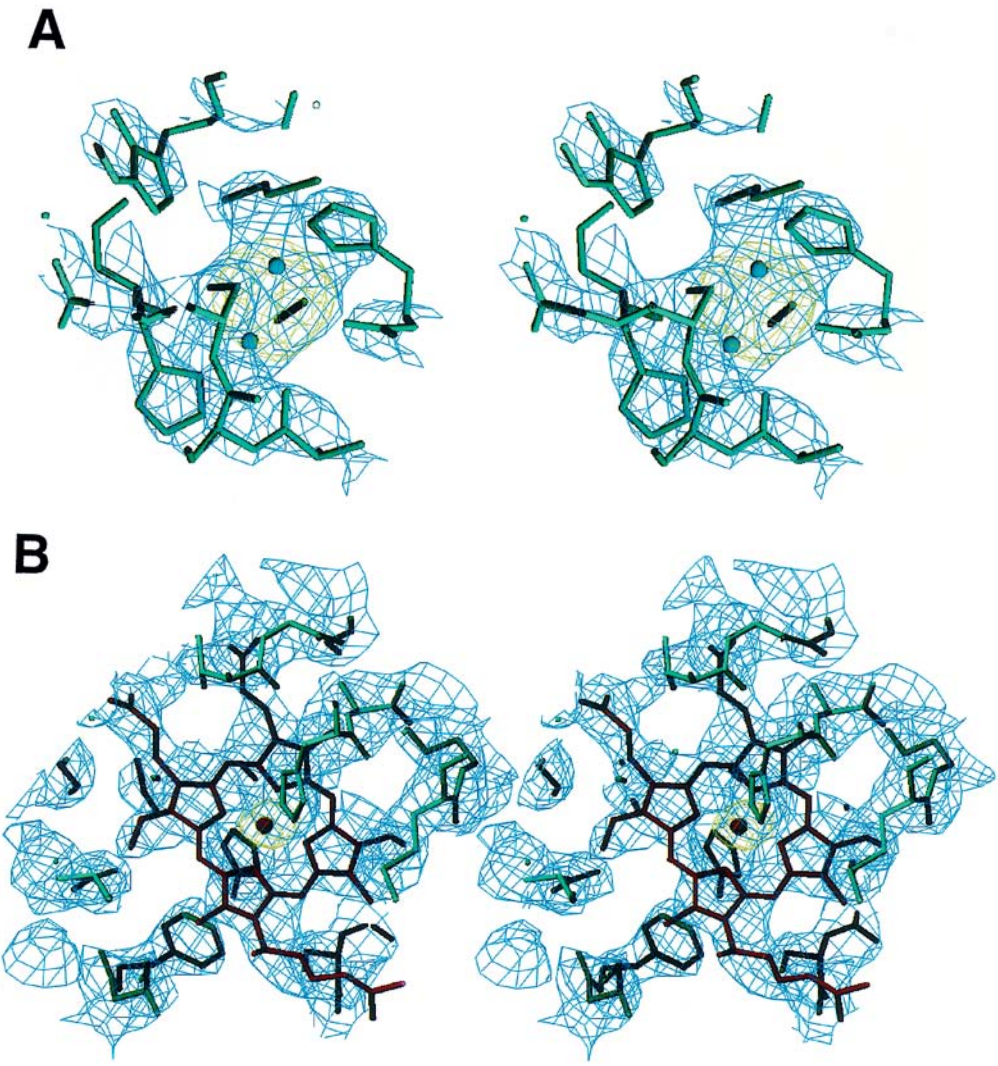

Fig. 4. Stereoviews of the Cu_A site and the heme a site. The blue cages are composed at 2σ of electron density at 2.8 Å resolution together with yellow cages, drawn at 10σ of the native anomalous difference Fourier at 4.5 Å resolution. **(A)** Cu_A site: The two blue balls show the positions of two copper atoms. **(B)** Heme a site: The red structure represents the porphyrin plane with a red ball showing the position of iron.

density maps at lower resolution, including those of the fully oxidized enzyme azide derivative at 2.9 Å resolution *(9,54)*, the fully reduced enzyme CO derivative at 2.8 Å resolution *(9)*, and the fully oxidized enzyme free from the inhibitors at 2.8 Å resolution *(6)*, although these electron density maps are not accurate enough to conclude the covalent linkage nonempirically. The covalent linkage is reported for the *Paraccocus* enzyme at 2.7 Å resolution *(55)*.

As shown in Fig. 5, the phenol-ring plane of Tyr244 and the imidazol-ring plane of His240 are not in the same plane to form a significant interaction between the two π-electron systems. The angle between the two planes is about 60°. However, the covalent linkage could be a part of a facile electron-transfer pathway from Cu_B to the ligand of Fe_{a3} (such as O_2 and –OOH), which is hydrogen-

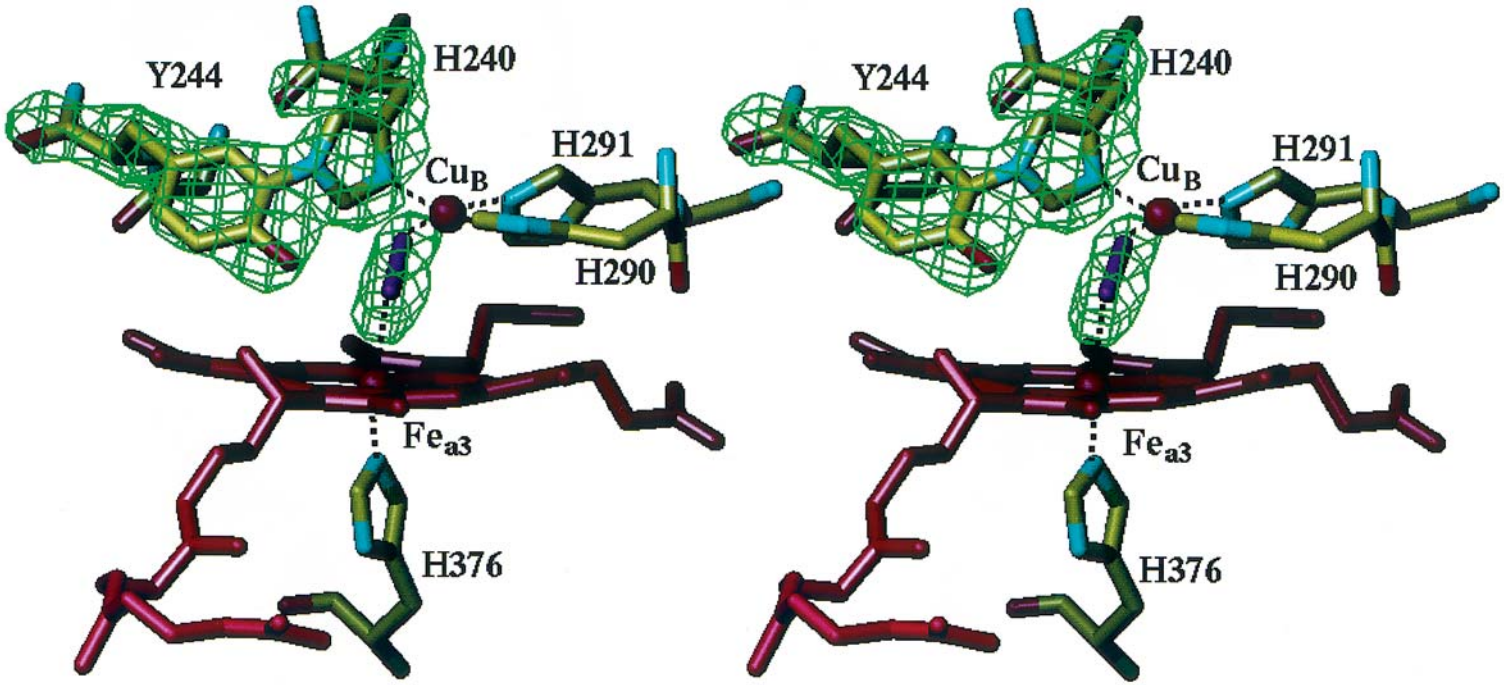

Fig. 5. X-ray structure of the O_2 reduction site of bovine heart cytochrome-*c* oxidase in the fully oxidized state at 2.3 Å resolution. The cages show the $|F_0–F_c|$ difference Fourier map of the oxidized form calculated by omitting His240, Tyr244, and any ligand between Fe_{a3} and Cu_B from the F_c calculation. The cages are drawn at the 7σ level ($1\sigma = 0.00456e^{-}/Å^3$).

bonded to the OH group of Tyr244. In the fully reduced form, no ligand is detectable between Cu_B and Fe_{a3} *(9)*. On reduction of the fully oxidized enzyme, the Fe_{a3}–Cu_B distance increases from 4.91 Å to 5.19 Å as a result of the movement of Cu_B relative to the fixed position of Fe_{a3} *(9)*. No other conformational change is induced on reduction in the Cu_B–Fe_{a3} site. Thus, in the fully reduced state, Cu_B has a trigonal planer geometry.

Three redox inactive metal sites are detectable in the electron density map of the enzyme at 2.3 Å resolution *(9)*. The magnesium site is located on the interface between subunits I and II. The carboxyl groups of Glu198 of subunit II and the two amino acids of subunit I, the imidazole of His368, and the peptide carbonyl group of Asp369 coordinate to the magnesium ion. In addition to these three ligands, three water molecules are coordinated to form a slightly distorted tetragonal bipyramid. The magnesium is located near the level of the mitochondrial innermembrane surface *(9)*. The zinc atom is coordinated by four SH groups of Cys60, Cys62, Cys82, and Cys85 in subunit Vb, which is encoded by a nuclear gene and is attached to subunits I and II on the matrix side *(6)*. A sodium ion site is detectable near the intermembrane surface of subunit I *(9)*. Three peptide carbonyl groups of Glu40, Gly45, and Ser441, a carboxyl group of Glu40, and a water molecule coordinate to the Na^+ ion to form a trigonal bipyramid. In the bacterial enzyme, the sodium ion is replaced with calcium and includes an extra negatively charged ligand to balance the charge *(55)*.

The physiological roles of these redox inactive metal sites are unknown. The magnesium and zinc ions have been proposed to be the intrinsic constituents because they were reproducibly found in many samples of purified bovine heart cytochrome-*c* oxidase *(56,57)*. However, the possibility exists that these metals are bound tightly to contaminant proteins and copurified with cytochrome-*c* oxidase. The X-ray structure showing specific binding of these metals to the intrinsic protein subunits indicates that these metals are intrinsic constituents of this enzyme. Prior to the solution of X-ray structures, the presence of sodium site had not been suggested. These X-ray structures are good examples of the importance of the determination of the composition of a large multicomponent protein.

5. MECHANISM OF O_2 REDUCTION BY CYTOCHROME-*C* OXIDASE

As described earlier, Cu_B in the reduced state is in a trigonal planar coordination environment with three histidine imidazole groups *(9)*. Usually, cuprous trigonal planar compounds are very stable and are poor ligand acceptors as well as poor electron donors. Thus, O_2 bound at Fe_{a3}^{2+} is unlikely to interact with Cu_B^{1+}. The coordination structure of Cu_B^{1+} is highly likely to contribute to the astonishingly high stability of the oxygenated form. On the other hand, the hydroxyl group of Tyr244 is fixed near the O_2 reduction site. The shortest distance between the OH group and an atomic model of O_2 placed on Fe_{a3} is estimated to be 3.4 Å. Considering the possible rearrangement of three-dimensional structure when O_2 is introduced to Fe_{a3}^{2+} site, the OH group of Tyr244 is placed close enough for formation of a hydrogen bond with the O_2 bound at Fe_{a3}^{2+}. The formation of the putative hydrogen bond between the Tyr244 OH group and the bound O_2 is rate limited by the rearrangement of the O_2 reduction site. Once the hydrogen bond is formed, the OH group could readily donate a hydrogen atom (a proton + an electron) to the bound O_2 to form a hydroperoxo intermediate (Fe_{a3}^{3+}–OOH) by a two-electron reduction process. Because the two-electron reduction process is very rapid, as described in Section 3.4. *(47)*, the formation of the hydroperoxo intermediate is likely to be rate limited by the rearrangement of the three-dimensional structure of the O_2 reduction site for the hydrogen-bond formation between O_2 and Tyr244. Thus, the process could be as slow as $t_{1/2} = 0.4$ ms *(53)*.

The resultant hydroxyl radical of Tyr244, after formation of the hydroperoxo intermediate, could be readily reduced with an electron equivalent from Cu_B^{1+} to produce a deprotonated phenol group of Tyr244, which is ready to accept a proton. Now, Cu_B is in the cupric state. Thus, it is ready to accept a negatively charged ligands. Then, in the next step, the hydroperoxo group bound to Fe_{a3}^{3+} could be deprotonated by transfer of the proton to Tyr244. The resultant peroxide bound to Fe_{a3}^{3+} is coordi-

nated to Cu_B^{2+}. The oxidation of Cu_B^{1+} facilitates the reaction step. Ligand-binding studies of cyanide and azide suggest the presence of a proton-accepting site near the O_2 reduction site. The availability of acidic protons could stimulate cleavage of the O–O bond and result in a two-electron abstraction process, possibly from Fe_{a3}^{3+} and Fe_a^{2+}. Thus, once the μ-peroxide intermediate is formed, the acidic protons from the proton-accepting site could trigger the O–O bond cleavage. In fact, formation of the second intermediate (P form) next to the oxygenated form is coupled to the oxidation of heme a. Also, the resonance Raman results, as described in Section 3.5., shows that the P form is a ferryl oxide form *(53)*.

The reaction step from the oxygenated form to the P form is essentially a four-electron reduction process. Molecular oxygen (O_2) in the oxygenated form must receives four electrons to break the O=O bond to provide two oxides (O^{2-}) and Fe_{a3} in the high oxidation state. This four-electron reduction of O_2 essentially at once may be the strategy that the enzyme uses for reduction of O_2 to water without the release of active oxygen species. This process produces an Fe_{a3} site in the high oxidation state, where the iron is Fe^{4+}. These high oxidation states of iron are very reactive but are trapped in the porphyrin system. Thus, they are much safer than the active oxygen species produced in the O_2-reduction site.

The X-ray structure of the fully oxidized form of bovine heart cytochrome-*c* oxidase as prepared has a peroxide bridging Cu_B^{2+} and Fe_{a3}^{3+} *(9)*. The stability of this form indicates that no acidic protons is available in the Cu_B^{2+}–Fe_{a3}^{3+} site in the state. The reactivity with cyanide *(14)* shows that the fully oxidized form as prepared is the "fast" form, which is considered to be an active enzyme form involved in the enzymic turnover *(58)*. However, the X-ray structure suggests that this form is a resting oxidized form and that the bridging peroxide prevents the Cu_B^{2+}–Fe_{a3}^{3+} site from being exposed spontaneously to O_2, which is likely to form active oxygen species by extracting electrons from the dimetalic site. It should be noted that no experimental evidence has been obtained for involvement of the "fast" form in the catalytic turnover. On the other hand, two water (OH^-/H_2O) molecules are assigned to the electron density between Cu_B^{2+} and Fe_{a3}^{3+} of the fully oxidized form of the *Paracoccus* enzyme at 2.7 Å resolution *(55)*. The electron density map of the fully oxidized form of bovine heart enzyme at 2.8 Å resolution is not accurate enough for differentiating peroxide from two water (OH^-/H_2O) molecules.

6. PROTON-TRANSFER MECHANISM

6.1. Possible Proton-Transfer Paths

Cytochrome-*c* oxidase must transfer protons for two purpose, for producing water molecules and for pumping protons. Usually, the interior of a globular proteins is filled with hydrophobic amino acid side chains to provide a very low dielectric constant to the inner environment. Thus, special structures are required for proton transfer through proteins. A hydrogen bond between two functional groups, both of which can be either hydrogen donor or acceptor, could serve as an effective proton-transfer path, as given in Fig. 6A. In the X-ray structure of bovine heart cytochrome-*c* oxidase, several cavities large enough to trap water molecules are observed but no clear electron density peaks are detectable. These structures suggest that the cavities contain mobile water molecules. Thus, hydronium ions could transfer protons inside the cavities. Hydroxide ions also carry protons.

It should be noted that a long hydrogen-bond network including many interconnecting hydrogen bonds is unlikely to be an effective proton-transfer path. Proton transfer through a single hydrogen bond is strictly reversible; that is, the forward reaction rate is identical to the reverse reaction rate. Thus, the fraction of the forward reaction decreases by 50% at each hydrogen bond. On the other hand, proton-transfer rates inside cavities are determined by the mobility of water molecules. Thus, the proton-transfer rate is essentially independent of the cavity size.

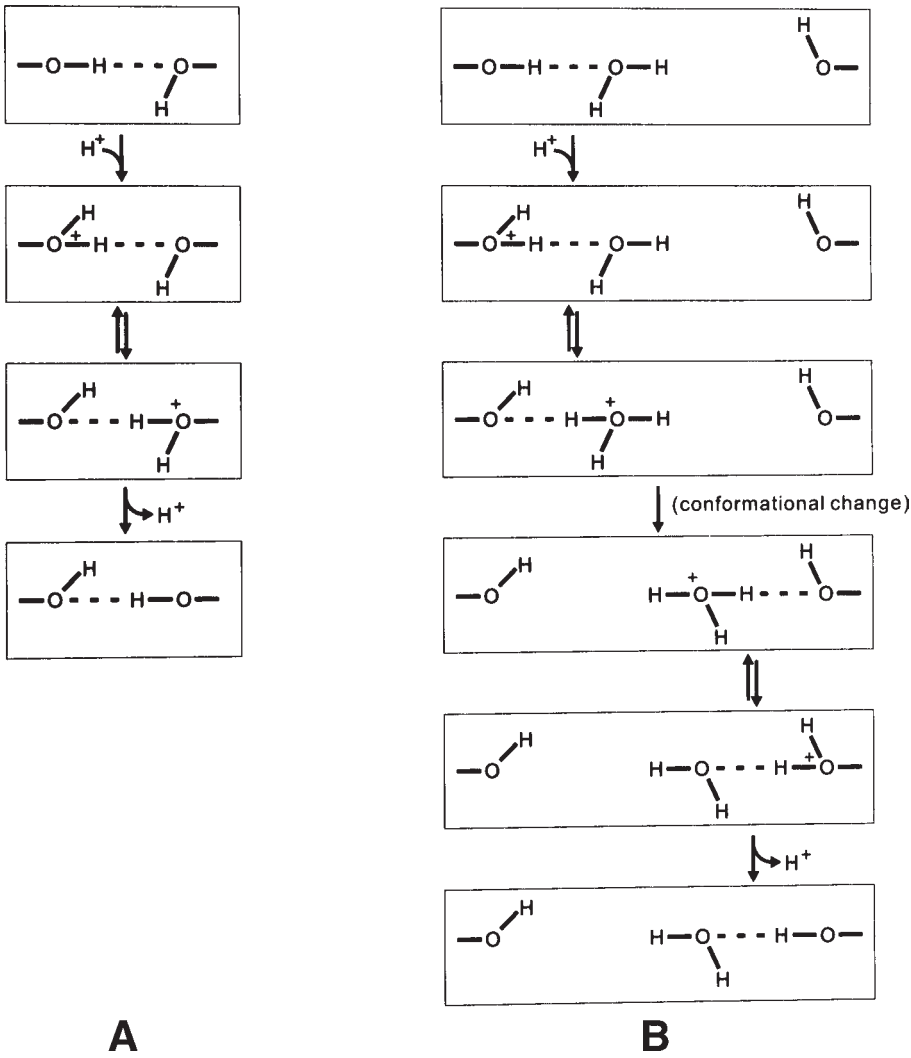

Fig. 6. Possible proton transfers through hydrogen bonds. **(A)** A possible proton-transfer pathway through a hydrogen bond between the two groups, both of which can be either a hydrogen donor or an acceptor. **(B)** A possible irreversible proton transfer with migration of a hydronium ion.

Proton transfer through a long hydrogen-bond network may be promoted by an arrangement of disconnecting points in the network where protons are transferred irreversibly with the aid of conformational changes. For example, a water molecule fixed by a hydrogen bond at a hydroxyl group as given in Fig. 6B, on receiving a proton from the hydroxide group, moves to other OH groups to form a new hydrogen bond. Then, a proton on the water molecule could be transferred to the OH group on the right-hand side. The migration of water could be irreversible if it is controlled by a conformational change inducing the polarity decrease in the environment of the hydronium ion, hydrogen-bonded to the left-hand hydroxyl group, down to the level significantly lower than that of the right-hand hydroxyl group. This irreversible conformational change provides an irreversible proton-transfer step from the left-hand hydroxyl group to the right-hand hydroxyl group. If this conforma-

tional change is coupled to the oxidation state of a metal center, a redox coupled proton transfer is facilitated by this system. The migration of water can be replaced with that of ionizable amino acid side chain. Proton transfers inside the protein both for water formation and for pumping protons must include such irreversible steps. In other words, protons for making water molecules must also be actively transported (pumped).

6.2. Proposed Mechanisms of Redox Coupled Proton Transfer

The first proposal for the proton pumping element of cytochrome-*c* oxidase included the redox coupled change in the coordination of the Cu_A site *(59)*. Unfortunately. this mechanism was not widely accepted, because the proton-pumping activity of *Escherichia coli* quinol oxidase, which does not have Cu_A site, was shown experimentally. Many researchers believe that cytochrome-*c* oxidase and quinol oxidase pump protons by an identical mechanism, although evidence to support this proposal is lacking.

Another proton-pumping element including the Cu_B site was proposed in 1994 *(60)*. This mechanism proposes that protons are pumped directly by a redox coupled coordination change in the Cu_B site. The key point of this proposal is that redox coupled movement of one of the three hisidine imidazole group responsible for pumping protons. This histidine cycle mechanism was quite widely accepted because all of the amino acids included in this mechanism are completely conserved in all biological species with terminal oxidases in the heme–copper terminal oxidase superfamily. Furthermore, an X-ray structure of *Parraccocus* cytochrome-*c* oxidase in the fully oxidized azide bound state lacks one of the histidine imidazoles bound to Cu_B, which suggests the mobility of the imidazole group *(7)*. Many researchers accepted that this X-ray structure supports the histidine cycle mechanism. However, X-ray structures of the bacterial enzyme in both fully oxidized and fully reduced states showed that all three histidine imidazoles are coordinated to Cu_B *(61)*. Furthermore, X-ray structures of bovine heart cytochrome-*c* oxidase in the fully oxidized, fully reduced, fully oxidized azide-bound and fully reduced CO-bound states clearly showed that three histidine imidazoles are bound to Cu_B *(9,54)*.

A drawback of this proposal is that no mechanism for sorting protons for pumping from those for making waters is given. If protons to be pumped are introduced to the O_2 reduction site, they would be readily used for water formation. Then, the protons cannot be pumped to the intermembrane side. One would state that the O_2 reduction and the proton pumping can occur in a separated timely manner. However, experimental results show that both the proton pumping and the proton transfer for water formation are coupled tightly with the electron transfer for the O_2 reduction *(62,63)*. Thus, the mechanism for the time sharing would not be simple. No experimental evidence supporting the time sharing has been obtained.

6.3. Redox Coupled Conformational Change in Bovine Heart Cytochrome-c Oxidase

Figure 7A shows a comparison of X-ray structures of bovine heart cytochrome-*c* oxidase in the fully oxidized and reduced states at 2.30 Å and 2.35 Å resolution, respectively *(9)*. A fairly large change in conformation is detectable in a loop region between helices I and II on the intermembrane side. No significant conformational change is detectable in other protein moiety of this enzyme. The conformational change includes the peptide backbone. Only the conformational change in Asp51 induces the change in the accessibility to the bulk water phase on the intermembrane side. In the fully oxidized state, Asp51 is completely buried within the interior of the protein, and water molecules in the bulk water phase are not able to access the amino acid side chain. On reduction of this enzyme, Asp51 moves toward the molecular surface to be exposed to the bulk water phase in the intermembrane side. On the other hand, as shown in Fig. 7B, Asp51 in the fully oxidized state has an effective accessibility to the bulk water phase on the matrix side, because Asp51 is connected to Arg38 via a hydrogen-bond network that includes a peptide bond. The Arg38 is located on the wall of a large cavity located close to heme a plane, which holds mobile water molecule. The cavity is connected to

the matrix space via a water path. Thus, Arg38 is equilibrated with the bulk water phase on the matrix side, so that Asp51 can take up protons from the matrix side. In this sense, Asp51 is accessible to the matrix side. In the reduced state, the hydrogen bond between Asp51 and the peptide NH group of Ser441 is broken and Asp51 loses the accessibility to the matrix space. Thus, the redox coupled movement of Asp51 strongly suggests that this is the site for proton pumping.

6.4. Proton Transfer Through a Peptide Bond

As shown in Fig. 7B, the hydrogen-bond network between Asp51 and Arg38 includes a peptide bond. This peptide bond is likely to facilitate a unidirectional proton transfer to Asp51. It has been well established that H/D exchange in a peptide NH group proceeds through an imidic acid intermediate (–C(OH)=N^+H–) because the peptide C=O is much more basic than the peptide NH *(64)*. The imidic acid releases the proton to give the enol form of the peptide. The enol form tautomerizes back to the keto form of the peptide, which is much more stable than the enol form. In this step, H/D exchange in NH group occurs in solution. In the enzyme, once the peptide carbonyl is protonated, the positive charge migrates to the nitrogen atom, which can then donate protons to the deprotonated carboxyl group of Asp51 hydrogen-bonded to the peptide NH, leaving the enol form of the peptide. The enol form will be readily transformed to the more stable keto form by migration of the proton on the enol OH to =N–. When the peptide is in the enol form, the reverse reaction to form the imidic acid is possible. However, once the enol form tautomerizes back to the keto form, the reverse reaction is unlikely to occur. Even if the NH group is protonated to give N^+H_2, the imidic acid intermediate cannot be formed from this form. The proton will then be readily taken up by the nearby COO^- group. Thus, the stability of the keto form versus the enol form contributes to the unidirectionality in the proton transfer. Furthermore, a conformational change of Asp51 also strongly contributes for the unidirectinality of the proton pump. The third factor contributing to the unidirectionality could be that oxidation of heme a decreases significantly the p*K* of the propionate groups. Dissociated protons from one of the propionates shown in Fig. 7B could be transferred to the peptide carbonyl to form an imidic acid. The positive charge on Arg38 may prevent the protons from approaching the large cavity in which water molecules are equilibrated with bulk solvent. The electrons taken from heme a are transferred irreversibly to the O_2-reduction site. When heme a is reduced again to increase the p*K* value of the dissociated propionate, the propionate will be reprotonated by water molecules in the large cavity via Arg38.

6.5. FTIR Studies on the Redox Coupled Conformational Change

The redox coupled conformational change in Asp51 is clearly detectable by comparison of the X-ray structure of the fully oxidized enzyme at 2.3 Å resolution with that of fully reduced enzyme at 2.35 Å resolution *(9)*. However, the resolution of the X-ray structure is not high enough for detection of the protonation state of Asp51. For this purpose, infrared spectroscopy is very useful. An infrared positive band near 1750 cm^{-1} assignable to the COOH group of Asp or Glu was observed in the difference spectrum of the oxidized versus reduced forms of bovine heart cytochrome-*c* oxidase. This band was not observed in the redox difference spectrum of *Paracoccus* cytochrome-*c* oxidase, which does not have aspartate in the corresponding position in the amino acid sequence *(65)*. Thus, the infrared band is likely to be the result of the redox coupled protonation change of Asp51 (COOH in the oxidized state and COO^- in the reduced state).

Recently, it has been claimed that the conformational change in Asp51 is controlled only by electrostatic attraction between Asp51 COO^- and Cu_A, which are located only 6 Å apart in the oxidize state *(66)*. However, these Fourier-transform infrared (FTIR) results do indicate that Asp51 does have a redox coupled protonation change. Furthermore, in the oxidized state, the carboxyl group is protonated so that no electrostatic interaction is possible for the –COOH group. On the other hand, in the reduced form, the carboxyl group is deprotonated, but the Cu_A site in the reduced form does not have any net charge. Thus, no electrostatic interaction is possible between them. However, during the

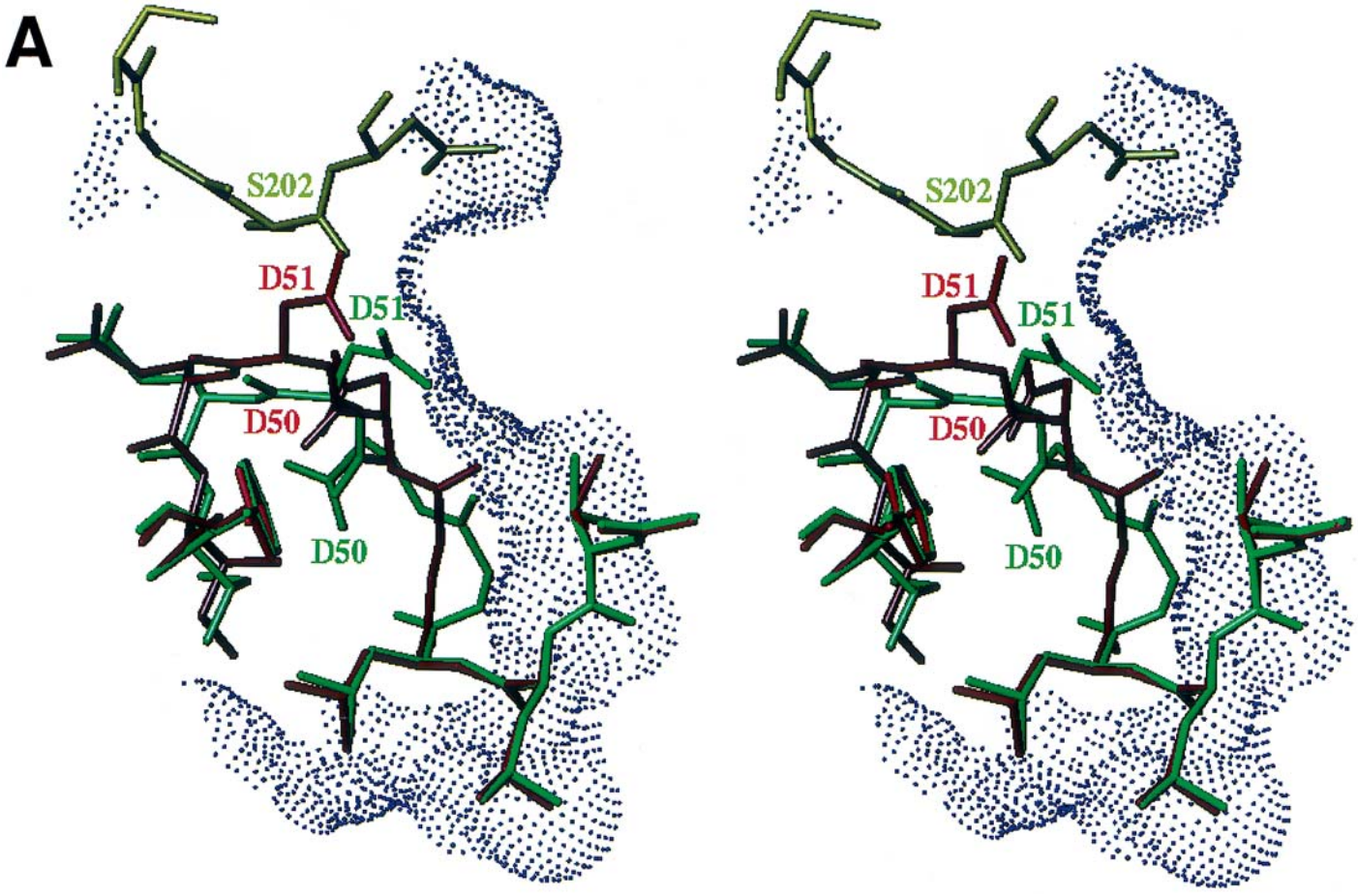

Fig. 7. Redox coupled conformational change in a loop between helices I and II of subunit I. A stereoview **(A)** and a schematic representation of the hydrogen-bond network connecting Asp51 with the matrix space **(B)**. **(A)** The molecular surface on the intermembrane side is shown by small dots. Red and green sticks represent the structures in the fully oxidized and reduced states.

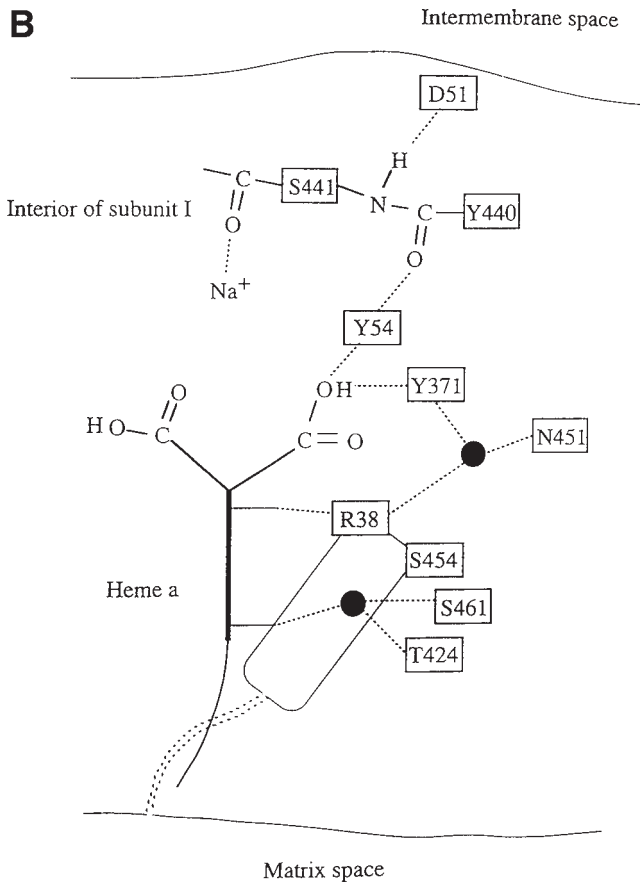

Fig. 7. (B) Dotted lines show hydrogen bonds. The rectangle represents a cavity near heme a. The two dotted lines connecting the matrix surface and the cavity represents the water path. The dark balls show the positions of fixed water molecules.

oxidation process of the reduced form of the enzyme, the oxidized form of Cu_A could trigger the conformational change of Asp51 COO^- by an electrostatic attraction.

6.6. Proton-Pumping Mechanisms in Cytochrome-c Oxidase in Various Biological Species

The key amino acid in the proton-pumping process of bovine heart cytochrome-*c* oxidase is conserved only in the animal kingdom. Plant cytochrome-*c* oxidase, bacterial cytochrome-*c* oxidase, and other enzymes in the heme-copper terminal oxidase superfamily do not have Asp51. Thus, the above proton-pump mechanism including Asp51 has not been accepted widely. An interpretation for the incomplete conservation of Asp51 is as follows: Reduction of O_2 without release of active oxygen species is an extremely complex and specific reaction. For this purpose, a heme–copper system is optimal. Thus, amino acids ligand to the metals must be conserved. On the other hand, proton pumping is much simpler chemically. Many amino acids, cofactors, and even water molecules can transfer protons. Thus, it is not surprising that Asp51 is not completely conserved. In fact, the *Paracoccus* enzyme contains a structure similar to that of the proton-pumping system in the bovine heart enzyme, although no COOH-containing amino acid is located at the position corresponding to that of Asp51 of the bovine heart enzyme. The structure suggests that the *Paracoccus* enzyme also pumps protons using a system that is closely similar to that of bovine heart enzyme, which does not include the

O_2-reduction site. Thus, the proton transfers for pumping is completely separated from the proton transfer for water formation.

According to the recent mutagenesis works for the bacterial channel-like structure corresponding to the possible proton pumping channel of the bovine heart enzyme, mutations of amino acids located on the wall of the water channel in the bottom half of the channel has no significant effect on the enzyme activity *(67,68)*. On the other hand, a mutation of Arg38 to Met in bovine number, which is at the starting point of the hydrogen-bond network, kills the enzyme *(68,69)*. These mutation results are consistent with the structure of the channel composed of the water channel and the hydrogen-bond network in the bottom and upper halves, respectively, with Arg38 at the interface.

REFERENCES

1. Ferguson-Miller, S. and Babcock, G. T. (1996). Heme/copper terminal oxidases. *Chem. Rev.* **96**, 2889–2907.
2. Wikström, M. K. F. (1977) Proton pump coupled to cytochrome c oxidase in mitochondria. *Nature* **266**, 271–273.
3. Malmström, M. G. (1973) Cytochrome oxidase: some current biochemical and biophysical problems. *Q. Rev. Biophys.* **6**, 389–431.
4. Malmström, B. G. (1990) Cytochrome c oxidase as a redox linked proton pump. *Chem. Rev.* **90**, 1247–1260.
5. Warburg, O. (1924) Über eisen, den sauerstoffübertragenden Bestandteil des Atmungsfermentes. *Biochem. Z.* **152**, 479–494.
6. Tsukihara, T, Aoyama, H., Yamashita, E., Tomizaki, T., Yamaguchi, H., Shinzawa-Itoh, K., et al. (1995) Structures of metal sites of oxidized bovine heart cytochrome-*c* oxidase at 2.8 Å. *Science* **269**, 1069–1074.
7. Iwata, S., Ostermeier, C., Ludwig, B., and Michel, H. (1995) Structure at 2.8 Å resolution of cytochrome-*c* oxidase from *Paracoccus* denitrificans. *Nature* **376**, 660–669.
8. Yakushiji, E. and Okunuki, K. (1941) Isolierung der a-Komponents des Cytochroms und ihre Eigenschaften. *Proc. Imp. Acad. Japan.* **17**, 38–40.
9. Yoshikawa. S., Shinzawa-Itho, K., Nakashima, R., Yaono, R., Yamashita, E., Inoue, N., et al. (1998) Redox-coupled crystal structural changes in bovine heart cytochrome-*c* oxidase. *Science* **280**, 1723–1729.
10. Garavito, R. M. and Picot, D. (1990) The art of crystallizing membrane proteins. *Methods* **1**, 57–69.
11. Shinzawa-Itoh, K., Ueda, H., Yoshikawa, S., Aoyama, H., Yamashita, E., and Tsukihara, T. (1995) Effects of ethyleneglycol chain length of dodecyl polyethyleneglycol monoether on the crystallization of bovine heart cytochrome-*c* oxidase. *J. Mol. Biol.* **246**, 572–575.
12. Caughey, W. S., Smythe, G. A., O'Keefe, D. H., Maskasky, J. E., and Smith, M. L. (1975) Heme A of cytochrome-*c* oxidase. Structure and properties: comparisons with hemes B, C, and S and derivatives. *J. Biol. Chem.* **250**, 7602–7622.
13. Caughey, W. S., Wallace, W. J., Volpe, J. A., and Yoshikawa, S. (1976) Cytochrome c oxidase. *The Enzymes*, 3rd ed. (P. D. Boyer, ed.), Academic, New York, Vol. 13, pp. 299–344.
14. Mochizuki, M., Aoyama, H., Shinzawa-Itho, K., Usui, T., Tsukihara, T., and Yoshikawa, S. (1999) Quantitative re-evaluation of the redox active sites of crystalline bovine heart cytochome-*c* oxidase. *J. Biol. Chem.* **274**, 33,403–33,411.
15. Kadenbach, B., Ungïbauer, M., Jarausch, J., Büge, U., and Kuhn-Nentwig, L. (1983) The complexity of respiratory complexes. *Trends Biochem. Sci.* **8**, 398–400.
16. Buse, G., Steffens, G. J., Steffens, G. C. M., Meinecke, L., and Hensel, S. (1986) Sequence analysis of complex membrane proteins (cytochrome c oxidase). *Advanced Methods in Protein Microsequence Analysis* (Wittman-Liebold ed.), Springer-Verlag, Berlin, pp. 340–351.
17. Tsukihara, T., Aoyama, H., Yamashita, E., Tomizaki, T., Yamaguchi, H., Shinzawa-Itoh, K., et al. (1996) The whole structure of the 13-subunit oxidized cytochrome-*c* oxidase at 2.8 Å. *Science* **272**, 1136–1144.
18. Robinson, N. C., Strey, F., and Talbert, L. (1980) Investigation of the essential boundary layer phospholipids of cytochrome-*c* oxidase using Triton X-100 delipidation. *Biochemistry* **19**, 3656–3661.
19. Robinson, N. C. (1982) Specificity and binding affinity of phospholipids to the high-affinity cardiolipin sites of beef heart cytochrome-*c* oxidase. *Biochemistry* **21**, 184–188.
20. Sedlák, E. and Robinson, N. C. (1999) Phopholipase A(2) digestion of cariolipin bound to bovine cytochrome-*c* oxidase alters both activity and quaternary structure. *Biochemistry* **38**, 14,966–14,972.
21. Keilin, D. and Hartree, E. F. (1938) Cytochrome a and cytochrome oxidase. *Nature* **141**, 870–871.
22. Keilin, D. and Hartree, E. F. (1939) Cytochrome and cytochrome oxidase. *Proc. R. Soc. Lond. Ser. B Biol. Sci.* **127**, 167–191.
23. Yonetani, T. (1959) Studies on cytochrome A III. Effect of synthetic detergents upon the activity of cytochrome A. *J. Biochem.* **46**, 917–924.
24. Vanneste, W. (1966) The stoichiometry and absorption spectra of components a and a-3 in cytochrome-*c* oxidase. *Biochemistry* **5**, 838–848.
25. Lappalainen, P., Watmough, N. J., Greenwood, C., and Saraste, M. (1995) Electron transfer between cytochrome-c and the isolated CuA domain: identification of substrate-binding residues in cytochrome-c oxidase. *Biochemistry* **34**, 5824–5830.
26. Wharton, D. C. and Tzagoloff, A. (1964) Studies on the electron transfer system LVII. The near infrared absorption band of cytochrome c oxidase. *J. Biol. Chem.* **239**, 2036–2041.

27. Beinert, H., Shaw, R. W., Hamsen, R. E., and Hartzell, C. R. (1980) Studies on the origin of the near-infrared (800–900 nm) absorption of cytochrome-*c* oxidase. *Biochim. Biophys. Acta* **591**, 458–470.
28. Yoshikawa, S., Mochizuki, M., Zhao, X.-J., and Caughey, W. S. (1995) Effects of overall oxidation state on infrared spectra of heme a3 cyanide in bovine heart cytochrome-c oxidase. Evidence of novel mechanistic roles for CuB. *J. Biol. Chem.* **270**, 4270–4279.
29. Reinhammer, B., Malkin, R., Jensen, P., Karlsson, B., Andreasson, L.-E., Aasa, R., et al. (1980) A new copper(II) electron paramagnetic resonance signal in two laccases and in cytochrome-*c* oxidase. *J. Biol. Chem.* **255**, 5000-5003.
30. Van Gelder, B. F. and Beinert, H. (1969) Studies of the heme components of cytochrome-*c* oxidase by EPR spectroscopy. *Biochim. Biophys. Acta* **189**, 1–24.
31. Riester, J., Zumft, W. G., and Kronech, P. M. H. (1989) Nitrous oxide reductase from *Pseudomonas stutzeri*. Redox properties and spectroscopic characterization of different forms of the multicopper enzyme. *Eur. J. Biochem.* **178**, 751–762.
32. Jin, H., Thomann, H., Coyle, C. L., and Zumft, W. G. (1989) Copper coordination in Nitrous oxide reductase from *Pseudomonas stutzeri*. *J. Am. Chem. Soc.* **111**, 4262–4269.
33. Scott, R. A., Zumft, W. G., Coyle, C. L., and Dooley, D. M. (1989) *Pseudomonas stutzeri* N_2O reductase contains CuA-type sites. *Proc. Natl. Acad. Sci. USA* **86**, 4082–4086.
34. Kroneck, P. M. H., Antholine, W. E., Kastrau, D. H. W., Buse, G., Steffens, G. C. M., and Zumft, W. G. (1990) Multifrequency EPR evidence for a bimetallic center at the CuA site in cytochrome-*c* oxidase. *FEBS Lett.* **268**, 274–276.
35. Tweedle, M. F., Wilson, L.J., Garcia-Iniguez, L., Babcock, G. T., and Palmer, G. (1978) Electronic state of heme in cytochrome oxidase III. The magnetic susceptibility of beef heart cytochrome oxidase and some of its derivatives from 7–200 K. Direct evidence for an antiferromagnetically coupled Fe (III)/Cu (II) pair. *J. Biol. Chem.* **253**, 8065–8071.
36. Moss, T. H., Shapiro, E., King, T. E., Beinert, H., and Hartzell, C. (1978) The magnetic susceptibility of cytochrome oxidase in the 4.2–1.5 K range. *J. Biol. Chem.* **253**, 8072–8073.
37. Thomson, A. J., Eglinton, D. G., Hill, B. C., and Greenwood, C. (1982) The nature of haem a3 in the oxidized state of cytochrome-*c* oxidase. Evidence from low-temperature magnetic-circular-dichroism spectroscopy in the near-infrared region. *Biochem. J.* **207**, 167–170.
38. Van Gelder, B. F. (1966) On cytochrome-*c* oxidase. I. The extinction coefficients of cytochrome a and cytochrome a3. *Biochim. Biophys. Acta* **118**, 36–46.
39. Tiesjema, R. H., Muijsers, A. O., and Van Gelder, B. F. (1973) Biochemical and biophysical studies on cytochrome-c oxidase. X. Spectral and potentiometric properties of the hemes and coppers. *Biochim. Biophys. Acta* **305**, 19–28.
40. Schroedl, N. A. and Hartzell, C. R. (1977) Oxidative titrations of reduced cytochrome aa3: anisotropic extinction behavior observed in the heme alpha-band region. *Biochemistry* **16**, 1327–1333.
41. Babcock, G. T., Vickery, L. E., and Palmer, G. (1978) The electronic state of heme in cytochrome oxidase II. Oxidation-reduction potential interactions and heme iron spin state behavior observed in reductive titrations. *J. Biol. Chem.* **253**, 2400–2411.
42. Blair, D. F., Ellis, W. R., Jr., Wang, H., Gray, H. B., and Chan, S. I. (1986) Spectrochemical study of cytochrome-*c* oxidase: pH and temperature dependences of the cytochrome potentials. Characterization of site-site interactions. *J. Biol. Chem.* **261**, 11,524–11,537.
43. Steffens, G. C. M., Biewald, R., and Buse, G. (1987) Cytochrome-c oxidase is a three-copper, t-heme-A protein. *Eur. J. Biochem.* **164**, 295–300.
44. Gibson, Q. H. and Greenwood, C. (1963) Reactions of cytochrome oxidase with oxygen and carbon monoxide. *Biochem. J.* **86**, 541–555.
45. Hill, B. C. (1994) Modeling the sequence of electron transfer reactions in the single turnover of reduced, mammalian cytochrome-*c* oxidase of oxygen. *J. Biol. Chem.* **269**, 2419–2425.
46. Mori, M. and Weil, J. A. (1967) The formation of and interaction between some peroxide binuclear cobalt complexes. *J. Am. Chem. Soc.* **89**, 3732–3744.
47. Yoshikawa, S., Choc, M. G., O'Toole, M. C., and Caughey, W. S. (1977) An infrared study of CO binding to heart cytochrome-*c* oxidase and hemoglobin A. Implications re O_2 reactions. *J. Biol. Chem.* **252**, 5498–5508.
48. Chance, B., Saronio, C., and Leigh, J. S., Jr. (1975) Functional intermediates in the reaction of membrane-bound cytochrome oxidase with oxygen. *J. Biol. Chem.* **250**, 9226–9237.
49. Blackmore, R. S., Greenwood, C., and Gibson, Q. H. (1991) Studies of the primary oxygen intermediate in the reaction of fully reduced cytochrome oxidase. *J. Biol. Chem.* **266**, 19,245–19,249.
50. Varotsis, C., Woodruff, W. H., and Babcock, G. T. (1990) Time-resolved Raman detection of υ (Fe-O) in an early intermediate in the reduction of O_2 by cytochrome c oxidase. *J. Am. Chem. Soc.* **112**, 1297.
51. Ogura, T., Takahashi, S., Shinzawa-Ihto, K., Yoshikawa, S., and Kitagawa, T. (1990) Observation of the Fe^{II}-O_2 stretching Raman band for cytochrome oxidase compound A at ambient temperature. *J. Am. Chem. Soc.* **112**, 5630–5631.
52. Han, S., Ching, Y.-C., and Rousseau, D. L. (1990) Primary intermediate in the reaction of oxygen with fully reduced cytochrome-*c* oxidase. *Proc. Natl. Acad. Sci. USA* **87**, 2491–2495.
53. Ogura, T., Takahashi, S., Hirota, S., Shinzawa-Itho, K., Yoshikawa, S., and Kitagawa, T. (1993) Time-resolved resonance Raman elucidation of the pathway for dioxygen reduction by cytochrome c oxidase. *J. Am. Chem. Soc.* **115**, 8527–8536.
54. Fei, M. J., Yamashita, E., Inoue, N., Yao, M., Yamaguchi, H., Tsukihara, T., et al. (2000) X-ray structure of azide-bound fully oxidized cytochrome-*c* oxidase from bovine heart of 2.9 Å resolution. *Acta. Crystallogr.* **D56**, 529–535.

55. Ostermeier, C., Harrenga, A., Ermler, U., and Michel, H. (1997) Structure of 2.7 Å resolution of the *Paracoccus* denitrificans two-subunit cytochrome-*c* oxidase complexed with an antibody FV fragment. *Proc. Natl. Acad. Sci. USA* **94**, 10,547–10,533.
56. Einansdottier, O. and Caughey, W. S. (1984) Zinc is a constituent of bovine heart cytochrome-*c* oxidase preparations. *Biochem. Biophys. Res. Commun.* **124**, 836–842.
57. Einansdottier, O. and Caughey, W. S. (1985) Bovine heart cytochrome-*c* oxidase preparations contain high affinity binding sites for magnesium as well as for zinc, copper, and heme iron. *Biochem. Biophys. Res. Commun.* **129**, 840–847.
58. Moody, A. J. (1996) "As prepared" forms of fully oxidised haem/Cu terminal oxidases. *Biochim. Biophys. Acta* **1276**, 6–20.
59. Gelles, J., Blair, D. F., and Chan, S. I. (1986) The proton-pumping site of cytochrome-*c* oxidase: a model of its structure and mechanism. *Biochim. Biophys. Acta* **853**, 205–236.
60. Wikström. M., Bogachev, A., Finel, M., Morgan, J. E., Puustinen, A., Raitio, M., et al. (1994) Mechanism of proton translocation by the respiratory oxidases. The histidine cycle. *Biochim. Biophys. Acta* **1187**, 106–111.
61. Michel, H. and Harrenga, A. (1999) the cytochrome-*c* oxidase from *Paracoccus* denitrificans does not change the metal center ligation upon reduction. *J. Biol. Chem.* **274**, 33,296–33,299.
62. Wikström, M. and Morgan, J. E. (1992) The dioxygen cycle. Spectral, kinetic, and thermodynamic characteristics of ferryl and peroxy intermediates observed by reversal of the cytochrome oxidase reaction. *J. Biol. Chem.* **267**, 10,266–10,273.
63. Verkhovsky, M. I., Jasaitis, A., Verkhovskaya, M. L., Morgan, J. E., and Wikström, M. (1999) Proton translocation by cytochrome-*c* oxidase. *Nature* **400**, 480–483.
64. Perrin, C., Lollo, C. P., and Johnston, E. R. (1984) NMR site-to-site rate constants and the mechanism of acid-catalyzed proton exchange in secondary amides. *J. Am. Chem. Soc.* **106**, 2749–2753.
65. Hellwig, P., Soulimane, T., Buse, G., and Mäntele, W. (1999) Similarities and dissimilarities in the structure-function relation between the cytochrome-*c* oxidase from bovine heart and from *Paracoccus* denitrificans as revealed by FT-IR difference spectroscopy. *FEBS Lett.* **458**, 83-86.
66. Michel, H. (1999) Cytochrome-*c* oxidase: catalytic cycle and mechanisms of proton pumping—a discussion. *Biochemistry* **38**, 15,129–15,140.
67. Pfitzner, U., Odenwald, A., Osterman, T., Weingard, T., Ludwig, B., and Richter, O.-M. H. (1998) Cytochrome-*c* oxidase (heme aa3) from *Paracoccus* denitrificans: analysis of mutations in putative proton channels of subunit I. *J. Bioenerg. Biomembr.* **30**, 89–97.
68. Lee, H.-M., Das, T. K., Rousseau, D. L., Mills, D., Feguson-Miller, S., and Gennis, R. B. (2000) Mutations in the putatiave H-channel in the cytochrome-c oxidase from Rhodobacter sphaeroides show that this channel is not important for proton conduction but reveal modulation of the properties of heme a. *Biochemistry* **39**, 2989–2996.
69. Kannt, A., Pfitzner, U., Ruitenberg, M., Hellwig, P., Ludwig, B., Mäntele, W., et al. (1999) Mutation of Arg-54 strongly influences heme composition and rate and directionality of electron tranfer in *Paracoccus* denitrificans cytochrome-*c* oxidase. *J. Biol. Chem.* **274**, 37,974–37,981.

8

The Fet3 Protein

A Multicopper Ferroxidase Essential to Iron Metabolism in Yeast

Daniel J. Kosman

1. INTRODUCTION

Iron homeostasis in eukaryotes is dependent on adequate copper nutrition. This physiologic linkage between copper and iron is the result of the enzymatic activity of one or more multicopper ferroxidases. Ferroxidases are enzymes that catalyze the reaction shown in reaction (1).

$$4Fe(II) + O_2 + 4H^+ \rightarrow 4Fe(III) + 2H_2O \qquad (1)$$

There are two ferroxidases in humans, ceruloplasmin and hephaestin, and two in the yeast *Saccharomyces cerevisiae*, Fet3p and Fet5p. In addition, each one of these copper proteins relies on a copper ATPase found in the membrane of a specific vesicular compartment for the copper necessary for each protein's activation. The copper pumping that any one of these ATPases does may be critical to copper homeostasis as well as for copper excretion, for example. These pumps, in turn, rely on a protein—a copper chaperone—that ferries the copper from the plasma membrane copper permease through the cytosol to this vesicular compartment. The permease relies on a plasma membrane cuprireductase to supply it with the Cu(I) as substrate for uptake. Nonetheless, irrespective of whether or how a defect in any one of these enzymes, transporters, chaperones, or pumps may contribute to a dysfunction in copper handling, there most certainly will be a direct impact on the copper incorporation into one or more of these ferroxidases leading to a secondary effect on iron homeostasis. The copper ferroxidases are central to this secondary nutritional, metabolic, essentially epistatic relationship between copper and iron in eukaryotes. The yeast protein Fet3, a paradigm for this subclass of multicopper oxidases, is the focus of this chapter.

2. THE THREE TYPES OF PROTEIN COPPER SITE

There are three types of copper site found in nature; copper proteins are classified on the basis of the "type" of copper site that they contain *(1)*. These three types of copper site differ as to coordination number, type of ligands, and geometry; these differences, in turn, are the basis for these sites' electronic signatures and chemical (redox) activity. Type-1 Cu(II) exhibits a very strong absorbance at approx 600 nm (ε = 5000 M^{-1} cm^{-1}). This absorbance imparts a striking blue color to type-1 copper-containing proteins at concentrations >100 μM. This absorbance is the result of a charge-

From: Handbook of Copper Pharmacology and Toxicology
Edited by: E. J. Massaro © Humana Press Inc., Totowa, NJ

transfer transition from the cysteine sulfur ligand that characterizes the type-1 site to the Cu(II). This Cys–S π to Cu^{2+} d_{x2-y2} transition also places significant unpaired electron spin density on the sulfur rather than on the copper. As a result, the type-1 Cu(II) has a correspondingly small parallel electron spin–nuclear spin hyperfine coupling evident in the continuous-wave electron paramagnetic resonance (cwEPR) spectrum ($A_{\|} = (43–95) \times 10^{-4}$ cm^{-1}). In addition to this Cys ligand, type-1 sites also have two histidine imidazole ligands. These three ligands typically describe a trigonal plane such that the geometry of the site overall can be described as distorted tetrahedral or distorted trigonal pyramid with the fourth ligand, if present, at the apex of this pyramid. However, it is the cysteine sulfur ligand common to all type-1 sites that dominates their electronic and chemical properties *(1,2)*.

Type-2 copper sites are "normal" in that they exhibit only the weak (forbidden) d–d transitions typical of Cu(II). They are "nonblue." Not surprisingly, they lack the cysteine sulfur ligand found at all type-1 sites while most commonly containing only histidine imidazole coordination by the protein. The absence of significant electron spin transfer to the ligands at type-2 Cu(II) results in these sites having the copper hyperfine coupling typical of (pseudo)square-planar–Cu(II) complexes containing nitrogenous and/or oxygenous ligands. $A_{\|}$ values for type–2 Cu(II) sites in proteins range from 140 to 190×10^{-4} cm^{-1}. The wave function that describes the unpaired electron in type-1 Cu(II) (spin density higher at the S) results also in a smaller spin-orbit coupling in comparison to the wave function that describes the unpaired electron at type-2 Cu(II). With the electron spin density higher at the metal in this latter case, there is greater spin-orbit coupling. This difference results in a larger contribution of orbital angular momentum to the magnetization of an electron at a type-2 Cu(II) and thus in a stronger interaction with the magnetic field. This is reflected in a larger $g_{\|}$ value for type-2 sites, typically >2.2; in contrast, $g_{\|}$ values for type-1 Cu(II) are closer to the free-electron value of 2.002.

Another feature that distinguishes type-2 from type-1 copper sites is that the former nearly always have at least one water molecule from solvent as one of the inner-sphere ligands; many have two solvent-derived exchangeable ligands. Type-1 Cu(II), in contrast, does not have a coordinated solvent-derived ligand. This structural difference is directly linked to the different function that the two sites play in the electron-transfer reactions involving copper proteins. Type 1 sites are restricted to outer-sphere electron-transfer processes, whereas type-2 sites catalyze reactions that involve a direct coordination of an electron donor or acceptor. Thus, in the case of the multicopper oxidases, the type-1 copper is the site of entry of the electron from the one-electron reductant, whereas dioxygen—the electron acceptor or oxidant—is reduced at the type-2 copper site.

Type-3 copper is the third type of Cu(II) site in biology. A type-3 site has two distinguishing electronic properties. The first is its relatively strong absorbance in the near ultraviolet (UV) at approx 330 nm (ε = 3–5000 M^{-1} cm^{-1}). This transition is indicated by a shoulder on the much stronger absorbance at approx 280 nm because of protein aromatic amino acid residues. Second, type-3 sites are diamagnetic despite the presence of Cu(II). The lack of a cwEPR spectrum, for example, is attributed to the fact that the type-3 Cu(II) site contains two copper atoms that are antiferromagnetically coupled through a bridging oxygen (–OH) atom. The absorbance at 330 nm is the result of charge transfer from this ligand onto the copper atoms. This bridging ligand is the hallmark of type-3 copper sites, at least in their fully oxidized state; in other respects, they vary as to the nature of the protein ligands, although most contain either or both histidine imidazole and tyrosine phenol ligands.

3. MULTICOPPER OXIDASES HAVE ONE EACH OF THE THREE TYPES OF COPPER SITES: FET3P

What distinguishes multicopper oxidases from other copper proteins is that they contain one each of these three types of copper sites *(1,3)*. Not only does this make them excellent models for *all* copper proteins, but because they have four redox active metal ions, they also serve as paradigms for other enzymes that couple a one-electron reductant to a four-electron oxidant, most notably cytochrome-*c* oxidase. Indeed,

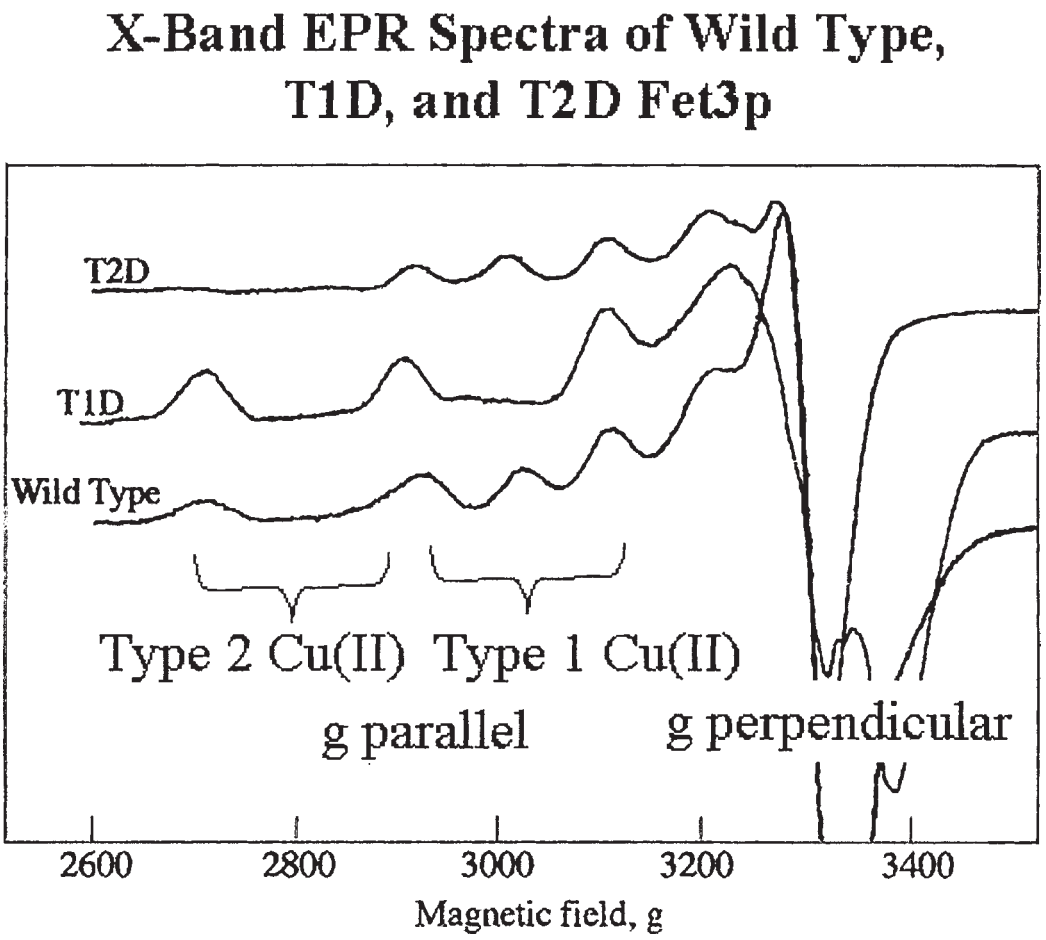

Fig. 1. Electron paramagnetic resonance spectra of wild-type and T1D and T2D mutants of Fet3p as indicated. Spectra were obtained at a microwave frequency of 9.5 GHz and 120 K. The samples were prepared in 25% (v/v) ethylene glycol/50 m*M* MES buffer (pH = 6.0). The instrument settings were constant with 10 mW microwave power, 100 kHz modulation frequency, 10 G modulation amplitude, 0.02 s time constant, and 60 s sweep time. (From ref. *4*.)

the three copper sites (and four copper atoms) in the multicopper oxidases play essentially equivalent roles in comparison to the two heme groups and two copper atoms in that enzyme.

Spectral data on the Fet3 protein illustrate the electronic properties of the three types of Cu(II) site found in multicopper oxidases *(4,5)*. The cwEPR spectrum shown in Fig. 1 for the wild-type protein has contributions from both the type-1 and type-2 Cu(II) electron Zeeman and nuclear spin interactions. The spectra for mutant proteins that lack either the type-2 copper (T2D) or type-1 copper (T1D) exhibit the EPR spectrum of the remaining Cu(II) site only (Fig. 1). These latter spectra show clearly the relatively smaller *A* and *g* values associated with the type-1 Cu(II) (seen in the T2D protein) in comparison to the type-2 Cu(II) (seen in the T1D protein) as was noted earlier. The UV-visible absorbance spectra of this set of three Fet3 proteins are shown in Fig. 2.

Shown also in Fig. 2 is the spectrum of a double-mutant protein. This is the T1D/T2D protein that lacks both the type-1 and type-2 copper atoms. Only the type-3 binuclear cluster contributes to the nonprotein absorbance in this protein, demonstrating that the shoulder at 330 nm seen in all of the spectra shown in Fig. 2 is the result of this cluster. This cluster contributes a broad absorbance

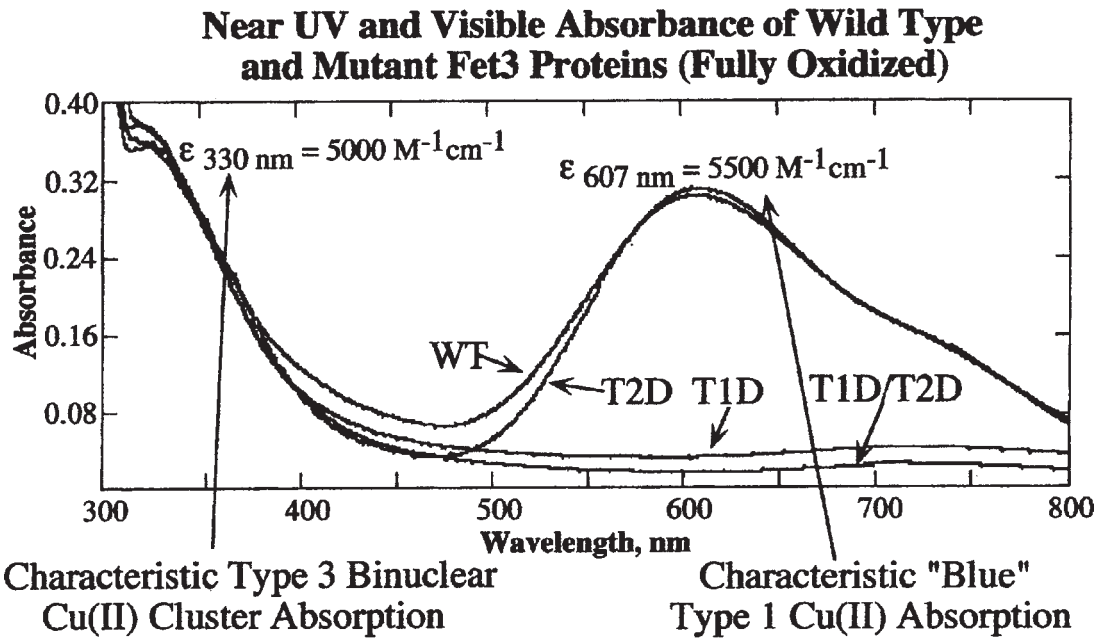

Fig. 2. Absorbance spectra of wild type, T1D, T2D, and T1D/T2D mutants of Fet3p as indicated. All samples were prepared in 50 m*M* MES buffer (pH = 6.0). Spectra were recorded following treatment of the samples with 0.5 m*M* hydrogen peroxide to ensure that all copper atoms present were in the cupric state. (From ref. *4*.)

centered at 720 nm, as the spectrum of this double mutant demonstrates also. The absorbance of the wild-type protein at 608 nm is clearly the result of type-1 Cu(II) because it is seen only in protein forms that possess this site (e.g., the wild-type and T2D mutant protein). The spin Hamiltonian and absorbance values for the copper sites in Fet3p are summarized in Table 1. In Fet3p as in all of the multicopper oxidases, the type-1 Cu(II) is the site of entry of electrons from the reducing substrate, whereas oxygen binds to and is reduced at the type-2 and type-3 binuclear clusters. In the ferroxidase reaction [reaction (1)], the reducing substrate is Fe^{2+}. Although all multicopper oxidases use organic reductants as substrate (e.g., *o*-dianisidine, *p*-phenylenediamine, and *p*-hydroquinone), hCp, Fet3p, and the other ferroxidases alone as a subclass have strong activity toward Fe^{2+}.

4. KNOWN STRUCTURES OF MULTICOPPER OXIDASES

Structures of three multicopper oxidases have been determined by X-ray crystallographic analysis: human ceruloplasmin (hCp), *Coprinus cinereus* (fungal) laccase (Lac), and *Cucurbita pepo* (zuccini) ascorbate oxidase (AO). hCp is the only ferroxidase whose structure has been determined crystallographically *(7,8)*. Lindley and his coworkers have published a 3.1-Å map (PDB accession number, 1KCW). This structure showed that as in Lac (1A65) *(9)* and AO (1AOZ) *(10–12)*, the type-2 and type-3 copper atoms in hCp are trigonally arranged with an atom-to-atom spacing of approx 3.5 Å. This "trinuclear" cluster is, in turn, approx 13 Å from the type-1 copper atom. This arrangement of the three copper sites is diagrammed in Fig. 3 using ligand assignments for Fet3p. These assignments are based on the sequence homologies among the multicopper oxidases, as shown in Fig. 4. In all cases, the numbering is based on the encoded protein, not the mature processed one. All of the encoded proteins contain leader signal-recognition sequences that are cleaved during their maturation. As noted earlier, the type-1 Cu(II) is the redox partner of the reducing substrate. The trinuclear cluster, in

Table 1
Spin Hamiltonian and Absorbance Parameters for the Copper Sites in Fet3p

Copper site	$g_{\|\|}$	$A_{\|\|}$ ($\times 10^{-4}$ cm^{-1})	$g_{\perp}$	λ_{max} (*nm*)	ε ($M^{-1}cm^{-1}$)
Type 1	2.19	89	2.05	608	5500
Type 2	2.24	195	2.05	Not resolvable, <100	
Type 3	Diamagnetic		330	~5000	
		~720		~300	

Source: Data from refs. *4–6*.

turn, is responsible for the four one-electron transfers to dioxygen that result in the production of two water molecules *(13)*.

The structures of the type-1 sites in hCp, Lac, and AO—and in Fet3p—differ in some details; nonetheless, the electron-transfer reactions at this site in the four proteins are all outer sphere in nature *(3)*. This mechanism is dictated by the fact that type-1 sites, as a class, do not have exchangeable solvent-accessible inner coordination sites to which a reductive ligand could bind. On the other hand, the relationship between the copper atom and the solvent-accessible surface of the protein does vary among these proteins. For example, the type-1 copper in hCp is completely buried *(7)*, whereas this site in *Coprinus cinereus* Lac is much closer to the surface *(9)*. This difference is apparent in Fig. 5, which displays Connelly surfaces adjacent to the type-1 sites in the two proteins. Connelly surfaces, in effect, show the solvent surface of a macromolecule. The green-hued surface patch in the Lac structure (Fig. 5, left) is the result of the N^{ε} of H494; clearly, the edge of this copper ligand is strongly exposed to solvent. In contrast, the corresponding histidine in hCp, H1045, is buried in the protein and completely shielded from solvent (Fig. 5, right). In both cases, the electron transfer from the substrate, irrespective of its nature, is outer sphere; however, given the striking difference in surface accessibility, the precise mechanism (route) for how the electron gets to the Cu(II) may be quite different in the two proteins.

5. ESEEM ANALYSIS OF FET3P COPPER-SITE STRUCTURE: THE TYPE-1 AND TYPE-2 CU(II) SITES

Although the structure of Fet3p is not known, electron spin-echo envelope modulation (ESEEM) data suggest that its type-1 copper has a solvent accessibility that is intermediate between the situation in hCp and Lac *(14)*. ESEEM is a pulsed EPR technique that resolves spin interactions that are weak compared to the interaction of the electron spin magnetization with the instrument magnetic field or with those fields resulting from strongly interacting nuclei. Those are the interactions detected in the cwEPR spectrum as in Fig. 1. Thus, ESEEM that is the result of the weak interaction (approx 1 MHz at a field of 3 kG) of the distal, noncoordinating N in an histidine imidazole found at a Cu(II) site in a protein can be resolved easily *(15)*. The ESEEM spectra of the unpaired electron at the type-1 Cu(II) (in the T2D mutant) is shown in Fig. 6A *(14)*. The depth and period of modulation of the electron spin magnetization can be correlated to the amount of spin density that is transferred from the Cu^{2+} to equatorially coordinated histidine imidazoles and the number of such ligands. The modulation depth of the ESEEM spectrum resulting from the type11 Cu(II) is therefore relatively weak because much of the spin density is on the S ligand of Cys484 at this site *(1,2)*. The Fourier transform of the modulation envelope gives the modulation frequencies that generate it. This transform is shown in Fig. 6B and can be best fit with a model that includes two equatorial but inequivalent imidazole ligands at the type-1 Cu^{2+}.

The ESEEM spectrum of the type-2 Cu^{2+} (in the T1D mutant) is substantially different, both because at this site there is significantly more spin density at the copper (no charge transfer involving

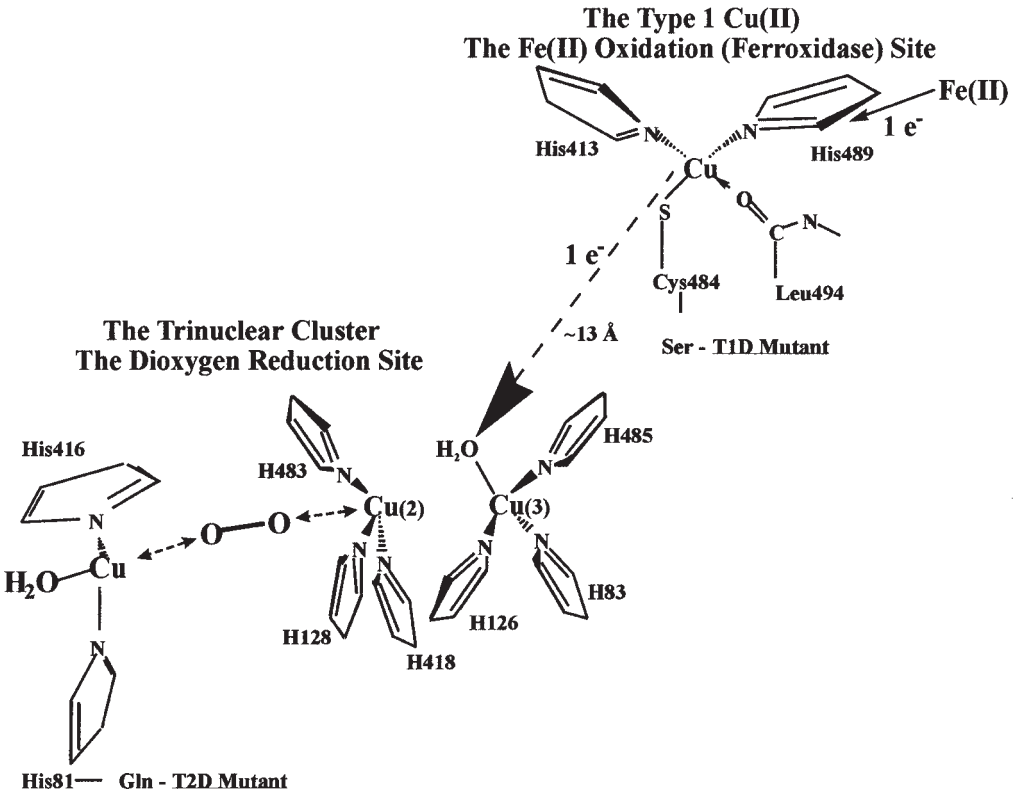

Fig. 3. Spatial relationship among the three copper sites in a multicopper oxidase. The structure (and residue numbering) is a representation of these sites in hCp. The trinuclear cluster is a near-isosceles triangle, approx 3.4 Å on a side. The notation $Cu_{(2)}$ and $Cu_{(3)}$ is taken from ref. *10* and corresponds to the notation Type 3" and Type 3', respectively, used by Zaitseva et al. *(7)*. Oxygen is thought to bind between the type-2 copper and $Cu_{(2)}$.

a cysteine sulfur) and because this copper atom is directly coordinated by solvent water. The first of these differences is apparent in the depth of modulation, as seen in Fig. 7A. The second is apparent in the weaker modulation seen at longer times. This is the result of ^1H associated with bound water molecules. The Fourier transform of the ESEEM data is given in Fig. 7B and is best fit by assuming one equatorial imidazole and, perhaps, a second imidazole ligand coordinated axially.

The spectra in Figs. 6 and 7 were taken in H_2O and therefore do have the potential to show a modulation resulting from ^1H of any water that might be coordinated to or magnetically "near" the type-2 Cu(II) as well. This modulation was well resolved in the type-2 Cu(II) spectrum as noted but was essentially absent in the type 1-Cu(II) one. In order to better resolve this modulation, however, one takes spectra in ^1H_2O and ^2H_2O and calculates the ratio of the experimental modulation patterns: in effect, the pattern in deuterium oxide provides the negative control for water proton modulation *(16)*. Again, the strength and pattern of this ratioed modulation can be interpreted in terms of how water might be coordinated to or how it might magnetically interact with the Cu(II). This is illustrated in the theoretical traces given in Fig. 8A,B for one equatorial water, or for one axial water, or for ambient water only ("outer-sphere" water). These three traces can be compared to the experimental trace for the ratioed envelope for the type-1 site in Fet3p. This experimental trace can be best modeled by a Cu(II) that has a "half-shell" of ambient water only, with no directly coordinated water molecules (Fig. 8D). The fit that is shown is for a model that has this "hemisphere" of water molecules at 3.75 Å from the type-1 Cu(II). In comparison to the known structures of Lac and hCp (Fig. 5), this result

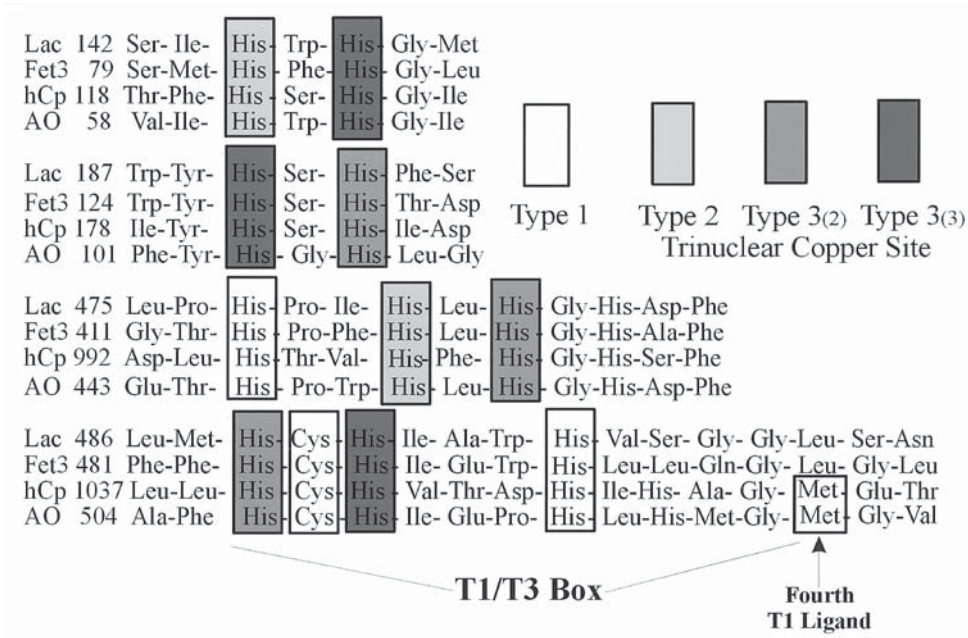

Fig. 4. Sequence alignments of the copper-binding motifs in multicopper oxidases. The sequences are for *Neurospora crassa* laccase (Lac), *Cucimus sativus* ascorbate oxidase (AO), and two ferroxidases, human ceruloplasmin (hCp) and Fet3p, from *Saccharomyces cerevisiae.* The key indicates the ligand assignments to the three copper sites found in these proteins. The sequence numbering is referenced to the ATG that encodes the start codon in the translated mRNA and not to the carboxyl terminal residue of the processed mature protein. Note that all of these are glycoproteins and are targeted to the endoplasmic reticulum. Thus, the nascent polypeptide contains a canonical signal-recognition sequence that is cleaved as part of the proteins' overall processing, which includes the posttranslational insertion of the four active-site copper atoms.

indicates that in Fet3p the N^{ε} of His489 (corresponding to His494 and 1045 in Lac and hCp, respectively) would be just at the protein surface and contributing little to the Connelly surface. On the other hand, the Hε2 hydrogen at His489 would be solvent exposed and H-bonded to water. Further ESEEM analysis was consistent with this inference. The type-1 Cu(II) sites in the three proteins are directly compared in the illustrations shown in Fig. 9.

In addition to the relative degree of solvent exposure represented in these models, the difference in coordination can also be seen. Lac (A) and Fet3p (C) have three-coordinate trigonal type-1 Cu(II) sites, whereas hCp (B) has a four-coordinate distorted tetrahedral structure. Type-1 copper sites in general exhibit this divergence, which can also be seen in the sequence alignments in Fig. 3: AO, like hCp, has the thioether of Met as a fourth ligand. What is interesting is that although this ligand does modulate the properties of type-1 Cu(II) to some extent, other features, such as protein-induced distortion, overall are much stronger determinants of type-1 copper structure and reactivity *(2,17)*.

The ratioed envelope for the type-2 Cu(II) spectrum is best fit with a combination of one equatorial water, one axial water, as well as a distribution of ambient water at a radius of 4–8 Å (Fig. 8E). Together with the Fourier transform shown in Fig. 7B that is attributable to a single equatorially coordinated histidine, the water modulation analysis suggests a structure of the type-2 Cu(II) site in Fet3p that is significantly different from what crystallographic analysis has indicated for the type-2 sites in hCp *(7,8)* and AO *(11,12)*. This site in these proteins appears to have two equatorial histidine imidazoles, and one equatorial water ligand in an essentially trigonal planar complex. This is illustrated in Fig. 10A. In contrast, Fet3p appears to have only one equatorial histidine imidazole, and one equatorial and one axial water. Inasmuch as the type-2 site in Fet3p has both conserved histidines

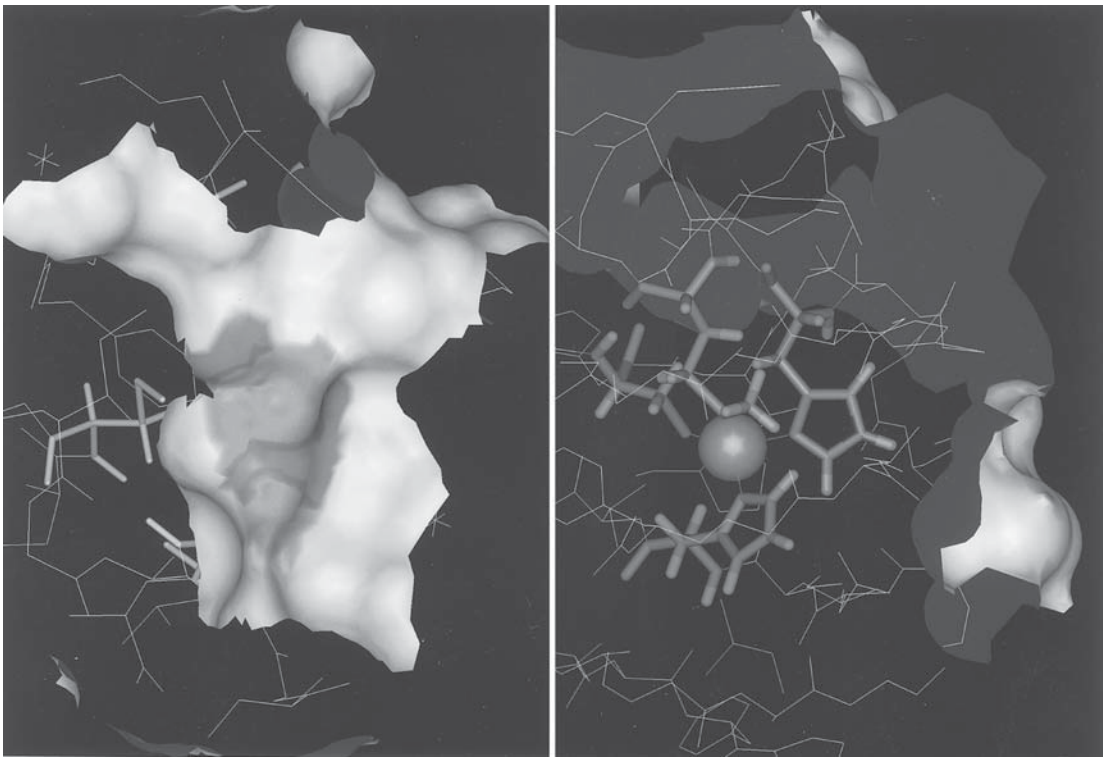

Fig. 5. The Connelly surface at the type-1 copper sites in *C. cinereus* Lac (left) and hCp (right). These surfaces were generated using InsightII software from Molecular Dynamics. The structure files came from the PDB; the accession numbers were 1A65 for Lac, and 1KCW for hCp. The type-1 site in hCp is completely shielded from solvent; H1045 (to the right), which is the closest ligand to the surface, is at least 7 Å from it. In contrast, the corresponding His ligand in Lac, His494, is strongly solvent exposed. The shading in the right panel is the result of the N^{ε} of this residue and the magenta indicates the adjacent ring carbons. Electron spin-echo envelope modulation data indicate that this site in Fet3p is more similar to Lac than to hCp.

(His81 and His416), it is possible that the second of these is an axial ligand at this site and therefore does not contribute to the modulation pattern. This model of the type-2 site is presented in Fig. 10B. A model for all three copper sites in Fet3p and there putative spatial relationship was given in Fig. 3.

6. EXAFS ANALYSIS OF FET3P COPPER-SITE STRUCTURE: THE BINUCLEAR TYPE-3 SITE

One recombinant Fet3p mutant has been particularly informative about the structure of the type-3 binuclear cluster in them. This is the T1D/T2D double mutant that contains only this type-3 site *(5)*. EXAFS (extended X-ray absorption fine structure) analysis of this protein contains contributions from electron ejection and scattering from only the type-3 copper atoms and thus provides direct structural information about this cluster. The *K*-edge XAS spectrum for this mutant in its oxidized and reduced states is shown in Fig. 11. The oxidized sample has a nearly featureless edge with a midpoint energy of 8990 eV typical of tetragonally distorted type-2 Cu(II) centers (i.e., ones with predominantly histidine imidazole coordination). The reduced type-3 cluster exhibited a pronounced shoulder at 8984 eV just below the midpoint energy of 8987 eV. The shoulder is characteristic of a

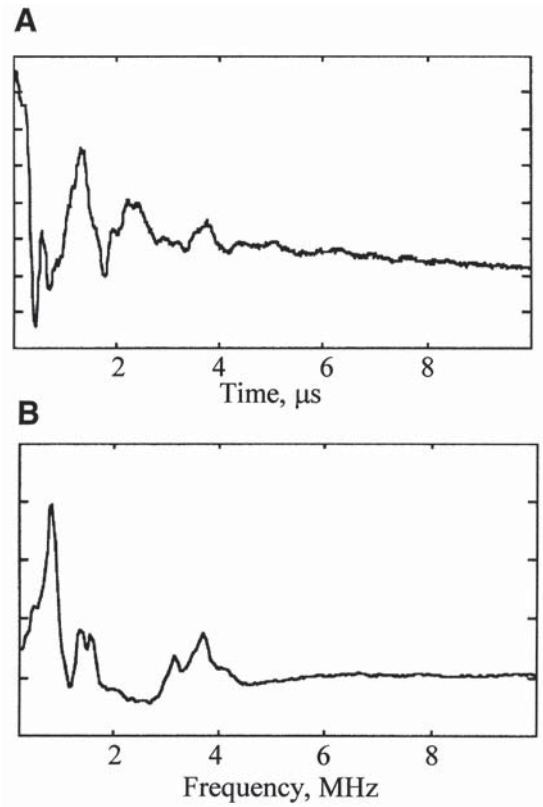

Fig. 6. ESEEM spectra for T2D Fet3p **(A)** the ESEEM spectrum of the type-1 Cu(II) site (T2D mutant) was collected at 2825 G with $\tau = 250$ ns. The measurement conditions were 8.80 GHz microwave frequency, 43 dB microwave power, and 4.2 K sample temperature. The sample was 0.5 m*M* Fet3p in pH = 6.0 MES buffer containing 25% ethylene glycol. **(B)** Fourier transform of the ESEEM data. (From ref. *14*.)

three-coordinate site with a significant doming of the Cu(I) out of the trigonal plane, presumably toward a more weakly bound fourth ligand.

The EXAFS analysis of the reduced and the oxidized T1D/T2D mutant protein and of the T1D mutant that had an intact trinuclear center gave a rather complete picture of the coordination at the type-3 cluster. The best fit of the EXAFS data in all cases included the coordination of three histidine imidazoles to each of the two type-3 coppers consistent with the *K*-edge results. Furthermore, the bridging oxygen ligand that electronically couples the two Cu(II) in the oxidized state was strongly evident in the data. Also evident was the scattering that gave a Cu–Cu distance in the cluster of 3.33 Å. The fitted data for the oxidized cluster are indicated in the structure shown in Fig. 12A.

The analysis of the data for the reduced protein was slightly more ambiguous. This ambiguity followed from the fact that the best fit required an additional single oxygen or nitrogen first shell atom at 2.49 Å distributed between the two copper atoms. This was at a considerably longer distance than the bridging O in the oxidized cluster (2.49 vs 1.91 Å; *see* Fig. 12A,B). Also, the Cu–Cu distance in the reduced cluster was greater because there was no evidence of Cu backscattering in the data. One interpretation of these data is given in Fig. 12B. In the model, the two copper atoms move apart upon reduction. The oxygen bridge is disrupted and the putative hydroxide is protonated, thus making cluster reduction electroneutral. (As presented in Fig. 12, the formal charge of both the oxidized and reduced states is +2; this is arbitrary, of course, because it depends on how one writes the

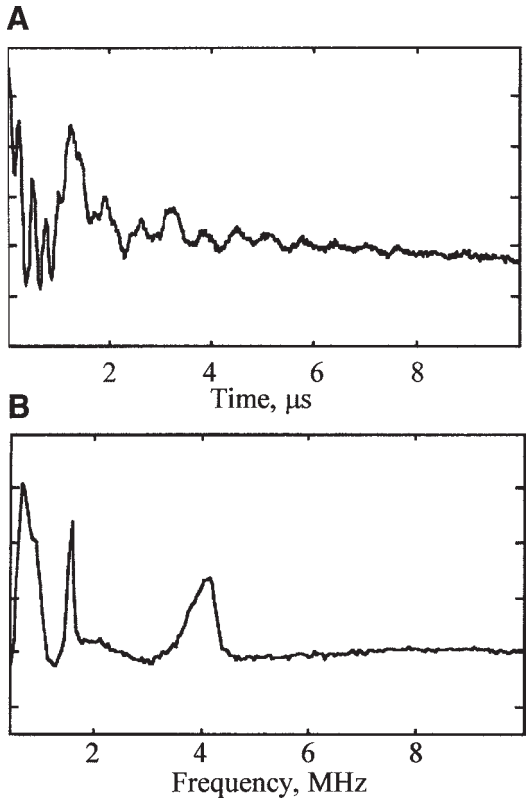

Fig. 7. ESEEM spectra for T1D Fet3p. **(A)** ESEEM spectrum of the type-2 Cu(II) site was collected at 2690 G with $\tau = 260$ ns. The measurement conditions were 8.80 GHz microwave frequency, 43 dB microwave power, and 4.2 K sample temperature. The sample was 0.5 m*M* Fet3p in pH = 6.0 MES buffer containing 25% ethylene glycol. **(B)** Fourier transform of the ESEEM data. (From ref. *14*.)

state of protonation/ionization of the bridging oxygen/hydroxide.) In this model, the two Cu(I) could now serve different roles in O_2 binding and reduction. The open "apical" coordination site on $Cu_{(2)}$ (*see* Fig. 12; *see also* Fig. 3) would be one binding site for the dioxygen molecule; the other site, tethering the O–O to the protein, would be the type-2 Cu(I), as has been indicated by several studies *(13)*. The other type-3 Cu(I), in addition to supplying one of the electrons for dioxygen reduction, serves as part of an acid catalyst, thereby also supplying proton(s) to the reduced oxygen species, O_2^{2-} and $HO^{\bullet}$. There certainly needs to be proton transfer coincident with electron transfer to the dioxygen. The EXAFS data on the T1D/T2D Fet3p are the first to suggest a model for this part of dioxygen reduction at the trinuclear cluster of a multicopper oxidase.

7. WHAT MAKES A MULTICOPPER OXIDASE A FERROXIDASE?

7.1. Human Ceruloplasmin

Human ceruloplasmin is composed of six plastocyaninlike domains (plastocyanin is a type-1 copper-containing protein) that are arranged in a trigonal array *(7)*. One result of this domain replication is a conformational fold that produces a distinct, negatively charged patch on the protein surface adjacent to the catalytically active type-1 Cu(II). This copper atom is in domain 6. Domains 2 and 4 contain type-1-like copper sites that do not participate in the ferroxidase reaction. Lindley and his co-workers

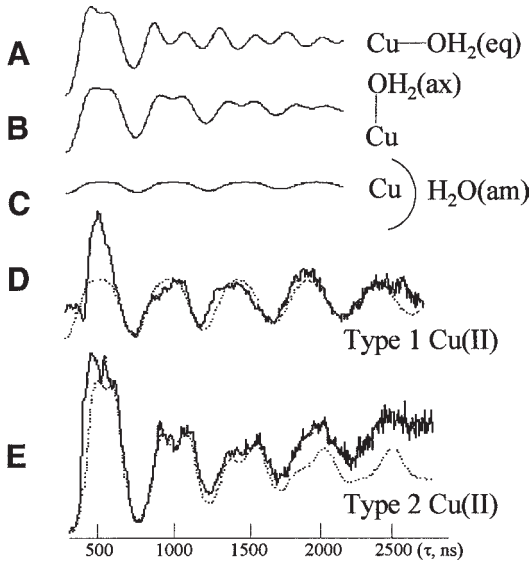

Fig. 8. Simulated and experimental two-pulse ^2H_2O (solvent water) ESEEM spectra. Theoretical ESEEM spectra for equatorial, axial, and ambient water are calculated as indicated. These can be compared to the experimental envelopes for the Fet3p type-1 and type-2 Cu(II) sites (solid lines) and the simulations for these envelopes assuming only ambient water for the type-1 copper and a combination of one equatorial, one axial, and ambient water (dotted lines) for the type-2 copper. (From ref. *14*.)

have proposed that this patch contains two ligand arrays essential to the ferroxidase reaction *(8)*. First, they interpreted a region of electron density adjacent to the type-1 Cu(II) as a "labile" copper-binding site that includes residues E291, E954, H959, and D1044. (This numbering is referenced to the mRNA sequence that includes the signal sequence cleaved during processing. This notation has been chosen to facilitate genome-based alignments.) They postulate that Fe^{2+} binds at this site and is oxidized in an outer-sphere electron transfer to the type-1 Cu(II). His959 and/or D1044 could provide the path for this process because both are in contact with the two histidine imidazoles that are ligands to the type-1 copper. Immediately adjacent to and on the solvent side of this "labile" site is a region in which additional electron density is observed when the crystals are soaked in Fe^{3+}. The authors refer to this as the Fe^{3+} holding site for the ferric ion product of the ferroxidase reaction. The ligands at this putative Fe^{3+} site are not well delineated. However, D249, E950, E951, and E976 are in the vicinity of this electron density. Also, the electron density resulting from E954 shifts away from the "labile" site toward this "holding" site, suggesting that this side chain could play a role in the channeling of the Fe^{3+} from one site to the other. As appealing as this model is, it is based on fairly limited structural data. Systematic structure–function studies have yet to be done to test this model (illustrated in Fig. 13).

7.2. Fet3p

Fet3p most certainly does not have the trimeric structure that Cp has and thus cannot have the ligand arrays that Lindley and co-workers propose for the "labile" and "holding" sites. In both sites, the ligands come from at least two of the six domains. There is nothing in the Fet3p sequence to indicate that Fet3p has a tertiary fold of this nature. On the other hand, Fet3p most reasonably has one or more ligand arrays that play a similar function. What the crystallographic data on hCp and their interpretation suggest is that these arrays would be composed of similar

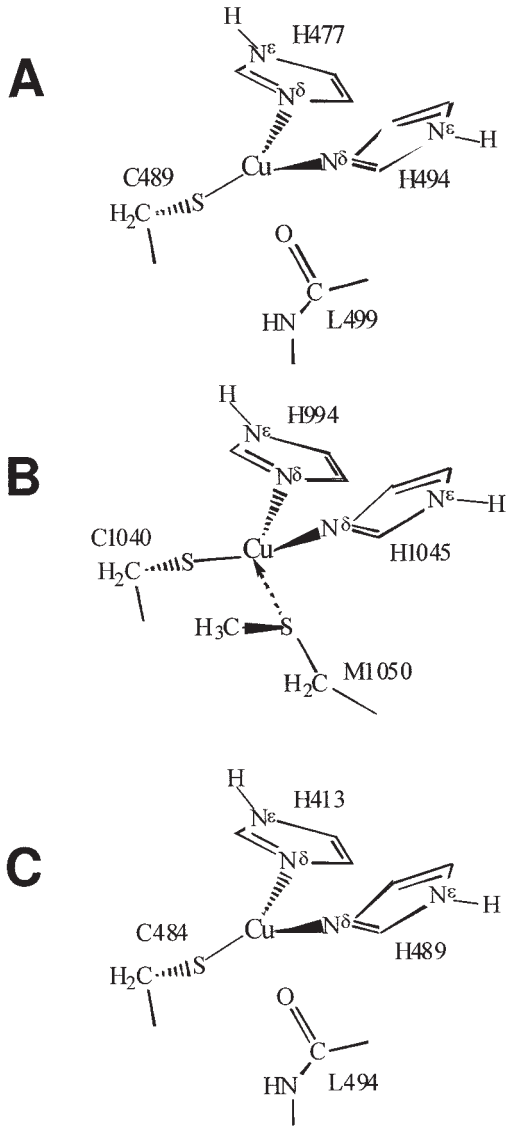

Fig. 9. Model of the type-1 Cu(II) structures in Lac, hCp, and Fet3p. The solvent accessibility is indicated by the shading. As shown in Fig. 5, His494 in Lac is strongly solvent exposed, whereas in hCp, His1045 is fully buried within the protein. ESEEM analysis (Fig. 8) suggests that this residue in Fet3p, His489, is at or near the surface of the protein, more similar to Lac than to hCp.

amino acid side-chain types, specifically D or E and H residues. Askwith and Kaplan based mutagenesis studies on the very reasonable assumption that such residues would provide this type of metal-ion coordination *(18)*. Based a homology modeling study carried out by Murphy et al. *(20)* and sequence alignments among the putative multicopper oxidases found in a variety of yeast genomes (shown in Fig. 14), they prepared several Fet3p mutants. These were tested in vivo for their ability to support iron uptake and in vitro for their ferroxidase activity as visualized by a histochemical enzyme stain of membrane extracts fractionated in polyacrylamide gels. Among these mutants were E227A, D228A, and E230A. These are found in “ferroxidase” Box 3

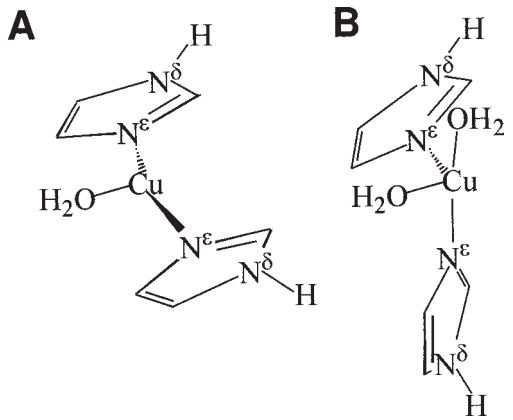

Fig. 10. Alternative type-2 Cu(II) coordination. **(A)** The structure of the type-2 site in AO and hCp is represented in which the two His ligands define a single, presumably equatorial plane. An equatorial H_2O is indicated by the fact that anions, including peroxide, the two-electron oxygen reduction intermediate, does bind equatorially in AO *(11)*. **(B)** The type-2 Cu(II) coordination proposed for Fet3p. ESEEM indicates that this site has only one equatorial His, and one equatorial and one axial water. The other His at this site may be axial because it does not contribute to the N modulation in the ESEEM pattern *(14)*.

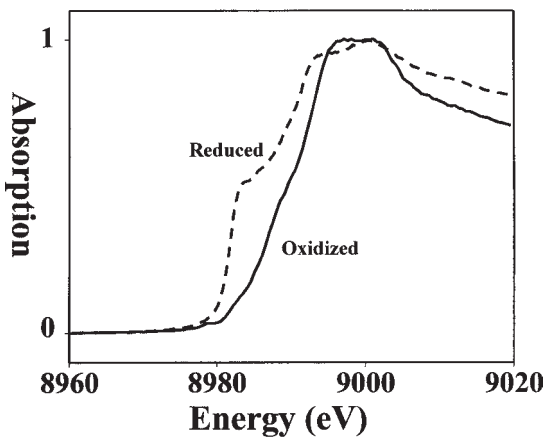

Fig. 11. XAS of the binuclear type-3 copper site in a Fet3p double mutant. The T1D/T2D Fet3p sample was 0.5 m*M* in pH = 6.0 MES buffer at 11–14 K. The data were collected at the Stanford Synchrotron Radiation Laboratory *(5)*. The XAS for the oxidized and reduced type-3 sites are indicated.

(Fig. 14), and except for the latter residue in Fio1p, they are fully conserved in all the yeast "ferroxidases" identified by sequence analysis to date. Based on the structural model, all were predicted to play a role in either the binding of Fe^{2+}, or the electron-transfer reaction, or both *(19,20)*. In fact, none of these mutants constructed by Askwith and Kaplan exhibited any significant loss of ferroxidase activity in this qualitative histochemical assay, and all supported a normal rate of iron uptake. Possibly, a more rigorous kinetic analysis would reveal some deficit in enzymic activity in one or more of these mutant proteins. However, in light of the normal physiologic activity of these several-mutant proteins, it is highly unlikely that any one of these residues plays a critical role in the structure and function of Fet3p.

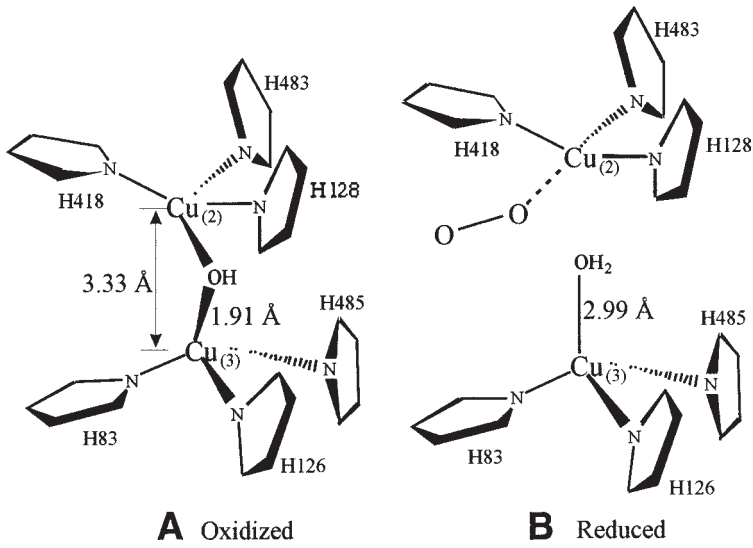

Fig. 12. Model for the coordination changes at the binuclear copper site in Fet3p upon reduction. This model is based on the fitting of the EXAFS data from the oxidized and reduced forms of T1D and T1D/T2D Fet3p. This fitting indicated three significant structural differences upon cluster reduction: (1) loss of the bridging oxygen ligand; (2) separation of the two copper atoms; (3) appearance of a nonbridging O/N ligand with a relatively long bond to one of the copper atoms. Also pictured in the model for the reduced state is the dioxygen liganded to $Cu_{(2)}$, as has been proposed based on a variety of spectral and kinetic data. The model here suggests that the proposed water at $Cu_{(3)}$ that results from protonation of the bridging (–OH) upon reduction could serve as an acid catalyst of the reduction of the bound O_2. (From ref. *5*.)

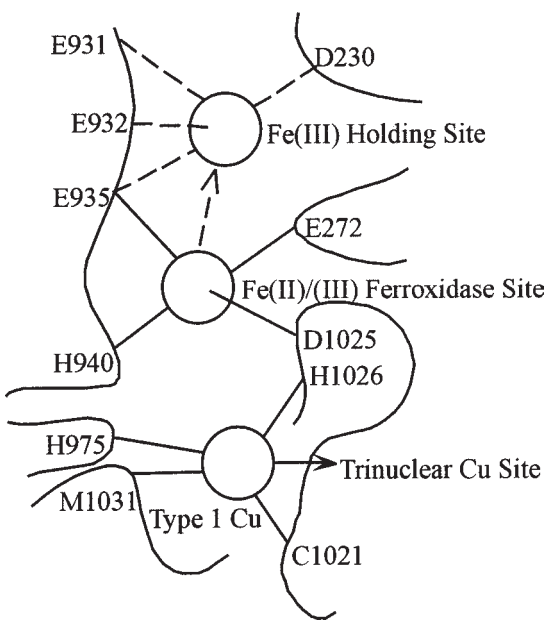

Fig. 13. Model of the iron-binding sites in hCp. Fe^{2+} oxidation is proposed to occur with the metal bound at a site adjacent to the type-1 copper. Crystallographic data suggest that E291, E954, H959, and D1044 are ligands to the iron at this site *(8)*. The Fe^{3+} produced is suggested to then migrate to a "holding site" that is closer to the protein surface. The ligation of this site is not resolved crystallographically; the residues indicated are potential ligands.

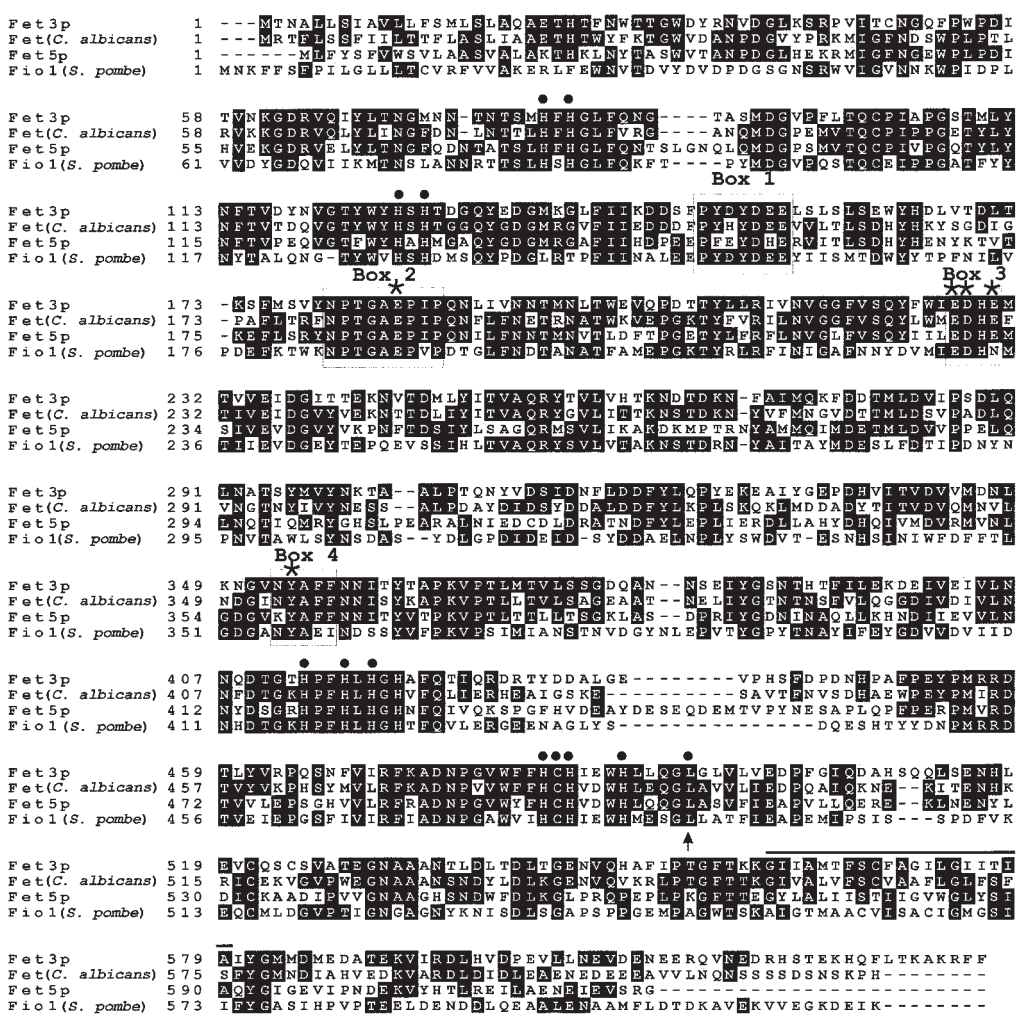

Fig. 14. Alignment of encoded sequences of Fet3p (gi6323703) and Fet5p (gi6321067) from *Saccharomyces cerevisiae*, and Fet homolog from *Candida albicans* (gi1684656), and Fio1p (gi1067210) from *Schizosaccharomyces pombe*. The copperligands are indicated by • . The four homology elements common to the fungal "ferroxidases" are noted as "boxes." Within two of these boxes, specific residues have been mutated. These are indicated by an asterisk (*). The arrow below the Leu residue in the type-1 site of these fungal proteins shows that, as a group, this site is trigonal in this class of multicopper oxidases. The bar above residues 560–579 in Fet3p indicates the predicted carboxyl-terminal membrane-spanning element in this protein; the alignment shows that this element is likely conserved in Fet5p (a known type-1 membrane protein) and the Fet homolog from *C. albicans* but is most likely absent in Fio1p. These sequences and others noted in the text can be retrieved from the website maintained by the National Center of Biotechnology Information (NCBI) using the accession numbers given (www.ncbi.nlm.nih.gov).

One of the two systems that has been developed to produce soluble, recombinant Fet3p involves expression of *FET3* in insect cells using the standard *Baculovirus* system *(21)*. The protein produced localizes to the cell membrane from which it can be released in soluble form by mild trypsin digestion. The protein released is in a copper-free *apo* form and must be incubated with copper in vitro to attain enzymatic activity. In this system, two mutants were constructed based on a model of Fet3p built on the structure of ascorbate oxidase *(19,20)*. In this model, residues E185 and Y354 were

located adjacent to the type-1 site and therefore were proposed to be involved in iron binding. The inclusion of Y354 in this set is somewhat surprising inasmuch as Y would preferentially bind Fe^{3+}, not Fe^{2+}. On the other hand, both residues are fully conserved among the yeast ferroxidase homologs (*see* Fig. 14, Box 2 and Box 4). In any event, only the E185A mutant exhibited strikingly different kinetics with Fe^{2+} as substrate. For this mutant, V_{max} was reduced 2.5-fold while K_m for Fe^{2+} was increased 6-fold. The result of these two changes was a 16-fold decrease in V_{max}/K_m for Fe^{2+} turnover. Steady-state results like these are ambiguous with respect to mechanism because these kinetic constants can reflect the contributions of several discreet steps in the overall enzymic reaction. Among these are the intermolecular and intramolecular electron-transfer steps, the electron transfers to O_2, and the release of H_2O. Therefore, it is not possible to conclude from this type of experiment that a particular amino acid residue is playing a specific role in only one of these steps.

Nonetheless, mutation at E185 expressed in the *Baculovirus* system did alter the ferroxidase activity of Fet3p, indicating that this residue could be a candidate for one of the ligands involved in iron binding and/or electron transfer into the type-1 Cu(II). These initial data indicated that the role of E185 needed to be thoroughly delineated as noted, particularly because it is found within one of the highly conserved motifs that appear to *distinguish* the yeast ferroxidases from those found in other eukaryotes (e.g., flies and mammals). Therefore, it could have played a specific role in the ferroxidase reaction of Fet3p and there may not be a functionally homologous residue in hCp.

On the other hand, one can reasonably question the choice of structural template in either of these modeling studies. As noted, Fet3p and hCp have little in common except the copper liganding motifs characteristicsof all multicopper oxidases (Fig. 4). Although more similar to Fet3p, AO, used by Buonaccorsi di Patti et al. in their modeling studies, also has a domain structure that sequence alignments indicate are not likely to be found in Fet3p. The most similar to Fet3p of those multicopper oxidases for which structural coordinates have been published is *C. cinereus* laccase. In a structure of Fet3p built *in silico* based on the Lac structure, E185 and Y354 are both over 20 Å away from the type-1 copper site (Kosman, unpublished). The location of E185 in Fet3p based on this model is shown in Fig. 15A. Of course, this model is no more likely to be correct than either of the other two. Clearly, truly useful knowledge about the structure of Fet3p with regard to residues with the potential to contribute to substrate specificity will come only from the crystallographically determined structure itself.

8. KINETIC EVALUATION OF FET3P STRUCTURE AND FUNCTION

A yeast system has been developed capable of producing the soluble recombinant Fet3p needed for detailed structural, spectroscopic and kinetic analysis *(4,5,13,21)*. This system has been successfully used to produce the copper-site-deleted mutants whose spectral properties were described in some detail earlier *(4,5,13,21)*. The amino acid replacements made in these mutants were shown in Fig. 3. This system is based on a truncation of the *FET3* gene at nucleotide +1666 (at amino acid residue 555); a nucleotide sequence encoding the FLAG epitope was appended at that point. The result of this manipulation was the production of a Fet3p that lacked its carboxyl-terminal membrane-spanning domain. Instead, it was epitope tagged at its C-terminus. Lacking its membrane domain, this protein was secreted into the growth medium rather than remaining tethered to the plasma membrane. This strategy is illustrated in Fig. 16. The protein produced was easily recovered from the growth medium by ion-exchange chromatography. The yield of pure protein was 5–10 mg/L, depending on the precise protein species being produced. This system has two significant advantages over the *Baculovirus* one. First, the protein is recovered directly from the growth medium without protease treatment. More importantly, unlike the *Baculovirus* expression system, the protein is processed normally within the yeast cell and therefore contains all of its copper prosthetic groups.

This protein has been used to determine the precise kinetic constants for the ferroxidase reaction catalyzed by Fet3p. These constants are given in Fig. 17; this figure also includes the kinetic constants for iron uptake by the yeast cell. The strong similarity between the two sets of kinetic constants is

consistent with the inference that the latter values are simply a reflection of the former, that is, that the ferroxidase reaction catalyzed by Fet3p [reaction (1)] is the rate-limiting step in iron uptake by the yeast cell. In particular, note that the K_m for O_2 is essentially the same in both reactions, approx 1 μ*M*. This underscores the tight coupling that must exist between iron uptake through the iron permease, Ftr1p, and the ferroxidase reaction catalyzed by Fet3p, as is indicated by the diagrams in Fig. 17.

The yeast-expression system has allowed for the production of the 100-mg quantities of Fet3p required for detailed structure–function studies. These studies have been of two general types: kinetic and spectroscopic/biophysical. Most recently, diffraction-quality crystals of Fet3p have been produced. A sample of these are shown in Fig. 18. These particular crystals are approx 300 μm in length and diffract to approx 3 Å, indicating that crystallographic structure determination of Fet3p will be accomplished in the near future (Taylor et al., unpublished results).

This structure will show whether any of the homology modeling studies alluded to above provided any real insight into Fet3p structure and function. As noted, the model based on the *C. cinereus* laccase is the more reliable based on the paradigms used to select among possible homologs in choosing a basis set for model building. In fact, this model did locate a pair of aspartic acid residues at positions 278 and 283 in the encoded protein that were on one side of a shallow cleft with His489 on the opposite side. His489 provides one of the two type-1 histidine imidazole ligands and would be the His that is at or near the protein surface. In this model, D278, in particular, is immediately adjacent to the site of entry of the electron from the ferrous ion substrate and thus could be part of the substrate-binding site for Fe^{2+} (Fig. 15B). In addition, the aspartic acid residues lie within a region of the protein that secondary-structure prediction indicates may be α-helical. This would put both D residues on the same face of this putative helix, indicating that both could be part of the "ferroxidase" site. Furthermore, these D residues are conserved in all of the yeast "Fet3p" homologs (Fig. 14).

The possible role of either E185 or D278 in the oxidase activity of Fet3p was investigated in the recombinant protein produced by the method outlined in Fig. 16. Both proteins had intact and spectroscopically normal type-1, type-2, and type-3 copper sites as determined by visible aborbance and cwEPR (e.g., as in Figs. 1 and 2). In contrast to the *Baculovirus*-produced protein, the E185 mutant exhibited only a modest decrease in activity (approx 50% of wild type under V/K_m conditions). Under the conditions of this assay, the D278 mutant was fully wild type in regard to enzymic activity. The former result was in contrast to that reported by Buonacorsi di Patti et al. *(19)*; their mutant protein had only approx 6% wild-type activity. However, their expression system did not give them sufficient protein for spectral assay so that they had no independent method by which to determine the state of the copper sites. In any event, none of these attempts to locate "ferroxidase" residues based on homology modeling have yielded much insight and thus the question "what makes Fet3p a ferroxidase" remains unanswered.

That Fet3p and hCp do indeed have specificity for Fe^{2+} as a substrate can be demonstrated directly by kinetic analysis. The copper-site mutants generated in the yeast-recombinant system have been particularly useful in two different types of experiments designed to explore the substrate specificity and overall reaction mechanism for Fet3p. First, the T2D protein allows for investigation of the electron transfer to the type-1 Cu(II) in the absence of turnover. This is because in the multicopper oxidase reaction, electron transfer from the type-1 copper—as Cu(I)—to the trinuclear cluster where O_2 is reduced, requires the type 2-Cu(II) *(1,3)*. Thus, the addition of Fe(II) or other substrate (*o*-dianisidine, *p*-phenylenediamine, hydroquinone) to the fully oxidized T2D protein results in the reduction of the type-1 Cu(II) without further turnover *(5)*. This reaction is shown in Fig. 19A with Fe(II) as substrate and in Fig. 19B with hydroquinone as the substrate *(22)*. The results demonstrate clearly the strong selectivity that Fet3p has toward Fe(II) in comparison to hydroquinone. The reaction with Fe(II) is complete within the instrument dead time (approx 2 ms); therefore, the k_{obs} must be >1200 s^{-1}. Under similar conditions of reactant concentrations, the k_{obs} for reduction of the type-1

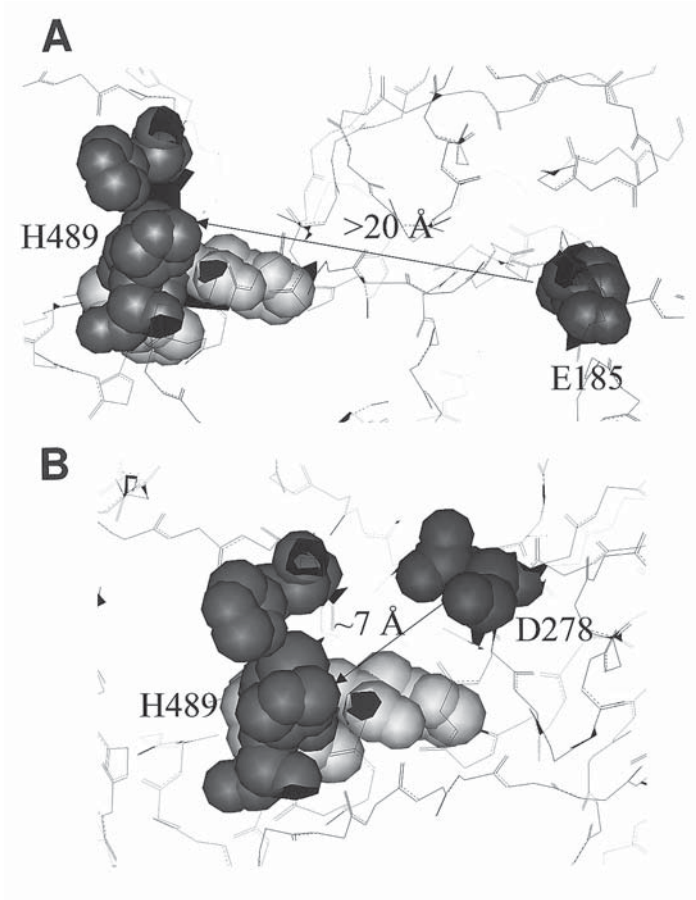

Fig. 15. Computer modeling of the ferroxidase site in Fet3p. Model proposed by Buonaccorsi di Patti et al. *(21)* based on the structure of ascorbate suggested that Glu185 was part of the Fet3p ferroxidase site. A model of Fet3p based on the more similar laccase structure *(9)* or a *de novo* model generated in InSightII places this residue >20 Å away from the type 1 Cu(II) (panel **A**). Instead, this model places residue D278 within 7 Å of this copper site (panel **B**) (Severance and Kosman, unpublished).

Cu(II) in Fet3p by hydroquinone was 0.008 s^{-1}. The large k_{obs} for the reaction with Fe(II) suggests that electron transfer takes place within a Fet3p–Fe(II) substrate complex, although it does not require it.

Using this stopped-flow technique, Machonkin and his co-workers have measured the rate constant for the Fet3p–hydroquinone reaction and compared it to the type-1 reduction rates for hCp and Lac *(22)*. The purpose of this comparison was to establish any possible correlation between solvent accessibility of the type-1 sites in these proteins (e.g., see comparisons shown in Figs. 5 and 9) and their reactivity. The second-order rate constants for the reaction of hCp and Fet3p with hydroquinone were 6.1×10^4 $M^{-1}s^{-1}$ and 3.5×10^5 $M^{-1}s^{-1}$, respectively. The value for the *C. cinereus* Lac reaction was $>10^7$ $M^{-1}s^{-1}$. This pattern of reactivity parallels the solvent accessibility of the type-1 site in the three proteins in that this site in hCp is completely buried while one edge of this site in *C. cinereus* is fully solvent accessible. As suggested by the ESEEM data, the Fet3p type-1 Cu(II) falls in between these two extremes *(14)*.

There was no similar correlation between reactivity toward Fe(II) and solvent exposure. Fet3p and hCp exhibited similar rates of type-1 Cu(II) reduction by Fe(II) (k_{obs} > 1200 s^{-1}), whereas the rate with *C. cinereus* Lac was >23 s^{-1}. In other words, laccases can use Fe(II) as the substrate but have no

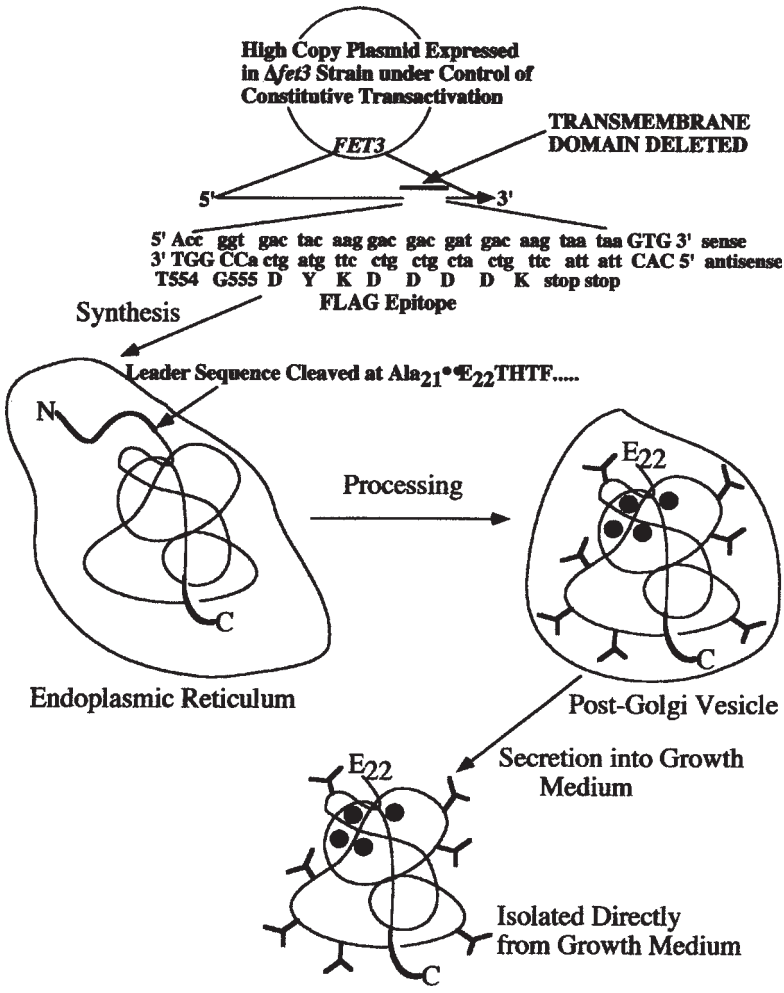

Fig. 16. Strategy for production of a recombinant, soluble Fet3 protein in yeast. (From ref. *4*.)

better than 1–2% of this activity in comparison to Fet3p and hCp. In addition, they are at least 100-fold better than the ferroxidases in the turnover of bulky organic reductants. Combining the structure and reactivity features of these proteins indicates that the type-1 sites in the ferroxidases are less accessible to these large reductants while possessing specificity elements that support the recognition and binding of Fe(II) as the substrate. As outlined earlier, some of these elements may have been identified in hCp; they remain uncharacterized in Fet3p.

Theoretically, the redox potential of the type-1 Cu(II) could provide the specificity toward a particular reductive substrate in comparison to another. Type-1 copper sites do exhibit a remarkable variability in reduction potential, from 240 mV in nitrite reductase *(23,24)* to >1 V for a noncatalytic type-1 copper in hCp *(25)*. This variability is certainly the result, in part, of the presence of the methionine ligand found in the four-coordinate type-1 sites (as in hCp and AO) that is absent in Lac and Fet3p, for example (cf. Figs. 4 and 9). Mutagenesis studies indicate that this ligand "tunes" the $E°'$ down by approx 100 mV *(26)*. On the other hand, the ferroxidase-active type-1 sites Fet3p and hCp have essentially identical reduction potentials (427 and approx 450 mV, respectively) despite the fact that the latter has Met coordination, whereas the former does not *(6,22)*. In summary, avail-

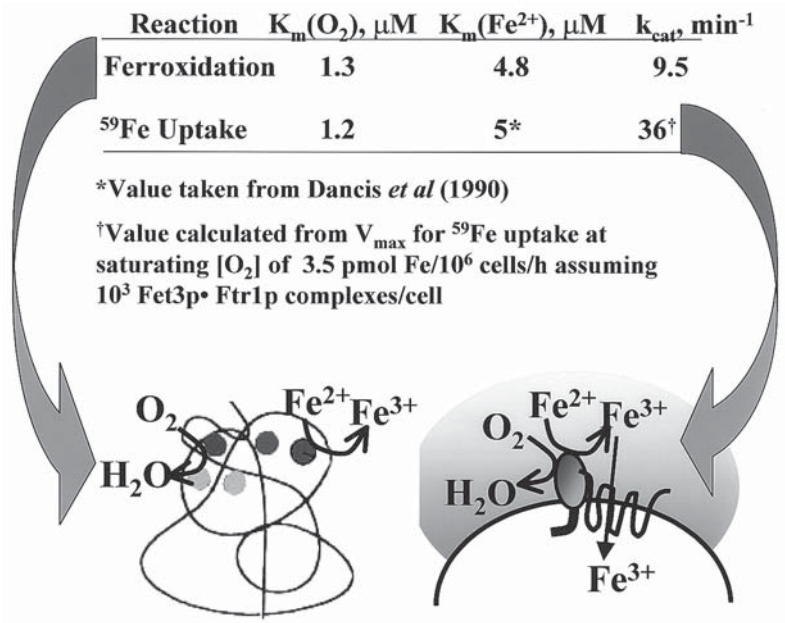

Fig. 17. Kinetic equivalence of ferroxidation and iron uptake in yeast. The ferroxidation kinetics were determined using soluble recombinant Fet3p, whereas ^{59}Fe uptake was determined in whole yeast cells. (Data are taken from ref. *4*.)

able data do not suggest that a simple linear free-energy relationship links substrate specificity to type-1 reduction potential in the multicopper oxidases, nor does the presence or absence of a Met ligand predict the $E°'$. Instead, ferroxidase activity appears to be an acquired trait resulting from protein elements that are in addition to the copper ligands and environment that directly modulate the spectral and redox properties of the type-1 copper atom itself.

9. WHERE DO WE GO FROM HERE?

The experimental tools and reagents are now in hand to develop a complete understanding of how the ferroxidases, Fet3p and hCp, and their congeners in the same and other organisms work, both in molecular and physiologic terms. Most certainly, a high-resolution structure of Fet3p will be available, as will data on structure–function studies on mutant forms of recombinant hCp. This information will go a long way to fill the current gaps in our understanding of ferroxidase structure and function. There will be data on the electrophysiology of Fe(II) oxidation by Fet3p and iron uptake through Ftr1p in a heterologous eukaryotic system (e.g., *Xenopus* oocytes or transfected Caco-2 cells). These studies would test models for the coupling mechanism that links Fe(II) oxidation to iron uptake. The cellular role of other ferroxidases (e.g., hephaestin) in human iron metabolism will have been established and that of the other ferroxidase/permease pair in yeast, Fet5p/Fth1p. The links between ferroxidases and the Fe^{2+} transporters—those in both the plasma and intracellular membranes—in the various cell types in mammals will become clearer.

Finally, as this new information becomes available, we will be come to an understanding of the evolution of the multicopper oxidase that had ferroxidase activity. Copper and iron, of course, are intimately associated with aerobic metabolism, although copper and iron enzymes are not confined to obligate aerobes. True, the ferroxidase reaction is explicitly an aerobic process. However, taking Fet3p as an example (K_m for O_2 = 1 m*M*, equivalent to a partial pressure under an 0.1% O_2 atmosphere), the ferroxidase reaction can proceed under microaerobic conditions. These conditions do not

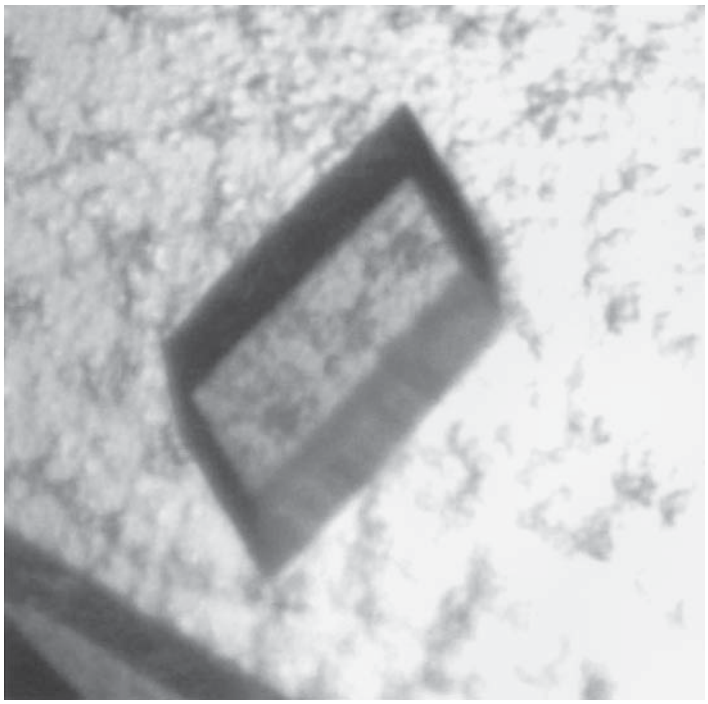

Fig. 18. Diffraction-quality crystals of Fet3p. These crystals, which are bright blue, diffract to approx 3 Å, but do not have suitable temperature behavior for analysis using synchrotron radiation. This is likely the result of the presence of approx 10% residual carbohydrate following endoglycosidase treatment. A recombinant form of Fet3p lacking carbohydrate is under construction.

obtain for yeast under most lab conditions, but they certainly do for hCp because free O_2 in the plasma is strongly buffered by hemoglobin and they certainly would have obtained in the early stages of geologic aerobiosis. Certainly, one of the early events in aerobiosis would have been evolution of the copper- and iron-requiring processes of respiration that enormously extended the energy-production capacity of facultative aerobes. Mechanisms for supplying iron to cells to support these respiratory functions would have been part of this early evolution. In this view, the ferroxidases may have been the first of the multicopper oxidases and may have been selected for specifically as a component of iron uptake in these first eukaryotes. There is an irony in this view in that the target for this cellular iron, whose uptake required the action of a copper ferroxidase, was itself a copper- and iron-dependent enzyme—cytochrome-*c* oxidase—and both enzymes were dioxygen reductases. On the other hand, this may not be irony, but a very reasonable evolutionary trick. After all, both enzymes are also multinuclear metallo-oxidases with surprising homologies despite their disparate overall structures and cofactors. Reasonably, they are part of the same adaptive stream; perhaps they also part of the same evolutionary tree. This question, too, may be brought closer to resolution in these next few exciting years of research on ferroxidases and iron homeostasis.

ACKNOWLEDGMENTS

The author gratefully acknowledges the efforts of Dr. Daniel Yuan that provided the essential nucleation site for the highly collaborative work on Fet3p that is reviewed in this chapter. This collaboration has included the laboratories of Dr. Ninian Blackburn, Dr. John McCracken, and Dr. Edward Solomon. The members of these labs that have participated in this collaboration are Martina

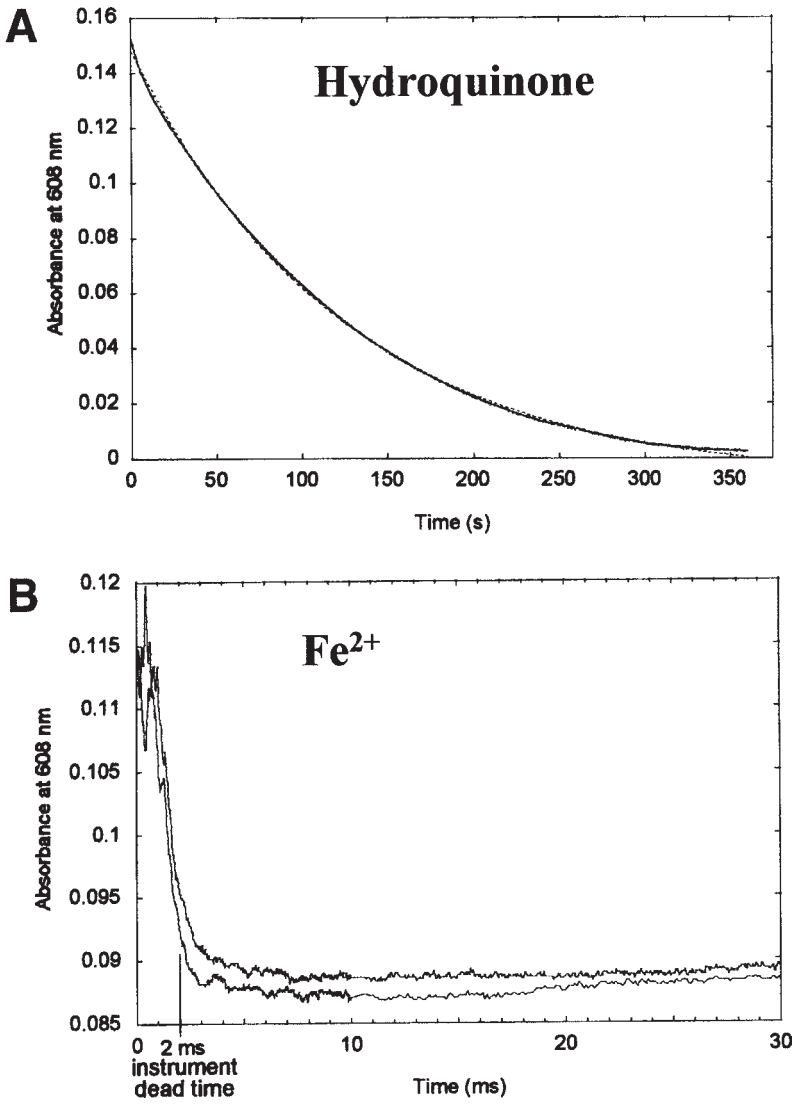

Fig. 19. Reduction of the type-1 Cu(II) in Fet3p by Fe^{2+} **(A)** and hydroquinone **(B)**. The reduction is followed by the 608-nm absorbance resulting from the type-1 CU(II). The [Fet3p} was 35 μ*M* in pH = 6.5 MES with [Fe^{2+}] = 343 μ*M* and [hydroquinone] = 565 μ*M*. (From ref. *22*.)

Ralle, Constantino Aznar, Timothy Machonkin, Liliana Quintanar, and Amy Palmer. All of the members of my own lab have contributed to this work but most particularly Richard Hassett, Scott Severance, Tzu-Pin Wang, and Kimberly Prohaska. Of course, little good happens in the Kosman lab without the critical assistance of Annette Romeo, and our work on Fet3p and the iron–copper connection owes much to her efforts. The support for this work by the NIH (DK53820) is gratefully acknowledged.

REFERENCES

1. Solomon, E. I. and Lowery, M. D. (1993) Electronic structure contributions to function in bioinorganic chemistry. *Science* **259**, 1575–1581.
2. Solomon, E. I., Penfield, K. W., Gewirth, A. A., Lowery, M. D., Shadle, S. E., Guckert, J. A., et al. (1996) Electronic

structure of the oxidized and reduced blue copper sites: contributions to the electron transfer pathway, reduction potential, and geometry. *Inorg. Chim. Acta* **243**, 67–78.
3. Solomon, E. I., Sundaram, U. M., and Machonkin, T. E. (1996) Multicopper oxidases and oxygenases. *Chem. Rev.* **96**, 2563–2605.
4. Hassett, R. F., Yuan, D. S., and Kosman, D. J. (1998) Spectral and kinetic properties of the Fet3 protein from *Saccharomyces cerevisiae*, a multinuclear copper ferroxidase enzyme. *J. Biol. Chem.* **273**, 23,274–23,282.
5. Blackburn, N. J., Ralle, M., Hassett, R., and Kosman, D. J. (2000) Spectroscopic analysis of the trinuclear cluster in the Fet3 protein from yeast, a multinuclear copper oxidase. *Biochemistry* **39**, 2316–2324.
6. Machonkin, T. E. and Solomon, E. I. (2000) *J. Am. Chem. Soc.* The thermodynamics, kinetics, and molecular mechanism of intramolecular electron transfer in human ceruloplasma. **122**, 12,547–12,560.
7. Zaitseva, I., Zaitsev, V., Card, G., Moshkov, K., Bax, B., Ralph, A., et al. (1996) The X-ray structure of human ceruloplasmin at 3.1 Å: nature of the copper centres. *J. Biol. Inorg. Chem.* **1**, 15–23.
8. Lindley, P. F., Card, G., Zaitseva, I., Zaitsev, V., Reinhammar, B., Selin-Lindgren, E., et al. (1997) An X-ray structural study of human ceruloplasmin in relation to ferroxidase activity. *J. Biol. Inorg. Chem.* **2**, 454–463.
9. Ducros, V., Brzozowski, A. M., Wilson, K. S., Brown, S. H., Ostergaard, P., Schneider, P., et al. (1998) Crystal structure of the type 2 Cu depleted laccase from *Coprinus cinereus* at 2.2 Å resolution. *Nature Struct. Biol.* **5**, 310–316.
10. Messerschmidt, A., Steigemann, W., Huber, R., Lang, G., and Kroneck, P. M. H. (1992) X-ray crystallographic characterization of type 2 depleted ascorbate oxidase from zucchini. *Eur. J. Biochem.* **209**, 597–602.
11. Messerschimidt, A., Luecke, H., and Huber, R. (1993) X-ray structures and mechanistic implications of three functional derivatives of ascorbate oxidase from zuccini. *J. Mol. Biol.* **230**, 997–1014.
12. Messerschmidt, A., Ladenstein, R., Huber, R., Bolognesi, M., Avigliano, L., Petruzzelli, R., et al. (1992) Refined cystal structure of ascorbate oxidase at 1.9 Å resolution. *J. Mol. Biol.* **224**, 179–205.
13. Shin, W., Sundaram, U. M., Cole, J. L., Zhang, H. H., Hedman, G., Hodgson, K. O., et al. (1996) Chemical and spectroscopic definition of the peroxide-level intermediate inthe multicopper oxidases: relevance to the catalytic mechanism of dioxygen reduction to water. *J. Am. Chem. Soc.* **118**, 3202–3215.
14. Aznar, C. P., Kosman, D. J., Hassett, R., Yuan, D., and McCracken, J. (2002) Pulsed EPR studies on the type 1 and type 2 Cu(II) sites in the yeast multicopper oxidase, Fet3p. *Biochemistry,* in press.
15. Cornelius, J. B., McCracken, J., Clarkson, R. B., and Belford, R. L. (1990) Electron spin echo envelope modulation angle selection studies of axial pyridine coordination to copper(II) benzoylacetonate. *J. Phys. Chem.* **94**, 6977–6982.
16. Hegg, E. L., Whiting, A. K., Saari, R. E., McCracken, J., Hausinger, R. P., and Que, L. J. (1999) Herbicide-degrading α-keto acid-dependent enzyme TfdA: metal coordination environment and mechanistic insights. *Biochemistry* **38**, 16,714–16,726.
17. Malmström, B. G. (1994) Rack-induced bonding in blue-copper proteins. *Eur. J. Biochem.* **223**, 711–718.
18. Askwith, C. C. and Kaplan, J. (1998) Site-directed mutagenesis of the yeast multicopper oxidase Fet3p. *J. Biol. Chem.* **273**, 22,415–22,419.
19. Buonaccorsi di Patti, M. C., Pascarella, S., Catalucci, D., and Calabrese, L. (1999) Homology modeling of the multicopper oxidase Fet3 gives new insights in the mechanism of iron transport in yeast. *Protein Eng.* **12**, 895-897.
20. Murphy, M. E., Lindley, P. F., and Adman, E. T. (1997) Structural comparison of cupredoxin domains: Domain recycling to construct proteins with novel functions. *Protein Sci.* **6**, 761–770.
21. Bonaccorsi di Patti, M. C., Felice, M. R., Camuti, A. P., Lania, A., and Musci, G. (2000) The essential role of Glu-185 and Tyr-354 residues in the ferroxidase activity of *Saccharomyces cerevisiae* Fet3. *FEBS Lett.* **472**, 283–286.
22. Machonkin, T. E., Quintanar, L., Palmer, A. E., Hassett, R., Severance, S., Kosman, D. J., et al. (2001) Spectroscopy and reactivity of the type 1 copper site in Fet3p from *Saccharomyces cerevisiae*: correlation of structure with reactivity in the multicopper oxidases. *J. Am. Chem. Soc.* **123**, 5507–5517.
23. Suzuki, S., Kohzuma, T., Deligeer, A., Yamaguchi, K., Nakamura, N., Shidara, S., et al. (1994) Spectroscopic, kinetic and thermodynamic characterization of the blue copper site in nitrite reductase. *J. Am. Chem. Soc.* **116**, 11,145–11,146.
24. LaCroix, L. B., Shadle, S. E., Wang, Y., Averill, B. A., Hedman, B., Hodgson, K. O., et al. (1996) Electronic structure of the perturbed blue copper site in nitrite reductase: Spectroscopic properties, bonding, and implications for the entatic/rack state. *J. Am. Chem. Soc*. **118**, 7775–7768.
25. Machonkin, T. E., Zhang, H. H., Hedman, B., Hodgson, K. O., and Solomon, E. I. (1998) *Biochemistry* **37** 9570–9578.
26. Xu, F., Palmer, A. E., Yaver, D.S., Berka, R. M., Gambetta, G. A., Brown, S. H., et al. (1999) *J. Biol. Chem*. **274** 12,372–12,375.

9

Interaction of Copper-Binding Proteins from *Enterococcus hirae*

Paul A. Cobine, Christopher E. Jones, Wasantha A. Wickramasinghe, Marc Solioz, and Charles T. Dameron

1. INTRODUCTION

Copper is imported into prokaryotic cells by CPx-type ATPases. CPx-type ATPases have the transmembrane characteristics typical of P-type ATPases involved in the translocation of many ions. A conserved Cys–Pro–X (X = C or H) sequence within the transmembrane channel and a variable number of distinct amino-terminal domains define the CPx classification *(1)*. The cytoplasmic subdomains of the CPx-ATPases have a MxCxxC or M/HxxMDHS/GxM metal-binding site (x = any amino acid). Intracellular copper is utilized in the activation of enzymes, such as cytochrome-*c* oxidase, superoxide dismutase, and lysyl oxidase. Copper also has the potential to cause cellular damage because of its redox properties. To overcome this dichotomy, the cell regulates copper levels and prevents toxicity with overlapping mechanisms: sequestration, export, and inhibition of entry.

Protection by sequestration can have numerous modes of action. Metals are secluded by binding to high-affinity peptides, such as metallothionein *(2)*, or can be stored in vesicles with import facilitated by ATPase pumps [e.g., the Menkes and Wilson proteins *(3)*]. Sequestration mechanisms result in an intracellular environment rich in chelating agents that limit the concentration of potentially toxic metals. In fact, studies on baker's yeast *Saccharomyces cerevisiae* have shown that cells contain very low levels of available free copper *(4)*. In spite of the chelating environment, essential copper reaches its target by utilizing a mechanism that both sequesters and directs the copper to copper-dependent proteins. This mechanism involves a class of proteins termed the copper chaperones.

Copper chaperones have been identified for the delivery of copper to copper-regulated DNA-binding proteins from bacteria, cytochrome-*c* oxidase from yeast, superoxide dismutase from yeast and humans, and Cu(I)-ATPases in yeast and humans *(5–7)*. The utilization of homologous metallochaperones across such a diverse range of organisms suggests that a common method of copper trafficking has evolved. The copper chaperone, CopZ, has a central role in copper routing in the gram-positive bacterium *Enterococcus hirae (8)*. The *E. hirae* copper homeostasis gene products are translated from the *cop* operon, which encodes four genes *copZ–copY–copA–copB*. The proteins expressed from the operon are the copper chaperone, a copper-regulated repressor CopY, and two ATPase pumps, CopA and CopB *(9)*. The current understanding of the *cop* system is that cellular copper levels are controlled by the import and export pumps (CopA and CopB) whose expression is regulated by CopY *(10)*.

From: Handbook of Copper Pharmacology and Toxicology
Edited by: E. J. Massaro © Humana Press Inc., Totowa, NJ

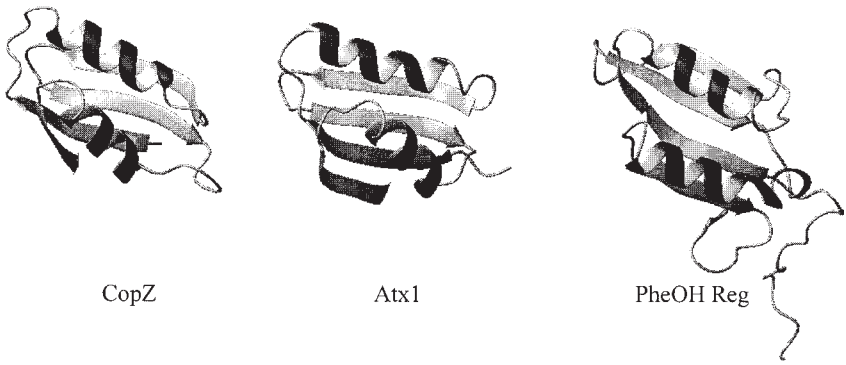

Fig. 1. The solution structure of CopZ traces the same global βαββαβ fold found in the copper chaperone Atx1 and the regulatory domain of phenylalanine hydroxylase. The two α-helices lay diagonally across four β-strands. CopZ and Atx1 share the same metal-binding loop (MxCxxC) between the first β-strand and the α-helix. (PDB accession nos. 1CPZ, 1CC8, 1PHZ).

Copper binds to CopZ in the cytoplasm and is subsequently transferred to CopY. The binding of copper to CopY leads to release of the repressor allowing expression of the operon to proceed.

2. COPZ: A COPPER CHAPERONE

CopZ has sequence homology to proteins involved in the homeostasis of numerous metals. These include the copper chaperone, Atx1 (*S. cerevisiae*), the mercury chaperone, MerP (*Shigella flexneri*), a domain in the copper chaperone for superoxide dismutase, CCS (*S. cerevisiae* and *Homo sapiens*) and as the N-terminal domains of the CPx-ATPases: Menkes disease (MNK), Wilson's disease (WND), and CopA (*H. sapiens* and *E. hirae*). The solution structure of CopZ reveals a conserved βαββαβ global fold and an exposed flexible loop that contains the MxCxxC metal-binding motif (Fig. 1) *(11)*. The two α-helices lie diagonally across four β-strands forming an "open-faced β-sandwich" *(12)*. This simple global fold is utilized for many different functions. The βαββαβ fold is found as a domain in phenylalanine hydroxylase *(13)* (Fig. 1), procarboxypeptidase *(14)*, and ferredoxin *(15)*. Solution structures of MerP *(16)* and MNKr4 *(17)* and the crystal structures of Atx1 *(18)* and CCS *(19)* have the same βαββαβ fold and reinforce the importance of the fold in the metallochaperone family. The ubiquitous nature of this global fold contrasts to the specificity of the copper chaperones for their target.

Spectral analysis of CopZ has revealed that the protein binds copper and silver *(20,21)*. Copper-binding stoichiometry of *apo*CopZ can be determined by monitoring the amplitude of the metal–ligand charge-transfer band (MLCT). The untraviolet (UV)–visible absorption spectra of Cu(I)CopZ displays the characteristic MLCT of a Cu(I)–sulfur transition near 250 nm (Fig. 2). The MLCT reaches a plateau at 1 mol equivalent of Cu(I). The cysteine residues of the metal-binding site are exposed on a loop between the first β-strand and the first α-helix with little protection from the surrounding environment *(11)*. CopZ displays no copper–thiolate luminescence characteristic of a Cu(I)S protein in which the Cu(I) is shielded from the solvent environment (Fig. 2). Protected sites are found in some copper-binding proteins such as metallothionein and the yeast transcription factor Ace1 *(22)*.

X-ray absorption studies of Cu(I)–CopZ have confirmed the coordination of Cu(I) through two sulfur ligands, with an average bond length of 2.244 Å *(21)*. Extended X-ray absorption fine-structure (EXAFS) studies of metals coordinated to other βαββαβ folded proteins have all resulted in large Debye–Waller factors indicative of static disorder *(23–26)*. All of these studies have derived bond lengths suggesting a coordination environment with a high proportion of Cu(I) bound to two cysteinyl sulfurs. Digonal coordination of cuprous copper in proteins was, until the discovery of

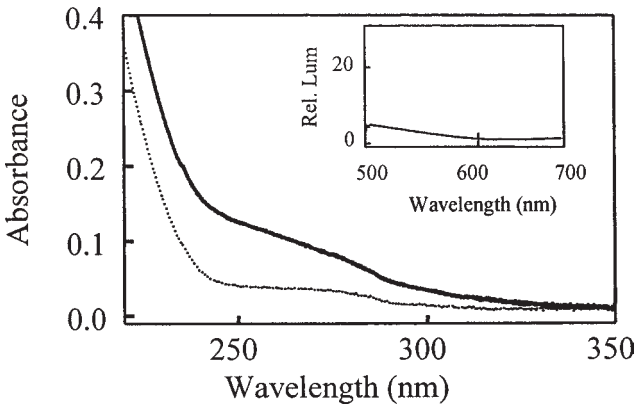

Fig. 2. Reconstitution of Cu(I) into the copper chaperone CopZ. The increase at 250 nm is the result of the formation of a Cu(I)–S metal–ligand charge-transfer band. Inset: Absence of Cu(I)–S luminescence at 600 nm in Cu(I)–CopZ (excited at 295 nm).

these proteins, thought to be rare although whole-cell EXAFS performed on *S. cerevisiae* did predict a high proportion of digonal copper *(27)*. By providing only two adjacent sulfurs as ligands, the copper chaperone has exerted pressure on copper to remain digonal. Because the d^{10} electronic configuration of Cu(I) enforces no stereochemical demands, the coordination is largely determined by the electrostatic and molecular mechanical factors *(28)*. A combination of direct ligands and the electrostatic configuration around the metal-binding loop provides a site suited to two-coordinate Cu(I). This site also allows for the ligand-exchange reactions thought to be involved in the metal transfer from the metallochaperones to the target. Ligand-exchange mechanisms have been proposed for the transfer of Cu(I) from a two-coordinate site to a two-coordinate site (Atx1-Ccc2) *(23)*, from a two-coordinate to a three-coordinate site (CopZ–CopY) *(21)*, and for the transfer of mercury (MerP–MerT) *(29)*.

3. COPY: A COPPER-REGULATED REPRESSOR

The expression of the *cop* operon is dependent on the intracellular concentration of copper. The expression of the operon is biphasic because the operon encodes both the import and export pumps. Transcription is represssed under normal copper conditions by a DNA-binding protein, CopY. CopY is a homodimer repressor that binds across the transcription start site to a 27-base-pair inverted repeat. DNA footprinting and site-directed mutagenesis of the regulatory region has revealed an ACA triplet at –61 and –30 (from translation start site) to be critical to DNA binding *(10)*. The secondary structure predicted for CopY suggests a multidomain protein. The first domain is predicted to have a helical bundle structure made up of three repeated α-helices making up a DNA-binding domain. A second domain is proposed as a metal-binding domain; this region lacks regular secondary structure and encompasses a $CxCx_4CxC$ motif (Fig. 3). The $CxCx_{4\text{-}5}CxC$ motif is repeated in the metallothionein family and in a number of transcription factors involved in the expression of metalloregulated proteins. These transcription factors include Ace1 (*S. cerevisiae*) *(22)*, AMT (*Candida glabrata*) *(30)*, Mac1 (*S. cerevisiae*) *(31)*, and Grisea (*Podospora anserina*) *(32)*. Interestingly, the Cys motif is found in a human homolog of unknown function (accession no. A161517) (Fig. 4).

CopY is one of the target molecules for Cu(I)–CopZ. DNA-binding activity of CopY is dependent on metal occupancy of the $CxCx_4CxC$ motif *(8,10)*. In the metallotransfer reaction, CopZ transfers univalent copper ions into the site occupied by the single divalent zinc, displacing the zinc. The size difference between CopZ/CopY coupled with atomic absorption spectroscopy enables metal transfer to be monitored *(8)*. Additionally, the $CxCx_{4\text{–}5}CxC$ homologs have been demonstrated to have lumi-

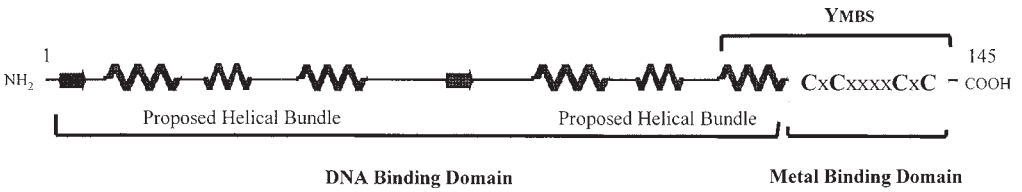

Fig. 3. CopY secondary-structure prediction and proposed domains. The cysteine residues of the metal-binding domain are highlighted.

CopY	mkqlnkkepvetie**C**n**C**ipgq.**C**e**C**kkq
AMT1	qekgitieedmlmsgnmdm**C**l**C**vrgep**C**r**C**harrkrtqksnkk
ACE1	cmcasarrpavgskedetr**C**r**C**degep**C**k**C**htkrkssrks
Mac1	evlthkgiflstq**C**s**C**.edes**C**p**C**vnclihrseeelns
Grisea	mvpvrkpgrplst**C**p**C**ppgkp**C**v**C**ggvrvaipkkq
MT2 β domain	mdpn**C**s**C**atggs**C**t**C**tgsckckeckcns
AF161517	fqsvsklnqgkp**C**t**C**igke.**C**q**C**krwhdmevysfsgl
Consensus	**CxC(4-5)CxC**

Fig. 4. Sequence alignment of $CxCx_{(4-5)}CxC$ motifs from bacteria, yeast, and humans. CopY is a repressor protein from *E. hirae.* AMT1 is a transcription activator for metallothionien from *C. glabrata.* ACE1 is a transcription activator for metallothionein from *S. cerevisiae.* Mac1 is transcription factor for the CTR/FRE proteins from *S. cerevisiae.* Grisea is a Mac1 ortholog from *Podospora ansernia.* MT2 β-domain is the N-terminal domain of metallothionien from *H. sapiens.* AF161517 is a human protein of unknown function.

nescent Cu(I)–S cores *(33)*. Copper coordinated to sulfur in a solvent-shielded environment is luminescent at room temperature *(28)*. Cu(I)–S luminescence is observed as the CopZ/CopY metal transfer proceeds. This Cu(I)–S luminescence is the result of Cu(I) binding to CopY, as the Cu(I)–S site in CopZ is solvent accessible. This can be exploited to determine the copper-binding stoichiometry of CopY. The increase in Cu(I)–CopY luminescence plateaus at 2.0 Cu(I)/CopY (Fig. 5). AMT titrated with copper beyond the plateau results in a decreased specific activity of the transcription factor *(30)*. The binding of these copper ions occurs in an all-or-nothing-type mechanism that has been identified previously in homologous $CxCx_{4-5}CxC$ proteins *(33)*.

X-ray absorption studies of Cu_2CopY confirmed the cuprous state and provided evidence for Cu(I)–S bonds of 2.26 Å. This bond length is best fit with three sulfur bonds; therefore, Cu(I) coordination in CopY requires the sharing of two sulfur ligands. A secondary scatter at 2.69 Å, usually attributed to a metal–metal interaction, is also evident from the EXAFS analysis *(21)*. These X-ray data suggest a tight $Cu(I)_2S_4$ core. The distorted planar geometry of three-coordinate copper and the sharing of ligands mean that the four sulfur groups should be mostly planar. Native CopY is isolated with 1 mol equivalent of Zn(II) per CopY. This zinc is displaced upon copper binding. In contrast to the Cu(I)–S planar geometry the zinc in Zn(II)–CopY should be coordinated in a tetrahedral geometry, with three sulfurs in a plane and one sulfur axial. The structural changes in the metal-binding domain when Cu(I) binds is dramatic enough to effect the DNA-binding activity of the protein. The addition of copper and reorientation of the metal-binding sulfurs affects DNA binding but does not

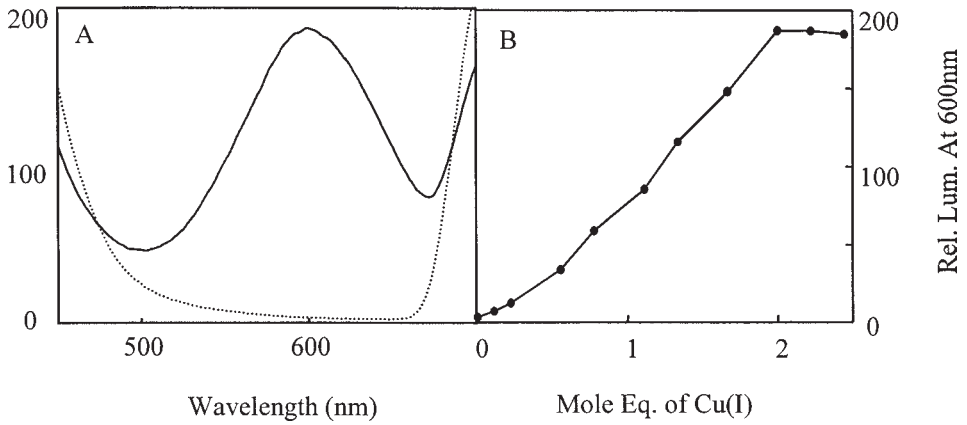

Fig. 5. Copper titration of CopY with Cu(I) as Cu(I)–CopZ. **(A)** The dotted line represents Zn(II)–CopY; the solid line represents 2Cu(I)–CopY. **(B)** The stepwise increase in relative luminescence at 600 nm for Cu(I)–CopY. The plateau represents the formation of a stable $Cu(I)_2 S_4$ core in CopY.

affect the dimer interaction of CopY. Gel filtration of the CopY species in the transfer reactions indicates no observable difference in size.

4. THE CHAPERONE–TARGET INTERACTION

Metallochaperones facilitate the transport of metal around the cell to its site of utilization. Therefore, metallochaperones may have at least dual specificity: one for the site of metal uptake and another for the target protein. The *S. cerevisiae* chaperones Atx1, Cox17, and CCS identified for CCC2, CCO, and SOD1 may deliver copper to a wide variety of copper-dependent enzymes, including the transcription factors Ace1 and Mac1. Current evidence suggests that the copper chaperones have limited targets and that the specificity for the target is high *(19)*. The yeast chaperone–target interactions, identified to date, appear to involve similarly structured domains and/or metal binding sites in the copper-transfer reaction. The Atx1–CCC2 interaction proceeds between two open-faced β-sandwiches with MxCxxC binding sites (same domains/same sites) *(34)*. The CCS–SOD1 interaction requires the formation of a heterodimer between CCS–SOD1 and results in the movement from a Cys–Cu-bridged complex to the SOD1 Cu site (same domains/different sites) *(35,36)*. The only confirmed target for *E. hirae*'s CopZ is CopY. The other potential targets for CopZ include the import and export ATPase pumps. The import pump, CopA, is similar to the Menkes, Wilson, and CCC2 ATPases in that the N-terminus contains a domain with a MxCxxC metal-binding site *(37)*. CopA has only one βαββαβ domain compared to six in the Menkes/Wilson proteins and two in CCC2. The interaction between CopA and CopZ represents a potential same domain/same site type interaction, similar to the Atx1–CCC2 interaction. CopB, the copper export ATPase, has a cytoplasmic domain rich in histidine residues *(38)*. If CopZ is the only copper chaperone in *E. hirae*, then it may have three different targets. A copper homeostasis model for *E. hirae* is summarized in Fig. 6, with the assumption that the CopZ is the only copper chaperone.

5. THE MECHANICS OF THE CHAPERONE-TARGET INTERACTION

CopZ transfers copper to CopY, leading to a structural change in CopY and a concomitant decrease in DNA-binding activity. A structural homolog of CopZ, MNKr2, the second Cu(I)-binding subdomain at the amino terminus of the Menkes protein, is unable to transfer copper to CopY *(8)*. CopZ does not transfer or exchange metal to either MNKr2 or the complete amino terminal of the

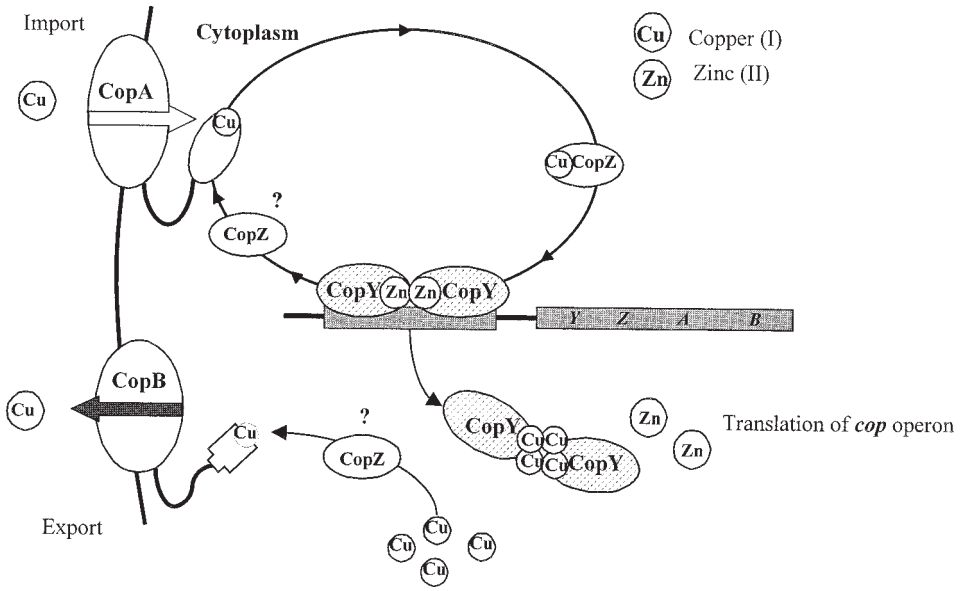

Fig. 6. Schematic representation of copper routing in *E. hirae*. The import and export ATPase pumps CopA and CopB control the intracellular concentration of copper by pumping metal across the membrane into and out of the cytoplasm. Cytoplasmic copper is transferred, by CopZ, to the repressor, CopY, which induces expression of the operon.

Menkes protein (unpublished data). The subdomains at the amino terminus of the Menkes ATPase have been shown to have a role in the copper regulated translocation of the Menkes protein from the trans-Golgi network to the plasma membrane *(39)*. Individually, the structure and metal-binding properties of the subdomains are identical to the reported properties of the metallochaperones *(40)*. Because MNKr2 is predicted to have the βαββαβ global fold and the MxCxxC motif seen in CopZ, the ability to recognize a target is not dependent on these general elements. The electrostatic surface of CopZ and its homologs have charged residues grouped into charged faces *(11,18)*. The organization of these faces appears to be individual for the different chaperones. Electrostatic interaction has been widely implicated in the interaction of the chaperones with targets. A charge relationship between CopZ and CopY was originally proposed when the *cop* operon was first described *(9)*. The structure of Atx1 and modeling of its target, CCC2, has revealed oppositely charged faces that are proposed to interact *(18)*. Site-directed mutagenesis of Atx1 has revealed the importance of particular lysine residues forming patches at the start of the first helix and the end of the second helix. Mutagenesis of these two patches resulted in a dysfunctional Atx1. Mutation of a single lysine residue located close to the MxCxxC motif indicated that this residue is necessary for both delivery of copper to CCC2 and Atx1's antioxidant role *(41)*. In the Menkes modules, MNKr4 and MNKr2, a phenylalanine occupies this position. A large number of Nuclear Overhauser Effect (NOE) contacts from this Phe to the methionine of the MxCxxC motif suggest that this Phe's role is to assist in the stabilization of the metal-binding loop *(17)*. Indeed, this residue may orientate the loop for correct copper binding.

The in vitro assay for copper transfer between CopZ and CopY linked to mutations of MNKr2 provides us with a powerful system to exploit gain-of-function mutations *(42)*. The Atx1 lysine residues, critical for chaperone–target docking in Atx1–CCC2, are not found at the same position in CopZ (Fig. 7). MNKr2 shares similar lysine positions to Atx1 but lacks the lysine arrangement of CopZ (Fig. 7). This may explain the inability of MNKr2 to deliver Cu(I) to CopY. Whereas Atx1 has lysine residues on the helical regions, CopZ has lysine patches on the β-sheet and these patches were

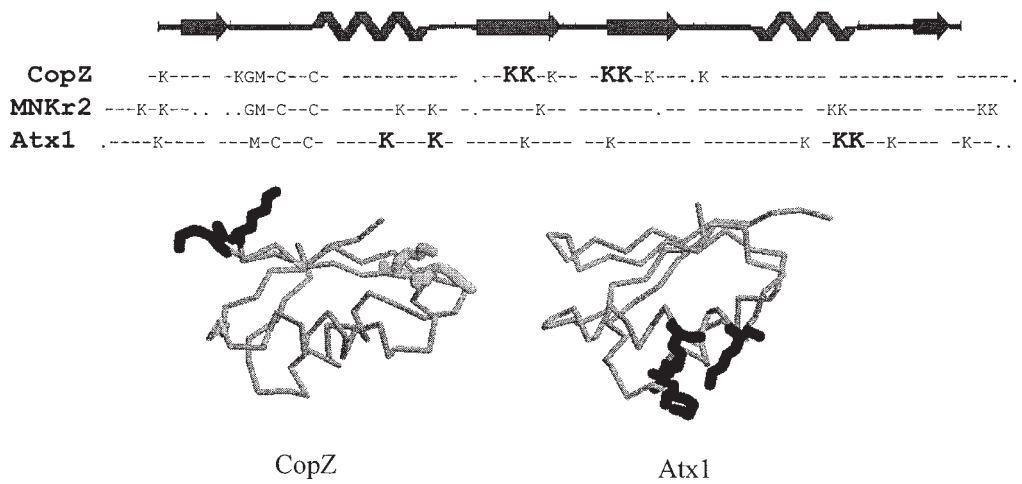

Fig. 7. The lysine arrangement in CopZ, MNKr2, and Atx1. The residues critical to the chaperone function in Atx1 (highlighted) are not present in CopZ. The residues highlighted in CopZ at positions 31, 32, 37, and 38 have been engineered into MNKr2. The structures of CopZ and Atx1 show that the lysine residues are on opposite sides of the molecules.

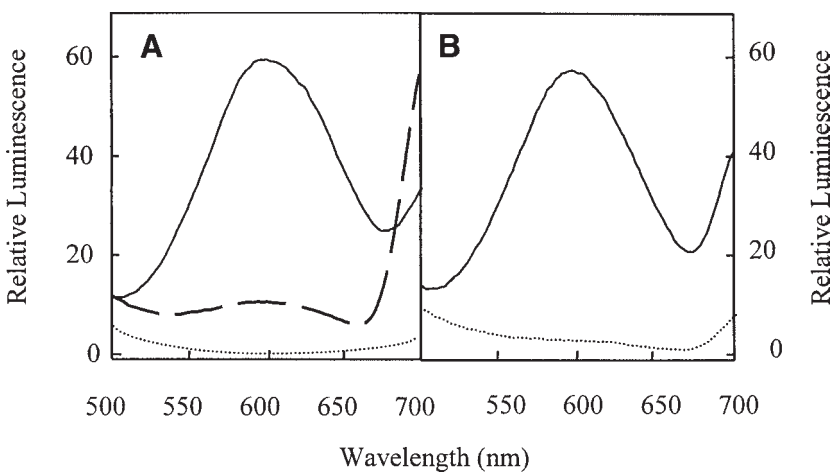

Fig. 8. Copper transfer of copper chaperone CopZ and homolog MNKr2. **(A)** The dotted line represents the luminescence of Cu(I)–CopZ; the dashed line indicates the luminescence of 2[Cu(I)–MNKr2]+Zn(II)–CopY; the solid line is Zn(II)–CopY +2[Cu(I)–CopZ], resulting in $Cu(I)_2$–CopY. **(B)** The dotted line represents Cu(I)–MNKr2 4K; the solid line is 2[Cu(I)–MNKr2 4K+Zn(II)–CopY], resulting in $Cu(I)_2$–CopY (i.e., the addition of lysine residues to MNKr2 along β-2/β-3 confers a gain of function mutation.

mimicked in MNKr2 mutants. The mutants produced in MNKr2 were QRDN31,32,37,38KKKK (4K), QR31,32KK ($2K^{31,32}$), and DN37,38KK ($2K^{37,38}$). When the ability of the mutants to transfer copper to CopY was assessed, the 4K mutant was able to function as a chaperone for CopY (Fig. 8). The $2K^{31,32}$ and $2K^{37,38}$ mutants were prepared to determine which end of the β-sheet was predominantly involved in docking to CopY. $2K^{37,38}$ is able to function equally well as the 4K mutant, but $2K^{31,32}$ was unable to transfer copper (Fig. 9). This indicates that specificity for a target may be conferred by the arrangement of charged patches on the surface of the chaperone. The nonfunctional $2K^{31,32}$ mutant residues lie at the very beginning of the second β-strand, which is at the opposite end of the molecule

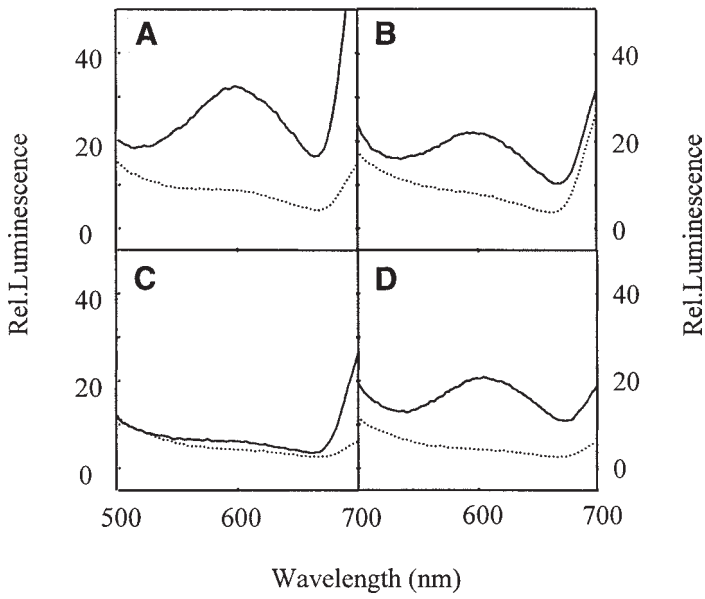

Fig. 9. Mutant MNKr2 interactions with native Zn(II)–CopY and the construct Y_{MBS}. **(A)** The dotted line is Cu(I)–MNKr2 $2K^{37,38}$; the solid line is 2[Cu(I)–MNKr2 $2K^{37,32}$]+ Zn(II)–CopY, resulting in transfer to $Cu(I)_2$–CopY. **(B)** The dotted line is Cu(I)–MNKr2 $2K^{37,38}$; the solid line is 2[Cu(I)–MNKr2 $2K^{37,38}$]+ Zn(II)–Y_{MBS}, resulting in $Cu(I)_2$–Y_{MBS}. **(C)** The dotted line is Cu(I)–MNKr2 $2K^{31,32}$; the solid line is 2[Cu(I)–MNKr2 $2K^{31,32}$]+ Zn(II)–CopY, resulting in no transfer of Cu(I). **(D)** The dotted line is Cu(I)–MNKr2 $2K^{31,32}$; the solid line is 2[Cu(I)–MNKr2 $2K^{31,32}$]+ Zn(II)–Y_{MBS}, resulting in $Cu(I)_2$–Y_{MBS}.

from the metal-binding motif. Interestingly, the nuclear magnetic resonance (NMR) structure of MNKr2 (unpublished results) indicates that these two residues are involved in the loop between helix 1 and strand 2 and contacts with other residues in the loop suggests that Q31 and R32 help define the transition from helix to strand. The $2K^{37,38}$ residues, D37 and N38, however, are located on the turn between the second and third strands, which is positioned adjacent to the loop containing the metal-binding motif. The solution structure of CopZ has a lack of definition in this region *(11)*. Perhaps the lack of constraint confers to this loop region the mobility the lysine residues require to both successfully dock with CopY and correctly position the metal-binding loop.

A truncated version of CopY (Y_{MBS}), containing the 32 terminal residues, which includes the metal-binding region and one helix, was also assessed on its ability to accept copper from MNKr2 and the MNKr2 mutants. Y_{MBS} exhibited no specificity (i.e., it would accept metal from CopZ, MNKr2, and mutants) (Fig. 9). This result suggests that CopY specificity for a chaperone exists, at least in part, outside the metal-binding motif. The recognition site is most likely a combination of charged residues in the metal-binding motif and the DNA-binding domain proximal in the tertiary structure. Determination of the residues of the recognition site and those involved in the transfer mechanism is necessary for a complete understanding of copper delivery to CopY.

6. CONCLUSION

The involvement of copper chaperones in directing metal to copper-dependent proteins has significantly increased our understanding of cellular copper homeostasis. The copper transport pathway in *E. hirae* represents a model for the interaction of proteins involved in copper homeostasis. Given the high level of homology between the *E. hirae* components and components of other copper pathways in

different organisms, the results from the *cop* system will add to the depth of understanding of chaperone-mediated copper homeostasis.

ACKNOWLEDGMENTS

C.T.D. acknowledges the assistance of the Australian Research Council, C.E.J. is the recipient of a National Health and Medical Research Council 'Dora Lush' Research Scholarship, and M.S. acknowledges the support of the Swiss National Foundation and the Novartis Foundation.

REFERENCES

1. Solioz, M. and Vulpe, C. (1996) CPx-type ATPase—a class of P-type ATPases that pump heavy metals. *TIBS* **21**, 237–241.
2. Vasak, M. and Hasler, D. W. (2000) Metallothioneins: new functional and structural insights. *Curr. Opin. Chem. Biol.* **4**, 177–183.
3. Harrison, M. D. and Dameron, C. T. (1999) Molecular mechanisms of copper metabolism and the role of the Menkes disease protein. *J. Biochem. Mol. Toxicol.* **13**, 93–106.
4. Rae, T. D., Schmidt, P. J., Pufahl, R. A., Culotta, V. C., and O'Halloran, T. V. (1999) Undetectable intracellular free copper: the requirement of a copper chaperone for superoxide dismutase. *Science* **284**, 805–808.
5. Harrison, M. D., Jones, C. E., Solioz, M., and Dameron, C. T. (2000) Intracellular copper routing: the role of copper chaperones. *TIBS* **25**, 29–32.
6. Rosenzweig, A. C. and O'Halloran, T. V. (2000) Structure and chemistry of the copper chaperone proteins. *Curr. Opin. Chem. Biol.* **4**, 140–147.
7. O'Halloran, T. V. and Culotta, V. C. (2000) Metallochaperones, an intracellular shuttle service for metal ions. *J. Biol. Chem.* **275**, 25,057–25,060.
8. Cobine, P., Wickramasinghe, W. A., Harrison, M. D., Weber, T., Solioz, M., and Dameron, C.T. (1999) The *Enterococcus hirae* copper chaperone CopZ delivers copper(I) to the CopY repressor. *FEBS Lett.* **445**, 27–30.
9. Odermatt, A. and Solioz, M. (1995) Two trans-acting metalloregulatory proteins controlling expression of the copper-ATPases of *Enterococcus hirae*. *J. Biol. Chem.* **270**, 4349–4354.
10. Strausak, D. and Solioz, M. (1997) CopY is a copper-inducible repressor of the *Enterococcus hirae* Copper ATPases. *J. Biol. Chem.* **272**, 8932–8936.
11. Wimmer, R., Herrmann, T., Solioz, M., and Wuthrich, K. (1999) NMR structure and metal interactions of the CopZ copper chaperone. *J. Biol. Chem.* **99**, 22,597–22,603.
12. Richardson, J. S. (1981) The anatomy and taxonomy of protein structures. *Adv. Protein Chem.* **34**, 167–339.
13. Kobe, B., Jennings, I.G., House, C.M., Michell, B.J., Goodwill, K.E., Santarsiero, B.D., et al. (1999) Structural basis of autoregulation of phenylalanine hydroxylase. *Nature Struct. Biol.* **5**, 442–448.
14. Vendrell, J., Billeter, M., Wider, G., Aviles, F. X., and Wutrich, K. (1991) The NMR structure of the activation domain isolated from porcine procarboxypeptidase B. *EMBO J.* **10(1)**, 11–15.
15. Kissinger, C. R., Sieker, L. C., Adman, E. T., and Jensen, L. H. (1991) Refined crystal structure of ferredoxin II from *Desulfovibrio gigas* at 1.7 A. *J. Mol. Biol.* **219(4)**, 693–715.
16. Steele, R. A. and Opella, S. J. (1997) Structures of the reduced and mercury-bound forms of MerP, the periplasmic protein from the bacterial mercury detoxification system. *Biochemistry* **36**, 6885–6895.
17. Gitschier, J., Moffat, B., Reilly, D., Wood, W.I., and Fairbrother, W.J. (1998) solution structure of the fourth metal-binding domain from the Menkes copper-transporting ATPase. *Nature Struct. Biol.* **5**, 47–54.
18. Rosenzweig, A. C., Huffman, D. L., Hou, M.Y., Wernimont, A. K., Pufahl, R. A., and O'Halloran, T. V. (1999) Crystal structure of the Atx1 metallochaperone at 1.02 A resolution. *Structure* **7**, 605–617.
19. Lamb, A. L., Wernimont, A. K., Pufahl, R. A., O'Halloran, T. V., and Rosenzweig, A. C. (1999) Crystal structure of the copper chaperone for superoxide dismutase. *Nature Struct. Biol.* **6**, 724–729.
20. Lu, Z. H., Cobine, P., Dameron, C. T., and Solioz (1999) How cells handle copper: a view from microbes. *J. Trace Elements Exp. Med.* **12**, 347–360.
21. Cobine, P. A., George, G. N., Wickramasinghe, W. A., Solioz, M., and Dameron, C. T. (2000) Coordination environment in the copper chaperone CopZ and its target, the repressor CopY. *Biochemistry*, in press.
22. Dameron, C. T., Winge, D. R., George, G. N., Sansone, M., Hu, S., and Hamer, D. (1991) A copper–thiolate polynuclear cluster in the ACE1 transcription factor. *Proc. Natl. Acad. Sci. USA* **88**, 6127–6131.
23. Pufahl, R. A., Singer, C. P., Peariso, K. L., Lin, S.-J., Schmidt, P. J., Fahrni, C. J., et al. (1997) Metal ion chaperone function of the soluble Cu(I) receptor Atx1. *Science* **278**, 853–856.
24. Cobine, P., George, G. N., Winzor, D. J., Harrison, M. D., Mogahaddas, S., and Dameron, C. T. (2000) Stoichiometry of complex formation between copper(I) and the N-terminal domain of the Menkes protein. *Biochemistry* **39**, 6857–6863.
25. Ralle, M., Cooper, M. J., Lutsenko, S., and Blackburn, N. J. (1998) The Menkes disease protein binds copper via novel 2-coordinate Cu(I)-cysteines in the N-terminal comain. *J. Am. Chem. Soc.* **120**, 13,525–13,526.
26. DiDonato, M., Narindrasorasaki, S., Forbes, J. R., Cox, D. W., and Sarkar, B. (1997) Expression, purification, and metal binding properties of the N-terminal domain from the Wilson disease putative copper-transporting ATPase (ATP7B). *J. Biol. Chem.* **272**, 33,279–33,282.

27. Desideri, A., Hartmann, H. J., Morante, S., and Weser, U. (1990) An EXAFS study of the copper accumulated by yeast cells. *Biol. Met.* **3**, 45–47.
28. Ford, P. C., Cariati, E., and Bourassa, J. (1999) Photoluminescence properties of multinuclear copper(I) compounds. *Chem. Rev.* **99(12)**, 3625–3648.
29. Brown, N. L., Camakaris, J., Lee, B. T. O., Williams, T., Morby, A. P., Parkhill, J., et al. (1991) Bacterial resistances to mercury and copper. *J. Cell. Biochem.* **46**, 106–114.
30. Thorvaldsen, J. L., Sewell, A. K., McCowen, C. L., and Winge, D. R. (1993) Regulation of metallothionein genes by the ACE1 and AMT1 transcription factors. *J. Biol. Chem.* **268**, 12,512–12,518.
31. Georgatsou, E., Mavrogiannis, L. A., Fragiadakis, G. S., and Alexandraki, D. (1997) The yeast Fre1p/Fre2p cupric reductases facilitate copper uptake and are regulated by the copper-modulated Mac1p activator. *J. Biol. Chem.* **272(21)**, 13,786–13,792.
32. Borghouts, C. and Osiewacz, H. D. (1998) GRISEA, a copper-modulated transcription factor from *Podospora anserina* involved in senescence and morphogenesis, is an orthology of MAC1 in *Saccharomyces cerevisiae*. *Mol. Gen. Genet.* **260(5)**, 492–502.
33. Winge, D. R., Graden, J. A., Posewitz, M. C., Martins, L. J., Jensen, L. T., and Simon, J. R. (1997) Sensors that mediate copper-specific activation and repression of gene expression. *J. Biol. Inorg. Chem.* **2**, 2–10.
34. Huffman, D. L. and O'Halloran, T. V. (2000) Energetics of copper trafficking between the Atx1 metallochaperone and the intracellular copper transporter, Ccc2. *J. Biol. Chem.* **275**, 18,611–18,614.
35. Schmidt, P. J., Rae, T. D., Pufahl, R. A., Hamma, T., Strain, J., O'Halloran, T. V., et al. (1999) Multiple protein domains contribute to the action of the copper chaperone for superoxide dismutase. *J. Biol. Chem.* **274(34)**, 23,719–23,725.
36. Eisses, J. F., Strasser, J. P., Ralle, M., Kaplan, J. H., and Blackburn, N. J. (2000) Domains I and III of the human copper chaperone for superoxide dismutase interact via a cysteine-bridged dicopper(I) cluster. *Biochemistry* **39(25)**, 7337–7342.
37. Odermatt, A., Suter, H., Krapf, R., and Solioz, M. (1993) Primary structure of two P-type ATPases involved in copper homeostasis in *Enterococcus hirae*. *J. Biol. Chem.* **268**, 12,775–12,779.
38. Solioz, M. and Odermatt, A. (1995) Copper and silver transport by copB-ATPase in membrane vesicles of *Enterococcus hirae*. *J. Biol. Chem.* **270**, 9217–9221.
39. Voskoboinik, I., Strausak, D., Greenough, M., Brooks, H., Petris, M., Smith, S., et al. (1999) Functional analysis of the N-terminal CXXC metal-binding motifs in the human Menkes copper-transporting P-tuype ATPase expressed in cultured mammalian cells. *J. Biol. Chem.* **274**, 22,008–22,012.
40. Harrison, M. D., Meier, S., and Dameron, C. T. (1999) Characterisation of copper-binding to the second subdomain of the Menkes protein (MNKr2). *Biochim. Biophys. Acta* **1453**, 254–260.
41. Portnoy, M. E., Rosenzweig, A. C., Rae, R., Huffman, D. L., O'Halloran, T. V., and Culotta, V. C. (1999) Structure–function analysis of the ATX1 metallochaperone. *J. Biol. Chem.* **274**, 15,041–15,045.
42. Cobine, P., Jones, C. E., Deecke, L. N., Wickramasinghe, W. A., and Dameron, C. T. (2000) Unlocking the key-lock mechanism for copper chaperones. *Metal Ions in Biology and Medicine* (Centeno, J. A., Collerry, P., Vernet, G., Finkelman, R. B., Gibb, H., and Etienne, J.-C., eds.), John Libbey Eurotext, Montrouge, France, Vol. 6, pp. 691–693.

III
Copper Transport

10
Copper Uptake in Eukaryotic Cells

Lisbeth Birk Møller and Nina Horn

1. INTRODUCTION

Copper is a trace element important for the function of many cellular enzymes, but it may be toxic if present in excess. Thus, a delicate balance between uptake and efflux of copper ions determines the amount of cellular copper. In biological systems, copper is effectively sequestered by binding to molecules such as glutathione or metallothionein or by cytoplasmic transport proteins called copper chaperones *(1)*. Consequently, free copper ions are virtually nonexistent in living organisms. The concentration of free copper ions has been estimated to be of the order of 10^{-18} to 10^{-13} *M* in yeast cells and in human blood plasma, respectively *(2,3)*. In this chapter we will give a brief overview of the routes taken by copper in humans from absorption in the intestine to extrusion into the bile, followed by a more detailed review of the molecular mechanism involved in copper uptake in mammalian cells. For comparison, we will also discuss the extensive knowledge about the mechanisms of Cu uptake in the yeast *Saccharomyces cerevisiae*.

2. THE ROUTES OF COPPER TRANSPORT IN HUMANS

2.1. Absorption of Copper and Intercellular Transport

In humans, dietary copper 0.6–1.6 mg/d is mainly absorbed in the small intestine where it is transferred across the mucosal barrier by a mechanism which seems to be nonenergy-dependent *(3)*. The high-affinity copper-uptake protein hCtr1 might be involved in this function.

From the mucosal cells, copper is transferred across the basolateral membrane into the interstitial fluid and portal blood by an energy-dependent mechanism. This appears to be the rate-limiting step and probably involves the copper transporting P-type ATPase encoded by the Menkes gene *(3,4)*.

Copper absorbed in the intestine is transported via the portal blood to the liver, kidney, and other tissues in the form of Cu(II)–albumin as well as Cu(II)–histidine and probably Cu(II)–transcuprein complexes. Although the amount of albumin is higher than the amount of transcuprein, the two proteins binds almost equal amounts of copper. However, albumin seems not to be critical for the normal distribution and metabolism of copper, as it has been shown that the Nagase analbuminemic rat, which has no albumin in its blood, shows normal copper transport *(3,5)*.

In the liver, copper is incorporated into ceruloplasmin during its biosynthesis and maturation, resulting in secretion into the blood plasma. The Wilson protein, a P-type ATPase homologous to the Menkes protein**,** is involved in the incorporation of copper into ceruloplasmin *(6)*. Although more

From: Handbook of Copper Pharmacology and Toxicology
Edited by: E. J. Massaro © Humana Press Inc., Totowa, NJ

than 95% of the copper in the plasma is bound to ceruloplasmin, it is unknown if this complex is involved in Cu mobilization from serum. It has been speculated that ceruloplasmin has no essential role in copper transport, because exchange of copper bound to ceruloplasmin is very slow *(6,7)*. However, failure to incorporate copper into ceruloplasmin results in an unstable protein and loss of its ferroxidase activity, which is important for the mobilization of iron *(8)*. In agreement with this, it was shown that patients suffering from aceruloplasminemia have normal copper metabolism but accumulation of iron in the liver and brain *(9)*.

2.2. Buffering and Storage Systems

Glutathione is a tripeptide found ubiquitously in all cells. It has been shown that excess intracellular copper in the intestine, liver, and probably other tissues are immediately bound to glutathione and subsequently to metallothionein *(10,11)*. Thus, inhibition of glutathione synthesis in hepatocytes with buthionine sulfoximine inhibits incorporation of ^{67}Cu into metallothionein by more than 50%. Moreover, glutathione has been shown to protect cells against copper toxicity *(10–12)*.

Metallothioneins are a group of low-molecular-weight cysteine-rich proteins found in vertebrates, invertebrates, and fungi *(13)*. Mammalian cells have multiple metallothionein proteins that can buffer the intracellular concentrations of several metal ions, such as Cu, Zn, Cd, and others, which induce and bind to metallothioneins to different extents *(14–17)*. In mammals, this induction is mediated by binding of metal-responsive transcription factor 1 (MRF-1) to metal-responsive elements (MRE), in the metallothionein promoters. These promoters have multiple copies of MRE elements, which contain a core consensus sequence, 5'–TGCPuCXC-3' conserved in all higher eukaryotes *(18)*.

In *S. cerevisiae* there are two metallothioneins: Cup1 and Crs5, of which Cup1 is the most important. Only Cu and Ag induce the *CUP1* and *CRS5* genes and this induction is mediated through a copper-binding transcription factor Ace1 *(19–21)*. The *CUP1* gene promoter contains four Ace1 binding sites, whereas the *CRS5* promoter contains only a single site *(22,23)*. Studies of both yeast and mammalian cells have shown that metallothioneins have no direct role in copper uptake as such, but are important for the storage of the metal ions *(24,25)* and for protection against copper toxicity *(10,26,27)*.

2.3. Copper Chaperones

Recently, a number of small cytosolic copper-binding proteins, called copper chaperones, have been shown to transport copper to specific copper-dependent target proteins. Hah1 transports copper to the Wilson and the Menkes proteins *(28,29)*; CCS transports copper to the cytoplasmic protein superoxide dismutase (Sod1) *(30,31)*; Cox17 transports copper to mitochondria for incorporation into cytochrome-*c* oxidase *(32,33)*. The presence of these copper chaperones is necessary to ensure that copper can reach its specific target protein. It is unknown how the chaperones become loaded with copper and whether copper-uptake proteins are directly involved in this process.

2.4. Copper Efflux Pumps

The Wilson and Menkes proteins are highly homologous P-type ATPases. Both proteins apparently contribute to the cellular export of copper, by two different mechanisms. They are involved in loading of secretory proteins with copper as well as in direct extrusion of copper from the cell. The biosynthetic loading takes place in the trans-Golgi network, where the Wilson and Menkes proteins are normally located. The Wilson protein is expressed primarily in the liver, where it transports copper to apoceruloplamin, whereas the Menkes protein is predominant in all other tissues *(34,35)*. Direct excretion of copper appears to take place when cells are subjected to elevated copper levels. Under these conditions, the Menkes protein move from the trans-Golgi network to the plasma membrane of CHO cells, presumably to mediate direct excretion of copper *(36)*. On the other hand, an increase in the concentration of copper in HepG2 cells results in movement of the Wilson protein into

a cytoplasmic vesicular compartment *(37)*. It is very likely that movement to the hepatocyte basolateral membrane, for extrusion of copper into the bile, follows this step. Thus, in liver sections from copper-loaded rats, it was found that the Wilson protein was distributed in multiple vesicular structures and concentrated near the bile canalicular plasma membrane *(38)*.

The Menkes protein is encoded by the *ATP7A* gene and mutations in this gene result in Menkes disease. Menkes disease is X-linked and characterized by severe neurodegeneration and connective tissue abnormalities, which can be ascribed to reduced activity of several copper-requiring enzymes. Fibroblasts from patients suffering from Menkes disease accumulate copper, and this is used diagnostically *(39)*. Wilson disease, which is caused by mutations in the *ATP7B* gene, is characterized by copper toxicity resulting from the loss of ability to export copper from the liver to the bile and the inability to incorporate copper into ceruloplasmin *(40–43)*.

3. COPPER UPTAKE IN YEAST CELLS

Two genes encoding high-affinity copper transporters, *CTR1* and *CTR3*, have been identified in the yeast *S. cerevisiae (44,45)*. In most commonly used *S. cerevisiae* laboratory strains, the *CTR3* gene is disrupted by a transposon. Inactivation of the *CTR1* gene in such a strain eliminates high-affinity copper uptake and makes the strain resistant to high external concentrations of copper. The defective copper uptake furthermore results in deficiency of Cu,Zn superoxide dismutase activity and the intracellular copper concentration appears to be reduced as judged from the reduced expression of a *lacZ* reporter gene fused to the copper-inducible *CUP1* promoter. On the other hand, overexpression of the *CTR1* gene leads to increased uptake of copper *(44,46)*.

High-affinity copper uptake is not severely impaired by the *CTR1* deletion in yeast strains where the *CTR3* gene is functional, reflecting the functional redundancy of the two genes. However, strains in which both genes are functional have a higher rate of copper uptake compared to strains mutated in either of the two genes *(45)*.

Both Ctr1 and Ctr3 are integral membrane proteins and have been localized to the cell surface, by microscopy of yeast strains transformed with plasmids expressing epitope-tagged Ctr1 or Ctr3 fusion proteins *(44,47)*. Both proteins are predicted to have similar membrane topologies with three transmembranal segments, an extracellular N-terminal domain, and an intracellular C-terminal domain *(44,47,48)*. By immunoprecipitation, Ctr1 has been shown to exist at least as a homodimer *(46)*, whereas Ctr3 apparently forms a trimer at the plasma membrane *(47)*. It is speculated that such homomultimeric complexes, having from 6–12 transmembrane domains might form a pore through which the copper substrate could be translocated.

In spite of their similar topology and function in copper uptake, the Ctr1 and Ctr3 proteins have limited primary sequence homology. The Ctr1 protein consists of 406 amino acid residues and has a relatively large N-terminal domain containing 11 potential copper-binding motifs of the type MXXM *(44)*. The Ctr3 protein consists of only 241 amino acid residues and lacks the numerous methionine-rich motifs found in Ctr1, but it contains several cysteine residues, some of which might be involved in metal binding *(45)*. Ctr1 is heavy glycosylated with O-linked sugars *(46)*, whereas Ctr3 migrates in sodium dodecyl sulfate (SDS)–polyacrylamide gels as a 27-kDa monomeric protein consistent with its predicted mass, suggesting little or no glycosylation *(47)*.

In addition to the high-affinity transporters Ctr1 and Ctr3, several putative low-affinity copper-uptake systems have been identified in the yeast. The Ctr2 protein is 189 amino acid residues long and has some homology to Ctr1 and Ctr3, and like these, it is predicted to have three membrane-spanning segments *(49)*. Ctr2 has been proposed to be a low-affinity uptake system for copper, as a mutation in the *CTR2* gene increased resistance to toxic copper concentrations and overproduction of Ctr2 provided increased resistance to copper starvation. However, overproduction of Ctr2 was not sufficient to complement a *ctr1 ctr3* mutant with respect to copper uptake *(49)*.

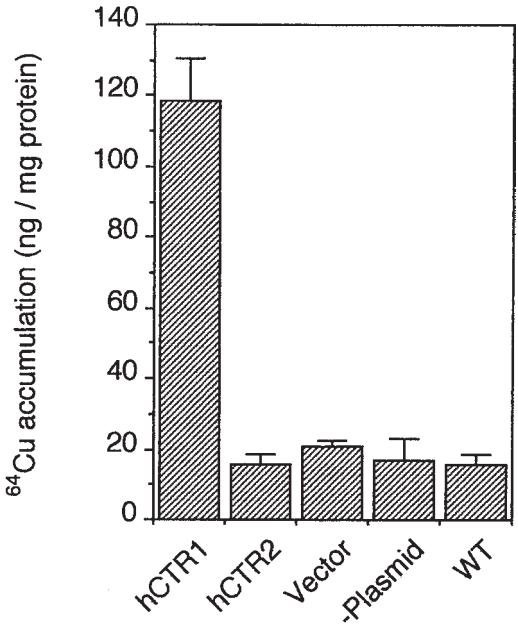

Fig. 1. Uptake of ^{64}Cu, by human fibroblast cultures. The culture designated WT is a primary cell line derived from a healthy individual. The remaining cultures were obtained from the same primary fibroblast culture that had been immortalized and transfected with plasmids as indicated. The amount of ^{64}Cu accumulation (ng/mg protein) during 20 h incubation in the presence of 10 μ*M* ^{64}Cu is shown. (Data from ref. *53*.)

Recently, the low-affinity Fe(II) permease Fet4p from *S. cerevisiae* has been demonstrated to function as a low-affinity copper permease *(50)*. Furthermore, three proteins, Smf1, Smf2, and Smf3, belonging to the Nramp family of metal transporters, have also been implicated in copper uptake, although they appear to have a higher affinity for manganese. It was found that EGTA arrested the growth of yeast strains in which one or more of the three *SMF* genes had been disrupted, and this growth arrest could be reversed by addition of 5 μ*M* Cu(II) *(51)*.

4. COPPER UPTAKE IN MAMMALIAN CELLS

A human protein potentially involved in high-affinity copper uptake, hCtr1, has been identified by complementation of a yeast *ctr1 ctr3* double mutant *(52)*. Expression of h*CTR1* in the uptake-deficient yeast mutant restores high-affinity iron uptake and permits growth on nonfermentable carbon sources. Furthermore, the human gene renders the yeast cells sensitive to copper overload, corrects the deficiency of Cu,Zn superoxide dismutase, and increases the cellular copper level as measured by atomic absorption spectrophotometry *(52)*. Recently, human fibroblasts, transfected with h*CTR1* cDNA have been shown to have a dramatically increased capacity for ^{64}Cu uptake, providing direct evidence that hCtr1 can function in copper uptake in human cells (*see* Fig. 1). So far, no human disorders of copper metabolism have been associated with the h*CTR1* gene, so it is presently unclear if other transporters might contribute to the uptake of copper ions in human cells.

A murine homolog of the h*CTR1* gene (m*CTR1*) has recently been cloned and shown to functionally complement yeast cells deficient in high-affinity copper uptake *(54)*. The possible generation of a m*CTR1* knockout mouse might provide additional insights into the physiological role of Ctr1 in mammalian copper metabolism. The mouse protein is highly homologous to hCtr1 (Fig. 2), and both are encoded by four exons separated by introns that are located at identical positions *(53,54)*. Interestingly, both proteins are also highly homologous to the predicted protein product of a rat cDNA

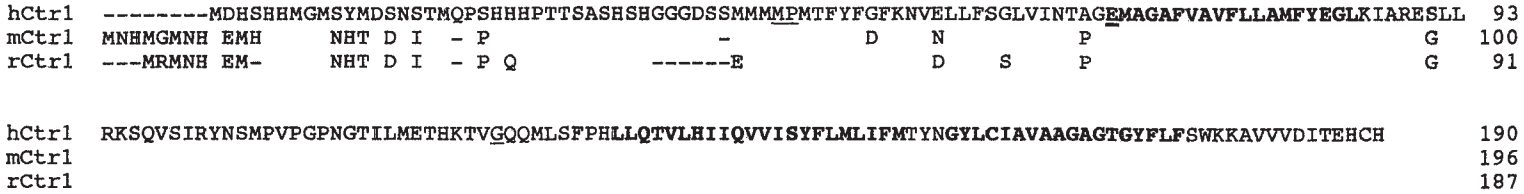

Fig. 2. Comparison of the protein sequences of hCtr1, mCtr1, and rCtr1, which consist of 190, 196, and 187 amino acid residues, respectively. Only derivations from the hCtr1 sequence are shown. Hyphens indicate the absence of an amino acid at the corresponding position. The predicted transmembrane segments in the hCtr1 sequence are shown in bold *(52)*. Nucleotides flanking the three introns in the hCtr1 and mCtr1 coding sequences respectively are underlined *(53,54)*. The Genbank accession no. of the h*CTR1* and the r*CTR1* sequences are U83460 and AF268030, respectively. The murine sequence was compiled from four EST sequences as described in ref. *53* (Genbank accession nos. AA124593, AA4867805, AI195572, AA250186).

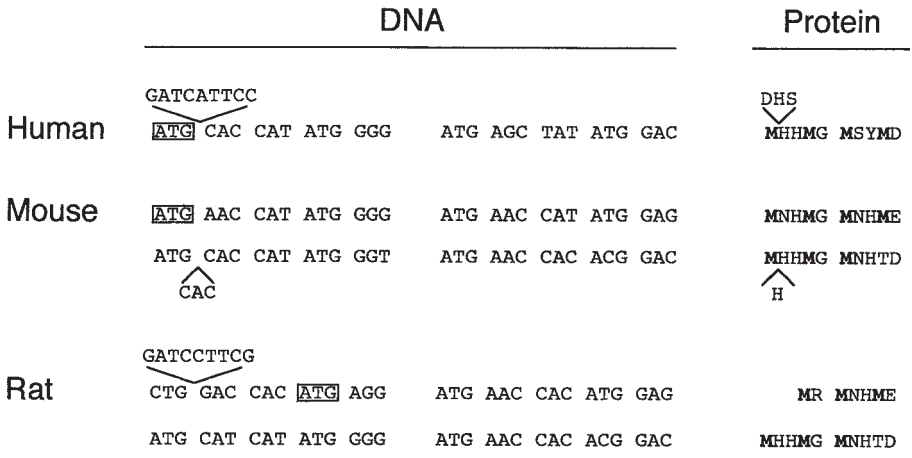

Fig. 3. Comparison of the DNA direct repeats in the beginning of the h*CTR1*, m*CTR1*, and r*CTR1* coding sequences. The initiation codon of the three genes is boxed. A 9-bp insertion in the first repeat of the human and rat sequence and a 3-bp insertion in the third repeat of the murine sequence have been "pulled out" to emphasize the similarity of the repeats. The methionines are shown in bold.

sequence, r*CTR1* (Fig. 2), but there is presently no experimental evidence relating to the function of this protein. Conflicting predictions have been presented for the initiation codon of the murine CTR1 gene *(53,54)*. In Figs. 2 and 3, we have assumed that the initiation codon is the first ATG codon in the m*CTR1* reading frame of the mouse cDNA.

The human Ctr1 protein is only 190 amino acids long and is predicted to contain three transmembrane segments like the yeast transporters. Interestingly, the primary structures of hCtr1 and a high-affinity copper transporter, Ctr4, from *S. pombe* suggest that these proteins have evolved by fusion of domains corresponding to the N-terminal domain of Ctr1 and the C-terminal domain of Ctr3 *(48)*. It is remarkable that the hCtr1 protein can substitute for the yeast Ctr1 protein, even though the N-terminal domain of the human protein is considerably shorter and contains only two putative copper-binding motifs, MXXM, whereas the yeast protein has 11 copies of this motif.

Interestingly, the beginning of the mouse and the rat *CTR1* coding sequences contains four imperfect repeats of a 15-bp-long consensus sequence ATG (A/C)AC CA(T/C) ATG G(G/A)(G/C) that may encode an MXXM motif, whereas only two of these repeats are present at the beginning of the human *CTR1* sequence (Fig. 3). Thus, it appears that the number of MXXM motifs even in these very closely related proteins may vary because of the expansion or deletion of such direct repeats in the DNA sequence. In this connection, the considerable sequence deviation between the N-terminal domains of the hCtr1, mCtr1, and rCtr1 proteins should be contrasted with the completely conserved amino acid sequences of their C-terminal domains (Fig. 2).

By DNA sequence analysis, Zhou and Gitschier *(52)* has identified another human gene, h*CTR2*, which is similar to h*CTR1*. The hCtr2 protein consists of 143 amino acid residues and is predicted to have the same membrane topology as hCtr1, but it lacks the counterpart of the putative copper-binding N-terminal domain. So far, there is no evidence of an involvement of hCtr2 in copper uptake, as expression of the h*CTR2* gene failed to complement the uptake deficiency of yeast mutant strains *(52)*. In agreement with this, copper uptake by human cells was not increased upon transfection with an h*CTR2* expressing plasmid (Fig. 1). The hCtr2 protein resembles the *S. cerevisiae* Ctr2 protein, as they both lack the counterpart the N-terminal domain of the Ctr1 proteins, the domain that has been implicated in the binding of copper by these proteins. Consequently, it has been speculated that the physiological function of hCtr2 and Ctr2 may be in the transport of substrates other than copper ions *(49,53)*.

5. REQUIREMENT FOR REDUCTION OF COPPER(II) PRIOR TO UPTAKE

In *S. cerevisiae*, high-affinity copper uptake mediated by Ctr1 and Ctr3 appears to be specific for transport of Cu(I) formed by prior reduction by the cell-surface Cu/Fe reductases Fre1/Fre2. The Fre1 and Fre2 proteins were originally identified as plasma membrane ferric reductases required for iron uptake *(55,56)*. Subsequent studies showed that the ability of Ctr1 and Ctr3 to function in high-affinity Cu uptake is dependent on the Fre1 reductase, as Cu uptake mediated by Ctr1 and Ctr3 was reduced to 90% and 70%, respectively, in the absence of Fre1 *(45)*. Comparison of copper uptake by mutant strains lacking Fre1 or Fre2 or both activities showed that Fre2 provides a minor but significant contribution to transport-related copper reduction under conditions of low Cu(II) concentration *(57)*. However, even the *fre1 fre2* double mutant was not as deficient with respect to copper uptake as mutants lacking the Ctr1 and Ctr3 proteins, perhaps owing to residual Cu reductase activity that might be ascribed to the *FRE3–FRE7* gene products. Furthermore, it has been shown that extracellular reductans such as ascorbate may suppress the dependence of Cu uptake on the plasma membrane reductase activities, presumably by facilitating nonenzymatic reduction of Cu(II) *(57,58)*.

In mammals, there is no consensus concerning the oxidation state of copper during uptake or the possible involvement of plasma membrane reductase activities. Several reports have suggested that copper is preferentially taken up in the form of Cu(II). Thus, the Cu(I)-specific chelator bathocuprione sulfonate did not inhibit the uptake of copper in the form of $CuHis_2$ into trophoblast cells isolated from human term placenta *(59)*. Ascorbate, which reduces Cu(II) to Cu(I), actually impaired apical uptake of copper from $CuCl_2$ into human differentiated intestinal Caco-2 cells *(60)*. In contrast, Percival and Harris *(61)* reported that ascorbate enhances copper transport from ceruloplasmin into human erythroleukemic K-562 cells, indicating that copper is taken up as Cu(I).

6. ENERGY REQUIREMENT OF COPPER UPTAKE

It has not been generally settled whether copper uptake is an energy-requiring process. In *S. cerevisiae*, it was found that Cu accumulation was saturable and subject to inhibition by the respiratory inhibitor sodium azide and the uncoupler dinitrophenol, particularly when cells were grown on nonfermentable carbon sources *(25)*. These results suggested that ATP is required to sustain net uptake of copper. Conflicting results have been reported concerning the energy requirement of copper uptake into mammalian cells. McArdle et al. *(62)* found no evidence for an ATP requirement in mouse hepatocytes, as inhibitors that substantially reduced intracellular ATP levels failed to reduce copper uptake. Studies of cultured trophoblast cells from human placenta also indicated that ATP was not required for copper uptake *(59)*. A recent study has suggested that apical uptake of Cu in human differentiated intestinal Caco-2 cells may not even be carrier mediated, as uptake appeared to be nonsaturable at copper concentrations up to 80 μ*M (60)*. However, Arrendo et al. *(63)* reported that copper uptake into Caco-2 cells was saturated at external copper concentrations of 4–6 μ*M*.

Given the similarity and functional equivalence of the human and yeast Ctr proteins, Caco-2 cells would be expected to have similar substrate specificity and uptake mechanism as yeast cells. The different results concerning the requirements for energy and substrate reduction in yeast and mammalian cells might, in part, derive from the failure to distinguish between passive adsorption of Cu on the cell surface and true intracellular uptake of Cu. It appears that the great majority of copper associated with cells of *S. cerevisiae* belongs to a pool of rapidly exchangeable copper adsorbed on the cell surface and that this exchange was not energy dependent *(25,64,65)*. Most of the cell-associated copper in mouse hepatocytes *(66)* and in *Escherichia coli* cells *(67)* also appears to be associated with such a rapidly exchangeable pool, which may severely complicate studies of the copper-uptake process.

7. REGULATION OF GENES INVOLVED IN COPPER METABOLISM

In yeast cells, copper uptake appears to be limited by the expression of the *CTR1* and *CTR3* genes *(45,46)* and this limitation is part of an intricate regulatory loop that controls the intracellular copper

concentration. Thus, copper transcriptionally downregulates the *CTR1* and *CTR3* genes as well as the *FRE1* gene, because their expression depends on a copper-sensitive transcriptional activator Mac1 *(68,69)*. Furthermore, the presence of a high copper concentration also inhibit copper uptake by inducing rapid degradation of both Mac1 and Ctr1 *(70,71)*, whereas copper does not affect the stability of Ctr3 *(47)*. Internalization of Ctr1 protein can be seen when cells are exposed to copper; however, the degradation of Ctr1 seems to be independent of endocytosis, as it also takes place in strains defective in endocytosis and vacuolar degradation. Together, these mechanisms assure a tight control of the intracellular copper concentration in yeast cells. It is presently unknown how copper uptake in mammalian cells is regulated. The finding that ^{64}Cu accumulation by human fibroblasts was greatly increased by transfection with the h*CTR1* gene suggests that Cu uptake in human cells, in analogy with yeast, is normally limited by the expression of the h*CTR1* gene (Fig. 3). However, expression of the mammalian *CTR1* genes is apparently not regulated in response to the cellular copper availability *(54)*. In this connection, it is noteworthy that efflux-deficient fibroblasts from Menkes disease patients hyperaccumulate copper in contrast to yeast cells deficient with respect to the homologous Ccc2 protein *(72)*. This difference might suggest that the control of copper uptake in human cells is less stringent than in yeast cells.

In yeast cells, copper is indirectly required for ferrous iron uptake, because iron uptake depends on a multicopper ferroxidase, Fet3, located in the plasma membrane. This link between copper and iron metabolism is reflected in the finding that FET3 and several of the genes involved in transport of copper to Fet3 are regulated by iron. Thus, the *FRE1* and *FRE2* genes encoding Fe (III)/Cu(II) membrane reductases as well as the *CCC2* and *ATX1* genes, which encode the copper pump, Ccc2 and its chaperone, respectively, are all regulated by the iron-responsive transcription factor Aft1 *(28,73,74)*.

The human homolog of Fet3, ceruloplasmin, is also involved in iron transport, but the major function of ceruloplasmin seems to be mediation of iron export via the protein transferrin *(75,76)*. However, recent results suggest that ceruloplasmin also stimulates cellular iron uptake *(77)*. In analogy with its yeast homolog the human ceruloplasmin gene is activated by iron deficiency *(77,78)*, but conflicting results have been reported concerning the regulation of this gene by copper. McArdle et al. *(17)* found no effect of copper on ceruloplasmin expression in mouse hepatocytes, whereas Daffada and Young *(79)* observed an increase of ceruloplasmin mRNA in HepG2 cells after administration of copper.

8. UNRESOLVED QUESTIONS

Although our knowledge about Cu uptake in mammalian cells has increased considerably over the last few years, there are still several important questions that remain unresolved. Thus, it still needs to be established whether copper uptake mediated by hCtr1 is energy dependent and whether copper is transported in the form of Cu(I) or Cu(II). Furthermore, it is presently unknown if other proteins besides hCtr contribute significantly to the uptake of copper by human cells. How the different cytoplasmic copper chaperones become loaded with copper also remains to be elucidated. Finally, our knowledge about the regulation of copper uptake in mammalian cells is very sparse. The recent cloning of several of the genes involved in copper homeostasis in mammalian cells and further mechanistic and physiological studies of their encoded gene products will probably provide the answers to these questions.

ACKNOWLEDGMENTS

Work in the authors' laboratory was supported by grants from the National Research Council, Novo Nordisk Foundation, and the Foundation of 1870.

REFERENCES

1. Pena, M. M. O., Lee, J., and Thiele, D. J. (1999) A delicate balance: homeostatic control of copper uptake and distribution. *J. Nutr.* **129**, 1251–1260.
2. Rae, T. D., Schmidt, P. J., Pufahl, R. A., Culotta, V. C., and O'Halloran, T. V (1999) Undetectable intracellular free copper: the requirement of a copper chaperone for superoxide dismutase. *Science* **284**, 805–808.
3. Linder, M. C. and Hazegh-Azam, M. (1996) Copper biochemistry and molecular biology. *Am. J. Clin. Nutr.* **63**, 797S–811S.
4. Kodama, K., Murata, Y., and Kobayashi, M.(1999) Clinical manifestations and treatment of Menkes disease and its variants. *Pediatr. Int.* **41**, 423–429.
5. Vargas, E. J., Shoho, A. R., and Linder, M. C. (1994) Copper transport in the Nagase analbuminemic rat. *Am. J. Physiol.* **267**, G259–G269.
6. Sato, M. and Gitlin, J. D. (1991) Mechanisms of copper incorporation during the biosynthesis of human ceruloplasmin. *J. Biol. Chem.* **266**, 5128–5134.
7. Kock, K. A., Pena, M. M., and Thiele, D. J. (1997) Copper-binding motifs in catalysis, transport, detoxification and signaling. *Chem. Biol*. **4**, 549–560.
8. Osaki, S. and Johnson, D. A. (1969) Mobilization of liver iron by ferroxidase (ceruloplasmin). *J. Biol. Chem.* **244**, 5757–5758.
9. Harris, Z. L., Takahashi, Y., Miyajima, H., Serizawa, M., MacGillivray, R. T. A., and Gitlin, J. D.(1995) Aceruloplasminemia: molecular characterization of this dosorder of iron metabolism. *Proc. Natl. Acad. Sci. USA* **92**, 2539–2543.
10. Freedman, J. H., Ciriolo, M. R., and Peisach, J. (1989) The role of glutathione in copper metabolism and toxicity. *J. Biol. Chem.* **264**, 5598–5605.
11. Steinebach, O. M. and Wolterbeek, H. T. (1994) Role of cytosolic copper, metallothionein and glutathione in copper toxicity in rat hepatoma tissue culture cells. *Toxicology* **92**, 75–90.
12. Keogh, J. P., Steffen, B., and Siegers, C. P. (1994) Cytotoxicity of heavy metals in the human small intestinal epithelial cell line I-407: the role of glutathione. *J. Toxicol. Environ. Health* **43**, 351–359.
13. *Metallothioneins. Synthesis, Structure and Properties of Metallothioneins, Phytochelatins and Metal–Thiolate Complexes* (Stillman, M. J., Shaw, C. F., III, and Suzuki, K. T. eds.), VCH, New York, 1992, pp. 55–127.
14. Culotta, V. C. and Hamer, D. H. (1989) Fine mapping of a mouse metallothionein gene metal response element. *Mol. Cell. Biol.* **9**, 1376–1380.
15. Masters, B. A., Ouaife, C. J., Ericksen, J. C., Kelly, E. J., Froelick, G. J., Zambrowicz, B. P., et al. (1994) Metallothionein III is expressed in neurons that sequester zinc in synaptic vesicles. *J. Neurosci.* **14**, 5844–5857.
16. Masters, B. A., Kelly, E. J., Ouaife, C. J., Brinster, R. L., and Palmiter, R. D. (1994) Targeted disruption of metallothionein I and II genes increases sensitivity to cadmium. *Proc. Natl. Acad. Sci. USA* **91**, 584–588.
17. McArdle, H. J., Mercer, J. F., Sargeson, A. M., and Danks, D. M. (1990) Effects of cellular copper content on copper uptake and metallothionein and ceruloplasmin mRNA levels in mouse hepatocytes. *J. Nutr.* **120**, 1370–1375.
18. Westin, G. and Schaffner, W. (1988) A zink-responsive factor interacts with a metal-regulated enhancer element (MRE) of the mouse metallothionein-I gene. *EMBO J.* **7**, 3763–3770.
19. Furst, P., Hu, S., Hackett, R., and Hamer, D. (1988) Copper activates metallothionein gene transcription by altering the conformation of a specific DNA binding protein. *Cell* **55**, 705–717.
20. Furst, P. and Hamer, D. (1989) Cooperative activation of a eukaryotic transcription factor: interaction between Cu(I) and yeast ACE1 protein. *Proc. Natl. Acad. Sci. USA* **86**, 5267–5271.
21. Butler, G. and Thiele, D. J. (1991) ACE2, an activator of yeast metallothionein expression which is homologous to SWI5. *Mol. Cell. Biol.* **11**, 476–485.
22. Thiele, D. J. and Hamer, D. H. (1986) Tandemly duplicated upstream control sequences mediate copper-induced transcription of the *Saccharomyces cerevisiae* copper-metallothionein gene. *Mol. Cell. Biol.* **6**, 1158–1163.
23. Culotta, V. C., Howard, W. R., and Liu, X. F. (1994) CRS5 encodes a metallothionein-like protein in *Saccharomyces cerevisiae*. *J. Biol. Chem.* **269**, 25,295–25,302.
24. Suzuki, K. T., Karasawa, A., Sunaga, H., Kodama, H., and Yamanaka, K. (1989) Uptake of copper from the bloodstream and its relation to induction of metallothionein synthesis in the rat. *Compar. Biochem. Physiol. C*. **94**, 93–97.
25. Lin, C. M. and Kosman, D. J. (1990) Copper uptake in wild type and copper metallothionein-deficient *Saccharomyces cerevisiae*. Kinetics and mechanism. *J. Biol. Chem.* **265**, 9194–9200.
26. Welch, J., Fogel, S., Cathala, G., and Karin, M. (1983) Industrial yeasts display tandem gene iteration at the CUP1 region. *Mol. Cell. Biol.* **3**, 1353–1361.
27. Steinebach, O. M. and Wolterbeek, H. T. (1994) Effects of copper on rat hepatoma HTC cells and primary cultured rat hepatocytes. *J. Inorg. Biochem.* **52**, 27–48.
28. Lin, S. J., Pufahl, R. A., Dancis, A., O'Halloran, T. V., and Culotta, V. C. (1997) A role for the *Saccharomyces cerevisiae* ATX1 gene in copper trafficking and iron transport. *J. Biol. Chem.* **272**, 9215–9220.
29. Pufahl, R. A., Singer, C. P., Peariso, K. L., Lin, S. J., Schmidt, P. J., Fahrni, C. J., et al. (1997) Metal ion chaperone function of the soluble Cu(I) receptor Atx1. *Science* **278**, 853–856.
30. Culotta, V. C., Klomp, L. W., Strain, J., Casareno, R. L., Krems, B., and Gitlin, J. D. (1997) The copper chaperone for superoxide dismutase. *J. Biol. Chem.* **272**, 23,469–23,472.
31. Gamonet, F. and Lauquin, G. J. (1998) The *Saccharomyces cerevisiae* LYS7 gene is involved in oxidative stress protection. *Eur. J. Biochem.* **251**, 716–723.

32. Glerum, D. M., Shtanko, A., and Tzagoloff, A. (1996) SCO1 and SCO2 act as high copy suppressors of a mitochondrial copper recruitment defect in *Saccharomyces cerevisiae*. *J. Biol. Chem.* **271**, 20,531–20,535.
33. Srinivasan, C., Posewitz, M. C., George, G. N., and Winge, D. R. (1998) Characterization of the copper chaperone Cox17 of *Saccharomyces cerevisiae*. *Biochemistry* **37**, 7572–7577.
34. Paynter, J. A., Gimes, A., Lockhardt, P., and Mercer, J. F. (1994) Expression of the Menkes gene homologue in mouse tissues lack of effect of copper on the mRNA levels. *FEBS Lett.* **351**, 186–190.
35. Yamaguchi, Y., Heiny, M. E., and Gitlin, J. D. (1993) Isolation and characterization of a human liver cDNA as a candidate gene for Wilson disease. *Biochem. Biophys. Res. Commun.* **197**, 271–277.
36. Petris, M. J., Mercer, J. F., Culvenor, J. G., Lockhart, P., Gleeson, P. A., and Camakaris, J. (1996) Ligand-regulated transport of the Menkes copper P-type ATPase efflux pump from the Golgi apparatus to the plasma membrane: a novel mechanism of regulated trafficking. *EMBO J.* **15**, 6084–6095.
37. Hung, I. H., Suzuki, M., Yamaguchi,Y., Yuan, D. S., Klausner, R. D., and Gitlin, J. D. (1997) Biochemical characterization of the Wilson disease protein and functional expression in the yeast Saccharomyces cerevisiae. *J. Biol. Chem.* **272**, 21461–21466.
38. Schaefer, M., Hopkins, R. G., Failla, M. L., and Gitlin, J. D. (1999) Hepatocyte-specific localization and copper-dependent trafficking of the Wilson's disease protein in the liver. *Am. J. Physiol.* **276**, G639–G646.
39. Horn, N. (1976) Copper incorporation studies on cultured cells for prenatal diagnosis of Menkes´ disease. *Lancet* **1**, 1156–1160.
40. Schilsky, M. L. (1994) Identification of the Wilson's disease gene: clues for disease pathogenesis and the potential for molecular diagnosis. *Hepatology* **20**, 529–533.
41. Schilsky, M. L., Stockert, R. J., and Sternlieb, I. (1994) Pleiotropic effect of LEC mutation: a rodent model of Wilson's disease. *Am. J. Physiol.* **266**, G907–G913.
42. Dijkstra, M., van den Berg, G. J., Wolters, H., In't Veld, G., Slooff, M. J., Heymans, H. S., Kuipers, F., and Vonk, R. J. (1996) Adenosine triphosphate-dependent copper transport in human liver. *J. Hepatol.* **25**, 37–42.
43. Terada, K., Aiba, N., Yang, X.-L., Iida, M., Nakai, M., Miura, N., et al. (1999) Biliary excretion of copper in LEC rat after introduction of copper transporting P-type ATPase, ATP7B. *FEBS Lett.* **448**, 53–56.
44. Dancis, A., Yuan, D. S., Haile, D., Askwith, C., Eide, D., Moehle, C., et al. (1994) Molecular characterization of a copper transport protein in *S. cerevisia*: an unexpected role for copper in iron transport. *Cell* **76**, 393–402.
45. Knight, S. A. B., Labbé, S., Kwon, L. F., Kosman, D. J., and Thiele, D. J. (1996) A widespread transposable element masks expression of a yeast copper transport gene. *Genes Dev.* **10,** 1917–1929.
46. Dancis, A., Haile, D., Yuan, D. S., and Klausner, R. D. (1994) The *Saccharomyces cerevisiae* copper transport protein (CTR1p). Biochemical characterization, regulation by copper and physiological role in copper uptake. *J. Biol. Chem.* **269**, 25,660–25,667.
47. Pena, M. M., Puig, S., and Thiele, D. J. (2000) Characterization of the *Saccharomyces cerevisiae* high affinity copper transporter ctr3. *J. Biol. Chem.* **275**, 33,244–33,251.
48. Labbé, S., Pena, M. M. O., Fernandes, A. R., and Thiele, D. J. (1999) A copper-sensing transcription factor regulates iron uptake genes in Schizosaccharomyces pombe. *J. Biol. Chem.* **274**, 36,252–36,260.
49. Kampfenkel, K., Kushnir, S., Babicychuk, E., Inzé, D., and Van Montagu, M. (1995) Molecular characterization of a putative *Arabidopsis thaliana* copper transporter and its yeast homologue. *J. Biol. Chem.* **270**, 28,479–28,486.
50. Hassett, R., Dix, D. R., Eide, D. J., and Kosman, D. J. (2000) The Fe(II) permease Fet4p functions as a low affinity copper transporter and supports normal copper trafficking in *Saccharomyces cerevisiae*. *Biochem. J.* **351**, 477–484.
51. Cohen, A., Nelson, H., and Nelson, N. (2000) The family of SMF metal-ion transporters in yeast cells. *J. Biol. Chem.* **275**, 33,388–33,394.
52. Zhou, B. and Gitschier, J. (1997) A human gene for copper uptake identified by complementation in yeast. *Proc. Natl. Acad. Sci. USA* **94,** 7481–7486.
53. Møller, L.B., Petersen, C., Lund, C., and Horn, N. (2000) Characterization of the hCTR1 gene: genomic organization, functional expression, and identification of a highly homologous processed gene. *Gene* **257**, 13–22.
54. Lee, J., Prohaska, J. R., Dagenais, S. L., Glover, T. W., and Thiele, D. J. (2000) Isolation of a murine copper transporter gene, tissue specific expression and functional complementation of a yeast copper transport mutant. *Gene* **254**, 87–96.
55. Dancis, A., Roman, D. G., Anderson, G. J., Hinnebusch, A. G., and Klausner, R. D. (1992) Ferric reductase of *Saccharomyces cerevisiae*: molecular characterization, role in iron uptake, and transcriptional control by iron. *Proc. Natl. Acad. Sci. USA* **89**, 3869–3873.
56. Georgatsou, E. and Alexandraki, D. (1994) Two distinctly regulated genes are required for ferric reduction, the first step of iron uptake in *Saccharomyces cerevisiae*. *Mol. Cell. Biol.* **14**, 3065–3073.
57. Gorgatsou, E., Mavrogiannis, L. A., Fragiadakis, G. S., and Alexandraki, D. (1997) The yeast Fre1p/Fre2p cupric reductases facilitate copper uptake and are regulated by the copper-modulated Mac1p activator. *J. Biol. Chem.* **272**, 13786–13792.
58. Hassett, R. and Kosman, D. J. (1995) Evidence for Cu(II) reduction as a component of copper uptake by *Saccharomyces cerevisiae*. *J. Biol. Chem.* **270**, 128–134.
59. Tong, K. K. and McArdle, H. J. (1995) Copper uptake by cultured trophoblast cells isolated from human term placenta. *Biochim. Biophys. Acta* **1269**, 233–236.
60. Ferruzza, S., Sambuy, Y., Cirolo, M. R., De Martino, A., Santaroni, P., Rotilio, G., et al. (2000) Copper uptake and intracellular distribution in the human intestinal Caco-2 cell line. *BioMetals* **13**, 179–185.
61. Percival, S. S. and Harris, E. D. (1989) Ascorbate enhances copper transport from ceruloplasmin into human K562 cells *J. Nutr.* **119**, 779–784.

62. McArdle, H. J., Gross, S. M., and Danks, D. M. (1988) Utake of copper by mouse hepatocytes. *J. Cell. Physiol.* **136**, 373–378.
63. Arredondo, M., Uauy, R., and González, M. (2000) Regulation of copper uptake and transport in intestinal cell monolayers by acute and chronic copper exposure. *Biochem. Biophys. Acta* **1474**, 169–176.
64. Lin, C. M., Crawford, B. F., and Kosman, D. J. (1993) Distribution of ^{64}Cu in *Saccharomyces cerevisiae*: kinetic analyses of partitioning. *J. Gen. Microbiol.* **139,** 1617–1626.
65. Lin, C. M., Crawford, B. F., and Kosman, D. J. (1993) Distribution of ^{64}Cu in *Saccharomyces cerevisiae*: cellular locale and metabolism. *J. Gen. Microbiol.* **139**, 1605–1615.
66. McArdle, H. J., Gross, S. M., Creaser, I., Sargeson, A. M., and Danks, D. M. (1989) Effects of chelators on copper metabolism and copper pools in mouse hepatocytes. *Am. J. Physiol.* **265**, G667–G672.
67. Petersen, C. and Møller, L. B. (2000) Control of copper homeostasis in *Escherichia coli* by a P-type ATPase, CopA, and a MerR-like transcriptional activator, CopR. *Gene*, **261**, 289–298.
68. Labbé, S., Zhu, Z., and Thiele, D.J, (1997) Copper-specific transcriptional repression of yeast genes encoding critical components in a copper transport pathway. *J. Biol. Chem.* **272**, 15,951–15,958.
69. Yamaguchi-Iwai, Y., Serpe, M., Haile, D., Yang, W., Kosman, D. J., Klausner, R. D., et al. (1997) Homeostatic regulation of copper uptake in yeast via direct binding of MAC1 protein to upstream regulatory sequences of FRE1 and CTR1. *J. Biol. Chem.* **272**, 17,711–17,718.
70. Zhu, Z., Labbé, S., Pena, M. M. O., and Thiele, D. J. (1998) Copper differentially regulates the activity and degradation of yeast Mac1 transcription factor. *J. Biol. Chem.* **273**, 1277–1280.
71. Ooi, C. E., Rabinovich, E., Dancis, A., Bonifacino, J. S., and Klausner, R. D. (1996) Copper-dependent degradation of the *Saccharomyces cerevisiae* plasma membrane copper transporter CTR1p in the apparent absence of endocytosis. *EMBO J.* **15**, 3515–3523.
72. Yuan, D. S., Stearman, R., Dancis, A., Dunn, T., Beeler, T., and Klausner, R. D. (1995) The Menkes/Wilson disease gene homologue in yeast provides copper to a ceruloplasmin-like oxidase required for iron uptake. *Proc. Natl. Acad. Sci. USA* **92**, 2632–2636.
73. Yamaguchi-Iwai, Y., Dancis, A., and Klausner, R. D. (1995) AFT1: a mediator of iron regulated transcriptional control in *Saccharomyces cerevisiae*. *EMBO J.* **14**, 1231–1239
74. Yamaguchi-Iwai, Y., Stearman, R., Dancis, A., and Klausner, R.D. (1996) Iron-regulated DNA binding by the AFT1 protein controls the iron regulon in yeast. *EMBO J.* **15**, 3377–3384.
75. Osaki, S., Johnson, D. A., and Frieden, E. (1966) The possible significance of the ferrous oxidase activity of ceruloplasmin in normal human serum. *J. Biol. Chem.* **241**, 2746–2751.
76. De Jong, G., Van Dijk, J. P., and Van Eijk, H. G. (1990) The biology of transferrin. *Clin. Chim. Acta* **190**, 1–46.
77. Mukhopadhyay, C. K., Attieh, Z. K., and Fox, P. L. (1988) Role of ceruloplasmin in cellular iron uptake. *Science* **279**, 714–717.
78. Mukhopadhyay, C. K., Mazumder, B., and Fox, P. L. (2000) Role of hypoxia-inducible factor-1 in transcriptional activation of ceruloplasmin by iron deficiency. *J. Biol. Chem.* **275**, 21,048–21,054.
79. Daffada, A. A. and Young, S. P. (1999) Coordinated regulation of ceruloplasmin and metallothionein mRNA by interleukin-1 and copper in HepG2 cells. *FEBS Lett.* **457**, 214–218.

11

The Role of PINA in Copper Transport, Circadian Rhythms, and Wilson's Disease

Jimo Borjigin, Xing Sun, and Michael M. Wang

1. INTRODUCTION

Circadian rhythms are found in virtually all organisms and are tightly coupled to environmental lighting conditions. These rhythms dictate our daily sleep schedule and hormonal fluctuations *(1)* and even influence our susceptibility to disease such as heart attacks *(2)*, strokes *(3)*, and seizures *(4)*. One of the best studied circadian rhythms is the activity of the pineal gland, an organ situated deep within the brain. The pineal exhibits dramatic diurnal fluctuations in secretion of the hormone melatonin, which is best known for its soporific effects in humans. Melatonin is the only vertebrate hormone that is known to universally link environmental light information to the body's physiological responses, including clock resetting, seasonal reproduction, and sleep *(5)*. To understand the molecular basis of the circadian regulation of the pineal gland, we identified a set of genes expressed exclusively in the nighttime pineal. One of these genes, the pineal night-specific ATPase (*PINA*) is the focus of this chapter. PINA is a novel splice form of ATP7B and a putative copper transporter, which is active in the pineal only at night. The identification of PINA suggests that dynamic regulation of copper may play an integral role in circadian rhythms, and the study of PINA's functional differences from ATP7B may prove useful in understanding metal-transporting ATPases.

2. ENZYMATIC SYNTHESIS OF MELATONIN

To understand the role of PINA in circadian biology, one must first review the physiology of the pineal gland. In all animals, the only known function of the pineal is the regulated synthesis of melatonin. Melatonin is synthesized from dietary tryptophan by the actions of four enzymes (Fig. 1). Tryptophan hydroxylase (TPH), the rate-limiting enzyme in serotonin synthesis, is responsible for the 5' hydroxylation of tryptophan, yielding 5-hydroxytrytophan (5-HTP). A nonspecific aromatic amino acid decarboxylase (AAADC) converts 5-HTP to 5-hydroxytryptamine (5-HT, serotonin). A pineal/retina-specific enzyme serotonin *N*-acetyltransferase (NAT) acetylates serotonin to form *N*-acetylserotonin (NAS). Finally, another pineal/retina-specific enzyme, hydroxyindole-*O*-methyltransferase (HIOMT), catalyzes the conversion of NAS to melatonin.

3. REGULATION OF MELATONIN SYNTHESIS

Melatonin synthesis is ultimately controlled by the suprachiasmatic nucleus (SCN) of the brain, which uses a biological clock and lighting information to rhythmically control neural pathways. One

From: Handbook of Copper Pharmacology and Toxicology
Edited by: E. J. Massaro © Humana Press Inc., Totowa, NJ

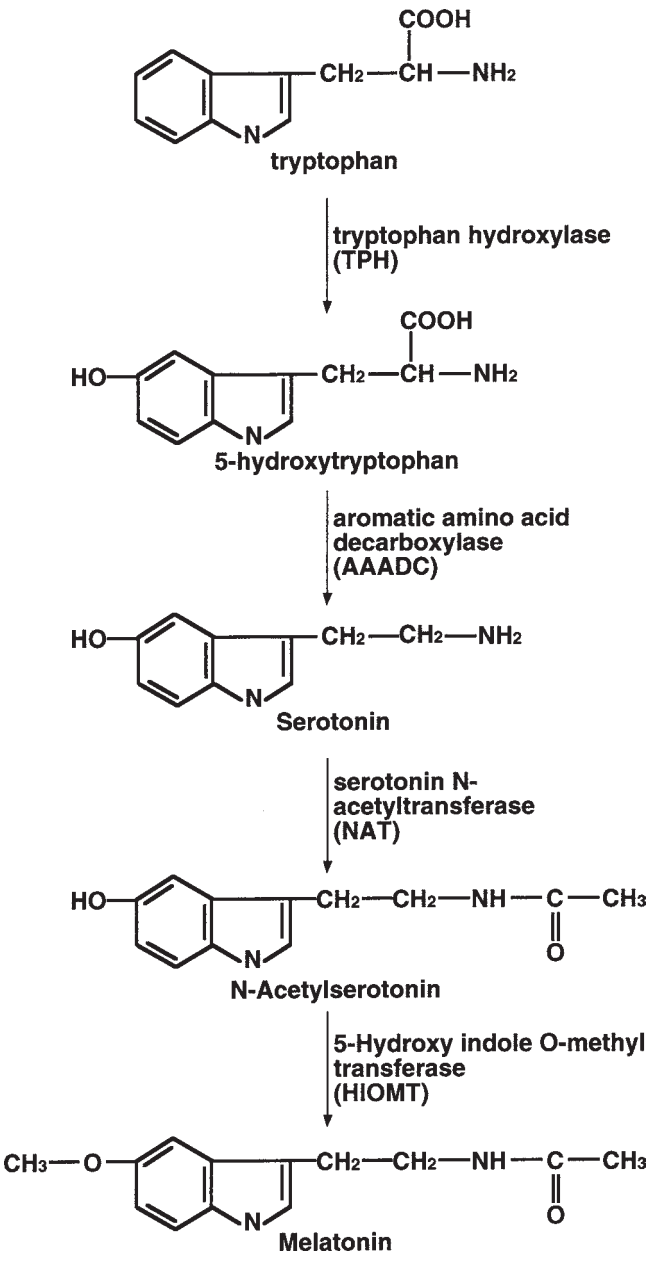

Fig. 1. Melatonin synthetic pathways (*see* text for details).

role of the SCN is to influence neurons of the superior cervical ganglion (SCG), which send axonal processes directly to the pineal gland. When stimulated, sympathetic SCG neurons release norepinephrine into the pineal, activating β-adrenergic receptors on the plasma membrane of pinealocytes. The receptors initiate a signaling cascade resulting in the production of cAMP, which stimulates the production of melatonin mainly by activating transcription of the *NAT* gene *(6)*. Although *NAT* mRNA levels correlate very well with melatonin production, additional effects of cAMP on protein stability and serotonin synthesis in the pineal are under active investigation.

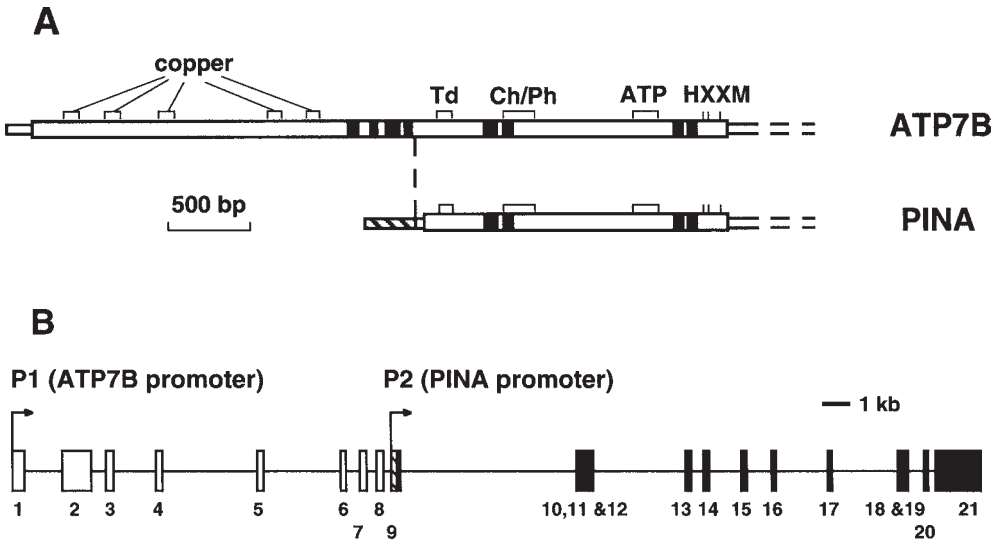

Fig. 2. Structure of *PINA* in comparison with *ATP7B*. **(A)** *PINA* cDNA structure. Functional domains that are conserved among copper transporters are marked as follows: copper, copper-binding domains; Td, transduction domain; Ch/Ph, channel/phosphorylation domain; ATP, ATP-binding domain. The potential copper-binding HXXM motif conserved in ATP7B proteins is also marked. The hatched region at the 5' end of *PINA* cDNA represents *PINA*-specific untranslated sequence. **(B)** *PINA* genomic structure. Transcriptional initiation site of *PINA* mRNA is located in the intron 8 *(9)* of *ATP7B* gene.

4. PINA AND PINEAL CIRCADIAN RHYTHMS

To understand the molecular regulation of the pineal gland at night, we attempted to identify nocturnal genes expressed in the pineal gland by performing subtractive hybridization *(7)*. *PINA* was among the first of these genes to be characterized.

Sequence analysis of *PINA* revealed that it is an alternatively spliced form of *ATP7B*, the copper-transporting ATPase mutated in Wilson's disease (WD) patients (Fig. 2A). In the *PINA* message, sequences encoding the N-terminal half of *ATP7B* are replaced by a unique untranslated 300-base-pair leader sequence. The *PINA* protein, therefore, represents only the C-terminal half of ATP7B. The 300-base-pair leader sequence has been shown to be part of an intron immediately upstream of exon 9 of *ATP7B*, suggesting that *PINA* is driven by a novel pineal/retina-specific promoter *(8)* nested within the center of the *ATP7B* gene *(9)* (Fig. 2B). The *PINA* promoter in fact contains a single CRE and multiple PIRE sites, which may be important for cAMP inducibility and pineal/retina tissue-specific transcription, respectively *(8)*.

Using probes unique for *PINA*, we determined that *PINA* is expressed exclusively in the pineal gland and the retina. Analysis by *in situ* hybridization demonstrates that *PINA* is expressed abundantly in selected populations of pinealocytes. In the retina, *PINA* is expressed in the retinal pigment epithelium and a subset of photoreceptors at night. Northern blot analysis also demonstrated dramatic temporal regulation of *PINA* mRNA that coincides precisely with the expression of *NAT* mRNA and increased melatonin production (Fig. 3). Like *NAT*, the expression of *PINA* is controlled by adrenergic stimulation of the pineal gland by the SCG *(10)*.

5. IMPLICATIONS OF FUNCTIONAL ANALYSIS OF PINA

Pineal night-specific ATPase is predicted to encode a 665-amino-acid protein with a molecular weight of 74 kDa. The protein contains only four of eight transmembrane domains predicted for

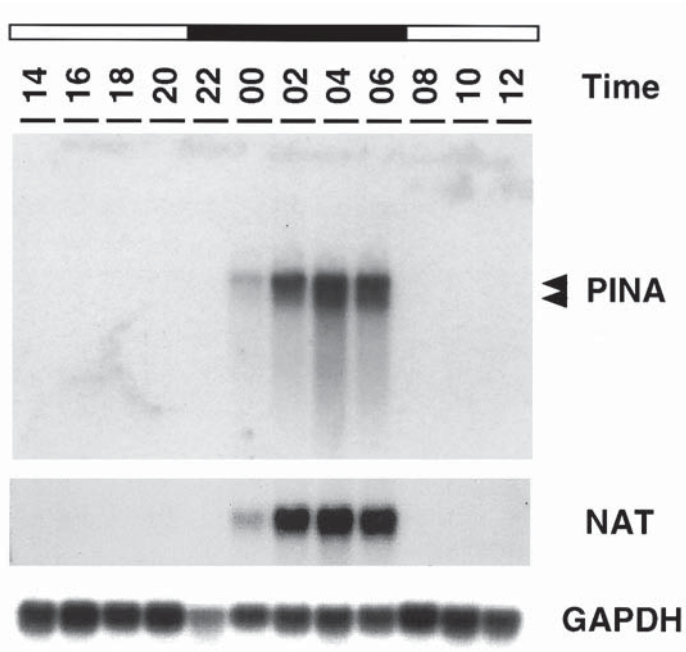

Fig. 3. Temporal expression pattern of PINA mRNA in adult pineals. Northern blot of pineal RNA collected from rats at 2-h intervals was hybridized sequentially with full-length PINA, NAT *(7)*, and GAPDH probes.

ATP7B *(11)* and retains the transduction, channel/phosphorylation, and ATPase catalytic domains. PINA does not contain five proposed metal-binding domains within the N-terminus of ATP7B, which have been postulated to bind copper and regulate activity of the transporter (Fig. 2A).

Surprisingly, despite the deletion of a bulk of the ATP7B protein, PINA functions as a copper transporter when introduced into yeast complementation assays, although its activity is much lower than the ATP7A protein analyzed as a control *(10)*. The functional integrity of PINA provides some useful insight into the structure requirements of other ATPases. PINA's structure suggests that previously identified critical N-terminal regions of ATP7B may not be essential for function. Moreover, regions conserved in the C-terminus may take on significance of greater magnitude than previously suspected.

We have sought to explain how PINA functions without N-terminal metal-binding motifs by examining its sequence for possible alternative metal-binding motifs in the C-terminus. The MXXM motif has been previously implicated in copper binding in bacterial copper transporters, but we did not find these motifs in PINA. Instead, we identified 3 copies of a HXXM motif in the C-terminus of the protein, which is also present in 11 copper-transporting proteins from bacteria and vertebrates *(10)*. In some bacterial proteins, the motif was repeated five times (Table 1). Based on this analysis, we suggest that the HXXM motif is involved in binding copper and that, in PINA, this is sufficient for copper transport. We further speculate that the N-terminal domain of ATP7B, missing in PINA, plays a regulatory, rather than essential, role in copper transport. Experimental verification is forthcoming.

6. ROLE OF PINA IN PINEAL PHYSIOLOGY

To determine a role for PINA in the normal pineal physiology, we have turned to the LEC rat, a strain in which *PINA* and *ATP7B* are mutated as a result of a large deletion in the C-terminal coding region *(12)*. These rats are well-established models of Wilson's disease in which copper builds up in the liver, resulting in liver failure and death *(13)*.

Table 1
A HXXM Motif Present in PINA/ATP7B and Proteins Involved in Copper Trafficking

Source	*Protein*	*HXXM motifs*[a]	*GeneBank accession no.*
Rat	PINA/ATP7B	$^{589/1375}$HGRM	Q64535
		$^{603/1389}$HVGM	
		$^{641/1427}$HGGM	
Human	ATP7B	^{1389}HGHM	P35670
		^{1403}HIGM	
Sheep	ATP7B	^{1368}HGHM	AF032881
Mouse	ATP7B	^{1386}HGRM	U38477
		^{1400}HIGM	
Human	ATP7A	^{696}HSSM	Q04656
Mouse	ATP7A	^{687}HSAM	Q64430
Chinese Hamster	ATP7A	^{686}HSSM	P49015
Enterococcus hirae	CopB	^{62}HGHM	P05425
		^{70}HSHM	
		^{75}HEDM	
		^{83}HSHM	
		^{88}HENM	
Pseudomonas syringae	CopA	^{376}HGSM	P12374
		^{409}HSKM	
		^{420}HGAM	
		^{428}HGAM	
		^{596}HMEM	
Pseudomonas syringae	CopB	37HSQM	P12375
		^{45}HSKM	
		^{53}HSQM	
		^{61}HSKM	
		^{69}HSQM	
Arabidopsis thaliana	COPT1	^{3}HDHM	Z49859
		^{34}HHHM	
		^{36}HMKM	

[a] The number represents position of the histidine residues.

Because the tissue specificity and circadian expression of *PINA* correlated well with *NAT* expression and melatonin synthesis, we suspected that PINA was involved in melatonin biosynthesis. Our investigations of PINA/ATP7B mutant LEC rats indeed revealed a defect in NAT protein stability, but, unfortunately, this was caused by an independent mutation in the NAT gene and not by the PINA mutation. We have now generated a novel line of rats in which three of the mutant LEC genes encoding NAT, PINA, and coat color have now been segregated: LPP (PINA–), LPN (NAT–), and LPW (wild type in all three loci). Using these strains of rats, we were able to address the role of PINA in normal pineal physiology. Using a novel on-line pineal microdialysis protocol, we have measured the circadian production of melatonin and its precursors in animals quantitatively and reproducibly. In normal rats (LPW; Fig. 4), we see low melatonin levels during the day and a sharp rise in melatonin synthesis shortly after lights off; melatonin output dramatically drops off minutes before lights on. The melatonin synthetic profile of LPP animals shows no significant differences over the course of the day or the night (LPP, Fig. 4), demonstrating that PINA is not essential for melatonin synthesis and secretion. Thus, the natural role of PINA remains unresolved presently.

Other postulated functions of PINA must account for its tissue distribution and temporal expression pattern, which suggest involvement in a pineal/retinal-specific nocturnal process. Melatonin

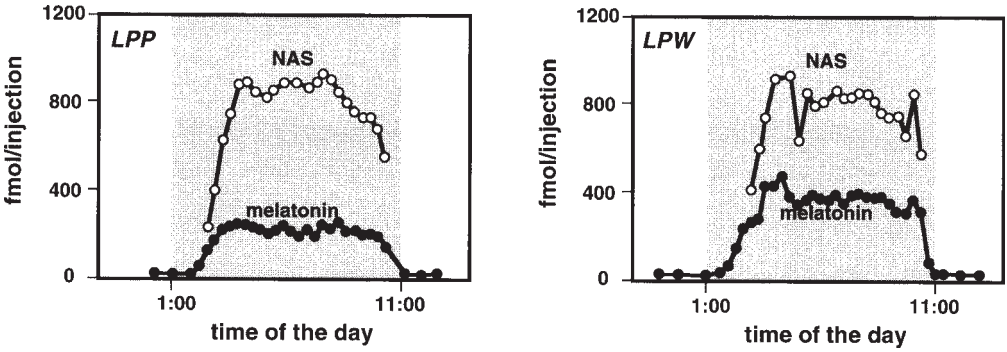

Fig. 4. Diurnal profile of pineal *N*-acetylserotonin (NAS, solid circle) and melatonin (open circle) release in wild-type (LPW) and PINA-defective (LPP) rats as determined by in vivo pineal microdialysis *(14)*. Lights were off at 1 am and on at 11 am (within the shaded area). The diurnal pattern is reproducible in 100% of the animals examined, with slight variations in the level of melatonin among individual rats. There is no statistical difference between LPP and LPW rat strains in the level of pineal melatonin secretion.

synthesis is regulated at a number of different levels; for example, flashes of light in the night rapidly inactivate hormone synthesis by activation of proteosomal degradation of NAT *(15)*; perhaps PINA participates in the nighttime regulation of NAT protein stability and therefore is only active in the night pineal. Alternatively, because little is known about pineal functions beyond its well-established duty as the body's source of melatonin, perhaps PINA plays a role in novel functions of the pineal that occur simultaneously with melatonin synthesis. In analogy to the role of ATP7B in copper loading of ceruloplasmin, PINA may help load nocturnally synthesized copper proteins in the pineal. PINA could also play a role in the concentration of copper within cellular compartments that may be necessary for the biosynthesis or processing of novel pineal secretion products. Clearly, an understanding of the role of PINA in the pineal may suggest novel, analogous functions for ATP7B in the liver.

7. PINA AND WILSON'S DISEASE

Wilson's disease (WD) is an autosomal recessive disorder resulting from mutations in the ATP7B gene. Patients with WD suffer from two main types of symptom: brain disorder and liver disease. For unknown reasons, the clinical presentation of WD patients span a broad spectrum; some patients suffer purely from liver disease, some from only brain disease, whereas others experience both types of symptom. Although patients do not pose eye complaints, the cornea of the eye is also affected in many patients, resulting in the hallmark brown discoloration of the cornea, which is very specific for neurological Wilson's disease, the Kayser–Fleischer ring.

The pathogenesis of WD is thought to result from a systemic overload of copper, which accumulates primarily in the three major targets of WD: the brain, eye, and liver. The etiological significance of copper is supported by the efficacy of treatments, which are principally aimed at chelation of free copper. Clearly, although multiple lines of experimental evidence have demonstrated that copper is toxic to hepatocytes and causes oxidative damage, it is less clearly established that copper is directly harmful to the neurons of the brain under normal circumstances. Could the case for copper toxicity in neurological WD be an oversimplification? Several pieces of evidence suggest that the brain disorder seen in WD is caused by more than simple copper overload. It is known, for example, that in human subjects with Wilson's disease and liver diseases, brain copper is elevated but there is sometimes no evidence of the characteristic neurological disorder. In cases of copper toxicity (Indian cirrhosis), there is clear liver failure, yet there have been no neurological symptoms described *(16–18)*. LEC rats, the animal model of Wilson's disease with mutant *ATP7B*, have clearly elevated brain copper levels, yet fail to demonstrate neurological dysfunction *(19,20)*. These observations temper the traditional

notions that copper alone causes neurotoxicity in WD. Alternatively, other factors affecting the brain or required for proper brain function may be released in the absence of functional ATP7B and PINA.

Coincidentally, in addition to the pineal, the retina and pigment epithelium expresses PINA but not ATP7B. Whether PINA dysfunction in the eye causes the Kayser–Fleischer ring remains to be determined, but consideration must be given in the future for a specific role of PINA in the development of brain dysfunction in Wilson's disease, particularly in light of conflicting data on the effects of copper on the brain.

8. CONCLUSIONS

The identification of PINA in the pineal gland and retina suggests that the pineal may carry out novel functions other than rhythmic melatonin synthesis. The functions may depend on copper transport. The highly parsimonious structure of PINA demonstrates that the critical regions required for ATP7B transporter function are clustered in the C-terminus of the ATP7B and indicates that novel protein partners may be required for native PINA function. The role of PINA in Wilson's disease remains to be proven.

REFERENCES

1. Moore-Ede, M. C., Sultzman, F. M., and Fuller, C. A. (1982) *The Clocks That Time Us–Physiology of the Circadian Timing System*. Harvard University Press, Cambridge, MA.
2. Purcell, H. and Mulcahy, D. (1995) Circadian rhythms and the onset of myocardial infarction: clinical implications. *J. Cardiovasc. Risk* **2**, 510–514.
3. Vermeer, S. E., Rinkel, G. J., and Algra, A. (1997) Circadian fluctuations in onset of subarachnoid hemorrhage. New data on aneurysmal and perimesencephalic hemorrhage and a systematic review. *Stroke* **28**, 805–808.
4. Quigg, M. (2000) Circadian rhythms: interactions with seizures and epilepsy. *Epilepsy Res*. **42**, 43–55.
5. Arendt, J. (1995) *Melatonin and the Mammalian Pineal Gland.* Chapman & Hall, London.
6. Borjigin, J., Li, X., and Snyder, S. H. (1999) The pineal gland and melatonin: molecular and pharmacologic regulation. *Annu. Rev. Pharmacol. Toxicol*. **39**, 53–65.
7. Borjigin, J., Wang, M. M., and Snyder, S. H. (1995) Diurnal variation in mRNA encoding serotonin N-acetyltransferase in pineal gland. *Nature* **378**, 783–785.
8. Li, X., Chen, S., Wang, Q., Zack, D. J., Snyder, S. H., and Borjigin, J. (1998) A pineal regulatory element (PIRE) mediates transactivation by the pineal/retina-specific transcription factor CRX. *Proc. Natl. Acad. Sci. USA* **95**, 1876–1881.
9. Thomas, G. R., Forbes, J. R., Roberts, E. A., Walshe, J. M., and Cox, D. W. (1995) The Wilson disease gene: spectrum of mutations and their consequences [published erratum appears in *Nature Genet.* 1995 Apr;**9(4)**:451]. *Nature Genet*. **9**, 210–217.
10. Borjigin, J., Payne, A. S., Deng, J., Li, X., Wang, M. M., Ovodenko, B., et al. (1999) A novel pineal night-specific ATPase encoded by the Wilson disease gene. *J. Neurosci*. **19**, 1018–1026.
11. Bull, P. C. and Cox, D. W. (1994) Wilson disease and Menkes disease: new handles on heavy-metal transport. *Trends Genet*. **10**, 246–252.
12. Wu, J., Forbes, J. R., Chen, H. S., and Cox, D. W. (1994) The LEC rat has a deletion in the copper transporting ATPase gene homologous to the Wilson disease gene. *Nature Genet*. **7**, 541–545.
13. Mori, M., Hattori, A., Sawaki, M., Tsuzuki, N., Sawada, N., Oyamada, M., et al. (1994) The LEC rat: a model for human hepatitis, liver cancer, and much more. *Am. J. Pathol*. **144**, 200–204.
14. Drijfhout, W. J., Grol, C. J., and Westerink, B. H. (1993), Microdialysis of melatonin in the rat pineal gland: methodology and pharmacological applications. *J. Neurochem.* **61**, 936–942
15. Gastel, J. A., Roseboom, P. H., Rinaldi, P. A., Weller, J. L., and Klein, D. C. (1998) Melatonin production: proteasomal proteolysis in serotonin N-acetyltransferase regulation. *Science* **279**, 1358–1360.
16. Sethi, S., Grover, S., and Khodaskar, M. B. (1993) Role of copper in Indian childhood cirrhosis. *Ann. Trop. Paediatr*. **13**, 3–5.
17. Muller, T., Feichtinger, H., Berger, H., and Muller, W. (1996) Endemic Tyrolean infantile cirrhosis: an ecogenetic disorder. *Lancet* **347**, 877–880.
18. Muller, T., van de Sluis, B., Muller, W., Pearson, P., and Wijmenga, C. (1999) Non-Indian childhood cirrhosis. *Eur. J. Med. Res*. **4**, 293–297.
19. Sato, M., Sugiyama, T., Daimon, T., and Iijima, K. (1994) Histochemical evidence for abnormal copper distribution in the central nervous system of LEC mutant rat. *Neurosci. Lett*. **171**, 97–100.
20. Saito, T., Itoh, T., Fujimura, M., and Saito, K. (1995) Age-dependent and region-specific differences in the distribution of trace elements in 7 brain regions of Long–Evans Cinnamon (LEC) rats with hereditary abnormal copper metabolism. *Brain Res*. **695**, 240–244.

12

The Identification of Motifs Involved in the Intracellular Trafficking of the Menkes Disease Protein

Michael J. Francis and Anthony P. Monaco

1. INTRODUCTION

Menkes disease is a severe neurodegenerative disorder arising from a defect in copper transport. The incidence of this disease has been estimated at 1 in 250,000 *(1)*, although in some populations it can be as high as 1 in 40,000 *(2)*. A less severe form of the disease, occipital horn syndrome (OHS) or X-cutis laxis, resulting from an allelic variant, has also been described. The clinical symptoms of both Menkes disease and OHS are caused by a lack of serum copper and copper-requiring enzymes, such as lysyl oxidase and cytochrome-*c* oxidase. In normal individuals, dietary copper is taken into the body and the majority is absorbed by the stomach and the small intestine. The copper is transported primarily with ceruloplasmin and is complexed to histidine and albumin. The copper is reduced to Cu(I) and taken up into the cell. In patients with Menkes disease, absorption of orally administered copper is much reduced, and the brain, blood, and liver show decreased levels of copper. However, in many other tissues, there is an increase in copper levels when compared to normal individuals, although there is still a defect in the function of copper-requiring enzymes *(3)*. Cultured fibroblasts from patients show both an excess accumulation of copper and efflux abnormalities from these cells *(4–7)*. These results suggest that the protein responsible for Menkes disease has a direct role in the intracellular transport of copper. This chapter discusses the role of motifs within the Menkes disease protein involved in this transport.

2. IDENTIFICATION, STRUCTURE, AND CELLULAR LOCALIZATION OF THE MENKES DISEASE GENE (*ATP7A*/*MNK*)

The gene responsible for Menkes disease (*ATP7A*) was identified in 1993 and is homologous to a bacterial family of P-type ATPases (8–10). These are integral membrane proteins that use an aspartyl phosphate to transport cations across membranes (Fig. 1). Conserved regions include heavy-metal-binding repeat sequences, GMXCXXC, a phosphatase domain, a DKTGT sequence involved in energy transduction, an ATP-binding domain, and eight transmembrane domains. The *ATP7A* gene has a 4.5 kb open reading frame and translates a protein of approximately 170 kDa. Deletions, mutations and reduced mRNA synthesis are all evidence that *ATP7A* is responsible for Menkes disease. Interestingly, mutations in the autosomal homolog of *ATP7A* (*ATP7B/WND*) are responsible for the phenotype observed in Wilson's disease patients, another disorder of copper transport. The abnormal

From: Handbook of Copper Pharmacology and Toxicology
Edited by: E. J. Massaro © Humana Press Inc., Totowa, NJ

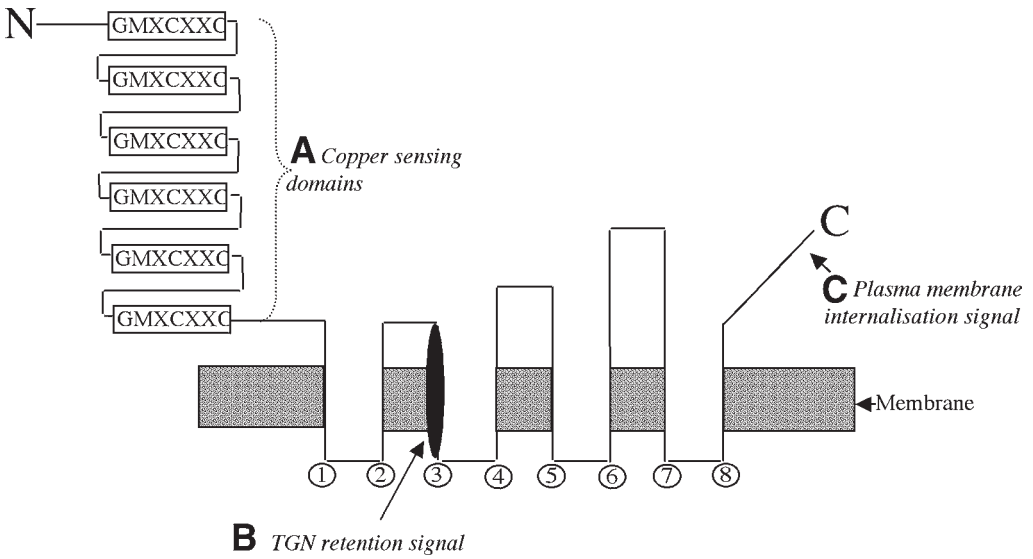

Fig. 1. Proposed gene structure of *ATP7A*/*MNK*, highlighting transmembrane domains (1–8) and proposed functional domains. The intracellular trafficking signals and motifs discussed in this chapter are shown in italics: **(A)** copper-sensing domains, **(B)** trans-Golgi network (TGN) retention signal, and **(C)** plasma membrane internalization signal.

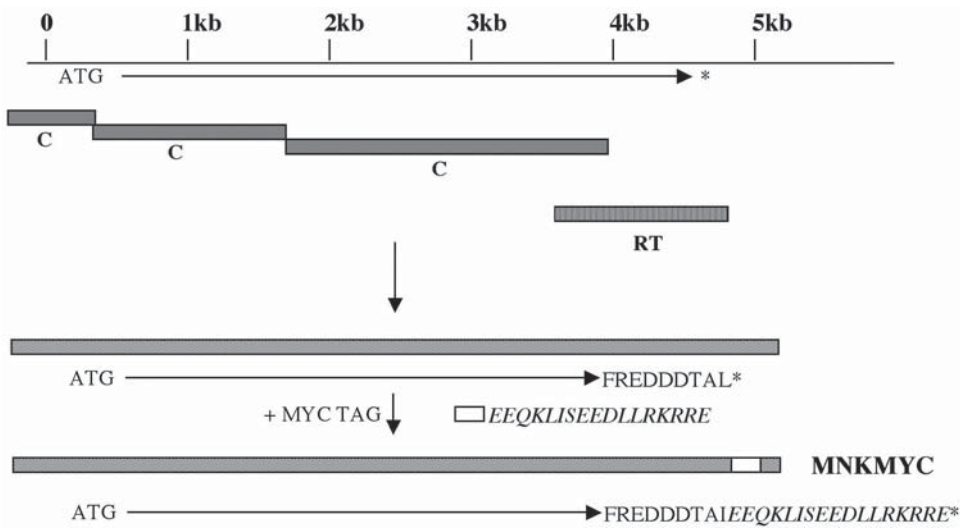

Fig. 2. Construction of the recombinant full-length MNK cDNA. CDNAs (C) isolated during the cloning of *ATP7A (8)* were ligated to a 3' RT-PCR product (RT). A MYC epitope tag was added in-frame at the 3' end, resulting in the construct MNKMYC. This full-length epitope-tagged cDNA was subsequently cloned into mammalian expression vectors for trafficking studies.

copper accumulation and retention phenotype observed in cell lines from Menkes patients has been corrected by the expression of the recombinant MNK and WND proteins in these cell lines *(11)*. Both the endogenous and the recombinant proteins at steady state are localized predominantly at the trans-Golgi network (TGN) *(12–16)*. On the addition of copper to cultured cells, a shift in equilibrium is observed and the protein is redistributed to the plasma membrane. The protein returns to the TGN on removal

of the copper. It is assumed from this that MNK has a role in copper efflux *(12,15,17)*. Although this trafficking does not require new protein synthesis, both the endocytic and exocytic routes are ATP dependent (12). These observations prompted studies into the characterization and identification of the motifs involved in this intracellular trafficking.

3. EXPRESSION STUDIES FROM A FULL-LENGTH MNK CDNA

In order to confirm the role of newly identified motifs within MNK that were involved in intracellular trafficking, it was essential to generate a full-length cDNA that could be expressed and the resulting protein visualized within mammalian systems. The disruption of putative trafficking motifs within this recombinant protein would help to confirm their role in the copper-induced relocalization of MNK.

3.1. Generation of Recombinant Construct

cDNAs and reverse transcription–polymerase chain reaction (RT-PCR) products isolated during the cloning of the *ATP7A* gene were ligated together to generate the full-length cDNA (Fig. 2). To distinguish between the almost ubiquitous expression of the endogenous protein and the recombinant protein, the recombinant protein was tagged with a specific epitope marker. An in-frame fusion of the MYC epitope (recognized by the monoclonal antibody 9E10) was inserted into the stop-codon position of MNK, resulting in the construct MNKMYC.

3.2. Recombinant MNK Protein Studies

MNKMYC was transfected into numerous human cell lines using a cationic lipid transfection reagent (Superfect-Qiagen). Lysates from the transfected cell lines were separated on a sodium dodecyl sulfate (SDS) polyacrylamide gel. The recombinant MNK protein was detected using the 9E10 antibody and a secondary anti-mouse antibody conjugated to HRP. A band of 180 kDa was observed in accordance with the predicted protein size (data not shown).

3.3. Intracellular Localization of Recombinant MNK

To determine whether the recombinant MNK localized to the same region of the cell as the endogenous form, the cellular localization of MNKMYC was detected using indirect immunofluorescence and confocal laser microscopy. Comparisons were made between the expression pattern of MNKMYC and the human TGN resident marker, TGN46. Figure 3 shows the protein expression of MNK in the human fibroblast cell line MRC5/V2. Both the staining patterns of MNKMYC (Fig. 3B) and TGN46 (Fig. 3A) are visible at a juxtanuclear reticulum location. The colocalization between these two proteins is confirmed by the yellow signal observed when the images are superimposed (Fig. 3C). As endogenous MNK and TGN46 are found in the TGN, these data confirm that the recombinant and endogenous MNK proteins reside in a morphologically identical organelle.

4. CHARACTERIZATION AND IDENTIFICATION OF MOTIFS INVOLVED IN INTRACELLULAR TRAFFICKING OF MNK

We focused our efforts on (1) understanding the role of the six N-terminal copper-binding domains in this copper-induced relocalization, (2) identifying motif(s) involved in retention of MNK to the TGN, and (3) identifying signals that mediate the internalization of MNK from the plasma membrane to the TGN.

4.1. Characterization of N-Terminal Copper-Binding Motifs

The N-terminal domains of both the Menkes protein (MNK) and the Wilson protein (WND) contain evolutionary conserved repeat sequences of the type GMXCXXCXXIE that bind copper, as well as zinc, cobalt, and nickel *(18–19)*. The number of these N-terminal repeats vary in the MNK/WND orthologs from one in *Enterococcus hirae* and two in *Schizosaccharomyces pombe*, to six in both

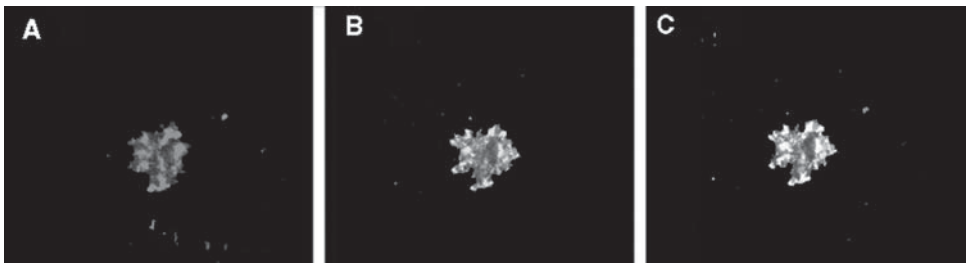

Fig. 3. Recombinant MNK localizes to the TGN. Recombinant MNK containing an in-frame fusion MYC epitope tag was detected by indirect immunofluorescence **(B)**. This signal is almost identical to that of the TGN marker TGN46 **(A)**. This similarity is confirmed by the overlap of the two signals **(C)**. (Reprinted from ref. *16* with permission from Oxford University Press.)

mammalian MNK and WND. The metal-binding properties of these repeats were first established by overexpressing the N-terminal domains of both MNK and WND in *Escherichia coli*. Both of these proteins can bind copper in vitro and in vivo, and five to six copper molecules are bound for every molecule of the N-terminal domain *(19)*.

Using reducing agents, it was also shown that the copper is most likely to be bound in the Cu(I) form. Further studies confirmed that copper binds as Cu(I) with a stoichiometry of one copper per domain *(20)*, and it is most likely to bind in a linear bi-coordinate manner to the two cysteine residues of the repeat *(21)*. One method employed to assay the role of these copper-binding domains on function has been the complementation of the ccc2 yeast mutant. The gene product of *ccc2* supplies copper to Fet3p, which is involved in iron import into the cell. A defective *ccc2* protein results in the cells unable to import iron and grow on iron-limited medium *(22,23)*. Both *ATP7A* and *ATP7B* can rescue the *ccc2* mutant phenotype *(24,25)*. Using this method to assay the effect of mutating the N-terminal repeats on function, the results of Payne and Gitlin inferred that the N-terminal motifs of *ATP7A* are functionally more important than the C-terminal motifs. The third copper-binding domain is the most important for MNK activity, whereas for *ATP7B*, the converse is true, and deletion of the first five repeats resulted in normal function *(26)*.

To monitor the role of these repeats in the copper-induced trafficking of MNK from the TGN to the plasma membrane, we performed exhaustive mutagenesis studies of these domains and observed the effects of increased cellular copper levels on intracellular trafficking of MNKMYC in a human fibroblast cell line. It had been previously demonstrated that, unlike the wild-type sequence (GMXCXXC), the mutant sequence, GMXSXXS, will not bind copper *(21,27)*. In our studies, both of the cysteine residues in the copper-binding domains (CBD), were mutagenised to serine (GMXSXXS). Figure 4 shows the effect of increasing copper concentrations on relocalization of wild-type MNK (CBDWT). Under normal physiological conditions, MNK has a perinuclear location. As the copper concentration increases, from 100 to 600 μM, a generally more punctate staining, leading to staining at the plasma membrane, is observed. Removal of copper from the media results in the protein returning to its perinuclear position. Mutagenesis of the cysteine residues to serine in all the repeats (CBDΔ1–6) abolishes movement to the plasma membrane (Fig. 5). To determine which of the copper-binding domains are involved in the trafficking of MNK to the plasma membrane, a series of mutants containing only one functional copper-binding domain were studied. For example, CBD1WT contains a functional copper-binding domain 1 only. All of these mutants behave identically to that of the wild-type protein and relocalize to the plasma membrane on the addition of copper (Fig. 6). These results suggest that in human fibroblasts, only one functional copper-binding domain is required for movement and that there is no observable difference in the trafficking of MNK from the involvement of any of the individual domains *(17)*.

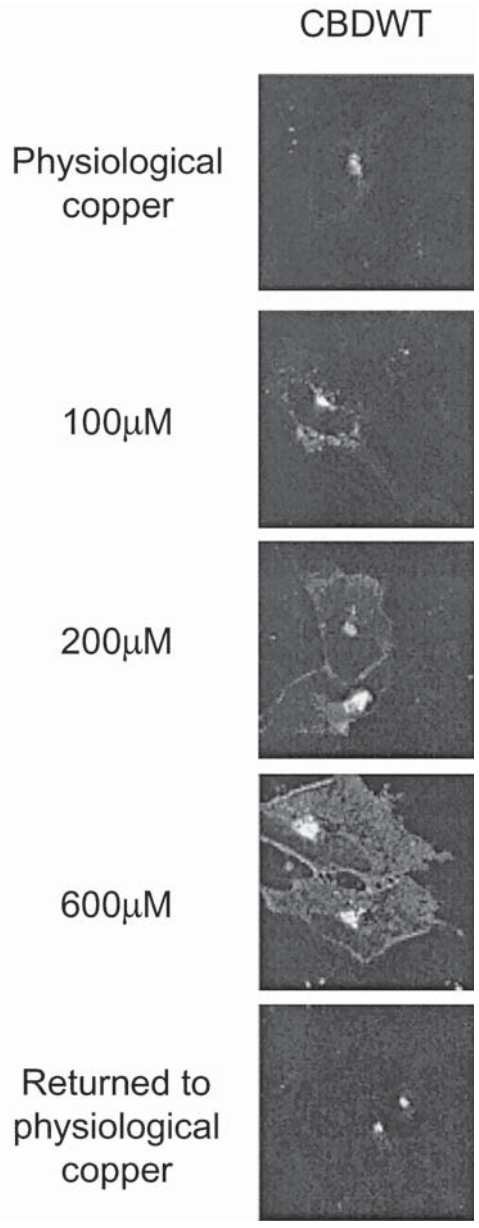

Fig. 4. MNK moves to the plasma membrane with increasing intracellular copper concentration. Copper was added to cells containing MNK. As the intracellular copper concentration increases (100–600 μ*M*), MNK moves from the TGN to the plasma membrane. The protein returns to the TGN on the removal of copper from the culture media. (Reprinted from ref. *17* with permission from Oxford University Press.)

Other studies have shown that in Chinese hamster ovary cells when CBD 4–6 of MNK are mutated, trafficking was abolished and the protein remained in the TGN *(28)*, suggesting that a CBD close to the membrane channel of MNK is essential for copper-induced trafficking. It has been proposed that the N-terminal repeats may function as a copper-sensing domain, with their progressive occupation with copper resulting in the relocalization of the protein *(12)*. All of the above data, although conflicting on the relative importance of each domain, suggest that not all of the copper-binding domains are required for the redistribution of the protein in high levels of copper.

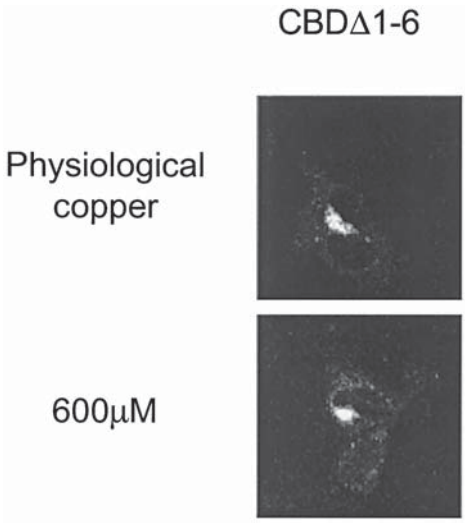

Fig. 5. Mutation of all copper-binding domains abolishes copper-induced relocalization. Each of the cysteine residues in all the six copper-binding domains (CXXC) at the N-terminus of MNK were mutagenised to serines. This mutagenised variant (CBDΔ1–6), although localized to the TGN, did not move to the plasma membrane on the addition of copper. (Reprinted from ref. *17* with permission from Oxford University Press.)

4.2. Using Reporter Molecules to Identify Intracellular Trafficking Motifs

To understand the copper-induced trafficking of MNK in more detail, studies were initiated into the identification of the motifs/domains involved. In order to identify these signals, we used the reporter molecule CD8. CD8 is a type-1 glycoprotein that is primarily localized to the plasma membrane. For these studies, it can be essentially divided into three domains: (1) lumenal domain; (2) transmembrane domain; (3) cytoplasmic domain (Fig. 7). The N-terminal lumenal domain, which in the wild-type protein sits exofacially to the cell, is recognized by the monoclonal antibody OKT8, which is used to follow the trafficking patterns of the protein within the cell.

The strategy employed involved the excision of either the transmembrane domain or cytoplasmic domain of CD8 and subsequent replacement with the comparative domains from MNK. If any of these newly introduced domains contains signals involved in MNK trafficking, it is likely that these signals will alter the trafficking characteristics of the fusion protein, when compared to the wild-type protein.

4.3. Identification of a Trans-Golgi Network Retention Signal

Many Golgi resident proteins such as TGN38 and β1,4-galactosyltransferase *(29)* are retained in the TGN by their transmembrane domain(s). It is therefore feasible that MNK is also retained in a similar manner. To study this, chimeric proteins consisting of the lumenal and cytoplasmic domain of the reporter molecule CD8 fused to different transmembrane domains of the MNK protein were generated. Localization of these chimeric proteins was monitored by indirect immunofluorescence. CD8 wild type (CD8-WT), as expected, localizes primarily to the plasma membrane (Fig. 8B). The insertion of the MNK trans-membrane domain 7 (TM7) into CD8 results in a staining pattern corresponding to the endoplasmic reticulum (Fig. 8H), suggesting that this protein is misfolding and not able to traverse through the secretory pathway. However, on replacing the transmembrane domain of CD8-WT with MNK transmembrane domain 3 (TM3), a staining pattern almost identical to that of the trans-Golgi network resident marker TGN46 is observed (Fig. 8E). The colocalization of these two proteins is confirmed on superimposition of these two images (Fig. 8F). These results suggest

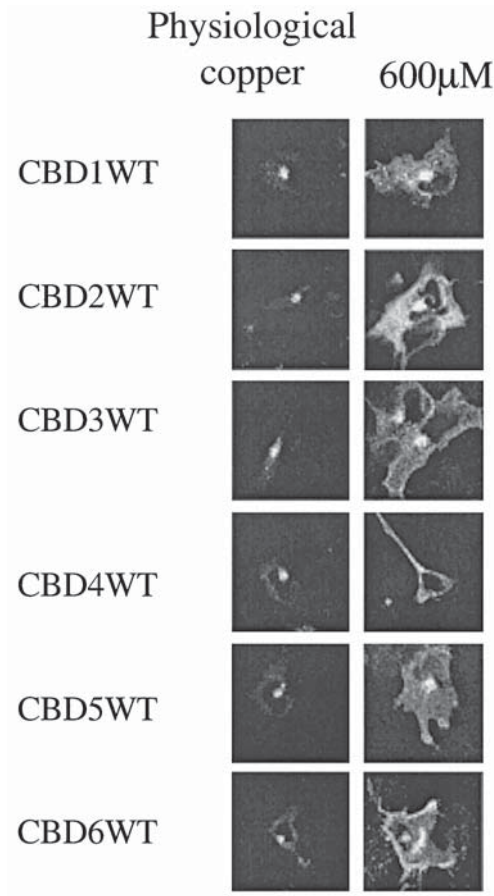

Fig. 6. Only one functional copper domain is required for copper-induced relocalization to the plasma membrane. Six mutants, each containing only one functional copper domain, were generated. All mutants were primarily resident at the TGN at basal copper levels, and all mutants trafficked to the plasma membrane on addition of media containing 600 μ*M* of copper. (Reprinted from ref. *17* with permission from Oxford University Press.)

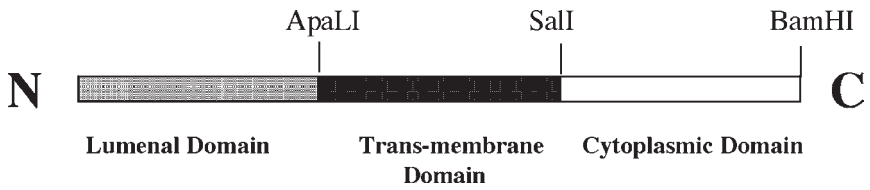

Fig. 7. Schematic representation showing the domains in CD8 used in this study. The N-terminus lumenal domain contains the epitope recognized by the monoclonal antibody OKT8. The transmembrane domain and cytoplasmic domain were excised and replaced with comparative domains from MNK using restriction-enzyme double digests *Apa*LI/*Sal*I and *Sal*I/*Bam*HI, respectively.

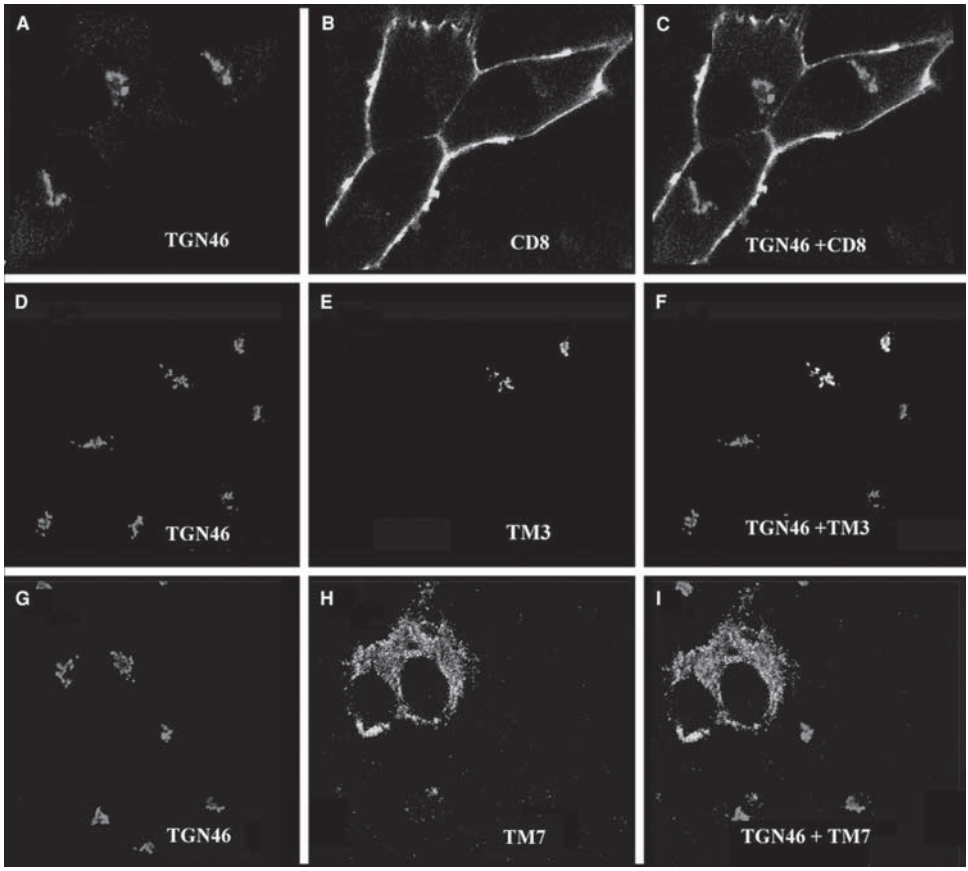

Fig. 8. Transmembrane domain 3 of MNK contains a trans-Golgi retention signal. Colocalization studies comparing the trans-Golgi resident protein TGN46 with CD8 fusion proteins containing transmembrane domain 3 or 7 were performed. Wild-type CD8 is localized to the plasma membrane **(B)** and does not colocalize with TGN46 **(A,C)**. The staining pattern of the fusion protein of CD8 containing transmembrane domain 3 of MNK **(E)** is almost identical to that of TGN46 **(D)**. The degree of overlap is confirmed by the bright signal **(F)**. The staining pattern of the fusion protein of CD8 containing transmembrane domain 7 of MNK is characteristic of the endoplasmic reticulum **(H)** and does not overlap with TGN46 **(I)**. (Reprinted from ref. *16* with permission from Oxford University Press.)

that there is a signal within a 38 amino acid (aa) stretch containing the TM3 of MNK sufficient to retain a protein at the TGN.

Interestingly, an alternatively spliced MNK product that skips exon 10 (containing TM3 and TM4) is present in low amounts in normal individuals. The protein from this transcript was localized to the endoplasmic reticulum *(30)* and the authors suggest that this arises because this aberrant splicing prevents correct protein folding or interferes with a Golgi "localization domain" *(30)*.

In summary, we identified a signal sufficient for the retention of fusion proteins at the TGN in a 38 amino acid stretch containing TM3, inferring that TM3 is an essential element in the localization of MNK to the TGN *(16)*. It is possible that the retentive qualities of TM3 are compromised on addition of copper, resulting in an increased proportion of the protein moving to the cell surface.

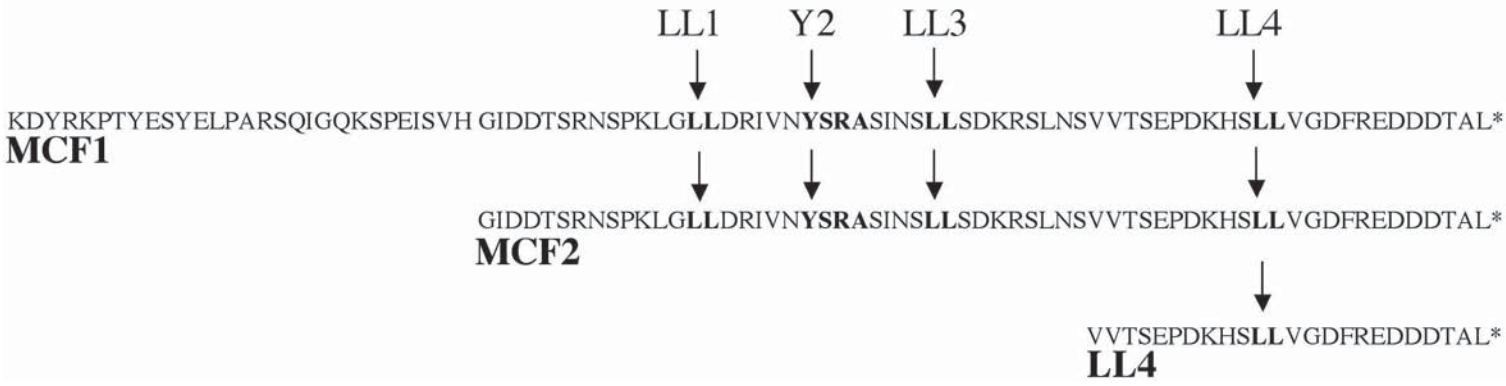

Fig. 9. C-terminus deletions of MNK. MCF1 (Menkes cytoplasmic fragment 1) contains the terminal 92 amino acids of MNK. This, along with the deleted fragment (MCF2), contains four putative internalisation motifs; three of the dileucine type, LL1, LL3, and LL4 and one of the tyrosine type, Y2 (YSRA). LL4 is the terminal 24-amino-acid fragment containing only 1 internalization type motif LL4 *(31)*.

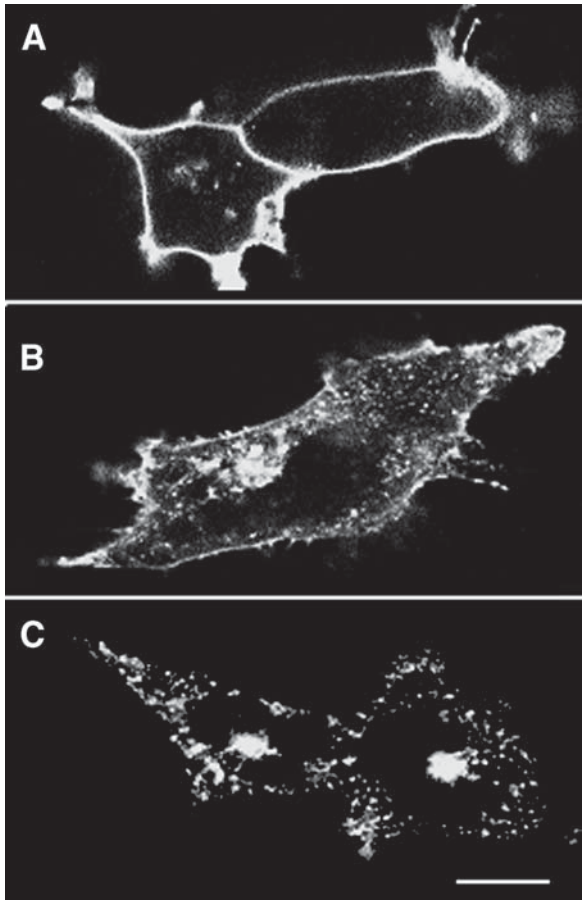

Fig. 10. A motif involved in plasma membrane internalization is contained within MCF1 and MCF2. The fusion proteins CD8-WT, CD8MCF1, and CD8MCF2 were transiently transfected into MRC5/V2 cells. The staining of CD8-WT is almost exclusively at the plasma membrane **(A)**; punctate staining indicative of internalization is observed with CD8MCF1 **(B)** and CD8MCF2 **(C)** *(31)*.

4.4. Identification of a Plasma Membrane Internalization Signal

In order to identify motif(s) involved in the return of MNK from the plasma membrane to the TGN, we focused on the C-terminus region of the protein (Menkes cytoplasmic fragment 1 [MCF1]). Many of the signals responsible for internalization of the proteins are located in the C-terminal cytoplasmic domains. MCF1 is 92 amino acids long and contains motifs similar to those involved in plasma membrane internalization (Fig. 9). These include the tyrosine and dileucine-based motifs. Deleted constructs containing the terminal 62 aa and 24 aa of MCF1 (MCF2 and LL4, respectively) were also generated. The cytoplasmic domain of CD8-WT was replaced with either MCF1, MCF2, or LL4 prior to transfection studies. The results of indirect immunofluorescence on transient transfections of CD8-WT, CD8MCF1, and CD8MCF2 in a human fibroblast cell line (MRC5/V2) are shown in Fig. 10.

These transient populations have been treated with cyclohexamide to inhibit new protein synthesis, prior to fixation and antibody staining. As expected, the staining of CD8-WT is almost exclusively at

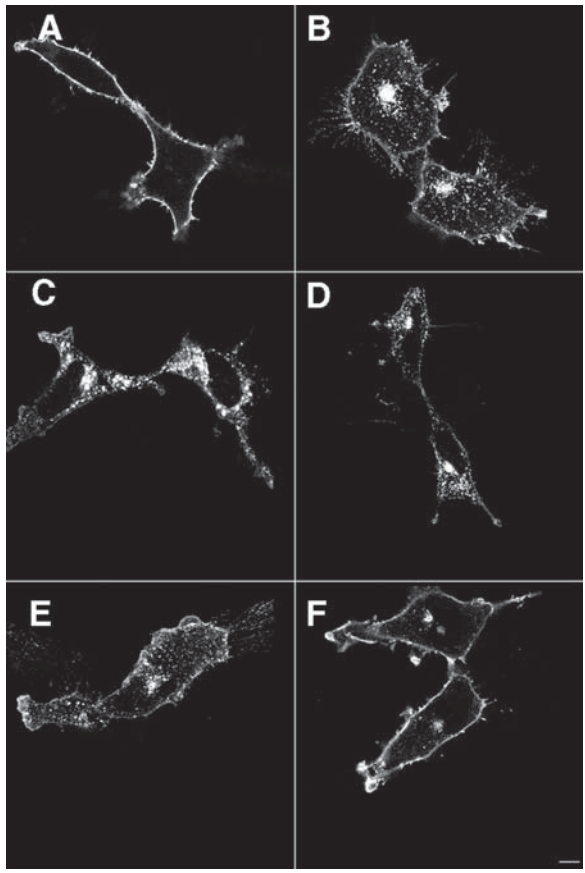

Fig. 11. A dileucine motif (LL4) is responsible for the internalization observed with the CD8/MNK fusion proteins. The putative internalization motifs in MCF2 (LL1, Y2, LL3, and LL4) were individually mutagenized, resulting in the constructs CD8ΔLL1, CD8ΔY2, CD8ΔLL3, and CD8ΔLL4, respectively. Plasma membrane staining was seen with CD8-WT **(A)** and punctate internalization patterns were seen with CD8MCF2 **(B)**, CD8ΔLL1 **(C)**, CD8ΔY2 **(D)**, and CD8ΔLL3 **(E)**, suggesting that each of these motifs were not involved in internalization. However, increased plasma membrane and no punctate staining was observed with CD8ΔLL4, suggesting that LL4 mediates internalization from the plasma membrane *(31)*.

the plasma membrane (Fig. 10A). However, both CD8MCF1 (Fig. 10B) and CD8MCF2 (Fig. 10C) show intense staining at a pericentriolar complex and punctate staining within the cell. This staining is characteristic of an internalization profile. The similarity of the CD8MCF1 and CD8MCF2 staining patterns imply that the motif responsible for this internalization is contained in both MCF1 and the smaller region MCF2. MCF2 contains four putative internalization motifs—three of the dileucine type (LL1, LL3, and LL4) and one tyrosine motif (Y2) (Fig. 9).

To determine which of these motifs is responsible for the internalization observed, site-directed mutagenesis was used to change each of the motifs. The dileucines were mutated to divalines and the tyrosine to a serine. This resulted in the following constructs: CD8ΔLL1, CD8ΔY2, CD8ΔLL3, and CD8ΔLL4. These constructs were transfected into human cell lines and the effect of these mutations on internalization monitored (Fig. 11).

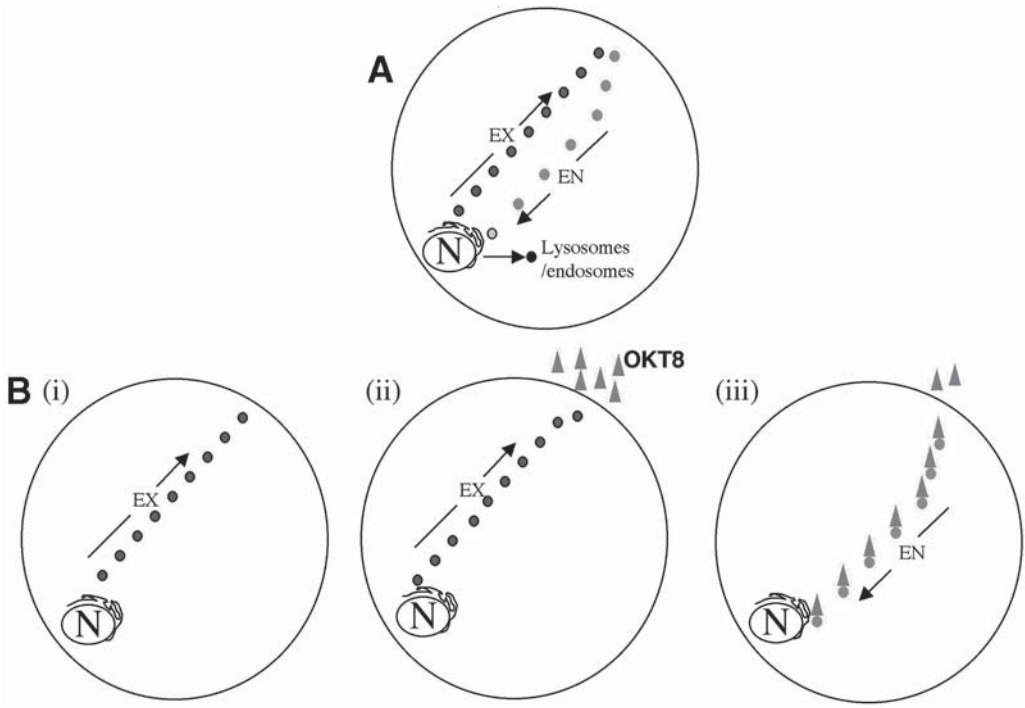

Fig. 12. Schematic representation detailing the endocytosis assay used in this assay. **(A)** At steady-state expression, all potential trafficking routes can be visualized. **(B)** (i) The CD8–MNK fusion protein trafficks by exocytosis (EX) to the plasma membrane. (ii) The cells in culture are bathed in the antibody OKT8 that recognizes and is allowed to bind to the lumenal domain of CD8. This domain lies exofacial to the cell. (iii) The fusion protein and bound antibody internalize by endocytosis (EN) and this route can be subsequently visualized by indirect immunofluorescence.

The expression patterns of CD8ΔLL1 (Fig. 11C), CD8ΔY2 (Fig. 11D), and CD8ΔLL3 (Fig. 11E) were almost identical to that of CD8MCF2 (Fig. 11B), demonstrating that the internalization profiles observed were independent of LL1, Y2, and LL3. However, the localization of CD8ΔLL4 (Fig. 11F) was primarily at the plasma membrane and very little, if any, punctate staining was present. This suggests that the dileucine motif, LL4, mediates the internalization of the CD8 fusion proteins. These experiments examine steady-state expression and it is therefore possible that the dileucine motif is important in the trafficking of the fusion protein to the plasma membrane. Therefore, mutation of this signal could prevent trafficking to the plasma membrane and therefore internalization.

To confirm the role of LL4 in internalization from the plasma membrane, an internalization assay was performed. This assay enables only the endocytic route to be observed (Fig. 12). Transient transfections of expression constructs CD8-WT (Fig. 13A), CD8MCF1 (Fig. 13B), and CD8LL4 (Fig. 13C) were analysed using this assay. The results clearly demonstrate that the punctate staining observed results from internalization from the plasma membrane and is mediated by LL4.

To determine which organelles in the endocytic pathway are used in this internalization, a series of colocalization experiments with known markers of the endocytic pathway were performed. These included CD63 (late endosomes), Lysotracker (lysosomes), transferrin receptor (recycling endosomes), and TGN46 (trans-Golgi network). Figure 14 compares the internalization profiles of CD8MCF1, the transferrin receptor containing recycling endosomes and TGN46. There is clearly a

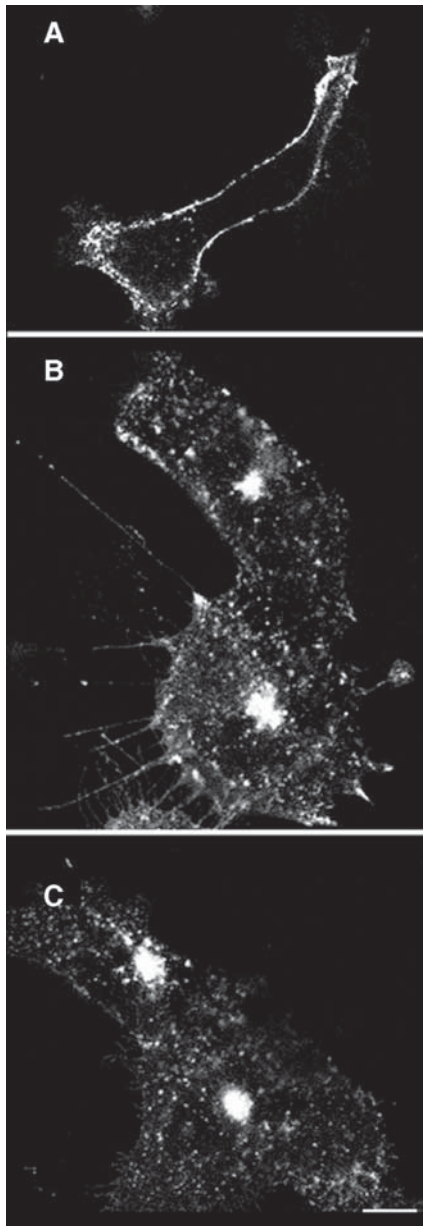

Fig. 13. Confirmation that the observed punctate patterning is a result of internalization from the plasma membrane. Expression patterns of CD8-WT, CD8MCF1, and CD8LL4 using the endocytosis assay described in Fig. 12. The CD8-WT signal remains at the plasma membrane **(A)**, whereas punctate staining is observed with both CD8MCF1 **(B)** and CD8LL4 **(C)**. This patterning arises as a result of internalization from the plasma membrane and confirms the role for LL4 in this internalization *(31)*.

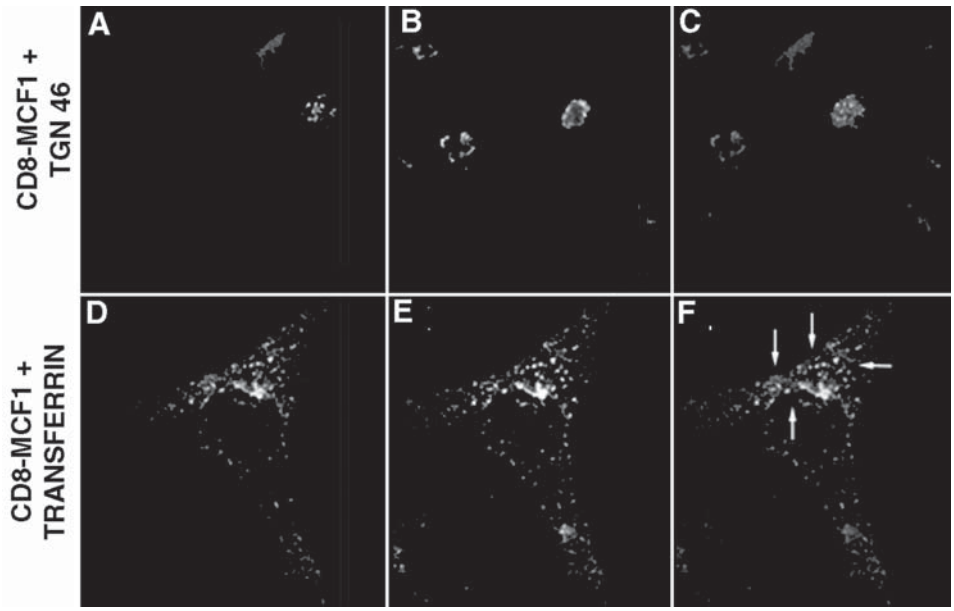

Fig. 14. Initial studies demonstrating that internalization of CD8MCF1 occurs via the transferrin receptor containing recycling endosomes. The staining pattern of the internalized CD8MCF1 was compared to that of TGN46 and the transferrin receptor. Although TGN46 **(A)** and CD8MCF1 **(B)** are resident in a similar region of the cell, there is no observable overlap between the two proteins **(C)**. The staining patterns of CD8MCF1 **(D)** and the transferrin receptor containing recycling endosomes **(E)** are almost identical. This is confirmed on overlapping of the two signals **(F)** *(31)*.

strong overlap with CD8MCF1 and the transferrin receptor (Fig. 14F), although no overlap with TGN46 (Fig. 14C).

To confirm this lack of overlap with TGN46, transfected cells were treated with colchicine. This drug disrupts the pericentriolar complex of the recycling endosomes and also the trans-Golgi network. On addition of colchicine, the accumulation of signal at the center of the cell in the recycling endosomes (Fig. 15B) and the juxtanuclear reticulum of the TGN (Fig. 15E) are no longer visible and the staining is now dispersed within the cell. On superimposition of the images, there is overlap between the dispersed signals of CD8MCF1 and the transferrin receptor (Fig. 15C), but no overlap between CD8MCF1 and TGN46 (Fig. 15F), indicating that CD8MCF1 is internalized through the recycling endosomes.

Although LL4 will internalize CD8 fusion proteins, it is possible that this is an artifactual signal that is activated by the reporter molecule system. To confirm that LL4 is a functional motif in MNK, LL4 was mutated in the full-length MNKMYC cDNA. The expression profile of this mutant protein was then observed. Although, at steady-state expression, MNK is primarily resident at the TGN, previous studies have shown that a small amount of MNK continously recycles between the TGN and plasma membrane. As the mutation of LL4 disrupts the internalization of MNK, there is a gradual accumulation of MNK at the plasma membrane (Fig. 16C,D) compared to the wild-type recombinant protein (Fig. 16A,B). This shows that the dileucine motif LL4 ($L_{1487}L_{1488}$ in the Menkes amino acid sequence) is essential for internalization from the plasma membrane and has been reported by other groups *(32)*.

These data provide us with two important pieces of trafficking information. First, the dileucine motif $L_{1487}L_{1488}$ mediates the internalization of MNK from the plasma membrane via the transferrin

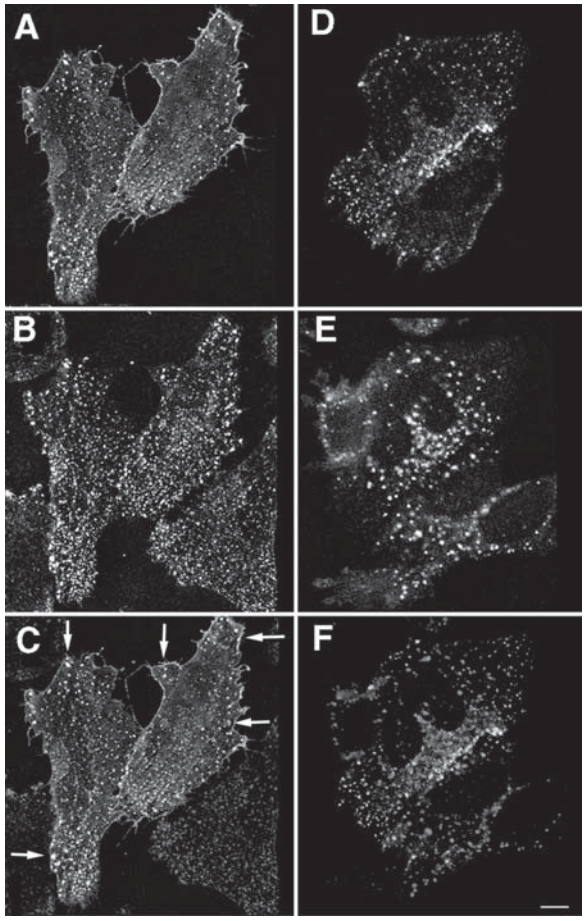

Fig. 15. Confirmation that LL4 mediates internalization via the recycling endosomes, but is not sufficient on its own to target the TGN. Transfected cells containing CD8MCF1 were treated with colchicine, which disrupts both the recycling endosomes and the TGN. After treatment with colchicine, significant colocalization is observed with CD8MCF1 **(A)** and the recycling endosomes **(B)**, shown in **(C)**. However, no colocalization **(F)** is observed with the disrupted patterns of CD8MCF1 **(D)** and the TGN **(E)** *(31)*.

containing recycling enzymes; second, $L_{1487}L_{1488}$ is not sufficient on its own to traffick the protein from the plasma membrane to the TGN *(12)*. Therefore, further sorting motifs are required. Current efforts are focusing on identifying these motifs.

5. SUMMARY

Over the last six years, since the discovery of the Menkes disease gene, considerable progress into understanding the mechanism behind the novel copper-induced cellular trafficking of MNK has been achieved. Trafficking studies of the Menkes protein suggests that there are at least three steps involved in the comprehensive trafficking of the MNK protein (Fig. 17). The first involves the binding of copper to the heavy-metal-binding repeats at the N-terminus, which may result in the disruption of the trans-Golgi retentive qualities of transmembrane domain 3. This disruption enables copper-bound MNK to traffick to the plasma membrane, presumably as a means to remove excess copper from the cell. Second, a dileucine motif enables the protein to enter the endocytic pathway on its return to the

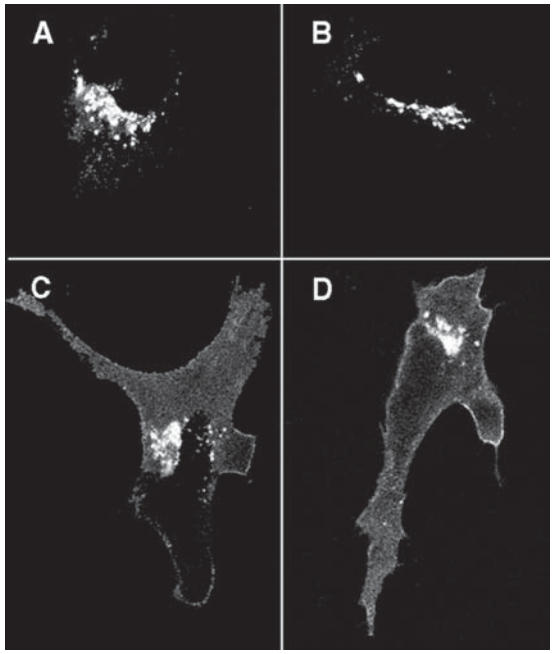

Fig. 16. LL4, ($L_{1487}L_{1488}$), mediates internalization of MNK. Although a small amount of protein is constituitively recycling between the TGN and plasma membrane, the protein expressed from the full-length cDNA (MNKMYC) is primarily resident at the TGN **(A, B)**. However, after 40 h, there is a gradual accumulation of MNKMYCΔLL4 **(C, D)**. This results from the inability of this mutant to internalize and is evidence that $L_{1487}L_{1488}$ is functional in MNK *(31)*.

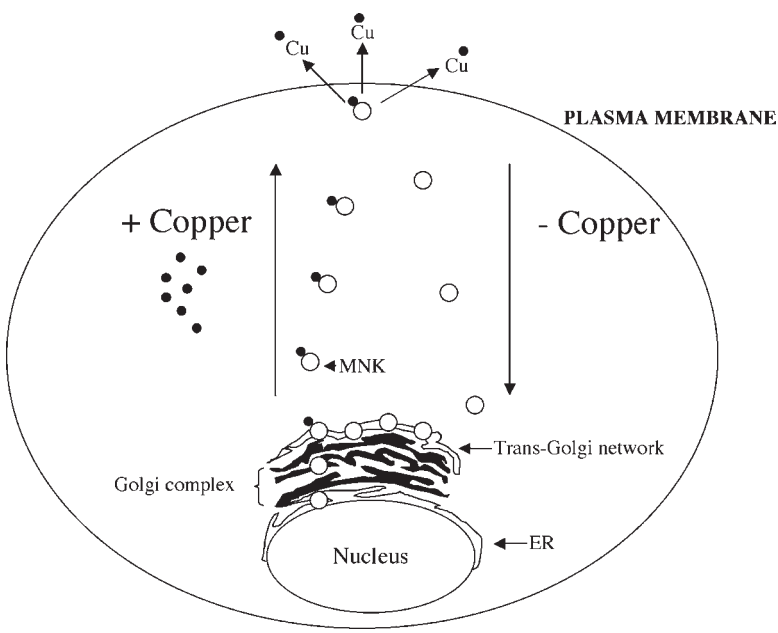

Fig. 17. Copper-induced relocalization of MNK. MNK is primarily resident at the TGN, retained by a signal within TM3. Copper binds to the N-terminal copper-binding domains, which may bring about a structural change within the protein, reducing the retentive qualities of TM3. MNK trafficks to the plasma membrane where it effluxes copper from the cell. On the removal of copper, MNK returns to the TGN via the recycling endosome, utilizing the dileucine motif ($L_{1487}L_{1488}$) at the C-terminus of the protein.

TGN, and, third, further unidentified motif(s) are required to sort the protein from the early/recycling endosomes to the TGN.

In conjunction with similar studies into the function and trafficking of WND, it will be important to build on these results and determine the similarity of both proteins in their functional properties. Depending on the outcome of these results, a suitable approach to therapy for Menkes disease may involve the upregulation or induction of expression of WND in tissues normally expressing MNK.

Menkes disease has become of great interest to researchers interested in the exocytic and endocytic trafficking of the cell and those investigating the mechansims behind copper homeostasis. Further studies will help to elucidate the mechanisms involved in this trafficking and, most importantly of all, may lead to novel therapies with which this fatal neurodegenerative disorder can be successfully treated.

ACKNOWLEDGMENTS

We thank Ian Goodyer and Rachael Daniels for helpful discussions, suggestions, and critical reading of the manuscript. This work was funded by the Wellcome Trust and A.P.M. is a Wellcome Trust Principal Research Fellow.

REFERENCES

1. Tonnesen, T., Kleijer, W. J., and Horn, N. (1991) Incidence of Menkes disease. *Hum. Genet.* **86,** 408–410.
2. Danks, D. M., Cartwright, E., Campbell, P. E., and Mayne, V. (1971) Is Menkes' syndrome a heritable disorder of connective tissue. *Lancet* **2,** 1089.
3. Horn, N., Tonnesen, T., and Tumer, Z. (1992) Menkes disease: an X-linked neurological disorder of the copper metabolism. *Brain Pathol.* **2,** 351–362.
4. Goka, T. J., Stevenson, R. E., Hefferan, P. M., and Howell, R. R. (1976) Menkes disease: a biochemical abnormality in cultured human fibroblasts. *Proc. Natl. Acad. Sci. USA* **73,** 604–606.
5. Horn, N. (1976) Copper incorporation studies on cultured cells for prenatal diagnosis of Menkes' disease. *Lancet* **1,** 1156–1158.
6. Tonnesen, T., Garrett, C., and Gerdes, A. M. (1991) High ^{64}Cu uptake and retention values in two clinically atypical Menkes patients. *J. Med. Genet.* **28,** 615–618.
7. Chan, W. Y., Garnica, A. D., and Rennert, O. M. (1978) Cell culture studies of Menkes kinky hair disease. *Clin. Chim. Acta* **88,** 495–507.
8. Chelly, J., Tumer, Z., Tonnesen, T., Petterson, A., Ishikawa-Brush, Y., Tommerup, N., et al. (1993) Isolation of a candidate gene for Menkes disease that encodes a potential heavy metal binding protein. *Nature Genet.* **3,** 14–19.
9. Mercer, J. F., Livingston, J., Hall, B., Paynter, J. A., Begy, C., Chandrasekharappa, S., et al. (1993) Isolation of a partial candidate gene for Menkes disease by positional cloning. *Nature Genet.* **3,** 20–25.
10. Vulpe, C., Levinson, B., Whitney, S., Packman, S., and Gitschier, J. (1993) Isolation of a candidate gene for Menkes disease and evidence that it encodes a copper-transporting ATPase. *Nature Genet.* **3,** 7–13.
11. La Fontaine, S. L., Firth, S. D., Camakaris, J., Englezou, A., Theophilos, M. B., Petris, M. J., et al. (1998) Correction of the copper transport defect of Menkes patient fibroblasts by expression of the Menkes and Wilson ATPases. *J. Biol. Chem.* **273,** 31,375–31,380.
12. Petris, M. J., Mercer, J. F., Culvenor, J. G., Lockhart, P., Gleeson, P. A., and Camakaris, J. (1996) Ligand-regulated transport of the Menkes copper P-type ATPase efflux pump from the Golgi apparatus to the plasma membrane: a novel mechanism of regulated trafficking. *EMBO J.* **15,** 6084–6095.
13. Dierick, H. A., Adam, A. N., Escara-Wilke, J. F., and Glover, T. W. (1997) Immunocytochemical localization of the Menkes copper transport protein (ATP7A) to the trans-Golgi network. *Hum. Mol. Genet.* **6,** 409–416.
14. Yamaguchi, Y., Heiny, M. E., Suzuki, M., and Gitlin, J. D. (1996) Biochemical characterization and intracellular localization of the Menkes disease protein. *Proc. Natl. Acad. Sci. USA* **93,** 14030–14,035.
15. La Fontaine, S., Firth, S. D., Lockhart, P. J., Brooks, H., Parton, R. G., Camakaris, J., et al. (1998) Functional analysis and intracellular localization of the human Menkes protein (MNK stably expressed from a cDNA construct in Chinese hamster ovary cells (CHO-K1). *Hum. Mol. Genet.* **7,** 1293–1300.
16. Francis, M. J., Jones, E. E., Levy, E. R., Ponnambalam, S., Chelly, J., and Monaco, A. P. (1998) A Golgi localization signal identified in the Menkes recombinant protein. *Hum. Mol. Genet.* **7,** 1245–1252.
17. Goodyer, I. D., Jones, E. E., Monaco, A. P., and Francis, M. J. (1999) Characterization of the Menkes protein copper-binding domains and their role in copper-induced protein relocalization. *Hum. Mol. Genet.* **8,** 1473–1478.
18. DiDonato, M. and Sarkar, B. (1997) Copper transport and its alterations in Menkes and Wilson diseases. *Biochim. Biophys. Acta* **1360,** 3–16.
19. Lutsenko, S., Petrukhin, K., Cooper, M. J., Gilliam, C. T., and Kaplan, J. H. (1997) N-terminal domains of human

copper-transporting adenosine triphosphatases (the Wilson's and Menkes disease proteins) bind copper selectively in vivo and in vitro with stoichiometry of one copper per metal-binding repeat. *J. Biol. Chem.* **272,** 18,939–18,944.
20. Harrison, M. D., Meier, S., and Dameron, C. T. (1999) Characterization of copper-binding to the second sub-domain of the Menkes protein ATPase (MNKr2). *Biochim. Biophys. Acta* **1453,** 254–260.
21. Gitschier, J., Moffat, B., Reilly, D., Wood, W. I., and Fairbrother, W. J. (1998) Solution structure of the fourth metal-binding domain from the Menkes copper-transporting ATPase. *Nat. Struct. Biol.* **5,** 47–54.
22. Yuan, D. S., Stearman, R., Dancis, A., Dunn, T., Beeler, T., and Klausner, R. D. (1995) The Menkes/Wilson disease gene homologue in yeast provides copper to a ceruloplasmin-like oxidase required for iron uptake. *Proc. Natl. Acad. Sci. USA* **92,** 2632–2636.
23. Stearman, R., Yuan, D. S., Yamaguchi-Iwai, Y., Klausner, R. D., and Dancis, A. (1996) A permease-oxidase complex involved in high-affinity iron uptake in yeast. *Science* **271,** 1552–1557.
24. Payne, A. S. and Gitlin, J. D. (1998) Functional expression of the Menkes disease protein reveals common biochemical mechanisms among the copper-transporting P-type ATPases. *J. Biol. Chem.* **273,** 3765–3770.
25. Forbes, J. R. and Cox, D. W. (1998) Functional characterization of missense mutations in ATP7B: Wilson disease mutation or normal variant? *Am. J. Hum. Genet.* **63,** 1663–1674.
26. Forbes, J. R., Hsi, G., and Cox, D. W. (1999) Role of the copper-binding domain in the copper transport function of ATP7B, the P-type ATPase defective in Wilson disease. *J. Biol. Chem.* **274,** 12,408–12,413.
27. Pufahl, R. A., Singer, C. P., Peariso, K. L., Lin, S. J., Schmidt, P. J., Fahrni, C. J., Culotta, V. C., et al. (1997) Metal ion chaperone function of the soluable Cu(I) receptor Atx1. *Science* **278,** 853–856.
28. Strausak, D., La Fontaine, S., Hill, J., Firth, S. D., Lockhart, P. J., and Mercer, J. F. (1999) The role of GMXCXXC metal binding sites in copper-induced redistribution of the Menkes protein. *J. Biol. Chem.* **274,** 11,170–11,177.
29. Teasdale, R. D., D'Agostaro, G., and Gleeson, P. A. (1992) The signal for Golgi retention of bovine beta 1,4-galactosyltransferase is in the transmembrane domain. *J. Biol. Chem.* **267,** 13,113.
30. Qi, M. and Byers, P. H. (1998) The signal for Golgi retention of bovine beta 1,4-galactosyltransferase is in the transmembrane domain. *Hum. Mol. Genet.* **7,** 465–469.
31. Francis, M. J., Jones, E. E., Levy, E. R., Martin, R. L., Ponnambalam, S., and Monaco, A. P. (1999) The Menkes protein (ATP7A; MNK) cycles via the plasma membrane both in basal and elevated extracellular copper using a C-terminal dileucine endocytic signal. *J. Cell Sci.* **112**, 1721–1732.
32. Petris, M. J. and Mercer, J. F. (1999) Identification of a dileucine motif within the C terminus domain of the Menkes disease protein that mediates endocytosis from the plasma membrane. *Hum. Mol. Genet.* **8,** 2107–2115.

13

Intracellular Copper Transport and ATP7B, the Wilson's Disease Protein

Kunihiko Terada and Toshihiro Sugiyama

1. INTRODUCTION

Copper is an essential trace metal for all living organisms because this metal serves as a cofactor for activating numerous enzymes critical for homeostasis. However, when copper exceeds the cellular needs, it is toxic through the production of highly reactive hydroxyl radicals that have deleterious effects on cellular components, including destabilization of plasma membranes and lysosomal membranes, disturbance of mitochondrial respiration, depletion of glutathione reserves, and damage of nucleic acids *(1)*. To prevent the accumulation of copper to the toxic level, cells are provided regulatory mechanisms that maintain the balance of intracellular copper.

Recently, a number of proteins that play significant roles in intracellular copper homeostasis were identified in various species, ranging from bacteria to humans. These proteins can be classified into copper chaperones *(2,3)* and copper transporters *(4)* (Table 1). Copper chaperones deliver copper to specific cytoplasmic compartments and target proteins, preventing inappropriate interactions of copper with other cellular components *(3)*. Members of copper chaperones include CopZ in *Enterococcus hirae*, Atx1, CCS, and Cox17 in yeast, HAH1, hCCS, and hCOX17 in humans *(3,5)*. On the other hand, copper transporters, which are integral membrane proteins, mediate cellular uptake and export of copper from cells *(4)*. Copper uptake is carried out by CopA in *E. hirae*, Ctr1 in yeast, and hCTR1 in humans *(4,5)*. The cytosolic copper taken up by these transporters binds to copper chaperones and is subsequently delivered to the secretory pathways by CopB in *E. hirae*, Ccc2 in yeast, Cua1 in *Caenorhabditis elegans*, and ATP7A and ATP7B in humans *(5,6)*. The majority of copper transporters, except for Ctr1 and hCTR1, belongs to the class of heavy-metal-transporting P-type ATPases that translocates various cations across membranes in a ATP-dependent manner *(4,7)*. However, Ctr1 and hCTR1, which are responsible for copper uptake in eukaryotes, are not copper ATPases, because they miss the ATP-binding domain, characteristic of P-type ATPases *(5)*.

Studies using the yeast Δccc2 strain have shown that Ccc2 delivers copper to Fet3 that resides in the secretory pathway, and this process is one of the key steps for high-affinity iron uptake systems indispensable for yeast growth *(8)*. In humans, two inherited diseases, Menkes disease and Wilson's disease, are the results of abnormal copper metabolism. Menkes disease, an X-linked disorder, is characterized by the systemic deficiency of copper resulting from the entrapment of this metal mainly in intestinal cells *(9)*. By contrast, Wilson's disease, an autosomal recessive disorder, is caused by copper toxicity that occurs primarily in the liver *(10)*. Interestingly, both disease states develop as

From: Handbook of Copper Pharmacology and Toxicology
Edited by: E. J. Massaro © Humana Press Inc., Totowa, NJ

Table 1
Copper Chaperones and Copper Transporters

	Bacteria	*Yeast*	*Human*
Copper chaperones	CopZ	Atx1	HAH1
		CCS	hCCS
		Cox17	hCOX17
Copper transporters			
P-type ATPases	CopA	Ccc2	ATP7A
	CopB		ATP7B
Others		Crt1	hCTR1
		Ctr3	

consequences of defective export of copper from intestinal cells in Menkes disease and from hepatocytes in Wilson's disease. Recent studies have revealed that copper ATPases play a central role in export pathways for copper *(11–14)*. Indeed, the disease-specific mutations, reported within the genes encoding ATP7A in Menkes disease and ATP7B in Wilson's disease, lead to the production of defective proteins *(11,15)*.

In this chapter, we first introduce Wilson's disease and its rodent models and show their contribution to our understanding of hepatic copper metabolism. Then, we discuss the functional features of ATP7B protein and its roles in hepatic copper transport.

2. WILSON'S DISEASE AND ITS RODENT MODELS

Wilson's disease is the consequence of toxic accumulation of copper initially in the liver and later in extrahepatic sites *(10)*. This disorder is inherited in an autosomal recessive manner and is present in approx 1 in 30,000 individuals in all populations. The hepatic accumulation of copper is the result of its reduced biliary excretion and disturbed incorporation into ceruloplasmin, a major copper-binding protein containing more than 90% of copper in plasma. Hepatic copper at toxic levels induces hepatocellular injury, and the released copper from the affected liver causes extrahepatic toxicity in the brain, kidneys, and eyes. The gene responsible for the disease was identified in 1993 by positional cloning and linkage disequilibrium analysis *(16,17)* and by searching for genes with homology to *ATP7A*, the gene responsible for Menkes disease *(18,19)*. The identified gene was localized to chromosome 13 and encodes a copper-transporting P-type ATPase, ATP7B. The presence of numerous disease-specific mutations, including point mutations, deletions, frame shifts, and splice errors within the gene, indicates that *ATP7B* is the correct gene for Wilson's disease *(17,20,21)*.

The Long–Evans Cinnamon (LEC) rat with a distinctive cinnamon-color coat is derived from Long–Evans agouti rats. Spontaneous hepatitis with jaundice occurs around 4 mo of age in this inbred strain of rats. This mutation, first noted in 1983, is inherited in an autosomal recessive manner. Initial studies for the LEC rat were reported in a monograph *(22)*. Before the discovery of the association of excess copper in the liver of LEC rats, interest in this strain focused on its propensity for the spontaneous development of hepatitis and liver cancer. Further investigations revealed an excessive accumulation of copper in the liver and a remarkable decrease in serum ceruloplasmin (CPN) activity in the LEC rat *(22–24)*. The similarity of these clinical features to those of Wilson's disease led to the notion that the LEC rat is an animal model of this disorder. Subsequent to the identification of *ATP7B* gene, *atp7b*, the rat gene homologous to *ATP7B*, was also cloned. A partial deletion at the 3' end of the gene was found in the LEC rat *(25)*. These molecular studies, as well as biochemical studies showing similar abnormalities in copper metabolism *(22–24,26)* proved that the LEC rat is a rodent model for Wilson's disease.

Table 2
Comparison of Wilson's Disease, LEC Rat, and Toxic Milk Mouse

	Wilson's disease	*LEC rat*	*Toxic milk mouse*
Inheritance	AR[a]	AR	AR
Gene	*ATP7B*	Rat *atp7b*	Mouse *atp7b*
Clinical			
Hepatitis	Yes	Yes	Yes
Liver cancer	Rare	Yes	Unknown
Laboratory findings			
Liver Cu	↑	↑	↑
Biliary Cu	↓	↓	Unknown
Ceruloplasmin activity	↓	↓	↓

[a]AR = autosomal recessive.

The laboratory findings including hepatic copper accumulation, reduced biliary copper excretion, reduced level of plasma copper, and a remarkable decrease of serum CPN activity are common for both Wilson's disease and LEC rat. Hepatocellular injury caused by copper toxicity is the major manifestation in both. Although neurological abnormalities are the onset in approx 40% of patients with Wilson's disease, these are rarely observed in the LEC rat. In addition, Kayser–Fleischer rings, deposits of copper in the cornea that occur in almost all neurologically affected patients with Wilson's disease, have not been reported in the LEC rat. Although a very few patients of Wilson's disease are known to develop liver cancer, more than 90% of the LEC rats, which survive the early phase of liver injury, develop liver cancers after 1 yr of age. The precise mechanism of carcinogenesis in the LEC rat is still uncovered, although the production of hydroxyl radicals by copper with subsequent damage to DNA is strongly suggested to trigger this process.

The toxic milk mouse, inherited in an autosomal recessive manner, is known to occur accumulation of hepatic copper and decrease in serum CPN activity, however, reduced excretion of biliary copper is not reported *(9)*. In addition, the production of copper-deficient milk by affected dams results in the death of pups *(9)*. The identification of causative mutation in murine *Atp7b* have proved that the toxic milk mouse is a true model of Wilson's disease *(27)*.

The clinical features manifested by Wilson's disease, the LEC rat, and the toxic milk mouse are summarized in Table 2.

3. EXPRESSION AND STRUCTURAL FEATURES OF ATP7B

The *ATP7B* gene is about 80 kb and contains 21 exons. Its transcript is approx 7.5 kb in size and expressed predominantly in liver, kidney, and placenta *(17,18,28)*. Alternative spliced forms of the gene have been identified in brain, kidney, and placenta *(28)*. Of these, the identification of pineal gland night-specific ATPase (PINA), expressed in pinealocytes, suggests its involvement in rhythmic copper metabolism in the pineal gland *(29)*. ATP7B protein is synthesized as a single-chain intracellular membrane protein of 165 kDa in human and rat liver, and its expression is regulated developmentally *(30)*. Based on the deduced amino acid sequence, ATP7B protein consists of 1465 amino acids and is predicted to be a copper-transporting P-type ATPase. ATP7B shows 54% amino acid identity with ATP7A, another mammalian copper-transporting P-type ATPase defective in Menkes disease *(28)*. This protein displays 82% identity with Atp7b protein, the rat counterpart of ATP7B. Each functional domain is well conserved in these proteins except that Atp7b lacks the fourth metal-binding domain. In the LEC rat, it is reported that approx 900 base pairs at the 3' end of *atp7b* is partially deleted *(25)* and expression of Atp7b is absent in the liver *(30)*.

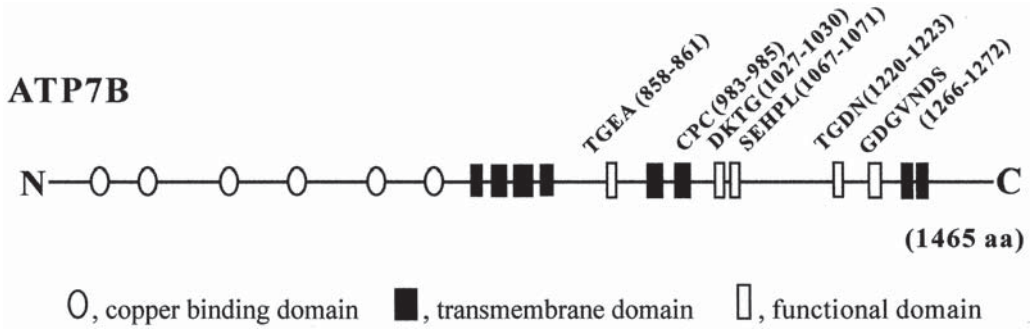

Fig. 1. Primary structure of ATP7B protein with key features. Human ATP7B consists of 1465 amino acids. The general features of P-type ATPases included in ATP7B are TGEA (phosphatase domain), DKTGT (phosphorylation domain), TGDN (ATP binding domain), and MVGDGVNDSP that connects the ATP-binding domain to the transmembrane segment. The unique features of ATP7B are six copper-binding sites, CPC and SEHPL involved with cation translocation, and eight transmembrane segments. The CPC domain locates within the sixth transmembrane region. Numbers in parentheses indicate amino acid positions of the functional domains.

P-Type ATPases translocate a variety of cations across cell membranes. This class of enzymes is characterized by formation of a covalent phosphorylated intermediate in their reaction cycle by the transfer of γ-phosphate of ATP to an aspartic acid residue of the protein and is inhibited by vanadate *(31)*. General features of P-type ATPases present in ATP7B are the TGEA motif (phosphatase domain), the DKTGT motif (phosphorylation domain), the TGDN motif (ATP-binding domain), and the sequence M*X*GDG*X*ND*X*P that connects the ATP-binding domain to the transmembrane segment. ATP7B is further classified as a heavy-metal-transporting P-type ATPase, which pumps copper, cadmium, or silver. The characteristic features of this class of ATPases are one to six repeated motifs for metal binding (GMTC*XX*C) at the N-terminus of the molecule, the CPC motif in the sixth transmembrane region, the SEHPL motif, and eight transmembrane segments *(3,7)*. A single copy of the GMTC*XX*C motif is found in bacterial CopA, two in yeast Ccc2, three in nematode CUA-1, five in rat Atp7b, and six in ATP7A and ATP7B *(3,6)*. The metal-binding motifs of ATP7B are specific for copper, and stoichiometric analysis showed that 6 mol of copper were bound to 1 mol of the N-terminus containing the six metal-binding regions of the protein *(32)*. The metal-binding motifs in ATP7A and ATP7B are shown to play essential roles in copper transport by the complementation of yeast Ccc2 *(11,15,33)*; however, each domain is not functionally equivalent. The CPC and SEHPL motifs of heavy-metal-transporting ATPases are assumed to be involved with metal translocation across membranes. This is supported by recent observations that mutations introduced into the CPC or SEHPL result in loss of ATP7B function in copper transport *(12,15)*. This class of proteins is called P_1-ATPases or CPx-type ATPases *(3,7)*. The primary structure of ATP7B is shown in Fig. 1.

4. INTRACELLULAR LOCALIZATION OF ATP7B

To accomplish their function, cellular proteins have to locate properly at specific intracellular sites. New information concerning the intracellular localization of ATP7B has emerged from studies with immunofluorescence and subcellular fractionation. These studies reveal that ATP7B is localized to the trans-Golgi network and to post-Golgi compartments, the latter likely being endosomes, in human hepatoblastoma cells and rat hepatocytes under basal conditions *(12,30,34–36)*. Other studies suggest the presence of ATP7B in mitochondria and at the canalicular pole of hepatocytes *(37,38)*. These results remain controversial and further studies are needed to resolve uncertainties.

ATP7B is known to behave differently depending on intracellular levels of copper. Exposure to copper induces a rapid movement of ATP7B from the Golgi compartments to as yet undefined post-Golgi vesicles *(12)*. This phenomenon is reversible and does not require *de novo* synthesis of protein. Rapid trafficking of ATP7A from the trans-Golgi network to the plasma membrane induced by copper has been reported *(39)*. Evidently, recycling of ATP7B between the trans-Golgi network and the post-Golgi compartments is regulated by the copper concentration, favoring the efficient discharge of cellular copper into the excretory compartments, yet the precise mechanism of the unique copper-induced protein trafficking remain to be determined.

5. BIOLOGICAL FUNCTION OF ATP7B

The properties of ATP7B described earlier strongly suggest that the protein plays a significant role in the intracellular transport of hepatic copper. The major export pathways for copper from hepatocytes consist of the secretion into blood following its incorporation into ceruloplasmin and the excretion into bile. The reconstitution of copper transport by the introduction of *ATP7B* cDNA into a yeast strain lacking Ccc2 and the subsequent reconstitution of copper incorporation into the copper protein Fet3 provide supporting evidence for the role of ATP7B in copper transport and ceruloplasmin biosynthesis *(12)*.

To further investigate the role of ATP7B in copper transport in vivo, *ATP7B* cDNA was introduced into the LEC rat by adenoviral-mediated gene delivery *(13)*. Transgene expression was observed in the liver and ATP7B was found to localize to the Golgi apparatus of hepatocytes. Secretion of holoCPN, the copper-bound form of the protein, was detected after viral infusion. These data indicate that ATP7B functions in copper export coupled with CPN synthesis and that the Golgi apparatus is the likely site for the incorporation of copper into CPN *(40,41)*. In addition, the elevated levels of copper content in the hepatic lysosomal fractions and the increased biliary excretion of copper were observed after the introduction of ATP7B, suggesting that ATP7B participates in the excretory pathway of copper, involving a vesicular transport of copper to lysosomes for delivery to the apical, canalicular membrane *(14,42)*. Together, these data provide the notion that ATP7B translocates copper into the Golgi compartments and into both the secretory and the excretory pathways for copper, thereby regulating the homeostasis of copper in liver cells.

Mutational analyses also support the requirement of ATP7B in hepatic copper transport, which explains the pathogenesis of Wilson's disease. Mutations of H1069Q in the SEHPL motif or N1270S in the M*X*GDG*X*ND*X*P sequence, reported in the patients, were shown to lose their copper-transport function by in vitro studies *(12,15,43)*, leading to a disturbance of intracellular copper transport in the disease. In addition, mutations introduced into the critical sites in ATP7B, such as the DKTGT/S motif and the CPC motif, were also found to alter the copper-transport function of ATP7B *(12,15)*. Regarding the copper-binding domains, although these domains are essential for copper transport, the sixth domain is sufficient to manifest the function *(15,33)*. These observations imply that intact ATP7B is necessary for regulating copper homeostasis in the liver.

In the intracellular trafficking of copper, ATP7B may act as a gate that controls the copper flow through the secretory and excretory pathways in liver.

6. COPPER TRANSPORT AND ATP7B

Liver is the main site of copper metabolism in the body, because mobilization of copper into the systemic circulation and into bile take place via hepatocytes.

Only half of dietary copper ingested, 0.8–1.5 mg/d, is absorbed from the upper intestine *(1)*. This process is probably mediated by hCTR1, identified by searching for proteins with homology to genes products associated with copper uptake in yeast *(44)*. The yeast Ctr1, identified through its effects on iron metabolism, was found to be necessary for the high-affinity copper transport *(45)*, and hCTR1 indeed replaced the function of Ctr1 in yeast *(44)*. hCTR1 is predicted to be a membrane-associated

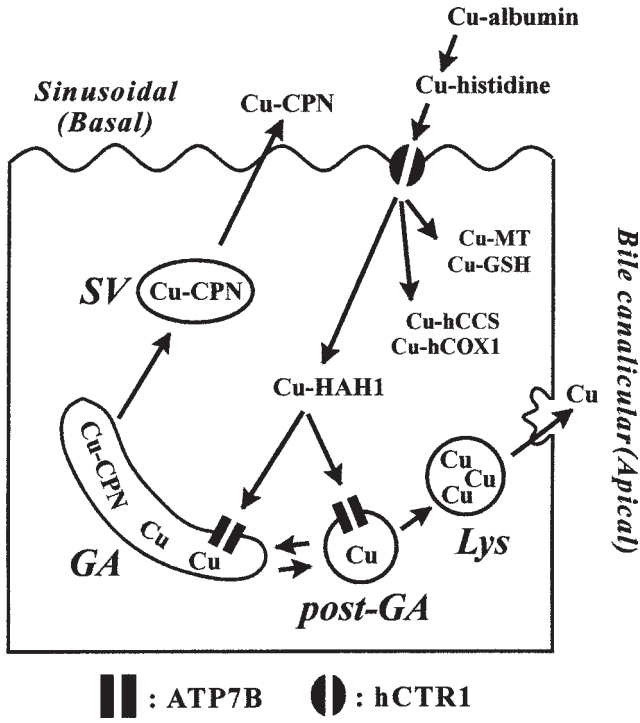

Fig. 2. Model of copper transport associated with ATP7B in hepatocyte. In the portal blood flow, copper is mostly bound with albumin via its N-terminal tripeptide (Asp-Ala-His) and then taken up into hepatocytes as a copper–histidine complex. This hepatic uptake is mediated by hCTR1. Subsequently, the cytosolic copper forms a complex with glutathione, metallothionein, or the copper chaperone. The copper chaperones hCOX17 and hCCS deliver copper to cytochrome-*c* oxidase in the mitochondria and the cytoplasmic copper/zinc superoxide dismutase, respectively. HAH1 distributes copper to ATP7B that resides in the trans-Golgi (GA) or in the post-Golgi compartments (post-GA), likely endosomes, and then copper is transported into these organelles by ATP7B. In the secretory pathway, after ceruloplasmin (CPN) incorporates copper at the Golgi, holoCPN (Cu-CPN) is secreted into blood through secretory vesicles (SV). In the excretory pathway, copper in the trans-Golgi or in the post-Golgi is excreted into bile through lysosomes (Lys). The recycling of ATP7B between the trans-Golgi and the post-Golgi is regulated by intracellular copper concentration. Under the basal condition, ATP7B resides in the trans-Golgi; however, it rapidly moves to the post-Golgi compartments when the level of intracellular copper is elevated.

transporter protein detectable in all human tissues, including intestine and liver *(44)*. Normally, the intestinal cells release copper under regulation of ATP7A, except in patients with Menkes disease in whom intestinal cells entrap copper because of defective ATP7A *(9)*. The released copper is mostly bound with albumin via its N-terminal tripeptide (Asp-Ala-His) in the portal blood, and then taken up into hepatocytes as a copper–histidine complex *(9)*. This hepatic uptake is also mediated by hCTR1. Subsequently, the cytosolic copper forms a complex with glutathione, metallothionein, or copper chaperone *(1,5)*. The copper chaperones hCOX17 and hCCS deliver copper to cytochrome-*c* oxidase in the mitochondria and the cytoplasmic copper/zinc superoxide dismutase, respectively *(4,5)*. Based on structural and functional similarities to the yeast Atx1, we assume that HAH1 distributes copper to ATP7B *(46)*. Then, copper is transported into the export pathways by ATP7B at the Golgi or post-Golgi compartments. In the export pathways, copper is secreted into blood, following its incorpora-

tion into CPN, and is excreted into bile through lysosomes. The latter process is more important for maintaining the hepatic concentration of copper, because the bile mobilizes three-quarters of the absorbed copper per day *(1)*. A unified model of hepatic copper transport is illustrated in Fig. 2.

7. CONCLUSIONS AND PERSPECTIVES

The identification of copper chaperones and copper transporters from bacteria to humans has provided useful information with respect to copper metabolism. Searching for novel proteins involved in these processes will help us resolve the various cellular pathways for copper transport. The characterization of two human copper transporters has greatly contributed to our understanding of the pathophysiology of Wilson's disease and Menkes disease. Although in vitro and in vivo studies have revealed the essential role of ATP7B in hepatic copper transport, further investigations are required for defining the precise localization of ATP7B and the physiological role of the copper-dependent recycling of ATP7B. In addition, although a ligand-transfer model was proposed recently, the mechanisms for copper transfer between ATP7B and chaperones have not been tested experimentally. Further research on these issues should contribute to a better understanding of the intracellular trafficking of copper and copper homeostasis in the body.

ACKNOWLEDGMENTS

We thank Dr. Irmin Sternlieb and Dr. Michael L. Schilsky for critical reading of the manuscript.

REFERENCES

1. Sternlieb, I. (1994) Copper and zinc, in *The Liver*: *Biology and Pathobiology*, 3rd ed. (Arias, I. M., Boyer, J. L., Fausto, N., Jakoby, W. B., Schachter, D. A., and Shafritz, D. A., eds.), Raven, New York, pp. 585–596.
2. Lippard, S. J. (1999) Free copper ions in the cell? *Science* **284**, 748–749.
3. Solioz, M. and Vulpe, C. (1996) CPx-type ATPases: a class of P-type ATPases that pump heavy metals. *Trends Biochem. Sci.* **21**, 237–241.
4. Harrison, M. D., Jones, C. E., Solioz, M., and Dameron, C. T. (2000) Intracellular copper routing: the role of copper chaperones. *Trends Biochem. Sci.* **25**, 29–32.
5. Pena, M. M. O., Lee, J., and Thiele, D. J. (1999) A delicate balance: homeostatic control of copper uptake and distribution. *J. Nutr.* **129**, 1251–1260.
6. Sambongi, Y., Wakabayashi T., Yoshimizu, T., Omote, H., Oka, T., and Futai, M. (1997) *Caenorhabditis elegans* cDNA for a Menkes/Wilson disease gene homologue and its function in a yeast *CCC2* gene deletion mutant. *J. Biochem.* **121**, 1169–1175.
7. Lutsenko, S. and Kaplan, J. H. (1995) Organization of P-type ATPases: significance of structural diversity. *Biochemistry* **34**, 15,607–15,613.
8. Yuan, D. S., Stearman, R., Dancis, A., Dunn, T., Beeler, T., and Klausner, R. D. (1995) The Menkes/Wilson disease gene homologue in yeast provides copper to a ceruloplasmin-like oxidase required for iron uptake. *Proc. Natl. Acad. Sci. USA* **92**, 2632–2636.
9. Danks, D. M. (1995) Disorders of copper transport, in *The Metabolic and Molecular Bases of Inherited Disease*, 7th ed. (Scriver, C. R., Beaudet, A. L., Sly, W. S., and Valle, D., eds.), McGraw-Hill, New York, pp. 2211–2235.
10. Scheinberg, I. H. and Sternlieb, I. (1984) *Wilson's Disease*. Major Problems in Internal Medicine, Vol. 23 (Smith Jr., L. H. ed.), W.B. Saunders, Philadelphia.
11. Payne, A. S. and Gitlin, J. D. (1998) Functional expression of the Menkes disease protein reveals common biochemical mechanisms among the copper-transporting P-type ATPases. *J. Biol. Chem.* **273**, 3765–3770.
12. Hung, I. H., Suzuki, M., Yamaguchi, Y., Yuans, D. S., Klausner, R. D., and Gitlin, J. D. (1997) Biochemical characterization of the Wilson disease protein and functional expression in the Yeast *Saccharomyces cerevisiae*. *J. Biol. Chem.* **272**, 21,461–21,466.
13. Terada, K., Nakako, T., Yang, X. L., Iida, M., Aiba, N., Minamiya, Y., et al. (1998) Restoration of holoceruloplasmin synthesis in LEC rat after infusion of recombinant adenovirus bearing WND cDNA. *J. Biol. Chem.* **273**, 1815–1820.
14. Terada, K., Aiba, N., Yang, X. L., Iida, Y., Nakai, M., Miura, N., et al. (1998) Biliary excretion of copper in LEC rat after introduction of copper transporting P-type ATPase, ATP7B. *FEBS Lett.* **448**, 53–56.
15. Iida, M., Terada, K., Sambongi, Y., Wakabayashi, T., Miura, N., Koyama, K., et al. (1998) Analysis of functional domains of Wilson disease protein (ATP7B) in *Saccharomyces cerevisiae*. *FEBS Lett.* **428**, 281–285.
16. Petrukhin, K., Fischer, S. G., Pirastu, M., Tanzi, R. E., Chernov, I., Devoto, M., et al. (1993) Mapping, cloning and genetic characterization of the region containing the Wilson disease gene. *Nature Genet.* **5**, 338–343.
17. Tanzi, R. E., Petrukhin, K., Chernov, I., Pellequer, J. L., Wasco, W., Ross, B., et al. (1993) The Wilson disease gene is a copper transporting ATPase with homology to the Menkes disease gene. *Nature Genet.* **5**, 344–350.

18. Bull, P. C., Thomas, G. R., Rommens, J. M., Forbes, J. R., and Cox, D. W. (1993) The Wilson disease gene is a putative copper transporting P-type ATPase similar to the Menkes gene. *Nature Genet.* **5**, 327–337.
19. Yamaguchi, Y., Heiny, M. E., and Gitlin, J. D. (1993) Isolation and characterization of a human liver cDNA as a candidate gene for Wilson disease. *Biochem. Biophys. Res. Commun.* **197**, 271–277.
20. Thomas, G. R., Forbes, J. R., Roberts, E. A., Walshe, J. M., and Cox, D. W. (1995) The Wilson disease gene: spectrum of mutations and their consequences. *Nature Genet.* **9**, 210–217.
21. Shah, A. B., Chernov, I., Zhang, H. T., Ross, B. M., Das, K., Lutsenko, S., et al. (1997) Identification and analysis of mutations in the Wilson disease gene (*ATP7B*): population frequencies, genotype-phenotype correlation, and functional analyses. *Am. J. Hum. Genet.* **61**, 317–328.
22. Mori, M, Yoshida, M. C., Takeichi, N., and Taniguchi, N., eds. (1993) *The LEC Rat, a New Model for Hepatitis and Liver Cancer.* Springer-Verlag, Tokyo.
23. Li, Y., Togashi, Y., Sato, S., Emoto, T., Kang, J. H., Takeichi, N., et al. (1991) Spontaneous hepatic copper accumulation in Long–Evans Cinnamon rats with hereditary hepatitis. *J. Clin. Invest.* **87**, 1858–1861.
24. Ono, T., Abe, S., and Yoshida, M. C. (1991) Hereditary low level of plasma ceruloplasmin in LEC rats associated with spontaneous development of hepatitis and liver cancer. *Jpn. J. Cancer Res.* **82**, 486–489.
25. Wu, J., Forbes, J. R., Chen, H. S., and Cox, D. W. (1994) The LEC rat has a deletion in the copper transporting ATPase gene homologous to the Wilson disease gene. *Nature Genet.* **7**, 541–545.
26. Suzuki, M. and Aoki, T. (1994) Impaired hepatic copper homeostasis in Long–Evans Cinnamon rats: reduced biliary excretion of copper. *Pediatr. Res.* **35**, 598–601.
27. Theophilos, M. B., Cox, D. W., and Mercer, J. F. B. (1996) The toxic milk mouse is a murine model of Wilson disease. *Hum. Mol. Genet.* **5**, 1619–1624.
28. Petrukhin, K., Lutsenko, S., Chernov, I., Ross, B. M, Kaplan, J. H., and Gilliam, T. C. (1994) Characterization of the Wilson disease gene encoding a P-type copper transporting ATPase: genomic organization, alternative splicing, and structure/function predictions. *Hum. Mol. Genet.* **3**, 1647–1656.
29. Borjigin, J., Payne, A. S., Deng, J., Li, X., Wang, M. M., Ovodenko, B., et al. (1999) A novel pineal night-specific ATPase encoded by the Wilson disease gene. *J. Neurosci.* **19**, 1018–1026.
30. Schaefer, M., Hopkins, R. G., Failla M. L., and Gitlin, J. D. (1999) Hepatocyte-specific localization and copper-dependent trafficking of the Wilson's disease protein in the liver. *Am. J. Physiol.* **276**, G639–G646.
31. Pedersen, P. L. and Carafoli, E. Ion motive ATPases. (1987) *Trends Biochem. Sci.* **12**, 146–150.
32. Lutsenko, S., Petrukhin, K., Cooper, M. J., Gilliam, T. C., and Kaplan, J. H. (1997) N-Terminal domains of human copper-transporting adenosine triphosphatases (the Wilson's and Menkes disease proteins) bind copper selectively in vivo and in vitro with stoichiometry of one copper per metal-binding repeat. *J. Biol. Chem.* **272**, 18,939–18,944.
33. Forbes, J. R., Hsi, G., and Cox, D. W. (1999) Role of the copper-binding domain in the copper transport function of ATP7B, the P-type ATPase defective in Wilson disease. *J. Biol. Chem.* **274**, 12,408–12,413.
34. Yang, X. L., Miura, N., Kawarada, Y., Terada, K., Petrukhin, K., Gilliam, T. C., et al. (1997) Two forms of Wilson disease protein produced by alternative splicing are localized in distinct cellular compartments. *Biochem. J.* **326**, 897–902.
35. Schaefer, M., Roelofsen, H., Wolters, H., Hofmann, W. J., Muller, M., Kuipers, F., et al. (1999) Localization of the Wilson's disease protein in human liver. *Gastroenterology* **117**, 1380–1385.
36. Harada, M., Sakisaka, S., Terada, K., Kimura, R., Kawaguchi, T., Koga, H., et al. (2000) Role of ATP7B in biliary copper excretion in a human hepatoma cell line and normal rat hepatocytes. *Gastroenterology* **118**, 921–928.
37. Lutsenko, S., and Cooper, M. J. (1998) Localization of the Wilson's disease protein product to mitochondria. *Proc. Natl. Acad. Sci. USA* **95**, 6004–6009.
38. Nagano, K., Nakamura, K., Urakami, K., Umezawa, K., Uchiyama, H., Koiwai, K., et al. (1998) Intracellular distribution of the Wilson's disease gene product (ATPase7B) after *in vitro* and *in vivo* exogenous expression in hepatocytes from the LEC rat, an animal model of Wilson's disease. *Hepatology* **27**, 799–807.
39. Petris, M. J., Mercer, J. F. B., Culvenor, J. G., Lockhart, P., Gleeson, P. A., and Camakaris, J. (1996) Ligand-regulated transport of the Menkes copper P-type ATPase efflux pump from the Golgi apparatus to the plasma membrane: a novel mechanism of regulated trafficking. *EMBO J.* **15**, 6084–6095.
40. Terada, K., Kawarada, Y., Miura, N., Yasui, O., Koyama, K., and Sugiyama, T. (1995) Copper incorporation into ceruloplasmin in rat livers. *Biochim. Biophys. Acta* **2170**, 58–62.
41. Murata, Y., Yamakawa, E., Iizuka, T., Kodama, H., Abe, T., Seki, Y., et al. (1995) Failure of copper incorporation into ceruloplasmin in the Golgi apparatus of LEC rat hepatocytes. *Biochem. Biophys. Res. Commun.* **209**, 349–355.
42. Harada, M., Sakisaka, S., Yoshitake, M., Shakado, S., Gondoh, K., Sata, M., et al. (1993) Biliary copper excretion in acutely and chronically copper-loaded rats. *Hepatology* **17**, 111–117.
43. Payne, A. S., Kelly, E. J., and Gitlin, J. D. (1998) Functional expression of the Wilson disease protein reveals mislocalization and impaired copper-dependent trafficking of the common H1069Q mutation. *Proc. Natl. Acad. Sci. USA* **95**, 10,854–10,859.
44. Zhou, B. and Gitschier, J. (1997) h*CTR1*: a human gene for copper uptake identified by complementation in yeast. *Proc. Natl. Acad. Sci. USA* **94**, 7481–7486.
45. Dancis, A., Yuan, D. S., Haile, D., Askwith, C., Eide, D., Moehle, C., et al. (1994) Molecular characterization of a copper transporter protein in *S. cerevisiae*: an expected role for copper in iron transport. *Cell* **76**, 393–402.
46. Klomp, L. W. J., Lin, S. J., Yuan, D. S., Klausner, R. D., Culotta, V. C., and Gitlin, J. D. (1997) Identification and functional expression of *HAH1*, a novel human gene involved in copper homeostasis. *J. Biol. Chem.* **272**, 9221–9226.

14

A Multicopper Oxidase-Based Iron-Transport System in Yeast

Jerry Kaplan

1. INTRODUCTION

Iron and copper are involved in redox reactions in all biological systems because of the ease by which these metals can gain and lose electrons. This property of facile electron loss has made these metals indispensable for a wide variety of biochemical reactions. The same redox properties that makes these metals so useful also renders them potentially toxic. Iron and copper can react with oxygen and oxygen metabolites to generate toxic radicals. This dualism of essential requirement and toxicity in excess has led to stringent regulation of metal uptake and storage systems. As all organisms must regulate and store these metals, there are similarities in the strategies that different organisms employ to maintain the concentration of iron or copper in biological fluids. The relationship between these two metals extends beyond their similar chemical and biological properties. Proper copper homeostasis is required for iron transport in eucaryotes; consequently, the metabolism of these two metals is closely entwined.

The earliest studies pointing to a role for copper in the metabolism of iron were based on clinical observations on patients with Wilson's disease (for review, *see* refs. *1* and *2*). In these patients, liver copper stores are excessively high, but plasma copper levels are extremely low. The major copper-containing protein in plasma is ceruloplasmin (Cp). In Wilson's patients there is a severe decrease in plasma Cp, and the Cp that is present is copper deficient. The absence of Cp was clearly related to the liver defect, but the role of Cp was unknown. In an attempt to better understand the functions of Cp, Cartwright and colleagues developed a nutritional model of copper deprivation using swine *(3)*. Developing piglets grow so rapidly that they quickly outgrow the maternal store of metals. When placed on a copper-free diet, the rapidly growing piglets become copper deficient and have low levels of plasma ceruloplasmin. The copper-deficient piglets were anemic, showing a microcytic or iron-limited anemia. The anemia, however, was not relieved by either increased dietary iron or by intravenous administration of iron. Histochemical examination of the intestinal duodenum revealed that the absorptive columnar cells were heavily iron loaded. This histological finding suggested that the defect in iron metabolism was not the result of an inability to absorb iron into the gut, but rather to a defect in the release of iron from intestine to plasma. Intravenous administration of iron, as iron–dextran or as heat-damaged red blood cells, revealed that the liver and spleen could accumulate iron but were unable to release that iron to plasma. These observations led to the conclusion that the defect in iron metabolism in the copper-deficient pig was not the result of a defect in uptake but to a defect in the release of iron from tissue to plasma.

From: Handbook of Copper Pharmacology and Toxicology
Edited by: E. J. Massaro © Humana Press Inc., Totowa, NJ

Because the deficit in copper metabolism resulted in a loss of holoCp, Cartwright and colleagues tested the hypothesis that Cp was involved in iron metabolism *(4)*. Injection of Cp into copper-deficient animals promoted an immediate increase in plasma iron, whereas injection of copper did not. If Cp were heat-treated or chemically inactivated prior to injection, plasma iron levels remained low. These results demonstrated that Cp played a role in iron metabolism. These observations were confirmed by Osaka et al. who showed that Cp would promote iron export from perfused rat liver *(5)*.

Iron released from tissues is bound to plasma transferrin, which then delivers iron to transferrin receptors. It was thought that Cp catalyzed the oxidation of ferrous to ferric iron, the ferric iron then binding to transferrin. This hypothesis was confirmed by in vitro measurements of the oxidase activity of Cp on both organic substrates and iron *(6,7)*. The oxidase activity is dependent on molecular oxygen, which is the terminal acceptor of the electrons removed from iron. Ferrous iron can be oxidized spontaneously. The presence of Cp, however, accelerates the reaction enormously, particularly at low oxygen tension *(6)*.

Ceruloplasmin is a member of a small family of proteins called multicopper oxidases (for review, *see* ref. *8*). These proteins are also known as the "blue oxidases," because of their characteristic blue color. Proteins belonging to this family are found in species as diverse as fungi, plants, and vertebrates. This protein family is distinguished by having copper bound in three different spectroscopic forms. The type-1 copper has an absorption maxima at 607 nm and is responsible for the blue color. Type 2 is spectroscopically silent in the visible range but has an electron spin resonance (ESR) signal. There are two type-3 coppers that are electronically linked; they do not have an ESR signal but can be detected spectroscopically at 330 nm. The type-2 and type-3 coppers are closely aligned, forming a trinuclear center. All multicopper oxidases show a similar mode of action; they oxidize four molecules of substrate with the concomitant reduction of molecular oxygen to water. Mechanistically, the enzymes oxidize substrates one molecule at a time, storing the abstracted electron. When the fourth molecule of substrate is oxidized, all four electrons then reduce molecular oxygen in one concerted reaction that does not generate reactive intermediates. This enzymatic oxidation of iron is in marked contrast to the spontaneous oxidation of iron, which does generate reactive oxygen intermediates. When the role of Cp was established in the early 1950s there was great reluctance to accept the role of Cp as a ferroxidase. Whereas all multicopper oxidases act on organic substrates, until 1990 only Cp was known to oxidize iron. It was believed that because iron oxidation was a thermodynamically favorable process, it that did not require an enzyme. Cp was then ascribed other roles, including as a plasma copper transporter.

1.1. Iron Metabolism in the Budding Yeast Saccharomyces cerevisiae

The experiments that confirmed the role of multicopper oxidases in iron metabolism in vertebrate systems came from studies on iron transport in yeast. Yeast, particularly the budding yeast *Saccharomyces cerevisiae* is perhaps the simplest of the eucaryotes, as they grow as single cells and can be both haploid and diploid The haploid status of yeast permits the selection of yeast mutants. Once a phenotype has been selected, genes responsible for modifying a specific phenotype can be identified by complementation using a genomic library. Because most yeast genes do not have introns, a yeast genomic library is functionally equivalent, although much easier to prepare than a cDNA library. Because all yeast genes have been cloned, only a small amount of sequence and subcloning is required to identify which gene on a genomic plasmid is responsible for modifying the mutant phenotype. A gene can modify a phenotype because it is allelic to the mutant gene or because it is a suppressor and metabolically bypasses the defective step. These two alternatives can easily be discriminated by deleting specific genes and examining the resulting phenotype. As yeast readily undergo homologous recombination, it is relatively easy to inactivate specific genes. The ability to inactivate specific genes permits a rigorous analysis of gene function; indeed, homologous recombination extends

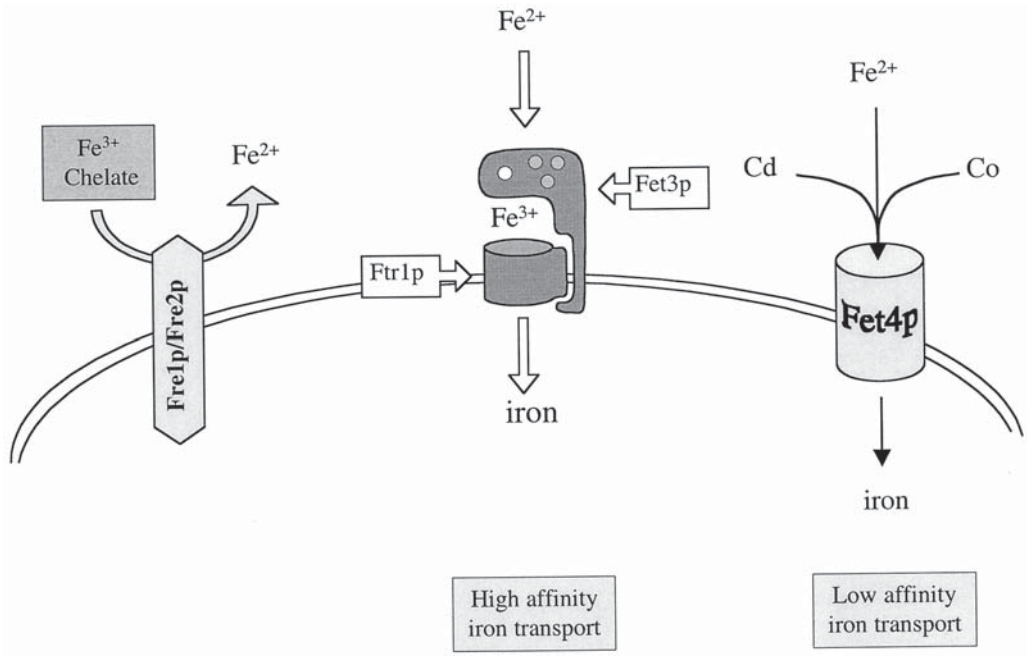

Fig. 1. Iron transport across the plasma membrane in the budding yeast *S. cerevisiae*. *See* text for details.

Koch's postulates to genetics. If the deletion strain is genetically and phenotypically identical to the mutant strain (i.e., a diploid between the two shows the mutant phenotype) and is phenotypically identical, then the identified gene is most probably the normal allele of the mutant gene.

Studies on yeast iron metabolism identified the existence of two different transport systems for elemental iron and a transport system for iron–siderophore complexes *(9)* (Fig. 1). Both transport systems for elemental iron recognize Fe(II) as a substrate. This was demonstrated by showing that Fe(II) chelators inhibited iron uptake, whereas Fe(III) chelators were unable to inhibit iron transport. Further, there was biochemical evidence for a cell surface reductase activity that converted Fe(III) to Fe(II) *(10)*. The most compelling work resulted from the cloning of the reductase gene. Dancis et al. identified a yeast mutant unable to grow on Fe(III) because of the lack of ferrireductase activity *(11)*. The gene for the ferrireductase was cloned by complementation analysis and was termed *FRE1*. Later studies identified a second cell-surface ferrireductase termed *FRE2 (12)*.

These reductases provide the substrate for the two elemental iron-transport systems. The low-affinity transport system encoded by the *FET4* gene is not specific for iron and can accumulate other transition metals *(13)*. The other system, comprised of the products of the *FET3* and *FTR1* genes, is a high-affinity transport system that is specific for iron (Fig. 2). The two transport systems are regulated differently. The high-affinity iron-transport system is induced when cells are grown on low-iron media. The low-affinity system is also negatively regulated by media iron, but the concentration required to turn off the system is usually not seen in most media formulations. The two systems are genetically separable, as they are the products of different genes. That the two systems are different both genetically and physiologically permitted a genetic approach to identifying the systems. Cells can be mutagenized and mutants in the high-affinity transport system can be identified by their inability to grow on low-iron media. These mutants were "rescued" by the addition of iron, as they could still obtain iron through the low-affinity transport system.

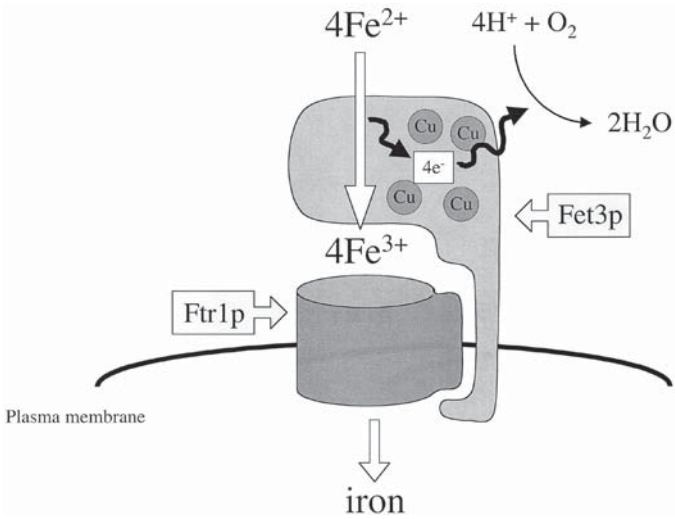

Fig. 2. Proposed model for high-affinity iron transport. *See* text for details.

1.2. Identification and Characterization of FET3

Using a selection system that was enriched for mutants unable to grow on low-iron media, Askwith et al. reported the identification of a mutant, *fet3*, that was unable to grow on low-iron media (14). This mutant had a normal surface reductase activity but was unable to accumulate 59Fe. A gene that could complement both the low-iron growth defect and the inability to accumulate radioactive iron was identified by complementation of the mutant strain with a genomic library. Genetic studies determined that the complementing gene was the normal allele of the mutated gene. The sequence of this gene, termed *FET3*, showed homology to members of the multicopper oxidase family. The closest homology was to ascorbate oxidase, but *FET3* showed significant homology to all multicopper oxidases. The homology was seen in a signature sequence that defines multicopper oxidases and in the sequences thought to ligate the coppers. A feature that distinguished Fet3p from the other known multicopper oxidases was the presence of a single transmembrane domain. Fet3p is made as a higher-molecular-weight precursor with an amino terminal extension. This extension is a leader sequence and gains entry of Fet3p into the secretory apparatus where Fet3p is glycosylated. The carboxyl terminal transmembrane domain is a membrane anchor tethering Fet3p to the membrane. Studies using epitope-tagged Fet3p demonstrated that Fet3p is a plasma membrane protein. At the time of its identification, most multicopper oxidases were found as secreted products in both plants and animals.

The sequence of Fet3p indicated that it was a multicopper oxidase. This indication was strengthened by the discovery that copper depletion results in an inability to grow on low-iron media. Copper depletion was accomplished either genetically through the identification of mutants unable to grow on copper *(15)* or through nutritional studies in which media copper was made limiting *(14)*. In either case, copper-deprived yeast does not have a functional high-affinity iron transport system. This work provided strong evidence that copper was required for high-affinity iron transport and supported the role of a multicopper oxidase in iron transport.

Studies on oxygen consumption provided further evidence for a putative ferroxidase in iron transport. Measurement of oxygen consumption by yeast showed both a *FET3*-dependent and *FET3*-independent oxygen consumption *(16)*. Most of the oxygen consumed by cells grown on iron-rich media was the result of mitochondrial consumption. In cells that were iron starved, however, there was an increased rate of oxygen consumption. If the *FET3* gene was deleted, then the enhanced rate of oxygen consumption was reduced and could be accounted for by mitochondrial respiration. Inhibi-

tion of respiration, either by pharmacological agents or by introduction of mutations into genes encoding respiratory proteins, resulted in a marked decrease in mitochondrial oxygen consumption, but not in *FET3*-induced oxygen consumption. Further studies demonstrated that the *FET3*-dependent rate of oxygen consumption was reduced in copper-starved yeast and could also be reduced by the addition to spheroplasts of an antibody directed against the extracellular domain of Fet3p but not by antibodies directed against the intracellular domain. Calculation of the ratio of the rates of *FET3*-dependent oxygen consumption and iron accumulation revealed a value of 4/1. This ratio conforms to the stoichiometry expected of a multicopper oxidase. The final piece of physiological data showing a role for a multicopper oxidase in iron consumption is that cells grown under anaerobic conditions are unable to accumulate iron by the *FET3*-dependent iron-transport system, rather, they employ the low-affinity iron-transport system that relies on the product of the *FET4* gene. Under anaerobic conditions, cells can only grow in media containing high concentrations of iron. A *fet3*-deletion strain that express the *FET4* gene product can grow, but a *FET4*-deletion strain cannot grow even though it has a good *FET3* gene. Further, the transcription of the *FET3* gene is repressed under anaerobic conditions *(17)*. These results show that *FET3* effects iron-dependent oxygen consumption, and without oxygen, cells are unable to take up iron by the Fet3p transport system.

Although the above studies showed that *FET3* was a multicopper oxidase, the specific role of the oxidase remained unclear. It is possible that Fet3p oxidizes a protein, rather than iron. The suggestion that Fet3p acted as a ferroxidase required the isolation of Fet3p and a direct measurement of ferroxidase activity. This was first accomplished by deSilva et al., who demonstrated that purified Fet3p could oxidize iron and that it could also load iron onto transferrin *(18)*. Examination of a number of potential substrates for multicopper oxidases showed iron to be the preferred substrate. The K_m for iron oxidation, 0.5 u*M* was very close to the K_m for iron transport. Purified Fet3p could iron load transferrin, although the rate of iron loading was low relative to that of ceruloplasmin. Reasons for the low rate may be that detergent was use to isolate Fet3p and as isolated Fet3p is heavily glycosylated. The presence of both detergent and carbohydrate may reduce the rate of transferrin iron loading through steric hindrance. Hasset et al. using molecular engineering produced a Fet3p that lacked a transmembrane domain *(19)*. This protein is secreted into the media, permitting its isolation without the use of detergents. The soluble Fet3p showed a similar rate of iron oxidation as the transmembrane containing Fet3p, both of which then had a lower rate of iron turnover than Cp. A highly active fragment of Fet3p can be released by proteases from the yeast *Pichia pastoris (20)*. This fragment lacks the transmembrane domain and can be isolated without the use of detergents. The isolated Fet3p oxidizes iron at the same rate as ceruloplasmin. It is unclear why the Fet3p from *Pichia* would have a faster rate of iron oxidation than the Fet3p from *S. cerevisiae*.

That purified Fet3p can oxidize iron suggests that it functions as an ferroxidase in iron transport. Mutagenesis studies designed to determine the molecular basis of iron oxidation support the view that the ferroxidase activity of Fet3p is essential for iron transport. Although there are many multicopper oxidases, all of which can oxidize organic substrates, only Fet3p and Cp (and its homologs) can also oxidize iron. A comparison of the sequence of Fet3p to the sequences of other multicopper oxidases led to the suggestion of several structural features of Fet3p that were thought to be responsible for iron oxidation. Askwith et al. made a series of site-specific mutants in an attempt to determine what features were responsible for iron oxidation *(21)*. Among the residues mutagenized were those thought to ligate the type-1 copper and thus were responsible for setting the oxidation potential. In most multicopper oxidases, a methionine is a ligand for the type-1 copper. In Fet3p, that methionine is replaced by leucine, suggesting a geometry typical of a high-redox-potential copper site. When that leucine was replaced by a methionine, the protein retained ferroxidase activity and the rate of iron uptake was reduced by less than twofold. Replacement of the leucine with other amino acids severely reduced both multicopper oxidase activity and cellular iron transport. Other residues suggested to be involved in iron oxidation (glutamic acid 227, aspartic acid 228, and glutamic acid 330) when changed to alanine did not affect either iron transport or ferroxidase activity. In a

more recent study, structural determinants for ferroxidase activity were based on modeling studies *(22)*. The amino acids Glu185 and Tyr354 were thought to be important for iron binding. Alteration of these amino acids by site-specific mutagenesis had an effect on ferroxidase activity *(23)*. Most impressively, alteration of Glu185 to Ala reduced ferroxidase activity by 95% but only reduced oxidase activity by 60%. This is the first result that suggests that the two enzymatic activities could be separated. Unfortunately, iron transport activity was not assayed. A measurement of iron transport could have provided compelling evidence that the ferroxidase activity of Fet3p is the critical aspect of its role in iron transport. If the ferroxidase activity of Fet3p is required for iron transport, then a prediction is that the Glu185Ala mutant would show a 95% decrease in iron transport. Even without this experiment, the consensus view is that Fet3p plays a role in iron transport as a result of its ferroxidase activity.

Although Fet3p is a ferroxidase converting Fe(II) into Fe(III), it only has a single transmembrane domain and is unlikely to transport iron across the bilayer. A genetic screen performed by Stearman et al. revealed a second gene required for high-affinity iron transport *(24)*. This gene, termed *FTR1*, encoded a protein with six transmembrane domains. Stearman et al. identified a sequence within Ftr1p comprising the amino acids REGLE, which is similar to a motif that implicated in the iron-binding region of mammalian L-chain ferritin. Mutation of these residues in Ftr1p abrogates its ability to transport iron. These authors also provided genetic evidence that Fet3p and Ftr1p form a complex. In the absence of Ftr1p, Fet3p did not localize to the cell surface. Similarly, in the absence of Fet3p, Ftr1p did not localize to the cell surface. These results suggest that both molecules must be synthesized simultaneously so that they can be assembled to form a complex that permits the correct targeting of either to the cell surface.

Confirmation that Fet3p and Ftr1p formed a functional complex came from studies of a homologous complex in different yeast *Schizosaccharomyces pombe*. The fission yeast, *S. pombe,* also has a ferroxidase-based high-affinity iron-transport system *(25)*. This system consists of an oxidase termed *fio1+* and a transmembrane transporter *fip1+*. These genes are highly homologous to the *S. cerevisiae* genes, with fio1p + sharing 38% identity and 60% similarity on the amino acid level with Fet3p and frp1p sharing 46% identity and 70% homology on the amino acid level percentage with Ftr1p. Expression of fio1p in a *S. cerevisiae* strain lacking *FET3* does not permit high-affinity iron uptake (Fig. 3). Thus, fio1p cannot partner with Ftr1p. If, however, fip1p is expressed at the same time as fio1p in the *S. cerevisiae fet3*-deletion strain, then the strain is capable of high-affinity iron transport. These results suggest that the oxidase and permease function as a unit and imply that Fet3p and Ftr1p are the only two plasma membrane proteins required to carry out iron transport.

Other yeasts, aside from *S. pombe* and *S. cerevisiae,* show an oxidase/permease-based iron-transport system. A ferroxidase was shown to be essential for iron transport in *Candida albicans* as deletion of the *C. albicans FET3* prevents high-affinity iron transport *(26,27)*. In one study, it was reported that the *C. albicans fet3*-deletion strain grew poorly in infected mice, suggesting that the *FET3* gene may be a virulence factor *(27)*. It is curious that the *C. albicans FET3* when expressed in a *S. cerevisiae fet3*-deletion strain complements the low-iron growth defect *(26)*. This result suggests that *C. abicans* Fet3p can form a complex with *S. cerevisiae* Ftr1p, whereas the *FET3* homolog of *S. pombe*, *fio1*$^{+}$, cannot. Biochemical studies have shown that *P. pastoris* also expresses a ferroxidase similar Fet3p *(19)*. It may well be that a ferroxidase/permease iron-transport system is common among yeasts.

The role of a ferroxidase in yeast iron transport, however, presents a conundrum. The reaction of Fe(II) with Fet3p generates Fe(III). Yet, the substrate for Fet3p is Fe(II) produced by the ferrireductases. The overall reaction is therefore:

$$\text{Fe(III)} + e^{-} \rightarrow \text{Fe(II) (ferriductase)}$$

$$\text{Fe(II)} + 4\text{H+} + \text{O}_2 \rightarrow \text{Fe(III)} + 2\text{H}_2\text{O (oxidase)}$$

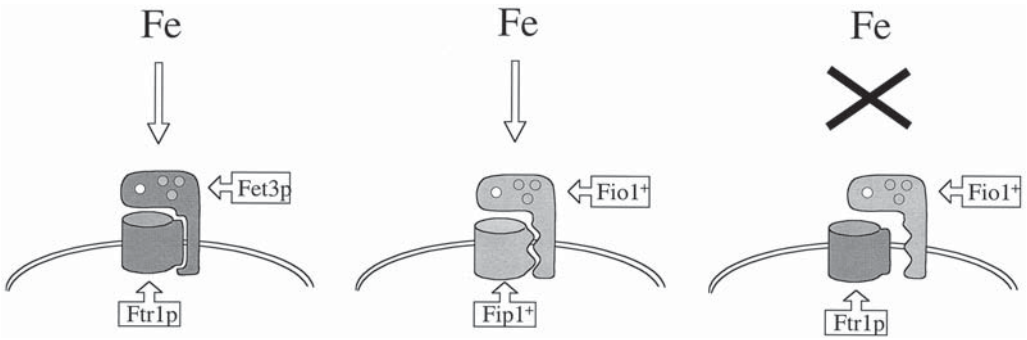

Fig. 3. Genetic evidence for complex formation between the multicopper oxidase and the transmembrane permease. *See* text for details.

Within the same domain, the cell surface, there are two diametrically opposed enzymatic reactions: a reduction and then an oxidation. Why do yeasts require iron to be first reduced and then oxidized? The explanation for this requirement is twofold. First, ferric iron is essentially insoluble and is not readily bioavailable. Iron is most often found as insoluble ferric hydroxide. Most bioavailable iron is found chelated to small organic molecules. There is little structural similarity in the organic chelates and, most often, iron is shielded from the media by organic molecules. Therefore, there is little basis for a chemical recognition of ferric chelates. Reduction of ferric iron by electron addition generates ferrous iron, which is much more soluble and can exist in aqueous fluids at measurable concentrations.

Ferric oxidation may be required to provide specificity to the transport process. To date, all known ferrous transport systems show a low degree of specificity, as they can mediate the accumulation of other transition metals. In yeast, for example, the *FET4*-transport system can also accumulate copper and cobalt in addition to iron *(13)*. In mammalian cells, DMT1 (also referred to as Nramp2 or DCT1) transports to iron, zinc, manganese, and cobalt *(28)*. In contrast, the two known Fe(III)-transport systems, *FET3/FTR1* in yeast and Cp and transferrin in vertebrates, are exquisitely specific for iron. There is no other relevant transition metal transported by these systems. (Aluminum and gallium can bind to transferrin.) The basis for specificity is the binding of iron to the transporter (*FET3*) or carrier, transferrin. As iron is insoluble, it needs specific ligands to generate high-affinity binding. The ligation of Fe(III) to amino acids imparts specificity on the binding process. Further, the enzyme reaction carried out by the multicopper oxidases generates Fe(III) without producing oxygen radicals.

1.3. Intracellular Processing and Assembly of Fet3p

All multicopper oxidases are glycosylated molecules that are either secreted or membrane bound. These molecules enter the secretory pathway as nascent polypeptides and are subsequently processed in the endoplasmic reticulum and Golgi apparatus. The assembly of an active Fet3p requires the addition of copper to the apo form to generate the active holo enzyme. Our understanding of the genes required for the copper loading of apoFet3p have been furthered by intense work that has been done defining the molecular basis of Menkes and Wilson's disease *(2,29)*. The genes responsible for these disorders are highly homologous ATP–copper transporters that are localized in post-Golgi vesicles. Like many of the genes involved in copper metabolism, there is a yeast homolog, termed *CCC2*. Genetic studies demonstrated that Ccc2p is the protein required for the copper loading of Fet3p *(30)*. In the absence of Ccc2p, an apoFet3 is transported to the cell surface. The apoFet3p lacks ferroxidase activity and is unable to mediate high-affinity iron transport. Ccc2p is found on a post-Golgi vesicle and it is thought that it is in this vesicle that apoFet3p obtains its copper. Exactly where or what this post-Golgi vesicle is has been clarified by studying the vacuolar assembly, an organelle that is analogous to the mammalian lysosome.

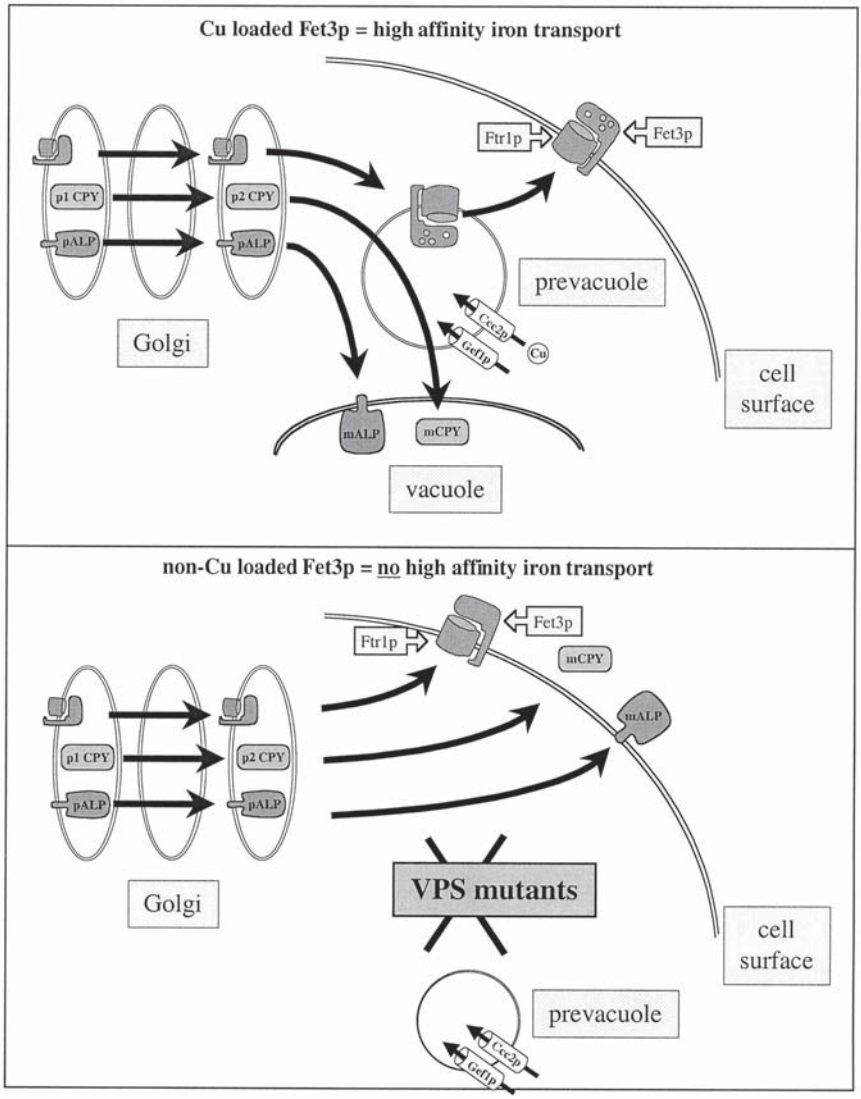

Fig. 4. Model for the intracellular processing of holoFet3p. CPY is a soluble vacuolar protein and ALP is a vacuolar membrane protein. These two proteins as well as apoFet3p and Ftr1p are synthesized in the rough endoplasmic reticulum and then transferred to the Golgi, where glycosylation takes place. apoFet3p is transferred from the Golgi to a vesicle that contains Ccc2p and Gef1p. It is in this vesicle that the copper is added to apoFet3p forming the holo enzyme. It is thought that CPY and ALP might also pass through this compartment. Mutations in genes that disrupt vesicular traffic at a post-Golgi step results in the transfer of apoFet3p, ALP, and CPY to the cell surface. The soluble enzyme CPY is secreted into the media, whereas apoFet3p stays on the cell surface. ALP contains endocytic signals that permit it to be internalized to the vacuole.

Genetic screens have led to the identification of many genes required for the transport of vacuolar components, both vacuolar enzymes and membrane components. Mutants defective in vacuole formation are termed *vps* or *vma* mutations *(31)*. Many of these mutants show an inability to grow on low-iron media *(32,33)*. This defect results from a defective high-affinity iron-transport system. The Fet3p delivered to the cell surface is not copper loaded and lacks ferroxidase activity. Golgi-derived vesicles containing appropriately glycosylated proteins, including apoFet3p and the vacuolar enzyme

carboxypeptidase Y (CPY), are delivered to the cell surface instead of the post-Golgi vesicle that normally houses the machinery for copper loading or the vacuole that normally houses CPY. These results position the Ccc2p vesicle between the trans-Golgi and the vacuole (Fig. 4).

In addition to the *VPS* genes, other genes are required for the copper loading of apoFet3p. One group of genes encodes subunits of the vacuolar H+-ATPase *(34)*. In the absence of a subunit of the enzyme, vacuoles and presumably other post-Golgi prevacuolar compartments are not acidified. A second gene encodes a member of the family of voltage-regulated chloride channels *(35)*. The yeast gene *GEF1* is highly homologous to the human gene *CLC5*, which encodes a vesicular chloride transporter that is specific to the kidney *(36)*. The yeast gene also encodes a vesicular protein that has been localized to the same vesicle as Ccc2p *(37,38)*. Defects in *gef1* also result in the presence of apoFet3p on the cell surface *(38,39)*.

A hypothesis has been presented to explain why a defect in a chloride channel would result in an apoFet3p *(38)*. In a membrane-bound vesicle, the introduction of cations such as Cu+ and H+ would quite rapidly result in an unfavorable membrane potential that prevents further introduction of cations, thereby limiting copper concentration and pH. Under normal conditions, this potential difference effects the opening of the voltage-gated chloride channel. Chloride enters the vesicle as a result of the electrical–chemical gradient. The introduction of anions into the vesicle neutralizes the positive potential difference resulting from cation accumulation. When the voltage potential has been dissipated, the chloride channel would close. The operation of the channel prevents the formation of an unfavorable gradient, permitting a high copper concentration and reduced pH. Disruption of chloride channels results in dysregulated vesicular ion homeostasis, reducing vesicular copper concentration and increasing vesicular pH. This hypothesis implies that there is a pH dependency to the copper loading of apoFet3p. To test this prediction, Davis-Kaplan et al. developed an in vitro system to measure the pH dependency of copper loading *(39)*. The system employed a mutant strain lacking Ccc2p. As mentioned earlier, in the absence of Ccc2p, an apoFet3p is placed on the cell surface. Cell-surface apoFet3p can be converted to holoFet3p at 0°C, suggesting that no metabolic energy is required. The assay for copper loading of apoFet3p is to expose cells to copper at different pH's at 0°C, wash the cells and then incubate them in copper-free buffers at 30°C to assay iron transport. The results of this experiment demonstrated that the copper loading of apoFet3p was pH dependent. The greatest degree of copper loading occurred at pH 4.5. This result confirms the role of the H+-ATPase in the maturation of Fet3p. The experiment, however, revealed an unusual feature in that copper loading of apoFet3p was chloride dependent. Without chloride, little copper loading occurred at all pH's examined. Chloride could be replaced by bromine and to a lesser extent by iodine, but not by other nonhalide anions. The requirement for chloride to load apoFet3p was confirmed by a second assay. holoFet3p as a multicopper oxidase can be assayed using organic substrates. An apoFet3p extracted from cells with a *CCC2* deletion has, as expected, no enzymatic activity on organic substrates. An apoFet3p copper loaded in vitro shows enzymatic activity. Using this assay, the copper loading of Fet3p was again shown to be chloride dependent.

The specific role of chloride in the loading of Fet3p is unknown. Trivial explanations such as chloride is required to maintain copper in solution have been ruled out. Examination of the kinetics of the chloride dependence of copper loading has shown an allosteric interaction between copper and chloride. In the presence of different concentrations of chloride, there is a sigmoidal relationship between copper and chloride. When chloride concentration is high, lower concentrations of copper effect the formation of a holoFet3p. The converse is also true, when copper concentration is high, lower concentrations of chloride are required to copper load Fet3p.

Examination of the literature reveals a precedent for chloride requirement for the metallation of a protein. The yeast enzyme leucine aminopeptidase 1, the product of the LAP1 gene, is a zinc-containing vacuolar exopeptidase. This enzyme requires both zinc and chloride for activity. In the absence of chloride, zinc will not bind to the enzyme. It was found that chloride bound to the enzyme, but only in the presence of zinc *(39,40)*. These studies showed a direct requirement of chloride for the

metallation of the enzyme. At present, it has not been demonstrated that chloride binds to Fet3p. Further, the studies on chloride binding do not rule out the hypothesis that disruption in the chloride channel prevents the formation of a holoFet3p by affecting ion homeostasis. It may well be that both disruption of iron homeostasis and the lack of chloride required for the direct metallation of the protein are responsible for the inability of *GEF1*-deletion strain to copper load apoFet3p.

The study of *FET3*, its biochemistry and physiology, has provided insight into both the mechanism of iron transport and the physiology of copper. As copper homeostasis is required for Fet3p activity, analysis of Fet3p function has led to the discovery of genes involved in copper metabolism. Further, analysis of the assembly of Fet3p has also led to insight into human iron metabolism. Finally, as the oxidase/permease iron-transport system may be a virulence factor for pathogenic fungi, the transport system them becomes a target for therapeutic approaches.

REFERENCES

1. Harris, Z. L. and Gitlin, J. D. (1996) Genetic and molecular basis for copper toxicity, *Am. J. Clin. Nutr.* **63**, 836S–841S.
2. Cox, D. W. (1996) Molecular advances in Wilson disease. *Prog. Liver Dis.* **14**, 245–264.
3. Lee, G. R., Nacht, S., Lukens, J. N., and Cartwright, G. E. (1968) Iron metabolism in copper-deficient swine. *J. Clin. Invest.* **47**, 2058–2069.
4. Ragan, H. A., Nacht, S., Lee, G. R., Bishop, C. R., and Cartwright, G. E. (1969) Effect of ceruloplasmin on plasma iron in copper-deficient swine. *Am. J. Physiol.* **217**, 1320–1323.
5. Osaki, S., Johnson, D. A., and Frieden, E. (1971) The mobilization of iron from the perfused mammalian liver by a serum copper enzyme, ferroxidase I. *J. Biol. Chem.* **246**, 3018–3023.
6. Osaki, S., Johnson, D. A., and Frieden, E. (1966), The possible significance of the ferrous oxidase activity of ceruloplasmin in normal human serum. *J. Biol. Chem.* **241**, 2746–2751.
7. Williams, D. M., Lee, G. R., and Cartwright, G. E. (1974) Ferroxidase activity of rat ceruloplasmin. *Am. J. Physiol.* **227**, 1094–1097.
8. Messerschmidt, A. and Huber, R. (1990) The blue oxidases, ascorbate oxidase, laccase and ceruloplasmin. Modelling and structural relationships. *Eur. J. Biochem.* **187**, 341–352.
9. Eide, D., Davis-Kaplan, S., Jordan, I., Sipe, D., and Kaplan, J. (1992) Regulation of iron uptake in Saccharomyces cerevisiae. The ferrireductase and Fe(II) transporter are regulated independently. *J. Biol. Chem.* **267**, 20,774–20,781.
10. Crane, R. H., Linnane, A. W., Low, H. (1982) Transmembrane ferricyanide reduction in yeast. *J. Bioenergy Biomembr.* **14**, 191–205.
11. Dancis, A., Klausner, R. D., Hinnebusch, A. G., and Barriocanal, J. G. (1990) Genetic evidence that ferric reductase is required for iron uptake in *Saccharomyces cerevisiae*. *Mol. Cell Biol.* **10**, 2294–2301.
12. Georgatsou, E. and Alexandraki, D. (1994) Two distinctly regulated genes are required for ferric reduction, the first step of iron uptake in *Saccharomyces cerevisiae*. *Mol. Cell Biol.* **14**, 3065–3073.
13. Dix, D. R., Bridgham, J. T., Broderius, M. A., Byersdorfer, C. A., and Eide, D. J. (1994) The FET4 gene encodes the low affinity Fe(II) transport protein of *Saccharomyces cerevisiae*. *J. Biol. Chem.* **269**, 26,092–26,099.
14. Askwith, C., Eide, D., Van Ho, A., Bernard, P. S., Li, L., Davis-Kaplan, et al. (1994) The FET3 gene of *S. cerevisiae* encodes a multicopper oxidase required for ferrous iron uptake. *Cell* 76, 403–410.
15. Dancis, A., Yuan, D. S., Haile, D., Askwith, C., Elde, D., Moehle, C., et al. (1994) Molecular characterization of a copper transport protein in *S. cerevisiae*: an unexpected role for copper in iron transport. *Cell* **76**, 393–402.
16. De Silva, D. M., Askwith, C. C., Eide, D., and Kaplan, J. (1995) The FET3 gene product required for high affinity iron transport in yeast is a cell surface ferroxidase. *J. Biol. Chem.* 270, 1098–1101.
17. Hassett, R. F., Romeo, A. M., and Kosman, D. J., Regulation of high affinity iron uptake in the yeast *Saccharomyces cerevisiae*. Role of dioxygen and Fe. *J. Biol. Chem.* 273, 7628–7636.
18. de Silva, D., Davis-Kaplan, S., Fergestad, J., and Kaplan, J. (1997) Purification and characterization of Fet3 protein, a yeast homologue of ceruloplasmin. *J. Biol. Chem.* 272, 14,208-14,213.
19. Hassett, R. F., Yuan, D. S., and Kosman, D. J. (1998) Spectral and kinetic properties of the Fet3 protein from *Saccharomyces cerevisiae*, a multinuclear copper ferroxidase enzyme. *J. Biol. Chem.* **273**, 23,274–23,282.
20. Bonaccorsi di Patti, M. C., Bellenchi, G. C., Bielli, P., and Calabrese, L. (1999), Release of highly active Fet3 from membranes of the yeast Pichia pastoris by limited proteolysis, *Arch. Biochem. Biophys.* **372**, 295–299.
21. Askwith, C. C. and Kaplan, J. (1998) Site-directed mutagenesis of the yeast multicopper oxidase Fet3p. *J. Biol. Chem.* 273, 22,415–22,419.
22. di Patti, M. C., Pascarella, S., Catalucci, D., and Calabrese, L. (1999) Homology modeling of the multicopper oxidase Fet3 gives new insights in the mechanism of iron transport in yeast. *Protein Eng.* **12**, 895–897.
23. Bonaccorsi di Patti, M. C., Felice, M. R., Camuti, A. P., Lania, A., and Musci, G., The essential role of Glu-185 and Tyr-354 residues in the ferroxidase activity of *Saccharomyces cerevisiae* Fet3. *FEBS Lett.* **472**, 283–286.
24. Stearman, R., Yuan, D. S., Yamaguchi-Iwai, Y., Klausner, R. D., and Dancis, A. (1996) A permease–oxidase complex involved in high-affinity iron uptake in yeast [see comments], *Science* **271**, 1552–1557.
25. Askwith, C. and Kaplan, J. (1997) An oxidase–permease-based iron transport system in *Schizosaccharomyces pombe* and its expression in *Saccharomyces cerevisiae*. *J. Biol. Chem.* 272, 401–405.

26. Eck, R., Hundt, S., Hartl, A., Roemer, E., and Kunkel, W. (1999) A multicopper oxidase gene from *Candida albicans*: cloning, characterization and disruption. *Microbiology* 145, 2415–2422.
27. Ramanan, N. and Wang, Y. (2000) A high-affinity iron permease essential for *Candida albicans* virulence. *Science* **288**, 1062–1064.
28. Gunshin, H., Mackenzie, B., Berger, U. V., Gunshin, Y., Romero, M. F., Boron, W. F., et al. (1997) Cloning and characterization of a mammalian proton-coupled metal-ion transporter. *Nature* **388**, 482–488.
29. Culotta, V. C., Lin, S. J., Schmidt, P., Klomp, L. W., Casareno, R. L., and Gitlin, J. (1999) Intracellular pathways of copper trafficking in yeast and humans. *Adv. Exp. Med. Biol.* **448**, 247–254.
30. Yuan, D. S., Stearman, R., Dancis, A., Dunn, T., Beeler, T., and Klausner, R. D. (1990) The Menkes/Wilson disease gene homologue in yeast provides copper to a ceruloplasmin-like oxidase required for iron uptake. *Proc. Natl. Acad. Sci. USA* **92**, 2632–2636.
31. Klionsky, D. J., Herman, P. K., and Emr, S. D. (1990) The fungal vacuole: composition, function, and biogenesis. *Microbiol. Rev.* **54**, 266–292.
32. Radisky, D. C., Snyder, W. B., Emr, S. D., and Kaplan, J. (1997) Characterization of VPS41, a gene required for vacuolar trafficking and high-affinity iron transport in yeast. *Proc. Natl. Acad. Sci. USA* **94**, 5662–5666.
33. Yuan, D. S., Dancis, A., and Klausner, R. D. (1997) Restriction of copper export in *Saccharomyces cerevisiae* to a late Golgi or post-Golgi compartment in the secretory pathway. *J. Biol. Chem.* **272**, 25,787–25,793.
34. Eide, D. J., Bridgham, J. T., Zhao, Z., and Mattoon, J. R. (1993) The vacuolar H(+)-ATPase of *Saccharomyces cerevisiae* is required for efficient copper detoxification, mitochondrial function, and iron metabolism. *Mol. Gen. Genet.* 241. 447–456.
35. Greene, J. R., Brown, N. H., DiDomenico, B. J., Kaplan, J., and Eide, D. J. (1993) The GEF1 gene of *Saccharomyces cerevisiae* encodes an integral membrane protein; mutations in which have effects on respiration and iron- limited growth. *Mol. Gen. Genet.* **241**, 542–553.
36. Gaxiola, R. A., Yuan, D. S., Klausner, R. D., and Fink, G. R. (1998) The yeast CLC chloride channel functions in cation homeostasis. *Proc. Natl. Acad. Sci. USA* **95**, 4046–4050.
37. Schwappach, B., Stobrawa, S., Hechenberger, M., Steinmeyer, K., and Jentsch, T. J. (1998) Golgi localization and functionally important domains in the NH2 and COOH terminus of the yeast CLC putative chloride channel Gef1p, *J. Biol. Chem.* 273, 15,110–15,118.
38. Gaxiola, R. A., Yuan, D. S., Klausner, R. D., and Fink, G. R. (1998) The yeast CLC chloride channel functions in cation homeostasis. *Proc. Natl. Acad. Sci. USA* **95**, 4046–4050.
39. Davis-Kaplan, S. R., Askwith, C. C., Bengtzen, A. C., Radisky, D., and Kaplan, J. (1998) Chloride is an allosteric effector of copper assembly for the yeast multicopper oxidase fet3p: An unexpected role for intracellular chloride channels [In Process Citation]. *Proc. Natl. Acad. Sci. USA* **95**, 13,641–13,645.
40. Rohm, K. H. (1985) Chloride as allosteric effector of yeast aminopeptidase I. *Arch. Biochem. Biophys.* **239**, 216–225.

IV

Molecular Pathogenesis of Diseases of Copper Metabolism

15

Molecular Basis of Diseases of Copper Homeostasis

Julian F. B. Mercer, David Kramer, and James Camakaris

1. INTRODUCTION

Copper is essential for life because it is a cofactor for a number of important enzymes, including cytochrome-*c* oxidase, lysyl oxidase, superoxide dismutase, and dopamine β-monooxygenase. The redox reactions carried out by these enzymes are facilitated by the ability of copper to shuttle between the two oxidation states Cu(I) and Cu(II). Deficiencies of copper can lead to profound effects, because of the reduced activity of these copper-dependent enzymes. The effects of copper deficiency are most marked during development, and severe deficiency in this period can prove to be fatal. The serious effects of copper deficiency in infancy are seen in the X-linked genetic disorder of copper transport, Menkes disease (MD) and the molecular basis of this disease will be discussed later in this chapter. The same redox properties that make copper a useful element render it dangerous in a free ionic state. Free copper, particularly Cu(I), can catalyze the formation of the highly reactive hydroxyl radicals that damage many cell components, including membranes, proteins, and nucleic acids *(1)*. The toxic effects of copper are demonstrated in another human genetic disorder, Wilson's disease (WD). This disease is characterized by excessive accumulation of copper in the liver, brain, and other organs and is fatal if untreated. All organisms have developed mechanisms to supply copper to essential enzymes without damaging cellular constituents and, in recent years, many of the molecules involved in copper homeostasis have been identified. Some interesting new mechanisms used by cells for handling this metal have been discovered. Two important steps forward in understanding the molecular basis of copper homeostasis were the isolation of the genes involved in human genetic disorders of copper—Menkes and Wilson's diseases. The coding sequences of these genes identified two important components of the copper homeostasis system, the copper ATPases, ATP7A and ATP7B. Genetic studies of micro-organisms, particularly yeast, have proven invaluable for the identification of some of the other molecules involved in cellular copper homeostasis, including copper-uptake molecules and intracellular copper carriers known as copper chaperones. The human orthologs of these genes have been isolated, demonstrating the generality of the copper-transport mechanisms.

This chapter will discuss the current knowledge of the molecular copper homeostatic mechanisms in mammals and the effect of the disruption of these mechanisms in the human genetic disorders of copper, Menkes and Wilson's diseases, and the animal models of these conditions. In addition, we will discuss some of the other copper-associated disorders, such as childhood copper-induced cirrho-

From: Handbook of Copper Pharmacology and Toxicology
Edited by: E. J. Massaro © Humana Press Inc., Totowa, NJ

ses, and the possibility that copper is a causative agent in neurological diseases such as the Alzheimer's disease and the prion diseases.

2. OVERVIEW OF COPPER HOMEOSTASIS IN HUMANS

2.1. Whole-Body Copper Homeostasis

There is a large body of early literature on the physiology of copper, which is now in the process of being reinterpreted in the light of the recent molecular advances. Here, we present only a brief summary of the overall process of copper transport; for more detailed information, the early work is well summarized in a number of reviews *(2–4)*. More recently, reviews incorporating the molecular advances have appeared *(5–7)*.

The amount of copper in the body is regulated by the rate of absorption of dietary copper across the intestinal epithelium vs the rate of excretion of copper into bile by hepatocytes. Although some regulation of copper status is achieved by alteration of the extent of absorption of dietary copper at the small intestine, changes in the rate of biliary excretion of copper appear to be principally responsible for overall copper balance. Figure 1 shows an outline of the major routes of copper in the body and the sites at which blocks occur in Menkes disease (MD) and Wilson's disease (WD).

Most dietary copper is absorbed in the small intestine (step 1, Fig. 1) and is transported across the basolateral membrane of the enterocyte into venules that collect into the portal vein *(2)*. This step is likely to involve the Menkes Cu-ATPase, ATP7A, because patients with Menkes disease accumulate copper within the intestinal epithelium. The regulation of absorption is discussed in more detail below (Section 2.3.). Once copper enters the blood, it either is bound to albumin *(8)*, complexed with histidine *(9)*, or attached to a macroglobulin termed transcuprein *(3)* and transported to the liver. The liver is a major player in copper homeostasis and rapidly removes most of the absorbed copper from the blood. About 50% of copper is taken up by the liver within 10 min of entry into the circulation *(10)*. Copper uptake by hepatocytes (step 2, Fig. 1) is a carrier-mediated process, not dependent on metabolic energy, and can occur from the copper–histidine complex *(11)*.

In the hepatocyte, copper is incorporated into the blue multicopper oxidase, ceruloplasmin *(2)*. The Wilson Cu-ATPase, ATP7B, is required for the incorporation of copper into ceruloplasmin; thus, this process is blocked in Wilson's disease (step 3a, Fig. 1) and low plasma ceruloplasmin is a feature of most patients with this disorder. Ceruloplasmin is the major copper protein in plasma and may play a part in supplying copper to tissues, a role supported, but not proven, by the finding of ceruloplasmin receptors in various tissues *(12)*. The role of ceruloplasmin in copper transport is still unclear, but the absence of any obvious disturbance of copper transport in the human disease, aceruloplasminemia, and the accumulation of iron in tissues of these patients suggest that the main role for this protein is in iron metabolism rather than copper transport *(13)*. If the amount of copper in the liver is excessive, copper is excreted in the bile (step 3b, Fig. 1). Biliary excretion of copper is the main regulatory step in maintaining overall copper homeostasis and requires ATP7B. Copper in the bile cannot be reabsorbed and is excreted in the feces *(2)*. The molecular basis of the regulation of biliary copper excretion is becoming clearer and is discussed in more detail later. Patients with WD have both defective biliary excretion and most do not incorporate copper into ceruloplasmin; thus, in this disease, copper accumulates in the liver to toxic levels.

Normally, very little copper is excreted in the urine, most apparently being resorbed in the kidney tubules (step 4, Fig. 1). In patients with WD, urinary copper secretion is elevated, presumably caused by copper release from the damaged liver *(4)*. In patients with Menkes disease and the mouse models of this disorder, copper becomes trapped in the proximal tubular cells of kidney, suggesting that ATP7A is required to pump the copper from these cells back into the circulation. This causes the apparently paradoxical situation of copper accumulation in some tissues of a patient suffering the effects of profound copper deficiency, but this copper is unavailable for the organ most sensitive to copper deprivation, the brain *(4,14)*. The copper concentration in the liver of Menkes patients is very

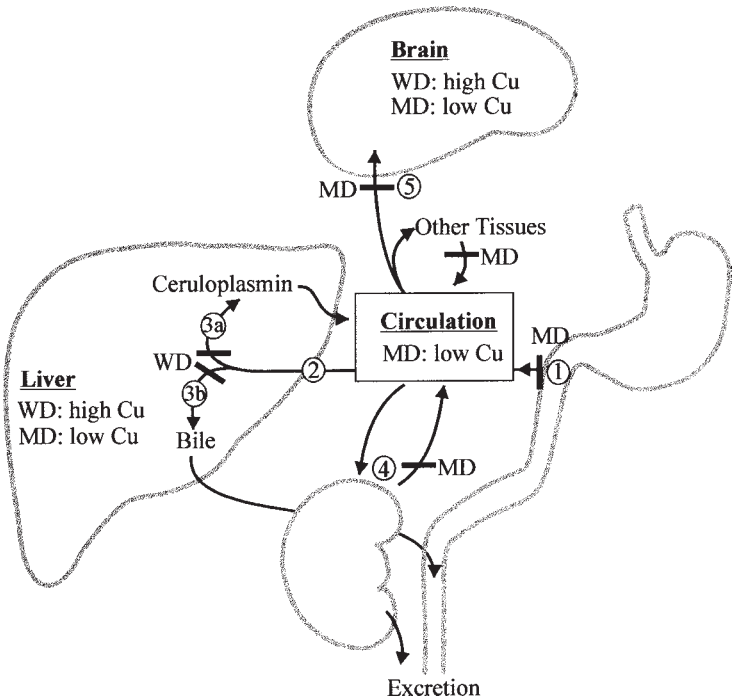

Fig. 1. An outline of the pathways of copper in the body and the blocks in Menkes (MD) and Wilson's disease (WD). Copper is absorbed in the small intestine (step 1) and the majority is taken up by the liver (step 2), which either incorporates the copper into ceruloplasmin (step 3a) that is secreted into the plasma, or if there is excess copper present, it is secreted into the bile (step 3b). Both steps 3a and 3b are defective in WD, leading to an accumulation of copper in the liver. Little copper is excreted in the urine, most is resorbed in the kidney tubules. In MD, blocks to copper transport occur at the small intestine, reducing the overall uptake of copper and across of the blood-brain barrier (step 4), resulting in a very low brain copper concentrations, which lead to severe neurological abnormalities. In addition, the efflux of copper from tissues to the circulation is blocked in MD, causing a paradoxical accumulation of copper even though the patient has a profound copper deficiency.

low, as ATP7B is functioning normally, providing what little copper is available for incorporation into ceruloplasmin.

The transport of copper into the brain (step 5, Fig. 1) is essential for normal brain development. To enter the brain, copper must traverse the vascular endothelial cells that comprise the blood-brain barrier. The requirement of ATP7A for this step has been directly demonstrated by the accumulation of copper in the astrocytes and vascular endothelium in the brain of mouse models of Menkes disease and ATP7A is expressed in these *(15)*. Thus, in human patients as well as in mutant mice, blood copper is probably trapped in the blood-brain barrier and not transported to neurones. The brain of patients with Menkes disease is severely copper deficient as a result of several blockages to copper transport: one at the small intestine, a second at the blood-brain barrier, and a third as a result of the entrapment of copper in peripheral tissues. The copper deficiency results in demylenation and other major neurological defects in these patients that are probably responsible for the fatal outcome of this disorder.

2.2. Cellular Copper Homeostasis

The underlying mechanisms of the physiological regulation of copper homeostasis are now becoming understood as a result of the advances in the molecular and cellular studies of the genes and proteins involved. An overriding principle that lies behind the types of mechanism that have been

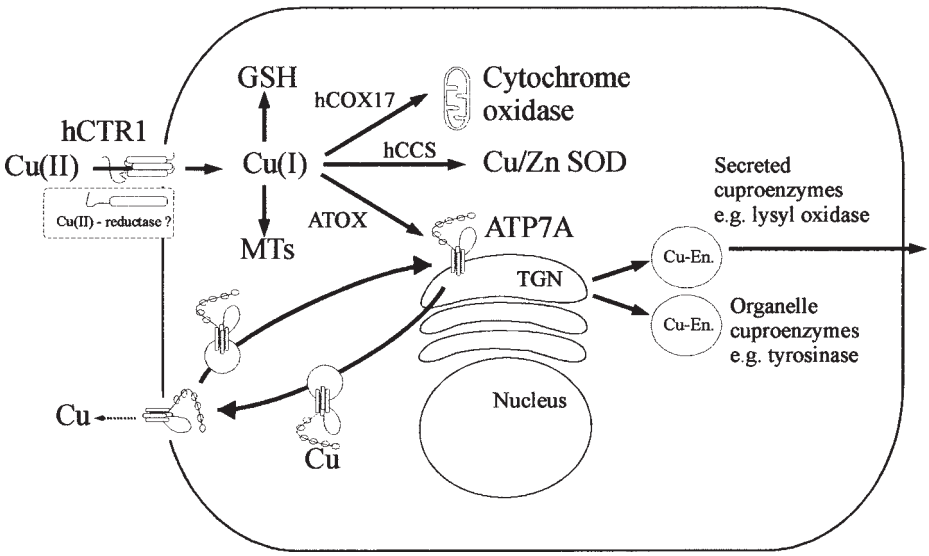

Fig. 2. Copper transport in a nonpolarized human cell such as a fibroblast. Copper enters the cell via the plasma membrane transporter, hCTR1, Cu(II) is thought to be reduced to Cu(I) by membrane reductases. As soon as copper enters the cell, it is distributed between the various copper chaperones, hCOX17, CCS, and ATOX 1, that carry the ion variously to the mitochondrion, Cu/Zn superoxide dismutase, or to ATP7A in the trans-Golgi network (TGN). ATP7A pumps copper into the TGN vesicles, where it is incorporated into secreted cuproenzymes, such as lysyl oxidase. ATP7A is constitutively recycling between the TGN and the plasma membrane, and the if copper levels in the cell increase, more ATP7A is found on the plasma membrane, allowing efflux of the metal ion. Cu(I) is also found on glutathione, and if the ATP7A-mediated efflux is insufficient to maintain low cytoplasmic copper levels, metallothioneins (MTs) are induced and bind the excess copper.

evolved to handle copper is the dual nature of copper in biological systems: Copper is both an essential cofactor for various Cu-dependent enzymes and a potential pro-oxidant. To function normally and to protect itself from potential damage a cell must be able to sense and respond to changes in intracellular copper levels. Different mechanisms will be activated in response to deficiency or excess as cells adopt an acquisition or detoxification mode depending on their copper status. Whole-body copper homeostasis depends on these mechanisms, which are modified in cells such as the intestinal enterocyte (acquisition) or the hepatocyte (detoxification). These modifications are discussed in more detail in Section 2.3. (*see* Figs. 3 and 4).

Much of our understanding of human cellular copper homeostasis has been gleaned from studies in yeast. Such comparisons have revealed a remarkable conservation of the molecules required for cellular copper homeostasis, but some important differences have been discovered. Figure 2 summarizes the current state of knowledge of copper homeostasis in a human cells such as a fibroblasts that require copper, but are not involved in the physiological regulation of whole-body copper status. Copper entry into the cell across the plasma membrane is mediated by the protein hCTR1 *(16)*. The human protein was identified following the discovery of the equivalent yeast protein Ctr1p encoded by the gene *CTR1*. In *Saccharomyces cerevisiae*, *CTR1* was discovered, paradoxically as a gene essential, not for copper transport but for iron transport *(17)*. This discovery provided a clear link between copper and iron transport that had been known for years but was not well understood. In *S. cerevisiae*, Cu is required for Fet3p, a multicopper oxidase related to the mammalian ceruloplasmin. Fet3p catalyzes the oxidation of $Fe2^{+}$ to $Fe3^{+}$, allowing entry of iron into the cell by a ferric transporter. The yeast Ctr1p is a 406-amino-acid protein with 3 putative transmembrane domains and has the motif M-X-X-M repeated 11 times in the extracellular (periplasmic) amino terminal domain

of the protein, these motifs presumably bind copper from the extracellular environment. The human ortholog is considerably smaller, consisting of 190 amino acids, and includes a methionine and histidine-rich N-terminal domain reminiscent of Ctr1p. hCTR1 also is thought to have three transmembrane domains but lacks much of the cytoplasmic region found in the yeast protein. This gene is expressed in all tissues so far examined, with liver, heart, and pancreas showing the highest levels of expression and the brain and muscle having the lowest levels. In yeast, Ctr1p specifically transports Cu(I); thus, a copper reductase is required on the plasma membrane to reduce the Cu(II) present in the oxidative extracellular environment. These reductases act on both Fe(III) and Cu(II), are known in yeast, and are products of the *FRE* genes (seven are known) *(18)*. It is unclear whether the transport of Cu(I) occurs by direct coupling of the reductases and Ctr1 at the plasma membrane. A reductase that uses NADH has been described in rat liver cells and may be required for mammalian plasma membrane copper transport *(19)*.

The potential pro-oxidant toxicity of copper necessitates that the Cu(I) ion be complexed at all times [copper is thought to be in the Cu(I) state in the cytoplasm]. It has been known for some time that intracellular copper is associated with glutathione (GSH) *(20)* and, after exposure of cells to excess copper, the small metal binding proteins metallothioneins (MTs) are induced *(21)*. More recently, experiments involving yeast mutants have uncovered a number of cytoplasmic copper carriers termed copper chaperones that accept and deliver copper to specific locations in the cell [reviewed in by Harrison et al. *(22)*]. Individual copper chaperones appear to be responsible for the specificity of delivery of copper to the different compartments of the cell, including the cytoplasm, the trans-Golgi network (TGN), and other less understood vesicles. The mechanisms whereby these chaperones are themselves loaded with copper and what determines the choice between the different chaperones once the copper enters the cell are unknown. Presumably, the regulation of the concentration of these chaperones is part of cellular copper homeostasis, but little is known about this process in mammalian cells.

The Cox17p chaperone in yeast has a role in delivering copper to mitochondria for incorporation into cytochrome oxidase *(23)*. Cox17p is a 69-amino-acid polypeptide present in the cytosol and the intermembrane space of the mitochondrion *(24)*. Inactivation of the *COX17* gene in yeast results in loss of cytochrome oxidase function as a result of a failure in the assembly of a functional multisubunit complex, leading to respiratory deficiency. The putative Cu-binding sites on Cox17p are tandem cysteine residues and two Cu(I) ions are bound in a binuclear cluster *(25)*. The human equivalent *COX17* has been identified by complementation of the cytochrome oxidase deficiency in a yeast strain with a null mutation in the *COX17* gene *(26)*. Little is known about the physiological role of the COX17 protein in mammalian cells, but a study of the expression patterns in rodent tissue show expression in a wide range of tissues, as expected from its role as a copper chaperone to cytochrome oxidase.

The copper chaperone for SOD1 (CCS, also known as LYS7 in yeast) transports copper to copper/zinc superoxide dismutase (SOD) and was identified by complementation of yeast mutant, which was SOD deficient but had an intact *SOD* gene *(27)*. In yeast, CCS is a 249-amino-acid protein that includes a single Cu-binding domain (MTCXXC) in the N-terminal region and the C-terminal half contains a domain with homology to SOD1. The human protein hCCS is 274 amino acids in length has 28% amino acid identity with the yeast protein *(27)*. An interaction with CCS and Cu/Zn SOD has been demonstrated and the localization of the two proteins in cells is identical, with a diffuse cytoplasmic and nuclear distribution *(28)*.

Another copper chaperone, Atx1 (antioxidant 1), was first identified as a suppressor of oxidative damage in yeast cells lacking SOD1 *(29)*. Atx1 is a 73-amino-acid cytosolic polypeptide with a singe amino terminal MTCXXC copper-binding motif. Atx1 binds one Cu(I) atom per polypeptide involving the thiol ligands of the two cysteines *(30)*. The Cu–Atx1 complex is proposed to move to the trans-Golgi network (TGN) where it interacts with the N-terminal MTCXXC residues of the yeast Menkes ortholog Ccc2 protein and copper is transferred by a series of two- or three-coordinate Cu-bridged

intermediates *(30)*. ATOX1 (formerly HAH1), the human ortholog of Atx1, has a 47% amino acid identity with Atx1 and contains an MTCXC domain *(31)*. ATOX1 is believed to transport copper from CTR1 to the Menkes and Wilson proteins in the TGN *(31)*.

The Menkes disease protein (ATP7A) and Wilson protein (ATP7B) are highly related copper-transporting P-type ATPases that have both biosynthetic and protective roles in cellular copper homeostasis in human cells under different copper conditions. During normal copper exposure, the Cu-ATPases are located in the TGN of the cell, where the metal is incorporated into various copper-dependent enzymes such as lysyl oxidase in fibroblasts (mediated by ATP7A as shown in Fig. 2) or ceruloplasmin in hepatocytes (mediated by ATP7B; *see* Fig. 4). If the copper levels in the cell start to rise, perhaps when the capacity of the copper chaperones is exceeded, a remarkable mechanism is activated that enables the cell to reduce its intracellular copper concentrations. This mechanism involves the Cu-induced trafficking of ATP7A and ATP7B to the plasma membrane of the cell (as shown in Fig. 2A for ATP7A) *(32)* or to a vesicular compartment (ATP7B; *see* Fig. 4A) *(33)*. In these locations, the excess copper can be effluxed from the cell or sequestered into a vesicle for later efflux. Because of its central role in copper homeostasis, the mechanism of copper-induced trafficking is of considerable interest and will be discussed in more detail in Section 2.3. Induction of the genes encoding the cysteine-rich metallothioneins (MTs), which avidly bind intracellular copper ions, provides a last line of defense against copper toxicity *(21)*. Presumably, this induction occurs when the capacity of the ATPases to efflux copper is insufficient to reduce the intracellular concentrations to a safe level.

2.3. Regulation of Copper Absorption and Excretion

The regulation of overall copper status of the body occurs by modification of the amount of dietary copper absorbed and the amount excreted in the bile. The uptake of dietary copper in the small intestine involves several main steps, each of which is a site of potential regulation: uptake, distribution and storage within the cell, and efflux across the basolateral membrane. The amount of copper absorbed from the diet has been found to depend on the copper content of the diet: When the dietary copper intake is very low, a high percentage is absorbed, and the amount absorbed is reduced as the copper content of the diet increases *(34)*. The molecular basis of this regulation is unclear, but a model can be proposed for the mechanism of copper uptake based on current knowledge of the components of cellular copper transport (Fig. 3A). It is possible that the main method of copper entry into the enterocyte involves hCTR1, which is expressed in the small intestine *(16)*. However, rats maintained on a diet containing only trace amounts of copper (<0.05 mg/kg) showed no increase in the level of *CTR1* mRNA in intestinal mucosa, suggesting that regulation of copper uptake does not involve changes in transcription of the *CTR1* gene. It is possible that copper regulation of CTR1 may occur by changes in location or levels of the protein, as in the Cu-dependent degradation of Ctr1p in *S. cerevisiae (35)*. Alternatively, the regulation of Cu uptake in response to copper availability may involve CTR1-independent mechanisms. For example, other transporters may contribute to copper uptake, such as the broad-specificity metal-ion transporter Nramp2 *(36)*, but such a system would not appear to have the specificity required for responses to changes in dietary intake of copper alone. High levels of dietary copper will induce the synthesis of metallothioneins to sequester the excess cytoplasmic copper. The metallothioneins may buffer the absorption of the metal, with the excess copper being eliminated when the epithelial cell is sloughed into the gut lumen. Such a mechanism has been suggested to underlie the reduction of copper absorption by high doses of zinc *(37)* used as a treatment for Wilson's disease *(38)*.

The transfer of copper across the basolateral membrane requires ATP7A, and as indicated in Fig. 3B, patients with Menkes disease accumulate copper in the enterocyte because this step is blocked. The copper then becomes associated with metallothioneins and is presumably lost when the enterocyte is sloughed off. The role, if any, of ATP7A in the normal regulation of copper uptake is unclear. The known copper-induced trafficking of the protein to the plasma membrane *(32)* would suggest that

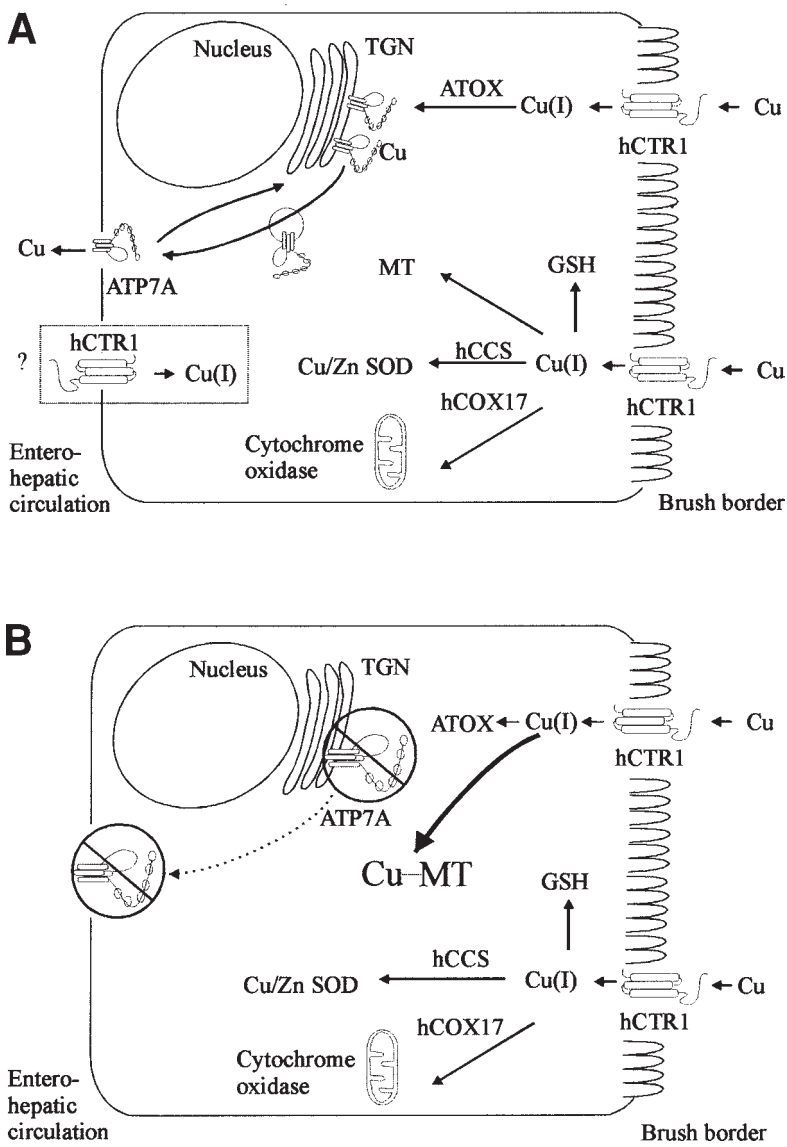

Fig. 3. **(A)** Model of copper transport in an intestinal enterocyte. Copper enters the cells via hCTR1 and it is possible that regulation of copper uptake is mediated by changes in the concentration or location of hCTR1. As with other cells, the copper is distributed within the cell by copper chaperones, but presumably a major pathway will be to ATP7A for the secretion of copper across the basolateral membrane. There is no definitive data on whether copper induces the movement of ATP7A to the basolateral membrane, but this is probable. It is not known whether the trafficking of ATP7A plays a part in regulating the amount of copper absorbed from the diet. **(B)** Model of copper transport in the enterocyte of an individual with Menkes disease. The absence of an active ATP7A results in accumulation of copper in the cell, as basolateral transport is not possible. The excess copper induces the transcription of MTs, which sequester the excess metal. This copper is lost to the body when the enterocyte sloughs off.

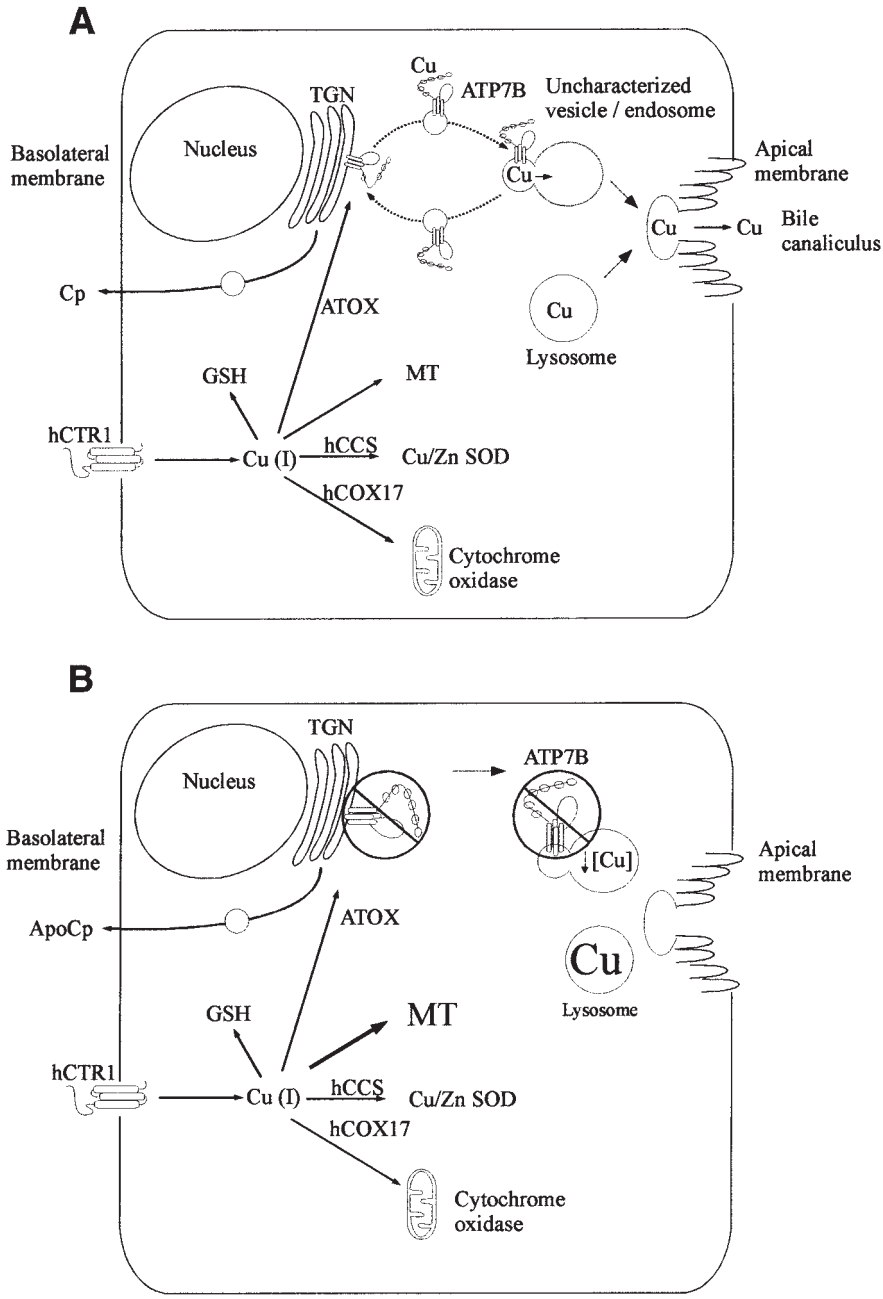

Fig. 4. **(A)** Copper-transport hepatocytes. The hepatocyte is the main regulator of copper efflux from the body, by means of copper transport across the biliary canalicular membrane (apical surface) of the hepatocyte. ATP7B is the main regulator of this process. When the liver copper concentration is low, ATP7B is located in the TGN, where it supplies copper to ceruloplasmin, which is secreted into the blood. If copper levels start to rise in the cytoplasm because of excess copper intake in the diet, ATP7B is induced to traffic to a vesicular compartment and possibly also to the apical membrane, pumping copper into vesicles that later discharge the copper into the bile. APT7B on the apical membrane may also pump copper directly out of the cell. If the dietary intake of copper is so high that the ATP7B-mediated efflux is insufficient, copper accumulates and induces metallothioneins. Some of this Cu–MT is taken up by lysosomes and some may be discharged by exocytosis into the bile. **(B)** Copper transport in hepatocytes of an individual with Wilson's disease. ATP7B is inactive, so no copper is incorporated in ceruloplasmin, leading to secretion of apoceruloplasmin (*continued*)

when copper levels are high in an enterocyte, ATP7A will be located on the basolateral membrane, presumably increasing copper uptake into the circulation. As this is contrary to the observed decrease in copper uptake when dietary levels are high, it may suggest that primary control over the amount of dietary copper absorbed is the modification of uptake across the apical surface, as discussed earlier. Nevertheless, the Cu-induced trafficking behavior of ATP7A in intestinal cells has not been reported and may show some differences from that observed in nonpolarized cells, so a possible role for ATP7A in regulating uptake cannot be excluded.

The liver is the primary regulator of copper status and this is achieved by modulation of the rate of biliary excretion, mainly mediated by ATP7B (Fig. 4A). This protein also delivers copper to ceruloplasmin in the TGN, thus explaining why patients with Wilson's disease have low biliary excretion of copper and usually have low levels of holoceruloplasmin in plasma (Fig. 4B). The liver removes excess copper by excretion in the bile and this mechanism is an important regulatory step in cases, such as an acute exposures to high copper, where the small-intestine regulatory mechanisms are insufficient or are too slow (e.g., induction of MT) to exclude the excess copper. The increased knowledge of the cell biology of ATP7B, discussed in Section 6., suggests that the increased copper efflux when the cell is exposed to excess copper is due to copper-induced trafficking of ATP7B to vesicles and/or the apical membrane of the hepatocyte, resulting in the efflux of copper into the bile. This efflux can be achieved either by exocytosis of the copper-laden vesicles or direct pumping of copper across the biliary canalicular membrane *(39)*, (Fig. 4A). Lysosomal exocytosis into the biliary canaliculae is thought to form part of the pathway for biliary excretion of copper *(40)*, but it is not clear whether these lysosomes described in this study correspond to the copper-loaded vesicles noted earlier. The exact details of this process are unclear, as there is still debate on whether ATP7B actually reaches the apical membrane *(41,42)*; nevertheless, the trafficking response of the protein is clearly the fundamental copper-sensing mechanism ultimately responsible for the increase in biliary copper excretion in copper-loaded animals.

When the dietary intake exceeds the capacity of the biliary excretion mechanisms, for instance as a result of dietary supplementation *(43)* or in Wilson's disease *(44)* (e.g., Fig. 4B), much of the excess metal is associated with MTs. In such copper-loaded livers, the copper also accumulates in lysosomes *(43)*. Glutathione appears to be involved in the biliary excretion of copper in copper-loaded livers *(39)*.

3. GENETIC COPPER-DEFICIENCY DISEASES

3.1. Features of the Genetic Copper Deficiencies

There are three clinically distinct X-linked copper deficiency disorders known in humans: classical Menkes disease (MD), occipital horn syndrome (OHS), and mild Menkes disease. All three are very rare diseases, with an estimated frequency of between 1 per 100,000 and 300,000 live births *(45)*. The rarity of these diseases, however, contrasts with the important role they continue to play in the understanding of copper homeostasis. Molecular analysis shows that all three genetic copper deficiencies result from mutations of *ATP7A*. A model proposing linking clinical phenotypes to the types of mutations in ATP7A has been recently proposed and is discussed later in more detail *(46)*.

The clinical features of MD were first described in 1962 by John Menkes *(47)*, and in 1972, David Danks realized that MD is a genetic copper-deficiency disorder, based on similar features found in copper-deficient sheep and pigs *(48)*. Patients with MD are profoundly copper deficient and usually die by the age of 3–4 yr. As noted previously (*see* Fig. 1), some tissues of MD patients have higher

Fig. 4. (*continued*) and low plasma levels of the protein. Biliary excretion is blocked, so intracellular copper accumulates to very high levels, inducing cytoplasmic metallothioneins, which, as the cell ages, are ingested by lysosymes and the cell develops Cu-laden lysosomes. Eventually, the cell's copper storage is exceeded and it dies from copper toxicity, the excess copper is released into the circulation, depositing in extrahepatic tissues, such as the brain.

than normal amounts of copper. For example, the kidney and gut may contain more than 10-fold higher concentrations of copper compared with normal. In contrast the brain has only 2% of total-body copper in Menkes patients compared with normal of 35%, emphasizing the severity of the deficiency of copper in this organ *(49)*. The phenomenon of copper accumulation in the presence of copper-deficiency symptoms is the result of normal cellular uptake of copper but reduced efflux *(4)*. As noted previously, cells that accumulate copper are those normally involved in the transport of copper, such as the small-intestine enterocytes and cells of the blood-brain barrier *(50)*, the proximal tubules of the kidney, and the placental cells of the affected fetus *(51)*. The small amount of copper absorbed from the diet by the patients gradually accumulates in these peripheral tissues, but is unavailable to the rest of the body. The liver of Menkes patients has very low copper concentrations compared with normal, and this reflects the overall copper deficiency of the patient—the liver does not accumulate copper, as ATP7A is only expressed at a low level in this organ and copper efflux is achieved by ATP7B.

A major clinical feature, and suspected eventual cause of death, of patients with MD is profound neurological abnormalities in the brain. These neurological defects are possibly caused by the low activity of cytochrome-*c* oxidase, a copper-dependent enzyme in the electron-transport chain. Low activity of other copper-dependent enzymes in the brain such as superoxide dismutase, peptidylglycine–α-amidating monooxygenase, and dopamine-β-hydroxylase may also contribute to the abnormalities *(14)*. MD patients also have connective tissue defects such as abnormalities of bone and weak vascular walls, resulting from reduced activity of lysyl oxidase. The connective tissue defects found in MD patients become the predominant features of the less severe condition, OHS. Lysyl oxidase is a copper-dependent enzyme that catalyzes the crosslinking of collagen and elastin, and the low activity of this enzyme is responsible for the aberrant connective tissue. Other clinical features of MD are caused by the low activity of specific cuproenzymes. Patients with MD are hypopigmented because of reduced activity of tyrosinase, a copper-dependent enzyme required for melanin synthesis. Hypothermia is also a feature of MD and is thought to be the result of low cytochrome-*c* oxidase activity. OHS patients have hyperelastic skin, arterial aneurisms, hernias, bladder diverticulae, and multiple skeletal abnormalities: Bony abnormalities of the occiput give rise to the name. Neurological abnormalities are not a feature of OHS although patients may be mildly mentally retarded. Another clinical phenotype, mild Menkes disease, has been described and a missense mutation in ATP7A has been identified in this patient *(52)*.

Cultured cells from Menkes patients accumulate copper and this property is used for prenatal diagnosis *(53,54)*. This excess copper results as a consequence of defective copper efflux from the cell *(55)*. Figure 5 shows the pattern of copper distribution in a fibroblast from a Menkes patient (compare to Fig. 1, a normal fibroblast). Efflux of copper from the cell cannot occur, because this step requires both an active ATP7A and copper-induced trafficking of ATP7A. A role for ATP7A in copper efflux was strongly supported by the increased rate of copper efflux observed in cultured cell lines that overexpress the Menkes gene *(56)*. Estimation of the rate of efflux of copper from cultured fetal cells is a more reliable method for prenatal diagnosis than simple cellular copper measurements *(55)*. The absence of an active ATP7A in the TGN explains the low activity of lysyl oxidase secreted by fibroblasts from MD patients *(57)* because the Menkes Cu-ATPase is required to pump copper across the TGN membrane. Cultured fibroblasts from patients with OHS also accumulate excess copper *(58)* and have defective copper efflux (Camakaris, unpublished data).

3.2. Treatment of Menkes Disease

Menkes disease patients have been treated by daily injections of copper salts or complexes, such as copper histidine *(59)*, but this treatment has not produced successful results in many patients *(14)*. In responding patients, Cu-therapy prolongs survival and results in clinical improvement, but treatment must be commenced as soon as possible after birth, before significant brain damage has occurred *(4,60,61)*. Even with early treatment, however, not all patients respond to therapy and Kaler has suggested that

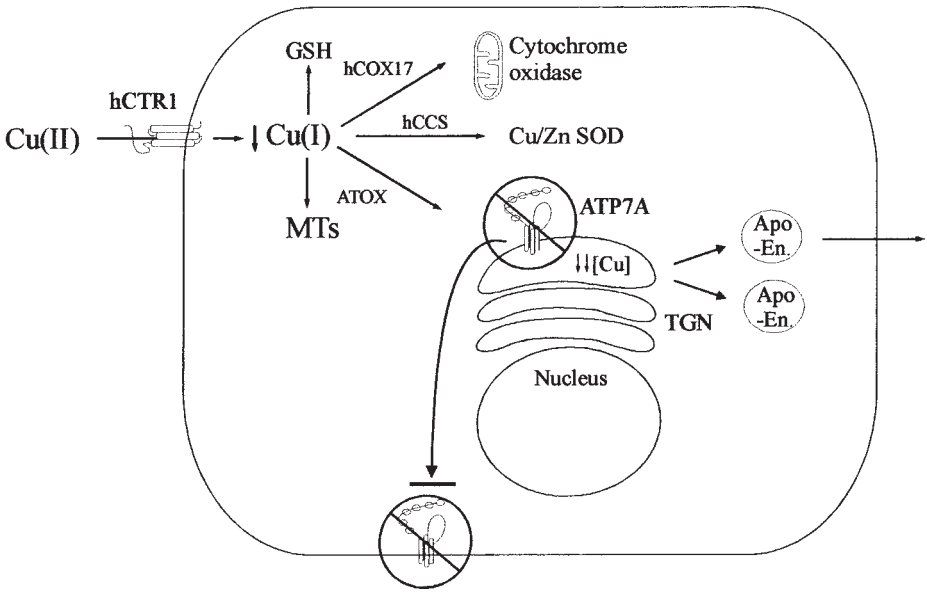

Fig. 5. Copper transport in a fibroblast from a Menkes disease patient. When cells are cultured in media with normal copper concentration, copper entry into the cell is normal, but efflux is blocked because of the absent ATP7A activity. The measurement of copper concentration in the cell or the rate of efflux of copper can be used for prenatal diagnosis of Menkes disease. The absence of ATP7A also prevents the incorporation of copper into secreted cuproenzymes, such as lysyl oxidase.

the responding patients are those who retain some residual ATP7A activity *(62)*. In patients who respond to therapy, the connective tissue abnormalities are not corrected and the patients acquire some of the clinical features of OHS *(60,61)*.

3.3. Mouse Models of Menkes Disease and Occipital Horn Syndrome

Mutations of the X-linked mottled locus (*Mo*) in mice result in varying degrees of copper deficiency and a diverse range of phenotypes. The mottled locus contains the gene *Atp7a*, the murine ortholog of *ATP7A (63,64)*. There are at least 21 known mutant alleles of the gene, and the mutant phenotypes can be divided into 4 broad groups: prenatal lethal, postnatal lethal, viable with mild generalized effects, and mild with pronounced connective tissue defects *(65)*. All except the prenatal lethal are models of the human genetic copper deficiencies. The brindled mouse (mutant allele: $Atp7a^{Mo\text{-}br}$) is a close homolog to classical MD, with most of the typical features of the human disorder; the affected male dies around 15 d after birth from the effects of profound copper deficiency. The blotchy mouse ($Atp7a^{Mo\text{-}blo}$) is viable and is a model of OHS. The copper deficiency in the blotchy mouse is less severe than in the brindled mouse, but the connective tissue abnormalities are more pronounced and lysyl oxidase levels in the blotchy mouse are lower than in the more severely affected brindled mouse *(66)*. The reason for the selective reduction of lysyl oxidase in the blotchy mouse and OHS has not been clarified, but a molecular explanation has been suggested *(46)* and is discussed in Section 7.1. The viable brindled mouse ($Atp7a^{Mo\text{-}vbr}$) is a possible model of mild Menkes disease, as this mouse has a less severe copper deficiency but does not exhibit the pronounced connective tissue defects seen in the blotchy mouse. The prenatal lethal mutants, which have no human equivalent, include the dappled ($Atp7a^{Mo\text{-}dp}$) mutant male, which dies between d 15 and d 17 of gestation. Mutations in *Atp7a* have been found in many of the mottled mutants, and these are discussed in Section 7.1.

Copper treatment of the brindled mouse prevents its death, provided that the copper is administered prior to 10 d postnatal *(67)*. The reason for the critical time period is not fully understood, but

there may be a critical copper-dependent period of brain development between 7 and 10 d in the mouse. It is thought that a similar critical period occurs in humans, and this would be consistent with the failure of copper therapy in older infants with Menkes disease *(4)*. Interestingly, the phenotypically very similar Jax-brindled mouse (*Atp7A*$^{mobr\text{-}J}$) does not appear to respond to copper therapy *(68)*; this difference is perhaps a clue to the variable success in treating MD patients *(65)*. A mutation in Atp7a has been found in the brindled mouse and is predicted to allow the formation of normal amounts of a partially functional protein *(69)*, which is consistent with Kaler's suggestion that the human MD patients who respond to therapy have some partially functional ATP7A *(70)*. Unfortunately, the mutation in the Jax-brindled mouse has not been described.

4. GENETIC COPPER-TOXICOSIS DISORDERS

4.1. Wilson's Disease

Wilson's disease (WD) is a genetic copper-toxicosis disorder affecting both the liver and central nervous system. In this disease, mutations of *ATP7B* result in reduction of biliary excretion of copper and low incorporation of copper into ceruloplasmin in the liver (Fig. 4B) *(4)*, but for unknown reasons, not all patients have low ceruloplasmin levels. Because the uptake of copper from the small intestine is normal in WD, the reduced copper excretion results in a net positive copper balance in the body and copper gradually accumulates to high concentrations in the liver *(4)*. The excess copper eventually causes severe liver damage, liver failure, and death. Copper also deposits in the brain, and neurological abnormalities are a major clinical feature of some patients. Disease symptoms appear at various ages, but rarely before the age of 5 yr; however, there are reported cases as young as 3 yr, which can be misdiagnosed because of the young age of the patient *(71)*. The neurological form of the disease usually presents during the teenage years. Attempts are being made to relate the type of mutation in *ATP7B* to the clinical phenotype and these will be discussed in Section 7.2. WD is commonly treated with the copper chelator penicillamine *(72)* or by reducing the uptake of copper in the small intestine with large doses of oral zinc *(73)*. In some cases, the use of the powerful copper chelator, ammonium tetrathiomolybdate, is proving to be a valuable alternative therapy *(74)*.

4.2. Other Possible Genetic Copper-Toxicosis Disorders

A group of similar childhood copper-toxicosis conditions have been described and are often associated with excess intake of copper in infancy. Indian childhood cirrhosis (ICC) is a fatal disease characterized by massive hepatic copper accumulation resulting from the consumption of milk containing high concentrations of copper. Since the practice of boiling milk in brass vessels has been discouraged, the disease is disappearing *(75)*. There is a high rate of parental consanguinity in families affected with this disease and up to 22% of siblings are affected, suggesting a genetic basis *(75)*. Clinically, ICC can be distinguished from Wilson's disease by the characteristic liver histology, early age of onset, normal ceruloplasmin and absence of neurological involvement *(75)*. Similar infantile copper-associated toxicity cases have been reported, and a clear autosomal recessive inheritance has been reported for the disease in Austria *(76)*. This disease is indistinguishable clinically from ICC and was found also to be the result of the consumption of milk that had been contaminated by copper. Like ICC, the disease has disappeared as the use of copper pots for boiling milk has declined. Mutations in ATP7B have been excluded as a causative factor *(77)*.

4.3. Animal Models of Wilson's Disease and ICC

There are two proven rodent models of WD, the Long–Evans Cinnamon (LEC) rat and the toxic milk (tx) mouse. The LEC rat accumulates high levels of hepatic copper in the first few months after birth *(78)* and this excess copper is the likely the cause of early-onset hepatitis. A deletion of the 3' portion of ATP7B has been reported thus demonstrating the LEC rat is a true model of WD *(79)*. Recent experiments have used this rat model to study the possibility of gene correction in WD *(80)*.

The autosomal recessive mutation toxic milk (*tx*) in mice causes the accumulation of hepatic copper in a similar manner to the LEC rat. The name, toxic milk, was derived from the observed death of pups suckling mutant dams and this was shown to be the result of copper-deficient milk produced by the mutant dam *(81)*. A missense mutation (met1356val) in the eighth transmembrane domain of the Atp7b in the *tx* mouse has been found, showing it to be a true model of WD *(82)*. Although this amino acid change does not appear particularly deleterious, it has been shown to severely affect the function of the protein *(83)*. A mouse "knockout" mutant with no detectable expression of Atp7b has been produced and has a phenotype very similar to that of the tx mouse *(84)*. The production of copper-deficient milk suggests that Atp7b has an important role in delivery of copper to milk, at least in the mouse. Consistent with this hypothesis, expression of Atp7b has been demonstrated in the mammary gland of mice, and the subcellular distribution of the protein in the tx mouse is abnormal *(85)*. Copper-deficient milk has not been reported in LEC rat dams or, indeed, in mothers with WD, and it would be of interest to further investigate whether the *tx* mouse is unique in this respect.

Two other animal models of copper toxicosis are of interest, normal sheep and a breed of dog, the Bedlington terrier. These animals accumulate hepatic copper and this phenotype may be the result of mutations of novel copper homeostasis genes, perhaps the orthologs of the gene that is involved in Austrian childhood cirrhosis. Sheep are prone to accumulate hepatic copper, because of a reduction in biliary copper excretion and, in this respect, sheep resemble patients with WD *(4)*. The molecular basis of this phenotype is unclear; however, sheep have two forms of ATP7B, one that closely resembles the protein in other mammals and an other that has a novel N-terminal extension of 79 amino acids *(86)*. It is possible that this novel form may play a part in the hepatic copper accumulation phenotype.

An autosomal recessive copper-toxicosis condition with many similarities to WD *(87)* is common in Bedlington terriers. Affected dogs accumulate hepatic copper due a defect in biliary excretion. Like WD, the disease is fatal if untreated, but can sometimes be controlled with penicillamine or high doses of zinc *(38)*. Unlike WD, however, plasma ceruloplasmin concentrations are normal and no neurological abnormalities have been detected *(87)*. Genetic mapping data excluded the possibility that a defect in the canine *ATP7B* gene was responsible for the copper toxicosis *(88)*.

5. ISOLATION OF THE GENES AFFECTED IN MENKES AND WILSON'S DISEASES

The Menkes gene was isolated by a positional cloning procedure based on a female with MD who had a balanced X:2 translocation chromosomal translocation *(89)*. The Menkes gene had been mapped to band Xq13.3 *(90)*, the site of the translocation breakpoint on the X chromosome. This observation together with the disease occurring in the female suggested that the translocation had disrupted the Menkes gene and the breakpoint was mapped to a 300-kb restriction fragment allowing cloning of the gene from YACs overlapping this region *(91–93)*. Three groups independently isolated cDNA clones from the Wilson's disease gene some using the YAC clones from the chromosomal region where Wilson's disease gene had been mapped, and primers based on the Menkes gene sequence *(94–96)*. These groups made the reasonable assumption, which proved to be correct, that the two genes might be related enough to allow polymerase chain reaction (PCR) amplification or probing of clones from the candidate YACs.

5.1. Structure and Expression of ATP7A and ATP7B Genes

The Menkes gene is large and complex, consisting of 23 exons, ranging from 77 to 4120 base pairs and spanning about 150 kb *(97,98)*. It encodes an mRNA of approximately 8.5 kb with a single open reading frame, with the ATG codon in exon 2 and the TAA stop codon in exon 23, followed by a 3.8-kb untranslated region. There is evidence for alternate splicing of the gene that may generate different 5' start sites *(99)*. An alternate form of mRNA lacking exon 10 is present in most tissues of normal

individuals *(97)*, which maintains the reading frame, although the protein product of this form lacks transmembrane domains 3 and 4 and has been shown to mislocalize to the endoplasmic reticulum *(100)*. The functional significance of this form is unclear, but a patient with OHS was shown to have the majority of his Menkes transcript as the exon 10 deleted form, suggesting that the corresponding protein may have some residual copper-transport activity *(101)*.

The Menkes gene is expressed in many tissues, although it is not an abundant mRNA: Northern blots have detected the message in kidney, lung, heart, brain, testis, gut mucosa, placenta, skeletal muscle, fibroblasts, lymphoblasts, and mammary gland carcinoma cells *(91–93,102,103)*. Very low levels of mRNA were found in mature liver, but in developing liver, the levels are much higher *(104)*, comparable to the kidney, but decline soon after birth *(102)*. High expression was detected in the choroid plexus of the brain. This observation and other evidence for expression of ATP7A in cells of the blood-brain barrier place this protein in position to regulate the entry of copper into the brain, consistent with the severe copper deficiency in the brain of Menkes patients *(105)*. A putative promoter region of the gene has been identified and a possible disease causing mutation was found *(106)*, but no detailed studies on the regulation of the promoter have appeared. There is no evidence that the expression of *ATP7A* is regulated by copper. In mouse tissues, no correlation of tissue copper levels and *Atp7a* expression was found *(102)*, and the gene has been found to be unresponsive to copper in cultured cells *(32)*.

The *ATP7B* gene has 21 exons and encodes an mRNA of 7.5 kb with a 162-base-pair 5' untranslated region *(107)*. The promoter of this gene has not been well characterized, but appears to have metal-regulatory elements resembling those found in metallothionein genes *(108)*, yet there is no evidence that this gene is copper responsive in mice *(82)*. The range of tissues expressing *ATP7B* is more restricted than *ATP7A*, but *ATP7B* is strongly expressed in the liver and to a lesser extent in kidney, brain, placenta, mammary gland and pancreas, intestine, hypothalamus, and ovary *(85,86,94,95)*. As noted for *ATP7A,* the expression pattern in the developing mammal differs from the adult with *ATP7B* showing a wider range of expression, perhaps suggestive of some specific function in the fetus *(104)*. Alternately spliced forms of *ATP7B* mRNA have been found. A shorter version of the protein has been detected in the cytosol *(109)*, and apparently brain-specific splicing has been reported *(110)*. A remarkable spliced form of the gene has been found expressed in the pineal gland and is regulated by light. Although the predicted protein lacks of all the N-terminal metal-binding sites, some copper-transport activity has been detected *(111)*. Further work is required to establish the significance of these alternate forms of the protein.

5.2. Structural Features of the ATP7A and ATP7B Proteins

The sequence of ATP7A predicts a 1500-amino-acid polypeptide and characteristic structural features identify it as a member of the extended family of transmembrane proteins known as P-type ATPases *(92)*. There are at least 80 known P-type ATPases found in all life forms. These enzymes are primarily involved in the ATP hydrolysis-dependent transmembrane movement of various cations, including H^+, Na^+, K^+, Ca^{2+}, and Mg^{2+} *(112)*. The term "P-type" refers to the existence of a high-energy phosphoryl-enzyme intermediate formed during the reaction cycle of ion translocation. The site of phosphorylation is an invariant aspartic acid in the sequence DKTG. ATP7B is predicted to be 1411 amino acids in length and is very similar to ATP7A with about 57% amino acid identity *(94)*. ATP7A and ATP7B are more similar to the bacterial heavy-metal-transporting P-type ATPases than to the classical mammalian ATPases that transport the alkali metals ions such as Ca^{2+} and Na^+. The cadmium transporter CadA has a very similar predicted structure to that of the Menkes protein *(113)* and bacterial copper-transporting P-type ATPases, CopA and CopB, have been described *(114,115)* as well as copper ATPases in yeast *(116,117)*. Hydrophobicity analysis of MNK predicts eight transmembrane domains *(92,118)*. The heavy-metal-transporting ATPases are distinct from the classical P-type ATPases in both membrane topology and primary sequence features. They have been classified as a subclass of the P-type ATPases, called P1-type ATPases or CPx type ATPases *(119,120)*.

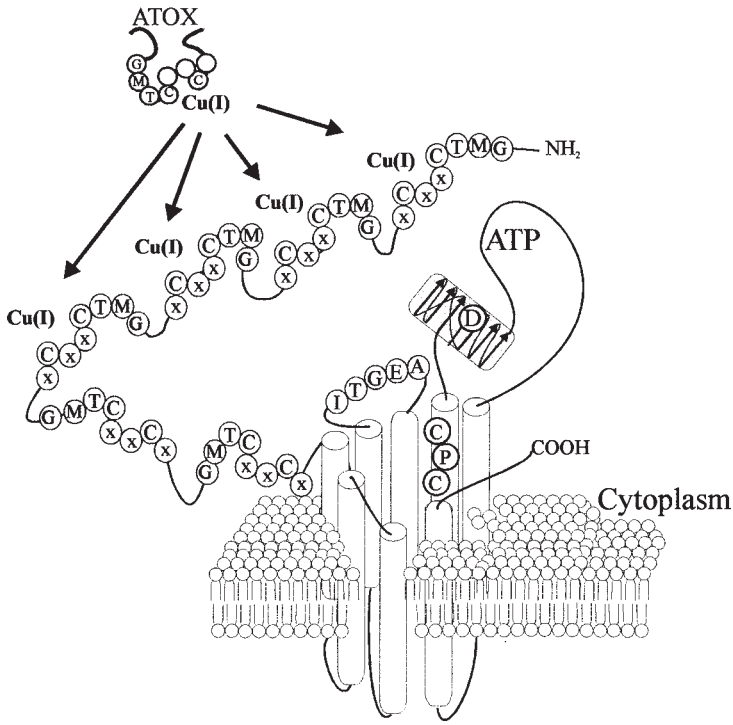

Fig. 6. Hypothetical three-dimensional representation of ATP7A/B based on the three-dimensional structure of the calcium ATPases *(121)*. The eight transmembrane domains are shown as cylinders traversing the lipid bilayer and forming a channel that allows copper to traverse the membrane. On the cytoplasmic side of the transmembrane channel, the cysteine residues in the CPC motif are thought to accept copper prior to translocation across the membrane. This copper is shown as coming from the N-terminal copper-binding sites, but the exact details of this transfer is unclear, and copper may also be directly available to the channel if concentrations are high in the cell. The metal-binding sites receive copper from the cytoplasmic chaperone ATOX1. The ATP-binding site in the large cytoplasmic loop is indicated (ATP) and the aspartic acid (D), which is phosphorylated, is shown as part of a β-pleated-sheet. The enzyme contains an endogenous phosphatase indicated by the motif ITGEA.

A hypothetical three dimensional representation of MNK is shown in Fig. 6, based on the recently described three-dimensional structure of the Ca^{2+} ATPase *(121)*. The eight transmembrane domains form a channel through which the copper traverses the membrane. As noted, all P-type ATPases have an ATP-binding site and an invariant aspartic acid residue (D in Fig. 6), which is phosphorylated and dephosphorylated during the reaction cycle of cation translocation. The CPC motif characteristic of heavy-metal P-type ATPases is indicated on the cytoplasmic edge of the channel. The cysteines are likely to bind copper during its translocation and are essential for the enzyme activity *(122)*. The proline is found in all P-type ATPases and is important for the conformational changes involved in cation transport. Evidence that ATP7A functions as a P-type ATPase was obtained using a vesicle assay for copper transport *(123)*, which showed that Cu transport was inhibited by orthovanadate, a specific inhibitor of P-type ATPases. The reaction only occurred in the presence of dithiothreitol, supporting the notion that Cu(I) is the ionic form of copper that is translocated. A major feature of the heavy-metal P-type ATPases is the presence of metal-binding sites (MBS) with a canonical sequence MTCXXC in the N-terminal region. ATP7A/B have six of these MBSs and the possible roles that these domains in accepting copper from the chaperone ATOX1 and regulating the trafficking of ATP7/B proteins is discussed next.

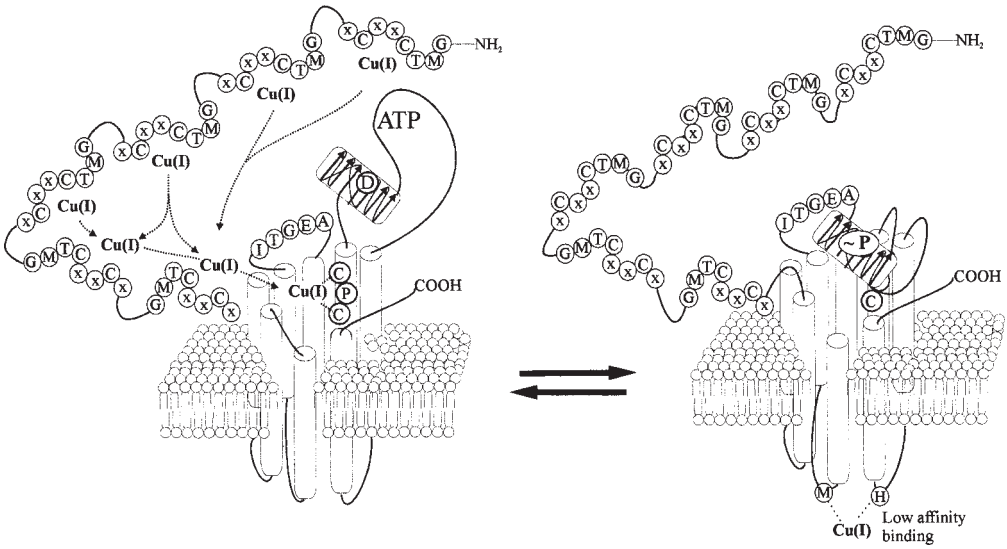

Fig. 7. Model of the conformational changes in ATP7A/B involved in Cu transport. The P-type ATPases undergo marked conformational changes associated with cation transport. Shown here are two basic forms of the enzyme, with copper bound to the high-affinity cytoplasmic site (CPC) and ATP bound to the enzyme (left diagram). Binding of copper to the metal-binding sites may induce conformational changes that facilitate the transfer of copper to the CPC site. Following phosphorylation of the aspartic acid, the high-affinity site is occluded and the copper is transported to the other side of the membrane, where it is bound to a low-affinity site (shown as methionines and histidines). The aspartic acid is dephosphorylated by the endogenous phosphatase and the enzyme returns to the original state.

Much of the understanding of the complex mechanism of ion transport catalyzed by these enzymes has come from the study of the calcium ATPases. This work has now reached the stage of an X-ray crystal structure at 2.6 A resolution *(121)*. Although the topology of the Cpx ATPases and the calcium ATPases differ, in that there are 8 transmembrane channels proposed for the former and 10 have been demonstrated in the latter, the fundamental ATPases core and reaction cycle are conserved. Thus, it is instructive to compare the two, particularly as the three-dimensional structure of the heavy-metal ATPases is not known. It is clear that P-type ATPases undergo considerable conformational changes during the reaction cycle, which can be distinguished by affinity for the metal ion, and various fluorescent changes. We have attempted to represent in Fig. 7the type of changes that may be involved. The binding of the cation to a high-affinity cytoplasmic site (CPC) allows the phosphorylation of the aspartic acid to form the phosphoenzyme, which has a distinct conformation that occludes the high-affinity cytoplasmic binding site and reveals a lower-affinity binding site on the luminal side. In this way, the cation is transferred across the membrane. The internal phosphatase removes the phosphate and the enzyme returns to the intial conformation, where the high-affinity binding site is exposed to the cytoplasm *(124)*. Commonly, only two conformational states are distinguished for P-type ATPases, E1 and E2; in the E1 state, the cation has access to the high-affinity cation-binding sites; for ATP7A, this the CPC in the channel and the corresponding region in the calcium ATPase is VAAIPE-309 forming the type-2 calcium binding site *(121)*. In the E2 state following the substantial conformation change consequent to the phosphorylation, the high-affinity site is occluded, and the metal is bound to the low-affinity sites *(125)*. For ATP7A, this low-affinity site could be the cluster of methionines and histidines on the luminal side (Fig. 7). The simplistic E1/E2 model has been criticized, in that the enzymes will certainly adopt more than just one conformation during the complete reaction cycle *(124)*. A deeper understanding of the conformational changes is necessary when

one attempts to understand the various disease phenotypes by consideration of the effects of disease-causing mutations at a molecular level and the mechanism of copper-induced trafficking of the copper ATPases, a mechanism that is a key part of cellular copper homeostasis. This process appears intimately tied to a unique feature of the mammalian Cu-ATPases, the six cytoplasmic copper-binding sites in the N-terminal region of the molecule.

Six copies of the metal-binding-site motif, MTCXXC are found in the N-terminal portion of MNK and have been shown to bind copper in vivo and in vitro *(126–128)* and a three-dimensional solution structure of MBS4 of ATP7A has been determined *(129)*. Interestingly, only one to three of these MBSs are present in the bacterial and yeast copper-ATPases *(115–117,130)* and in Cad A. Several studies have investigated the role of these MBSs in copper transport and there is significant disagreement as to whether they are essential for copper transport. Payne and Gitlin showed by progressive mutagenesis of the CXXC motifs of ATP7A to SXXS, a motif that cannot bind copper, that mutation of the first three MBSs abolished copper transport despite the presence of intact MBS4–6, suggesting that the first three MBS had a critical role *(131)*. In contrast, Forbes and Cox, using the same yeast complementation assay, found that only MBS6 of ATP7B was needed for copper-transport activity *(132)*. These conflicting results might indicate that there are fundamental differences between ATP7A and ATP7B in the way in which the six copper-binding sites function *(132)*. Although this seems inherently unlikely in view of the close relationship of the two proteins, there are differences between the two proteins in the N-terminal domain; for example, there is a 78-amino-acid deletion between the first and second metal-binding site in ATP7B relative to ATP7A. The effect of mutation of the copper-binding sites was assessed using an assay for Cu-ATPases in mammalian cell vesicles *(133)*. This work clearly demonstrated that Cu transport into vesicles did not require any of the MBSs; moreover, in whole cells expressing the mutant with all six Cu sites mutated, copper accumulated into vesicles. Previous work had demonstrated that this particular mutant ATP7A had lost its Cu-induced trafficking ability *(134)*. Thus, it appeared that copper accumulation was the result of an active transporter pumping copper into vesicles, but which could not subsequently traffic to the plasma membrane to allow copper release from the cell *(133)*.

At least a partial resolution to the discrepancies noted above has come from studies on the interaction of the copper chaperone, Atx1 in yeast and ATOX1 in mammals, with the N-terminal Cu-binding sites. Interestingly, these chaperones closely resemble a single copper-binding domain of the Cu-ATPases, having the same GMTCXXC motif. Atx1 has been shown to bind copper in a two- or three-coordinate metal cluster, and a direct interaction between Atx1 and the cytosolic domains of the yeast ortholog of ATP7A/B was demonstrated *(30)*. Thus, Atx1 accepts copper from the plasma membrane transporter, Ctr1, and transports the metal through the cytoplasm to CCC2, where the copper is transferred to the Cu site of CCC2 by a series of rapid associative changes involving two- and three-coordinate copper *(30)*. A model has been proposed in which the copper chaperones transfer copper to the N-terminal copper sites and the copper is subsequently donated to the metal at the CPC site in the channel *(132)*. Larin et al. *(135)* demonstrated that ATOX1 was capable of independent interaction with individual MBSs. MBS1–4 appeared to interact with roughly equal efficiency, but the last two, MBS5 and MBS6, failed to interact. Thus, the results indicate that the fifth and sixth metal-binding sites may well have a different function from the first four. Consistent with this differentiation of function between the metal-binding sites, Forbes et al. found that the first three metal domains (MBS1–3) could not replace MBS5 and MBS6 for copper transport *(132)*. In addition, the most recent studies on the stoichiometry of the copper binding to ATP7A suggest that four Cu(I) ions are bound in an environment shielded from solvent *(128)*. This study, however, did not identify which Cu sites were involved in the binding.

A possible model for integrating these observations is that ATOX1 delivers copper to the first four metal-binding sites, and the metal is subsequently transferred to MBS5 and MBS6, from where it is donated to the CPC in the channel, but direct donation of copper from other MBSs cannot be excluded. Some of the possible paths of copper movement between the MBSs and the CPC are indicated by

dotted lines in Fig. 7. These transfer processes are presumably occurring under normal physiological conditions (i.e., with cytoplasmic copper concentrations within the low to normal range). When cytoplasmic copper concentrations increase as a result of the exposure of the cell to elevated copper concentration, the capacity of the ATOX1 delivery system may be exceeded. Under such conditions, copper may be bound to low-molecular-mass ligands, such as glutathione, and delivered directly to the CPC residues in the channel. This mechanism would explain how an ATP7A molecule with all six copper-binding sites mutated could still pump copper into vesicles in cells exposed to high copper *(133)*.

Whatever the exact role of the various copper-binding sites in copper transport, it is clear that copper binding to this region causes significant conformational changes that are presumably related to the copper-transport cycle *(127,128)*. These changes might be linked, but not necessarily directly, to the conformational changes that accompany the metal transport through the channel. DiDonato et al. showed that a 70-kd fragment containing the six copper-binding domains of ATP7B underwent both secondary- and tertiary-structure changes upon copper binding *(127)*. It has been speculated by a number of authors that the presence of six Cu sites in these proteins may serve as some kind of sensor of the copper concentrations in the cell *(32,92)*. The conformational changes that the N-terminal region undergoes upon copper binding has been suggested to be part of the signaling mechanism that stimulates the copper-induced trafficking of ATP7A and ATP7B *(127,128,132)*. There is also evidence that the N-terminal region of ATP7B interacts with part of the cytoplasmic loop containing the ATP-binding site in a copper-dependent manner. This interaction was proposed to be part of the overall conformational changes in the protein that are involved in both copper transport and copper-induced trafficking *(136)*. To explore these ideas further, we now discuss the studies on the cell biology of ATP7A/7B and Cu-induced trafficking of these ATPases.

6. THE CELL BIOLOGY OF THE CU-ATPASES

Copper homeostasis mediated by both ATP7A/B is dependent on both copper-transport activity and the localization of these proteins to the correct cellular compartment. Both proteins have two major roles in copper homeostasis: delivery of copper to secreted cuproenzymes and efflux of copper from cells. One of the key questions to be answered once the genes were isolated was how a single protein could carry out these both of these functions. The answer to this question is that the dual role is achieved by the alteration of the location of the protein within the cell. The biosynthetic role is carried out when the proteins are in the TGN, and TGN localization has been demonstrated for both ATP7A *(32,137,138)* and ATP7B *(33,42)*. The efflux role occurs when the proteins are either located on the plasma membrane (ATP7A) *(32)* or on an intracellular vesicular compartment (ATP7B) *(33,42)*. When copper concentrations in the cell are in the normal physiological range, the proteins are found on the TGN, but exposure of cells to high concentrations of copper results in a relocalization of ATP7A within 30 min to the plasma membrane *(32)* or a compartment that may be the late endosome/subapical endosome in the case of ATP7B *(41,83)*. The relocalization of ATP7A was shown to be rapidly reversible when excess copper was removed and not to require new protein synthesis *(32)*. In this study, it was found that the concentration of ATP7A mRNA and protein did not change when cells were exposed to copper, suggesting that the ATP7A gene was not copper responsive. This aspect of copper homeostasis depended solely on a posttranslational mechanism: copper-induced trafficking.

The initial studies on the trafficking of ATP7A/B were carried out the nonpolarized Chinese hamster ovary cells, but in the physiological situation, these proteins will often function in polarized cells and this raised the question as to which membrane, apical or basolateral, the proteins are targeted. It is probable that ATP7A will traffic to the basolateral membrane; however, it has proven difficult to express ATP7A in polarized cells to prove this point (Petris, personal communication), so the membrane target of ATP7A remains to be established. For ATP7B, the situation is clearer; Roelofsen et al. *(41)* have provided convincing data that, in polarized cultured hepatocytes, this protein traffics in four stages:

(1) at low copper concentrations ATP7B is in the TGN; (2) within 30 min of exposure of the cells to copper, the protein is present in randomly distributed vesicular structures; (3) the vesicles appear to fuse and form clusters that accumulate at the apical pole of the cells; and (4) within 2–3 h, ATP7B is detected on the apical membrane. It is likely that stages 1–3 occur when ATP7B is expressed in nonpolarized Chinese hamster ovary cells, as ultrastructural studies have shown the presence of ATP7B on large vesicular structures that resemble late endosomes *(83)*. These large vesicles may well be equivalent to the subapical vesicles noted by Roelofsen et al. *(41)*. These conclusions, based on studies in cultured cells, are supported by the distribution of ATP7B in rat liver. Schaefer et al. found that in copper-deficient rats, ATP7B was localized in the TGN of hepatocytes, but when animals were copper loaded, the protein was distributed in multiple vesicular structures *(42)*, but these authors did not find any ATP7B on the canalicular membrane. Further evidence that trafficking of the Cu-ATPases is indeed a physiologically relevant process was provided by the finding that both ATP7A and ATP7B are located in the TGN of nonlactating breast tissue, but are redistributed to vesicular structures in the lactating tissue *(85,139)*. Although the physiological stimulus for the change in intracellular location of the proteins in the lactating gland has not been determined, these studies suggest that the trafficking of ATP7A/B is an important part of the delivery of copper into breast milk. The role of ATP7B in this process was suspected from the finding that milk produced by the toxic milk mouse mutant was copper deficient *(81)* and the Atp7B knockout mouse accumulated copper in the mammary gland *(84)*. Interestingly, the mutant Atp7B in the tx mouse does not relocalize in response to lactation (85), a behavior that is reminiscent of the lack of Cu-induced relocalization observed in a mutant forms of ATP7A found in cells from a patient with mild Menkes disease *(52)*. Indeed, a number of diverse mutations appear to prevent copper-induced trafficking of both ATP7A and ATP7B, but the reason for this is unclear *(140,141)*. The differential effects of mutations on copper transport and trafficking has the potential to generate diverse disease phenotypes, as will be discussed in Section 7.

The importance of Cu-induced trafficking in copper homeostasis has encouraged a number of studies to investigate the way in which copper may stimulate the movement of the protein. Attention has focused on the six metal-binding sites. These studies have used site-directed mutagenesis to alter the MBSs to a non-Cu-binding form (usually changing CXXC to SXXS) or by deletion of one or more of the metal-binding sites. With ATP7A Strausak et al. found that mutation of the first three MBSs did not have any appreciable effect on copper-induced trafficking, but that a molecule in which MBS1–3 were intact and MBS4–6 were mutated was incapable of relocalizing in high copper *(134)*. This work also showed that the first four MBSs could be deleted and the truncated molecule could still traffic in response to Cu. Work by Goodyer et al. showed that an ATP7A molecule with any one of the six MBSs intact could still undergo Cu-induced trafficking *(142)*, a result in apparent contradiction to the finding of Strausak et al. that the mutant with MBS1–3 intact could not traffic. The reason for this discrepancy is at present unclear. Both studies agree, however, that at least one intact MBS is necessary for the trafficking to occur. Although similar studies with ATP7B have yet to be reported, Roelofsen et al. have suggested that the binding of copper to one or more of the copper-binding sites may induce a change in conformation in the protein that exposes an apical targetting signal *(41)*. The same argument could be applied to ATP7A, but in this case, the signal may be a basolateral targeting signal. Discovery of such targeting signals, if they exist, will be an important advance in the analysis of the molecular basis of copper homeostasis.

The Cu-ATPases contain other protein motifs that are important for determining the cellular location of the proteins. Petris et al. and Francis et al. have shown that a dileucine motif in the C-terminal region of ATP7A is required for correct TGN localization *(143,144)*. Mutation of the dileucine to dialanine resulted in a molecule that was constitutively located on the plasma membrane. This effect was shown to be the result of the requirement of the dileucine for retrieval of ATP7A from the plasma membrane to the TGN (i.e., that the dileucine is an endocytic targeting motif). A trileucine motif is found in a corresponding region of ATP7B that may also be responsible for retrieval of this molecule,

but this has yet to be demonstrated. A 38-amino-acid sequence in transmembrane 3 of ATP7A was identified as a Golgi localization signal, presumably necessary for the retention of the protein in the TGN *(100)*. Use of ATP7A labeled with a c-myc epitope tag showed that the molecule is undergoing constitutive recycling from the TGN to the plasma membrane, even in basal copper *(145)*. Importantly in the presence of copper, the endocytosis of the protein was not inhibited, suggesting that the mechanism of copper-induced trafficking was not the result of the inhibition of endocytosis, but stimulation of exocytosis. Full characterization of Cu-induced trafficking, the interplay of the various targeting motifs, and the importance of conformational changes in these processes promise to be a fascinating area of investigation for numbers of years to come. Indeed, further characterization of the processes responsible for docking, trafficking, and protein retrieval from the plasma membrane and vesicles and the effect of mutations on these processes will be crucial to the understanding of the regulation of copper homeostasis and the clinical effects of mutations in these molecules.

7. MOLECULAR BASIS FOR THE VARIABLE CLINICAL PHENOTYPES IN MENKES DISEASE

Many mutations causing classical MD and the milder variants have been identified *(146)*. The classical disease appears to result when mutations prevent the formation of any functional protein; for example, partial or complete deletions of *ATP7A* are found in about 15% of MD patients *(93)*, and the disease-causing missense mutations are the result of amino acid changes that would be expected to cause major disruption to the protein, such as large charged residues occuring in the hydrophobic transmembrane domains, indicating that the disease is caused by complete loss of ATP7A activity *(147)*. RNA splicing abnormalities are quite common in classical Menkes disease and usually result in complete loss of normal *ATP7A* mRNA. Other mutations found include premature stop codons, frame shifts, and nonsense mutations *(147)*. In one patient with mild MD, a missense mutation in transmembrane domain 7 has been found. The mutant protein was located in the TGN, but, surprisingly, did not relocate to the plasma membrane in response to Cu *(52)*. The milder course of the disease suggests that the mutant protein retains some Cu-transport activity. One possible explanation for the clinical features of this patient (mild neurological effects and mild connective tissue disease) could be the localization of a partially active protein in the TGN able to deliver sufficient Cu to lysyl oxidase. Thus, OHS does not develop, but because of the defective trafficking of the protein, the distribution of copper in the body is still abnormal *(46)*.

All cases of OHS so far described have been the result of splice-site mutations that still permit the production of small amounts of normal protein *(148)*. A possible explanation for the pronounced connective tissue defects is that the ability of the cells to efflux copper is reduced because of the amount of active ATP7A is so small. Thus, exposure of the cell to only a small amount of copper (even the amount of copper in a Cu-deficient patient) is sufficient to raise the intracellular copper enough to induce relocalization of the protein to the plasma membrane *(46)*. If so, even in quite low copper concentrations, no ATP7A would be found in the TGN; hence, copper is not supplied to lysyl oxidase.

Thus, the variable clinical phenotype resulting from mutations of ATP7A can be explained by a combination of the different effects mutations can have on the protein function, such as reduction in copper-transport activity, altered intracellular location, and defective trafficking in response to copper.

7.1. Mutations of Atp7a in the Mottled Mice

Similar conclusions about the molecular basis of the different phenotypes observed in the mottled mouse mutants have emerged from the studies of the mutations in these mice. The murine ortholog of ATP7A was obtained in 1994 and mRNA abnormalities of the expression of MNK in a number of the mottled mutants was demonstrated *(63,64)*. Subsequent work has identified mutations in *Atp7a* in most of the mottled mutants. The main difference between the murine and human diseases is that

complete loss of Atp7a activity has a more severe effect in the mouse, resulting in prenatal lethality. This difference may suggest that the mouse has a greater requirement for copper at a critical phase of development than humans and, thus, is more sensitive to reduction in the activity of Atp7a. There is a quite diverse range of mutations that cause prenatal lethality in mice *(65)*. The first of the prenatal-lethal mutants to be described was the dappled mouse *(149)* and, subsequently, the causative mutation was found in the *Atp7a* promoter, explaining the lack of *Atp7a* mRNA *(150)*. Other mutations causing prenatal lethality are A1364D missense mutation in mottled 11H in which a charged residue is placed in transmembrane domain 7, and a severe splice-donor-site mutation *(151)*. The viable brindled mouse is a possible model for mild Menkes disease *(65)* and is caused by a mutation K1037T adjacent to the invariant aspartic acid that is phosphorylated. Presumably, this mutation causes a reduction in phosphorylation, rather than complete abolition; otherwise, the disease would be more severe. In the closest mouse model of Menkes disease, there is a deletion of two amino acids in the first cytoplasmic loop of the Atp7a *(69)*. Normal amounts of protein are present in cells and tissues of the mouse, but the protein does not traffic when cells are exposed to copper *(140)*. This result demonstrates that the mutation has a severe effect on the trafficking function of the protein, but, presumably, the protein must retain some copper-transport activity, otherwise the mutant male would die *in utero*. The presence of a partially active transporter fixed in the TGN would explain why lysyl oxidase activity in the brindled mouse can be restored by copper treatment *(66)*.

Two higher molecular-weight forms of *Atp7a* mRNA in addition to mRNA of the normal size have been detected in tissues of the blotchy mouse *(63,64)* and a mutation of the minor splice signals were found in the *Atp7a* gene, which is presumably responsible for the aberrant splicing *(152)*. Trace amounts amount of Atp7a have been detected in Western blots of blotchy mouse fibroblasts *(140)*. As noted earlier, similar mild splice-site mutations have been found in OHS patients, supporting the concept that mutations in *ATP7A* that allow a small amount (perhaps less than 2%) of normal protein to be produced result in pronounced connective tissue abnormalities *(148)*. As previously noted, if this residual ATP7A were located on the plasma membrane even when cells are exposed to normal or low copper concentrations, lysyl oxidase would not receive any copper *(46,140)*. This model explains why, in contrast to the brindled mouse, copper treatment of the blotchy mutant does not restore lysyl oxidase activity.

7.2. Molecular Basis of the Phenotypic Variability in Wilson's Disease

The age of onset of WD varies from 2 to more than 40 yr, and patients can present with either hepatic or neurological symptoms. Some WD patients have normal plasma ceruloplasmin, but most have low levels. The reason for this variable presentation is unclear, but some indication has been obtained by analysis of the types of mutation found in patients. A study of WD has demonstrated a wide range of mutations, although, in contrast to MD, large deletions of ATP7A have not been found in patients *(71)*. Over 200 mutations have been described and are listed in a database (http://www.medgen.med.ualberta.ca/database). In North America, 38% of WD chromosomes harbor the His1069Gln mutation and other population groups have different common mutations. The correlation between genotype and phenotype is complicated by the fact that many WD patients are compound heterozygotes (i.e., they carry different ATP7B mutations on each chromosome 13). Patients who are homozygous for severe mutations have an earlier onset of disease and are sometimes not recognized as WD because of this fact *(71)*. In some cases, the alternate splicing appears to have allowed splicing out of the exon containing a severe mutation resulting in a milder phenotype *(153)*. Milder mutations may present with later-onset neurological disease *(153)*. Similar to MD variants, mutations that cause mislocalization of the protein or changes in Cu-induced trafficking may result in distinct phenotypes, such as WD patients with normal ceruloplasmin *(141)*. The clinical severity of WD might also be influenced by environmental factors, such as the amount of copper ingested, or allelic variants of modifying genes, such as metallothioneins. Such factors could explain why the common His1069Gln mutations is associated with a range of clinical presentations *(154)*.

8. COPPER AND NEURODEGENERATIVE DISEASES

Some very interesting recent findings have linked copper to various devastating neurological conditions and a common theme that emerges is the possibility of Cu-induced free-radical production leading to neuronal damage. Amyotrophic lateral sclerosis (ALS), a neurodegenerative disease affecting motor neurones, leads to progressive muscular weakness, atrophy, and death. An autosomal dominant form of ALS is caused by mutations in Cu/Zn superoxide dismutase (SOD). It appears that the disease results from a gain of function of Cu/Zn SOD, associated with abnormal forms of the protein in which copper is bound in a manner that allows the generation of reactive oxygen species *(155)*. Alzheimer's disease is a progressive neurodegenerative disease characterized by amyloid plaques and neuronal cell loss. A major constituent of the plaques is the amyloid-β protein (APP). APP is a copper-binding molecule and can reduce Cu(II) to Cu(I) *(156)*; it may be involved in copper transport in neurones, so potentially mutations in this protein could lead to increased Cu(I) and associated free-radical generation *(156)*. Disturbances of copper metabolism have been noted in Alzheimer's patients, and may result in toxic gain of function through the interaction of copper with APP and toxicity as a result of the action of copper, and APP has been demonstrated in cultured neurones *(157)*. These finding have led to suggestions that Alzheimer's disease could possibly be treated with copper chelators, and preliminary trials with a mouse model of the disease have shown that the copper chelator bathocuprein promotes solubilization of amyloid aggregates *(158)*. The infectious prion proteins (PrPSc) that are the causative agents in Creutzfeld–Jakob disease, kuru, fatal familial insomnia, and "mad cow disease" are toxic conformational variants of a normal cellular protein (PrPC). The normal physiological role of the prion protein is unkown, but it has been observed that it binds copper *(159)* and that it recycles between the plasma membrane and endosomes *(160)*. The conformation of the prion protein has been shown to be altered by binding of metal ions, including copper *(161)*, and copper has been shown to facilitate the formation of the protease-resistant infectious confomer PrP^{Sc} *(162)*. These observations suggests both that the prion protein may normally function in copper homeostasis and that the interaction of copper with the infectious form may be part of the causation of the disease. Parkinson disease appears to be associated with abnormalities of iron and copper. Patients have reduced levels of ceruloplasmin in their cerebrospinal fluid and this might be related to the raised iron levels in the basal ganglia, as ceruloplasmin is needed for iron mobilization *(163)*.

9. CONCLUSIONS

The study of copper transport has clearly entered a new era with the isolation of the genes affected in Menkes and Wilson's diseases and the study of the protein products encoded by these genes. Analysis of the mutations that cause MD and WD is aiding understanding of the molecular basis of the various disease phenotypes and is assisting prenatal diagnosis. In addition, studies on the function of ATP7A and ATP7B are revealing new aspects of copper transport and new trafficking mechanisms that are of general interest to cell biologists. There is still much to be discovered about the complex functions of the copper ATPases, and the next few years should yield some fascinating insights into the detailed role that these molecules play in the delicate balance that is needed for copper homeostasis. The discovery of the intracellular copper chaperones has provided a major leap forward in understanding of the distribution of copper within the cell. Many questions, however, remain to be answered before the full details of copper homeostasis in humans are resolved. Little is known about the targeting of copper within cells or the signals directing copper proteins to various locations in the cell. How are the cell membranes protected from copper damage? How is copper distribution around the body regulated? An area that we have not discussed in this chapter in any detail is the delivery of copper to the fetus and neonate and the effect of mutations on this process. This is an important area of investigation because the growing mammal is at most risk of copper deficiency, but is also very sensitive to copper toxicity. What role is copper actually playing in the

neurological diseases discussed in the last section? Are there other copper-related diseases yet to be recognized, because of mutations in the various copper chaperones or other components of the copper homeostatic system? Despite these and many other questions, in contrast to even 10 yr ago, it is possible to believe that within another 10 yr the answers to these questions will be found and the molecular basis of copper transport will be substantially worked out. One can confidently expect that the discovery of gene(s) involved in the childhood copper-associated cirrhosis conditions, the Bedlington terrier, and the reason for the copper sensitivity of the sheep will be discovered and new genes will be added to the growing cast of players involved in copper homeostasis. The links between the molecules regulating cellular copper homeostasis and the physiological and pathophysiological effects of copper should be clarified. We hope that these discoveries will be accompanied by corresponding improvements in the treatments of the various disorders involving this essential but dangerous element.

REFERENCES

1. Kumar, S., Rowse, C., and Hochstein, P. (1978) Copper-induced generation of superoxide in human red cell membrane. *Biochem. Biophys. Res. Commun.* **83,** 587–593.
2. Linder, M. C. (1991) *Biochemistry of Copper*. Biochemistry of the Elements (Frieden, E., ed.), Plenum, New York.
3. Linder, M. C., Lomeli, N. A., Donley, S., Mehrbod, F., Cerveza, P., Cotton, S., et al. (1999) Copper transport in mammals. *Adv. Exp. Biol. Med.* **448,** 1–16.
4. Danks, D. M. (1995) Disorders of copper transport, in *The Metabolic and Molecular Basis of Inherited Disease*, 7th ed. (Scriver, C. R., Beaudet, A. L., Sly, W. M., and Valle, D., eds.), McGraw-Hill, New York, Vol. 1, pp. 2211–2235.
5. Harris, E. D. (2000) Cellular copper transport and metabolism. *Annu. Rev. Nutr.* **20,** 291–310.
6. Vulpe, C. D. and Packman, S. (1995) Cellular copper transport. *Annu. Rev. Nutr.* **15,** 293–322.
7. Pena, M. M. O., Lee, J., and Thiele, D. J. (1999) A delicate balance: Homeostatic control of copper uptake and distribution. *J. Nutr.* **129,** 1251–1260.
8. Owen, C. A. (1965) Metabolism of radiocopper (Cu64) in the rat. *Am. J. Physiol.* **209,** 900–904.
9. Harris, D. I. M. and Sass-Kortsak, A. (1967) The influence of amino acids on copper uptake by rat liver slices. *J. Clin. Invest.* **46,** 659–677.
10. Sass-Kortsak, A. (1965) Copper metabolism. *Adv. Clin. Chem.* **8,** 24–31.
11. McArdle, H. J. (1992) The transport of copper across the cell membrane: different mechanisms for different metals? *Proc. Nutr. Soc.* **51,** 199–209.
12. Goode, C. A., Dinh, C. T., and Linder, M. C. (1989) Mechanism of copper transport and delivery in mammals: review and recent findings. *Adv. Exp. Med. Biol.* **258**, 131–144.
13. Harris, Z. L., Takahashi, Y., Miyajima, H., Serizawa, M., MacGillivray, R. T., and Gitlin, J. D. (1995) Aceruloplasminemia: molecular characterization of this disorder of iron metabolism. *Proc. Natl. Acad. Sci. USA* **92,** 2539–2543.
14. Kaler, S. G. (1994) Menkes disease. *Adv. Pediatr.* **41,** 262–303.
15. Murata, Y., Kodama, H., Mori, Y., Kobayashi, M., and Abe, T. (1998) Mottled gene expression and copper distribution in the macular mouse, an animal model for Menkes disease. *J. Inherited Metab. Dis.* **21,** 199–202.
16. Zhou, B. and Gitschier, J. (1997) hCTR1: a human gene for copper uptake identified by complementation in yeast. *Proc. Natl. Acad. Sci. USA* **94,** 7481–7486.
17. Dancis, A., Yuan, D. S., Haile, D., Askwith, C., Elde, D., Moehle, C., et al. (1994) Molecular characterization of a copper transport protein in *S. cerevisiae*: an unexpected role for copper in iron transport. *Cell* **76,** 393–402.
18. Hassett, R. and Kosman, D. J. (1995) Evidence for Cu(II) reduction as a component of copper uptake by *Saccharomyces cerevisiae*. *J. Biol. Chem.* **270,** 128–134.
19. van den Berg, G. J., and Mc Ardle, H. J. (1994) A plasma membrane NADH oxidase is involved in copper uptake by plasma membrane vesicles isolated from rat liver. *Biochim. Biophys. Acta* **1195,** 276–280.
20. Freedman, J. H., Ciriolo, M. R., and Peisach, J. (1989) The role of glutathione in copper metabolism and toxicity. *J. Biol. Chem.* **264**, 5598–5605.
21. Hamer, D. H. (1986) Metallothionein. *Ann. Rev. Biochem.* **55**, 913–951.
22. Harrison, M. D., Jones, C. E., Solioz, M., and Dameron, C. T. (2000) Intracellular copper routing: the role of copper chaperones. *Trends Biochem. Sci.* **25,** 29–32.
23. Glerum, D. M., Shtanko, A., and Tzagoloff, A. (1996) Characterization of COX17, a yeast gene involved in copper metabolism and assembly of cytochrome oxidase. *J. Biol. Chem.* **271**, 14,504–14,509.
24. Beers, J., Glerum, D. M., and Tzagoloff, A. (1997) Purification, characterization and localization of yeast Cox17p, a mitochondrial copper shuttle. *J. Biol. Chem.* **272**, 33,191–33,196.
25. Srinivasan, C., Posewitz, M. C., George, G. N., and Winge, D. R. (1998) Characterization of the copper chaperone Cox17 of *Saccharomyces cerevisiae*. *Biochemistry* **37,** 7572–7577.
26. Amaravadi, R., Glerum, D. M., and Tzagoloff, A. (1997) Isolation of a cDNA encoding the human homolog of COX17, a yeast gene essential for mitochondrial copper recruitment. *Hum. Genet.* **99,** 329–333.

27. Culotta, V. C., Klomp, L. W. J., Strain, J., Casareno, R. L. B., Krems, B., and Gitlin, J. D. (1997) The copper chaperone for superoxide dismutase. *J. Biol. Chem.* **272,** 23,469–23,472.
28. Casareno, R. L. B., Waggoner, D., and Gitlin, J. D. (1998) The copper chaperone CCS directly intereacts with copper/zinc superoxide dismutase. *J. Biol. Chem.* **273**, 23,625–23,628.
29. Lin, S.-J., Pufahl, R. A., Dancis, A., O'Halloran, T. V., and Culotta, V. C. (1997) A role for the *Saccharomyces cerevisiae ATX1* gene in copper trafficking and iron transport. *J. Biol. Chem.* **272**, 9215–9220.
30. Pufahl, R. A., Singer, C. P., Peariso, K. L., Lin, S.-L., Schmidt, P. J., Fahrni, V., et al. (1997) Metal ion chaperone function of the soluble Cu(I) receptor Atx1. *Science*, **278**, 853–856.
31. Klomp, L. W., Lin, S.-J., Yuan, D. S., Klausner, R. D., Culotta, V. C., and Gitlin, J. D. (1997) Identification and functional expression of HAH1, a novel human gene involved in copper homeostasis. *J. Biol. Chem.* **272**, 9221–9226.
32. Petris, M. J., Mercer, J. F. B., Culvenor, J. G., Lockhart, P., Gleeson, P. A., and Camakaris, J. (1996) Ligand-regulated transport of the Menkes copper P-type ATPase efflux pump from the Golgi apparatus to the plasma membrane: a novel mechanism of regulated trafficking. *EMBO J.* **15,** 6084–6095.
33. Hung, I. H., Suzuki, M., Yamaguchi, Y., Yuan, D. S., Klausner, R. D., and Gitlin, J. D. (1997) Biochemical characterization of the Wilson's disease protein and functional expression in the yeast *Saccharomyces cerevisiae*. *J. Biol. Chem.* **272,** 21,461–21,466.
34. Turnlund, J. R., Keyes, W. R., Peiffer, G. L., and Scott, K. S. (1998) Copper absorption, excretion and retention by young men consuming low dietary copper determined by using the stable isotope ^{65}Cu. *Am. J. Clin. Nutr.* **67,** 1219–1225.
35. Ooi, C. E., Rabinowich, E., Dancis, A., Bonifacino, J. S., and Klausner, R. D. (1996) Copper-dependent degradation of the *Saccharomyces cerevisiae* plasma membrane copper transporter Ctr1p in the apparent absence of endocytosis. *EMBO J.* **15,** 3515–3523.
36. Gunshin, H., Mackenzie, B., Erger, U. V., Gunshin, Y., Romero, M. F., Boron, W. F., et al. (1997) Cloning and characterization of a mammalian proton-coupled metal-ion transporter. *Nature* **388,** 482–488.
37. Hall, A. C., Young, B. W., and Bremner, I. (1979) Intestinal metallothionein and the mutual antagonism between copper and zinc in the rat. *J. Inorg. Biochem.* **11,** 57–66.
38. Brewer, G. J., Yuzbasiyangurkan, V., Lee, D. Y., and Appelman, H. (1989) Treatment of Wilson's disease with zinc. 6. Initial treatment studies. *J. Lab. Clin. Med.* **114**, 633–638.
39. Nederbragt, H. (1989) Effect of the glutathione-depleting agents diethylmaleate, phorone and buthionine sulfoximine on biliary copper excretion in rats. *Biochem. Pharmacol.* **38**, 3399–3406.
40. Gross, J. B., Jr., Myers, B. M., Kost, L. J., Kuntz, S. M., and LaRusso, N. F. (1989) Biliary copper excretion by hepatocyte lysosomes in the rat. Major excretory pathway in experimental copper overload. *J. Clin. Invest.* **83**, 30–39.
41. Roelofsen, H., Wolters, H., Van Luyn, M. J. A., Miura, N., Kuipers, F., and Vonk, R. J. (2000) Copper-induced apical trafficking of ATP7B in polarized hepatoma cells provides a mechanism for biliary copper excretion. *Gastroenterology* **119,** 782–793.
42. Schaefer, M., Hopkins, R. G., Failla, M. L., and Gitlin, J. D. (1999) Hepatocyte-specific localization and copper-dependent trafficking of the Wilson's disease protein in the liver. *Am. J. Physiol.* **276,** G639–G646.
43. Evering, W. E. N. D., Haywood, S., Bremner, I., and Trafford, J. (1991) The protective role of metallothionein in copper-overload: I. Differential distribution of immunoreactive metallothionien in copper-loaded rat liver and kidney. *Chem.–Biol. Interact.* **78,** 283–295.
44. Elmes, M. E., Clarkson, J. P., Mathy, N. J., and Jasani, B. (1989) Metallothionein and copper in liver disease with copper retention—a histopathological study. *J. Pathol.* **158,** 131–137.
45. Tonnesen, T., Kleijer, W. J., and Horn, N. (1991) Incidence of Menkes disease. *Hum. Genet.* **86,** 408–410.
46. Mercer, J. F. B. (2001) The molecular basis of copper transport diseases. *Trends Mol. Med.* **7,** 64–69.
47. Menkes, J. H., Alter, M., Stegleder, G. K., Weakley, D. R., and Sung, J. H. (1962) A sex-linked recessive disorder with retardation of growth, peculiar hair, and focal cerebral and cerebellar degeneration. *Pediatrics* **29,** 764–779.
48. Danks, D. M., Campbell, P. E., Stevens, B. J., Mayne, V., and Cartwright, E. (1972) Menkes's kinky hair syndrome: an inherited defect in copper absorption with wide-spread effects. *Pediatrics* **50,** 188–201.
49. Horn, N., Heydorn, K., Damsgaard, E., Tygstrup, I., and Vestermark, S. (1978) Is Menkes syndrome a copper storage disorder? *Clin. Genet.* **14,** 186–187.
50. Kodama, H. (1993) Recent developments in Menkes disease. *J. Inherited Metab. Dis.* **16,** 791–799.
51. Xu, G. Q., Yamano, T., and Shimada, M. (1994) Copper distribution in fetus and plaenta of the macular mutant mouse as a model of Menkes kinky hair disease. *Biol. Neonate* **66,** 302–310.
52. Ambrosini, L. and Mercer, J. F. B. (1999) Defective copper-induced trafficking of the Menkes protein in patients with mild and copper-treated classical Menkes disease. *Hum. Mol. Genet.* **8,** 1547–1555.
53. Camakaris, J., Danks, D. M., Ackland, L., Cartwright, E., Borger, P., and Cotton, R. G. H. (1980) Altered copper metabolism in cultured cells from human Menkes' syndrome and mottled mouse mutants. *Biochem. Genet.* **18,** 117-131.
54. Horn, N. (1976) Copper incorporation studies on cultured cells for prenatal diagnosis of Menkes disease. *Lancet* **1,** 1156–1158.
55. Camakaris, J., Danks, D. M., Phillips, M., Herd, S., and Mann, J. R. (1982) Copper metabolism in Menkes' syndrome and mottled mouse mutants, in *Inflammatory Diseases and Copper* (Sorenson, J. R. J., ed.), Humana, Totowa, NJ, pp. 85–96.
56. Camakaris, J., Petris, M., Bailey, L., Shen, P., Lockhart, P., Glover, T. W., et al. (1995) Gene amplification of the Menkes (MNK; ATP7A) P-type ATPase gene of CHO cells is associated with copper resistance and enhanced copper efflux. *Hum. Mol. Genet.* **4,** 2117–2123.

57. Royce, P. M., Camakaris, J., and Danks, D. M. (1980) Reduced lysyl oxidase activity in skin fibroblasts from patients with Menkes' syndrome. *Biochem. J.* **192,** 579–586.
58. Peltonen, L., Kuivaniemi, H., Palotie, A., Horn, N., Kaitila, I., and Kivirikko, K. I. (1983) Alterations in copper and collagen metabolism in the Menkes syndrome and a new type of the Ehrlers–Danlos syndrome. *Biochemistry* **22,** 6156–6163.
59. Sarkar, B., Lindertat-Walsh, K., and Clarke, J. T. (1993) Copper-histidine therapy for Menkes disease. *J. Pediatr.* **123,** 828–830.
60. Tümer, Z., Horn, N., Tonnesen, T., Christodoulou, J., Clarke, J. T. R., and Sarkar, B. (1995) Early copper–histidine treatment for Menkes disease. *Nature Genet.* **12,** 11–13.
61. Christodoulou, J., Danks, D. M., Sarkar, B., Baerlocher, K. E., Casey, R., Horn, N., et al. (1998) Early treatment of Menkes disease with parenteral copper-histidine: long-term follow-up of four treated patients. *Am. J. Med. Genet.* **76,** 154–164.
62. Kaler, S. G. (1996) Menkes disease mutations and response to early copper histidine treatment. *Nature Genet.* **13,** 21–22.
63. Levinson, B., Vulpe, C., Elder, B., Martin, C., Verley, F., Packman, S., et al. (1994) The mottled gene is the mouse homologue of the Menkes disease gene. *Nature Genet.* **6,** 369–373.
64. Mercer, J. F. B., Grimes, A., Ambrosini, L., Lockhart, P., Paynter, J. A., Dierick, H., et al. (1994) Mutations in the murine homologue of the Menkes disease gene in dappled and blotchy mice. *Nature Genet.* **6,** 374–378.
65. Mercer, J. F. B., Ambrosini, L., Horton, S., Gazeas, S., and Grimes, A. (1999) Animal models of Menkes disease. *Adv. Exp. Biol. Med.* **448,** 97–108.
66. Royce, P. M., Camakaris, J., Mann, J. R., and Danks, D. M. (1982) Copper metabolism in mottled mouse mutants. *Biochem. J.* **202,** 369–371.
67. Mann, J. R., Camakaris, J., Danks, D. M., and Walliczek, F. G. (1979) Copper metabolism in mottled mouse mutants 2. Copper therapy of brindled (Mobr) mice. *Biochem. J.* **180,** 605–612.
68. Kelley, E. J. and Palmiter, R. D. (1996) A murine model of Menkes disease reveals a physiological function of metallothionein. *Nature Genet.* **13,** 219–222.
69. Grimes, A., Hearn, C., Lockhart, P., Newgreen, D., and Mercer, J. F. B. (1997) Molecular basis of the brindled mouse mutant (Mo^{br}): a murine model of Menkes disease. *Hum. Mol. Genet.* **6,** 1032–1042.
70. Kaler, S. G., Das, S., Levinson, B., Goldstein, D. S., Holmes, C. S., Patronas, N. J., et al. (1996) Successful early copper therapy in Menkes disease associated with a mutant transcript containing a small in-frame deletion. *Biochem. Mol. Med.* **57,** 37–46.
71. Thomas, G. R., Forbes, J. R., Roberts, E. A., Walshe, J. M., and Cox, D. W. (1995) The Wilson's disease gene: spectrum of mutations and their consequences. *Nature Genet.* **9,** 210–216.
72. Walsh, J. M. (1973) Copper chelation in patients with Wilson's disease. *Q. J. Med.* **42,** 441–450.
73. Brewer, G. J., Yuzbasiyan-Gurkan, V., and Young, A. B. (1987) Treatment of Wilson's disease. *Semin. Neurol.* **7,** 209–220.
74. Brewer, G. J., Dick, R. D., Johnson, V., Wang, Y., Yuzbasiyan-Gurkan, V., Kluin, K., et al. (1994) Treatment of Wilson's disease with ammonium tetrathiomolybdate. *Arch. Neurol.* **51,** 545–554.
75. Pandit, A. and Bhave, S. (1996) Present interpretation of the role of copper in Indian childhood cirrhosis. *Am. J. Clin. Nutr.* **63**, 830S–834S.
76. Muller, T., Feichtinger, H., Berger, H., and Muller, W. (1996) Endemic Tyrolean infantile cirrhosis: an ecogenetic disorder. *Lancet* **347,** 877–880.
77. Wijmenkga, C., Muller, T., Murli, I. S., Brunt, T., Feichtinger, H., Schonitzer, D., et al. (1998) Endemic Tyrolean infantile cirrhosis is not an allelic variant of Wilson's disease. *Eur. J. Hum. Genet.* **6,** 624–628.
78. Li, Y., Togashi, Y., Sato, S., Emoto, T., Kang, J.-H., Takeichi, N., et al. (1991) Spontaneous hepatic copper accumulation in long-evans cinnamon rats with hereditary hepatitis: a model of Wilson's disease. *J. Clin. Invest.* **87,** 1858–1861.
79. Wu, J., Forbes, J. R., Chen, H. S., and Cox, D. W. (1994) The LEC rat has a deletion in the copper transporting ATPase homologous to the Wilson's disease gene. *Nature Genet.* **7,** 541–545.
80. Terada, K., Aiba, N., Yang, X.-L., Iida, M., Nakai, M., Miura, N., et al. (1999) Biliary excretion of copper in LEC rat after introduction of copper transporting P-type ATPase, ATP7B. *FEBS Lett.* **448,** 53–56.
81. Rauch, H. (1983) Toxic milk, a new mutation affecting copper metabolism in the mouse. *J. Heredity* **74,** 141–144.
82. Theophilos, M., Cox, D. W., and Mercer, J. F. B. (1996) The toxic milk mouse is a murine model of Wilson's disease. *Hum. Mol. Genet.* **5**, 1619–1624.
83. La Fontaine, S., Theophilos, M. B., Firth, S. D., Parton, R. G., and Mercer, J. F. B. (2001) Effect of the tx mutation on the intracellular localization of the murine Wilson Cu-ATPases (Wnd). *Hum. Mol. Genet.* **10,** 361–370.
84. Buiakova, O. I., Xu, J., Lutsenko, S., Zeitlin, S., Das, K., Das, S., et al. (1999) Null mutation of the murine ATP7B (Wilson's disease) gene results in intracellular copper accumulation and late-onset hepatic nodular transformation. *Hum. Mol. Genet.* **8**, 1665-1671.
85. Michalczyk, A. A., Rieger, J., Allen, K., Mercer, J. F. B., and Ackland, M. L. (2000) Defective trafficking of the Wilson's disease protein ATP7B in the mammary gland of the toxic milk mouse. *Biochem. J.* **352,** 565–571.
86. Lockhart, P. J., Wilcox, S. A., Dahl, H.-H. M., and Mercer, J. F. B. (2000) Cloning, mapping and expression analysis of the sheep Wilson's disease gene homologue. *Biochim. Biophys. Acta* **1491,** 229–239.
87. Su, L.-C., Ravanshad, S., Owen, C. A., McCall, J. T., Zollman, P. E., and Hardy, R. M. (1982) A comparison of copper loading disease in Bedlington terriers and Wilson's disease in humans. *Am. J. Physiol.* **243,** G226–G230.
88. van de Sluis, B. J. A., Breen, M., M., N., van Wolferen, M., de Jong, P., Binns, M. M., et al. (1999) Genetic mapping of the copper toxicosis locus in Bedlington terriers to dog chromosome 10, in a region syntenic to human chromosome region 2p13–p16. *Hum. Mol. Genet.* **8**, 501–507.

89. Kapur, S., Higgins, J. V., Delp, K., and Rogers, B. (1987) Menkes syndrome in a girl with X-autosome translocation. *Am. J. Med. Genet.* **26,** 503–510.
90. Tumer, Z., Tommerup, N., Tonnesen, T., Kreuder, J., Craig, I. W., and Horn, N. (1992) Mapping of the Menkes locus to Xq13.3 distal to the X-inactivation center by an intrachromosomal insertion of the segment Xq13.3–q21.2. *Hum. Genet.* **88,** 668–672.
91. Mercer, J. F. B., Livingston, J., Hall, B. K., Paynter, J. A., Begy, C., Chandrasekharappa, S., et al. (1993) Isolation of a partial candidate gene for Menkes disease by positional cloning. *Nature Genet.* **3,** 20–25.
92. Vulpe, C., Levinson, B., Whitney, S., Packman, S., and Gitschier, J. (1993) Isolation of a candidate gene for Menkes disease and evidence that it encodes a copper-transporting ATPase. *Nature Genet.* **3,** 7–13.
93. Chelly, J., Tumer, Z., Tonnerson, T., Petterson, A., Ishikawa-Brush, Y., Tommerup, N., et al. (1993) Isolation of a candidate gene for Menkes disease that encodes a potential heavy metal binding protein. *Nature Genet.* **3,** 14–19.
94. Bull, P. C., Thomas, G. R., Rommens, J. M., Forbes, J. R., and Cox, D. C. (1993) The Wilson's disease gene is a putative copper transporting P-type ATPase similar to the Menkes gene. *Nature Genet.* **5,** 327–337.
95. Tanzi, R. E., Petrukhin, K., Chernov, I., Pellequer, J. L., Wasco, W., Ross, B., et al. (1993) The Wilson's disease gene is a copper transporting ATPase with homology to the Menkes disease gene. *Nature Genet.* **5,** 344–350.
96. Yamaguchi, Y., Heiny, M. E., and Gitlin, J. D. (1993) Isolation and characterization of a human liver cDNA as a candidate gene for Wilson's disease. *Biochem. Biophys. Res Commun.* **197,** 271–277.
97. Dierick, H. A., Ambrosini, L., Spencer, J., Glover, T. W., and Mercer, J. F. B. (1995) Molecular structure of the Menkes disease gene (ATP7A). *Genomics* **28,** 462–469.
98. Tumer, Z., Vural, B., Tonnesen, T., Chelly, J., Monaco, A. P., and Horn, N. (1995) Characterization of the exon structure of the Menkes disease gene using vectorette PCR. *Genomics* **26,** 437–442.
99. Harris, E. D., Reddy, M. C., Qian, Y., Tiffany-Castiglioni, E., Majumdar, S., and Nelson, J. (1999) Multiple forms of the Menkes Cu-ATPase. *Adv. Exp. Med. Biol.* **448,** 39–51.
100. Francis, M. J., Jones, E. E., Levy, E. R., Ponnambalam, S., Chelly, J., and Monaco, A. P. (1998) A golgi localization signal identified in the Menkes recombinant protein. *Hum. Mol. Gen.* **7**, 1245–1252.
101. Qi, M. and Byers, P. H. (1998) Constitutive skipping of alternatively spliced exon 10 in the ATP7A gene abolishes Golgi localization of the Menkes protein and produces the occipital horn syndrome. *Hum. Mol. Genet.* **7,** 465–469.
102. Paynter, J. A., Grimes, A., Lockhart, P., and Mercer, J. F. B. (1994) Expression of the Menkes gene homologue in mouse tissues: lack of effect of copper on the mRNA levels. *FEBS Lett.* **351,** 186–190.
103. Ackland, L. M., Cornish, J., Paynter, J. A., Grimes, A., Michalczyk, A., and Mercer, J. F. B. (1997) Expression of Menkes (ATP7a) and Wilson (ATP7b) disease genes in mammary carcinoma cells. *Biochem. J.* **328**, 237–243.
104. Kuo, Y.-M., Gitschier, J., and Packman, S. (1997) Developmental expression of the mouse mottled and toxic milk genes suggests distinct functions for the Menkes and Wilson's disease copper transporters. *Hum. Mol. Genet.* **6,** 1043–1049.
105. Qian, Y., Tiffany-Castiglioni, E., Welsh, J., and Harris, E. D. (1998) Copper efflux from murine microvascular cells requires expression of the Menkes disease Cu-ATPase. *J. Nutr.* **128,** 1276–1282.
106. Levinson, B., Conant, R., Schnur, R., Das, S., Packman, S., and Gitschier, J. (1996) A repeated element in the regulatory region of the MNK gene and its deletion in a patient with occipital horn syndrome. *Hum. Mol. Genet.* **5,** 1737–1742.
107. Petrukhin, K., Lutsenko, S., Chernov, I., Ross, B. M., Kaplan, J. H., and Gilliam, T. C. (1994) Characterization of the Wilson's disease gene encoding a copper transporting ATPase: genomic organization, alternative splicing, and structure/function predictions. *Hum. Mol. Genet.* **3,** 1647–1656.
108. Oh, W. J., Kim, E. K., Park, K. D., Hahn, S. H., and Yoo, O. J. (1999) Cloning and characterization of the promoter region of the Wilson's disease gene. *Biochem. Biophys. Res. Commun.* **259,** 206–211.
109. Yang, X., Kawardada, Y., Terada, K., Petrukhin, K., Gilliam, T. C., and Sugiyama, T. (1997) Two forms of Wilson's disease protein produced by alternative splicing are localized in distinct cellular compartments. *Biochem. J.* **326,** 897–902.
110. Petrukhin, K., Fischer, S. G., Pirastu, M., Tanzi, R. E., Chernov, I., Devoto, M., et al. (1993) Mapping, cloning and genetic characterization of the region containing the Wilson's disease gene. *Nature Genet.* **5,** 338–343.
111. Borjigin, J., Payne, A. S., Deng, J., Li, X., Wang, M. M., Ovodenko, B., et al. (1999) A novel pineal night-specific ATPase encoded by the Wilson's disease gene. *J. Neurosci.* **19**, 1018–1026.
112. Kuhlbrandt, W., Auer, M., and Scarborough, G. A. (1998) Structure of the P-type ATPases. *Curr. Opin. Struct. Biol.* **8,** 510–516.
113. Silver, S., Nucifora, G., Chu, L., and Misra, T. K. (1989) Bacterial resistance ATPases: primary pumps for exporting toxic cations and anions. *Trends Biochem. Sci.* **14,** 76–80.
114. Solioz, M., Odermatt, A., and Krapf, R. (1994) Copper pumping ATPases: common concepts in bacteria and man. *FEBS Lett.* **346,** 44–47.
115. Odermatt, A., Suter, H., Krapf, R., and Solioz, M. (1993) Primary structure of two P-type ATPases involved in copper homeostasis in *E. hirae*. *J. Biol. Chem.* **268,** 12,775–12,779.
116. Fu, D., Beeler, T. J., and Dunn, T. M. (1995) Sequence, mapping and disruption of CCC2, a gene that cross-complements the Ca^{2+} sensitive phenotype of csg1 mutants and encodes a P-type ATPase belonging to the Cu^{2+} ATPase subfamily. *Yeast* **11,** 283–292.
117. Rad, M. R., Kirchrath, L., and Hollenberg, C. P. (1994) A putative P-type Cu^{2+} transporting ATPase on chromosome II of *Saccharomyces cerevisiae*. *Yeast* **10,** 1217–1225.
118. Vulpe, C., Levinson, B., Whitney, S., Packman, S., and Gitschier, J. (1993) Isolation of a candidate gene for Menkes disease and evidence that it encodes a copper-transporting ATPase. *Nature Genet.* **3,** 273.

119. Solioz, M. and Vulpe, C. (1996) CPX-type ATPases: a class of P-type ATPases that pump heavy metals. *Trends Biochem. Sci.* **21,** 237–241.
120. Lutsenko, S. and Kaplan, J. H. (1995) Organization of P-type ATPases: significance of structural diversity. *Biochemistry* **34,** 15,607–15,613.
121. Toyoshima, C., Nakasako, M., Nomura, H., and Ogawa, H. (2000) Crystal structure of the calcium pump of sarcoplasmic reticulum at 2.6 A resolution. *Nature* **405,** 647–655.
122. Forbes, J. R. and Cox, D. W. (1998) Functional characterization of missense mutations in ATP7B: Wilson's disease mutation or normal variant? *Am. J. Hum. Genet.* **63,** 1663–1674.
123. Voskoboinik, I., Brooks, H., Smith, S., Shen, P., and Camakaris, J. (1998) ATP-dependent copper transport by the Menkes protein in membrane vesicles isolated from cultured Chinese hamster ovary cells. *FEBS Lett.* **438,** 178–182.
124. Jencks, J. P. (1989) How does a calcium pump pump calcium. *J. Biol. Chem.* **264,** 18,855–18,858.
125. MacLennan, D. H., Clarke, D. M., Loo, T. W., and Skerjanc, I. S. (1992) Site-directed mutagenesis of the Ca^{2+} ATPase of sarcoplasmic reticulum. *Acta Physiol. Scand.* **146,** 141–150.
126. Lutsenko, S., Petrukhin, K., Cooper, M. J., Gilliam, C. T., and Kaplan, J. H. (1997) N-Terminal domains of human copper-transporting adenosine triphosphatases (the Wilson's and Menkes disease proteins) bind copper selectively *in vivo* and *in vitro* with stoichiometry of one copper per metal-binding repeat. *J. Biol. Chem.* **272,** 18,939–18,944.
127. DiDonato, M., Hsu, H.-F., Narindrasorasak, S., Que, L., and Sarkar, B. (2000) Copper-induced conformational changes in the N-terminal domain of the Wilson's disease copper-transporting ATPase. *Biochemistry* **39,** 1890–1896.
128. Cobine, P. A., George, G. N., Winzor, D. J., Harrison, M. D., Mogahaddas, S., and Dameron, C. T. (2000) Stoichiometry of complex formation between copper (I) and the N-terminal domain of the Menkes protein. *Biochemistry* **39,** 6857–6863.
129. Gitschier, J., Moffat, B., Reilly, D., Wood, W. I., and Fairbrother, W. J. (1998) Solution structure of the fourth metal-binding domain from the Menkes copper-transporting ATPase. *Nature Struc. Biol.* **5,** 47–53.
130. Silver, S. and Phung, L. T. (1996) Bacterial heavy metal resistance: new surprises. *Annu. Rev. Microbiol.* **50,** 753–789.
131. Payne, A. S. and Gitlin, J. D. (1998) Functional expression of the Menkes disease protein reveals common biochemical mechanisms among the copper-transporting P-type ATPases. *J. Biol. Chem.* **273,** 3765–3770.
132. Forbes, J. R., Hsi, G., and Cox, D. W. (1999) Role of the copper-binding domain in the copper transport function of ATP7B, the P-type ATPase defective in Wilson's disease. *J. Biol. Chem.* **274,** 12,408–12,413.
133. Voskoboinik, I., Strausak, D., Greenough, M., Brooks, H., Smith, S., Mercer, J. F. B., et al. (1999) Functional analysis of CXXC metal-binding motifs in human Menkes copper transporting P-type ATPase. *J. Biol. Chem.* **274,** 22,008–22,012.
134. Strausak, D., La Fontaine, S., Hill, J., Firth, S. D., Lockhart, P. J., and Mercer, J. F. B. (1999) The role of GMXCXXC metal binding sites in the copper-induced redistribution of the Menkes protein. *J. Biol. Chem.* **274,** 11,170–11,177.
135. Larin, D., Mekios, C., Das, K., Ross, B., An-Suei, Y., and Gilliam, T. C. (1999) Characterization of the interaction between the Wilson and Menkes disease proteins and the cytoplasmic copper chaperone, HAH1P. *J. Biol. Chem.* **274,** 28,497–28,504.
136. Tsivkovskii, R., MacArthur, B. C., and Lutsenko, S. (2001) The lys1010–lys1325 fragment of the Wilson's disease protein binds nucleotides and interacts with the N-terminal domain of this protein in a copper-dependent manner. *J. Biol. Chem.* **276,** 2234–2242.
137. Yamaguchi, Y., Heiny, M. E., Suzuki, M., and Gitlin, J. D. (1996) Biochemical characterization and intracellular localization of the Menkes disease protein. *Proc. Natl. Acad. Sci. USA* **93,** 14,030–14,035.
138. Dierick, H. A., Adam, A. N., Escara-Wilke, J. F., and Glover, T. W. (1997) Immunocytochemical localization of the Menkes copper transporter (ATP7A) to the trans compartment of the Golgi complex. *Proc. Natl. Acad. Sci. USA* **6,** 409–416.
139. Ackland, M. L., Anikijenko, P., Michalczyk, A., and Mercer, J. F. B. (1999) Expression of the Menkes copper-transporting ATPases, MNK, in the lactating human breast: possible role in copper transport into milk. *J. Histochem. Cytochem.* **47,** 1553–1562.
140. La Fontaine, S., Firth, S. D., Lockhart, P., Brooks, H., Camakaris, J., and Mercer, J. F. B. (1999) Activity and intracellular localization of Mnk, the murine homologue of the Menkes protein in cells from blotchy (Moblo) and brindled (Mobr) mouse mutants. *Hum. Mol. Genet.* **8,** 1069–1075.
141. Forbes, J. R. and Cox, D. W. (2000) Copper-dependent trafficking of Wilson's disease mutant ATP7B proteins. *Hum. Mol. Genet.* **9,** 1927–1935.
142. Goodyer, I. D., Jones, E. E., Monaco, A. P., and Francis, M. J. (1999) Characterization of the Menkes protein copper-binding domains and their role in copper-induced protein relocalization. *Hum. Mol. Genet.* **8**, 1473–1478.
143. Petris, M. J., Camakaris, J., Greenough, M., La Fontaine, S., and Mercer, J. F. B. (1998) A C-terminal di-leucine is required for localization of the Menkes protein in the transGolgi network. *Hum. Mol. Genet.* **7,** 2063–2071.
144. Francis, M. J., Jones, E. E., Levy, E. R., Martin, R. L., Ponnambalam, S., and Monaco, A. P. (1999) Identification if di-leucine motif within the C terminus domain of the Menkes disease protein that mediates endocytosis from the plasma membrane. *J. Cell Sci.* **112,** 1721–1732.
145. Petris, M. J. and Mercer, J. F. B. (1999) The Menkes protein (ATP7A, MNK) cycles via the plasma membrane in basal and elevated extracellular copper using a C-terminal di-leucine endocytic signal. *Hum. Mol. Genet.* **8,** 2107–2115.
146. Tümer, Z., Lund, C., Tolshave, J., Vural, B., Tonnesen, T., and Horn, N. (1997) Identification of point mutations in 41 unrelated patients affected with Menkes disease. *Am. J. Hum. Genet.* **60,** 63–71.
147. Das, S., Levinson, B., Whitney, S., Vulpe, C., Packman, S., and Gitschier, J. (1994) Diverse mutations in patients with Menkes disease often lead to exon skipping. *Am. J. Hum. Genet.* **55,** 883–889.

148. Moller, L. B., Tumer, Z., Lund, C., Petersen, C., Cole, T., Hanusch, R., et al. (2000) Similar splice-site mutations of the ATP7A gene lead to different phenotypes: classical Menkes disease or occipital horn syndrome. *Am. J. Hum. Genet.* **66,** 1211–1220.
149. Phillips, R. J. S. (1961) "Dappled," a new allele at the mottled locus in the house mouse. *Genet. Res.* **2,** 209–295.
150. Levinson, B., Packman, S., and Gitschier, J. (1997) Deletion of the promoter region in the Atp7a gene of the *mottled dappled* mouse. *Nature Genet.* **16,** 224–225.
151. Cecchi, C., Biasotto, M., Tosi, M., and Avner, P. (1997) The *mottled* mouse as a model for human Menkes disease: identification of mutations in the *Atp7a* gene. *Hum. Mol. Genet.* **6,** 425–433.
152. Das, S., Levinson, B., Vulpe, C., Whitney, S., Gitschier, J., and Packman, S. (1995) Similar splicing mutations of the Menkes/mottled copper-transporting ATPase gene in occipital horn syndrome and the blotchy mouse. *Am. J. Hum. Genet.* **56,** 570–576.
153. Thomas, G. R., Jensson, O., Gudmundsson, G., Thorsteinsson, L., and Cox, D. W. (1995) Wilson's disease in Iceland: a clinical and genetic study. *Am. J. Hum. Genet.* **56,** 1140–1146.
154. Duc, H. H., Hefter, H., Stremmel, W., Castaneda-Guillot, C., Hernadez, H. A., Cox, D. W., et al. (1998) His1069Gln and six novel Wilson's disease mutations: analysis of relevance for early diagnosis and phenotype. *Eur. J. Hum. Genet.* **6,** 616–623.
155. Lyons, T. J., Nerisissian, A., Huang, H., Yeom, H., Nishida, C. R., Graden, J. A., et al. (2000) The metal binding properties of the zinc site of yeast copper-zinc superoxide dismutase: implications for amyotrophic lateral sclerosis. *J. Biol. Inorg. Chem.* **5,** 189–203.
156. Multhaup, G., Schlicksupp, A., Hesse, L., Beher, D., Ruppert, T., Masters, C. L., et al. (1996) The amyloid precursor protein of Alzheimer's disease in the reduction of copper(II) to copper(I). *Science* **271,** 1406–1409.
157. White, A. R., Multhaup, G., Maher, F., Bellingham, S., Camakaris, J., Zheng, H., et al. (1999) The Alzheimer's disease amyloid precursor protein modulates copper-induced toxicity and oxidative stress in primary neuronal cultures. *J. Neurosci.* **19,** 9170–9179.
158. Cherny, R. A., Barnham, K. J., Lynch, T., Volitakis, I., Li, Q. X., Mclean, C. A., et al. (2000) Chelation and interchelation: complementary properties in a compound for the treatment of Alzheimer's disease. *J. Struct. Biol.* **130,** 209–216.
159. Brown, D. R., Qin, K., Herms, J. W., Madlung, A., Manson, J., Strome, R., et al. (1997) The cellular prion protein binds copper in vivo. *Nature* **390,** 684–687.
160. Pauly, P. C. and Harris, D. (1998) Copper stimulates the endocytosis of the prion protein. *J. Biol. Chem.* **273,** 33,107–33,110.
161. Wadsworth, J. D. F., Hill, A. F., Joiner, S., Jackson, G. S., Clarke, A. R., and Collinge, J. (1999) Strain-specific prion-protein conformation determined by metal ions. *Nature Cell Biol.* **1,** 55–59.
162. McKenzie, D., Bartz, J., Mirwald, J., Olander, D., Marsh, R., and Aiken, J. (1998) Reversibility of scrapie inactivation is enhanced by copper. *J. Biol. Chem.* **273,** 25,545–25,547.
163. Boll, M., Sotelo, J., Otero, E., Clcaraz-Zubeldia, M., and Rios, C. (1999) Reduced ferroxidase activity in the cerebrospinal fluid from patients with Parkinson's disease. *Neurosci. Lett.* **265,** 155–158.

16

Disturbances of Copper Homeostasis and Brain Function

Giuseppe Rotilio, Maria Rosa Ciriolo, Maria Teresa Carrì, and Luisa Rossi

1. INTRODUCTION

Copper is involved in electron-transporting chains of chloroplasts and mitochondria and is essential for the activity of enzymes involved in the oxygen metabolism, including cytochrome-*c* oxidase, superoxide dismutase, dopamine-β-hydroxylase, tyrosinase, lysyl oxidase, and peptidil–glycine α-amidating monooxygenase *(1)*. These copper-dependent enzymes are crucial to several processes of oxidative metabolism, namely respiration, detoxification, neurotransmitter synthesis, pigmentation, and maturation of connective tissue.

The evolutionary recruitment of copper to fulfill its physiological role in life is based on its redox properties (i.e., its readiness to be reduced by reducing substrates and then reoxidized by oxygen). Redox cycles in living organisms are regulated in such a way as to make reoxidation by oxygen usable as a source of chemical energy to be stored in "energy-rich" phosphate bonds. However, this redox reactivity leads to the risk of damage to cell and tissues if copper is not properly transported to the sites of biosynthesis of its target enzymes. In fact, potentially harmful events may take place if biological handling of copper is deranged from the proper track. When, for instance, copper is present in excess, production of potentially toxic free radicals from reaction of the reduced form of copper with oxygen may give rise to partially reduced and very reactive oxygen species (ROS), like superoxide (O_2^-), hydrogen peroxide (H_2O_2), and the hydroxyl radical (OH·) (Table 1) *(2)*. This happens when metal oxidation occurs outside the proper sites on specialized proteins ($4e^-$ oxidases) where oxygen is fully reduced to water by the concerted transfer of four electrons. Furthermore, copper can bind to nucleophiles such as essential cell thiols (glutathione, sulfydril side chains of enzyme active sites and of membrane proteins, etc.), leading to protein inactivation.

All of the potentially dangerous effects brought about by copper in living systems may be included within the concept of "oxidative stress." In fact, oxidative stress is the consequence of an imbalance between oxidant and antioxidant factors within a definite compartment. This may be the result of either excess of ROS, deficiency in defense, or intrinsic higher vulnerability of the tissue or cell implicated in the process. Excess ROS may derive from leakage of electrons from respiratory chain transporters under a variety of conditions of mitochondrial damage and microsomal overstimulation *(3)*. The defense system includes enzymes like Cu,Zn superoxide dismutase, which converts O_2^- into

From: Handbook of Copper Pharmacology and Toxicology
Edited by: E. J. Massaro © Humana Press Inc., Totowa, NJ

Table 1
Copper-Induced Production of Oxygen Radicals

$AH_2 + Cu(II)$	$\rightarrow AH\cdot + Cu(I) + H^+$
$AH\cdot + O_2$	$\rightarrow A + O_2^- + H^+$
$Cu(I) + O_2$	$\rightarrow Cu(II) + O_2^-$
$O_2^- + O_2^- + 2H^+$	$\rightarrow H_2O_2 + O_2$
$Cu(II) + O_2^-$	$\rightarrow Cu(I) + O_2$
$Cu(I) + H_2O_2$	$\rightarrow OH\cdot + OH^- + Cu(II)$

Note: AH_2 is any divalent reducing compound.

Table 2
Antioxidant Defense

Mechanism	*Natural defensive compounds*
	Prevention
Metal sequestration and transport	Metallothionein, glutathione (GSH), ferritin, transferrin, ceruloplasmin
"Coupled" electron-transfer chain	Ubiquinone, cytochrome-*c* oxidase
	Interception
Noncatalytic (scavengers)	Vitamin E, vitamin C, urate, glutathione, bilirubin, flavonoids
Catalytic (enzymes)	Superoxide dismutases, catalase, peroxidases, ceruloplasmin, ancillary enzymes: GSH transferases, GSH-regenerating enzymes
	Repair
	Phospholipid–glutathione peroxidase, DNA-repair enzymes

H_2O_2, and catalase and peroxidases, which inactivate H_2O_2 and molecules that entrap free radicals (scavengers) or transition metals (Table 2) *(4)*. Copper is janus faced because, on one hand, it plays a major role as source of damage and, on the other hand, it is responsible for impaired defense when deficient. As a matter of fact, the main defense molecules are copper-containing enzymes, either preventing the production of oxidizing species (such as cytochrome-*c* oxidase, which permits the concerted reduction of oxygen with minimal leaking of intermediate reduction products outside the mitochondrial membrane) or intercepting already formed radicals (such as Cu,Zn superoxide dismutase).

In addition, it should be underscored that copper is too redox active to exist in an unbound form in the biological systems without causing oxidative damage. Proper handling or sequestering of copper ions, under either high-affinity (physiological transport) or low-affinity (metal overload) regimes are vital processes in preventing metal reactions with O_2^- and H_2O_2 to yield the indiscriminate high-potential oxidant $OH\cdot$. In this regard, copper chaperones and copper thioneins are the proteins involved under high-affinity and low-affinity regimes, respectively. Metallothionein is a small protein involved in metal detoxification, rich in cysteines, and capable of binding up to 12 reduced copper ions: the synthesis of this protein is induced at the transcriptional level by metals. Therefore, it represents one of the first lines of defense against the risk of free-copper accumulation *(5)*. Furthermore, the ubiquitous

cysteine-containing tripeptide glutathione reacts directly with copper(I), thus protecting the cells from its toxicity, but it is also capable to donate copper to copper proteins *(6–9)*. In the latest years, an intricate network of copper binding and delivering low-molecular-weight proteins, playing a chaperone function, constitutively expressed in eukaryotic cells, has been detected *(9–11)*. This system, in humans, include: the CTR1 protein, involved in the passive entrance of copper in cells; the HAH1 protein, which delivers copper to the trans-Golgi-located copper pumps, which, in turn, are involved in the synthesis of the secretory proteins; COX17, which donates copper to cytochrome-*c* oxidase; and the CCS chaperone, which facilitates copper loading onto Cu,Zn superoxide dismutase. Furthermore, in mammals, copper in plasma travels bound either to low-molecular-weight molecules (like histidine) or to protein carriers (such as ceruloplasmin or albumin) *(1,9)*.

It is to be expected, in view of these considerations, that different tissues have different susceptibilities to copper toxicity, depending on inherent properties of their structural components and their metabolic and functional activities. In particular, the brain is among the most susceptible tissues to injuries caused by deficits or excesses of copper because it is extremely sensitive to oxidative stress. This is the consequence of a variety of factors: a high flux of reactive oxygen species may derive from a high rate of oxidative metabolism during the production of ATP in mitochondria and from specific metabolic pathways like dopamine oxidation *(12)* or nitric oxide (NO) production during glutammatergic transmission *(13)*. NO is a physiological messenger molecule *(14)* produced from the enzymatic oxidation of L-arginine by NO synthases. The biological consequences of NO formation in cellular systems are governed by a complex and, as yet, not completely elucidated network of competing reactions of NO, which is a free-radical itself, with O_2^-, ROS, transition metals, and thiols *(15)*. Such reactions yield various reactive nitrosative species, including nitrosyl–metal complexes, *S*-nitroso thiols, N_2O_3, and peroxynitrite ($ONOO^-$).

The brain is also well known for its low content of antioxidative enzymes with respect to other tissues *(16,17)*; this represents another risk factor of oxidative stress. Furthermore, it is a target prone to damage from oxidative attack: it has high concentrations of polyunsaturated fatty acids and a high ratio of membrane surface area to cytoplasmic volume. Last but not least, it has been demonstrated that transition metals increase with age in the brain *(18,19)* and this may be of relevance because the majority of neurodegenerative diseases occur in the elderly.

Oxidative damage ultimately leads to neuronal cell death that may have the features of necrosis or programmed cell death. The prevalence of a kind of cell death in neurodegeneration depends on the intensity of the initial insult: milder stress initiates the chain of events ultimately leading to programmed cell death, proceeding through a well-established program, involving intrinsic, evolutionary highly conserved molecular components *(20)*, whereas devastating damage leads to necrosis *(21)*. It is conceivable that the persistence of mild oxidative insult in neural cells, possibly the result of metal-sustained oxidative stress or to NO production, commits neurons to die via apoptosis. In fact, apoptotic cells have been consistently found in both acute and chronic neurodegenerative diseases *(22)*. It could be of interest to investigate whether copper-dependent factors play some role in the intricate pattern of events underlying neural apoptosis.

The object of this chapter will be to survey recent data on risks for brain deriving from deficits or excesses of copper, in the light of the considerations outlined earlier. The matter will be mainly organized around the more and more clearly emerging relationships between copper and major neurodegenerative diseases (Table 3). Some of these cases of neurodegenerative diseases derive from well-established genetic mutations affecting copper transport, such as those occurring in Menkes' and Wilson's diseases and thus they represent models for the effects on brain of severe disturbances of copper metabolism *(23,24)*. In other diseases, copper is more or less directly involved in the associated molecular changes, and this is the case of Alzheimer's disease, Parkinson's disease, familial amyotrophic lateral sclerosis, and prion disease *(25)*. Altogether, these clinical situations are very useful for the identification of molecular mechanisms underlying the risks of copper toxicity for brain because of either deficits or excesses or aberrant coordination of the metal.

Table 3
Copper Involvement in Neurodegenerative Disorders

Disease (origin)	*Protein interacting with copper*	*Physiological protein function*	*Consequence of protein deficiency*
Menkes (genetic)	Cu-ATPase	Copper transport	Copper deficiency
Wilson (genetic)	Cu-ATPase	Copper transport	Copper overload
ALS (sporadic or familial)	SOD1	Superoxide dismutation	Acquisition of pro-oxidant properties
Alzheimer (sporadic or familial)	APP	Unknown	APP fragmentation, Aβ-deposition
Prion diseases (sporadic, familial, or infectious)	PrP	Unknown	PrP structural modification, PrP^{Sc} stabilization
Parkinson (sporadic or familial)	α-Synuclein	Unknown	Aggregation

2. GENETIC SOURCES OF COPPER TOXICITY IN BRAIN

The importance of unperturbed homeostasis of copper for brain is well elucidated by the symptoms of Menkes' disease and Wilson's disease, two inherited disorders of copper metabolism resulting from genetically determined loss of function of very similar ATPases localized to the plasma membrane and trans-Golgi network of the cell, which are involved both in copper efflux from cells and in copper incorporation into secretory copper–proteins *(9,24)*. Copper-transporting ATPases share the same common organization including six copper-binding domains, eight hydrophobic transmembrane domains, a domain involved in the transduction of energy from ATPase activity to ion transport, and a cation channel *(26)*. Although they utilize a common structural frame and an identical mechanism of action, the key importance of the two diseases, to understand how deficits or excesses of copper affect the brain, resides in the tissue-specific expression of the two ATPases implicated in either disease. Menkes' copper pump is mainly expressed in intestine, placenta, brain, and kidney, whereas Wilson's pump is expressed predominantly in the liver and hardly in the brain *(9)*.

2.1. Menkes' Disease

Menkes' syndrome is an X-linked (Xq13.3) recessive disorder associated to copper deficiency, lethal in the early childhood *(27)*. The most striking feature of this disease is the coarse and hypopigmented hair; therefore, it is also called "kinky or steely hair disease." Menkes' children show impaired synthesis of collagen and elastin. Furthermore, they are severely mentally retarded: altered brain development and neurodegeneration have been detected by postmortem histological assay *(28)*. In particular, diffuse atrophy, focal degeneration of gray matter, and prominent neuronal loss has been detected in the cerebellum. Purkinje cells show abnormal dendridic arborization and focal axonal swelling. These features are present at birth, indicating that copper is essential for prenatal growth and development of the central nervous system. The molecular basis of this syndrome has recently been discovered, by identifying a mutated gene (*ATP7A*) encoding for a P-type cation-transporting ATPase *(29–31)*. All types of mutations have been found: nonsense, missense, duplications, and deletion. Approximately 200 mutations have been identified, responsible for classical or milder form of the disease. As a primary effect, the impairment of the copper ATPase results in defective copper export from intestinal cells, leading to systemic copper deficiency. Thus, copper accumulates in intestine, kidney, and cultured fibroblasts, whereas brain and liver are copper deficient. Systemic depletion of copper-dependent enzymes may justify the phenotype and the symptoms of Menkes patients.

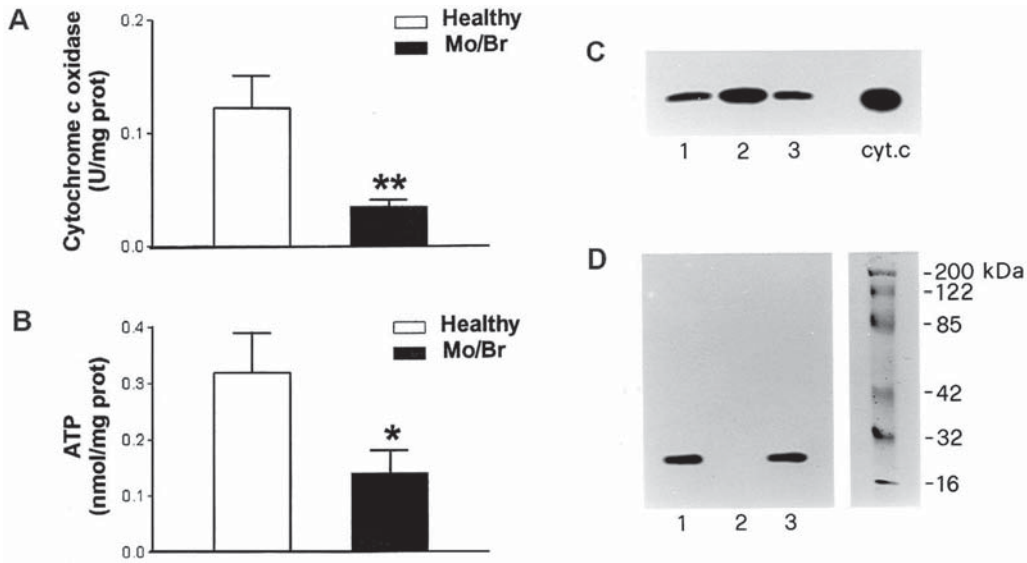

Fig. 1. Mitochondrial impairment and markers of apoptosis in the brain of mottled/brindled mice. Fourteen-day-old mice were used. **(A)** Cytochrome-*c* oxidase activity in total brain homogenates was assayed spectrophotometrically; **(B)** ATP levels were assessed by a luminescent method; **(C)** Cytochrome-*c* in the cytosol was measured by Western blotting using a monoclonal antibody; **(D)** Bcl-2 protein was measured by Western blotting using a polyclonal antibody. Lanes 1 and 3: healthy control mice; Lane 2: mottled/brindled. For details, *see* ref. *34*.

The cause of the neurological abnormalities observed in Menkes disease is still to be ascertained. As mentioned earlier, copper content is particularly low in the brain, because ATPase also transports copper across the blood-brain barrier and lower activities of copper-dependent enzymes may strongly contribute to the altered development of the central nervous system *(32)*. However, the mechanisms accounting for prenatal cerebral and cerebellar degeneration remain unknown, implying the existence of an as yet unidentified copper-dependent factor, which plays an essential role in neuronal growth and differentiation.

In the brain of the $Mo^{br/Y}$ mouse, the closest animal model of Menkes' disease *(32,33)*, we have recently shown *(34)* that copper deficiency leads to specific decrease in brain of cytochrome-*c* oxidase and Cu,Zn superoxide dismutase activities. In addition, a dramatic change of markers for apoptosis were detected in the brain: loss of the antioxidant Bcl-2 protein, which also plays a fundamental role in brain development and morphogenesis *(35)*, release of cytochrome-*c* from the mitochondria, and depletion of ATP (Fig. 1). Histological analysis of brain revealed a high percentage of apoptotic cells in the neocortex and the hippocampus *(34)*. These results clearly show that a copper deficit may cause mitochondrial damage in the brain consequent to inactivation of cytochrome-*c* oxidase. In turn, this event may trigger leakage of oxygen radicals out of damaged mitochondria, leading to neurodegeneration via oxidative stress-mediated apoptosis. Treatment of Menkes' disease consists in intravenous administration of the copper–histidine complex *(27)*. The crucial role of cytochrome-*c* oxidase alteration in neurodegeneration is demonstrated by studies on the timing of treatment of $Mo^{br/Y}$ with copper, showing that delayed treatment results in irreversible changes of cytochrome-*c* oxidase of the brain, leading to irresponsiveness to the treatment *(36)*.

2.2. Wilson's Disease

Wilson's disease (hepatolenticular degeneration) is an autosomal recessive disorder of copper transport *(23)*, which maps to chromosome 13q14.3 *(37,38)*, biochemically characterized by accumulation

of copper in the liver and brain of affected patients. This disease thus represents a model for intoxication by copper excesses. The age of onset of the disease range from the age of 9 yr up to 50. Diagnosis mainly relies on hepatic dysfunction; however, Wilson's patients may display hepatic symptoms and/or neurological symptoms. At the earliest stage of the disease copper accumulates in the cytosol of hepatocytes, thus inducing synthesis of metallothionein and copper-bound metallothionein ends up into lysosomes. High copper levels induce hepatocytes necrosis, followed by increased copper release into the bloodstream, leading to hemolysis. Finally, copper levels increase in other organs such as the kidney, brain, and cornea. In the latter, copper accumulation produces pigmented rings (Kayser–Fleisher rings), which represent the hallmark of the latest stage of the disease. In brain, deposition of copper occurs in the basal ganglia, resulting in gliosis and neuronal loss. Progressive neurodegeneration leads to neurological symptoms, including tremors, dystonia, slurring of speech, and rigidity *(39)*. Behavioral disturbances are also present with changes of personality, depression, and schizophrenia. Although liver symptoms are most common in affected children, neurological disturbances are more typical of the adult onset of the disease. Increased levels of liver copper are the result of impaired biliary excretion of the metal. Mutation of the copper-transport liver ATPase expressed mainly in the liver, which shows a 55% amino acid identity with the Menkes disease protein *(37,40–42)*, represents the genetic rationale of this disease. This protein is responsible for the secretory pathway of copper both for efflux of copper into the bile and copper incorporation into ceruloplasmin. Therefore, in addition to impairment of copper efflux into bile, hepatic synthesis of holo-ceruloplasmin is inhibited and secretion is impaired because of degradation of the copper-free protein. Thus, ceruloplasmin absence in the plasma is a diagnostic marker of this disease *(43)*.

Treatment of Wilson's disease includes oral administration of copper chelators (such as D-penicillamine, trientine, tetrathiomolibdate) or induction of metallothionein synthesis by zinc administration *(43)*. The efficacy of these drugs for neurological manifestations is not successful. Both penicillamine and trientine may even lead to worsening because of the redistribution of copper into the brain.

Therefore, both deficits and excesses of copper induce neurodegeneration, very likely because of increased oxidative stress in both cases. According to the models provided by the two genetic diseases just described, the lack of copper may lead to neurodegeneration because of the inactivation of cytochrome-*c* oxidase and mitochondrial function, and consequent increased O_2^- production in the respiratory chain. Excesses of copper will create conditions that are favourable to O_2^-, yielding a redox cycle with oxygen, and to thiol binding in proteins and membranes.

3. COPPER IN LATE-ONSET NEURODEGENERATIVE DISEASES

Neurodegenerative diseases that are characterized by late-onset in life offer a very interesting matter of analysis as far as risks related to copper are concerned, insofar as aberrant copper chemistry rather than excessive or deficient metal availability seems to be implicated as a causative factor of neurodegeneration, again strongly associated to overproduction of oxygen free radicals.

3.1. Amyotrophic Lateral Sclerosis

3.1.1. Molecular Basis of the Disease

Amyotrophic lateral sclerosis (ALS) is a progressive lethal disease, leading to death in a few years after the early symptoms. The target of neurodegeneration is quite specific, because only cortical and spinal motoneurones are affected, with consequent progressive impairment of all muscular activities, eventually leading to respiratory compromise and death. ALS occurs both as a sporadic (SALS) and a familial (FALS) disorder, with inherited cases accounting for about 10% of patients *(44)*. The only gene conclusively linked to FALS so far is the one coding for the dimeric enzyme Cu,Zn superoxide dismutase (SOD1) (21q22) showing autosomal dominant mutations *(45,46)*. Linkage studies have revealed that mutations in SOD1 are responsible for 10–15% of FALS *(47)*. In spite of this intricate

Table 4
Redox Reactions of SOD1

A: With Superoxide (O_2^-)
$SOD1 \cdot Cu(II) + O_2^- \rightarrow SOD1 \cdot Cu(I) + O_2$
$SOD1 \cdot Cu(I) + O_2^- + 2H^+ \rightarrow SOD1 \cdot Cu(II) + H_2O_2$
B: With Hydrogen Peroxide (H_2O_2)
$SOD1 \cdot Cu(II) + H_2O_2 \rightarrow SOD1 \cdot Cu(I) + O_2^- + 2H^+$
$SOD1 \cdot Cu(I) + H_2O_2 \rightarrow SOD1 \cdot Cu(II) + OH\cdot + OH^-$
C: With Peroxynitrite ($ONOO^-$)
$SOD1 \cdot Cu(II) + ONOO^- \rightarrow SOD1 \cdot CuO \cdots NO_2^+$
$SOD1 \cdot CuO \cdots NO_2^+ + H\text{–tyr–protein} \rightarrow SOD1 \cdot Cu(II) + OH^- + NO_2\text{–tyr–protein}$

etiopathological pattern, the phenomenology of the disease is identical in all sporadic and familial cases. This has stimulated a great deal of interest in studying the relationships between the enzyme involved in the few genetically determined cases and the neurodegeneration typical of the disease.

SOD1 is a very efficient enzyme, considered to be a primary defense barrier in oxidative stress because it catalyzes the disproportionation of two molecules of O_2^- into dioxygen and H_2O_2 at a rate very near the diffusion-controlled limit. The site of enzyme activity resides on the copper, which is involved in a redox cycle with the superoxide substrate *(48)*. To date, there are more than 60 SOD1 point mutations reported in FALS families, distributed in all the 5 exons of the gene *(49)*. Interestingly enough, mutants associated to the most severe cases of FALS are fully active. Conversely, mutants with very low enzymatic activity are associated to mild forms of the disease. For instance, mutant H46R, which is almost completely inactive since affecting the active site *(50)*, is reported typical of a "mild" Japanese form of FALS (average duration 17 yr) *(51)*. Conversely, G93A mutants are fully active but are associated with a severe form of the disease *(52)*. The most frequent mutation, A4V, is found in almost 50% of patients in North America and is associated with a severe form of FALS, although SOD1 activity is only slightly reduced *(49)*. This mutation affects a residue involved in the formation of contacts at the dimer interface, as several other FALS-typical mutations. Furthermore, different mutations affecting the active site result in different effects in terms of the severity of the disease. For instance, mutation H48Q confers to the protein scarce dismutating activity, but was described for patients severely affected, with a rapid course (8 mo), at difference with H46R *(49)*.

These results primed the hypothesis that neurodegeneration in FALS is not related to the loss of function by SOD1, but to a gain of additional noxious properties by the enzyme.

3.1.2. Additional Functions of SOD1 in FALS

In addition to redox cycling with O_2^- substrate (Table 4), copper in the active site of SOD1 can also react with the peroxide product (Table 4). Whereas cycle A will remove O_2^- from any potentially harmful interaction with metals or other radicals to generate more potent oxidants like OH· (*see* Table 1), cycle B becomes a generator of OH· and envisages a paradoxical pro-oxidant activity of SOD1. However, cycle B can be effective only under a certain set of circumstances, because it is much less kinetically favored than cycle A, unless in the presence of large excesses of H_2O_2 or in the presence of enzyme variants with abnormal affinity for H_2O_2. The latter case may be the result of either distorted copper coordination or altered geometry of the active-site channel. In fact, markers of oxidative stress such as peroxidated lipids, oxidized proteins, and DNA are elevated in several experimental systems, ranging from both sporadic and FALS patients to transgenic mice *(53–55)*.

Some of the FALS-typical enzyme variants have been purified and some of them indeed showed an increased propensity for the reaction with H_2O_2 *(56–58)*. At least two of the ALS-linked mutant SOD1 (A4V and G93A) can increase the rate of formation of OH· in vitro, as demonstrated through

the electron spin resonance (ESR) technique, by the use of spin traps *(56–58)*. Those spin-trapping experiments were criticized by some authors *(59)* and the relevance of such reactions in vivo has also been questioned. For instance, conflicting evidence for increased $OH^{\cdot}$ formation was obtained in transgenic FALS mice *(54,55,60)*. Furthermore, Marklund et al. *(61)* did not find increased peroxidase activity with another FALS mutant, D90A.

Imperfectly folded mutant SOD1 may catalyze the nitration of tyrosines through use of peroxynitrite as a substrate (Table 4). The group of Beckman has found that, in agreement with previous reports in vitro (62), mutant FALS–SOD1s have decreased affinity for zinc in vivo and this might enhance catalysis of tyrosine nitration by peroxynitrite (63,64). Indeed, the presence of elevated free-nitrotyrosine levels has been reported in transgenic mice expressing SOD1 mutants (60).

These findings could explain how SOD1 enzymes act as antioxidants and pro-oxidants at the same time. In fact, antioxidant activities (i.e., superoxide dismutation) and pro-oxidant activities (i.e., peroxidase and nitration reactions) utilize similar redox mechanisms. Wild-type SOD1 seems to achieve its specificity by restricting access of potential substrates other than O_2^{-}: structural perturbations in FALS–SOD1 mutants may allow access of alternative substrates to the copper center, leading to more diverse catalytic redox reactions. Both hypotheses, of FALS–SOD1 peroxidative activity and tyrosine nitration, point to a different, increased availability of active-site copper to the substrate as a prerequisite for the gain of function of SOD1s typical of FALS patients. Enhanced peroxidase activity of FALS–SOD1 is copper dependent, in that it can be blocked by stoichiometric copper-chelating agents as diethyldithiocarbamate and D-penicillamine in vitro, whereas the peroxidase activity of the wild-type enzyme is unaffected unless copper is removed from the active site by an excess of chelators (56,65). Furthermore, the metal-binding properties of the FALS mutant proteins and their redox behavior are altered. It has been proposed that alteration of the properties of the zinc site will alter the metal-binding affinity of the copper site as well, possibly inducing a loosening of the protein structure (62). This hypothesis has been recently supported by the finding that zinc-deficient SOD1 (both wild-type and FALS mutants) acquire toxic properties (64).

Direct measurements of purified recombinant FALS–SOD1 have demonstrated a decrease in copper binding for yeast G85R mutant (66) and human H46R (50) but not for other mutants, such as yeast G93A (66). In H46R, a critical residue for maintenance of the geometry of the active site is substituted. This mutant is structurally stable but lacks significant enzyme activity and has impaired capability of binding catalytic copper (50). Recombinant mutated protein was expressed in the Escherichia coli strain QC779, which is defective in bacterial SODs. We showed that this protein contains about 5% copper; the copper ESR signal for H46R increases in intensity upon titration with copper chloride, but the spectrum displays an axial geometry, at variance with the tetraedrally distorted square planar geometry of the wild-type enzyme, thus suggesting that arginine in the 46 position does not correctly coordinate the copper. Furthermore, reconstituted protein displays only poor dismutating activity. In a recent article, it has been confirmed that this particular FALS mutant does not bind copper at the copper-specific site; rather, copper ions either compete for zinc at the active site or bind to a surface solvent-exposed residue near the dimer interface, individuated as Cys111 (67). Based on several evidences obtained in their yeast model system, Corson et al. (68), by analyzing several FALS–SOD1 mutants overexpressed in Sacchoromyces cerevisiae, have suggested that aberrant copper-mediated chemistry catalysed by a less tightly folded mutant enzyme might be responsible for SOD1-linked FALS phenotype.

3.1.3. Mutant SOD1 Involvement in FALS-Associated Neurodegeneration

The molecular mechanisms hypothesized to underlie SOD1 toxicity in FALS are under study in our laboratory in models of neural cells. We devised a model system made of several human neuroblastoma SH-SY5Y cell lines where the ratio of expression of mutant SOD1 to endogenous SOD1 approximated 1:1, a situation resembling that of heterozigous patients *(69)*. Mutant SOD1s were chosen as to have the opposite situation in terms of residual dismutating activity and relevance to the

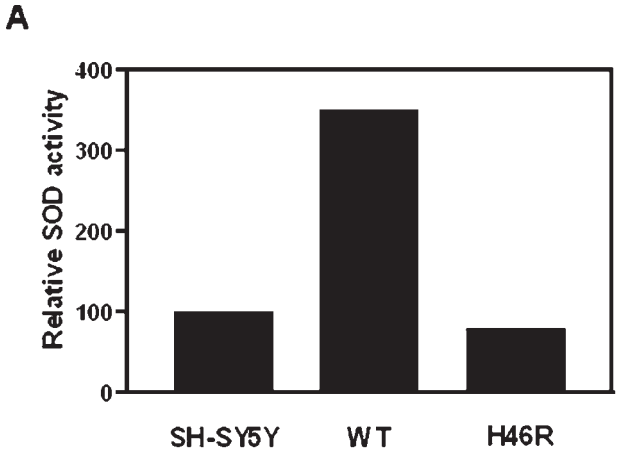

B

Viable cells (%)

	SH-SY5Y	WT	H46R
+ PQ	90.0 ± 5.2	85.2 ± 4.9	26.3 ± 3.9
+ PQ + D-pen	78.2 ± 7.1	78.0 ± 7.8	82.2 ± 4.1

Fig. 2. D-Penicillamine protects SH-SY5Y neuroblastoma cells transfected with H46R FALS mutant from paraquat-induced toxicity. **(A)** SOD1 activity measured spectrophotometrically; **(B)** cell survival evaluated by trypan blue dye exclusion and expressed as percentage of corresponding untreated cell line. WT: cells transfected with wild-type SOD1. For details, *see* ref. *70*.

severity of the disease (i.e., the H46R or the G93A variants). In those studies, mutations have been introduced in the cDNA-encoding human SOD1 and several monoclonal cell lines have been established constitutively expressing either the wild-type or the mutant enzymes. Cells overexpressing the G93A mutant, in addition to a significant increase in SOD1 protein and activity, also showed a loss of mitochondrial membrane potential, an increased sensitivity to valinomycin, and a parallel increase in cytosolic calcium concentration. Therefore, mitochondrial damage and calcium levels may represent early factors in the pathogenesis of FALS.

When SH-SY5Y cells have been transfected with plasmids directing constitutive expression of H46R mutant, they showed increased levels of immunoreactive SOD1. However, they have much lower dismutase activity than wild-type transfected or control neuroblastoma cells. This led us to the conclusion that expression of this mutant enzyme affects the activity of the endogenous enzyme, through formation of unstable or partially inactive heterodimers *(70)*. In fact, misfolded SOD1 have been reported in spinal cords from transgenic mice expressing several FALS mutants in the presence or in the absence of overexpression of wild-type human SOD1 *(71)*. Overall data indicate that FALS–SOD1 is made less stable by mutations and is capable of forming precipitates independently of the coexpression of wild-type protein. However, this seems not to be a general rule for FALS–SOD1s, as many other mutants do not aggregate *(72)* and the possibility that SOD1 aggregation is the consequence of a dysfunction in some other cell component is still open.

In our transfected cell system, we have also observed that expression of mutant H46R induces a selective increase in sensitivity to paraquat-induced cell death. This cannot arise only from reduced

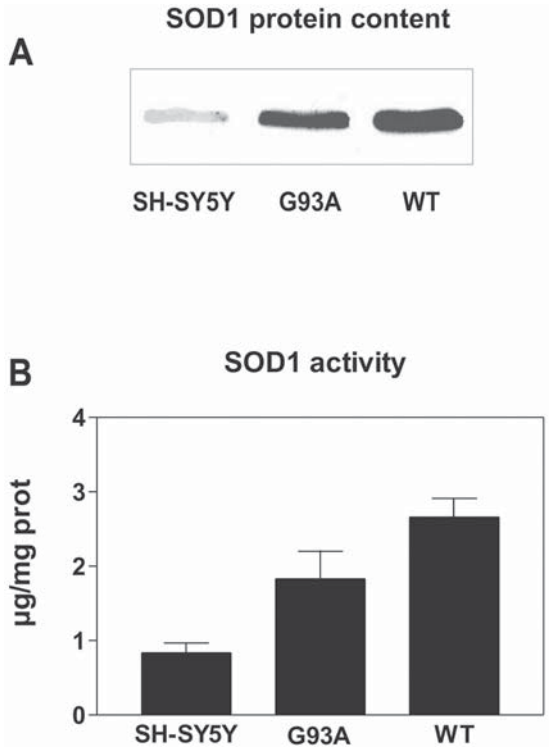

Fig. 3. SOD1 protein and activity in SH-SY5Y neuroblastoma cells transfected with WT or G93A FALS mutant enzyme. **(A)** Protein content was assessed by Western blotting using a polyclonal antibody. **(B)** SOD1 activity was measured by a polarographic method. For details, *see* ref. *80*.

SOD1 activity, which still remains about 75% of that of control cells (Fig. 2A), but may be likely ascribed to aberrant metal chemistry of this mutant enzyme. In fact, cells could be protected by treatment with the copper chelator D-penicillamine (Fig. 2B). Our data are in line with a previous report *(73)* in a different system, where cell death of adenovirus-infected PC12 cells expressing FALS–SOD1s was partially inhibited by administration of a copper chelator. Survival of transgenic mice expressing a different FALS mutation (G93A) was extended by administration of D-penicillamine *(74)*.

The actual mechanism of motor neuron loss (whether necrosis or apoptosis) in ALS is still actively debated. Although activation of proapoptotic Bax protein and inactivation of antiapoptotic Bcl-2 has been reported in sporadic ALS patients *(75)*, some authors have not been able to detect apoptotic cells in FALS–SOD1 transgenic mice *(76)*. However, mutations associated with FALS convert SOD1 from an antiapoptotic gene to a proapoptotic gene in yeast and in conditionally immortalized mammalian neural cells *(77)*. Furthermore, caspase-1 is activated in neural cells and tissue with SOD1-FALS *(78)* and inhibition of caspase-1 and caspase-3 delays progression of disease and extends survival in FALS–SOD1 transgenic mice *(79)*. Furthermore, NO-dependent apoptosis seems to be increased by FALS–SOD1 in motor neurons *(64)*.

In order to extend the mechanistic understanding of SOD1 action in FALS, we challenged our model of neuroblastoma cells transfected with the G93A mutant with NO *(80)*. Cells were treated with several NO donors, including nitroso-glutathione (GSNO), which represents the physiological intracellular dispenser of NO *(81)*. The G93A transfected cells showed an increased amount of both SOD1 protein and activity, comparable to that of wild-type SOD1 transfected cells (Fig. 3). However, they

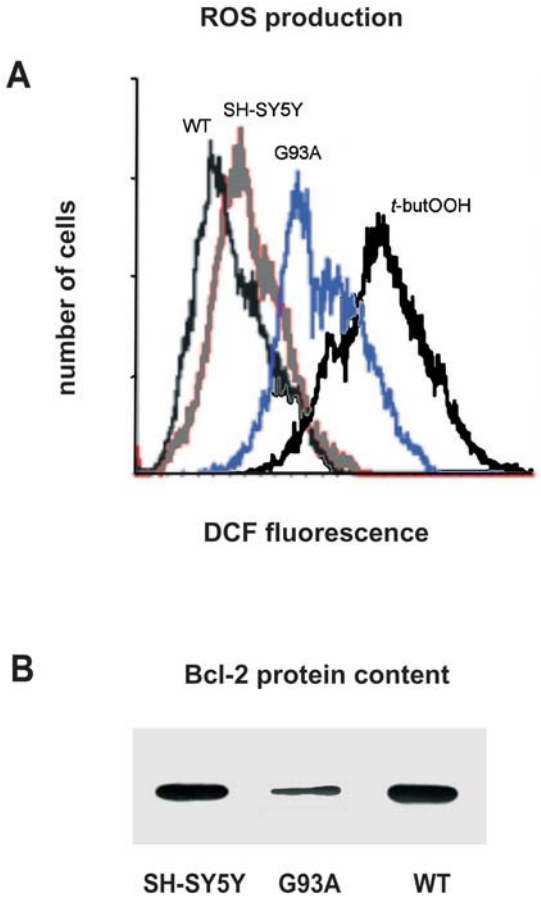

Fig. 4. Pro-oxidant status of SH-SY5Y cells transfected with FALS mutant G93A. **(A)** Intracellular ROS were detected by incubation with 2'-7'-dichlorofluorescein diacetate (DCF), followed by FACScan analysis. *Tert*-butyl-hydroperoxide (*t*-butOOH) was used as a positive control. **(B)** Bcl-2 immunoreactive protein was measured by Western blotting using a monoclonal antibody. For details, *see* ref. *80*.

had an increased flux of ROS (Fig. 4A), as if a pro-oxidant status lurked within them. In addition, they also showed a lower basal level of the antiapoptotic, antioxidant protein Bcl-2 (Fig. 4B). When exposed to NO donors, they showed an increased susceptibility to undergo apoptosis, with respect to control SH-SY5Y cells, whereas wild-type SOD1 transfected cells were spared. NO-mediated apoptosis in these models was associated with a canonical sequence of events, including Bcl-2 downregulation, increased expression, and phosphorylation of the tumor suppressor protein p53 and of the product of one its target genes, the cell cycle inhibitor p21 *(80)*. Furthermore, cytochrome-*c* was released from the mitochondria (Fig. 5A), thus leading to activation of the cysteine protease caspase-3 (Fig. 5B). Interestingly, pretreatment of cells with the copper chelator D-penicillamine protected cells transfected with the G93A SOD1 mutant from NO-induced apoptosis (Fig. 6), thus conferring them with behavior typical of the wild-type SOD1 transfected cells. In other words, it seems that G93A cells behave as the wild-type ones when the copper is properly constrained. These results confirm the role of aberrant copper chemistry both in oxygen radical formation and in NO susceptibility, as we already showed for the H46R mutant (70). In conclusion, high levels of SOD1

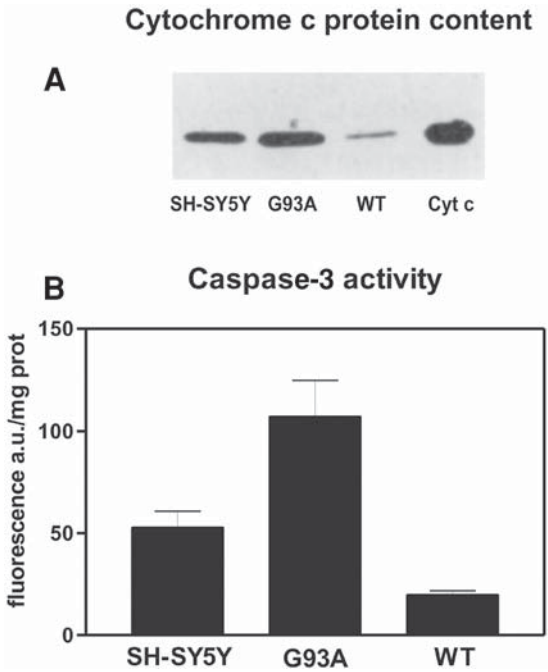

Fig. 5. Molecular markers of apoptosis in SH-SY5Y cells upon GSNO treatment. **(A)** Immunoreactive cytochrome-*c* in cell cytosol was detected by Western blotting by a monoclonal antibody; **(B)** caspase-3 activity was measured fluorometrically. For details, *see* ref. *80*.

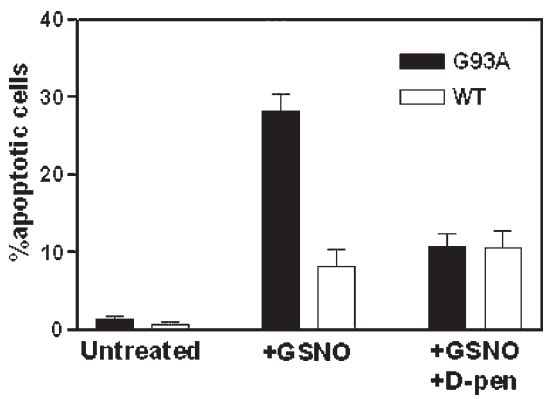

Fig. 6. Increased susceptibility of G93A cells to GSNO is abolished by D-penicillamine. Apoptotic cells were detected by FACScan analysis, upon propidium iodide staining. For details, *see* ref. 80.

activity protect cells from apoptosis, unless other nasty side activities are present; in that case, they may become a damage mediator and be proapoptotic.

In conclusion, neurodegeneration in FALS appears to be a consequence of aberrant copper chemistry deriving from improper handling of the metal by one of its physiological carriers, even though its concentration limits are normal. In such circumstances, copper can become available in the cell to harmful reactions that generate oxidative stress. This is actually the most likely mechanism of copper toxicity in other late-onset neurodegenerative diseases.

3.2. Alzheimer's Disease

The argument of improper copper binding as possible mediator of brain injury is relevant to Alzheimer's disease (AD), the most common cause of senile dementia with both familial and sporadic forms. It is a progressive neurodegenerative disorder characterized by neuronal cell loss or dysfunction. The neocortex and the hippocampus are both severely affected, but neurodegeneration is selective *(82)*: thus, learning, behavior, and memory functions are impaired. Neurochemical hallmarks of this disease include the presence of proteinaceous deposits in neurons (neurofibrillary tangles) as well as in the extracellular space (cerebrovascular and neuritic plaques) *(83)*. The principal component of these deposits is a peptide of 39–43 amino acids (about 4 kDa), called amyloid β protein (Aβ), which has an important role in neuronal dysfunction because it is toxic to neurons *(84)*. This peptide derives from the processing of a full-length, transmembrane protein, called amyloid precursor protein (APP), displaying several different isoforms, as a result of alternative splicing of a single gene. It consists of a large N-terminal extracellular region, a transmembrane domain, and a small cytoplasmic tail. All of the family components show binding sites for zinc, iron, and copper. Zinc binds to the extracellular domain and may regulate protein folding; furthermore, it has been recently suggested that it may favor precipitation of Aβ, converting it into a less harmful form than the soluble one *(85)*. Copper also binds to the extracellular region to a cysteine-rich domain by two conserved histidines *(86)*. The physiological role of APP is not clear: however, owing to its membrane location and its capability of copper binding, a possible involvement in neuronal copper transport has been suggested *(87)*. When bound copper(II) is reduced to copper(I), an intramolecular electron transfer may occur, leading to the formation of a disulfide bridge *(88)*. Copper(I) may in turn be oxidized back by H_2O_2 with the production of $OH^{\cdot}$ and random fragmentation of APP. Copper(II) may favor the aggregation process of Aβ *(89)*, especially under conditions representing physiological acidosis resembling those present in the inflammated brain parenchyma *(90)*. Conversely, zinc may exert a preventive role of free-radical formation by quenching abnormal Aβ-mediated redox activity *(85)*. It should also be kept in mind that zinc, iron, and copper are more concentrated than normal in the neuropil of Alzheimer patients and are further concentrated in the core and periphery of plaques *(91)* and that this increase may be the result of metals binding to Aβ. This is a very important point because Aβ is present as a soluble protein in normal fluid and tissues and tends to form aggregates also in healthy aged individuals, although the aggregates forming in Alzheimer's brain are much less soluble. A plausible hypothesis would be that exposure to excessive amounts of these metals or predisposition to their selective accumulation is a risk factor for the onset of the disease.

The Aβ interaction with redox active copper is a significant source of oxidative stress in AD *(92,93)*. There is wide consensus indicating increased oxidative stress in the brain of Alzheimer patients, represented by increased protein oxidation *(94,95)*, increased lipid peroxidation *(96)*, and damage to both nuclear and mitochondrial DNA *(97,98)*. Mitochondrial dysfunction is implicated in AD and it has even been proposed as a causative genetic factor in the pathogenesis of familial forms *(82)*. There is also evidence that Aβ impairs the activity of mitochondrial respiratory chain and reports evidenced decrease of the activity of cytochrome-*c* oxidase *(99–101)*, although this may be a secondary event *(102)*. Cortical, cerebellar, and hippocampal neuronal cultures derived from knockout APP mice were less susceptible than wild-type cells to physiological concentrations of copper, in terms of decreased levels of lipid peroxidation *(103)* and copper(II) markedly potentiates the neurotoxicity exhibited by Aβ in cell cultures *(104)*.

3.3. Parkinson's Disease

Recently, some evidence for the involvement of copper in the mechanism underlying the onset of Parkinson's disease (PD) has also emerged. This disease is characterized by resting tremor, rigidity, bradykinesia or slowness, and postural instability. Hallmarks of this disease include degeneration of dopaminergic neurons in the substantia nigra, with intracytoplasmic inclusions known as Lewy bodies

(105). Degeneration also involves neurons in the locus ceruleus, nucleo basalis, hypothalamus, and cerebral cortex. Established etiology of this disease involves environmental factors (exposure to pesticides, herbicides, industrial chemicals) and genetic factors (approx 5–10% of PD patients have a familial form of parkinsonism with an autosomal-dominant pattern of inheritance). Familial PD was linked to the q21–23 region of chromosome 4 *(106)*; mutations in the gene coding for the protein α-synuclein, leading to replacements of the alanine residue in position 30 or 53 with threonine or proline, respectively, were identified *(107,108)*. Although the physiological role of α-synuclein is still largely unknown, accumulation of this small protein seems to be a crucial event in the development of PD, because it is an abundant component of Lewy bodies in all of the cases of the disease. Furthermore, mutation of this protein in the familial cases might favor the accumulation process.

The pathogenesis of PD may involve oxidative stress, because oxidized marker molecules have been detected in the brains of PD patients *(105)*. Oxidative insult may derive from several sources. Among those, increased turnover of dopamine, the oxidation of which leads to the formation of H_2O_2 *(12)* or derangements in mitochondrial complex I activity *(109)*. The relevance of oxidative stress for this disease is also strengthened by the finding that in the PD brain, the antioxidant glutathione decreases *(110)* and that oxidized proteins *(111)*, DNA *(112)*, and lipids *(113)* are present in PD brain. Furthermore, excitotoxic damage mediated by NO and peroxynitrite seems to be relevant to cell damage, because, for instance, NO-dependent nitration of tyrosine residues on cellular proteins has been found in PD *(114)*. The mechanism of cell death in PD seems to involve apoptosis, repeatedly detected in postmortem PD brains *(105)*.

A direct involvement of copper in the pathogenesis and/or progression of PD has been envisaged. Defects of cytochrome-*c* oxidase in nigral neurones of PD patients have been found *(115)*, as well as a significantly lower ceruloplasmin concentration and ceruloplasmin activity and Cu,Zn superoxide dismutase activity in blood *(116)*. More interestingly, it has been demonstrated that copper(II) induces α-synuclein to form self-oligomers and that the acidic C-terminus of the protein is essential for the copper effect *(117)*. Interestingly enough, fragments of α-synuclein represent the non-Aβ component of senile plaques in AD, thus reinforcing the role of copper in AD progression. Therefore, abnormal copper homeostasis can be considered a risk factor also for the development of PD.

3.4. Prion Diseases

Prion diseases represent a class of neurodegenerative diseases, including scrapie in sheep, bovine spongiform encephalopaty in cattle and Creutzfeldt–Jacob disease in humans. Most humans affected by prion disease present rapidly progressive dementia, sometimes accompanied by cerebellar ataxia. Postmortem analysis shows spongiform degeneration and astrocytic gliosis. The human prion disease can exist as sporadic, genetic, or infectious forms. Prusiner proposed that prions are transmissible particles that are devoid of nucleic acids and seem to be composed exclusively of a modified protein *(118)*. Several studies have demonstrated that the critical pathogenetic event is the misfolding of a benign 33 to 35 kDa glycoprotein (PrP), anchored to the outer surface of the plasma membrane of the neurones by the C-terminus, to form the infectious isoform (PrP^{Sc}). This isoforms is protease resistant and accumulates mainly in the brain. The main structural modification consists of an increased β-sheet content and diminished α-helix *(119)*.

It has been proposed that PrP may be a copper-binding protein *(120)*. A link between copper and prion diseases has early been envisaged when cuprizone, a copper-chelating agent, was shown to induce neuropathological changes in mice similar to those found in the prion disease *(121)*. The highly flexible and conserved N-terminal domain of mammalian PrP shows four octapeptide tandem repeat regions (PHGGGWGQ): it has been demonstrated that both synthetic peptides *(122,123)*, containing three or four copies of this octapeptide, and recombinant PrP *(124)* preferentially bind copper over other metals, with a micromolar affinity. The coordination sphere of copper involves four histidines belonging to four distinct octarepeats in a square planar geometry, with cooperation of binding. This constrains the region into a rather compact structure, thus leading up to four ligated copper(II)

per PrP protein *(125)*. Copper binding induces a conformational shift from a predominant α-helical to a β-sheet structure *(126–128)* and stabilizes the conformation of the infectious form in experiments of reversible denaturation *(129)*. From the bulk of these data, it can be suggested that the metal may play at least a complementary role in the etiology of prion disease.

Little is known about the normal function of PrP in the brain. As for APP, owing to its plasma membrane location, it could be a candidate for copper sensing, copper brain metabolism, and exchange of copper(II) with other copper-binding molecules. However, on this subject, literature data are controversial. Indeed, copper rapidly and reversibly stimulates endocytosis of PrP in N2a mouse neuroblastoma cells stably transfected with PrP *(130)*. Furthermore, the brain of PrP gene-ablated mice show reduction of copper levels in addition to a reduction of the activity of Cu,Zn superoxide dismutase, altered electrophysiological response in the presence of excess copper, and altered cellular phenotype *(131)*. Decreased Cu,Zn superoxide dismutase activity in cultured cerebellar cells from these mice makes them more sensitive to oxidative stress *(132)*. Therefore, imbalance in antioxidant functions has been proposed as a causative factor for prion disease *(133)*. However, recently, the role of PrP in copper brain uptake and distribution has been questioned by the finding that brain copper content and the activity of both Cu,Zn superoxide dismutase and cytochrome-*c* oxidase are not related to the expression level of PrP *(134)*. Another controversial point regards copper redox activity when bound to PrP. Brown et al. *(135)* demonstrated that PrP, either as a recombinant or immunoprecipitated from brain tissue, shows dismutating activity, thus addressing to copper-bound PrP a role in cellular resistance to oxidative stress and Ruiz et al. showed a potential physiological role of copper reduction by PrP *(136)*. On the other hand, there is also evidence that PrP binds copper ions in a redox inactive state, rendering dismutation and copper-induced generation of ROS impossible *(137)*.

In conclusion, recent results on the molecular mechanisms underlying the impairment of brain function in the most common neurodegenerative diseases suggest an intriguing role for copper. This metal really seems to represent a pivotal factor both in the development and in the health of the central nervous system. Genetic disruption of copper homeostasis, as it occurs in Wilson's and Menkes' diseases, is always associated with neurodegeneration, no matter whether the content of the metal is increased or diminished. Furthermore, aberrant copper chelation to neural proteins may lead to increased oxidative challenge to neurones, thus triggering processes ultimately leading to cell death. The observation that neurodegeneration mostly occur as programmed cell death gives support to the hypothesis that an as yet unknown copper-dependent factor may be involved in apoptosis.

ACKNOWLEDGMENT

This work was partially supported by Ministero della Sanità (Progetto Finalizzato 1998-2000), by MURST–CNR (Biotechnology Program L. 95/95) and by CNR (Progetto Strategico Biologia dell'Invecchiamento e sue Conseguenze sul Sistema Assistenziale).

REFERENCES

1. Pena, M. M. O., Lee, J., and Thiele, D. J. (1999) A delicate balance: homeostatic control of copper uptake and distribution. *J. Nutr.* **129**, 1251–1260.
2. Halliwell, B. (1992) Reactive oxygen species and the central nervous system. *J. Neurochem.* **59**, 1609–1623.
3. Cross, A. R. and Jones, O. T. G. (1991) Enzymic mechanism of superoxide production. *Biochim. Biophys. Acta* **1057**, 281–298.
4. Sies, H. (1993) Strategies of antioxidant defense. *Eur. J. Biochem.* **215**, 213–219.
5. Hamer, D. H. (1986) Metallothionein. *Annu. Rev. Biochem.* **55**, 913–951.
6. Freedman, J. H., Ciriolo, M. R. and Peisach, J. (1988) The role of glutathione in copper metabolism and toxicity. *J. Biol. Chem.* **264**, 5598–5605.
7. Ciriolo, M. R., Desideri, A., Paci, M., and Rotilio, G. (1989) Reconstitution of Cu,Zn-superoxide dismutase by the Cu (I)–glutathione complex. *J. Biol. Chem.* **265**, 11,030–11,034.
8. Da Costa Ferreira, A. M., Ciriolo, M. R., Marcocci, L., and Rotilio, G. (1993) Copper (I) transfer into metallothionein mediated by glutathione. *Biochem. J.* **292**, 673–676.

9. Harris, E. D. (2000) Cellular copper transport and metabolism. *Annu. Rev. Nutr.* **20**, 291–310.
10. Valentine, J. S. and Gralla, E. B. (1997) Delivering copper inside yeast and human cells. *Science* **278**, 817–818.
11. O'Halloran, T. V. and Culotta, V. C. (2000) Metallochaperones an intracellular shuttle service for metal ions. *J. Biol. Chem.* **275**, 25,057–25,060.
12. Spina, M. B. and Cohen, G. (1989) Dopamine turnover and glutathione oxidation: implications for Parkinson disease. *Proc. Natl. Acad. Sci. USA* **86**, 1398–1400.
13. Facchinetti, F., Dawson, V. L., and Dawson, T. M. (1998) Free radicals as mediator of neuronal injury. *Cell. Mol. Neurobiol.* **18**, 667–682.
14. Moncada, S., Palmer, R. M. J., and Higgs, E. A. (1991) Nitric oxide: physiology, pathophysiology, and pharmacology. *Pharmacol. Rev.* **43**, 109–142.
15. Stamler, J. S., Singel, D. J., and Loscalzo, J. (1992) Biochemistry of nitric oxide and its redox-activated forms. *Science* **258**, 1898–1902.
16. Rossi, L., Ciriolo, M. R., Marchese, E., De Martino, A., Giorgi, M., and Rotilio, G. (1994) Differential decrease of copper content and of copper binding to superoxide dismutase in liver, heart and brain of copper-deficient rats. *Biochem. Biophys. Res. Commun.* **203**, 1028–1034.
17. Chance, B., Sies, H., and Boveris, A. (1979) Hydroperoxide metabolism in mammalian organs. *Physiol. Rev.* **59**, 527–605.
18. Keen, C.L., and Hurley, L.S. (1980) Developmental changes in concentration of iron, copper and zinc in mouse tissues. *Mech. Ageing Dev.* **13**, 161–176.
19. Morita, A., Kimura, M., and Itokawa, I. (1994) The effect of aging on the mineral status of female mice. *Biol. Trace Element Res.* **42**, 165–177.
20. Miller, L. J. and Marx, J. (1998) Apoptosis. *Science* **281**, 1301–1326.
21. Bonfoco, E., Krainc, D., Ankarcrona, M., Nicotera, P., and Lipton, S. A. (1995) Apoptosis and necrosis: two distinct events induced, respectively, by mild and intense insults with *N*-methyl-D-aspartate or nitric oxide/superoxide in cortical cell cultures. *Proc. Natl. Acad. Sci. USA* **92**, 7162–7166.
22. Leist, M. and Nicotera, P. (1998) Apoptosis, excitotoxicity, and neuropathology. *Exp. Cell Res.* **239**, 183–201.
23. DiDonato, M. and Sarkar, B. (1997) Copper transport and its alterations in Menkes and Wilson diseases. *Biochim. Biophys. Acta* **1360**, 3–16.
24. Cox, D. W. (1999) Disorders of copper transport. *Br. Med. Bull.* **55**, 544–555.
25. Waggoner, D. J., Bartnikas, T. B., and Gitlin, J. D. (1999) The role of copper in neurodegenerative disease. *Neurobiol. Dis.* **6**, 221–230.
26. Harris, Z. L. and Gitlin, J. D. (1996) Genetic and molecular basis for copper toxicity. *Am. J. Clin. Nutr.* **63**, 836S–841S.
27. Tumer, Z. and Horn, N. (1997) Menkes disease: recent advances and new aspects. *J. Med. Gen.* **34**, 265–274.
28. Menkes, J. H., Alter, M., Stegleder, G., Weakley, D. R., and Sung, J. H. (1962) A sex-linked recessive disorder with retardation of growth, peculiar hair and focal cerebral and cerebellar degeneration. *Pediatrics* **29**, 764–779.
29. Chelly, J., Tumer, Z., Tossesen, T., Petterson, A., Ishikawa-Brush, Y., Tommerup, N., et al. (1993) Isolation of a candidate gene for Menkes disease that encodes a potential heavy metal binding protein. *Nature Genet.* **3**, 14–19.
30. Mercer, J. F. B., Livingston, J., Hall, B., Paynter, J. A., Begy, C., Chandrasekharappa, S., et al. (1993) Isolation of a partial candidate gene for Menkes disease by positional cloning. *Nature Genet.* **3**, 20–25.
31. Vulpe, C., Levison, B., Whitney, S., Packman, S., and Gitschier, J. (1993) Isolation of a candidate gene for Menkes disease and evidence that it encodes a copper-transporting ATPase. *Nature Genet.* **3**, 7–13.
32. Mercer, J. F. B. (1998) Menkes syndrome and animal models. *Am. J. Clin. Nutr.* **67**, 1022S–1028S.
33. Yajima, K. and Suzuki, K. (1979) Neuronal degeneration in the brain of the brindled mouse. *Acta Neuropatol.* **45**, 17–25.
34. Rossi, L., De Martino, A., Marchese, E., Piccirilli, S., Rotilio, G., and Ciriolo, M. R. (2000) Neurodegeneration in the animal model of Menkes disease involves Bcl-2 linked apoptosis. *Neuroscience* **103**, 181–188.
35. Sadoul, R. (1998) BCL-2 family members in the development and degenerative pathologies of the nervous system. *Cell Death Differ.* **5**, 805–815.
36. Fuji, T., Ito, M., Tsuda, H., and Mikawa, H. (1990) Biochemical study on the critical period for treatment of the mottled brindled mouse. *J. Neurochem.* **55**, 885–889.
37. Petrukhin, K., Fischer, S. G., Pirastu, M., E., et al. (1993) Mapping, cloning and genetic characterization of the region containing the Wilson disease gene. *Nature Genet.* **5**, 338–343.
38. Chelly, J. and Monaco, A. P. (1993) Cloning the Wilson disease gene. *Nature Genet.* **5**, 317–318.
39. Dobyns, W. B., Goldstein, N. P., and Gordon, H. (1979) Clinical spectrum of Wilson's disease (hepatolenticular degeneration). *Mayo Clin. Proc.* **54**, 35–42.
40. Bull, P. C., Thomas, G. R., Rommens, J. M., Forbes, J. R., and Cox, D. W. (1993) The Wilson disease gene is a putative copper transporting P-type ATPase similar to the Menkes gene. *Nature Genet.* **5**, 327–337.
41. Tanzi, R. E., Petrukhin, K., Chernov, I., Pellequer, J. L., Wasco, W., Ross, B., et al. (1993) The Wilson disease gene is a copper transporting ATPase with homology to the Menkes disease gene. *Nature Genet.* **5**, 344–350.
42. Yamaguchi, Y., Heiny, M. E., and Gitlin, J. D. (1993) Isolation and characterisation of a human liver cDNA as a candidate gene for Wilson disease. *Biochem. Biophys. Res. Commun.* **197**, 271–277.
43. Brewer, G. J. (1995) Pratical recommendations and new therapies for Wilson's disease. *Drugs* **50**, 240–249.
44. Morrison, B. M. and Morrison, J. H. (1999) Amyotrophic lateral sclerosis associated with mutations in superoxide dismutase: a putative mechanism of degeneration. *Brain Res. Rev.* **29**, 121–135.

45. Deng, H.-X., Hentati, A., Tainer, J. A., et al. (1993) Amyotrophic lateral sclerosis and structure defects in Cu,Zn superoxide dismutase. *Science* **261**, 1047–1051.
46. Rosen, D. R., Siddique, T., Patterson, D., A., et al. (1993) Mutations in Cu/Zn superoxide dismutase gene are associated with familiar amyotrophic lateral sclerosis. *Nature* **362**, 59–62.
47. Rowland, L. P. (1995) Amyotrophic lateral sclerosis: human challenge for neuroscience. *Proc. Natl. Acad. Sci. USA* **92**, 1251–1253.
48. Bannister, J. V., Bannister, W. H., and Rotilio, G. (1987) Aspects of the structure, function and application of superoxide dismutase. *CRC Crit. Rev. Biochem.* **22**, 111–180.
49. Orrell, R. W. (2000) Amyotrophic lateral sclerosis: copper/zinc superoxide dismutase (SOD1) gene mutations. *Neuromuscul. Disord.* **10**, 63–68.
50. Carrì, M.T., Battistoni, A., Polizio, F., Desideri, A., and Rotilio, G. (1994) Impaired copper binding by the H46R mutant of human Cu,Zn superoxide dismutase, involved in amyotrophic lateral sclerosis. *FEBS Lett.* **356**, 314–316.
51. Ogasawara, M., Matsubara, Y., Narisawa, K., et al. (1993) Mild ALS in Japan associated with novel SOD mutation. *Nature Genet.* **5**, 323–324.
52. Borchelt, D. R., Lee, M. K., Slunt, H. S., Guarnieri, M., Xu, Z. S., Wong, P. C., et al. (1994) Superoxide dismutase 1 with mutation linked to familial amyotrophic lateral sclerosis possesses significant activity. *Proc. Natl. Acad. Sci. USA* **91**, 8292–8296.
53. Ferrante, R. J., Browne, S. E., Shinobu, L. A., Bowling, A. C., Baik, M. J., Mac Garvey, U., et al. (1997) Evidence of increased oxidative damage in both sporadic and familial amyotrophic lateral sclerosis. *J. Neurochem.* **69**, 2064–2074.
54. Bogdanov, M. B., Ramos, L. E., Xu, Z. and Beal, M.F. (1998) Elevated "hydroxyl radical" generation in vivo in an animal model of amyotrophic lateral sclerosis. *J. Neurochem.* **71**,1321–1324.
55. Liu, D., Wen, J., Liu, J., and Li, L. (1999) The roles of free radicals in amyotrophic lateral sclerosis: reactive oxygen species and elevated oxidation of protein, DNA and membrane phospholipids. *FASEB J.* **13,** 2318–2328.
56. Wiedau-Pazos, M., Goto J. J., Rabizadeh S., Gralla, E. B., Roe, J. A., Lee, M. K., et al. (1996) Altered reactivity of superoxide dismutase in familial amyotrophic lateral sclerosis. *Science* **271**, 515–518.
57. Yim, H. S., Kang, J. H., Yim, M. B., Kwak, H. S., Chock, P. B., and Stadtman, E. R. (1996) A gain-of-function of an amyotrophic lateral sclerosis-associated Cu,Zn-superoxide dismutase mutant: an enhancement of free radical formation due to a decrease in Km for hydrogen peroxide. *Proc. Natl. Acad. Sci. USA* **93**, 5709–5714.
58. Yim, H.-S., Kang, J.-H., Chock, P. B., Stadtman, E. R., and Yim, M. B. (1997) A familial amyotrophic lateral sclerosis-associated A4V Cu,Zn-superoxide dismutase mutant has a lower K_m for hydrogen peroxide. Correlation between clinical severity and the K_m value. *J. Biol. Chem.* **272**, 8861–8863.
59. Singh, R. J., Karoui, H., Gunther, M. R., Beckman, J. S., Mason, R. P., and Kalyanaraman, B. (1998) Reexamination of the mechanism of hydroxyl radical adducts formed from the reaction between familial amyotrophic lateral sclerosis associated Cu,Zn superoxide dismutase mutants and H_2O_2. *Proc. Natl. Acad. Sci. USA* **95**, 6675–6680.
60. Bruijn, L. I., Beal, M. F., Becher, M. W., Shulz, J. B., Wong, P. C., Price, D. L., et al. (1997) Elevated free nitrotyrosine levels, but no protein-bound nitrotyrosine or hydroxyl radicals, throughout amyotrophic lateral sclerosis like disease implicate tyrosine nitration as an aberrant in vivo property of one familial ALS-linked superoxide dismutase 1 mutant. *Proc. Natl. Acad. Sci. USA* **94**, 7606–7611.
61. Marklund, S. L., Andersen, P. M., Forsgren, L., Nilsson, P., Ohlsson, P. I., Wikander, G., et al. (1997) Normal binding and reactivity of copper in mutant superoxide dismutase isolated from amyotrophic lateral sclerosis patients. *J. Neurochem.* **69**, 675–681.
62. Lyons, T. J., Liu, H., Goto, J. J., Nersissian, A., Roe, J. A., Graden, J. A., et al. (1996) Mutations in copper–zinc superoxide dismutase that cause amyotrophic lateral sclerosis alter the zinc binding site and the redox behaviour of the protein. *Proc. Natl. Acad. Sci. USA* **93**, 12,240–12,244.
63. Crow, J. P., Sampson, J. B., Zhuang, Y. X., Thompson, J. A., and Beckman, J. S. (1997) Decreased zinc affinity of amyotrophic lateral sclerosis-associated superoxide dismutase mutants leads to enhanced catalysis of tyrosine nitration by peroxynitrite. *J. Neurochem.* **69**, 1936–1944.
64. Estevez, A. G., Crow, J. P., Sampson, J. B., Reiter, C., Zhuang, J., Richardson, G. J., et al. (1999) Induction of nitric oxide-dependent apoptosis in motor neurons by zinc-deficient superoxide dismutase. *Science* **286**, 2498–2500.
65. Bredesen, D. E., Wiedau-Pazos, M., Goto, J. J., Rabizadeh, S., Roe, J. A., Gralla, E. B., et al. (1996). Cell death mechanisms in ALS. *Neurology* **47(Suppl 2)**, S36–S39.
66. Nishida, C.R., Gralla, E. B., and Valentine, J. S. (1994) Characterization of three yeast copper–zinc superoxide dismutase mutants analogous to those coded for in familial amyotrophic lateral sclerosis. *Proc. Natl. Acad. Sci. USA* **91**, 9906–9910.
67. Goto, J. J., Zhu, H., Sanchez, R. J., Nersissian, A., Gralla, E. B., Valentine, J. S., et al. (2000) Loss of in vitro metal ion binding specificity mutant in copper-zinc superoxide dismutases associated with familiar amyotrophic lateral sclerosis. *J. Biol. Chem.* **275**, 1007–1014.
68. Corson, L. B., Strain, J. J., Culotta, V. C., and Cleveland, D. W. (1998) Chaperone-facilitated copper binding is a property common to several classes of familial amyiotrophic lateral sclerosis-linked superoxide dismutase mutants. *Proc. Natl. Acad. Sci. USA* **95,** 6361–6366.
69. Carrì, M. T., Ferri, A., Battistoni, A., Famhy, L., Gabbianelli, R., Poccia, F., et al. (1997) Expression of a Cu,Zn superoxide dismutase typical of familial amyotrophic lateral sclerosis induces mitochondrial alteration and increase of cytosolic Ca^{2+} concentration in transfected neuroblastoma SH-SY5Y cells. *FEBS Lett.* **414**, 365–368.
70. Gabbianelli, R., Ferri, A., Rotilio, G., and Carrì, M. T. (1999) Aberrant copper chemistry as a major mediator of oxidative stress in a human cellular model of amyotrophic lateral sclerosis. *J. Neurochem.* **73**, 1175–1180.

71. Bruijn, L. L., Houseweart, M. K., Kato, S., Anderson, K. L., Anderson, S. D., Ohama, E., et al. (1998) Aggregation and motor neuron toxicity of an ALS-linked SOD1 mutant independent from wild type SOD1. *Science* **281**, 1851–1854.
72. Ratovitski, T., Corson, L. B., Strani, J., Wong, P. Cleveland, D. W., Culotta, V. C., et al. (1999) Variation in the biochemical/biophysical properties of mutant superoxide dismutase 1 enzymes and the rate of disease progression in familial amyotrophic lateral sclerosis kindreds. *Hum. Mol. Genet.* **8**, 1451–1460.
73. Ghadge, G. D., Lee, J. P., Bindokas, V. P., Jordan, J., Ma, L., Miller, R. J., et al. (1997) Mutant superoxide dismutase-1-linked familial amyotrophic lateral sclerosis: molecular mechanisms of neuronal death and protection. *J. Neurosci.* **17**, 8756–8766.
74. Hottinger, A. F., Fine, E. G., Gurney, M. E., Zurn, A. D., and Aebscher, P. (1997) The copper chelator D-penicillamine delays onset of disease and extends survival in a transgenic mouse model of familial amyotrophic lateral sclerosis. *Eur. J. Neurosci.* **9**, 1548–1551.
75. Mu, X. J., He, J., Anderson, D. W., Trojanowski, J. Q., and Spriger, J. E. (1996) Altered expression of Bcl-2 and Bax messengers RNA in amyotrophic lateral sclerosis spinal cord motor neurons. *Ann. Neurol.* **40**, 379–386.
76. Migheli, A., Atzori, C., Piva, R., Tortarolo, M., Girelli, M., Schiffer, D., et al. (1999) Lack of apoptosis in mice with ALS. *Nature Med.* **9**, 966–967.
77. Rabizadeh, S., Gralla, E. B., Borchelt, D. R., Gwinn, R., Valentine, J. S., Sisodia, S., et al. (1994) Mutations associated with amyotrophic lateral sclerosis convert superoxide dismutase from an antiapoptotic gene to a proapoptotic gene: studies in yeast and neural cells. *Proc. Natl. Acad. Sci. USA* **92**, 3024–3028.
78. Pasinelli P., Borchelt D. R., Houseweart M. K., Cleveland D. W., and Brown R. H. Jr. (1998) Caspase-1 is activated in neural cells and tissue with amyotrophic lateral sclerosis-associated mutations in copper-zinc superoxide dismutase. *Proc. Natl. Acad. Sci. USA* **95**, 15,763–15,768.
79. Li, M., Ona, V. O., Guégan, C., Chen, M., Jackson-Lewis V., Andrews, L. J., et al. (2000) Functional role of caspase-1 and caspase-3 in an ALS transgenic mouse model. *Science* **288**, 335–339.
80. Ciriolo, M. R., De Martino, A., Lafavia, E., Rossi, L., Carrì, M. T., and Rotilio, G. (2000) Cu,Zn superoxide dismutase-dependent apoptosis induced by nitric oxide in neuronal cells. *J. Biol. Chem.* **275**, 5065–5072.
81. Inoue, K., Akaike, T., Miyamoto, Y., Okamoto, T., Sawa, T., Otagiri, M., et al. (1999) Nitrosothiol formation catalysed by ceruloplasmin. *J. Biol. Chem.* **274**, 27,069–27,075.
82. Bonilla, E., Tanji, K., Hirano, M., Vu, T. H., Di Mauro, S., and Schon, E. A. (1999) Mitochondrial involvement in Alzheimer's disease. *Biochem. Biophys. Acta* **1410**, 171–182.
83. Holtzman, D. M. and Mobley, W. C. (1991) Molecular studies in Alzheimer's disease. *Trends Biochem. Sci.* **16**, 140–144.
84. Yankner, B. A., Duffy, L. K., and Kirshner, D. A. (1990) Neurotrophic and neurotoxic effects of amyloid β protein: reversal by tachykinin neuropeptides. *Science* **250**, 279–282.
85. Cuajungco, M. P., Goldstein, L. E., Nunomura, A., Smith, M. A., Lim, J. T., Atwood, C. S., et al. (2000) Evidence that the β-amyloid plaques of Alzheimer's disease represent the redox-silencing and entombment of Aβ by zinc. *J. Biol. Chem.* **275**, 19,439–19,442.
86. Hesse, L., Beher, D., Masters, C. L., and Multhaup, G. (1994) The beta A4 amyloid precursor protein binding to copper. *FEBS Lett.* **349**, 109–116.
87. Selkoe, J. (1998) The cell biology of beta-amyloid precursor protein and presenilin in Alzheimer's disease. *Trends Cell Biol.* **8**, 447–453.
88. Multhaup, G., Schlicksupp, A., Hesse, L., Beher, D., Ruppert, T., Masters, C. L., et al. (1996) The amyloid precursor protein of Alzheimer's disease in the reduction of copper (II) to copper (I). *Science* **271**, 1406–1409.
89. Multhaup, G., Ruppert, T., Schlicksupp, A., Hesse, L., Bill, E., Pipkorn, R., et al. (1998) Copper-binding amyloid precursor protein undergoes a site-specific fragmentation in the reduction of hydrogen peroxide. *Biochemistry* **37**, 7224–7230.
90. Atwood, C. S., Moir, R. D., Huang, X., Scarpa, R. C., Bacarra, M. E., Romano, D. M., et al. (1998) Dramatic aggregation of Alzheimer Aβ by Cu (II) is induced by conditions representing physiological acidosis. *J. Biol. Chem.* **273**, 12,817–12,826.
91. Lovell, M. A., Robertson, J. D., Teesdale, W. J., Campbell, J. L. and Markesbery, W. R. (1998) Copper, iron and zinc in Alzheimer's disease senile plaques. *J. Neurol. Sci.* **158**, 47-52.
92. Markesbery, W. R. and Carney, J. M. (1999) Oxidative alterations in Alzheimer's disease. *Brain Pathol.* **9**, 133-146.
93. Smith, M. A., Rottkamp, C. A., Nunomura, A., Raina, A. K., and Perry, G. (2000) Oxidative stress in Alzheimer's disease. *Biochim. Biophys. Acta* **1502**, 139–144.
94. Smith, C. D., Carney, J. M., Starke-Reed, P. E., Oliver, C. N., Stadtman, E. R., Floyd, R. A., et al. (1991) Excess brain protein oxidation and enzyme dysfunction in normal aging and Alzheimer's disease. *Proc. Natl. Acad. Sci. USA* **88**, 10,540–10,543.
95. Markesbery, W. R. (1997) Oxidative stress hypothesis in Alzheimer's disease. *Free Radical Biol. Med.* **23**, 134–147.
96. Coyle, J. and Puttfarcken, P. (1993) Oxidative stress, glutamate, and neurodegenerative disorders. *Science* **262**, 689–695.
97. Mecocci, P., MacGarvey, U., and Beal, M. F. (1994) Oxidative damage to mitochondrial DNA is increased in Alzheimer's disease. *Ann. Neurol.* **36**, 747–751.
98. Lyras, L., Cairns, N. J., Jenner, A., Jenner, P., and Halliwell, B. (1997) An assessment of oxidative damage to proteins, lipids, and DNA in brain from patients with Alzheimer's disease. *J. Neurochem.* **68**, 2061–2069.
99. Parke, W. D., Jr., Filley, C. M., and Parks, J. K. (1990) Cytochrome oxidase deficiency in Alzheimer's disease. *Neurology* **40**, 1302–1303.

100. Mutisya, E. M., Bowling, A. C., and Beal, M. F. (1994) Cortical cytochrome oxidase activity is reduced in Alzheimer's disease. *J. Neurochem.* **63**, 2179–2184.
101. Kish, S. J., Bergeon, C., Rajput, A., Dozic, S., Mastrogiacomo, F., Chang, L.-J., et al. (1992) Brain cytochrome oxidase in Alzheimer's disease. *J. Neurochem.* **59**, 776–779.
102. Kish, S. J., Mastrogiacomo, F., Guttman, M., Furukawa, Y., Taanman, J., Dozic, S., et al. (1999) Decreased brain protein levels of cytochrome oxidase subunit in Alzheimer's disease and in hereditary spinocerebellar ataxia disorders: a nonspecific change? *J. Neurochem.* **72**, 700–707.
103. White, A. R., Multhaup, G., Maher, F., Bellingham, S., Camakaris, J., Zheng, H., et al. (1999) The Alzheimer's disease amyloid precursor protein modulates copper-induced toxicity and oxidative stress in primary neuronal cultures. *J. Neurosci.* **19**, 9170–9179.
104. Huang, X., Cuajungco, M. P., Atwood, C. S., Hartshorn, M. A., Tyndall, J. D. A., Hanson, G. R., Stokes, K. C., et al. (1999) Cu (II) potentiation of Alzheimer Aβ neurotoxicity. *J. Biol. Chem.* **274**, 37,111–37,116.
105. Olanow, C. W. and Tatton, W. G. (1999) Etiology and pathogenesis of Parkinson's disease. *Annu. Rev. Neurosci.* **22**, 123–144.
106. Polymeropoulos, M. H., Lavedan, C., Leroy, E., Ide, S. E., Dehejia, A., et al. (1997) Mutation in the a-synuclein gene identified in families with Parkinson's disease. *Science* **276**, 2045–2047.
107. Polymeropoulos, M. H., Higgins, J. J., Golbe, L. I., Johnson, W. G., Ide, S. E., et al. (1996) Mapping of a gene for Parkinson's disease to chromosome 4q21-q23. *Science* **274**, 1197–1199.
108. Kruger, R., Kuhn, W., Muller, T., Woitalla, D., Graeber, M., Kosel, S., et al. (1998) Ala30Pro mutation in the gene encoding α-synuclein in Parkinson's disease. *Nature Genet.* **18**, 106–108.
109. Zhang, Y., Dawson, V. L., and Dawson, T. M. (2000) Oxidative stress and genetics in the pathogenesis of Parkinson's disease. *Neurobiol. Dis.* **7**, 240–250.
110. Jenner, P. and Olanow, C. W. (1996) Oxidative stress and the pathogenesis of Parkinson's disease. *Neurology* **47**, 161–170.
111. Alam, Z. I., Daniel, S. E., Lees, A. J., Mardsen, C. D., Jenner, P., and Halliwell, B. (1997) A generalised increase in protein carbonyls in the brain in Parkinson's but not incidental Lewy body disease. *J. Neurochem.* **69**, 1326–1329.
112. Alam, Z. I., Jenner, A., Daniel, S. E., et al. (1997b) Oxidative DNA damage in the parkinsonian brain: a selective increase in 8-hydroxyguanine in substantia nigra? *J. Neurochem.* **69**, 1196–1203.
113. Dexter, D. T., Holley, A. E., Flitter, W. D., Slater, T. F., Wells, F. R., Daniel, S. E., et al. (1994) Increased levels of lipid hydroperoxides in the parkinsonian substantia nigra: an HPLC and ESR study. *Mov. Disord.* **9**, 92–97.
114. Good, P. F., Hsu, A., Werner, P., Perl, D. P., and Olanow, C. W. (1998) Protein nitration in Parkinson's disease. *J. Neuropathol. Exp. Neurol.* **57**, 388–342.
115. Itoh, K., Weis, S., Mehraein, P. and Muller-Hocker, J. (1997) Defects of cytochrome c oxidase in the substantia nigra of Parkinson's disease: an immunohistochemical and morphometric study. *Mov. Disorders* **12**, 9–16.
116. Torsdottir, G., Kristinsson, J., Sveinbjornsdottir, S., Snaedal, J., and Johannesson, T. (1999) Copper, ceruloplasmin, superoxide dismutase and iron paramenters in Parkinson's disease. *Pharmacol. Toxicol.* **85**, 239–243.
117. Paik, S. R., Shin, H-J., Lee, J.-H., Chang C.-S., and Kim, J. (1999) Copper (II)-induced self-oligomerization of α-synuclein. *Biochem. J.* **340**, 821–828.
118. Prusiner, S. B. (1998) Prions. *Proc. Natl. Acad. Sci. USA* **95**, 13,363–13,383.
119. Weissmann, C. (1999) Molecular genetics of transmissible spongiform encephalopathies. *J. Biol. Chem.* **274**, 3–6.
120. Prince, R. C. and Gunson, D. E. (1998) Prions are copper-binding proteins. *Trends Biochem. Sci.* **23**, 197–198.
121. Kimberlin, R. H., Millson, G. C., Bountiff, L., and Collins, S. C. (1974) A comparison of the biochemical changes induced in mouse brain cuprizone toxicity and by scrapie infection. *J. Compar. Pathol.* **84**, 263–270.
122. Hornshaw, M. P., Mcdermott, J. R., Candy, J. M., and Lakey, J. H. (1995) Copper binding to the N-terminal tandem repeat region of mammalian and avian prion protein: structural studies using synthetic peptides. *Biochem. Biophys. Res. Commun.* **214**, 993–999.
123. Hornshaw, M. P., Mcdermott, J. R., and Candy, J. M. (1995) Copper binding the N-terminal tandem repeat regions of mammalian and avian prion protein. *Biochem. Biophys. Res. Commun.* **207**, 621–629.
124. Stockel, J., Safar, J., Wallace, A. C., Cohen, F. E., and Prusiner, S. B. (1998) Prion protein selectively binds copper (II) ions. *Biochemistry* **37**, 7185–7193.
125. Viles, J. H., Cohen, F. E., Prusiner, S. B., Goodin, D. B., Wright, P. E., and Dyson, H. J. (1999) Copper binding to the prion protein: structural implications of four identical cooperative bindings sites. *Proc. Natl. Acad. Sci. USA* **96**, 2042–2047.
126. Miura, T., Hori, A., and Takeuchi, H. (1996) Metal-dependent alpha-helix formation promoted by the glycine-rich octapeptide region of prion protein. *FEBS Lett.* **396**, 248–252.
127. Whittal, R. M., Ball, H. L., Cohen, F. E., Burlingame, A. L., Prusiner, S. B., and Baldwin, M. A. (2000) Copper binding to octarepeat peptides of the prion protein monitored by mass spectrometry. *Protein Sci.* **9**, 332–343.
128. Qin, K., Yang, Y., Chishti, M. A., Meng, L. J., Kretzschmar, H. A., Yip, C. M., et al. (2000) Copper (II)-induced conformational changes and protease resistance in recombinant and cellular PrP. Effect of protein age and deamidation. *J. Biol. Chem.* **275**, 19,121–19,131.
129. McKenzie D., Bertz, J., Mirwald, J., Olander, D., Marsh, R., and Aiken, J. (1998) Reversibility of scrapie inactivation is enhanced by copper. *J. Biol. Chem.* **273**, 25,545–25,547.
130. Pauly, P. C. and Harris, D. A. (1998) Copper stimulates endocytosis of the prion protein. *J. Biol. Chem.* **273**, 33,107–33,110.
131. Brown, D. R., Kefeng, Q., Herms, J W., Madlung, A., Manson, J., Strome, R., et al. (1997) The cellular prion protein binds copper *in vivo*. *Nature* **390**, 684–687.

132. Brown, D. R., Schulz-Schaeffer, W. J., Schimdt, B., and Kretzscmar, H. A. (1997) Prion protein-deficient cells show altered response to oxidative stress due to decreased SOD-1 activity. *Exp. Neurol.* **146**, 104–112.
133. Wong, B. S., Pan, T., Liu, R., Petersen, R. B., Jones, I. M., Gambetti, P., et al. (2000) Prion disease: a loss of antioxidant function? *Biochem. Biophys. Res. Commun.* **275**, 249–252.
134. Waggoner, D. J., Drisaldi, B., Bartnikas, T. B., Casareno, R. L., Prohaska, J. R., Gitlin, J. D., et al. (2000) Brain copper content and cuproenzyme activity do not vary with prion protein expression level. *J. Biol. Chem.* **275**, 7455–7458.
135. Brown, D. R., Wong, B. S., Hafiz, F., Clive, C., Haswell, S. J., and Jones, I. M. (2000) Normal prion protein has an activity like that of superoxide dismutase. *Biochem. J.* **344 (Pt. 3)**, 767.
136. Ruiz, F. H., Silva, E., and Inestrosa, N. C. (2000) The N-terminal tandem repeat region of human prion protein reduces copper: role of tryptophan residues. *Biochem. Biophys. Res. Commun.* **269**, 491–495.
137. Shiraishi, N., Ohta, Y., and Nishikimi, M. (2000) The octapeptide repeat region of prion protein binds Cu (II) in the redox-inactive state. *Biochem. Biophys. Res. Commun.* **267**, 389–402.

17

Role of Copper and Other Transition Metal Ions in the Pathogenesis of Parkinson's Disease, Prion Diseases, Familial Amyotrophic Lateral Sclerosis, and Alzheimer's Disease

Gerd Multhaup, Hermann H. Dieter, Konrad Beyreuther, and Thomas A. Bayer

1. INTRODUCTION

During the last few years, there has been growing evidence based on experimental data that Cu and other transition metal ions may have important roles in the pathogenesis of a series of hereditary and sporadic disorders of the central nervous system (CNS). It is suggested that metal ions such as Cu exert toxicity during electron-transfer reactions and also play a structural role by changing the conformation of proteins upon specific binding. In contrast, Zn is assumed to play a purely structural role because it exists exclusively in one oxidation state. According to presently accumulating knowledge, Cu complexes are especially sensitive to redox reactions (in the form of "free") -Cu ions in the Fenton-type reaction). On the other hand, copper is an essential element—being a cofactor of detoxifying enzymes such as of Cu/Zn-superoxide dismutase (SOD). According to the high-affinity binding of Cu to the native amyloid precursor protein (APP) and the prion protein (PrP), Cu is suggested to exert conformation stabilizing functions, to act as a redox active detoxifying cofactor, and is involved in metabolic transport (APP) or absorption–secretory (PrP and APP) functions. Currently, there are no data to confirm the hypothesis that an enhanced exogeneous exposure to Cu (or other transition metal ions) may accelerate the progression of neurodegenerative diseases or even to show a significant association with increased metal-ion levels in general, or what may occur with a higher frequency in response to exogenous exposure. In contrast, a causal relationship has been shown for neurodegenerative symptoms and chronic inhalatory exposure of Mn because of its unique ability to cross the blood-brain barrier via the olfactory epithelium.

Nevertheless, and considering the accumulating evidence of the possible involvement of Cu and Fe in the pathogenesis of most of these diseases (Fig. 1), it is highly recommended that more attention should be paid to the possibility that neurodegenerative processes may be triggered especially by Cu and Fe via environmental exposure or by an altered endogenous exposure (i.e., from nutrition).

2. PARKINSON'S DISEASE

Parkinson's disease (PD) affects 2% of the population over the age of 65. Neuropathologically, this disorder is characterized by intracellular inclusions (Lewy bodies), neuronal cell loss, and notable

From: Handbook of Copper Pharmacology and Toxicology
Edited by: E. J. Massaro © Humana Press Inc., Totowa, NJ

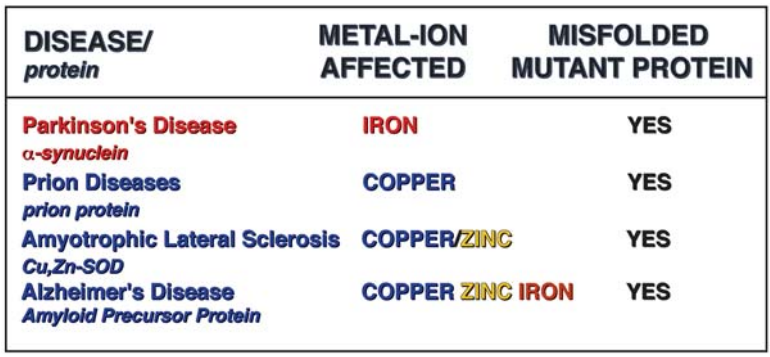

Fig. 1. Possible involvement of transition metal ions in neurodegenerative disorders. Iron, copper, and aluminium induce amyloidlike aggregate formation of α-synuclein in vitro (Parkinson); copper induces conformational changes in PrP and can convert the prion protein to a protease-resistant form (prion disease); copper in the mutant Cu,Zn-SOD catalyzes deleterious oxidation reactions (familial amyotrophic lateral sclerosis); copper initiates amyloid Aβ aggregation and may act as a sink, thus disturbing metal-ion homeostatis by drawing copper ions away from the amyloid precursor protein (Alzheimer's disease).

depigmentation of the substantia nigra *(1)*. The neurons that degenerate use dopamine as a transmitter, which leads to dopamine deficiency in the striatum, the main dopaminergic innervation target. Lewy bodies are intracytoplasmic circular inclusions and are the hallmark pathological finding in Lewy-body dementia. Lewy bodies and Lewy neurites stain very strongly for α-synuclein, a 140-amino-acid protein of unknown function that is abundantly expressed in the presynaptic nerve terminals of the brain. The protein α-synuclein is the main component of the filamentous inclusions in all cases of Parkinson's disease. An overexpression of α-synuclein in transgenic mice *(2)* led to a loss of dopaminergic terminals in the basal ganglia with motor impairments. Mice lacking α-synuclein display functional deficits in the nigrostriatal dopamine system *(3)*. Thus, it is suggested that α-synuclein is an essential activity-dependent negative regulator of dopamine neurotransmission.

2.1. Genetics

The primary cause of PD generally remains unknown. After age, a positive family history is the second most important risk factor for developing the illness. PD in most patients is sporadic, although patients with autosomal dominant *(4–6)* or recessive disease *(7,8)* have been reported. The autosomal dominant form is the most common form among familial cases *(9)*. Clinical features with Lewy bodies were similar to those in sporadic PD, but the mean age of the disease onset was younger (45 yr) and the mean duration of the illness (average 9 yr) was shorter. The gene could be localized to chromosome 4q21–q23, where the gene for α-synuclein had been mapped *(10,11)*. Missense mutations have been described in the α-synuclein gene in two unrelated kindreds with early-onset familial PD *(11,12)*. The mutations change residues 53 (A53T) in a large Italian-American kindred and 30 (A30P) of α-synuclein in a German pedigree. Both mutations lie in the repeat region of α-synuclein. The mutations may change the conformation into a β-sheet structure and thus initially promote the aggregation. Interactions with other cellular components may lead to aggregation into filaments and assembly into Lewy bodies and Lewy neurites, which finally leads to a gain of toxic function. One of these components was identified to be Cu(II), when a Cu(II)-induced self-aggregation of α-synuclein had been observed *(13,14)*. Even an overexpression of wild-type α-synuclein was found to be toxic and mutations were found to exhibit even greater toxicity, most likely the result of activity as a protein chaperone *(15)*. When α-synuclein was observed to bind to tau and to stimulate the protein kinase A-catalyzed phosphorylation of tau serine residues 262 and 356 *(16)*, a linking between two diseases was provided: the tau gene was found to be mutated in another rare autosomal dominant inherited dementia, termed frontotemporal dementia, and parkinsonism was linked to chromosome 17, FTDP17 *(17)*.

Deletions in parkin, a novel gene of unknown function, have been associated with the autosomal recessive form of a rare juvenile parkinsonism (AR-JP) in Japanese families. The gene was identified by positional cloning *(18)* and mapped to chromosome 6q25.2–27 near the SOD-2 locus of the Mn-SOD gene *(7)*. Autosomal recessive juvenile parkinsonism shows marked clinical similarity to PD, and the linkage to the 6q25.2–27 region was found in a group of 15 families from 4 distinct ethnic backgrounds *(19)*. Recombination events restricted the JP locus to a 6.9-c*M* region and excluded SOD-2 *(19)*. The disease phenotype was associated with deletions between exons 3 and 7 (of 12 exons encoding a protein of 465 amino acids) *(20)*.

A genetic predisposition appears to be important in the pathogenesis of the much more common sporadic PD, because the prevalence of PD among relatives of PD patients has been shown to be five times higher than in the general population *(21)*. This view is in accordance with a recent finding where a susceptibility locus for PD was mapped to chromosome 2p13 *(22)*. According to the mean age of onset and the low penetrance of the mutation (less than 40%), this locus has been suggested to play a possible role not only in familial PD, but also in sporadic PD *(22)*.

2.2. PD and Oxidative Stress

The term "stress" describes a state of disturbed homeostasis, harmony, and equilibrium. In PD, the relationships between oxidative damage and PD have been proposed for years and widely studied. In all forms of the disease, mitochondrial failure and oxidative stress occur and are probably secondary to other primary genetic or environmental factors. In addition, mitochondrial failure and oxidative stress are linked: If either one takes place, the other follows. Thus, mitochondrial failure and oxidative stress are considered to be the major contributors to the progress of nigral cell death in PD *(23–27)*.

Several lines of evidence underline the presence of oxidative stress in nigral neurons in PD, including the following:

- Increase in iron content
- Increase in superoxide dismutase activity
- Increase in protein oxidation
- DNA damage
- Increase in lipid oxidation
- Decrease in the level of the reduced form of glutathione

Postmortem analysis showed increased levels of iron, implying deranged iron metabolism *(23,25)*. Thus, PD is characterized by a high deposition of iron and a low concentration of ferritin in the substantia nigra. In addition, more severely affected patients had a higher iron content. This is why the iron concentration measured by magnetic resonance correlated with the severity of clinical symptomatology *(28)*. However, no significant differences were observed between PD patients' and control subjects' dietary intake of iron from food or supplements *(29–33)*.

2.3. Possible Involvement of Transition Metal Ions in PD

In various subcortical brain regions, populations of astroglia progressively accumulate iron-mediated peroxidase-positive cytoplasmic inclusions. The mechanism mediating the pathological deposition of redox active brain iron in PD is unknown, but recent studies showed that nigral gliosomes in old rats were immunoreactive for ubiquitin and a mitochondrial epitope. Redox active iron in aging nigral astroglia was detected by X-ray emission and was suggested to predispose the nervous system to neurodegenerative processes *(34)*. In a minority of nigral gliosomes, copper was also detected in peroxidase-positive astrocyte inclusions in the substantia nigra *(34)*. The cerebrospinal fluid (CSF) levels of Zn(II) were significantly decreased in PD patients as compared with controls, whereas the serum levels of Zn(II), Fe(III), Cu(II), and Mg(II) did not differ significantly between PD patients and controls *(35)*. This could be related to the oxidative stress hypothesis, when transition metals,

such as iron and copper, occupy binding sites of Zn(II) and undergo redox reactions. Also, Zn(II) itself can reduce oxidative stress by binding to thiol groups, thereby decreasing their oxidation.

Chronic exposure to copper, manganese, and the combinations of lead–copper and iron–copper led to an increased association with PD, suggesting occupational exposures to metals as risk factors for PD *(36)*. Particularly, iron and hydrogen peroxide have been shown to induce aggregate formation of α-synuclein in vitro *(14,37)*. Likewise, iron(II) could promote the aggregation of α-synuclein in vivo because iron accumulates in the substantia nigra with age and iron(II) can stimulate free-radical production.

In an iron-induced animal model of parkinsonism, manganese protected nigral neurons from iron-induced oxidative injury and dopamine depletion in a dose-dependent basis *(38)*. In brain homogenates, a molar excess of manganese inhibited lipid peroxidation caused by iron *(38)*. Here, manganese most likely served as an atypical antioxidant because it competed with iron to catalyze the Fenton reaction. In contrast to this, it has been found that Mn alters brain aconitase activity in mitochondrial fractions from rat brain, possibly leading to a disruption of mitochondrial energy production and cellular Fe metabolism in the brain *(39)*. The symptoms of Mn-induced neurotoxicity resemble those of PD.

2.4. A Unifying Hypothesis

Although the pathophysiological mechanisms of cell death in PD is unknown, therapeutic implications also support the free-radical/oxidative stress hypothesis in PD. The inhibition of MAO-B, a predominantly glial enzyme in the brain, by drugs such as selegiline may protect against activation of some toxins and free radicals formed from the MAO-B oxidation of dopamine. However, it has also been suggested that selegiline may act through an increase of neurotrophic factor activity and upregulate molecules such as glutathione, SOD, catalase, and Bcl-2 protein, which all protect against oxidative stress and thus can often be effective only early in the course of PD *(40,41)*. New approaches designed to attenuate the effects of oxidatve stress include enhancing the survival of neurons by giving brain-derived neurotrophic factors and by providing antioxidants such as vitamin E. So far, only selegiline has been shown to be successful in prolonging the survival of patients with PD *(42)*. Recently, autotransplantation based on promising results in a rodent model system for PD disease has been suggested in a nonhuman primate model with the carotid body as an autologous dopamine source *(43)*.

2.5. Lewy Bodies

Clearly, mutations in α-synuclein lead to the occurence of Lewy bodies and Parkinson's disease *(11)*. Thus, mutations as primary events in either tau or α-synuclein can lead to their cognate pathologies. Synuclein is a neuron-specific protein localized in the presynaptic nerve terminals *(44)*. The expression is more prominent in the cerebrocortical areas than in the basal ganglia *(45)*. Lewy bodies are not restricted to PD, because α-synuclein is also the precursor of the nonamyloid component of the senile plaque in Alzheimer's disease in vitro *(46)*. Recently, this review has been challenged by the finding that α-synuclein cannot be detected immunohistochemically in senile plaques of Alzheimer's disease (AD) brains *(47)*. Abnormal filamentous inclusions within some nerve cells is a characteristic shared by AD, PD, dementia with Lewy bodies, Huntington's disease, and other trinucleotide repeat disorders that lead to degeneration of affected nerve cells.

The primary cause of PD is still unknown, as is the molecular mechanism of nigral cell death. However, mitochondrial failure and oxidative stress leading to a disturbed metal-ion homeostasis appear to play an important role in nigral degeneration. The vulnerable neurons in PD may be particularly sensitive to oxidative stress that may be induced by iron, although other transition metal ions such as copper might play a role because ceruloplasmin (CP), the major plasma antioxidant, and copper-transport protein are significantly elevated in PD.

3. PRION DISEASES

The name "prion" diseases was given to transmissible pathogens causing scrapie and other transmissible neurodegenerative diseases and distinguish these pathogens from others, including viroids and viruses. Prion diseases are a group of neurodegenerative diseases that affect animals and humans. Examples of prion diseases include scrapie of sheep, transmissible mink encephalopathy (TME), chronic wasting disease (CWD) of mule deer and elk, bovine spongiform encephalopathy (BSE) of cattle, feline spongiform encephalopathy (FSE), exotic ungulate encephalopathy, and the human diseases kuru, Creutzfeld–Jacob disease (CJD), Gerstmann–Sträussler–Scheinker syndrome (GSS), and fatal familial insomnia of humans *(48)*.

3.1. Genetics

Most cases of human prion diseases are sporadic. About 10% are familial and could be linked to a number of mutations in the PrP gene *(49,50)*. During the course of prion diseases, a largely protease-resistant aggregated form of PrP accumulates in the brain *(50,51)*. It has been hypothesized that the mutations promote a spontaneous conversion of the normal cellular protein, called PrP^{C}, into an abnormally folded isoform PrP^{Sc}. Sporadic CJD may come about when an extremely rare event leads to spontaneous conversion of PrP^{C} to PrP^{Sc} and gives rise to a conversion cascade. PrP^{Sc} has been suggested to induce the neurodegeneration and gliosis characteristic of prion diseases. PrP^{Sc} may either be the agent of transmission or at least associated with it. The abnormally folded isoform PrP^{Sc} was classified as a new infectious agent causing prion diseases that can transmit an infection without an essential nucleic acid *(52)*. The expression of the normal form of the prion protein PrP^{c} is essential for the replication of the infectious prion, for controlling the development of pathology, and for modulating the duration of the disease *(53–55)*. Although the neurodegeneration requires the expression of PrP^{C}, some inherited prion diseases show PrP^{Sc} at the detection limit *(56)*. This observation led to the discovery of three topological forms of PrP^{C}, a secreted form secPrP, derived from the glycosylphospholipid (GPI)-anchored prion protein and two transmembrane forms, one with the C-terminal of the protein in the lumen (^{Ctm}PrP), and the other with the N-terminal of the protein within the lumen (^{Ntm}PrP) *(57)*. The elevated expression of the transmembrane-spanning topological form ^{Ctm}PrP was sufficient to cause neurodegeneration in transgenic mice, although the mechanism of action remains unclear *(57)*. From this, neurodegeneration was suggested to occur through ^{Ctm}PrP accumulation in all prion diseases after PrP^{Sc} had been formed. A causal relationship between PrP^{Sc} accumulation and ^{Ctm}PrP formation was observed by the finding that the effectiveness of accumulated PrP^{Sc} required to induce neurodegenerative disease was dependent on the disposition of host-encoded PrP to be made in the ^{Ctm}PrP form *(58)*. Alternatively, a direct increase in ^{Ctm}PrP could explain why Gerstmann–Sträussler–Scheinker disease has not been transmissible and why PrP^{Sc} could not be detected in the brain of these patients *(58)*.

3.2. The Prion Protein

Enriching fractions of Syrian hamster (SHa) brain for scrapie prion infectivity led to the initial discovery of the prion protein (PrP^{C}) with 209 amino acids that is processed from a 254-amino-acid precursor *(59,60)*. Determination of the N-terminal sequence of the protease resistant form of PrP^{Sc} enabled the retrieval of molecular clones encoding PrP from cDNA libraries *(50,61)*. During the past few years, the gene encoding the prion protein has been sequenced from many mammalian sources. The PrP gene codes for a highly conserved 33- to 35-kDa brain sialoglycoprotein, mainly expressed in neuronal and glia cells among species with a highly conserved structure *(50,61–64)*. The normal cellular role of the prion protein remains enigmatic, although there is evidence of presynaptic localization and that the prion protein is required for normal synaptic function *(65)*. More evidence for this is presented by knockout mice that show disrupted circadian rhythmus, loss of Purkinje cells, and abnormalities in long-term potentiation *(66–68)*. Physiological roles of PrP have been proposed from

the findings that PrP is located at the cell surface and binds copper, suggesting a role as transporter, ligand, or receptor *(69)*.

In the pathological process of prion disease, PrP^{C} is converted into the infectious prion protein. PrP^{Sc} is induced to aggregate into PrP-amyloid by the formation of intermolecular β-sheets. This process mediates a resistance against proteolytic degradation to the scrapie isoform PrP27-30 that consists of amino acids 90–123 (i.e., hamster sequence) *(70)* and is accompanied by neuronal loss and astrogliosis *(71)*. The converted protein can be incorporated into growing aggregates leading to amyloidlike plaques in infected brains *(72–74)*. The inhibition of PrP^{C} transport to the cell surface blocks the formation of PrP^{Sc}, finally confirming that PrP^{Sc} arises from alternate or misprocessing of PrP^{Sc} *(75)*.

The secondary structure of the full-length PrP (i.e., hamster sequence 29–231) is identical to those of PrP (90–231) and the N-terminal half of protein residues 29–124 is unstructured *(76)*. Residues 60–91 consist of four octarepeat sequences (i.e., PHGGGWGQ) that represent the most conserved parts of PrP in mammals *(77)*. The chicken PrP is the most divergent protein in an otherwise highly homologous family and has a similar N-terminal region of nine hexapeptide tandem repeats (i.e., PHNPGY) *(77–79)*. Also, a few prion cases have been linked to the presence of additional octarepeat sequences *(80)*.

3.3. PrP as a Copper-Binding Protein

As early as 1992, octarepeats of prion proteins containing histidine and tryptophan residues functioning as ligands for transition metals were proposed for the spontaneous conversion of the PrP^{C} (i.e., cellular) isoform into PrP^{Sc} (i.e., scrapie) isoform triggered by the coordination of these metals *(81)*. A copper-charged affinity column can be used to purify PrP^{C} *(82)*, and synthetic peptides corresponding to the octarepeat region of the prion protein revealed an affinity for Cu(II) with a K_d of 6.7 μ*M (78)*. At neutral and basic pH, the single octapeptide PHGGGWGQ and a peptide containing four octarepeats form a 1:1 complexes with Cu(II) *(83)*, whereas the latter chelates two Cu(II) ions at pH 6 but four at pH 7.4 *(84)* and also has the ability to reduce Cu(II) *(85)*. The full-length protein shows a similar preferential binding of Cu(II) with a K_d of 14 μ*M (86)*. The only other cation that was able to substitute for Cu(II) was manganese *(87)*. Recently, a plausible structure for the bridged complex of four Cu(II) ions with PrP residues 58–91 was proposed, indicating that the histidine residues in each octarepeat are coordinated to the Cu(II) ion *(88)*. Unlike the synthetic peptides from the chicken prion N-terminus, the mature chicken prion protein does not bind copper *(89)*.

During metabolic breakdown of mammalian PrP^{C}, the N-terminus containing this repeat region is cleaved off *(90)* and the remaining C-terminal part lacks the copper-binding domain, retains the infectivity, and does not bind any longer to copper-charged affinity columns *(91)*. The conversion of PrP^{c} to PrP^{Sc} has been discussed to occur in a Fenton-like reaction when Cu(II) bound to the octapeptide region in PrP^{C} enables the degradation of the N-terminal domain of PrP^{C} *(92)*. An involvement of copper in the process of infectivity was found when the addition of copper to hamster PrP^{Sc}-enriched fractions facilitated restoration of both infectivity and protease resistance of previously denatured PrP^{Sc} *(93)*. This study demonstrated that loss of scrapie infectivity can be a reversible process modulated by copper ions and suggests an indirect role of Cu(II) in this process.

Although the octapeptide repeat is not required for infectivity of PrP^{Sc}, this region is highly conserved between species, implying that this domain could represent a physiological unit. A consensus has almost been reached that Cu(II) may be a folding partner that promotes a definite conformation of the PrP^{C} region containing glycine repeats that otherwise possess a low propensity for a defined secondary structure *(94)*. When the predicted secondary and tertiary structures of PrP^{C} was published, only little secondary structure in these peptides was found *(95)*. Thus, residues 29–124 of PrP^{C} are highly flexible and unstructured in the absence of Cu(II) *(76)*, but the octarepeat region of the holoprotein at physiological Cu(II) concentrations no longer can be considered unstructured.

Copper ions might induce an α-helical motif in the N-terminus of the protein to act as a template for the formation of the α-helices in the rest of the protein. Indeed, Cu(II) binding to the repeat segment of PrP^C can induce formation of the α-helical structure on the C-terminal side of the peptide chain *(96)*. The lack of copper binding might play a role in the pathogenesis because infectivity of prions is based on the β-sheet conformation of the protein, rather than on the α-helical structure and the acquisition of partial resistance to digestion with proteinase K *(91,97)*. The importance of the N-terminal region of PrP was underlined when PrP transgenes were found to restore the susceptibility to the disease *(98)*. PrP amino-proximal deletions of residues 32–121 or 32–134 caused severe ataxia and neuronal death in knockout mice shortly after birth, whereas the wild-type PrP gene abolished this effect *(98)*. In contrast to the mammalian homologs, the chicken prion protein N-terminal tandem amino acid repeats seem to fold without a cofactor and represent a stable protease-resistant domain.

The prion protein seems to be balanced between radically different folds *(99)* with a high-energy barrier between the β-conformation and the native α-conformation. This balance would be influenced by PrP ligands (for the sporadic casese), such as Cu(II), and inherent factors (i.e., for familial cases) such as the mutations causing inherited prion diseases *(100)*. Evidence for the dependence of PrP^{Sc} conformation on the binding of copper and zinc is provided by the observation that conformational isomers can be interconverted by altering their metal-ion charge *(101)*.

The transmembrane form with the C-terminal of the protein in the lumen (^{Ctm}PrP) was shown to be responsible for the spontaneous development of clinical signs and neuropathology in transgenic mice. According to the data mentioned earlier, this form could act as a sink for Cu(II), when Cu(II) binds to the N-terminal repeat regions located in the cytoplasm. This could lead to a disturbed copper homeostasis: first, as a result of the ability to gain Cu(II) from other copper binding molecules and, second, as a result of the lost benefit of copper binding on the structure, because the transmembrane domain separates the N-terminal from the C-terminal of ^{Ctm}PrP and thereby inhibits the switch to a "healthy" α-conformation of the C-terminal portion of the molecule in the lumen *(57)*. Independent from these ideas, mechanisms have been discussed if ^{Ctm}PrP is causing the disease, either by PrP^{Sc} promoting the formation of ^{Ctm}PrP or by hindering its aggregation *(102)*.

3.4. PrP Has a Functional Role in Cu(II) Metabolism

The specificity of copper-binding suggests that PrP^C might somehow be involved in catalytic reactions *(103)*. The normal PrP was found to have an activity like that of superoxide dismutase *(104)*. The dismutase activity was abolished by depletion of the octapeptide-repeat region that is involved in copper binding. PrP^C was found to be endocytosed constitutively from the plasma membrane via clathrin-coated pits and was finally recycled back to the cell surface *(105)*. A dramatic effect on this cycle was found when copper was observed to stimulate the endocytosis of the prion protein *(106)*. A possible explanation could be that as a result of an altered conformation, Cu(II)-charged PrP^C is bound by a putative receptor that lets PrP^C accumulate in clathrin-coated pits *(106)*. Upon internalization, PrP^C could then deliver Cu(II) to an endocytic compartment where bound copper ions dissociate from PrP^C and the protein travels back to the cell surface to start another cycle.

Although other proteins have been identified as candidates for copper transport across the plasma membrane in yeast and humans *(107,108)*, it has been suggested that PrP^C is a principal copper-binding protein in brain. Both synaptosomes and endosomes from wild-type mice showed a significantly higher copper content than PrP knockout mice *(109)* as a result of measurements showing that cell membranes deficient in PrP^C are also deficient in copper. Thus, PrP^C was proposed to act as a transporter to regulate the Cu(II) content of intracellular compartments. Additional evidence for this was provided by another report that identified a link between increasing levels of PrP^C expression and increased levels of glutathione peroxidase *(110)*. Altered expression levels of PrP^C also altered Cu,Zn-SOD antioxidant enzyme activity by regulating copper incorporation into the enzyme *(111)*. An antioxidant activity was assigend to PrP^C when neurons from PrP knockout mice were found to be

significantly more susceptible to hydrogen peroxide toxicity than wild-type neurons *(112)* and methionine residues of PrP were uniquely susceptible to oxidation *(113)*. Even PrP^{C} itself was found to possess a SOD-like activity *(114)*. Nevertheless, the results on the role of PrP in Cu metabolism are still under controversial discussion because contradictory findings have been published recently indicating that Cu content and cuproenzyme activity do not vary with PrP expression levels in mice *(115)*.

Most recently, the generation of a PrP^{Sc}-like conformation in living cells has been reported *(116)*. A reducing environment and the absence of glycosylation favored the conversion of full-length PrP to a molecule with all signature characteristics of PrP^{Sc}. Thus, mistargeting PrP and/or retrograde transport of misfolded PrP could facilitate the initial production of PrP^{Sc}.

4. AMYOTROPHIC LATERAL SCLEROSIS

Amyotrophic lateral sclerosis (ALS) is an age-dependent degenerative disorder of motor neurons with sporadic and inherited forms. The disease is characterized by a progressive loss of motor neurons in the spinal cord and brain. The cause of ALS is not known. The incidence of the disease worldwide is 1–2 cases per 100,000. Pathologically, the degeneration of lower motor neurons of the spinal cord and brainstem and loss of large motor neurons in the cerebral cortex are prominent features causing weakness and spasticity *(117)*. The selective vulnerability of motor neurons is relative because peripheral nerves reveal reduced numbers of large myelinated axons, axonal degeneration, and distal axonal atrophy *(117)*.

4.1. Genetics/FALS

Multiple mechanisms have been postulated to be the cause of the sporadic form of the disease, including excitotoxicity *(118,119)*, oxidative injury *(120)*, cytoskeletal abnormalities with aggregates containing SOD1 *(121)*, and autoimmunity *(122,123)*. Up to 70% of sporadic cases have varying loss of the glutatmate transporter, EAAT2 *(118,124)*. Aberrant EAAT2 mRNA species seem to account for the regional selective loss of EAAT2, most likely the result of RNA processing errors *(125)*.

Amyotrophic lateral sclerosis is inherited in about 10% of cases, and of those cases, about 20% have been linked to mutations in sod1, the gene that encodes human copper–zinc superoxide dismutase (Cu,Zn-SOD) *(126,127)*. To date, more than 60 different dominantly inherited point mutations have been found.

No correlation between SOD activity and the frequency or severity of the disease has been demonstrated so far, suggesting that mutant SOD does not cause FALS because of a deficiency in SOD activity. In addition, an elevation of wild-type Cu,Zn-SOD in Down's syndrome causing the symptoms of the disease could be excluded, a lack of correlation of symptoms with overdosage was found in partial trisomy 21 *(128,129)*.

Familial ALS mutations in Cu,Zn SOD are dominant and are currently believed to exert their effects because of a gain of function instead of a loss of function. There is increasing evidence for a gain of toxic function. First, the expression of FALS mutant human Cu,Zn-SOD in transgenic mice causes motor neuron disease, whereas expression of wild-type human Cu,Zn-SOD does not *(130–132)*. Second, Cu,Zn-SOD knockout mice do not develop a FALS-like syndrome *(133)*, although female homozygous knockout mice showed a markedly reduced fertility compared with that of wild-type and heterozygous knock-out mice. Further studies revealed that these mice ovulated and conceived normally, but exhibited a marked increase in embryonic lethality *(134)*. Third, human Cu,Zn-SOD is antiapoptotic, whereas the expression of FALS mutant protein can be proapoptotic in cultured cells *(135)*. Fourth, some FALS mutations retain near-normal levels of enzyme activity or stability *(136)* and mutant SOD1 subunits do not alter the metabolism or activities of wild-type SOD1 in a dominant negative fashion *(137)*. Fifth, poorly or unstably folded mutants are sufficient to cause the formation of SOD1-containing aggregates that are toxic to motor neurons *(138,139)*. Recently,

the gain of function has been best exemplified by Estevez and colleagues who showed that an altered Cu(II) coordination by Zn(II)-deficient SOD was responsible for the conversion of the antioxidant activity into a pro-oxidant activity of SOD *(140)*.

4.2. Superoxide Dismutase

The lack of a changed phenotype in SOD1 null mice indicates that the enzyme is probably not necessary for normal development and life, but rather may be involved with other antioxidant enzymes in the response to oxidative stress. This might also be taken as another argument for the appealing hypothesis that SODs are not only enzymes that rapidly dismutate O_2^- radicals, but that they can also act as metal storage proteins and are otherwise involved in metal-ion homeostasis *(141)*.

A role for Cu,Zn-SOD in the free-radical theory of senescence was provided by the shortened life-span of *Drosophila* with a mutational defect in Cu,Zn-SOD, and by *Candida elegans*, which had only half the normal complement of SOD *(142,143)*. Mice lacking SOD exhibited a shortened life-span *(144)* but appeared normal while young and were less able to recover from axonal injury *(133)*. A lack of Mn-SOD imposed more serious consequences by shortening the life-span and exhibiting faulty mitochondrial activities in several tissues, especially the heart *(145,146)*. Thus, Mn-SOD may play a more critical role than Cu,Zn-SOD in antioxidant defense mechanisms under normal physiological conditions *(147)*. This is supported by the findings that mice lacking Mn-SOD die at very young age *(145,146)*.

Homodimeric Cu,Zn-SOD acts to disproportionate two molecules of superoxide anion to hydrogen peroxide and water in a reaction mediated through cyclic reduction and oxidation of copper bound to the active site [*(148)*; i.e., reactions (1) and (2)].

$$O_2^- + \text{Cu(II)Zn-SOD} \rightarrow O_2 + \text{Cu(I)Zn-SOD} \quad (1)$$

$$O_2^- + \text{Cu(I)Zn-SOD} + 2H^+ \rightarrow H_2O_2 + \text{Cu(II)Zn-SOD} \quad (2)$$

Cu,Zn-SOD is a cytosolic antioxidant enzyme that lowers concentrations of superoxide by disproportionation to give hydrogen peroxide and dioxygen [i.e., reaction (3)].

$$2O_2^- + 2H^+ \rightarrow O_2 + H_2O_2 \quad (3)$$

The mechanism involves alternate reduction and reoxidation of the copper ion at the active site of the enzyme [i.e., reactions (1) and (2)]. Approximately one-third of the total cellular SOD1 exists as the apoprotein *(149)*. The incorporation of copper into SOD1 in intact cells is absolutely dependent on the presence of the SOD1-specific copper chaperone CCS that belongs to a group of small cytoplasmic proteins involved in copper trafficking *(150)*. A colocalization of CCS and SOD1 in mammalian tissues of the CNS *(150)* already suggested that CCS can directly insert copper into the enzyme and is active at very low copper concentrations *(151)*. Moreover, there is a physiological requirement for CCS in vivo, and it has been proposed that in the absence of CCS, intracellular SOD1 exists with one Zn(II) bound per SOD1 dimer *(152)*.

Cu,Zn-Superoxide dismutase has also been known for some time to catalyze reactions of hydrogen peroxide with certain substrates in competition with autoinactivation by the enzyme itself [i.e., reaction (6)] *(153)*. The mechanism for this peroxidative activity of Cu,Zn-SOD involves alternate reduction and reoxidation of the copper ion in the enzyme, but this time by hydrogen peroxide [i.e., reactions (4)–(6)].

$$H_2O_2 + \text{Cu(II)Zn-SOD} \rightarrow O_2^- + \text{Cu(I)Zn-SOD} + 2H^+ \quad (4)$$

$$H_2O_2 + \text{Cu(I)Zn-SOD} \rightarrow OH^- + (\cdot\,OH)\text{Cu(II)Zn-SOD} \quad (5)$$

$$\text{Spin trap} + (\cdot\,OH)\text{Cu(II)Zn-SOD} \rightarrow \text{Oxidized spin trap} + \text{Cu(II)Zn-SOD} \quad (6)$$

Spin-trap reagents in vitro and physiological substrates in vivo are oxidized by hydrogen peroxide in a reaction catalyzed by Cu,Zn-SOD [i.e., reactions (4) and (5)] and are able to inhibit the inactivation of the enzyme *(154,155)*. Three hypotheses have been proposed to account for the possible involvement of copper in the gain of function of the human FALS mutant Cu,Zn-SOD:

- Copper ions in the mutant enzymes could catalyze deleterious oxidation reactions of substrates by hydrogen peroxide *(154,155)*.
- Copper ions in the mutant enzymes could be catalyzing nitration of tyrosine residues by peroxynitrite *(156–158)*.
- Copper could be leaching out of the mutant proteins and could be inducing toxic effects at another site in the cell.

Most likely, FALS mutations in Cu,Zn-SOD cause a change in the structure of the enzyme that results in an enhancement of the ability of the enzyme-bound copper ion to catalyze destructive oxidative reactions in substrates with peroxides. SOD mutations may destabilize SOD or the dimer and may lead to misfolding *(136,159)*. Misfolding and perturbed dimer formation could lead to aggregation of the protein with a subsequent gain-of-function toxicity *(139)*.

The toxicity of mutant SOD has been proposed to involve an increase in peroxynitrite formation *(156)*, an increase in peroxidase activity *(160,161)*, a loss of shielding of metal ions *(162)*, and aggregation of the enzyme *(139)*. The idea that the FALS mutant Cu,Zn-SOD enzymes may have more accessible active sites is supported by recent crystallographic studies of the G37R mutant *(163)*. In this variant, spinal motor neurons are the most profoundly affected cells, showing axonal and dendritic abnormalities that include SOD1 accumulations in irregularly swollen portions of motor axons, abnormal axonal cytoskeleton architecture, and small vacuoles, derived from damaged mitochondria, in both axons and dendrites *(4,162,164–166)*.

4.3. Deposits

The different mutations can be associated with different types of cellular pathology in mice. The presence of G85R SOD1 had no effect on the level or the activity of wild-type SOD1 *(121)*, but astrocytes contain SOD1 aggregates induced by mutant human G85R SOD1 expression. This is supported by ubiquitin-immunoreactive Lewy-body-like inclusions in astrocytes, which are observed before clinical signs appear *(121)*. At later stages, motor neurons also contain SOD1 and ubiquitin-positive aggregates.

Aggregates of SOD1 are common to disease caused by different mutants, raising the possibility that coaggregation of unidentified components or aberrant catalysis by misfolded mutants may underly mutant-mediated toxicity. Similar SOD1 aggregates have also been reported for some human sporadic and familial ALS cases *(167–169)*. Wild-type protein was a component of aggregates in human disease, but the wild-type protein was not required for aggregation, neither for stabilizing the mutant nor for contributing to aggregates nucleated by mutant SOD1.

4.4. Role of Copper

Although the absence of influence of SOD1 activity on mutant toxicity was supposed to challenge the idea that toxicity derives from oxidative stress arising from superoxide *(121)*, one has to take into consideration that copper may play an important role in the as-yet-unidentified mechanism leading to misfolded aggregated mutants. Administration of the antioxidant vitamin E and selenium (which raises concentrations of the antioxidant enzyme glutathione peroxidase) modestly delays both the onset and progression of disease without affecting survival, although riluzole and gabapentin (two putative inhibitors of the glutamatergic system) do not influence the onset or progression of disease but prolong survival *(170)*. Oral administration of D-penicillamine (a copper chelator) delays the onset of disease *(171)*. Coexpression of the antiapoptotic protein Bcl-2 and even mutant SOD1 extends survival but has no influence on disease progression *(172)*. Expression of two FALS-related mutant

SODs (A4V and V148G) caused cell death in differentiated PC12 cells, superior cervical ganglion neurons, and hippocampal pyramidal neurons. Death could be prevented by Cu chelators, Bcl-2, glutathione, vitamin E, and inhibitors of caspases.

4.5. Conclusion

The extraordinary metabolic activity of motor neurons at least partly resulting from their large surface area and dependence on intracellular transport proteins *(173)* puts them at a heightened risk of damage from free-radical species that are generated as a result of the mutant SOD expression. Other factors present in the CNS may confer a selective vulnerability to motor neurons.

5. ALZHEIMER'S DISEASE

Age is by far the most important risk factor for dementia, because susceptibility to dementia and Alzheimer's disease increases exponentially with age. However, Alzheimer's disease is clearly distinguishable from normal age-related changes, indicating that it is a specific disease process. The proportion of individuals with AD increases by approx 30–40% with each decade of life to a peak after the age of 80.

5.1. Genetic Background

Three identified genes are involved in the autosomal dominant forms of early-onset AD. Mutations in the gene encoding the amyloid precursor protein (APP) and two homologous genes, presenilin 1 (PS-1) and presenilin 2 (PS-2), result in a dominantly inherited form of the disease that usually begins prior to the age of 60 yr and has been found to alter amyloid β (Aβ) protein metabolism. Screening a population-based sample of patients with early-onset AD (<65 yr) revealed APP mutations in 0.5% of the patients, PS-1 mutations in 6%, and PS-2 mutations in 1% *(174)*.

Alzheimer's disease is a multifactorial disease in which several genetic and environmental factors have been implicated. The disease can often result from an interplay of different genetic and environmental risk factors. Familial and sporadic forms of Alzheimer's disease (Fig. 2) occurring later in life have been associated with the e4 polymorphism in the gene encoding apolipoprotein E (APOE). The APOE gene is an important genetic determinant for early-onset AD and for the predominant late-onset form of the disease, which affects 90–95% of all patients. APOE-e4 lowers the typical age of late-onset AD *(175)* and APOE-e4 also decreases the age at onset of familial AD with an APP mutation (176). Each allele lowers the age of onset by 7–9 years *(177)*.

5.2. Brain Lesions

Alzheimer's disease is characterized pathologically by neuronal degeneration and the deposition of amyloid plaques and neurofibrillary tangles in the brains of affected individuals. Amyloid deposits are primarily composed of the Aβ amyloid protein of which the Aβ1–40 isoform is the predominant soluble species in biological fluids and the Aβ1–42 isoform is the predominant species in developing plaque deposits *(178–186)*. When transgenic mouse models, which overexpress mutant human APP, were immunized with Abeta42, either before the onset of AD-type neuropathologies (at 6 wk of age) or at an older age (11 mo), immunization of the young animals essentially prevented the development of Aβ plaque formation *(187)*.

Neuritic plaques and neurofibrillary tangles are the major neuropathological lesions that allow a definitive diagnosis of AD postmortem. Neuritic plaques are spherical multicellular lesions that are usually found in moderate or large numbers in limbic structures and in the association neocortex. They are composed of extracellular deposits of the amyloid Aβ protein with degenerating axons and dendrites within and intimately surrounding the amyloid deposit. In regions that are less affected, such as the cerebellum and the thalamus, Aβ deposits are of a primarily diffuse type with an amor-

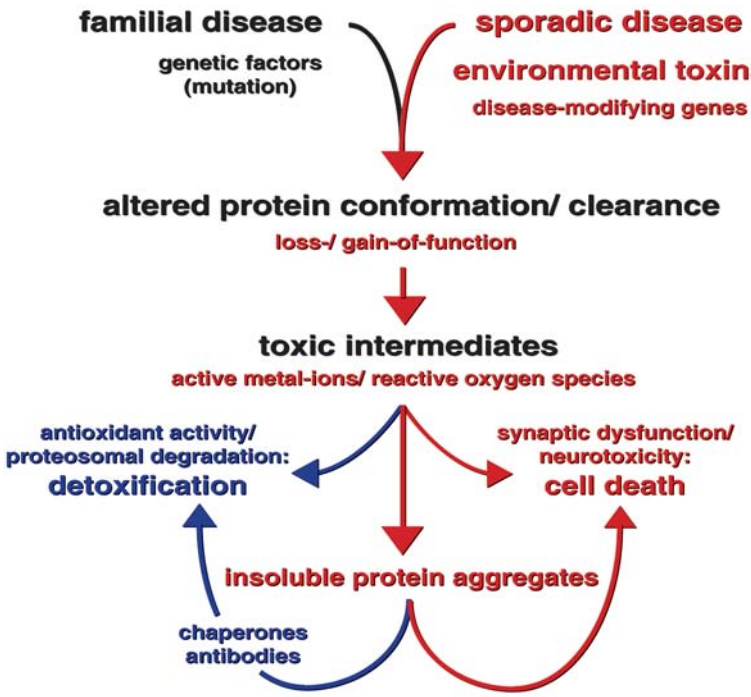

Fig. 2. Accumulation of amyloid Aβ is invariably associated with the pathology of AD. Overexpression of APP, or disease-modifying genes, shorten the time of onset. Early accumulations of amyloid Aβ constitute the first abnormality, possibly representing toxic forms of Aβ. If there is no detoxification, extracellular deposition occurs that is central to the pathogenesis of the disease. Vaccination with amyloid Aβ can dramatically reduce amyloid deposition in a mouse model of AD.

phous and nonfibrillar form of Aβ, as found in brains of aged normal humans that often contain Aβ deposits.

Neurofibrillary tangle is the other classical lesion that occurs independently in AD. The tangles occur in large numbers in the AD brain, the entorhinal cortex, hippocampus, amygdala, and association cortices of lobes. The subunit protein of the paired helical filaments (PHF) is the tau protein, present in tangles as bundles of paired, helically wound tau aggregates. These intraneuronal proteinaceous inclusions are often ubiquitinated deposits, similar to those found in other neurodegenerative disorders, such as Parkinson's and Lewy-body disease. Although the tau gene has not been found to be the site of mutations in familial AD, mutations in tau have been discovered in families with frontotemporal dementia with parkinsonism linked to chromosme 17 (FTDP-17) *(17,188,189)*.

5.3. The Amyloid Precursor Protein

The amyloid precursor protein is a transmembrane glycoprotein that undergoes extensive alternative splicing *(190)*. APP belongs to a multigene family that contains at least two other homologs known as amyloid precursor-like proteins (APLP1 and APLP2) *(191–194)*. APP and APLPs share most of the domains and motifs of APP, including a hydrophobic membrane-spanning domain, N- and O-glycosylation sites, metal-ion-binding domains, and the Kunitz-type protease inhibitor (KPI) domain (not found in APLP1). Only APP contains the Aβ region and can be cleaved by β- and γ-secretase to generate Aβ. Thus, APLPs cannot contribute to Aβ deposition in Alzheimer's disease, but they may compensate for the function of APP.

The normal functions of APP and APLPs are not well understood. There exists at least some evidence for neuritic and protective roles *(195–198)*. APP binds Zn(II) at higher nanomolar concentrations *(199–*

202) and an altered APP metabolism or expression level is believed to result in neurotoxic processes *(108,196,203–207)*. APP can reduce Cu(II) to Cu(I) in a cell-free system, potentially leading to increased oxidative stress in neurons *(108)*. The domain that contributes to such activities is the copper-binding domain *(208)* residing between residues 135 and 158 of APP, a region that shows strong homolgy to APLP2 but not to APLP1. Five years after the initial identification of the amino acid residues involved in the redox reaction, it has been confirmed by Ruiz et al. that cysteine 144 is a key residue in the reduction of Cu(II) to Cu(I) by soluble APP *(108,208,209)*.

Potentially, APP–Cu(I) complexes may be involved to reduce hydrogen peroxide to form an APP–Cu(II)–hydroxyl radical intermediate *(204,205)*. Recently, it has been discovered that APP residues 135–158 consisting of cysteine and Cu-coordinating histidine residues can modulate copper-mediated lipid peroxidation and neurotoxicity in culture of APP knockout ($APP^{0/0}$) and wild-type (wt) neurons *(206)*. The wt neurons were found to be more susceptible than the $APP^{0/0}$ neurons to physiological concentrations of copper but not to other metals. The increased levels of lipid peroxidation products in wt neurons were most likely the result of copper-mediated oxidative stress. Similar effects were obtained with the APP142–166 peptide containing the APP copper-binding domain. The specificity for the increased copper-mediated toxicity by the APP142–166 peptide was shown by the failure of a mutant peptide to bind copper and to potentiate toxicity and the failure of the wt peptide to mediate toxicity from zinc or iron *(207)*. Because an inhibition of copper toxicity was observed in the presence of the copper(I) chelator bathocuproine (BC) in wt cultures of neurons, the increased toxicity in wt neurons could be related to Cu(I) production of APP or secondary reactions of Cu(I), leading to an inbalance of cellular antioxidants.

The amyloid precursor protein and APLP2 are most likely involved in maintaining copper levels in tissues of adult mice *(210)*. $APP^{0/0}$ mice have significantly increased copper but not zinc or iron levels in the cerebral cortex and liver, compared to age and genetically matched wt mice. $APLP2^{0/0}$ mice also revealed increases in copper in the cerebral cortex and liver. These findings suggest that the APP family can modulate copper homeostasis and that APP/APLP2 expression may be involved in copper efflux from the liver and cerebral cortex *(108,210)*. The fact that $APP^{0/0}$ but not $APLP2^{0/0}$ neurons revealed increased resistance to copper toxicity in vitro may be explained by the observation that APLP2 has only 60% of the copper redox activity of APP *(204,211)*. The redox activity may be directly linked to toxicity and could be critical for the potential ability of APP and APLP2 to transport copper. This point of view is supported by the finding that Cu(II) reduction modulates copper uptake in eucaryotic cells *(212)*. Most importantly, copper was found to influence APP processing in a cell culture model system when copper was observed to greatly reduce the levels of amyloid Aβ peptide and copper also caused an increase in the secretion of the APP ectodomain *(213)*. An increase in intracellular APP levels that paralleled the decrease in Aβ generation suggested that additional copper was acting on two distinct regulating mechanisms (i.e., Aβ production and the other on APP synthesis) *(213)*.

5.4. APP in Antioxidant Responses

Neurotrophic factors and neuronal injury upregulate APP expression and induce secretion of APP *(197,214,215)*. The addition of sAPP to culture medium protects cortical and hippocampal neurons from neurotoxic insults induced by hypoglycemia and excitatoxic amino acids. APP was reported to act by stabilizing intracellular Ca^{2+} levels and reducing oxidative stress *(216–218)*. Also overexpression of human APP in cell lines and transgenic mice can result in protection against oxidative stress and resistance to excitotoxicity *(215,219)*. In contrast to these experiments with exogenous sAPP or transfected cell lines, no differences in cell survival were observed in $APP^{0/0}$ compared with $APP^{+/+}$ neurons when both were exposed to various oxidative insults *(207)*.

5.5. Metal-Ion Homeostasis in AD

Metal-ion homeostasis is severely dysregulated in AD *(220–225)*. Increased concentrations of copper, iron, and zinc are detected in the neuropil of the AD-affected brain where they are highly

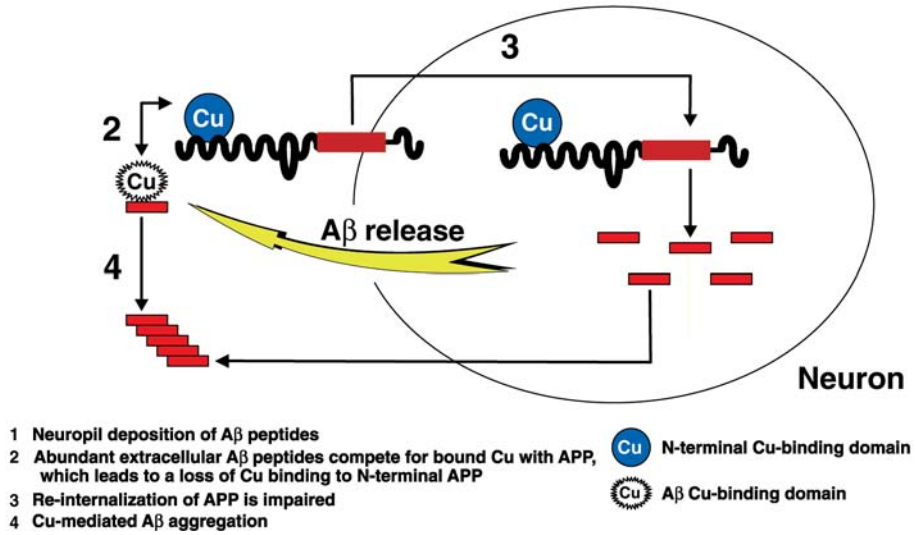

Fig. 3. Possible involvement of copper in Alzheimer's disease. First, APP transport is disturbed by intracellular accumulations of amyloid Aβ. Second, the transport of APP to synaptic sites is inhibited followed by a loss of cell surface APP. Third, reinternalization of APP–Cu complexes is impaired, leading to increased levels of copper in the neuropil. Fourth, increased extracellular copper may trigger amyloid Aβ aggregation extracellularly.

concentrated within amyloid plaques and reach concentrations of up to 0.4 m*M* (Cu) and 1 m*M* (Fe and Zn) *(223,226,227)*. A likely reason is that Aβ binds equimolar amounts of Cu(II) and Zn(II) at pH 7.4 *(199,200,228–230)*. Human Aβ can directly produce hydrogen peroxide by a mechanism that involves the reduction of the metal ions Fe(III) or Cu(II), setting up conditions for Fenton-type chemistry *(231)*.

In the presence of submicromolar concentrations of zinc and copper, synthetic peptides of Aβ aggregate into amyloid *(230)*. Evidence that these metal ions may play a role in cerebral amyloid assembly is provided by the observation that Cu/Zn selective chelators enhance solubility of Aβ from postmortem brain tissue of AD patients and transgenic mouse brains *(232)*. In addition, by histological fluorescent techniques, it has been shown that Zn(II) is present in amyloid deposits in human brain *(233)* and in plaques of transgenic mice *(234)*. Most likely, an abnormal zinc and/or copper homeostasis mediated by APP initiates the Aβ deposition followed by the formation and accumulation of Aβ that acts as a sink, drawing in metal ions into its mass and away from APP (Fig. 3). This might be further facilitated by the mildly acidic conditions that have been reported in AD brains and that allows copper to completely displace zinc from synthetic Aβ aggregates *(230,235)*, reflecting the fact that copper and zinc are biologically antagonistic *(236)*. Under acidic conditions, Aβ1–40 strongly favors copper binding over zinc in the presence of an equimolar amount of both metal ions *(237)*. Also, the affinity of copper for Aβ1–42 is seven orders of magnitude higher than for Aβ1–40, most likely the result of a higher β-sheet content of Aβ42 because β-sheet or β-barrel conformations frequently mediate the high-affinity copper binding of cuproproteins *(238)*. Although it remains to be determined whether Aβ is at all metal bound in vivo, Aβ-mediated cytotoxicity could be shown to be potentiated by Cu(II) and was greatest for the variant Aβ1–42 in vitro *(239)*. Thus, the early unifying hypothesis for free-radical-based neurotoxicity of Aβ *(240)* was recently attributed to metal-catalyzed redox reactions *(231,241)*.

A marked enrichment of copper, iron, and zinc was observed in AD neuropil and amyloid plaques *(223)*. In addition, a 2.2-fold increase of the concentration of copper in the CSF of AD patients was

found accompanied by an increase of the copper-transport protein ceruloplasmin *(242)*. A marked accumulation of ceruloplasmin has been described within neurons, astrocytes, and neuritic plaques in AD hippocampus, where it may reflect a response to increased copper levels *(243)*.

5.6. Oxidative Metabolism

Energy metabolism studies showed that glucose-6-phosphate dehydrogenase activities and heme oxygenase-1 (HO-1) levels were increased in AD brains *(244,245)*. The increased G6PDH activity might be the result of the fact that glycolytic enzyme activity is decreased and more NADPH is demanded by detoxifying systems. A considerable number of oxidative stress markers are found in AD brains, such as increased protein carbonyl formation in the inferior parietal lobule and hippocampus *(246,247)*, protein nitration *(226,248)*, lipid peroxidation *(240,249–252)*, DNA oxidation *(253,254)*, and advanced Maillard reaction products *(255)*. Indirect evidence that the AD brain is under oxidative stress can be concluded from reports that treatment of individuals with antioxidants such as vitamin E and selegeline *(256)* and with anti-inflammatory medications *(257–259)* delay the progression of the disease.

5.7. Copper and AD Pathology

The possibility that copper may contribute to AD pathology is suggested by the perturbed ceruloplasmin and copper levels in AD patients *(223,243)* and the production of free radicals by APP–Cu complexes and increased Aβ aggregation in the presence of zinc and/or copper *(203,230)*. Aβ can generate ROS from transition metals *(260)* and deplete neuronal glutathione levels *(261,262)*. On the other hand, redox activities of APP and APLP2 (with APLP2 having only 60% of the copper redox activity) may not only be critical to the ability of the proteins to transport copper but may also be involved in radical production during copper uptake that requires Cu(II) reduction *(108)*.

ACKNOWLEDGMENTS

We are indebted to Dr. Scott Baker (ICA), André Kemmling, and Gudrun Jürgens for their assistance in the compilation of this work. We also thank Professor Colin L. Masters, Australia, and Professor Nibaldo Inestrosa, Chile, for helpful comments.

REFERENCES

1. Forno, L. S. (1996) *J. Neuropathol. Exp. Neurol.* **55(3)**, 259–272.
2. Masliah, E., Rockenstein, E., Veinbergs, I., Mallory, M., Hashimoto, M., Takeda, A., et al. (2000) *Science* **287(5456)**, 1265–1269.
3. Abeliovich, A., Schmitz, Y., Farinas, I., Choi-Lundberg, D., Ho, W. H., Castillo, P. E., Shinsky, N., et al. (2000) *Neuron* **25(1)**, 239–252.
4. Morrison, P. J., Godwin-Austen, R. B., and Raeburn, J. A. (1996) *J. Med. Genet.* **33(6)**, 504–506.
5. Dobyns, W. B., Ozelius, L. J., Kramer, P. L., Brashear, A., Farlow, M. R., Perry, T. R., et al. (1993) *Neurology* **43(12)**, 2596–2602.
6. Wooten, G. F., Currie, L. J., Bennett, J. P., Harrison, M. B., Trugman, J. M., and Parker, W. D., Jr. (1997) *Ann. Neurol.* **41(2)**, 265–268.
7. Matsumine, H., Saito, M., Shimoda-Matsubayashi, S., Tanaka, H., Ishikawa, A., Nakagawa-Hattori, Y., et al. (1997) *Am. J. Hum. Genet.* **60(3)**, 588–596.
8. Yamamura, Y., Sobue, I., Ando, K., Iida, M., and Yanagi, T. (1973) *Neurology* **23(3)**, 239–244.
9. Golbe, L. I., Di Iorio, G., Sanges, G., Lazzarini, A. M., La Sala, S., Bonavita, V., et al. (1996) *Ann. Neurol.* **40(5)**, 767–775.
10. Spillantini, M. G., Divane, A., and Goedert, M. (1995) *Genomics* **27(2)**, 379–381.
11. Polymeropoulos, M. H., Lavedan, C., Leroy, E., Ide, S. E., Dehejia, A., Dutra, A., et al. (1997) *Science* **276(5321)**, 2045–2047.
12. Kruger, R., Kuhn, W., Muller, T., Woitalla, D., Graeber, M., Kosel, S., et al. (1998) *Nature Genet.* **18(2)**, 106–108.
13. Paik, S. R., Lee, J. H., Kim, D. H., Chang, C. S., and Kim, J. (1997) *Arch. Biochem. Biophys.* **344(2)**, 325–334.
14. Paik, S. R., Shin, H. J., Lee, J. H., Chang, C. S., and Kim, J. (1999) *Biochem. J.* **340(Pt. 3)**, 821–828.
15. Ostrerova, N., Petrucelli, L., Farrer, M., Mehta, N., Choi, P., Hardy, J., and Wolozin, B. (1999) *J. Neurosci.* **19(14)**, 5782–5791

16. Jensen, P. H., Hager, H., Nielsen, M. S., Hojrup, P., Gliemann, J., and Jakes, R. (1999) *J. Biol. Chem.* **274(36)**, 25,481–25,489.
17. Hutton, M., Lendon, C. L., Rizzu, P., Baker, M., Froelich, S., Houlden, H., et al. (1998) *Nature* **393(6686)**, 702–705.
18. Kitada, T., Asakawa, S., Hattori, N., Matsumine, H., Yamamura, Y., Minoshima, S., et al. (1998) *Nature* **392(6676)**, 605–608.
19. Jones, A. C., Yamamura, Y., Almasy, L., Bohlega, S., Elibol, B., Hubble, J., et al. (1998) *Am. J. Hum. Genet.* **63(1)**, 80–87.
20. Leroy, E., Anastasopoulos, D., Konitsiotis, S., Lavedan, C., and Polymeropoulos, M. H. (1998) *Hum. Genet.* **103(4)**, 424–427.
21. Uitti, R. J., Shinotoh, H., Hayward, M., Schulzer, M., Mak, E., and Calne, D. B. (1997) *Can. J. Neurol. Sci.* **24(2)**, 127–132.
22. Gasser, T., Muller-Myhsok, B., Wszolek, Z. K., Oehlmann, R., Calne, D. B., Bonifati, V., et al. (1998) *Nature Genet.* **18(3)**, 262–265.
23. Jenner, P. and Olanow, C. W. (1998) *Ann. Neurol.* **44(3 Suppl. 1)**, S72–S84.
24. Jenner, P. (1998) *Mov. Disord.* **13 (Suppl. 1),** 24–34.
25. Jenner, P. G. and Brin, M. F. (1998) *Neurology* **50(6 Suppl. 6)**, S39–S43; discussion S44–S48.
26. Mizuno, Y., Hattori, N., and Matsumine, H. (1998) *J. Neurochem.* **71(3)**, 893–902.
27. Mizuno, Y., Yoshino, H., Ikebe, S., Hattori, N., Kobayashi, T., Shimoda-Matsubayashi, S., et al. (1998) *Ann. Neurol.* **44(3 Suppl. 1)**, S99–S109.
28. Ye, F. Q., Allen, P. S., and Martin, W. R. (1996) *Mov. Disord.* **11(3)**, 243–249.
29. Logroscino, G., Marder, K., Graziano, J., Freyer, G., Slavkovich, V., Lojacono, N., et al. (1998) *Mov. Disord.* **13 (Suppl. 1)**, 13–16.
30. Jellinger, K., Paulus, W., Grundke-Iqbal, I., Riederer, P., and Youdim, M. B. (1990) *J. Neural Transm. Park Dis. Dement Sect* **2(4)**, 327–340.
31. Jellinger, K., Kienzl, E., Rumpelmair, G., Riederer, P., Stachelberger, H., Ben-Shachar, D., et al. (1992) *J. Neurochem.* **59(3)**, 1168–1171.
32. Hirsch, E. C., Brandel, J. P., Galle, P., Javoy-Agid, F., and Agid, Y. (1991) *J. Neurochem.* **56(2)**, 446–451.
33. Mann, V. M., Cooper, J. M., Daniel, S. E., Srai, K., Jenner, P., Marsden, C. D., et al. (1994) *Ann. Neurol.* **36(6)**, 876–881.
34. Schipper, H. M., Vininsky, R., Brull, R., Small, L., and Brawer, J. R. (1998) *Exp. Neurol.* **152(2)**, 188–196.
35. Jimenez-Jimenez, F. J., Molina, J. A., Aguilar, M. V., Meseguer, I., Mateos-Vega, C. J., Gonzalez-Munoz, M. J., et al. (1998) *J. Neural. Transm.* **105(4–5)**, 497–505.
36. Gorell, J. M., Johnson, C. C., Rybicki, B. A., Peterson, E. L., Kortsha, G. X., Brown, G. G., et al. (1997) *Neurology* **48(3)**, 650–658.
37. Hashimoto, M., Hsu, L. J., Xia, Y., Takeda, A., Sisk, A., Sundsmo, M., et al. (1999) *Neuroreport* **10(4)**, 717–721.
38. Sziraki, I., Mohanakumar, K. P., Rauhala, P., Kim, H. G., Yeh, K. J., and Chiueh, C. C. (1998) *Neuroscience* **85(4)**, 1101–1111.
39. Zheng, W., Ren, S., and Graziano, J. H. (1998) *Brain Res.* **799(2)**, 334–342.
40. Jenner, P. and Olanow, C. W. (1996) *Neurology* **47(6 Suppl. 3)**, S161–S170.
41. Lang, A. E. and Lozano, A. M. (1998) *N. Engl. J. Med.* **339(16)**, 1130–1143.
42. Ebadi, M., Srinivasan, S. K., and Baxi, M. D. (1996) *Prog. Neurobiol.* **48(1)**, 1–19.
43. Luquin, M. R., Montoro, R. J., Guillen, J., Saldise, L., Insausti, R., Del Rio, J., et al. (1999) *Neuron* **22(4)**, 743–750.
44. Jakes, R., Spillantini, M. G., and Goedert, M. (1994) *FEBS Lett.* **345(1)**, 27–32.
45. Maroteaux, L. and Scheller, R. H. (1991) *Brain Res. Mol. Brain Res.* **11(3–4)**, 335–343.
46. Ueda, K., Fukushima, H., Masliah, E., Xia, Y., Iwai, A., Yoshimoto, M., et al. (1993) *Proc. Natl. Acad. Sci. USA* **90(23)**, 11,282–11,286.
47. Bayer, T. A., Jakala, P., Hartmann, T., Havas, L., McLean, C., Culvenor, J. G., et al. (1999) *Neurosci. Lett.* **266(3)**, 213–216.
48. Prusiner, S. B. (1991) *Science* **252(5012)**, 1515–1522.
49. Prusiner, S. B. (1992) *Curr. Opin. Neurobiol.* **2(5)**, 638–647.
50. Oesch, B., Westaway, D., Walchli, M., McKinley, M. P., Kent, S. B., Aebersold, R., et al. (1985) *Cell* **40(4)**, 735–746.
51. McKinley, M. P. and Prusiner, S. B. (1991) *Curr. Topics Microbiol. Immunol.* **172**, 75–91.
52. Prusiner, S. B. (1989) *Annu. Rev. Microbiol.* **43**, 345–374.
53. Bueler, H., Aguzzi, A., Sailer, A., Greiner, R. A., Autenried, P., Aguet, M., et al. (1993) *Cell* **73(7)**, 1339–1347.
54. Moore, R. C., Hope, J., McBride, P. A., McConnell, I., Selfridge, J., Melton, D. W., et al. (1998) *Nature Genet.* **18(2)**, 118–125.
55. Westaway, D., Carlson, G. A., and Prusiner, S. B. (1995) *Trends Microbiol.* **3(4)**, 141–147.
56. Hsiao, K. K., Groth, D., Scott, M., Yang, S. L., Serban, H., Rapp, D., et al. (1994) *Proc. Natl. Acad. Sci. USA* **91(19)**, 9126–9130.
57. Hegde, R. S., Mastrianni, J. A., Scott, M. R., DeFea, K. A., Tremblay, P., Torchia, M., et al. (1998) *Science* **279(5352)**, 827–834.
58. Hegde, R. S., Tremblay, P., Groth, D., DeArmond, S. J., Prusiner, S. B., and Lingappa, V. R. (1999) *Nature* **402(6763)**, 822–826.
59. Bolton, D. C., McKinley, M. P., and Prusiner, S. B. (1982) *Science* **218(4579)**, 1309–1311.
60. Prusiner, S. B. (1982) *Science* **216(4542)**, 136–144.

61. Chesebro, B., Race, R., Wehrly, K., Nishio, J., Bloom, M., et al. (1985) *Nature* **315(6017)**, 331–333.
62. Kretzschmar, H. A., Stowring, L. E., Westaway, D., Stubblebine, W. H., Prusiner, S. B., and Dearmond, S. J. (1986) *DNA* **5(4)**, 315–324.
63. Cashman, N. R., Loertscher, R., Nalbantoglu, J., Shaw, I., Kascsak, R. J., Bolton, D. C., et al. (1990) *Cell* **61(1)**, 185–192.
64. Bendheim, P. E., Brown, H. R., Rudelli, R. D., Scala, L. J., Goller, N. L., Wen, G. Y., et al. (1992) *Neurology* **42(1)**, 149–156.
65. Herms, J., Tings, T., Gall, S., Madlung, A., Giese, A., Siebert, H., et al. (1999) *J. Neurosci.* **19(20)**, 8866–8875.
66. Tobler, I., Gaus, S. E., Deboer, T., Achermann, P., Fischer, M., Rulicke, T., et al. (1996) *Nature* **380(6575)**, 639–642.
67. Sakaguchi, S., Katamine, S., Nishida, N., Moriuchi, R., Shigematsu, K., Sugimoto, T., et al. (1996) *Nature* **380(6574)**, 528–531.
68. Collinge, J., Whittington, M. A., Sidle, K. C., Smith, C. J., Palmer, M. S., Clarke, A. R., et al. (1994) *Nature* **370(6487)**, 295–297.
69. Brown, D. R., Schulz-Schaeffer, W. J., Schmidt, B., and Kretzschmar, H. A. (1997) *Exp. Neurol.* **146(1)**, 104–112.
70. Nguyen, J., Baldwin, M. A., Cohen, F. E., and Prusiner, S. B. (1995) *Biochemistry* **34(13)**, 4186–4192.
71. DeArmond, S. J. and Prusiner, S. B. (1995) *Brain Pathol.* **5(1)**, 77–89.
72. Merz, P. A., Somerville, R. A., Wisniewski, H. M., and Iqbal, K. (1981) *Acta Neuropathol. (Berl.)* **54(1)**, 63–74.
73. Diringer, H., Gelderblom, H., Hilmert, H., Ozel, M., Edelbluth, C., and Kimberlin, R. H. (1983) *Nature* **306(5942)**, 476–478.
74. Prusiner, S. B., McKinley, M. P., Bowman, K. A., Bolton, D. C., Bendheim, P. E., Groth, D. F., et al. (1983) *Cell* **35(2 Pt. 1)**, 349–358.
75. Caughey, B., Race, R., and Chesebro, B. (1989) *Prog. Clin. Biol. Res.* **317**, 619–636.
76. Donne, D. G., Viles, J. H., Groth, D., Mehlhorn, I., James, T. L., Cohen, F. E., et al. (1997) *Proc. Natl. Acad. Sci. USA* **94(25)**, 13,452–13,457.
77. Harris, D. A., Falls, D. L., Johnson, F. A., and Fischbach, G. D. (1991) *Proc. Natl. Acad. Sci. USA* **88(17)**, 7664–7668.
78. Hornshaw, M. P., McDermott, J. R., Candy, J. M., and Lakey, J. H. (1995) *Biochem. Biophys. Res. Commun.* **214(3)**, 993–999.
79. Gabriel, J. M., Oesch, B., Kretzschmar, H., Scott, M., and Prusiner, S. B. (1992) *Proc. Natl. Acad. Sci. USA* **89(19)**, 9097–9101.
80. Poulter, M., Baker, H. F., Frith, C. D., Leach, M., Lofthouse, R., Ridley, R. M., et al. (1992) *Brain* **115(Pt. 3)**, 675–685.
81. Sulkowski, E. (1992) *FEBS Lett.* **307(2)**, 129–130.
82. Pan, K. M., Stahl, N., and Prusiner, S. B. (1992) *Protein Sci.* **1(10)**, 1343–1352.
83. Miura, T., Hori-i, A., Mototani, H., and Takeuchi, H. (1999) *Biochemistry* **38(35)**, 11,560–11,569.
84. Whittal, R. M., Ball, H. L., Cohen, F. E., Burlingame, A. L., Prusiner, S. B., and Baldwin, M. A. (2000) *Protein Sci.* **9(2)**, 332–343.
85. Ruiz, F. H., Silva, E., and Inestrosa, N. C. (2000) *Biochem. Biophys. Res. Commun.* **269(2)**, 491–495.
86. Stöckel, J., Safar, J., Wallace, A. C., Cohen, F. E., and Prusiner, S. B. (1998) *Biochemistry* **37(20)**, 7185–7193.
87. Brown, D. R., Hafiz, F., Glasssmith, L. L., Wong, B. S., Jones, I. M., Clive, C., et al. (2000) *EMBO J.* **19(6)**, 1180–1186.
88. Viles, J. H., Cohen, F. E., Prusiner, S. B., Goodin, D. B., Wright, P. E., and Dyson, H. J. (1999) *Proc. Natl. Acad. Sci. USA* **96(5)**, 2042–2047.
89. Marcotte, E. M. and Eisenberg, D. (1999) *Biochemistry* **38(2)**, 667–676.
90. Chen, S. G., Teplow, D. B., Parchi, P., Teller, J. K., Gambetti, P., and Autilio-Gambetti, L. (1995) *J. Biol. Chem.* **270(32)**, 19,173–19,180.
91. Pan, K. M., Baldwin, M., Nguyen, J., Gasset, M., Serban, A., Groth, D., et al. (1993) *Proc. Natl. Acad. Sci. USA* **90(23)**, 10,962–10,966.
92. Ishikawa, Y., Ito, S., Nishino, S., Ohba, S., and Nishida, Y. (1998) *Z. Naturforsch. [C]* **53(5–6)**, 378–382.
93. McKenzie, D., Bartz, J., Mirwald, J., Olander, D., Marsh, R., and Aiken, J. (1998) *J. Biol. Chem.* **273(40)**, 25,545–25,547.
94. Liautard, J. P. (1991) *FEBS Lett.* **294(3)**, 155–157.
95. Huang, Z., Gabriel, J. M., Baldwin, M. A., Fletterick, R. J., Prusiner, S. B., and Cohen, F. E. (1994) *Proc. Natl. Acad. Sci. USA* **91(15)**, 7139–7143.
96. Miura, T., Hori-i, A., and Takeuchi, H. (1996) *FEBS Lett.* **396(2–3)**, 248–252.
97. Prusiner, S. B. (1997) *Science* **278(5336)**, 245–251.
98. Shmerling, D., Hegyi, I., Fischer, M., Blattler, T., Brandner, S., Gotz, J., et al. (1998) *Cell* **93(2)**, 203–214.
99. Jackson, G. S., Hosszu, L. L., Power, A., Hill, A. F., Kenney, J., Saibil, H., et al. (1999) *Science* **283(5409)**, 1935–1937.
100. Collinge, J. (1997) *Hum. Mol. Genet.* **6(10)**, 1699–1705.
101. Wadsworth, J. D., Hill, A. F., Joiner, S., Jackson, G. S., Clarke, A. R., and Collinge, J. (1999) *Nature Cell. Biol.* **1(1)**, 55–59.
102. Doyle, D. and Rogers, M. (1998) *Trends Genet.* **14(5)**, 171–173.
103. Prince, R. C. and Gunson, D. E. (1998) *Trends Biochem. Sci.* **23(6),** 197–198
104. Brown, D. R. and Mohn, C. M. (1999) *Glia* **25(3)**, 282–292.
105. Shyng, S. L., Huber, M. T., and Harris, D. A. (1993) *J. Biol. Chem.* **268(21)**, 15,922–15,928.
106. Pauly, P. C., and Harris, D. A. (1998) *J. Biol. Chem.* **273(50)**, 33,107–33,110.
107. Valentine, J. S. and Gralla, E. B. (1997) *Science* **278(5339)**, 817–818.

108. Multhaup, G., Schlicksupp, A., Hesse, L., Beher, D., Ruppert, T., Masters, C. L., et al. (1996) *Science* **271(5254)**, 1406–1409.
109. Brown, D. R., Qin, K., Herms, J. W., Madlung, A., Manson, J., Strome, R., et al. (1997) *Nature* **390(6661)**, 684–687.
110. Brown, D. R., Schmidt, B., and Kretzschmar, H. A. (1997) *Int. J. Dev. Neurosci.* **15(8)**, 961–972.
111. Brown, D. R. and Besinger, A. (1998) *Biochem. J.* **334(Pt. 2)**, 423–429.
112. White, A. R., Collins, S. J., Maher, F., Jobling, M. F., Stewart, L. R., Thyer, J. M., et al. (1999) *Am. J. Pathol.* **155(5)**, 1723–1730.
113. Wong, B. S., Wang, H., Brown, D. R., and Jones, I. M. (1999) *Biochem. Biophys. Res. Commun.* **259(2)**, 352–355.
114. Brown, D. R., Wong, B. S., Hafiz, F., Clive, C., Haswell, S. J., and Jones, I. M. (1999) *Biochem. J.* **344 (Pt. 1)**, 1–5.
115. Waggoner, D. J., Drisaldi, B., Bartnikas, T. B., Casareno, R. L., Prohaska, J. R., Gitlin, J. D., et al. (2000) *J. Biol. Chem.* **275(11)**, 7455–7458.
116. Ma, J. and Lindquist, S. (1999) *Nature Cell Biol.* **1(6),** 358–361.
117. Brownell, B., Oppenheimer, D. R., and Hughes, J. T. (1970) *J. Neurol. Neurosurg. Psychiatry* **33(3)**, 338–357.
118. Shaw, P. J., Chinnery, R. M., and Ince, P. G. (1994) *Brain Res.* **655(1–2)**, 195–201.
119. Rothstein, J. D. (1996) *Neurology* **47(4 Suppl. 2)**, S19–S25; discussion S26.
120. Bowling, A. C. and Beal, M. F. (1995) *Life Sci.* **56(14)**, 1151–1171.
121. Bruijn, L. I., Houseweart, M. K., Kato, S., Anderson, K. L., Anderson, S. D., Ohama, E., et al. (1998) *Science* **281(5384)**, 1851–1854.
122. Smith, C., Mitchinson, M. J., Aruoma, O. I., and Halliwell, B. (1992) *Biochem. J.* **286(Pt. 3)**, 901–905.
123. Appel, S. H., Smith, R. G., Engelhardt, J. I., and Stefani, E. (1994) *J. Neurol. Sci.* **(124 Suppl.)**, 14–19.
124. Rothstein, J. D., Martin, L. J., and Kuncl, R. W. (1992) *N. Engl. J. Med.* **326(22)**, 1464–1468.
125. Lin, C. L., Bristol, L. A., Jin, L., Dykes-Hoberg, M., Crawford, T., Clawson, L., et al. (1998) *Neuron* **20(3)**, 589–602.
126. Horton, W. A., Eldridge, R., and Brody, J. A. (1976) *Neurology* **26(5)**, 460–465.
127. Rosen, D. R., Siddique, T., Patterson, D., Figlewicz, D. A., Sapp, P., Hentati, A., et al. (1993) *Nature* **362(6415)**, 59–62.
128. Leschot, N. J., Slater, R. M., Joenje, H., Becker-Bloemkolk, M. J., and de Nef, J. J. (1981) *Hum. Genet.* **57(2)**, 220–223.
129. De La Torre, R., Casado, A., Lopez-Fernandez, E., Carrascosa, D., Ramirez, V., and Saez, J. (1996) *Experientia* **52(9)**, 871–873.
130. Gurney, M. E., Yamamoto, H., and Kwon, Y. (1992) *J. Neurosci.* **12(8)**, 3241–3247.
131. Gurney, M. E. (1997) *J. Neurol. Sci.* (**152 Suppl. 1),** S67–S73.
132. Dal Canto, M. C. and Gurney, M. E. (1997) *Acta Neuropathol. (Berl.)* **93(6)**, 537–550.
133. Reaume, A. G., Elliott, J. L., Hoffman, E. K., Kowall, N. W., Ferrante, R. J., Siwek, D. F., et al. (1996) *Nature Genet.* **13(1)**, 43–47.
134. Ho, Y. S., Gargano, M., Cao, J., Bronson, R. T., Heimler, I., and Hutz, R. J. (1998) *J. Biol. Chem.* **273(13)**, 7765–7769.
135. Rabizadeh, S., Gralla, E. B., Borchelt, D. R., Gwinn, R., Valentine, J. S., Sisodia, S., et al. (1995) *Proc. Natl. Acad. Sci. USA* **92(7)**, 3024–3028.
136. Borchelt, D. R., Lee, M. K., Slunt, H. S., Guarnieri, M., Xu, Z. S., Wong, P. C., et al. (1994) *Proc. Natl. Acad. Sci. USA* **91(17)**, 8292–8296.
137. Borchelt, D. R., Thinakaran, G., Eckman, C. B., Lee, M. K., Davenport, F., Ratovitsky, T., et al. (1996) *Neuron* **17(5)**, 1005–1013.
138. Bruijn, L. I., Becher, M. W., Lee, M. K., Anderson, K. L., Jenkins, N. A., Copeland, N. G., et al. (1997) *Neuron* **18(2)**, 327–338.
139. Durham, H. D., Roy, J., Dong, L., and Figlewicz, D. A. (1997) *J. Neuropathol. Exp. Neurol.* **56(5)**, 523–530.
140. Estevez, A. G., Crow, J. P., Sampson, J. B., Reiter, C., Zhuang, Y., Richardson, G. J., et al. (1999) *Science* **286(5449)**, 2498–2500.
141. Fee, J. A. (1991) *Mol. Microbiol.* **5(11)**, 2599–2610.
142. Phillips, J. P., Campbell, S. D., Michaud, D., Charbonneau, M., and Hilliker, A. J. (1989) *Proc. Natl. Acad. Sci. USA* **86(8)**, 2761–2765.
143. Ishii, N., Takahashi, K., Tomita, S., Keino, T., Honda, S., Yoshino, K., et al. (1990) *Mutat. Res.* **237(3–4)**, 165–171.
144. Fridovich, I. (1997) *J. Biol. Chem.* **272(30)**, 18,515–18,517.
145. Li, Y., Huang, T. T., Carlson, E. J., Melov, S., Ursell, P. C., Olson, J. L., et al. (1995) *Nature Genet.* **11(4)**, 376–381.
146. Lebovitz, R. M., Zhang, H., Vogel, H., Cartwright, J., Jr., Dionne, L., Lu, N., et al. (1996) *Proc. Natl. Acad. Sci. USA* **93(18)**, 9782–9787.
147. Melov, S., Schneider, J. A., Day, B. J., Hinerfeld, D., Coskun, P., Mirra, S. S., et al. (1998) *Nature Genet.* **18(2)**, 159–163.
148. McCord, J. M. and Fridovich, I. (1969) *J. Biol. Chem.* **244(22)**, 6056–6063.
149. Petrovic, N., Comi, A., and Ettinger, M. J. (1996) *J. Biol. Chem.* **271(45)**, 28,331–28,334.
150. Culotta, V. C., Klomp, L. W., Strain, J., Casareno, R. L., Krems, B., and Gitlin, J. D. (1997) *J. Biol. Chem.* **272(38)**, 23,469–23,472.
151. Rae, T. D., Schmidt, P. J., Pufahl, R. A., Culotta, V. C., and O'Halloran, T. V. (1999) *Science* **284(5415)**, 805–808.
152. Lyons, T. J., Liu, H., Goto, J. J., Nersissian, A., Roe, J. A., Graden, J. A., et al. (1996) *Proc. Natl. Acad. Sci. USA* **93(22)**, 12,240–12,244.
153. Hodgson, E. K., and Fridovich, I. (1975) *Biochemistry* **14(24)**, 5294–5299.
154. Yim, M. B., Chock, P. B., and Stadtman, E. R. (1990) *Proc. Natl. Acad. Sci. USA* **87(13)**, 5006–5010.
155. Yim, M. B., Chock, P. B., and Stadtman, E. R. (1993) *J. Biol. Chem.* **268(6)**, 4099–4105.

156. Beckman, J. S., Carson, M., Smith, C. D., and Koppenol, W. H. (1993) *Nature* **364(6438)**, 584.
157. Beal, M. F. and Matthews, R. T. (1997) *Mol. Aspects Med.* **18 (Suppl.)**, S169–S179.
158. Bruijn, L. I., Beal, M. F., Becher, M. W., Schulz, J. B., Wong, P. C., Price, D. L., et al. (1997) *Proc. Natl. Acad. Sci. USA* **94(14)**, 7606–7611.
159. Deng, H. X., Hentati, A., Tainer, J. A., Iqbal, Z., Cayabyab, A., Hung, W. Y., et al. (1993) *Science* **261(5124)**, 1047–1051.
160. Wiedau-Pazos, M., Goto, J. J., Rabizadeh, S., Gralla, E. B., Roe, J. A., Lee, M. K., et al. (1996) *Science* **271(5248)**, 515–518.
161. Yim, M. B., Kang, J. H., Yim, H. S., Kwak, H. S., Chock, P. B., and Stadtman, E. R. (1996) *Proc. Natl. Acad. Sci. USA* **93(12)**, 5709–5714.
162. Wong, P. C., Pardo, C. A., Borchelt, D. R., Lee, M. K., Copeland, N. G., Jenkins, N. A., et al. (1995) *Neuron* **14(6)**, 1105–1116.
163. Hart, P. J., Liu, H., Pellegrini, M., Nersissian, A. M., Gralla, E. B., Valentine, J. S., et al. (1998) *Protein Sci.* **7(3)**, 545–555.
164. Gurney, M. E., Pu, H., Chiu, A. Y., Dal Canto, M. C., Polchow, C. Y., Alexander, D. D., et al. (1994) *Science* **264(5166)**, 1772–1775.
165. Dal Canto, M. C. and Gurney, M. E. (1995) *Brain Res.* **676(1)**, 25–40.
166. Borchelt, D. R., Wong, P. C., Becher, M. W., Pardo, C. A., Lee, M. K., Xu, Z. S., et al. (1998) *Neurobiol. Dis.* **5(1)**, 27–35.
167. Shibata, N., Hirano, A., Kobayashi, M., Sasaki, S., Kato, T., Matsumoto, S., et al. (1994) *Neurosci. Lett.* **179(1–2)**, 149–152.
168. Chou, S. M., Wang, H. S., and Komai, K. (1996) *J. Chem. Neuroanat.* **10(3–4)**, 249–258.
169. Kato, M., Saito, H., and Abe, K. (1997) *J. Neurochem.* **68(5)**, 1889–1895.
170. Gurney, M. E., Cutting, F. B., Zhai, P., Doble, A., Taylor, C. P., Andrus, P. K., et al. (1996) *Ann. Neurol.* **39(2)**, 147–157.
171. Hottinger, A. F., Fine, E. G., Gurney, M. E., Zurn, A. D., and Aebischer, P. (1997) *Eur. J. Neurosci.* **9(7)**, 1548–1551.
172. Kostic, V., Jackson-Lewis, V., de Bilbao, F., Dubois-Dauphin, M., and Przedborski, S. (1997) *Science* **277(5325)**, 559–562.
173. Collard, J. F., Cote, F., and Julien, J. P. (1995) *Nature* **375(6526)**, 61–64.
174. Selkoe, D. J. (1998) *Trends Cell Biol.* **8(11)**, 447–453.
175. Saunders, A. M., Strittmatter, W. J., Schmechel, D., George-Hyslop, P. H., Pericak-Vance, M. A., Joo, S. H., et al. (1993) *Neurology* **43(8),** 1467–1472.
176. Levy-Lahad, E. and Bird, T. D. (1996) *Ann. Neurol.* **40(6)**, 829–840.
177. Corder, E. H., Saunders, A. M., Strittmatter, W. J., Schmechel, D. E., Gaskell, P. C., Small, G. W., et al. (1993) *Science* **261(5123)**, 921–923.
178. Glenner, G. G., Wong, C. W., Quaranta, V., and Eanes, E. D. (1984) *Appl. Pathol.* **2(6)**, 357–369.
179. Masters, C. L., Simms, G., Weinman, N. A., Multhaup, G., McDonald, B. L., and Beyreuther, K. (1985) *Proc. Natl. Acad. Sci. USA* **82**, 4245–4249.
180. Masters, C. L., Multhaup, G., Simms, G., Pottgiesser, J., Martins, R. N., and Beyreuther, K. (1985) *EMBO J.* **4(11)**, 2757–2763.
181. Shoji, M., Golde, T. E., Ghiso, J., Cheung, T. T., Estus, S., Shaffer, L. M., et al. (1992) *Science* **258(5079)**, 126–129.
182. Haass, C., Schlossmacher, M. G., Hung, A. Y., Vigo Pelfrey, C., Mellon, A., Ostaszewski, B. L., et al. (1992) *Nature* **359(6393)**, 322–325.
183. Seubert, P., Vigo Pelfrey, C., Esch, F., Lee, M., Dovey, H., Davis, D., et al. (1992) *Nature* **359(6393)**, 325–7.
184. Vigo-Pelfrey, C., Lee, D., Keim, P., Lieberburg, I., and Schenk, D. B. (1993) *J. Neurochem.* **61(5)**, 1965–1968.
185. Roher, A. E., Palmer, K. C., Yurewicz, E. C., Ball, M. J., and Greenberg, B. D. (1993) *J. Neurochem.* **61(5)**, 1916–1926.
186. Roher, A. E., Chaney, M. O., Kuo, Y. M., Webster, S. D., Stine, W. B., Haverkamp, L. J., et al. (1996) *J. Biol. Chem.* **271(34)**, 20,631–20,635.
187. Schenk, D., Barbour, R., Dunn, W., Gordon, G., Grajeda, H., Guido, T., et al. (1999) *Nature* **400(6740)**, 173–177.
188. Spillantini, M. G., Murrell, J. R., Goedert, M., Farlow, M. R., Klug, A., and Ghetti, B. (1998) *Proc. Natl. Acad. Sci. USA* **95(13)**, 7737–7741.
189. Poorkaj, P., Bird, T. D., Wijsman, E., Nemens, E., Garruto, R. M., Anderson, L., et al. (1998) *Ann. Neurol.* **43(6),** 815–825.
190. Sandbrink, R., Masters, C. L., and Beyreuther, K. (1994) *J. Biol. Chem.* **269(19)**, 14,227–14,234.
191. Wasco, W., Bupp, K., Magendantz, M., Gusella, J. F., Tanzi, R. E., and Solomon, F. (1992) *Proc. Natl. Acad. Sci. USA* **89(22)**, 10,758–10,762.
192. Sprecher, C. A., Grant, F. J., Grimm, G., O'Hara, P. J., Norris, F., Norris, K., et al. (1993) *Biochemistry* **32(17)**, 4481–4486.
193. Slunt, H. H., Thinakaran, G., Von Koch, C., Lo, A. C., Tanzi, R. E., and Sisodia, S. S. (1994) *J. Biol. Chem.* **269(4)**, 2637–2644.
194. Bayer, T. A., Cappai, R., Masters, C. L., Beyreuther, K., and Multhaup, G. (1999) *Mol. Psychiatry* **4(6),** 524–528.
195. Schubert, D., LaCorbiere, M., Saitoh, T., and Cole, G. (1989) *Proc. Natl. Acad. Sci. USA* **86(6)**, 2066–2069.
196. Milward, E. A., Papadopoulos, R., Fuller, S. J., Moir, R. D., Small, D., Beyreuther, K., et al. (1992) *Neuron* **9(1)**, 129–137.
197. Mattson, M. P., Cheng, B., Culwell, A. R., Esch, F. S., Lieberburg, I., and Rydel, R. E. (1993) *Neuron* **10(2)**, 243–254.

198. Cappai, R., Mok, S. S., Galatis, D., Tucker, D. F., Henry, A., Beyreuther, K., et al. (1999) *FEBS Lett.* **442(1)**, 95–98.
199. Bush, A. I., Multhaup, G., Moir, R. D., Williamson, T. G., Small, D. H., Rumble, B., et al. (1993) *J. Biol. Chem.* **268(22)**, 16,109–16,112.
200. Bush, A. I., Pettingell, W. H., Multhaup, G., Paradis, D. M., Vonsattel, J. P., Gusella, J. F., et al. (1994) *Science* **265(5177)**, 1464–1467.
201. Multhaup, G., Bush, A. I., Pollwein, P., and Masters, C. L. (1994) *FEBS Lett.* **355(2)**, 151–154.
202. Multhaup, G. (1994) *Biochimie* **76(3–4)**, 304–311.
203. Multhaup, G., Ruppert, T., Schlicksupp, A., Hesse, L., Beher, D., Masters, C. L., et al. (1997) *Biochem. Pharmacol.* **54(5)**, 533–539.
204. Multhaup, G., Ruppert, T., Schlicksupp, A., Hesse, L., Bill, E., Pipkorn, R., et al. (1998) *Biochemistry* **37(20)**, 7224–7230.
205. Multhaup, G., Hesse, L., Borchardt, T., Ruppert, T., Cappai, R., Masters, C. L., et al. (1999) *Adv. Exp. Med. Biol.* **448**, 183–192.
206. White, A. R., Reyes, R., Mercer, J. F., Camakaris, J., Zheng, H., Bush, A. I., et al. (1999) *Brain Res.* **842(2)**, 439–444.
207. White, A. R., Multhaup, G., Maher, F., Bellingham, S., Camakaris, J., Zheng, H., et al. (1999) *J. Neurosci.* **19(21)**, 9170–9179
208. Hesse, L., Beher, D., Masters, C. L., and Multhaup, G. (1994) *FEBS Lett.* **349(1)**, 109–116.
209. Ruiz, F. H., Gonzalez, M., Bodini, M., Opazo, C., and Inestrosa, N. C. (1999) *J. Neurochem.* **73(3)**. 1288–1292.
210. White, A. R., Zheng, H., Galatis, D., Maher, F., Hesse, L., Multhaup, G., et al. (1998) *J. Neurosci.* **18(16)**, 6207–6217.
211. Multhaup, G. and Masters, C. L. (1999) *Met. Ions Biol. Syst.* **36**, 365–387.
212. Hassett, R. and Kosman, D. J. (1995) *J. Biol. Chem.* **270(1)**, 128–134.
213. Borchardt, T., Camakaris, J., Cappai, R., Masters, C. L., Beyreuther, K., and Multhaup, G. (1999) *Biochem. J.* **344(Pt. 2)**, 461–467.
214. Nakamura, Y., Takeda, M., Niigawa, H., Hariguchi, S., and Nishimura, T. (1992) *Neurosci Lett.* **136(1)**, 95–98.
215. Schubert, D. and Behl, C. (1993) *Brain Res.* **629(2),** 275–282.
216. Mattson, M. P., Barger, S. W., Cheng, B., Lieberburg, I., Smith-Swintosky, V. L., and Rydel, R. E. (1993) *Trends Neurosci.* **16(10)**, 409–414.
217. Goodman, Y. and Mattson, M. P. (1994) *Exp. Neurol.* **128(1)**, 1–12.
218. Barger, S. W., Horster, D., Furukawa, K., Goodman, Y., Krieglstein, J., and Mattson, M. P. (1995) *Proc. Natl. Acad. Sci. USA* **92(20)**, 9328–9332.
219. Mucke, L., Abraham, C. R., and Masliah, E. (1996) *Ann. NY Acad. Sci.* **777**, 82–88.
220. Ehmann, W. D., Markesbery, W. R., Alauddin, M., Hossain, T. I., and Brubaker, E. H. (1986) *Neurotoxicology* **7(1)**, 195–206.
221. Samudralwar, D. L., Diprete, C. C., Ni, B. F., Ehmann, W. D., and Markesbery, W. R. (1995) *J. Neurol. Sci.* **130(2)**, 139–145.
222. Deibel, M. A., Ehmann, W. D., and Markesbery, W. R. (1996) *J. Neurol. Sci.* **143(1–2)**, 137–142.
223. Lovell, M. A., Robertson, J. D., Teesdale, W. J., Campbell, J. L., and Markesbery, W. R. (1998) *J. Neurol. Sci.* **158(1)**, 47–52.
224. Thompson, C. M., Markesbery, W. R., Ehmann, W. D., Mao, Y. X., and Vance, D. E. (1988) *Neurotoxicology* **9(1)**, 1–7.
225. Cornett, C. R., Markesbery, W. R., and Ehmann, W. D. (1998) *Neurotoxicology* **19(3)**, 339–345.
226. Smith, M. A., Harris, P. L., Sayre, L. M., and Perry, G. (1997) *Proc. Natl. Acad. Sci. USA* **94(18)**, 9866–9868.
227. Suh, Y. H. (1997) *J. Neurochem.* **68(5)**, 1781–1791
228. Bush, A. I., Pettingell, W. H., Jr., Paradis, M. D., and Tanzi, R. E. (1994) *J. Biol. Chem.* **269(16)**, 12,152–12,158.
229. Huang, X., Atwood, C. S., Moir, R. D., Hartshorn, M. A., Vonsattel, J. P., Tanzi, R. E., et al. (1997) *J. Biol. Chem.* **272(42)**, 26,464–26,470.
230. Atwood, C. S., Moir, R. D., Huang, X., Scarpa, R. C., Bacarra, N. M., Romano, D. M., et al. (1998) *J. Biol. Chem.* **273(21),** 12,817–12,826.
231. Huang, X., Atwood, C. S., Hartshorn, M. A., Multhaup, G., Goldstein, L. E., Scarpa, R. C., et al. (1999) *Biochemistry* **38(24)**, 7609–7616.
232. Cherny, R. A., Legg, J. T., McLean, C. A., Fairlie, D. P., Huang, X., Atwood, C. S., et al. (1999) *J. Biol. Chem.* **274(33)**, 23,223–23,228.
233. Suh, S. W., Jensen, K. B., Jensen, M. S., Silva, D. S., Kesslak, P. J., Danscher, G., et al. (2000) *Brain Res.* **852(2)**, 274–278.
234. Lee, J. Y., Mook-Jung, I., and Koh, J. Y. (1999) *J. Neurosci.* **19(11)**, RC10.
235. Yates, C. M., Butterworth, J., Tennant, M. C., and Gordon, A. (1990) *J. Neurochem.* **55**(5)**,** 1624–1630.
236. Owen, C. A. (1982) *Biological Aspects of Copper: Occurrence, Assay, and Interrelationships*, Copper in Biology and Medicine Series, Noyes, Park Ridge, NJ.
237. Atwood, C. S., Huang, X., Moir, R. D., Tanzi, R. E., and Bush, A. I. (1999) *Met. Ions Biol. Syst.* **36,** 309–364.
238. Silva, J. R. R. F. d. and Williams, R. J. P. (1991) *The Biological Chemistry of the Elements: The Inorganic Chemistry of Life*, Clarendon, Oxford University Press, Oxford.
239. Huang, X., Cuajungco, M. P., Atwood, C. S., Hartshorn, M. A., Tyndall, J. D., Hanson, G. R., et al. (1999) *J. Biol. Chem.* **274(52)**, 37,111–37,116.
240. Hensley, K., Carney, J. M., Mattson, M. P., Aksenova, M., Harris, M., Wu, J. F., et al. (1994) *Proc. Natl. Acad. Sci. USA* **91(8)**, 3270–3274.

241. Dikalov, S. I., Vitek, M. P., Maples, K. R., and Mason, R. P. (1999) *J. Biol. Chem.* **274(14),** 9392–9399.
242. Basun, H., Forssell, L. G., Wetterberg, L., and Winblad, B. (1991) *J. Neural Transm. Park Dis. Dement Sect* **3(4)**, 231–258.
243. Loeffler, D. A., LeWitt, P. A., Juneau, P. L., Sima, A. A., Nguyen, H. U., DeMaggio, A. J., et al. (1996) *Brain Res.* **738(2)**, 265–274.
244. Tokutake, S., Nagase, H., Morisaki, S., and Oyanagi, S. (1995) *Neurosci. Lett.* **185(2)**, 99–102.
245. Martins, R. N., Harper, C. G., Stokes, G. B., and Masters, C. L. (1986) *J. Neurochem.* **46(4)**, 1042–1045.
246. Smith, C. D., Carney, J. M., Starke Reed, P. E., Oliver, C. N., Stadtman, E. R., Floyd, R. A., et al. (1991) *Proc. Natl. Acad. Sci. USA* **88(23)**, 10,540–10,543.
247. Smith, C. D., Carney, J. M., Tatsumo, T., Stadtman, E. R., Floyd, R. A., and Markesbery, W. R. (1992) *Ann. NY Acad. Sci.* **663,** 110–119.
248. Good, P. F., Werner, P., Hsu, A., Olanow, C. W., and Perl, D. P. (1996) *Am. J. Pathol.* **149(1)**, 21–28.
249. Balazs, L. and Leon, M. (1994) *Neurochem. Res.* **19(9)**, 1131–1137.
250. Lovell, M. A., Ehmann, W. D., Mattson, M. P., and Markesbery, W. R. (1997) *Neurobiol. Aging* **18(5)**, 457–461.
251. Subbarao, K. V., Richardson, J. S., and Ang, L. C. (1990) *J. Neurochem.* **55(1)**, 342–345.
252. Sayre, L. M., Zelasko, D. A., Harris, P. L. R., Perry, G., Salomon, R. G., and Smith, M. A. (1997) *J. Neurochem.* **68(5)**, 2092–2097.
253. Mecocci, P., MacGarvey, U., and Beal, M. F. (1994) *Ann. Neurol.* **36(5)**, 747–751.
254. Nunomura, A., Perry, G., Hirai, K., Aliev, G., Takeda, A., Chiba, S., et al. (1999) *Ann. NY Acad. Sci.* **893**, 362–364.
255. Smith, M. A., Richey, P. L., Taneda, S., Kutty, R. K., Sayre, L. M., Monnier, V. M., et al. (1994) *Ann. NY Acad. Sci.* **738**, 447–454.
256. Sano, M., Ernesto, C., Thomas, R. G., Klauber, M. R., Schafer, K., Grundman, M., et al. (1997) *N. Engl. J. Med.* **336(17)**, 1216–1222.
257. Breitner, J. C. (1996) *Annu. Rev. Med.* **47**, 401–411.
258. Rother, M., Kittner, B., Rudolphi, K., Rossner, M., and Labs, K. H. (1996) *Ann. NY Acad. Sci.* **777,** 404–409.
259. Schubert, P., Ogata, T., Rudolphi, K., Marchini, C., McRae, A., and Ferroni, S. (1997) *Ann. NY Acad. Sci.* **826,** 337–347.
260. Bondy, S. C., Guo-Ross, S. X., and Truong, A. T. (1998) *Brain Res.* **799(1)**, 91–96.
261. Freedman, J. H., Ciriolo, M. R., and Peisach, J. (1989) *J. Biol. Chem.* **264(10)**, 5598–5605.
262. Muller, W. E., Romero, F. J., Perovic, S., Pergande, G., and Pialoglou, P. (1997) *J Neurochem* **68**(6)**,** 2371-7.

18

Molecular Genetics and Clinical Aspects of Menkes Disease and Occipital Horn Syndrome

Hiroko Kodama

1. INTRODUCTION

Menkes disease (MNK) is an X-linked recessive disorder characterized by progressive neuronal degeneration and connective tissue abnormalities, first described by Menkes and co-workers in 1962 *(1)*. In 1972, Danks et al. demonstrated that MNK is associated with copper deficiency as a result of a defect in intestinal copper absorption, which results in copper accumulation in the intestine *(2,3)*. This observation, together with the discovery of a mutant strain of mice serving as a model of MNK, mottled mutant mice, led to many studies on copper metabolism and the pathophysiology of this disease *(4,5)*. Moreover, patients with a milder MNK phenotype have been reported. These patients are generally said to have "mild MNK," whereas the typical phenotype is referred to as "classical MNK." In this chapter, classical MNK and mild MNK are referred to as MNK and mild MNK, respectively. Occipital horn syndrome (OHS), first described by Lazoff et al. in 1975 *(6)*, is considered to represent the mildest form of MNK.

In 1993, approx 30 yr after Menkes' original report, the Menkes disease gene was identified as a gene encoding a copper-transporting P-type ATPase (ATP7A) *(7–9)*. Both mild MNK and OHS have been identified as genetic disorders resulting from mutations in the *ATP7A* gene *(10,11)*. Moreover, mottled mice have been reported to have mutations in the mottled gene (*atp7a*), the murine homolog of the ATP7A gene *(11–16)*. The discovery of the *ATP7A* gene led to vigorous studies on the function and metabolism of ATP7A and the intracellular copper transport system, as well as studies on the molecular genetics and clinical aspects of MNK.

2. MOLECULAR GENETICS

2.1. Background

The Menkes disease gene has been mapped to Xq13.3 and it is organized into 23 exons. It encodes a copper-transporting ATPase (ATP7A) consisting of 1500 amino acid residues, with a molecular mass of 165 kDa. The ATP7A gene is expressed in almost all tissues, except for the liver. The ATP7A protein contains six metal-binding domains near the N-terminus, a phosphorylation domain, a phosphatase domain, and eight transmembrane domains (Fig. 1). When the intracellular copper concentration is within the normal range, ATP7A is localized in the trans-Golgi network and it acts to

From: Handbook of Copper Pharmacology and Toxicology
Edited by: E. J. Massaro © Humana Press Inc., Totowa, NJ

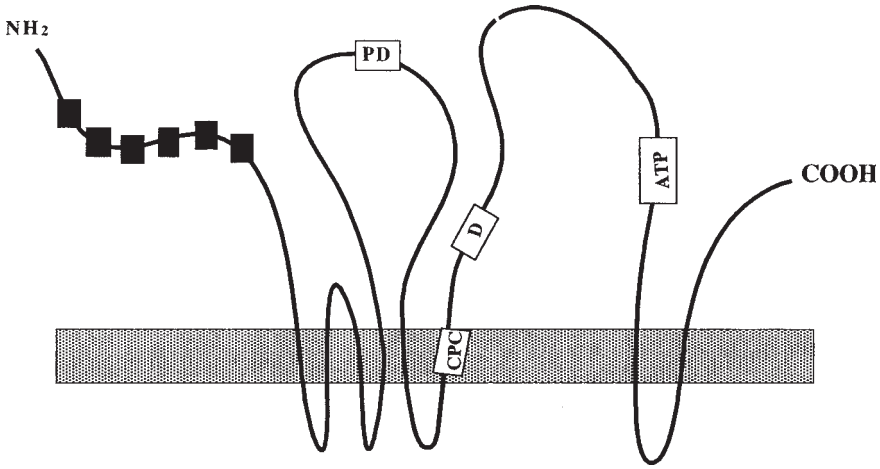

Fig. 1. Predicted structure of the Menkes copper-transporting ATPase (ATP7A). ■, six copper-binding domains; PD, phosphatase domain; CPC, cation channel; D, phosphorylation domain; ATP, ATP-binding domain.

transport copper from the cytosol into the Golgi apparatus and, subsequently, to exclude copper from the cells. When the intracellular copper concentration increases, ATP7A is transported to the plasma membrane *(17,18)*.

2.2. Gene Defects

Patients with MNK exhibit a large variety of mutations in the *ATP7A* gene. Tümer et al. summarized a total of 191 different mutations affecting the *ATP7A* gene, mainly in European and American patients with MNK and OHS *(19)*. The mutations consisted of 7 chromosome mutations, 35 partial gene deletions, 39 deletion/insertion point mutations, 35 nonsense mutations, 43 splice-site mutations, and 32 missense mutations. These findings indicate that patients with MNK or OHS have no common mutations. The mutations in the *ATP7A* gene in 17 unrelated Japanese patients with classical MNK have been identified, and each patient was found to have a different mutation (Table 1). Splice-site mutations were found in two patients, and in both of these cases, only abnormal transcripts were found by reverse transcription–polymerase chain reaction (RT-PCR) analysis. All of the mutations identified in patients with MNK seem to have an important influence on the structure and function of ATP7A.

Mild MNK and OHS are very rare. To our knowledge, the mutations in patients with mild MNK and OHS have been reported in only 10 cases (Table 2) *(10,11,20–25)*. One patient with mild MNK was found to have a missense mutation, and the mutant protein was located in the trans-Golgi network, but it failed to be transported to the plasma membrane in response to an increase intracellular copper concentration *(20)*. Another patient with mild MNK was found to have a splice-site mutation resulting in the production of both normal and mutant transcripts. In patients with OHS reported by Kaler et al. and Qi et al., it seems that each of the mutations resulted in the production of a partially functional ATP7A protein. Seven of the mutations identified in patients with OHS are splice-site mutations. Five of these splice-site mutations have been reported to result in the production of the normal transcript as well as abnormal transcripts. A splice-site mutation in the *ATP7A* gene has also been identified in a Japanese patient with OHS (Table 2) *(23)*. This mutation was found to be the same as one in a patient reported by Møller et al. *(22)*. However, the level of normal mRNA in Møller et al's patient was 2–5% of that in unaffected individuals, whereas the level of normal mRNA in the Japanese patient was 19%. These differences suggest that the production of normal ATP7A mRNA

Table 1
***ATP7A* Mutations and Serum Levels of Copper and Ceruloplasmin in Japanese Patients with Menkes Disease**

	Exon no.	*Nucleotide changes*[a]	*Consequence*	*Serum Cu (μg/dL)*	*Cerulo-plasmin (mg/dL)*
		Insertion/Deletion			
O.H.	7	del 1893AG	I582FS584X	20	6
T.Y.	8	ins 2030 A	E628FS644X	8	8
I.Y.	10	del 2459AGAG	E771FS774X	18	12
O.T.	15	ins 3219 AT	I1024FS1026X	16	7
Y.Y.	20	del 4150G	R1335FS1341X	18	5
T.R.	21	del 4159TCT	del 1339L	8	10
		Nonsense			
I.K.	3	644C→T	Q167X	9	8
H.S.	5	1605C→A	S487X	10	3
K.S.	6	1730G→T	E529X	16	6
N.S.	8	2078C→T	R645X	10	3
Y.K.	15	3083C→T	R980X	3	3
S.Y.	15	3101C→T	R986X	16	11
		Missense			
K.Y.	9	2303T→C	C720R	4	3
H.T.	10	2324G→A	G727R	26	6
T.K.	21	4177TA→AT	S1344R,I1345F	35	11
		Splice site			
M.D.	16	DS(AAACAGgtac→AAACgtac)	Skips exon 16	10	7
Y.N.	22 and IVS22	DS(ACTTTCTTCTCTCTTAAA CTgtaagtatgatagcttttgct cac→ACTTTctcac)	Skips exon 22	13	5

[a]Codon and nucleotide numbers are according to the *ATP7A* cDNA sequence published by Vulpe et al. *(7).* DS = donor site.

varies among patients with the same splice-site mutation, although the mechanism responsible for the variation remains unclear.

2.3. Genotype–Phenotype Correlation

The phenotypes can been classified into classical MNK (referred to as MNK in this chapter), mild MNK, and OHS. Almost all patients with MNK have similar clinical courses and the laboratory findings are similar. However, some patients have been reported to exhibit severer clinical features, such as congenital skull fractures and neonatal hemorrhage *(26–28)*. On the other hand, some patients seem to exhibit slightly milder phenotypes. In the two patients with missense mutations listed in Table 1, the reduction in serum copper concentrations was milder than that in other patients with MNK. The G727R missense mutation in case H.T. is the same mutation as that found in a patient reported by Das et al., in whose case the normal-sized ATP7A mRNA was detected by Northern blot analysis *(29)*. The missense mutations S1344R and I1345F in case T.K. result in changes in amino acid residues between the fourth and fifth transmembrane domains, but this is not a highly conserved region of the protein. The mutant protein produced in each of these patients may retain some partial ATP7A function, but the level of activity seems to be extremely low.

Table 2
ATP7A Mutations in Patients with Mild MNK and Patients with OHS

Study (ref.)	*Nucleotide changes*[a]	*Consequence*	*mRNA transcripts size: amount of normal size one (% of normal level)*
Mild Menkes disease			
Kaler et al. *(10)*	nt 4268 + 3a→t	Skips 118-bp exon	Normal and smaller; 19%
Ambrosini et al. *(20)*	C4230T	Ala1362Val	
Occipital horn syndrome			
Levinson et al. *(21)*	Deletion of a repeated element in the regulatory region of the *ATP7A*		Normal; normal amount
Møller et al. *(22)*	GTTgtaagtaagattt→ GTTgtaagattt	Skips exon 6	Normal and smaller; 2–5%
Gu et al. *(23)*	GTTgtaagtaagattt→ GTTgtaagattt	Skips exon 6	Normal and smaller; 19%
Ronce et al. *(24)*	C2055T	Ser637Leu, skips exon 8, skips exon 10, and skips exon 8–10	Normal size containing the missense mutation, and smaller;
Qi et al. *(25)*	IVS10+3a→t	Skips exon 10	Only smaller;
Kaler et al. *(10)*	A2642G	Skips 92-bp exon	Normal size containing the missense mutation, and smaller; 36%
Das et al. *(11)*	nt 3062–4a→g	Skips 195-bp exon	Normal and smaller; normal amount
Das et al. *(10)*	nt 3656+5g→a	Skips 217-bp exon	Normal and smaller; very little amount

[a]According to Vulpe et al. *(7)*.

As described in Section 2.2., most of the patients with OHS have splice-site mutations that allow some normal ATP7A mRNA to be produced, suggesting that the milder phenotype displayed by these patients is the result of the presence of some normal ATP7A mRNA, resulting in partial ATP7A function. The levels of ATP7A activity required to avoid the classical MNK phenotype or to avoid the disease symptoms completely are not yet known. A quantitative and sensitive analysis of ATP7A activity will clarify the correlation between residual ATP7A activity and the severity of symptoms in patients, as well as the correlation between genotype and phenotype.

3. PATHOPHYSIOLOGY

In almost all normal cells, except for hepatocytes, ATP7A is localized in the trans-Golgi membrane. ATP7A acts to transport copper from the cytosol into the Golgi apparatus and then serves to excrete copper. In the cells of individuals with MNK, copper accumulates in the cytosol and cannot be excreted from the cells. Copper accumulation in the intestine results in a failure of copper absorption, leading to copper deficiency, especially in the serum, liver, and brain. The characteristic features of MNK can be explained by decreases in activity of copper-dependent enzymes (Fig. 2 and Table 3). These decreases in enzyme activity are caused by defective copper absorption and/or disturbances in intracellular copper transport. In patients with MNK and in the animals serving as a model of this disease, the levels of activity of several copper-dependent enzymes, including dopamine β-hydroxy-

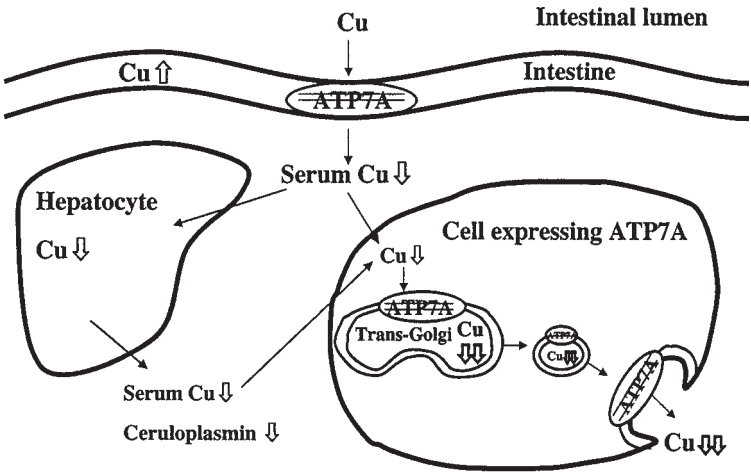

Fig. 2. Disruption of copper homeostasis in Menkes disease, with decreases and increases in copper levels shown.

Table 3
Reduced Activities of Copper-Dependent Enzymes and Clinical Findings of Menkes Disease

Reduced copper-dependent enzyme activities	*Findings in Menkes disease*
Cytochrome-*c* oxidase	Mitochondrial abnormalities, neurological damage, hypothermia, muscle weakness
Dopamine β-hydroxylase	Abnormalities in catecholamines in the serum and cerebrospinal fluid, hypotension
Peptidylglycine α-amidating monooxygenase	Unknown
Lysyl oxidase	Decreased strength of collagen and elastin (arterial abnormalities, bladder diverticula, loose skin and joints)
Tyrosinase	Reduced pigmentation of hair and skin
Sulfhydryl oxidase	Pili torti
Ceruloplasmin	Decreased levels of circulating copper
Copper-zinc superoxide dismutase	Failure of free radical detoxification

lase, cytochrome-*c* oxidase, and Cu/Zn superoxide dismutase, are improved by parenteral administration of copper, indicating that the decreased levels of activity of these enzymes are the result of only the defective copper absorption *(30–32)*. However, the level of activity of lysyl oxidase seems not to be improved by copper administration. The level of lysyl oxidase activity is significantly reduced in cultured fibroblasts from patients with MNK, even in the presence of a high copper concentration *(33,34)*. These findings suggest that the incorporation of copper into lysyl oxidase is disturbed in the affected cells.

On the other hand, significant accumulation of copper occurs in cells of the proximal tubules of the kidney, in which copper metabolism seems to occur in a manner similar to that in intestinal cells *(35,36)*.

4. CLINICAL FEATURES

The characteristic clinical features of MNK, mild MNK, and OHS are shown in Table 4. In the neonatal period, some patients with classical MNK display hypothermia, hyperbilirubinemia, and

Table 4
Clinical Findings for Patients with Classical Menkes Disease, Mild Menkes Disease, and OHS

	Classical[a]	*Mild*[a]	*OHS*[a]
Premature delivery	+	–	–
Neurological problems			
Intractable convulsions	++	+/–	+/–
Developmental delay	++	+	+/–
Dysarthria	Not applicable	++	+/–
Ataxia	Not applicable	++	+/–
Hair abnormalities	++	+	+/–
Arterial abnormalities	++	+	+
Bone changes	++	+	+
Hypothermia	+	–	–
Hypotonic muscles	++	+	+
Cutis laxa	+	+	++
Hypopigmented skin	+	+	–
Bladder diverticula	+	+	+
Recurrent urinary infections	+	+	+
Diarrhea	+	+	+
Gastrointestinal hemorrhage, polyps *(58)*	+	?	?
Retinal degeneration, iris cysts	+	?	?

+, ++ = finding present with increasing severity; +/– = finding sometimes present; – = finding usually not present.

mild hair abnormalities. However, patients are seldom diagnosed as MNK in the neonatal period because these abnormalities also sometimes appear in unaffected premature babies. Physicians usually begin to suspect that a child may have MNK after the age of 3 mo, when the characteristic MNK features, including seizures, delayed development, marked muscular hypotonia, and abnormal hair, become prominent. However, the initiation of treatment at this time is too late to prevent neurological disturbances (*see* Section 7.). Therefore, early diagnosis of MNK before the appearance of a severe delay in development is extremely important. The most striking finding concerning patients with MNK is the depigmented and friable hair (Fig. 3). A retrospective study examining the cases of 10 patients with MNK revealed that the hair abnormalities began to progress before the appearance of seizures and developmental delay in all cases *(37)*. This seems to be an important clinical clue for early diagnosis. Unfortunately, most pediatricians do not notice these symptoms because this disease is very rare and they seldom have the opportunity to observe a patient with MNK. Thus, pediatricians and neonatologists must be taught to recognize these characteristics to ensure the early diagnosis of patients with MNK.

In patients with MNK, bladder diverticula form and become huge and sometimes rupture *(38)*. Radiographs of the skeleton show a variety of abnormalities, including osteoporosis, metaphyseal spurring, a disphyseal periosteal reaction, and wormian bones in the skull. Fractures often occur in the extremities and vertebrae. Neuroimaging reveals cerebral atrophy, impaired myelination, tortuous and enlarged intracranial vessels, and subdural hemorrhage. Recurrent respiratory and urinary tract infections often occur. Convulsions are usually intractable and the clinical course worsens inexorably. Patients with MNK are bedridden and cannot sit alone, smile, or speak. Most patients die from infection or neurological disturbances by the age of 3 yr, although some survive until the age of 14 *(39)*. The patient in case O.H. in Table 1 is a profoundly handicapped patient who had not received parenteral administration of copper, but survived until the age of 24. One case of macrocephaly and

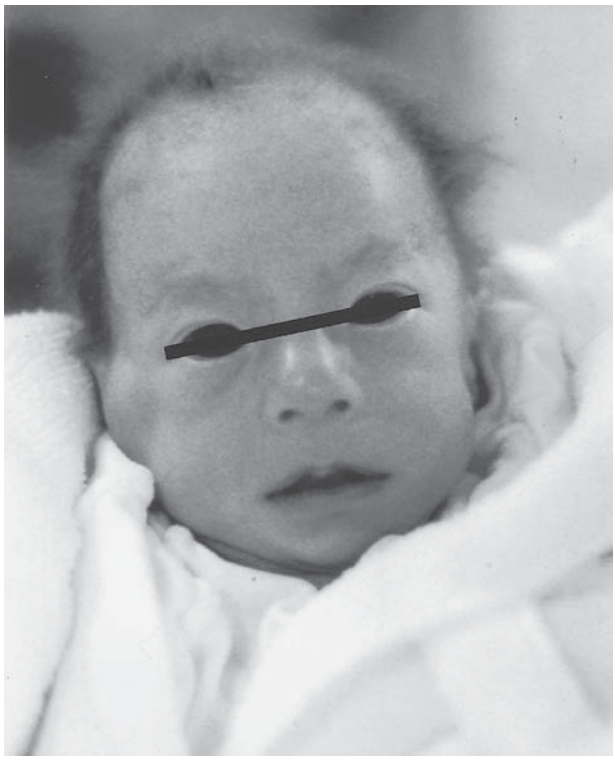

Fig. 3. A 3-mo-old patient with classical Menkes disease. His hair is depigmented, lusterless, and kinky.

one of congenital skull fractures have been reported *(28,40)*. A few females affected with MNK who have cytogenetically abnormal karyotypes have also been reported *(41,42)*.

Occipital horn syndrome is the mildest type of MNK. The most noticeable difference in clinical features from patients with MNK is that patients with OHS have little or no neurological disturbance and live until adulthood. However, some patients with OHS have recurrent seizures *(43)*. The predominant clinical features of OHS are mild muscle hypotonia and connective tissue abnormalities, including exostosis in the occipital bones, bladder diverticula, and laxity of the skin and joints (Figs. 4 and 5).

Mild MNK is extremely rare and its clinical features are intermediate between those of MNK and OHS. Since the clinical spectrum of MNK and OHS is very wide, patients with neurological retardation, ataxia and connective tissue abnormalities should be evaluated for biochemical evidence of defective copper transport.

5. LABORATORY FINDINGS

Table 5 shows the characteristic laboratory findings in cases of MNK. The biochemical data most useful for diagnosis are low serum copper and ceruloplasmin levels. However, it should be noted that serum copper and ceruloplasmin levels are also very low in unaffected babies, especially in premature babies, and gradually increase to adult levels (Table 6) *(44)*. In babies in whose cases MNK is suspected, therefore, serum copper and ceruloplasmin levels should be examined serially to determine whether the normally expected increase in copper and ceruloplasmin levels fails to appear. Serum copper and ceruloplasmin levels cannot be improved by oral administration of copper, but rise significantly after copper injection. Copper concentrations are significantly high in cultured fibroblasts derived from these patients, and this is useful for diagnosis.

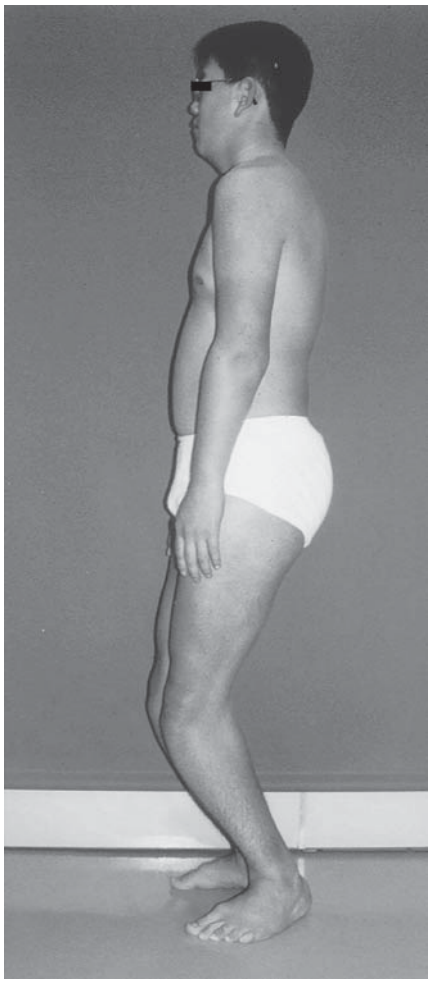

Fig. 4. A 14-yr-old patient with occipital horn syndrome. Mild muscle hypotonia is observed.

Abnormal catechol levels in the serum and cerebrospinal fluid are caused by a decrease in dopamine β-hydroxylase activity *(10,45)*. The level of activity of lysyl oxidase, a key enzyme in the synthesis of the crosslinks in collagen, is also reduced, leading to connective tissue abnormalities. No biochemical markers for evaluating the connective tissue abnormalities have been reported. However, we examined the level of deoxypyridinoline, a degradation product of collagen, in the urine of 10 patients with MNK, and it was found to be significantly lower than the normal level (unpublished data). Based on these findings, it seems possible that the urine deoxypyridinoline level may be a useful marker for evaluating the connective tissue abnormalities in patients with MNK.

Copper accumulates significantly in the cells of the proximal tubules of the kidney. In three patients with MNK given copper injections, the urinary β_2-microglobulin level was found to be significantly high, but amino aciduria, proteinuria, glucosuria, or hematuria was not observed (unpublished data). These results suggest that the accumulation of copper produces only a slight disturbance in renal function.

In patients with OHS, serum copper and ceruloplasmin levels are usually low. In some patients with OHS, however, normal levels of serum copper and ceruloplasmin have been reported *(23,46,47)*. These findings indicate that a diagnosis of OHS cannot be excluded on the basis of normal serum

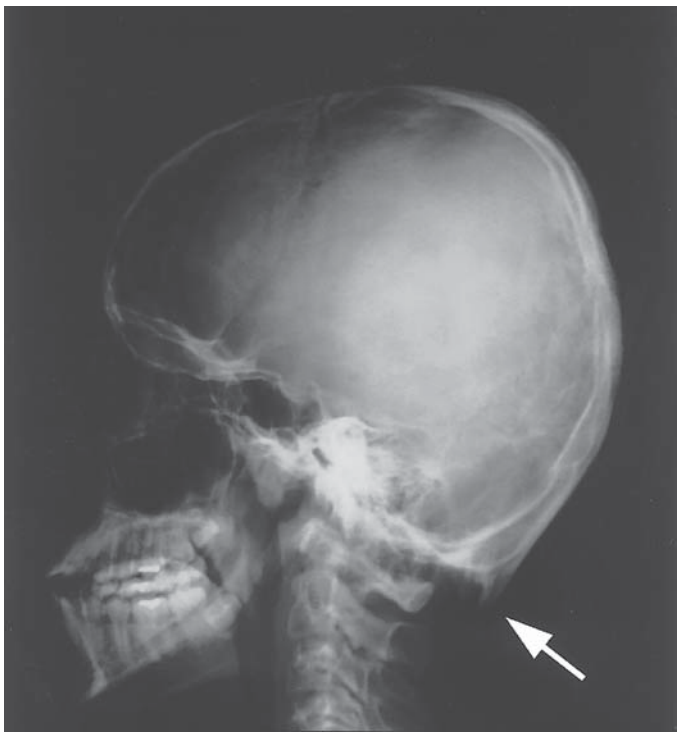

Fig. 5. Occipital horns (arrow) in a 14-yr-old patient with occipital horn syndrome.

Table 5
Laboratory Findings for Patients with Menkes Disease and OHS

	Menkes disease			*Normal*	
	Classical type	*Mild type*	*OHS*	*Age 1 mo*	*Children and adults*
Serum copper concentration (μg/dL)	>30	14–77	23–80	70±8	98±20
Serum ceruloplasmin (mg/dL)	>15	4–20	9–29	15–32	24–45
Serum DOPA:DHPG	6.2–34.2	18.9–120	5.4		1.7~3.3
Cerebrospinal fluid DOPA:DHPG	1.2–4.6	1.4	1.1		0.3~0.7
Serum copper and ceruloplasmin after oral administration of copper	No increase		No increase	Increase	
Copper content of cultured fibroblasts (ng/mg protein)[a]	90–201 (*n*=30)		155–362 (*n*=3)	24–33 (*n*=30)	

Note: DOPA: β-dihydroxyphenylalanine; DHPG: dihydroxyphenylglycol.
[a] Data obtained from the Department of Pediatrics, Teikyo University School of Medicine.

levels of copper and ceruloplasmin. On the contrary, the copper concentration is significantly high in cultured fibroblasts from patients with OHS (Table 5). The copper levels in cultured fibroblasts from patients with OHS are indistinguishable from those in fibroblasts from patients with MNK. These findings indicate that the copper concentration in fibroblasts does not reflect the severity of the phenotype or the amount of residual ATP7A activity. However, the copper concentration in cultured fibroblasts is a useful indicator for establishing a diagnosis of OHS as well as MNK.

Table 6
Serum Copper Level in Low-Birth-Weight Infants (μg/dL)

	Birth weight (g)		
Age	*<1500*	*1501–2000*	*2001–2500*
0	36±38	34±13	29±11
1 wk	38±19	40±21	64±31
1 mo	56±25	46±16	71±24
2 mo	58±27	77±25	92±42
3 mo	70±32	83±15	105±26

6. DIAGNOSIS

Diagnosing patients with MNK who are older than 3 mo is not difficult; their diagnosis is based on their symptoms, low serum levels of copper and ceruloplasmin, and characteristic radiological changes. The diagnosis can be confirmed by further biochemical findings, such as lack of improvement in serum copper and ceruloplasmin levels after oral administration of copper and high levels of copper in cultured fibroblasts. However, early diagnosis is very difficult. During the neonatal period, the clinical features of patients with MNK and their serum copper and ceruloplasmin levels cannot be distinguished from those of unaffected infants. The retention of ^{64}Cu in uptake studies with cultured fibroblasts and an elevated ratio of dihydroxyphenylalanine (DOPA) to dihydroxyphenylglycol (DHPG) in the serum have been reported to be useful indicators for early diagnosis *(48)*. However, these assays cannot be easily and quickly performed in the case of most infants suspected of having MNK. A much simpler test for early diagnosis is to ascertain whether serum copper and ceruloplasmin levels fail to increase after oral administration of copper.

A DNA-based diagnostic test is now available. However, a large number of different mutations in the *ATP7A* gene have been documented. Moreover, a few patients with MNK or OHS have been found to have no mutations in exons of the *ATP7A* gene (unpublished data). Therefore, even if a mutation is not found, MNK or OHS can not be excluded as a potential diagnosis.

Heterozygote females can be diagnosed based on pili torti in their hair and/or an elevated copper concentration in cultured fibroblasts. DNA-based diagnosis is very useful for carrier detection when the mutant ATP7A has been identified in the index patient.

DNA-based diagnosis is also very useful for prenatal diagnosis when the mutation in the family has been identified. If the mutation cannot be identified, prenatal diagnosis is still possible by analyzing the copper concentration or by measuring ^{64}Cu uptake in cultured chorionic villi or amniotic cells *(49,50)*.

7. TREATMENT

The currently accepted treatment for patients with MNK is parenteral administration of copper. Among the different forms of copper used in such cases (i.e., copper–histidine, copper–acetate, and copper–ethylenediaminetetraacetic acid (EDTA), copper–histidine has been reported to be taken up by the brain most effectively *(51)*. Treatment by parenteral administration of copper-histidine immediately improves the serum copper and ceruloplasmin levels as well as the hair abnormalities in patients with MNK. Christodoulou et al. have reported that neurological degeneration can also be prevented when treatment is initiated before the age of 2 mo *(52)*. In some patients with MNK, however, early treatment does not normalize the neurological outcome *(53)*. Such different responses to early treatment may arise from differences in the residual levels of ATP7A activity or differences in the processing of copper–histidine *(51)*. When treatment is initiated in patients older than 2 mo, the neurological disturbances cannot be improved. These findings indicate that the newborn period is critical for normal neurodevelopment and that a certain level of copper is essential. This period is

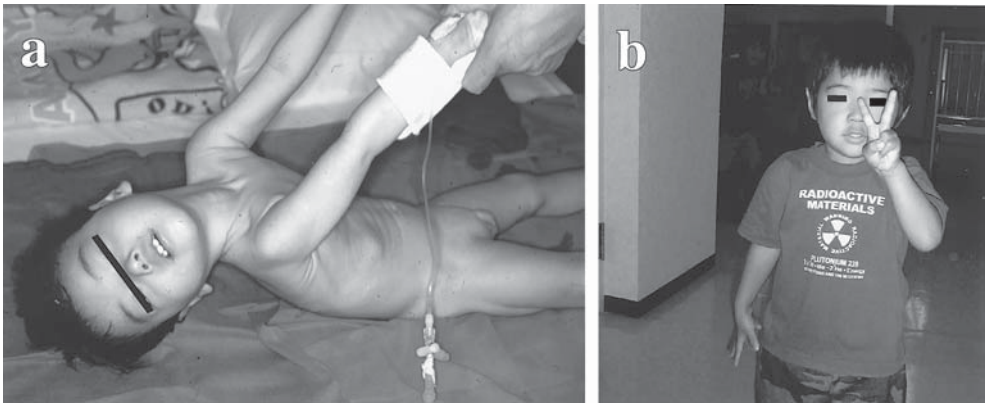

Fig. 6. Two siblings with classical Menkes disease. **(a)** Photograph of the 2-yr-old elder brother who has been treated since the age of 8 mo. His hair has become normal, but his neurological disturbances could not be improved. **(b)** Photograph of the 2-yr-old younger brother who has been treated with copper-histidine injections since the age of 22 d.

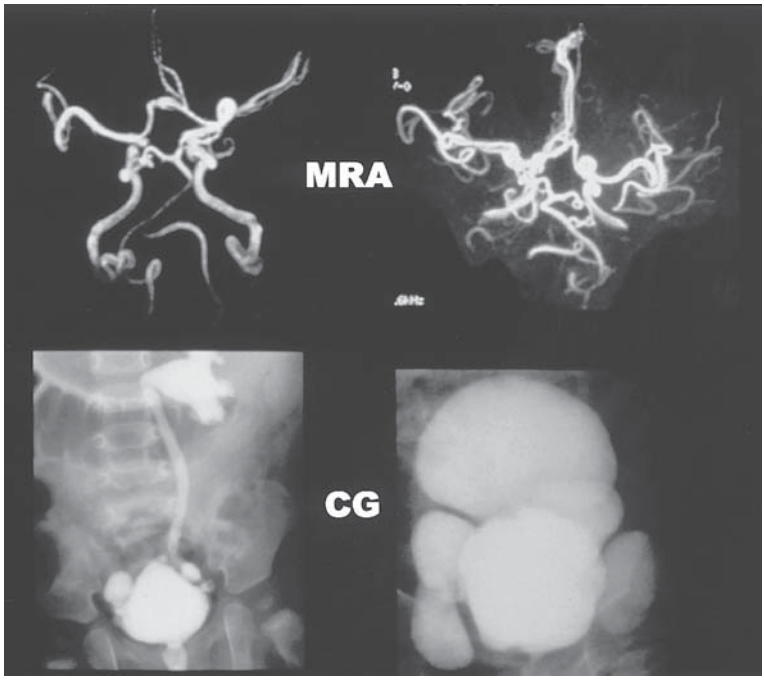

Fig. 7. X-ray films of the elder brother. Left and right films were taken at the age of 8 mo when the treatment was started, and at the age of 2 yr, respectively. The elongation and tortuousness of the brain vessels are shown (upper, magnetic resonance angiograms); the development of bladder diverticula (lower, cystograms) are progressive.

also associated with prematurity of the blood-brain barrier. In the mouse model of MNK, copper accumulates in the blood-brain barrier *(54,55)*. Thus, parenterally administered copper is probably trapped in the blood-brain barrier of patients and is not transported to the neurons after the barrier matures. Therefore, early treatment is very important to prevent the neurological disturbances in patients with MNK.

Two siblings with MNK who were treated with subcutaneous injections of copper–histidine and who exhibited typical clinical courses of MNK are described here. The elder patient was diagnosed as having MNK at the age of 8 mo based on the characteristic clinical features and biochemical findings of MNK. Treatment with copper–histidine was initiated at the age of 8 mo. The serum copper and ceruloplasmin levels have been maintained within the normal range since the initiation of treatment. The hair abnormalities have also improved (Fig. 6a). However, the neurological disturbances have not improved at all. Moreover, the connective tissue abnormalities have progressed in spite of ongoing treatment (Fig. 7). At the time of the elder brother's diagnosis, the younger brother was in his 28th gestational week and was prenatally diagnosed as having MNK on the basis of high copper levels in the amniocytes (30.7 ng/mg protein; normal: 12.3 ± 4.4). A planned cesarean section was performed in the 36th gestational week, and subcutaneous copper–histidine therapy was initiated at the age of 22 d. His neurological development has been completely normal (Fig. 6b). At his present age of 3 yr, he can run and he speaks a lot. However, radiological examination has revealed a small diverticulum of the bladder and spurs on the metaphyses of the long bones. The elder brother seems to have followed the typical clinical course of MNK when treatment is started late, whereas the younger patient seems to have followed the course of patients with MNK who receive early treatment.

As shown by these two patients, a serious problem that remains unsolved is that parenteral administration of copper cannot completely improve the connective tissue disorder, even when treatment is started at an early age. Patients who receive early treatment and develop well neurologically often display the clinical characteristics of patients with OHS. Because copper transport from the cytosol to the Golgi apparatus is disturbed in the affected cells, the parenterally administered copper may not reach the organelles (probably the trans-Golgi network), where copper is incorporated into lysyl oxidase. More effective means of treatment must be found to prevent the connective tissue abnormalities. A more effective means of treatment would also be beneficial for patients with OHS, for whom there is presently no available treatment.

ACKNOWLEDGMENTS

This work was supported by grants from the Ministry of Education, Science and Culture in Japan (06670829, 07770607, and 07770608). The author thanks Ms. Y. Murata, Y.H. Gu, K. Okamoto, E. Sato, and Y. Nakamura for their technical assistance and Dr. N. Haga for providing Figs. 4 and 5.

REFERENCES

1. Menkes, J. H., Alter, M., Steigleder, G. K., Weakley, D. R., and Sung, J. H. (1962) A sex-linked recessive disorder with retardation of growth, peculiar hair, and focal cerebral and cerebellar degeneration. *Pediatrics* **29**, 764–769.
2. Danks, D. M., Campbell, P. E., Stevens, B. J., Mayne, V., and Cartwright, E. (1972) Menkes' kinky hair syndrome: an inherited defect in copper absorption with widespread effects. *Pediatrics* **50**, 188–201.
3. Danks, D. M., Cartwright, E., Stevens,B. J., and Townley, R. R. W. (1973) Menkes' kinky hair disease. Further definition of the defect in copper transport. *Science*. **179**, 1140–1142.
4. Hunt, D. M. (1974) Primary defect in coppert transport underlies mottled mutants in the mouse. *Nature* **249**, 852–853.
5. Nishimura, M. (1975) A new mutant mouse, macular(ML). *Exp. Anim.* **24**, 185 (in Japanese).
6. Lazoff, S. G., Ryback, J. J., Parker, B. R., and Luzzatti, L. (1975) Skeletal dysplasia, occipital horns, diarrhea and obstructive uropathy: a new hereditary syndrome. *Birth Defects* **11**, 71–74.
7. Vulpe, C., Levinson, B., Whitney, S., Packman, S., and Gitschier, J. (1993) Isolation of a candidate gene for Menkes disease and evidence that it encodes a copper-transporting ATPase. *Nature Genet.* **3**, 7–13.
8. Chelly, J., Tümer, Z., Tønnesen, T., Petterson, A., Ishikawa-Brush, Y., Tommerup, N., et al. (1993) Isolation of a candidate gene for Menkes disease that encodes a potential heavy metal binding protein. *Nature Genet.* **3**, 14–19.
9. Mercer, J. F., Livingston, J., Hall, B., Paynter, J. A., Begy, C., Chandrasekharappa, S., et al. (1993) Isolation of a partial candidate gene for Menkes disease by positional cloning. *Nature Genet.* **3**, 20–25.
10. Kaler, S. G., Gallo, L. K., Proud, V. K., Percy, A. K., Mark, Y., Segal, N. A., et al. (1994) Occipital horn syndrome and a mild Menkes phenotype associated with splice site mutations at the MNK locus. *Nature Genet.* **8**, 195–202.
11. Das, S., Levinson, B., Vulpe, C., Whitney, S., Gitschier, J., and Packman, S. (1995) Similar splicing mutations of the Menkes/mottled copper-transporting ATPase gene in occipital horn syndrome and the blotchy mouse. *Am. J. Hum. Genet.* **56**, 570–576.

12. Levinson, B., Vulpe, C., Elder, B., Martin, C., Verley, F., Packman, S., et al. (1994) The mottled gene is the mouse homologue of the Menkes disease gene. *Nature Genet.* **6**, 369–373.
13. Cecchi, C., Biasotto, M., Tosi, M., and Avner P. (1997) The mottled mouse as a model for human Menkes disease: identification of mutations in the Atp7a gene. *Hum. Mol. Genet.* **6**, 425–433.
14. Grimes, A., Hearn, C. J., Lockhart, P., Newgreen, D. F., and Mercer J. F. B. (1997) Molecular basis of the brindled mouse mutant (Mobr): a murine model of Menkes disease. *Hum. Mol. Genet.* **6**, 1037–1042.
15. Reed, V. and Boyd, Y. (1997) Mutation analysis provides additional evidence that mottled is the mouse homologue of Menkes' disease. *Hum. Mol. Genet.* **6**, 417–423.
16. Murata, Y., Kodama, H., Abe, T., Ishida, N., Nishimura, M., Levinson, B., et al. (1997) Mutation analysis and expression of the mottled gene in the macular mouse model of Menkes disease. *Pediatr. Res.* **42**, 436–442.
17. Petris, M. J., Mercer, J. F. B., Culvenor, J. G., Lockhart, P., Gleeson, P. A., and Camakaris, J. (1996) Ligand-regulated transport of the Menkes copper P- type ATPase efflux pump from the Golgi apparatus to the plasma membrane: a novel mechanism of regulated trafficking. *EMBO* **15**, 6084–6095.
18. Goodyer, I. D., Jones, E. E., Monaco, A. P., and Francis, M. J. (1999) Characterization of the Menkes protein copper-binding domains and their role in copper-induced protein relocalization. *Hum. Mol. Genet.* **8**, 1473–1478.
19. Tümer, Z., Møller, L. B., and Horn, N. (1999) Mutation spectrum of ATP7A, the gene defective in Menkes disease. *Adv. Exp. Med. Biol.* **448**, 83–95.
20. Ambrosini, L. and Mercer, J. F. (1999) Defective copper-induced trafficking and of the Menkes protein in patients with mild and copper-treated classical Menkes disease localization. *Hum. Mol. Genet.* **8**, 1547–1555.
21. Levinson, B., Conant, R., Schnur, R., Das, S., Packman, S., and Gitschier J. (1996) A repeated element in the regulatory region of the MNK gene and its deletion in a patient with occipital horn syndrome. *Hum. Mol. Genet.* **5**, 1737–1742.
22. Møller, L.B., Tümer, Z., Lund, C., Petersen, C., Cole, T., Hanusch, R., et al. (2000) Similar splice-site mutations of the ATP7A gene lead to different phenotypes: classical menkes disease or occipital horn syndrome. *Am. J. Hum. Genet.* **66**, 1211–1220.
23. Gu, Y. H., Kodama, H., Murata, Y., Mochizuki, D., Yanagawa, Y., Ushijima, H., et al. (2001) ATP7A gene mutation in 16 patients with Menkes disease and a patient with occipital horn syndrome. *Am. J. Med. Genet.* 217–222.
24. Ronce, N., Moizard, M. P., Robb, L., Toutain, A., Villard, L., and Moraine C. (1997) A C2055T transition in exon 8 of the ATP7A gene is associated with exon skipping in an occipital horn syndrome family. *Am. J. Hum. Genet.* **61**, 233–238.
25. Qi, M. and Byers, P. H. (1998) Constitutive skipping of alternatively spliced exon 10 in the ATP7A gene abolishes Golgi localization of the menkes protein and produces the occipital horn syndrome. *Hum. Mol. Genet.* **7**, 465–469.
26. Geller, T. J., Pan, Y., and Martin, D. S. (1997) Early neuroradiologic evidence of degeneration in Menkes' disease. *Pediatr. Neurol.* **17**, 255–258.
27. Jankov, R. P., Boerkoel, C. F., Hellmann, J., Sirkin, W. L., Tumer, Z., Horn, N., et al. (1998) Lethal neonatal Menkes' disease with severe vasculopathy and fractures. *Acta Paediatr.* **87**, 1297–1300.
28. Ubhi, T., Reece, A., and Craig, A. (2000) Congenital skull fracture as a presentation of Menkes disease. *Dev. Med. Child. Neurol.* **42**, 347–348.
29. Das, S., Levinson, B., Whitney, S., Vulpe, C., Packman, S., and Gitschier J. (1994) Diverse mutations in patients with Menkes disease often lead to exon skipping. *Am. J. Hum. Genet.* **55**, 883–889.
30. Wenk, G. and Suzuki, K. (1983) Congenital copper deficiency: copper therapy and dopamine-beta-hydroxylase activity in the mottled (brindled) mouse. *J. Neurochem.* **41**, 1648–1652.
31. Meguro, Y., Kodama, H., Abe, T., Kobayashi, S., Kodama, Y., and Nishimura M. (1991) Changes of copper level and cytochrome c oxidase activity in the macular mouse with age. *Brain Dev.* **13**, 184–186.
32. Yoshimura, N., Hatayama, I., Sato, K., and Nishimura, M. (1993) Complete recovery of cytochrome oxidase and superoxide dismutase activities in the brain of brindled mice receiving copper therapy. *J. Intellect. Disabil. Res.* **37**, 561–569.
33. Peltonen, L., Kuivaniemi, H., Palotie, A., Horn, N., Kaitila, I., and Kivirikko, K. I. (1983) Alterations in copper and collagen metabolism in the Menkes syndrome and a new subtype of the Ehlers-Danlos syndrome. *Biochemistry* **22**, 6156–6163.
34. Kemppainen,R., Hamalainen, E. R., Kuivaniemi, H., Tromp, G., Pihlajaniemi, T., and Kivirikko, K. I. (1996) Expression of mRNAs for lysyl oxidase and type III procollagen in cultured fibroblasts from patients with the Menkes and occipital horn syndromes as determined by quantitative polymerase chain reaction. *Arch. Biochem. Biophys.* **328**, 101–106.
35. Nooijen, J. L., De Groot. C. J., Van den Hamer, C. J., Monnens, L. A., Willemse, J., and Niermeijer, M.F. (1981) Trace element studies in three patients and a fetus with Menkes' disease. Effect of copper therapy. *Pediatr. Res.* **15**, 284–289.
36. Kodama, H., Abe, T., Takama, M., Takahashi, I., Kodama, M., and Nishimura, M. (1993) Histochemical localization of copper in the intestine and kidney of macular mice: light and electron microscopic study. *J. Histochem. Cytochem.* **41**, 1529–1535.
37. Ozawa, H., Nakamoto, N., and Kodama, H. (2002) Clinical manifestations for early diagnosis of the patient with classical Menkes disease. *No to Hatztatsu* (in Japanese, Abstract English).
38. Oshio, T., Hino, M., Kirino, A., Matsumura, C., and Fukuda, K.(1997) Urologic abnormalities in Menkes' kinky hair disease: report of three cases. *J. Pediatr. Surg.* **32**, 782–784.
39. Gerdes, A. M., Tønnesen, T., Pergament, E., Sander, C., Baerlocher, K. E., Wartha, R., et al. (1988) Variability in clinical expression of Menkes syndrome. *Eur. J. Pediatr.* **148**, 132–135.

40. Jayawant, S., Halpin, S., and Wallace, S. (2000) Menkes kinky hair disease: an unusual case. *Eur. J. Pediatr.* **4**, 131–134.
41. Sugio, Y., Sugio, Y., Kuwano, A., Miyoshi, O., Yamada, K., Niikawa, N., et al. (1998) Translocation t(X;21)(q13.3; p11.1) in a girl with Menkes disease. *Am. J. Med. Genet.* **79**, 191–194.
42. Abusaad, I., Mohammed, S. N., Ogilvie, C. M., Ritchie, J., Pohl, K. R., and Docherty, Z. (1999) Clinical expression of Menkes disease in a girl with X;13 translocation. *Am. J. Med. Genet.* **87**, 354–359.
43. Jacome, D. E. (1999) Epilepsy in Ehlers–Danlos syndrome. *Epilepsia* **40**, 467–473.
44. Higashi, A., Matsuda, I., Masumoto, T., Saikusa, H., Yabuso, M., and Oka, Y. (1985) Serum zinc and copper concentrations in low birth weight infants during first three months of life: correlation to birth weight and different feedings. *Tohoku J. Exp. Med.* **146**, 253–263.
45. Kaler, S. G., Goldstein, D. S., Holmes, C., Salerno, J. A., and Gahl, W. A. (1993) Plasma and cerebrospinal fluid neurochemical pattern in Menkes disease. *Ann. Neurol.* **33**, 171–175.
46. Tsukahara, M., Imaizumi, K., Kawai, S. and Kajii, T. (1994) Occipital horn syndrome: report of a patient and review of the literature. *Clin. Genet.* **45**, 32–35.
47. Herman, T. E., McAlister, W. H., Boniface, A., and Whyte, M. P. (1992) Occipital horn syndrome. Additional radiographic findings in two new cases. *Pediatr. Radiol.* **22**, 363–365.
48. Kaler, S. G. (1994) Menkes disease. *Adv. Pediatr.* **41**, 263–304.
49. Tønnesen, T., Gerdes, A. M., Damsgaard, E., Miny, P., Holzgreve, W., Sondergaard, F. et al. (1989) First-trimester diagnosis of Menkes disease: intermediate copper values in chorionic villi from three affected male fetuses. *Prenat. Diagn.* **9**, 159–165.
50. Heydorn, K., Damsgaard, E., and Horn, N. (1999) Accumulated experience with prenatal diagnosis of Menkes disease by neutron activation analysis of chorionic villi specimens. *Biol. Trace Element Res.* **71–72**, 551–561.
51. Sarkar, B. (1999) Treatment of Wilson and Menkes disease. *Chem. Rev.* **99**, 2535–2544.
52. Christodoulou, J., Danks, D. M., Sarkar, B., Baerlocher, K. E., Casey, R., Horn, N., et al. (1998) Early treatment of Menkes disease with parenteral copper–histidine: long-term follow-up of four treated patients. *Am. J. Med. Genet.* **76**, 154–164.
53. Kaler, S. G., Buist, N. R., Holmes, C. S., Goldstein, D. S., Miller, R. C., and Gahl, W. A. (1995) Early copper therapy in classic Menkes disease patients with a novel splicing mutation. *Ann. Neurol.* **38**, 921–928.
54. Kodama, H., Meguro, Y., Abe, T., Rayner, M. H., Suzuki, K. T., Kobayashi, S., et al. (1991) Genetic expression of Menkes disease in cultured astrocytes of the macular mouse. *J. Inherit. Metab. Dis.* **14**, 896–901.
55. Kodama, H. (1993) Recent developments in Menkes disease. *J. Inherit. Metab. Dis.* **16**, 791–799.
56. Murata, Y., Kodama, H., Mori, Y., Kobayashi, M., and Abe, T. (1998) Mottled gene expression and copper distribution in the macular mouse, an animal model for Menkes disease. *J. Inherit. Metab. Dis.* **21**, 199–202.
57. Cunningham, S., Crofton, P. M., Marshall, T. G., and Fitzpatrick, D. R. (1999) A case of Menkes syndrome with pyloric stenosis: an effect of copper deficiency on NOS1? *J. Inherit. Metab. Dis.* **22**, 1978.
58. Kaler, S. G., Westman, J. A., Bernes, S. M., Elsayed, A. M., Bowe, C. M., Freeman, K. L., Wu, C. D., and Wallach, M. T. (1993) Gastrointestinal hemorrhage associated with gastric polyps in Menkes disease. *J. Pediatr.* **122,** 93–95.

19

The Meaning of Alternative Transcripts of the Menkes Disease Gene

Edward D. Harris, Manchi C. M. Reddy, and Sudeep Majumdar

1. INTRODUCTION

The Menkes disease gene (*MNK*) codes for a membrane-bound Cu-transporting ATPase that maintains cellular Cu homeostasis and prevents Cu toxicity. Properties of the gene product, ATP7A, are described elsewhere in this book. In this chapter, we focus is on a lesser known, and perhaps lesser appreciated, function of *MNK*: the competency of it or a related gene locus to synthesize smaller transcripts that may code for proteins or peptides functional in cytosolic and nuclear Cu transport. A growing body of evidence supports the existence of abridged or modified transcripts with Menkes-like sequences. Whether modified transcripts are spliced variants of the primary ATP7A mRNA or are unique mRNAs synthesized through a second genetic locus has not been resolved. Data that support a second genetic locus for the Menkes disease gene or perhaps a second transcription start site include the following observations:

1. Repeats of identical alternative transcripts in numerous human cells
2. Evidence for an unattached second promoter region upstream from exon 1
3. Evidence for novel insertion sequences in the 5' region between exon 1 and exon 2
4. Nonconforming splice sites
5. Nonconforming bases in alternative transcripts
6. A noncoding exon upstream from exon 1

In this chapter, we survey the information that may help understand the meaning of alternative transcripts.

2. ATP7A TRANSCRIPT AND VARIANTS

The complete coding sequence of ATP7A, the Menkes disease gene product, is expressed over a span of 23 exons contained within an 8.3 to 8.5-kb mRNA. Exon 1 is noncoding and exon 2 has the translation start site *(1,2)*. Internal exons are correlated with specific structural features of the protein. For example, the first seven encode the six Cu-binding sites featuring the motif, GMTCXSC, which constitutes about 40% of the mass of the ATP7A protein. By species comparisons, this domain has the greatest number of permissible residue substitutions *(3)*. Exons 9 and 10 each code for two transmembrane domains and the smaller of the two loops that extend into the cytosol. Exons 15–23 delineate the ion channel and the larger cytoplasmic loop with phosphorylation and ATP-binding

From: Handbook of Copper Pharmacology and Toxicology
Edited by: E. J. Massaro © Humana Press Inc., Totowa, NJ

Table 1
Known Alternative Transcripts from SY5Y Cell cDNAs and Potential Protein Products

Band	*Exons present*	*Feature*	*Estimated molecular weight (kDa)*
4.7a	1–23	Intact ATP7A	170
4.7b	1–9, 11–23[a]	Lacks exon 10	145
1.8	1–2, 16–23[a]	Lacks exons 3–15; 8 nonconforming bases	57
0.8	1–3, 22[b]	45-bp insert at 5' end	11.2

[a]In frame.
[b]Out-of-frame stop codon.

sites. Although the purified protein has yet to be isolated and its function confirmed by reconstitution experiments, transfecting cells expression vectors encoding the full-length ATP7A cDNA yields clones with varying levels of the ATP7A protein *(4)* and corrects the Cu efflux defect in fibroblasts from Menkes patients *(5)*.

Smaller transcripts thought to be derived from ATP7A mRNA were first detected as reverse transcription–polymerase chain reaction (RT-PCR)-amplified oligonucleotides *(6)* and later characterized as a finite series of structurally related mRNAs consistent in appearance within and between cells lines *(7)*. cDNAs of two such transcripts have novel inserts in the 5' flanking region or lack internal exons. These transcripts have been detected in extracts from normal fibroblasts, HepG2 cells, Caco-2 cells, BeWo cells, and SY5Y neuroblastoma cells, which disassociates them from any Menkes disease mutations. An extensive body of evidence, including RNase protection assays, genomic DNA sequencing data, nested PCR assays, has determined them not to be spliced products of the larger ATP7A structure nor derived from the Wilson disease gene. This laboratory has cloned and sequenced alternative transcripts to learn their structure and biological meaning. The data in Table 1 summarize some of the unique features. A full discussion is given in the following subsections.

2.1. ATP7A2–16

One of the first alternative transcripts characterized in the laboratory featured an in-frame link between exon 2 and 16 (band 1.8 in Table 1), excluding exons 3–15, four of the six Cu-binding sites, six of the eight transmembrane domains, and the CPC channel. The putative protein product, a 57-kDa protein, has one Cu-binding site (coded by exon 2), the phosphorylation site, the ATP-binding site, and two transmembrane domains *(6)*. Based on Western blot analysis, a protein with the calculated molecular mass of ATP7A2–16 was visible in extracts from undifferentiated BeWo cells, but was not seen when the cells were induced to differentiate *(6)*. A movement toward differentiation restored Cu efflux function to the undifferentiated BeWo cells, reversing Cu accumulation *(8)*. The detection of the 57-kDa protein in undifferentiated cells correlated with the expression of ATP7A2–16 mRNA. Perhaps, of interest was the observation that ATP7A2–16 mRNA is expressed in liver hepatoma ($HepG_2$) cells. Based on Northern analysis, others have concluded that ATP7A mRNA is not strongly expressed in liver tissue *(9,10)*. The data suggest a tissue-specific and developmentally specific suppression of ATP7A mRNA and a concomitant augmented expression of ATP7A2-16 mRNA.

A puzzling observation was the consistent and reproducible occurrence of seven nonconforming bases in the open reading frame of ATP7A2–16 . The substitutions were cDNAs cloned from a number of human cells. This observation supports the suggestion that ATP7A mRNA may not be the parent structure of ATP7A2–16 (i.e., the truncated mRNA is not a spliced product of the larger mRNA). Currently, the origin of ATP7A2–16 is unknown, but the possibility of the mRNA arising

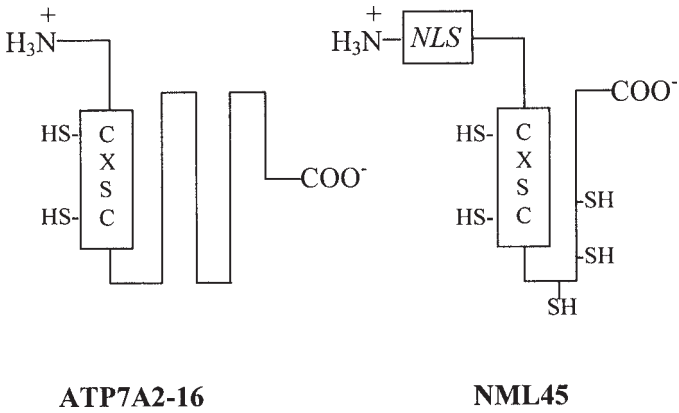

Fig. 1. Schematic diagram of ATP7A2–16 and NML45. Both alternative transcript products feature one Cu-binding site. NML45 is characterized by a nuclear localization sequence on the N-terminus and a –SH rich region near the C-terminus of the peptide.

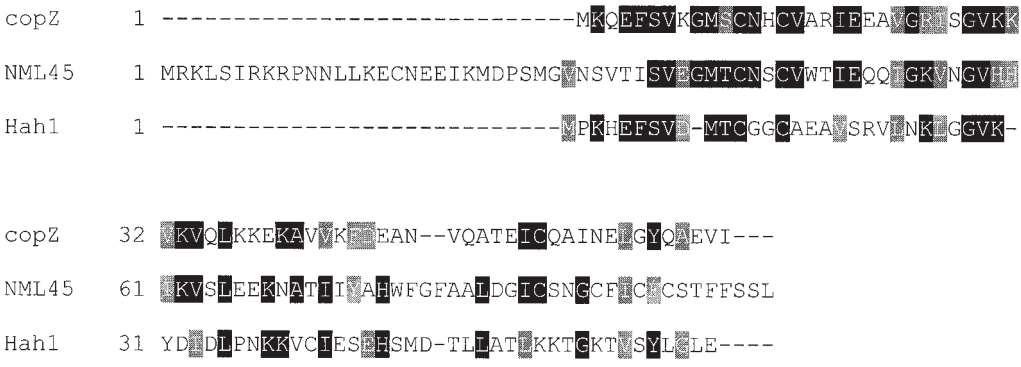

Fig. 2. Amino acid sequence alignment of NML45 with copZ and Hah1. Residues showing identity in position in black. Gray indicates conservative substitutions.

from a second gene locus or genetic polymorphism cannot be dismissed. Stronger evidence for another *MNK* gene locus is discussed next.

2.2. NML45

Recently characterized in this laboratory, NML45 is a transcript variant that has a 45-bp nucleotide insert interposed between exon 1 and 2 *(11)*. An ATG sequence in frame with the downstream ATG start site is on the extreme 5' end of the insert. Because the ATP7A translation start site is 21 bases downstream from the exon 1–2 junction, the 45 + 21 adds 66 bp to an ATP7A transcript (i.e., assuming that the upstream site is the start site). The 66 bp would then encode a 22-amino-acid extension to the N-terminus. The 22 residues in the extension, MRKLSIRKRPNNLLKECNEEIK, are projected by PSORT analysis to encode a nuclear localization sequence (NLS) (viz., RK…RKRP), a structural feature required of proteins to gain access into the nucleus *(12)*. A construct of NML45 cDNA with the green fluorescent protein has provided evidence for nuclear localization dependent on the extension residues and not internal sequences *(11)*. Further sequence analysis revealed that the NML45 transcript is not a full-length ATP7A mRNA, but rather a truncated transcript with an open

reading frame for a 103-residue 11.2-kDa protein. An out-of-frame link joins sequences in exon 3 to exon 22, which gives rise to a cysteine-rich region featuring the motif CxxxCxxCxC, a potential binding site for heavy metals (Fig. 1). In addition, exon 2 sequences in the transcript code for the GMTCXXC motif that engages Cu. Because of its novel 45-bp insert and nuclear localization, the transcript has been designated "nuclear-Menkes-like (NML) 45." The protein product of NML45 mRNA has not been isolated or characterized.

The function of NML45 is unknown. Sequence comparisons between NML45, Atox1 (formerly Hah1), a cytosolic copper metallochaperone *(13)*, and copZ, a nuclear derepressor of membrane-bound ATPases in *Enterococcus hirae (14)* is shown in Fig. 2. Excluding 22 residues in the N-terminal signal sequence, 25 of the 81 (31%) in NML45 are an identical match with residues in copZ, but only 15 of the 81 (18%) match the sequence and position with Atox1. When conserved substitutions are included in the analysis, the percentage of residues in NML45 is 36 out of 81, or about 44%. The structural similarity suggests an analogous functional overlap between NML45 and copZ.

3. REGULATION OF MNK GENE EXPRESSION

Less is known about the regulation of *MNK* gene expression than any other feature of the gene. Perhaps the strongest evidence for cell-type specificity is the failure of mature liver cells to express the transcript for ATP7A *(9,15)*. In our studies, we showed that developmentally arrested BeWo cells failed to express a *MNK* transcript, but did so when the cells were induced to differentiate either by growing them on bicameral filter surfaces or treating them with sodium butyrate *(8)*. The induction by either of these methods restored Cu efflux functions to the cells. Camakaris and colleagues selected Chinese hamster ovary (CHO) cells that differed in the degree of ATP7A expression, which made it possible to isolate and propagate clones with superior tolerance to Cu toxicity *(16)*. It is still uncertain as to whether the expression of ATP7A is influenced by hormonal or growth factors or even Cu levels in the cell. In an effort to overcome this larger unknown, investigators have turned to characterizing the promoter region of the gene.

4. MNK GENE PROMOTER

Initial attempts to clone a promoter in the 5' flanking region of the *MNK* gene by Levinson et al. led to the discovery of a 1.3-kb GC-rich region containing a 98-bp tandem tri-repeat. Also found were a series of E- boxes, an AFT-1 site, and a site for binding of a cAMP responsive protein *(17)*. Notably absent was a TATA box near the transcription start site. The initial characterization also gave evidence for metal responsive elements (MREs) that were harbored within the E-box sequences. Importantly, a patient known to have occipital horn syndrome, a mild form of Menkes disease, had segments from two of the three 98-bp tri-repeats deleted from the 5' region. Contrary to data reported by Qi and Byers *(18)*, no evidence was found for any deletion in the ORF of the gene, suggesting that OHS was associated more with the promoter region and regulation of *MNK* expression than mutations in structural domains of the ATP7A. Although Levinson et al. provided the first comprehensive investigation of an *MNK* promoter, their work did not corroborate earlier sequence data of the 5' region by Chelly et al. Indeed, Levinson et al. did not acknowledge Chelly et al. in their article and thus may not have been aware of the potential for sequence variations in the 5' flanking region of exon 1.

In their studies *(10)*, Chelly et al. prepared phage libraries constructed from genomic sequence in two 100-kb YAC clones using flanking markers *DXS56* and *PGK1*. A *Hin*dIII fragment (designated 5–3) was then used as a probe to screen clones in a kidney cDNA library. Two cDNAs (cMNK1 and cMNK3) that differed in size and in sequences at the 5' end were detected. Both hybridized to an 8.5-kb mRNA in a Northern analysis, but only cMNK3 recognized a second 5.5-kb mRNA. Chelly et al. contemplated that cMNK3 contained a chimeric cDNA insert. Importantly, cMNK3 hybridized to an autosomal chromosome presumably because of the hypothetical insert. The basis for this reaction

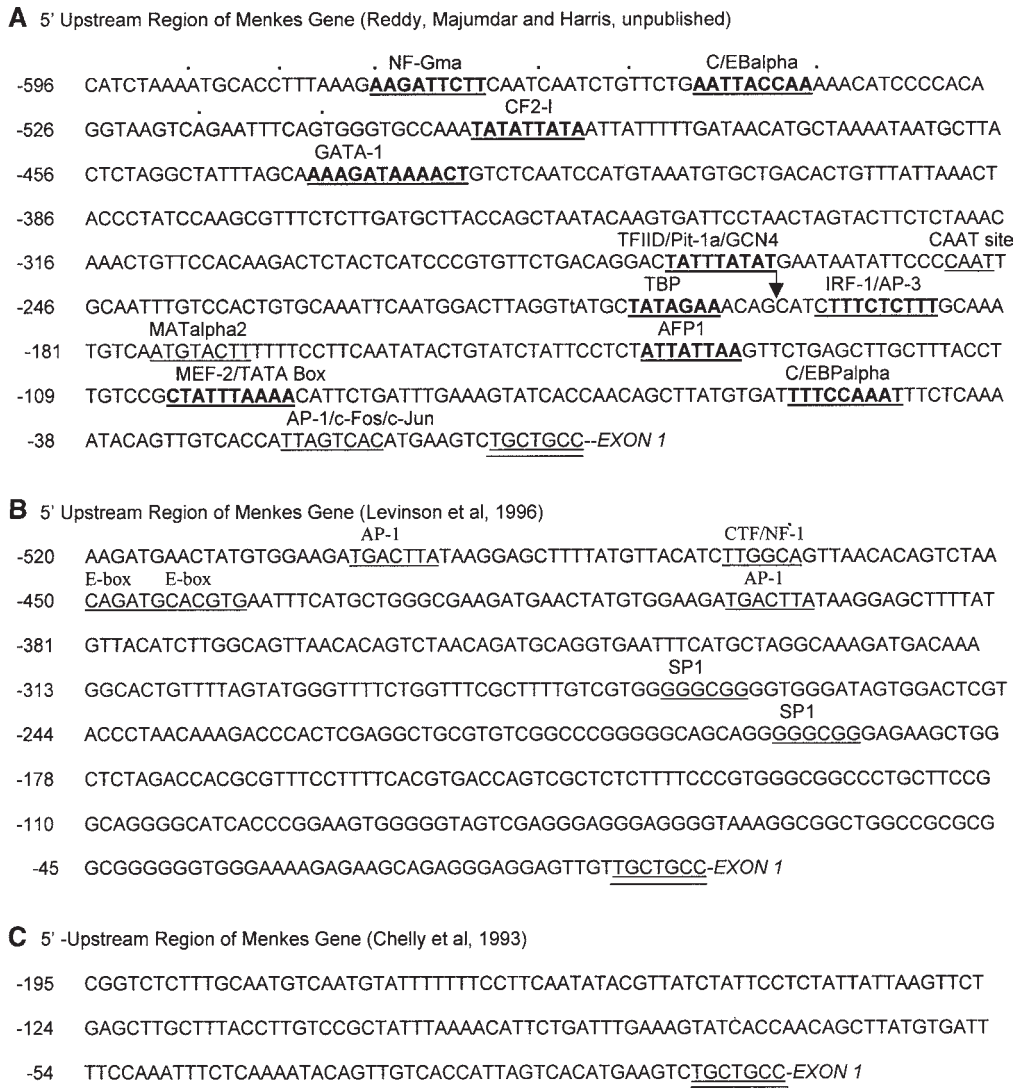

Fig. 3. Base sequences in the 5' flanking region of exon 1. **(A)** Sequences upstream by Chelly et al. Arrow indicates the end of exon 0; **(B)** sequences reported by Levinson et al; **(C)** cDNA sequences determined by Chelly et al. Known promoter elements are underlined. Double line indicates common bases.

was not pursued further. The genomic DNA sequence data reported by Levinson et al. did not show the 196 bp observed by Chelly et al. Only the first seven bases flanking exon 1 were in agreement (*see* Fig. 3). The data, therefore, suggest that Chelly et al. had evidence for novel upstream sequences. It should be noted that the genomic structure of the *MNK* gene had not been determined at the time of Chelly et al.'s studies, and hence demarcations between introns and exons were not known

5. EVIDENCE FOR A SECOND PROMOTER

In our work, we used a genomic walking protocol to determine if the promoter described by Levinson et al. was connected to the 196 bp of Chelly et al. DNA from a human genomic library was amplified using a primer that anchored nucleotides in the 196-bp region. The experiments succeeded

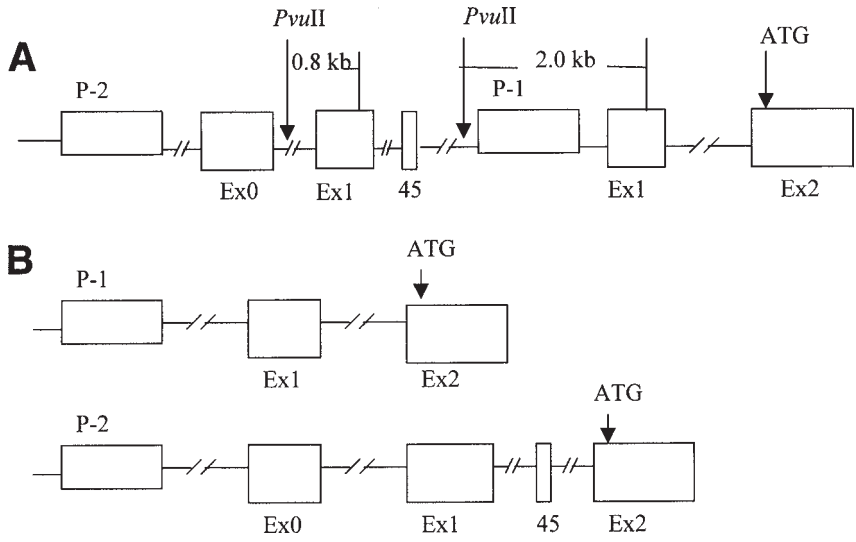

Fig. 4. Organization and mapping of the *MNK* 5' flanking region. **(A)** Two separate loci with contiguous promoters linked to a common untranslated exon which through splicing links to the coding region; **(B)** two separate loci each with a different promoter. Only P-2 connects with exon 0. Exon 1 is common to both loci. In (A) a suspected *Pvu*II sites flanking P-1 gives rise to a 2.0-kb DNA fragment extending from exon 1. This fragment when cloned was found to contain P-1, the promoter described by Levinson et al. *(17)*. The 0.8-kb fragment is believed to originate in an unknown *Pvu*II site between upstream exon 1 and exon 0.

in amplifying a genomic fragment that had Chelly et al.'s sequences and 1.3 kb of nucleotides upstream, in all, about 1.5 kb upstream from exon 1. Partial sequence data for this segment is shown in Fig. 3A. None of the bases beyond the first seven matched the sequences of Levinson et al. (Fig. 3B). Instead, the first 600 bases contained 14 sites that matched cis-acting sites in promoters including 2 TATA boxes, a CAAT site, and AP-1 and AP-3 sites, all significant regulatory sites for controlling eukaryotic gene expression.

In further studies, we took advantage of the fact that the promoter of Levinson et al. lacked a *Pvu*II restriction site and repeated the upstream analysis on a *Pvu*II digest of the genomic DNA. A second genomic walking analysis on the fragments again used the exon 1 primer as a downstream anchor. Two equally strong well-defined bands of 0.8 and 2.0-kb were generated. The 2.0-kb band upon cloning and sequencing matched the sequences reported by Levinson et al. (Fig. 4B), confirming a connection between Levinson et al.'s promoter and exon 1. No evidence for a second promoter sequences were found in the 2.0-kb fragment. The data, therefore, suggest two distinctly dissimilar promoters in the region flanking exon 1. That neither the sequences reported by Chelly et al. nor Levinson et al. had a *Pvu*II site leads us to conclude that the 0.8-kb band may a fragment that joins exon 1 to an intron that is proximal to exon 1. This hypothesis is currently being investigated.

6. ANALYSIS OF THE SECOND PROMOTER

Figure 3A shows sequence data for 600 bases of the 1.5-kb fragment obtained by genomic walking. Sequence data of Levinson et al. and Chelly et al. are shown for comparative purposes (Fig 3B,C). With the exception of three bases on the 5' end, the genomic DNA sequences match perfectly with the cDNA sequences reported by Chelly et al. and deviate sharply from those reported by Levinson et al. beyond the TGCCGCC at the 5' junction with exon 1. Six of the 14 cis-acting elements that engage

Table 2
Activating Sequences in Wilson's and Menkes Disease Gene Promoters

	WD[a]	*MNK P-1*[a]	*MNK P-2*[a]
CAAT box	+	–	+
MRE	+	+	–
E-Boxes	+	+	+
TATA boxes	–	+	+
AP-1	+	+	+
AP-2	+	–	+
AP-3	–	–	+

[a]WD, Wilson's disease gene *(19)*; MNK P-1, Menkes disease gene promoter 1 *(17)*; MNK P-2, Menkes disease gene promoter 2 (Reddy et al., unpublished).

known transcription factors are located in the 196 bp flanking exon 1. Because Chelly et al. reported this 196-bp sequence in a cDNA, the data suggest an untranslated exon further upstream from exon 1. We have referred to the 196 bp as exon 0 and define its position as between exon 1 downstream and P-2, the second promoter site. Table 2 compares P-2 with the Wilson's disease gene promoter and Levinson et al. (P-1). As noted, P-2 has no GC-rich region, and E-boxes and tandem repeats are not seen. P-1 and P-2, however, are connected to exon 1. The Wilson promoter reported by Oh et al. *(19)* bears no structural similarity to either P-1 or P-2. It is highly instructive and, at the moment puzzling, that exon 0 as genomic sequences is richly endowed with cis-activating elements flanking and perhaps regulating the expression of a gene whose identity has not been determined.

Figure 4 shows two interpretations for *MNK* promoter organization. Option A assumes both promoters regulate a common gene with P-1 downstream from P-2. Option B assumes P-1 and P-2 are promoters for two separate loci of *MN*K. The loci need not be on the same DNA segment nor the same chromosome. Option B places exon 0 after P-2 and further suggests that P-2 regulates the gene that gives rise to NML45. P-1 connects exon 1 directly to exon 2. Data are insufficient to conclude whether P-1, P-2 control *MNK* expression. Genomic sequence data does not support a close juxtaposition of the two. The data, however, support P-2 on the 5' flanking region of exon 0 upstream from P-1. Being upstream of P-1, exon 0 with its cis-acting elements is positioned strategically to enhance the activity of P-1. The upstream analysis of P-1 by us and by Levinson et al., however, has failed to locate exon 0 or P-2 within 2 kb of P-1. This observation does not support a tandem arrangement of two promoters converging on a common exon. Option B considers that P-1 and P-2 control genes of dissimilar loci not necessarily on the same chromosome. Because Levinson et al. analyzed DNA from the X chromosome in their analysis, P-1 is likely to be X-chromosomal. The chromosome location of P-2 is unknown, but exon 0 may hold the key to learning its precise position.

Levinson et al.'s sequence data did not extend beyond exon 1, whereas, based on overlapping cDNA clones, Chelly et al. linked exon 0 to exon 7. Thus, P-2 would appear to be a candidate for the promoter that controls expression of full-length ATP7A. This hypothesis will be revised pending the establishment of a connection between P-1 and downstream exons. On the other hand, two promoters in tandem and converging on a common untranslated exon would suggest developmental or tissue-specific expression of *MNK*. Mutation analysis has linked OHS to the promoter of Levinson et al. It thus becomes imperative to learn which promoter regulates expression of the full-length ATP7A and which one serves other purposes. These data become very important in light of the discovery of alternative transcripts for the Menkes gene and finding that one of these could be linked with the nuclear localization of Cu *(11)*.

7. SUMMARY AND CONCLUSIONS

Current understanding holds that internal Cu transport in mammalian cells employs a series of smaller peptides (metallochaperones) and membrane-transporting ATPases (ATP7A, ATP7B) to move Cu within the cytosol and organelles *(20)*. With the exception of Atox1 *(21)*, the chromosomal origin of mammalian copper chaperones is unknown. Expression of ATP7A is cell type and developmental-stage-specific. *MNK* or a related gene code for at least two mRNA transcripts that differ from ATP7A in their 5' flanking and coding sequences. All have a single metal-binding motif structurally analogous to the heavy-metal motif in ATP7A. A prudent method for generating NML45 (or ATP7A2–16) is by targeted specific splicing of a larger mRNA. This hypothesis, however, is difficult to accept because of a reproducible pattern of specific base substitution, exon skipping, and insertion sequences in the alternative transcripts that have no connection with mature ATP7A mRNA sequences. Thus, one is led to consider a second gene devoted primarily to synthesizing smaller peptides. The finding of a second promoter upstream from exon 1 strengthens a two-loci hypothesis. As yet, we have been unable to link P-2 or P-1 with the synthesis of alternative mRNAs. If such a link exists, it will be possible to resolve the meaning of a second promoter and the alternative transcripts and perhaps further the understanding of spatial and temporal regulation of *MNK* gene expression.

ACKNOWLEDGMENTS

Funding for the research was provided in part from USDA grant 98-35200-6055 and grant P30-ES09106 awarded to the Center for Environment and Rural Health at Texas A&M University.

REFERENCES

1. Dierick, H., Ambrosini, L., Spencer, J., Glover, T. W., and Mercer, J. F. B. (1995), Molecular structure of the Menkes disease gene (*ATP7A*). *Genomics* **28**,462–469.
2. Tumer, Z., Vural, B., Tonnesen, T., Chelly, J., Monaco, A. P., and Horn, N. (1995) Characterization of the exon structure of the Menkes disease gene using vectorette PCR. *Genomics* **26**,437–442.
3. Qian, Y., Tiffany-Castiglioni, E., and Harris, E. D. (1998) Sequence of a Menkes-type Cu-transporting ATPAse from rat C6 glioma cells: comparison of the rat protein with other mammalian Cu-transporting ATPases. *Mol. Cell. Biochem.* **181**,49–61.
4. La Fontaine, S., Firth, S. D., Lockhart, P. J., et al. (1998) Functional analysis and intracellular localization of the human Menkes protein (MNK) stably expressed from a cDNA construct in Chinese hamster ovary cells (CHO-K1). *Hum. Mol. Genet.* **7**,1293–1300.
5. La Fontaine, S., Firth, S. D., Camakaris, J., Englezou, A., Theophilos, M. B., Petris, M., et al. (1998) Correction of the copper transport defect of Menkes patient fibroblasts by expression of the Menkes and Wilson ATPases. *J. Biol. Chem.* **273(47)**, 31,375–31,380.
6. Reddy, M. C. M. and Harris, E. D. (1998) Multiple transcripts coding for the Menkes gene: evidence for alternative splicing of Menkes mRNA. *Biochem. J.* **334**,71–77.
7. Harris, E. D., Reddy, M. C. M., Qian, Y., Tiffany-Castiglioni, E., Majumdar, S., and Nelson, J. (1999) Multiple forms of the Menkes Cu-ATPAse. *Adv. Exp. Med. Biol.* **448**,39–51.
8. Qian, Y., Majumdar, S., Reddy, M. C. M., and Harris, E. D. (1996) Coincident expression of Menkes gene with copper efflux in human placental cells. *Am. J. Physiol.* **270**,C1880–C1884.
9. Mercer, J. F. B., Livingston, J., Hall, B., et al. (1993) Isolation of a partial candidate gene for Menkes disease by positional cloning. *Nature Genet.* **3**,20–25.
10. Chelly, J., Tümer, Z., Tonnesen, T., et al. (1993) Isolation of a candidate gene for Menkes disease that encodes a potential heavy metal binding protein. *Nature Genet.* **3**,14–19.
11. Reddy, M. C. M., Majumdar, S., and Harris, E. D. (2000) Evidence for a Menkes-like protein with a nuclear targeting sequence. *Biochem. J.* **350**,855–863.
12. Nakai, K. and Horton, P. (1999) PSORT: a program for detecting sorting signals in proteins and predicting their subcellular localization. *Trends Biochem. Sci.* **24**,34–36.
13. Klomp, L. W., Lin, S. J., Yuan, D. S., Klausner, R. D., Culotta, V. C., and Gitlin, J. D. (1997) Identification and functional expression of HAH1, a novel human gene involved in copper homeostasis. *J. Biol. Chem.* **272**,9221–9226.
14. Cobine, P., Wickramasinghe, W. A., Harrison, M. D., Weber, T., Solioz, M., and Dameron, C. T. (1999) The *Enterococcus hirae* copper chaperone CopZ delivers copper(I) to the CopY repressor. *FEBS Lett.* **445**,27–30.
15. Vulpe, C., Levinson, B., Whitney, S., Packman, S., Gitschier, J. (1993) Isolation of a candidate gene for Menkes disease and evidence that it encodes a copper-transporting ATPase. *Nature Genet.* **3**,7–13.
16. Camakaris, J., Petris, M. J., Bailey, L., et al. (1995) Gene amplification of the Menkes (MNK; ATP7A) P-type ATPase gene of CHO cells is associated with copper resistance and enhanced copper efflux. *Hum. Mol. Genet.* **4**,2117–2123.

17. Levinson, B., Conant, R., Schnur, R., Das, S., Packman, S., and Gitschier, J. (1996) A repeated element in the regulatory region of the MNK gene and its deletion in a patient with occipital horn syndrome. *Hum. Mol. Genet.* **5**,1737–1742.
18. Qi, M. and Byers, P.H. (1998) Constitutive skipping of alternatively spliced exon 10 in the ATP7A gene abolishes Golgi localization of the Menkes protein and produces the occipital horn syndrome. *Hum. Mol. Genet.* **7**,465–469.
19. Oh, W. J., Kim, E. K., Park, K. D., Hahn, S. H., and Yoo O. J. (2000) Cloning and characterization of the promoter region of the Wilson Disease gene. *Biochem. Biophys. Res. Commun.* **259**,206–211.
20. Harris, E. D. (2000) Cellular copper transport and metabolism. *Annu. Rev. Nutr.* **20**,291–310.
21. Hamza, I., Klomp, L. W., Gaedigk, R., White, R. A., and Gitlin, J. D. (2000) Structure, expression, and chromosomal location of the mouse Atox1 gene. *Genomics* **63(2)**,294–297.

20

Expression Profiling in Menkes Disease

Zeynep Tümer, Nina Horn, and Lars Riff Jensen

1. INTRODUCTION

The main focus in genomic research is starting to shift from structural genomics to functional genomics and proteomics, which deal with the function of genes and their products. Each cell expresses different sets of genes at different levels as the result of different situations such as development, environmental influences, and disease. Each physiological and pathological situation can thus be characterized by a specific set of gene transcripts (transcriptome) and protein products (proteome). To identify the transcriptomes in Menkes disease, we have employed differential display (DD) of mRNA, a technique which displays mRNA species expressed by a cell population and that is used to detect differences in gene expression between different cell types or under altered conditions *(1)*. The primary defect in the Menkes disease is in the cellular export protein ATP7A, and several copper enzymes are affected secondarily *(2)*. Alhough we can predict the role of some of the copper enzymes in the development of the multisystemic Menkes disease, it is likely that several other enzymes/proteins also contribute to disease progression.

2. COPPER

2.1. The Normal Copper Metabolism

The transition metal copper is important for the activation of dioxygen, which is essential for the survival of all living aerobic organisms. Because of its reversible interchange between two oxidation states (cuprous and cupric), copper serves as a cofactor for a number of oxygen-processing enzymes involved in diverse metabolic processes. These include cellular respiration, neurotransmitter biosynthesis, maturation of peptide hormones, free-radical scavenging, crosslinking of elastin, collagen and keratin, melanin production, and iron homeostasis *(2)*. Copper has further been implicated in myelination *(3)* and in the regulation of the circadian rhythm *(4)* and may also be necessary for coagulation and angiogenesis *(5)*.

Their ability to interact directly with oxygen paradoxically renders both cupric and cuprous ions highly toxic in excess, because they act as electron-transfer intermediates and catalyze the formation of hydroxyl radicals, which have detrimental effects on cellular components. A fine regulation of copper homeostasis is therefore vitally important for all living organisms.

From: Handbook of Copper Pharmacology and Toxicology
Edited by: E. J. Massaro © Humana Press Inc., Totowa, NJ

Copper is absorbed from the intestine and its transfer is dependent on the copper export mechanism that is deficient in Menkes disease (ATP7A). The metal is subsequently transported to the liver, the central organ of copper storage and homeostasis. In the liver, copper is either secreted to the blood bound to ceruloplasmin or excreted to the bile, and both processes are controlled by the copper pump that is defective in Wilson's disease (ATP7B). The main excretion route for copper is via bile and urinary loss is negligible *(2)*.

In blood, the main copper complexing molecules are ceruloplasmin (90%), albumin (5%), and certain amino acids, especially histidine. Ceruloplasmin has long been regarded as the main copper transporter, but its primary role was recently shown to be in the iron metabolism as a ferroxidase *(6)*. The major copper-transport form in blood is likely to be albumin, although analbuminemia as a result of a genetic defect does not lead to an imbalance in copper metabolism *(7)*. Albumin-bound copper is in equilibrium with amino-acid-bound copper and these two forms probably constitute a buffer system that secures the availability of sufficient copper to tissues as well as protecting against copper toxicity.

The brain is likely to access circulating copper across both brain barriers, the blood-brain barrier at the cerebral endothelium and the blood-cerebrospinal fluid barrier at the choroid plexus, through a controlled copper transfer. Under physiological circumstances, circulating ceruloplasmin will not enter the brain, but a membrane-bound form is synthesized within the central nervous system *(8,9)*. Similarly, albumin is not transported into the brain, but a newly identified protein with the same copper-binding motif may play a similar role in cerebrospinal fluid *(10)*.

2.2. Cellular Copper Transport

Cellular copper transport has been investigated extensively during recent years both in humans and yeast. In the following, we will summarize our current knowledge about the cellular copper transport and the reader will be referred to recent reviews for the original references *(2,11,12)*.

Uptake of copper across the plasma membrane appears to occur via an energy-independent membrane carrier, CTR1. By analogy with yeast, the metal is likely to be reduced from the cupric to cuprous state prior to uptake. However, in humans, the reductase(s) involved in this process is yet unknown.

Copper-requiring enzymes are found in all cellular compartments and it is essential to prevent the metal from causing cellular damage during its transfer. The "free" copper pool in the cell is extremely low and, indeed, far below the affinity of most copper-dependent enzymes. Efficient delivery of copper to the enzymes is achieved by a number of copper-chelating transporters (copper chaperones), which guide the copper ion to different cellular locations while protecting the cellular components from the toxic effects of copper. Copper chaperones are highly specific for their targets and cannot functionally substitute for each other in their respective pathways. The copper chaperones participate directly in the loading of the metal into the recipient molecule, and once the metal has been inserted into the target protein, the chaperone is available again for metal delivery. Of the three chaperones identified, CCS (copper chaperone for superoxide dismutase [SOD]) targets copper to the cytosolic Cu,Zn superoxide dismutase (SOD1) and COX17 guides copper to the mitochondria for insertion into cytochrome-*c* oxidase (COX). COX17 delivers copper to the mitochondria inner membrane, where the proteins SCO1 and SCO2 subsequently secure the insertion of the metal into COX. The third copper chaperone, HAH1 (human Atx1 homolog) guides copper to the secretory pathway, where the membrane-bound copper ATPases, ATP7A and ATP7B reside. These two highly similar proteins belong to a family of cation pumps, including sodium, potassium and calcium pumps, which utilize ATP for the active transport of a cation across a membrane. ATP7A and ATP7B are involved in the delivery of copper to the secreted copper enzymes and in the export of surplus copper from cells. The cellular copper homeostasis seems to be regulated primarily by the export pump. At increased copper concentrations, the protein is reversibly translocated to the plasma membrane, where it pumps copper

out of the cell. In liver, this function is carried out by ATP7B, the protein defective in Wilson's disease, and in other tissues, it is carried out by by ATP7A, the protein defective in Menkes disease.

3. MENKES DISEASE

Menkes disease (MD) is a multisystemic lethal disorder of copper metabolism, inherited as an X-linked recessive trait. Progressive neurodegeneration and connective tissue manifestations together with peculiar "kinky" hair are the main manifestations *(2,13)*. Although many patients present a severe clinical course, variable forms can be distinguished, and the occipital horn syndrome (OHS) is the mildest recognized form. Clinical and physiopathological features of MD are attributable to deficiency of one or more important copper-requiring enzymes secondary to a defect in ATP7A.

3.1. Intracellular Copper Transport in Menkes Disease

Elimination of copper from cells is the basic disturbance in MD and almost all of the tissues except for the liver and the brain will accumulate copper to abnormal levels. When functional defects in MD are discussed, the body tissues and organs therefore can be viewed in three categories: liver, brain, and other tissues.

In the liver, the copper level is low, but can be corrected by copper supplementation. This indicates that the low copper level is not a result of disturbed hepatic copper metabolism, but a secondary effect resulting from the requirement of the metal in other tissues. In the normal liver, ATP7A mRNA expression is very low *(14–16)*, suggesting that its role is taken over by ATP7B. A defect in ATP7B will result in copper accumulation in the liver, with subsequent overflow to other organs as seen in Wilson's disease *(17)*.

The reason for the low copper content in the brain of MD patients is, however, different. The mammalian brain is one of the richest copper-containing organs in the body *(18,19)*. The regulation of brain copper level is not well understood, but because MD leads to low copper levels in the brain, ATP7A probably participates in this process. In MD patients, copper is likely to be trapped in both barriers of the brain, whereas the neurons and glial cells are deprived of copper *(20–23)*. The brain is therefore unique in that it is the only organ deprived of copper, whereas for the other organs and tissues, copper deficiency is functional.

In tissues and organs other than liver and brain, the ATP7A defect leads to intracellular copper accumulation *(24)*. Excess copper induces synthesis of metallothionein, a small and cystein-rich intracellular copper-binding protein, which functions as a copper scavenger. The disturbance of copper metabolism is also reflected in easily accessible cell types like cultured skin fibroblasts *(25)* and Epstein–Barr-virus transformed lymphocytes (cultured lymphoblasts) *(26)* of MD patients, making these cell types useful in vitro models. Furthermore, copper accumulation in cultured fibroblasts is also used as a reliable and definitive diagnostic test for MD *(2,13)*.

3.2. Copper Enzymes

Menkes disease is a multisystemic disorder involving several copper-dependent enzymes *(2,27)*. Understanding the pathological pathways in different systems in MD requires knowledge of these metalloenzymes and their function, which will be summarized in the following subsection. In the brain the activity of all copper-dependent enzymes is low because of deprivation of copper in this organ. However, systemic changes are caused by the lack of incorporation of copper into the secreted or vesicular enzymes secondary to malfunction of ATP7A.

3.2.1. Dopamine β-Hydroxylase

Dopamine β-hydroxylase (DHB) is a critical enzyme in the catecholamine biosynthetic pathway converting dopamine into noradrenaline and (subsequently) adrenaline. Deficient activity of DBH will expectedly lead to autonomic failure and this will contribute to central nervous system (CNS) degeneration and other symptoms like ataxia, hypotension, hypothermia, and diarrhea observed in MD patients.

In addition to copper, the enzyme requires ascorbate as a cofactor *(28)*. DBH is localized in secretory vesicles in nerve terminals and in the adrenal medulla, but it is not expressed in fibroblasts. Because of its vesicular location, the enzyme has to pass through the secretory pathway of the cells, and it is likely that copper is added at this stage. Biosynthesis of DBH does not appear to be copper dependent, and reduced enzyme activity as a result of low copper levels in the brain can be corrected by the addition of copper *(29,30)*.

Recently, a novel monooxygenase (MOX) that is homologous to DBH has been identified in senescent fibroblasts *(31)*. MOX maintains the active copper site, but because it lacks a signal peptide sequence, it is probably not secreted. The substrate of this enzyme is yet unknown.

3.2.2. Peptidyl α-Amidating Monooxygenase

Peptidyl α-amidating monooxygenase (PAM) is involved in the maturation of several growth factors and neural peptide hormones involved in hypothalamic–pituitary regulation, as well as in intestinal function *(32)*. Dysfunction of this complex system will expectedly lead to numerous neurological disturbances although the specific nature has not been delineated yet. The deficiency of one of the peptide hormones, vasopressin, may, for example, contribute to the development of hypotension in MD patients. PAM has only been studied in three milder Menkes patients. The plasma activities were found to be normal, but the activity could be stimulated by addition of copper *(33)*.

Peptidyl α-amidating monooxygenase is structurally similar to DBH, and it also requires copper and ascorbic acid as cofactors *(28)*. PAM is found in both secreted and membrane-associated forms, and its biosynthesis is likely to require copper loading in the secretory pathway in analogy with DBH. Copper can easily be removed from PAM and restored again *(32)*.

Peptidyl α-amidating monooxygenase is widely expressed including fibroblasts. Because of the strong molecular and mechanistic similarities between DBH and PAM, information obtained about PAM by studying fibroblasts may be extrapolated to DBH to some extent.

3.2.3. Lysyl Oxidase Gene Family

Lysyl oxidase (LOX) is a secreted enzyme that catalyzes crosslinking of elastin and collagen, and it is found extracellularly attached to its substrates. A deficiency of LOX will virtually affect all organs containing connective tissue. In Menkes disease, skin, bones, and blood vessels are profoundly affected, leading to symptoms like loose skin and joints, osteoporosis, abnormal facies, hernias, bladder diverticula, arterial aneurysms, petechial hemorrhage. Apart from its role in the connective tissue disturbance, LOX deficiency also has an indirect contribution to the CNS degeneration through arterial changes *(2)*. Decreased LOX activity has been demonstrated in cultured skin fibroblasts of MD patients by several researchers *(34–41)*.

In addition to its well-known role in extracellular matrix formation, several new biological functions have also been attributed to LOX, ranging from developmental regulation to tumor suppression and cell growth control. Identification of other lysyl-oxidase-like genes indicates that they may be responsible for some of these diverse functions. In addition to LOX, three distinct genes have been isolated, lysyl-oxidase-like gene, LOXL1 *(42,43)*, lysyl-oxidase-like gene 2, LOXL2 *(44)*, and lysyl-oxidase-related gene, LOR1 *(45)*. The predicted amino acid sequences of all of the members of this gene family contain a copper-binding site and the two conserved residues (Lys and Tyr), which are known to participate in the formation of the intramolecular quinone cofactor. LOX and LOXL1 are both acting extracellularly and evidence exists to indicate that they crosslink different types of collagen *(46)*. The LOR gene probably also functions extracellularly and it is overexpressed in senescent fibroblasts *(45)*. LOXL2 lacks a hydrophobic export signal sequence necessary for extracellular transport and, hence, it is likely to function within the cell.

Lysyl oxidase (and hence also the other members of this gene family) is particularly sensitive to impaired delivery of copper, because activation of the enzyme is a two-step process requiring copper at both steps. Copper catalyzes the formation of the cofactor, but it is also part of the active catalytic center. After the synthesis of prolysyl oxidase, the enzyme is copper loaded and the cofactor is formed

before secretion as part of the Golgi or trans-Golgi processing. Copper deficiency will affect the formation of the cofactor and, hence, the enzymatic activity of LOX. Thus, LOX activity in the body is solely dependent on the amount of copper available during the biosynthesis of the enzyme. Copper added after secretion of the enzyme is unable to catalyze the intramolecular cofactor formation and restore the enzymatic activity of LOX. Although the mechanisms by which copper is delivered to lysyl oxidase are not well studied, it is very likely that ATP7A is involved in this process, as LOX secretion and copper efflux use the same pathway. This hypothesis is supported by studies in rat, which showed that the relative levels of LOX and ATP7A mRNA transcripts were quantitatively similar throughout embryonic and early fetal life *(47)*.

Lysyl oxidase is present in high concentrations in dense connective tissue and the fibroblast is one of the principal cell types expressing lysyl oxidase. The study of MD fibroblasts may also provide information about the function and regulation of the new homologous genes in relation to copper homeostasis.

3.2.4. Copper-Containing Amine Oxidase

Copper-containing amine oxidase (CAO) comprises a heterogeneous group of tissue-specific amine oxidases that participate in wound healing, growth regulation, differentiation, and, possibly, apoptosis *(48)*. The preferred substrates are polyamines and diamines and CAO may hereby also influence neurological functions. In the brain, CAO is required for the deamination of putrescine and is necessary for the formation of the neurotransmitter GABA (γ-aminobutyric acid) *(49)*. Disturbance of CAO may therefore add to the neurological symptoms observed in MD patients, but this enzyme has not been studied in MD yet.

Similar to LOX, CAO uses a quinone cofactor that is formed by a copper-catalyzed modification of a single amino acid in the protein and this probably occurs in the secretory pathway, as the enzyme is either secreted or membrane anchored. Unlike LOX, enzymatic activity of a form of CAO can be restored by copper addition after the protein has been synthesized and secreted *(50)*. CAO is found in numerous tissues, including vascular smooth muscle, lung, eye, adipose tissue, placenta, and, in particular, intestine and plasma. A form is also expressed in fibroblast *(51)*.

3.2.5. Cytochrome-c Oxidase

Cytochrome-*c* oxidase (COX) is the terminal oxidase in the respiratory chain and important for energy formation. Adequate energy supply is crucial for normal nerve conduction as well as other metabolic processes. COX is located in the mitochondrial inner membrane and requires copper for the correct assembly of the enzyme complex. COX is obviously affected in the copper-deplete brain tissue of Menkes patients *(52–54)* adding to the neurodegenerative processes. A restricted ATP production because of COX deficiency in the CNS can cause seizures as observed frequently in MD patients.

Muscle weakness is a common symptom in MD and a compromised mitochondrial function has also been observed in muscle tissue of patients *(52,55–57)*, even though copper levels are elevated in this tissue. It has recently been shown that in cultured hepatoma cells, copper regulated expression of cytochrome-*b*, a mitochondrially encoded membrane-bound protein that is part of the mitochondrial respiratory chain *(58)*. Copper may therefore affect the respiratory chain and, hence, the energy production also through this protein. Identification of differentially expressed genes in fibroblasts may therefore help in defining the physiopathological mechanisms giving rise to these abnormalities.

3.2.6. Superoxide Dismutase

In several metabolic processes, highly reactive superoxide anions (free radicals) are produced and they have to be eliminated immediately because of their toxic nature. An important class of antioxidant enzymes is the SODs, which converts superoxide anions into oxygen and hydrogen peroxide and exists in three distinct forms. Two of these forms (SOD1 and SOD3) contain copper, and the third one, the mitochondrial SOD, contains manganese (SOD2).

SOD1 (Cu,Zn-SOD) is located in the cytoplasm and peroxisomes of all cell types, showing high activity in metabolically active organs such as the liver and kidney and low activity in, for example, skeletal muscle *(59)*. Copper is inserted into the enzyme in the cytosol by means of the chaperone CCS after the enzyme has been synthesized *(11)*. A diminished function of SOD1 in the brain of MD patients will result in further accumulation of free radicals, leading to peroxidation of lipids and neuronal degeneration. On the other hand, in the peripheral tissues (erythrocytes and cultured lymphoblasts), SOD1 activity is not reduced *(24,60)*, suggesting that copper delivery to SOD1 is independent of ATP7A and its diminished function in the brain is the result of copper deficiency. Furthermore, SOD1 activity is significantly increased in cultured lymphoblasts of MD patients, and the increased synthesis of SOD1 may play a protective role against copper toxicity *(60)*.

The second copper-containing superoxide dismutase, SOD3, is also known as extracellular SOD (EC-SOD). It is secreted from a few well-dispersed cell types, such as fibroblasts and glia cells, but the principal source is vascular smooth-muscle cells *(61–63)*. It is found in the interstitial matrix of several tissues, but SOD3 content is very high in some organs such as lungs *(59,64)*. The biological significance is still poorly described. As SOD3 is a secreted enzyme, the metal is likely to be inserted in the secretory pathway and, hence, dependent on a normal ATP7A function. We are currently studying this enzyme in Menkes fibroblasts (unpublished results).

3.2.7. Ceruloplasmin

Ceruloplasmin is a ferroxidase and catalyzes the oxidation of highly reactive ferrous ions to less toxic ferric ions, which, in turn, are bound to transferrin. During this oxidation process, ferrous ions can react with molecular oxygen and form superoxide radicals. Ceruloplasmin is synthesized as a holoprotein and copper ions are incorporated during the biosynthesis. The availability of copper does not influence the rate of synthesis or secretion of apoceruloplasmin, but failure of copper incorporation during biosynthesis will result in secretion of an apoprotein that is devoid of oxidase activity and is easily degradable *(65)*. Ceruloplasmin is synthesized primarily in the liver, and ATP7B transports copper into the hepatocyte secretory pathway for incorporation into ceruloplasmin.

A membrane-anchored form of ceruloplasmin is synthesized in various tissues and cell types, including cultured fibroblasts *(66)*. Most importantly, the same form is also synthesized within the brain *(8,9,67)*. Ceruloplasmin production within the CNS is necessary for iron homeostasis. As observed in aceruloplasminemia, an abolished activity of ceruloplasmin will lead to iron accumulation at certain brain regions and cause progressive neurodegeneration and lipid peroxidation *(68)*. Low activity of brain ceruloplasmin secondary to low copper levels may also lead to similar consequences in MD.

3.2.8. Hephaestin

The gene encoding for the so-called hephaestin protein has recently been identified and the protein product is predicted to play an important role in intestinal iron absorption *(69)*. It is homologous to ceruloplasmin and contains similar copper-binding sites. In addition, it contains a transmembrane domain, suggesting that the ceruloplasmin-like domain is located in an extracytosolic compartment or in the extracellular space. Based on its homology to ceruloplasmin, it has been proposed that hephaestin is a ferroxidase necessary for iron release from intestinal epithelial cells. Studies in mouse show that hephaestin expression is high in the small intestine and colon and contrasts that of ceruloplasmin, which is not expressed in the intestine, but highly expressed in liver. How copper is delivered to hephaestin has not been delineated yet, but ATP7A might be involved in this process. Reduced iron absorption may partly explain the anemia observed in some MD patients.

3.2.9. Clotting Factors V and VIII

The blood-clotting factors V and VIII contain copper and the copper-binding site is structurally related to that of ceruloplasmin. This suggests a role for copper in these coagulation factors, although the specific nature is yet unknown. It has been suggested that copper may play a role in the correct folding of these proteins *(70)* and failure of incorporation of the metal might impair their synthesis or

function. Both proteins are secreted and they are primarily synthesized in the liver. Copper is likely to be delivered to these proteins in the secretory pathway by ATP7B.

3.2.10. Copper-Dependent Sulfhydryl Oxidase

Disulfide bridges between the cysteine residues are required for the stability and function of a large number of proteins, including keratin *(71,72)*. Several enzymes are involved in disulfide metabolism. Sulfhydryl oxidases contribute to disulfide bridge formation by catalyzing the oxidation of sulfhydryl groups to disulfides. Sulfhydryl oxidases have been purified from a number of mammalian sources *(73–75)*, but skin is the only tissue where a possibly copper-dependent form has been described *(76)*.

Abnormal hair structure in MD patients indicates that keratinization is a copper-dependent process. It is likely that lack of copper impairs the function of copper-containing sulfhydryl oxidase resulting in deficient crosslinking of keratin, which normally provides a more durable structure to hair and skin. The hair from MD patients have a normal sulfur content, but free-sulfhydryl groups are increased and disulfide bonds are reduced grossly *(77)*. Copper therapy can normalize the hair structure in MD patients.

3.2.11. Tyrosinase

Tyrosinase is a copper-dependent enzyme that catalyzes several steps in the biosynthesis of melanin pigment, which neutralizes the harmful effect of the sun. Dysfunction of tyrosinase will lead to hypopigmentation of the skin and hair as observed in MD patients. Tyrosinase is expressed in melanocytes and is stored in melanosomes. Tyrosinase is not expressed in fibroblasts, but, very recently, Petris and colleagues *(78)* have expressed the enzyme in normal and Menkes fibroblasts using a cDNA construct. In this elegant study, they have shown that ATP7A was required for tyrosinase activation, suggesting that ATP7A had a role in delivering copper to the secretory pathway and to tyrosinase.

3.2.12. Copper-Dependent Ceramide Hydroxylase

In yeast, sphingolipid biosynthesis is a copper-dependent process controlled by the activity of the ATP7A/ATP7B ortholog (CCC2) *(79)*. A key component of sphingolipid is ceramide that may be hydroxylated at one or more sites of the fatty acid side chains. This process may also occur in humans, providing an explanation for the dysmyelination observed in MD patients *(80)*. The copper-dependent hydroxylation clearly occurs in the Golgi apparatus, but the molecular mechanisms remain to be identified and characterized in both man and yeast. It is not known at what stage of the biosynthesis the hydroxylation occurs.

3.2.13. Other Copper Proteins

Dysfunction of copper-containing proteins like the prion protein and the amyloid precursor protein (APP) may also add to the neurological disturbances in MD, but further investigations are necessary to support this hypothesis.

4. DIFFERENTIAL DISPLAY

4.1. Overview of the Procedure

Differential mRNA display by polymerase chain reaction (DD-PCR) is an mRNA fingerprinting technique described in early 1990s for detecting gene-expression levels and identifying differentially expressed genes through arbitrary amplification and comparison of different mRNA resources *(1)*. A major area of application for DD has been the identification of genes differentially expressed in tumor tissues compared to the corresponding normal tissues.

The general strategy of DD is to amplify partial cDNA fragments with PCR using subsets of reverse transcribed mRNAs and displaying these fragments on a denaturing polyacrylamide gel. In

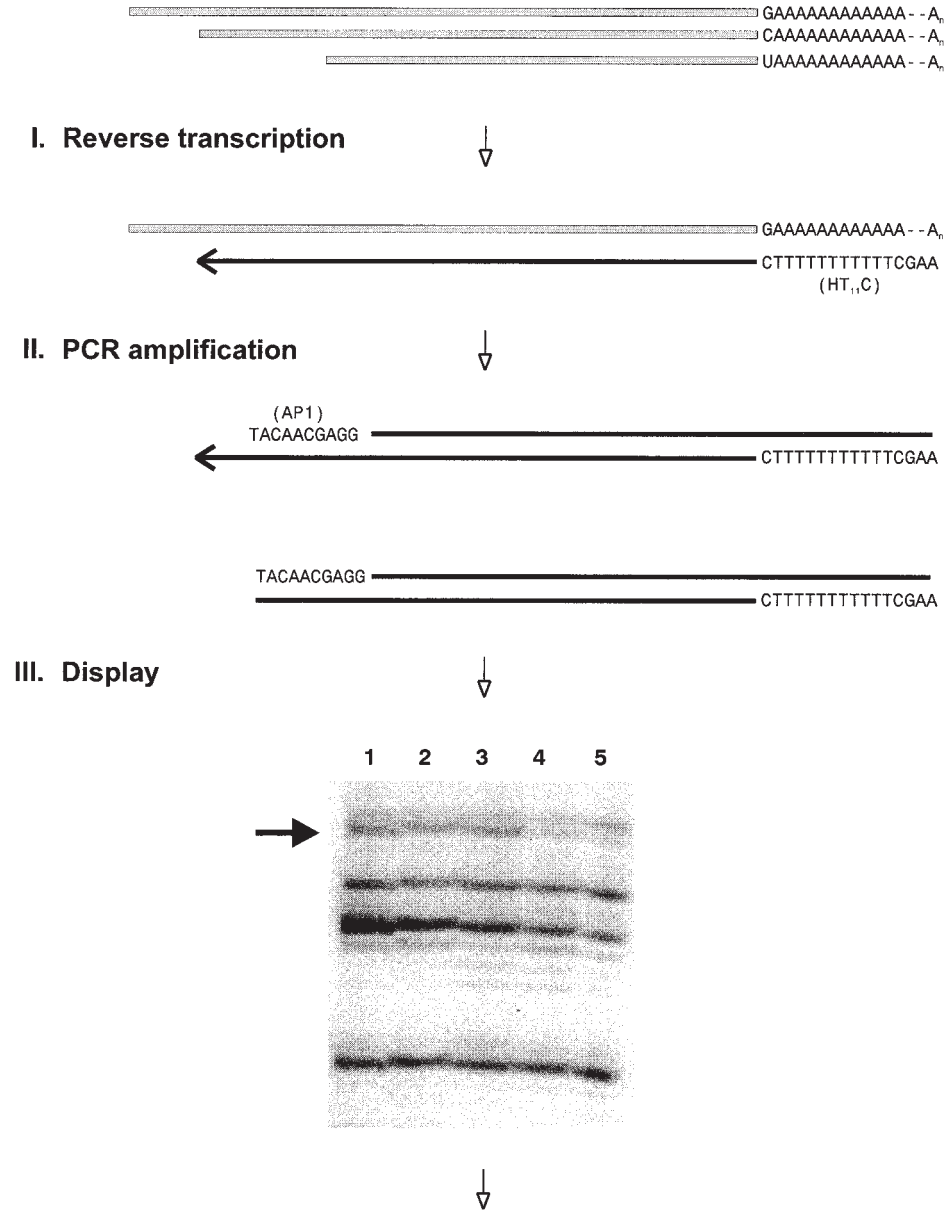

Fig. 1. Outline of the differential display of mRNA technique. **(I)** Reverse transcription: mRNAs (gray bar) are reverse transcribed using Superscript II RNase H^- Reverse Transcriptase (Life Technologies), dNTPs, and an anchored oligo-dT primer ($HT_{11}V$) to produce single-stranded DNA complements (black bar) of of mRNA. H 5' *Hin*dIII restriction site overhang (AAGC); V denotes G, A, or C; and T_{11} 11 thymidine nucleotides. The 3' nucleotide (V) anchor the $HT_{11}V$ oligonucleotide to the 5' end of the poly(A) tail of the mRNA. A_n stands for the end of the mRNA strand. With this procedure three different subpopulations of mRNAs are generated. **(II)** PCR amplification: One of 26 arbitrary decamer primers (AP) is then used in combination with one of the [α-^{32}P]-ATP labeled $HT_{11}V$ primers to amplify a subset of mRNA 3' termini from the cDNAs generated. **(III)** Display: The labeled cDNA fragments are then displayed on a 6% denaturing polyacrylamide gel. **(IV)** A band of interest (indicated by an arrow), such as one overexpressed in Menkes fibroblasts (lanes 1–3) compared to the control fibroblasts (lanes 4 and 5) is investigated further as described in the text.

our DD studies, we have used a slightly modified form of the original description *(81)*, as summarized below and schematized in Fig. 1. The mRNAs were reverse transcribed using one of three anchored oligo-dT primers (designated as $HT_{11}A$, $HT_{11}C$, or $HT_{11}G$) annealing to the poly(A) tails present on most eukaryotic mRNAs and generating three subpopulations of mRNA. The cDNA species were subsequently amplified with PCR, where a short primer (a decamer) with arbitrary sequence served as the 5' primer and the 3' primer was the anchored oligo-dT labeled with [α-^{32}P]-ATP *(82)*. The PCR products were separated by electrophoresis on a 6% denaturing polyacrylamide gel, the gels were dried, and the fragments were visualized by autoradiography. Individual bands that indicate differentially regulated mRNAs were recovered from dried polyacrylamide gels by eluting in water and purifying with ethanol precipitation. The fragments were subsequently reamplified with PCR using the same primer set. The reamplified fragments were separated by agarose gel electrophoresis, recovered by eluting in water and directly sequenced using Cy5-labeled oligo-dT primers in an ALFexpress automatic DNA sequencer (Pharmacia Biotech AB). Search for sequence similarities has been carried out using public databases such as BLAST *(83)* and FASTA *(84)*. To verify the expression patterns of the bands of interest, specific primers were designed for each fragment and RT-PCR and/or Northern blot hybridization was conducted.

This procedure generates up to 500-bp-long fragments representing mainly the 3' ends of mRNA species. In this study, we have used 26 different decamers for each of the three mRNA subpopulations and an estimated population of 20,000 expressed mRNA should be effectively screened by this approach *(82)*.

Differential display is a widely used technique because it is fast, inexpensive, sensitive, and relatively simple. Alhough powerful, DD has several drawbacks, including reproducibility, presence of false positives, and confirmation of differential expression of the candidate clones. Several reports have described improvements of the initial method dealing with these problems. As to our experience, isolation of high-quality and intact RNA, careful sample treatment, quality of the enzymes used for reverse transcription and PCR amplification, elimination of DNA contamination, and replicate and duplicate experiments are some of the important points that should be taken into consideration when carrying out DD.

4.2. Preliminary Results

In the first attempt to identify known/unknown proteins that might be involved in the pathogenesis of Menkes disease, we have compared mRNA expression profiles of cultured fibroblasts of three MD patients with two controls. One of the patients had the OHS phenotype and a splice-site mutation affecting the donor site of intron 15 (unpublished result). The two other patients had the classical severe form of Menkes disease and one of them had a partial deletion of *ATP7A* including exons 3–23 and the other patient had a nonsense mutation in exon 4 (Arg409Ter) (unpublished results). Biochemical studies did not reveal any significant difference in the amount of copper accumulated or retained in fibroblasts with different mutations.

Using 26 different decamers for each of the 3 subsets of mRNA, we have generated 78 displays corresponding to approx 5000–7000 fragments for each individual cell. A total of 147 fragments ranging between 50 and 500 bp have been selected for sequencing and 119 of them could be sequenced successfully. For each fragment, approx 30–300 base pairs were sequenced. Of the 119 fragments sequenced, 38 fragments matched genes coding for known proteins; 36 showed sequence similarity to expressed sequence tags (ESTs) or known proteins found in the databases; 29 did not show any sequence similarity to already known expressed sequence (ESTs); and 16 fragments showed sequence similarity to theoretical proteins or genomic sequences (as of November 2000). One of the fragments of interest was matching to lysyl oxidase gene, which will be discussed in Section 5.2.

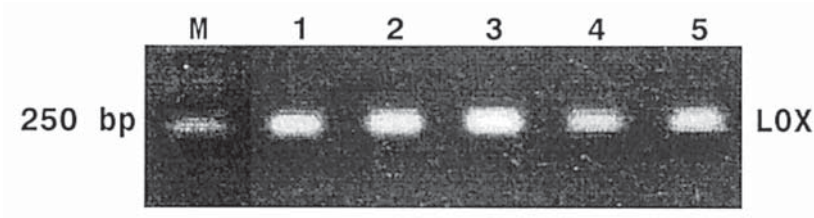

Fig. 2. Expression of LOX mRNA. RT-PCR was carried out with LOX-specific oligonucleotides using total RNA isolated from fibroblasts of MD patients and controls. The results suggest increase in LOX mRNA levels in the patient with the OHS phenotype (lane 1) as well as in the patients with the classical severe form (lanes 2 and 3) compared to controls (laned 4 and 5). M = molecular-weight marker.

5. EXPRESSION PROFILING IN MENKES DISEASE

5.1. Using Fibroblasts

Disturbance in copper homeostasis in MD is reflected in cultured skin fibroblasts, where a number of copper-dependent enzymes are expressed (*see* Section 3.2.). Fibroblasts thus provide a useful model for studying the effect of the disturbed copper metabolism on various copper-requiring enzymes and transport pathways through defining the differentially expressed genes.

Fibroblast is an excellent cell type, especially in studying connective tissue disturbance, which is a principal manifestation in Menkes disease, where lysyl oxidase deficiency plays a substantial role (Section 3.2.3.). However, neurodegeneration observed in MD is the result of a more complicated mechanism, where arterial abnormalities and disturbance of several copper enzymes add to the symptoms. The human brain is the most complex region of the body in terms of the diversity of gene expression and the brain copper metabolism is the result of a complex interplay of several copper enzymes in various cell types. Transcription profile obtained from the fibroblasts will, therefore, have obvious limitations in reflecting the gene expression profile of the brain. Still a simpler and easily accessible cell type like the fibroblast can provide useful information and may possibly direct the attention to new interactions.

5.2. LOX as a Differentially Expressed Gene in MD Fibroblasts

One of the differentially expressed genes in our displays was, indeed, lysyl oxidase and our initial studies with RT-PCR suggested an upregulation of LOX mRNA levels (Fig. 2). A likely explanation is that *LOX* levels are regulated by a positive feedback mechanism, where mRNA transcription is upregulated as a response to a defective posttranslational processing of LOX and/or elevated intracellular copper levels. Supporting this hypothesis, the majority of protein-bound copper secreted from skin fibroblasts was found to be associated with LOX, suggesting that this enzyme is a vehicle for copper egress from connective tissue cells *(85)*.

However, our results are not in line with the results of previous studies. In rat skin fibroblasts, copper deficiency influenced functional activity of lysyl oxidase but not the steady-state levels of mRNA *(86)*. Similarly Yeowell and colleagues *(87)* did not observe a significant change in the steady-state level of LOX mRNA in MD fibroblasts. In contrast to these studies, levels of lysyl oxidase mRNA transcripts were decreased in Menkes and OHS fibroblasts *(41,88)*. Further studies are necessary to understand the physiopathology of LOX and to reach a consensus in how LOX mRNA expression is reguated in MD.

6. OTHER STUDIES

A few studies have been published studying the influence of copper status on gene expression using the DD technique. One of the studies was carried out on the hepatocytes of copper-deficient

rats *(89)*. Among the 10 cDNAs confirmed to be differentially expressed were 2 mitochondrial rRNA genes, the intracellular gene-encoding ferritin, the iron storage protein, and fetuin which encodes tyrosine kinase inhibitor associated with rat insulin receptor. Elucidation of the influence of copper on the regulation of these genes requires further studies.

The other study was carried out to investigate the affect of Cu toxicity on cultured human hepatoma cells (HepG2) and they showed that copper regulated transcription of cytochrome-*b (58)*. Increased levels of copper led to substantial increase in cytochrome-*b* transcription, whereas the transcription was suppressed with low levels of copper. It is suggestive that cytochrome-*b* has a role in the mitochondrial response to both deficiency and toxicity of copper. Mitochondrial damage has been shown previously under altered copper levels, including Menkes cells *(90)*. Most interestingly in our initial studies, we have also observed differential expression of cytochrome-*b* in Menkes fibroblasts. Further studies are necessary to elucidate the role of cytochrome-*b* in the mitochondrial dysfunction observed in Menkes disease.

7. FUTURE PROSPECTS

Although mRNA is not an ultimate product of a gene, understanding the gene regulation at transcript levels is the first step in understanding the molecular pathways. Identification of the expressed genes in an abnormal condition compared to a normal condition will thus give insights into the normal physiology and the disease state. The technique of choice in profiling gene expression at transcription level is shifting to cDNA microarrays, which exploits the wide genetic information in databases and the technological improvements. Although this technique depends on the availability of cDNA clones (in contrast to DD), it enables quantitative monitoring and analysis of expression profiles of thousands of genes simultaneously. Microarray technology is far from being comprehensive at present, but virtually every transcript of the human genome can be analyzed simultaneously by this technology, allowing a broad view of gene-expression changes in physiological and pathological situations. However, more traditional techniques such as DD have been excellent tools in identifying genes and will still be widely used, at least for a while, as they are inexpensive and rapid and can be performed in any laboratory.

As transcriptional profiles are not exactly correlated to protein-expression levels, studies with proteomes, which will reflect dynamically and exactly the state of biological systems, are necessary to get a full picture of biological processes. It is obvious that both functional genomics and proteomics offer abundant information on gene-expression patterns and the ultimate goal will be the correlation of these studies.

Functional genomic and proteomic studies in humans, animal models, or yeast systems may give insights into the several intracellular processes where copper is a possible etiological factor. These include primary disorders of copper metabolism such as Menkes and Wilson's disease or more common neurodegenerative diseases like Alzheimer's or Parkinson's disease.

REFERENCES

1. Liang, P. and Pardee, A. B. (1992) Differential display of eukaryotic messenger RNA by means of the polymerase chain reaction. *Science* **257**, 967–971.
2. Horn. N. and Tümer, Z. (2002) Menkes steely hair disease and the occipital horn syndrome, in *Connecitve tissue and Its Heritable Disorders: Molecular, Genetic, and Medical Aspects*, 2nd ed. (Royce, P. M. and Steinmann, B., eds.), Wiley, New York, in press.
3. Horn, N., Tønnesen, T., and Tümer, Z. (1992) Menkes disease: an x-linked neurological disorder of the copper metabolism. *Brain Pathol.* **2,** 351–362.
4. Borjigin, J., Payne, A. S., Deng, J., Li, X., Wang, M. M., Ovodenko, B., et al. (1999) A novel pineal night-specific ATPase encoded by the Wilson's disease gene. *J. Neurosci.* **19,** 1018–1026.
5. Pena, M. M., Lee, J., and Thiele, D. J. (1999) A delicate balance: homeostatic control of copper uptake and distribution. *J. Nutr.* **129,** 1251–1260.
6. Mukhopadhyay, C. K., Attieh, Z. K., and Fox, P. L. (1998) Role of ceruloplasmin in cellular iron uptake. *Science* **279**, 714–717.

7. Kallee, E. (1996) Bennhold's analbuminemia: a follow-up study of the first two cases (1953-1992). *J. Lab. Clin. Med.* **127**, 470–480.
8. Patel, B. N. and David, S. (1997) A novel glycosylphosphatidylinositol-anchored form of ceruloplasmin is expressed by mammalian astrocytes. *J. Biol. Chem.* **272,** 20,185–20,190.
9. Patel, B. N., Dunn, R. J., and David, S. (2000) Alternative RNA splicing generates a glycosylphosphatidylinositol-anchored form of ceruloplasmin in mammalian brain. *J. Biol. Chem.* **275,** 4305–4310.
10. Harford, C. and Sarkar, B. (1995) Neuromedin C binds Cu(II) and Ni(II) via the ATCUN motif: implications for the CNS and cancer growth. *Biochem. Biophys. Res. Commun.* **209**, 877–882.
11. O'Halloran, T. V. and Culotta, V. C. (2000) Metallochaperones, an intracellular shuttle service for metal ions. *J. Biol. Chem.* **275**, 25,057–25,060.
12. Chinenov,Y. V. (2000) Cytochrome c oxidase assembly factors with a thioredoxin fold are conserved among prokaryotes and eukaryotes. *J. Mol. Med.* **78**, 239–242.
13. Tümer, Z. and Horn, N. (1997) Menkes disease: recent advances and new aspects. *J. Med. Genet.* **34**, 265–274.
14. Vulpe, C., Levinson, B., Whitney, S., Packman, S., and Gitschier, J. (1993) Isolation of a candidate gene for Menkes disease and evidence that it encodes a copper-transporting ATPase. *Nature Genet.* **3**, 7–13.
15. Chelly, J., Tümer, Z., Tønnesen, T., Petterson, A., Ishikawa-Brush, Y., Tommerup, N., et al. (1993) Isolation of a candidate gene for Menkes disease that encodes a potential heavy metal binding protein. *Nature Genet.* **3**, 14–19.
16. Mercer, J. F. B., Livingston, J., Hall, B., Paynter, J. A., Begy, C., Chandrasekharappa, S., et al. (1993) Isolation of a partial candidate gene for Menkes disease by positional cloning. *Nature Genet.* **3**, 20–25.
17. Cox, D., Tümer, Z., and Roberts, E. A. (2000) Disorders of copper metabolism, in *Inborn Metabolic Diseases*, 3rd ed. (Fernandes, J., Saudubray, J., and van den Berghe, G., eds.), Springer-Verlag, Berlin, pp. 385–391.
18. Osterberg, R. (1980) Physiology and pharmacology of copper. *Pharmacol. Ther.* **9**, 121–146.
19. Nalbandyan, R. M. (1983) Copper in brain. *Neurochem. Res.* **8**, 1211–1232.
20. Kodama, H. (1993) Recent developments in Menkes disease. *J. Inherited Metab. Dis.* **16,** 791–799.
21. Qian., Y., Tiffany-Castiglioni, E., Welsh, J., and Harris, E. D. (1998) Copper efflux from murine microvascular cells requires expression of the Menkes disase Cu-ATPase. *J. Nutr.* **128**, 1276–1282.
22. Nishihara, E., Furuyama, T., Yamashita, S., and Mori, N. (1998) Expression of copper trafficking genes in the mouse brain. *Neuroreport* **9**, 3259–3263.
23. Iwase, T., Nishimura, M., Sugimura, H., Igarashi, H., Ozawa, F., Shinmura, K., et al. (1996) Localization of Menkes gene expression in the mouse brain; its association with neurological manifestations in Menkes model mice. *Acta Neuropathol.* **91**, 482–488.
24. Horn, N. (1984) Copper metabolism in Menkes disease, in *Metabolism of Trace Metals in Man: Developmental Biology and Genetic Implications* (Rennert, O. M. and Chan, W. Y., eds.), CRC, Boca Raton, FL, Vol. 2, pp. 25–52.
25. Horn, N. (1976) Copper incorporation studies on cultured cells for prenatal diagnosis of Menkes' disease. *Lancet* **1**, 1156–1158.
26. Riordan, J. R. and Jolicoeur-Paquet, L. (1982) Metallothionein accumulation may account for intracellular copper retention in Menkes' disease. *J. Biol. Chem.* **257,** 4639–4645.
27. Tümer. Z. and Horn, N. (1999) Hereditary disorders of copper metabolism, in *Genetic Aberrancies and Neurodegenerative Disorders* (Mattson, M., ed.), Advances in Gerontology, Vol. 3, Jai, New York, pp. 355–389.
28. Southan, C. and Kruse, L. I. (1989) Sequence similarity between dopamine beta-hydroxylase and peptide alpha-amidating enzyme: evidence for a conserved catalytic domain. *FEBS Lett.* **255**, 116–120.
29. Hunt, D. M. (1977) Catecholamine biosynthesis and the activity of a number of copper-dependent enzymes in the copper-deficient mottled mouse mutants. *Compar. Biochem. Physiol.* **57**, 79–83.
30. Skotland, T. and Ljones, T. (1979) The enzyme-bound copper of dopamine beta-monooxygenase. Reaction with copper chelators, preparation of the apoprotein, and kinetics of the reconstitution by added copper. *Eur. J. Biochem.* **94**, 145–151.
31. Chambers, K. J., Tonkin, L. A., Chang, E., Shelton, D. N., Linskens, M. H., and Funk, W. D. (1998) Identification and cloning of a sequence homologue of dopamine beta-hydroxylase. *Gene* **218**, 111–120.
32. Prigge, S. T., Mains, R. E., Eipper, B. A., and Amzel, L. M. (2000) New insights into copper monooxygenases and peptide amidation: structure, mechanism and function. *Cell. Mol. Life. Sci.* **57,** 1236–1259.
33. Prohaska, J. R., Tamura, T., Percy, A. K., and Turnlund, J. R. (1997) In vitro copper stimulation of plasma peptidylglycine alpha-amidating monooxygenase in Menkes disease variant with occipital horns. *Pediatr. Res.* **42**, 862–865.
34. Royce, P. M., Camakaris, J., and Danks, D. M. (1980) Reduced lysyl oxidase activity in skin fibroblasts from patients with Menkes' syndrome. *Biochem. J.* **192,** 579–586.
35. Royce, P. M. and Steinmann, B. (1990) Markedly reduced activity of lysyl oxidase in skin and aorta from a patient with Menkes' disease showing unusually severe connective tissue manifestations. *Pediatr. Res.* **28**, 137–141.
36. Byers, P. H., Siegel, R. C., Holbrook, K. A., Narayanan, A. S., Bornstein, P., and Hall J. G. (1980) X-linked cutis laxa: defective cross-link formation in collagen due to decreased lysyl oxidase activity. *N. Engl. J. Med.* **303**, 61–65.
37. Kuivaniemi, H., Peltonen, L., Palotie, A., Kaitila, I., and Kivirikko, K. I. (1982) Abnormal copper metabolism and deficient lysyl oxidase activity in a heritable connective tissue disorder. *J. Clin. Invest*. **69**, 730–733.
38. Kuivaniemi, H., Peltonen, L., and Kivirikko, K. I. (1985) Type IX Ehlers–Danlos syndrome and Menkes syndrome: the decrease in lysyl oxidase activity is associated with a corresponding deficiency in the enzyme protein. *Am. J. Hum. Genet.* **37**, 798–808.

39. Peltonen, L., Kuivaniemi, H., Palotie, A., Horn, N., Kaitila, I., and Kivirikko, K. I. (1983) Alterations in copper and collagen metabolism in the Menkes syndrome and a new subtype of the Ehlers–Danlos syndrome. *Biochemistry* **22**, 6156–6163.
40. Wakai, S., Ishikawa, Y., Nagaoka, M., Minami, R., and Hayakawa,T. (1991) Occipital horn syndrome (Ehlers–Danlos syndrome type IX) with severe psychomotor retardation and muscle atrophy—a first Japanese case. *Rinsho Shinkeigaku* **31**, 534–538.
41. Kemppainen, R., Hamalainen, E. R., Kuivaniemi, H., Tromp, G., Pihlajaniemi, T., and Kivirikko, K. I. (1996) Expression of mRNAs for lysyl oxidase and type III procollagen in cultured fibroblasts from patients with the Menkes and occipital horn syndromes as determined by quantitative polymerase chain reaction. *Arch. Biochem. Biophys.* **328**, 101–106.
42. Kenyon, K., Modi, W. S., Contente, S., and Friedman, R. M. (1993) A novel human cDNA with a predicted protein similar to lysyl oxidase maps to chromosome 15q24–q25. *J. Biol. Chem.* **268**, 18,435–18,437.
43. Kim, Y., Boyd, C. D., and Csiszar, K. (1995) A new gene with sequence and structural similarity to the gene encoding human lysyl oxidase. *J. Biol. Chem.* **270,** 7176–7182.
44. Jourdan-Le Saux, C., Tronecker, H., Bogic, L., Bryant-Greenwood, G. D., Boyd, C. D., and Csiszar, K. (1999) The LOXL2 gene encodes a new lysyl oxidase-like protein and is expressed at high levels in reproductive tissues. *J. Biol. Chem.* **274**, 12,939–12,944.
45. Saito, H., Papaconstantinou, J., Sato, H., and Goldstein, S. (1997) Regulation of a novel gene encoding a lysyl oxidase-related protein in cellular adhesion and senescence. *J. Biol. Chem.* **272**, 8157–8160.
46. Kim, Y., Peyrol, S., So, C. K., Boyd, C. D., and Csiszar, K. (1999) Coexpression of the lysyl oxidase-like gene (LOXL) and the gene encoding type III procollagen in induced liver fibrosis. *J. Cell. Biochem.* **72,** 181–188.
47. Tchaparian, E. H., Uriu-Adams, J. Y., Keen, C. L., Mitchell, A. E., and Rucker, R. B. (2000) Lysyl oxidase and P-ATPase-7A expression during embryonic development in the rat. *Arch. Biochem. Biophys.* **379,** 71–77.
48. Houen, G. (1999) Mammalian Cu-containing amine oxidases (CAOs): new methods of analysis, structural relationships, and possible functions. *APMIS* **96(Suppl.),** 1–46.
49. Seiler, N. (2000) Oxidation of polyamines and brain injury. *Neurochem. Res.* **25,** 471–490.
50. Klinman, J.P. (1996) New quinocofactors in eukaryotes**.** *J. Biol. Chem.* **271**, 27,189–27,192.
51. Buffoni, F., Pino, R., and Dal Pozzo, A. (1995) Effect of tripeptide–copper complexes on the process of skin wound healing and on cultured fibroblasts. *Arch. Int. Pharmacodyn. Ther*. **330**, 345–360.
52. Maehara, M., Ogasawara, N., Mizutani, N., Watanabe, K., and Suzuki, S. (1983) Cytochrome c oxidase deficiency in Menkes kinky hair disease. *Brain Dev.* **5,** 533–540.
53. Robain, O., Aubourg, P., Routon, M. C., Dulac, O., and Ponsot, G. (1988) Menkes disease: a Golgi and electron microscopic study of the cerebellar cortex. *Clin. Neuropathol.* **7,** 47–52.
54. Sparaco, M., Hirano, A., Hirano, M., DiMauro, S., and Bonilla, E. (1993) Cytochrome c oxidase deficiency and neuronal involvement in Menkes' kinky hair disease, immunohistochemical study. *Brain Pathol.* **3**, 349–354.
55. Morgello, S., Peterson, H. C., Kahn, L. J., and Laufer, H. (1988) Menkes kinky hair disease with "ragged red" fibers. *Dev. Med. Child Neurol.* **30**, 808–820.
56. Inagaki, M., Hashimoto, K., Yoshino, K., Ohtani, K., Nonaka, I., Arima, M., et al. (1988) Atypical form of Menkes kinky hair disease with mitochondrial NADH–CoQ reductase deficiency. *Neuropediatrics* **19**, 52–55.
57. Pedespan, J. M., Jouaville, L. S., Cances, C., Letellier, T., Malgat, M., Guiraud, P., et al. (1999) Menkes disease: study of the mitochondrial respiratory chain in three cases. *Eur. J. Paediatr. Neurol.* **3**, 167–170.
58. Levenson, C. W., Song, Y., Narayanan, V. S., Fitch, C. A., and Yeiser, E. C. (1999) Regulation of mitochondrial cytochrome b mRNA by copper in cultured human hepatoma cells and rat liver. *Biol. Trace. Element Res*. **70**, 149–164.
59. Marklund S. L. (1984) Extracellular superoxide dismutase and other superoxide dismutase isoenzymes in tissues from nine mammalian species. *Biochem. J.* **222,** 649–655.
60. Petrovic, N., Comi, A., and Ettinger, M. J. (1996) Copper incorporation into superoxide dismutase in Menkes lymphoblasts. *J. Biol. Chem.* **271**, 28,335–28,340.
61. Marklund, S. L. (1990) Expression of extracellular superoxide dismutase by human cell lines. *Biochem. J.* **266,** 213–219.
62. Oury, T. D., Day B. J., and Crapo, J. D. (1990) Extracellular superoxide dismutase in vessels and airways of humans and baboons. *Free Radical Biol. Med.* **20,** 957–965.
63. Strαlin, P., Karlsson, K., Johansson B. O., and Marklund, S. L. (1995) The interstitium of the human arterial wall contains very large amounts of extracellular superoxide dismutase. *Arterioscler. Thromb. Vasc. Biol.* **15**, 2032–2036.
64. Marklund, S. L. (1984) Extracellular superoxide dismutase in human tissues and human cell lines. *J. Clin. Invest.* **74,** 1398–1403.
65. Gitlin, J. D., Schroeder, J. J., Lee-Ambrose, L. M., and Cousins, R. J. (1992) Mechanisms of caeruloplasmin biosynthesis in normal and copper-deficient rats. *Biochem. J.* **282**, 835–839.
66. Mittal, B. and David, S. (1994) A monoclonal antibody that recognizes an adhesion molecule expressed by certain cells of neuroectodermal and mesenchymal origin. *Mol. Cell. Neurosci.* **5,** 63–77.
67. Mittal, B. and David, S. (1994) The role of an astrocyte surface molecule in neuronal migration in the developing rat cerebellum. *Mol. Cell. Neurosci.* **5**, 78–86.
68. Waggoner, D. J., Bartnikas, T. B., and Gitlin, J. D. (1999) The role of copper in neurodegenerative disease. *Neurobiol. Dis.* **4,** 221–230.
69. Vulpe, C.D., Kuo, Y.M., Murphy, T.L., Cowley, L., Askwith, C., Libina, N., et al. (1999) Hephaestin, a ceruloplasmin homologue implicated in intestinal iron transport, is defective in the sla mouse. *Nature Genet.* **21**, 195-199.

70. Kaufman, R. J., Pipe, S. W., Tagliavacca, L., Swaroop, M., and Moussalli, M. (1997) Biosynthesis, assembly and secretion of coagulation factor VIII. *Blood Coagul. Fibrinolysis* **8**, S3–S14.
71. Yu, J., Yu, D. W., Checkla, D. M., Freedberg, I. M., and Bertolino, A. P. (1993) Human hair keratins. *J. Invest. Dermatol.* **101(1 Suppl.)**, 56S–59S.
72. Wang, H., Parry, D. A., Jones, L. N., Idler, W. W., Marekov, L. N., and Steinert, P. M. (2000) In vitro assembly and structure of trichocyte keratin intermediate filaments. A novel role for stabilization by disulfide bonding. *J. Cell Biol.* **25**, 1459–1468.
73. Hoober, K. L., Joneja, B., White, H. B. , III, and Thorpe, C. (1996) A sulfhydryl oxidase from chicken egg white. *J. Biol. Chem.* **271**, 30,510–30,516.
74. Hoober, K. L., Sheasley, S. L., Gilbert, H. F., and Thorpe, C. (1999) Sulfhydryl oxidase from egg white. A facile catalyst for disulfide bond formation in proteins and peptides. *J. Biol. Chem.* **274**, 22,147–22,150.
75. Hoober, K. L., Glynn, N. M., Burnside, J., Coppock, D. L., and Thorpe, C. (1999) Homology between egg white sulfhydryl oxidase and quiescin Q6 defines a new class of flavin-linked sulfhydryl oxidases. *J. Biol. Chem.* **274**, 31,759–31,762.
76. Yamada, H., Suga, Y., Takamori, K., and Ogawa, H. (1994) Stoichiometry of the reaction catalyzed by skin sulfhydryl oxidase. *J. Dermatol.* **21**, 394–396.
77. Danks, D. M. (1983) Copper deficiency and the skin, in *Biochemistry and Physiology of the Skin* (Goldsmith, L. A., ed.), Oxford University Press, New York, pp. 1102–1112.
78. Petris, M. J., Strausak, D., and Mercer, J. F. (2000) The Menkes copper transporter is required for the activation of tyrosinase. *Hum. Mol. Genet.* **9**, 2845–2851.
79. Beeler, T. J., Fu, D., Rivera, J., Monaghan, E., Gable, K., and Dunn, T. M. (1997) SUR1 (CSG1/BCL21), a gene necessary for growth of Saccharomyces cerevisiae in the presence of high Ca^{2+} concentrations at 37 degrees C, is required for mannosylation of inositolphosphorylceramide. *Mol. Gen. Genet.* **255**, 570–579.
80. Hara, A. and Taketomi, T. (1986) Cerebral lipid and protein abnormalities in Menkes' steely-hair disease. J*pn. J. Exp. Med.* **56,** 277–284.
81. Liang, P. and Pardee, A. B. (1998) Differential display. A general protocol. *Mol. Biotechnol.* **10**, 261–267.
82. Bauer, D., Muller, H., Reich, J., Riedel, H., Ahrenkiel, V., Warthoe, P., et al. (1993) Identification of differentially expressed mRNA species by an improved display technique (DDRT-PCR). *Nucleic Acids Res.* **21**, 4272–4280.
83. http://www.ncbi.nlm.nih.gov/BLAST/
84. http://www.ebi.ac.uk/fasta3/
85. Kosonen, T., Uriu-Hare, J. Y., Clegg, M. S., Keen, C. L., and Rucker, R .B. (1997) Incorporation of copper into lysyl oxidase. *Biochem. J.* **327**, 283–289.
86. Rucker, R. B., Romero-Chapman, N., Wong, T., Lee, J., Steinberg, F. M., McGee, C., et al. (1996) Modulation of lysyl oxidase by dietary copper in rats. *J. Nutr.* **126**, 51–60.
87. Yeowell, H. N., Marshall, M. K., Walker, L. C., Ha, V., and Pinnell, S. R. (1994) Regulation of lysyl oxidase mRNA in dermal fibroblasts from normal donors and patients with inherited connective tissue disorders. *Arch Biochem. Biophys.* **308,** 299–305.
88. Gacheru, S., McGee, C., Uriu-Hare, J. Y., Kosonen, T., Packman, S., Tinker, D., et al. (1993) Expression and accumulation of lysyl oxidase, elastin, and type I procollagen in human Menkes and mottled mouse fibroblasts. *Arch. Biochem. Biophys.* **301,** 325–329.
89. Wang, Y. R, Wu, J. Y., Reaves, S. K., and Lei, K. Y. (1996) Enhanced expression of hepatic genes in copper-deficient rats detected by the messenger RNA differential display method. *J. Nutr.* **126**, 1772–1781.
90. Kodama, H., Okabe, I., Yanagisawa, M., and Kodama, Y. (1989) Copper deficiency in the mitochondria of cultured skin fibroblasts from patients with Menkes syndrome. *J. Inherited Metab. Dis.* **12**, 386–389.

21

Regulation by Copper of the Expression of Human Bis, a New Gene Involved in the Cellular Stress Response to Metals

Maria Gabriella Pagliuca, Rosa Lerose, and Arturo Leone

1. INTRODUCTION

It is widely accepted that copper is an essential trace element required for survival by all organisms from bacteria to humans *(1)*. Because of their chemical properties, copper ions are able to adopt distinct redox states, either in an oxidized [Cu(II)] or in a reduced state [Cu(I)]. Consequently, Cu ions are involved as important cofactors in redox reactions catalyzed by proteins controlling fundamental biological functions, like mithocondrial respiration or cell growth and development. Severe alterations in the activities of these enzymes cause disease states or pathologic conditions. The most common effects of copper deficiency include anemia, neutropenia, bone abnormalities, and malabsorption syndrome *(2)*.

Excess copper is toxic, depending on the concentrations of the metal present in the environment *(3)*. The molecular mechanisms underlying the cytotoxicity of copper have been defined only partially [i.e., direct inactivation of essential enzymes through binding to some sulfhydryl groups *(4)* or production of reactive oxygen species [ROS] *(5)*]. The redox activity of this metal ion strongly resembles the chemistry of iron (Fe): Cu readily participates in reactions resulting in the production of highly ROS, including hydroxyl radicals. The latter are believed to be responsible for devastating cellular effects like lipid peroxidation of membranes, direct oxidation of proteins, and cleavage of DNA and RNA molecules. Indeed, the generation and action of ROS are thought to be among the major contributing factors to the development of cancer, diseases of the nervous system, and aging *(6)*. In addition to the generation of ROS, Cu may manifest its toxicity by displacing other metal cofactors from their natural ligands in key cellular signaling proteins. An example is the replacement of Zn(II) by Cu(II) in the zinc-finger DNA-binding domain of the human estrogen receptor. Such displacement changes the tertiary structure of the protein, causing, in vitro, a defective binding to its cognate target DNA sequences. In vivo, such a mechanism would interfere with its role in the hormone-dependent signal transduction pathway *(7)*. Precise regulatory mechanisms must be present in the cell to prevent the accumulation of Cu ions to toxic levels and to preserve their essential levels. Alterations in these balances cause severe lethal diseases, as demonstrated in two inherited disorders of copper metabolism in humans, the Menkes and the Wilson's diseases *(8)*.

A number of mammalian genes are transcriptionally regulated by heavy metals *(9)*. These genes include those coding for metallothioneins *(MTs) (10,11)* and the 70-kDa heat-shock protein *(HSP70) (12)*.

From: Handbook of Copper Pharmacology and Toxicology
Edited by: E. J. Massaro © Humana Press Inc., Totowa, NJ

Repeated cis-acting DNA elements, the metal-responsive elements (MREs), present in multiple copies in the promoter region of MT genes, regulate the response of these genes to various heavy metals such as Cd, Zn, Cu, and Hg *(13,14)*. One MRE-binding transcription factor, named MTF-1, has been described in detail so far, although the mechanisms controlling the signaling process are still unclear *(15)*. The MT proteins are small, with sequences conserved during the evolution, and characterized by a high content of cysteine residues (approx 33%). The mammalian proteins are generally 61 amino acids long with a molecular weight of 6000 Daltons and contain 20 cysteines in the sequence Cys-Cys or Cys-X-Cys. These amino acids are the coordination sites for the binding of up to 7 Zn(II) or Cd(II) atoms; in the case of copper, a total of 12 ions can be bound, with a tetrahedral geometry *(11,16)*. MTs play a role in resistance to metal toxicity, including copper toxicity *(17)*, although other functions in the storage, transport, and distribution of the different heavy metals in the cells have been reported *(18)*.

The *Hsp* genes are known to be regulated by various stresses other than heat, including exposure to amino acid analogs, heavy metals, and oxidizing agents *(19)*. The Hsp proteins are divided into subfamilies characterized by their molecular mass *(20)*. The 70-kDa and 60-kDa *Hsp* gene families participate to the folding, assembly, and translocation of proteins between the intracellular compartments *(19,20)*. Other Hsps are involved in the degradation of misfolded proteins *(21)*. Many Hsps are constitutively expressed; in situations of stress, the transcription of these genes is increased, with oligomerization and binding of heat-shock factors (HSFs) to heat-shock elements (HSE) present in multiple copies in the promoter regions of Hsp *(22)*. This mechanism of activation of transcription appears to be in common for heat and heavy metals, like copper and zinc *(23)*. Hsps have a distinct domain structure with an ATP-binding site located at the amino terminal end and a carboxyterminal domain with high affinity for misfolded or aberrant proteins and polypeptides. Although both the inducible form of Hsp70 and its cognate constitutive equivalent Hsc70 by itself may exert some protective effects on denatured or misfolded proteins, they generally act in concert with other cellular components which themselves associate with Hsc70 *(24)*. At the moment, Hsp70 function appears to be modulated by two classes of proteins: (1) chaperone enhancers, such as Hip, which stimulate Hsp70 chaperone activity and the assembly of Hsp70 into macromolecular chaperone-containing complexes, and Hsp40 (Hdj-1) which promotes the Hsp70 ATPase activity *(25)*; (2) chaperone inhibitors, as exemplified by Bag-1 *(26,27)*. Bag-1 associates in vivo and in vitro with Hsp70 and inhibits its protein refolding activity *(28,29)*. Two domains play a critical role in the cellular activity of Bag-1: a C-terminal region, which binds to the Hsp70 ATPase domain and an N-terminal ubiquitinlike domain *(30,31)*. In human HeLa cells, three Bag-1 isoforms have been characterized on the basis of their diverse molecular masses, because of the different start sites for translation initiation *(32)*. Recently, an evolutionarily conserved family of Bag-like proteins has been described, characterized by a common region of roughly 50 amino acid residues at the carboxyl termini—named the "Bag domain"—mediating the binding to the ATPase sites of Hsp70 and Hsc70, and a markedly different N-terminal region, unique for each Bag protein *(33)*. Two members have been most recently isolated, *Bag-4* or SOOD, silencer of death domains, a cloned 60-kDa protein that lacks death domains but specifically binds to and inhibits the death domains of tumor necrosis factor receptor type 1 (TNFR-1) and receptor 3 (DR3) *(34,35)*, and Bis, the product of *Bag-3* gene, a Bcl-2-binding protein that synergizes with Bcl-2 in preventing cell death *(36)*.

In this chapter, we describe that exposure of HeLa cells to copper positively regulates the expression of *Bis* gene, together with Hsp70 and MTs genes. This regulation constitutes a novel data, because *Bag-1*, at the moment the best characterized gene in the *Bag* gene family, is not regulated by stress (temperature, heavy metals). Moreover, copper has a distinct effect on the cell localization of Bis protein: Following growth of the cells in high concentrations of the metal, the protein mobilizes from the cytosol to a perinuclear compartment. Therefore, Bis appears as a new protein involved in the prevention of cellular toxicity by copper.

```
MSAATHSPMM QVASGNGDRD PLPPGWEIKI DPQTGWPFFV DHNSRTTTWN   50
DPRVPSEGPK ETPSSANGPS REGSRLPPAR EGHPVYPQLR PGYIPIPVLH  100
EGAENRQVHP FHVYPQPGMQ RFRTEAAAAA PQRSQSPLRG MPETTQPDKQ  150
RGQVAAAAAA QPPASHGPER SQSPAASDCS SSSSSASLPS SGRSSLGSHQ  200
LPRGYISIPV IHEQNVTRPA AQPSFHQAQK THYPAQQGEY QTHQPVYHKI  250
QGDDWEPRPL RAASPFRSSV QGASSREGSP ARSSTPLHSP SPIRVHTVVD  300
RPQQPMTHRE TAPVSQPENK PESKPGPVGP ELPPGHIPIQ VIRKEVDSKP  350
VSQKPPPPSE KVEVKVPPAP VPCPPPSPGP SAVPSSPKSV ATEERAAPST  400
APAEATPPKP GEAEAPPKHP GVLKVEAILE KVQGLEQAVD NFEGKKTDKK  450
YLMIEEYLTK ELLALDSVDP EGRADVRQAR RDGVRKVQTI LEKLEQKAID  500
VPGQVQVYEL QPSNLEADQP LQAIMEMGAV AADKGKKNAG NAEDPHTETQ  550
QPEATAAATS NPSSMTDTPG NPAAP                             575
```

Fig. 1. Sequence of the Bis protein. Amino acid sequence of human Bis, deduced from the cDNA sequence reported in GenBank; the residues comprising the Bag domain are underlined and the WW domain is framed.

2. RESULTS

2.1. Cloning and Tissue Expression of Bis

A partial clone of Bis, the product of the *Bag-3* gene, a member of the Bcl-2 associated athanogene family of Bcl-2-binding proteins *(36)*, was originally isolated from a cDNA library obtained from HeLa cells grown for 10 h in the presence of 250 μ*M* ZnCl2 *(37)*. Comparison by Blast analysis with the *Bag-3* gene sequence present in GenBank confirmed that the nucleotide sequence of this clone corresponded to Bis sequences in the region between nucleotides 915 and 1728. The full-length 2.-kb Bis cDNA was obtained through reverse transcription–polymerase chain reaction (RT-PCR), using primers deduced from the published sequence *(33)* and as template RNA from zinc-induced HeLa cells *(37)*.

Domain analysis of Bis reveals the previously reported Bag domain and a WW region (Fig. 1). The WW domain is a small globular module composed of 38–40 semiconserved amino acids and is involved in mediating protein–protein interaction *(38)*. Functionally, it is similar to the SH3 domain in the binding to polyproline ligands *(39)*.

The tissue expression profile of the Bis gene was obtained by Northern blot and showed that a single specie of 2.6-kb mRNA was present in a variety of adult human tissues, with high levels in skeletal muscle, heart, and lung (Fig. 2).

2.2 Regulation of the Expression of the Bis Gene by Copper

Because our clone of Bis was isolated from a library made from RNA of zinc-induced HeLa cells, we next examined if copper regulated the expression of this gene. Thus, HeLa cells were exposed for different times to 250 μM and 500 μM CuSO4 and experiments of Northern blot were performed

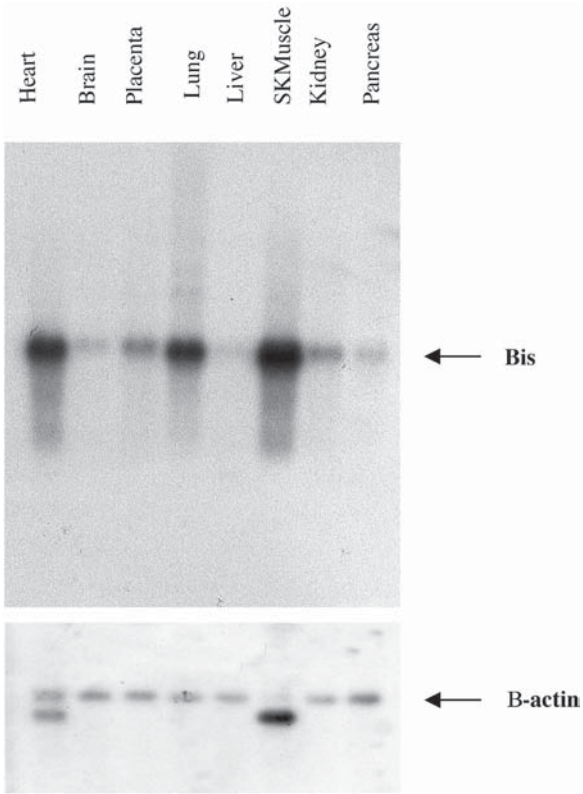

Fig. 2. Tissue expression of the Bis gene. The tissue distribution of Bis mRNA was examined in Northern blot experiments using RNAs from human adult tissues (CLONTECH) and a ^{32}P-labeled human Bis probe, nucleotide region 915–1728 (GenBank). Levels of RNA were normalized for equal amounts of β-actin mRNA.

using as probe the Bis cDNA region between nucleotides 915 and 1728. In Fig. 3 are shown the results: Bis probe hybridized to a single mRNA species, which was accumulated with time-dependent kinetics following exposure to the cited concentrations of copper (Fig. 3A). *Bis* mRNA was highly accumulated between 1 and 6 h after exposure to 250 μM CuSO4 (Fig. 3A: lanes 1, 3, 5, 7, and 9) or 500 μM $CuSO_4$ (Fig. 3A: lanes 2, 4, 6, 8, and 10) with respect to the controls (Fig. 3A–C). Because copper is a known positive regulator of Hsp synthesis (23), we next examined if in the same experimental conditions *Hsp70* expression was activated also. Northern blot experiments were performed on the same samples, using as a probe the human *Hsp70* cDNA. We found that *Hsp70* mRNA was highly accumulated in cells grown in the presence of 250 μM and 500 μM $CuSO_4$, with a kinetic very similar to Bis (Fig. 3B). Finally, a probe of the human MTI-e cDNA, which hybridizes to all the different MT mRNA isoforms, was used to determine the activation of MT genes in these experimental conditions. The kinetic of expression of MTs (Fig. 3A) overlapped with the copper-mediated responses of Bis (Fig. 3C) and Hsp70 genes (Fig. 3B). Therefore copper appear to regulate with similar time-dependent kinetics the expression of Bis together with two other well characterized metal-regulated genes. The lower panel of the figure shows the hybridization of a human ribosomal 28S RNA probe as internal control (Fig. 3D).

2.3 Subcellular Localization of Bis Protein Cells Grown in Absence or in the Presence of High Concentrations of Copper

To examine the intracellular localization of the Bis protein, we used indirect immunofluorescence technique. A polyclonal rabbit antiserum was generated against the last 16 amino acids of the carboxy-

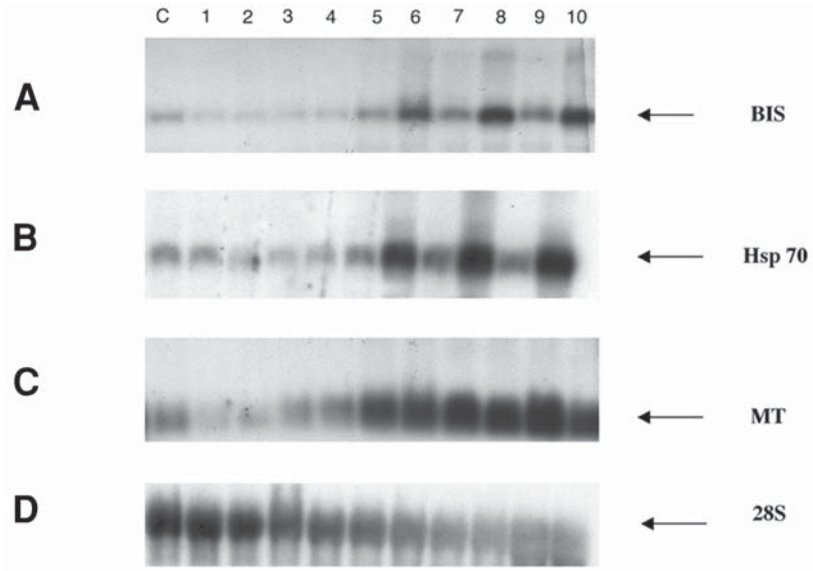

Fig. 3. Kinetics of accumulation of *Bis*, *MT*, and *Hsp70* mRNAs in HeLa cells following exposure to copper. HeLa cells (lanes C, controls) were grown for 12 h in Dulbecco's modified minimal essential medium (DMEM) high glucose (Sigma) supplemented with 2 m*M* glutamine and 100 U/mL penicillin, 50 µg/mL streptomycin, and 10% fetal calf serum (Gibco). Before each experiment, the medium was replaced with DMEM containing 0.1% fetal calf serum. After 20 h, the cells were treated for different times (1 h, lanes 1 and 2; 2 h, lanes 3 and 4; 3 h, lanes 5 and 6; 5 h, lanes 7 and 8; 6 h, lanes 9 and 10) with 250 µ*M* $CuSO_4$ (lanes 1, 3, 5, 7, and 9) or 500 µ*M* (lanes 2, 4, 6, 8, and 10). RNA was extracted with guanidine thiocyanate buffer and 10 µg of total RNA per sample were separated on a 1.5% agarose gel in the presence of formaldehyde and transferred to nylon membranes (Hybond N+, Amersham). The membranes were hybridized in stringent conditions to the following probes: *Bis* cDNA, nucleotide region 915–1728; *hHsp* 70 *(40)* (kind gift of Dr. Gabriella Santoro) and *hMTI-e (41)* full-size cDNAs. Levels of RNA were normalized for equal amounts of 28S RNA in each lane.

terminal tail of Bis protein and was used to detect the subcellular localization of Bis protein in control HeLa cells or in the same cells grown for different times in the presence of 250 µ*M* $CuSO_4$. In control cells, Bis protein appeared equally distributed in the cytoplasm (Fig. 4A). When HeLa cells were exposed to copper for 3 and 6 h Bis showed a perinuclear accumulation (Fig. 4B,C). Because Hsp70 has been shown to interact with the Bis protein, we next examined if the cellular localization of Hsp70 changed in cells exposed to copper. Using an antibody against the inducible form of Hsp70 (iHsp70), we observed that following exposure to the metal, the iHsp70 protein concentrated in the RER as well in a perinuclear compartment (Fig. 5B,C). These data are in agreement with the formation of complexes between iHsp70 and Bis in cadmium-exposed cells, demonstrated in immunoprecipitation experiments *(37)*.

2.4. Synthesis and Regulation of Bis Protein in HeLa Cells

The synthesis of the Bis protein was analyzed in vitro and in vivo. The full-length *Bis* cDNA was subcloned in pBluescript KS, transcribed in the corresponding mRNA, and translated in vitro in the presence of radioactive amino acids. The resulting in vitro translated polypeptide corresponded to 84 kDa, the expected molecular mass of the Bis protein (Fig. 6A, lane 1). We next examined if the same polypeptide was present in HeLa cells and copper regulated its synthesis. Cells were grown in presence or absence of 250 µ*M* $CuSO_4$ for 10 h and Western blot experiments were performed on the protein lysates, separated on sodium dodecyl sulfate–polyacrylamide gel electrophoresis (SDS/

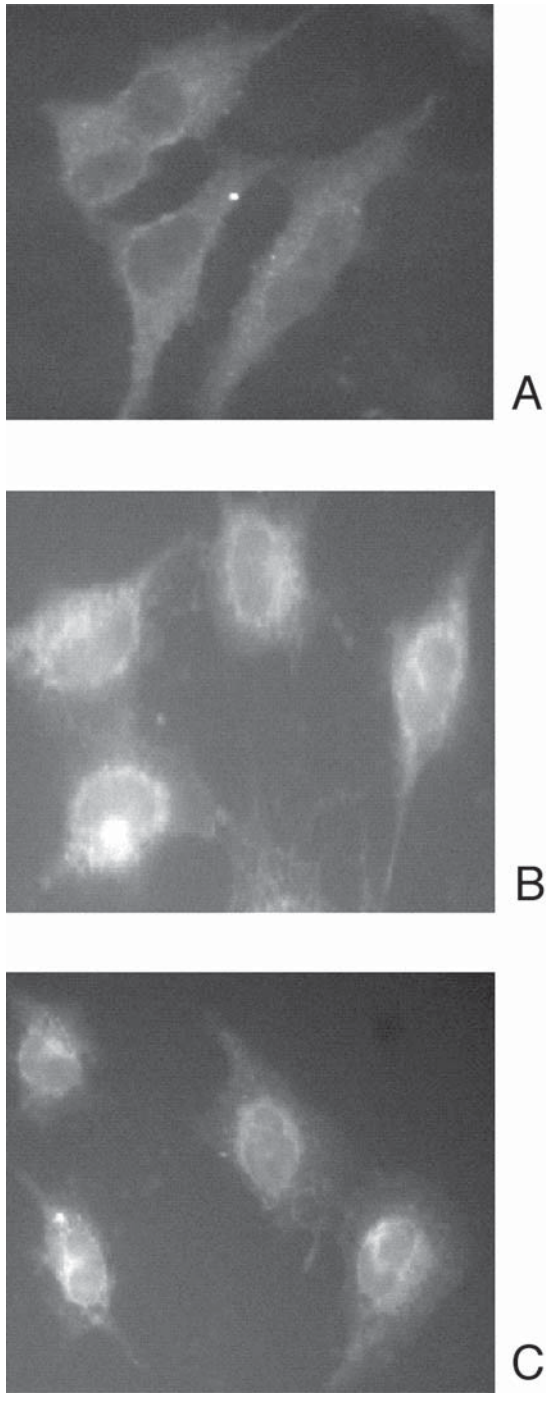

Fig. 4. Copper-regulated cellular trafficking of Bis protein. HeLa cells were grown as described previously in the absence **(A)** or presence of 250 μ*M* $CuSO_4$ for 3 h **(B)** and 6 h **(C)**, plated on glass coverslips and fixed with 3.7% formaldehyde in phosphate-buffered saline (PBS) for 20 min at room temperature, washed two times with PBS, and permeabilized with 0.1% Triton X-100 in PBS for 5 min. The cells were then treated with Bis antibody (dilution 1:400) for 20 min at room temperature, washed with PBS three times, and incubated with goat anti-rabbit FITC-conjugated IgG (dilution 1:100) (Sigma) for 20 min before observation under a fluorescence microscope.

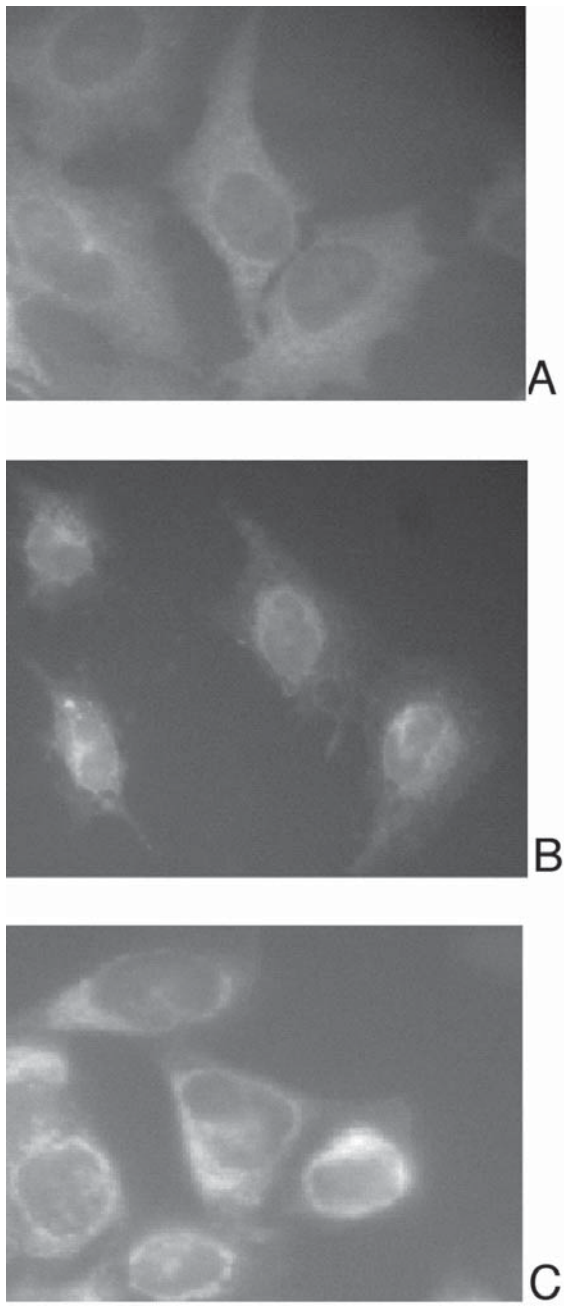

Fig. 5. Localization of Hsp70 in cells exposed to copper. HeLa cells were grown as described previously in the absence **(A)** or presence of 250 μ*M* $CuSO_4$ for 3 h **(B)** and 6 h **(C),** plated on glass coverslips were fixed in 3.7% formaldehyde in PBS for 20 min at room temperature, washed with PBS two times, and permeabilized with 0.1% Triton X-100 in PBS for 5 min. The cells were treated for 20 min at room temperature with a mouse monoclonal antibody raised against the inducible form of Hsp70 (dilution 1:200), and after three washes with PBS, the cells were incubated for 20 min with a FITC-conjugated anti-mouse IgG antibody (dilution 1:100) (Sigma) before observation under a fluorescence microscope.

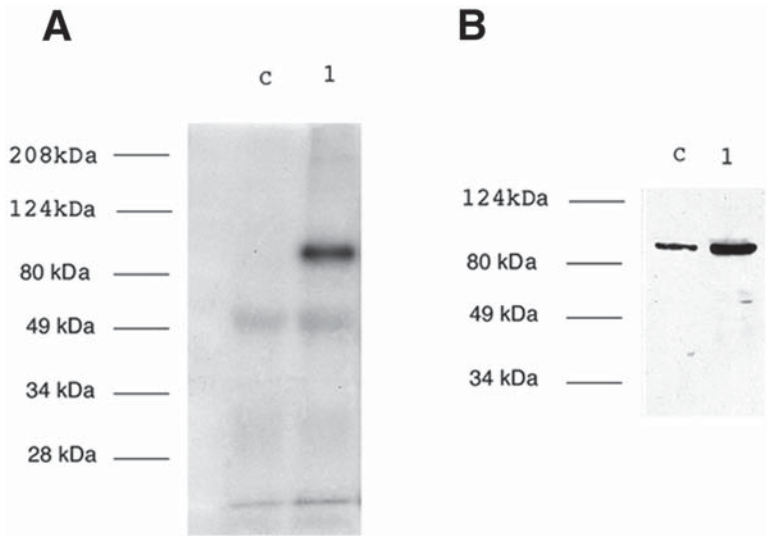

Fig. 6. In vitro and in vivo synthesis of the Bis protein. **(A)** The plasmid (pBluescript KS), containing the full-length *Bis* cDNA, was linearized by digestion with XhoI and was transcribed and translated in vitro using the TNT-coupled reticulocyte lysate system and T3 RNA polimerase (Promega), a mixture of amino acids minus methionine and 2 µL of 14.3 mCi/mL [^{35}S] methionine (Amersham) according to the manufacturer's instructions. A reaction without the plasmid was also performed as a negative control. The translated product were reduced, alkylated, and separated on 10% SDS-PAGE gel *(42)* and revealed by autoradiography. (c) Negative control; 1, transcribed and translated *Bis* cDNA. **(B)** HeLa cells were grown as described previously in the absence **(C)** or presence of 250 µ*M* $CuSO_4$ for 10 h (lane 1). Total cell extracts were reduced, alkylated. and separated on 10% SDS-PAGE *(42)*. Western blot was performed using the rabbit polyclonal anti-Bis antibody. Migration of the ^{14}C-labeled protein molecular-weight markers are indicated on the left.

PAGE), using our anti-Bis antibody. As shown in Fig. 6, the Bis protein was indeed present in control cells (Fig. 6B, lane C) and its synthesis was positively regulated by copper (Fig. 6B, lane 1).

3. DISCUSSION

It is well proved that copper is an essential trace element required for the activity of a number of essential enzymes *(2)*; at the same time, high concentrations of the metal can be toxic for the cells if its levels are not physiological *(3,43)*. Different biochemical mechanisms have been established during evolution to avoid the accumulation of toxic free-copper ions within the cell; the best characterized—and so far the most important—are the enzymatic activities of copper transporters, controlling the amounts of the metal within the different cellular compartments *(44)* and the transcription of genes whose protein products bind the excess of metal (i.e., MTs) *(10,11)* or protect the cells from metal-dependent stress (i.e., Hsps) *(12,20)*. More recently, the production of the intracellular reducing agent glutathione has also been considered to be part of the mentioned mechanisms *(45)*.

The existence of genetic diseases where copper homeostasis is deeply altered provides the opportunity to elucidate the pathways that regulate the levels of the metal within the cell and to identify the genes and the proteins involved, as illustrated in the cases of the X-linked Menkes disease and the autosomal recessive Wilson's disease *(8)*. Progressive neurodegeneration and connective tissue disturbances are the main manifestations of Menkes disease and most of the clinical features delineate a picture of copper deficiency, explained by the malfunction of one or more copper enzymes (i.e., tyrosinase, lysyl oxidase, others). The protein product of the Menkes gene (*MNK* or *ATP7A*) is a transmembrane copper-binding P-type ATPase, the first intracellular copper transporter described in mammals and presents a widespread expression in several organs, with the exception of the liver

(46). The latter is, instead, the preferential tissue for the expression of the Wilson gene (*WND* or *ATP7B*), which codifies for another copper-binding P-type ATPase, highly homologous to the MNK protein *(47)*. Wilson's disease patients are characterized in the greatest number of cases by liver cirrhosis, due to the toxic effects of accumulation of copper in the hepatocytes *(8)*. Interestingly, both ATP7A and ATP7B proteins are localized in the trans-Golgi network and traffic toward an endosomal compartment following exposure of the cells to the metal *(48,49)*. Experiments carried on primary cell lines from patients indicate that both ATPases are involved in the control of the effluxes of copper from the cells *(8)*.

Exposure of cells and organisms to high levels of copper activates two class of gene, *MTs* and *Hsps*, with different roles in the protection from heavy-metal toxicity: MTs act as primary chelators of the free-copper ions, whereas Hsps are induced to preserve the native folding of proteins damaged by those copper ions which escape from the chelating action of MTs *(50)*. We found that Bis, the product of the *Bag-3* gene, initially described as the Bcl-2-binding protein *(36),* is a copper-regulated gene. In HeLa cells grown in two different concentrations of copper, the levels of *Bis* mRNA increased with time-dependent kinetics comparable to those of *MTs* and *Hsp70* mRNAs (Fig. 3). Because the transcriptional regulation of the Bis gene by copper could be mediated either by the HSEs *(22)* or MREs *(13,14)*, we searched for both of these cis-acting sequences in the promoter region of *Bis*—also named *Bag-3*—present in the GenBank. Both types of sequence are present in 1500 nucleotides upstream the transcription start analyzed so far, in strong agreement with the data present in this chapter. A more detailed functional analysis of the promoter region will clarify the role of MRE and HSE in the copper-mediated transcriptional activation of the Bis gene.

Bis gene is highly expressed in the skeletal muscle and heart, followed by the lung (Fig. 2). We do not know at the moment if this is part of other tissue-specific types of gene regulation, or reflects the participation of the *Bis* gene to particular aspects of heavy-metal gene regulation in these tissues, or both mechanisms should be considered. Examples of the latter case are the human *MTIe* and *MT1f* genes, which present both metal and tissue-specific types of regulation *(41)*.

The Bis polypeptide is member of the family of the Bag proteins and has a M_r of a 84 kDa with two important domains: a WW domain located at the N-terminal region and the Bag domain near the C-terminal region, the latter needed for the interaction with Hsp70/Hsc70 (Figs. 1 and 6) *(33)*. Using our antibody against the C-terminal of Bis, we confirmed that the Bis in basal condition is localized in cytoplasm *(36)*. Following exposure of cells to copper, we observed that the protein concentrated with time in a perinuclear region, corresponding to a localization between the rough endoplasmic reticulum and the Golgi apparatus (Fig. 4 and data not shown). Interestingly, also the inducible form of Hsp70 distributes in part in this perinuclear staining, following copper-mediated stress (Fig. 5 and data not shown). The metal-dependent relocalization of the Bis protein strongly resembles the mentioned trafficking of ATP7A and ATP7B proteins from the trans-Golgi network to an endosomal compartment in cells grown in high concentrations of copper *(48,49)*. The compartments involved and the different functions of these genes tend to exclude common mechanisms of cell trafficking, but it is interesting to note that, in both cases, elevation in the extracellular concentrations of copper causes an intracellular relocalization of proteins controlling the amounts of the metal within the different cellular compartments (ATP7A and ATP7B) or participate to the mechanisms of protection of the cells from metal-dependent stress (Bis/Hsp70). New studies are needed to elucidate if proteins other than Hsp70 interact with Bis in stressed cells, eventually through domains different from the Bag region (i.e., WW domain, others), and actively participate to its trafficking. Domain analyses of the Bis/Bag3 protein reveal the previously reported the BAG region and the WW domain, plus seven putative protein kinase C (PKC) sites, five putative CKII phosphorylation sites, several potential tyrosine phosphorylation sites, and a series of proline-rich PXXP repeats of SH3 binding type (D'Ursi et al., data not published). Novel data support this hypothesis: a clone called CAIR-1 (CAI stressed-1) with a nucleotide sequence corresponding to BAG-3 has been recently isolated from human melanoma cells (A2058) exposed chronically to escalating quantities of the calcium entry blocker (CAI) *(51)*. The expression

of the CAIR-1/*Bag3* gene is increased in CAI-treated cells, and the protein forms a ternary complex with two other peptides: HSP70 through the BAG domain and PLC-γ via the PXXP repeats.

ACKNOWLEDGMENTS

A.L. wishes to thank the Dipartimento di Biochimica e Biotecnologie Mediche, Naples, Italy for its generous hospitality in the use of laboratories to perform some of the published experiments and Ornella Moltedo for her expert technical assistance. This work was supported by the following grants to A.L.: Intramural 60% fund, Università di Salerno; P.F. "Biotechnology," C.N.R.; "Stress proteins," Ministero dell'Università e della Ricerca Scientifica e Tecnologica (M.U.R.S.T.).

REFERENCES

1. Linder, M. C. and Goode,C. A. (1991) Introduction and overview of copper as an element essential for life, in *Biochemistry of Elements* (Frieden. E., ed.), Plenum, New York, p. 316.
2. Uauy, R., Olivares, M., and Conzalez, M. (1998) Essentiality of copper in humans. *Am. J. Clin. Nutr.* **67(Suppl.)**, 797s–811s.
3. Bremner, I. (1998) Manifestation of copper excess. *Am. J. Clin. Nutr.* **67(Suppl.)**, 1069–1073s.
4. Nakamura, M. and Yamazaki, I. (1972) One-electron transfer reaction in biochemical system VI. Changes in electron transfer mechanism of lipoamide dehydrogenase by modification sulfhydryl groups. *Biochem. Biophys. Acta* **267**, 249–257.
5. Halliwell, B. and Gutteridge, J. M. C. (1984) Oxigen toxicity, oxygen radicals, transition metals and diseases. *Biochem. J.* **219**, 1–46.
6. Halliwell, B. and Gutteridge, J. M. (1990) Role of free radicals and catalytic metal ions in human disease: An overview. *Methods Enzymol.* **186**, 1–85.
7. Predki, P. F. and Sakar, B. (1992) Effect of replacement of "zinc finger" zinc on estrogen receptor DNA interactions. *J. Biol. Chem.* **267**, 5842–5846.
8. Danks, D. M. (1995) Disorders of copper transport, in *The Metabolic and Molecular Bases of Inherited Disease* (Scriver, C. R., Beaudet, A. L., Sly, W. S., and Valle, D., eds.), vol. 18, McGraw-Hill, New York, pp. 2211-2235.
9. Thiele, D. J. (1992) Metal regulated transcription in eukaryotes. *Nucl. Acid. Res.* **20**,1183–1191.
10. Bremner, I. and Beattie, J. H. (1990). Metallothionein and the trace minerals. *Annu. Rev. Nutr.* **10**, 63–83.
11. Ripa S. and Ripa R. (1999) Metallothionein. *Boll. Chim. Farm.* **138**, 11S–18S.
12. Feldman, D. E., and Frydman, J. (2000) Protein folding in vivo: the importance of molecular chaperones. *Curr. Opin. Struct. Biol.* **10**, 26–33.
13. Richards, RI., Heguy, A., and Karin, M. (1984) Structural and functional analysis of the human metallothionein-Ia gene:differential induction by metal ions and glucocorticoids. *Cell* **37**, 263–272.
14. Stuart, G. W., Searle, P. F., Chen, H. Y., Brinster, R. L., and Palmiter, R. D. (1984) A 12-base-pair DNA motif that is repeated several times in metallothionein gene promoters confers metal regulation to a heterologous gene. *Proc. Natl. Acad. Sci. USA* **81**, 7318–7322.
15. Westin, G., and Schaffner, W. (1988). A zinc-responsive factor interacts with a metal-regulated enhancer element (MRE) of the mouse metallothionein gene. *EMBO J.* **7**, 3763–3770.
16. Rosen, D. R., Siddique, T., and Patterson, D. (1993) Mutations in Cu/Zn superoxide dismutase gene are associated with familial anyotropic lateral sclerosis. *Nature* **362**, 59–62.
17. Winge, D. R. and Miklossy, K. A. (1982) Differences in the polymorphic forms of metallothionein. *Arch. Biochem. Biophys.* **214**, 80–88.
18. Moltedo, O., Verde, C., Capasso, A., Parisi, E., Bonatti, S., Alvarez-Hernandez, et al. (2000) Zinc transport and metallothionein secretion in the intestinal human cell line Caco-2. *J. Biol. Chem.* **275**, 31,819–31,825.
19. Morimoto, R. I. (1998) Regulation of the heat shock transcriptional response: cross talk between a family of heat shock factors, molecular chaperones, and negative regulators. *Genes Dev.* **24**, 3788–3796.
20. Welch, W. J. (1992) Mammalian stress response: cell physiology, structure/function of stress proteins, and implications for medicine and disease. *Physiol. Rev.* **72**, 1063–1081.
21. Hayes, S. A. and Dice, J. F. (1996) Roles of molecular chaperones in protein degradation. *J. Cell Biol.* **132**, 255–258.
22. Morano K. A. and Thiele D. J. (1999) Heat shock factor function and regulation in response to cellular stress, growth, and differentiation signals. *Gene Express* **7**, 271–282.
23. Hatayama, T., Asai, Y., Wakatsuki, T., Kitamura, T., and Imahara. H. (1993) Regulation of hsp70 synthesis induced by cupric sulfate and zinc sulfate in thermotolerant HeLa cells. *J. Biochem.* **114**, 592–597.
24. Gebauer, M., Zeiner, M., and Gehring, U. (1997) Proteins interacting with the molecular chaperone hsp70/hsc70: physical associations and effects on refolding activity. *FEBS Lett.* **417**, 109–113.
25. Freeman, B. C., Myers, M. P., Schumacher, R., and Morimoto, R. I. (1995) Identification of a regulatory motif in Hsp70 that affects ATPase activity, substrate binding and interaction with HDJ-1. *EMBO J.* **14**, 2281–2292.
26. Takayama, S., Sato, T., Krayewski, S., Kochel, K., Irie, S., Millan, J. A., et al. (1995) Cloning and functional analysis of Bag-1: a novel Bcl-2 binding protein with anti-cell death activity. *Cell* **80,** 279–284.
27. Wang, H.-G., Takayama, S., Rapp, U. R., and Reed, J. C. (1996) Bcl-2 interacting protein, Bag-1, binds to and activates the Kinase Raf-1. *Proc. Natl. Acad. Sci. USA* **93,** 7063–7068.

28. Takayama, S., Bimston, D. N., Matsuzawa, S., Freeman, B. C., Aime-Sempe, C., Xie, Z., et al. (1997) Bag-1 modulates the chaperone activity of Hsp70/hsc70. *EMBO J.* **16**, 4887–4896.
29. Zeiner, M., Gebauer, M., and Gehring, U. (1997) Mammalian protein RAP46: an interaction partner and modulator of 70kDa heat shock proteins. *EMBO J.* **16,** 5883–5890.
30. Packham, G., Brimmel, M., and Cleveland, J. L. (1997) Mammalian cells express two differently localized Bag-1 isoforms generated by alternative translation initiation. *Biochem. J.* **328**, 807–813.
31. Froesch, B. A., Takayama, S., and Reed, I. C. (1998) BAG-1L protein enhances androgen receptor function. *J. Biol. Chem.* **273**, 11,660–11,666.
32. Luders, J., Demand, J., and Hohfeld, J. (2000). The ubiquitin-related BAG-1 provides a link between the molecular chaperones Hsc70/Hsp70 and the proteosome. *J. Biol. Chem.* **275**, 4613–4617.
33. Takayama, S., Xie, Z., and Reed, J. C. (1999) An evolutionarily conserved family of Hsp70/Hsc70 molecular chaperone regulators. *J. Biol. Chem.* **274,** 781–786.
34. Frisch, S. M. 1999. Evidence for a function of death-receptor-related, death-domain-containing proteins in anoikis. *Curr. Biol.* **9,** 1047-1049.
35. Jiang, Y., Woronicz, J. D., Liu, W., and Goeddel, D. V. (1999) Prevention of constitutive TNF receptor 1 signaling by silencer of death domain. *Science* **283**, 543–546.
36. Lee, J-H., Takahashi, T., Yasuhara, N., Inazawa, J., Kamada, S., and Tsujimoto, Y. (1999) Bis, a Bcl-2 binding protein that synergized with Bcl-2 in preventing cell death. *Oncogene* **18,** 6183–6190.
37. Pagliuca, M. G., Lerose, R., Cigliano, S. and Leone, A. (2002). The expression and cellular localization of human Bis, a negative regulator of Hsp70 activity, is dependent by heavy metals and temperature, in preparation.
38. Bork. P. and Sudol, M. (1994) The WW domain: a signaling site in dystrophin? *Trends Biochem. Sci.* **19**, 531–533.
39. Macias, M. J., Hyvonen, M., Baraldi, E., Schultz, J., Sudol, M., Saraste, M., et al. (1996) Structure of WW domain of a kinase-associated protein complexed with a proline-rich peptide. *Nature* **382**, 646–649.
40. Macejak, D., Rayfield, M., and Luftig, R. (1990) Isolation and characterization of human HSP70 expressed in *Escherichia coli. Arch. Biochem. Biophys.* **280**, 53–60.
41. Schmidt, C. J. and Hamer, D. H. (1986) Cell specificity and an effect of ras on human metallothionein gene expression. *Proc. Natl. Acad. Sci. USA* **83**, 3346–3350.
42. Bonatti, S. (1983) *Biosynthesis of Sindbis virus membrane glycoproteins in vitro*. Methods Enzymol. **96**, 512-9.
43. Peña, M. M. O., Lee, J., and Thiele, D. J. (1999) A delicate balance: homeostatic control of copper uptake and distribution. *J. Nutr.* **14**, 1251–1260.
44. Radisky, D. and Kaplan, J. (1999) Regulation of transition metal transport across the yeast plasma membrane. *J. Biol. Chem.* **274**, 4481–4484.
45. Abe, T., Yamamura, K., Gotoh, S., Kashimura, M., and Higashi, K. (1998) Concentration-dependent differential effects of *N*-acetyl-L-cysteine on the expression oh HSP70 and methallothionein genes induced by cadmium in human amniotic cells. *Biochem. Biophys. Acta* **1380**, 123–132.
46. Yamaguchi, Y., Heiny, M. E., and Gitlin, J. D. (1993) Isolation and characterization of human liver cDNA as a candidate gene for Wilson disease. *Biochem. Biophys. Res. Commun.* **197**, 271–277.
47. Mercer, J. F. B., Livingston, J., Hall, B., Paynter, J. A., Begy, C., Chandrasekharappa, S., et al. (1993) Isolation of a candidate gene for Menkes disease that encodes a potential heavy metal binding protein. *Nature Genet.* **3**, 20–25.
48. Schaefer, M., Hopkins, R. G., Failla, M. L., and Gitlin, J. D. (1999) Hepatocyte-specific localization and copper-dependent trafficking of the Wilson's disease protein in the liver. *Am. J Physiol.* **276**, 639–646.
49. Petris, M. J. and Mercer, J. F. (1999) The Menkes protein (ATP7A; MNK) cycles via the plasma membrane both in basal and elevated extracellular copper using a C-terminal di-leucine endocytic signal. Hum. Mol. Genet. **8**, 2107–2015.
50. Murata, M., Gong, P., Suzuki, K., and Koizumi, S. (1999) Differential metal response and regulation of human heavy metal-inducible genes. *J. Cell. Physiol.* **180**, 105–113.
51. Doong, H., Price, J., Kim, Y. S., Gasbarre, C., Probst, J., Liotta, LA., et al. (2000) CAIR-1/BAG-3 forms an EGF-regulated ternary complex with phospholipase C-g and Hsp70/Hsc70. *Oncogene* **19**, 4385–4395.

22

Non-Indian Childhood Cirrhosis

Using a Founder Population to Identify the Underlying Genetic Defect

Cisca Wijmenga

1. INTRODUCTION

Inherited liver cirrhosis is rarely observed in infancy or childhood in Western countries, but, recently, 138 cases of an endemic form of infantile cirrhosis were reported from several families in the Tyrol, Austria. These infants had received high amounts of dietary copper released from copper vessels used to prepare their formula milk. Extensive studies in this Tyrolean population suggested that the so-called non-Indian childhood cirrhosis (NICC) occurred only in children with a genetic defect (in homozygous form). These Tyrolean NICC families could be traced back for 10 generations and it was shown that the majority of the families were related to each other. A founder effect was therefore suggested as the most likely reason for the increased frequency of NICC in the Tyrol (i.e., the patients are all descendants of one common ancestor, who introduced the disease mutation into the population many generations ago). Thus, all of the patients in this population should carry the same NICC mutation and share relatively large regions of DNA around the disease locus. This should result in a strong association between the NICC mutation and alleles of marker loci in the surrounding chromosome region. Hence, a genetic approach aimed at pinpointing such an association was considered a good strategy for identifying the underlying genetic defect in these Tyrolean NICC families. However, because of the lethal outcome of the disease, the mapping of the NICC gene had to focus on obligate gene carriers (i.e., both of the patients' parents). A genomewide screen is being undertaken to scan every chromosome for the presence of the NICC gene. So far, the genetic study has excluded some genes known to be associated with copper, such as *ATP7B* and h*CTR1*, as candidate genes for NICC. In addition, approx 70% of the total human genome has also been excluded from containing the NICC gene.

2. COPPER TOXICITY

Copper is one of the essential heavy metals in the life of all organisms, including man; it plays an essential role in cellular respiration, free-radical defense, neurotransmitter function, connective tissue biosynthesis, and cellular iron metabolism *(1)*. Because copper is a necessary metal, it is important that the daily intake of copper in the diet is sufficiently high to maintain these essential functions. The normal human body contains between 70 and 100 mg of copper. Some 15% of the copper taken

From: Handbook of Copper Pharmacology and Toxicology
Edited by: E. J. Massaro © Humana Press Inc., Totowa, NJ

up by the diet is transported into a variety of tissues and the remaining 85% copper is excreted (about 98% of which is excreted via the bile and 2% via the urine) *(1)*.

The acceptable range of oral intake lies between 1.3 and 13 mg Cu/d for adults and between 0.6 and 1 mg Cu/d for children *(2)*. Copper is found in a wide variety of foods, including cereals, meat, fruits, and vegetables, but drinking water can also be a major source of copper intake, especially where copper water pipes are corroded. The World Health Organization (WHO) recommended that the copper concentration in drinking water should not exceed 2000 μg/L *(3)*.

High copper concentrations can induce acute and chronic intoxications in many organisms by damaging DNA, membrane lipids, and proteins *(4)*. Wilson's disease has long been recognized as a genetic disorder characterized by massive copper accumulation, mainly in the liver and brain *(1)*. More recently, the gene defect underlying Wilson's disease has been identified and shown to be a copper-transporting P-type ATPase (*ATP7B*), which is located on chromosome 13, region q14 *(5,6)*. *ATP7B* has been shown to play an important role in the incorporation of copper into ceruloplasmin in the trans-Golgi compartment *(7,8)*.

Indian childhood cirrhosis (ICC) is another disorder resulting from a defect in copper metabolism. ICC was initially only recognized in India *(9)*, but Walker-Smith and Blomfield *(10)* described the disease for the first time outside of India. They reported an Australian boy of non-Indian origin who died at the age of 15 mo from liver cirrhosis resulting from the consumption of drinking water contaminated with copper. His liver histology was later recognized as being identical to ICC *(11,12)*. ICC has also been seen more recently in Austria *(13)*, Germany *(14–18)*, Ireland *(19)*, Italy *(20)*, Japan *(21)*, Kuwait *(22)*, Mexico *(23)*, Saudi Arabia *(24)*, Singapore *(25)*, the United Kingdom *(19,26)* and the United States *(27–30)*. For an overview, *see also* ref. *31*. The non-Indian diseases have been labeled idiopathic copper toxicosis (ICT) or non-Indian childhood cirrhosis (NICC).

Idiopathic copper toxicosis is a prototype of a liver disease attributed to the ingestion of excess copper. However, a recent study by Scheinberg and Sternlieb *(32)* suggests that ICT cannot be caused solely by increased dietary intake of copper. An epidemiological study in the Massachusetts area, where copper concentrations in drinking water used to be high (8 mg/L; under low pH conditions), did not report deaths from any form of liver disease, suggesting that ICT occurs only in children with a predisposing genetic defect. Because we now know that a genetic component is involved, it would be more appropriate to use the term NICC instead of ICT, as idiopathic means "arising spontaneously without recognizable course." Yet, the term ICT is still frequently used in the literature.

3. NICC IN THE TYROL AND GERMANY

Between 1900 and 1974, a group of 138 infants from the Austrian province of Tyrol suffered from childhood liver cirrhosis *(13,33)*. All of the children with symptoms died before the age of 3 yr. The clinical features of the fatal liver cirrhosis observed in the Tyrol showed striking similarities to ICC and ICT. Although the hepatic copper content was not determined in these children, the hepatic morphology was characteristic of ICC/ICT. The high levels of dietary copper were attributed to the formula milk used for feeding the infants; it was routinely prepared in untinned copper and brass vessels until the early 1970s. The disappearance of the disease after 1974 coincided with a change in baby feeding practices and the replacement of untinned copper and brass kitchen vessels. These observations further supported the significant role played by copper cooking utensils. However, the fact that 231 siblings remained healthy although they had been exposed to the same copper-enriched diet as the 138 diseased children implied a genetic predisposition. Segregation analysis suggested that the disease was transmitted as an autosomal recessive disorder, involving equal numbers of both sexes *(13)*. The social and geographical isolation of this population probably led to a high rate of consanguineous marriages (possibly unrecognized as such), resulting in an increased frequency of homozygous offspring *(13)*.

The families affected by Tyrolean NICC were found to be related to each other and they all lived in a rural area of approx 2500 km^2 *(13)*. Back in 1780, the entire population of this area comprised

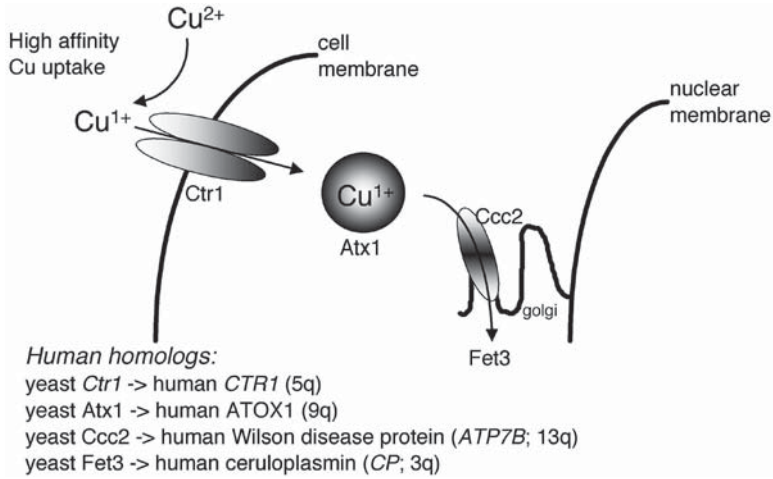

Fig. 1. A simplistic scheme of copper transport into the secretory pathway in yeast. Before the copper ions are taken up by the high-affinity copper transporter Ctr1, the copper II ions are reduced to copper I ions. Inside the cell, copper is transported by the copper chaperone (Atx1) to Ccc2 in the trans-Golgi network, where it is incorporated into ferroxidase (Fet3). In humans, homologous genes have been identified for *Ctr1*, *Atx1*, *Ccc2*, and *Fet3*. It is anticipated that these human genes will exhibit very similar functions. For an overview, *see* ref. *35*.

approx 17,500 inhabitants, increasing to 57,030 inhabitants by 1995 (T. Müller, personal communication). A part of the large Tyrolean NICC pedigree *(13)* containing the nuclear families A, B, C, and I *(34)* could be linked to a common ancestor 10 generations ago. These 4 families came from a small, isolated village, which comprised 2230 individuals in 1760 and 5196 in 1996. The village population presumably expanded only by reproduction rather than by migration of people into the community. Because many people left this rural area because there was insufficient work, the expansion of the population must have been greater than suggested by the numbers given above. Nevertheless, the gene pool is unlikely to have received new mutations in the NICC genes.

A similar large cluster of NICC families has been found in northern Germany *(18)*. Five families with eight NICC cases were identified in Emsland, northern Germany, in a well-defined rural area. Pedigree analysis showed that the families were linked to a common ancestor many generations ago (at least eight). Copper water pipes were suggested as the source of high copper concentrations in tap water. Like the Tyrolean cases, the infants were not breast-fed but fed with formula milk prepared with tap water *(18)*. In addition, the inheritance pattern of NICC in the Emsland families was consistent with an autosomal recessive inheritance of the disease.

4. BASIC DEFECT AND PATHOGENESIS OF NICC

Copper has unambiguously been implicated as a key factor in the development of NICC, because of (1) abnormally high hepatic copper concentrations, (2) identifiable sources of environmental copper exposure in the large majority of cases, (3) disappearance of the disease after a change in cooking habits, and (4) successful treatment of NICC patients with D-penicillamine. It is hypothesized that NICC and ICC are ecogenetic disorders in which an as yet unknown genetic defect only manifests when dietary copper is elevated and a homozygous gene defect is present. The genes whose products are involved in copper metabolism are interesting candidates for this disorder. Much of our knowledge on copper transport and distribution comes from studying the yeast *Saccharomyces cerevisiae (35)*. The genes involved in copper metabolism have been highly conserved between eukaryotic organisms (Fig. 1). An example of a conserved gene is the yeast *Ccc2* gene *(36)*, which is homologous to the human *ATP7B* gene involved in Wilson's disease. Given the clinical and pathological similarities

between NICC and Wilson's disease, several authors have proposed that ICC and NICC might, in fact, represent allelic variants of Wilson's disease by showing mutations in the *ATP7B* gene *(37–40)*.

The hypothesis that ICC and NICC might be allelic variants of Wilson's disease was originally based on the hepatic copper accumulation observed for all of these copper-overload syndromes *(13,40–42)*. The genetic component that was recognized in ICC *(43)* and NICC *(40)* has been used as a further argument to support this concept. The possibility that all of these disorders are caused by mutations in the same gene has not been ruled out, albeit that the clinical and biochemical differences between Wilson's and non-Wilsonian copper toxicosis appear to outweigh their similarities. Wilson's disease is generally believed not to manifest before the age of 6 yr, whereas ICC and NICC usually present in the first few years of life *(13,32)*. However, recent studies indicate a wider spectrum of clinical variability, particularly with respect to age of onset, than has generally been considered typical for Wilson's disease *(38)*. We were therefore interested in investigating whether *ATP7B* mutations could cause Tyrolean NICC.

5. GENE MAPPING BASED ON IDENTITY BY DESCENT

The high frequency of NICC in an isolated rural area in the Tyrol suggested a founder effect (i.e., the affected individuals are all descendants of a common ancestor who introduced the NICC mutation into the population many generations ago) (Fig. 2). If there had been a lack of selective pressure against this mutant allele, the allele could have spread through the population so that a large majority of individuals would have inherited the same mutant gene identical by descent (IBD) either as a gene carrier or as a patient. In theory, the location of the gene mutation in patients should be revealed by *homozygosity mapping*, a mapping approach based on the inheritance of two identical copies of the disease locus by the affected child from a common ancestor (i.e., homozygosity by descent [HBD]) *(44)* (Fig. 3).

The size of the region around a disease locus that shows HBD in an affected inbred individual is determined by the number of meiotic steps that separate the affected individual from the common ancestor who carried a single copy of the disease gene on one of his/her chromosomes. In every meiotic step, recombination will lead to a reduction of the shared chromosomal segment (*see* Fig. 3). This mapping method therefore works extremely well when the patient is the product of a first- or second-cousin marriage (first cousins are separated by four meiotic steps, and second cousins by six meiotic steps) (Fig. 4). Relatively large regions (i.e., haplotypes) of approx 20–30 centiMorgans (cM) around the disease locus can be expected to be IBD in patients produced from these marriages *(45)*. The sensitivity with which homozygous regions can be detected is based on the resolution of the genetic markers used for mapping studies. Currently, most marker maps for genomewide mapping studies are spaced 5–10 cM apart. As the number of meiotic steps between a patient and a common founder increases, the homozygous region around the disease gene mutation becomes more difficult to observe. This is expected to be the case for Tyrolean NICC *(13,33,34)*. Nevertheless, disease chromosomes should still share a reasonable amount of DNA around their disease mutation (e.g., chromosomes A and B in Fig. 2). These conserved regions of IBD around disease mutations can be identified by a search for haplotypes shared between individual patients.

More recently, founded populations (approx 8–15 generations ago) have become excellent resources for mapping rare diseases with a simple inheritance pattern: We can search for segments that are *shared by patients* and then demonstrate that this sharing is IBD (Fig. 4). This haplotype sharing approach has been extremely useful in mapping a number of rare disease genes, including the gene involved in benign recurrent hepatic cholestasis (BRIC) *(46)*, Byler's disease *(47)*, and North American childhood cirrhosis *(48)*. The BRIC gene, for example, was localized to chromosome 18 by performing a genomewide screen on only three patients from a religiously isolated fishing community in the Netherlands. Although the chromosomes of these three BRIC patients had undergone at least six meioses since their shared origin, the BRIC haplotype was still shared over a region of more than 20 cM *(46)*.

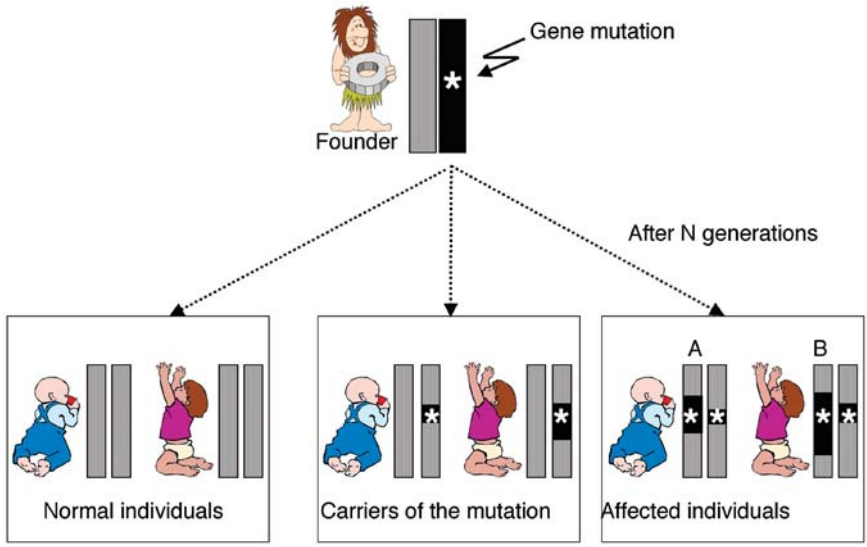

Fig. 2. A schematic representation of the effects of a founder effect in a population that expanded mainly by reproduction. The chromosome with the disease mutation (indicated by an asterisk) is transmitted by the founder through many generations; because of recombination, the size of the DNA flanking the mutation (in black) has been reduced. In the current population—consisting of normal, carriers, and affected individuals—each mutation is identical to the one that was already present in the founder of the population. However, the size of the ancestral DNA flanking the mutation (depicted in black) is different on each chromosome. The two bars represent a pair of homologous chromosomes.

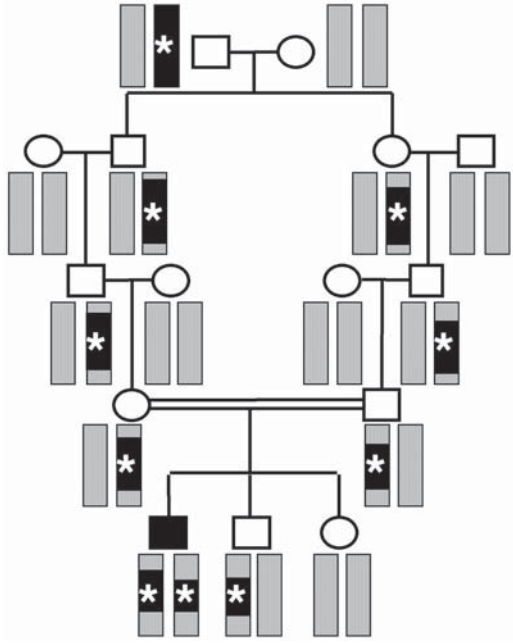

Fig. 3. The principle of homozygosity mapping. Homozygosity for the disease mutation (indicated by an asterisk) is the result of the inheritance of two copies of the mutant gene. Because this mutation was originally present in one of the two founders of this family, the two copies of the mutant gene (and its surrounding DNA) are identical by descent. The patient is therefore not only homozygous for the mutation responsible for the disease but also for the DNA directly flanking the mutation (i.e., the black region).

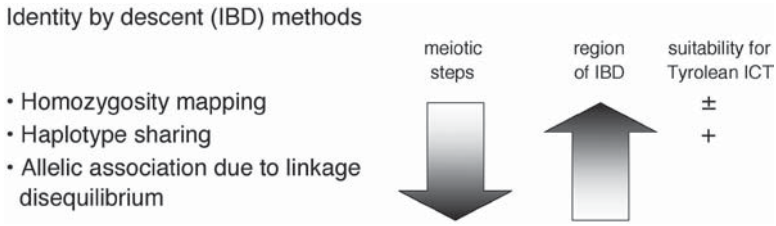

Fig. 4. The suitability of the different identity by descent methods is determined by the number of meiotic steps that separate patients or chromosomes from each other.

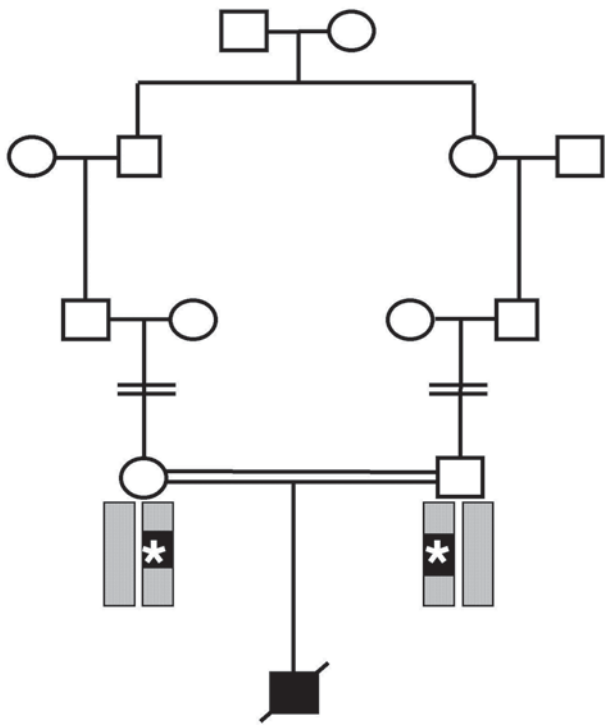

Fig. 5. The situation found in the Tyrolean NICC families. Haplotype sharing around the disease mutation can only be carried out using the obligate gene carriers (i.e., the patients' parents).

The situation for the Tyrolean NICC is, however, more complicated. The disease is lethal when left untreated, although now treatment can be either medication (e.g., D-penicillamine) or a liver transplantation. In the Tyrol, there is only one patient who has received a liver transplant and who is still alive and available for study (unpublished). All of the remaining patients have died from liver cirrhosis *(13)*. Nevertheless, pairs of parents were identified who had had at least one NICC child (thus, both the parents must be obligate carriers for the NICC mutation on one of their chromosomes and, consequently, each parent was expected to have one copy of a [partly] shared haplotype [Fig. 5]). For families A, B, C, and I *(34)*, the number of meiotic steps between the parents ranged from 5 to 19. Such relationships should result in IBD sharing of about 6 cM (for 20 meiotic steps) to more than 20 cM (for 5 meiotic steps) *(45)*.

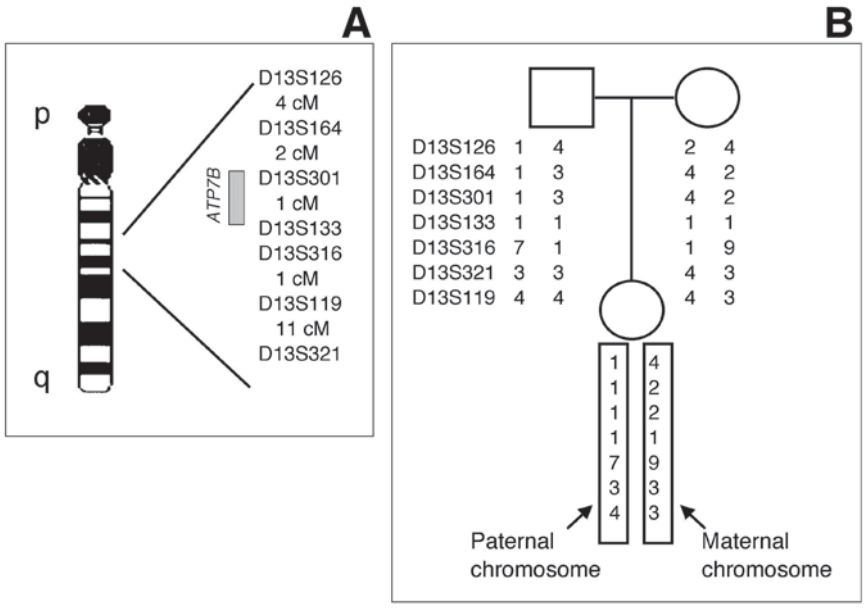

Fig. 6. (A) Map of the genetic markers surrounding the *ATP7B* gene on 13q14. The distance between the markers is given in centiMorgans. **(B)** An example of how haplotypes are constructed in small families (comparable to the Tyrolean NICC families). The alleles present in the child are used to determine which combination of alleles (i.e., haplotype) is inherited from the father and which from the mother. In this way, the two chromosomes in both parents can be arranged in two haplotypes (i.e., a grandpaternal and a grandmaternal chromosome).

6. EXCLUDING *ATP7B* AS A CANDIDATE GENE FOR TYROLEAN NICC

Seven individual genetic markers within or in the immediate vicinity of *ATP7B* at chromosome location 13q14.3 (Fig. 6A) were typed in 15 Tyrolean NICC parents. These 15 gene carriers have a total of 30 chromosomes, at least 15 of which are expected to carry the NICC mutation. The marker alleles were manually arranged into haplotypes (Fig. 6B) and compared between the obligate carriers to see if a shared chromosomal segment surrounding the *ATP7B* gene could be identified. The constructed haplotypes for NICC carriers did not demonstrate any sharing *(34)*. These results were strengthened by the observation that D13S301, a genetic marker located within intron 1 of the *ATP7B* gene, showed strong evidence against being associated with Tyrolean NICC. For D13S301, seven different alleles were identified among 15 obligate gene carriers. If a mutation within the *ATP7B* gene was involved in Tyrolean NICC, all of the gene carriers should share one identical mutant copy of the *ATP7B* gene. As a consequence, this mutant copy should be identifiable by virtue of a particular D13S301 allele. However, the most commonly observed D13S301 allele was allele three and only 7 of the 15 obligate gene carriers shared this allele. These data indicated that the Tyrolean NICC phenotype is a distinct genetic entity, clearly separate from Wilson's disease, and involving another, as yet unidentified, genetic locus.

7. TOWARD IDENTIFYING THE NICC GENE

Apart from *ATP7B*, there are a few other copper-related genes that were considered candidates for Tyrolean NICC, namely the copper transporter *CTR1 (49)* and the copper chaperone *HAH1* or *ATOX1 (50)* (Fig. 1). Using the same strategy as that used for *ATP7B,* we were able to exclude *CTR1* as a candidate gene for Tyrolean NICC, as we found no shared haplotype between the 15 NICC parents and the haplotypes constructed from genetic markers within and surrounding the *CTR1* gene on

chromosome 5q (unpublished data). However, the exact location of the *ATOX1* gene on chromosome 9q with respect to the genetic markers used was not known at that time (1998), so that we were unable to test the region encompassing the *ATOX1* gene for haplotype sharing in the Tyrolean NICC parents.

We therefore set out to screen the entire genome for the presence of a NICC gene using the same eight Tyrolean families. In total, the study consisted of 32 individuals: 15 obligate gene carriers (the patients' parents) and 17 siblings. Although the genetic status of the siblings is unknown, they were important for two reasons: (1) to check for typing inconsistencies; the genotypes observed in the siblings should be present in the parents; (2) to reconstruct parental haplotypes; the children are necessary to reconstruct the paternal, maternal, and grandparents' chromosomes by identifying which set of marker alleles (i.e., haplotype) is inherited from each of the parents (*see also* Fig. 6B).

In order to perform a genomewide screen, we have a panel of 450 polymorphic markers commonly used for genetic mapping studies. Dr. James Weber at the Marshfield Medical Research Foundation (Marshfield, WI, USA) in collaboration with the Cooperative Human Linkage Center (Iowa City, IA, USA) developed this panel *(51,52)*. These markers, based on the presence of simple tandem repeat sequences in the human genome, the so-called microsatellite repeats *(53,54)*, can be detected by amplifying the DNA containing each marker by polymerase chain reaction (PCR), followed by size separation on an automated DNA sequence analyzer. The markers employed in this study are mainly trinucleotide and tertranucleotide repeats, which show an average heterozygosity of 76%. This means that, for each marker, 76% of the individuals tested will reveal two different alleles (i.e., that they are heterozygous). The 450 markers cover all 22 autosomes and the sex chromosomes. Because the total human genome measures about 3300 cM *(55)*, the average distance between the markers is about 8 centiMorgan. One cM in genetic distance corresponds to a physical distance of about 1 million base pairs.

Each of the 32 individuals involved in the genomewide screen was tested with the 450 genetic markers, resulting in a total of 14,400 genotypes (Fig. 7). The statistical analysis of the data was performed in two ways: (1) testing single markers by association analysis based on linkage disequilibrium; if a haplotype is shared between obligate gene carriers, the frequency of the individual marker alleles comprising this haplotype should be overrepresented on chromosomes containing the disease mutation *(34)*; (2) by simultaneously testing multiple markers by constructing haplotypes from any two or three consecutive markers and then looking for sharing between the 15 obligate gene carriers (the patients' parents). The search for shared haplotypes on a genomewide scale proved to be fairly complicated. The statistical programs currently available were not developed for situations in which the patients are unavailable and we therefore had to develop our own software tools. Such a statistical analysis requires weeks of computation time because of the large number of haplotypes that need to be compared to each other. In addition, such an approach is extremely sensitive to the order of markers along the chromosome and to the distance between consecutive markers. The order and distances of the current marker maps are based on a set of reference families from the Centre d'Étude du Polymorphisme Humain (CEPH) *(56)*. Although the order of the markers is becoming more reliable with the increasing availability of physical data on the human genome, the genetic distances between the markers still show rather broad confidence limits.

The lod (a statistic for evaluating pedigrees for linkage) score was calculated for each of the 450 markers tested. In this situation the lod score represents the likelihood of association between the NICC gene and a particular marker. A lod score of +3 or higher (likelihood >1000:1) should be regarded as evidence for association; we regarded a lod score of –1 or lower (likelihood <1:10) as evidence against association. The lod scores between +3 and –1 are inconclusive, although every lod score above +1 is of potential interest for further investigation.

The single-marker analysis using 450 genetic markers allowed us to exclude 67% of the genome as a possible site for the Tyrolean NICC gene (these where all chromosomal regions where the lod score reached a value of –1 or lower). These markers mapped to all chromosomes. A total of 58 gaps remained (for an example, *see* Fig. 8A) that needed to be analyzed using additional markers. The

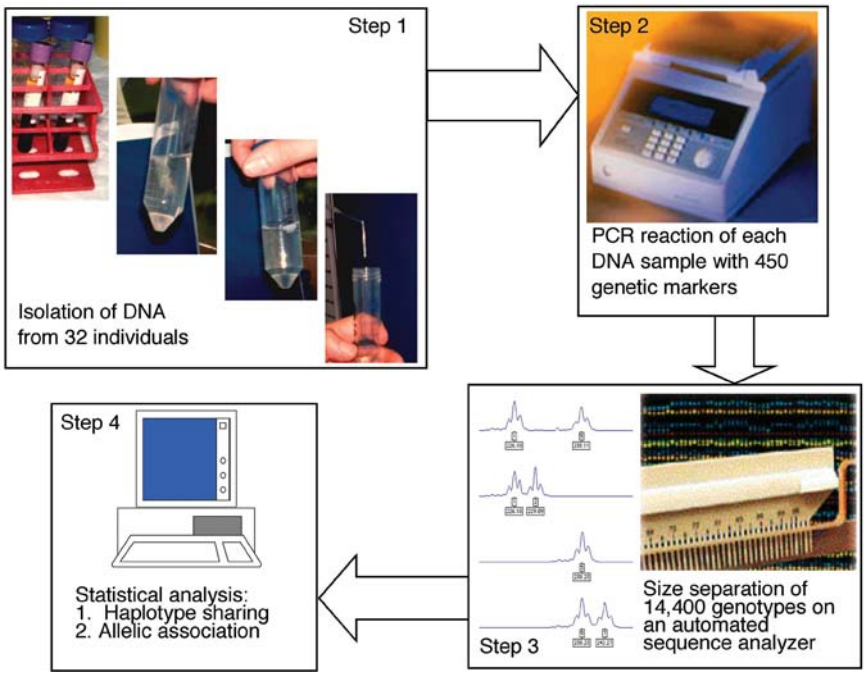

Fig. 7. Overview of the different laboratory steps taken in a genomewide screening approach.

sizes of these gaps ranged from 5 to 45 cM. Six regions on chromosomes 6, 11, 13, 14, 17, and 19 were identified that showed some degree of association with certain marker alleles (for an example, *see* Fig. 8A). Some of the 58 gaps have been filled with additional markers, allowing us to exclude an ever larger part of the human genome as a possible site for the Tyrolean NICC gene. Once we have scrutinized the total human genome, we will start to follow up those regions that show association by constructing haplotypes using a dense set of markers (i.e., one genetic marker every centiMorgan).

8. COMPLICATING FACTORS IN MAPPING THE TYROLEAN NICC GENE

Although the Tyrolean population exhibiting NICC is an excellent resource for mapping the underlying gene defect using an IBD approach, there are a number of complicating factors in this study. The power of a haplotype-sharing approach is partly determined by the age of the mutation (Fig. 4). In general, such an approach works best when the common ancestor is no further than 10–12 generations away. Although we anticipate that the founder who brought in the Tyrolean NICC mutation lived no more than 10–12 generations ago, we have no proof that this is the case. If the mutation has been present in the Tyrolean population for a much longer time, the density of the current marker set might not be sufficient. However, this problem could, in part, be overcome by adding more markers to increase the resolution of the map. Nevertheless, we should realize that the reliability of the study is still lessened by two factors: (1) the small number of chromosomes being studied and (2) the complexity of screening obligate gene carriers. Because the NICC patients are unavailable, we cannot determine which of the two homologous chromosomes in each parent carries the NICC mutation (i.e., we do not know which combinations of haplotypes in the parents to compare in order to identify the mutation).

In the meantime, we have been able to increase the number of people in the study by collecting more DNA samples from the Tyrol. DNA is now available from 11 Tyrolean NICC families, comprising 18 obligate gene carriers, 1 surviving NICC patient, and 23 healthy siblings. In addition,

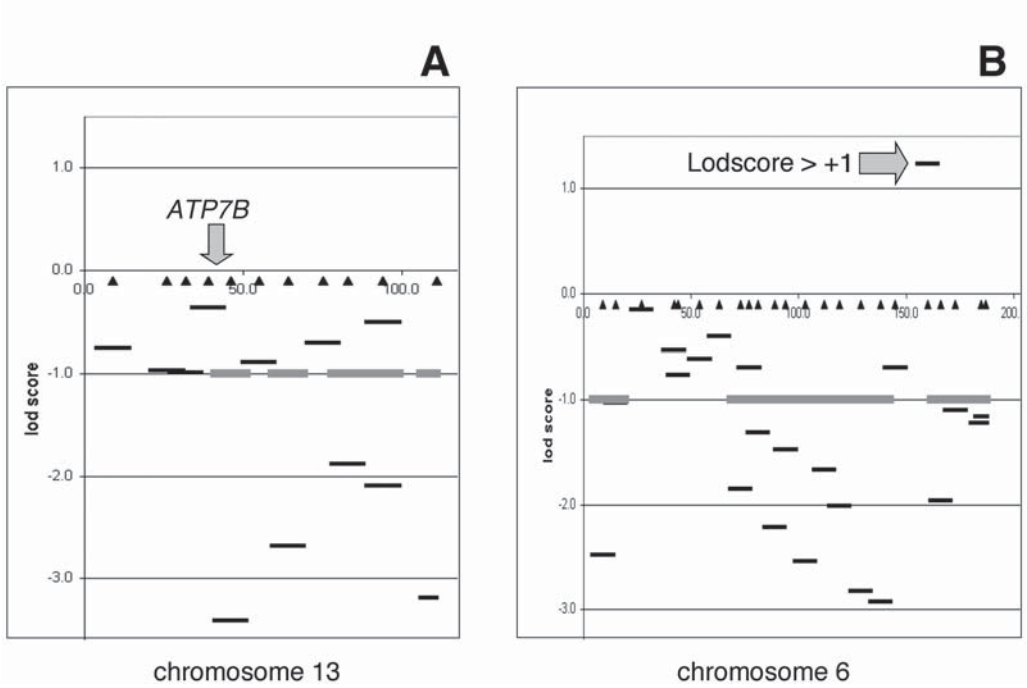

Fig. 8. Two examples of results from the genomewide association analysis in the eight Tyrolean NICC families. The *X*-axes represents the length of the chromosome (in cM); the position of the individual markers is indicated by a triangle. The *Y*-axes shows the lod score values. The black horizontal bars give the lod score value for the corresponding marker (indicated by the triangle in the center of the bar); the gray horizontal bars are the regions that were excluded for the presence of the NICC gene. **(A)** The data from chromosome 13. The part of the chromosome containing the *ATP7B* gene was excluded in this study. **(B)** The data from chromosome 6. The majority of chromosome 6 can be excluded. However, marker D6S1007 (at approx 160 cM) shows a lod score larger than +1 (indicated by an arrow). This region needs to be further investigated with a much denser set of markers.

DNA samples have also been collected from 7 German NICC families, comprising 3 surviving NICC patients, 13 gene carriers (i.e., parents), and 13 healthy siblings. This material will be used for follow-up studies on the genomewide screen being performed for the Tyrol.

In addition, we have also collected DNA from 13 ICC families in India. Given the similarities in phenotypes between ICC and NICC and the intake of high environmental copper as a precipitating factor, it is conceivable that both diseases are the result of mutations in the same gene. These ICC families have two advantages over the Tyrolean NICC families: (1) The patients are still alive because they were diagnosed in time and treated successfully and (2) the patients parents' are more closely related than the parents in the Tyrolean families. We now have DNA from a total of 12 ICC patients and 51 relatives for a genomewide screen. The parents in some of these families are first-degree relatives, which may allow the identification of homozygosity around the ICC locus.

9. IS THERE AN ANIMAL MODEL FOR NICC?

The identification of an animal model with phenotypic similarities to Tyrolean NICC could prove a useful tool to studying the disease mechanism because it is usually easier to map genes in animal models because of (1) inbreeding of the strains, (2) the large size of pedigrees, and (3) the shorter generation time. There are a few current animal models in which ingestion of copper has produced cirrhosis of the liver: the copper toxicosis in Bedlington terriers *(57,58)* and in sheep *(59,60)*. Copper toxicosis in North Ronaldsay sheep (so-called Ronaldsay copper toxicosis or RCT) shows many

similarities with NICC. The North Ronaldsay sheep are an inbred population that do well on the island of North Ronaldsay, in the Orkneys, Scotland, because the sea grass contains very low copper concentrations (Cu < 5 ppm). When these sheep are brought to the mainland, where they switch to a normal diet, copper accumulates in the liver and they develop hepatic copper toxicosis. The histological features include Mallory bodies and pericellular fibrosis, very similar to the pathology of NICC. However, there are currently no good marker maps available for the sheep genome to carry out genetic studies.

Copper toxicosis in Bedlington terriers was suggested as a good model for Tyrolean NICC because of the similarities in inheritance pattern and phenotype: hepatic copper toxicosis and normal ceruloplasmin levels *(61,62)*, although the terriers show no eye and brain lesions as in Wilson's disease *(61,62)*. We were recently able to show that the copper toxicosis in Bedlington terriers is not the result of a mutation in the canine *ATP7B* gene *(63)*. The copper toxicosis gene has recently been mapped to canine chromosome 10, region q26. This part of the dog genome is homologous to human 2p13–p16 *(63,64)*. Based on genetic and physical mapping, the location of the copper toxicosis gene in Bedlington terriers has now been refined to a region of less than 5 million base pairs. Although the resources available for the dog genome are also rather limited, the cloning of the copper toxicosis gene will benefit from the progress being made in the human genome. So far, the genes and their order on canine 10q26 is identical to those on human 2p13–p16 *(64)*. Once the complete sequence of human 2p13–p16 is released, it will therefore be possible to screen all of the canine homologs of the genes present in 2p13–p16 for mutations in Bedlington terriers that have copper toxicosis.

However, the genomewide screen in the Tyrolean NICC families did not reveal any evidence for association with markers from 2p13–p16, indicating that copper toxicosis in Bedlington terriers and Tyrolean NICC are two distinct genetic entities as a result of mutations in two different genes associated with copper metabolism.

10. LOOKING AHEAD

The fact that Tyrolean NICC has almost disappeared since untinned copper vessels have been replaced by modern household vessels raises the question of why it is still important to search for the NICC gene. First, our knowledge on copper homeostasis in humans is still limited. The identification of the NICC gene and insight into the function of its product, the protein, may broaden our understanding of the cellular processes that occur after copper has been taken up by the body. Second, childhood cirrhosis as a result of copper toxicosis is not limited to the Tyrolean population. The identification of the gene could make it possible to identify people who are either a carrier of the disease or at risk of developing copper toxicosis because they have a mutation in both alleles of the gene. The identification of high-risk people is currently only possible in families who have been exposed to high environmental copper and who have already had a child suffering from NICC.

What we do not know is whether the frequency of NICC mutations differs among different populations. Because NICC only manifests when an affected person is exposed to high amounts of dietary copper (and this may only be true in infants), many gene carriers may go unrecognized. Yet, in the absence of any selective pressure, such a mutation can easily spread through populations and occur quite frequently. The study by Scheinberg and Sternlieb *(32)* suggests that the number of gene carriers is low in the Massachusetts area. However, it cannot be excluded that these numbers could be biased if, for instance, the children in this area were breastfed and exposed to the high copper concentrations in tap water only later in life. Nevertheless, the regional differences observed in the recognized cases of NICC and ICC suggest that the disease gene frequency may differ between different parts of the world. Identifying the responsible gene would allow us not only to address the question about the frequency of occurrence of the NICC gene but would also enable us to study the effects of prolonged copper exposure in people with this genetic mutation, both children and adults.

The families (both ICC and NICC) that have now been collected and used for genetic studies, as well as the increased density of genetic markers, should provide a good starting point for mapping the

underlying gene(s). This work should also resolve the question of whether ICC and NICC are different allelic variants of the same gene. In addition, identifying the genetic defect underlying copper toxicosis in Bedlington terriers would add to our current understanding of the cellular pathways involved in copper uptake, distribution, and excretion.

11. GLOSSARY

Allele: Different forms of a gene or a genetic marker

CentiMorgan (cM): A unit of genetic distance. One centiMorgan approximately equivalent to 1.10^6 pairs.

Haplotype: A series of alleles found at linked loci on a single chromosome.

Heterozygous: The presence of different alleles at a given locus on both chromosomes.

Heterozygosity value: Probability that an individual will be heterozygous at the locus.

Identity by descent (IBD): Alleles in an individual or in two people that are identical because they have both been inherited from the same common ancestor.

Linkage disequilibrium (or allelic association): Nonrandom association of alleles at linked loci.

Lod score: A measure of the likelihood of genetic linkage between loci. The log (base 10) of the odds that the loci are linked rather than unlinked. For a mendelian character, a lod score greater than +3 is evidence of linkage; one that is less than –2 is evidence against linkage.

Locus: A unique chromosomal location defining the position of a genetic marker or gene.

Marker: A genetic marker is a polymorphic DNA sequence derived from a single chromosomal location.

Meiotic step: Number of meioses between two individuals.

Polymorphism: Locus with two or more alleles: one of which has a frequencey of > 1%.

Recombination: A new set of marker alleles on a given chromosome because of the cross over of homologous chromosomes in meiosis.

ACKNOWLEDGMENTS

I would like to thank Jackie Senior for critically reading and improving the manuscript. The work on NICC in the Tyrol and the Bedlington terriers cited in this chapter has been supported by grants from the International Copper Association and the Netherlands Organization for Scientific Research (NWO).

REFERENCES

1. Danks, D. M. (1995) Disorders of copper transport, in *The Molecular and Metabolic Basis of Inherited Diseases* (Scriver, C. R, Beaudet, A. L., Sly, W. S., and Valle, D., eds.), McGraw-Hill, New York, pp. 2211–2235.
2. FAO/IAEA/WHO Expert Consultation (1996) Copper, in *Trace Elements in Human Nutrition and Health*, World Health Organization, Geneva, pp. 123–143.
3. WHO (1993) *Guidelines for Drinking Water Quality, Vol. 1, Recommendations*, 2nd ed. World Health Organization, Geneva.
4. Agarwal, K., Sharma, A., and Talukder, G. (1989) Effects of copper on mammalian cell components. *Chem. Biol. Interact.* **69**, 1–16.
5. Bull, P. C., Thomas, G. R., Rommens, J. M., Forbes, J. R., and Cox, D. W. (1993) The Wilson disease gene is a putative copper transporting P-type ATPase similar to the Menkes gene. *Nature Genet.* **5**, 327–337.
6. Petrukhin, K. and Gilliam, T. C. (1994) Genetic disorders of copper metabolism. *Curr. Opin. Pediatr.* **6**, 698–701.
7. Nagano K., Nakamura K., Urakami K. I, Umeyama K., Uchiyama H., Koiwai K., et al. (1998) Intracellular distribution of the Wilson's disease gene product (ATPase7B) after in vitro and in vivo exogenous expression in hepatocytes from the LEC rat, an animal model of Wilson's disease. *Hepatology* **27**, 799–807.
8. Forbes, J. R. and Cox, D. W. (2000) Copper-dependent trafficking of Wilson disease mutant ATP7B proteins. *Hum. Mol. Genet.* **9**, 1927–1935.
9. Dayal, R. S., Mathur, G. P., Prasad, R., and Wahi, P. N. (1968) Indian childhood cirrhosis. Clinico-pathological study of 100 cases. *Indian Pediatr.* **5**, 17–23.
10. Walker-Smith, J .A. and Blomfield, J. (1973) Wilson's disease or chronic copper poisoning? *Arch. Dis. Child* **48**, 476–479.

11. Portmann, B., Walker-Smith, J. A., and Tanner, M. S. (1980) Wilson's disease, chronic copper poisoning, or Indian childhood cirrhosis? *Arch. Dis. Child* **55**, 163–164.
12. Portmann, B., Tanner, M. S., Mowat, A. P., and Williams, R. (1978) Orcein-positive liver deposits in Indian childhood cirrhosis. *Lancet* **8078**, 1338–1340.
13. Müller, T., Feichtinger, H., Berger, H., and Müller, W. (1996) Endemic Tyrolean infantile cirrhosis: an ecogenetic disorder. *Lancet* **9005**, 877–880.
14. Bent, S. and Bohm, K. (1995) Copper-induced liver cirrhosis in a 13-month old boy. *Gesundheitswesen* **57**, 667–669.
15. Muller-Hocker, J., Meyer, U., Wiebecke, B., Hubner, G., Eife, R., Kellner, M., et al. (1988) Copper storage disease of the liver and chronic dietary copper intoxication in two further German infants mimicking Indian childhood cirrhosis. *Pathol. Res. Pract.* **183**, 39–45.
16. Muller-Hocker, J., Weiss, M., Meyer, U., Schramel, P., Wiebecke, B., Belohradsky, B. H., et al. (1987) Fatal copper storage disease of the liver in a German infant resembling Indian childhood cirrhosis. *Virchows Arch. A. Pathol. Anat. Histopathol.* **411**, 379–385.
17. Trollmann, R., Neureiter, D., Lang, T., Dorr, H. G., and Behrens, R. (1999) Late manifestation of Indian childhood cirrhosis in a 3-year-old German girl. *Eur. J. Pediatr.* **158**, 375–378.
18. Müller, T., Schafer, H., Rodeck, B., Haupt, G., Koch, H., Bosse, H., et al. (1999) Familial clustering of infantile cirrhosis in Northern Germany: a clue to the etiology of idiopathic copper toxicosis. *J. Pediatr.* **135**, 189–196.
19. Baker, A., Gormally, S., Saxena, R., Baldwin, D., Drumm, B., Bonham, J., et al. (1995) Copper-associated liver disease in childhood. *J. Hepatol.* **23**, 538–543.
20. Maggiore, G., De Giacomo, C., Sessa, F., and Burgio, G. R. (1987) Idiopathic hepatic copper toxicosis in a child. *Pediatr. Gastroenterol. Nutr.* **6**, 980–983.
21. Nagasaka, H., Kobayashi, K., Yorifuji, T., Kage, M., Kimura, A., Takayanagi, M., et al. (1999) Indian childhood cirrhosis-like disease in a Japanese boy undergoing liver transplantation. *J. Pediatr. Gastroenterol. Nutr.* **29**, 598–600.
22. Aljajeh, I. A., Mughal, S., al-Tahou, B., Ajrawi, T., Ismail, E. A., and Nayak, N. C. (1994) Indian childhood cirrhosis-like liver disease in an Arab child. A brief report. *Virchows Arch.* **424**, 225–227.
23. Valencia, M. P., Gamboa, M. J., and Mediana, J. (1993) Copper overload and cirrhosis in four Mexican children. *Lab. Invest.* **68**, 10P (abstract).
24. Abiodun, P. O., Albarki, A. A., Dewan, M., and Annobil, S. H. (2000) Indian childhood-like cirrhosis in three Saudi Arabian siblings. *Ann. Trop. Paediatr.* **20**, 61–66.
25. Lim, C. T. and Choo, K. E. (1979) Wilson's disease in a 2 year old child. *J. Singapore Paediatr. Soc.* **21**, 99–102.
26. Horslen, S. P., Tanner, M. S., Lyon, T. D., Fell, G. S., and Lowry, M. F. (1994) Copper associated childhood cirrhosis. *Gut* **35**, 1497–1500.
27. DuBois, R. S., Rodgerson, D. O., Martineau, G., Shroter, G., Giles, G., Lilly, J., et al. (1971) Orthotopic liver transplantation for Wilson's disease. *Lancet* **7698**, 505–508.
28. Lefkowitch, J. H., Honig, C. L., King, M. E., and Hagstrom, J. W. (1982) Hepatic copper overload and features of Indian childhood cirrhosis in an American sibship. *N. Engl. J. Med.* **307**, 271–277.
29. Adamson, M., Reiner, B., Olson, J. L., Goodman, Z., Plotnick, L., Bernardini, I., et al. (1992) Indian childhood cirrhosis in an American child. *Gastroenterology* **102**, 1771–1777.
30. Ludwig, J., Farr, G. H., Freese, D. K., and Sternlieb, I. (1995) Chronic hepatitis and hepatic failure in a 14-year-old girl. *Hepatology* **22**, 1874–1879.
31. Müller, T., Müller, W., and Feichtinger, H. (1998) Idiopathic copper toxicosis. *Am. J. Clin. Nutr.* **67**, 1082S–1086S.
32. Scheinberg, I. H. and Sternlieb, I. (1994) Is non-Indian childhood cirrhosis caused by dietary copper? *Lancet* **233**, 1002–1004.
33. Müller, T., van de Sluis, B., Müller, W., Pearson, P., and Wijmenga, C. (1999) Non-Indian childhood cirrhosis. *Eur. J. Med. Res.* **4**, 293–297.
34. Wijmenga, C., Müller, T., Murli, I. S., Brunt, T., Feichtinger, H., Schonitzer, D., et al. (1998) Endemic Tyrolean infantile cirrhosis is not an allelic variant of Wilson's disease. *Eur. J. Hum. Genet.* **6**, 624–628.
35. Peña, M. M. O., Lee, J., and Thiele, D. J. (1999) A delicate balance: homeostatic control of copper uptake and distribution. *J. Nutr.* **129**, 1251–1260.
36. Yuan, D. S, Stearman, R., Dancis, A., Dunn, T., Beeler, T., and Klausner, R. D. (1995) The Menkes/Wilson disease gene homologue in yeast provides copper to a ceruloplasmin-like oxidase required for iron uptake. *Proc. Natl. Acad. Sci. USA* **92**, 2632–2636.
37. Petrukhin, K., Fischer, S. G., Piratsu, M., Tanzi, R. E., Chernov, I., Devoto, M., et al. (1993) Mapping, cloning and genetic characterisation of the region containing the Wilson disease gene. *Nature Genet.* **5**, 338–343.
38. Thomas, G. R., Forbes, J. R., Roberts, E. A., Walshe, J. M., and Cox, D. W. (1995) The Wilson disease gene: spectrum of mutations and their consequences. *Nature Genet.* **9**, 210–217.
39. Cox D. W. (1995) Genes of the copper pathway. *Am. J. Hum. Genet.* **56**, 828–834.
40. Scheinberg, I. H. and Sternlieb, I. (1996) Wilson disease and idiopathic copper toxicosis. *Am. J. Clin. Nutr.* **63**, 842–845.
41. Tanner, M. S., Portmann, B., Mowat, A. P., Williams, R., Pandit, A. N., Mills, C. F., et al. (1979) Increased hepatic copper concentration in Indian childhood cirrhosis. *Lancet* **8128**, 1203–1205.
42. Popper, H., Goldfischer, S., Sternlieb, I., Nayak, N. C., and Madhavan, T. V. (1979) Cytoplasmic copper and its toxic effects. Studies in Indian childhood cirrhosis. *Lancet* **8128**, 1205–1208.
43. Tanner, M. S (1986) Indian childhood cirrhosis, in *Recent Advances in Paediatrics* (Meadow, S. R., ed.), Churchill Livingstone, Edinburgh, Vol. 8, pp. 103–120.
44. Lander, E. S. and Botstein, D. (1987) Homozygosity mapping: a way to map human recessive traits with the DNA of inbred children. *Science* **236**, 1567–1570.

45. Terwilliger, J. D., Shannon, W. D., Lathrop, G. M., Nolan, J. P., Goldin, L. R, Chase, G. A., et al. (1997) True and false positive peaks in genomewide scans: applications of length-biased sampling to linkage mapping. *Am. J. Hum. Genet.* **61**, 430–438.
46. Houwen, R. H. J., Baharloo, S., Blankenship, K., Raeymaekers, R., Juyn, J., Sandkuijl, L. A., et al. (1994) Genome screening by searching for shared segments: mapping a gene for benign recurrent intrahepatic cholestasis. *Nature Genet.* **8**, 380–386.
47. Carlton, V. E. H., Knisely, A. S, and Freimer, N. B. (1995) Mapping of a locus for progressive familial intrahepatic cholestasis (Byler disease) to 18q21-q22, the benign recurrent intrahepatic cholestasis region. *Hum. Mol. Genet.* **4**, 1049–1053.
48. Bétard, C., Rasquin-Weber, A., Brewer, C., Drouin, E., Clark, S., Verner, A., et al. (2000) Localization of a recessive gene for North American Indian childhood cirrhosis to chromosome region 16q22 and identification of a shared haplotype. *Am. J. Hum. Genet.* **67**, 222–228.
49. Zhou B. and Gitschier, J. (1997) hCTR1: a human gene for copper uptake identified by complementation in yeast. *Proc. Natl. Acad. Sci. USA* **94**, 7481–7486.
50. Klomp, L. W., Lin, S. J., Yuan, D. S., Klausner, R. D., Culotta, V. C., and Gitlin, J. D. (1997) Identification and functional expression of HAH1, a novel human gene involved in copper homeostasis. *J. Biol. Chem.* **272**, 9221–9226.
51. Murray, J. C., Buetow, K. H., Weber, J. L., Ludwigsen, S., Scherpbier-Heddema, T., Manion, F., et al. (1994) A comprehensive human linkage map with centimorgan density. Cooperative Human Linkage Center (CHLC). *Science* **265**, 2049–2054.
52. Marshfield Clinic, http://research.marshfieldclinic.org/genetics
53. Litt, M. and Luty J. A. (1989) A hypervariable microsatellite revealed by in vitro amplification of a dinucleotide repeat within the cardiac muscle actin gene. *Am. J. Hum. Genet.* **44**, 397–401.
54. Weber, J. L. and May, P. E. (1989) Abundant class of human DNA polymorphisms which can be typed using the polymerase chain reaction. *Am. J. Hum. Genet.* **44**, 388–396.
55. Morton, N. E. (1991) Parameters of the human genome. *Proc. Natl. Acad. Sci. USA* **88**, 7474–7476.
56. Dausset, J., Cann, H., Cohen, D., Lathrop, M., Lalouel, J. M., and White, R. (1990) Centre d'Étude du Polymorphisme Humain (CEPH): collaborative genetic mapping of the human genome. *Genomics* **6**, 575–577.
57. Sternlieb, I. (1981) Copper toxicosis of the Bedlington terrier. *J. Rheumatol.* **7(Suppl.)**, 94–95.
58. Haywood, S., Fuentealba, I. C., Foster, J., and Ross, G. (1996) Pathobiology of copper-induced injury in Bedlington terriers: ultrastructural and microanalytical studies. *Anal. Cell Pathol.* **10**, 229–241.
59. MacLachlan, G. K. and Johnston, W. S. (1982) Copper poisoning in sheep from North Ronaldsay maintained on a diet of terrestrial herbage. *Vet. Rec.* **111**, 299–301.
60. Whitaker, D. A. (1997) Copper toxicosis in sheep. *Vet. Rec.* **141**, 556.
61. Twedt, D. C., Sternlieb, I., and Gilbertson, S. R. (1979) Clinical, morphologic, and chemical studies on copper toxicosis of Bedlington Terriers. *J. Am. Vet. Med. Assoc.* **175**, 269–275.
62. Hunt, D. M., Wake, S. A., Mercer, J. F., and Danks, D. M. (1986) A study of the role of metallothionein in the inherited copper toxicosis of dogs. *Biochem. J.* **236**, 409–415.
63. Van de Sluis, B. J. A., Breen, M., Nanji, M., van Wolferen, M., de Jong, P., Binns, M., et al. (1999) Genetic mapping of the copper toxicosis locus in Bedlington terriers to dog chromosome 10, in a region syntenic to human chromosome region 2p13–p16. *Hum. Mol. Genet.* **8**, 501–507.
64. Van de Sluis, B., Kole, S., Holmes, N. G., Pearson, P. L., Rothuizen, J., van Oost, B. A., et al. (2000) Refined genetic and comparative physical mapping of the canine copper toxicosis locus. *Mamm. Genome* **11**, 455–460.

V
Copper Toxicity and Therapeutics

23

Biological Effects of Chronic Copper Exposure

Magdalena Araya, Mauricio González, Manuel Olivares, and Ricardo Uauy

1. INTRODUCTION

Together with chromium, iron, cobalt, manganese, nickel, and zinc, copper represent the elements that are nutritionally essential. Copper is both essential and toxic to humans depending on the amounts ingested. It occurs as metal (Cu°) or as ion, which serves as important catalytic cofactor because of its ability to adopt distinct redox states, either oxidized (Cu^{2+}) or reduced (Cu^{1+}). In biological systems copper ions occur mainly in the cupric state because this is more stable.

There has been some discussion about copper body requirements. In adults, to cover copper essentiality, the current recommendation is 30 µg/kg body weight/d, which equates to approx 2 mg/d for an average adult. At earlier ages, daily intake of dietary copper has been set at 130–200 µg/kg/d from 0 to 6 mo and 80–120 µg/kg/d from 6 mo to 10 yr *(1,2)*. These amounts must be obtained from the diet (water and foods) because other sources, such as air (breathing or through the skin), are irrelevant in most daily life conditions. In Western societies, the consumption of mineral supplements is another source of copper that may become a relevant proportion of daily copper ingestion. Because most natural drinking waters have low copper concentrations, copper originating from foods rather than water is more relevant for nutritional purposes. However, soft acidic waters, especially when going through new copper pipes, may deliver higher amounts of copper *(3–5)*; whether these amounts are enough to trigger acute toxic effects in susceptible individuals has been systematically investigated only in the last few years.

In nutrition, copper deficiency has been historically relevant because it is associated with anemia that does not respond to iron administration *(6–8)*. At the other extreme of the curve, long-standing high exposure leads to copper deposit in the liver, which probably represents a safe physiological phenomenon in its early phases. How liver accumulation proceeds to tissue damage and appearance of chronic toxic effects remains to be elucidated. Thus, the range in which copper homeostasis is effective is not clear.

Copper delivered in water, especially as plain water on an empty stomach, has better chances of interacting with the stomach wall than that delivered in a complex dietary bolus. In this latter mixing with other components of the diet may modify its bioavailability and, therefore, its absorption rate. Because it is difficult to measure actual exposure–bioavailability–absorption of copper, the concept of safe lower and safe upper limits of oral intake have been proposed, based on gastrointestinal effects from acute and subacute exposures. The International Programme on Chemical Safety, IPCS

From: Handbook of Copper Pharmacology and Toxicology
Edited by: E. J. Massaro © Humana Press Inc., Totowa, NJ

(9), defined the lower limit of acceptable range of oral intake (AROI) at 20 µg/kg/d in adults and at 50 µg/kg/d in infants. The upper limit of AROI for adults was defined as uncertain, most likely to be in the range of the several but not many milligrams per day *(10)*. When copper content in drinking water is low (<0.01 mg Cu/L), over 90% of the copper intake depends on the diet. Instead, when copper concentration in drinking water is higher (1–2 mg Cu/L), water may provide up to 50% of the daily copper intake. Although toxic effects are clear with rather high long-standing copper doses, they are poorly known when copper exposure is mildly increased. At which copper concentrations the first adverse effects are elicited, when chronic effects take place, to what extent they may be reversible in their early stages are all questions that remain unanswered. In this chapter, we will review aspects related to exposure, absorption, and adaptive responses to copper overload at the cell, systems, and organs and whole-body levels. The cutoff points for a No Adverse Effects Level (NOAEL) *(11)* and AROI *(9)* for water will be discussed, particularly in the light of recently finished studies on acute copper toxicity.

2. COPPER HOMEOSTASIS AND METABOLISM

The relationship between copper dietary exposure and the body copper nutritional status is complex because copper homeostasis allows a wide range of copper dietary intake without resulting on adverse effects. This homeostasis includes the capacity to regulate copper absorption, retention, and excretion. About one-half of the copper ingested is absorbed *(12)*. Absorption occurs mainly in the duodenum and ileum, but some absorption would also take place in the stomach *(13)*.

Studies in cell lines suggest that previous copper status affect the way the cells handle copper offered from the medium *(14)*. How this may impact on the whole body as a result of supplementation programs in humans is not clear and deserves study. Also, in intestinal cell lines (Caco2), copper seems to have a direct effect on epithelial permeability depending on the chemical form of copper offered *(14,15)*. There are few data on the copper effects on permeability in humans; in a recent study on apparently healthy adult volunteers who ingested a single dose of 10 mg Cu/L as copper sulfate, a significant increase of gastric but not intestinal permeability was observed *(16)*. This supports the idea that early acute effects depend mainly on events occurring in the stomach.

Although adaptation takes place when copper exposure varies, changes in copper absorption seem to be more efficient to decreases than to increases of dietary copper. Thus, a 10-fold increase in dietary copper resulted in only a twofold increase of copper absorption *(17)*. In another study by Turnlund et al. *(18)*, these authors observed no significant changes in plasma copper, ceruloplasmin, superoxide dismutase (SOD) (in erythrocytes), and in urinary copper excretion over the range of 0.8 to 7.5 mg/d, suggesting that copper homeostasis is efficient within this range. The stability of copper homeostasis was supported by the recent Foodcue study in which adult volunteers received 3 mg of copper sulfate daily or 3 or 6 mg of copper glycine chelate daily. Results showed that intake of copper as high as 7 mg/d had no pro-oxidant activity; rather, it seemed to result in protection of red blood cells against oxidation *(19)*.

In response to dietary increase, endogenous copper excretion through the bilis increases while urinary excretion remains unchanged, suggesting that copper endogenous excretion is more important in controlling the fraction of copper retained by the body than the rate of absorption or urinary excretion *(17)*. Details of copper excretion through the bilis will be given later in this chapter. When dietary copper intake is very high, there is a latency to detect a response, the balance remains positive for some days and then becomes negative *(17)*, suggesting that excess copper remain in the enterocytes until these are shed into the lumen.

When copper entry to the body is greater than the needs, it is deposited, mainly in the liver. However, deposit by itself does not necessarily mean tissue damage. It is well known that at birth, healthy full-term neonates have copper concentrations in their liver that may be similar to those observed in individuals with copper-associated cirrhosis *(20)*. Understanding how copper is handled by the very young child remains a most challenging question.

3. ACUTE TOXICITY IN HUMANS

There is a wide range of acute toxic effects associated with copper ingestion. Most of them represent accidental intake of contaminated foods or fluids or deliberate ingestion of large amounts of copper salts with suicidal purpose *(21–24)*. This has led to the description of a range of responses, starting with vomiting, diarrhea, and abdominal pain to extreme cases of multiple-organ failure, shock, and death. In recent years, attention has focused to the early toxic effects that copper may elicit, mainly when it is ingested in drinking waters. Acute responses originate in the stomach and depend on copper ions that stimulate receptors, which, in turn, stimulate the vagus nerve eliciting a reflex response of nausea/vomit *(25–27)*. When the copper dose is somewhat larger, in addition to the vagal response, direct stimulation of the hypothalamic vomit center triggers retching and vomiting. The mechanism to explain diarrhea associated to larger copper doses is not well understood.

To characterize the early acute responses to copper exposure, the copper concentration at which gastrointestinal symptoms appeared (nausea, vomiting, abdominal pain, and diarrhea) were assessed, following a "worst-scenario" design in apparently healthy adult volunteers *(28)*. In these studies, including both genders and ages from 18 to 60 yr the NOEL was 2 mg Cu/L and the lowest observed adverse effect level (LOAEL) was 4 mg Cu/L. The first and most frequent symptom reported was nausea, which was transient, appeared within 5 min after ingestion, and did not repeat. Analysis of copper doses in water vs responses showed that in testing up to 12 mg Cu/L, close to a half of the subjects did not report symptoms. The incidence of vomiting was 11.5%; it first appeared at 6 mg/L, with a twofold increase between 10 and 12 mg/L. Interestingly, diarrhea and abdominal cramps were rare within the range of concentrations studied. Because nausea is a nonspecific response that many factors may modulate, the same volunteers were reassessed for intraindividual variability, receiving, on a second opportunity, the copper concentration at which they first reported symptoms. This showed that a large proportion (87.5%) of subjects confirmed their "threshold" concentration when this was 10 or 12 mg Cu/L. Instead, only 44.4% of them confirmed the positive responses when their "threshold" was 4 or 6 mg Cu/L. These data are relevant when assessing the safety of drinking waters. Using the dose-response curve and the 95% confidence limits, the copper concentration at which 5% of the population would respond was 2.0 and 4.2 mg Cu/L, depending on whether the first or confirmed nausea response was used for calculations.

The "worst-scenario" design used to calculate a dose-response curve required an overnight fasting and that the volunteers ingest a fixed volume of 200 mL distilled deionized water containing graded amounts of copper sulfate, all of which is not a common practice in daily life. For this reason and after completion of the first set of trials, the same subjects were invited to participate in a second set of sessions aimed at evaluating whether and how concentrations defined as confirmed threshold modified when copper was delivered in an orange-flavored drink. This was defined as a common breakfast drink. In these conditions, subjects reporting nausea dropped from 54% to 18%. The shift to the right of the dose-response curve was expected because the orange drink contained numerous potential copper binders. The lowest concentration of copper associated with nausea was 8 mg/L *(28)*.

During these studies. all subjects who tasted the copper in the test solution described it as metallic, bad, disgusting. With the hypothesis that the capacity of tasting copper in the test solution would increase the rate of response, the same subjects underwent an additional set of trials aimed at determining the individual's threshold for tasting copper in solution. No relationships were found between tasting and outcome report, thus disproving the hypothesis. Zacarías et al. assessed in detail the curves of tasting; dislike and rejection of solutions containing graded concentrations of copper (unpublished observations). It is interesting that at low copper concentrations (2 and 4 mg Cu/L), the curve of rejection of copper sulfate in water runs very close to the curve of nausea (Fig. 1).

To further characterize the early adverse responses to copper taking into account variables that may influence intravariability and intervariability of the response, an international protocol including apparently health adult volunteers from the United States, North Ireland, and Chile was conducted.

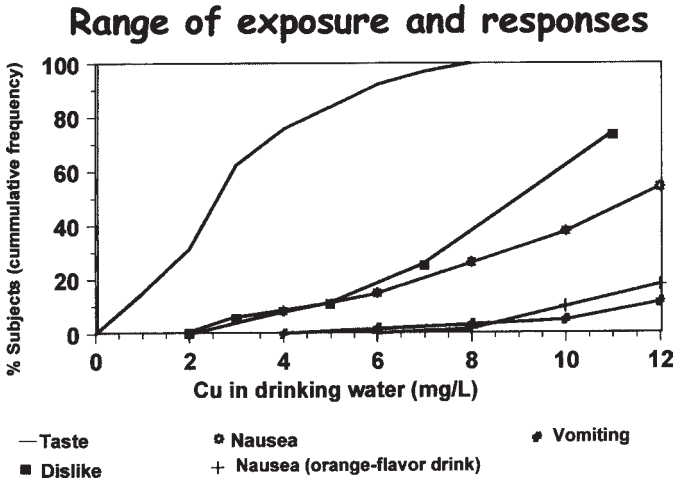

Fig. 1. Taste, "dislike," nausea, and vomiting curves in apparently healthy volunteers after drinking graded amounts of copper sulfate in water or an orange drink.

Nausea was confirmed to be the earliest and most frequent response after ingestion of copper sulfate after overnight fasting. Using the pool data, an acute NOAEL was calculated at 4 mg Cu/L *(28a)*.

In the above-discussed studies, we assessed the effects of administering a single bolus of copper delivered in water. There are few surveys of controlled copper ingestion during nonexperimental short-term trials. In a pioneer study, Pizarro et al. evaluated women who lived in Santiago, Chile, and who drank waters containing 0, 1, 3, or 5 mg elemental Cu/L (as copper sulfate) for 15 d. Results showed that consumption of waters with concentration ≥3 mg elemental Cu/L resulted in a significant increase of symptoms reported (nausea, vomiting, abdominal pain, and diarrhea) *(29)*. Olivares et al. evaluated infants fed with formula bottles prepared with water containing 2 mg Cu/L during their first year of life *(30)*. Children grew normally and exhibited normal liver function parameters throughout the study period; no changes on diarrhea or other illnesses were detected. The safety of this value, established by WHO as a provisional safe guideline for copper in drinking water, was again confirmed in children and adults in a large community survey recently finished (Araya et al., unpublished). In another recent field survey during which 1600 adults drank daily fluids prepared with waters containing graded copper concentrations, gastrointestinal symptoms significantly increased at 4 mg Cu/L (Araya et al., unpublished).

4. BASIS TO UNDERSTAND TOXIC EFFECTS ASSOCIATED WITH CHRONIC EXPOSURE TO COPPER

In mammals, adaptation to high and low copper exposure depends on general mechanisms of cellular copper management that control plasmatic levels of this metal. In different tissues, biochemical and molecular studies have led to a better understanding of how different organs adapt to copper excess and deficit. These studies provide evidence on the molecular components that participate in copper metabolism. In this section, we will discuss the molecular mechanisms involved in three important steps of copper intracellular metabolism of intestinal and hepatic tissues: (1) transport of copper into the cells; (2) intracellular storage of copper; (3) export of copper from the cells. These mechanisms will be discussed considering whether their alteration may introduce toxic effects to the organism.

4.1. Chronic Effects at Intestinal Tissues Level

The process of copper transport and absorption must supply adequate amounts of systemic copper to fulfill the requirement of a variety of copper-dependent enzymes *(31)*; at the same time, intestinal mechanisms must exist to prevent copper excess in the organism. As mentioned in Section 2., copper

absorption in humans occurs in the small intestine, after processing of food in the stomach, duodenum, and jejunum *(13,32)*. In general, evidence indicates that intestinal tissue is able to modulate the rate of copper absorption; however, the cellular and molecular mechanisms involved in this function have not been identified, leaving the precise limits of intestinal copper adaptation undetermined.

In eukariotic cells, the redox state of copper is important to the process of copper uptake and may be a first point of regulation in the absorption pathway. In the intestinal lumen, copper is mainly bound to proteins, and during the uptake process, there is equilibrium between cuprous [Cu(I)] and cupric forms [Cu(II)]. Dietary components such as phytates, amino acids (mainly histidine and cysteine), ascorbate, and other reducing agents modulate the predominance of one or the other copper ions, determining the bioavailability of copper *(33)*. Protein(s) with storage or reductase activity such as cellular prion (PrP^c) or amyloid precursor protein (APP), respectively, have been identified in the apical epithelial membrane *(34–36)*. However, their physiological potential capacity to modulate the concentration and uptake of the cuprous form in enterocytes has been not evaluated. Several reports indicate that structural alterations of APP and PrP^c affect neuronal copper homeostasis, suggesting the participation of this metal in pathologies such as Alzheimer's disease, Parkinson's disease, and amyotropic lateral sclerosis *(37–41)*. Two types of copper transporter have been identified in the epithelial plasmatic membrane: DCT1 *(42,43)* and human copper transporter 1 (hCTR1) and 2 (hCTR2) *(44)*. Although there is no evidence of mutations affecting their function, any alteration of them (sorting to membrane, interaction with other plasmatic proteins, etc.) could lead to defective copper homeostasis.

Distribution and storage of copper in epithelial cells can be envisioned as a highly regulated process. Once copper is in the cytoplasm of the intestinal cells, it is rapidly transferred to the tripeptide glutathion (gamma-L-Glu-L-Cys-Gly, GSH) and/or to the protein metallothionein (MT) *(45)*. In intestinal cells, close to 80% of the newly absorbed Cu is found in the cytoplasm, essentially bound to MT and GSH *(32)*. GSH and MTs are important intracellular reducing agents for Cu(II) and complexation agents for Cu(I). The high thermodynamic stability of Cu(I)–S bonds in both Cu(I)–GSH and Cu(I)–MT complexes, coupled with their kinetic fragility, provide efficient and specific pathways for intracellular copper storage and transport *(45,46)*. To investigate the role of MT in copper homeostasis, mice bearing these targeted deletions were crossed with the mottled-brindled-J (Mo-brJ) strain of mice, which lack a functional copy of the Menkes protein *(47)*. The Mo-brJ mice died from copper deficiency because of the inability to export copper out of the intestine, into circulation. Mutant mice accumulate copper in the intestine, which induce the expression of *MT-I* and *MT-II* genes, leading to an increase of copper–MT complexes. Considering that MT binds copper with high affinity, it was proposed that elimination of MT from the intestine might enhance copper efflux into the circulation. However, the work of Kelly and Palmiter *(48)* showed that inactivation of *MT-I* and *MT-II* genes in the *MT–/–, Mo-brJ* mutant exacerbated the phenotype of Mo-brJ mice. These results support the idea that the elevated MT levels observed in Menkes disease are mitigating copper toxicity rather than exacerbating the disease. In addition, they showed that in the absence of a functional mechanism of copper export, MT is required for a normal embryonic development.

Recently, a new group of proteins named "chaperones" have been associated with intracellular copper sorting *(49,50)*. These proteins bind copper and are involved in copper transfer from the cell surface to specific intracellular copper proteins. In humans, copper chaperone HAH1 (or ATOX1) has been shown to deliver copper to the Wilson's disease protein ATP7B, in the Golgi apparatus *(51)*. COX17 is involved in transferring copper to cytochrome oxidase in the mitochondria *(52,53)* and CCS is involved in delivering copper to SOD1 *(54)*. Thus, regulation of intracellular copper levels corresponds to the summation of relative contributions of each of these components that may be modified as a function of epithelial cell requirements.

The newly absorbed Cu bound to MT, to chaperones, and to GSH must be continuously released from them to regenerate the capacity of these molecules to form the Cu complex. The process as a whole induces an apical-to-basolateral cellular flux of the metal (*see* Fig. 2), which permits transfer-

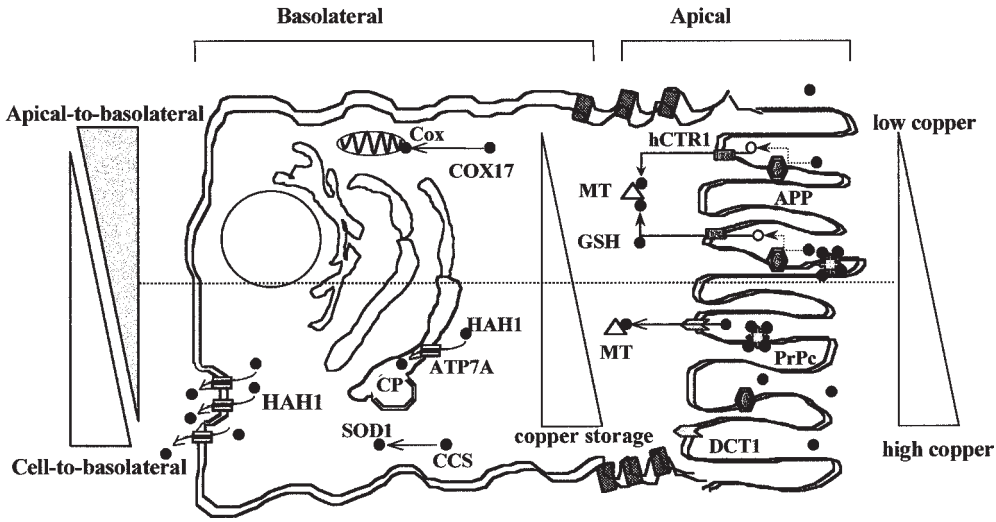

Fig. 2. Schematic representation of the effect of copper preloading on cellular copper homeostasis. The figure illustrates the absorption process of copper at cellular levels and the different components involved in the interaction with this metal.

ring copper from the intestinal lumen to the portal circulation *(32,45)*. Our results indicate that in Caco-2 cells grown in a low copper medium, 64% of the cellular-to-basolateral flux corresponds to newly incorporated copper (^{64}Cu). This suggests that in these conditions, copper uptake is strongly associated to efflux pathway(s) (Fig. 2). In contrast, only a minor fraction (4%) of the ^{64}Cu was delivered to the basolateral domain, when copper concentration was increased in the medium. In these latter conditions, the intracellular copper was elevated and the copper efflux was enhanced *(14)*. When copper offered to the cell is high, copper uptake by the cell may be higher than the concentration of the copper-chelating agents, making it possible that intracellular copper becomes toxic unless the cells can induce protective mechanisms. Induction of MT is one protective mechanism *(55)*. Another mechanism is given by the facilitation of copper efflux during excess, by increasing the expression, and by a copper-dependent redistribution of the copper transporter Menkes P-type ATPase (MNK) *(56–60)*. These evidences along with our studies on copper transport in Caco-2 led us to propose the model schematized in Fig. 2. In monolayer intestinal cells (Caco-2) chronically exposed to high extracellular copper concentration, the trans-cellular traffic of copper is shifted from a direct (uptake/efflux) pathway to an indirect (copper storage/efflux) pathway. Thus, the overall process results in an increase on both storage and cellular-to-basolateral cellular flux of copper.

4.2. Chronic Effects at Hepatic Tissues Level

Once copper enters portal circulation, the metal is transported bound to albumin, transcuprein, amino acids (histidine, threonine, cysteine), or peptides containing these amino acids *(61–63)*. Hepatic tissue removes copper from circulation by rapidly trapping it into chelating copper proteins that transfer copper to cuproenzymes or ceruloplasmin. Copper returns to the extrahepatic circulation mainly bound to ceruloplasmin, and copper excess is excreted into the bile *(32,45,64)*.

Whatever the mechanism involved in copper uptake, the metal is preferentially transported as Cu(I). Because vitamin C reduces Cu(II) to Cu(I), it stimulates Cu uptake into liver plasma membranes and isolated hepatocytes *(65,66)*; a reductase system that uses NADH to reduce Cu has been described in liver cells *(65)*.

The processes of storing and exporting copper in the liver are critical to maintaining the physiological level of this element in plasma. Hepatic cells possess protective mechanisms that allow them to act as a buffering system against extracellular copper fluctuations. Measurement of intracellular copper concentration in cells growing in a culture medium containing 0.44 μmol/L of Cu revealed that hepatic cell lines (HepG2) contained significantly more copper than HeLa (from adenocarcinoma of cervix), NIH 3T3 (fibroblasts of embryo), N2A (neuroblastoma), and B12 (glioblastoma) cell lines. In these four cell lines, analyzed the order of relative abundance for trace metals was Cu < Fe < Zn *(67,68)*. Analysis of the subcellular distribution of copper indicated that Cu was mainly in the cytosol fraction (81.7%) *(69)*, whereas only about 30% of the newly incorporated ^{64}Cu was recovered in this fraction *(70)*. Considering that only about 10% of total proteins is present in the cytoplasmatic fraction, copper concentration was highly enriched in this fraction (13.1±1.2 nmol/mg protein) as compared to the corresponding homogenate (1.35 ± 0.24 nmol/mg protein) *(69)*. In this context, it has been reported that free ions in the intracellular [Cu] pool are limited to less than one free-copper ion per cell, suggesting that a pool of free-copper ions is not used in physiological activation of metalloenzymes *(71)*. These studies also suggest that in hepatic cells, copper is handled by mechanisms that control intracellular levels of the metal and its return to the extrahepatic system by bile excretion *(32,45,64)*. One of these mechanisms consists of the increase in the number of intracellular copper-chelator units (such as MT or GSH) that can sequester copper excess *(45,55,72–77)*.

Studies on different cell lines (including HepG2 cells) *(72)* exposed to graded copper concentration have shown great complexity on the MT gene expression *(78,79)*. As an example, Sadhu and Gedamu *(80)* have shown that exposure of HepG2 cells to heavy metals results in a differential increase in the relative amounts of MT transcripts. To date, the functional significance of the multiple MT isoforms is unknown. Whether each isoform contributes separately to copper homeostasis or there is redundancy in their cellular roles is not known. GSH is the main nonproteinaceous component that binds intracellular copper. It has a well-defined role in hepatic copper turnover and also has the potential to carry copper into bile during the copper excretion process *(81)*. It has been proposed that GSH functions as a first chelating agent for incoming Cu(I), binding the metal as soon as it enters the cell *(74,82)*. The role of GSH as an intermediate in intracellular copper distribution has been evaluated in hepatic cells by using a GSH synthesis inhibitor that has no effect on MT levels *(74)*. Results of those studies showed a significant decreased in MT-bound copper levels, supporting a model in which Cu(I) is complexed by GSH immediately after entering the cell and then transferred from GSH to MT, where is stored.

A second protective mechanism used by hepatic cells is based on transporters that facilitate copper excretion during excess *(32,45,46,83,84)*, so that the amount of copper excreted into the bile is directly proportional to the excess of absorbed copper *(85)*. Transport of hepatic copper across the canalicular membrane follows at least three routes:

1. Lysosomal exocytosis: Under certain conditions such as chronic copper overload, copper tends to accumulate in liver lysosomes *(84)*. ^{64}Cu orally administered to Wilson patients, who have gross accumulation of hepatic copper, results in a similar specific activity both in lysosomes and the bile, suggesting that lysosomes may be a source of biliary copper *(86)*.
2. Glutathione-mediated copper excretion. Evidence indicate that depletion of hepatic GSH leads to a decrease in biliary copper, suggesting coupling between hepatic transport of GSH and copper excretion into bile; this mechanism requires that copper conjugation with GSH occurs within the hepatic cell *(45)*. Studies with mutant Eisai hyperbilirrubinuric (EHB) rats suggested that Cu–GSH complexes are secreted via a GSH-conjugated transporting system located in the canalicular membrane. These studies indicate that the intracellular levels of GSH available to form Cu–GSH complexes and the activity of a GSH-conjugated transporting system are necessary for hepatic copper excretion *(87–89)*.
3. P-Type ATPase facilitated copper excretion. Mutations in the *ATP7B* gene lead to excessive hepatic copper accumulation because of impaired biliary copper excretion *(90)*. Biochemical and immunohistochemi-

cal studies have localized the Wilson protein mainly to the trans-Golgi reticulum and late endosomes *(49,85,90)*. However, Dijkstra et al. *(87)*, using liver plasma membrane vesicles, provided biochemical evidence for the presence of a vanadate-inhibited copper transport in human liver, which was mainly localized at the canalicular domain of the hepatocyte plasma membrane. The presence of inmunoreactive Wilson proteins in canalicular membrane in HePG2 cells was confirmed using antibodies against ATP7B protein after treatment with copper, suggesting that copper induces trafficking of its own transporter from the trans-Golgi network to the apical membrane, where it may facilitate biliary copper excretion *(90)*. Thus, the ATPase may represent another pathway of biliary copper excretion that works in concert with lysosomal exocytosis and GSH-mediated excretion.

Alternatively, a redistribution of copper by chaperon units (HAH1) would promote an increase of copper flux at specific cellular compartments in which copper efflux is carried out by the ATP7B–ceruloplasmine system *(49)*. Based on structural analysis of ATP7B, it was assumed that copper binds as Cu(I) to cysteine residues on the copper-binding site of this protein *(91)*. Once copper is incorporated to the secretory pathway, it may be delivered to plasma, bound to ceruloplasmin *(92)*, or it can be used to be incorporated into newly synthesized cuproproteins *(51,93)*.

Copper is secreted from the liver to blood and then distributed to the various organs. Ceruloplasmin (CP) is a blue multicopper oxidase that contains 80–90% of the copper found in the sera of vertebrate species *(85)*. The crystal structure of CP confirms the presence of six tightly bound copper ions, three of them forming type-1 copper centers involved in electron-transfer processes. Three other copper ions (one type 2 and two type 3) are in a single trinuclear center, which is the oxygen-activating site during the catalytic cycle of the enzyme *(92)*. Copper in CP is not exchangeable, suggesting that CP does not function as an essential copper-transport protein *(84)*. Normal copper metabolism in patients with aceruloplasminemia support this concept. There is 5–10% of copper bound to nonceruloplasmin components, which is exchangeable. Several studies demonstrate that copper in plasma is bound to albumin and histidine. Albumin seems to play a regulatory role in controlling the copper flow between plasma and tissues. Histidine competes with albumin for copper and a ternary complex was found to be the rate-determining step in the exchange of copper between histidine and albumin *(84)*. Histidine has been shown to enhance copper uptake in human trophoblast cells, in the presence of serum; this has been interpreted as the result of copper release from albumin *(94)*. The relevance of this copper-transport mechanism in plasma deserves further investigation.

5. CHRONIC TOXICITY IN HUMANS

In humans, chronic toxic effects of copper associated with specific gene mutations such as Wilson's disease are well known *(95–98)*. Rare cases of childhood cirrhosis with fatal outcome have led to postulate that genes other than Wilson's would be associated with these cases (idiopathic copper cirrhosis, idiopathic copper toxicosis). In these patients, interaction between genes and the environment that provides normal/higher copper exposure determine the appearance of clinical manifestation *(99–102)*. In all of patients, the diagnosis is made when subclinical or clinical manifestations led to the suspicion of functional liver failure or altered copper metabolism and these are demonstrated by routine laboratory measurements. In contrast to genetic conditions, the effects of chronic high copper exposure are less clear, mainly in relation to the duration of exposure and the actual copper ingestion required for triggering the effects. There are well-characterized cases of copper-associated cirrhosis in which high exposure was the result of the use of copper containers in which milk was stored and boiled *(98,99)*. In the case of Indian children, the mean daily intake was calculated at 0.9 mg/kg/d. In adults, there is an interesting case of a man who developed cirrhosis after ingesting 30 mg Cu/d for 2 yr and 60 mg/d during a third year. If we assume that for a normal adult male, the mean weight is about 70 kg and we use for calculation the maximum daily total exposure of 0.5 mg Cu/kg/d, this man's intake was 86% and 172% of this value when ingesting the

first and second dose, respectively. Both for genetic and nongenetically determined conditions, it is necessary to develop markers able to detect homeostasis rupture and early accumulation effects before tissue damage occurs and is irreversible. This is especially relevant to individuals that lack the susceptibility genes.

Because of obvious ethical concerns, liver biopsies cannot be used in normal individuals to evaluate the upper limit of the safe range of human copper intake. Noninvasive methods to evaluate copper excess are urgently needed. In an effort to measure the effect of a higher but physiological copper burden in infants, we explored the use of erythrocyte MT as a potential indicator of copper load, using a copper dose within the range recommended by WHO for this age group *(30)*. One hundred twenty-eight healthy infants at 3 mo of age were randomly assigned to receive either 50 or 150 µg/kg body weight of copper for 9 mo. Bottles prepared with formula plus waters containing different copper concentrations provided the copper dose. In addition to erythrocyte MT, we monitored in blood serum copper, ceruloplasmin, and SOD at 3-mo intervals, demonstrating no changes between the groups *(30)*. Results may be interpreted as suggesting a lack of adaptive responses to the higher/lower copper intakes studied or, alternatively, that the biochemical indices used were not sensitive enough to detect changes at the ranges evaluated.

About 90% of copper in blood is bound to ceruloplasmin. Elevation of the nonceruloplasmin-bound copper level has been observed in patients with Wilson's disease, with idiopathic copper toxicosis *(103,104)* and in human neonates on total parenteral nutrition *(105)*. Direct measurement of nonCP pool is rarely done; most authors calculate this pool on the basis of serum copper and CP assuming that 1 mol of CP binds six copper atoms. Correlation between non-CP-bound copper and serum copper, calculated in the way mentioned and applied to the 128 well-nourished infants who received 50 or 150 µg Cu/kg/d gave $r = 0.86$ *(30)*. The strong correlation observed suggests that when serum copper exceeds the lower normal limit (14 µmol/L = 90 µg/dL), ceruloplasmin would be fully saturated if no other binding compound was available. The non-CP-bound copper increases linearly within the normal range; because free copper is not physiologically present in the serum, this suggests tight binding by other compounds. In adults, we recently finished an assessment of 106 subjects who received <0.01 or 4 mg Cu/L (as copper sulfate) in their daily fluid intake, for 2 mo. Preliminary results show that correlation between non-CP-bound copper and total serum copper was $r = 0.55$ (Araya et al., unpublished).

Ongoing studies are currently evaluating whether a non-CP copper pool may become a marker of early copper load. Further research is necessary to determine its performance, including specificity and sensitivity.

REFERENCES

1. National Academy of Sciences (1989) *Recommended Dietary Allowances*, 10th ed., National Academy of Sciences, Washington, DC, pp. 224–230.
2. WHO/FAO/IAEA (1996) Copper, in *Trace Elements in Human Nutrition and Health*, World Health Organization, Geneva, pp. 123–143.
3. USA Environmental Protection Agency (1995) *Effect of pH, DIC, Orthophosphate and Sulfate on Drinking Water Cupro Solvency*, Office of Research and Development, Washington, DC, EPA/600/R-95/085.
4. US Environmental Protection Agency(1994) Drinking water; maximum contaminant level goal and national primary drinking water regulation for lead and copper. *Fed. Reg.* **59**, 33,860–33,864.
5. National Research Council.(1980) *Drinking Water and Health*, National Academy Press, Washington, DC, Vol. 3.
6. Cordano, A., Baertl, J., and Graham, G. G. (1964) Copper deficiency in infants. *Pediatrics* **34**, 324–336.
7. Graham, G. G. and Cordano, A. (1964) Copper depletion and deficiency in the malnourished infant. *John Hopkins Med. J.* **124**, 129–150.
8. Cordano, A., Placko, R. P., and Graham, G. G. (1966) Hypocupremia and neutropenia in copper deficiency. *Blood* **28**, 280–283.
9. International Programme on Chemical Safety (IPCS) (1999) *Principles and Methods for the Assessment of Risk from Essential Trace Elements*, World Health Organization, Geneva.
10. International Programme on Chemical Safety (IPCS) (1998) *Environmental Health Criteria 200. Copper*, World Health Organization, Geneva.

11. Olivares, M. and Uauy, R. (1996) Limits on metabolic tolerance to copper and biological basis for present recommendations and regulations. *Am. J. Clin. Nutr.* **63**, 846S–852S.
12. Turnlund, J. R. (1988) Copper nutriture, bioavailability, and the influence of dietary factors. *J. Am. Diet. Assoc.* **88**, 303–308.
13. Rucker, R. B., Lönnerdal, B., and Keen, C. L. (1993) Intestinal absorption of nutritionally important trace elements, in *Physiology of the Gastrointestinal Tract* (Johnson, L.R., ed.), Raven, New York, pp. 2183–2202.
14. Arredondo, M., Uauy, R., and González, M. (2000) Regulation of copper uptake and transport in intestinal cell monolayers by acute and chronic copper exposure. *Biochim. Biophys.* **1474**, 169–176.
15. Ferruza, S., Scarino, M. L., Rotilio, G., Ciriolo, M. R., Santaroni, P., Muda, A. O., et al. (1999) Copper treatment alters the permeability of tight junctions in cultured human intestinal Caco-2 cells. *Am. J. Physiol.* **277**, G1138–G1148.
16. Gotteland, M., Araya, M., Pizarro, F., and Olivares, M. (2001) Effect of acute copper exposure on gastrointestinal permeability in healthy volunteers. *Dig. Dis. Sci.*, **46**, 1909–1914.
17. Turnlund, J. R., Keyes, W. R., Anderson, H. L., and Acord, L. L. (1989) Copper absorption and retention in young men at three levels of dietary copper by use of the stable isotope ^{65}Cu. *Am. J. Clin. Nutr.* **49**, 870–878.
18. Turnlund, J. R., Keen, C. L., and Smith, R. G. (1990) Copper status and urinary and salivary copper in young men at three levels of dietary copper. *Am. J. Clin. Nutr.* **51**, 658–664.
19. Rock, E., Mazur, A., O'Connor, J. M., Bonham, M. P., Rayssiguier, Y., and Strain, J. J. (2000) The effect of copper supplementation on red blood cell oxidizability and plasma antioxidants in middle-aged healthy volunteers. *Free Radical Biol. Med.* **28**, 324–329.
20. Klein, D., Scholz, P., Drasch, G. A., Müller-Höcker, J., and Summer, K H. (1991) Metallothionein, copper and zinc in fetal and neonatal human liver: changes during development. *Toxicol. Lett.* **56**, 61–67.
21. US Environmental Protection Agency, Environmental Criteria and Assessment Office (1987) *Summary Review of the Health Effects Associated with Copper*, Environmental Protection Agency, Cincinnati, OH, EPA 600/8–87/001.
22. National Institute of Public Health and Environmental Protection (1989) *Integrated Criteria Document Copper.* Appendix to report N°. 758474009. National Institute of Public Health and Environmental Protection, Bilthoven, The Netherlands.
23. US Environmental Protection Agency, Environmental Criteria and Assessment Office (1985) *Drinking Water Criteria Document for Copper (Final Draft).* Environmental Protection Agency, Cincinnati, OH, EPA 600/X-84/190-1.
24. Low, B. A., Donohue, J. M., and Bartley, C. B. (1996) Backflow prevention failures and copper poisonings associated with post-mixed soft drink dispensers. NSF International, Ann Arbor, MI.
25. Wang, S. C. and Borison, H. L. (1951) Copper sulfate emesis: a study of afferent pathways for the gastrointestinal tract. *Am. J. Physiol.* **164**, 520–526.
26. Niijima, A., Jiang, Z. Y., Dauton, N. G., and Fox, R. A. (1987) Effect of copper sulfate on the rate of afferent discharge in gastric branch of the vagus nerve in the rat. *Neurosci. Lett.* **80**, 71–74.
27. Kayashima, N., Tanka, M., Iwasaki, M., and Hayama, T. (1978) Site of oral copper sulfate in dogs. (I) Threshold of various portions of gastrointestinal tract to locally applied copper sulfate. *Jpn. J. Pharmacol.* **28**, 775–781.
28. Olivares, M., Araya, M., Pizarro, F., and Uauy, R. (2001) Nausea threshold in apparently healthy individuals who drink fluids containing graded concentrations of copper. *Reg. Toxicol. Pharmacol.* **33**, 271–275.

28a. Araya, M., McGoldrick, M. C., Klevay, L., Strain, J. J., Robson, P., Olivares, M., et al. (2001) Determination of an acute no-observed-adverse-effect-level (NOAEL) for copper in water. *Regul. Toxicol. Pharmacol.* **34**, 137–145.

29. Pizarro, F., Olivares, M., Uauy, R., Contreras, P., Rebelo, A., and Gidi, V. (1999) Acute gastrointestinal effects of graded levels of copper in drinking water. *Environ. Health Perspect.* **107**, 117–121.
30. Olivares, M., Pizarro, F., Speisky, H., Lönnerdal, B., and Uauy, R. (1998) Copper in infant nutrition: safety of World Health Organization provisional guideline value for copper content in drinking water. *J. Pediatr. Gastroenterol. Nutr.* **26**, 251–257.
31. Uauy, R., Olivares, M., and González, M. (1998) Essentiality of copper in humans. *Am. J. Clin. Nutr.* **67**, 952S–959S.
32. Linder, M. C. and Hazegh-Azam, M. (1996) Copper biochemistry and molecular biology. *Am. J. Clin. Nutr.* **63**, 797S–811S.
33. Lönnerdal, B. (1996) Bioavailability of copper. *Am. J. Clin. Nutr.* **63**, 821S–829S.
34. Multhaup, G., Schlicksupp, A., Hesse, L., Beher, D., Ruppert, T., Masters, C. L., et al. (1996) The amyloid precursor protein of Alzheimer's disease in the reduction of copper(II) to copper(I). *Science* **271**, 1406–1409.
35. Brown, D. R., Qin, K., Herms, J.W., Madlung, A., Manson, J., Strome, R., et al. (1997) The cellular prion protein binds copper in vivo. *Nature* **390**, 684–687.
36. Pammer, J., Cross, H. S., Frobert, Y., Tschachler. E., and Oberhuber, G. (2000) The pattern of prion-related protein expression in the gastrointestinal tract. *Virchows Arch.* **436**, 466–472.
37. Waggoner, D. J., Bartnikas, T. B., and Gitlin, J. D. (1999) The role of copper in neurodegenerative disease. *Neurobiol. Dis.* **6**, 221–230.
38. Wong, P. C., Waggoner, D., Subramaniam, J. R., Tessarollo, L., Bartnikas, T. B., Culotta, V. C., et al. (2000) Copper chaperone for superoxide dismutase is essential to activate mammalian Cu/Zn superoxide dismutase. *Proc. Natl. Acad. Sci. USA* **97,** 2886–2891.
39. Goto, J. J., Zhu, H., Sánchez, R. J., Nersissian, A., Gralla, E. B., Valentine, J. S., et al. (2000) Loss of in vitro metal ion binding specificity in mutant copper–zinc superoxide dismutases associated with familial amyotrophic lateral sclerosis. *J. Biol. Chem.* **275**, 1007–1014.
40. Bush, A. I. (2000) Metals and neuroscience. *Curr. Opin. Chem. Biol.* **4**, 184–191.
41. Torsdottir, G., Kristinsson, J., Sveinbjornsdottir, S., Snaedal, J., and Johannesson, T. (1999) Copper, ceruloplasmin, superoxide dismutase and iron parameters in Parkinson's disease. *Pharmacol. Toxicol.* **85**, 239–243.

42. Gunshin, H., Mackenzie, B., Berger, U. V., Gunshin, Y., Romero, M. F., Boron, W. F., et al. (1997) Cloning and characterization of a proton-coupled mammalian metal ion transporter. *Nature* **388**, 482–488.
43. Tandy, S., Williams, M., Leggett, A., López-Jímenez, M., Dedes, M., Ramesh, B., et al. (2000) Nramp2 expression is associated with pH-dependent iron uptake across the apical membrane of human intestinal Caco-2 cells. *J. Biol. Chem*. **275**, 1023–1019.
44. Zhou, B. and Gitschier, J. (1997) hCTR1: a human gene for copper uptake identified by complementation in yeast. *Proc. Natl. Acad. Sci. USA* **94**, 7481–7486.
45. Dijkstra, M., Vonk, R. J., and Kuipers, F. (1996) How does copper get into bile? New insights into the mechanism(s) of hepatobiliary copper transport. *J. Hepatol.* **24**, 109–120.
46. Corazza, A., Harvey, I., and Sadler, P. J. (1996) 1H,13C-NMR and X-ray absorption studies of copper(I) glutathione complexes. *Eur. J. Biochem.* **236**, 697–705.
47. Jornot, L. and Junod, A. F. (1993) Variable glutathione levels and expression of antioxidant enzymes in human endothelial cells. *Am. J. Physiol.* **264**, L482–L489.
48. Kelly, E. J. and Palmiter, R. D. (1996) A murine model of Menkes disease reveals a physiological function of metallothionein. *Nature Genet*. **13**, 219–222.
49. Ellis, R. J. (2000) Chaperone substrates inside the cell. *Trends Biochem. Sci*. **25**, 210–212.
50. Harrison, M. D., Jones, C. E., Solioz, M., and Dameron, C. T. (2000) Intracellular copper routing: the role of copper chaperones. *Trends Biochem Sci*. **25**, 29–32.
51. Klomp, L. W., Lin, S., Yuan, D. S., Klausner, R. D., Culotta, V. C., and Gitlin, J. D. (1997) Identification and functional expression of Hah1, a novel human gene involved in copper homeostasis. *J. Biol. Chem.* **272**, 9221–9226.
52. Amaravadi, R., Glerum, D. M., and Tzagoloff, A. (1997) Isolation of a cDNA encoding the human homolog of COX17, a yeast gene essential for mitochondrial copper recruitment. *Hum. Genet*. **99**, 329–333.
53. Glerum, D. M., Shtanko, A., and Tzagoloff, A. (1997) Characterization of COX17, a yeast gene involved in copper metabolism and assembly of cytochrome oxidase. *J. Biol. Chem.* **271**, 14,504–14,509.
54. Casareno, R. L., Waggoner, D., and Gitlin, J. D. (1998) The copper chaperone CCS directly interacts with copper/zinc superoxide dismutase. *J. Biol. Chem.* **273**, 23,625–23,628.
55. Freedman, J. H. and Peisach, J. (1989) Resistance of cultured hepatoma cells to copper toxicity: purification and characterization of the hepatoma metallothionein. *Biochim. Biophys. Acta* **992**, 145–154.
56. Chelly, J., Tümer, Z., Tønneson, T., Petterson, A., Ishikawa-Brush, Y., Tommerup, N., et al. (1993) Isolation of a candidate gene for Menkes disease that encodes a potential heavy metal binding protein. *Nature Genet*. **3,** 14–19.
57. Camakaris, J., Petris, M., Bailey, L., Shen, P., Lockhart, P., Glover, T. W., et al. (1995) Gene amplification of the Menkes (MNK; ATP7A) P-type ATPase gene of CHO cells is associated with copper resistance and enhanced copper efflux. *Hum. Mol. Genet*. **4**, 2117–2123.
58. Petris, M. J., Mercer, J. F. B., Culvenor, J. G., Lockhart, P., Gleeson, P. A., and Camakaris, J. (1996) Ligand-regulated transport of the Menkes copper P-type ATPase efflux pump from the Golgi apparatus to the plasma membrane: a novel mechanism of regulated trafficking. *EMBO*. **15**, 6084–6095.
59. Yamaguchi, Y., Heiny, M. E., Suzuki, M., and Gitlin, J. (1996) Biochemical characterization and intracellular localization of the Menkes disease protein. *Proc. Natl. Acad. Sci. USA* **93**, 14,030–14,035.
60. Petris, M. J., and Mercer, J. (1999) The Menkes protein (ATP7A; MNK) cycles via the plasma membrane both in basal and elevated extracellular copper using a C-terminal di-leucine endocytic signal. *Hum. Mol. Genet*. **8**, 2107–2115.
61. Neumann, P. Z. and Sass-Kortsak, A. (1967) State of copper in human serum: evidence for amino acid-bound fraction. *J. Clin. Invest.* **46**, 646–658.
62. Weiss, K. C. and Linder, M. C. (1985) Copper transport in rats involving a new plasma protein. *Am. J. Physiol*. **249**, E77–E88.
63. Harris, E. D. (2000) Cellular copper transport and metabolism. *Annu. Rev. Nutr*. **20**, 291–310**.**
64. Harada, M., Sakisaka, S., Yoshitake, M., Shakadoh, S., Gondoh, K., Sata, M., et al. (1993) Biliary copper excretion in acutely and chronically copper-loaded rats. *Hepatology* **17**, 111–117.
65. Bingham, M. J. and McArdle, H. J. (1994) A comparison of copper uptake by liver plasma membrane vesicles and uptake by isolated cultured rat hepatocytes. *Hepatology* **20**, 1024–1031.
66. van der Berg, G. J. and Beynen, A. C. (1992) Influence of ascorbic acid supplementation on copper metabolism in rats. *Br. J. Nutr*. **68**, 701–715.
67. González, M., Ruiz, F., Uauy, R., and Inostrosa, N. C. (1997) Intracellular changes on trace metals and metallothioneins are associated to variations in the extracellular copper concentration in mammalian cells. 1st International Meeting on Copper Homeostasis and Its Disorders: Molecular and Celular Aspects, Italy, p. 24.
68. González, M., Tapia, L., Alvarado, M., Tornero, J. D., and Fernández, R., (1999) Intracellular determination of trace elements by total reflection X-ray fluorescence spectroscopy in mammalian cultured cells. *J. Anal. Atomic Spectrom*. **14**, 885–888.
69. Uauy, R., Olivares, M., and González, M. (1999) Mechanisms for whole body, tissue and cellular adaptation to low and high copper exposure in humans. 2nd International Meeting on Copper Homeostasis and Its Disorders: Molecular and Cellular Aspects, p. 48.
70. Stockert, R. J., Grushoff, P. S., Morell, A. G., Bentley, G. E., O'Brien H. A., Scheinberg, I. H., et al. (1986) Transport and intracellular distribution of copper in a human hepatoblastoma cell line, HepG2. *Hepatology* **6**, 60–64.
71. Rae, T. D., Schmidt, P. J., Pufahl, R. A., Culotta, V. C., and O'Halloran, T. V. (1999) Undetectable intracellular free copper: the requirement of a copper chaperone for superoxide dismutase. *Science* **284**, 805–808.

72. Schilsky, M. L., Blank, R. R., Czaja, M. J., Zern, M. A., Scheinberg, I. H., Stockert, R. J., et al. (1989) Hepatocellular copper toxicity and its attenuation by zinc. *J. Clin. Invest.* **84**, 1562–1568.
73. Sato, M. and Bremner, I. (1993) Oxygen free radicals and metallothionein. *Free Radical Biol. Med.* **14**, 325–337.
74. Steinebach, O. M. and Wolterbeek, H. T. (1994) Role of cytosolic copper, metallothionein and glutathione in copper toxicity in rat hepatoma tissue culture cells. *Toxicology* **92**, 75–90.
75. Poutney, D. L., Schauweker, I., Zarn, J., and Vasak, M. (1994) Formation of mammalian Cu8-MT in vitro: evidence for the existence of two Cu(I)4-thiolate cluster. *Biochemistry* **33**, 9699–9705.
76. Blalock, T., Dunn, M., and Cousins, R. (1988) Metallothionein gene expression in rats: tissue-specific regulation by dietary copper and zinc. *J. Nutr.* **118**, 222–228.
77. Thorvaldsen, J., Sewell, A. Q., McCowen, C., and Winge, D. (1993) Regulation of metallothionein genes by the ACE1 and AMT1 transcription factors. *J. Biol. Chem.* **268**, 12,512–12,518.
78. Thiele, D. (1992) Metal-regulated transcription in eukaryotes. *Nucleic Acids Res.* **20**, 1183–1191.
79. Pawels, M., Van Weyenbergh, J., Soumillion, A., Prost, P., and De Ley, M. (1994) Induction by zinc of specific MT isoforms in human monocytes. *Eur. J. Biochem.* **220**, 105–110.
80. Sadhu, Ch. and Gedamu, L. (1988) Regulation of human metallothionein (MT) genes. *J. Biol. Chem.* **263**, 2679–2684.
81. Mohan, P., Failla, M., Bremner, I., Arthurd-Smith, A., and Kerzner, B. (1995) Biliary copper excretion in the neonatal rat: role of glutathione and metallothionein. *Hepatology* **21**, 1051–1057.
82. Freedman, J. H., Ciriolo, M. R., and Peisach, J. (1989) The role of glutathione in copper metabolism and toxicity. *J. Biol. Chem.* **264**, 5598–5605.
83. Buckley, W. T. (1996) Application of compartmental modeling to determination of trace element requirements in humans. *J. Nutr.* **126**, 2312S–2319S.
84. DiDonato, M. and Sarkar, B. (1997) Copper transport and its alterations in Menkes and Wilson diseases. *Biochim. Biophys. Acta* **1360**, 3–16.
85. Harris, Z. L. and Gitlin, J. D. (1996) Genetic and molecular basis for copper toxicity. *Am. J. Clin. Nutr.* **63**, 836S–841S.
86. Sternlieb, I., Van den Hamer, C. J., Morell, A. G., Alpert, S., Gregoriadis, G., and Scheinberg, I. H. (1973) Lysosomal defect of hepatic copper excretion in Wilson's disease (hepatolenticular degeneration). *Gastroenterology* **64**, 99–105.
87. Dijkstra, M., van den Berg, G. J., Wolters, H., In't Veld G., Slooff, M. J., Heymans, H. S., et al. (1996) Adenosine triphosphate-dependent copper transport in human liver. *J. Hepatol.* **25**, 37–42.
88. Sugawara, N., Lai, Y., Yuasa, M., Dhar, S. K., and Arizono, K. (1996) Biliary excretion of copper, manganese, and horseradish peroxidase in Eisai hyperbilirubinemic mutant rats (EHBRs) with defective biliary excretion of glutathione. *Biol. Trace. Element Res.* **55**, 181–189.
89. Sugawara, N., Lai, Y. R., Arizono, K., and Ariyoshi, T. (1996) Biliary excretion of exogenous cadmium, and endogenous copper and zinc in the Eisai hyperbilirubinuric (EHB) rat with a near absence of biliary glutathione. *Toxicology* **112**, 87–94.
90. Roelofsen, H., Wolters, H., Van Luyn, M. J., Miura, N., Kuipers, F., and Vonk, R. J. (2000) Copper-induced apical trafficking of ATP7B in polarized hepatoma cells provides a mechanism for biliary copper excretion. *Gastroenterology* **119**, 782–793.
91. Bingham, M. J., Burchell, A., and McArdle, H. J. (1995) Identification of an ATP-dependent copper transport system in endoplasmic reticulum vesicles isolated from rat liver. *J. Physiol.* **482**, 583–587.
92. Bingham, M. J., Ong, T. J., Ingledew, W. J., and McArdle, H. J. (1996) ATP-dependent copper transporter, in the Golgi apparatus of rat hepatocytes, transports Cu(II) not Cu(I). *Am. J. Physiol.* **271**, G741–G746.
93. Kaplan, J. and O'Halloran, T. V. (1996) Iron metabolism in eukaryotes: Mars and Venus at it again. *Science* **271**, 510–512.
94. Vulpe, Ch. and Packman, S. (1995) Cellular copper transport. *Annu. Rev. Nutr.* **15**, 293–322.
95. Lönnerdal, B. (1996) Bioavailability of copper. *Am. J. Clin. Nutr.* **63**, 821S–829S.
96. Danks, D. M. (1995) Disorders of copper transport, in *The Metabolic and Molecular Bases of Inherited Disease*, (Scriver, C. L., Beaudet, A. L., Sly, W. S, and Valle, D, eds.), McGraw-Hill, New York, pp. 2211–2235.
97. Scheinberg, I. H. and Sternlieb, I. (1996) Wilson disease and idiopathic copper toxicosis. *Am. J. Clin. Nutr.* **63**, 842S–855S.
98. Tanner, M. S. (1998) Role of copper in Indian childhood cirrhosis. *Am. J. Clin. Nutr.* **67**, 1074S–1081S.
99. Tanner, M. S., Kantarjian, A. H., Bhave, S. A., and Pandit, A. N. (1983) Early introduction of copper-contaminated animal milk as possible cause of Indian chilhood cirrhosis. *Lancet* **2**, 992–995.
100. Müller, T., Feichtinger, H., Berger, H., and Müller, W. (1996) Endemic Tyrolean cirrhosis: an ecogenetic disorder. *Lancet* **347**, 877–880.
101. Müller, T., Müller, W., and Feichtinger, H. (1998) Idiopathic copper toxicosis. *Am. J. Clin. Nutr.* **67**, 1082S–1086S.
102. Müller-Höcker, J., Meyer, U., Wiebeche, B., and Hübner, G. (1988) Copper storage disease of the liver and chronic dietary copper intoxication in two further German infants mimicking Indian childhood cirrhosis. *Pathol. Res. Pract.* **183**, 39–45.
103. Ogihara, H., Ogihara, T., Miki, M., Yasuda, H., and Mino, M. (1995) Plasma copper and antioxidant status in Wilson's disease. *Pediat. Res.* **37**, 219–226.
104. Eife, R., Weiss, M., Müller-Höcker, J., Lang, T., Barros, V., Sigmund, B., et al. (1999) Chronic poisoning by copper in tap water: copper intoxication with predominant systemic symptoms. *Eur. J. Med. Res.* **4**, 224–228.
105. Soo, T. L., Simmer, K., Carlson, L., and McDonald, L. (1988) Copper and very low birthweight babies. *Arch. Dis. Child.* **63**, 79–81.

24

Copper Toxicity to Tight Junctions in the Human Intestinal Caco-2 Cell Line

Simonetta Ferruzza, Yula Sambuy, Andrea Onetti-Muda, Fabio Nobili, and Maria Laura Scarino

1. COPPER AND INTESTINAL TOXICITY

Copper in humans plays different roles: It is an essential nutrient, but, depending on the dose, it can act as a toxic substance. However, it remains controversial where to set the limits between essential and toxic levels of intake.

Sensitive and accurate indicators of copper toxicity at the level of the gastrointestinal tract are still missing, and those available (e.g., nausea, vomiting, abdominal pain) do not discriminate from other toxicants and respond at high levels of ingested copper *(1)*. Setting the toxic levels is therefore difficult and most information on copper toxicity in humans derive from data collected in clinical cases of acute poisoning *(2–4)*.

The oral absorption of xenobiotics is a critical factor for their fate into the body and is mainly controlled by their passage across the intestinal ephitelium. The barrier function of the intestinal mucosa is guaranteed by the presence and the function of the tight junctions, which are highly organized and finely regulated structures joining adjacent epithelial cells. However, tight junctions do not represent an absolute diffusion barrier and restrict diffusion in a manner that depends on the molecular weight and on the charge of the tracer; furthermore, paracellular permeabilty is regulated by different physiological and pathological stimuli *(5–8)*.

In the present study, we investigated the effects of ionic copper and of copper chelates on the tight junctions' structure and function using a human intestinal in vitro model, the Caco-2 cell line, in order to elucidate the effect of copper on the permeability of the intestinal epithelium and the mechanisms of copper interaction with tight junctions.

In addition, such a study contributes to the establishment of a more sensitive end point of the effect of copper at the intestinal level (i.e., modification in intestinal permeability), which could help toxicologist in establishing upper limits of tolerable copper intake.

2. THE HUMAN INTESTINAL CACO-2 CELL MODEL FOR TRANSPORT AND TOXICITY STUDIES

2.1. The Model

The Caco-2 cell line was established by Fogh and co-workers in 1977 from a human colon adenocarcinoma and was originally used for the screening of the cytotoxic effects of antitumoral drugs and

From: Handbook of Copper Pharmacology and Toxicology
Edited by: E. J. Massaro © Humana Press Inc., Totowa, NJ

for the study of resistance mechanisms *(9)*. Later, it was demonstrated that Caco-2 cells can spontaneously differentiate both morphologically and functionally, when maintained at confluency, into a polarized epithelium resembling that of the mature small intestine *(10–13)*. Differentiated Caco-2 cells develop ultrastructural characteristics, such as functional tight junctions and microvilli on the apical (AP) surface, which are typical of the small intestinal absorptive enterocytes. In addition, during differentiation, the cells progressively express hydrolase activities associated with the AP membrane (sucrase–isomaltase, lactase, aminopeptidase N and dipeptidylpeptidase IV), normally expressed on the microvilli of the absorptive enterocyte of the small intestine. Although a transient expression of these enzyme activities is observed in the fetal human colon around the 15th wk of gestation, these enzymes are not present in the mature colon *(14)*. Conversely, electrical properties, ionic conductivity, and permeability characteristics of the differentiated Caco-2 cells resemble those of the colon crypt cells *(15,16)*. In addition, transport activities of both small intestinal and colonic type have been observed in Caco-2 cells *(17)*. Overall, some but not all small intestinal functions have been shown to be expressed in the differentiated Caco-2 cell line, leading to the conclusion that these cells, because of their tumoral origin, may not represent a single cytotype, but they exhibit some biochemical characteristics of the normal adult intestine, others of the fetal colon, and others of the normal adult colon *(18)*.

Caco-2 cells can be grown and differentiated on permeable filter supports leading to the formation of a monolayer of differentiated cells joined by functional tight junctions separating the AP medium in the upper chamber from the basolateral (BL) medium in the lower chamber (Fig. 1). Such arrangement mimics the barrier function of the intestinal epithelium, facing the intestinal lumen on the AP side and the blood capillaries and connective tissue on the basal side. Caco-2 cells on filters have been extensively employed to study polarized uptake and transepithelial transport of nutrients and xenobiotics, including several heavy metals *(19–26)*. In addition, in toxicology, this model has frequently been used to study the effect and the metabolism of natural and synthetic compounds *(27–31)*.

Figure 1 shows a schematic representation of the Caco-2 cell monolayer on the polycarbonate filter insert with AP medium on the luminal side and BL medium on the mucosal side. Differentiated Caco-2 cells on the filter can also be viewed in cross-section by optical microscopy after inclusion in polyacrylate resin and staining of 3-µm sections with hematoxylin–eosin. Cells are disposed in a monolayer and they are well polarized with nuclei on the basal side and brush border on the AP side (Fig. 2).

2.2. Cell Culture

The human intestinal Caco-2 cell line was obtained from Alain Zweibaum (INSERM, Villejuif, Paris, France). Caco-2 cells were grown and maintained as previously described *(21)* in Dulbecco's modified minimum essential medium (DMEM) containing 25 m*M* glucose, 3.7 g/L $NaHCO_3$, and supplemented with 4 m*M* L-glutamine, 1% nonessential amino acids (containing 8.9 mg/L L-alanine, 15 mg/L L-asparagine, 13.3 mg/L L-aspartate, 14.7 mg/L L-glycine, 11.5 mg/L L-proline, 10.5 mg/L L-serine), 1×10^5 U/L penicillin, 100 µg/L streptomycin, and 10% heat-inactivated fetal calf serum (complete culture medium). Tissue culture media and supplements were obtained from Euroclone UK Ltd (Pero, Milan, Italy). For experiments monitoring the effects of copper on tight-junction permeability, the cells were seeded on polycarbonate filter cell culture chamber inserts (Transwell, 12 mm diameter, 1.13 cm^2 area, 0.45 µm pore diameter; Costar Europe, Badhoevedorp, The Netherlands). Cells were seeded at a density of 4×10^5 cells/cm^2 and were allowed to differentiate for 16–19 d after confluency; the medium was regularly changed three times a week.

2.3. Assays of Tight-Junction Permeability

After seeding on the filters, Caco-2 cells start growing and, given the high seeding density, reach confluency within 2 d. After confluency, Caco-2 cells initiate a process of differentiation that lasts

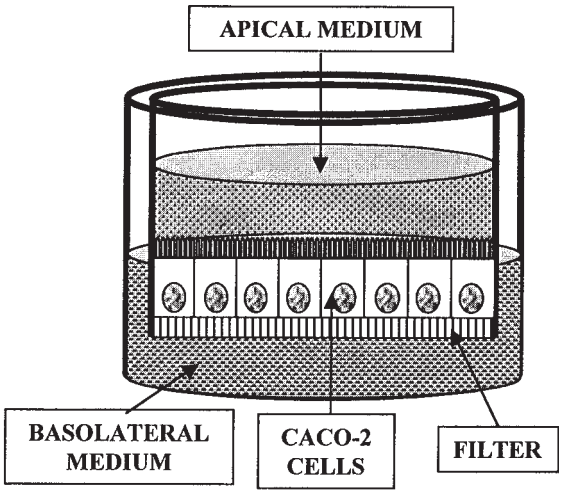

Fig. 1. Schematic view of Caco-2 cells' monolayer cultured on permeable filter culture inserts. Caco-2 cells on polycarbonate filter inserts after differentiation form a monolayer of cells coupled by tight junctions separating the AP from the BL medium. This system allows free access to both compartments and permits studies of the vectorial transport of molecules in both directions and of the toxic effects to the barrier function of the intestinal epithelium.

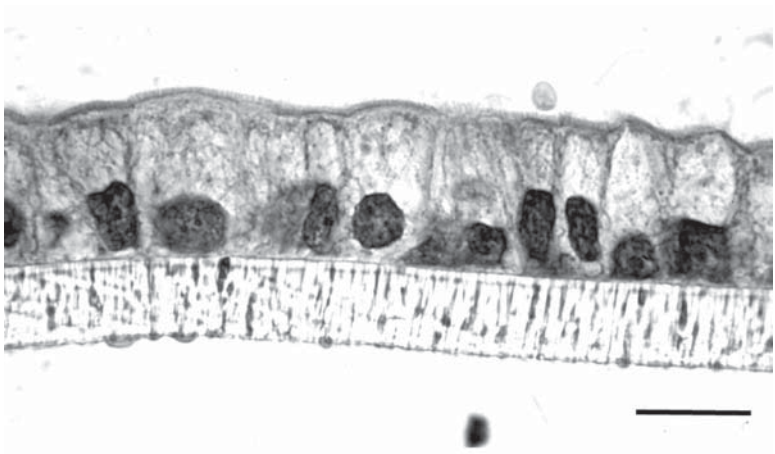

Fig. 2. Microphotograph of differentiated Caco-2 cells on a polycarbonate filter. Caco-2 cells grown on a filter and differentiated for 19 d were embedded in metacrylate resin (JB4; Polysciences Inc., Warrington, PA) and cut into 3-μ*M*-thick sections, stained with hematoxylin–eosin and observed by light microscopy. The cells appear well polarized with basal nuclei and a regular brush border on the AP surface. Bar = 8 μm.

2–3 wk and leads to the formation of a monolayer of cells coupled by functional tight junctions. The establishment of tight junctions can be followed during the differentiation process by measuring the transepithelial electrical resistance (TEER) of the cell monolayer *(21,32)* or the transepithelial passage of radioactively labeled mannitol *(33)*. In addition to mannitol, other molecules of different molecular weight (MW) and Stoke radius have been utilized as extracellular markers of paracellular flow, including PEG 4000 *(17,34,35)*, inulin *(27,36,37)*, and phenol red *(22,38,39)*.

2.3.1. Measurement of Transepithelial Electrical Resistance

Analysis of TEER to passive ion flow relies on a simplified equivalent circuit model viewing the epithelium as a parallel circuit consisting of a paracellular pathway (composed of tight-junction resistance in series with subjunctional lateral space resistance) and a transcellular pathway (as the AP and BL membranes in series). Because the tight junction is often rate limiting to paracellular solute movement, alterations in TEER are commonly used as an index of tight-junction permeability *(5)*. It has, however, to be noted that activation of membrane channels may lead to large changes in TEER that are independent of altered paracellular solute transport, as described in ref. *5*. In addition, TEER measure is influenced by the ionic composition of the medium, such that in particular experimental conditions (i.e., changes in pH or different composition of AP and BL media), the TEER may change independently of paracellular solute permeability. Therefore, TEER measures alone cannot be considered as accurate indicators of paracellular permeability. It is therefore advisable to couple the TEER assay with an analysis of transepithelial flux of an extracellular marker (*see* Section 2.3.2.).

The permeability of the tight junctions was determined by measuring the TEER of filter-grown cell monolayers in a complete culture medium, unless otherwise stated, using a commercial apparatus (Millicell ERS; Millipore Co., Bedford, MA) employing Ag–AgCl electrodes, according to the manufacturer's instructions *(21)*. Briefly, the resistance system was calibrated and the electrical resistance of the cell monolayer was measured by placing one electrode on either side of the polycarbonate filter. Because TEER is influenced by temperature *(17)*, it is important to control the temperature at which TEER is measured. In the present study TEER was always measured at 37°C in a water bath. TEER was expressed as Ohm · centimeter squared ($\Omega \cdot cm^2$) after subtracting from the reading the resistance of the supporting filter and multiplying it by the surface area of the monolayer.

2.3.2. Permeability to Extracellular Markers

The analysis of transepithelial flux of inert solutes such as mannitol (MW 182) or inulin (MW 4000) has often been used to determine the permeability characteristics of the tight junctions *(32,33,40)*. Whereas the detection of mannitol and inulin relies on their radioactive label (either ^3H or ^{14}C), a nonradioactive alternative for flux measurement is phenol red (MW 354) *(38,39)*. Analysis of solute movement across epithelial tight junctions is often reported as a percentage of the tracer, which moves from one side of the epithelium to the other per unit time *(32,33,40)*. Alternatively, solute passage across cell monolayers can be expressed as the apparent permeability coefficient (P_{app}), which is reported in units of mass per area per unit time, thus normalizing for filters of different size. Flux measurements, expressed as P_{app} (cm/s), were calculated using the following equation:

$$P_{app} = KV_tA^{-1} \quad (1)$$

where K is the steady-state rate of change in concentration in the receiver chamber (C_t/C_0) vs time (s); C_t is the concentration in the receiver compartment at the end of each time interval, C_0 is the initial concentration in the AP chamber at each time interval (mol/mL), V_t is the volume of the receiver chamber (mL), and A is the surface area of the filter membrane (cm^2) *(41)*.

When using extracellular flux markers labeled with ^3H, the production of ^3H_2O upon spontaneous degradation of the compound with time has to be considered, as water can move across paracellular and transcellular pathways *(42,43)*. This problem can be overcome by using fresh reagents or ^{14}C-labeled compounds. Phenol red has the advantages of a nonradioactive marker, but it exhibits some disadvantages: The phenol red in the cell growth medium has to be well washed away before the assay and the colorimetric assay is subject to interference from other colored substances that may be used to treat the cell monolayer. In addition, because the passage of phenol red in differentiated "tight" Caco-2 cell monolayers is very low, the influence of the blank value may be high, thus increasing the variability of the measurement.

The transepithelial passage of the radiolabeled extracellular marker D-1[^{3}H(N)]-mannitol (specific activity 706.7 GBq/mmol) (NEN Life Sciences Products, Zaventem, Belgium) across the cell monolayer

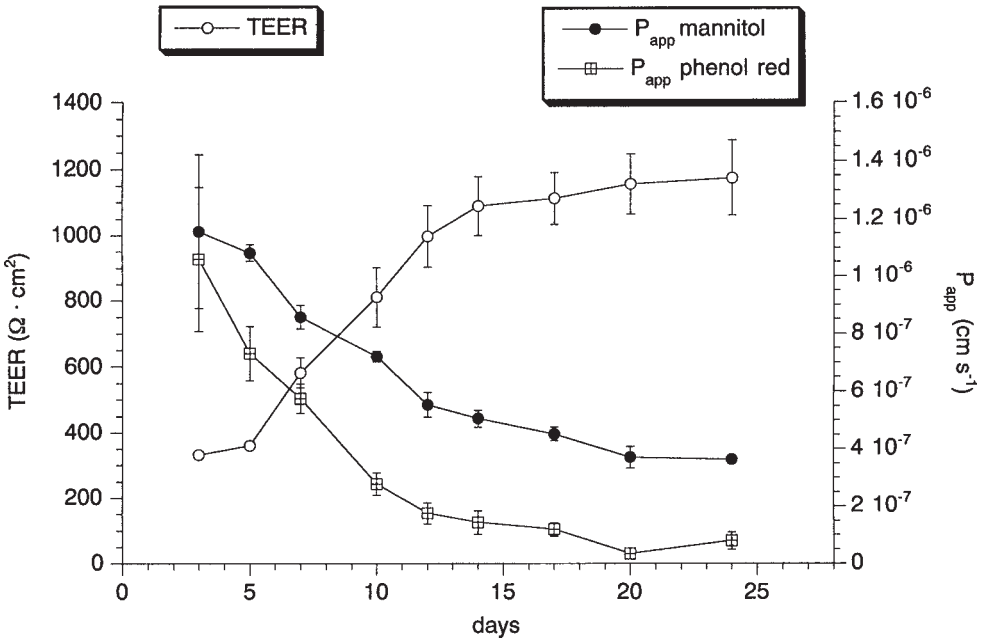

Fig. 3. Establishment of functional tight junctions during differentiation of Caco-2 cells. After seeding Caco-2 cells on the filters (d 0) TEER and transepithelial flux of ^{3}H-mannitol and of phenol red were measured during the process of spontaneous differentiation (from 3 to 24 d) as described in Sections 2.3.1. and 2.3.2. TEER is expressed as Ohm · centimeter squared and the AP to BL flux of the two extracellular markers ^{3}H-mannitol and phenol red as P_{app}, calculated as in Eq. 1. Data are the means ± SD from a representative experiment performed in triplicate.

was determined by adding approx 40 µ*M* ^{3}H-mannitol (1/1000 of stock solution) in serum-free DMEM to the AP compartment, and after 60 min of incubation at 37°C, the radioactivity in the BL compartment was measured in the liquid scintillation counter (LS1801; Beckmann Instruments, Inc., Irvine, CA) *(32,40)*.

The transepithelial passage of phenol red was measured after washing cells in Hank's balanced salt solution (137 m*M* NaCl, 5.36 m*M* KCl, 0.44 m*M* KH_2PO_4, 0.34 m*M* Na_2PO_4, 1 m*M* $CaCl_2$, 1 m*M* $MgCl_2$, 5.6 m*M* glucose [HBSS]) additioned with 10 m*M* *N*-2-hydroxyethyl piperazine-*N*-4-butanesulfonic acid (HEPES) at pH 7.4. 1 m*M* phenol red in HBSS/HEPES (pH 7.4) was added to the AP compartment, and after incubation for 60 min at 37°C, the BL medium was collected. After the addition of 100 µL 0.1 *N* NaOH to 1 mL of BL medium, the absorbance at 560 nm was measured in the spectrophotometer (DU-70, Beckmann Instruments) and the concentration of phenol red calculated from the absorbance of a standard curve after subtraction of the blank obtained by incubating control cells in HBSS/HEPES in the absence of phenol red *(39)*. The transepithelial flux of ^{3}H-mannitol and phenol red were expressed as P_{app} according to Eq. 1.

2.3.3. Establishment of Functional Tight Junctions During Differentiation of Caco-2 Cells

As shown in Fig. 3, after seeding Caco-2 cells on filters (d 0) and measuring TEER and transepithelial flux of mannitol and phenol red during the process of spontaneous differentiation (from 3 to 24 d), a progressive increase in TEER was observed, accompanied by a decrease in the AP to BL permeability to mannitol and phenol red. After 14 d from seeding, all parameters reached a plateau that remained stable up to 24 d, corresponding to a TEER of 1133 ± 88 Ω · cm^2 and a P_{app} for mannitol of $4.2 \times 10^{-7} \pm 6.5 \times 10^{-8}$ cm/s and of phenol red of $1.0 \times 10^{-7} \pm 4.8 \times 10^{-8}$ cm/s. The P_{app} of

the two flux markers, mannitol and phenol red, decreased in parallel during the process of differentiation, exhibiting differences in absolute values that arise from the different size of the two molecules.

The P_{app} of mannitol in differentiated Caco-2 cells is of the same order of magnitude as that previously reported by other authors *(44,45)*, although higher P_{app} (10^{-6} cm/s) have also been reported *(17,46)*. These differences probably reflect differences in permeability of Caco-2 cells from various sources or passage number, often reported in the literature *(17,47,48)*.

3. EFFECT OF COPPER ON TIGHT-JUNCTIONS PERMEABILITY

3.1. Introduction

The effect of copper on epithelial permeability was investigated by our group using the Caco-2 cell line *(49)*. In ref. *49*, $CuSO_4$ was added either to the AP or to the BL compartment at pH 7.4 in complete medium for 24 h. Under these conditions, copper was chelated by amino acids and proteins (e.g., albumin) present in the complete medium and an increase in monolayer permeability was only observed after treatment with 100 μ*M* $CuSO_4$ from the BL side, which resulted in cellular damage, as shown by a decrease in total protein content *(49)*. Further studies demonstrated that ionic Cu(II), added to the AP side of filter-grown differentiated Caco-2 cells in saline solution at pH 6.0 and at pH 7.0, decreased the monolayer permeability in a dose-dependent way from 20 to 100 μ*M* after 3 h of treatment, but only at pH 6.0 *(50)*. These results demonstrate that copper speciation can play a crucial role in modifying intestinal permeability.

When ingested with food, copper is complexed with low-molecular-weight ligands such as amino acids and organic acids, which can influence its bioavailability. Moreover, copper can be given as a nutritional supplement, both as a salt or as a complex with organic molecules *(51)*. However, the stability of such complexes should be assessed after gastric transit at low pH and the gradual increase in pH occurring in the small intestine. Ionic copper can also be present in drinking water as a result of contamination from wells or pipes, especially in slightly acidic conditions.

In order to investigate the effect of different chemical species of copper on intestinal permeability Caco-2 cells were treated with $CuCl_2$, $Cu(His)_2$, and $Cu(Gly)_2$ (chelazome™).

3.2. Materials and Methods

To investigate the effects of copper on the permeability of tight junctions, Caco-2 cells were treated for 3 h at 37°C with increasing concentrations of $CuCl_2$ in HBSS containing 10 m*M* morpholinoethane sulfonic acid (MES) (pH 6.0) in the AP compartment. The BL compartment contained HBSS additioned with 10 mM HEPES at pH 7.4, 0.4 % copper-free bovine serum albumin (BSA), and 120 μ*M* reduced glutathione. The BSA had previously been extensively dialyzed against 0.2 *M* acetate buffer, pH 5.0, to remove copper.

Experiments were performed maintaining the medium in the AP compartment at pH 6.0 and that in the BL compartment at pH 7.4; these conditions reproduce the pH gradient existing in vivo across the mucosa of the small intestine.

The $Cu(His)_2$ complex was freshly prepared by dropwise addition of 2 m*M* $CuCl_2$ in HBSS under continuous vortexing to 4 m*M* L-histidine in HBSS at pH 6.0. The complex was then diluted in HBSS to the required concentration. The copper Chelazome amino acid chelate 2.5% copper complex [$Cu(Gly)_2$], provided by Albion Laboratories (Clearfield, UT), was dissolved in HBSS at the required concentration at pH 6.0 and used fresh.

At the end of copper treatment, the cell monolayer was washed with HBSS and the permeability of the tight junctions was determined by measuring the TEER of filter-grown cell monolayers at 37°C in complete buffered culture medium, as described in Section 2.3.1. When TEER was followed during copper treatment, the measurements were taken in HBSS. For TEER measurements, electrodes were pre-equilibrated for 2 h in the appropriate medium (i.e., HBSS or complete medium). The

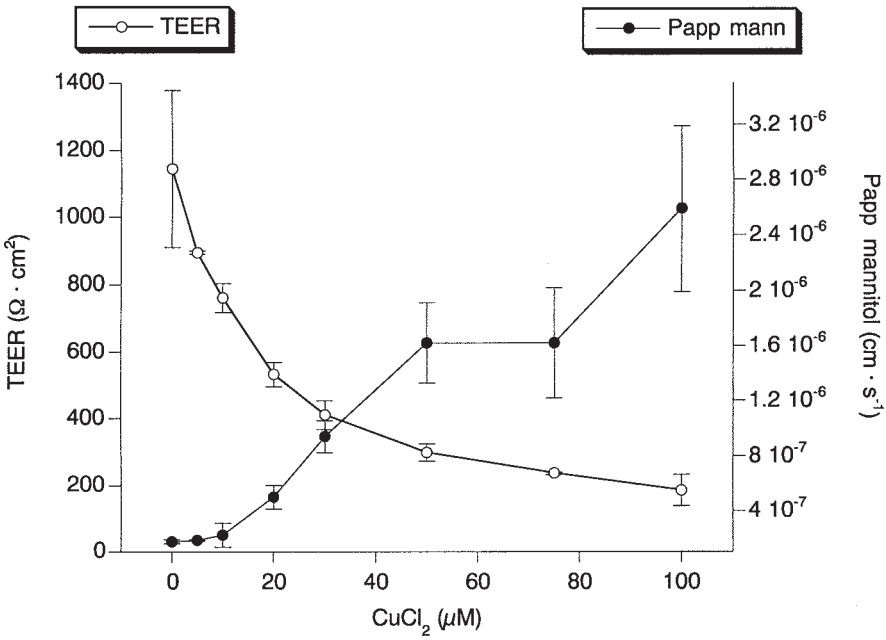

Fig. 4. The dose dependence of copper effect on tight-junction permeability. Caco-2 cells were treated with increasing concentrations of $CuCl_2$ (5–100 μ*M*) in the AP compartment for 3 h at pH 6.0. Following copper treatment, TEER and ^{3}H-mannitol flux were monitored on the same filters. Data are the means ± SD of triplicate filters from a representative experiment.

transepithelial passage of the radiolabeled extracellular marker D-1[^{3}H(N)]-mannitol (specific activity 706.7 GBq/mmol) across the cell monolayer were determined as described in Section 2.3.2.

In recovery experiments, the tight-junction permeability after treatment was monitored by measuring TEER and the cells were transferred in buffered complete culture medium and maintained at 37°C in the incubator or, for brief periods of time, in a water bath, recording TEER values at set intervals up to 26 h.

To ascertain if the recovery after copper treatment was dependent on *de novo* protein or mRNA synthesis, cells were treated with 30 μ*M* $CuCl_2$ for 3 h prior to transfer into complete buffered culture medium containing 10 μ*M* cycloheximide or 0.25 μg/mL actinomycin D. TEER values were recorded at set time intervals both during copper treatment and during recovery, after copper removal and transfer to buffered complete culture medium at 37°C up to 26 h.

3.3. Results and Discussion

Differentiated Caco-2 cells were treated for 3 h with increasing concentrations of $CuCl_2$ in HBSS at AP (pH 6.0), and TEER and ^{3}H-mannitol permeability were monitored simultaneously. As shown in Fig. 4, the decrease in TEER with increasing concentrations of $CuCl_2$ exhibited a half-maximal dose of approx 20 μ*M*. The increase in mannitol passage started at 20 μ*M* and continued progressively up to 100 μ*M*. These data clearly demonstrate that the relationship between transepithelial flux and TEER is nonlinear. This derives from the fact that, in parallel circuits, components of low resistance can dominate the net resistance, even if present at low frequency. Conversely, flux measurements are essentially the sum of fluxes across all junctional pathways *(5)*. Given these considerations, it can be seen that, particularly at values of several hundred Ohm · centimeter squared (as in the case of Caco-2 cell monolayers), very small increments in junctional permeability produced large decreases in TEER (Fig. 4). Conversely, at low TEER values (< 200 Ω · cm^2), relatively large changes in

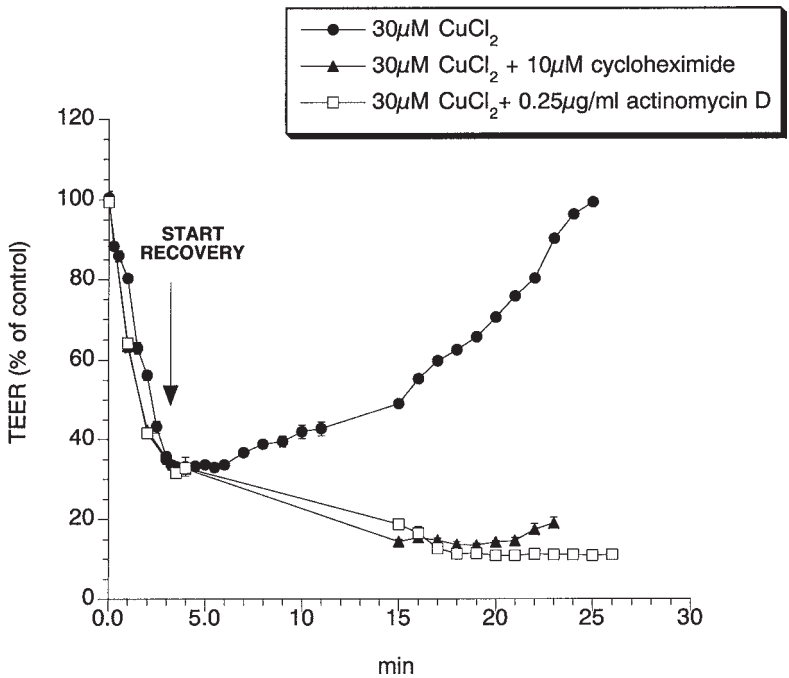

Fig. 5. Time-course of recovery from copper-induced changes to TEER in Caco-2 cells. Caco-2 cells were treated for 3 h with 30 μ*M* $CuCl_2$ at pH 6.0 in the AP compartment with or without 0.25 μg/mL actinomycin D or 10 μ*M* cycloheximide. TEER was monitored at set time intervals during copper treatment and during the subsequent recovery period in complete culture medium without added copper, up to 26 h. Data from a representative experiment performed in triplicate are shown as means ± SD and are expressed as the percent of their respective control (i.e., no additions, with actinomycin D or with cycloheximide).

transjunctional flux of hydrophilic solutes is often associated with very modest changes in TEER. Therefore, depending on the degree of alteration of tight-junctional permeability induced by the toxic agent under study, either TEER or transepithelial flux can better describe the effect. In the case of $CuCl_2$ below 50 μ*M* (for 3 h), TEER modifications are more sensitive indicators of the damage, whereas above this concentration, changes in mannitol flux probably discriminate better the alteration in permeability.

As previously shown, the effect of $CuCl_2$ on the permeability of tight junctions in Caco-2 cells reached a maximum at AP, pH 6.0, and was closely correlated with the AP uptake of copper *(40,50)*. In addition, no damage to cell membranes after treatment with up to 100 μ*M* $CuCl_2$ for 3 h was detected by lactate dehydrogenase (LDH) release assay *(40)*.

To determine whether the effects of copper on tight junctions were reversible, after 3 h of treatment with 30 μ*M* $CuCl_2$, exogenous copper was removed and the cells were transferred to complete buffered medium at 37°C and the TEER values were monitored at regular time intervals for up to 25 h. As shown in Fig. 5, upon copper removal, the TEER, after an initial lag, slowly started to increase, reaching control values after approx 22 h. The addition of either 0.25 μg/mL actinomycin D or 10 μ*M* cycloheximide during the period of recovery indicated that mRNA or protein synthesis inhibitors completely prevented the recovery from occurring after copper removal (Fig. 5).

Reversibility of toxic effects to tight-junction permeability has previously been reported for cytochalasin B, ethanol, and some absorption enhancers, although in contrast to what observed with copper, in these cases the recovery was fast (within 3–4 h) and did not require mRNA or protein synthesis *(52–54)*. These results, together with the observation that, during recovery, copper did not

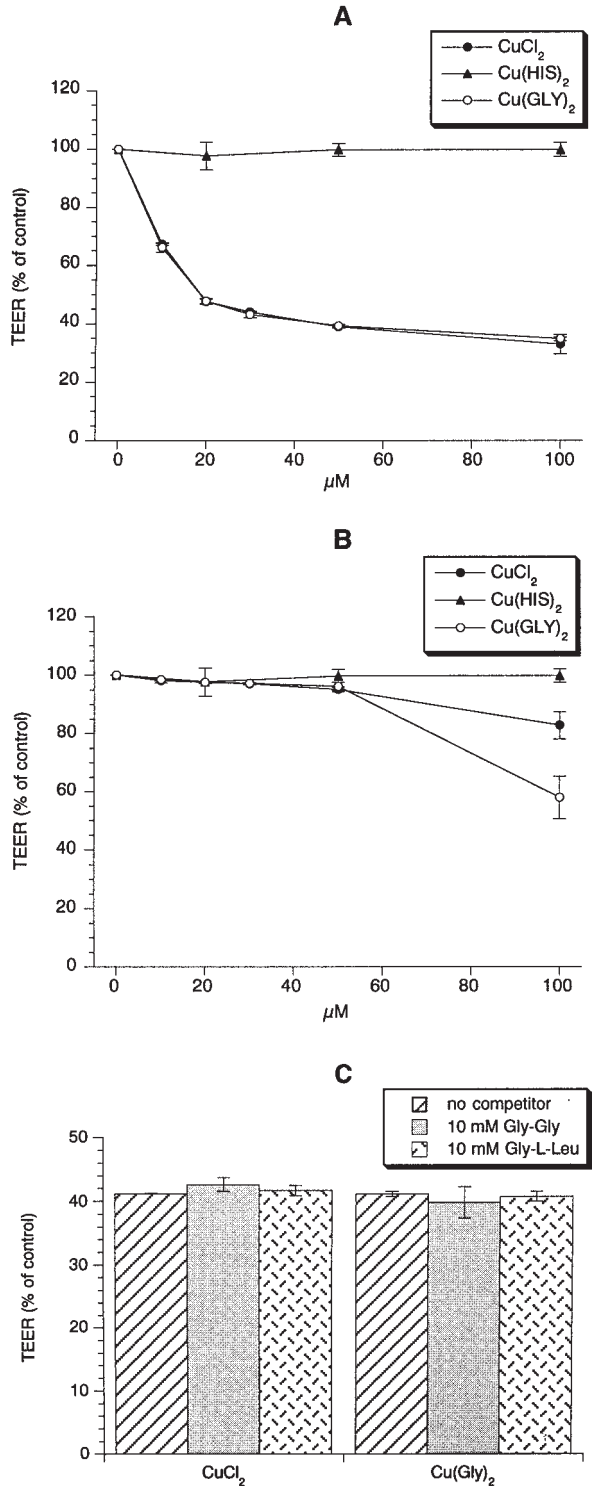

Fig. 6. Effect of different copper chelates on tight-junction permeability in Caco-2 cells. **(A)** Caco-2 cells were treated in the AP compartment for 3 h at pH 6.0 with either $CuCl_2$, $Cu(His)_2$, or $Cu(Gly)_2$ in the concentration range 10–100 μ*M*, and the TEER was measured at the end of the treatment. Data, expressed as the percentage of control, are the means ± SD of triplicate filters from a representative experiment. **(B)** Following copper treatment as detailed in (A), copper was removed and the cells were transferred to buffered culture medium and TEER was measured after 24 h. Data, expressed as the percentage of control, are the means ± SD of (*continued*)

leave the cell *(40)*, suggest that copper acts intracellularly on protein(s) that are involved in the maintenance of tight-junction closure, resulting in an increase in the permeability of the junctions. During the long recovery period in which mRNA transcription and subsequent protein synthesis are required to restore tight-junction functionality, copper does not leave the cell but redistributes to other intracellular ligands, including metallothionein and Cu,Zn-superoxide dismutase *(55)*.

When copper was presented to the Caco-2 cell monolayer complexed with L-histidine [$Cu(His)_2$] or complexed with glycine, as the copper Chelazome $Cu(Gly)_2$ the effect on TEER were markedly different (Fig. 6A). Copper in the form of $Cu(HiS)_2$ had no effect on tight-junction permeability: Between 20 and 100 μ*M* $Cu(His)_2$ did not, in fact, produce the decrease in TEER observed with corresponding concentrations of $CuCl_2$. Conversely, copper in the form of $Cu(Gly)_2$ reduced TEER as a function of the concentration to the same extent as $CuCl_2$. The effects of $Cu(Gly)_2$ were fully reversible after 23 h in complete culture medium, similar to what was observed with $CuCl_2$ at the same concentration (Fig. 6B). In addition, the effect of 30 μ*M* $Cu(Gly)_2$ for 3 h on TEER was not modified by the presence of an excess of dipeptides (10 m*M* Gly-Gly or Gly-L-Leu) in the AP medium (Fig. 6C). These results indicate that $Cu(His)_2$ at the concentrations employed in the present study does not induce changes to tight-junction permeability and this may be related to the reduced AP uptake of this copper complex compared to $CuCl_2$ previously reported in Caco-2 cells *(40)*.

The copper Chelazome may enter the intestinal cells intact via the intestinal dipeptide transporters *(56,57)* and then be hydrolyzed intracellularly. However, this is unlikely, as an excess Gly-Gly or Gly-L-Leu did not reduce the effect of $Cu(Gly)_2$ on tight-junction permeability. Conversely, the similar effect on tight junctions exerted both by ionic copper and by copper Chelazome indirectly suggest that this complex may be dissociated before entering the intestinal cell. Similarly, the bioavailability of zinc Chelazome in rats fed marginal levels of zinc was found to be the same as that of zinc carbonate *(58)*.

4. MORPHOLOGICAL EVALUATION OF COPPER EFFECTS ON CULTURED HUMAN INTESTINAL CACO-2 CELLS

Several toxic stimuli resulting in an increase in tight-junction permeability in Caco-2 cells, including xenobiotics and natural toxins, have been shown to induce depolymerization of the F-actin cytoskeleton *(5,27,53,59,60)* and perturbation of tight-junction proteins *(34,52,53,61)*. We have therefore investigated the morphological effect of copper in Caco-2 cells on the F-actin cytoskeleton and on junctional proteins by fluorescent microscopy and by confocal laser scanning microscopy (CLSM) and on the cell ultrastructure by transmission electron microscopy (TEM).

4.1. Fluorescent Labeling of F-Actin and Nuclei and Localization of Junctional Proteins by Immunofluorescence

4.1.1. Materials and Methods

For morphological studies, cells were seeded on cell culture chamber inserts fitted with transparent membranes (P.E.T. track-etched membrane, 25 mm diameter, 4.71 cm^2 area, 0.4 μm pore diameter; Becton Dickinson Labware Europe, Meylan Cedex, France). Cells were treated from the AP compartment with 50–300 μ*M* $CuCl_2$ or with 200 μ*M* $Cu(His)_2$ in HBSS, pH 6.0 for 3 h at 37°C, and after rinsing with phosphate-buffered saline containing 1 m*M* $CaCl_2$ and 1 m*M* $MgCl_2$ (PBS^+), they

(Continued from Fig. 6 caption)

triplicate filters from a representative experiment. **(C)** Caco-2 cells were treated with 30 μ*M* $CuCl_2$ or 30 μ*M* $Cu(Gly)_2$ for 3 h at pH 6.0, with or without 10 m*M* Gly-Gly or Gly-L-Leu in the AP compartment and the TEER was measured after treatment. Data, expressed as the percentage of their respective control, are the means ± SD of triplicate filters from a representative experiment.

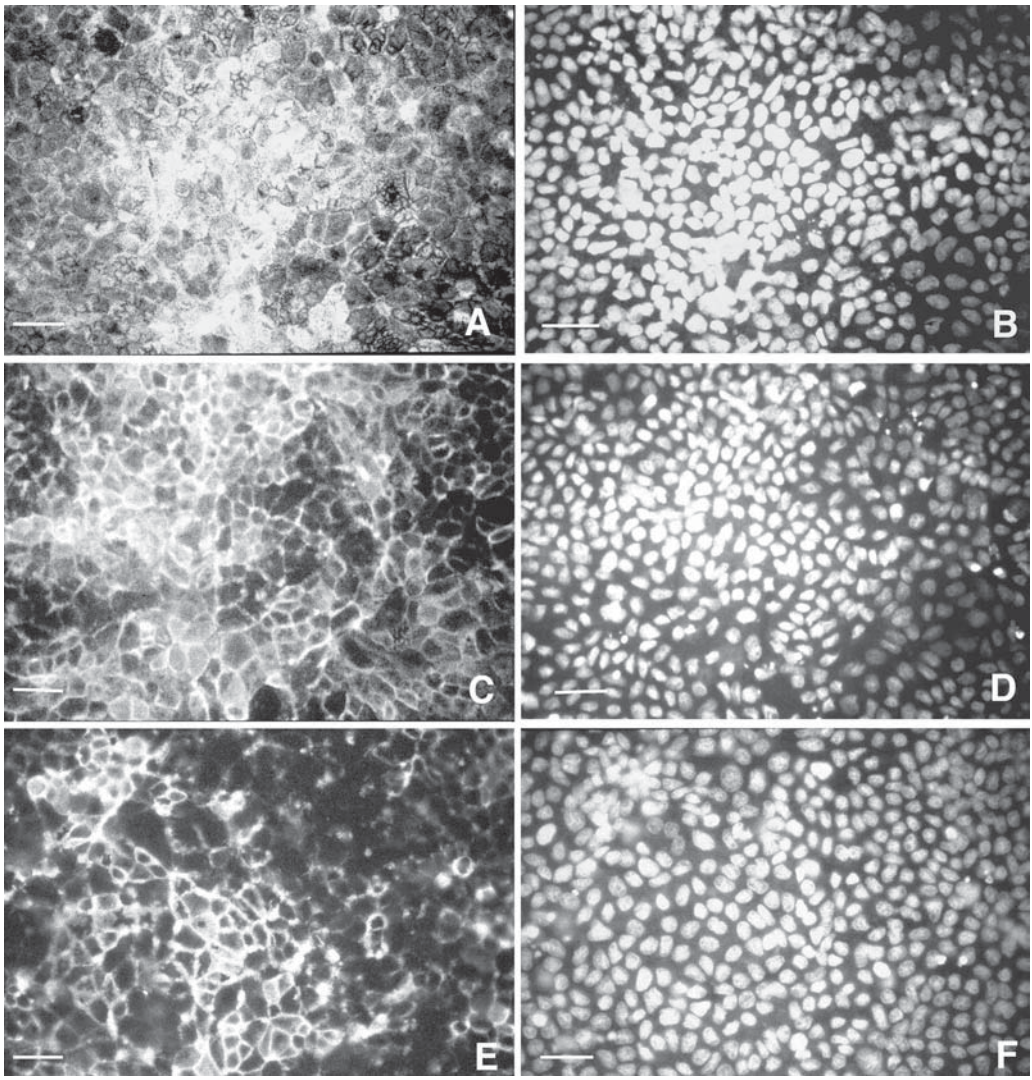

Fig. 7. Fluorescence microscopy of F-actin localized by FITC-phalloidin binding **(A, C, E)** and of nuclei stained with propidium iodide (**B, D, F**) in Caco-2 cells either untreated **(A, B)** or treated from the AP side for 3 h at pH 6.0 with 50 µ*M* **(C, D)** or 300 µ*M* **(E, F)** $CuCl_2$. Bars = 25 µ*M*.

were fixed with 2.5% paraformaldehyde in PBS^+. Free aldehydes were quenched using 50 m*M* NH_4Cl in PBS^+. For immunofluorescent localization of junctional proteins, cells were permeabilized with 0.075% saponin in PBS^+ and the cells were treated with primary antibody and secondary tetramethylrodamine isothiocyanate (TRITC)-conjugated antibody according to conventional techniques. The mouse monoclonal anti-E-cadherin was supplied by Zymed Laboratories Inc. (San Francisco, CA) and the secondary TRITC-conjugated affinity purified goat anti-mouse IgG was from Cappel, (Organon Tecknika Co., Durham, NC). For-F-actin localization cells were incubated for 30 min with 1.7 µg/mL phalloidin (1.28 µ*M*) conjugated with fluorescein isothiocyanate (FITC) in PBS^+ containing 0.075% saponin and 0.2% BSA. After rinsing, filters were mounted in Vectashield (Vector Laboratories, Burlingame, CA). When labeling of nuclei was required, before mounting, the filters were incubated for 30 min at 37°C in 20 µg/mL RNAse A (from bovine pancreas [Boehringer Mannheim

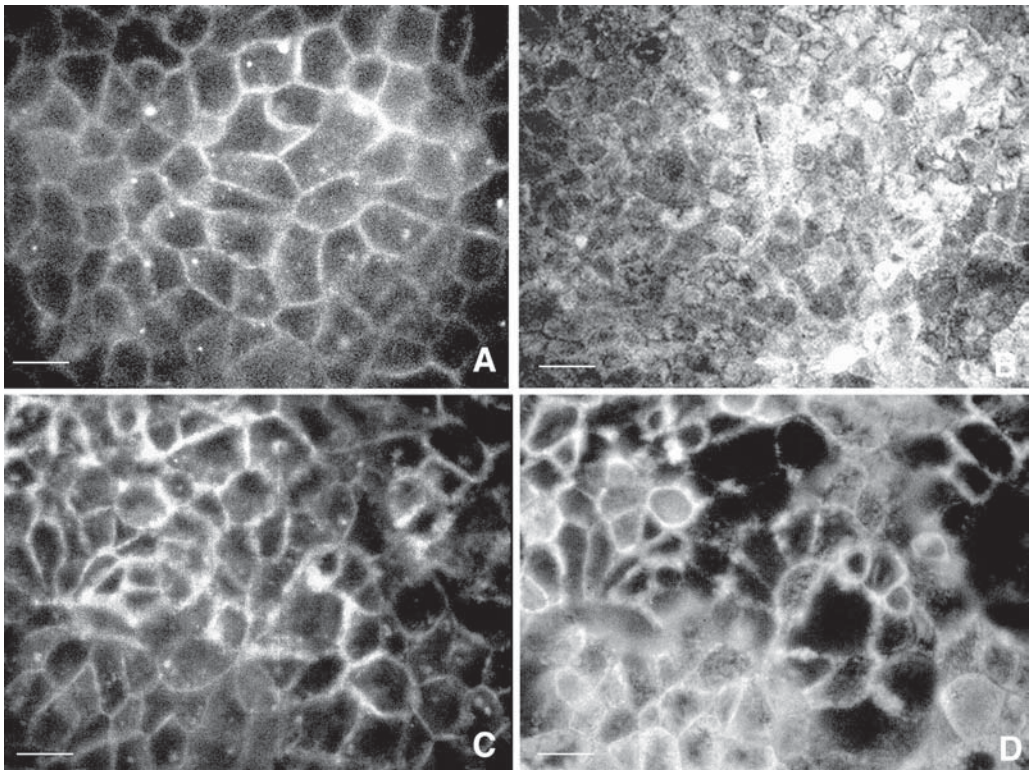

Fig. 8. Immunofluorescence microscopy of the adherens junction protein E-cadherin **(A, C)** and double staining of F-actin by FITC-phalloidin binding **(B, D)** of control cells **(A, B)** and cells treated for 3 h with 50 μ*M* $CuCl_2$ **(C, D)**. In areas where F-actin staining was strongly decreased by copper treatment **(D)**, E-cadherin distribution **(C)** appeared similar to that in control cells **(A)**. Bars = 10 μ*M*.

Italia, Monza, Italy], previously boiled for 10 min to denature DNAse), rinsed in PBS^+ and stained with 0.001% propidium iodide (Sigma-Aldrich Srl, Gallarate, Milan, Italy) in PBS^+ for 10 s and rinsed extensively. The cells were viewed with a fluorescent microscope (Axioscope 2; C. Zeiss, Jena, Germany) or with a confocal laser microscope (CLSM Sarastro 2000; Molecular Dynamics, Sunnyvale, CA). Vertical and horizontal scans were reconstructed through Image Space software (Molecular Dynamics). In particular, images were collected either with the usual scanning method (i.e. laser scans of subsequent *x*-*y*-planes at various *z*-positions in the specimen) or with cross-sections through datasets along the *x*-*z*-plane (i.e., vertical scans), which provide a direct insight into the axial extension of the scanned structures.

4.1.2. Results and Discussion

Alterations in tight-junction permeability are often associated with changes at the level of the actin cytoskeleton. We therefore investigated the distribution of F-actin in control and in copper-treated cells by staining with fluorescent phalloidin. Figure 7A shows the organization of F-actin in control cells, whereas Fig. 7B shows the nuclei in the same microscopic field stained with propidium iodide. Treatment with 50 μ*M* $CuCl_2$ for 3 h led to a marked reduction of F-actin staining in small areas of the cell monolayer (Fig. 7C); nuclear staining of the same microscopic field revealed that the cell monolayer was intact following copper treatment (Fig. 7D). Increasing the concentration of copper to 300 μ*M* $CuCl_2$ produced large areas of the cell monolayer in which the F-actin signal was either absent or strongly reduced and highly disorganized (Fig. 7E). Even in these extreme cases however, the nuclear staining showed lack of cellular loss (Fig. 7F).

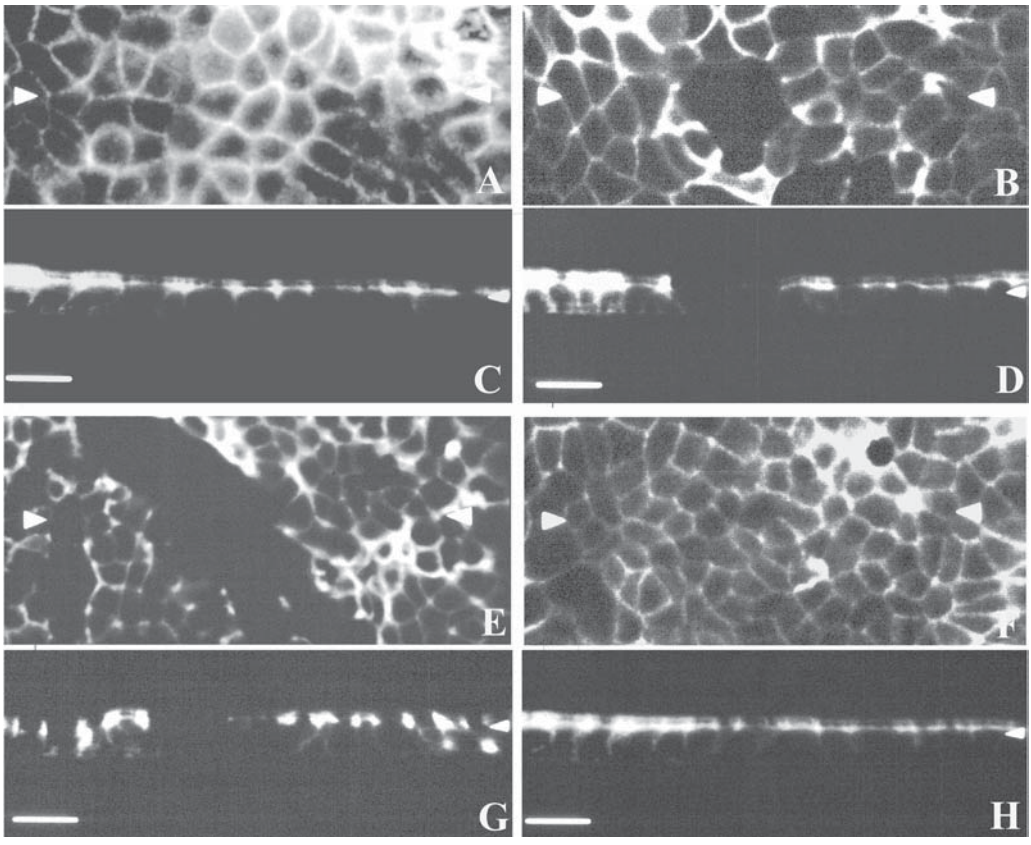

Fig. 9. Confocal laser scanning microscopy of F-actin localized by FITC-phalloidin binding in Caco-2 cells either untreated **(A, C)** or treated from the AP side with 50 μ*M* $CuCl_2$ **(B, D)**, 200 μ*M* $CuCl_2$ (**E, G**) or 200 μ*M* $Cu(His)_2$ **(F, H)**. Arrowheads indicate where horizontal **(A, B, E, F)** and vertical **(C, D, G, H)** scans were taken. Bars = 20 μ*M*.

Double-labeling with an antibody for the adherens junction protein E-cadherin and with FITC-phalloidin showed that following treatment with 300 μ*M* $CuCl_2$ for 3 h, in those areas where the F-actin signal was strongly reduced (Fig. 8D), the E-cadherin signal was correctly localized at the cell periphery (Fig. 8C) and was of the same intensity as in control cells (Fig. 8A). This observation is in accord with recent data indicating that tight junctions in differentiated Caco-2 cells are uncoupled from adherens junctions *(62)*. However, we had previously reported that also the tight-junction proteins ZO1 and occludin did not undergo gross changes in expression and localization following copper treatment *(40)*. Therefore, the mechanisms of copper-induced alteration of tight-junction permeability do not appear to affect the localization of junctional proteins.

Confocal laser scanning microscopy allows a more accurate localization of intracellular signals in polarized cells such as the Caco-2 cells, as it permits acquisition of thin optical sections of relatively thick cell layers, allows exact microphotometry, gathers optical sections for vertical sectioning or three-dimensional reconstruction, and eliminates out-of-focus fluorescence in the plane of focus of the image *(63)*.

As shown in Fig. 9A in a horizontal scan of control cells taken just below the AP surface, the F-actin signal was concentrated in a bundle running around the cell periphery. In a vertical scan of the same cells, the F-actin signal was prominent near the AP surface and along the brush border (Fig. 9C). In cells treated with 50 μ*M* $CuCl_2$ the horizontal scan showed areas of the cell monolayer com-

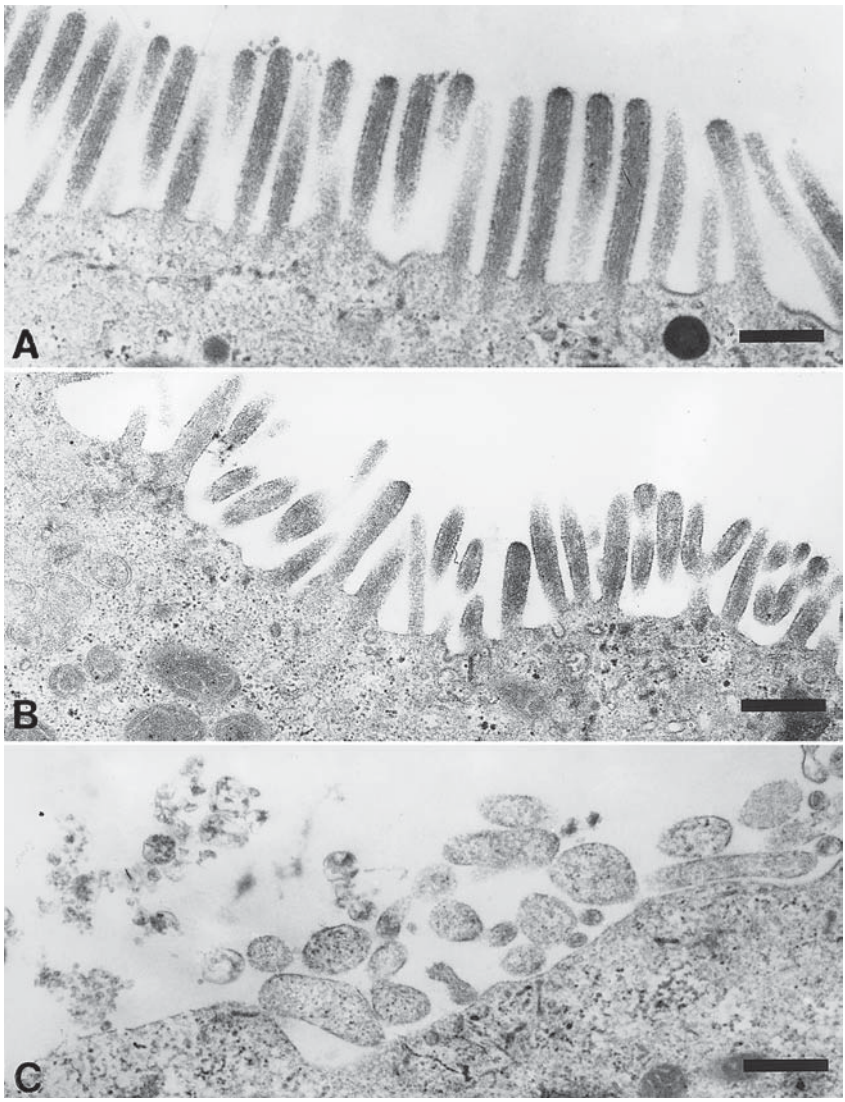

Fig. 10. Transmission electron microscopy of Caco-2 cells treated with copper. Control Caco-2 cells (**A**) and cells treated with 50 μM **(B)** or 200 μ*M* $CuCl_2$ (**C**) in the AP compartment for 3 h at pH 6.0. Ultrastructural changes to microvilli are evident after copper treatment with major disorganization (**B**), swelling and detachment occurring at increasing concentration of copper (**C**). Bars: **A** = 450 nm, **B** = 530 nm, **C** = 590 nm.

posed of a few cells in which the F-actin signal appeared to be absent (Fig. 9B). In the vertical scan taken across these areas, the loss of F-actin staining near the AP membrane and brush border was evident (Fig. 9D). Following treatment with 200 μ*M* $CuCl_2$, the areas showing reduced and altered F-actin staining increased in size and frequency. Figures 9E (horizontal scan below the AP surface) and 9G (vertical scan) showed a large area of the cell monolayer exhibiting strongly decreased staining for F-actin, and the cells all around this patch exhibited reduced and disorganized F-actin signal. Conversely, F-actin staining in cells treated with 50–200 μ*M* $Cu(HiS)_2$ was similar to that in untreated cells [Fig. 9F,H showing horizontal and vertical scans, respectively, of cells treated with 200 μ*M* $Cu(HiS)_2$ for 3 h].

A depolymerizing effect of copper on F-actin has previously been observed in *Mytilus galloprovincialis* emocytes *(64)*. Although copper is able to bind with high affinity to a COOH-terminal cysteine residue of actin, this binding does not appear to affect its state of polymerization *(65)*. However, the effect of copper on F-actin may be indirect and may be mediated by cytosolic factors such as actin-associated proteins, as recently demonstrated for cadmium in an in vitro actin polymerization assay employing cytosol preparations of mesangial cells *(66)*.

4.2. Ultrastructural Studies by Transmission Electron Microscopy

4.2.1. Materials and Methods

To evaluate the effects of copper on the ultrastructure of intestinal Caco-2 cells, copper-treated and control cells were prepared for transmission electron microscopy (TEM).

One-half of the filters used for F-actin-localization experiments were fixed for 1 h in 2.5% glutaraldehyde in 0.1 *M* phosphate buffer (pH 7.4) and postfixed in 1% OsO_4 for 30 min. The samples were dehydrated and embedded in Agar 100 resin (Agar Scientific Ltd., Stansted, Essex, UK). Ultrathin sections were cut (Ultracut E, Reichert Jung Optische Werke, Vienna, Austria), stained, and observed in the electron microscope (CM 10; Philips, Eindhoven, The Netherlands). A rapid and convenient method for processing of filter-grown cells for TEM has been published *(67)* and may also be applied to Caco-2 cells.

4.2.2. Results and Discussion

Figure 10A shows the ultrastructure of microvilli in control-differentiated Caco-2 cells: The microvilli are well aligned and regular in shape and height. Following treatment with 50 μ*M* $CuCl_2$ for 3 h, the ultrastructure of microvilli appeared distorted, with some branched microvilli (Fig. 10B). At higher concentrations, copper induced gross distortions and dilation of microvilli, often detaching from the cell surface (Fig. 10C). Similar changes in microvilli morphology have been reported in kidney proximal tubule cells *(68)* and in isolated rat hepatocytes *(69)* in which F-actin depolymerization had been induced by ATP depletion or by changes in intracellular calcium. Hepatocytes of copper-loaded rats also exhibited ultrastructural alterations of the microvilli *(70)*. The ultrastructural changes to microvilli are probably the result of the copper-induced depolymerization of the major scaffold of microvilli formed by F-actin bundles, as also shown by CLSM data demonstrating a complete loss of F-actin signal in the area of the brush border (Fig. 9).

5. POSSIBLE MECHANISMS OF THE COPPER EFFECT ON INTESTINAL TIGHT JUNCTIONS

5.1. Copper and Oxidative Stress

Like other transition metals, copper is able to produce reactive oxygen species in aqueous solutions and hence to produce oxidative damage to the cell. The toxic oxygen metabolites have many intracellular effects, including enhanced lipid peroxidation, DNA damage, and altered calcium and sulfhydryl homeostasis *(71)*.

To test whether the effect of copper ions on tight-junction permeability was mediated by the production of reactive oxygen species (ROS) we used a set of antioxidants (mannitol, dimethylsulfoxide, and a soluble derivative of vitamin E). None of these ROS scavengers, added during the treatment of Caco-2 cells with 30 μ*M* $CuCl_2$ at pH 6.0 for 4 h in the AP compartment, was able to counteract the effect of copper ions on the tight junctions as measured by ^{3}H-mannitol passage and by TEER measure *(50)*.

It had previously been demonstrated that hydrogen peroxide was able to increase paracellular permeability in Caco-2 cells via activation of protein tyrosine phosphorylation *(72)*. In a more recent work, this group further demonstrated that hydrogen peroxide but not superoxide anions nor the

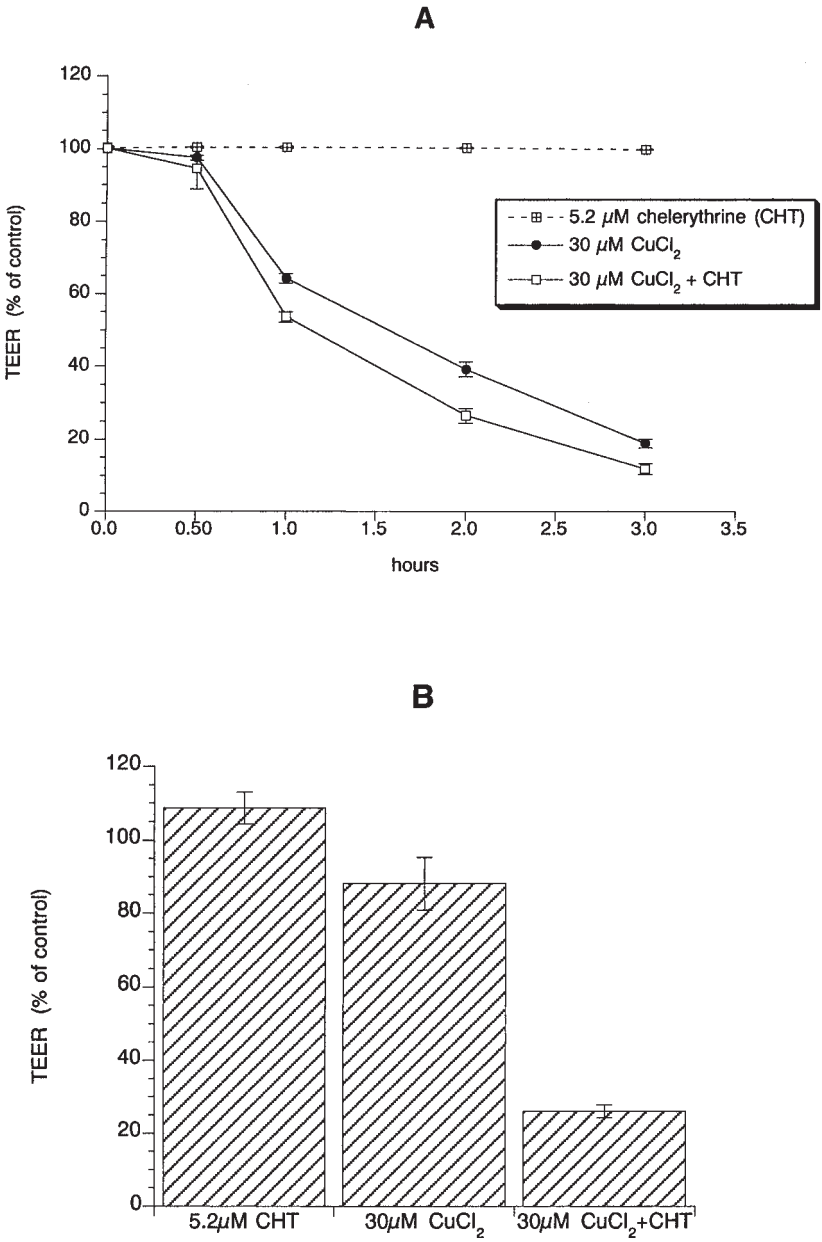

Fig. 11. Effect of PKC inhibition on the copper decrease in TEER and subsequent recovery following copper removal. **(A)** Caco-2 cells were treated with 30 μ*M* $CuCl_2$ in the AP compartment at pH 6.0 with or without the addition of 5.2 μ*M* chelerythrine chloride (CHT) an inhibitor of PKC, in the AP and BL media. TEER was monitored during the treatments. Data, expressed as a percentage of their respective control, are the means ± SD from a representative experiment performed in triplicate. **(B)** Following the treatment described in (**A**), copper was removed and the cells were transferred to the complete culture medium for recovery, and the TEER was measured after 24 h. Data, expressed as a percentage of their respective control, are the means ± SD from a representative experiment performed in triplicate.

hydroxyl radical were able to decrease paracellular permeability in Caco-2 cells *(73)*. Because the hydroxyl radical is the main radical species produced by copper ions via the Fenton reaction, we therefore suggest that, under the conditons used in our experiments, copper ions are unlikely to produce alterations in tight-junction permeability via an oxidant-induced mechanism.

5.2. Protein Kinase C

The assembly of tight junctions is tightly regulated by a network of signal transduction pathways that include, among others, protein kinase C (PKC) *(74)*. The role of PKC in tight-junction formation, however, appears to be multifaceted, and this may explain some conflicting results reported in the literature on the effects of PKC activators and inhibitors on tight-junction permeability. PKC activation by phorbol esters has been reported to decrease TEER in Caco-2 cells *(75)*. Similarly, in renal LLCPK1 cells, activation of protein kinase by phorbol esters led to a decrease in TEER associated with occludin dephosphorylation and delocalization from the tight junctions to the cytoplasm *(76)*. An opposite effect of phorbol esters on tight-junction permeability has recently been reported in Caco-2 cells: PKC inhibition prevented the increase in TEER observed upon activation of PKC, suggesting a role of PKC in the regulation of TEER via decreased phosphorylation of the regulatory light chain of myosin II *(77)*.

In order to investigate a possible role of PKC in the copper-induced changes in tight-junction permeability and during the recovery period, Caco-2 cells were treated with 30 μ*M* $CuCl_2$ at pH 6.0 for 3 h with or without the PKC inhibitor chelerythrine chloride (Sigma-Aldrich Srl) *(78)* in the AP and BL compartments, and TEER was monitored during treatment. Chelerythrine chloride was used at 5.2 μ*M* in HBSS/HEPES at pH 7.4 in the BL and in HBSS/MES at pH 6.0 in the AP compartment. After copper removal, cells were transferred to complete cell culture medium with or without 5.2 μ*M* chelerythrine in both compartments, and the TEER was measured after 24 h. As shown in Fig. 11, inhibition of PKC activity by chelerythrine did not markedly modify the effect of copper on TEER (Fig. 11A), but it prevented the restoration of monolayer permeability after 24 h of recovery (Fig. 11B).

The lack of effect of PKC inhibition on the copper-induced increase in tight-junction permeability does not point to an involvement of copper in the phosophorylation events controlling tight-junction permeability. Inhibition of PKC had no effect on control cells, confirming that its activity is not required for the maintenance of already established tight monolayers *(79)*. Conversely, PKC inhibition prevented the recovery of TEER following copper removal, suggesting a role of PKC in the reassembly of the F-actin cytoskeleton as reported in T84 and IEC6 intestinal cells *(80–82)*.

6. CONCLUSIONS

The human intestinal Caco-2 cell line has proved a useful model for studying the effect of copper on tight-junction permeability at the functional and structural level.

We demonstated in this work that copper has a specific toxic effect at the intestinal level, disrupting the barrier function that is established and maintained by tight junctions.

The copper-induced decrease in tight-junction permeability in Caco-2 cells is mediated by a perturbation of the F-actin cytoskeleton, depends on copper speciation, and is reversible after copper removal. The molecular mechanism responsible for the observed alteration to tight-junction permeability produced by copper in Caco-2 cells are still unknown.

An abnormal increase in intestinal paracellular permeability may be an important pathogenic factor in various intestinal and systemic diseases, allowing indiscriminate flow to the mucosal space and to the circulation of molecules that can act as allergens, inflammatory mediators, and toxins.

Food contaminants such as copper or other xenobiotics able to modify tight-junction permeability may play an important role, following both acute or chronic ingestion, in the ever-increasing incidence of food allergies, especially in infants.

The Caco-2 cell model and the use of tight-junction permeability as a sensitive and specific end point in the assessement of intestinal copper toxicity could be recommended as an in vitro method to help in the establishment of maximum tolerable levels of copper in food and water.

ACKNOWLEDGMENTS

This work was supported by the European Community, FOODCUE contract no FAIR-CT95-0813. We wish to thank Thompson and Joseph (LdT, Norwich, UK) for providing us with copper-chelazome. We thank A. Di Giacinto for preparation of TEM specimens and L. Virgili for photographic work.

REFERENCES

1. Pizarro, F., Olivares, M., Gidi, V., and Araya, M. (1999) The gastrointestinal tract and acute effects of copper in drinking water and beverages. *Rev. Environ. Health* **14,** 231–238.
2. McMullen, W. (1971) Copper contamination of soft drinks from bottle pourers. *Health Bull.(Edinb.)* **29**, 94–96.
3. Spitalny, K., Brondum, J., Vogt, R., Sergent, H., and Kappel, S. (1984) Drinking-water-induced copper intoxication in a Vermont family. *Pediatrics* **74**, 1103–1106.
4. Jantsch, W., Kulig, K., and Rumack, B. (1985) Massive copper sulfate ingestion resulting in hepatotoxicity. *Clin. Toxicol.* **22**, 109–116.
5. Madara, J. (1998) Regulation of the movement of solutes across tight junctions. *Annu. Rev. Physiol.*, **60**, 143–159.
6. Mitic, L. and Anderson, J. (1998) Molecular architecture of tight junctions. *Annu. Rev. Physiol.* **60**, 121–142.
7. Matter, K. and Balda, M. (1999) Occludin and the functions of tight junctions. *Int. Rev. Cytol.* **186**, 117–146.
8. Mitic, L., Van Itallie, C., and Anderson, J. (2000) Molecular physiology and pathophysiology of tight junctions. I. Tight junctions structure and function: lessons from mutant animals and proteins. *Am. J. Physiol. Gastrointest. Liver Physiol.* **279**, G250–G254.
9. Fogh, J., Fogh, J. M., and Orfeo, T. (1977) One hundred and twenty seven cultured human tumor cell lines producing tumors in nude mice. *J. Natl. Cancer Inst.* **59**, 221–226.
10. Pinto, M., Robine-Leon, S., Appay, M., Kedinger, M., Triadou, E., Dussaulx, E., et al. (1983) Enterocyte-like differentiation and polarization of the human colon carcinoma cell line Caco-2 in culture. *Biol. Cell* **47**, 323–330.
11. Matsumoto, H., Erickson, R., Gum, J., Yoshioka, M., Gum, E., and Kim, Y. (1990) Biosyntesis of alkaline phosphatase during differentiation of the human colon cancer cell line Caco-2. *Gastroenterology* **98**, 1199–1207.
12. Levy, P., Robert, A., and Picard, J. (1988) Biosynthesis of glycosaminoglycans in the human colonic tumor cell line Caco-2: structural changes occurring with the morphological differentiation of the cells. *Biol. Cell* **62**, 255–264.
13. Levy, P., Cherqui, G., Robert, A., Wicek, D., and Picard, J. (1989) Changes in glycosaminoglycan sulfatation and protein kinase C subcellular distribution during diferentiation of the human colon tumor cell line Caco-2. *Experientia* **45**, 588–591.
14. Zweibaum, A., Laburthe, M., Grasset, E., and Louvard, D. (1991) Use of cultured cell lines in studies of intestinal cell differentiation and function, in *Handbook of Physiology: The Gastrointestinal System* (Field, M. and Frizzel, R. A., eds.), American Physiology Society, Bethesda, MD, Vol. 4, pp. 223–255.
15. Grasset, E., Pinto, M., Dussaulx, E., Zweibaum, A., and Desjeux, J. F. (1984) Epithelial properties of human colonic carcinoma cell line Caco 2: electrical parameters. *Am. J. Physiol.* **247**, C260–C267.
16. Grasset, E., Bernabeu, J., and Pinto, M. (1985) Epithelial properties of human colonic carcinoma cell line Caco-2: effect of secretagogues. *Am. J. Physiol.* **247**, C260–C267.
17. Delie, F. and Rubas, W. (1997) A human colonic cell line sharing similarieties with enterocytes as a model to examine oral absorption: Advantages and limitations of the Caco-2 model. *Crit. Rev. Therap. Drug Carrier Syst.* **14**, 221–286.
18. Harris, D. S., Slot, J. W., Geuze, H. J., and James, D. E. (1992) Polarized distribution of glucose transporter isoforms in Caco-2 cells. *Proc. Natl. Acad. Sci. USA* **89**, 7556–7560.
19. Alvarez-Hernandez, X., Nichols, G. M., and Glass, J. (1991) Caco 2 cell line: a system for studying intestinal iron transport across epithelial cell monolayers. *Biochim. Biophys. Acta* **1070**, 205–208.
20. Alvarez-Hernandez, X., Madigosky, S., Stewart, B., and Glass, J. (1994) Iron status affects aluminium uptake and transport by Caco-2 cells. *J. Nutr.* **124**, 1574–1580.
21. Ferruzza, S., Ranaldi, G., Di Girolamo, M., and Sambuy, Y. (1995) The transport of lysine across monolayers of human cultured intestinal cells (Caco-2) depends on Na^+-dependent and Na^+-independent mechanisms on different plasma membrane domains. *J. Nutr.* **125**, 2577–2585.
22. Fleet, J. and Wood, R. (1999) Specific, 1,25,(OH)2D3-mediated regulation of transcellular calcium transport in Caco-2 cells. *Am. J. Physiol.* **276**, G958–G964.
23. Han, O., Failla, M. L., Hill, A. D., Morris, E. R., and Smith, J. C. (1994) Inositol phosphates inhibit uptake and transport of iron and zinc by a human intestinal cell line. *J. Nutr.* **124**, 580–587.
24. Jumarie, C., Campbell, P., Berteloot, A., Houde, M., and Denizeau, F. (1997) Caco-2 cell line used as an in vitro model to study cadmium accumulation in intestinal epithelial cells. *J. Membr. Biol.* **158**, 31–48.
25. Leblondel, G. and Allain, P. (1999) Manganese transport by Caco-2 cells. *Biol. Trace Element Res.* **67**, 13–28.

26. Raffaniello, R., Lee, S.-Y., Teichberg, S., and Wapnir, R. (1992) Distinct mechanisms of zinc uptake at the apical and basolateral membranes of Caco-2 cells. *J. Cell. Physiol.* **152**, 356–361.
27. De Angelis, I., Vincentini, O., Brambilla, G., Stammati, A., and Zucco, F. (1998) Characterization of furazolidone apical-related effects to human polarized intestinal cells. *Toxicol. Appl. Pharmacol.* **152**, 119–127.
28. Martinsson, T. (1999) Ropivacaine inhibits serum-induced proliferation of colon adenocarcinoma cells in vitro. *J. Pharm. Exp. Ther*. **288**, 660–664.
29. Bjorge, S., Hamele, K., Homan, R., Rose, S., Turluck, D., and Wright, D. (1991) Evidence for glucuronide conjugation of *p*-nitrophenol in the Caco-2 cell model. *Pharm. Res.* **8**, 1441–1443.
30. Boulenc, X., Bourrie, M., Fabre, I., Roque, C., Joyeux, H., Berger, Y., et al. (1992) Regulation of cytochrome P4501A1 gene expression in a human intestinal cell line, Caco-2. *J. Pharm. Exp. Ther.* **263**, 1471–1478.
31. Prueksaritanont, T., Gorham, L., Hochman, J., Tran, L., and Vyas, K. (1996) Comparative studies of drug-metabolising enzymes in dog, monkey and human small intestines and in Caco-2 cells. *Drug Metab. Dispos*. **24**, 634–642.
32. Ranaldi, G., Islam, K., and Sambuy, Y. (1994) D-Cycloserine uses an active transport mechanism in the human intestinal cell line Caco 2. *Antimicrob. Agents Chemother.* **38**, 1239–1245.
33. Ranaldi, G., Islam, K., and Sambuy, Y. (1992) Epithelial cells in culture as a model for the intestinal transport of antimicrobial agents. *Antimicrob. Agents Chemother.* **36**, 1374–1381.
34. Duizer, E., Gilde, A., Versantvoort, C., and Groten, J. (1999) Effects of cadmium chloride on the paracellular barrier function of intestinal epithelial cells. *Toxicol. Appl. Pharmacol.* **155**, 117–126.
35. Kotze, A., Thanou, M., Luessen, H., de Boer, B., Verhoef, J., and Junginger, H. (1999) Effect of the degree of quaternization on N-trimethyl chitosan chloride on the permeability of intestinal epithelial cells (Caco-2). *Eur. J. Pharm. Biopharm.* **47**, 269–274.
36. Manna, C., Galletti, P., Cucciolla, V., Moltedo, O., Leone, A., and Zappia, V. (1997) The protective effect of the olive oil polyphenol (3,4-dihydroxyphenyl)-ethanol counteracts reactive oxygen metabolite-induced cytotoxicity in Caco-2 cells. *J. Nutr.* **127**, 286–292.
37. Ma, T., Tran, D., Hoa, N., Nguyen, D., Merryfield, M., and Tarnawsky, A. (2000) Mechanism of extracellular calcium regulation of intestinal epithelial tight junction permeability: role of cytoskeletal involvement. *Microsc. Res. Tech*. **119**, 156–168.
38. Jovov, B., Wills, N., and Lewis, S. (1991) A spectroscopic method for assessing confluence of epithelial cell cultures. *Am. J. Physiol.* **261**, C1196–C1203.
39. Fleet, J. and Wood, R. (1994) Identification of calbindin D9k mRNA and its regulation by 1,25 dihydroxyvitamin D3 in Caco-2 cells. *Arch. Biochem. Biophys.* **308**, 171–174.
40. Ferruzza, S., Scarino, M., Rotilio, G., Ciriolo, M., Santaroni, P., Onetti Muda, A., et al. (1999) Copper treatment alters the permeability of tight junctions in cultured human intestinal Caco-2 cells. *Am. J. Physiol.* **277**, G1138–G1148.
41. Tavelin, S., Milovic, V., Ocklind, G., Olsson, S., and Arturrson, P. (1999) A conditionally immortalized epithelial cell line for studies of intestinal drug transport. *J. Pharmacol. Exp. Toxicol.* **290**, 1212–1221.
42. Ma, T. and Verkman, A. (1999) Aquaporin water channels in gastrointestinal physiology. *J. Physiol.* **517**, 317–326.
43. Snigirevskaya, E. and Komissarchik, Y. (2000) Structural correlates of the transepithelail water transport. *Int. Rev. Cytol.* **198**, 203–275.
44. Stewart, B., Chan, O., Lu, R., Reyner, E., Schmid, H., Hamilton, H., et al. (1995) Comparison of intestinal permeabilities determined in multiple in vitro and in situ models: relationship to absorption in humans. *Pharm. Res.* **12**, 693–699.
45. Artursson, P. and Karlsson, J. (1991) Correlation between oral drug absorption in humans and apparent drug permeability coefficients in human intestinal epithelial (Caco 2) cells. *Biochem. Biophys. Res. Commun.* **175**, 880–885.
46. Rubas, W., Jezyk, N., and Grass, G. M. (1993) Comparison of the permeability characteristics of the human colonic epithelial (Caco-2) cell line to colon of rabbit, monkey, and dog intestine and human drug absorption. *Pharm. Res.* **10**, 113–118.
47. Walter, E. and Kissel, T. (1995) Heterogeneity in the human intestinal cell line Caco-2 leads to differences in transepithelial transport. *Eur. J. Pharm. Sci.* **3**, 215–230.
48. Yu, H., Cook, T., and Sinko, P. (1997) Evidence for diminished functional expression of intestinal transporters in Caco-2 cell monolayers at high passage. *Pharm Res.* **14**, 757–762.
49. Rossi, A., Poverini, R., Di Lullo, G., Modesti, A., Modica, A., and Scarino, M. (1996) Heavy metal toxicity following apical and basolateral exposure in the human intestinal cell line Caco-2. *Toxicol. In Vitro* **10**, 27–36.
50. Ferruzza, S., Sambuy, Y., Rotilio, G., Ciriolo, M., and Scarino, M. (1999) The effect of copper on tight junctional permeability in a human intestinal cell line (Caco-2), in Coppert Transport and Its Disorders: Molecular and Cellular Aspects. (Leone, A. and Mercer, J., eds.), vol, 448, Plenum, New York, pp. 215–222.
51. Wapnir, R. (1998) Copper absorption and bioavailability. *Am. J. Clin. Nutr.* **67(Suppl.)**, 1054S–1060S.
52. Ma, T., Hollander, D., Tran, L., Nguyen, T., Hoa, N., and Bhalla, D. (1995) Cytoskeletal regulation of Caco-2 intestinal monolayer paracellular permeability. *J. Cell. Physiol.* **164**, 533–545.
53. Ma, T., Nguyen, D., Bui, V., Nguyen, H., and Hoa, N. (1999) Ethanol modulation of intestinal epithelial tight junction barrier. *Am. J. Physiol.* **276**, G965–G974.
54. Sakai, M., Imai, T., Ohtake, H., Azuma, H., and Otagiri, M. (1997) Effect of absorption enhancers on the transport of model compounds in Caco-2 cell monolayers: assessment by confocal laser scanning microscopy. *J. Pharm. Res.* **86**, 779–785.
55. Ferruzza, S., Sambuy, Y., Ciriolo, M., De Martino, A., Santaroni, P., Rotilio, G., et al. (2000) Copper uptake and intracellular distribution in the human intestinal Caco-2 cell line. *BioMetals* **13**, 179–185.

56. Ganapathy, V. and Leibach, F.H. (1991) Proton-coupled solute transport in the animal cell plasma membrane. *Curr. Opin. Cell Biol*. **3**, 695–701.
57. Thwaites, D. T., Hirst, B. H., and Simmons, N. L. (1993) Direct assessment of dipeptide/H^+ symport in intact human intestinal (Caco-2) epithelium: a novel method utilising continuous intracellular pH measurement. *Biochem. Biophys. Res. Commun.* **194**, 432–438.
58. Fairweather-Tait, S., Fox, T., Wharf, S., and Ghani, N. (1992) A preliminary study of the bioavailability of iron- and zinc-glycine chelates. *Food Addit. Contam*. **9**, 97–101.
59. Okada, T., Narai, A., Matsuanga, S., Fusetani, N., and Shimizu, M. (2000) Assessment of the marine toxins by monitoring the integrity of human intestinal Caco-2 cell monolayer. *Toxicol. In Vitro* **14**, 219–226.
60. Brunet, J., Cotte-Laffitte, J., Linxe, C., Quero, A., Geniteau-Legrende, M., and Servin, A. (2000) Rotavirus infection induces an increase in intracellular calcium concentration in human intestinal epithelial cells: role in microvillar actin alteration. *J. Virol.* **74**, 2323–2332.
61. Peiffer, I., Blanc-Potard, A., Bernet-Camard, M., Guignot, J., Barbat, A., and Servin, A. (2000) Afa/Dr diffusely adherin Escherichia coli C1845 infection promotes selective injuries in the junctional domain of polarized human intestinal Caco-2/TC7 cells. *Infect. Immunol.* **68**, 3431–3442.
62. Gomez, S., del Mont Llosas, M., Verdu, J., Roura, S., Lloreta, J., Fabre, M., et al. (1999) Independent regulation of adherens junction by tyrosine phosphorylation in Caco-2 cells. *Biochim. Biophys. Acta* **1452**, 121–132.
63. Wright, S., Centonze, V., Stricker, S., De Vries, P., Paddock, S., and Schatten, G. (1993) Introduction to confocal microscopy and three-dimensional reconstruction. *Methods Cell Biol.* **38**, 1–45.
64. Fagotti, A., Di Rosa, I., Simoncelli, F., Pipe, R., Panara, F., and Pascolini, R. (1996) The effects of copper on actin and fibronectin organization in *Mytilus galloprovincialis* in haematocytes. *Dev. Compar. Immunol.* **20**, 383–391.
65. Kim, E. and Reisler, E. (1996) Intermolecular coupling between loop 38-52 and the C-terminus in actin filaments. *Biophys. J.* **71**, 1914–1919.
66. Wang, Z. and Templeton, D. (1996) Cellular factors mediate cadmium-dependent actin depolymerization. *Toxicol. Appl. Pharmacol.* **139**, 115–121.
67. Parton, R. (1995) Rapid processing of filter-grown cells for epon embedding. *J. Histochem. Cytochem*. **43**, 731–733.
68. Nurko, S., Sogabe, K., Davis, J., Roeser, N., Defrain, M., Chien, A., et al. (1996) Contribution of actin cytoskeleton alterations to ATP depletion and calcium-induced proximal tubule cell injury. *Am. J. Physiol.* **270**, F39–F52.
69. Lange, J., Schlieps, K., Lange, K., and Knoll-Kohler, E. (1997) Activation of calcium signaling in isolated rat hepatocytes is accompanied by shape changes of microvilli. *Exp. Cell Res.* **234**, 486–497.
70. Fuentealba, I. and Haywood, S. (1988) Cellular mechanisms of toxicity and tolerance in the copper-loaded rat. I. Ultrastructural changes in the liver. *Liver* **8**, 372–380.
71. Stohs, S. and Bagchi, D. (1995) Oxidative mechanisms in the toxicity of metal ions. *Free Radical Biol. Med.* **18**, 321–336.
72. Rao, R., Baker, R., Baker, S., Gupta, A., and Holycross, M. (1997) Oxidant-induced disruption of intestinal epithelial barrier-function: role of protein tyrosine phosphorylation. *Am. J. Physiol.* **273**, G812–G823.
73. Rao, R., Li, L., Baker, S., Baker, S., and Gupta, A. (2000) Glutathione oxidation and PTPase inhibition by hydrogen peroxide in Caco-2 cell monolayer. *Am. J. Physiol*. **279**, G332–G340.
74. Balda, M. and Matter, K. (1998) Tight junctions. *J. Cell Sci.*, **111**, 541–547.
75. Stenson, W., Easom, R., Riehl, T., and Turk, J. (1993) Regulation of paracellular permeability in Caco-2 cell monolayers by protein kinase C. *Am. J. Physiol.* **28**, G955–G962.
76. Clarke, H., Peralta Soler, A., and Mullin, J. (2000) Protein kinase C activation leads to dephosphorylation of occludin and tight junction permeability increase in LL-PK1 epithelial cell sheets. *J. Cell Sci.* **113**, 3187–3196.
77. Turner, J., Angle, J., Black, E., Joyal, J., Sacks, D., and Madara, J. (1999) PKC-dependent regulation of transepithelial resistance: roles of MLC and MLC kinase. *Am. J. Physiol.* **277**, C554–C562.
78. Jarvis, W., Turner, A., Povirk, L., Traylor, R., and Grant, S. (1994) Induction of apoptotic DNA fragmentation and cell death in HL60 human promyelocytic leukemia cells by pharmacological inhibitors of protein kinase C. *Cancer Res*. **54**, 1707–1714.
79. Denker, B. and Nigam, S. (1998) Molecular structure and assembly of the tight junction. *Am. J. Physiol.* **274**(Renal Physiol. **43**), F1–F9.
80. Hecht, G., Robinson, B., and Koutsouris, A. (1994) Reversible disassembly of an intestinal epithelial monolayer by prolonged exposure to phorbol esters. *Am. J. Physiol.* **266**, G214–G221.
81. Tai, Y., Flick, J., Levine, S., Madara, J., Sharp, G., and Donowitz, M. (1996) Regulation of tight junction resistance in T84 monolayers by elevation in intracellular Ca^{2+}: a protein kinase C effect. *J. Membr. Biol*. **149**, 71–79.
82. Fasano, A., Fiorentini, C., Donelli, G., Uzzau, S., Kaper, J., Margaretten, K., et al. (1995) Zonula occludens toxin modulates tight junctions through protein kinase C-dependent actin reorganization in vitro. *J. Clin. Invest*. **96**, 710–720.

25

Cellular Responses to Copper in Aquatic Organisms

Importance of Oxidative Stress and Alteration of Signal Transduction

Aldo Viarengo, Bruno Burlando, and Claudia Bolognesi

1. INTRODUCTION

Copper (Cu) is a metal that can be found as an essential cofactor of several metalloproteins fundamental for cell and organism physiology *(1,2)*. The concentration of organic Cu in organisms is tightly regulated *(3,4)*. Despite its weak effect on terrestrial vertebrates, copper is considered an extremely toxic cation, as it is able to affect the physiological status of invertebrates and protists at nanomolar concentrations *(5)*. Also, aquatic vertebrates, such as teleost fish, are sensitive to Cu and to heavy-metal cations, probably the result of the metals toxic effects on the gills and the gastrointestinal tract, which are essential for the osmoregulation of these organisms *(6–8)*.

It must be noted, however, that Cu is generally introduced with the diet and does not usually represent a toxicological problem for mammals and, more generally, for terrestrial vertebrates: As an example, the metal concentration in the drinking water may reach values as high as 2 mg/L, without any symptoms of toxicity in humans *(9)*. However, numerous reports have demonstrated that in the case of Cu deficiency and in diseases characterized by the alteration of Cu homeostasis *(10,11)*, Cu toxicity becomes evident in mammals and humans. Cu is a transition metal belonging to group B of the periodic table of elements, including the essential metal Zn, the highly toxic environmental inorganic pollutants Cd and Hg, and the rare metals Ag and Au. These metals exert their biological effects as a result of common chemical properties such as a high affinity for sulfhydryl (SH) groups and acidic residues in proteins as well as the binding to ion imidazolic groups of protein nucleic acid, substrates and metabolites (S > N > O) *(12,13)*.

Interestingly, Cu is the only element of group B that may shift between an oxidized (Cu^{2+}) and a reduced status (Cu^{+}) in the cellular environment which significantly changes its affinity for SH groups (Hg^{2+}> Cu^{+} > Cd^{2+}> Cu^{2+} > Zn^{2+}). Moreover, similar to Fe^{2+}, in the presence of the physiological metabolite H_2O_2, Cu^{+} is oxidized in the Fenton-like reaction:

$$Cu^{+} (Fe^{2+}) + H_2O_2 \rightarrow Cu^{2+}(Fe^{3+}) + OH^{-} + {}^{\bullet}OH^{-}$$

thereby becoming a reactive oxygen species (ROS) producer able to enhance the cellular levels of hydroxyl radical ($OH^{\times}$) *(14)*. Hydroxyl radicals are extremely reactive and have been found to stimulate lipid peroxidation in cell membranes *(15)*. Moreover, copper can also react with lipoperoxide, producing peroxyradicals ($ROO^{\bullet}$) and the more reactive alkoxy radicals ($RO^{\bullet}$):

From: Handbook of Copper Pharmacology and Toxicology
Edited by: E. J. Massaro © Humana Press Inc., Totowa, NJ

$$ROOH + Cu^{2+} \rightarrow ROO^{\bullet} + Cu^{+} + H^{+}$$

$$ROOH + Cu^{+} \rightarrow RO^{\bullet} + Cu^{2+} + OH^{-}$$

These redox properties may render Cu and Fe cations particularly able to induce oxidative stress at the cellular and organism level.

For the purpose of this chapter, the mechanisms will be described by which an excess of Cu, through oxidative stress, may alter the physiological status of aquatic organisms. Examples of toxic effects on particular cell types or tissues aid in understanding the mechanisms of well-known Cu effects at the organism level. In order to offer a more comprehensive description of Cu effects at the subcellular level, results on aquatic organisms will be compared with others obtained on mammalian cells.

2. CELLULAR MECHANISMS OF Cu HOMEOSTASIS

Copper homeostasis should include all cellular processes that are essential for the maintenance of a physiological level of Cu in the cell, as well as the related levels of antioxidants suitable to inactivate the ROS produced by copper through redox cycling reactions.

Recent reports based mainly on yeast and vertebrates (3) have clarified that the main Cu entry pathway is related to the presence of a carrier (CTR) able to transfer Cu(I) from the external medium into the cytosol *(16)*. In the oxidative extracellular environment, copper is usually present as Cu(II), but on the cell surface, a Cu reductase reduces Cu(II) to Cu(I), that is eventually transferred into the cytosol *(3)*. It must be stressed, however, that the cells of protozoa and invertebrates, in particular the digestive cells of the hepatopancreas, are able to assume most of copper complexed to partially digested food by endo/phagocytosis.

The metal that enters the cell may be detoxified by different mechanisms. Cu may be bound by a specific sulfhydryl-rich protein called metallothionein (MT), showing an extremely high affinity for Cu(I) cations *(17,18)*. MT binds another essential metal, Zn, and other metal cations such as Hg^{2+} and Cd^{2+} that are usually considered as highly toxic environmental pollutants. The synthesis of MT is stimulated by Cu ions, as well as by other heavy metals, that penetrate into the cells *(5,19)*. Despite its inducibility, MT binds stoichiometrically to Cu ions that penetrate into the cytosol and rapidly eliminates only limited amounts of Cu. In addition, also glutathione (GSH), although with a lower affinity than MT, plays an important role in binding Cu(I). GSH-bound Cu may actually represents a significant percentage of total Cu present in the cytosolic environment *(20)*.

A second, more recently discovered, component of the Cu homeostasis system is a Cu-dependent ATPase that actively pumps the ion outside of the cell in the presence of high copper concentrations. This pump represents a key element for the survival of many cell types *(4)*, whereas dysfunction thereof is related to the well-known Wilson's and Menkes diseases *(21,22)*. The data available on the Cu ATPase mainly come from yeast, plant, and vertebrate cells where the enzyme has been identified both at the plasma membrane *(23)* and in the endoplasmic reticulum *(4)*. Recent studies demonstrate that this system also plays a fundamental role in the slime mold *Dictyostelium discoideum* (Burlando, unpublished data). However, more research is needed to clarify the importance of this Cu translocase in invertebrate cells, for which there is a lack of information.

The lysosomal vacuolar system has been shown to play an important role in sequestering part of the cellular excess of heavy metals *(24)*. In these organelles, Cu is bound to peroxidation products (lipofuscin) or to polymerized MT *(25–27)*. The fact that most cells can excrete the content of residual bodies renders this system important in the maintenance of tolerable Cu levels.

It was also reported that the formation of mineral granules, both P_i-pyrophosphate *(28)* and sulfur-containing granules *(29)*, is involved in Cu detoxification in different marine invertebrates, such as mollusks *(30,31)* and crustaceans *(32,33)*.

As for the incorporation of Cu in different cellular metalloproteins, it was initially hypothesized that MT may act as a transfer element for the redistribution of Cu to the different apoproteins *(17)*.

More recently, it was shown that, in vertebrates, a class of low-molecular-weight proteins, named Cu chaperones, has an important role in Cu redistribution. A growing body of evidence indicates that this class of proteins may play a fundamental role in cellular Cu handling *(4,34)*.

As mentioned earlier, under physiological conditions, cytosolic Cu^+ will produce ROS as a result of the presence of H_2O_2. In order to neutralize the possible toxic effects of ROS, a complex of antioxidant systems is present in the cell *(35)*. A group of antioxidant enzymes, including superoxide dismutase (SOD), catalase, and glutathione peroxidase, is involved in ROS scavenging. To complement the action of these enzymes, there are both cytosolic hydrophylic scavengers, such as GSH, MT, and ascorbic acid, and lipophylic scavengers present in membranes, such as vitamin E, carotenoids, and so forth.

In invertebrates, the quantitative composition of this complex antioxidant system shows seasonal variations *(36,37)*, suggesting that to avoid oxidative damage the cellular levels of free Cu (and Fe) and of antioxidants should be tightly regulated.

Considering the subcellular level, Cu-induced oxidative stress was found to affect different organelles (viz. plasmamembrane, endoplasmic reticulum, lysosomes and peroxisomes, mitochondria, and the nucleus).

3. EFFECTS OF Cu ON CELL COMPARTMENTS

3.1. Effects on the Plasma Membrane and the Endoplasmic Reticulum

The lipid peroxidation process stimulated by ROS involves an increase of malondialdehyde (MDA), other toxic aldehydes, and, more generally, carbonyl compounds *(38,39)*. When the Cu concentration in the cell overwhelms both metal homeostasis and the antioxidant defense system, free-Cu cations will alter cell functions and, consequently, organism physiology, both by direct binding to proteins and nucleic acids and by oxidative stress.

It has been shown that 50 μ*M* Cu and 100 μ*M* ascorbate, when added in vitro to membrane preparations obtained from mussel tissues, stimulate lipid peroxidation *(40)*. Moreover, it has been also demonstrated that exposure of mussels to a sublethal Cu concentration of 0.6 μ*M* for 4 d stimulates the lipid peroxidation process, as shown by enhanced concentrations of MDA and of other toxic aldehydes, such as hydroxinonenal, in the digestive gland tissue *(41)*. Similar results have been obtained with different mollusks exposed to copper *(42,43)*.

Exposure to Cu also causes oxidative alteration of gills, with a significant enhancement of MDA concentration and a decrease in GSH content. Immunohistochemical analysis has shown that this is associated to a disruption of the tubulin structure of the ciliated epithelium *(44)*, thereby explaining metal effects on ciliary activity, filtration rates, and the consequent decrease of scope for growth *(45–47)*.

However, it must be mentioned that the addition of 100–200 μ*M* Cu to tissue homogenates greatly inhibits the MDA reaction with thiobarbituric acid (*48*; Viarengo, unpublished data). This implies that in this kind of study, MDA tissue levels should be analyzed by high-performance liquid chromatography (HPLC) analyses *(49)* rather than by the TBA-based colorimetric method, although other colorimetric methods may be worth testing *(50)*. This might explain the limited number of articles concerning Cu effects on membrane lipid peroxidation. However, analysis of lipofuscin granules that accumulate in lysosomes is generally considered a good indication of oxidative stress, and, accordingly, a drastic increase of lipofuscin accumulation was found in the lysosomes of Cu-exposed mussels *(5)*. Cu-induced oxidative stress was demonstrated to occur also in the tissues of fish *(51)*, crustaceans *(52)*, and protozoa *(53)*.

A series of articles has demonstrated that the activity of ATPase-driven cation pumps, such as Na/K ATPase and Ca-ATPase, are affected by Cu *(40,54–56)*. However, differences between in vivo and in vitro results have been found. Data on fish gill plasma membrane pointed out that although Cu and other heavy metals are able to inhibit the Ca-ATPase activity in vitro, exposure of fish to low Cu

concentrations in long-term experiments actually increases this enzymatic activity *(56)*. Similar results have been obtained in metal-exposed mollusks *(40)*. These findings can be explained by the large number of SH residues in the Ca-ATPase. It can be hypothesised that, in the short term, the reaction of sulfhydryls with Cu(I) cations, together with SH oxidation by ROS, may inhibit the catalytic activity of the enzymes. However, in the long term, the enzyme activity would tend to increase as a result of a higher number of Ca-ATPase molecules synthesized by cells as an adaptive response to the Cu-polluted environment *(56)*. This view seems to be confirmed by data indicating that fish osmoregulation is affected by short treatments with Cu, whereas after longer Cu exposure, osmoregulation is recovered *(6,57)*.

Research on marine mussels has clearly demonstrated that, at micromolar concentrations, Cu significantly inhibits the in vitro Ca-ATPase activity of gill cell plasma membranes *(40)*. It has also been shown that Cu acts by preventing the formation of the phosphorylated Ca-ATPase intermediate, an essential step for Ca^{2+} transport across the plasma membrane *(40)*. Interestingly, Hg shows a stronger effect than Cu when added in vitro to the reaction mixture, but the copper inhibition effect on P-enzyme formation is strongly enhanced in the presence of ascorbic acid *(40)*. Under the latter condition, copper undergoes redox cycling, subsequently causing ROS production and lipid peroxidation, this explaining the higher inhibitory effects of copper on the Ca-ATPase activity. Also, in the reducing environment created by the ascorbic acid part of the copper is present in solution as Cu(I) cations that have a higher affinity for SH residues, thus directly inhibiting the enzyme activity. Such experimental conditions, resembling the reducing environment of the cytosol, are particularly suitable to point out the toxicity potential of the metal on plasma membrane cation transport.

Interestingly, when Cu is added to the reaction medium in the presence of other heavy metals, such as Cd and Hg, it shows additive inhibitory effects on the Ca^{2+}-ATPase *(40,58)*.

Results obtained in vitro have been confirmed by in vivo experiments showing that a 4-day exposure of mussels to a sublethal Cu concentration of 0.6 μ*M* strongly affects both Na/K ATPase and Ca-ATPase activities (approx 80%) *(59)*. However, after 7 d of metal exposure, the activity of the two enzymes is completely restored. In the same experiments, the concentrations of GSH and MDA follow a similar trend, with a drastic reduction of GSH (–40%) and an increase of MDA after 4 d of metal exposure, and a recovery of normal levels after 7 d.

Research on mussels has also shown that in gills, digestive gland and the mantle Cu affects the rate of amino acid uptake, probably as a result of an alteration of different amino acid carriers present in the plasma membrane *(60)*.

In conclusion, the data concerning Cu effects on transmembrane ion and amino acid transport can explain results obtained in the 1970s, showing that copper pollution in the aquatic environment affects osmoregulation not only in osmoregulator (euryhaline) animals but also in osmoconformer (stenohaline) organisms of estuarine habitats, such as mussels *(6)*.

Concerning Cu effects on endoplasmic reticulum, experiments on rat hepatic microsomal vesicles demonstrated that Cu (in the range of 5–20 μ*M*) inhibits Ca uptake and evokes a rapid Ca efflux *(61)*. Similar data were obtained using preparations of rat sarcoplasmic reticulum *(62)*. More recently, by using vesicles of the sarcoplasmic reticulum obtained from the adductor muscle of *Pecten jacobeus*, it has been demonstrated that a mixture of Cu and ascorbate at micromolar concentrations is able to evoke a prompt Ca release (Viarengo, unpublished results). Such an effect is associated with an oxidative burst and is reduced in the presence of millimolar amounts of GSH. In similar experiments using Fe/ascorbate, it has been shown that the Ca^{2+} release from SR is principally the result of Ca^{2+} channel opening operated by free radicals, most likely through SH oxidation. However, at a later stage, the activity of the SR Ca-ATPase is also inhibited by the oxidative effect of ROS produced through Cu redox cycling *(63)*.

It has been assessed also that in mussels exposed to 80 μg/L Cu for 7 d a significant reduction in the rate of protein synthesis also occurs *(60)*. Another important effect of Cu (but also of highly toxic metals such as Hg and Cd) is the inhibition of mixed-function oxygenase (MFO) activity present in

the smooth endoplasmic reticulum *(64)*. As known, MFO plays a fundamental role in steroid metabolism, as well as in the oxidation of lipophilic organic xenobiotic compounds *(65–67)*. Concerning the intermediate metabolism, it has been shown that when the metal is present in seawater at 0.6 μ*M*, it stimulates the GSH transferase activity in the gills and digestive gland of mussels *(5)*, thus possibly explaining the mechanism by which Cu drastically reduces the concentration of GSH in these tissues. Moreover, Cu also affects the cellular levels of amino acids in metal-exposed mussels *(68)*, which is likely to depend on a reduction in the amino acid uptake *(60)* and on an alteration of amino acid metabolism. In this regard, it has been found that Cu specifically inhibits the activity of aspartate and alanine transferase in the gills of the mollusk *Ruditapes philippinarum (69)*. As known, transaminases play an important role in regulating the intracellular amino acid pool. In addition, in intertidal marine invertebrates, transaminases are important during the anaerobiosis phase of the initial period of emersion, when aspartate represents the main energy substrate and alanine represents one of the principal end products *(69)*. Interestingly, Cu does not affect the activity of transaminases in vitro *(70)*.

3.2. Effects on Mitochondria

Different reports have shown that Cu may affect the rate of oxygen consumption in various aquatic organisms *(5)*. In mussels exposed to 200 μg/L Cu, the oxygen consumption is drastically reduced (about 50%), leading to a reduced survival of animals *(71)*. Moreover, 0.5–1 mg/L Cu was found to be toxic for shrimps (*Poeneus japonicus*) when exposed for 4 d to the metal. Among the alterations, a decrease in the number and size of mitochondria was described, together with a disorganization of their structure *(72)*.

In the liver of the rainbow trout, *Salmo gairdneri*, after exposure to 30–100 μg/L of Cu, a low respiratory control ratio (RCR) and a high inhibition of respiration rate indicated that the metal highly affects the mitochondrial function *(73)*. On the other hand, by using the alga *Nitzschia closterum*, it has been reported that 1.6 μ*M* Cu, a concentration able to inhibit cellular division, does not affect cell respiration rate and ATP production *(74)*. Similarly, Cu concentrations ranging from 2.5 to 40 ppm alter the osmoregulatory function of the crab *Carcinus maenas* and *Cancer irroratus*, but have no effect on the oxygen consumption of gill cells *(75)*.

The high copper concentrations used in experiments revealing effects on mitochondria suggest that only when a high level of Cu accumulates in the cytosol do detrimental effects on mitochondria occur. Support of this explanation comes from the exposure of mussels to sublethal concentrations of Cu (40 μg/L). In this case, the first cytotoxic effect is a destabilization of lysosomal membranes, followed by an alteration of mitochondrial membranes. Despite the effect of copper on mitochondria, only small variations of adenylate energy charge (AEG) are detected *(76)*. This may be a consequence of the metal decreasing the total cell metabolism and, consequently, producing a reduction in ATP utilization.

Concerning the mechanism of Cu action on mitochondria, it has been shown that an uptake of Cu^{2+} in the presence of energy gives rise to K^+ uptake from K^+-cointaining media, with accompanying swelling and respiratory stimulation. However, depending on the concentrations of Cu^{2+} and K^+, an inhibition of respiration follows *(77)*. More recent results have confirmed that Cu^+, at micromolar levels, promotes electrochemical K^+/H^+ exchange and facilitates the K^+ uniport probably by activating mitochondrial K^+ channels sensitive to glibenclamide *(78)*. Other causes for mitochondrial dysfunction induced by Cu could reside in the stimulation of ROS production and lipid peroxidation. Recent data *(79)* demonstrated that Cu toxicity in rat hepatocytes is related to the oxidative stress resulting from ROS production. Interestingly, by using different ROS scavengers, it was shown that this occurs as the result of mitochondrial ROS production independent of the cytosolic radical formation resulting from Cu redox cycling. In the fish, an impairment of mitochondrial function after Cu exposure was found to depend on lipid peroxidation of mitochondrial membrane *(80)*. Under these

conditions, also the uptake of Ca^{2+} may be compromised, thus reducing the efficiency of mitochondria as a last barrier against Ca^{2+} cytotoxicity deriving from an alteration of calcium homeostasis.

A different mechanism of action of Cu on the mitochondrial activity is the inhibition of enzymes of the Krebs cycle. It has been reported that in the kidney of the scallop *Placopecten magellanicus*, exposed to 20 µg/L Cu for 2 mo, isocitrate dehydrogenase is significantly reduced *(81)*. As a result of the essential role of this enzyme in the production of reduced equivalents needed for ATP synthesis, this effect may also contribute to the Cu-induced alteration of mitochondrial activity in aquatic organisms.

In conclusion, these data might explain contradictory results obtained in relation to Cu exposure and the effects on mitochondrial respiration rate.

3.3. Effects on Lysosomes

The lysosomal vacuolar system represents the main cellular site for the degradation of both endogenous and exogenous macromolecules *(82)*. Moreover, lysosomes are a preferential site for heavy-metal accumulation *(33,83–85)*.

Although the lysosomal acidic environment should not represent optimal conditions for metal-cation accumulation, different studies have demonstrated that metal binds to lysosomal lipofuscin granules. Lipofuscin is a complex mixture consisting of end products from protein and lipid oxidation. These oxidized compounds are not perfectly digested by the lysosomal enzymes and therefore tend to accumulate in these organelles, representing the main component of residual bodies. During formation of lipofuscin granules, metal cations react with acidic groups of oxidated lipids and proteins on the granule surface and, upon further growth of the granules, metal ions become sterically trapped in the lipofuscin structure. At a later stage, lipofuscin is eliminated by most cells through the exocytosis of residual bodies *(86)*.

Copper may follows this type of metal accumulation, but, at least in mussel, it is also accumulated into lysosomes by polymerization of Cu-binding metallothioneins driven to lysomes by protein turnover. Because of the acidic pH of lysosomes, metallothionein loses Zn cations and tends to polymerize by intermolecular disulfide bridges *(18)*.

Although lysosomes may accumulate high amounts of copper, this cation is able to alter the physiology of these organelles. It has been demonstrated that when marine organisms are exposed to a low cation concentration, one of the most evident symptoms of toxicity is the destabilization of lysosomal membranes *(42,87)*. This latter parameter is actually considered one of the most powerful biomarkers used in the monitoring of the effects of environmental pollutants.

The destabilization of lysosomal membranes is an essential step for the fusion of lysosomes with endoexophagosomes, leading to the formation of secondary lysosomes that are the active site of macromolecule degradation. A correlation between lysosomal membrane destabilization and activation of protein catabolism was demonstrated in mussel digestive gland cells exposed to phenantrene *(88)* and to Hg^{2+} (Burlando, unpublished results). This suggests that also Cu-induced lysosomal membrane destabilization should involve an increase in protein catabolism, at least in the first phase of lysosomal activation. In line with this view is the fact that copper also activates Cu proteases present in mollusk lysosomes *(89)*.

However, it is well known that long-term treatments with Hg, Cd, or with organic xenobiotics inactivate lysosomal enzymes and thereby slow down protein catabolism *(88,90)*. In the case of metals, this may be the result of the binding to SH domains in lysosomal hydrolases, thereby causing an inhibition of hydrolytic activities.

Moreover, different heavy metals are able to increase the lysosomal pH, most likely by inhibiting the proton pump present in the lysosomal membrane *(91)*. Interestingly, metal effects on lysosomal membranes add to the effects of hormones, such as 17 β estradiol, that physiologically act at the cellular level by enhancing lysosomal protein catabolism. Therefore, copper effects on lysosomes in

mussel cells may also be dependent on the hormonal status, which, in invertebrates, shows seasonal changes in relation to gonadal maturation. Little is known about the molecular mechanisms by which Cu (and other metals) activates lysosomal protein catabolism. However, it is important to note that the copper effect is additive to that of other metals such as Hg and Cd *(91)*.

3.4. Copper Genotoxicity

Copper compounds have been tested for genotoxic and mutagenic effects by using a variety of assays. Because of contradictory results, even with the same Cu compound, the mutagenic potency of copper is equivocal *(92–94)*. $CuCl_2$ was found to be genotoxic in the Mutatox and SOS assays using *Escherichia coli* VA4567 and *E. coli* 4537 *(95)*. However, copper did not show a mutagenic effect with the *S. typhimurium* or *E. coli*/mammalian microsome mutagenicity tests using the standard plate incorporation assay or the preincubation method *(96)*. $CuSO_4$ in a range of 1–1000 m*M* was negative in the SOS chromotest *(96)*. The lack of effects with the Ames and *E. coli* tests could be explained by the lower heavy-metal bioavailability produced by the use of solid culture media *(92)*. On the other hand, copper compounds have been reported to be mutagenic on mammalian cells in culture *(97,98)*. Cu accumulates in the nuclear fraction of cultured hepatocytes and induces a statistically significant unscheduled DNA synthesis *(94)*.

At micromolar concentrations, copper has been shown to enhance DNA damage in several biological systems: It increases the lethal effects of ionizing radiation and is involved in DNA damage by microwaves and ultraviolet (UV) radiation *(99,100)*. In plant bioassays using *Tradescandia*, *Vicia faba*, or *Allium cepa*, Cu did not affect micronuclei frequency *(101)*.

In aquatic organisms, Cu is highly accumulated by a number of organisms at different trophic levels *(102,103)* and reveals an induction of chromosomal damage. In vitro studies with cultured heart cells of *Crassostrea gigas* demonstrated an increase in micronuclei frequency by $CuSO_4$ *(104)*.

An in vivo study in *Mytilus galloprovincialis* revealed a dose-dependent increase of micronuclei frequency in gill cells of mussels exposed to 5–40 µg/L of $CuCl_2$. In addition, $CuCl_2$ caused a statistically significant increase in DNA damage measured by the alkaline elution technique at a concentration of 40 µg/L *(105)*. The mutagenic effects of copper may be caused by ROS produced through the Fenton reaction *(106,107)*.

As for the mechanisms of Cu-dependent genotoxicity, copper is an essential component of chromatin that accumulates preferentially in heterochromatic regions, destabilizing DNA. Therefore, high copper dosages could induce both clastogenic effects and spindle disturbances, as suggested by chromatin disintegration and a decrease of the mitotic index induced by high concentrations of $CuSO_4$ in plants *(108)*.

The mutagenic activity of copper might be attributed to its property of inducing infidelity in DNA synthesis. The large spectrum of genotoxic effects of copper includes single- and double-strand breaks, intrastrand crosslinks, and DNA oxidation-induced base modifications, also by the presence of oxygen radicals and related species. Fenton-mediated DNA damage has been widely demonstrated *(106,109,110)*.

However, apart from direct Cu interactions with chromatin, the Cu(II) form deriving from Cu redox cycling can also bind to nitrogen and oxygen, as well as to phosphate groups present in the deoxynucleotide bases. These interactions accelerate the hydrolysis of the glycosylic bound with the release of a purine base. If unrepaired, these apurinic sites could lead to misincorporations during DNA replication. Cu(II) preferentially binds to GC pairs in DNA. The reaction has been carried out in the presence of air, suggesting that the Cu(II)-induced DNA damage could have been caused by the generation of free radicals *(111)*.

Recent experiments established that the binding of copper to DNA is essential for the generation of double-strand breaks, crosslinks, and oxidized bases in Fenton reactions, indicating that a site-specific hydroxyl radical generating mechanism is involved in their formation *(112)*.

4. EFFECTS OF Cu ON CELL SIGNALING AND NEUROTRANSMISSION

Because of the high sensitivity of aquatic invertebrates to Cu and, in general, to heavy metals, even a moderate increase of the Cu concentration in the environment is sufficient to detect cellular alteration. Therefore, the question arises as to whether the biological effects of low concentrations of Cu in aquatic environments is really the result of the entry of metal into the cells and to its action on the different cellular compartments.

In this regard, it must be considered that for correct functioning, the cell is largely dependent on a complex system of chemical messengers, which are able to maintain cellular homeostasis and to modulate responses that render the organism able to adapt to environmental changes and biological requirements. Signal transduction mechanisms allow cells to react to exogenous stimuli (hormones, growth factors, neurotransmitters, etc.). Therefore, possible Cu-induced alterations of cell signaling may produce the drastic physiological changes described earlier as "direct" or "oxidative stress mediated" metal effects. Moreover, structural alterations of hormone receptors may alter the correct performance of "endocrine adaptive responses" *(113)*. These effects may be partially dependent on Cu alterations of the endocrine system (endocrine disruption) or as a result of the close relationship between endocrine and nervous systems to toxic effects on neuronal cells.

4.1. Effects of Cu on the Tyrosine Kinase Cascade

Tyrosine kinase receptors are activated by a variety of exogenous stimuli, such as growth factors, insulin, and so forth. Autophosphorylation of the receptor activates a complex protein phosphorylation cascade leading to metabolic changes and altered gene transcription *(114)*.

Recent data have demonstrated that in RTH 149 hepatoma trout cells, exposure to micromolar concentrations of Cu for 5–10 min causes a net increase of tyrosine phosphorylation in different proteins, with molecular weight ranging from 35 to 135 kDa *(115)*. The use of specific antibodies indicated that, in these cells, Cu activates homologs of ERK MAP kinases. In addition, in the presence of micromolar concentrations of H_2O_2 that *per se* slightly stimulate tyrosine phosphorylation, the Cu effect on ERK kinases is enhanced and a marked phosphorylation of a P38 homolog appears *(115)*. MAP kinases are involved in the activation of different DNA promoters that qualitatively and quantitatively modify DNA transcription and protein synthesis and, ultimately, affect cellular physiology. Moreover, the P38 MAP kinase is involved in a specific response to oxidative stress *(116)*. Similarly, in ameboid cells of the slime mold *Dictyostelium discoideum*, exposure to Cu causes a significant increase of tyrosine phosphorylation (Burlando, unpublished data).

4.2. Effects on Ca Homeostasis

Cytosolic free calcium is an important component of the cell signaling machinery. Transient increases of cytosolic Ca^{2+} play an essential role in the regulation of a variety of physiological processes in the cell *(117)*. As mentioned in Section 3.1., it has been assessed that the metal is able to inhibit Ca^{2+} and Na^+/K^+ ATPases present in the plasma membrane *(40,56,118)*. Plasma membrane Ca^{2+}-ATPase (PMCA) plays a pivot role in Ca^{2+} extrusion from the cell, and in various organisms, this enzyme is activated by Ca^{2+} or Ca^{2+}–calmodulin *(40)*. In this way, the increase of cytosolic free Ca^{2+} stimulates the translocase, eventually restoring the physiological cytosolic concentration of the cation. A second important mechanism for Ca^{2+} extrusion present in the plasma membrane is the Na^+/Ca^{2+} exchanger, whose functioning depends on the activity of the Na^+/K^+-ATPase that maintains a suitable transmembrane Na^+ gradient.

The Ca^{2+} ATPases present in calciosomes and in the sarcoplasmic reticulum (SERCA) are also inhibited by Cu, although the metal primarily acts by opening the Ca^{2+} channels of the endoplasmic reticulum *(119)*, thereby producing a fast Ca^{2+} release from intracellular stores (*62*, Viarengo unpublished results).

In studies on cell calcium, important advancements have been obtained with the use of fluorescent Ca^{2+} probes. These tools could be also extremely useful for the detection of cytosolic Ca^{2+} alterations

induced by heavy metals, but, on the other hand, it has been also assessed that nanomicromolar amounts of Cu cations are able to quench the fluorescence of Ca^{2+} probes, such as Fluo 3 and Fura 2, in free solution *(120)*. However, recent findings have demonstrated that micromolar concentrations of GSH (or cysteine) completely reverse Cu effects on Ca^{2+} probes in free solution, suggesting that a similar protective effect may also occur in living cells *(121)*.

In marine mussels, the same submicromolar concentration of Cu (0.6 μ*M*) that affects Ca^{2+} homeostasis in gill cells also induces a sustained Ca^{2+} increase in the cytosol of hemolymph and digestive gland cells *(44,122)*. This Ca^{2+} increase is only slightly reduced if the cells are exposed to the metal in a Ca^{2+}-free medium or pretreated with verapamil, an inhibitor of voltage-dependent Ca^{2+} channels. On the contrary, in the digestive gland cells, the pretreatment with thapsigargin, an agent able to deplete intracellular Ca^{2+} stores, strongly decreases the $[Ca^{2+}]_i$ rise evoked by the metal. These results indicate that Cu exerts a first effect on cytoplasmic Ca^{2+} stores and only at a later stage does it affect plasma membrane Ca^{2+} homeostasis mechanisms. Similar results have been obtained by using the hypotricous marine ciliate *Euplotes crassus* as an experimental system. In protozoa, the membrane potential is modulated by Ca^{2+}/K^+; therefore, these cells are very sensitive to Ca^{2+} homeostasis alterations. In this case, exposure to 1 μ*M* and 5 μ*M* Cu^{2+} for 10 min produces a Ca^{2+} increase of 56% and 500%, respectively *(123)*.

The results of recent studies on RTH 149 trout hepatoma cells have confirmed that also in aquatic vertebrates, Cu at micromolar concentrations is able to induce a sustained increase in the concentration of cytosolic Ca^{2+} *(115)*.

In conclusion, the data demonstrate that Cu toxicity may depend, at least in part, on the alteration of Ca^{2+} homeostasis. It is usually assumed that a sustained increase of Ca^{2+} may cause the activation of cytosolic neutral proteases, phospholipases, nuclear endonuclease, and a marked alteration of the cytoskeleton, eventually leading to cell death *(124,125)*. However, little has been done to correlate changes in cell physiology resulting from sublethal accumulation of Cu to its effects on cell signaling. Only recently, it has been demonstrated that destabilization of lysosomal membranes and the effect on protein catabolism because of Cu (and other heavy metals, such as Hg and Cd) are mainly dependent on an increase of cytosolic Ca^{2+} concentration. This study has clarified that the effects of Ca^{2+} on lysosomal activity is mediated by the activation of a cytosolic Ca^{2+}-dependent phospholipase A2, as lysosomal membranes remains stable in cells pretreated with phopholipase A2 inhibitors *(115)*. These results represent the first demonstration that sublethal Cu fluctuation may modulate cell physiology, at least in part, by affecting signal trasduction pathways.

However, other cell signaling pathways may be affected by Cu as well; it has been demonstrated *(126)* that micromolar Cu concentrations inhibit in vitro the binding of cAMP to cAMP-dependent protein kinase as well as the catalytic activity of this kinase. Moreover, it has recently been proposed that nitric oxide affects Cu activation of the transcription factor Ace 1 in yeast cells, thereby modulating, at least in part, the cytotoxic effect of Cu *(127)*.

Another important aspect of the indirect interference of Cu with the physiological activities of different tissues and organs is related to its ability to alter the hormonal response of cells. In primary cultures of mussel digestive gland cells, Cu significantly reduces the amplitude of the Ca^{2+} spikes elicited by bradikinin (BK) and ATP. In the case of digestive gland cells treated with epidermal growth factor (EGF), Cu decreases the number of cells which are responsive to this hormone *(122)*. Interestingly, these chemical messengers act through different biochemical pathways; EGF induces a physiological Ca^{2+} response via a Ca^{2+} influx from the extracellular medium, ATP acts by a Ca^{2+} release from intracellular Ca stores, and BK realizes an initial Ca^{2+} release from internal stores followed by an influx of Ca^{2+} from the extracellular medium *(122,128)*. In the case of BK and ATP, copper does not alter the activity of the intracellular Ca stores by inhibition of the Ca-ATPase. In this regard, it must be mentioned that "in vitro" experiments on mussel digestive gland homogenates have demonstrated that Cu inhibits the activity of phospholipase C (PLC). This enzyme is involved in the production of diacyl glycerol (DG) and of inositol 3,4,5 triphosphate (IP3) *(129)* that modulates the

cytosolic Ca^{2+} concentration by opening IP3-sensitive Ca^{2+} channels in calciosomes. The importance of this finding has been confirmed by exposure of mussels to 0.6 μ*M* Cu, which led to a significant reduction in the phospholipase C activity in gills (–20%) and digestive gland (–47%) *(130)*.

Similar results have been obtained utilizing skeletal muscle preparation *(131)*. Also in these experiments, micromolar concentrations of Cu were able to inhibit the IP3 production. Likewise, it can be expected that the levels of diacylglycerol become proportionally reduced. On the other hand, it has been also demonstrated that Cu inhibits the in vitro activity of protein kinase C, as well as its regulatory ligands *(126)*. Interestingly, the accumulation of Cu in the cytosol is likely to alter lipophylic hormones such as corticosteroids *(113)*. As a typical example of what has now been termed endocrine disruption, it has been recently reported that in Cu-exposed rainbow trouts (2.4 μ*M* for 5 d), the blood levels of cortisol are enhanced about fourfold *(113)*. On the contrary, the expression of the glucocorticoid receptor (GR) in gill cells is decreased. In particular, it was found that Cu decreases the number of chloride cells showing immunoreactivity for GR *(113)*. It is possible that Cu (and other heavy metals) may interfere with the steroid binding to the GR and, subsequently, with the receptor binding to glucocorticoid response elements (GRE) in the genome *(132,133)*. Moreover, Cu may alter the correct crosstalk of GR with other transcription factors *(134,135)*. As an alternative explanation, the Cu-induced increase in the level of cortisol in fish blood *(136,137)* may stimulate chloride cells to downregulate the GR expression, as demonstrated in cortisol-treated fish *(138–141)*.

4.3. Effects of Cu on Nervous Cells

In neurones, Cu is known to block the conduction of the action potential *(142–145)*. Cu was found to depolarize neuronal somata in snails *(146)*, and similar results were obtained utilizing *Helix pomatia* and *Limnaea stagnalis (147)*. Moreover, subsequent studies have demonstrated that in *Aplysia californica*, Cu activates specific ionic channels *(148)*. In *H. pomatia*, Cu evoked an ionic current as the result of an increased ion permeability. It was found that the Cu-activated current is biphasic and composed of overlapping outward and inward components. The outward component is the resulf of a Cu^{2+}-induced block of the steady-state outward Cl^- current, whereas the inward component is assumed to flow through Ca^{2+}-activated nonselective cationic channels *(149)*.

It has been demonstrated also that in mammalian neurones, Cu inhibits the binding of γ-aminobutyrric acid (GABA) to GABAa receptors, in which GABA activates a Cl^- flux through the receptor channel, as well as to GABAb receptors, whose activation decreases the activity of adenylate cyclase. GABAb receptors were found to be an order of magnitude more sensitive to the metal than GABAa receptors. Similar effects were demonstrated for other metals (Zn^{2+}> Cu^{2+}> Co^{2+}> Na^{2+}> Mn^{2+}> Fe^{2+}) *(150)*.

Moreover, it was found that Cu^{2+} decreases GABA-mediated Cl^- uptake into membrane vesicles prepared from rat neuronal cells. These data seem to indicate that Cu and other heavy metals, such as Zn, may contribute to modulate GABA receptors *(151)*.

Finally, it must be mentioned that also in the case of metal-induced alteration of cell signaling and hormonal responses, the Cu capability to stimulate ROS production may represent an important component of the molecular mechanisms of metal action. In fact, it has been clearly demonstrated that oxidative stress *per se* is able to modulate some pathways of cell signaling *(152)*.

5. CONCLUDING REMARKS

The data presented here describe different effects of Cu at the molecular and cellular level. When the cellular levels of Cu cations become cytotoxic, interference with different cell compartments occurs. The main detrimental effects include an activation of protein degradation in lysosomes, the inhibition of protein synthesis, altered ATP production in mitochondria, and toxic effects at the nuclear level by oxidative damage to DNA. The plasma membrane, being the first target of exogenous metal cations, represents an important site of Cu action and the metal's injury on the various active transport mechanisms may explain the alteration of osmoregulation in various aquatic organisms.

In addition, a relevant portion of physiological changes observed in animals exposed to toxic Cu doses may be the result of the effects of Cu cations on the nervous and endocrine systems. At the cellular level, this is caused in particular by an altered functioning of receptors of neurotransmitters and hormones and by the intracellular disturbance of signaling pathways. These latter processes may considerably affect the adaptive responses of animals to environmental stress, and this could particularly enhance the sensitivity of the organism to the noxious effects of copper.

REFERENCES

1. Hoar, W. S. (ed.) (1975) *General and Comparative Physiology.* Prentice-Hall, Englewood Cliffs, NJ.
2. Linder, M. C. (ed.) (1991) *Biochemistry of Copper*, Plenum, New York.
3. Peña, M. N. O., Lee, J., and Thiele, D. J. (1999) A delicate balance: homeostatic control of copper uptake and distribution . *Am. Soc. Nutr. Sci.* **129**, 1251–1260.
4. Camakaris, J., Voskoboinik, I., and Mercer, J. F. (1999) Molecular mechanisms of copper homeostasis. *Biochem. Biophys. Res. Commun.* **261**, 225–232.
5. Viarengo, A. (1989) Heavy metals in marine invertebrates: mechanisms of regulation and toxicity at the cellular level. *Aquat. Sci*. **1**, 295–317.
6. Bouquegneau, J. M. and Gilles, R. (1979) Osmoregulation and pollution of the aquatic medium, in *Metabolism and Osmoregulation in Animals* (Gilles, R., ed.), New York, pp. 563–580.
7. Nussey, G., Van Vuren, J. H. J., and Du Preez, H. H. (1995) Effect of copper on the haematology and osmoregulation of the Mozambique tilapia, *Oreochromis mossambicus* (Cichliadae). *Compar. Biochem. Physiol.* **111C**, 369–380.
8. Hansen, H. J. M., Olsen, A. G., and Rosenkilde, P. (1996) The effect of Cu on gill and esophagus lipid metabolism in the Rainbow Trout (*Onchorynchus mykiss*). *Compar. Biochem. Physiol.* **113C**, 23–29.
9. Pizarro, F., Olivares, M., Gidi, V., and Araya, M. (1999) The gastrointestinal tract and acute effects of copper in drinking water and beverages. *Rev. Environ. Health* **14**, 231–238.
10. Barceloux, D. G. (1999) Copper. *J. Toxicol. Clin. Toxicol.* **37**, 217–230.
11. Di Donato, M. and Sarkar, B. (1997) Copper transport and its alterations in Menkes and Wilson diseases. *Biochim. Biophys. Acta* **1360**, 3–16.
12. Eichorn, G. L. (ed.) (1973) *Inorganic Biochemistry*, Elsevier, Amsterdam.
13. Freeman, H. C. (1973) Metal complexes of amino acid and peptides, in *Inorganic Biochemistry* (Eichorn, G. L., ed.), Elsevier, Amsterdam, pp. 121–127.
14. Stohs, S. J. and Bagchi, D. (1995) Oxidative mechanisms in the toxicity of metal ions. *Free Radical Biol. Med.* **18**, 321–336.
15. Halliwell, B. and Gutteridge, M. C. (1984) Oxigen toxicity, oxigen radicals, transition metals and disease. *Biochem. J.* **219**, 1–14.
16. Lin, C. M. and Kosman, D. J. (1990) Copper uptake in wild type and copper metallothionein-deficient *Saccharomyces cerevisiae*. Kinetics and mechanism. *J. Biol. Chem.* **265**, 9194–9200.
17. Kagi, J. K. R. and Kojima, Y. (1987) Chemistry and biochemistry of metallothionein, in *Metallothionein II Experientia.* Birkhauser, Basel, Suppl. vol. 52, pp. 25–61.
18. Viarengo, A., Pertica, M., Mancinelli, G., Zanicchi, G., Bouquegneau, J. M., and Orunesu, M. (1984) Biochemical characterization of Cu-thioneins isolated from the tissues of mussels exposed to the metal. *Mol. Physiol.* **5**, 41–52.
19. Hamer, D. H. (1986) Metallothionein. *Annu. Rev. Biochem.* **55**, 913–951.
20. Freedman, J. H., Ciriolo, M. R., and Peisach, J. (1989) The role of glutathione in copper metabolism. Characterization of a heavy metal ion transporter in the lysosomal membrane. *FEBS Lett.* **436**, 223–227.
21. Menkes, J. H. (1999) Menkes disease and Wilson disease: two sides of the same copper coin. Part I: Menkes disease. *Eur. J. Paediatr. Neurol.* **3**, 147–158.
22. Menkes J. H. (1999) Menkes disease and Wilson disease: two sides of the same copper coin. Part II: Wilson disease. *Eur. J. Paediatr. Neurol.* **3**, 245–253.
23. Havelaar, A. C., De Gast, I. L., Snijders, S., Beerens, C. E., Mancini, G. M., and Verheijen, F. W. (1998) Characterization of a heavy metal ion transporter in the lysosomal membrane. *FEBS Lett.* **436(2)**, 223–227
24. Petris, M. J., Mercer, J. F., Culvenor, J. G., Lockhart, P., Gleeson, P. A., and Camakaris, J. (1996) Ligand-regulated transport of the Menkes copper P-type ATPase efflux pump from the Golgi apparatus to the plasma membrane: a novel mechanism of regulated trafficking. *EMBO J.* **15**, 6084–6095.
25. Viarengo, A., Zanicchi, G., Moore, M. N., and Orunesu, M. (1981) Accumulation and detoxication of copper by the mussel *Mytilus Galloprovincialis* Lam.: a study of subcellular distribution in the digestive gland cells. *Aquat. Toxicol.* **1**, 147–157.
26. George, S. G. (1983) Heavy metal detoxication in *Mytilus* kidney. An in vitro study of Cd and Zn binding to isolated tertiary lysosomes. *Compar. Biochem. Physiol.* **76C**, 59–65.
27. George, S. G. (1983) Heavy metal detoxification in the mussel *Mytilus edulis*. Composition of Cd-containing kidney granules (tertiary lysosomes). *Compar. Biochem.Physiol.* **76C**, 53–57.
28. Simkiss, K. (1981) Calcium pyrophosphate and cellular pollution. *Trends Biochem. Sci.* **6**, 3–9.
29. Martoja, M., Vu, T. T., and Elkaim, B. (1980) Bioaccumulation du cuivre chez *Littorina littorea* L. (Gasteropode Prosobranche): signification physiologique et ecologique. *J. Exp. Marine Biol. Ecol.* **43**, 251–270.

30. George, S. G., Pirie, B. J. S., Cheyne, A. R., Coombs, T. L., and Grant, P. T. (1978) Detoxication of metals by marine bivalves: an ultrastructural study of the compartmentation of copper and zinc in the oyster, *Ostrea edulis*. *Marine Biol.* **45**, 147–156.
31. Mason, A. Z. and Nott, J. A. (1981) The role of intracellular biomineralized granules in the regulation and detoxification of metals in gastropods with special reference to the marine prosobranch *Littorina littorea*. *Aquat. Toxicol.* **1**, 239–245.
32. Al-Mohanna, S. Y. and Nott, J. A. (1982) The accumulation of metals in the hepatopancreas of the shrimp *Penaeus Semisulcatus* de Haan (Crustacea: Decapoda) during the moult cycle. Proceedings of the Conference on Marine Environmental Pollution, p. 195.
33. Pirie, B., Liu, F., and George, S. (1985) Ultrastructural localisation of copper and zinc in the Polychaete *Nereis diversicolor* from a highly contaminated estuary. *Marine Environ. Res.* **17**, 197–203.
34. Lin, S. J., Pufahl, R. A., Dancis, A., O'Halloran, T. V., and Culotta, V. C. (1997) A role for *Saccharomyces cerevisiae* ATX1 gene in copper trafficking and iron transport. *J. Biol. Chem.* **272**, 9215–9220.
35. Chen, L. H. and Lowry, S. R. (1989) Cellular antioxidant defense system. *Prog. Clin. Biol. Res.* **287**, 247–256.
36. Viarengo, A., Canesi, L., Pertica, M., and Livingstone, D. R. (1991) Seasonal variations in the antioxidant defence systems and lipid peroxidation of the digestive gland of mussels. *Compar. Biochem. Physiol.* **100C**, 187–190.
37. Lovas, M., Szabò, L., Matkovics, H., and Fischer, R. (1987) Seasonal antioxidant enzyme changes in earthworm (*Lumbricus terrestris*). *Compar. Biochem. Physiol.* **87C**, 63–64.
38. Slater, T. (1984) Free radical mechanisms in tissue injury. *Biochem. J.*, 115–222.
39. Poli, G., Dianzani, M. U., Cheeseman, K. H., Slater, T. F., Lang, J., and Esterbauer, H. (1985) Separation and characterisation of the aldehydic products of lipid peroxidation stimulated by carbon tetrachloride or ADP-iron in isolated rat hepatocytes and rat liver microsomal suspensions. *Biochem. J.* **227**, 629–638.
40. Viarengo, A., Mancinelli, G., Pertica, M., Fabbri, R., and Orunesu, M. (1993) Effects of heavy metals on the Ca^{2+}-ATPase activity present in gill cell plasma-membrane of mussels (*Mytilus galloprovincialis* Lam.) *Compar. Biochem. Physiol.* **106C**, 660–665.
41. Viarengo, A., Canesi, L., Pertica, M., Poli, G., Moore, M. N., and Orunesu, M. (1990) Heavy metal effects on lipid peroxidation in the tissues of *Mytilus galloprovincialis* Lam. *Compar. Biochem. Physiol.* **97C**, 37–42.
42. Ringwood, A. H., Conners, D. E., and Di Novo, A. (1998) The effects of copper exposures on cellular responses in oysters. *Marine Environ. Res.* **46**, 591–595.
43. Romeo, M. and Gnassia-Barelli, M. (1997) Effect of heavy metals on lipid peroxidation in the Mediterranean clam *Ruditapes decussatus*. *Compar. Biochem. Physiol.* **118C**, 33–37.
44. Viarengo, A., Arena, N., Canesi, L., Alia, F. A., and Orunesu, M. (1994) Structural and biochemical alteration in the gills of copper-exposed mussels, in *Contaminants in the Environment* (Renzoni, A., Mattei, N., Lari, L., and Fossi, C. eds.), Lewis Publishers, Inc., Boca Raton, pp. 135–144.
45. Moore, M. N., Widdows, J., Cleary, J. J., Pipe, R., Salkeld, R. N., Donkin, S. V., et al. (1984) Responses of the mussels *Mytilus edulis* to copper and phenanthrene: interactive effects. *Marine Environ. Res.* **14**, 167–173.
46. Widdows, J. and Johnson, D. 1988. Physiological energetics of *Mytilus edulis*: scope for growth. *Marine Ecol. Prog.* **46**, 113–119.
47. Grace, A. L. and Gainey, L. F., Jr. (1987) The effects of copper on the heart rate and filtration rate of *Mytilus edulis*. *Marine Pollut. Bull.* **18**, 87–93.
48. Stacey, N. H., Curtis, D., and Classen (1980) Copper toxicity in isolated rat hepatocytes. *Toxicol. Appl. Pharmacol.* **58**, 211–220.
49. Esterbauer, H., Lang, J., Zadravec, S., and Slater, T. (1984) Detection of malondialdehyde by high-performance liquid chromatography. *Methods Enzymol.* **105**, 319–328.
50. Esterbauer, H., Shaur, R. J., and Zollner, H. (1991) Chemistry and biochemistry of 4-hydroxynonenal, malonaldeyde and related aldehydes. *Free Radical Biol. Med.* **11**, 81–128.
51. Romeo, M., Benanni, N., Gnassia Barelli, M., Lafaurie, M., and Girard, J. P. (1999) Cadmium and copper display different responses towards oxidative stress in the kidney of the sea bass *Dicentrarchus labrax*. *Aquat. Toxicol.* **48**, 185–194.
52. Brouwer, M. and Brouwer T. H. (1998) Biochemical defense mechanisms against copper-induced oxidative damage in the blue crab, Callinectes sapidus. *Arch. Biochem. Biophys.* **351**, 257–264.
53. Okamoto, O. K. and Colepicolo, P. (1998) Response of superoxide dismutase to pollutant metal stress in the marine dinoflagellate *Gonyaulax polyedra*. *Compar. Biochem. Physiol.* **119C**, 67–73.
54. Tallineau, C., Barriere, M., Boulard, M., Boulard-Heitzmann, P., Pontcharraud, R., Reiss, D., and Guillard O. (1984) Evidence for the involvement of $(Cu\text{-}ATP)^{2-}$ in the inhibition of human erythrocyte (Ca^{2+} + Mg^{2+})-ATPase by copper. *Biochim. Biophys. Acta* **775**, 51–56.
55. Whittaker, W. P., Michaelson, I. A., and Kirkland, R. J. A. (1970) The effect of copper on membrane enzymes. *Biochim. Biophys. Acta* **196**, 116–119.
56. Sheppard, K. L. and Simkiss, K. (1978) The effects of heavy metal ions on Ca^{2+} ATPase extracted from fish gills. *Compar. Biochem. Physiol.* **61**, 69–72.
57. Mckim, J. M., Christensen, G. M., and Hunt, E. P. (1970) Changes in the blood of brook trout (*Salvelinus fontinalis*) after short-term and long-term exposure to copper. *J. Fish. Res. Bd. Can.* **27**, 1883–1889.
58. Viarengo, A., Mancinelli, G., Burlando, B., Panfoli, I., and Marchi, B. (1999) The SR Ca^{2+} ATPase of the antarctic scallop *Adamussium colbecki*: cold adaptation and heavy metal effects. *Polar Biol.* **21**, 369–375.
59. Viarengo, A., Pertica, M., Mancinelli, G., Burlando, B., Canesi, L., and Orunesu, M. (1996). *In vivo* effects of copper on the calcium homeostasis mechanism of mussel gill cell plasma membranes. *Compar. Biochem. Physiol.* **113C**, 421–425.

60. Viarengo, A., Pertica, M., Mancinelli, G., Capelli, R., and Orunesu, M. (1980) Effects of copper on the uptake of aminoacids, on protein synthesis and on ATP content in different tissues of *Mytilus Galloprovincialis* Lam. *Marine Environ. Res.* **4**, 152–185.
61. Zhang, G. H., Yamaguchi, M., Kimura, S., Higham, S., and Kraus-Friedmann, N. (1990) Effects of heavy metal on rat liver microsomal Ca^{2+} ATP-ase and Ca^{2+} sequestering. Relation to SH groups. *J. Biol. Chem.* **265**, 2184–2189.
62. Prabhu, S. D. and Salama, G. (1990) The heavy metal ions Ag^{+} and Hg^{2+} trigger calcium release from cardiac sarcoplasmic reticulum. *Arch. Biochem. Biophys.* **277**, 47–45.
63. Burlando, B., Viarengo, A., Pertica, M., Ponzano, E., and Orunesu, M. (1997) Effects of free oxygen radicals on Ca^{2+} release mechanisms in the sarcoplasmic reticulum of scallop (*Pecten jacobaeus*) adductor muscle. *Cell Calcium* **22**, 83–90.
64. Viarengo, A., Bettella, E., Fabbri, R., Burlando, B., and Lafaurie, M. (1997) Heavy metal inhibition of EROD activity in liver microsomes from the bass *Dicentrarchus labrax* exposed to organic xenobiotics: role of GSH in the reduction of heavy metal effects. *Marine Environ. Res.* **44**, 1–11.
65. Stegeman, J. J. (1981) Polynuclear aromatic hydrocarbons and their metabolism in the marine environment, in *Polyciclic Hydrocarbons and Cancer*, Academic, New York, p. 3.
66. Lee, R. F. (1981) Mixed function oxygenases (MFO) in marine invertebrates. *Marine Biol. Lett.* **2**, 87–93.
67. Livingstone, D. R. and Farrar, S. (1984) Tissue and subcellular distribution of enzyme activities of mixed-function oxygenase and benzo-a-pyrene metabolism in the common mussel *Mytilus Edulis*. *L. Sci. Total Environ.* **39**, 209–215.
68. Hummel, H., Bogaards, R., De Wolf, L., Sinke, J., and Poortvliet, T. (1994) Evaluation of free amino acids as a biochemical indicator of metal pollution. *Marine Environ. Res.* **38**, 303–312.
69. Blasco, J. and Puppo, J. (1999) Effects of heavy metals (Cu, Cd and Pb) on aspartate and alanine aminotransferase in *Ruditaoes philippinarum* (Mollusca: Bivalvia). *Compar. Biochem. Physiol.* **C122**, 253–263.
70. Puppo, J. and Blasco, J. (1975) Partial characterisation of alanine aminotransferase from gills and digestive gland of the bivalve *Ruditapes philippinarum*. *Compar. Biochem. Physiol.* **111**, 99–109.
71. Scott, D. and Major, C. (1972) The effect of copper (II) on survival, respiration, and heart rate in the common blue mussel *Mytilus edulis*. *Biol. Bull.* **143**, 679–684.
72. Soegianto, A., Charmantier, D. M., Trilles, J. P., and Charmantier, G. (1999) Impact of copper on the structure of gills and epipodites of the shrimp *Penaeus japonicus* (Decapoda). *J. Crustac. Biol.* **19**, 209–223.
73. Arillo, A., Calamari, D., Margiocco, C., Melodia, F., and Mensi, P. (1984) Biochemical effects of long-term exposure to cadmium and copper of Rainbow trout (*Salmo gairdneri*): validation of water quality criteria. *Ecotoxicol. Environ. Safety* **8**, 106–117.
74. Stauber, J. L. and Florance, T. M. (1987) Mechanism of toxicity of ionic copper and copper complexes to algae. *Marine Biol.* **94**, 511–519.
75. Calabrese, A., MacInnes, J. R., Nelson, D. A., Greig, R. A., and Yevich, P. P. (1984) Effects of long-term exposure to silver or copper on growth, bioaccumulation and histopathology in the blue mussel *Mytilus edulis*. *Marine Environ. Res.* **11**, 253–259.
76. Viarengo, A., Secondini, A., Scoppa, P., Moore, M. N., and Orunesu M. (1985) Effetti del Cu^{2+} e del Cd^{2+} sull'attività mitocondriale e sulla carica energetica adenilica delle cellule della ghiandola digestiva di mitili. *Atti riunione Congiunta SIB, SIF, SINU*, Pisa.
77. Zaba, B. N. and Harris, E. J. (1976) Uptake and effects of copper in rat liver mitochondria. *Biochem J.* **160**, 707–714.
78. Wojtczak, L., Nikitina, E. R., Czyz, A., and Skulskii, I. A. (1996) Cuprous ions activate glibenclamide-sensitive potassium channel in liver mitochondria. *Biochem. Biophys. Res. Commun.* **223**, 468–473.
79. Pourahmad, J., O'Brien, P. J., and Giam, C.S. (2000) A comparison of hepatocyte cytotoxic mechanism for Cu^{2+} and Cd^{2+}. *Toxicology* **143**, 263–273.
80. Totaro, A., Pisanti, E., Glees, F. A., and Contimillo, A. (1986) The effect of copper pollution on mitochondrial degeneration. *Marine Environ. Res.* **18**, 245–251.
81. Gould, E., Greig, R. A., Rusanowsky, D., and Marks, B. C. (1985) Metal-exposed sea scallops *Placopecten magellanicus* (Gmelin): a comparison of the effects and uptake of cadmium and copper, in *Marine Pollution and Physiology* (Vernberg, F. J., Thurberg, F. P., Calabrese, A., and Vernberg, W. B., eds.), The Belle W. Baruch Library in Marine Science, University of South Carolina, Columbia, Vol. 13, pp. 157–186.
82. Glaumann, H. and Ballard, F. J. (eds.) (1987) *Lysosomes: Their Role in Protein Breakdown.* Academic, London.
83. Sternlieb, I. and Goldfisher, S. (1976) Heavy metals and lysosomes, in *Lysosomes in Biology and Pathology*, (Dingle, J.T. and Dean R. T., eds.), Elsevier Science, New York, pp. 185–200.
84. Moore, M. N. (1977) Lysosomal responses to environmental chemical in some marine invertebrates, in *Pollutant Effects on Marine Organisms* (Giam, C. S., ed.), Heat & Co., Lexington, MA.
85. Chassard-Bouchaud, C. (1981) Role des lysosomes dans le phenomene de concentration du cadmium. Microanalyse par spectrographie des rayons X. *C.R. Acad. Sci.* III **293**, 261–265.
86. George, S. G. and Viarengo, A. (1985) A model of heavy metal homeostasis and detoxication in mussels, in *Marine Pollution and Physiology: Recent Advances* (Vernberg, F. J., Thurberg, F. P., Calabrese, A., and Vernberg, W. B., eds.), University of South Carolina Press, Columbia, pp. 125–143.
87. Reddy, N. M. and Venkateswara, P. (1987) Copper toxicity to the fresh water snail, *Lymnaea luteola. Bull. Environ. Contam. Toxicol.* **39**, 50–55.
88. Moore, M. N. and Viarengo, A. (1987) Lysosomal membrane fragility and catabolism of cytosolic proteins: evidence for a direct relationship. *Experientia* **43**, 320–323.

89. Iordachescu, D., Dumitru, I. F., and Niculescu, S. (1978) Activation by copper ions of mytilidases-acid proteolytic enzymes obtained from *Mytilus galloprovincialis. Compar. Biochem. Physiol.* **61B**, 119.
90. Webb, M. (1979) Interactions of cadmium with cellular components, in *The Chemistry, Biochemistry and Biology of Cadmium* (Webb, M., ed.), Elsevier Science, Amsterdam, pp. 285–340.
91. Viarengo, A., Marro, A., Marchi, B., and Burlando, B. (2000) Single and combined effects of heavy metals and hormones on lysosomes of haemolymph cells from the mussel *Mytilus galloprovincialis*. *Marine Biol.* **137**, 907–912.
92. Codina, J. C., Perez-Torrente, C., Perez-Garcia, A., Cazorla, F. M., and De Vicente, A. (1995) Comparison of microbial tests for the detection of heavy metal genotoxicity. *Arch. Environ. Contam. Toxicol.* **29**, 260–265.
93. Rossman, T. G., Molina, M., and Meyer, L. W. (1984) The genetic toxicology of metal compounds. Induction of lambda prophage in *E. coli*-WP2. *Environ. Mutagen* **6**, 59–69.
94. Denizeau, F. and Marion, M. (1989) Genotoxic effects of heavy metals in rat hepatocytes. *Cell Biol. Toxicol.* **5**, 15–25.
95. Quillardet, P., Huisman, O., D'Ari, R., and Hofnuug, N. (1982) SOS contest: a direct assay of induction of SOS function in E. coli K.12 to misure the genotoxicity. *Proc. Natl. Acad. Sci. USA* **79**, 5971–5975.
96. Olivier, P. and Marsin, D. (1987) Study of the genotoxic potential of 48 inorganic derivates with the SOS chromotest. *Mutat. Res.* **189**, 263–269.
97. Hollstein, M., McCann, J., Angelosanto, F. A., and Nichols, W. W. (1979) Short-term tests for carcinogens and mutagens. *Mutat. Res.* **65**, 132–226.
98. Flessel, C. P. (1978) Metals as mutagens, in *Inorganic and Nutritional Aspects of Cancer* (Schrauzer, G. N., ed.), Plenum, New York, pp. 117–128.
99. Samuni, A., Chevion, M., and Czpaski, G. (1984) Roles of copper and O_2 in the radiation induced inactivation of T7 bacteriophage. *Radiat. Res.* **99**, 562–572.
100. Sagripanti, J. L., Swicord, M. L., and Davis, C. C. (1987) Microwave effects on plasmid DNA. *Radiat. Res.* **110**, 219–231.
101. Steinkellner, H., Mun-Sik, K., Helma, C., Ecker, S., Ma, T. H., Horak, O., et al. (1998) Genotoxic effects of heavy metals: comparative investigation with plant bioassays. *Environ. Mol. Mutagen.* **31**, 183–191.
102. Klerks, P. L. and Weis, J. S. (1987) Genetic adaptation to heavy metals in aquatic organisms: a review. *Environ. Pollut.* **45**, 173–205.
103. Janus, J. A., Canton, J. H., Van Gestel, C. A. M., and Heijna-Merkus, A. (1989) Integrated Criteria Document: Copper Effects. Appendix to Report no. 758474009, National Institute for Public Health and Environmental Protection (RIVM), Bilthoven, The Netherlands.
104. Burgeot, T., His, E., and Galgani, F. (1995) The micronucleus assay in *Crassostrea gigas* for the detection of seawater genotoxicity. *Mutat. Res.* **342**, 125–140.
105. Bolognesi, C., Landini, E., Roggieri, P., Fabbri, R., and Viarengo, A. (1999) Genotoxicity biomarkers in the assessment of heavy metal effect in mussels: experimental studies. *Environ. Mol. Mutagen* **33**, 287–292.
106. Regoli, F. (1998) Trace metals and antioxidant enzymes in gills and digestive gland of the Mediterranean mussel *Mytilus galloprovincialis*. *Arch. Environ. Contam. Toxicol.* **34**, 48–63.
107. Ueda, J., Takai, M., Shimazu, Y., and Ozawa, T. (1998) Reactive oxigen species generated from the reaction of copper(II) complexes with biological reductants cause DNA strand scission. *Arch. Biochem. Biophys.* **357**, 231–239.
108. Sharma, A. and Talukdar, G. (1987) Effects of metals on chromosomes of higher organisms. *Environ. Mutagen* **9**, 191–226.
109. Cai, L., Koropatnick, J., and Cherian, M. G. (1995) Metallothionein protects DNA from copper-induced but not iron-induced cleavage in vitro. *Chem. Biol. Interact.* **96**, 143–155.
110. Tkeshelashvili, L. K., McBride, T., Spence, K., and Loeb, L. A. (1991) Mutation spectrum of copper-induced DNA damage. *J. Biol. Chem.* **266**, 6401–6406.
111. Schaaper, R. M., Koplitz, R. M., Tkeshelashvili, L. K., and Loeb, L. A. (1987) Metal-induced lethality and mutagenesis: possible role of apurinic intermediates. *Mutat. Res.* **177**, 179–188.
112. Lloyd, D. R. and Phillips, D. H. (1999) Oxidative DNA damage mediated by copper (II), iron (II) and nickel (II) Fenton reactions: evidence for site-specific mechanisms in the formation of double-strand breaks, 8-hydroxydeoxyguanosine and putative intrastrand cross-links. *Mutat. Res.* **424**, 23–36.
113. Bonga, S. E. W. (1997) The stress response in fish. *Physiol. Rev.* **77**, 591–625.
114. Van Der Geer, P., Hunter, T., and Lindberg, R. A. (1994) Receptor protein-tyrosine kinases and their signal transduction pathways. *Annu. Rev. Cell Biol.* **10**, 251–337.
115. Burlando, B., Panfoli, I., Magnelli, V., Cerrato, N., Marchi, B., and Viarengo, A. (2000) Heavy metals effects on calcium and tyrosine kinase-dependent signal transduction pathways. *Compar. Biochem. Physiol.* **126A(Suppl. 1)**, 20–25.
116. Widmann, C, Gibson, S, Jarpe, M. B., and Johnson, G. L. (1999) Mitogen-activated protein kinase: conservation of a three-kinase module from yeast to human. *Physiol. Rev.* **79**, 143–180.
117. Berridge, M. J. (1997) Elementary and global aspects of calcium signalling. *J. Physiol.* **499**, 291–306.
118. Simkiss, K. (1984) Effects of Metal Ions on respiratory structures, in *Toxine, Drugs and Pollutants in Marine Animals* (Bolis, L., Zadunaisky, J., and Gilles, R., eds.), Springer Verlag, Berlin, pp 138–145.
119. Viarengo, A. (1994) Heavy metal cytotoxicity in marine organisms: effects on Ca^{2+} homeostasis and possible alteration of signal trasduction pathways. *Adv. Compar. Environ. Physiol.* **20**, 85–105.
120. Martell, A. E. and Smith, R. M. (eds.) (1974) *Critical Stability Constants*. *Volume 1: Amino Acids*, Plenum, New York.
121. Marchi, B., Burlando, B., Panfoli, I., and Viarengo, A. (2000) Interference of heavy metal cations with fluorescent Ca^{2+} probes does not affect Ca^{2+} measurements in living cells. *Cell Calcium* **28**, 225–231.

122. Canesi, L., Ciacci, C., and Gallo, G. (2000) Hg^{2+} and Cu^{2+} interfere with agonist-mediated Ca^{2+} signaling in isolated Mytilus digestive gland cells. *Aquat. Toxicol.* **49**, 1–11.
123. Viarengo, A., Accomando, R., Ferrando, I., Beltrame, F., Fato, M., and Marcenaro, G. (1996) Heavy metal effects on cytosolic free Ca^{2+} level in the marine protozoan *Euplotes crassus* evaluated by confocal laser scanning microscopy. *Compar. Biochem. Physiol.* **113C**, 161–168.
124. Orrenius, S., Thor, D., Di Monte, D., Bellomo, G., Nicotera, P., Ross, D., et al. (1985) Mechanism of oxidative cell injury studied in intact cell, in *Mechanism of Cell Liver Injury*, Taylor and Francis, London, pp. 238–243.
125. Schanne, F. A. X., Kane, A. B., Young, E. E., and Farber, J. L. (1979) Calcium dependence of toxic cell death: a final common pathway. *Science* **206**, 700–706.
126. Speizer, A. L., Watson, M. J., Kanter, J. R., and Brunton, L. L. (1989) Inhibition of phorbol ester binding and protein kinase C activity by heavy metals. *J. Biol. Chem.* **264**, 5581–5585.
127. Chiang, K.T., Shinyashiki, M., Switzer, C.H., Valentine, J.S., Gralla, E.B., Thiele, D.J., et al. (2000) Effects of nitric oxide on the copper-responsive transcription factor Ace1 in *Saccharomyces cerevisiae*: cytotoxic and cytoprotective actions of nitric oxide. *Arch. Biochem. Biophys.* **377**, 296–303.
128. Canesi, L., Ciacci, C., Orunesu, M., and Gallo, G. (1997) Effects of epidermal growth factor on isolated digestive gland cells from mussels (*Mytilus galloprovincialis* Lam.). *Gen. Comp. Endocrinol.* **107**, 221–228.
129. Panfoli, I., Burlando, B., and Viarengo, A. (2000) Effects of heavy metals on the phospholipase C activity present in gills and digestive gland cells of the marine mussel *Mytilus galloprovincialis*. Lam. *Compar. Biochem. Physiol.* **127B**, 391–397.
130. Prentki, M., Biden, T. J., Janjic, D., Irvine, R. F., Berridge, M. J., and Wollheim, C. B. (1984) Rapid mobilization of Ca^{2+} from rat insulinoma microsomes by inositol-1,4,5-trisphosphate. *Nature* **309**, 562–563.
131. Shute, J. K. and Smith, M. E. (1985) Inhibition of phosphatidylinsitol phosphodiesterase activity in skeletal muscle by metal ions and drugs which block neuromuscular transmission. *Biochem. Pharmacol.* **34**, 2571–2475.
132. Freedman, L. P., Luisi, B. F., Korszun, Z. R., Basavappa, R., Sigler, P. B., and Yamamoto, K. R. (1988) The function and structure of the metal coordination sites within the glucocorticoid receptor DNA binding domain. *Nature* **334**, 543–546.
133. Dunderski, J., Stanosevic, J., Ristic, B., Trajkovic, D., and Matic, G. (1992) In vivo effects of cadmium on rat liver glucocorticoid receptor functional properties. *Int. J. Biochem.* **24**, 1065–1072.
134. ‘Makino, Y., Tanaka, H., Dahlman-Wright, K., and Makino, I. (1996) Modulation of glucocorticoid-inducible gene expression by metal ions. *Mol. Pharmacol.* **49:** 612–620.
135. Reichardt, H. M. and Schutz, G. (1988) Glucocorticoid signalling. Multiple variations of a common theme. *Mol. Cell. Endocrinol.* **146**, 1–6.
136. Munoz, M. J., Carballo, M., and Tarazona, J. V. (1991) The effect of sublethal levels of copper and cyanide on some biochemical parameters of rainbow trout along subacute exposition. *Compar. Biochem. Physiol.* **100C**, 577–582.
137. Brown, J. A. (1993) Endocrine responses to environmental pollutants, in *Fish Ecophysiology* (Rankin, J. C. and Jensen, F. B., eds.), Chapman & Hall, London, pp. 276–295.
138. Pottinger, T. G. (1990) The effect of stress and exogenous cortisol and receptor-like binding of cortisolin the liver of rainbow trout, *Oncorhynchus mykiss*. *Gen. Compar. Endocrinol.* **78**, 194–203.
139. Lee, P. C., Goodrich, M., Struve, M., Yoon, H. I., and Weber, D. (1992) Liver and brain glucocorticoid receptor in rainbow trout, *Oncorhynchus mykiss:* down-regulation by dexamethasone. *Gen. Compar. Endocrinol.* **87**, 222–231.
140. Maule, A. G. and Schreck, C. B. (1990) Glucocorticoid receptor in leukocytes and gill of juvenile coho salmon (*Oncorhynchus kisutch*). *Gen. Compar. Endocrinol.* **77**, 448–455.
141. Uchida, K., Kaneko, T., Tagawa, M., and Hirano, T. (1998) Localization of cortisol receptor in branchial chloride cells in chum salmon fry. *Gen. Compar. Endocrinol.* **109**, 175–181.
142. Lorente De No, R. (1974) A study of nerve physiology. *Stud. Rockfeller Inst. Med. Res.* **132**, 179–180.
143. Del Castillo-Nicolau, J. and Hufschmidt, H. J. (1951) Reversible possible poisoning of nerve fibers by heavy-metal ions. *Nature* **167**, 146–147.
144. Smith, H. M. (1958) Effects of sulphydryl blockade on axonal function. *J. Cell. Compar. Physiol.* **51**, 161–171.
145. Arhem, P. (1980) Effects of some heavy metal ions on the ionic currents of myelinated fibres from *Xenopus laevis*. *J. Physiol.* **306**, 219–231.
146. Ciarandini, D. J., Stefani, E., and Gerschenfeld, H. M. (1967) Inhibition of membrane permeability to chloride by copper in molluscan neurons. *Nature* **213**, 97–99.
147. Rozsa, K. S. and Salanki, J. (1990) Heavy metals regulate physiological and behavioural events by modulating ion channels in neuronal membranes of molluscs. *Environ. Monitor. Assess.* **14**, 363–375.
148. Weinreich, D. and Wonderlin, W. F. (1987) Copper activates an unique inward current in molluscan neurons. *J. Physiol.* **394**, 429–443.
149. Tibor, K., Gyori, J., Oleg, N., Osipenko, O. N., Silva, B., and Maginyan, S. B. (1991) Copper-induced non-selective permeability changes in intracellulary perfused snail neurons. *J. Toxicol.* **11**, 349–354.
150. Drew, C. A., Spence, I., and Johnston, G. A. R. (1991) The effect of metal cations of the first transition series on GABA binding GABA-A and GABA-B binding sites in rat brain. *J. Neurochem.* **57**, 1–10.
151. Smart, T. G. and Costanti, A. (1989) The vertebrate neuronal GABA-A receptor complex is modulated by group IIB divalent cations. *Br. J. Pharmacol.* **96**, 328–333.
152. Suzuki, Y. J., Forman, H. J., and Sevanian, A. (1997) Oxidants as stimulators of signal transduction. *Free Radical Biol. Med.* **22**, 269–285.

26

Selective Removal of Copper Accumulating in the Form Bound to Metallothionein by Tetrathiomolybdate

Kazuo T. Suzuki and Yasumitsu Ogra

1. INTRODUCTION

Copper (Cu) in the body is present in the form of either a monovalent (cuprous, Cu^{+}) or divalent (cupric, Cu^{2+}) state. Cuprous ions are readily oxidized to cupric ions and Cu cannot exist in the form of cuprous ions without being coordinated by appropriate ligands. In other words, Cu in the monovalent form readily reduces chemicals, as in the case of the production of reactive oxygen species. At the same time, cupric ions are reduced to monovalent Cu in the presence of reducing agents (i.e., thiol groups in abundant glutathione in the body). As a result, Cu is essential in the biological redox reaction for the normal function in the body and its deficiency is fatal to the body. At the same time, Cu is extremely toxic when it exists in excess.

The body has to regulate the concentration of Cu within a certain range; namely, the body utilizes Cu efficiently in a deficient state, whereas detoxifies it in an excessive state. These homeostatic mechanisms are current topics in relation to the mechanisms underlying the genetic Menkes disease *(1–3)* and Wilson's disease *(4)*. The latter genetic disease is now known to be caused by an excessive accumulation of Cu owing to the mutation of the responsible transporter for Cu in the liver *(5–7)*. Following the identification of the transporter genes of *ATP7A* and *ATP7B*, the intracellular carrier proteins (chaperones) were discovered and the mechanisms underlying the homeostasis of Cu have been further developed *(8–11)*.

Therapies for Wilson's disease have been of concern and the removal of Cu accumulating in the form bound to metallothionein (MT) is pivotal for the therapy. The direct and selective removal of Cu by tetrathiomolybdate (TTM) may supply not only a unique therapy for the disease but also a means to study the homeostatic mechanisms of Cu. The powerful but selective removal of Cu by TTM can be applied not only for the excessive metals accumulating in Wilson's disease but also for the essential Cu in the progression of cancer *(12)*.

The following sections describe the removal of excess Cu accumulating in a form bound to MT by TTM from the viewpoints of the mechanisms and the selectivity in terms of among various kinds of metals and also among Cu in different chemical environments.

From: Handbook of Copper Pharmacology and Toxicology
Edited by: E. J. Massaro © Humana Press Inc., Totowa, NJ

2. BACKGROUND FOR THE ACCUMULATION OF COPPER-BINDING METALLOTHIONEIN IN WILSON'S DISEASE

2.1. Copper Accumulating in the Body and Its Toxicity

2.1.1. Excessive Copper Accumulating in the Body Is Bound to Metallothionein

Copper in the liver, kidneys, and other organs and tissues of the normal functioning body is present in nontoxic forms, bound mainly to Cu enzymes and, when in excess, to MT, an inducible low-molecular-weight protein rich in cysteinyl residues having a high capacity to bind heavy metals such as zinc (Zn), Cu, and cadmium (Cd) *(13)*. On the other hand, Cu accumulating in the liver of Wilson's disease patients and its animal model, Long–Evans rats with a cinnamonlike coat color (LEC rats), is bound mainly to MT (Cu–MT and Cu,Zn–MT) because of the mutation of the transporter of Cu for the efflux of Cu, ATP7B *(14–16)*.

2.1.2. Copper–Metallothionein Becomes a Pro-Oxidant by Producing Monovalent Copper in the Liver of LEC Rats

Copper and zinc are bound to MT through thiol groups of cysteinyl residues in MT (i.e., all metals are bound to MT through mercaptide [metal–sulfur] bonds by forming two thiolate clusters [α- and β-domains]) *(13)*. The stability of the metal–thiolate clusters was found to decrease in the order Cu > Cd >Zn *(17)* and excessive Cu bound to MT is limited in its availability; hence, it is not toxic as far as Cu is present bound to MT. However, the protein moiety of MT is metabolically degraded and resynthesized continuously as in the case of general proteins. Therefore, when Cu accumulates more than the capacity of the synthesis of MT, Cu not sequestered to MT (so-called free-Cu ions) appears in the cell *(18–20)*.

Copper bound to MT is in the monovalent state (cuprous), and divalent Cu (cupric ions) is reduced to monovalent Cu before being bound to MT, abundant thiol groups on MT being the potent reducing agent for Cu *(21,22)*. The affinity of Cu to MT is greater than that of Zn, and Cu is easily bound to MT by replacing Zn on MT *(21)*. When all Zn on MT is replaced with Cu, further reduction of divalent Cu occurs at the expense of thiol groups coordinating to Cu on MT, thereby liberating monovalent Cu from MT together with the newly reduced Cu. As a result, divalent Cu is reduced to monovalent Cu with thiol groups on MT until all thiol groups are oxidized as depicted schematically in Fig. 1.

Monovalent Cu is a potent reducing agent and catalyzes one electron reduction of reactive oxygen species (i.e., reduces hydrogen peroxides to hydroxyl radicals by the Fenton reaction [Fig. 2]) *(23–25)*. The supply of monovalent Cu produces the reactive oxygen species in the medium, which is assumed to cause acute hepatitis in LEC rats, the animal model of Wilson's disease. The sequestration of radicals/reactive oxygen species is one of the well-known biological roles of MT together with the protection of the body from the harmful effect of heavy metals. However, the production of reactive oxygen species under the present condition suggests that MT becomes a pro-oxidant when Cu accumulates more than the capacity to synthesize Cu–MT (Fig. 1).

2.2. Selective Removal of Copper Bound to Metallothionein

2.2.1. Copper Accumulating in the Form Bound to Metallothionein by the Defective ATP7B

The concentration of Cu in the body is maintained homeostatically within a certain level. However, in the liver of Wilson's disease patients and its animal model, LEC rats, Cu accumulates in a form bound to MT owing to the mutation of the Cu-binding ATPase for the efflux of Cu (ATP7B) that is expressed in the liver *(5–7,14)*. ATP7B is responsible for the transport of Cu in the cytoplasm into the Golgi apparatus *(26–28)* and also into the bile *(29)*. In the normal functioning body, the Cu transported into the Golgi apparatus is supplied to ceruloplasmin (CP) and secreted into the blood-

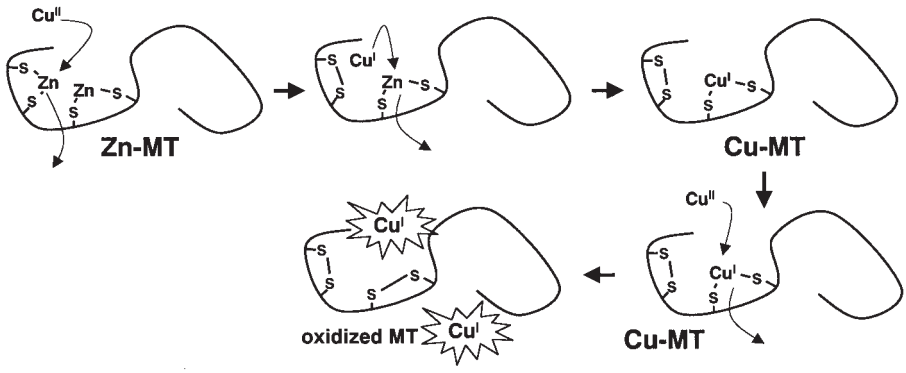

Fig. 1. Production of monovalent Cu by metallothionein depending on Zn and Cu on metallothionein. Although Zn and Cu are coordinated with four (tetrahedral) and three (trigonal) thiol groups on MT, respectively, only two thiol groups are depicted for Zn and Cu to simplify the reaction in this figure.

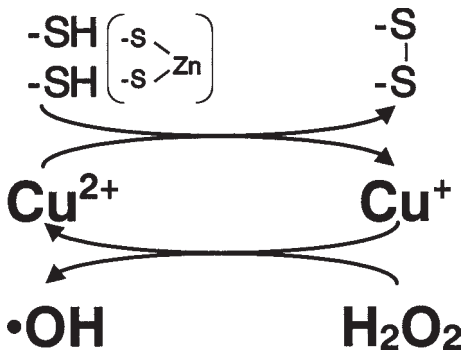

Fig. 2. Production of reactive oxygen species by one electron reduction of oxygen molecules.

stream in a form bound to CP. Excessive Cu is excreted into the bile, the chemical form of Cu transported into the bile being assumed to be cuprous ions as a result of the function of ATP7B. The schematic diagram for the role of ATP7B is shown in Fig. 3.

As ATP7B is not functioning genetically in the livers of patients with Wilson's disease and LEC rats, Cu is not transported into the Golgi apparatus and accumulates in the cytoplasm. Excessive accumulation of Cu is toxic to the body and the body induces the synthesis of MT to sequester the excess Cu in a nontoxic form, Cu,Zn–MT *(15,16)*. As a result, Cu accumulates in the liver in the form bound to MT without showing toxic effects until it accumulates up to the limit of the capacity of MT synthesis *(18–20)*.

In the normal subjects and rats without the defective ATP7B, the ATP7B is localized on the Golgi membrane and transports Cu from the cytoplasm into the Golgi apparatus under the certain concentration of Cu. However, when the concentration of Cu in the cytoplasm increases more than the certain level, ATP7B is translocated on the plasma membrane and exports Cu from the cytoplasm into the bile *(28)*.

In Wilson's disease patients and LEC rats, the two major excretion routes for Cu through the transporter ATP7B are not functioning. As a result, Cu accumulates in the liver and induces the synthesis of MT, resulting in the accumulation of Cu,Zn–MT followed by Cu–MT.

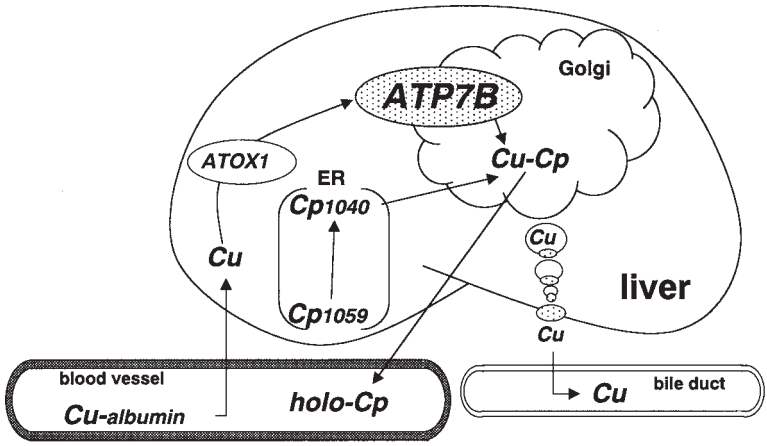

Fig. 3. Schematic diagram for the transport of Cu into the Golgi apparatus and the bile by ATP7B.

2.2.2. How to Decrease the Concentration of Copper Accumulating in the Form Bound to Metallothionein

The concentration of Cu accumulating in the form bound to MT can be decreased either by reducing the intake of Cu or by removing the Cu accumulating in the liver. The former approach is possible by feeding diets and water of low Cu content, by competing the uptake/absorption of Cu with Zn *(30,31)*, or by inhibiting the uptake/absorption of Cu by complexing with chelating agents, trientine, and D-penicillamine *(31–34)*. The chelating agents may remove Cu not bound to CP in the bloodstream as well. However, the affinity of Cu to MT is greater than those of these chelating agents, and the Cu bound to MT in the liver cannot be removed. The former approach with diets of low Cu content may be possible for experimental animals but not practical for humans. The use of chelating agents is effective in retarding the onset of hepatitis *(35)*. However, chelating agents are not powerful enough to remove Cu accumulating in the form bound to MT in the liver *(36)*.

Contrary to the strategies mentioned earlier, the removal of Cu directly from MT seems to be more effective in reducing the concentration of Cu accumulating in the form bound to MT in the liver. This approach is possible only with the chelating agent, TTM *(37)*. TTM was used to antagonize the toxicity of Cu based on the observations that Cu and molybdenum (Mo) form a complex in the presence of sulfur under anaerobic conditions in the gastrointestinal tract and that the availability of both metals becomes negligible by the complex formation in livestock *(38)*.

The mechanisms underlying the complex formation between TTM and Cu and its application to the removal of Cu from the livers of patients of Wilson's disease and LEC rats are described in Chapter 5.

3. EXPERIMENTAL PROCEDURES

3.1. Preparation of Tetrathiomolybdate

When hydrogen sulfide is bubbled into an ammonium polymolybdate (oxymolybdate) solution (0.5 g/5 mL ammonia solution; Wako Pure Chemicals Ind., Osaka, Japan), yellow crystals of ammonium dithiomolybdate (DTM) appear at first, and further bubbling of hydrogen sulfide produces dark red crystals of ammonium salt of TTM *(39)*. The precipitate was washed twice with ethanol (–25°C) and then dried *in vacuo*. DTM and TTM can be identified, based on their contents of sulfur and molybdenum (Mo), by inductively coupled argon plasma mass–spectrometry (ICP–MS) and their molecular weights can be determined by fast atomic bombardment mass spectrometry.

Tetrathiomolybdate is easily hydrolyzed to molybdate, especially under acidic conditions, by liberating insoluble sulfide ions. Fresh TTM crystals (amorphous) without containing hydrolyzed (degraded) ones are soluble in saline up to 50 mg/mL saline. DTM is more labile than TTM.

Sodium salt of TTM can be prepared instead of ammonium salt. However, the ammonium salt is much easily prepared in a pure form than the sodium salt.

3.2. Preparation of Copper-Containing Metallothionein from a Liver Supernatant of LEC Rats

In the present experiment, Cu,Zn,Cd-containing MTs were prepared to evaluate the specificity of TTM against diverse metals in the form bound to MT. LEC rats aged 8–12 wk (about 120–200 μg Cu/g liver) were injected intraperitoneally with cadmium chloride at a dose of 2 mg Cd/kg body weight 24 h before dissection. Livers of the LEC rats were removed, and then homogenized in 50 m*M* Tris-HCl buffer solution (pH 7.4), containing 0.25 *M* glucose, which had been bubbled with 99.999% nitrogen, under an atmosphere of nitrogen with a glass–Teflon homogenizer. The homogenate was ultracentrifuged at 105,000*g* for 60 min at 2°C, and then a 1-mL portion of the supernatant was sealed in a tube under nitrogen and was heated at 72˚C for 5 min to remove heat-labile high-molecular-weight proteins. After centrifugation at 1600*g* for 5 min, heat-treated supernatants in appropriate portions for later use were sealed under nitrogen and stored at –30˚C or lower. MT, especially Cu containing MT, is susceptible to oxidation by air and samples should be protected from air during the preparation procedures and storage. Repeated freezing and thawing of samples are not recommended and samples should be stored in appropriate portions for later use.

3.3. HPLC-ICP Analysis

A 0.1 mL portion of the supernatant was subjected to high-performance liquid chromatography (HPLC)–ICP MS analysis on a G3000SW column (7.5 × 600 mm, with a guard column of 7.5 × 75 mm, Tosoh, Tokyo, Japan) by elution with 50 m*M* Tris-HCl buffer solution (pH 8.4) at a flow rate of 1.0 mL/min followed by direct introduction of the eluate into a mass spectrometer with ionization by inductively coupled argon plasma (ICP-MS; HP4500, Yokogawa Analytical Systems, Musashino, Tokyo) *(39,40)*. Cu and Mo (and other elements) in the eluate were monitored continuously at m/z = 65 and 95, respectively. Although ^{63}Cu (69.2%) is more abundant than the other ^{65}Cu (30.8%), the former isotope was not recommended owing to the isobaric interference with $^{23}Na^{40}Ar^{+}$ and the latter isotope, ^{65}Cu, is recommended for the determination for biological samples. On the other hand, ^{95}Mo, the third abundant isotope (15.9%) is recommended for avoiding interference with sulfate. Distributions of Cu and Mo (and other elements) were drawn with an in-house developed program (appropriate programs are now available commercially).

4. MECHANISMS UNDERLYING THE SELECTIVE REMOVAL OF COPPER FROM COPPER-BINDING MT BY TTM

4.1. Formation of Three Different Complexes Between Copper and TTM In Vitro Depending on the Relative Molar Ratio of TTM to Copper

Tetrathiomolybdate forms different complexes with Cu (Cu^{2+}) in vitro depending on the relative ratio of TTM to Cu, which can be monitored spectroscopically by the change at the characteristic absorbances of 240, 315, and 465 nm. When Cu is present in the form bound to MT (i.e., Cu–MT or Cu,Zn–MT), three different complexes are formed on a gel filtration HPLC column by the HPLC-ICP MS method depending on the relative ratio of TTM to Cu as represented by the assumed structures shown in Fig. 4.

When a TTM solution in 50 m*M* Tris-HCl (pH 7.4) is added into a Cu,Zn–MT solution to the molar ratio of Mo/Cu less than unity (Mo/Cu<1), the Cu and Zn peaks of MT become eluted faster than the original retention time of MT at 18.4 (MT-I) and 20.0 min (MT-II) on the HPLC-ICP MS *(41)*.

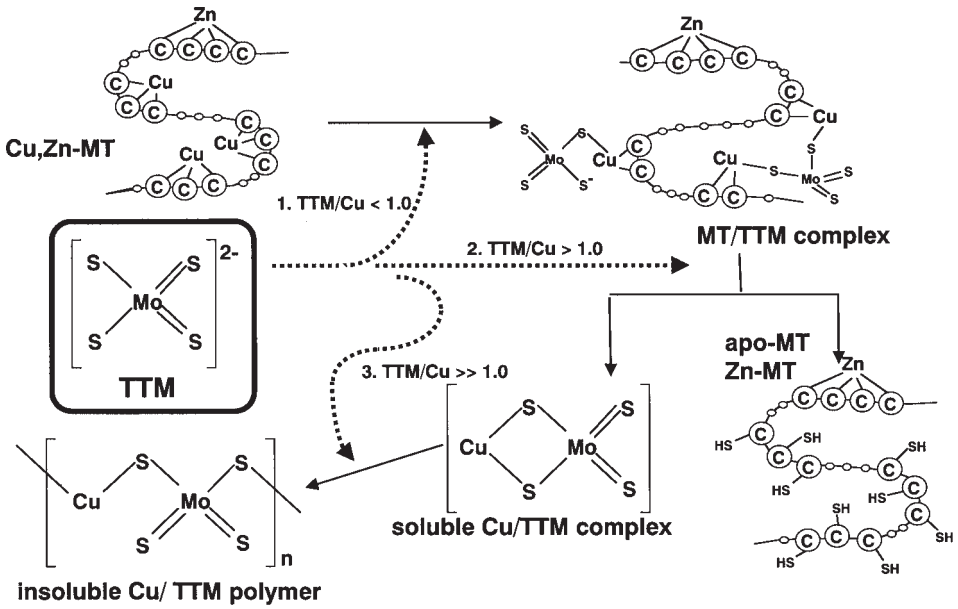

Fig. 4. Schematic formation of three different complexes between copper and TTM depending on the relative ratio of TTM/Cu in metallothionein.

The Mo peak of TTM becomes eluted at the same retention time as those of Cu and Mo from the original retention time of TTM at 20.8 min, suggesting the formation of a new complex between MT and TTM, tentatively named the MT/TTM complex *(41)*.

When TTM is added into a Cu,Zn,Cd–MT solution at the molar ratio of Mo/Cu greater than unity but less than 2 (1<Mo/Cu<2), the Cu and Mo peaks of the Cu/TTM complex become precipitated in the absence of proteins or become eluted together with high-molecular-weight proteins in the presence of a liver supernatant of LEC rats, Zn and Cd being eluted at the original retention time of MT. When a blood plasma or albumin is present instead of a liver supernatant or together with a liver supernatant, the Cu and Mo peaks are eluted at the same retention time as that of albumin, suggesting the formation of a ternary complex among the Cu removed from MT, Mo in TTM, and albumin. The changes in the elution profiles of the three metals suggest the removal of Cu from MT to form the soluble Cu/TTM complex. The Cu/TTM complex is not eluted out from the columns under the present separation conditions in the absence of proteins. The Cu/TTM complex binds readily to proteins and is then eluted out from columns *(42,43)*.

The addition of TTM to a Cu,Zn,Cd–MT solution at the molar ratio of TTM/Cu greater than 2 insolubilized the Cu and Mo by leaving soluble Zn,Cd–MT. The precipitated Cu/TTM complex was named the insoluble Cu/TTM complex *(41)*.

The production of the three different complexes can be explained by the following scheme: The first step is the formation of the metal–sulfur bridges between MT and TTM (i.e., S_{MT}–Cu–S_{TTM}). The second step is the cleavage of S_{MT}–Cu bond by the participation of TTM to form the soluble Cu/TTM complex. The soluble Cu/TTM complex is ready to bind to proteins with the highest affinity to albumin. The soluble Cu/TTM complex is readily bound to proteins and not eluted from a gel filtration column in the absence of proteins. However, further production of the Cu/TTM complex results in the formation of the polymeric Cu/TTM complex (the insoluble Cu/TTM complex) and it is precipitated in a nonsoluble form. These steps are given schematically in Fig. 4.

Zn,Cd–MT and/or apo-MT released from the MT/TTM complex at the second step can be stabilized in the presence of Zn or Cd ions in the reaction medium by forming Zn,Cd–MT and/or Zn–MT or Cd–MT

whose thiol groups are fully occupied by Zn and/or Cd. Zn,Cd–MT, Zn–MT, and Cd–MT released from the MT/TTM complex in the presence of Zn or Cd ions are eluted as sharp peaks at the corresponding retention times of MT.

4.2. Removal of Copper Accumulating in the Liver of Lec Rats by TTM In Vivo

4.2.1. A Single Intravenous Injection of TTM

A single intravenous injection of TTM into LEC rats removes Cu from the liver in different ways depending on the dose. At the low and middle doses of 2 and 10 mg TTM/kg body weight of LEC rats (Cu accumulating in the liver at the concentration of approximately 200 μg Cu/g liver), the Cu removed from the liver is excreted into the bloodstream and bile together with equimolar Mo. Mo injected in a form of TTM disappears from the bloodstream within 0.5 h, and then the metal appears again in the plasma in a form bound to albumin together with Cu, the molar ratio of Mo/Cu bound to albumin is approximately unity *(40,44–48)*. The Cu removed from the liver appears more in the bile than in the plasma together with equimolar Mo, both Cu and Mo in the bile being not eluted out from a gel filtration HPLC column under the conventional conditions mentioned earlier. As a result, the Cu removed from the liver is effluxed into the bile and plasma at the molar ratio of approx 7/3, and Mo does not remain in the liver at the low dose *(45)*. The results indicate that the MT/TTM complex observed in vitro at a low dose of TTM is detectable also in vivo, suggesting that the Cu/TTM complex is liberated from the MT/TTM complex.

At the high dose of 50 mg TTM/kg body weight, although the Cu removed from the liver is excreted into the bloodstream and bile together with equimolar Mo, the amounts of Cu and Mo do not increase in a dose-dependent manner and both metals are insolubilized in the liver. The insolubilized Cu/TTM complex is resolubilized slowly with time and excreted into the plasma and bile *(40)*.

Tetrathiomolybdate thus removes Cu from Cu–MT in the form of the Cu/TTM complex at any dose, and equimolar Cu and Mo are effluxed from the liver in the form of soluble Cu/TTM complex into the bile and plasma, the relative amount of the Cu/TTM complex effluxed into the bile and plasma being approximately 7/3 at any dose even though the efflux is retarded at a high dose of TTM owing to the insolubilization and resolubilization processes (Section 4.2.2.).

4.2.2. Repeated Intraperitoneal Injections of TTM

Repeated intraperitoneal injections of TTM at a dose of 10 mg/kg body weight for eight consecutive days are sufficient to remove about a half the amount of Cu in the liver and to reduce the concentration of Cu in the liver of LEC rats from approx 240 to 80 μg/g liver *(41,49)*. The remaining Cu in the liver was not bound to MT but insolubilized *(41,49)*; that is, TTM *removed* Cu from MT completely and excessive amounts of TTM formed the insoluble Cu/TTM complex. The Cu insolubilized in the liver was gradually solubilized within days and excreted into both the bile and bloodstream, maintaining the molar ratio of Mo/Cu of approx 1. The relative excretion of both metals into bile and plasma were approx 70% and 30%, respectively *(45)*. Loading of TTM at a higher dose than the present dose of 10 mg/kg or for a longer period than 10 d even at the dose of 10 mg/kg was toxic because of excessive removal of Cu (Section 4.2.4.).

4.2.3. Selectivity in the Removal of Copper by TTM: Selective to Copper Among Various Metals

Tetrathiomolybdate binds Cu through the Mo–S–Cu bridge and this bridge is specific to the three participating elements. Therefore, although TTM can form a complex with metals other than Cu, such as Zn and Cd, the complex formation between TTM and metals (elements) is selective to Cu in the body. In fact, complexes between TTM and metals other than Cu were not detected in vivo. Excessive TTM that does not participated in the formation of complexes with Cu is hydrolyzed to molybdate, this hydrolysis being facilitated in the liver *(44)*. Thus, TTM is highly selective to Cu among diverse metal ions in the ternary complex.

4.2.4. Selectivity in the Removal of Copper by TTM: Selective to Copper Among Copper Species

Tetrathiomolybdate can remove Cu from free-Cu ions (Cu bound nonspecifically to proteins) and Cu bound to MT (Cu coordinated only with thiol groups). However, TTM cannot remove Cu bound to most of Cu enzymes such as Cu,Zn-superoxide dismutase (SOD1) and ceruloplasmin (CP). Cu bound to SOD1 and CP is sometimes decreased after repeated injections of TTM. However, this is assumed not to be the result of direct removal of Cu from those enzymes, but from their chaperones during the metabolic turnover of their enzymes (i.e., Cu is liberated from degraded Cu enzymes is bound to chaperons before being transferred to newly synthesized apo-enzymes).

Because MT is most abundant among Cu-containing proteins in the liver of LEC rats, TTM dominantly removes Cu from MT in vivo in LEC rats. TTM can remove Cu from SOD1 and/or other Cu-containing proteins in LEC rats only after complete removal of Cu from MT. This suggests that an excessive dose of TTM causes a Cu deficiency as the chronic side effect.

The primary translation product of CP, CP_{1059} is processed to CP_{1040} in the endoplasmic reticulums (ER), and then trafficked to the Golgi apparatus, where Cu is supplied to give Cu–CP_{1040}, Cu being supplied into the Golgi apparatus by Atox1 and Atp7b, and then glycosylated to the mature form holo-CP and the holo-CP is secreted into the plasma *(50–52)*. In the liver of Wilson's disease patients and its animal model, LEC rats, Cu is not supplied to the Golgi apparatus because of the mutation of the gene encoding Atp7b that is present on the Golgi membrane and responsible to the transport of Cu from the cytosol to the Golgi apparatus. CP is, thus, secreted into the plasma in the form of apo-Cp in Wilson's disease patients and LEC rats *(53–57)*.

4.3. Side Effects of Tetrathiomolybdate

Two types of side effects, acute and chronic effects, are known to occur by treating TTM. The chronic effect is a deficiency of Cu caused by an excessive removal of Cu (Section 4.2.4.), and the acute effect is a toxicity of sulfide caused by the production of sulfide ions by the hydrolysis of TTM. As TTM can sequester both free Cu and Cu bound to MT or chaperones, excessive TTM depletes the Cu that should be supplied for the maturation of Cu enzymes, resulting in the causation of Cu deficiency in the body *(39)*. Therefore, excessive treatment with TTM is fatal and has to be avoided.

Tetrathiomolybdate is susceptible to hydrolysis, especially under acidic conditions, to produce sulfide ions. This means that the hydrolysis is accelerated in the gastric juice as the acute effect.

It was observed that a high dose of TTM (50 mg/kg body weight) caused kidney damage, resulting in the increase of blood urea nitrogen *(45)*. However, the mechanism underlying this acute nephrotoxicity of TTM is not known.

A lower dose and treatment with a sufficient interval via nonoral (parenteral) route are recommended to avoid both types of the side effects.

5. CONCLUSION

Tetrathiomolybdate is highly effective in removing excessive Cu accumulating in the body from the viewpoints of selectivity not only to Cu among diverse metal ions but also to Cu in the form of free ions and the metal coordinated by only thiol groups. As the typical Cu in the latter form can be removed by TTM (TTM-removable Cu), the two types of Cu-binding proteins are mentioned: one is MT and chaperones, and the other is free Cu ions or Cu ions bound nonselectively to proteins or other biological constituents. TTM is effective only to the TTM-removable Cu and does not remove Cu in Cu enzymes. As a result, TTM is quite safe as long as it is not applied in excess in terms of TTM-removable Cu during the metabolic turnover.

REFERENCES

1. Tønnesen, T., Kleijer, W. J., and Horn, N. (1991) Incidence of Menkes disease. *Hum. Genet.* **86**, 408–410.
2. Tønnesen, T., Peterson, A., Kruse, T. A., Gerdes, A. M., and Horn, N. (1992) Multipoint linkage analysis in Menkes disease. *Am. J. Hum. Genet.* **50**, 1012–1017.
3. Sarkar, B., Lingertat-Walsh, K., and Clarke, J. T. (1993) Copper–histidine therapy for Menkes disease. *J. Pediatr.* **123**, 828–830.
4. Monaco, A. P. and Chelly, J. (1995) Menkes and Wilson's diseases. *Adv. Genet.* **33**, 233–253.
5. Bull, P. C., Thomas, G. R., Rommens, J. M., Forbes, J. R., and Cox, D. W. (1993) The Wilson's disease gene is a putative copper transporting P-type ATPase similar to the Menkes gene. *Nature Genet.* **5**, 327–337.
6. Petrukhin, K., Fischer, S. G., Pirastu, M., Tanzi, R. E., Chernov, I., Devoto, M., et al. (1993) Mapping, cloning and genetic characterization of the region containing the Wilson's disease gene. *Nature Genet.* **5**, 338–343.
7. Tanzi, R. E., Petrukhin, K., Chernov, I., Pellequer, J. L., Wasco, W., Ross, B., et al. (1993) The Wilson's disease gene is a copper transporting ATPase with homology to the Menkes disease gene. *Nature Genet.* **5**, 344–350.
8. Amaravadi, R., Glerum, D. M., and Tzagoloff, A. (1997) Isolation of a cDNA encoding the human homolog of COX17, a yeast gene essential for mitochondrial copper recruitment. *Hum. Genet.* **99**, 329–333.
9. Culotta, V. C., Klomp, L., Strain, J., Casareno, R., Krems, B., and Gitlin, J. D. (1997) The copper chaperone for superoxide dismutase. *J. Biol. Chem.* **272**, 23,469–23,472.
10. Klomp, L. W., Lin, S. J., Yuan, D. S., Klausner, R. D., Culotta, V. C., and Gitlin, J. D. (1997) Identification and functional expression of HAH1, a novel human gene involved in copper homeostasis. *J. Biol. Chem.* **272**, 9221–9226.
11. Huang, I. H., Casareno, R. L., Labesse, G., Mathews, F. S., and Gitlin, J. D. (1998) HAH1 is a copper-binding protein with distinct amino acid residues mediating copper homeostasis and antioxidant defense. *J. Biol. Chem.* **273**, 1749–1754.
12. Brem, S. (1999) Angiogenesis and cancer control: from concept to therapeutic trial. *Cancer Control* **6**, 436–458.
13. Suzuki, K. T., Imura, N., and Kimura, M. (eds.) (1993) *Metallothionein III*, Birkhäuser, Basel.
14. Wu, J., Forbes, J. R., Chen, H. S., and Cox, D. W. (1994) The LEC rat has a deletion in the copper transporting ATPase gene homologous to the Wilson's disease gene. *Nature Genet.* **7**, 541–545.
15. Sugawara, N., Sugawara, C., Sato, M., Katakura, M., Takahashi, H., and Mori, M. (1991) Copper metabolism in LEC rats aged 30 and 80 days old: induction of Cu–metallothionein and status of zinc and iron. *Res. Commun. Chem. Pathol. Pharmacol.* **72**, 353–362.
16. Sakurai, H., Fukudome, A., Tawa, R., Kito, M., Takeshima, S., Kimura, M., et al. (1992) Unusual accumulation of copper related to induction of metallothionein in the liver of LEC rats. *Biochem. Biophys. Res. Commun.* **184**, 1393–1397.
17. Rupp, H. and Weser, U. (1978) Circular dichroism of metallothioneins: a structural approach. *Biochim. Biophys. Acta* **533**, 209–226.
18. Suzuki, K. T., Kanno, S., Misawa, S., and Sumi, Y. (1993) Changes in hepatic copper distribution leading to hepatitis in LEC rats. *Res. Commun. Chem. Pathol. Pharmacol.* **82**, 217–224.
19. Suzuki, K. T. (1995) Disordered copper metabolism in LEC rats, an animal model of Wilson's disease: role of metallothionein. *Res. Commun. Mol. Pathol. Pharmacol.* **89**, 221–240.
20. Suzuki, K. T. (1996) Participation of metallothionein in disordered copper metabolism and toxicity. *Environ. Sci.* **4**, 149–162.
21. Suzuki, K. T. and Maitani, T. (1981) Metal-dependent properties of metallothionein. Replacement in vitro of zinc in zinc-thionein with copper. *Biochem. J.* **199**, 289–295.
22. Stillman, M. J., Shaw, C.F., III, and Suzuki, K. T. (eds.) (1992) *Metallothioneins*, VCH, New York.
23. Sakurai, H., Satoh, H., Hatanaka, A., Sawada, T., Kawano, K., Hagino, T., et al. (1994) Unusual generation of hydroxyl radicals in hepatic copper–metallothionein of LEC (Long–Evans Cinnamon) rats in the presence of hydrogen peroxide. *Biochem. Biophys. Res. Commun.* **199**, 313–318.
24. Suzuki, K. T., Rui, M., Ueda, J., and Ozawa, T. (1996) Production of hydroxyl radicals by copper-containing metallothionein: roles as pro-oxidant. *Toxicol. Appl. Pharmacol.* **141**, 231–237.
25. Suzuki, K. T., Rui, M., Ueda, J., and Ozawa, T. (1997) Production of ascorbate and hydroxyl radicals in the liver of LEC rats in relation to hepatitis. *Res. Commun. Mol. Pathol. Pharmacol.* **96**, 137–146.
26. Forbes, J. R., Hsi, G., and Cox, D. W. (1999) Role of the copper-binding domain in the copper transport function of ATP7B, the P-type ATPase defective in Wilson's disease. *J. Biol. Chem.* **274**, 12,408–12,413.
27. Harada, M., Sakisaka, S., Kawaguchi, T., Kimura, R., Taniguchi, E., Koga, H., et al. (2000) Copper does not alter the intracellular distribution of ATP7B, a copper-transporting ATPase. *Biochem. Biophys. Res. Commun.* **275**, 871–876.
28. Forbes, J. R. and Cox, D. W. (2000) Copper-dependent trafficking of Wilson's disease mutant ATP7B proteins. *Hum. Mol. Genet.* **9**, 1927–1935.
29. Nagano, K., Nakanura, K., Urakami, K., Umeyama, K., Uchiyama, H., Koiwai, K., et al. (1998) Intracellular distribution of the Wilson's disease gene product (ATPase 7B) after in vitro and in vivo exogenous expression in hepatocytes from the LEC rat, an animal model of Wilson's disease. *Hepatology* **27**, 799–807.
30. Friedman, L. S. (1993) Zinc in the treatment of Wilson's disease: how it works. *Gastroenterology* **104**, 1566–1568.
31. Walshe, J. M. and Munro, N. A. (1995) Zn-induced deterioration in Wilson's disease aborted by treatment with penicillamine, dimercaprol, and a novel zero copper diet. *Arch. Neurol.* **52**, 10–11.

32. Walshe, J. M. (1982) Treatment of Wilson's disease with trientine (triethylene tetramine) dihydrochloride. *Lancet* **1**, 643–647.
33. Scheinberg, I. H., Sternlieb, I., Schilsky, M., and Stockert, R. J. (1987) Penicillamine may detoxify copper in Wilson's disease. *Lancet* **2**, 95.
34. Gibbs, K. and Walshe, J. M. (1990) Liver copper concentration in Wilson's disease: effect of treatment with "anti-copper" agents. *J. Gastroenterol. Hepatology* **5**, 420–424.
35. Sone, H., Maeda, M., Wakabayashi, K., Takeichi, N., Mori, M., Sugimura, T., et al. (1996) Inhibition of hereditary hepatitis and liver tumor development in Long–Evans Cinnamon rats, by a copper chelating agent, trientine dihydrochloride. *Hepatology* **23**, 764–770.
36. McQuaid, A. and Mason, J. (1990) A comparison of the effects of penicillamine, trientine, and trithiomolybdate on (35S)-labeled metallothionein in vitro; implications for Wilson's disease therapy. *J. Inorg. Biochem.* **41**, 87–92.
37. Brewer, G. J., Dick, R. D., Johnson, V., Wang, Y., Yuzbasiyan-Gurkan, V., Kluin, K., et al. (1994) Treatment of Wilson's disease with ammonium tetrathiomolybdate. I. Initial therapy in 17 neurologically affected patients. *Arch. Neurol.* **51**, 545–554.
38. Suttle, N. F. (1991) The interactions between copper, molybdenum, and sulphur in ruminant nutrition. *Annu. Rev. Nutr.* **11**, 121–140.
39. Ogra, Y., Komada, Y., and Suzuki, K. T. (1999) Comparative mechanism and toxicity of tetra- and dithiomolybdates in the removal of copper. *J. Inorg. Biochem.* **75**, 199–204.
40. Ogra, Y., Chikusa, H., and Suzuki, K. T. (2000) Metabolic fate of the insoluble copper/tetrathiomolybdate complex formed in the liver of LEC rats with excess tetrathiomolybdate. *J. Inorg. Biochem.* **78**, 123–128.
41. Ogra, Y., Ohmichi, M., and Suzuki, K. T. (1996) Mechanisms of selective copper removal by tetrathiomolybdate from metallothionein in LEC rats. *Toxicology* **106**, 75–83.
42. Suzuki, K. T. and Ogra, Y. (1995) Formation of copper–metallothionein/tetrathiomolybdate complex is the first step in removal of Cu from LEC rats. *Res. Commun. Mol. Pathol. Pharmacol.* **88**, 187–195.
43. Ogra, Y. and Suzuki, K. T. (1995) Removal and efflux of copper from Cu–metallothionein as Cu/tetrathiomolybdate complex in LEC rats. *Res. Commun. Mol. Pathol. Pharmacol.* **88**, 196–204.
44. Ogra, Y. and Suzuki, K. T. (1998) Targeting of tetrathiomolybdate on the copper accumulating in the liver of LEC rats. *J. Inorg. Biochem.* **70**, 49–55.
45. Komatsu, Y., Sadakata, I., Ogra, Y., and Suzuki, K. T. (2000) Excretion of copper complexed with thiomolybdate into the bile and blood in LEC rats. *Chem.–Biol. Interact.* **124**, 217–231.
46. Suzuki, K. T., Yamamoto, K., Kanno, S., Aoki, Y., and Takeichi, N. (1993) Selective removal of copper from metallothionein in the liver of LEC rats by tetrathiomolybdate. *Toxicology* **83**, 149–158.
47. Suzuki, K. T., Yamamoto, K., Ogra, Y., Kanno, S., Aoki, Y., and Takeichi, N. (1994) Mechanisms for removal of copper from metallothionein by tetrathiomolybdate. *J. Inorg. Biochem.* **54**, 157–165.
48. Ogra, Y. Ohmichi, M., and Suzuki, K. T. (1995) Systemic dispositions of molybdenum and copper after tetrathiomolybdate injection in LEC rats. *J. Trace Elements Med. Biol.* **9**, 165–169.
49. Suzuki, K. T., Ogra, Y., and Ohmichi, M. (1995) Molybdenum and copper kinetics after tetrathiomolybdate injection in LEC rats: specific role of serum albumin. *J. Trace Elements Med. Biol.* **9**, 170–175.
50. Aldred, A. R., Grimes, A., Schreiber, G., and Mercer, J. F. . (1987) Rat ceruloplasmin. Molecular cloning and gene expression in liver, choroid plexus, yolk sac, placenta, and testis. *J. Biol. Chem.* **262**, 2875–2878.
51. Fleming, R. E. and Gitlin, J. D. (1990) Primary structure of rat ceruloplasmin and analysis of tissue-specific gene expression during development. *J. Biol. Chem.* **265**, 7701–7707.
52. Suzuki, K. T. and Kuroda, T. (1994) Direct transfer of copper from metallothionein to superoxide dismutase: a possible mechanism for differential supply of Cu to SOD and ceruloplasmin in LEC rats. *Res. Commun. Mol. Pathol. Pharmacol.* **86**, 15–23.
53. Scheinberg, I. H. and Gitlin, D. (1952) Deficiency of ceruloplasmin in patients with hepatolenticular degeneration (Wilson's disease). *Science* **166**, 484–485.
54. Yamada, T., Agui, T., Suzuki, Y., Sato, M., and Matsumoto, K. (1993) Inhibition of the copper incorporation into ceruloplasmin leads to the deficiency in serum ceruloplasmin activity in Long–Evans cinnamon mutant rat. *J. Biol. Chem.* **268**, 8965–8971.
55. Nakamura, K., Endo, F., Ueno, T., Awata, H., Tanoue, A., and Matsuda, I. (1995) Excess copper and ceruloplasmin biosynthesis in long-term cultured hepatocytes from Long–Evans Cinnamon (LEC) rats, a model of Wilson's disease. *J. Biol. Chem.* **270**, 7656–7660.
56. Murata, Y., Yamakawa, E., Iizuka, T., Kodama, H., Abe, T., Seki, Y., et al. (1995) Failure of copper incorporation into ceruloplasmin in the Golgi apparatus of LEC rat hepatocytes. *Biochem. Biophys. Res. Commun.* **209**, 349–355.
57. Terada, K., Kawarada, Y., Miura, N., Yasui, O., Koyama, K., and Sugiyama, T. (1995) Copper incorporation into ceruloplasmin in rat livers. *Biochim. Biophys. Acta* **1270**, 58–62.

27

Control of Copper in Wilson's Disease and Diseases of Neovascularization, such as Cancer

George J. Brewer

1. INTRODUCTION

Over the last 20 yr our group has worked on the development of new anticopper drugs for the treatment of Wilson's disease. This has led to the development of zinc and tetrathiomolybdate for specific indications in Wilson's disease, which we will discuss in detail shortly.

Tetrathiomolybdate has turned out to be a very safe and potent anticopper agent, and over the last 5 yr we have been able to take advantages of those properties to begin evaluating this drug as a therapy in diseases of neovascularization, such as cancer. The rationale here is that angiogenesis has a strong dependency on adequate levels of copper. When copper levels are reduced such that the patient is in a state of mild copper deficiency, angiogenesis is inhibited. Thus, this chapter will have two sections: The first dealing with the control of copper in Wilson's disease, and the second dealing with control of copper in disease of neovascularization.

2. WILSON'S DISEASE

2.1. Overview of Wilson's Disease

2.1.1. Abnormal Copper Balance and the Genetic Basis for Wilson's Disease

Wilson's disease is an autosomal recessive disorder of copper accumulation and copper toxicity *(1–6)*. It is a relatively rare disease, thought to have a frequency in most populations of about 1 in 30,000 to 1 in 40,000 *(2)*. A failure of biliary excretion of excess copper is the cause of the copper accumulation *(7–9)*. Most diets contain 0.75–1.5 mg of copper, averaging about 1.0 mg *(10–13)*. The requirement for copper appears to be about 0.75 mg/d for adults, which means that, in most cases, the small excess in dietary copper must be excreted and lost from the body *(1)*. Copper is unusual among cations in that its balance is regulated not by the gut or by the kidney, but by the liver. The liver excretes excess copper in the bile, packaged in some manner to prevent its reabsorption, and the excess copper is lost in the stool *(14)*.

The gene responsible for Wilson's disease has been cloned and is called *ATP7B (15–17)*. The gene codes for a copper-binding ATPase that has membrane-binding properties. Exactly how this protein functions in the biliary excretion of copper has not been completely clarified as yet. An epistatic effect of this genetic defect is a reduction in circulating ceruloplasmin (Cp) in the blood. Cp is a

From: Handbook of Copper Pharmacology and Toxicology
Edited by: E. J. Massaro © Humana Press Inc., Totowa, NJ

copper-containing protein synthesized by the liver and released into the blood, and in most patients with Wilson's disease, the serum level of Cp is quite low.

Some evidence suggests that copper is transported into the lumen of the Golgi apparatus and secretory vesicles by ATP7B *(18)*. Some of this copper may be used for incorporation into apoceruloplasmin, and this mature, fully oxidase-active Cp is then secreted into blood containing six to seven atoms of copper. These data suggest that ATP7B function in copper transport is coupled with synthesis of mature, copper-containing Cp. Our group has hypothesized that this circle is completed by a role for Cp to be the packaging mechanism for excretion of regulatory copper in the bile *(14)*. Cp is protease resistant, and we find the right amount of copper contained in Cp crossreacting material in the bile of normal subjects to account for copper balance regulation. This crossreacting material is missing in the bile of normal subjects *(14)*.

In all populations studied so far, there have been a large number of different mutations in the *ATP7B* gene which produce the disease *(19)*. Generally, no one mutation is extremely predominant. For example, in the US Caucasian population, the most common mutation accounts for about 30% of the mutations, but the next, only 10%, and after that, the percentage falls off rapidly. Over 100 disease-producing mutations in this gene are now known, and most patients are compound heterozygotes. Because of the large number of mutations, development of a simple DNA diagnostic test is not practical with current technology.

2.1.2. Clinical Presentation

As a result of the genetic defect, homozygous patients with Wilson's disease accumulate a small amount of copper every day of their lives. At first it is stored in the liver, but its storage capacity is soon exceeded and damage to the liver begins as early as 3–4 yr of life *(2)*. The patient may present with liver disease, with the most common age of presentation being the late teenage years *(1–3)*. However, the age of presentation can be quite broad, ranging from 5–6 yr of age up until the 40s *(1)*. The clinical picture may be that of hepatitis, and if it is episodic, a diagnosis of chronic active hepatitis may be entertained. However, copper, and not a virus, is the culprit in this situation. Alternatively, the patient may present with hepatic decompensation, ranging from mild to fulminant in severity. Table 1 lists the types of hepatic presentation and some of the characteristic findings in each.

As the copper storage capacity of the liver is exceeded, increasing levels of copper appear in the blood, and then in organs of the body other than the liver. After the liver, the next most sensitive organ seems to be the brain, and patients may present with a neurologic disorder affecting control of muscles, called a movement disorder *(5,6)*. Table 2 lists the various symptoms most commonly seen in the neurological presentation. Note that there is no muscle weakness or sensory abnormality. Typically, these patients present in the late teenage years or early twenties, although, again, the age of presentation can be quite broad, ranging form early childhood to as late as 50 yr.

A fairly significant number of the patients, perhaps half of those who are going to present neurologically, will develop psychiatric symptoms prior to the neurologic symptoms. Table 3 lists the types of psychiatric symptomatology that are commonly seen in Wilson's disease *(20)*. As can be seen from Table 3, the types of symptoms are quite diverse, with inability to focus, depression, and loss of control of emotions being the most common.

Table 4 lists other abnormalities that can be seen in Wilson's disease and are sometimes the first presenting symptoms *(1,2)*.

2.1.3. Diagnosis

2.1.3.1. Recognition

It is very important that Wilson's disease be recognized and diagnosed as early as possible to minimize the amount of permanent liver and brain damage. Because the disease is treatable, further damage can be prevented once diagnosis is made and treatment started. The most troublesome aspect in regard to early diagnosis is recognition by the physician of the possibility of the disease in a patient

Table 1
Types of Hepatic Presentation

Type	*Clinical appearance*	*Laboratory findings*
Hepatitis	Asymptomatic, or possible mild jaundice	Elevated transaminase enzymes, possible mild elevated bilirubin
Episodic hepatitis	Same as hepatitis	Same as hepatitis
Chronic cirrhosis	Asymptomatic, possible complications of portal hypertension, such as bleeding varices, or possible hepatic failure	Elevated transaminase enzymes; possible abnormalities of liver function tests; possible leukopenia and/or thrombocytopenia
Hepatic failure		
Mild	Mild jaundice and fluid accumulation	Elevated transaminase enzymes; mild elevation of bilirubin; low albumin; possible mild abnormalities of other liver function tests
Moderate	Moderate jaundice, fluid accumulation, and other signs of liver failure	All abnormalities under "mild" are more severe
Severe	Deep jaundice, marked fluid accumulation, and other signs of liver failure	All abnormalities under "mild" are more severe

Table 2
Common Neurological Symptoms

Dysarthria
Dystonia
Tremor
Incoordination
Drooling
Parkinsonism-like facies and movements

Table 3
Common Behavioral Abnormalities

Difficulty focusing on tasks
Extreme emotionality
Depression
Insomnia
Loss of inhibitions

Table 4
Other Clinical Abnormalities

Loss of menstruation
Gallstones
Renal stones
Arthritis, particularly of knees
Abnormal losses of amino acids, etc., in urine

presenting with appropriate symptoms. Because the disease is relatively rare, physicians often do not think of a possible Wilson's diagnosis when they see patients with the kinds of liver, neurologic, or psychiatric presentations discussed earlier.

In Tables 5–7 are provided useful tips for physicians on the situations to be especially alert for the possible diagnosis of Wilson's disease *(5)*. It should be noted that relative youth is an important differential diagnostic criterion. A young patient presenting with parkinsonism has a much higher risk of having Wilson's disease than somebody in their sixties.

2.1.3.2. Screening

Once the diagnosis is considered a possibility, the next step is to decide on which screening tests to use to determine if Wilson's disease is likely or unlikely. Table 8 provides guidance in this regard. Let us consider symptomatic patients first, and then deal with affected but presymptomatic patients second. If the patient is symptomatic, a 24-h urine copper test is virtually diagnostic *(1,4–6)*. As shown in Table 8, if the value is over 100 μg/24 h the diagnosis is very likely Wilson's disease. It should be noted that if the patient has received even brief treatment with a chelator such as penicillamine or trientine, there is a rebound period during which the basal urine copper may be lower than 100 μg/24 h, even though the patient is affected (unpublished observations). A second caveat is that if the patient has had obstructive liver disease for some time, an elevated urine copper may not be indicative of Wilson's disease *(1)*. This is because the liver is responsible for excretion of copper, and with chronic obstruction, hepatic copper levels can build up, and then urinary copper levels build up to be over 100. However, in the absence of evidence of obstructive liver disease, urine copper is an excellent screening tool and is always elevated in symptomatic patients.

The Kayser–Fleischer (K-F) ring examination (Table 8) using a slit lamp in the hands of an ophthalmologist is a very reliable diagnostic tool in patients who present with neurologic or psych-iatric symptoms *(1)*. It is very rare for a patient of this type not to have K-F rings. This tool is much less useful in the hepatic presentation, where approximately half of the patients do not show these rings *(1)*.

Measurement of serum ceruloplasmin (Cp) is a useful guide but is not diagnostic. It is quite low in 85% of affected patients but can be only minimally reduced or even normal in 15% of patients *(1)*. It is particularly likely to be normal in patients with active liver disease, because it is an acute-phase reactant. Complicating this, carriers of the Wilson's disease gene (i.e., individuals with one copy of the disease gene) show a reduced Cp in upward of 15% of cases *(1)*. Because the carrier state is frequent compared to the affected state, finding a low Cp can be quite misleading. Thus, the Cp value should be used as a guide to affect index of suspicion, but not to rule in or rule out the diagnosis.

We *(1)* and others *(2)* do not recommend the use of a penicillamine loading test, looking at urinary excretion of copper, because this procedure has never been studied to the point that the values in gene carriers are known to be clearly differentiated from those in affected individuals. We *(1)* do not recommend the use of the radiocopper diagnostic test developed by Sternlieb et al. *(21)* for the same reason. The results in gene carriers, at least in our hands, appear to overlap with affected individuals, making the test unreliable for distinguishing between these two genotypes *(1)*.

It is important to be able to screen and diagnose the presymptomatic patients with Wilson's disease (Table 8). These are patients who have two abnormal Wilson's disease genes, but have not yet become clinically ill. Prophylactic therapy in these patients can be used to prevent them from becoming clinically ill. Generally, these patients will be diagnosed as part of a family workup, after diagnosis of a patient, as siblings are at 25% risk for also being affected. However, occasionally, patients of this type will be picked up because of elevated serum transaminase enzymes during a routine medical examination or because of the observation of the presence of K-F rings.

It cannot be emphasized too strongly that an intensive screening of the siblings of an affected individual should be carried out, because of the very high 25% risk of each sibling being affected but in a presymptomatic state. In general, the screening tests discussed earlier are applicable, but it needs to be pointed out that urine copper values can be in a gray zone in presymptomatic siblings (Table 8).

Table 5
Liver Disease Situations Indicative of Wilson's Disease Screening

Viral-negative hepatitis under age 50
Viral-positive hepatitis, if certain aspects do not fit, if under age 50
Cirrhosis, under age 40
Cirrhosis, age 40–60, if a definite etiology cannot be established
Acute unexplained liver failure

Table 6
Neurologic Disease Situations Indicative of Wilson's Disease Screening

Isolated tremor under age 50
Dysarthria under age 50
Dystonia under age 50
Incoordination developing, under age 50
Diagnosis of parkinsonism, under age 50

Table 7
Psychiatric Disease Situations Indicative of Wilson's Disease Screening

Behavioral abnormalities in previously normal people, under age 40
Suspected substance abuse, denied by patient, under age 40

Table 8
Screening and Diagnostic Tests

Test	*Interpretation*
24-h Urine copper	Normal: 20–50 µg Symptomatic Wilson's disease: over 100 µg to very high Presymptomatic Wilson's disease: 65 µg to very high Wilson's disease carriers: normal to 75 µg May be falsely elevated over 100 µg in obstructive liver disease
Kayser–Fleischer rings (examined by slit lamp)	Normal and Wilson's disease carriers: Absent Symptomatic neurological/psychiatric Wilson's disease: present Symptomatic hepatic Wilson's disease: present in 50% Presymptomatic Wilson's disease: present in 40% May be falsely present in obstructive liver disease
Serum ceruloplasmin	Normal: 20–35 mg/dL Wilson's disease (symptomatic and presymptomatic): very low to low in 85% of patients, but normal in 15%; tends to be normal in liver presentation Wilson's disease carriers: normal to low; below normal in 15%
Liver copper	Normal: 20–50 µg/g dry weight of tissue Wilson's disease (symptomatic and presymptomatic): over 200 µg Wilson's disease carriers: normal to 125 µg May be falsely elevated to over 200 µg in obstructive liver disease

Normal urine copper is 20–50 μg/24 h, and in symptomatic Wilson's disease, it is over 100. Between 50 and 100 is a gray zone. In our experience, the urine copper in presymptomatic siblings who ultimately prove to have Wilson's disease can range from about 65 μg/24 h to several hundred micrograms *(22,23)*. Siblings who ultimately prove to be gene carriers can have urine copper values ranging from normal to as high as 85 μg/24 h *(23)*. Patients who fall into the gray zone between about 60 and 100 μg/24 h during a family workup will usually require liver biopsy to make a certain diagnosis (*see* the next subsection).

2.1.3.3. Definitive Diagnosis

Liver biopsy with a quantitative measure of copper is the gold standard for diagnosis (Table 8). Copper levels are elevated in all affected (untreated) patients to above 200 μg/g dry weight, even in presymptomatic patients *(1,23)*. Copper stains of the liver should not be relied upon. They will be positive only if the copper is sequestered in sufficient concentrations in certain cells or areas to give a positive stain. If the copper is diffusely cytosolic, it will not show up positive on a stain, even though the copper levels are very elevated. We also refer again to the diagnostic problem that chronic obstructive liver disease poses to a diagnosis of Wilson's disease. Obstructive liver disease can elevate the hepatic copper level well up into the Wilson's disease range. In this situation, elevated hepatic copper levels are obviously not reliable for diagnosis of Wilson's disease.

Not all patients need to have a liver biopsy for diagnosis of Wilson's disease *(5)*. Table 9 provides the constellation of findings that are adequate for definitive diagnosis. It can be noted, for example, that if the patient presents neurologically or psychiatrically, the presence of K-F rings or elevated urine copper are adequate for the diagnosis. The same would be true for a patient with hepatic presentation, but in hepatic presentations where the K-F rings are not present, an elevated urine copper should probably be substantiated by a liver biopsy. In this case, the histological appearance can help exclude the presence of obstructive disease, and the presence of elevated hepatic copper in the absence of obstructive disease makes the diagnosis definitive.

2.2. Control of Copper in Wilson's Disease

2.2.1. Available Drugs for Anticopper Drug Therapy

2.2.1.1. Zinc

Considerable information on zinc is given in Table 10. Zinc acts by blocking the absorption of copper by inducing intestinal cell metallothionein *(24)*. Then, as copper enters the intestinal cell, the metallothionein, which has a very high affinity for copper, complexes the copper and prevents its serosal transfer. The intestinal cells have a life-span of about 6 d and then slough into the lumen of the bowel, carrying the complexed copper with it for loss in the stool. This mechanism serves not only to block the absorption of food copper, but reabsorption of endogenously secreted copper from saliva, gastric juice, and other endogenous sources. In this manner, zinc puts the patient into a modest negative copper balance *(25–30)*. The adult dose of zinc is 50 mg three times a day, with each dose separated from food and beverages other than water by at least 1 h. Giving zinc with food allows it to be complexed to organic phosphate compounds called phytates, as well as to fiber and other vegetable constituents, that prevent its entry into intestinal cells to induce metallothionein. The dose of zinc in children is somewhat reduced depending on body weight and age (25 mg twice daily until age 6, then 25 mg three times daily until age 16 or body weight of 125 lbs.). Zinc was approved as a therapy for Wilson's disease by the Food and Drug Administration in January 1997.

2.2.1.2. Trientine

Trientine (Table 10) was introduced in 1982 by Walshe *(31)* as a substitute for penicillamine in patients who became penicillamine intolerant. Trientine acts by copper chelation and increasing the urinary excretion of copper. It may also have some effect on blocking copper absorption. The adult

Table 9
Adequate Diagnostic Findings Short of Liver Biopsy

Findings	*Exceptions*
Urine copper [a] over 100 µg/24 h K.F.[b] rings on slit-lamp examination	Patients with obstructive liver disease
Typical neurological syndrome K.F. rings	
Typical neurological syndrome Urine Copper[a] over 100 µg/24 h	
Hepatic presentation K.F. rings	Patients with obstructive liver disease
Hepatic disease presentation Urine copper[a] over 100 µg/24 h	Patients with obstructive liver disease

[a]Caution: 24-h urine copper values can be falsely elevated by copper contamination of collecting materials, and not all laboratories can measure urine copper accurately.

[b]K.F. stands for Kayser–Fleischer rings. *Caution*: not all ophthalmologists have enough experience to recognize K.F. rings, although they rarely say that they are present when they are not.

dose is either 250 mg four times a day or 500 mg twice a day, each dose separated from food and beverages other than water by 0.5 h before and 2 h after food ingestion.

Although trientine has some toxicity, it is much safer than penicillamine and, therefore, should be used instead of penicillamine when chelation therapy is indicated. The potential toxicities of trientine are indicated in Table 10. Trientine is officially approved for use in the United States as a substitute for penicillamine after the patient proves intolerant to penicillamine, but it should always be used first, instead of penicillamine, whenever a chelator is indicated.

2.2.1.3. Tetrathiomolybdate

This is a drug (Table 10) under development by our group for treating the acutely ill Wilson's disease patient presenting with neurologic or psychiatric symptoms *(32–34)*. Tetrathiomolybdate (TM) has a unique mechanism of action in that it forms a three-way complex with copper and protein. When given with meals, TM complexes with food copper and food protein and prevents the absorption of that copper. When given between meals, some of the TM is absorbed into the blood, and there it complexes with the freely available copper and albumin, rendering that copper, which is potentially toxic in Wilson's disease, unavailable for cellular uptake and, therefore, nontoxic.

The dose of TM is usually 20 mg three times daily with meals and 20 mg three times daily between meals. Its toxicity is limited to overtreatment. The drug is so potent that it can deplete the bone marrow of copper, causing anemia or leukopenia. This state is easily reversible by stopping the drug temporarily and then resuming at a lower dose. This drug is not yet officially approved for use. It is being studied as an experimental drug at the University of Michigan and Mount Sinai Medical Center in New York.

2.2.1.4. Penicillamine

Penicillamine (Table 10) was the first oral drug developed for Wilson's disease (in 1956) and was, like trientine, developed by Walshe *(35)*. As with trientine, it acts by chelation and urinary excretion of copper. It is an effective drug and was the only available treatment for Wilson's disease for many years. The survival of a generation of Wilson's disease patients can be attributed to the development and use of penicillamine. However, the drug has a very long list of toxicities (*see* Table 10) and should no longer be used for Wilson's disease, because there are safer alternatives. One of the frightening things about this drug is that when it is used in the acutely ill Wilson's disease patient presenting with neurological disease, it causes worsening in 50% of these patients *(36)*. Twenty-five percent

Table 10
Available Drugs for Anticopper Therapy

Drug	*Trade name*	*Mechanism*	*Recommended use*	*Advantages*	*Disadvantages*	*Toxicity*
Zinc acetate	Galzin[a]	Blocks copper absorption	Maintenance Presymptomatic Pregnancy Pediatric Initial, with TM or a chelator	Effective Nontoxic	Slow acting	Mild abdominal discomfort in some patients
Trientine	Syprine[b]	Chelator, increased urinary excretion of copper	Initial, with zinc	Effective Moderately fast-acting	Moderately toxic Not well studied	Bone marrow suppression Proteinuria Autoimmune disorders Not adequately studied
D-Penicillamine	Cuprimine[b]	Chelator, increased urinary excretion of copper	None	Effective Fast-acting	Long list of acute, subacute, and chronic toxicities. High frequency of making patients presenting with neurological disease worse	Acute hypersensitivity Proteinuria Bone marrow suppression Effects on immune system Effects on collagen and skin Can make neurological disease worse
Ammonium tetrathiomolybdate	None	Forms complex with copper and protein. In gastrointestinal tract, it makes copper unabsorbable. In blood, it renders copper nontoxic	Initial neurologic	Effective Very fast-acting Little toxicity	Not commercially available Not studied for maintenance use	Overtreatment produces reversible anemia

[a]Manufactured by Gate Pharmaceutical Co., Montgomeryville, PA.
[b]Manufactured by Merck, Sharp, and Dohme, Denmark.

Table 11
Recommended Anticopper Therapies According to Disease Status

Disease status	*Recommended therapy*
Maintenance therapy	First choice: zinc Second choice: trientine
Initial therapy	
Hepatic presentation	First choice: zinc and trientine Second choice: trientine
Neurologic or psychiatric presentation	First choice: tetrathiomolybdate and zinc Second choice: trientine and zinc Third choice: zinc
Presymptomatic therapy	First choice: zinc Second choice: trientine
Pediatric maintenance therapy	First choice: zinc Second choice: trientine
Pregnancy	First choice: zinc Second choice: trientine

Table 12
Recommended Treatment Monitoring

Therapy	*Monitoring tests*	*Frequency*
Zinc maintenance	Urine copper and zinc	Every 6 mo at start, then every 12 mo
	Freely available blood copper	Whenever blood is drawn
	Blood counts and liver function tests	Every 12 mo
Trientine maintenance	Urine copper	Every 6 mo at start, then every 12 mo
	Freely available blood copper	Whenever blood is drawn
	Blood counts, urinalysis and liver function tests	Every week when first starting drug for 4 wk, then every month for 4 mo, then every 4 mo for 12 mo, then once or twice a year

of that original sample never recover to their prepenicillamine baseline. The mechanism of this may be the mobilization of hepatic copper, resulting in further elevation of copper in the brain. The dose and use of penicillamine in relation to food is similar to trientine.

2.2.2. Anticopper Drug Therapy Recommendations

2.2.2.1. Maintenance Therapy

We divide the therapy of Wilson's disease into initial and maintenance therapy, and then some special cases (Table 11). Initial therapy is that period of time when anticopper therapy is being given to lower the copper level sufficiently to eliminate further copper toxicity. Depending on the drug used, this may be a period of 2–6 mo. After that, patients must take an anticopper medication for the rest of their lives to prevent the reaccumulation of copper and resumption of copper toxicity. We call this latter period maintenance therapy. Table 11 gives our preferred treatments for maintenance therapy in Wilson's disease. Zinc therapy is strongly recommended because it is completely effective and it has a very low level of toxicity *(25–30,37–44)*. Our second choice would be trientine because it is an effective copper chelator and has a lower level of toxicity than the other chelator available, penicillamine (Table 11). At this time, we do not recommend either penicillamine or tetrathiomolybdate for maintenance therapy.

It is important for every Wilson's disease patient to receive some monitoring during their lifetime to ensure that therapy is going well. When zinc therapy is being used, we recommend evaluations every 6 mo during the early follow-up period (Table 12). After confidence is built up in the adequacy of the compliance of a patient, perhaps after 1 or 2 yr of experience, the interval can be decreased to once a year. The monitoring should include a 24-h urine zinc and copper measurement, which can be done with a mail-in system. The zinc measurement is to evaluate compliance. In a patient on an adequate therapeutic dose, taking the dose properly, the urinary excretion of zinc should be at least 2 mg/24 h. Anything less than this indicates that the patient is not complying completely with the program. The urine copper is a useful monitoring tool as well. In the absence of chelation therapy, the urinary excretion of copper reflects the body loading of copper. In zinc-treated patients during the maintenance phase, we like to see this value below 125 μg/24 h (normal being 20–50 μg/24 h). (Note, however, that an occasional patient will exhibit urine copper values well over this amount while complying well and while under good copper control. This may be the result of a low renal threshold for copper.) It is not necessary for the urine copper value to come down to normal, although it will slowly decrease over years of therapy. If the urine copper value starts going up, particularly if urine zinc values have gone down, this is an indication of lack of compliance and an indication that the patient may soon get into clinical trouble. This calls for a warning to the patient by the medical team to improve their compliance. It is a good idea in any Wilson's disease patient being followed to monitor blood counts and liver function tests once yearly.

In fully compliant patients, it is possible, after several years of therapy, to eventually overtreat Wilson's disease patients with any of the anticopper therapies listed in Table 10. In the case of zinc therapy, this will usually be indicated by the urine copper level moving down into the low normal range. Any urine copper value in the lower half of normal ought to be a warning of possible overtreatment and incipient copper deficiency. The first sign of copper deficiency would be a hypochromic microcytic type anemia followed, sometimes, by leukopenia. We recommend that when the urine copper levels drop to the lower half of the normal range, the dose of zinc be decreased, generally to 25 mg twice a day. It is also useful to follow "freely available blood copper," which is the serum copper minus the ceruloplasmin (Cp) copper. The Cp in milligrams per deciliter is multiplied by 3 and this number subtracted from the serum copper in micrograms per deciliter. Normal values for freely available blood copper are 10–15 μg/dL.

Trientine therapy can be monitored by following urine copper levels (Table 12). Because the drug acts by increasing urinary excretion of copper, it can be anticipated that in the first few months of therapy, urine copper values will be over 0.5 mg/24 h. Gradually, as the patient is depleted of excess copper, this may come down to the area of 0.2–0.5 mg/d. During the first year of trientine therapy, blood studies and urinalysis should be done on a regular basis, as indicated in Table 12, to make sure that the patient is not undergoing some type of toxicity related to trientine.

2.2.2.2. Initial Therapy

For a patient presenting with hepatic disease, it is necessary to triage the patient to determine whether that they are likely to recover with medical therapy or may require hepatic transplantation. We use the prognostic index of Nazer et al. *(45)* as a guide for this purpose. If it is found that the liver disease is sufficiently severe that the patient is not likely to recover short of hepatic transplantation, the patient and the family should be so advised, and, with their concordance, hepatic transplantation planned. If the patient falls in the area of a good prognostic index, then we recommend proceeding with medical therapy, which we will discuss later in this subsection. If the patient is somewhat borderline and the decision is made to opt for medical therapy, it is important to watch the patient carefully, and if there is any indication of deterioration of hepatic function, reopen the question of hepatic transplantation. If a patient is to be transplanted, it is always best to do so in a nonemergency situation.

The therapy we recommend for a patient with hepatic presentation that is to be treated medically is a combination of zinc and trientine (Table 11). The trientine is used to get an initial brisk negative copper balance, and zinc is used not only to block absorption of copper but to induce hepatic metallothionein, which, in the process of sequestering copper, may help protect the liver. We have used this approach in seven patients who had mild hepatic decompensation with low albumin, mildly elevated bilirubin, and often ascites (unpublished). These patients made a recovery to normal liver function, although of course, they will have lifelong cirrhosis.

For the initial therapy of the neurologically or psychiatrically presenting patient (Table 11), our first choice is tetrathiomolybdate (TM). As previously discussed, TM is a rapid-acting drug that gains quick control over copper toxicity without a significant risk of making the neurological symptoms worse *(32–34)*. We indicated earlier that this risk is about 50% with penicillamine *(36)*, and by comparison, in an open study with TM, only 2 of 55 patients worsened, using rigorous neurological criteria (*34*; unpublished data). We use TM for 8 wk, usually concomitant with zinc, and then transition the patient to maintenance therapy with zinc.

The second choice for initial therapy of those patients presenting with neurologic or psychiatric disease is trientine, preferably with zinc (Table 11). Trientine has not been tried in this setting. Because it is a somewhat gentler drug that penicillamine, it may not be associated with the same risk of initial worsening. We are currently comparing trientine to TM in a double-blind study of neurologically presenting patients.

The third choice for this type of patient would be zinc therapy (Table 11). The reason this is not higher on our list is that zinc is rather leisurely acting, and it takes upward of 6 mo to gain control of copper toxicity with zinc alone. During this time, the disease may progress. However, this is the method used by the Hoogenraad group in the Netherlands and they claim good results *(46)*.

We recommend against use of penicillamine in neurologically presenting patients because of the great risk of making the patient worse neurologically when this therapy is used *(36)*.

2.2.2.3. Presymptomatic Therapy

Our recommendations for presymptomatic therapy (Table 11) closely follow those for maintenance therapy, because patients who are not yet acutely ill from copper toxicity can be viewed as comparable to patients in maintenance therapy. Thus we use zinc for our first recommended therapy *(22)*, with trientine being second on our list.

2.2.2.4. Pediatric Maintenance Therapy

Our recommendations are again for the use of zinc as a first choice (Table 11), with doses reduced for age and weight *(30)*, as previously discussed. Again, trientine would be our second choice.

2.2.2.5. Therapy During Pregnancy

It is very important that the pregnant Wilson's disease patient continue on anticopper therapy, because discontinuing therapy in order to protect the fetus has led to disastrous results, with Wilson's disease regression in a number of patients *(1,2)*. The problem has been that penicillamine is a known teratogen in animal studies *(47)* and has produced a penicillamine teratogenic syndrome in about 5% of human patients in whom it has been used *(48–50)*. Thus, we and others strongly recommend against its use during pregnancy *(50,51)*.

Our drug of choice for the therapy of pregnant patients is zinc (Table 11), because we have had good experience with it *(51)* and because it has been shown to be nonteratogenic in animal studies *(52)*. We have treated 26 pregnancies in 19 women with zinc during pregnancy. We have observed one major and one minor birth defect. Trientine can also be considered (Table 11). There is much less experience with it, but the experience that has been reported has not indicated a high rate of teratogenicity *(53)*. Obviously, more data need to be collected on both zinc and trientine to decide which is the optimal therapy during pregnancy.

2.2.3. Other Copper Management Issues

2.2.3.1. Diet

For many years, it was traditional to put patients with Wilson's disease on low-copper diets. However, the tables listing the amount of copper in foods are grossly inaccurate, and in many cases, they greatly overestimate the amount of copper actually present in those foods *(1)*. We have measured copper in various foods and find only two that we recommend be somewhat limited in the diet of Wilson's disease patients *(1)*. One of these is liver. Food lot animals are fed high concentrations of minerals in order to enhance growth, and the copper ends up being concentrated in the liver. Thus, a single helping of liver from a food lot animal can provide the amount of copper normally ingested in a week. This is dangerously high. We recommend that patients during the first year of therapy not eat any liver whatsoever. After that, a small bit of liver paté is acceptable. The other food that is somewhat high in copper is shellfish. It is not as high as liver, but it is higher than other foods. We recommend that during the first year of therapy, patients not ingest shellfish, but after that, they can have up to one meal per week. Other than this, we do not limit the diet. We find that most sources of chocolate, beans, peanuts, mushrooms, and vegetables previously reported to have high levels of copper really do not *(1)*. So, the dietary management is quite simple: First year, no liver or shell fish; after that, only small amounts of liver and only one meal of shellfish per week.

2.3.3.2. Drinking and Cooking Water

Occasionally, drinking water sources have a high level of copper. These will usually be found in homes with copper pipes in which the water is acidic, causing copper from the piping to be leached into the water. Because this soluble inorganic copper is readily absorbed, it is worthwhile to check the copper levels of the patient's drinking water sources and restrict them if they are too high. The Environmental Protection Agency allows 1.2 parts per million (ppm, which equals mg/L) in drinking water. We believe this level of copper is too high for Wilson's disease patients. If the copper level is over 0.1 ppm, we recommend that the patient not use that water source. Although this level of copper would be unlikely to cause problems, it is an indication of copper leaching, in which case, water at certain times of the day, such as first-draw water, could be considerably higher.

2.3. Prognosis

2.3.1. Recovery

Recovery of both neurological and hepatic function after initiation of adequate anticopper therapy takes place over the 2-yr period after that. It must be emphasized that the drugs only control copper. The body must repair the injury. Clinically detectable improvement occurs beginning about 6 mo after therapy initiation and is mostly compete by 24 mo. Neurological recovery is generally quite good, depending, in part, on the severity of disability at the beginning of treatment. Hepatic function usually returns to normal over this same time period, although patients are generally left with some underlying cirrhosis.

2.3.2. Compliance

We have emphasized in several places in this report that compliance needs to be monitored and patients need to be reminded to take their drug properly if compliance falls off. One might think that compliance would be a relatively minor problem in a disease in which the symptoms have, in most cases, occurred in the patients themselves, or at least in relatives, and in which it is clear that treatment makes a major difference. However, our experience, even in our carefully followed cohort of patients, is that there is an underlying major compliance problem of at least 10% *(1)*. Beyond this, there are more minor episodes of poor compliance that affect approx 30–35% of the patients. It must be remembered that this is a lifelong therapy and that patients are going through various phases of their lives. These are usually young patients, often in the process of leaving home to go to college or

to seek employment. Their lifestyles are changing, and taking their drug, if they have been asymptomatic for a period of time, may become a relatively low priority. Thus, it becomes extremely important to monitor these patients on a regular basis, at least for the first 2 or 3 yr, to establish a pattern of good compliance. We urge that patients be monitored every 6 mo during this period. Then, if the results have been uniformly good, monitoring can taper off to once a year.

Obviously, then, the prognosis depends heavily on the patients' rigorous compliance with their anticopper therapy. If the patient's compliance falls off, they do not have the luxury of many years until they become ill again. The length of time it originally took them to become ill may mislead them to think that after "decoppering therapy," they again have many years of noncompliance before becoming sick again. They do not, because the liver is now damaged and does not have the copper storage capacity that it once did. Thus, patients get into trouble if they completely stop their anticopper drug for periods varying from 3 mo to 2 yr *(1)*.

2.3.3. Risk Factors

Beyond poor compliance, other risk factors in this disease include those associated with significant cirrhosis or severe neurological deficit. All patients with Wilson's disease, even the presymptomatic ones, will have some degree of liver damage, and the often have mild to moderate cirrhosis. Manifestations of this will often be a mild thrombocytopenia and/or leukopenia as a result of hypersplenism. Generally speaking, these blood count abnormalities are not medically relevant. With control of copper toxicity, the cirrhosis, the hypersplenism, and the reduced white blood cell and platelet counts are not progressive. A more significant problem associated with cirrhosis is bleeding from esophageal or gastric varices. This risk is highest in patients who present with liver disease, but can also occur in patients who present neurologically or who are presymptomatic. Any evidence of gastrointestinal bleeding in a patients with Wilson's disease, whether it be black stools or vomiting of blood, should be an immediate indication for a trip to the emergency room of the nearest hospital. Although this bleeding is often mild and easily controlled, it can be severe and life-threatening.

On the neurological side, a risk factor is aspiration in patients who are having serious problems with dysphagia. Such patients should have a gastrostomy during the period of initial treatment in order to avoid this risk. The swallowing function usually improves over the course of a year of therapy and then the gastrostomy can be removed. Chronic aspiration can lead to chronic pulmonary disease, aspiration pneumonia, and a potentially serious outcome.

In summary, in well-complying patients without severe liver disease or severe neurological deficit, life expectancy is normal or near normal. This outlook becomes less positive if there are compliance problems, severe neurological disability, or severe liver disease.

3. CONTROL OF COPPER IN DISEASE OF NEOVASCULARIZATION

3.1. Cancer

3.1.1. Background in Cancer and Angiogenesis

Folkman *(54–56)* has pointed out the dependence of the growth of solid tumors on new blood vessel growth, most often referred to as angiogenesis (in this chapter, angiogenesis and neovascularization are synonymous terms). He pointed out that cancer cells can divide and grow into a small cluster up to 2 mm in diameter without a blood supply, the cells receiving their nutrition by simple diffusion. After that, however, a vasculature is required to supply nutrients to the inner part of the cell mass, hence the need for angiogenesis for tumor growth. Because angiogenesis is generally not required in adults, except for wound healing and during the menstrual cycle, Folkman has pointed out that inhibition of angiogenesis is a possible mechanism for inhibiting further tumor growth.

In recent years, this field of research has virtually exploded, with much research on angiogenic promoters and inhibitors and with ideas for potential antiangiogenic therapies. It is beyond the scope

of this chapter to review that literature and there are already excellent reviews of the field *(57,58)*. We will restrict ourselves here to the role of copper in angiogenesis and antiangiogenesis.

3.1.2. Role of Copper in Angiogenesis

In the 1980s, a series of investigations established the role of copper in angiogenesis *(59–61)*. Much of this early work was done in the rabbit cornea model. In one study, it was shown that copper placed in the cornea was itself angiogenic *(59)*. Copper could be in the form of copper sulfate or in a protein molecule such as ceruloplasmin *(60)*. Apoceruloplasmin, without copper, was not angiogenic. Later, rabbits were made mildly copper deficient, and angiogenesis in their corneas was compared to that in control animals. Prostaglandin E_1 was markedly angiogenic in controls, but lost much of its angiogenic properties in copper-deficient rabbits *(61)*. Thus, the concept began to emerge that not only is copper proangiogenic, but mild copper deficiency is antiangiogenic.

Brem and colleagues then extended this concept to tumors *(62,63)*. They produced mild copper deficiency in rats and rabbits by using penicillamine and a low-copper diet, and they transplanted tumor tissue into the brains of these and normal control animals. In copper-deficient rabbits or rats, the growth of these implanted tumors was greatly reduced compared to control animals. However, there was no benefit in terms of survival, probably because of equivalent cerebral edema and brainstem herniation in the treated and control animals. The lack of a survival benefit may have discouraged these investigators, because this work was not pursued.

3.1.3. Preclinical Studies of Tetrathiomolybdate

In the process of developing tetrathiomolybdate (TM) for Wilson's disease and becoming aware of its great potency and safety as an anticopper agent, I became interested in testing this drug as an antiangiogenic agent in cancer.

My first approach, in 1991, was to do a rat tumor model study (unpublished). We injected a rat tumor cell line under the skin of rats and then waited for tumors to develop under the skin, which we could feel and measure. The idea was that when tumors were obvious, we could treat half of the animals with TM and see if we could slow or stop tumor growth compared to control animals. However, the tumors began to get smaller spontaneously, presumably because the immune system of these rats was able to control this particular tumor. Thus, this model system did not work for our purposes.

I then switched to a mouse model. We injected MCA-205 murine sarcoma cells under the skin. This time the tumors grew as they were supposed to. As soon as we could feel the tumors under the skin, we put half of the mice on TM treatment of 1.25 mg by once-a-day stomach gavage. Over the next 3 wk, we measured the tumors of the TM-treated animals versus controls. By d 17, we were able to show a statistically significant reduction in growth of the tumors in the TM-treated mice. This difference was maintained until the animals were sacrificed on d 23. We dissected out the tumors and weighed them. The tumors in the TM-treated mice weighed significantly less than the tumors in the control animals. This positive experiment has not been published.

In 1995, I began to work with an oncologist at the University of Michigan, Dr. Sofia Merajver, who was also interested in antiangiogenesis. She designed a mouse tumor model study using HER2/neu transgenic mice, and together we conducted it. In this mouse model, the mice carry a gene defect that causes all of the female mice to get breast cancer during the first year of life. Half of the mice were treated with TM by once-daily gavage, and half were controls, that received a placebo gavage. By 275 d, 17 of 22 control animals had developed large, often multiple, breast tumors, but none of the 15 TM-treated animals had developed detectable tumors *(64)*. When we sacrificed TM-treated animals and looked at the breast tissue under the microscope, small clusters of cancer cells could be seen. Five treatment animals were released from TM therapy, and within 12 d, all had palpable tumors. Thus, the cancer was there (remember Folkman said it could grow to about 2 mm without blood vessels), but it had not grown into a visible tumor because it could not grow blood vessels. Angiogen-

esis had been prevented by TM. Tumor-bearing control animals were treated with TM, and in three out of five cases, tumor volume was reduced.

To evaluate the animal's copper status during TM therapy, we developed serum ceruloplasmin (Cp) levels as a surrogate marker of copper status *(64)*. Serum copper itself is not useful during TM therapy, because the complex of albumin, copper, and TM builds up in the circulation and the total serum copper actually increases during TM therapy, although available copper decreases. Cp is a copper-containing protein synthesized by the liver, and the amount synthesized and released into the blood is directly correlated with copper availability in the liver *(65)*. It was our objective to reduce the Cp to about 20–30% of baseline and hold it there. The mouse work validated Cp as a useful surrogate marker of copper status very nicely.

3.1.4. Clinical Studies of Tetrathiomolybdate in Cancer

When we saw the effectiveness of TM in preventing cancer growth in the genetic mouse model, we not only were encouraged that we might be able to treat human cancers (i.e., stop their growth), but perhaps we could *prevent* some types of cancer in patients with a high risk of cancer as a result of a genetic predisposition. Of course, prophylactic use will have to wait until the safety of the drug and this copper-deficiency approach is firmly established. The next priority was to see if we could stop the growth of cancers already present in patients.

The concept to be tested in clinical studies was that, although copper is an essential trace element and the body's normal cells require a certain amount of it, the level of copper required for angiogenesis is higher than that required for the health of normal cells. The idea, then, is to use TM to decrease copper levels into this "window" between the levels required for angiogenesis and the levels required for vital cellular functions.

The kind of patients we decided to start with in our first clinical trial were patients with cancers that had metastasized or were otherwise inoperable and who had gone through other available therapies such as radiation and chemotherapy. In other words, these were patients who had run out of options.

One of the objectives of early studies of a drug is to study the dose required and to evaluate possible toxicity. The FDA refers to these as phase I objectives. Of course, we as investigators are also always interested in whether the drug shows effectiveness (also called efficacy) in these early patients. Initial examination of efficacy is called a phase II study. To the extent we are able to look at effectiveness, in this case whether TM stopped tumor growth, a phase I study is also partly phase II.

We enrolled and studied 18 patients in our first clinical trial, which was designed to be a phase I study but looking at efficacy wherever possible *(66)*. These patients had a wide variety of solid tumors, including breast, prostate, kidney, colon, chondrosarcoma, hemangioma, malignant melanoma, pancreas, and hemiangioendothelioma. We used 90–120 mg of TM divided into six doses for initial induction. We accomplished phase I objectives very nicely *(66)*. TM proved easy to use in these patients, and copper status easy to determine and follow using Cp levels. As Cp levels reached our target of 5–15 mg/dL (normal is 20–35), we backed off on the dose in most patients. The amount of TM required to maintain Cp in the target range varied from about 20–120 mg. The only toxicity we encountered was overtreatment in an occasional patient, which leads to a reversible anemia *(66)*.

Six of the 18 patients were in good enough condition to stay on TM long enough so that we could look at phase II objectives—Was the drug effective in stopping the growth of the tumor? Indeed it was. The tumor growth was stopped and stabilized in the six patients who had tumor types including breast, chondrosarcoma, kidney, angiosarcoma, and hemiangioendothelioma for periods ranging up to 21 mo as of this writing. A few new patients have been added to this phase I/II study while waiting to get on with a number of phase II studies looking at specific tumor types. We now have a total of eight patients with disease stabilization times ranging from 5 to 21 mo.

Table 13
Diseases of Neovascularization That May Be Targets for Tetrathiomolybdate Therapy

Cancer, including metastatic and inoperable
Macular degeneration, wet type
Diabetic retinopathy
Rheumatoid arthritis
Psoriasis

3.2. Other Diseases of Neovascularization

In addition to cancer, TM may be useful for other diseases where angiogenesis is a problem (*see* Table 13). One example is a type of eye disease called wet-type macular degeneration, in which uncontrolled blood vessel growth in the retina causes rapidly progressive blindness. We already have started a few patients with this disease on TM therapy.

Another disease of angiogenesis is diabetic retinopathy, in which blood vessels proliferate in the retinas of diabetic patients, again causing blindness. In rheumatoid arthritis, the material that grows into the joint and causes pain and inflammation is very blood vessel rich. The skin plaques in psoriasis are underlaid by a proliferation of blood vessels.

Thus, if TM continues to be effective as an antiangiogenic agent and nontoxic, it is obvious from Table 13 that there are many diseases in which it might be therapeutically useful.

ACKNOWLEDGMENTS

This research was supported in part by Food and Drug Administration grants FD-R-000179 and FD-U-000505. The work with zinc therapy was also assisted by Gate Pharmaceutical Co., Montgomeryville, PA. We also acknowledge the assistance and support of the General Clinical Research Center of the University of Michigan Hospitals, supported in part by NIH grant M01-RR00042.

REFERENCES

1. Brewer, G. J. and Yuzbasiyan-Gurkan, V. (1992) Wilson disease. *Medicine* **71**, 139–164.
2. Scheinberg, I.H. and Sternlieb, I. (1984) Wilson's disease, in *Major Problems in Internal Medicine*, Vol. 23. (Smith, L. H., Jr., ed.), W.B. Saunders, Philadelphia.
3. Schilsky, M. L. (1993) Wilson disease: genetic basis of copper toxicity and natural history. *Semin. Liver Dis.* **16**, 83–95.
4. Brewer, G. J. (2000) Recognition, diagnosis and management of Wilson's disease. *Proc. Soc. Exp. Biol. Med.* **223,** 39–49.
5. Brewer, G. J., Fink, J. K., and Hedera, P.(1999) Diagnosis and treatment of Wilson's disease. *Semin. Neurol.* **19**, 261–270.
6. Brewer, G. J. (2000) Wilson's disease. (2000) *Curr. Treat. Options Neurol.* **2**, 193–203.
7. Frommer, D. J. (1974) Defective biliary excretion of copper in Wilson's disease. *Gut* **15**, 125–129.
8. Gibbs, K. and Walshe, J. M. (1980) Biliary excretion of copper in Wilson's disease. *Lancet* **2**, 538–539.
9. O'Reilly, S., Weber, P. M., Oswald, M., and Shipley, L. (1971) Abnormalities of the physiology of copper in Wilson's disease. III. The excretion of copper. *Arch. Neurol*, **25**, 28–32.
10. Hill, G. M., Brewer, G. J., Prasad, A. S., Hydrick, C. R., and Hartmann, D. E. (1987) Treatment of Wilson's disease with zinc: I. Oral zinc therapy regimens. *Hepatology* **7**, 522–528.
11. Holden, J. M, Wolf, W. R., and Mertz, W. (1979) Zinc and copper in self selected diets. *J. Am. Diet. Assoc*. **75**, 23–28,.
12. Klevay, L. M, Reck, S. J., and Barcome, D. P. (1979) Evidence of dietary copper and zinc deficiencies. *JAMA* **241**, 1916–1918.
13. Reiser, S., Smith, J. C., Jr., Mertz, W., Holbrok, J. T., Scholfield, D. J., Powell, A. S., et al. (1985) Indices of copper status in humans consuming a typical American diet containing either fructose or starch. *Am. J. Clin. Nutr.* **42**, 242–251.
14. Iyengar, V., Brewer, G. J., Dick, R. D., and Owyang, C. (1988) Studies of cholecystokinin-stimulated biliary secretions reveal a high molecular weight copper-binding substance in normal subjects that is absent in patients with Wilson's disease. *J. Lab. Clin. Med.* **111**, 267–274.
15. Tanzi, R. E., Petrukhin, K., Chernov, I., Pellequer, J. L., Wasco, W., Ross, B., Romano, et al. (1993) The Wilson disease gene is a copper transporting ATPase with homology to the Menkes disease gene. *Nature Genet.* **5**, 44–50.
16. Yamaguchi, Y., Heiny, M. E., and Gitlin, J. D. (1993) Isolation and characterization of a human liver cDNA as a candidate gene for Wilson disease. *Biochem. Biophys. Res. Commun.* **197**, 271–277.

17. Bull, P. C., Thomas, G. R., Rommens, J. M., Forbes, J. R., and Cox, D. W. (1993) The Wilson's disease gene is a putative copper transporting P-type ATPase similar to the Menkes gene. *Nature Genet.* **5**, 327–337.
18. Terada, K., Schilsky, M. L., and Sugiyama, T. (1998) ATP7B (WND) protein. *Int. J. Biochem. Cell Biol.* **30**, 1063–1067.
19. Kennedy, S. and Cox, D. W. (1999) Wilson disease mutation database. Provided by University of Alberta (http://www.medgen.med.ualberta.ca/database.html), accessed May 22, 2000.
20. Akil, M., Schwartz, J. A., Dutchak, D., Yuzbasiyan-Gurkan, V., and Brewer, G. J. (1991) The psychiatric presentations of Wilson's disease. *J. Neurol. Psychol. Clin. Neurosci.* **3**, 377.
21. Sternlieb, I., Morell, A. G., Bauer, C. D., Combes, B., DeBobes-Sternberg, S., and Scheinberg, I. H. (1961) Detection of heterozygous carrier of the Wilson's disease gene. *J. Clin. Invest.* **40**, 707–715.
22. Brewer, G. J., Dick, R. D., Yuzbasiyan-Gurkan, V., Johnson, V., and Wang, Y. (1994) Treatment of Wilson's disease with zinc. XIII: therapy with zinc in presymptomatic patients from the time of diagnosis. *J. Lab. Clin. Med.* **123**, 849–858.
23. Yuzbasiyan-Gurkan, V., Johnson, V., and Brewer, G. J. (1991) Diagnosis and characterization of presymptomatic patients with Wilson's disease and the use of molecular genetics to aid in the diagnosis. *J. Lab. Clin. Med.* **118**, 458–465.
24. Yuzbasiyan-Gurkan, V., Grider, A., Nostrant, T., Cousins, R. J., and Brewer, G. J. (1992) The treatment of Wilson's disease with zinc: X. Intestinal metallothionein induction. *J. Lab. Clin. Med.* **120**, 380–386.
25. Brewer, G. J., Hill, G. M., Prasad, A. S., Cossack, Z. T., and Rabbani, P. (1983) Oral zinc therapy for Wilson's disease. *Ann. Intern. Med.* **99**, 314–320.
26. Hill, G. M., Brewer, G. J., Prasad, A. S., Hydrick, C. R., and Hartmann, D. E. (1987) Treatment of Wilson's disease with zinc: I. Oral zinc therapy regimens. *Hepatology* **7**, 522–528.
27. Hill, G. M., Brewer, G. J., Juni, J. E., Prasad, A. S., and Dick, R. D. (1986) Treatment of Wilson's disease with zinc: II. Validation of oral 64copper uptake with copper balance. *Am. J. Med. Sci.* **12**, 344–349.
28. Brewer, G. J., Yuzbasiyan-Gurkan, V., and Dick, R. (1990) Zinc therapy of Wilson's disease: VIII. Dose response studies. *Trace Elements Exp. Med.* **3**, 227–234.
29. Brewer, G. J., Yuzbasiyan–Gurkan, V., Johnson, V., Dick, R. D., and Wang, Y. (1993) Treatment of Wilson's disease with zinc: XII. Dose regimen requirements. *Am. J. Med. Sci.* **305,** 199–202.
30. Brewer, G. J., Dick, R. D., Johnson, V. D., Brunberg, J. A., Kluin, K. J., and Fink, J. K. (1998) The treatment of Wilson's disease with zinc XV. Long-term follow-up studies. *J. Lab. Clin. Med.* **132**, 264–278.
31. Walshe, J. M. (1982) Treatment of Wilson's disease with trientine (triethylene tetramine) dichloride. *Lancet* **1**, 643–647.
32. Brewer, G. J., Dick, R. D., Yuzbasiyan-Gurkan, V., Tankanow, R., Young, A. B., and Kluin, K. J. (1991) Initial therapy of Wilson's disease patients with tetrathiomolybdate. *Arch. Neurol.* **48,** 42–47.
33. Brewer, G. J., Dick, R. D., Johnson, V., Wang Y., Yuzbasiyan-Gurkan, V., Kluin, K., et al. (1994) Treatment of Wilson's disease with tetrathiomolybdate I. Initial therapy in 17 neurologically affected patients. *Arch. Neurol.* **51**, 545–554.
34. Brewer, G. J., Johnson, V., Dick, R. D., Kluin, K. J., Fink, J. K., and Brunberg, J. A. (1996) Treatment of Wilson's disease with ammonium tetrathiomolybdate: II. Initial therapy in 33 neurologically affected patients and follow-up on zinc therapy. *Arch. Neurol.* **53**, 1017–1025.
35. Walshe, J. M. (1956) Penicillamine. A new oral therapy for Wilson's disease. *Am. J. Med.* **156**, 487–495.
36. Brewer, G. J., Terry, C. A., Aisen, A. M., and Hill, G. M. (1987) Worsening of neurological syndrome in patients with Wilson's disease with initial penicillamine therapy. *Arch. Neurol.* **44**, 490–494.
37. Yuzbasiyan-Gurkan, V., Brewer, G. J., Abrams, G. D., Main, B., and Giacherio, D. (1989) Treatment of Wilson's disease with zinc: V: Changes in serum levels of lipase, amylase and alkaline phosphatase in Wilson's disease patients. *J. Lab. Clin. Med.* **114**, 520–526.
38. Brewer, G. J., Yuzbasiyan-Gurkan, V., Lee, D. Y., and Appelman, H. (1989) The treatment of Wilson's disease with zinc VI. Initial treatment studies. *J. Lab. Clin. Med.* **114**, 633–638.
39. Brewer, G. J., Yuzbasiyan-Gurkan, V., and Johnson, V. (1991) The treatment of Wilson's disease with zinc: IX. Response of serum lipids. *J. Lab. Clin. Med.* **118**, 466–470.
40. Brewer, G. J., Yuzbasiyan–Gurkan, V., Johnson, V., Dick, R.D., and Wang Y. (1993) Treatment of Wilson's disease with zinc: XI. Interaction with other anticopper agents. *J. Am. Coll. Nutr.* **12**, 26–30.
41. Brewer, G. J., Johnson, V., and Kaplan, J. (1997) Treatment of Wilson's disease with zinc: XIV. Studies of the effect of zinc on lymphocyte function. *J. Lab. Clin. Med.* **129**, 649–652.
42. Hoogenraad, T. U., Koevoet, R., and De Ruyter Korver, E. G. W. M. (1979) Oral zinc sulfate as long-term treatment in Wilson's disease (hepatolenticular degeneration). *Eur. Neurol.* **18**, 205–211.
43. Hoogenraad, T. U., Van den Hamer, C. J. A., Koevoet, R., and De Ruyter Korver, E. G. W. M. (1978) Oral zinc in Wilson's disease. *Lancet* **2**, 1262–1263.
44. Hoogenraad, T. U., Van Hattum, J., and Van den Hamer, C. J. A. (1987) Management of Wilson's disease with zinc sulfate. Experience in a series of 27 patients. *J. Neurol. Sci.* **77**, 137–146.
45. Nazer, H., Ede, R. J., Mowat, A. P., and Williams, R. (1986) Wilson's disease: clinical presentation and use of prognostic index. *Gut* **27**, 1377–1381.
46. Hoogenraad, T. U. (1996) Wilson's disease, in *Major Problems in Neurology*, Vol. 30 (Warlow, C. P. and van Gijn, J., eds.). W.B. Saunders, London.
47. Keen, C. L., Mark-Savage, B., Lönnerdal, B., and Hurley, L. S. (1983) Teratogenic effects of D-penicillamine in rats: relation to copper deficiency. *Drug Nutr. Interact.* **2**, 17–34.
48. Mjolnerod, O. K., Dommerud, S. A., Rasmussen, K., and Gjeruldsen, S. T. (1971) Congenital connective tissue defect probably due to D-penicillamine treatment in pregnancy. *Lancet* **1**, 673–675.
49. Solomon, L., Abrams, G., Dinner, M., and Berman, L. (1977) Neonatal abnormalities associated with D-penicillamine treatment during pregnancy. *N. Engl. J. Med.* **296**, 54–55.

50. Rosa, F. W. (1986) Teratogen update: penicillamine. *Teratology* **33**, 127–131.
51. Brewer, G. J., Johnson, V. D., Dick, R. D., Fink, J. K., Kluin, K. J., and Hedera, P. (2000). Treatment of Wilson's disease with zinc. XVII. treatment during pregnancy. *Hepatology* **31**, 364–370.
52. Food and Drug Administration. *Teratologic Evaluation of FDA 71-49 (Zinc Sulfate)*. Food and Drug Research Laboratories, Inc. Prepared for Food and Drug Administration, United States Department of Commerce, Washington, DC, Publications PD-221 805, February 1973, and PB 267, June 1974.
53. Walshe, J. M. (1986) The management of pregnancy in Wilson's disease treated with trientine. *Q. J. Med.* **58**, 81–87.
54. Folkman, J. (1972) Anti-angiogenesis: new concept for therapy of solid tumors. *Ann. Surg.* **175**, 409–416.
55. Folkman, J. (1995) Angiogenesis in cancer, vascular, rheumatoid, and other disease. *Nature Med.* **1**, 27-31.
56. Folkman, J. (1997) Antiangiogenic therapy, in *Cancer: Principles and Practice of Oncology* (De Vito, V., Rosenberg, and Hellman, eds.), Lippencott-Raven, Philadelphia, pp. 3075–3085.
57. Beckner, M. E. (1999) Factors promoting tumor angiogenesis. *Cancer Invest.* **17**, 594–623.
58. Brem, S. (1999) Angiogenesis and cancer control: from concept to therapeutic trial. *Cancer Control* **6**, 436–458.
59. Parke, A., Battacherjee, P., Palmer, R. M., and Lazarus, N. R. (1988) Characterization and quantification of copper sulfate-induced vascularization of the rabbit cornea. *Am. J. Clin. Pathol.* **137**, 1121–1142.
60. Raju, K. S., Alesandrii, G., Zinche, M., and Gullino, P. M. (1982) Ceruloplasmin, copper ions, and angiogenesis. *J. Natl. Cancer Inst.* **69**, 1183–1188.
61. Zinche, M., Jones, J., and Gullino, P. M. (1982) Role of prostoglandin E and copper in angiogenesis. *J. Natl. Cancer Inst.* **69**, 475–482.
62. Brem, S. S., Zagzag, D., Tsanaclis, A. M. C., Gatley, S., Elkouby, M. P., and Brein, S. E. (1990) Inhibition of angiogenesis and tumor growth in the brain. Suppression of endothelial cell turnover by penicillamine and the depletion of copper, an angiogenic cofactor. *Am. J. Pathol.* **137**, 1121–1147.
63. Brem, S., Tsanaclis, A. M., and Zagzag, D. (1990) Anticopper treatment inhibits pseudopdial protrusion and invasive spread of 9L gliosarcoma cells in the rat brain. *Neurosurgery* **26**, 391–396.
64. Merajver, S. D., Irani, J., van Golen, K., and Brewer, G. (1998) Copper depletion as an anti-angiogenic strategy in HER2-neu transgenic mice. Proceedings of the AACR Special Conference on Angiogenesis and Cancer, p. B11.
65. Linder, M. C., Houle, P. A., Isaacs, E., Moor, J. R., and Scott, L. E. (1979) Copper regulation of ceruloplasmin in copper-deficient rats. *Enzyme* **24**, 23–35.
66. Brewer, G. J., Dick, R. D., Grover, D. K., LeClaire, V., Tseng, M., Wicha, M., et al. (2000) Treatment of metastatic cancer with tetrathiomolybdate, and anticopper, antiangiogenic agent: I. Phase I study. *Clin. Cancer Res.* **6**, 1–10.

28

Copper-Rich Metallothionein Polymers During the Development of Fulminant Hepatitis in LEC Rats

Effect of D-Penicillamine

Dominik Klein, Josef Lichtmannegger, and Karl H. Summer

1. INTRODUCTION

The progressive accumulation of copper in hepatocytes of humans and animals may lead to hepatocellular necrosis *(1-3)*. In Wilson's disease, an inherited disorder of copper metabolism in humans, the excretion of copper into bile is impaired. The phenotype of the disease is caused by a mutation of the *ATP7B* gene leading to a nonfunctioning gene product, a copper-transporting P-type ATPase *(4)*.

Recently, an animal model for this disease, the Long–Evans Cinnamon (LEC) rat has been described *(5,6)*. The LEC rat has a mutation in the gene homologous to the human Wilson's disease gene *(7)* and shows most of the features of the disease such as extensive copper accumulation in the liver and decreased serum levels of ceruloplasmin. LEC rats spontaneously develop hepatic injury, acute hepatitis with jaundice approx 4 mo after birth, and half of them die of fulminant hepatitis. Those who survive exhibit chronic hepatitis and, eventually, hepatocellular carcinoma *(5,8,9)*. Both the development of hepatitis and hepatocarcinogenesis in these animals have been prevented by D-penicillamine (DPA) *(10,11)*, a drug routinely used in treating Wilson's disease *(12–14)*.

The mechanism of how excess copper damages the hepatocyte or what chemical form of copper is toxic and the molecular mechanism of the DPA action are yet unclear. The hepatocellular accumulation of copper is generally associated with elevated levels and increased binding of copper to metallothionein (MT), a low-molecular-weight cysteine-rich protein. MT synthesis can be induced by copper and other metals. Whereas the binding of copper to MT is well known for the cytosol, the contribution of MT in the binding of copper in the particulate fraction has not been adequately investigated. There is, however, indication for a role of MT in the binding of copper in the lysosomes. For example, a correlation between copper and sulfur was observed in hepatic lysosomes of patients with Wilson's disease and chronic cholestasis *(15)*, and MT was identified as a lysosomal copper-containing protein in the livers of dogs with inherited copper toxicosis *(16,17)*.

The present study focuses on the subcellular association of copper in the liver of LEC rats at various stages of hepatitis and the effects of DPA on copper and copper-binding proteins of both parenchymal and mesenchymal liver cells.

From: Handbook of Copper Pharmacology and Toxicology
Edited by: E. J. Massaro © Humana Press Inc., Totowa, NJ

2. ANIMALS AND TREATMENT

The LEC rats were purchased from Charles River Japan, Inc. (Yokohama, Japan). Wistar rats inbred strain Neuherberg, Germany, were used as controls. The animals were fed a commercial diet (Altromin, Lage, Germany) with a copper content of 11 mg/kg and received tap water *ad libitum*. The LEC rats were divided into six groups according to age and treatment: untreated animals aged 62 ± 2 d, 77 ± 1 d, and 86 ± 1 d, animals aged 107 ± 1 d after treatment with DPA from d 64, and animals aged 84 ± 1 d and 93 ± 1 d, respectively, after treatment with DPA from d 77 (*see* below). LEC rats treated with DPA from d 64 were allowed free access to DPA hydrochloride (DPA–HCl) in deionized water (538.8 mg/L, pH adjusted to 3.5 with 1 *M* NaOH) at a target dose of 100 mg/kg body weight/d. These animals were killed at d 107 ± 1. In addition, LEC rats aged 77 d were treated with DPA (311 mg DPA–HCl/mL, pH approx 2.5) by gastric intubation with a total of nine doses each of 500 mg/kg. One dose was administered at d 77, 81, and 82, and two doses daily at d 78–80. From d 80 until they were killed at d 84 ± 1 and d 93 ± 1, respectively, these animals also received water *ad libitum* containing DPA at the above-mentioned concentration. For comparison, the oral dose of DPA in the therapy of Wilson's disease for adults and adolescents is 1–2 g/d.

3. RESULTS

In LEC rats aged up to 64 d, serum AST activity, bilirubin levels, morphology, and histopathology of the liver were normal (Table 1). At the age of 77 d, when treatment with DPA by gastric intubation was started, serum AST activity and, with the exception of one animal, serum bilirubin were elevated and bilirubinuria was observed. Light microscopic examination of the liver revealed numerous single-cell necroses, hyalin-spherical cytoplasmic inclusions, enlarged nuclei, a slight increase in mesenchymal cells, and an increased number of bile canaliculi and oval cells (data not shown). LEC rats aged 86 d suffered from systemic jaundice. Light microscopically, the liver appeared similar to that of the 77-d-old animals but, by far, more mesenchymal cells, partly yellowish pigmented, were observed (data not shown). LEC rats aged 107 d that received DPA from d 64 through drinking water showed barely elevated serum AST activity and normal bilirubin values. Some enlarged nuclei but few single-cell necroses and mesenchymal cells were noted (data not shown). In LEC rats aged 84 and 93 d, treated with DPA from d 77, serum AST and bilirubin values were normal, and the bilirubinuria had disappeared. The liver showed a slightly increased number of bile canaliculi, very few single-cell necroses and enlarged nuclei, and few mesenchymal cells (data not shown).

Ultrastructural findings of hepatocytes of LEC rats aged 77 d with beginning hepatitis (Fig. 1A–C) included dilatation of cisternae of the rough endoplasmic reticulum and dilated mitochondrial cristae. Numerous lysosomal electron-dense particles were noted, which were located mainly in hepatocytes, less in Kupffer cells. In contrast, in the liver of jaundiced LEC rats (age 86 d), the abundance of lysosomes packed with electron-dense material were detected in Kupffer cells (Fig. 1D). Livers of 84-d-old LEC rats treated with DPA from d 77 showed normal nuclei, rough endoplasmic reticulum, and mitochondria. Lysosomes of both hepatocytes and Kupffer cells only infrequently showed electron-dense material (Fig. 1E,F).

The highest levels of total copper concentrations were observed in 77-d-old rats with beginning hepatitis (Fig. 2). Jaundiced LEC rats aged 86 d exhibited about 20% lower hepatic copper concentrations. After treatment with DPA, hepatic copper levels were even lower than those of morphologically and histologically normal 62-d-old rats ($p < 0.05$, not shown).

In the cytosol, copper was almost exclusively bound to MT, independent of age, occurrence of liver disease, and treatment with DPA (not shown). In diseased LEC rats aged 77 and 86 d, the majority of copper was recovered from the noncytosolic fraction of the liver. Upon DPA treatment, the mean copper values decreased by about 60%, mostly representing the noncytosolic copper.

The distribution of copper in hepatic lysosomes and mitochondria is shown in Fig. 3A. High levels of the metal were recovered from the high-density fraction no. 1 of the slightly diseased animals aged

Table 1
Assignment of the LEC Rats to the Experimental Groups

Group (no. of animals)	*Age (d) range (mean ± SD)*	*Serum AST (U/L) range*	*Serum bilirubin (mg/dL) range*	*Liver pathology (mean ± SD)*
			(mean ± SD)	
Wistar controls (*n*=9)	55–62 (57 ± 2)	190–311 (246 ± 38)	<0.5–0.6	Normal
LEC, age 62 d (*n*=6)	59–64 (62 ± 2)	161–304 (244 ± 48)	<0.5	Normal
LEC, age 77 d (*n*=4)	77–79 (77 ± 1)	510–1090 (867 ± 210)	<0.5–3.6	Abnormal
LEC, age 86 d (*n*=6)	85–87 (86 ± 1)	860–1605 (1409 ± 283)	12.8–44.5 (30.7 ± 12.9)	Abnormal
LEC + DPA from d 64, age 107 d (*n*=4)	106–107 (107 ± 1)	377–497 (430 ± 60)	<0.5	Abnormal
LEC + DPA from d 77, age 84 d (*n*=3)	84–85 (84 ± 1)	261–281 (272 ± 10)	<0.5	Abnormal
LEC + DPA from d 77, age 93 d (*n*=4)	92–93 (93 ± 1)	213–452 (305 ± 104)	<0.5	Abnormal

77 d and particularly of the animals with systemic jaundice aged 86 d. These animals showed also clearly increased copper levels in the lysosome-specific fractions no. 9. The relatively high concentration of copper in fraction no. 10 derives from cytosolic contamination. Rats treated with DPA from d 64 to 107 showed only marginally elevated copper levels in the density fractions. The concentrations of MT in the fractions (Fig. 3B) paralleled those of copper. Accordingly, treatment of 77-d-old rats with DPA significantly decreased the MT levels in the high-density fraction no. 1 by 75%. MT in this fraction, however, was insoluble and could be analyzed only after solubilization with guanidinium thiocyanate and 2-mercaptoethanol.

Ultrastructurally, the insoluble material consisted of lysosomes containing electron-dense granules (Fig. 4A). Using energy-dispersive X-ray microanalysis, the electron-dense material could be attributed to copper (Fig. 4B).

High-performance liquid chromatography (HPLC) analysis of the solubilized material revealed a copper-containing component of 7.3 kDa, corresponding to 50% of the apparent molecular weight of native MT (Fig. 5). This component crossreacted with MT-specific antibodies in an enzyme-linked immunosorbent assay (ELISA) (not shown). A similar material, although at lower concentration, was isolated in addition to native MT, also from the lysosome-specific fraction no. 9 of the density gradient (Fig. 5).

The solubilization of the MT polymers by DPA was investigated in vitro. In the presence of 185 m*M* DPA, both copper and MT were solubilized almost totally within 5 min (results not shown). After HPLC analysis, copper was recovered at a relative elution volume of 2.0, corresponding to an apparent molecular weight of 6.6 kDa (Fig. 6). This fraction was bluish purple with an absorption maximum at 520 nm, which has been reported to be specific for thiol–copper(II) complexes *(20)*. In contrast, copper in the cytosol was virtually not mobilized by DPA (Fig. 6).

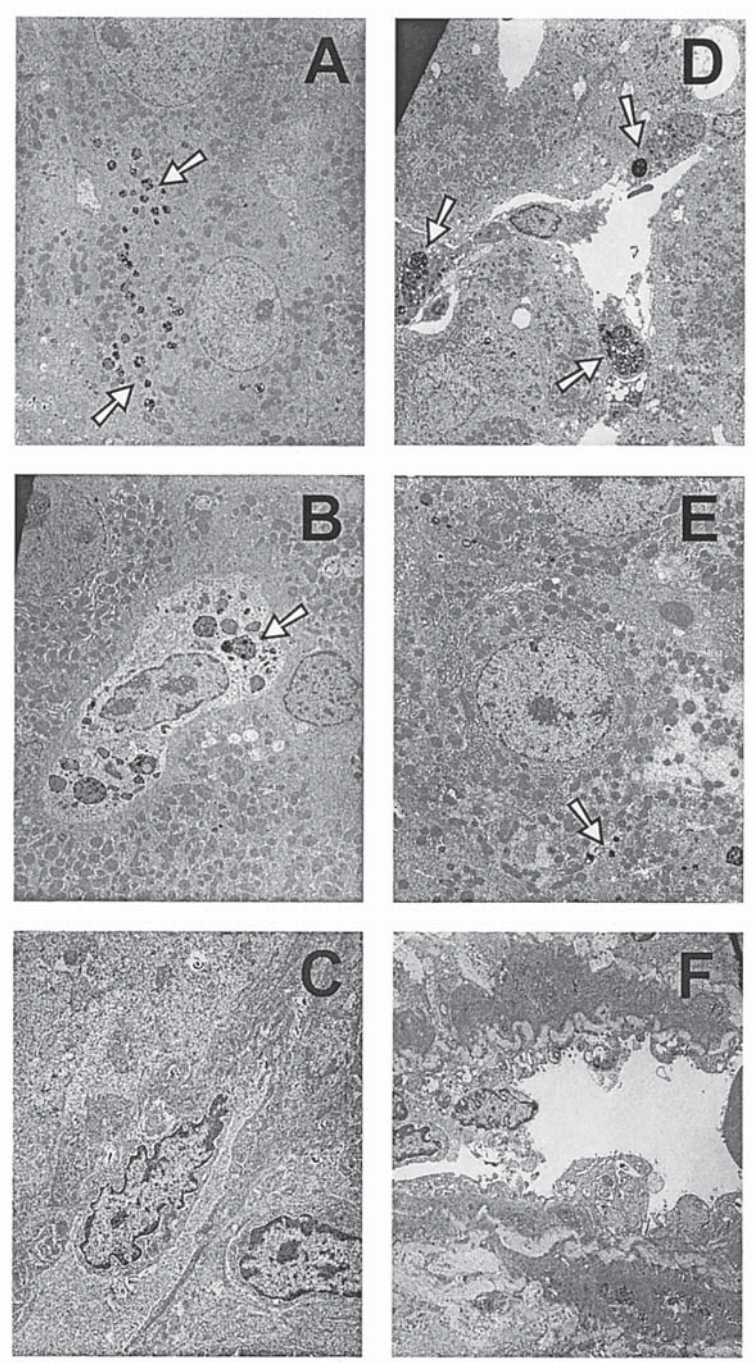

Fig. 1. Transmission electron micrographs from the livers of LEC rats aged 77 d **(A–C)**, aged 87 d with systemic jaundice **(D)**, and aged 84 d after treatment with D-penicillamine from d 77 **(E, F)**. Original magnification: **A, B, E**: 2.650×, **C**: 5.000×, **D**: 1.670×, **F**: 4.320×. Arrows indicate the localization of electron-dense particles. [From Klein, D., et al., *J. Hepatol.* **32**, 193–201 (2000), with permission.]

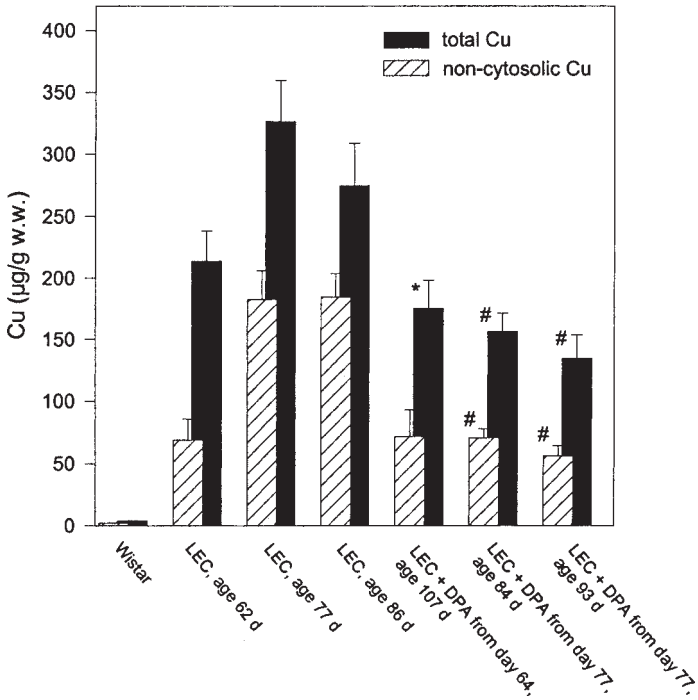

Fig. 2. Total and noncytosolic copper contents in the liver of LEC rats with and without treatment with D-penicillamine (DPA) (mean ± SD, n = 3–11). *Significantly different from LEC rats, age 62 d ($p < 0.05$); #significantly different from LEC rats, age 77 d ($p<0.05$). [From Klein, D., et al., *J. Hepatol.* **32**, 193–201 (2000), with permission.]

4. DISCUSSION

In agreement with the key role of copper for the development of hepatitis in LEC rats, the metal accumulated in the liver with age. During the progression of hepatitis, the metal shifted from the cytosolic to the noncytosolic compartment of the liver. The decrease in the concentration of hepatic copper in severely affected animals is considered to result from the leakage of cytosolic copper from necrotic hepatocytes into blood. Accordingly, in these animals, elevated copper levels were observed in the blood and kidney *(21)*.

Here, we report that in the LEC rat, the noncytosolic copper was mainly detected in lysosomes. Also in Wilson's disease, the localization of hepatic copper varies with the stage of the disease: In the early stage, copper is diffuse in the cytoplasm of hepatocytes, whereas later, when fibrosis and cirrhosis are the predominant histopathological features, the metal is mainly located in hepatocyte lysosomes *(22)*.

There is considerable uncertainty on the subcellular site of hepatic injury caused by excess copper. From studies with Wilson's disease patients, it has been postulated that hepatic copper in the cytosol, which is predominant in the early stage of the disease, is toxic *(22)*. In the liver of our LEC animals, copper levels were also fairly high in the cytosol before the onset of acute hepatitis; however, the total of copper was bound to MT. Consistent with the role of MT in detoxifying metals, these findings do not support a prominent role of cytosolic copper in initiating hepatotoxicity.

The assumption that the accumulation of copper in lysosomes represents a detoxification pathway *(23)* is questionable because findings in humans *(1)* and animals *(24,25)* suggest that, in particular, hepatocytes packed with copper-loaded lysosomes are the cells that undergo necrosis *(26)*. Undoubtedly, the molecular association of copper within the lysosomes is of crucial importance with regard to its

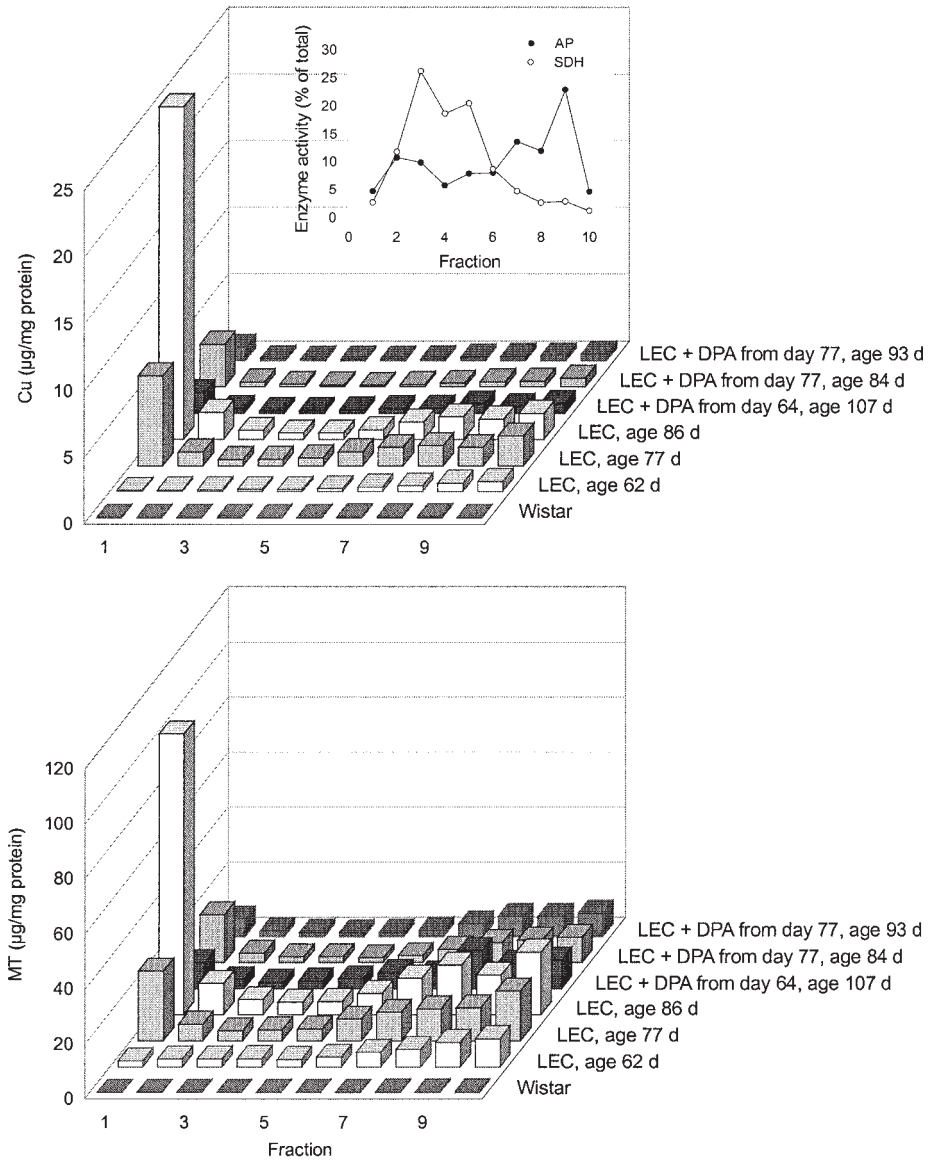

Fig. 3. Copper (top) and MT (bottom) in density gradient fractions of crude lysosomes from livers of LEC rats (mean values, $n = 3–11$). Crude lysosomes were obtained by differential centrifugation as described in ref. *18*. To separate lysosomes from mitochondria, crude lysosomes were layered on a Nycodenz gradient of the following composition: 1 mL 40%, 1 mL 33%, 3 mL 28%, 2 mL 27% and 2 mL 24% (w/v) Nycodenz in 10 m*M* Tris-HCl (pH 7.4) and centrifuged at 74,100g_{max} (swing-out rotor) for 3 h. After centrifugation, the gradient was fractionated in aliquots of 1 mL. The inset shows a typical distribution profile of the lysosome-specific acid phosphatase (AP) and the mitochondria-specific succinate dehydrogenase (SDH) activities. MT was determined by the thiomolybdate-method *(19)* after incubating the sample with guanidinium thiocyanate and 2-mercaptoethanol as described in ref. *18*. [In part from Klein, D., et al., *J. Hepatol.* **32**, 193–201 (2000), with permission.]

toxicity. As shown here, the lysosomal copper was associated with insoluble material, which could be solubilized under reducing conditions. The solubilized product had an apparent molecular weight of 7.3 kDa and crossreacted with MT-specific antibodies. Accordingly, the insoluble material is considered to consist of polymers of degradation products of copper-containing MT. The formation of

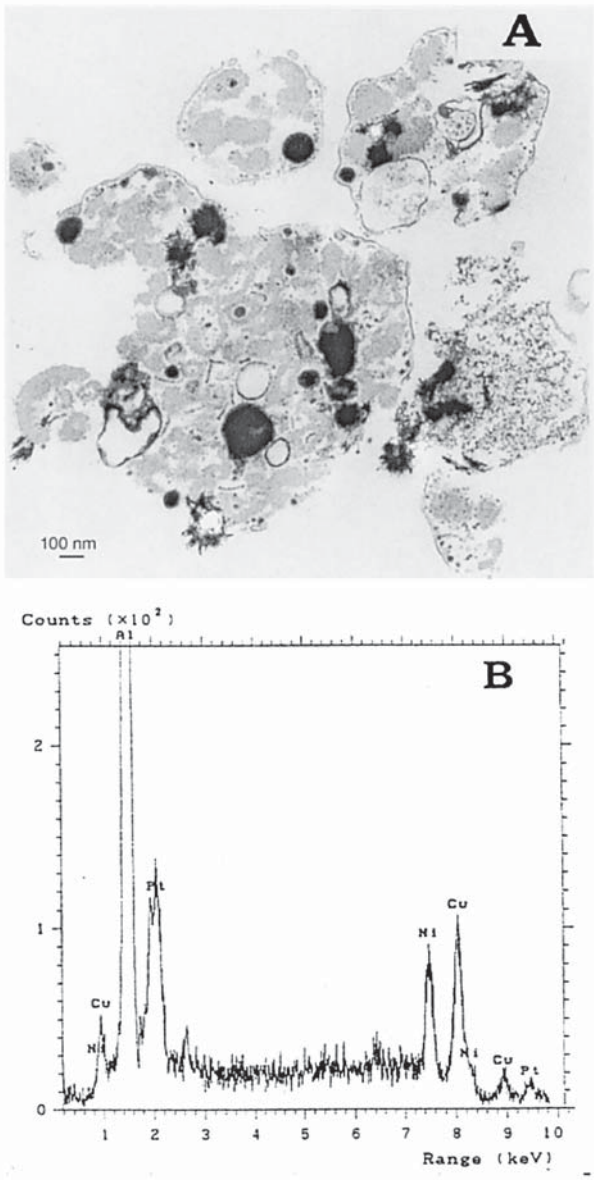

Fig. 4. (A) Electron micrograph of the high-density fraction (fraction no. 1 of the density gradient) of crude lysosomes from a jaundiced LEC rat (original magnification 52,400×). **(B)** Energy-dispersive X-ray microanalysis of the lysosomal electron-dense matrix. Aluminum (Al), nickel (Ni), and platinum (Pt) peaks are derived from the stub, the grid, and the surface coating of the specimen, respectively. [From ref. *18*, with permission.]

these polymers relates to the uptake of highly copper-loaded MT from the cytosol into the lysosomes. Generally, the fate of MT in the lysosome is mainly determined by the metal composition of the protein: Because of the acidic pH of the lysosomal matrix, zinc-containing MT will easily lose the metal, and the apoprotein, consequently, will be degraded *(27)*. Because metal removal from copper–MT requires a lower pH *(28)*, the lysosomal pH of typically 4.7 is likely not low enough to remove significant amounts of copper from highly copper-loaded MT, thus rendering the protein fairly stable

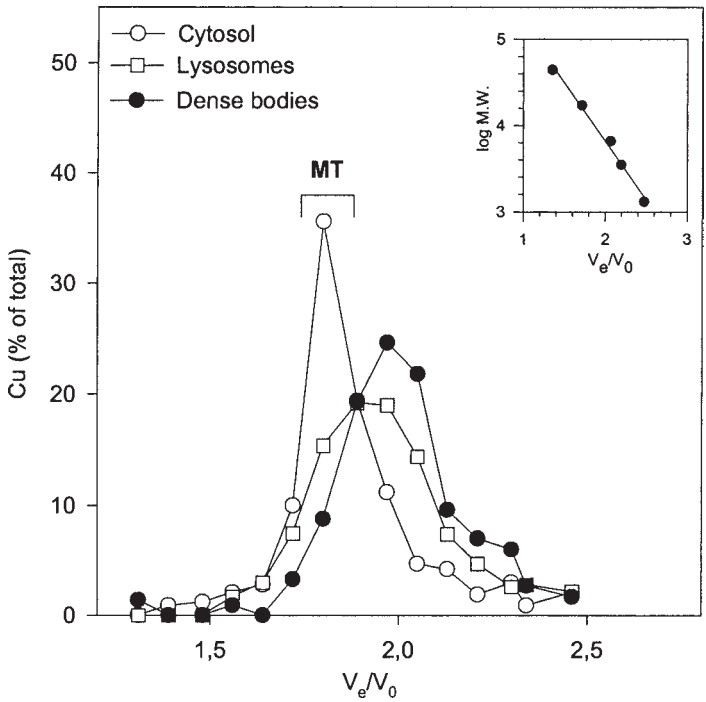

Fig. 5. HPLC gel chromatography of cytosol, solubilized lysosomes (density gradient fraction no. 9) and solubilized dense bodies (gradient fraction no. 1) from the liver of a jaundiced rat. The inset shows the relative elution volumes of chicken ovalbumin (molecular weight [MW] 44,000), equine myoglobin (MW 17,000), aprotinin (MW 6500), β-endorphin (MW 3465), and angiotensin (MW 1297). The bracket indicates the relative elution volume of native MT from rat liver. (From ref. *18*, with permission.)

against proteolysis. Consistently, copper-containing MT in vitro was reported to be fairly resistant against hydrolysis by lysosomal enzymes *(29)*. Furthermore, in vivo, the intralysosomal pH has been found to be increased after copper overload *(25)*. Our results suggest that the highly copper-loaded MT in lysosomes is only partly degraded. The resulting proteolysis-resistant product presumably represent the β-domain of MT, which in copper-containing MT *(30,31)* is more stable than the α-domain. The β-domain then might polymerize and form an oxidized, insoluble material that apparently cannot be excreted into bile. The polymerization process likely proceeds through a radical-mediated mechanism involving iron which has been shown to be massively elevated in the hepatocyte lysosomes of LEC rats *(18)*. The degradation products of copper-containing MT obviously are polymerized through disulfide bridges because the solubilization of the polymer by guanidinium thiocyanate required the presence of 2-mercaptoethanol. Therefore, it is reasonable to assume that copper associated with the polymer is more loosely bound and therefore more reactive than copper bound to native MT. Supporting this assumption, copper in the copper-rich granules is histochemically stainable with rhodanine, whereas copper bound to native MT is not *(32,33)*. The reactive polymer-associated copper may initiate lipid peroxidation of lysosomal membranes, resulting in lysosomal rupture and release of hydrolytic enzymes into the cytoplasm.

According to our ultrastructural findings, copper is massively located in Kupffer cells in the liver of jaundiced LEC rats. This is most likely the result of phagocytotic copper uptake from necrotic or apoptotic hepatocytes. Once within the macrophages, this material seems to further aggregate to copper-rich granules. The accumulation of high amounts of presumably reactive copper in Kupffer cells may amplify the liver damage either directly or through stimulation of these cells. A similar

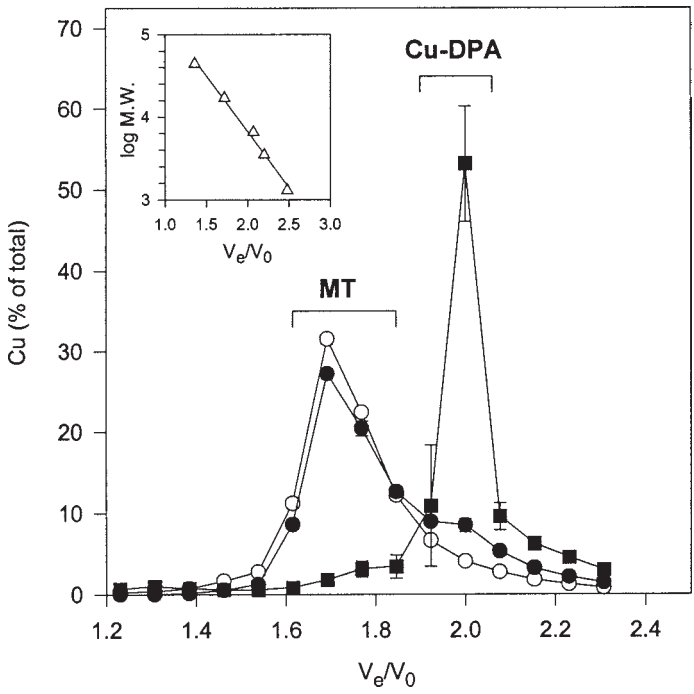

Fig. 6. Copper elution profile of gel chromatographically separated liver cytosol (circles) from a LEC rat aged 77 d and copper-rich polymers (squares) from a jaundiced LEC rat before (open symbols) and after (closed symbols) incubation with D-penicillamine (DPA, 185 m*M*, 5 min, mean ± SD, $n = 3$). The brackets indicate the elution volume of native metallothionein (MT) from rat liver and a mixture of copper:DPA of 1:1.250 mol/mol, respectively. The inset shows the relative elution volumes of protein standards (*see* Fig. 5). [From Klein, D., et al., *J. Hepatol.* **32**, 193–201 (2000), with permission.]

stimulatory role of Kupffer cells has been also reported in chemical- and metal-induced hepatotoxicity *(34,35)*.

The therapeutic principle of DPA in treating Wilson's disease is thought to involve the depletion of excess copper in the liver through chelation or to facilitate copper detoxification through induction of MT. Accordingly, in Wilson's disease, DPA treatment resulted in diminished levels of hepatic copper *(36)*, although a negative copper balance is probably not maintained after the first year of treatment *(33)*. Scheinberg et al. *(37)* reported that the removal of copper from the liver is incomplete and inconsistent, and the hepatic copper levels may remain elevated even after years of therapy. These findings led the authors to suggest that DPA detoxifies copper by induction of MT rather than removes the metal from the liver *(33)*. Induction of MT, however, has been described only in rats and mice after single intraperitoneal administration of the drug *(38,39)* and in our LEC rats there was no evidence of MT induction after DPA treatment (results not shown).

Consistent with earlier findings *(10, 11)*, DPA administered to nondiseased LEC animals prevented the onset of fulminant hepatitis. The drug particularly inhibited the disease-specific accumulation of copper in the noncytosolic fraction. In diseased LEC rats, DPA treatment resulted in the reversal of liver damage. In these animals DPA sequestered copper particularly from the lysosomes (i.e., it mobilized the metal likely from the MT polymers). In agreement, upon ultrastructural examination, the electron-dense particles were absent and, simultaneously, the copper content of the polymer-containing fractions declined. The mobilization of copper from the polymers by DPA could also be demonstrated in vitro and obviously involves their solubilization and the formation of copper–DPA complexes. DPA is known to form stable high-molecular-weight complexes with copper *(20,40)*

and is able to undergo disulfide-exchange reactions *(40)*. Thus, the solubilization is likely to proceed through the reduction of the disulfide bridges of the polymers.

According to the in vitro findings and in agreement with findings of others *(42,43)*, DPA did not remove copper that was bound to MT in liver cytosol. Also in our LEC rats, most of the cytosolic MT-bound copper remained in this compartment after DPA treatment. The poor availability of MT-bound copper for binding to DPA may explain the observation that copper concentrations in normal livers of LEC rats treated with DPA for 3 mo were half of those observed in untreated animals but still 30 times greater than those of control animals *(10)*. This, again, supports the assumption that elevated levels of cytosolic copper bound to MT is of minor importance for the hepatotoxicity of the metal. Assuming our findings on LEC rats are applicable to Wilson's disease, DPA particularly mobilizes copper, which is not bound to cytosolic MT. This fits well to the observation *(37)* that patients with Wilson's disease may not be truly decoppered by DPA.

ACKNOWLEDGMENTS

The authors wish to thank Dr. U. Heinzmann, GSF-Institute of Pathology, and Prof. Dr. P. Schramel, GSF-Institute of Ecological Chemistry for the electron microscopy work and the metal determinations, respectively. This work was supported in part by BWPLUS, grant no. PUG U 98003.

REFERENCES

1. Sternlieb, I. (1980) Copper and the liver. *Gastroenterology* **78**, 1615–1628.
2. Schilsky, M. L. and Sternlieb, I. (1993) Animal models of copper toxicosis. *Anim. Mod. Liver Res.* **37**, 357–377.
3. Pandit, A. N. and Bhave, S. A. (1983) Copper and Indian childhood cirrhosis. *Indian Pediatr.* **20**, 893–899.
4. Bull, P. C., Thomas, G. R., Rommens, J. M., Forbes, J. R., and Cox, D. W. (1993) The Wilson disease gene is a putative copper transporting P-type ATPase similar to the Menkes gene. *Nature Genet.* **5**, 327–337.
5. Yoshida, M. C., Masuda, R., Sasaki, M., Takeichi, N., Kobayashi, H., Dempo, K., et al. (1987) New mutation causing hereditary hepatitis in the laboratory rat. *J. Hered.* **78**, 361–365.
6. Li, Y., Togashi, Y., Sato, S., Emoto, T., Kang, J. H., Takeichi, N., et al. (1991) Spontaneous hepatic copper accumulation in Long–Evans Cinnamon rats with hereditary hepatitis. *J. Clin. Invest.* **87**, 1858–1861.
7. Wu, J., Forbes, J. R., Chen, H. S., and Cox, D. W. (1994) The LEC rat has a deletion in the copper transporting ATPase gene homologous to the Wilson disease gene. *Nature Genet.* **7**, 541–545.
8. Sasaki, M., Yoshida, M. C., Kagami, K., Takeichi, N., Kobayashi, H., Dempo, K., et al. (1985) Spontaneous hepatitis in an inbred strain of Long–Evans rats. *Rat News Lett.* **14**, 4–6.
9. Takeichi, N., Kobayashi, H., Yoshida, M. C., Sasaki, M., Dempo, K., and Mori, M. (1988) Spontaneous hepatitis in Long–Evans rats: a potential animal model for fulminant hepatitis in man. *Acta Pathol. Jpn.* **38**, 1369–1375.
10. Togashi, Y., Li, Y., Jong-Hon, K., Takeichi, N., Fujioka, Y., Nagashima, K., et al. (1992) D-Penicillamine prevents the development of hepatitis in Long–Evans Cinnamon rats with abnormal copper metabolism. *Hepatology* **15**, 82–87.
11. Jong-Hon, K., Togashi, Y., Kasai, H., Hosokawa, M., and Takeichi, N. (1993) Prevention of spontaneous hepatocellular carcinoma on Long–Evans Cinnamon rats with hereditary hepatitis by the administration of D-penicillamine. *Hepatology* **18**, 614–620.
12. Walshe, J. M. (1956) Penicillamine: a new oral therapy for Wilson's disease. *Am. J. Med.* **2**, 487–495.
13. Parkes, D. (1984) Wilson's disease. *Br. Med. J.* **288**, 1180–1181.
14. Lingam, S., Wilson, J., Nazer, H., and Mowat, A. P. (1987) Neurological abnormalities in Wilson's disease are reversible. *Neuropediatrics* **18**, 11–12.
15. Hanaichi, T., Kidokoro, R., Hayashi, H., and Sakamoto, N. (1984) Electron probe X-ray analysis on human hepatocellular lysosomes with copper deposits: copper binding to a thiol-protein in lysosomes. *Lab. Invest.* **51**, 592–597.
16. Lerch, K., Johnson, G. F., Grushoff, P. S., and Sternlieb, I. (1985) Canine hepatic lysosomal copper protein: identification as metallothionein. *Arch. Biochem. Biophys.* **243**, 108–114.
17. Johnson, G. F., Morell, A. G., Stockert, R. J., and Sternlieb, I. (1981) Hepatic lysosomal copper protein in dogs with an inherited copper toxicosis. *Hepatology* **1**, 243–248.
18. Klein, D., Lichtmannegger, J., Heinzmann, U., Müller-Höcker, J., Michaelsen, S., and Summer, K. H. (1998) Association of copper to metallothionein in hepatic lysosomes of Long–Evans cinnamon (LEC) rats during the development of hepatitis. *Eur. J. Clin. Invest.* **28**, 302–310.
19. Klein, D., Bartsch, R., and Summer, K. H. (1990) Quantitation of Cu-containing metallothionein by a Cd-saturation method. *Anal. Biochem.* **189**, 35–39.
20. Kato, N., Nakamura, M., and Uchiyama, T. (1999) ^{1}H NMR studies of the reactions of copper(I) and copper(II) with D-penicillamine and glutathione. *J. Inorg. Biochem.* **75**, 117–121.
21. Klein, D., Michaelsen, S., Sato, S., Luz, A., Stampfl, A., and Summer, K. H. (1987) Binding of copper to metallothionein in tissues of the LEC rat with inherited abnormal copper accumulation. *Arch. Toxicol.* **71**, 340–343.

22. Goldfischer, S. and Sternlieb, I. (1968) Changes in the distribution of hepatic copper in relation to the progression of Wilson's disease (hepatolenticular degeneration). *Am. J. Pathol.* **53**, 883–901.
23. Goldfischer, S., Popper, H., and Sternlieb, I. (1980) The significance of variations in distribution of copper in liver disease. *Am. J. Pathol.* **99**, 715–723.
24. Lindquist, R. R. (1968) Studies on the pathogenesis of hepatolenticular degeneration. III. The effect of copper on rat liver lysosomes. *Am. J. Pathol.* **53**, 903–927.
25. Myers, B. M., Prendergast, F. G., Holman, R., Kuntz, S. M., and LaRusso, N. F. (1993) Alterations in hepatocyte lysosomes in experimental hepatic copper overload in rats. *Gastroenterology* **105**, 1814–1823.
26. Kumaratilake, J. S. and McHowell, J. C. (1989) Lysosomes in the pathogenesis of liver injury in chronic copper poisoned sheep: An ultrastructural and morphometric study. *J. Compar. Pathol.* **100**, 381–390.
27. Mehra, R. K. and Bremner, I. (1985) Studies on the metabolism of rat liver copper–metallothionein. *Biochem. J.* **227**, 903–908.
28. Hunziker, P. E. (1991) Metal removal from mammalian metallothioneins. *Methods Enzymol.* **205**, 451–452.
29. Bremner, I. and Mehra, R. K. (1983) Metallothionein: some aspects of its structure and function with special regard to its involvement in copper and zinc metabolism. *Chemica Scripta* **21**, 117–121.
30. Presta, A., Green, A. R., Zelazowski, A., and Stillman, M. J. (1995) Copper binding to rabbit liver metallothionein. Formation of a continuum of copper(I)–thiolate stoichiometric species. *Eur. J. Biochem.* **227**, 226–240.
31. Li, H. and Otvos, J. D. (1996) ^{111}Cd NMR studies of the domain specificity of Ag^+ and Cu^+ binding to metallothionein. *Biochemistry* **35**, 13,929–13,936.
32. Sumi, Y., Kawahara, S., Kikuchi, Y., Sawada, J. I., Suzuki, T., and Suzuki, K. T. (1993) Histochemical and immunohistochemical localization of copper, iron and metallothionein in the liver and kidney of LEC rats. *Acta Histochem. Cytochem.* **26**, 5–9.
33. Scheinberg, I. H. and Sternlieb, I. (1984) Wilson's disease, in *Major Problems in Internal Medicine* (Smith, L. H., Jr., ed.), W. B. Saunders, Philadelphia.
34. Sauer, J. M., Waalkes, M. P., Hooser, S. B., Kuester, R. K., McQueen, C. A., and Sipes, I. G. (1997) Suppression of Kupffer cell function prevents cadmium induced hepatocellular necrosis in the male Sprague–Dawley rat. *Toxicology* **121**, 155–164.
35. Edwards, M. J., Keller, B. J., Kauffman, F. C., and Thurman, R. G. (1993) The involvement of Kupffer cells in carbon tetrachloride toxicity. *Toxicol. Appl. Pharmacol.* **119**, 275–279.
36. Gibbs, K. and Walshe, J. M. (1990) Liver copper concentration in Wilson's disease: effect of treatment with "anti-copper" agents. *J. Gastroenterol. Hepatol.* **5**, 520–524.
37. Scheinberg, I. H., Sternlieb, I., Schilsky, M., and Stockert, R. J. (1987) Penicillamine may detoxify copper in Wilson's disease. *Lancet* **2,** 95.
38. Goering, P. L., Tandon, K., and Klaassen, C. D. (1985) Induction of hepatic metallothionein in mouse liver following administration of chelating agents. *Toxicol. Appl. Pharmacol.* **80**, 467–472.
39. Heilmaier, H. E., Jiang, J. L., Greim, H., Schramel, P., and Summer, K. H. (1986) D-penicillamine induces rat hepatic metallothionein. *Toxicology* **42**, 23–31.
40. Vallon, J. J. and Badinand, A. (1968) A polarographic study of the redox and complex-forming reactions of penicillamine, *N*-acetylpenicillamine and copper (I). *Anal. Chim. Acta* **42**, 445–454.
41. Joyce, D. A. (1989) D-Penicillamine pharmacokinetics and pharmacodynamics in man. *Pharmac. Ther.* **42**, 405–427.
42. McQuaid, A. and Mason, J. (1990) A comparison of the effects of penicillamine, trientine, and trithiomolybdate on (^{35}S)-labeled metallothionein in vitro; implications for Wilson's disease therapy. *J. Inorg. Biochem.* **41**, 87–92.
43. McQuaid, A., Lamand, M., and Mason, J. (1992) The interactions of penicillamine with copper in vivo and the effect on hepatic metallothionein levels and copper/zinc distribution: the implications for Wilsons's disease and arthritis therapy. *J. Lab. Clin. Med.* **119**, 744–750.

VI
Copper Metabolism and Homeostasis

29

Sensory Protein Modification

A New Feature in Copper Balancing

Zhiwu Zhu, Jose Heredia, and Ryan Teves

1. INTRODUCTION

How cells sense changes in copper ion concentration is a central question in copper-ion homeostasis. This is because the essential yet toxic biological nature of copper ions depends on its intracellular concentration. The importance of copper ions in living organisms is explained by its role as a cofactor for a number of enzymes involved in cellular physiology *(1)*. Its toxic nature is generally thought to be the result of excess copper ions that can participate in reactions that generate reactive oxygen molecules such as O_2^- and $HO^\bullet$ *(2)*. Copper ions might also displace other metal ions such as Zn^{2+} from their respective protein molecules, perturbing or disrupting their functions *(3,4)*. Copper-ion exposure is also known to change the intracellular redox state *(5)*, which may also trigger toxic effects. A recent investigation found higher mutation frequencies of the tumor suppressor p53 in Wilson's disease patients who had accumulated excess copper ions in the liver and other organs *(6)*. The presence of copper ions is necessary for the radiation of γ-rays to cause DNA conformational changes from a right-handed to a left-handed helical form *(7)*. While avoiding an excessive accumulation of copper ions, cells must also prevent copper-ion deficiency that deprives the functions of copper-dependent enzymes, as is seen in Menkes syndrome patients *(8–10)*. Clearly, in order to maintain a "just right" concentration, cells must have the ability to differentiate the physiological from the toxic copper level.

Remarkable progress has been achieved in the past decade in the elucidation of molecular mechanisms underlying detoxification *(11–14)*, uptake, and distribution of copper ions *(15–28)*. This progress largely accounts for the current molecular understanding of copper-ion homeostasis. Moreover, this progress makes it possible for us to now begin to address the above question. We believe that one of the challenges we are facing is to develop, at the molecular level, a quantitative picture of copper-ion homeostasis. In this chapter, we will review our recent research progress and that of others toward that goal, and re-examine data in the literature within a framework of quantitative understanding of copper-ion homeostasis. Within this context, we will then propose a thermodynamic model. We will also review the recent development in the investigation of copper-ion signaling. Above all, we would like to raise and draw our attention to a fundamental aspect of copper-ion homeostasis: how cells differentiate the physiological from the toxic copper ion level.

From: Handbook of Copper Pharmacology and Toxicology
Edited by: E. J. Massaro © Humana Press Inc., Totowa, NJ

2. QUANTITATIVE COPPER-ION HOMEOSTASIS

What is the exact concentration of the physiological copper-ion level? What is the exact level at which copper ions become toxic? These are two obvious and natural questions in copper-ion homeostasis, considering that the copper ion is either a nutrient or toxicant, depending on its concentration. Surprisingly, the questions have not attracted much attention and investigation, which explains that our current quantitative understanding of copper-ion homeostasis is very much empirical. A recent study *(29)*, for the first time, indicates that determining the exact concentrations of physiological and toxic copper levels is possible at the molecular level.

2.1. Mac1p Senses Two Different Copper Ion Levels

Organisms such as yeast have a remarkable ability to adapt to drastically varying copper-ion conditions. Yeast gene expression differs greatly under different copper-ion conditions *(30)*, which implies that yeast can detect the changes in copper-ion concentrations. The transcription factor Mac1p plays a pivotal role in yeast copper-ion homeostasis. Mac1p controls copper-ion uptake by regulating the expression of genes encoding high-affinity copper-ion transporters *CTR1* and *CTR3 (29,31–38)*. Mac1p has also been shown to participate directly in copper-ion detoxification through a mechanism independent of *CTR1* and *CTR3 (39)*. We have also found that Mac1p might regulate the degradation of Ctr1p in response to toxic copper levels, by a yet to be explored mechanism independent of its regulatory role in *CTR1* transcription (Zhu, unpublished results; *40*). A long-standing question in understanding how Mac1p senses copper ions and regulates *CTR1* and *CTR3* transcription was whether copper ions affect the binding of Mac1p to the copper-ion-responsive elements (CuREs) in the promoters of *CTR1* and *CTR3*. This question has been solved recently in our laboratory *(29)*.

The DNA binding of Mac1p was found to be disrupted by copper ions and isoelectronic Ag^+, indicating that Mac1p, much like Ace1p and Amt1p, senses the cuprous ions, Cu^+. This finding suggests that increases in copper-ion concentrations disrupt the DNA binding of Mac1p and result in the subsequent inactivation of *CTR1* and *CTR3* transcription *(29)*. Surprisingly, the same study also found that in order for Mac1p to bind to the CuREs, Mac1p first has to bind Cu^+ ions. Together, the DNA binding of Mac1p is, on one hand, Cu^+-coordination dependent and, on the other hand, disrupted by copper ions. It is this finding that indicates that Mac1p is able to sense two different levels of copper ions and that the two different copper-ion concentrations exert distinct effects on the DNA binding of Mac1p and, therefore, on the expression of *CTR1* and *CTR3 (29)*. Then, what are the biological natures of these two copper-ion levels sensed by Mac1p? We found that mutations within the known conserved copper-ion-binding motif of the DNA-binding domain completely abolished the ability of Mac1p to activate *CTR1* and *CTR3* transcription and that mutant cells were unable to grow on medium containing a nonfermentable carbon source ethanol (YPE), a copper-ion-requiring condition *(41)*. Growth of the mutant on YPE can, however, be restored by the addition of exogenous $CuSO_4$, but not by other metal ions (unpublished results; *31*). Clearly, by activating *CTR1* and *CTR3* gene expression, the function of this motif is to maintain an adequate copper-ion concentration for growth under copper-ion-requiring conditions. The mutant protein failed to bind the CuREs in the *CTR1* promoter *(41)*; however, purified protein of the separated DNA-binding domain bound the DNA, in a copper-ion-coordination-dependent fashion *(42)*. These data together indicate that Cu^+ coordination of the conserved metal-ion-binding motif triggers Mac1p to bind to *CTR1* and *CTR3* promoters and is critical for yeast growth at the copper-ion-requiring condition *(41)*. In contrast, mutations within the REP-I motif of the activation domain had no effect on the activation of *CTR1* and *CTR3* transcription, but disrupted the inactivation of this transcription by increases in the copper-ion concentration *(41)*. The mutant cells were able to grow on YPE, but showed a sensitive phenotype on copper-ion-containing medium. The REP-I motif is important for Mac1p to sense and detoxify excess copper ions, but not for cells to acquire adequate copper ions *(41)*. Considering the role of Mac1p in yeast copper-ion homeostasis, it is reasonable to conclude that through the metal-ion-binding

motifs in its DNA-binding and activation domains, Mac1p senses both the physiological and toxic copper-ion levels, respectively.

As discussed earlier, Mac1p senses two different copper-ion levels through its DNA-binding and activation domains, indicating that the two domains have different affinities to Cu^+ and that Mac1p function is governed, in part, by a thermodynamic principle. It is now possible for us to determine the exact concentration for physiological and toxic copper levels. This can be accomplished by in vitro measuring of the copper-ion-binding affinities for both the DNA-binding and activation domains.

2.2. *Decision-Making Between Uptake and Detoxification: A Thermodynamic Model*

Among the known mechanisms of yeast copper-ion homeostasis, detoxification and uptake are responsive to changes in copper-ion concentrations *(14,33)*. The two mechanisms, however, respond oppositely, with uptake activated and detoxification repressed when copper ion is deficient, uptake repressed and detoxification activated under copper-rich conditions. Cells have to orchestrate these two processes to maintain an intracellular copper-ion concentration—not too low, not too high, but "just right." Then, just what does dictate this decision-making of yeast cells? Mechanistically, copper-ion uptake *(15,16)*, controlled by Mac1p, is independent of copper-ion detoxification, activated by Ace1p *(13)*. The question becomes even more prominent if we take into consideration the sequence homology between the regulatory factors of these two processes, Mac1p and Ace1p *(31)*.

The role of Mac1p in yeast copper-ion homeostasis was first recognized through its sequence homology to the two other known copper-ion-sensing factors Ace1p in *Saccharomyces cerevisiae* and Amt1p in *C. glabrata (31)*. The homology only lies within the first 40 residues of NH_2-terminal DNA-binding domains. Importantly, it is within these 40 residues that the known Cu^+-binding motif resides. As a means to sensing copper ions, both Ace1p and Amt1p coordinate copper ions through this motif and then bind to the promoters of *CUP1*, *CRS5*, and other metallothionein (MT) genes, resulting in transcriptional activation *(14)*. Our study show that this mechanism is conserved in Mac1p *(29)*; however, it also raises an important question. Because both Mac1p and Ace1p have an almost identical Cu^+-binding motif in their DNA-binding domains, under copper-limiting conditions, why are Mac1p Cu^+ bound and active in CuRE binding, but not the Ace1p? The answer will be instrumental in understanding how yeast keeps a balanced copper level.

Here, I propose a model, not only in an attempt to answer the above question but also to account for the existing data in literature on both Ace1p and Mac1p. The model was basically established from our finding on how Mac1p functions (as described earlier). I propose that the principle governing the decision-making of yeast in balancing the intracellular copper-ion concentration is the intrinsic Cu^+-binding affinities of the regulatory factors, such as Mac1p and Ace1p. It is virtually a model of thermodynamics of copper-ion binding. This model predicts that the DNA-binding domain of Mac1p has a higher affinity to Cu^+ than the DNA-binding domain of Ace1p does. This predication is supported by the data that have already been reported and here I cite a few. In vivo footprinting studies have found that Ace1p binds to the *CUP1* promoter only when cells were exposed to exogenous copper ions *(43)*; in contrast, Mac1p binds to the CuREs in the *CTR3* promoter in the absence of exogenous copper ions *(33)*. An in vitro electrophoretic mobility shift assay has shown that exogenous copper ions have to be added to reactions in order to detect DNA-binding activity of Ace1p in yeast extracts prepared from cells that were grown in standard growth medium *(44)*. Under similar conditions, the DNA-binding activity of Mac1p was detected without the addition of exogenous copper ions *(29)*. Furthermore, DNA-binding activity of the separated DNA-binding domain of Mac1p was detected in yeast extracts prepared from cells that were grown even in the presence of copper-ion-specific chelator bathocuproine disulfonate (BCS) *(35)*. Studies of the transcriptional activation of *CUP1* or *CTR1* and *CTR3* by chimeric proteins, Ace1-VP16 or Mac1-VP16, also supports the model *(18,36)*. Certainly, proof of this model will come from biochemical studies measuring

Cu^+-binding affinities of these two proteins. Nonetheless, it is warranted to draw attention to this fundamental aspect of the metal ion–protein interaction in copper-ion homeostasis.

2.3. Phosphorylation of Copper-Sensing Factor Mac1p…"Joining the Rank"

As reflected in the above discussion, a general mechanism by which cells sense metal ions is the direct metal-ion coordination by regulatory protein factors *(45)*. This mechanism, no doubt, dominates metal-ion signaling. However, the prevailing mechanism for cellular signaling is the phosphorylation of protein *(46)*. The recent discoveries of phosphorylation modification of Mac1p and Aft1 *(29,47)*, therefore, expanded our current description of metal-ion signaling. This progress revealed a previously unknown area in metal ions in biology and allows us to foresee an exciting field of investigation. Further studies of this new mechanism, likely, will deepen our understanding of the roles of metal ions in living organisms and will also enable us to comparatively examine metal-ion signaling with other nonmetal signal transduction mechanisms to gain a better understanding of cellular homeostasis.

As discussed earlier, Mac1p posses a remarkable ability to be able to sense two different levels of copper ions. We have found that this ability is established, in part, with the phosphorylation of Mac1p *(29)*. This modification of Mac1p was discovered in our pursuit to detect the DNA-binding activity of Mac1p in yeast extracts, as was reported recently *(29)*. Our investigation also led to the finding that yeast keeps the majority of Mac1p nonphosphorylated under physiological conditions. Interestingly, overexpression of Mac1p results in hyperphosphorylation. Phosphorylation modification is required for Mac1p to bind to the CuREs in the *CTR1* promoter *(29)*. As discussed already, the DNA binding of the phosphorylated Mac1p is disrupted by the addition of copper ions or its isoelectronic Ag^+. These data indicate that the phosphorylated Mac1p is, therefore, the sensor for the increases in copper-ion concentration and that the phosphorylation modification of Mac1p is a key event in copper-ion signaling *(29)*. This is likely a general mechanism for yeast to sense metal ions, as the iron-responsive regulatory factor Aft1 is also found to undergo phosphorylation modification *(47)*. Aft1 regulates gene expression of high-affinity iron-transporting machinery in a fashion analogous to Mac1p *(48)*.

Based on this development, we now can ask whether changes in copper-ion concentration affect Mac1p phosphorylation. We have subsequently found that copper starvation, by the addition of BCS in growth medium, increases the level of phosphorylated Mac1p in yeast *(41)*. In contrast, increases in the copper-ion concentration, by the addition of $CuSO_4$ in the growth medium, trigger degradation of the phosphorylated Mac1p *(41)*. Therefore, the phosphorylation and degradation of Mac1p are two important steps in the yeast copper-ion signaling pathway. Then, it is critical to determine the mechanism by which the signal of changes in copper-ion concentration is propagated. Two findings are particularly worth noting here. We have discovered that the REP-IIA mutant is completely phosphorylated, suggesting that the role of the REP-II motif is to limit the phosphorylation of Mac1p *(41)*. A recent study, using the two-hybrid assay, has reported that Mac1p interacts with the product of the *PPT1* gene *(49)*. The *PPT1* encodes a serine/threonine protein phsophatase, and the function of *PPT1*, and its human homolog, is currently unknown *(50)*. Together, these findings suggest that the copper-ion signal is propagated at least through the protein–protein interaction between Ppt1p and Mac1p. Because the REP-II is a typical metal-ion-binding motif *(34)*, the result also implies that metal-ion binding of the REP-II motif may function as a switch, to control the protein–protein interaction in response to the changes in copper-ion concentration. Copper-ion signaling in yeast, therefore, involves metal-ion binding, phosphorylation, degradation, and protein–protein interaction of the sensory factor, Mac1p.

3. CONCLUSION

As is apparent in the above discussion, these latest findings have uncovered a new territory in the field of copper-ion homeostasis. They have also raised important questions for future investigation.

To delineate the copper-ion signaling pathway is of particular importance and biochemical studies will enable us to determine the exact molecular mechanism of copper-ion signal transduction. Further studies will, no doubt, yield important insights into the understanding of copper-ion homeostasis.

REFERENCES

1. Linder, M. C. (ed.) (1991) *Biochemistry of Copper*, Plenum, New York.
2. Halliwell, B. and Gutteridge, J. M. C. (1990) Role of free radicals and catalytic metal ions in human disease: an overview, in *Methods in Enzymology*, *Volume 186* (Parker, L. and Glazer, A. N., eds.), Academic, San Diego, CA, pp. 1–85.
3. Hutchens, T. W., Allen, M. H., Li, C. M., and Yip, T. T. (1992) Occupancy of a C2–C2 type "zinc-finger" protein domain by copper. *FEBS Lett.* **309**, 170–174.
4. Predki, P. F. and Sarkar, B. (1992) Effect of replacement of "zinc-finger" zinc on estrogen receptor DNA interactions. *J. Biol. Chem.* **267**, 5842–5846.
5. Fortuniak, A., Zadzinski, R., Bilinski, T., and Bartosz, G. Biochem. (1996) Glutathione depletion in the yeast *Saccharomyces cerevisiae*. *Biochem. Mol. Biol. Int.* **38**, 901–910.
6. Hussain, S. P., Raja, K., Amstad, P. A., et al. (2001) Increased p53 mutation load in nontumorous human liver of Wilson disease and hemochromatosis: oxyradical overload diseases. *PNAS* **97**, 12,770–12,775.
7. Trumbore, C. N., Ehrlich, R. S., and Myers, Y. N. (2001) Changes in DNA conformation induced by gamma irradiation in the presence of copper. *Radiat. Res.* **155**, 453–465.
8. Danks, D. M. (1989) in *The Metabolic Basis of Inherited Disease* (Scriver, C. R., Beaudet, A. L., Sly, W. S., and Valle, D., eds.), McGraw-Hill, New York, pp. 1411–1431.
9. Harris, Z. L. and Gitlin, J. D. (1996) Genetic and molecular basis for copper toxicity. *Am. J. Clin. Nutr.* **63**, 836s–841S.
10. Vulpe, C. D. and Packman, S. (1995) Cellular copper transport. *Annu. Rev. Nutr.* **15**, 293–322.
11. Karin, M. (1985) Metallothioneins: proteins in search of functions. *Cell* **41**, 9–10.
12. Hamer, D. H. (1986) Metallothionein. *Annu. Rev. Biochem.* **55**, 913–951.
13. Thiele, D. J. (1992) Metal-regulated transcription in eukaryotes. *Nucleic Acids Res.* **20**, 1183–1191.
14. Zhu, Z. and Thiele, D. J. (1996) Toxic metal-responsive gene transcription, in *Stress-Inducible Cellular Responses* (Feige, U., Morimoto, R. I., Yahara, I., and Polla, B. S., eds.), Birkhauser, Basel, pp. 307–320.
15. Dancis, A., Yuan, D. S., Haile, D., Askwith, C., Eide, D., Moehle, C., et al. (1994) Molecular characterization of a copper transport protein in *S. cerevisiae*: an unexpected role for copper in iron transport. *Cell* **76**, 393–402.
16. Knight, S. A. B., Labbé, S., Kwon, L. F., Kosman, D. J., and Thiele, D. J. (1996) A widespread transposable element masks expression of a yeast copper transport gene. *Genes Dev.* **10**, 1917–1929.
17. Zhou, B. and Gitschier, J. (1997) hCTR1: a human gene for copper uptake identified by complementation in yeast. *Proc. Natl. Acad. Sci. USA* **94**, 7481–7486.
18. Peña, M. M. O., Puig S., and Thiele, D. J. (2000) Characterization of the *Saccharomyces cerevisiae* high affinity copper transporter Ctr3 *J. Biol. Chem.* **275**, 33,244–33,251.
19. Labbé, S., Peña, M. M. O., Fernandes, A. R., and Thiele, D. J. (1999) A Copper-sensing transcription factor regulates iron uptake genes in *Schizosaccharomyces pombe*. *J. Biol. Chem.* **274**, 36,252–36,260.
20. Valentine, J. S. and Gralla, E. B. (1997) Delivering copper inside yeast and human cells. *Science* **278**, 817–818.
21. Lin, S. J. and Culotta, V. C. (1995) The ATX1 gene of *Saccharomyces cerevisiae* encodes a small metal homeostasis factor that protects cells against reactive oxygen toxicity. *Proc. Natl. Acad. Sci. USA* **92**, 3784–3788.
22. Lin, S. J., Pufahl, R. A., Dancis, A., O'Halloran, T. V., and Culotta, V. C. (1997) A role of the *Saccharomyces cerevisiae* ATX1 gene in copper trafficking and iron transport. *J. Biol. Chem.* **272**, 9215–9220.
23. Pufahl, R. A., Singer, C. P., Peariso, K. L., Lin, S.-J., Schmidt, P. J., Fahrni, C. J., et al. (1997) Metal ion chaperone function of the soluble Cu(I) receptor Atx1. *Science* **278**, 853–856.
24. Hung, I., Casareno, R. L. B., Labesse, G., Mathews, F. S., and Gitlin, J. D. (1998) HAH1 is a copper-binding protein with distinct amino acid residues mediating copper homeostasis and antioxidant defense. *J. Biol. Chem.* **273**, 1749–1754.
25. Glerum, D. M., Shtanko, A., and Tzagoloff, A. (1996) Characterization of *COX17*, a yeast gene involved in copper metabolism and assembly of cytochrome oxidase. *J. Biol. Chem.* **271**, 14,504–14,509.
26. Beers, J., Glerum, D. M., and Tzagoloff, A. (1997) Purification, characterization, and localization of yeast Cox17p, a mitochondrial copper shuttle. *J. Biol. Chem.* **272**, 33,191–33,196.
27. Culatto, V. C., Klomp, L. W. J., Stain, J., Casareno, R. L. B., Krems, B., and Gitlin, J. D. (1997) The copper chaperone for superoxide dismutase. J. *Biol. Chem.* **272**, 23,469–23,472.
28. Casareno, R. L. B., Waggoner, D., and Gitlin, J. D. (1998) The copper chaperone CCS directly interacts with copper/zinc superoxide dismutase. J. *Biol. Chem.* **273**, 23,625–23,628.
29. Jose, H., Crooks, M., and Zhu, Z. (2001) Phosphorylation and Cu^+ coordination-dependent DNA binding of the transcription factor Mac1p in the regulation of copper transport. *J. Biol. Chem.* **276**, 8793–8797.
30. Gross, C., Kelleher, M., Iyer, V. R., Brown, P. O., and Winge, D. R. (2000) Identification of the copper regulon in *Saccharomyces cerevisiae* by DNA microarrays. *J. Biol. Chem.* **275**, 32,310–32,316.
31. Jungmann, J., Reins, H.-A., Lee, J., Romeo, A., Hassett, R., Kosman, D., et al. (1993) MAC1, a nuclear regulatory protein related to Cu-dependent transcription factors is involved in Cu/Fe utilization and stress resistance in yeast. *EMBO J.* **12**, 5051–5056.
32. Yamaguchi-Iwai, Y., Serpe, M., Haile, D., Yang, W., Kosman, D. J., Klausner, R. D., et al. (1997) Homeostatic regulation of copper uptake in yeast via direct binding of MAC1 protein to upstream regulatory sequences of *FRE1* and *CTR1*. *J. Biol. Chem.* **272**, 17,711–17,718.

33. Labbé, S., Zhu, Z., and Thiele, D. J. (1997) Copper-specific transcriptional repression of yeast genes encoding critical components in the copper transport pathway. *J. Biol. Chem*. **272**, 15,951–15,958.
34. Zhu, Z., Labbé, S., and Thiele, D. J. (1998) Copper differentially regulates the activity and degradation of yeast Mac1 transcription factor. *J. Biol. Chem*. **273**, 1277–1280.
35. Jensen, L. T., Posewitz, M. C., Srinivasan, C., and Winge, D. R. (1998) Mapping of the DNA binding domain of the copper-responsive transcription factor Mac1 from *Saccharomyces cerevisiae*. *J. Biol. Chem*. **273**, 23,805–23,811.
36. Jensen, L. T. and Winge, D. R. (1998) Identification of a copper-induced intramolecular interactions in the transcription factor Mac1 from *Saccharomyoces cerevisiae*. *EMBO J*. **17**, 5400–5408.
37. Graden, J. A. and Winge, D. R. (1997) Copper-mediated repression of the activation domain in the yeast Mac1p transcription factor. *Proc. Natl. Acad. Sci. USA*, **94**, 5550–5555.
38. Serpe, M., Joshi, A., and Kosman, D. J. (1999) Structure–function analysis of the protein-binding domains of Mac1p, a copper-dependent transcriptional activator of copper uptake in *Saccharomyces cerevisiae*. *J. Biol. Chem*. **274**, 29,211–29,219.
39. Peña, M. M., Koch, H. A., and Thiele, D. J. (1998) Dynamic regulation of copper uptake and detoxification genes in *Saccharomyces cerevisiae*. *Mol. Cell. Biol*. **18**, 2514–2523.
40. Eng Ooi, C., Rabinovich, E., Dancis, A., Bonifacino, J. S., and Klausner, R. D. (1996) Copper-dependent degradation of the Saccharomyces cerevisiae plasma copper transporter Ctr1p in the apparent absence of endocytosis. *EMBO J*. **15**, 3515–3523.
41. Zhu, Z., Jose, H., and Maria, D. (2002), in preparation.
42. Yongxing, W., Kwasi, A., Cremin, J., and Zhu, Z. (2002), in preparation.
43. Huibregtse, J. M., Engelke, D., and Thiele, D. J. (1989) Copper-induced binding of cellular factors to yeast metallothionein upstream activation sequences. *Proc. Natl. Acad. Sci. USA* **86**, 65–69.
44. Gralla, E., Thiele, D. J., Silar, P., and Valentine, J. S. (1991) ACE1, a copper-dependent transcription factor, activates expression of the yeast copper, zinc superoxide dismutase gene. *Proc. Natl. Acad. Sci. USA* **88**, 8558–8562.
45. O'Halloran, T. V. (1993) Transition metals in control of gene expression. *Science* **261**, 715–725.
46. Bhalla, U. P. and Iyengar, R. (1999) Emergent properties of networks of biological signaling pathways. *Science* **283**, 381–387.
47. Casaa, C., Aldea, M., Espinet, C., Gallego, C., Gil, R., and Herrero, E. (1997) The Aft1 transcriptional factor is differentially required for expression of high-affinity iron uptake genes in *Saccharomyces cerevisiae*. *Yeast* **13**, 621–637.
48. Stearman, R., Yuan, D. S., Yamaguchi-Iwai, Y., Klausner, R. D., and Dancis, A. (1996) A permease–oxidase complex involved in high-affinity iron uptake in yeast. *Science* **271**, 1552–1557.
49. Ito, T., Chiba, T., Ozawa, R., Yoshida, M., Hattori, M., and Sakaki, Y. (2001) A comprehensive two-hybrid analysis to explore the yeast protein interactome. *Proc. Natl. Acad. Sci. USA* **98**, 4569–4574.
50. Stark, M. J. (1996) Yeast protein serine/threonine phosphatases: multiple roles and diverse regulation. *Yeast* **12**, 1647–1675.

30

Comparative Analysis of Copper and Iron Metabolism in Photosynthetic Eukaryotes vs Yeast and Mammals

Sharon La Fontaine, Jeanette Quinn, and Sabeeha Merchant

1. INTRODUCTION

Copper and iron are essential micronutrients for all organisms because of their function as cofactors in enzymes that catalyze redox reactions in fundamental metabolic processes. Prominent examples of such enzymes include cytochrome oxidase in respiration, plastocyanin in photosynthesis, superoxide dismutase in oxidative stress, and ceruloplasmin in iron metabolism. Copper and iron carry out very similar functions in biology because both exhibit stable, redox-interchangeable ionic states with the potential to generate less stable electron-deficient intermediates during multielectron redox reactions involving oxygen chemistry. The major difference between copper and iron in biological systems derives from their individual ligand preferences and coordination geometries. The bioavailability of copper and iron is low so that organisms are faced with the challenge of acquiring sufficient copper and iron for cellular requirements while avoiding the buildup of levels that could lead to cellular toxicity. Over the last decade, it has become apparent that organisms have developed a suite of strategies to combat such challenges, so that an intricate balance between uptake, utilization, storage and detoxification, and efflux pathways for copper and iron exists.

A paradigm for copper and iron metabolism in eukaryotic cells has been developed through studies with the baker's yeast *Saccharomyces cerevisiae* (reviewed in refs. *1* and *2*). Genetic analysis of iron transport in *S. cerevisiae* has revealed a dependence of iron metabolism on adequate copper nutrition and this molecular connection has provided valuable insight into the basis for the well-established link between copper and iron nutrition in mammals. With the objective of comparing copper and iron metabolism in photosynthetic eukaryotes with that in yeast and mammals, this chapter summarizes the present state of knowledge of the relevant pathways in yeast and mammals, especially the basis for the copper–iron link, followed by a discussion of copper and iron metabolism in the model photosynthetic organisms *Arabidopsis thaliana* and *Chlamydomonas reinhardtii* and concludes with evidence for a copper–iron link in Chlamydomonas. The relevant pathways in other model organisms such as *Drosophila* and *Caenorhabditis elegans* will not be covered in this chapter, as our objective is to provide a background for comparison to plants rather than to embark on a comprehensive review of these processes in all model organisms.

From: Handbook of Copper Pharmacology and Toxicology
Edited by: E. J. Massaro © Humana Press Inc., Totowa, NJ

2. YEAST COPPER–IRON LINK

2.1. Copper

2.1.1. Uptake

In *S. cerevisiae*, high-affinity copper uptake is mediated by the *CTR1* and *CTR3* gene products (Ctr1p and Ctr3p, respectively) *(2–5)* and is associated with copper reductase activity of Fre1p and Fre2p to reduce Cu^{2+} to Cu^{1+} prior to uptake *(6,7)*. *CTR1*, *CTR3*, and *FRE1* are transcriptionally activated in response to copper deficiency by the copper-dependent transcriptional activator Mac1p *(2,8–10)*. Copper-dependent endocytosis of Ctr1p at low copper concentrations and degradation of Ctr1p in copper-replete cells provides an additional posttranslational level of regulation *(11)*. Three putative low-affinity copper-transport systems also have been described: Fet4p *(12)*, Smf1/Smf2 *(13,14)*, and Ctr2 *(15)*.

2.1.2. Distribution, Storage, and Regulation

Inside the cell, copper is bound by cytoplasmic copper chaperones and delivered to specific destinations within the cell. These chaperones include Cox17p, Lys7p, and Atx1p, for copper delivery to cytochrome oxidase in the mitochondria, cytosolic and mitochondrial superoxide dismutase, and the copper transporter Ccc2p in the secretory pathway, respectively *(2,16–20)*. Ccc2p is required for loading copper onto Fet3p, a multicopper oxidase, required for high-affinity iron transport across the plasma membrane *(21)*. The chloride-ion channel Gef1p, located in the same compartment, is also required for copper loading onto Fet3p *(22,23)*. Sco1p and Sco2p were identified as integral membrane proteins within the inner mitochondrial membrane and may be involved in the transfer of copper from Cox17p to cytochrome oxidase *(5,24,25)*.

With increased intracellular copper levels, copper-storage proteins such as the metallothioneins encoded by *CUP1* and *CRS5* are induced and sequester the copper *(8)*. Storage of copper in the vacuole may be an additional mechanism of preventing copper toxicity *(5)*.

Mac1p and Ace1p are the two copper-responsive transcriptional activators in *S. cerevisiae (2,9,10)*. Under copper-deficient conditions, Mac1p activates the expression of six genes, *CTR1, CTR3, FRE1, FRE7, YFR055w,* and *YJL217w*. With elevated copper levels, Ace1p activates the expression of copper-detoxification proteins, Cup1p and Crs5p.

2.2. Iron

2.2.1. Uptake

Iron uptake into *S. cerevisiae* involves several different assimilatory pathways depending on the chemical source of iron and its concentration. In general, all of the pathways require reduction of Fe^{3+} to Fe^{2+} by one or more products of the *FRE1–FRE7* genes *(14,26)*. Under iron-limiting conditions, high-affinity uptake is mediated by the inducible Fet3p/Ftr1p complex in the plasma membrane *(1,14,27)*. Fet3p is a multicopper oxidase *(28)* whose active sites are related to multicopper oxidases such as laccase, ascorbate oxidase, and ceruloplasmin. Fet3p functions to oxidize Fe^{2+} to Fe^{3+} at the cell surface; Fe^{3+} is then delivered from Fet3p to the associated Fe^{3+} permease, Ftr1p, for transport into the cell *(14,27)*. Highly related pathways operate in other fungi. In *Schizosaccharomyces pombe*, Frp1 is related to the Fre reductases, and Fio1/Fip1 forms an iron-uptake complex related to Fet3p/Ftr1p *(29)*. The fungal pathogen *Candida albicans* also uses a similar pathway, involving a surface-associated reductase, Cfl1p *(30)*, two Ftr1p-related permeases, CaFtr1 and CaFtr2 *(31)*, and a Fet3p-like component *(30)*. Expression of the permeases and their associated oxidases is regulated by iron nutritional status *(27,29)*, whereas some reductases are regulated by iron status and others by both copper and iron—the latter category functioning in both copper and iron assimilation *(10,14)*. Under iron-replete conditions, low-affinity systems, such as Fet4p,

with broad transition metal specificity *(12,32)*, or Smf1/Smf2, which were originally identified as manganese transporters *(13)*, operate. When iron is available in complex with siderophores, it can enter cells either through the Fet3p/Ftr1p complex after reduction by the Fre proteins and subsequent release of the iron from the siderophore, or if the Fet3p/Ftr1p is inoperable, by the ARN family of siderophore transporters through an endocytic pathway *(33–38)*.

2.2.2. Distribution, Storage, and Regulation

Whereas the Fet3p component of iron assimilation is conserved from yeast to man, the mechanism of iron storage appears diverse. *S. cerevisiae* lacks genetic information for ferritin *(8)*; rather, iron (with other ions) is stored in the vacuole *(39,40)*. A homolog of the oxidase–permease complex Fet3p/Ftr1p, designated Fet5p/Fth1, was localized to the vacuole and proposed to function under iron starvation conditions to mobilize stored iron from the vacuole *(41)*.

Another key organelle in iron metabolism is the mitochondrion. Not only is it an important target site for iron utilization, but it is also a major player in the maintenance of cellular iron homeostasis. Yfh1p regulates mitochondrial iron accumulation, possibly at the level of efflux *(42,43)*, Ccc1p limits mitochondrial iron uptake *(44)*, Nfs1p is involved in maintaining or synthesizing cytosolic Fe–S proteins *(45,46)*, Atm1p is a transporter of the inner mitochondrial membrane *(47)*, and Ssc2p is a protein of the Hsp70 class of chaperones with a role in Yfh1p maturation *(48)*. Although there are as yet no defined chaperones for the delivery of iron to specific intracellular targets, the IscA family of proteins are candidates for iron delivery to sites of iron–sulfur cluster assembly *(49)*.

Iron uptake in *S. cerevisiae* is regulated in response to cellular iron levels via the iron-responsive transcriptional activator Aft1p. Under iron-limiting conditions, Aft1p-mediated activation leads to induction of *FRE1, FRE2, FTR1, FET3, FET5*, and *FTH1*, as well as the induction of expression of the genes involved in copper transport, *CCC2* and *ATX1 (8)*. A further level of regulation of iron uptake exists that is mediated through Tpk2, a catalytic subunit of the yeast A kinases (PKA) *(50)*. According to the proposed model, during fermentative growth on glucose Tpk2, activated by cAMP, represses genes involved in iron uptake, but as the glucose is depleted, Tpk2 activity is inhibited, thus relieving the repression of the iron-transport genes. This derepression allows iron transport into the cell for incorporation into respiratory enzymes and permits growth on nonfermentable carbon sources.

2.3. Copper–Iron Link

In *S. cerevisiae*, the copper–iron link is evident at both the level of protein biosynthesis and function and at the level of gene regulation. Copper is required for the assembly and function of the high-affinity Fet3p/Ftr1p iron-uptake complex, and thus for high-affinity iron uptake. Therefore, *S. cerevisiae* cells that are copper deficient are also iron deficient. The iron-uptake genes are regulated as a function of iron availability, so that the expression of these genes is activated in cells that are starved for iron. Because the Fre1 reductase functions in copper and iron uptake, its expression is induced by both copper and iron deficiency, whereas the copper-transport genes (*CCC2* and *ATX1*), whose activity is critical for the production of functional iron-uptake proteins, are induced by iron deficiency, but not by copper deficiency *(51–54)*. In addition, in *S. pombe*, a copper-responsive transcription factor, Cuf1, activates *CTR4* gene expression for copper uptake under copper-starvation conditions while mediating repression of the iron-uptake genes under these same conditions to prevent futile expression of these genes when there is insufficient copper cofactor available to produce functional iron-uptake proteins *(55)*. Therefore, an intricate system of interplay among transport, storage, chaperone and regulatory proteins exists to maintain copper and iron homeostasis in *S. cerevisiae* and *S. pombe*.

3. MAMMALIAN COPPER–IRON LINK

Although evidence for a physiological link between copper and iron metabolism in mammals was elucidated approximately 75 yr ago *(56,57)*, the molecular basis for such a link is only now beginning

to unfold. The discovery of ceruloplasmin *(58)*, the ceruloplasmin homologs Fet3p in yeast *(28)* and Hephaestin in mice *(60)* and a role for all of them in iron metabolism have been pivotal in furthering our understanding of the copper–iron connection in mammals *(1,59)*.

3.1. Copper

3.1.1. Absorption

The first step in the proposed scheme for copper transport through the body is the absorption of dietary copper through the intestinal mucosa *(61,62)*, although the precise mechanism of copper absorption is not known. A candidate protein for copper uptake into intestinal cells is hCtr1, a homolog of the yeast high-affinity copper transporter Ctr1p *(63)*. Recently, the mouse homolog was shown to be essential *(64)*. Inside the cell, copper is likely to be bound by the human counterparts of the yeast intracellular copper chaperones, Atox1 (Hah1), hCox17, and hCCS, for copper delivery to the secretory pathway, mitochondria, and Cu/Zn-superoxide dismutase (SOD), respectively *(5,17,18,65–67)*. In intestinal enterocytes and the majority of nonhepatic cells, Atox1 delivers copper to the Ccc2p homolog, the Menkes protein (MNK) located at the trans-Golgi network (TGN) *(66)*. MNK, in turn, transports copper into the TGN lumen for incorporation into copper-dependent enzymes that are transported by the secretory pathway, such as lysyl oxidase *(68)*. An additional role of MNK is in the efflux of excess copper from the cell, which is achieved through a mechanism whereby copper concentrations above a certain threshold level stimulate a steady-state shift in the distribution of MNK from the TGN to the plasma membrane *(69,70)*. Under normal steady-state conditions, MNK continually recycles between the TGN and plasma membrane *(71,72)*. Therefore, MNK located at the basolateral surface of intestinal epithelial cells may also serve to transport copper across the basolateral membrane into the bloodstream.

3.1.2. Distribution

Albumin, the major copper carrier in the circulation, transports copper via the portal blood to the liver *(73)*. Here, the MNK counterpart and homolog of Ccc2p, the Wilson protein (WND), is also located at the TGN and relocalizes in elevated copper to an unidentified vesicular compartment, possibly en route to the biliary canalicular membrane *(74–76)*. In the liver, WND functions to excrete the excess copper into the bile *(77)* and to transport much of the copper that enters hepatic cells into the TGN lumen for incorporation into ceruloplasmin *(78)*. The ceruloplasmin holoenzyme, which contains six copper atoms *(79)*, is secreted from the liver and carries > 95% of total serum copper for delivery to tissues *(80)*. In addition, ceruloplasmin, via its ferroxidase activity, mediates iron release from the liver, also for delivery to tissues *(81)*.

3.1.3. Regulation

In mammals at a whole-body level, copper absorption from the small intestine is, to some extent, regulated, with increased uptake when the animal is copper deficient and decreased uptake when the diet is adequate in copper *(82)*. Details of the molecular mechanisms regulating absorption remain to be elucidated. The control of copper excretion, which is also an important part of the protection against excess copper exposure, is regulated by the liver, with excess copper being disposed of through the bile *(83)*. Within the cell, excess copper is detoxified by at least two mechanisms; sequestration by metal-binding proteins such as metallothioneins (MT) and enhanced export by the copper ATPases, MNK, and WND *(84)*. Although a definitive biological role for MTs remains elusive despite years of research, MTs are known to be small cysteine-rich proteins that bind heavy metals, including copper, zinc, and cadmium, through cysteine thiolates *(85,86)*. There are 17 genes encoding four isoforms of mammalian MTs (MT-1 to MT-4), each of which have subtypes. Induction of MT synthesis occurs at the level of transcription by heavy metals themselves (Zn^{2+}, Cu^{2+}, and Cd^{2+}) through metal-regulatory elements (MREs) tandemly arranged within the 5´ flanking regions of MT genes *(87,88)*. In contrast, the regulation of copper export by MNK and WND occurs at a post-translational and enzymatic level that couples copper efflux to the intracellular copper concentration *(69,74,75,77)*.

3.2. Iron

3.2.1. Absorption

The current model of iron uptake and utilization begins with the absorption of iron from nutritional sources across the intestinal epithelium. Iron, taken into the body as Fe^{3+}, is reduced to Fe^{2+} by Dcytb and perhaps other as yet unidentified ferrireductases and transported across the apical surface of enterocytes lining the gut by the divalent metal-ion transporter DMT1 (DCT1, Nramp2) *(89–92)*. The HFE protein has a role in regulating intestinal iron absorption *(91,93,94)*. HFE associates at the cell surface with β_2-microglobulin and the transferrin receptor, but the significance of these associations remains to be fully elucidated *(91)*. However, the discovery of a reciprocal regulation of HFE and DMT1 *(95)* led to the proposal that HFE regulates trafficking of DMT1 to the plasma membrane and therefore iron uptake, depending on cellular iron concentrations *(96)*. Inside the cell, Fe^{2+} is incorporated into iron-containing proteins, bound to ferritin for storage and detoxification, or it is directed to the mitochondria for heme synthesis and assembly of nonheme iron proteins (97). The Frataxin protein regulates mitochondrial iron accumulation although its precise function remains to be defined *(1)*. Although chaperones for delivering iron to intracellular targets are believed to exist, these putative chaperones have not been identified *(98)*.

3.2.2. Distribution

Iron also is transported across the basolateral surface of enterocytes into the blood for transport throughout the body. This export of iron from the enterocyte is mediated by a basolateral transporter Ferroportin1 *(99)*/IREG1 *(100,101)*, although the species of iron transported has not been established. Iron is carried throughout the body, fulfilling the physiological iron requirements of cells and tissues, bound to the plasma protein transferrin. The loading of iron onto transferrin requires oxidation from Fe^{2+} to Fe^{3+}, which may be mediated by either or both of the multicopper ferroxidases, Hephaestin and ceruloplasmin. Hephaestin may act together with Ferroportin1 at the basolateral surface of enterocytes to oxidize Fe^{2+} to Fe^{3+} prior to export into the plasma *(102)*. Alternatively or in addition, plasma ceruloplasmin oxidizes Fe^{2+} to Fe^{3+} subsequent to export into blood plasma for loading onto transferrin. An additional important role of ceruloplasmin is the mobilization of iron from tissues such as the liver where ceruloplasmin is synthesized *(59)*. In cells other than those of the intestine, iron is taken up bound to transferrin. The transferrin receptor at the cell surface binds diferric transferrin and is internalized and taken up into endosomes *(103)*. The Fe^{3+} is released from transferrin into the acidified endosome and reduced to Fe^{2+} *(97)*, followed by transport into the cytoplasm by DMT1 *(89,104)*.

3.2.3. Regulation

The regulation of intestinal iron uptake is mediated through iron-dependent transcriptional and translational control of DCT1 *(105)*. The iron concentration within the cell is controlled by reciprocal regulation of ferritin and the transferrin receptor at the posttranscriptional level. This regulation is mediated by iron-regulatory proteins (IRPs) 1 and 2 that bind iron-responsive elements (IREs) located in the 5' and 3' untranslated regions of ferritin and transferrin receptor mRNAs, respectively, to modulate the amount of each protein that is produced based on the cellular iron status *(90,91,97,106–108)*. IREs or IRE-like elements have been identified in the UTRs of other proteins, including an IRE-like element within the 5' UTR of the IREG1 mRNA and the 3' UTR of DMT1 mRNA *(90,91,106)*, but regulation of DMT1 and IREG1 by mechanisms involving this element have not been characterized.

3.3. Copper–Iron Link

Although the existence of a copper–iron link was documented in nutritional studies many decades ago, the discovery of the molecular basis for this link is relatively recent. In particular, the multicopper ferroxidases form the basis of the copper–iron connection. Ceruloplasmin is central to interorgan copper and iron metabolism. The copper atoms carried by ceruloplasmin not only serve to satisfy the

copper requirements of body tissues but are also critical for its catalytic function as a ferroxidase for iron mobilization and release from the liver for transport around the body. The assumption is that copper is also critical for the ferroxidase function of Hephaestin, mediating iron absorption from the small intestine into the bloodstream. Hence, iron metabolism is critically dependent on copper both at the level of absorption from dietary sources and transport around the body.

Clearly, there are parallels between the yeast and human copper–iron transport systems that extend to the fact that the dependence of iron metabolism on copper has been maintained over a vast evolutionary distance. Many of the metabolic catalysts are conserved, such as Atx1p/Atox1, Ccc2p/Menkes–Wilson ATPases, Fet3p/ceruloplasmin–Hephaestin, Yfh1p/Frataxin, Ctr1p/hCtr1, Cox17p/hCox17, Lys7/CCS, and the Sco proteins; yet others are distinct between yeast and man, such as Ftr1p vs IREG1 or DMT1, and Dcytb vs the Fre reductases.

4. COPPER–IRON LINK IN PHOTOSYNTHETIC ORGANISMS

Besides having the same copper and iron requirements as human and yeast cells, photosynthetic organisms have additional requirements for these metals in the plastid, where they are utilized as the redox active cofactors in many metabolic processes, including, in particular, the proteins involved in photosynthetic electron transfer in the chloroplast. Iron-containing cytochromes, Fe–S centers (>20 atoms per PSII/PSI unit), and copper-requiring plastocyanin are abundant proteins in photosynthetic organisms. Metal metabolism in this context presumably requires a completely separate set of factors in addition to those required for cellular and mitochondrial iron and copper metabolism. A further challenge for photosynthetic organisms is that biologically useful levels of soil copper and iron are low. The variability in the mineral composition of soils means that for plants to survive and grow they must adapt to the variation in supply of copper and iron. As with yeast and humans, the essential elements of copper and iron metabolism include transport, storage and detoxification, and utilization. The transport process can be further subdivided into reduction, uptake, and intraorganellar and intracellular transport. The storage and detoxification of copper and iron may involve not only sequestration by cellular proteins but also compartmentalization into vacuoles and plastids, which, in turn, requires proteins for transport into these compartments. Most of our knowledge about copper and iron metabolism in photosynthetic organisms comes from studies on the vascular plant *Arabidopsis thaliana*, the unicellular green alga *Chlamydomonas reinhardtii*, and the cyanobacterium *Synechocystis* 6803, which serves as a model for chloroplast biology. The biology of metal metabolism in these organisms is ripe for study because the mechanisms of copper and iron homeostasis in photosynthetic organisms are less well characterized than in humans and yeast.

4.1. Arabidopsis

Arabidopsis thaliana is a small weed in the mustard family, formally known as the family Brassicaceae. It has become an invaluable tool for studying plant physiology, biochemistry, development, and molecular genetics, and joins organisms such as *Escherichia coli*, yeast, *Drosophila*, *Caenorhabditis elegans*, and mice as vehicles for providing insight into fundamental biological processes.

4.1.1. Copper: Transport and Distribution

Copper assimilation and its regulation in plants is largely uncharacterized. Two approaches are commonly used: the identification of genes or expressed sequence tags (ESTs) encoding metal transporters based on sequence relationships, and functional complementation of well-characterized *S. cerevisiae* mutants.

4.1.1.1. COPT1

One of the first Arabidopsis genes encoding a copper transporter to be identified by the latter approach was *COPT1*, which encodes a highly hydrophilic protein that was capable of rescuing a *S. cerevisiae ctr1* strain defective in high-affinity copper uptake *(15)*. In copper-replete plants, *COPT1*

Table 1
Copper Transporters, Chaperones, and Homeostasis Factors in *Arabidopsis thaliana*

Gene	*Homolog*	*Putative function*	*Experimental evidence*	*Reference/ accession*
COPT1	Functional homolog of *S. cerevisiae CTR1*	Copper transporter; distributive	Rescues *S. cerevisiae ctr1* mutant	*15*
COPT1 homologs	*COPT1*	*Copper transporter*	Based on sequence similarity	CAB51175 chromosome 2, section 151
RAN1	Wilson/Menkes proteins, *S. cerevisiae CCC2*	ATP-dependent intracellular copper transporter	Rescues *S. cerevisiae ccc2* mutant	*110*
RAN1 homolog	*RAN1*	ATP-dependent copper transporter	Based on sequence similarity	AAF19707
PAA1	Wilson/Menkes proteins, *Synechococcus PacS*	ATP-dependent copper transporter in plastid	Based on sequence similarity	*111,112*
COX17 homologs	Yeast, mammalian *COX17*	Copper chaperone *(cytochrome* oxidase assembly factor)	Based on sequence similarity	*113* BAB02169 chromosome 1 and BAC F8L10
CCS1 homologs	Yeast *LYS7*, mammalian *CCS1*	Cu/Zn-SOD copper chaperone	Rescues *lys7* mutant; binds metal	*114* AF061517 AF179371 BE038022
CCH	Yeast *ATX1*, mammalian *ATOX1*	Copper chaperone	Rescues *S. cerevisiae atx1* mutant	*115*
CutA homolog	*E. coli CutA*	Copper homeostasis protein; plastid localization	Binds copper; is imported into plastids	AF327524 *112,116*
SCO1 homolog	Yeast, mammalian *SCO1*	Copper transport	Based on sequence similarity	AAF07830
COX11 homolog	Yeast, mammalian *COX11*	Cytochrome oxidase Cu_B center assembly factor; possible copper chaperone	Based on sequence similarity	AAG00893

is expressed in flowers, stems, and leaves, but not in roots *(109)*, suggesting that the gene product might function in distribution rather than in assimilation. The expression of *COPT1* in copper-deficient plants has not yet been analyzed. Two sequences, highly related to *COPT1*, are evident in the complete genome of Arabidopsis; the genes seemed to be expressed, but their function in metal metabolism has not been determined (Table 1). Perhaps one of these may represent an assimilatory pathway component. Two less closely related sequences that are not known to be expressed also were identified.

4.1.1.2. RAN1 and the CPX Family of Metal Transporters

The family of ethylene receptors comprises an important function for copper in plants. These molecules use copper as a cofactor at the binding site for this gaseous plant signaling molecule *(117)*. Genetic analysis of the ethylene signaling pathway in Arabidopsis led to the identification of the *RAN1* locus, which encodes a copper transporter related in sequence and in function to *CCC2* of *S.*

cerevisiae (118,119). In plants, RAN1 is proposed to function by analogy to Ccc2p to load copper proteins such as the ethylene receptors. Phenotypic analysis of a strong *ran1–3* allele suggests that RAN1 may function also to load copper proteins in addition to the ethylene receptors.

A homolog of RAN1 has been annotated in the Arabidopsis genome as a copper-transporting ATPase, but its functional relationship to RAN1 is not known (Table 1). The occurrence of highly related sequences in the EST database for other plant species suggests that the RAN1 homolog is expressed. Williams and co-workers *(120)* have noted that the Arabidopsis genome encodes additional CPx-type metal-transporting ATPases, including PAA1 identified previously as a putative plastid-localized copper transporter *(111)*, HMA1 and HMA4, and more recent database analyses reveal yet more sequences in this family. A reverse genetic approach to their study should add much to our knowledge of plant metal-transport mechanisms.

In the meantime, cyanobacteria, which are useful models for chloroplast biology, have been used to deduce a role for CPx-type transporters in metal delivery to the plastid *(121–125)*. Two such proteins, PacS located in the thylakoid membrane *(121)* and CtaA *(122)*, were found to be required for copper delivery to plastocyanin in the thylakoid lumen, and by analogy, these authors proposed that similar proteins might function in the plastid thylakoid membrane and envelope, respectively, for delivery to plastid copper enzymes *(125)*. PAA1 is one good candidate for a plastid-localized copper transporter *(111)*. Synechocystis mutants disrupted for PacS and CtaA function displayed an increased requirement for iron *(125)*, suggesting a connection between copper and iron metabolism in this organism and, perhaps by extension, in plastids as well (*see* Section 4.2.).

4.1.1.3. Copper Chaperones

A copper metallochaperone, designated Atx1, was recently identified in *Synechocystis* PCC6803 and shown to interact with the CtaA copper importer to acquire and then deliver copper to the PacS copper ATPase (*125a*). An Arabidopsis homolog of a copper chaperone (mammalian *ATOX1* and Saccharomyces *ATX1*) was identified as a gene that was upregulated during senescence (Table 1). This gene, called *CCH*, can functionally complement an *atx1* mutant yeast strain for both antioxidant and copper-chaperone activity *(115)*, and the encoded protein may also function in intercellular copper transport in plants *(126)*. Because *CCH* is induced during senescence, a role in sequestering copper following degradation of copper-containing proteins has also been proposed. *RAN1* is upregulated during leaf senescence as well, suggesting that CCH and RAN1 may function together to recycle copper during senescence *(127)*. Genes encoding functional metallothioneins had been identified previously in *A. thaliana (128)*. One of these, *MT1*, is induced during leaf senescence and also in leaves with higher than normal copper concentrations, whereas another, *MT2*, is expressed in leaves prior to senescence. It is suspected that these metallothionein-like proteins may function in copper homeostasis to prevent copper toxicity from copper released during degradation of senescing leaf proteins *(127)*.

Homologs of two other copper chaperones, Cox17p and Lys7p/CCS1, also are found in the Arabidopsis genome (Table 1). CCS1, which binds metal *(114)*, is proposed to be targeted to the plastid as is appropriate because Cu,Zn-SOD is present in this organelle in plants. These homologs can complement the appropriate Saccharomyces mutant, suggesting that the pathways for copper delivery are conserved between plants, mammals, and fungi, but it should be noted that their function and subcellular localization in plants has not yet been studied. It is certainly possible that the plant homologs have analogous rather than homologous functions. Genome analysis has revealed Sco1 and Cox11 homologs as well (Table 1), but these have not been subject to experimental analysis at any level.

A number of other sequences and putative open reading frames with the chaperone-like metal-binding site MxCxGC (or simply a CxxC metal-binding site) can be found in the Arabidopsis genome. One family of these proteins has been characterized and consists of C-terminal prenylated proteins that bind transition metals *(129)*. Because these proteins might be membrane associable, one hypoth-

esis is that they may function in copper delivery to extracellular plasma membrane or secreted copper proteins. Another possibility is that they might be involved in some other aspect of metal homeostasis, such as metal sequestration for resistance.

4.1.2. Iron: Acquisition and Storage

4.1.2.1. Copper-Idependent Acquisition

All plants must extract iron from insoluble Fe^{3+} complexes in the soil and convert it to the more soluble Fe^{2+} form for transport into the cell. Two types of iron acquisition mechanisms have been described for plants: Strategy I and Strategy II. Neither pathway seems to require a copper-containing ferroxidase as noted for animals, fungi (*see* Sections 2.2. and 3.2.) and algae (*see* Section 4.2.2.). Nevertheless, the mechanisms of iron movement within the plant, from the roots to the shoots, is not well characterized at the molecular level, and there is some indication that copper deficiency can cause a localized iron deficiency. Therefore, a connection with copper may yet be discovered.

In Strategy I plants (dicotyledons and nongraminaceous monocotyledons), Fe^{3+} is released from chelates by reduction and Fe^{2+} is taken up by a Fe^{2+}-specific transporter. A putative ferric chelate reductase-encoding gene, *FRO2*, was identified on the basis of its relationship to yeast (*FRE*) and mammalian (gp91phox) homologs *(130)*. *FRO2* is upregulated in iron deficiency and complements *frd1* mutants. Roots of the *frd1* mutants display impaired ferric chelate reductase activity and iron uptake *(131,132)*; hence *FRO2* is a key component of iron assimilation. Several homologs of *FRO2* are found in the Arabidopsis genome (Table 2); their function is not known yet but it is assumed that they participate in iron assimilation or distribution within the plant. A cytochrome-b_5 reductase, encoded by *NFR*, with Fe^{3+}-chelate reductase activity also was cloned from maize and a homolog was identified in Arabidopsis *(138)*. Because the protein is localized to the tonoplast, its role in assimilation is questioned, but a role in intracellular iron or copper homeostasis is still open *(140)*. Nevertheless, genetic evidence for NFR function in metal metabolism is not yet available. In addition to iron reduction, iron solubility in the rhizosphere is increased through activation of a specific H^+-ATPase. The gene *AHA2* encodes one member of a large family of H^+-ATPases in Arabidopsis; it is upregulated under iron deficiency and therefore assigned function in iron assimilation *(109)*.

Two types of iron transporters are known in plants: IRT1 and the NRAMP family (Table 2). IRT1 was identified independently by functional complementation of *S. cerevisiae fet3/fet4* or *smf1* mutants *(133–135)*, whereas the NRAMP family from plants was identified on the basis of their homology to fungal and mammalian NRAMPs and tested for function by complementation of *fet3/fet4* or *smf1 S. cerevisiae* mutants *(136,137)*. In Arabidopsis, *IRT1* is expressed in roots and is upregulated under iron-deficient growth conditions, implying a role in Fe uptake *(133)*. IRT1 is one member of a large family of divalent cation transporters called the ZIP family that is distributed widely in nature *(135)*. The NRAMP family of transporters *(120)*, including NRAMP 1, 3, and 4, is also implicated in iron assimilation by virtue of their increased expression in iron-deficient plants and their ability to rescue *fet3/fet4* mutants *(136,137)*. Both the IRT1 and NRAMP type of transporters seem to have broad metal specificity for divalent, cations but their physiological specificity may well be more narrow. Because both types of transporters take up Fe^{2+}, a role for a ferroxidase (as in mammals, fungi, and algae) is not evident.

The Strategy II iron acquisition mechanism is found in grasses (graminaceous monocotyledons). The roots of these plants secrete phytosiderophores which chelate Fe^{3+}, and a siderophore transporter, YS1, takes up the resulting complex *(139,141)*. YS1, which was cloned from an *Ac*-tagged *ys1* allele, belongs to the major facilitator superfamily. The mutants display interveinal chlorosis that can be rescued by direct application of iron to the leaves or via the xylem after the roots are excised *(142)*. Like the enzymes involved in phytosiderophore biosynthesis, iron–phytosiderophore uptake is induced under iron-deficient conditions through increased expression of the *YS1* gene. Arabidopsis contains 8 *YS1*-like genes, designated *YSL1* through *YSL8*, but whether they all function in siderophore metabolism remains to be determined *(139)*.

Table 2
Iron Assimilation Components in *Arabidopsis thaliana*

Gene	*Homolog*	*Function*	*Experimental evidence*	*Reference*
IRT1	ZIP family	Iron transporter	Rescues *S. cerevisiae ftr3/4*double mutant; expressed in roots; induced in Fe deficiency	*133–135*
Nramp1, Nramp3, Nramp4	Nramp family	Iron transporters	Rescues *S. cerevisiae ftr3/4* double mutant; increase in mRNA accumulation in Fe deficiency	*136,137*
FRO2	*S. cerevisiae FRE1, S. pombe FRP1,* and mammalian gp91phox	Iron-chelate reductase	Increased accumulation of *FRO2* mRNA in Fe deficiency; complements *frd1* mutant	*130*
FRO2 homologs	*FRO2*	Iron-chelate reductases	Based on similarity to *FRO2*	*130*
NFR homolog	Maize *NFR*	Iron reductase	Based on sequence similarity	*138*
YSL1-8	Maize *YS1*	Siderophore uptake	Based on sequence similarity	*139*

4.1.2.2. Iron Storage

Iron is stored within plants in ferritin, which is localized in the plastids in the stroma *(143)*. Ferritin is found primarily in roots and leaves of young plants with much lower levels in mature plants *(144)*. The native molecule consists of 24 subunits of a single type of chain that is related to animal ferritin chains with an additional plant-specific N-terminal sequence in the mature protein known as the extension peptide. The plant ferritin chain has the iron oxidation site found in animal ferritin H chains and also the carboxylates of the L chain that are responsible for efficient mineralization of the core.

Ferritin has a storage function; it accumulates in seeds during maturation and is mobilized by degradation of the protein during germination *(141)*. The abundance of ferritin in the stroma of the plastid decreases as chloroplasts develop, and this corresponds to the movement of iron from the stroma to the thylakoid membrane where iron-containing electron-transfer proteins reside. Ferritin is found only at low levels in mature plants. When ferritin is incorrectly expressed in mature plants, it results in iron-deficiency chlorosis, confirming that ferritin sequesters iron and supporting the model that ferritin serves as an iron reservoir for iron supply to the photosynthetic apparatus in developing leaves *(145)*. Ferritins probably function also for transient iron storage (e.g., as is necessary during senescence or other situations where iron proteins are degraded) *(144)*. This might explain the anomalous finding that mRNAs encoding ferritin are upregulated during Fe deficiency; in Fe-deficiency-induced chlorosis, Fe might be released as PSI is degraded (*see* Section 4.2.2.2.). Thus, plant ferritin accumulation is regulated at the level of transcription in response to iron levels among other stimuli *(146)*. In soybean, transcriptional regulation is mediated by an iron-regulatory element (FRE) and iron-sensing trans-acting factor *(147)*, whereas in *A. thaliana* and maize, an iron-dependent regulatory sequence (IDRS) was recently identified within the promoter region of the respective ferritin genes (*AtFer1* and *ZmFer1*) and shown to be involved in iron-responsive transcriptional control *(148)*.

4.1.3. Copper–Iron Link

Evidence in support of a definitive link between copper and iron metabolism in vascular plants remains to be firmly established. It is well accepted that ferric reductase is specifically induced in response to iron deficiency. However, in pea plants, copper deficiency also stimulates elevated root ferric reductase activity, as well as rhizosphere acidification, another response that is induced by iron deficiency *(149,150)*. Cohen et al. *(149)* suggested that the copper–iron-deficiency-induced activity derives from a single ferric reductase enzyme and, furthermore, that the copper deficiency causes a localized iron deficiency in the plant, which consequently leads to induction of the ferric reductase activity, a scenario that parallels the human and yeast copper–iron link.

In Arabidopsis, iron deficiency leads to an increase in both ferric reductase activity and copper-chelate reductase activity at the root surface *(131)*. Both activities are absent in *frd1-1* mutants *(131)* and are restored in transgenic plants expressing *FRO2 (130)*. Although these data suggested that the ferric reductase can also reduce Cu^{2+} to Cu^{1+}, the accumulation of copper (as well as manganese and zinc) was not inhibited in *frd1-1* mutants, leading to the conclusion that other factors must be involved in regulating divalent cation influx *(131)*.

Much is still to be learned about the complex mechanisms underlying copper and iron homeostasis in plants, from uptake by the roots to transport into, and storage and utilization by the cells of the various plant tissues. Although molecular approaches to identify and functionally characterize plant genes and proteins are proceeding at a rapid pace, significant insights into plant metal metabolism also can be gained from studying other model photosynthetic organisms such as the unicellular green alga, *Chlamydomonas reinhardtii*.

4.2. Chlamydomonas

The unicellular green alga *Chlamydomonas reinhardtii* is also a genetically tractable organism that can be grown on very highly defined media consisting of simple salts, which facilitates studies involving trace micronutrients such as copper. Therefore, it has served as a model for the analysis of copper metabolism in the context of the photosynthetic apparatus. The organism grows heterotrophically as well as photoautotrophically, so that mutants affected in metal supply to the photosynthetic apparatus can be maintained and analyzed *(151)*. Under photoautotrophic conditions, the chloroplast is a sink organelle for metal micronutrients like copper and iron, whereas under heterotrophic conditions, copper and iron are distributed to both the mitochondrion as well as the plastid. The mechanisms for metal homeostasis involving the plastid are only beginning to be studied. The recent generation of an EST database for *C. reinhardtii* has provided an opportunity for comparative analysis of metal metabolism in this organism relative to plants and animals.

4.2.1. Copper: Adaptation to Deficiency

4.2.1.1. Plastocyanin vs Cytochrome-c_6

Chlamydomonas reinhardtii has provided a fascinating system for the study of biological compensation for copper deficiency since Wood (1978) *(152)* recognized that the organism remains photosynthetically competent in copper-deficient medium by replacing an abundant copper protein, plastocyanin, with an iron-containing cytochrome, cytochrome-c_6. Our laboratory has since discovered that this occurs through regulated proteolysis of apoplastocyanin (so that the protein is degraded in –Cu cells but accumulates as the holoprotein in +Cu cells), and transcriptional activation of the *Cyc6* gene (encoding cytochrome-c_6) *(153,154)*. Interestingly, the degree of transcriptional activation is proportional to the perceived copper deficiency *(155)*. In a fully copper-supplemented medium (> 400 n*M* for a late log-phase culture), the photosynthetic apparatus maintains several million molecules of plastocyanin per cell. When the medium copper concentration falls below the amount necessary to provide copper at this stoichiometry, the *Cyc6* gene is activated to the extent necessary to compensate for the loss of plastocyanin. Genetic analysis of plastocyanin mutants (*pcy* strains) demonstrated that the activation of the *Cyc6* gene responded to perception of copper levels rather than to the perception of holoplastocyanin deficiency because strains lacking plastocyanin (e.g., frame shift

or stop codon in the structural gene for preapoplastocyanin) still display copper-responsive *Cyc6* expression *(156,157)*. Therefore, a copper sensor must exist in this organism.

4.2.1.2. Copper Assimilation

In addition to the regulation of alternate (Cu vs Fe) carriers for the photosynthetic apparatus, there are other adaptations to copper deficiency. As is the case generally for nutrient deficiencies, an assimilatory pathway is activated in copper deficiency *(158)*. This pathway involves a reductase component and a transporter. Because the pathway is activated coordinately (with respect to medium copper concentration) with *Cyc6* expression, it is likely that the assimilatory components are downstream targets of the same signal transduction pathway. When medium copper content is measured in Chlamydomonas cultures grown in copper-deficient versus copper-sufficient or copper-excess conditions, one notes that there is no residual copper in the medium as long as this nutrient is below that required to fill the active site of all copper enzymes. Once the copper content of the medium exceeds that required to saturate the copper enzymes, net copper uptake ceases and the excess copper remains in the medium. The mechanism underlying this tight homeostatic control is not known. Is there a balance between an influx versus efflux transporter? Or is the uptake transporter regulated at multiple points (e.g., posttranslationally and also transcriptionally) to achieve this level of control? In this context it should be noted that activation of assimilatory pathways puts the organism at risk for toxicity when the nutrient is resupplied. Hence, it is reasonable to imagine multiple levels of control operating to balance intracellular copper levels in the face of deficiency on the one hand and overload on the other.

Chlamydomonas does not seem to have genetic information for metallothioneins and probably uses only phytochelatins for detoxification of copper, cadmium, mercury, and other heavy metals *(159–161)*, although it is possible that the metallothioneins of Chlamydomonas have not yet been discovered. Perhaps genomics will provide the answer to this question.

4.2.1.3 other targets

Three other plastid-localized enzymes are regulated by copper availability in Chlamydomonas: coproporphyrinogen oxidase (Cpx1) encoded by *Cpx1 (161)*, and two putative diiron enzymes encoded by *Crd1* and *Cth1 (162)*. The function of the latter is not known, but one possibility is that they are required for iron metabolism in the plastid. Because Chlamydomonas uses a multicopper oxidase for iron assimilation (*see* Section 4.2.2.), copper-deficient cells probably have to devise mechanisms for bypassing this step in order to remain iron replete. The existence of such mechanisms is evident from the finding that copper-deficient cells are not iron deficient *(158)*. Indeed, *crd1* mutants behave as if they exhibit a localized iron deficiency in the plastid. Crd1 and Cth1 are hypothesized to have similar functions, whereby Cth1 is used in copper-replete cells that are not iron challenged, whereas Crd1 is used in copper-deficient cells that may be adapting to a less effective iron-assimilating pathway owing to reduced plasma membrane ferroxidase activity.

Coprogen oxidase catalyzes a step in tetrapyrrole biosynthesis, leading to heme and chlorophyll in the plastid. The increased activity of coprogen oxidase in –Cu cells has been attributed to an increased demand for heme (e.g., for cyt-c_6 synthesis) in this situation. Nevertheless, this remains an unsatisfactory explanation because the fraction of the tetrapyrrole pool (various chlorophylls and hemes) in cyt-c_6 is very small. With the discovery of a copper-requiring enzyme in iron assimilation and the logical corollary of a copper-independent backup pathway operating in copper-deficient cells, one must re-evaluate the function of *Cpx1* in –Cu cells. Increased expression of the gene does not result in relocalization to a different compartment, such as the mitochondrion *(163)*. One possibility is that increased flux through the tetrapyrrole pathway draws iron into the plastid.

The EST database has revealed several other copper metabolizing proteins (Table 3). For some of these, the function can be predicted by analogy to the function of the homologs, but for others, such as CutA and CutC homologs, genetic analysis is required. In the meantime, expression studies and subcellular localization will provide some clues.

Table 3
Homologs of Copper Transporters, Chaperones and Other Copper-Metabolizing Factors in *Chlamydomonas reinhardtii*

Gene	*Homolog*	*Putative function*	*Experimental evidence*	*Accession*
Ccc2	Arabidopsis *Ran1*	Copper transport	Based on sequence similarity. Blast score (EST): vs *A. thaliana* RAN1= 1e-8; vs Menkes protein = 2e-6	BE761354
Atx1	Arabidopsis *CCH* and *S. cerevisiae Atx1*	Copper chaperone/ delivery for Ran1/Ccc2	Rescues *S. cerevisiae atx1* mutant; transcripts induced up to 6.5× in Fe deficiency. Blast score: vs *A. thaliana* CCH =3e-13 vs *S. cerevisiae* Atx1p = 8e-4	AF280056
Cox17	Human and Arabidopsis *Cox17* homologs	Copper chaperone for cytochrome oxidase assembly	Rescues *cox17* mutant weakly. Blast score: vs human Cox17 = 1e-11 vs *A. thaliana* = 2e-11 vs *S. cerevisiae* = 2e-4	AF280543
Sco1	Related to *S. cerevisiae Sco1* and its Arabidopsis homolog	Copper delivery to cytochrome oxidase	Based on sequence similarity. Blast score (EST): vs *A. thaliana* = 2e-30; vs *S. cerevisiae*/human = 5e-22	AV620545
Cox11	Related to *S. cerevisiae Cox11* and its Arabidopsis homolog	Cytochrome oxidase Cu_B center assembly factor	Based on sequence similarity. Blast score (BE129228): vs *A. thaliana* = 9e-29; vs human = 5e-31 vs *S. cerevisiae* = 2e-29	BE129228 AV631011
CutA	Arabidopsis, human *CutA*	Copper homeostasis protein	Based on sequence similarity. Blast score (EST): vs *A. thaliana* = 3e-36 vs human = 6e-26 vs *E. coli* CutA = 2e-19	BE237847
CutC	Human, *E. coli CutC*	Copper homeostasis protein	Based on sequence similarity. Blast score (EST): vs human homolog = 2e-37 vs *E. coli* CutA = 2e-28	AV387727

4.2.1.4. Hypoxic Expression of Copper-Deficiency Targets

Cyc6, *Cpx1*, *Crd1*, and *Cth1* are each regulated also by hypoxia *(162,164)*. A simple model to explain this observation is that hypoxic cells are copper deficient, but this was ruled out by demonstrating that hypoxic cells make holoplastocyanin *(165)*. Further, the expression pattern of these genes in response to –Cu vs $–O_2$ is not the same; *Cpx1* and *Crd1* are more strongly activated by hypoxia

than by copper deficiency, whereas the converse is true for *Cyc6*. Promoter analysis of *Cpx1* identified a hypoxia-responsive element that is not required for the nutritional copper response, strengthening the argument for separation of the two responses. For the *Crd1* gene, the hypoxic response is shown to be physiologically significant because the *crd1* mutant recapitulates the copper-deficiency chlorotic phenotype, indicating that Crd1 function is required for adaptation to hypoxia. The mechanism of hypoxia perception in Chlamydomonas and its relationship to copper sensing is not known, but insights may emerge when the molecular details of Crr1 (the copper response regulator, *see* below) are revealed. Because copper deficiency and hypoxia probably co-occur in nature, it may be that the ability to respond to either signal allows the organism to anticipate and, hence, adapt more rapidly to copper deficiency.

4.2.1.5. A Master Regulator

Genetic analysis of the nutritional copper sensor led to the identification of two mutants at the *CRR1* locus that are blocked in activation of all of the above genes (Eriksson and Merchant, unpublished). Because these genes are not activated by copper deficiency or by hypoxia in these mutants, it was concluded that Crr1 must be involved in both signal transduction pathways. Whether Crr1 functions also in mediating the response to copper toxicity has not been tested.

4.2.2. Iron: Assimilation and Deficiency

4.2.2.1. Iron Assimilation

As in other organisms, iron uptake by Chlamydomonas involves reductases *(158,166–168)*. The reductases are induced in iron deficiency and may be the same enzyme as that induced in –Cu cells *(158)*. The EST database does not reveal homologs corresponding to the Saccharomyces *FRE* genes nor to the Arabidopsis *FRO* genes, but a putative homolog of *NFR* has been identified (Table 4). It should be a simple matter to assess its role in metal metabolism by testing its expression in copper- or iron-deficient cells.

The discovery of a multicopper oxidase encoded by *Fox1* in Chlamydomonas with significant similarity to mammalian ceruloplasmin and hephaestin was startling *(169,170)*. First, it had been assumed that iron assimilation in Chlamydomonas was independent of copper because copper-deficient cells do not appear iron deficient. Second, multicopper oxidases have not previously been implicated in iron metabolism in plants. A role for the *Fox1* gene product in iron assimilation is suggested by its pattern of expression, which shows greater than 100-fold induction under iron-deficient conditions, the parallel expression of an Ftr1-like permease *(169)*, and the localization of Fox1 to the plasma membrane by Buckhout and co-workers *(170)*. Components potentially involved in loading the oxidase with copper, such as the Ccc2 transporter and the Atx1 metallochaperone homologs (Table 3), also are found in Chlamydomonas. The latter is induced under –Fe conditions, albeit not as strongly as *Fox1* and *Ftr1*. Ccc2 and Atx1 homologs of Chlamydomonas are more related to the plant homologs RAN1 and CCH, respectively, than to the human or Saccharomyces counterparts (Table 3). Ccc2 and Atx1 of Chlamydomonas and plants probably function to load a variety of copper-containing enzymes in the secretory pathway in addition to Fox1. In plants, RAN1 is required for loading copper into the active site of the ethylene receptor *(118)* and perhaps other enzymes as well. Loss of RAN1 is not lethal in the plant, probably because of the occurrence of a homolog (Table 1). In Chlamydomonas, Ccc2/Ran1 is likely to be required for loading Fox1, but there may also be other copper proteins that are substrates for Ccc2/Ran1.

4.2.2.2. Iron Deficiency

One of the characteristic symptoms of iron deficiency in a photosynthetic organism is the development of chlorosis (chlorophyll deficiency). When heterotrophic Chlamydomonas cells are transferred from the usual medium (18 μ*M* iron–EDTA) to iron-deficient medium (0.1 μ*M* iron–EDTA), photosystem I and light harvesting proteins are lost (Moseley, et al., unpublished). Iron assimilation components are activated prior to development of chlorosis, which occurs only if assimilatory mechanisms remain

Table 4
Homologs of Iron Transporters and Iron-Metabolizing Enzymes in *Chlamydomonas reinhardtii*

Gene	*Homolog*	*Putative function*	*Experimental evidence*	*Reference/ accession*
Fox1	Related to mammalian ceruloplasmin and Hephaestin	Ferroxidase required for iron assimilation or distribution	Transcripts induced up to 400× in Fe deficiency; plasma membrane localized Blast score: vs hephaestin =1e-131 vs ceruloplasmin =1e-113	Unpublished; *170*
Ftr1	Related to *C. albicans* CaFtr1	Fe^{3+} transporter	Transcripts induced up to 230× in Fe deficiency; 2× RExxE motifs in cDNA Blast score (partial cDNA sequence): vs *C. albicans* CaFtr1 =4e-10	Unpublished
Fer1	Related to plant and animal ferritins	Iron storage in plastid	Based on sequence similarity; increased expression in Fe deficiency. Blast score (assembled sequence): vs *A. thaliana* ferritin 1 =7e-47 vs Xenopus ferritin H chain 2 = 4e-30	AV632653 AV619384 BE227588 AV623127 AV395232
Nramp homolog	Arabidopsis *Nramp*	Divalent metal ion transport	Based on sequence similarity. Blast score (assembled sequence): vs *A. thaliana* NRAMP1 = 4e-22	AV625564 AV389837 BE452312 BE452998
IscA1	*Azotobacter vinelandii IscA*	Iron–sulfur cluster assembly	Based on sequence similarity. Blast score (assembled sequence): vs *A. vinelandii* IscA = 2e-22	AV618923 AW721159 BE725819 BE725818 BE726308 BE726307
IscA2	*Azotobacter vinelandii IscA*	Iron–sulfur cluster assembly	Based on sequence similarity. Blast score (assembled sequence): vs *A. vinelandii* IscA = 9e-94	AV636381 AV633541 AV386551 BE725609
IscU	*Pseudomonas aeruginosa IscU*	Iron–sulfur cluster assembly	Based on sequence similarity. Blast score (assembled sequence): vs *P. aeruginosa* IscU = 2e-46 vs *A. thaliana* homolog = 1e-55	AV397853 AV619693 AV620447 AV624765 AV623500 AV623764 AV623473 AV638761 AV621762 AV625355

inadequate because of limited iron nutrition. It is possible that the threshold for cellular responses (such as activation of Fox1) and organelle responses (such as degradation of chlorophyll proteins) is different and/or that separate iron sensors occur in each compartment.

Paradoxically, the *Fer1* gene, encoding a plastid ferritin, is also induced in iron-deficient cells. Because ferritin has an iron-storage function, the increase in its mRNA in –Fe cells is counterintuitive. Two models have been offered to explain this observation; first, that increased ferritin might allow the cell to handle overload when iron is resupplied to the deficient cells. However, this model does not sit well when one considers that ferritin overexpression causes iron deficiency. It is more likely that ferritin may serve to buffer iron as it is released from degrading PSI and recycled to other compartments (such as the mitochondrion). This model is supported by the finding that iron deficiency impacts the chloroplast more severely than it does respiration. It also is compatible with the increase in *Fer1* gene expression in degreening N-starved Chlorella cells *(171)*.

4.2.2.3. Iron Metabolism Components

Based solely on BLAST searches, other candidates for iron-metabolizing components have been identified in Chlamydomonas (Table 4). These include components required for assembly of iron–sulfur clusters (*Isc* genes) and candidate metal transporters (*Nramp*). Comparison of Chlamydomonas metal-metabolizing components with those of plants and animals leads us to wonder whether Chlamydomonas is half beast/half plant. Some components have their closest homologs in mammals, such as the ferroxidase, whereas others have their closest homolog in plants, such as Ccc2/Ran1.

4.2.3. Copper–Iron Link

Unlike yeast cells, wild-type copper-deficient Chlamydomonas cells do not exhibit symptoms of iron deficiency (chlorosis in the case of photosynthetic organisms) when grown under copper-deficient conditions. In fact, copper-deficient and copper-supplemented Chlamydomonas cells grow equally well *(162,169)*. This suggests that either a copper–iron link equivalent to that established for yeast and mammals does not exist in Chlamydomonas or, alternatively, that this organism has backup systems that function when the copper-dependent iron uptake/metabolism is compromised. Our recent results (Section 4.2.2.) with iron-responsive expression of putative iron metabolizing proteins further supports the idea that copper-requiring components are required for iron metabolism in Chlamydomonas.

A survey of copper and iron proteins reveals several reactions for which both copper- and iron-containing proteins are known. Key examples are hemocyanin/hemoglobin, cytochrome oxidase/alternative oxidase, Cu,Zn-SOD/Fe-SOD, copper/heme nitrite reductases, membrane–methane monooxygenase/soluble methane monooxygenase, plastocyanin/cytochrome-c_6. The copper enzymes are believed to be more recent additions to the biochemical repertoire relative to iron enzymes *(172)*. The similarity in catalytic ability between copper and iron enzymes raises the question of whether the substitution of a copper enzyme with a "backup" iron version might represent a general metabolic adaptation to copper deficiency. Azurin and cytochrome-c_{551} in *Pseudomonas aeruginosa* form a pair analogous to plastocyanin and cytochrome-c_6, and it has been suggested, although not documented in vivo, that they might function interchangeably. A fascinating example of another pair of iron and copper proteins became known more recently following the discovery that a membrane-bound methane monooxygenase is a multicopper oxidase *(173)*. The enzyme catalyzes the hydroxylation of methane to methanol using O_2 as a substrate. A soluble version of this enzyme is well characterized and contains a diiron active site *(174)*. Some methanotrophic bacteria have both types of enzymes, and which one is used depends on copper availability in the medium, with control being effected by transcriptional regulation *(175)*. When copper is available, transcription of the gene encoding the diiron-hydroxylase is repressed, whereas synthesis of the copper enzyme is stimulated. The copper enzyme is the protein of choice when both copper and iron are available. The retention of genetic information for the diiron enzyme implies that both must be required in the natural environment; in a hypoxic environment, Cu^{1+} might be lost in insoluble precipitates, but Fe^{2+} might be more

readily available. As mentioned earlier, in Chlamydomonas, the copper-deficiency responses can be mimicked by hypoxia *(164)*. One explanation for this is that oxygen deficiency signals incipient copper deficiency and the response to hypoxia allows the organism to anticipate and, hence, survive copper-deficient conditions.

5. CONCLUDING REMARKS

Studies of copper–iron crosstalk in photosynthetic organisms are still in their infancy and many issues remain to be addressed. The full extent of the putative backup system for iron metabolism in copper-deficient Chlamydomonas must be elucidated. In an organism designed to undertake two fundamental metabolic processes (respiration and photosynthesis), the existence of such a backup system would appear to represent a shrewd evolutionary development. Does such a system also exist in vascular plants? With the current data explosion derived from complete genome sequences, EST databases, and microarray expression analysis, the resolution of such fundamental issues ought to be attainable in the very near future.

ACKNOWLEDGMENTS

The authors would like to thank Janette Kropat for helpful comments. This work is supported by grants from the National Institutes of Health (GM42143) (S.M.), the Australian Research Council International Researcher Exchange scheme (X00001622) (S.L. and S.M.), and a National Health and Medical Research Council R. Douglas Wright Fellowship (S.L.).

REFERENCES

1. Askwith, C. and Kaplan, J. (1998) Iron and copper transport in yeast and its relevance to human disease. *Trends Biochem. Sci.* **23**, 135–138.
2. Labbe, S. and Thiele, D. J. (1999) Pipes and wiring: the regulation of copper uptake and distribution in yeast. *Trends Microbiol.* **7**, 500–505.
3. Dancis, A., Haile, D., Yuan, D. S., et al. (1994) The *Saccharomyces cerevisiae* copper transport protein (Ctr1p). *J. Biol. Chem.* **269**, 25,660–25,667.
4. Pena, M. M. O., Puig, S., and Thiele, D. J. (2000) Characterization of the *Saccharomyces cerevisiae* high affinity copper transporter Ctr3. *J. Biol. Chem.* **275**, 33,244–33,251.
5. Pena, M. M. O., Lee, J., and Thiele, D. J. (1999) A delicate balance: homeostatic control of copper uptake and distribution. *J. Nutr.* **129**, 1251–1260.
6. Georgatsu, E., Mavrogiannis, L. A., Fragiadakis, G. S., et al. (1997) The yeast Fre1p/Fre2p cupric reductases facilitate copper uptake and are regulated by the copper-modulated Mac1p activator. *J. Biol. Chem.* **272**, 13,786–13,792.
7. Hassett, R. and Kosman, D. J. (1995) Evidence for Cu(II) reduction as a component of copper uptake by *Saccharomyces cerevisiae*. *J. Biol. Chem.* **270**, 128–134.
8. Eide, D. J. (1998) The molecular biology of metal ion transport in *Saccharomyces cerevisiae*. *Annu. Rev. Nutr.* **18**, 441–469.
9. Gross, C., Kelleher, M., Iyer, V. R., et al. (2000) Identification of the copper regulon in *Saccharomyces cerevisiae* by DNA microarrays. *J. Biol. Chem.* **275**, 32,310–32,316.
10. Winge, D. R., Jensen, L. T., and Srinivasan, C. (1998) Metal-ion regulation of gene expression in yeast. *Curr. Opin. Chem. Biol.* **2**, 216–221.
11. Ooi, C. E., Rabinovich, E., Dancis, A., et al. (1996) Copper-dependent degradation of the *Saccharomyces cerevisiae* plasma membrane transporter Ctr1p in the apparent absence of endocytosis. *EMBO J.* **15**, 3515–3523.
12. Hassett, R., Dix, D. R., Eide, D. J., et al. (2000) The Fe(II) permease Fet4p functions as a low affinity copper transporter and supports normal copper trafficking in *Saccharomyces cerevisiae*. *Biochem. J.* **351**, 477–484.
13. Cohen, A., Nelson, H., and Nelson, N. (2000) The family of *SMF* metal ion transporters in yeast cells. *J. Biol. Chem.* **275**, 33,388–33,394.
14. Radisky, D. and Kaplan, J. (1999) Regulation of transition metal transport across the yeast plasma membrane. *J. Biol. Chem.* **274**, 4481–4484.
15. Kampfenkel, K., Kushnir, S., Babiychuk, E., et al. (1995) Molecular characterization of a putative *Arabidopsis thaliana* copper transporter and its yeast homologue. *J. Biol. Chem.* **47**, 28,479–28,486.
16. Harrison, M., Jones, C. E., and Dameron, C. T. (1999) Copper chaperones: function, structure and coper-binding properties. *J. Biol. Inorg. Chem.* **4**, 145–153.
17. Harrison, M. D., Jones, C. E., Solioz, M., et al. (2000) Intracellular copper routing: the role of copper chaperones. *TIBS* **25**, 29–32.
18. O'Halloran, T. V. and Culotta, V. C. (2000) Metallochaperones, an intracellular shuttle service for metal ions. *J. Biol. Chem.* **275**, 25,057–25,060.

19. Valentine, J. S. (1997) Delivering copper inside yeast and human cells. *Science,* **278**, 817–818.
20. Culotta, V. C., Sturtz, L., Jensen, L., et al. (2001) Metals and oxidative stress: new insights from yeast. *J. Exp. Bot.* **52(Suppl.)**, 61.
21. Yuan, D. S., Stearman, R., Dancis, A., et al. (1995) The Menkes/Wilson disease gene homologue in yeast provides copper to a ceruloplasmin-like oxidase required for iron uptake. *Proc. Natl. Acad. Sci. USA,* **92**, 2632–2636.
22. Davis-Kaplan, S. R., Askwith, C. C., Bengtzen, A. C., et al. (1998) Chloride is an allosteric effector of copper assembly for the yeast multicopper oxidase Fet3p: An unexpected role for intracellular chloride channels. *Proc. Natl. Acad. Sci. USA* **95**, 13,641–13,645.
23. Gaxiola, R. A., Yuan, D. S., Klausner, R. D., et al. (1998) The yeast CLC chloride channel functions in cation homeostasis. *Proc. Natl. Acad. Sci. USA,* **95**, 4046–4050.
24. Glerum, D. M., Shtanko, A., and Tzagoloff, A. (1996) *SCO1* and *SCO2* act as high copy suppressors of a mitochondrial copper recruitment defect in *Saccharomyces cerevisiae*. *J. Biol. Chem.* **271**, 20,531–20,535.
25. Rentzsch, A., Krummeck-Weiβ, G., Hofer, A., et al. (1999) Mitochondrial copper metabolism in yeast: mutational analysis of Sco1p involved in the biogenesis of cytochrome *c* oxidase. *Curr. Genet.* **35**, 10–-108.
26. Martins, L. J., Jensen, L. T., Simons, J. R., et al. (1998) Metalloregulation of *FRE1* and *FRE2* homologs in *Saccharomyces cerevisiae*. *J. Biol. Chem.* **273**, 23,716–23,721.
27. Stearman, R., Yuan, D. S., Yamaguchi-Iwai, Y., et al. (1996) A permease–oxidase complex involved in high-affinity iron uptake in yeast. *Science* **271**, 1552–1557.
28. Askwith, C., Eide, D., Van Ho, A., et al. (1994) The *FET3* gene of *S. cerevisiae* encodes a multicopper oxidase required for ferrous iron uptake. *Cell* **76**, 403–410.
29. Askwith, C. and Kaplan, J. (1997) An oxidase–permease-based iron transport system in *Schizosaccharomyces pombe* and its expression in *Saccharomyces cerevisiae*. *J. Biol. Chem.* **272**, 401–405.
30. Hammacott, J. E., Williams, P. H., and Cashmore, A. M. (2000) *Candida albicans CFL1* encodes a functional ferric reductase activity that can rescue a *Saccharomyces cerevisiae fre1* mutant. *Microbiology* **146**, 869–876.
31. Ramanan, N. and Wang, Y. (2000) A high-affinity iron permease essential for *Candida albicans* virulence. *Science* **288**, 1062–1064.
32. Dix, D., Bridgham, J., Broderius, M., et al. (1997) Characterization of the FET4 protein of yeast. Evidence for a direct role in the transport of iron. *J. Biol. Chem.* **272**, 11,770–11,777.
33. Yun, C.-W., Ferea, T., Rashford, J., et al. (2000) Desferrioxamine-mediated iron uptake in *Saccharomyces cereivisiae*. Evidence for two pathways of iron uptake. *J. Biol. Chem.* **275**, 10,709–10,715.
34. Yun, C.-W., Tiedeman, J. S., Moore, R. E., et al. (2000) Siderophore–iron uptake in *Saccharomyces cerevisiae*. Identification of ferrichrome and fusarinine transporters. *J. Biol. Chem.* **275**, 16,354–16,359.
35. Heymann, P., Ernst, J. F., and Winkelmann, G. (1999) Identification of a fungal triacetylfusarinine C siderophore transport gene (TAF1) in *Saccharomyces cerevisiae* as a member of the major facilitator superfamily. *Biometals* **12**, 301–306.
36. Heymann, P., Ernst, J. F., and Winkelmann, G. (2000) Identification and substrate specificity of a ferrichrome-type siderophore transporter (Arn1p) in *Saccharomyces cerevisiae*. *FEMS Microbiol. Lett.* **186**, 221-227.
37. Lesuisse, E., Blaiseau, P. L., Dancis, A., et al. (2001) Siderophore uptake and use by the yeast *Saccharomyces cerevisiae*. *Microbiology* **147(Pt. 2)**, 289–298.
38. Lesuisse, E., Simon-Casteras, M., and Labbe, P. (1998) Siderophore-mediated iron uptake in *Saccharomyces cerevisiae*: the SIT1 gene encodes a ferrioxamine B permease that belongs to the major facilitator superfamily. *Microbiology* **144(Pt. 2)**, 3455–3462.
39. Klionsky, D. J., Herman, P. K., and Emr, S. D. (1990) The fungal vacuole: composition, function and biogenesis. *Microbiol. Rev.* **54**, 266–292.
40. Raguzzi, F., Lesuisse, E., and Chrichton, R.R. (1988) Iron storage in *Saccharomyces cerevisiae*. *FEBS Lett.* **231**, 253–258.
41. Urbanowski, J. L. and Piper, R. C. (1999) The iron transporter Fth1p forms a complex with the Fet5 iron oxidase and resides on the vacuolar membrane. *J. Biol. Chem,* **274**, 38,061–38,070.
42. Babcock, M., Silva, D. D., Oaks, R., et al. (1997) Regulation of mitochondrial iron accumulation by Yfh1, a putative homolog of frataxin. *Science* **276**, 1709–1712.
43. Radisky, D. C., Babcock, M. C., and Kaplan, J. (1999) The yeast frataxin homologue mediates mitochondrial iron efflux. *J. Biol. Chem.* **274**, 4497–4499.
44. Chen, O. S. and Kaplan, J. (2000) *CCC1* supresses mitochondrial damage in the yeast model of Friedreich's ataxia by limiting mitochondrial iron accumulation. *J. Biol. Chem.* **275**, 7626–7632.
45. Kispal, G., Csere, P., Prohl, C., et al. (1999) The mitochondrial proteins Atm1p and Nfs1p are essential for biogenesis of cytosolic Fe/S proteins. *EMBO J.* **18**, 3981–3989.
46. Li, J., Kogan, M., Knight, S. A. B., et al. (1999) Yeast mitochondrial protein, Nfs1p, coordinately regulates iron-sulphur cluster proteins, cellular iron uptake, and iron distribution. *J. Biol. Chem.* **274**, 33,025–33,034.
47. Leighton, J. and Schatz, G. (1995) An ABC transporter in the mitochondrial inner membrane is required for normal growth of yeast. *EMBO J.* **4**, 188–195.
48. Knight, S. A. B., Sepuri, N. B. V., Pain, D., et al. (1998) Mt-Hsp70 homolog, Ssc2p, required for maturation of yeast frataxin and mitochondrial iron homeostasis. *J. Biol. Chem.* **273**, 18,389–18,393.
49. Jensen, L. and Culotta, V. (2000) Role of *Saccharomyces cerevisiae* ISA1 and ISA2 in iron homeostasis. *Mol. Cell. Biol.* **20**, 3919–3927.
50. Robertson, L. S., Causton, H. C., Young, R. A., et al. (2000) The yeast A kinases differentially regulate iron uptake and respiratory function. *Proc. Natl. Acad. Sci. USA* **97**, 5984–5988.

51. Dancis, A., Roman, D. G., Anderson, G. J., et al. (1992) Ferric reductase of *Saccharomyces cerevisiae*: molecular characterization, role in iron uptake, and transcriptional control by iron. *Proc. Natl. Acad. Sci. USA* **89**, 3869–3873.
52. Jungmann, J., Reins, H., Lee, J., et al. (1993) MAC1, a nuclear regulatory protein related to Cu-dependent transcription factors is involved in Cu/Fe utilization and stress resistance in yeast. *EMBO J.* **12**, 5051–5056.
53. Lin, S.-J., Pufahl, R. A., Dancis, A., et al. (1997) A role for the *Saccharomyces cerevisiae ATX1* gene in copper trafficking and iron transport. *J. Biol. Chem.* **272**, 9215–9220.
54. Yamaguchi-Iwai, Y., Stearman, R., Dancis, A., et al. (1996) Iron-regulated DNA binding by the AFT1 protein controls the iron regulation in yeast. *EMBO J.* **15**, 3377–3384.
55. Labbe, S., Pena, M. M. O., Fernandes, A. R., et al. (1999) A copper-sensing transcription factor regulates iron uptake genes in *Saccharomyces pombe*. *J. Biol. Chem.* **274**, 36,252–36,260.
56. Elvehjem, C. A. (1935) The biological significance of copper and its relation to iron metabolism. *Physiol. Rev.* **15**, 471–507.
57. Hart, E. B., Steenbock, H., Waddell, J., et al. (1928) Iron in nutrition. VII. Copper as a supplement to iron for hemoglobin building in the rat. *J. Biol. Chem.* **77**, 797–812.
58. Holmberg, C. G. and Laurell, C. B. (1948) Investigations in serum copper. II. Isolation of the copper-containing protein, and a description of some of its properties. *Acta Chem. Scand.* **2**, 550–556.
59. Eisenstein, R. S. (2000) Discovery of the ceruloplasmin homologue hephaestin: new insight into the copper/iron connection. *Nutr. Rev.* **58**, 22–26.
60. Vulpe, C. D., Kuo, Y. M., Murphy, T. L., et al. (1999) Hephaestin, a ceruloplasmin homologue implicated in intestinal iron transport, is defective in the sla mouse. *Nature Genet.* **21**, 195–199.
61. Crampton, R. F., Matthews, D. M., and Poisner, R. (1965) Observations on the mechanism of absorption of copper by the small intestine. *J. Physiol.* **178**, 111–126.
62. Van Campen, D.R. (1971) Absorption of copper from the gastrointestinal tract, in *Intestinal Absorption of Metal Ions, Trace Elements and Radionuclides* (Skoryna, S. C. and Waldron-Edwards, D., eds.), Pergamon, Oxford, pp. 211–227.
63. Zhou, B. and Gitschier, J. (1997) h*CTR1*: a human gene for copper uptake identified by complementation in yeast. *Proc. Natl. Acad. Sci. USA* **94**, 7481–7486.
64. Lee, J. and Thiele, D. J. (2001) Essential role for mammalian copper transporters in copper homeostasis and embryonic development. *J. Exp. Bot.* **52(Suppl.)**, 84.
65. Hamza, I., Schaefer, M., Klomp, L. W. J., et al. (1999) Interaction of the copper chaperone HAH1 with the Wilson disease protein is essential for copper homeostasis. *Proc. Natl. Acad. Sci. USA* **96**, 13,363–13,368.
66. Larin, D., Mekios, C., Das, K., et al. (1999) Characterization of the interaction between the Wilson and Menkes disease proteins and the cytoplasmic copper chaperone, HAH1P. *J. Biol. Chem.* **274**, 28,497–28,504.
67. Hamza, I., Chen, J., Gitlin, J. D., et al. (2001) Critical role for metallochaperone Atox1 in perinatal copper homeostasis. *J. Exp. Bot.* **52(Suppl.)**, 84.
68. Petris, M. J., Strausak, D. and Mercer, J. F. B. (2000) The Menkes copper transporter is required for the activation of tyrosinase. *Hum. Mol. Genet.* **9**, 2845–2851.
69. Petris, M. J., Mercer, J. F. B., Culvenor, J. G. et al. (1996) Ligand-regulated transport of the Menkes copper P-type ATPase efflux pump from the Golgi apparatus to the plasma membrane: a novel mechanism of regulated trafficking. *EMBO J.* **15**, 6084–6095.
70. Petris, M. J., Mercer, J. F. B., and Camakaris, J. (1999) The cell biology of the Menkes disease protein. *Adv. Exp. Biol. Med.* **448**, 53–66.
71. Petris, M. J., Camakaris, J., Greenough, M., et al. (1998) A C-terminal di-leucine is required for localization of the Menkes protein in the *trans*-Golgi network. *Hum. Mol. Genet.* **7**, 2063–2071.
72. Petris, M. J. and Mercer, J. F. B. (1999) The Menkes protein (ATP7A; MNK) cycles via the plasma membrane both in basal and elevated extracellular copper using a C-terminal di-leucine endocytic signal. *Hum. Mol. Genet.* **8**, 2107–2115.
73. Linder, M. C., Wooten, L., Cerveza, P., et al. (1998) Copper transport. *Am. J. Clin. Nutr.* **67**, 965S–971S.
74. Hung, I. H., Suzuki, M., Yamaguchi, Y., et al. (1997) Biochemical characterization of the Wilson disease protein and functional expression in the yeast *Saccharomyces cerevisiae*. *J. Biol. Chem.* **272**, 21,461–21,466.
75. Schaefer, M., Hopkins, R. G., Failla, M. A., et al. (1999) Hepatocyte-specific localization and copper-dependent trafficking of the Wilson's disease protein in the liver. *Am. J. Physiol.* **276**, G639–G646.
76. Suzuki, M. and Gitlin, J. D. (1999) Intracellular localization of the Menkes and Wilson's disease proteins and their role in intracellular copper transport. *Pediatr. Int.* **41**, 436–442.
77. Terada, K., Aiba, N., Yang, X.-L. et al. (1999) Biliary excretion of copper in LEC rat after introduction of copper transporting P-type ATPase, ATP7B. *FEBS Lett.* **448**, 53–56.
78. Terada, K., Nakako, T., Yang, X.-L., et al. (1998) Restoration of holoceruloplasmin synthesis in LEC rat after infusion of recombinant adenovirus bearing WND cDNA. *J. Biol. Chem.* **273**, 1815–1820.
79. Sato, M. and Gitlin, J. D. (1991) Mechanisms of copper incorporation during the biosynthesis of human ceruloplasmin. *J. Biol. Chem.* **266**, 5128–5134.
80. Holmberg, C. G. and Laurell, C. B. (1948) Investigations in serum copper. II. Isolation of the copper containing protein and a description of some of its properties. *Acta Chem. Scand.* **2**, 550–556.
81. Winzerling, J. J. and Law, J. H. (1997) Comparative nutrition of iron and copper. *Annu. Rev. Nutr.* **17**, 501–526.
82. Linder, M.C. (1991) *Biochemistry of Copper*, Plenum, New York.
83. Evans, G. W. (1973) Copper homeostasis in the mammalian system. *Physiol. Rev.* **53**, 535–569.
84. Dameron, C. T. and Harrison, M. D. (1998) Mechanisms for protection against copper toxicity. *Am. J. Clin. Nutr.* **67(Suppl.)**, 1091S–1097S.

85. Miles, A. T., Hawksworth, G. M., Beattie, J. H., et al. (2000) Induction, regulation, degradation, and biological significance of mammalian metallothioneins. *Crit. Rev. Biochem. Mol. Biol.* **35**, 35–70.
86. Vasak, M. and Hasler, D. W. (2000) Metallothioneins: new functional and structural insights. *Curr. Opin. Chem. Biol.* **4**, 177–183.
87. Labbe, S., Simard, C., and Seguin, C. (1997) Metallothionein gene regulation in mouse cells, in *Metal Ions in Gene Regulation* (Silver, S. and Walden, W., eds.), Chapman & Hall, New York, pp. 231–249.
88. Remondelli, P., Moltedo, O., Pascale, M. C., et al. (1999) Metal regulation of metallothionein gene transcription in mammals. *Adv. Exp. Med. Biol.* **448**, 223–236.
89. Andrews, N. C. (1999) The iron transporter DMT1. *Int. J. Biochem. Cell Biol.* **31**, 991–994.
90. Aisen, P., Wessling-Resnick, M., and Leibold, E. A. (1999) Iron metabolism. *Curr. Opin. Chem. Biol.* **3**, 200–206.
91. Schneider, B. D. and Leibold, E. A. (2000) Regulation of mammalian iron homeostasis. *Curr. Opin. Clin. Nutr. Metab. Care* **3**, 267–273.
92. Tandy, S., Williams, M., Leggett, A., et al. (2000) Nramp2 expression is associated with pH-dependent iron uptake across the apical membrane of human intestinal Caco-2 cells. *J. Biol. Chem.* **275**, 1023–1029.
93. Bennett, M. J., Lebron, J. A., and Bjorkman, P. J. (2000) Crystal structure of the hereditary haemochromatosis protein HFE complexed with transferrin receptor. *Nature* **403**, 46–53.
94. Riedel, H. D., Muckenthaler, M. U., Gehrke, S. G., et al. (1999) HFE downregulates iron uptake from transferrin and induces iron-regulatory protein activity in stably transfected cells. *Blood* **94**, 3915–3921.
95. Han, O., Fleet, J. C., and Wood, R. J. (1999) Reciprocal regulation of HFE and Nramp2 gene expression by iron in human intestinal cells. *J. Nutr.* **129**, 98–104.
96. Nelson, N. (1999) Metal ion transporters and homeostasis. *EMBO J.* **18**, 4361–4371.
97. Haile, D. J. (1999) Regulation of genes of iron metabolism by the iron-response proteins. *Am. J. Med. Sci.* **318**, 230–240.
98. Conrad, M. E., Umbreit, J. N., and Moore, E. G. (1999) Iron absorption and transport. *Am. J. Med. Sci.* **8**, 213–229.
99. Donovan, A., Brownlie, A., Zhou, Y., et al. (2000) Positional cloning of zebrafish *ferroportin 1* identifies a conserved vertebrate iron exporter. *Nature* **403**, 776–781.
100. McKie, A. T., Marciani, P., Rolfs, A., et al. (2000) A novel duodenal iron-regulated membrane protein (Ireg1) implicated in basolateral transfer of iron to the circulation. *Mol. Cell,* **5**, 299–309.
101. Abboud, S. and Haile, D. J. (2000) A novel mammalian iron-regulated protein involved in intracellular iron metabolism. *J. Biol. Chem.* **275**, 19,906–19,912.
102. Kaplan, J. and Kushner, J. P. (2000) Mining the genome for iron. *Nature* **403**, 712–713.
103. Andrews, N. C., Fleming, M. D., and Gunshin, H. (1999) Iron transport across biologic membranes. *Nutr. Rev.* **57**, 745–748.
104. Tabuchi, M., Yoshimori, T., Yamaguchi, K., et al. (2000) Human NRAMP2/DMT1, which mediates iron transport across endosomal membranes, is localized to late endosomes and lysosomes in HEp-2 cells. *J. Biol. Chem.* **275**, 22,220–22,228.
105. Rolfs, A. and Hediger, M. A. (2001) Intestinal metal ion absorption: an update. *Curr. Opin. Gastroenterol.* **17**, 177–183.
106. Eisenstein, R. S. and Blemmings, K. P. (1998) Iron regulatory proteins, iron responsive elements and iron homeostasis. *J. Nutr.* **128**, 2295–2298.
107. Kühn, L. C. (1998) Iron and gene expression: molecular mechanisms regulating cellular iron homeostasis. *Nutr. Rev.* **56**, S11–S19.
108. Thomson, A. M., Rogers, J. T., and Leedman, P. J. (1999) Iron-regulatory proteins, iron-responsive elements and ferritin mRNA translation. *Int. J. Biochem. Cell Biol.* **31**, 1139–1152.
109. Fox, T. C. and Guerinot, M. L. (1998) Molecular biology of cation transport in plants. *Annu. Rev. Plant Physiol. Plant Mol. Biol.* **49**, 669–696.
110. Hirayama, T., Kieber, J. J., Hirayama, N., et al. (1999) *RESPONSE TO ANTAGONIST1*, a Menkes/Wilson disease-related copper transporter, is required for ethylene signaling in *Arabidopsis*. *Cell,* **97**, 383–393.
111. Tabata, K., Kashiwagi, S., Mori, H., et al. (1997) Cloning of a cDNA encoding a putative metal-transporting P-type ATPase from *Arabidopsis thaliana. Biochim. Biophys. Acta* **1326**, 1–6.
112. Pilon, M., Burkhead, J., and Pilon-Smits, E. A. H. (2001) Metal homeostasis in Arabidopsis chloroplasts: the roles of the copper binding protein AtCutAp and the P-type ATPase Paa1p. *J. Exp. Bot.* **52(Suppl.)**, 65.
113. Kaneko, T., Kato, T., Sato, S., et al. (2000) Structural analysis of Arabidopsis thaliana chromosome 3. II. Sequence features of the regions of 4,251,695 bp covered by ninety P1, TAC and BAC clones. *DNA Res.* **7**, 217–221.
114. Zhu, H., Shipp, E., Sanchez, R. J., et al. (2000) Cobalt(2+) binding to human and tomato copper chaperone for superoxide dismutase: Implications for metal ion transfer mechanism. *Biochemistry* **39**, 5413–5421.
115. Himelblau, E., Mira, H., Lin, S. J., et al. (1998) Identification of a functional homolog of the yeast and human homeostasis gene *ATX1* from *Ardabidopsis. Plant Physiol.* **117**, 1227–1234.
116. Lin, X., Kaul, S., Rounsley, S. D., et al. (1999) Sequence and analysis of chromosome 2 of the plant *Arabidopsis thaliana. Nature* **402**, 761–768.
117. Bleecker, A. B. and Kende, H. (2000) Ethylene: a gaseous signal molecule in plants. *Annu. Rev. Cell Dev. Biol.* **16**, 1–18.
118. Hirayama, T. and Alonso, J. M. (2000) Ethylene captures a metal! Metal ions are involved in ethylene perception and signal transduction. *Plant Cell Physiol.* **41**, 548–555.
119. Woeste, K. E. and Kieber, J. J. (2000) A strong loss-of-function mutation in *RAN1* results in constitutive activation of the ethylene repsonse pathway as well as a rosette-lethal phenotype. *Plant Cell* **12**, 443–455.
120. Williams, L. E., Pittman, J. K., and Hall, J. L. (2000) Emerging mechanisms for heavy metal transport in plants. *Biochim. Biophys. Acta* **1465**, 104–126.

121. Kanamaru, K., Kashiwagi, S., and Mizuno, T. (1994) A copper-transporting P-type ATPase found in the thylakoid membrane of the cyanobacterium *Synechococcus sp.* PCC7942. *Mol. Microbiol.* **13**, 369–377.
122. Phung, L. T., Ajlani, G. and Haselkorn, R. (1994) P-type ATPase from the cyanobacterium Synechococcus 7942 related to the human Menkes and Wilson disease gene products. *Proc. Natl. Acad. Sci. USA* **91**, 9651–9654.
123. Rutherford, J. C., Cavet, J. S., and Robinson, N. J. (1999) Cobalt-dependent transcriptional switching by a dual-effector MerR-like protein regulates a cobalt-exporting variant CPx-type ATPase. *J. Biol. Chem.* **274**, 25,827–25,832.
124. Thelwell, C., Robinson, N. J., and Turner-Cavet, J. S. (1998) An SmtB-like repressor from Synechocystis PCC 6803 regulates a zinc exporter. *Proc. Natl. Acad. Sci. USA* **95**, 10,728–10,733.
125. Tottey, S., Rich, P. R., Rondet, S. A. M., et al. (2001) Two Menkes-type ATPases supply copper for photosynthesis in *Synechocystis* PCC6803. *J. Biol. Chem.* **276**, 19,999–20,004.
125a. Tottey, S., Rondet, S. A., Borrelly, G. P., Robinson, P. J., Rich, P. R. and Robinson, N. J. (2002) A copper metallochaperone for photosynthesis and respiration reveals metal-specific targets, interaction with an importer, and alternative sites for copper acquisition. *J. Biol. Chem.* **277**, 5490–5497.
126. Mira, H., Martinez-Garcia, F., and Penarrubia, L. (2001) Evidence for the plant-specific intercellular transport of the Arabidopsis copper chaperone CCH. *Plant J.* **25**, 521–528.
127. Himelblau, E. and Amasino, R. M. (2000) Delivering copper within plant cells. *Curr. Opin. Plant Biol.* **3**, 205–210.
128. Zhou, J. and Goldsbrough, P. B. (1994) Functional homologues of fungal metallothionein genes from *Arabidopsis*. *Plant Cell* **6**, 875–884.
129. Dykema, P. E., Sipes, P. R., Marie, A., et al. (1999) A new class of proteins capable of binding transition metals. *Plant Mol. Biol.* **41**, 139–150.
130. Robinson, N. J., Procter, C. M., Connolly, E. L., et al. (1999) A ferric-chelate reductase for iron uptake from soils. *Nature* **397**, 694–697.
131. Yi, Y. and Guerinot, M. L. (1996) Genetic evidence that induction of root Fe(III) chelate reductase activity is necessary for iron uptake under iron deficiency. *Plant J.* **10**, 835–844.
132. Guerinot, M. L., Grotz, N., Hibbard, S., et al. (2001) Molecular characterization of the uptake of iron and other divalent cations in *Arabidopsis*. *J. Exp. Bot.* **52(Suppl.)**, 62.
133. Eide, D., Broderius, M., Fett, J., et al. (1996) A novel iron-regulated metal transporter from plants identified by functional expression in yeast. *Proc. Natl. Acad. Sci. USA* **93**, 5624–5628.
134. Korshunova, Y., Eide, D., Clark, W. G., et al. (1999) The IRT1 protein from *Arabidopsis thaliana* is a metal transporter with a broad substrate range. *Plant Mol. Biol.* **40**, 37–44.
135. Guerinot, M. L. (2000) The ZIP family of metal transporters. *Biochim. Biophys. Acta* **1465**, 190–198.
136. Curie, C., Alonso, J. M., Jean, M. L., et al. (2000) Involvement of NRAMP1 from *Arabidopsis thaliana* in iron transport. *Biochem. J.* **347**, 749–755.
137. Thomine, S., Wang, R., Ward, J. M., et al. (2000) Cadmium and iron transport by members of a plant metal transporter family in *Arabidopsis* with homology to *Nramp* genes. *Proc. Natl. Acad. Sci. USA* **97**, 4991–4996.
138. Bagnaresi, P., Thoiron, S., Mansion, M., et al. (1999) Cloning and characterization of a maize cytochrome-b5 reductase with Fe3+-chelate reduction capability. *Biochem. J.* **338(Pt. 2)**, 499–505.
139. Curie, C., Panaviene, Z., Loulergue, C., et al. (2001) Maize yellow stripe1 encodes a membrane protein directly involved in Fe(III) uptake. *Nature* **409**, 346–349.
140. Bagnaresi, P., Mazars-Marty, D., Pupillo, P., et al. (2000) Tonoplast subcellular localization of maize cytochrome b5 reductases. *Plant J.* **24**, 645–654.
141. Briat, J.-F. and Lobreaux, S. (1997) Iron transport and storage in plants. *Trends Plant Sci.* **2**, 187–193.
142. Bell, W. D., Bogorad, L., and McIlrath, W. J. (1958) Response of the yellow-stripe maize mutant (ys1) to ferrous and ferric iron. *Bot. Gaz.* **120**, 36–39.
143. Theil, E. C. (1987) Ferritin: structure, gene regulation, and cellular function in animals, plants and microorganisms. *Annu. Rev. Biochem.* **56**, 289–315.
144. Briat, J. F., Lobreaux, S., Grignon, N., et al. (1999) Regulation of plant ferritin synthesis: how and why. *Cell. Mol. Life Sci.* **56**, 155–166.
145. Van Wuytswinkel, O., Vansuyt, G., Grignon, N., et al. (1999) Iron homeostasis alteration in transgenic tobacco overexpressing ferritin. *Plant J.* **17**, 93–97.
146. Briat, J. F. and Lobreaux, S. (1998) Iron storage and ferritin in plants. *Metal Ions Biol. Syst.* **35**, 563–584.
147. Wei, J. and Theil, E. C. (2000) Identification and characterization of the iron regulatory element in the ferritin gene of a plant (soybean). *J. Biol. Chem.* **275**, 17,488–17,493.
148. Petit, J.-M., Wuytswinkel, O. V., Briat, J.-F., et al. (2001) Characterization of an iron dependent regulatory sequence (IDRS) involved in the transcriptional control of *AtFer1* and *ZmFer1* plant ferritin genes by iron. *J. Biol. Chem.* **276**, 5584–5590.
149. Cohen, C. K., Norvell, W. A., and Kochian, L. V. (1997) Induction of root cell plasma membrane ferric reductase. *Plant Physiol.* **114**, 1061–1069.
150. Welch, R. M., Norvell, W. A., Schaefer, S. C., et al. (1993) Induction of iron (III) and copper (II) reduction in pea (*Pisum sativum* L.) roots by Fe and Cu status: does the root-cell plasmalemma Fe(III)-chelate reductase perform a general role in regulating uptake? *Planta* **190**, 555–561.
151. Harris, E. H. (1989) *The Chlamydomonas Sourcebook: A Comprehensive Guide to Biology and Laboratory Use*, Academic, San Diego, CA.

152. Wood, P. M. (1978) Interchangeable copper and iron proteins in algal photosynthesis. Studies on plastocyanin and cytochrome *c*-552 in *Chlamydomonas*. *Eur. J. Biochem.* **87**, 8–19.
153. Li, H. H. and Merchant, S. (1995) Degradation of plastocyanin in copper-deficient *Chlamydomonas reinhardtii*. *J. Biol. Chem.* **270**, 23,504–23,510.
154. Quinn, J. M. and Merchant, S. (1995) Two copper-responsive elements associated with the Chlamydomonas Cyc6 gene function as targets for transcriptional activators. *Plant Cell* **7**, 623–638.
155. Hill, K. L. and Merchant, S. (1992) In vivo competition between plastocyanin and a copper-dependent regulator of the *Chlamydomonas reinhardtii* cytochrome c_6 gene. *Plant Physiol.* **100**, 319–326.
156. Li, H. H., Quinn, J., Culler, D., et al. (1996) Molecular genetic analysis of plastocyanin biosynthesis in *Chlamydomonas reinhardtii*. *J. Biol. Chem.* **271**, 31,283–31,289.
157. Merchant, S. and Bogorad, L. (1987) Metal ion regulated gene expression: use of a plastocyanin-less mutant of *Chlamydomonas reinhardtii* to study the Cu(II)-dependent expression of cytochrome *c*-552. *EMBO J.* **6**, 2531–2535.
158. Hill, K. L., Hassett, R., Kosman, D., et al. (1996) Regulated copper uptake in *Chlamydomonas reinhardtii* in response to copper availability. *Plant Physiol.* **112**, 697–704.
159. Howe, G. and Merchant, S. (1992) Heavy metal-activated synthesis of peptides in *Chlamydomonas reinhardtii*. *Plant Physiol.* **98**, 127–136.
160. Cobbett, C. S. (2000) Phytochelatin biosynthesis and function in heavy-metal detoxification. *Curr. Opin. Plant Biol.* **3**, 211–216.
161. Hill, K. L. and Merchant, S. (1995) Coordinate expression of coproporphyrinogen oxidase and cytochrome c6 in the green alga *Chlamydomonas reinhardtii* in response to changes in copper availability. *EMBO J.* **14**, 857–865.
162. Moseley, J., Quinn, J., Eriksson, M., et al. (2000) The *Crd1* gene encodes a putative di-iron enzyme required for photosystem I accumulation in copper deficiency and hypoxia in *Chlamydomonas reinhardtii*. *EMBO J.* **19**, 2139–2151.
163. Quinn, J. M., Nakamoto, S. S., and Merchant, S. (1999) Induction of coproporphyrinogen oxidase in *Chlamydomonas* chloroplasts occurs via transcriptional regulation of *Cpx1* mediated by copper-response elements and increased translation from a copper-deficiency-specific form of the transcript. *J. Biol. Chem.* **274**, 14,444–14,454.
164. Quinn, J. M., Barraco, P., Eriksson, M., et al. (2000) Coordinate copper- and oxygen-responsive *Cyc6* and *Cpx1* expression in *Chlamydomonas* is mediated by the same element. *J. Biol. Chem.* **275**, 6080–6089.
165. Quinn, J. M., Eriksson, M., Moseley, J. L., and Merchant, S. (2002) Oxygen deficiency responsive gene expression in *Chlamydomonas reinhardtii* through a copper-sensing signal transduction pathway. *Plant Physiol.* **128**, 463–471.
166. Eckhardt, U. and Buckout, T. J. (1998) Iron assimilation in *Chlamydomonas reinhardtii* involves ferric reduction and is similar to Strategy I higher plants. *J. Exp. Bot.* **49**, 1219–1226.
167. Lynnes, J. A., Derzaph, T. L. M., and Weger, H. G. (1998) Iron limitation results in induction of ferricyanide reductase and ferric chelate reductase activities in *Chlamydomonas reinhardtii*. *Planta* **204**, 360–365.
168. Weger, H. G. (1999) Ferric and cupric reductase activities in the green alga *Chlamydomonas reinhardtii*: experiments using iron-limited chemostats. *Planta* **207**, 377–384.
169. Quinn, J. M., LaFontaine, S., Gohre, V., et al. (2000) Copper-dependent and copper-independent iron metabolism in *Chlamydomonas reinhardtii*. *Plant Physiol.* S961.
170. Herbik, A. and Buckhout, T. J. (2001) Is a ferroxidase involved in the high-affinity iron uptake in Chlamydomonas? *J. Exp. Bot.* **52(Suppl.)**, 80.
171. Hortensteiner, S., Chinner, J., Matile, P., et al. (2000) Chlorophyll breakdown in *Chlorella protothecoides*: characterization of degreening and cloning of degreening-related genes. *Plant Mol. Biol.* **42**, 439–450.
172. Osterberg, R. (1974) Origins of metal ions in biology. *Nature* **249**, 382–383.
173. Nguyen, H. H., Shiemke, A. K., Jacobs, S. J., et al. (1994) The nature of the copper ions in the membranes containing the particulate methane monooxygenase from *Methylococcus capsulatus* (Bath). *J. Biol. Chem.* **269**, 14,995–15,005.
174. Lipscombe, J. D. (1994) Biochemistry of the soluble methane monooxygenase. *Annu. Rev. Micobiol.* **48**, 371–399.
175. Neilsen, A. K., Gerdes, K., and Murrell, J. C. (1997) Copper-dependent reciprocal transcriptional regulation of methane monooxygenase genes in *Methylococcus capsulatus* and *Methylosinus trichosporium. Mol. Microbiol.* **25**, 399–409.

31

Copper and the Morphological Development of *Streptomyces*

Erik Vijgenboom and Bart Keijser

1. INTRODUCTION

Redox active metal ions such as copper are potentially dangerous to a cell because of their habit of engaging in all kinds of reaction generating, among others, reactive oxygen species. However, these metal ions play a crucial role as a cofactor in a variety of enzymes and electron-transport proteins. Recently, it has become evident that copper ions play an intriguing role in the morphogenesis of *Streptomyces*. This Gram-positive bacterium undergoes a complicated cycle of morphological differentiation to ensure its propagation. Here, we review what is currently known about *Streptomyces* morphogenesis and the link with copper, and what developments are to be expected in the near future.

2. THE LIFE CYCLE OF *STREPTOMYCES*

From a bacterial point of view, the filamentous Gram-positive soil bacteria *Streptomyces* have a very complex lifestyle (Fig. 1A). Their vegetative mycelium consists of a network of branched hyphae. Perhaps, as a consequence of their hyphal growth habit, they rely on the formation of exospores for propagation. In addition they produce a wide range of secondary metabolites (antibiotics, fungicides). Because of the fascinating and complex multicellular processes of development *Streptomyces* are the system of choice for studies of prokaryotic morphological and physiological development, but they are also an attractive industrial organism.

The complete life cycle of *Streptomyces* consists of two phases: the vegetative growth and the reproductive growth. Vegetative growth is characterized by the production of branched hyphae with irregular crosswalls dividing the hyphae in compartments. Growth mainly occurs through extension of cell walls at the hyphal tips. At variable intervals, septation occurs, resulting in multigenome compartments because partitioning of sibling DNA molecules does not take place. In the final stage of vegetative growth, when entering the stationary phase, many streptomycetes produce a variety of secondary metabolites, which include 60% or more of the known antibiotics. Because of nutrient limitation, stress response, and cellular signaling, streptomycetes initiate the reproductive growth stage by the formation of aerial mycelium. These hyphae grow perpendicular onto the vegetative mycelium and erect themselves from the plane of the agar. The vegetative mycelium supplies the nutrients needed for aerial growth, so the aerial mycelium is both physically and physiologically dependent on the vegetative mycelium. The early stages of aerial hyphae formation show straight

From: Handbook of Copper Pharmacology and Toxicology
Edited by: E. J. Massaro © Humana Press Inc., Totowa, NJ

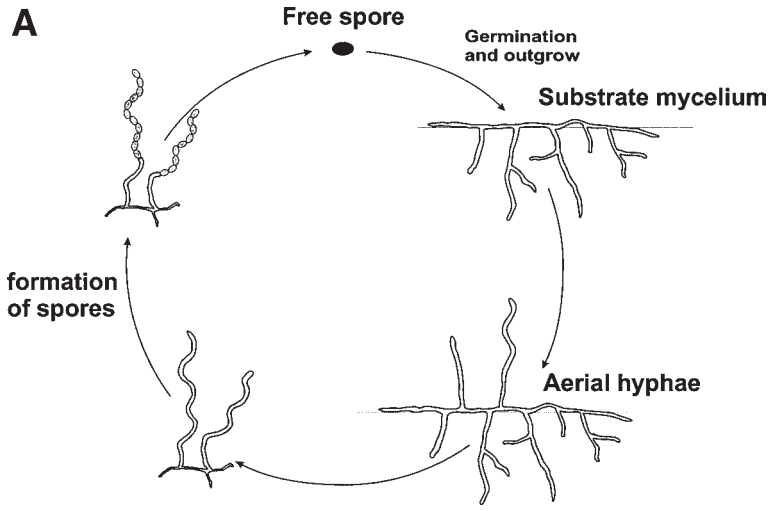

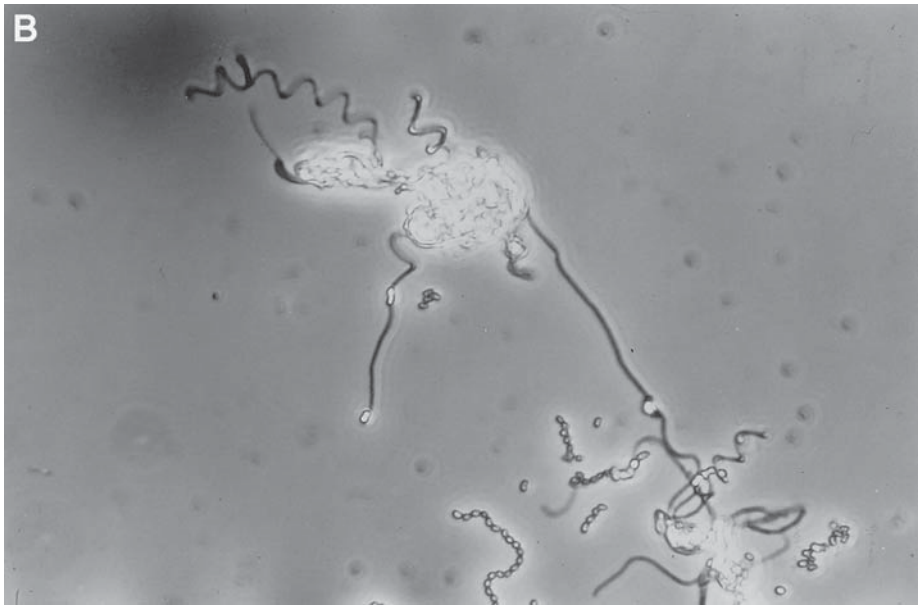

Fig. 1. (A) The life cycle of streptomycetes. The first step in the development of a new colony is the germination of a spore. Two germ tubes are formed that develop into a branched vegetative mycelium. One of the factors involved in the germination is cAMP *(1)*. The reproductive part of the life cycle is initiated by the erection of aerial hyphae. At this point, the vegetative mycelium becomes a substrate mycelium that feeds the aerial mycelium. Developmental mutants affected in this process are designated *bld* (bald) mutants because they lack the fluffy white aerial mycelium. After coiling and regular septation, spores are developed at the tips of the aerial hyphae. Mutants blocked in this stage of differentiation are called *whi* (white) mutants because they do not develop the gray color of the pigment associated with the spores. **(B)** Photograph of vegetative mycelium (straight hyphae in the center), aerial hyphae (coiled hyphae at the top), and spore chains (bottom) taken with a phase-contrast microscope.

hyphae that eventually will start to coil. In the final stage of the reproductive growth, regular-sized compartments are formed at the tips of the aerial hyphae that develop into spores (Fig. 1B). During spore formation, partitioning of the genomes does occur, resulting in one genome per compartment. For most *Streptomyces* strains, the reproductive cycle is only switched on when grown on solid media. A few *Streptomyces* strains are capable of spore production in liquid broth, so-called submerged sporulation *(2–5)*, but this will be not discussed here.

The various stages of differentiation during growth on solid media can easily be followed because the formation of aerial hyphae gives colonies a white and fluffy appearance, whereas upon spore formation, colonies turn gray because of the production of a gray spore pigment. The onset of the physiological differentiation, production of secondary metabolites, is intimately associated with the start of morphological development, suggesting that these two processes share common regulatory elements. As for the morphogenesis, the physiological differentiation can be monitored easily because many of the secondary metabolites are pigmented.

Insight in the underlying processes that initiate developmental pathways has been gained by studying mutants that are disturbed in their ability to differentiate. Screening programs using NTG -, UV –, or transposon mutagenesis rendered two classes of developmental mutants: those no longer able to form aerial hyphae, the *bld* (bald) mutants, and those disturbed in their capacity to form mature gray spores, the *whi* (white) mutants.

Analogies between the developmental process in *Streptomyces* and other spore-producing microorganisms such as *Bacillus subtilis* have been drawn *(6–8)*. These ideas suggest that although the morphogenesis in these bacteria is rather different, endospore versus exospore, unicellular versus hyphal growth, the basic layout of developmental routes can be similar or at least contain similar components.

2.1. bld Mutants

The majority of developmental mutants have been generated in *Streptomyces coelicolor* A(3)2; therefore, this strain will be discussed in more detail. Strains lacking the ability to produce aerial hyphae are classified as *bld* (bald) mutants. A dozen or more *bld* mutants have been described in literature, but only a few have been studied at the molecular level. Many of these mutants are not only impaired in the earliest stages of morphogenesis but are also affected in their secondary metabolism and catabolite repression *(9)*. Changes in secondary metabolism in *S. coelicolor* are obvious because two of the secondary metabolites, the blue-pigmented polyketide antibiotic actinorhodin (Act) and the red-pigmented tripyrolle undesylprodigiosin (Red), are colored. Most *bld* mutants turned out to be conditionally affected in their ability to initiate aerial mycelium growth. On media with glucose as the carbon source, they display the characteristic bald appearance, whereas on mannitol containing media, these mutants do produce aerial hyphae and spores *(10)*. In some of the mutants, growth on a poor carbon source, such as mannitol, also results in a partial restoration of antibiotic production. One explanation for the medium-dependent phenotype of the *bld* mutants is the existence of at least two developmental pathways in this phase of the differentiation: one only active on minimal medium containing mannitol and the other on complex-rich media.

An interesting observation was made when *bld* mutants were grown on solid medium, one next to the other, without actual contact between the hyphae. Of each pair of *bld* mutants, one was observed to stimulate the development of aerial hyphae formation of the other in the border region between the two strains. This stimulation was always a one-way communication: one strain acted as the donor and the other as the recipient that was rescued for aerial hyphae formation. Analysis of pairs of all *bld* mutants showed that most of them could be arranged in a hierarchical order *(11–13)*. Each mutant was able to stimulate the development of all mutants lower in this cascade. An explanation of this cascade is the involvement of at least five extracellular signals, where the presence of each signal causes the production or export of the next. So far, only one substance (signal 1) that would qualify as a signaling compound has been partially purified. This signal is a 665-Dalton peptide supposed to

contain at least serine and glycine residues, and proposed to be associated with the function of the *bldK* gene cluster *(14)*. The *bldK* locus consists of five genes with similarity to the oligopeptide–permease family of ATP-binding cassette (ABC) membrane-spanning transporters. The *bldK* mutation does not only result in a block in differentiation but also confers resistance to the toxic tripeptide bialaphos, confirming that the *bldK* gene product is an oligopeptide importer *(12)*.

One would expect to find more elements of the proposed *bld*-signaling cascade by analyzing the gene products of the *bld* genes. However, this approach has not been successful until now. The best characterized mutant, *bldA*, does not encode a protein but an extremely rare leucyl tRNA molecule translating the UUA codon. These codons are very infrequent in genes of *Streptomyces* because the high GC contents (70%) of the genome and a strong bias for a G or C at the third position of codons *(15)*. The involvement of this tRNA in the regulation of the onset of aerial mycelium formation could be through regulatory proteins of which the mRNAs contain one or more UUA codons. However, this appears not to be the case. Only for the regulatory proteins of the synthesis clusters of *act* and *red* has a clear regulatory role of *bldA* been found *(16–18)*. Therefore, the molecular basis of the bald phenotype of the *bldA* mutant is still not clear.

The *bldB* and *bldD* mutants are putative transcriptional regulators with unidentified targets (19,20). One mutant, *bldF*, has an extremely high production of the red pigment and it is not clear whether the phenotype is the result of this overproduction or an additional block of the developmental pathway *(21)*. One of the most recently characterized *bld* mutants is *bldN (22)*. BldN is an extracytoplasmic function RNA polymerase sigma factor but does not fit cleanly in the proposed "bld-cascade." A target for BldN is one of the two promoters of *bldM* that encodes a response regulator and belongs to the last step of the bld-cascade. An explanation for the fact that not all *bld* genes fit in the cascade could be an indirect role in the production of extracellular signaling molecules.

In a different approach to get information on the morphological differentiation, extracellular proteins produced during development have been studied. One of them, SapB, has a molecular weight of 2 kDa, consists of 18 amino acids, is most likely modified on the sixth amino acid residue, and is believed to be produced nonribosomal *(9)*. Purified SapB turned out to be able to restore aerial mycelium formation in a *bld* mutant. This implied that SapB is an important factor in morphogenesis, although the aerial hyphae erected by the *bld* mutants upon the addition of SapB did not coil, septate, and form chains of spores as the wild-type aerial hyphae do *(23)*. In this context, the sole function of SapB seems to be the facilitation of the erection of vegetative hyphae and so mimicking the early stages of the developmental controlled formation of aerial hyphae. Therefore, SapB does not appear to have a regulatory function concerned with the onset of differentiation. On minimal medium supplied with mannitol, *bld* mutants do form aerial hyphae and spores, but do not produce detectable amounts of SapB *(24)*. This supports the hypothesis that at least two pathways of aerial mycelium formation do exist and that SapB is not required *per se* for aerial hyphae formation. This kind of morphogenic protein is not unique to *S. coelicolor*. Streptofactin, a similar protein isolated from *S. tendae*, can restore aerial hyphae formation to *S. tendae bld* mutants as well as *S. coelicolor bld* mutants *(25)*. Also, SC3, a hydrophobin isolated from the fungus *Schizophyllum commune*, does restore erection of vegetative hyphae to some extent *(26)*. What do these proteins have in common? They all are surface-active peptides that lower the surface tension and have the tendency to concentrate at hydrophobic–hydrophilic interfaces. The model for the action of these hydrophobinlike peptides discerns two actions: (1) reduction of surface tension to allow the hydrophilic vegetative hyphae to break through the liquid surface and (2) providing the aerial hyphae with a hydrophobic coat. The function of SapB in formation of aerial hyphae seems to be restricted to the first action, the reduction of the surface tension. Although the surface of *S. coelicolor* aerial hyphae is hydrophobic, no SapB could be detected *(26)*.

2.2. *whi* Mutants

Mutants that fail to produce mature gray pigmented spores are called *whi* (white) mutants. In total, eight loci have been identified in which mutations result in the *whi* phenotype. The *whiE* mutants are all affected in the locus that contains the genes for the production of the spore pigment that has

resemblance to the polyketides. These mutants are, from a morphological point of view, not defective. The functions of most of the gene products of the other *whi* genes are not elucidated. Six loci harbor the genes involved in early sporulation events. Mutations in these genes result in a diminished formation of sporulation septa. The *whiG* gene codes for a σ-factor and *whiG* mutants are arrested in the earliest stages of aerial hyphae development and have straight aerial hyphae. The WhiG protein is expressed throughout growth, indicating that its activity must be repressed during vegetative growth. This is most likely done by an anti-σ factor, which is in agreement with the characteristics of the σ-factor family, of which WhiG is a member *(27)*. Once the aerial hyphae start to coil, the *whiB* and *whiA* gene products come into play. Disruption mutants of these genes have extremely long aerial hyphae, suggesting that the WhiB and WhiA proteins somehow have control over the final length of the aerial hyphae *(28,29)*. The function of both proteins is unknown. WhiB belongs to a group of small proteins with many charged residues and four cysteines in a particular order. WhiB-like proteins have only been detected in actinomycetes *(30)*.

One of several genes involved in the late stages of aerial hyphae development, spore formation and maturation, is *whiH*. Mutations in this gene, either point mutations or disruptions, result in strains that have a pale gray color as the result of low *whiE* expression. Further characteristics of this mutant are condensation and aberrant partitioning of the nucleoids *(29)*. Mutations in the *whiD* locus result in strains with defective spores. The size of the spores is irregular and inspection by scanning electron microscope indicates also possible lysis of spores *(31)*.

Under the assumption that the available genetic map of eight *whi* loci was not complete, a renewed effort was made to identify new *whi* mutants. This approach has resulted in five sporulation loci that are distinct from the known ones *(32)*. Another approach using insertional mutagenesis has come up with several genes involved in morphogenesis, among which there is one new *whi* mutant *(33)*. Studies not directly aimed at the identification of developmental mutants have shown that not all developmental genes show up in mutant screens using mutagens such as UV and NTG. The gene *ssgA*, encoding for a small protein with unknown function, was identified in *S. griseus* as the suppressor of submerged sporulation *(34)*. In *S. coelicolor*, an ortholog of the *ssgA* gene was isolated that upon overexpression stimulates the septum formation in liquid-grown cultures. Disruption of the *ssgA* gene resulted in a mutant defective in spore formation but capable of aerial hyphae production. Therefore, *ssgA* classifies as a *whi* gene and has a crucial function in septum formation *(35)*.

2.3. Other Factors Affecting Development

Evidence for the involvement of γ-butyrolactones in the regulation of the onset of secondary metabolism and the onset of differentiation is accumulating. Similar small diffusible signaling molecules operate in various other bacteria as regulators of a wide variety of processes *(36)*. A-factor (2-isocapryloyl-3*R*-hydroxymethyl-γ-butyrolactone) was the first of these bacterial hormones to be identified in *S. griseus (37)* and shown to act in nanomolar concentration as a "all-or-none" switch for both morphological development and streptomycin production. Later, several butyrolactone autoregulators were purified form *S. coelicolor (38,39)*. The butyrolactone receptors are supposed DNA-binding proteins that take care of the regulation of genes needed for secondary metabolism and morphogenesis *(40–42)*. Another diffusible signal molecule suggested to serve in the regulation of antibiotic synthesis and morphological development is cAMP. An adenylate cyclase disruption mutant is conditionally impaired in aerial hyphae production and displays a severe delay in germ-tube formation *(1,43)*.

Many other genes have been reported that, upon mutation, disturb morphological development and/or secondary metabolism. The AfsK/AfsR couple consists of a serine/threonine kinase and its target protein. These components of a signal transduction pathway are present in *S. griseus* and *S. coelicolor* but do not seem to control the same developmental steps. In *S. coelicolor*, the AfsK/R system is needed for secondary metabolism, whereas the same system is needed for morphological development in *S. griseus (44)*. Mutations in the *abs* loci uncouple antibiotic biosynthesis from morphological

development. None of the four antibiotics/pigments of *S. coelicolor* are produced in an *absA* mutant, but sporulation was unaffected *(45)*. Another group of these mutants, defined as the *absB* locus, were identified as RNase III mutants *(46)*.

Last but not least, the RNA polymerase σ factors should be mentioned. Streptomycetes produce a range of σ factors that are implicated in the transcriptional regulation of a variety of genes, including some involved in differentiation *(47–49)*. The best known examples are WhiG (*see* Section 2.2.) and σ^F that are required for normal spore maturation *(27)*.

3. COPPER AND DIFFERENTIATION

Studying the aspects of *Streptomyces* differentiation held more surprises. Extracting an agar plug with a brass cork borer from a plate with confluent growth of vegetative *S. lividans* mycelium resulted in a stimulation of development of aerial hyphae and of spores in the mycelium in the immediate surroundings where the plug was taken. This effect was not the result of mechanical stress because the stimulation of the development did not occur when a plastic device was employed to extract an agar plug. The source for the developmental induction was found to be the result of copper, one of the components of the alloy of which the cork borer was made (Kieser and Melton, unpublished). The effects of copper ions on reproductive growth was confirmed by Ueda et al. *(50)*, who showed that a mutant of *S. tanashiensis*, deficient in both antibiotic production and sporulation, was restored in both aspects when extra copper salts were added to the medium. Although stimulation of the actinorhodin production in *S. coelicolor* by copper ions was also reported *(50)*, this observation could not be reproduced by others *(51)*. However, copper ions do seem to have an effect on (secondary) metabolism. The characteristic earthy odor of many streptomycetes and fungi is the result of geosmin (*trans*-1,10-dimethyl-*trans*-9-decanol) production. This volatile compound has a very low odor threshold. Dionigi et al. *(52)* observed that geosmin production is stimulated specifically by copper ions not only in *S. tendae* but also in the fungus, *Penicillum expansum*. The impact of copper ions on morphogenesis is not restricted to streptomycetes. The GRISEA mutant of the filamentous fungus *Podospora anserina* has a diminished production of aerial hyphae and a longer life-span than the wild type. This phenotype was reversed to wild-type characteristics upon the addition of extra copper salts to the medium (53). The protein encoded by the *grisea* gene turned out to be an ortholog of Mac1, a copper-dependent transcription factor of *Saccharomyces cerevisae (54)*. The wild-type grisea gene complements a *mac1* mutant of *S. cerevisae*. The implication of these results is that GRISEA has a role in copper homeostasis in *P. anserina* similar to that of Mac1 in *S. cerevisae*. The observed phenotype for the *grisea* mutant shows a serious impact on morphogenesis, life-span control, and senescence, suggesting that disturbance of copper homeostasis does have a broad spectrum of effects and is better manifested in filamentous fungi than in yeast.

In *S. lividans*, an increase of the concentration copper in the growth media R2YE from 0.2 to 2 μ*M* was sufficient to advance the switch from vegetative growth to the production of aerial hyphae by approx 24 h (Fig. 2). The abundance of aerial hyphae and spores formed, as judged from the "fluffy white appearance" and the intensity of the gray spore pigment, respectively, is higher in the presence of copper ions than eventually observed in control strains without extra copper added. The closely related strain *S. coelicolor* did not respond to the addition of extra copper. However, it should be noted that this strain is "quicker" when it comes to development than *S. lividans*. In the presence of 2 μ*M* copper, salt differentiation in *S. lividans* is about as quick as that of *S. coelicolor*. The action of copper ions is unique and specific, no other metal ions stimulated the production of aerial hyphae and spores *(50,51)*.

The importance of copper during the switch from vegetative growth to the reproductive growth was substantiated further by the effect of reduction of the bioavailable copper concentration by the addition of copper chelators. In media, equilibrium exists between Cu(I) and Cu(II). The reduced Cu(I) form is constantly oxidized by oxygen, whereas the oxidized species Cu(II) is reduced by reducing equivalents present in the growth medium. Upon binding of Cu(I) by the specific chelator

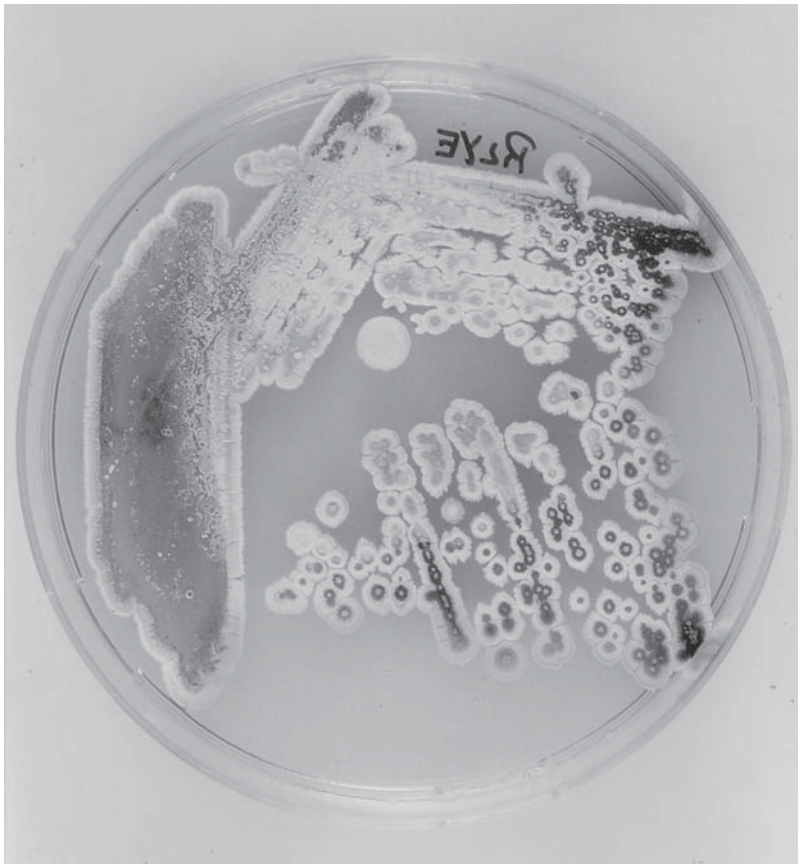

Fig. 2. Induction of development by copper. On the complex R2YE medium, *S. lividans* is slower in development than the closely related strain *S. coelicolor*. However, extra copper ions accelerate differentiation. This figure shows that immediately around a cotton filter disk that contains copper sulfate, aerial hyphae and spores develop faster than in the more distant regions of growth. Titration experiments have shown that raising the concentration of copper ions from 0.2 to 2 μ*M* is sufficient.

BCDA (bathocuproinedisulfonic acid), the equilibrium will shift toward the Cu(I) species and eventually all copper will be bound by the chelator.

Streptomyces coelicolor and *S. lividans* grown on medium containing BCDA (20 μ*M*) failed to produce aerial hyphae and spores (Fig. 3A). However, the presence of this copper chelator was not an impediment for vegetative growth or secondary metabolism. The BCDA effect could be reversed by the addition of extra copper ions (Fig. 3B). Remarkably, the developmental block that occurred after the addition of BCDA could still be relieved by the addition of extra copper salts after 1 wk. Therefore, the effect of BCDA is not the result of the toxicity of this chelator but rather the result of the diminished bioavailability of copper *(51)*. The devastating effect of the reduction of the available copper ions by addition of BCDA on morphogenesis was observed only on rich yeast-extract-containing media such as R2YE. In contrast, neither this effect on differentiation nor the stimulation of differentiation by extra copper was present on minimal media containing mannitol as the carbon source. These observations support the idea that at least two pathways can be induced that lead into development.

None of the *bld* mutants could be stimulated to produce aerial hyphae by the addition of extra copper. The inability to restore development of the *bld* mutants by elevating the copper-ion concentration may indicate that we are dealing with a linear cascade and not two separate pathways. In the linear-cascade

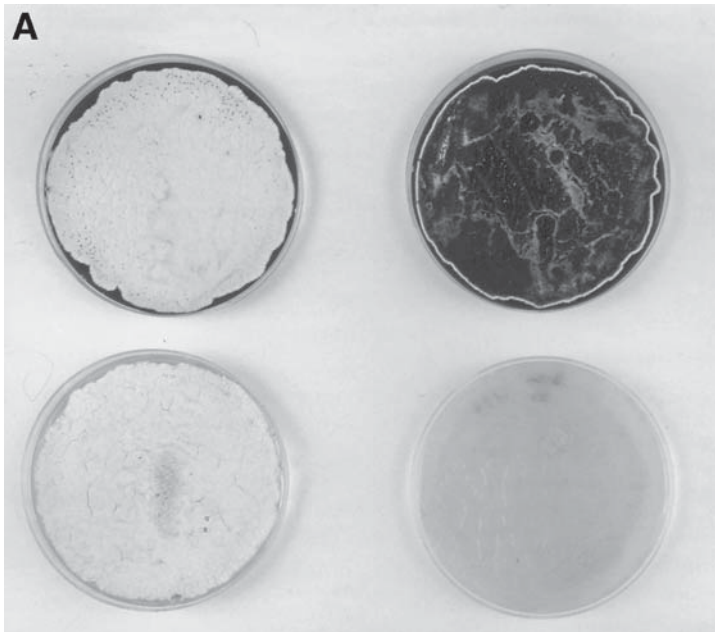

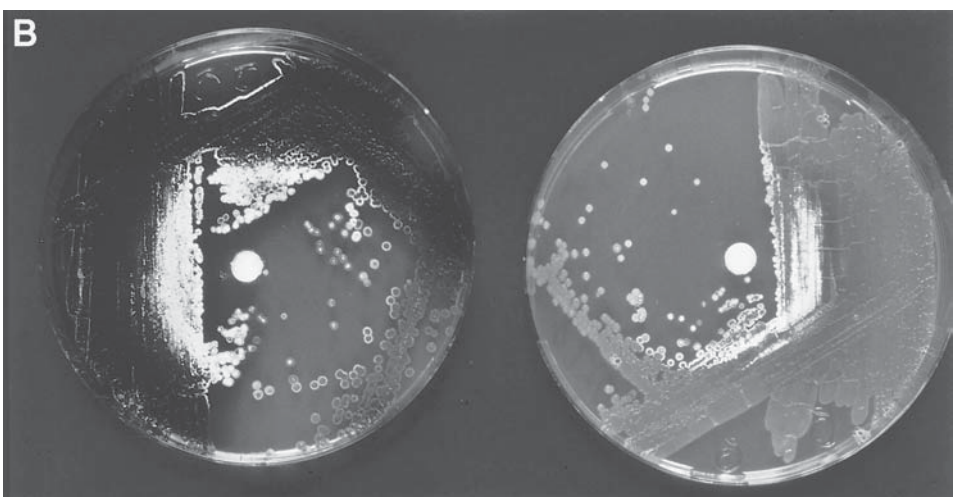

Fig. 3. (A) Inhibition of morphological development by the Cu(I)-specific chelator BCDA. Confluent lawns of *S. lividans* (bottom) and *S. coelicolor* (top) have developed aerial hyphae and spores after 7 d incubation at 30°C (left). On R2YE agar plates with 25 μ*M*, BCDA added, morphological development is blocked and does not proceed further than vegetative mycelium. The production of secondary metabolites is not inhibited. **(B)** Copper counteracts the inhibition of BCDA. *S. coelicolor* (left) and *S. lividans* (right) were grown on R2YE agar plates containing 25 μ*M* BCDA. The addition of copper sulfate via a cotton filter induces development of aerial hyphae and spores in a circular zone around the filter.

model, the effect of the copper ions would play a role higher up in the "bld-cascade." However, the *bld* mutants suffer from pleiotropic effects that could affect the putative "copper pathway" as well.

The mechanism responsible for the strong enhancement of the differentiation by the addition of copper and for the developmental block that occurs after the addition of copper-specific chelators is not well understood in streptomycetes. Considering the observations made in *P. anserina*, deregulation of cellular copper metabolism is obvious. Assuming that *S. lividans* is lagging behind in development

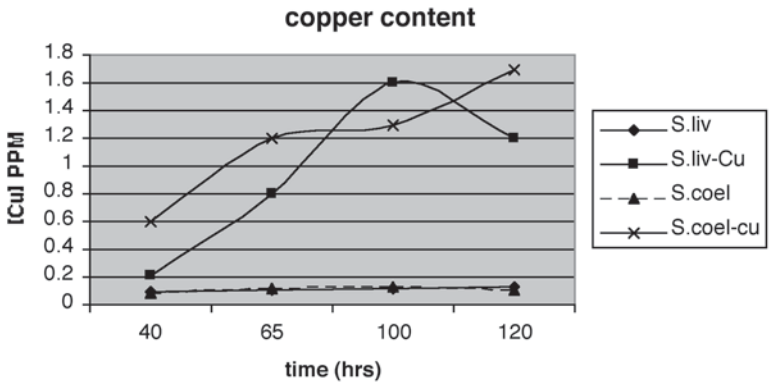

Fig. 4. Copper content of *S. lividans* and *S. coelicolor*. The copper content of mycelium of *S. lividans* and *S. coelicolor* grown in medium with and without extra copper added was determined by atomic absorption. Mycelium was concentrated by centrifugation and dissolved in nitric acid. The copper concentration (in ppm) is expressed per milligram of mycelium (wet weight). Samples were taken during vegetative growth (around 40 h), just before aerial hyphae started to appear (65 h), during full aerial hyphae development (100 h), and during sporulation (120 h).

because of a malfunction in copper homeostasis, one would expect to see different intracellular copper levels in surface-grown cultures of *S. lividans* and *S. coelicolor*. Atomic absorption measurements of the cellular copper concentrations of *S. lividans* and *S. coelicolor* mycelium harvested at various moments during growth on solid medium showed the same constant copper content during growth for both strains. A particular increase at the onset of differentiation was not detected (Fig. 4). On growth media with extra copper added, the mycelium does contain higher copper levels that increase in time, but, again, there is no major difference between *S. lividans* and *S. coelicor* (Keijser, unpublished). This may rule out that copper needs to be imported in higher amounts during one specific stage of growth.

3.1. The ram Cluster

Complementation of morphological mutants with genomic libraries of the wild-type strain is a powerful and successful technique to clone the corresponding gene *(32)*. Several clones of a genomic library of the closely related strain *S. coelicolor* complemented the copper-dependent phenotype of *S. lividans*. The *S. lividans* transformants produced aerial hyphae approx 24–36 h earlier than the parent strain. Extra copper addition to the medium could not achieve a further advancement of the onset of differentiation *(51)*. Sequencing and Southern blot analysis showed that, without exception ,these complementing clones were derived from the same region of the *S. coelicolor* genome. They contain the *ram* cluster that was previously identified as a clone that resulted in rapid aerial mycelium formation *(55)*. This locus consists of five genes encoding a putative membrane-bound serine/threonine kinase (*ramC*), a transcription factor of the two-component response regulator family (*ramR*), two ABC transporters (*ramAB*), and a small ORF (*ramS*) that does not have any homology to known sequences in the database (Fig. 5). The *ramC* gene is not required for the complementation because this ORF was not intact on all of the complementing clones. Integration of a single copy of the *ramSABR* genes in the genome of *S. lividans* was sufficient to get full complementation of the copper-dependent differentiation. Introduction of *ramS* or *ramR* alone had no effect *(51)*.

3.2. The Role of Ram Proteins in the Onset of Aerial Hyphae Formation

The need of *S. lividans* for the *S. coelicolor ram* genes to get timely aerial hyphae formation suggests the absence of a (active) *ram* cluster in the former strain. Surprisingly, a complete *ram*

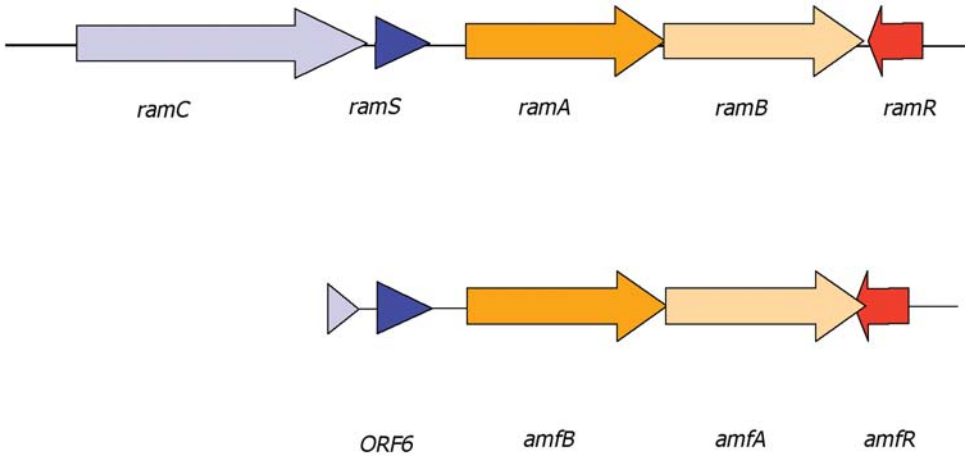

Fig. 5. Organization of the *ram* and *amf* clusters. The *ram* cluster consists of five genes: a membrane-bound serine/threonine kinase (*ramC*), a small peptide (*ramS*), two ABC transporters (*ramA* and *ramB*), and a transcription factor (*ramR*). The stop codon of *ramA* overlaps with the start codon of *ramB*, suggesting translational coupling of the two ORFs. The *amf* cluster consists of the same number of genes. The *ramC* ortholog is not cloned/sequenced completely, but the available C-terminal sequence suggests that the ORF upstream of ORF6 is similar to *ramC*. The *amfC* gene reported in the literature *(56)* does not belong to this cluster of genes.

cluster is present in *S. lividans* and is shown to be fully capable of complementing the copper-dependent phenotype when present in at least two copies *(51)*. In order to get better insight in the participation of the proteins encoded by these genes in development, *ramABR* disruption mutants were constructed and the transcriptional regulation and organization was analyzed. Introduction of an extra copy of *ram* dramatically increased the low level of transcription of *S. lividans*. Transcription, arising in part from promoters upstream of *ramS*, was found to be confined to the growth phase in which aerial hyphae are formed, underscoring the role of this cluster during this developmental stage *(51)*. This was further illustrated by the phenotype of *S. lividans ramABR* mutants. The disruption of *ramABR* in *S. lividans* resulted in a loss of the ability to form aerial hyphae and spores, whereas disruption in *S. coelicolor* resulted in a severe delay of the onset of aerial hyphae formation but not a *bld* phenotype (Fig. 6). Vegetative growth and secondary metabolism were not affected by the mutation. Interestingly, normal development was restored when grown in the presence of excess copper. In addition, when grown in close proximity to differentiating wild-type strains, the development of *ramABR* mutants was also restored (Fig. 7). This is indicative for extracellular complementation. The *ram* disruption mutant is no longer capable of exporting a signal molecule whereas the wild type strain is and can provide the mutant with this signaling molecule. The role of RamR as a transcription factor could be either in the regulation of the production of this signal, the regulation of *ramAB* transcription, or the regulation of the expression of an unknown factor.

One of the *bld* mutants (*bldA*) does respond to the *ram* mutant when grown next to one another. All other mutants tested, *bldD*, *bldF*, and *bldG*, do not respond nor does the *ram* mutant react to the *bld* mutants *(51)*. However, this analysis is not extensive enough to conclude whether *ram* is or is not part of the proposed "bld-cascade" *(11)*.

The data do not strongly support a direct association between *ram* and copper. A model in which *ram* and copper are part of independent morphological pathways seems the simplest solution for the moment. In this model, the copper-dependent pathway is induced under high copper-ion conditions

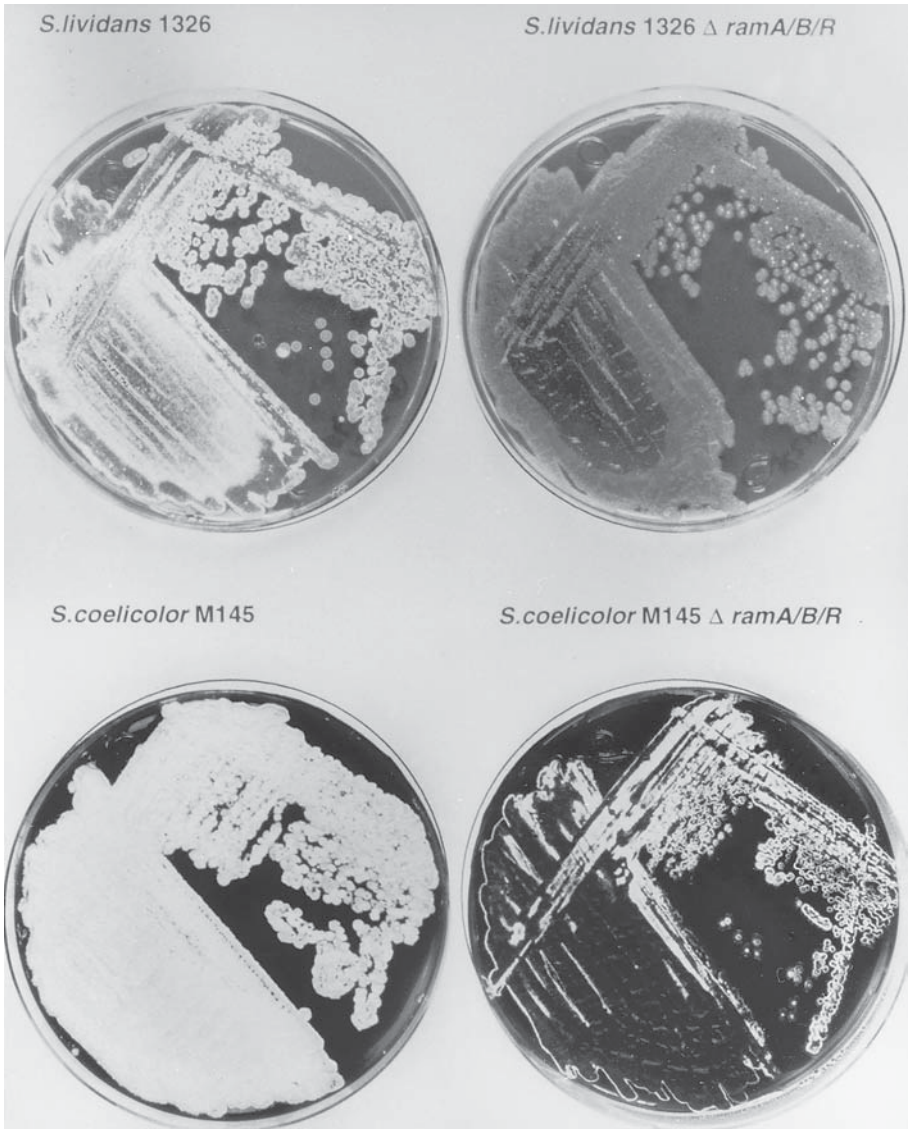

Fig. 6. Phenotype of *ram* disruption mutants. Wild-type strains (left) and *ram* disruption mutants (right) of *S. lividans* and *S. coelicolor* were grown on R2YE (0.2 μ*M* copper). The *S. lividans* mutant has a bald phenotype, whereas the *S. coelicolor* mutants is still capable of aerial hyphae formation, albeit much slower than the wild type.

(>2 μ*M*) and development then becomes *ram* independent. The observation that a strong reduction of the available copper results in a block of differentiation could be explained by the need of a specific copper protein during development that could operate during both the *ram*-dependent and the high-copper-dependent routes. This is supported by the fact that vegetative growth is not inhibited by the Cu(I)-specific chelator BCDA (i.e., enough copper is still available for the copper proteins active during this growth phase). The only condition when *ram* is essential for timely development is in the presence of "normal" copper levels. Under these conditions, the *ram* dependence is absolute for *S. lividans*, whereas *S. coelicolor* seems to have yet another route to its disposal that allows slow development even in the absence of *ram* (Fig. 8).

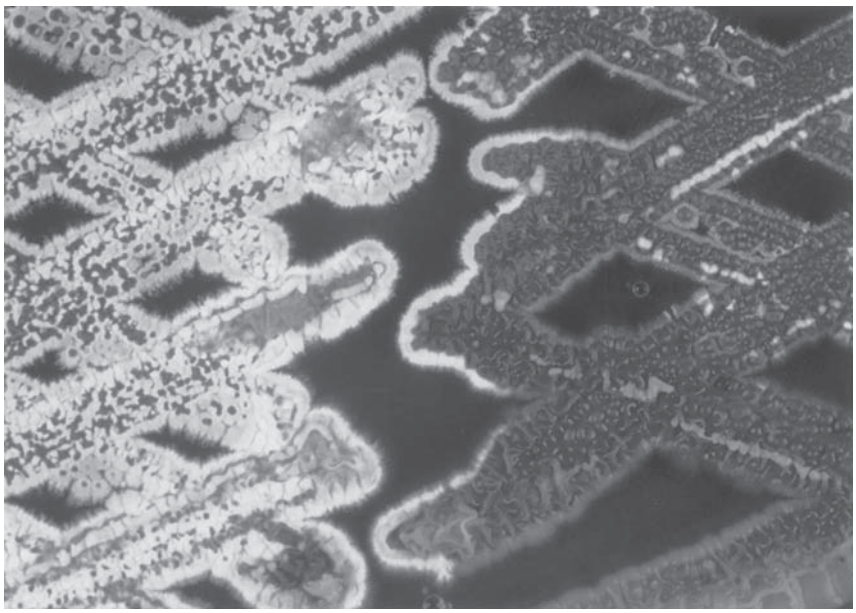

Fig. 7. Communication between the *ram* disruption mutant and the wild-type strain. Wild-type *S. lividans* (left) and the *ramABR* disruption mutant (right) grown on solid medium under conditions where the mutant alone does not form aerial hyphae and spores. The edge of patches of mutant hyphae growing closest to the wild-type mycelium show the typical white color of aerial hyphae. This is indicative for an extracellular factor that induces development in the mutant and is produced by the wild-type strain. Therefore, the *ramABR* mutant is either not capable of secreting this factor or unable to produce it. The former would be in agreement with the putative function of RamAB.

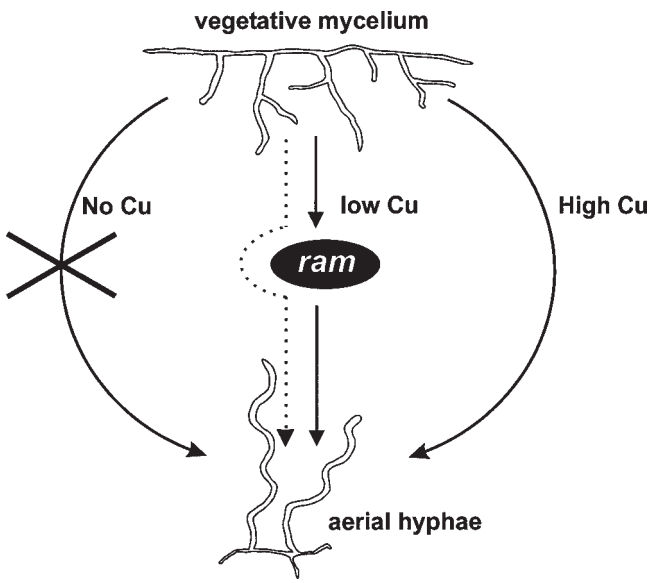

Fig. 8. Copper and the onset of aerial hyphae formation. Binding of all copper ions to the copper-specific chelator BCDA blocks the switch from vegetative growth to aerial mycelium formation (left). The *ram*-dependent pathway operates during growth on R2YE (0.2 μ*M* copper), whereas under the same conditions, a second pathway that is *ram* independent but slower (dotted line) seems to be active in *S. coelicolor*. Higher copper levels (>2 μ*M*) render *S. coelicolor* and *S. lividans ram* independent.

3.3. The amf Cluster

In *S. griseus*, one of the important factors determining morphological differentiation as well as physiological differentiation is A-factor. This bacterial hormone belongs to the family of γ-butyrolactones. A developmental mutant, HH1, that is deficient in A-factor production has a bald phenotype (no aerial hyphae formation) and no longer produces streptomycin *(6)*. A gene cluster complementing this mutant for morphological development but not for A-factor and streptomycin production is *amf*. The organization of the *S. griseus amf* cluster and the *S. coelicolor ram* cluster are very similar (Fig. 5). Two genes (*amfAB*) encode ABC transporters and a third gene (*amfR*), transcribed in the opposite direction, encodes a response regulator of a two-component regulator system. The *amf* cluster also contains a *ramS* ortholog and an upstream ORF with similarity to *ramC*. The overall similarity of the gene products of *ramAB* and *amfAB* is sufficiently high to assume that these transporters have a similar function. This does not necessarily mean that they transport the same molecule and operate at the same point of the developmental cascades in *S. griseus* and *S. coelicolor*.

The participation of the membrane-bound transporters AmfAB in the onset of aerial hyphae formation in *S. griseus* is, in fact, dubious. The *amfB* gene was shown to be dispensable for complementation of strain HH1, whereas *amfR* and *amfA* were needed *(57)*. Later, it was demonstrated in wild-type *S. griseus* that the disruption of only *amfR* results in a bald phenotype. This mutant could be complemented by *amfR*, including some upstream sequences but without *amfA (58)*.

4. GENOME ANALYSIS

A milestone for the understanding of the physiology of *Streptomyces* will be the completed nucleotide sequence determination of the 8-Mb linear genome of *S. coelicolor* (*Streptomyces coelicolor* Genome Project, http://www.sanger.ac.uk/Projects/S_coelicolor/, Sanger Centre, UK). This project has been initiated after the generation of a cosmid library covering the genome *(59)*. The ongoing annotation at the Sanger Centre provides the community with a first impression of the proteins encoded on this, for bacterial standards, large genome. The availability of the genome sequence facilitates more detailed searches for specific proteins and families of proteins. Blast searches using the sequences of known copper proteins and copper-binding motifs have been used to make an inventory of putative copper proteins in *S. coelicolor*. This inventory can provide better guidance to the experiments aimed at the understanding of the close relationship between copper ions and morphogenesis in *Streptomyces*.

In microorganisms, copper-containing proteins can roughly be divided in three categories: (1) electron-transfer proteins, (2) redox enzymes, and (3) copper-transport and homeostasis proteins. The first two categories of copper proteins have redox active copper centers. The function of proteins belonging to the latter group is transport and/or storage of copper ions and keeping copper redox inactive. In this way, these proteins protect the cell from the lethal effects of free-copper ions and they can deliver the copper ion at the site where it is required. Each of these categories of copper-containing proteins is characterized by one or more amino acid motifs, including the copper ligands. Representative proteins of each category and the known amino acid sequence motifs have been used to screen the *S. coelicolor* genome database for putative copper proteins. No hits have been found with searches for electron-transfer proteins, but several hits were recorded in the other two categories. Search criteria were, among others, copper-binding sites (type I, type II, or type III), heavy-metal-associated motif (HMA), and cysteine-rich sequences such as in metallothioneins *(60)* and in the copper fist domain of Mac1 *(61)*. The most convincing examples of putative copper-binding proteins in *S. coelicolor* are discussed in the following subsections and are listed in Table 1. The localization of these proteins is depicted in Fig. 9. It must be emphasized that the similarity searches deliver an indication of copper binding as a cofactor and a prediction of the function of the proteins. Detailed biochemical and genetic studies should provide definite proof of their copper-binding capacity and their role in physiology.

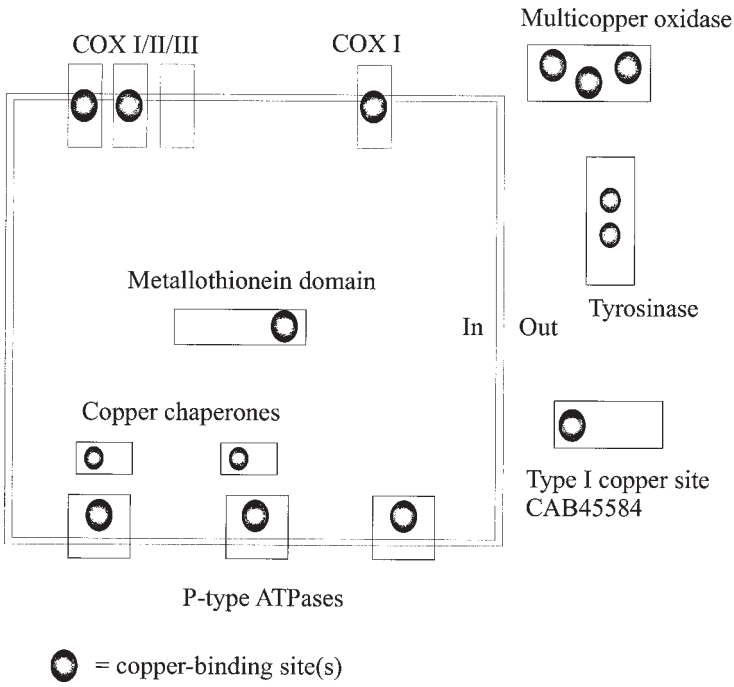

Fig. 9. Localization of putative copper proteins in *S. coelicolor*.

Table 1
Putative Copper-Binding and/or Transporting Proteins in *S. coelicolor*

Database no.	*Putative classification*	*Localization*	*Motif*
CAB96031	Metal transporter, P-type ATPase	Membrane	GMTCASC
CAB96030	Metal chaperone	Cytoplasm	GMSCGHC
CAB65641	Metal transporter, P-type ATPase	Membrane	GMTCAAC
SCC57A.02	Metal transporter, P-type ATPase	Membrane	GMTCASC
SCC46.15	Metal chaperone	Cytoplasm	GMSCGHC
CAB94657	Cytochrome-*c* oxidase subunit I	Membrane	Heme *a* and a_3 binding and Cu_B site
CAB39882	Cytochrome-*c* oxidase subunit I	Membrane	Heme *a* and a_3 binding and Cu_B site
CAB39883	Cytochrome-*c* oxidase subunit II	Membrane	Cu_A site
CAB45586	Multicopper oxidase	Extracellular	Type I, II, III site
CAB45584	Unknown with blue copper site	Extracellular	Type I copper site, CTIPGHGQM
CAB92266	Tyrosinaselike	Extracellular	Type III copper site, Cu_A and Cu_B
CAB50963	Unknown with metallothioneinlike domain	Cytoplasm	Cysteine rich at the C-terminus

Blast and motif searches were performed with the blast server provided on the *S. coelicolor* Genome project website. Amino acid sequence analysis for putative signal sequences were performed with SignalP *(62)*. Folding was carried out at 3D-pssm *(63)*.

4.1. Cytochrome-c Oxidase

The large family of terminal oxidases includes cytochrome-*c* oxidase (COX) and quinol oxidase (QOX) *(64,65)*. The bacterial members of this family consist of three subunits and have significant sequential and structural similarity. Subunits III and I are most conserved within the oxidase family.

```
                                                  *
MDRRGFNRRVLLGGAAAATSLSIAPEVAGAAPAAKGITARTAPAGGEVRH
LKMYAEKLADGQMGYGFEKGKASVPGPLIEVNEGDTLHIEFTNTMDVRAS

 T2  T3
LHVHGLDYEISSDGTAMNKSDVEPGGTRTYTWRTHKPGRRDDGTWRPGSA

   T3  T3
GYWHYHDHVVGTEHGTGGIRNGLYGPVIVRRKGDVLPDATHTIVFNDMTI

                                          T1    T2  T3
NNRKPHTGPDFEATVGDRVEIVMITHGEYYHTFHMHGHRWADNRTGILTG

                                                T3 T1 T3     T1        T1
PDDPSRVIDNKITGPADSFGFQIIAGEGVGAGAWMYHCHVQSHSDMGMVG
LFLVKKPDGTIPGYEPHEHGGATAKSGESGEPTGGAAAHEHEH
```

Fig. 10. Type I, II, and III copper-site ligands of CAB45584. Amino acid sequence (343 residues) of the putative multicopper oxidase (CAB45584) of *S. coelicolor*. The ligands of the type I, type II, and type III coppers are indicated by T1, T2, and T3, respectively. The signal peptidase cleavage site as predicted by SignalP *(62)* is indicated by an asterisk.

The main difference between the oxidases is their substrate, cytochrome-*c* or quinols. Subunit I contains the redox active copper Cu_B and binds the two hemes, *a* and a_3. In subunit II, the Cu_A site is located. The third subunit has the least sequence similarity and its role in the oxidase activity is still a matter of debate. Genes for a terminal oxidase of this family were expected to be present on the *Streptomyces coelicolor* genome because it has an aerobic metabolism. CAB39882 and CAB39883 show the highest similarity with subunit I and with subunit II of cytochrome-*c* oxidases, respectively. The two genes are located in a region of the genome encoding several other proteins involved in respiration, including the subunit III of COX.

The other copy of subunit I (CAB94657) is 87% similar to CAB39882 and is similar to many other subunits I of COX and QOX in the database. However, there are no genes for the oxidase subunit II and III located in the upstream or downstream sequences in this region of the genome. It remains to be investigated what the function of this protein is.

4.2. Multicopper Oxidase

The best known representatives of the multicopper oxidases are laccase and ascorbate oxidase (reviewed in ref. *66*). These enzymes contain three copper centers, type I, type II, and type III, each characterized by specific absorption bands. Two signatures (Prosite, SIB) in the primary amino acid sequence are indicative for multicopper oxidases. One pattern is specific for copper-binding domains, whereas the other pattern also recognizes domains that have lost their copper-binding ability. In addition, four amino acid sequences containing the copper ligands can be distinguished. Two regions are located in the N-terminal half of the protein and the other two are found in the C-terminal half. Together, these sequences make up the three copper centers.

CAB45586 contains all of the above and, strictly on amino acid similarity, should be considered as a member of the multicopper oxidase family. However, this *S. coelicolor* protein is much smaller than the known multicopper oxidases, 343 amino acids compared to >600 residues. The four amino acid motifs involved in copper binding are situated closer together in the primary amino acid sequence than is the case in other multicopper oxidases (Fig. 10). The amino acid residues 70–300 show similarity (40–45%) with the 2 domains containing the 4 sequences involved in copper binding of the copper resistance protein A (*copA*) of *Pseudomonas syringae (67)*, the copper resistance protein

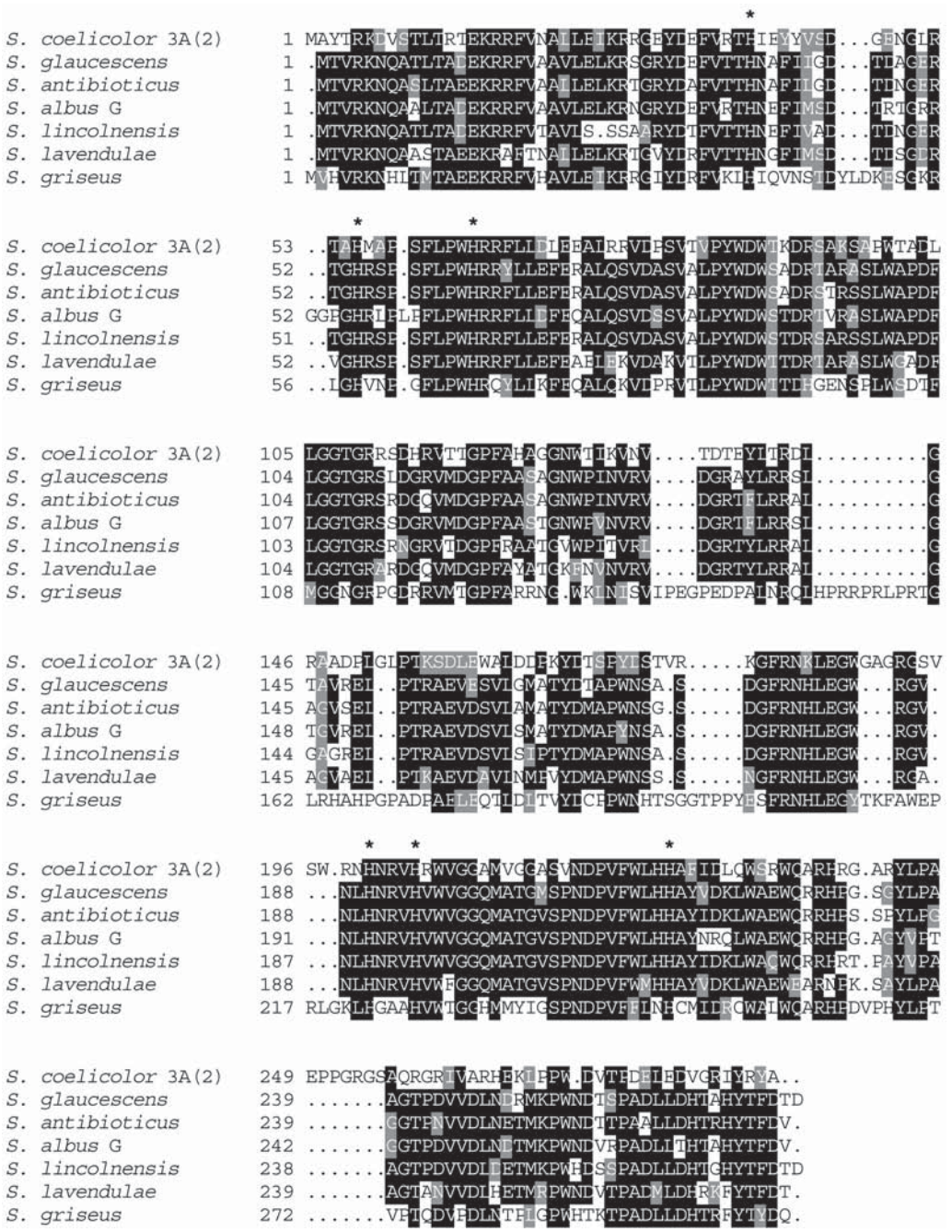

Fig. 11. Multiple-sequence alignment of the *S. coelicolor* tyrosinase-like protein and all known streptomycetes tyrosinases. Alignment of the sequences was carried out with the program MultAlin *(75)* and shading with the program BoxShade (www.ch.embnet.org/software/). The conserved histidine ligands of Cu_A and Cu_B are indicated by an asterisk.

pcoA of *Escherichia coli (68)*, ceruloplasmin, coagulation factor V, laccase, and ascorbate oxidase. At the extreme N-terminal end and at the C-terminal end, no significant similarity shows up in the database.

The first 30 N-terminal amino acids of CAB45586 are predicted to be a signal sequence *(62)*. Therefore, this multicopper oxidase is most likely exported and fulfills its function outside the cell.

4.3. CAB45584

CAB45584 is a protein of 729 amino acids with a putative N-terminal signal sequence. The first 130 amino acid residues of the mature protein have similarity with a putative blue copper protein of Arabidopsis and with auracyanin B of *Chloroflexus aurantiacus (69)*. The blue copper proteins are characterized by a type I copper site with the signature $CX_{1-2}P/GX_{0-1}HX_{2-4}M/Q$ where the C, H, and M are copper ligands. The fourth copper ligand is located many residues upstream of the cysteine. In parts of the 500 N-terminal amino acids, weak similarity with glycosyl hydrolases such as endoglucanase D of *Cellumonas fimi* is found. However, this class of enzymes has not been reported to contain a copper cofactor. Therefore, a prediction of the enzymatic function of CAB45584 will need more research than just *in silico* studies to define its function and copper content.

4.4. Tyrosinase-Like Protein

Tyrosinases are enzymes that catalyze the hydroxylation of monophenols to diphenols and the oxidation of diphenols to quinones (reviewed in ref. *70*). The latter are precursors of melanines and can spontaneously polymerize to these well-known brown pigments. For the reactions with monophenols, tyrosinases have to bind oxygen. This is accomplished by a dinuclear Cu site (Cu_A and Cu_B) present in the enzyme. Three histidine residues bind each copper and together they form the so-called type III site *(71,72)*. Not only do monooxygenases such as tyrosinase have this type of copper-binding site. In hemocyanins, the type III copper site is used to transport and store oxygen *(73)*. The third member of the type III copper-site family is catechol oxidase *(74)*, which can carry out the oxidation of diphenols but not the hydroxylation of monophenols.

Tyrosinases are widespread in nature and occur in all kingdoms. The protein identified in the *S. coelicolor* genome sequence does contain the conserved histidines involved in copper binding and has similarity with tyrosinases from other *Streptomyces* strains. However, the similarity is lower than found between the known tyrosinases (Fig. 11). In strains producing tyrosinase, the gene encoding tyrosinase, *melC2*, is always preceded by a small ORF, *melC1*, that encodes a histidine-rich protein that is proposed to be the copper chaperone of apotyrosinase and also involved in secretion of tyrosinase *(76,77)*. *Streptomyces* tyrosinase is an extracellular enzyme but does not have an N-terminal signal sequence. This feature is also present in *S. coelicolor*. Immediately upstream of the gene encoding CAB92266, in fact the start codon of the *melC2* ortholog, is located within this ORF; a small ORF is located with many histidine residues and similarity to *melC1* (Fig. 12). All tyrosinase-expressing *Streptomyces* strains do produce melanin, but *S. coelicolor* does not. Taking this into consideration, it suggests that CAB92266 is an extracellular copper enzyme but most likely does not have monophenols as substrate and is not a monophenol monooxygenase. If the protein turns out to be a tyrosinase, its expression must be strongly downregulated under "normal" growth conditions or the enzymatic product cannot polymerize to form melanines.

4.5. CAB50963

This protein consists of 310 amino acids. The C-terminal domain is rich in cysteines (23 out of 68 amino acids) and has a similarity to metallothioneins. The amino-terminal domain does not show significant similarity to proteins in the databases. The protein has been described first for *S. albogriseolus* as a putative repressor of the expression of an extracellular protease *(79)*. Metallothioneins are small proteins (68 amino acids) that bind heavy metals such as Cu, Zn, Cd, and

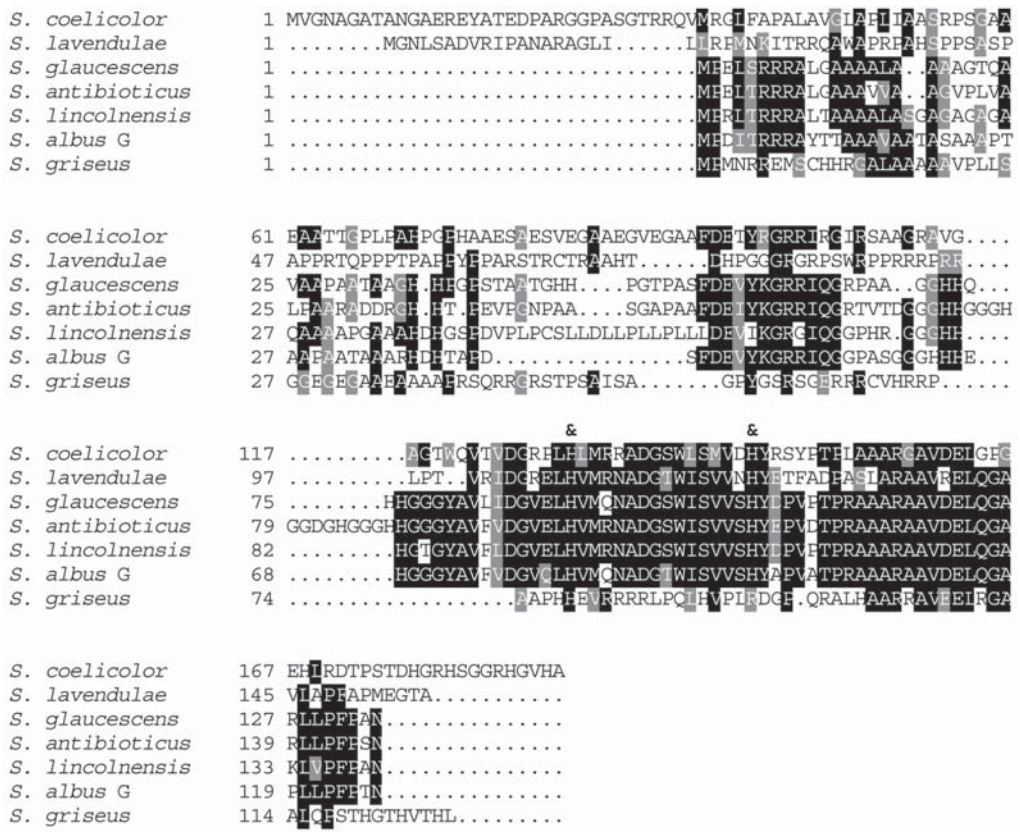

Fig. 12. Alignment of the *S. coelicolor* MelC1 with all known *Streptomyces* MelC1s. The histidine residues proposed to be involved in copper binding and apotyrosinase maturation are indicated with an **&** *(78)*. The signal peptidase cleavage site as predicted by SignalP *(62)* is behind amino acid residue 62, resulting in a abnormally long signal sequence. An alternative translational start site is present (Met at position 35), but this AUG codon is not preceded by an obvious ribosome-binding site, whereas the first methionine codon is.

Hg *(80)*. They function as metal sinks in the cell. The appearance of a metallothioneinlike domain in a much larger protein that may be involved in transcription regulation could turn out to be an interesting link with metal homeostasis.

4.6. Metal Transport

The physiological requirement for copper puts the cell in a difficult position. These redox active metals should not be present in the cells in a free state because of their capacity to engage in all kinds of redox reactions that can damage many macromolecules. Therefore, organisms have developed systems to import, sequester, distribute, and export metal ions depending on the intracellular need and the extracellular availability. For the acquisition of metals, the first barrier is the outer membrane. One of the families of proteins taking care of metal transport across membranes are the P-type ATPases containing a heavy-metal-associated domain (HMA) in the N-terminal sequence. The well-studied CopA of *Enterococcus hirae* belongs to this family *(81)*. The HMA contains a short sequence, GMXCXXC, involved in metal binding. This motif has been used to screen the *S. coelicolor* genome. Three genes were identified that encode for integral membrane proteins with all characteristics of the heavy-metal pumps (Fig. 13A). They have eight transmembrane domains, a phosphatase domain

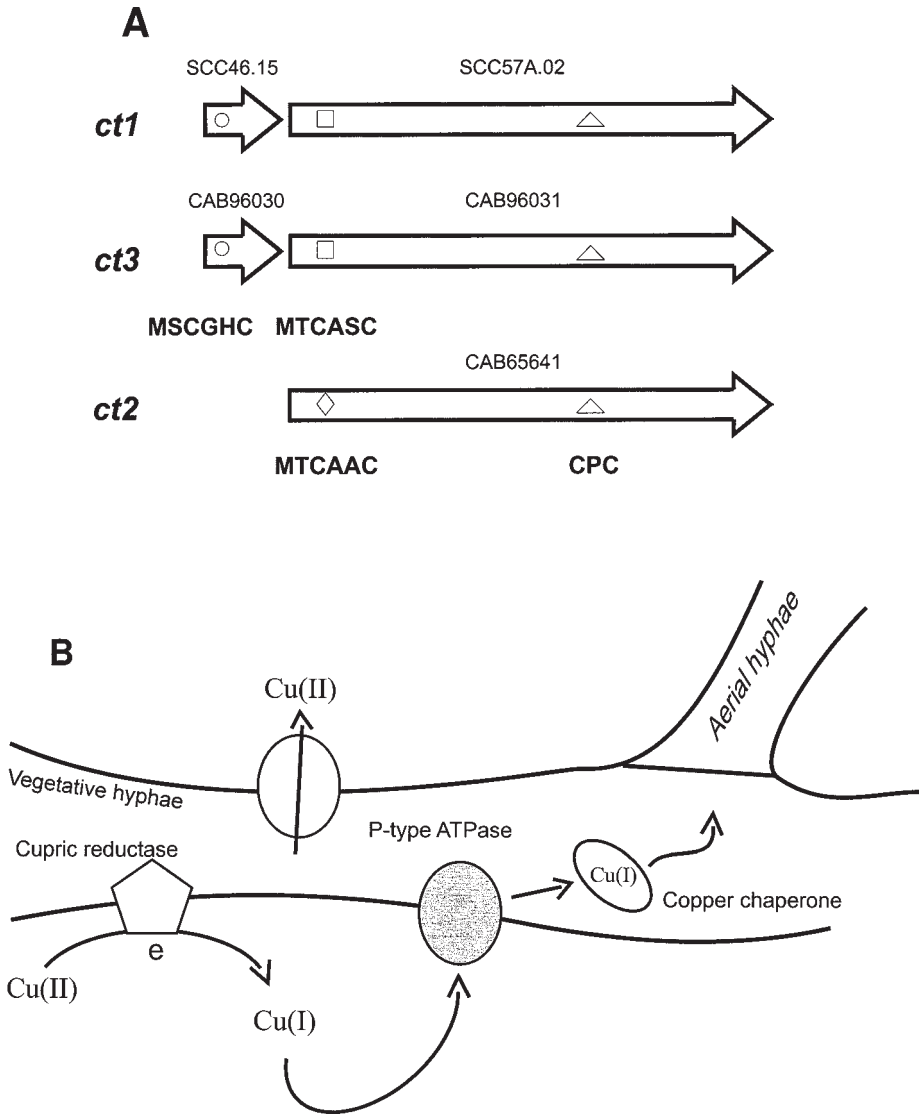

Fig. 13. **(A)** Gene organization of the copper P-type ATPases and copper chaperones. **(B)** Model for the copper trafficking in *S. coelicolor*. Two of the P-type ATPases are proposed to be involved in copper uptake, whereas the third ATPase, which is not linked to a chaperone, is concerned with copper efflux in analogy with CopA of *E. coli (82)*. The two copper-uptake ATPases do not necessarily have to be present at the same time in the same membranes. A scenario in which one of them is expressed during vegetative growth and the other during aerial hyphae development could be feasible. The cupric reductase is assumed to be a membrane-bound enzyme because all cupric reductase activity in *Streptomyces* was found to be mycelium associated (Vijgenboom, unpublished).

(TGE), a conserved phosphorylation site (DKTGT), an ATP-binding domain (GDGVN), and the CPC motif in the sixth transmembrane domain that is conserved in all P-type ATPases involved in transport of the soft metal ions [Cu(I), Cd(II), Ag(I), or Zn(II)]. The N-terminal cytoplasmic domain contains the GMTCAA/SC motif that is indicative for heavy-metal binding. This motif is capable of binding several heavy-metal ions, but the N-terminal domains of ATPases that transport a particular metal ion show a slightly greater similarity *(83)*. This criterion classifies the *S. coelicolor* P-type

ATPases as copper transporters. The conclusion is supported by the fact that upstream of two of the three ATPases, a small protein is encoded with similarity to CopZ *(84,85)*. This protein is a member of the family of copper chaperones that obtain the copper ion from the ATPase and take care of its distribution in the cell. The copper chaperones contain an N-terminal metal-binding motif very similar to that of the ATPases, GMSCGHC in the case of *S. coelicolor*. The presence of three putative copper-transporting ATPases in *S. coelicolor* raises several questions. Are all three ATPases involved in copper uptake? Where are the ATPases located, in the vegetative mycelial membrane or maybe in the septum separating vegetative and aerial hyphae? What are the targets of the copper chaperones? The answers to these questions of course have to await further studies, but an educated guess for two of them can be made right now. The two ATPases that are coexpressed with a copper chaperone are most likely involved in copper uptake. The third ATPase could be concerned with copper export, as has been shown for CopA of *E. coli (82)*. One of the targets for the copper chaperones could be a transcriptional regulator as shown for the CopZ-CopY couple *(86)* or cytochrome-*c* oxidase, as shown in *Saccharomyces cerevisae (87)*. A model for copper trafficking is depicted in Fig. 13B. The proposed cupric reductase has not been identified in the *S. coelicolor* genome sequence, but a cupric-reductase activity is present in intact vegetative mycelium of *S. lividans* and *S. coelicolor* (Vijgenboom, unpublished).

5. CONCLUSION

The lifestyle of the filamentous bacterium *Streptomyces* is interesting from many points of view. In this chapter, we have highlighted one aspect, the link between available copper ions and morphogenesis. An unexpected result of the reviewed studies is that *Streptomyces* has several pathways at its disposal to initiate the formation of aerial hyphae: a copper-dependent route, a *ram*-dependent route and an as yet not defined carbon-source-dependent pathway. Future studies have to reveal whether these pathways are really independent or whether they somehow interact and communicate.

The insight in the nature of the intimate relation between copper and aerial hyphae formation is far from complete. The availability of the *S. coelicolor* genome sequence allows for a more direct approach, as outlined in the last part of this chapter. All putative copper enzymes that came out of the search are either membrane bound (COX, ATPase) or extracellular (multicopper oxidase, CAB45584, tyrosinase). The cytoplasmic proteins seem to be involved in copper sensing (MT domain) and trafficking (chaperones). The reason for a relation between copper uptake and morphological development is not immediately obvious from the identification of these putative copper proteins. However, it should be mentioned that the aerial hyphae are not in direct contact with the source of nutrients and cofactors, the medium, but depend on uptake via the vegetative mycelium. In the near future many revelations may be expected, not only on this topic but also on all other fields studied in streptomycetes.

REFERENCES

1. Susstrunk, U., Pidoux, J., Taubert, S., Ullmann, A., and Thompson, C. J. (1998) Pleiotropic effects of cAMP on germination, antibiotic biosynthesis and morphological development in Streptomyces coelicolor. *Mol. Microbiol.* **30**, 33–46.
2. Daza, A., Martin, J. F., Dominguez, A., and Gil, J. A. (1989) Sporulation of several species of *Streptomyces* after nutritional downshift. *J. Gen. Microbiol.* **135**, 2483–2491.
3. Glazebrook, M. A., Doull, J. L., Stuttard, C., and Vining, L. C. (1990) Sporulation of *Streptomyces venezuelae* in submerged cultures. *J. Gen. Microbiol.* **136**, 581–588.
4. Huber, F. M., Piper, R. L., and Mertz, F. P. (1987) Sporulation of *Streptomyces roseosporus* in submerged culture. *J. Ind. Microbiol.* **2**, 235–241.
5. Kendrick, K. and Ensign, J. C. (1983) Sporulation of *Streptomyces griseus* in submerged culture. *J. Bacteriol.* **155**, 357–366.
6. Horinouchi, S. (1996) *Streptomyces* genes involved in aerial mycelium formation. *FEMS Microbiol. Lett.* **141**, 1–9.
7. Chater, K. F. (1998) Taking a genetic scalpel to the *Streptomyces* colony. *Microbiology* **144**, 1465–1478.
8. Kelemen, G. H. and Buttner, M. J. (1998) Initiation of aerial mycelium formation in *Streptomyces*. *Curr. Opin. Microbiol.* **1**, 656–662.

9. Pope, M. K., Green, B. D., and Westpheling, J. (1996) The *bld* mutants of *Streptomyces coelicolor* are defective in the regulation of carbon utilization, morphogenesis and cell-cell signalling. *Mol. Microbiol.* **19**, 747–756.
10. Champness, W. (1988) New loci required for *Streptomyces coelicolor* morphological and physiological differentiation. *J. Bacteriol.* **170**, 1168–1174.
11. Willey, J., Schwedock, J., and Losick, R. (1993) Multiple extracellular signals govern the production of a morphogenetic protein involved in aerial mycelium formation by *Streptomyces coelicolor*. *Genes Dev.* **75**, 895–903.
12. Nodwell, J. R., McGovern, K., and Losick, R. (1996) An oligopeptide permease responsible for the import of an extracellular signal governing aerial mycelium formation in *Streptomyces coelicolor*. *Mol. Microbiol.* **22**, 881–893.
13. Nodwell, J. R., Yang, M., Kuo, D., and Losick, R. (1999) Extracellular complementation and the identification of additional genes involved in aerial mycelium formation in *Streptomyces coelicolor*. *Genetics* **151**, 569–584.
14. Nodwell, J. R. and Losick, R. (1998) Purification of an extracellular signalling molecule involved in production of aerial mycelium by *Streptomyces coelicolor*. *J. Bacteriol.* **180**, 1334–1337.
15. Bibb, M. J., Findlay, P. R., and Johnson, M. W. (1984) The relationship between base composition and codon usage in bacterial genes and its use for the simple and reliable identification of protein-coding sequences. *Gene* **30**, 157–166.
16. White, J. and Bibb, M. J. (1997) *bldA* dependence of undecyl-prodigiosin production in *Streptomyces coelicolor* A3(2) involves a pathway-specific regulatory cascade. *J. Bacteriol.* **179**, 627–633.
17. Fernandez-Moreno, M. A., Caballero, J. L., Hopwood, D. A., and Malpartida, F. (1991) The *act* cluster contains regulatory and antibiotic export genes, direct targets for translational control by the *bldA* tRNA of *Streptomyces*. *Cell* **66**, 769–780.
18. Guthrie, E. P., Flaxman, C. S., White, J., Hodgson, D. A., Bibb, M. J., and Chater, K. F. (1998) A response-regulator-like activator of antibiotic synthesis from *Streptomyces coelicolor* A3(2) with an amino-terminal domain that lacks a phosphorylation pocket. *Microbiology* **144**, 727–738.
19. Elliot, M., Damji, F., Passantino, R., Chater, K., and Leskiw, B. (1998) The *bldD* gene of *Streptomyces coelicolor* A3(2): a regulatory gene involved in morphogenesis and antibiotic production. *J. Bacteriol.* **180**, 1549–1555.
20. Pope, M. K., Green, B., and Westpheling, J. (1998) The *bldB* gene encodes a small protein required for morphogenesis, antibiotic production, and catabolite control in *Streptomyces coelicolor*. *J. Bacteriol.* **180**, 1556–1562.
21. Puglia, A.-M. and Capelletti, E. (1984) A bald, superfertile, UV-resistant strain of *Streptomyces coelicolor* A3(2). *Microbiologica* **7**, 263–266.
22. Bibb, M. J., Molle, V., and Buttner, M. J. (2000) σ^{BldN}, an extracytoplasmic function RNA polymerase sigma factor required for aerial mycelium formation in *Streptomyces coelicolor* A3(2). *J. Bacteriol.* **182**, 4606–4616.
23. Tillotsen, R. D., Wösten, H. A. B., Richter, M., and Willey, J. M. (1998) A surface active protein involved in aerial hyphae formation in the filamentous fungus *Schizophyllum commune* restores the capacity of a bald mutant of the filamentous bacterium *Streptomyces coelicolor* to erect aerial structures. *Mol. Microbiol.* **30**, 595–602.
24. Willey, J., Santamaria, R., Guijarro, J, Geistlich, M., and Losick, R. (1991) Extracellular complementation of a developmental mutation implies a small sporulation protein in aerial mycelium formation by *S. coelicolor*. *Cell* **65**, 641–650.
25. Richter, M., Willey, J. M., Süßmuth, R., Jung, G., and Fiedler, H-P (1998) Streptofactin, a novel biosurfactant with aerial mycelium inducing activity from *Streptomyces tendae* Tu 901/8c. *FEMS Microbiol. Lett.* **163**, 165–171.
26. Wösten, H. A. B. and Willey, J. M. (2000) Surface-active proteins enable microbial aerial hyphae to grow into the air. *Microbiology* **146**, 767–773.
27. Kelemen, G. H., Brown, G. L., Kormanec, J., Potúcková, L., Chater, K. F., and Buttner, M. (1996) The position of the sigma factor genes *whiG* and *sigF* in the hierarchy controlling the development of spore chains in the aerial hyphae of *Streptomyces coelicolor* A3(2). *Mol. Microbiol.* **21**, 593–603.
28. Aínsa, J. A., Ryding, N. J., Hartley, N., Findlay, K. C., Bruton, C. J., and Chater, K. F. (2000) WhiA, a protein of unknown function conserved among Gram-positive bacteria, is essential for sporulation in *Streptomyces coelicolor* A3(2). *J. Bacteriol.* **182**, 5470–5478.
29. Flärdh, K., Findlay, K. C., and Chater, K. F. (1999) Association of early sporulation genes with suggested developmental decision points in *Streptomyces coelicolor* A3(2). *Microbiology* **145**, 2229–2243.
30. Soliveri, J. A., Gomez, J., Bishai, W. R., and Chater, K. F. (2000) Multiple paralogous genes related to the *Streptomyces coelicolor* developmental regulatory gene *whiB* are present in *Streptomyces* and other actinomycetes. Microbiology **146**, 333–343.
31. Molle, V., Palframan, W. J., Findlay, K. C., and Buttner, M. (2000) WhiD and WhiB, homologous proteins required for different stages of sporulation in *Streptomyces coelicolor* A3(2). *J. Bacteriol.* **182**, 1286–1295.
32. Ryding, N. J., Bibb, M. J., Molle, V., Findlay, K. C., Chater, K. F., and Buttner, M. J. (1999) New sporulation loci in *Streptomyces coelicolor* A3(2). *J. Bacteriol.* **181**, 5419–5425.
33. Gehring, A. M., Nodwell, J. R., Beverley, S. M., and Losick, R. (2000) Genomewide insertional mutagenesis in *Streptomyces coelicolor* reveals additional genes involved in morphological differentiation. *Proc. Natl. Acad. Sci. USA* **97**, 9642–9647.
34. Kawamoto, S. and Ensign, J. C. (1995) Cloning and characterization of a gene involved in regulation of sporulation and cell division in *Streptomyces griseus*. *Actinomecetologica* **9**, 136–151.
35. van Wezel, G. P., van der Meulen, J., Kawamoto, S., Luiten, R. G. M., Koerten, H. K., and Kraal, B. (2000) *ssgA* is essential for sporulation of *Streptomyces coelicolor* A3(2) and affects hyphal development by stimulating septum formation. *J. Bacteriol.* **182**, 5653–5662.
36. England, R., Hobbs, G., Bainton, N., and Roberts, D. (eds.) (1999) *Microbial Signaling and Communication*, Cambridge University Press, Cambridge.

37. Horinouchi, S. and Beppu, T. (1992) Autoregulatory factors and communication in actinomycetes. *Annu. Rev. Microbiol.* **46**, 377–398.
38. Kawabuchi, M., Hara, Y., Nihira, T., and Yamada, Y. (1997) Production of butyrolactone autoregulators by *Streptomyces coelicolor* A3(2). *FEMS Microbiol. Lett.* **157**, 81–85.
39. Takano, E., Nihira, T., Hara, Y., Jones, J. J., Gershater, C. J. L., Yamada, Y., et al. (2000) *J. Biol. Chem.* **275**, 11,010–11,016.
40. Kinoshita, H., Tsuji, T., Ipposhi, H., Nihira, T., and Yamada, Y. (1999) Characterization of binding sequences for butyrolactone autoregulator receptors in streptomycetes. *J. Bacteriol.* **181**, 5075–5080.
41. Onaka, H., Nakagawa, T., and Horinouchi, S. (1998) Involvement of two A-factor receptor homologues in *Streptomyces coelicolor* A3(2) in the regulation of secondary metabolism and morphogenesis. *Mol. Microbiol.* **28**, 743–753.
42. Ohnishi, Y., Kameyama, S., Onaka, H., and Horinouchi, S. (1999) The A-factor regulatory cascade leading to streptomycin biosynthesis in *Streptomyces griseus*: identification of a target gene of the A-factor receptor. *Mol. Microbiol.* **34**, 102–111.
43. Kang, D.-K., Li, X.-M., Ochi, K., and Horinouchi, S. (1999) Possible involvement of cAMP in aerial mycelium formation and secondary metabolism in *Streptomyces griseus*. *Microbiology* **145**, 1161–1172.
44. Umeyama, T., Lee, P-C., Ueda, K., and Horinouchi, S. (1999) An AfsK/AfsR system involved in the reponse of aerial mycelium formation to glucose in *Streptomyces griseus*. *Microbiology* **145**, 2281–2292.
45. Adamidis, T., Riggle, P., and Champness, W. (1990) Mutations in a new *Streptomyces coelicolor* locus which globally block antibiotic biosynthesis but not sporulation. *J. Bacteriol.* **172**, 2962–2969.
46. Price, B., Adamidis, T., Kong, R., and Champness, W. (1999) A *Streptomyces coelicolor* antibiotic regulatory gene, *absB*, encode an RNase III holmolog. *J. Bacteriol.* **181**, 6142–6151.
47. Potuckova, L., Kelemen, G. H., Findlay, K. C., Lonetto, M. A., Buttner, M. J., and Kormanec, J. (1995) A new RNA polymerase sigma factor, sigma F, is required for the late stages of morphological differentiation in Streptomyces spp. *Mol. Microbiol.* **17**, 37–48.
48. Paget, M. S. B., Chamberlin, L., Atrih, A., Foster, S. J., and Buttner, M. J. (1999) Evidence that the extracytoplasmic function sigma factor sigmaE is required for normal cell wall structure in Streptomyces coelicolor A3(2). *J. Bacteriol.* **181**, 204–211.
49. Paget, M. S., Kang, J. G., Roe, J. H., and Buttner, M. J. (1998) σ^R, an RNA polymerase sigma factor that modulates expression of the thioredoxin system in response to oxidative stress in Streptomyces coelicolor A3(2). *EMBO J.* **17**, 5776–5782.
50. Ueda, K., Tomaru, Y., Endoh, K., and Beppu, T. (1997) Stimulatory effect of copper on antibiotic production and morphological differentiation in *Streptomyces tanashiensis*. *J. Antibiot.* **50**, 693–695.
51. Keijser, B. J. F., van Wezel, G. P., Canters, G. W., Kieser, T., and Vijgenboom, E. (2000) The *ram*-dependence of *streptomyces lividans* differentiation is bypassed by copper. *J. Mol. Microbiol. Biotechnol.* **2**, 565–574.
52. Dionigi, C. P., Ahten, T. S., and Wartelle, L. H. (1996) Effects of several metals on spore, biomass, and geosmin production by Streptomyces tendae and Penicillium expansum. *J. Ind. Microbiol.* **17**, 84–88.
53. Marbach, K., Fernández-Larrea, J., and Stahl, U. (1994) Reversion of a long-living undifferentiated mutant of *Podospora anserina* by copper. *Curr. Genet.* **26**, 184–186.
54. Borghouts, C. and Osiewacz, H. D. (1998) GRISEA, a copper-modulated transcription factor from *Podospora anserina* involved in senescence and morpgogenesis, is an ortholog of MAC1 in *Saccharomyces cerevisae*. *Mol. Gen. Genet.* **260**, 492–502.
55. Ma, H. and Kendall, K. (1994) Cloning and analysis of a gene cluster from *Streptomyces coelicolor* that causes accelerated aerial mycelium formation in *Streptomyces lividans*. *J. Bacteriol.* **176**, 3800–3811.
56. Yonekawa, T., Ohnishi, Y., and Horinouchi, S. (1999) Involvement of *amfC* in physiological and morphological development in *Streptomyces coelicolor* A3(2). *Microbiology* **145**, 2273–2280.
57. Ueda, K., Miyake, K., Horinouchi, S., and Beppu, T. (1993) A gene cluster involved in aerial mycelium formation in *Streptomyces griseus* encodes proteins similar to the response regulators of two-component regulatory systems and membrane translocators. *J. Bacteriol.* **175**, 2006–2016.
58. Ueda, K., Hsheh, C-W., Tosaki, T., Shinkawa, H., Beppu, T., and Horinouchi, S. (1998) Characterization of an A-factor-responsive repressor for *amfR* essential for onset of aerial mycelium formation in *Streptomyces griseus*. *J. Bacteriol.* **180**, 5085–5093.
59. Redenbach, M., Kieser, H. M., Denapaite, D., Eichner, A., Cullum, J., Kinashi, H., et al. (1996) A set of ordered cosmids and a detailed genetic and physical map for the 8 Mb Streptomyces coelicolor A3(2) chromosome. *Mol. Microbiol.* **21**, 77–96.
60. Kägi, J. H. R. (1991) Overview of metallothionein. *Methods Enzymol.* **205**, 613–626.
61. Jungmann, J., Reins, H. A., Lee, J., Romeo, A., Hassett, R., Kosman, D., et al. (1993) MAC1, a nuclear regulatory protein related to Cu-dependent transcription factors is involved in Cu/Fe utilization and stress resistance in yeast. *EMBO J.* **12**, 5051-5056.
62. Nielsen, H., Engelbrecht, J., Brunak, S., and von Heijne, G. (1997) Identification of prokaryotic and eukaryotic signal peptides and prediction of their cleavage sites. *Protein Eng.* **10**, 1–6.
63. Kelley, L. A., MacCallum, R. M., and Sternberg, M. J. E. (2000) Enhanced genome annotation using structural profiles in the program 3D-PSSM. *J. Mol. Biol.* **299**, 501–522.
64. Castresana, J., Lübben, M., Saraste, M. and Higgins, D. G. (1994) Evolution of cytochrome oxidase, an older enzyme than atmospheric oxygen. *EMBO J.* **13**, 2516–2525.

65. Chepuri, V., Lemieux, L., Au, D. C. T., and Gennis, R. B. (1990) The sequence of the cyo operon indicates substantial structural similarities between the cytochrome o ubiquinol oxidase of *Escherichia coli* and the aa3-type family of cytochrome c oxidases. *J. Biol. Chem.* **265**, 11,185–11,192.
66. Solomon, E. I., Sundaram, U. M., and Machonkin, T. E. (1996) Multicopper oxidases and oxygenases. *Chem. Rev.* **96**, 2563–2605.
67. Lim, C. K. and Cooksey, D. A. (1993) Characterization of chromosomal homologs of the plasmid-borne copper resistance operon of Pseudomonas syringae. *J. Bacteriol.* **175**, 4492–4498.
68. Brown, N. L., Barrett, S. R., Camakaris, J., Lee, B. T. and Rouch, D. A. (1995) Molecular genetics and transport analysis of the copper-resistance determinant (pco) from *Escherichia coli* plasmid pRJ1004. *Mol. Microbiol.* **17**, 1153–1166.
69. McManus, J. D., Brune, D. C., Han, J., Sanders-Loehr, J., Meyer, T. E., Cusanovich, M. A., et al. (1992) Isolation, characterization, and amino acid sequences of auracyanins, blue copper proteins from the green photosynthetic bacterium Chloroflexus aurantiacus. *J. Biol. Chem.* **267**, 6531–6540.
70. Sanchez-Ferrer, A., Rodriguez-Lopez, J. N., Garcia-Canovas, F., and Garcia-Carmona, F. (1995) Tyrosinase: a comprehensive review of its mechanism. *Biochem. Biophys. Acta* **1247**, 1–11.
71. Huber, M. and Lerch, K. (1988) Identification of two histidines as copper ligands in *Streptomyces glaucescens* tyrosinase. *Biochemistry* **27**, 5610–5615.
72. Tsai, T.-Y. and Lee, Y.-H. W. (1998) Roles of copper ligands in the activation and secretion of *Streptomyces* tyrosinase. *J. Biol. Chem.* **273**, 19,243–19,250.
73. Cuff, M. E., Miller, K. I., van Holde, K. E., and Hendrickson, W. A. (1998) Crystal structure of a functional unit from Octopus hemocyanin. *J. Mol. Biol.* **278**, 855–870.
74. Klabunde, T., Eicken, C., Sacchettini, J. C., and Krebs, B. (1998) Crystal structure of a plant catechol oxidase containing a dicopper center. *Nature Struct. Biol.* **5**, 1084–1090.
75. Corpet, F. (1988) Multiple sequence alignment with hierarchical clustering. *Nucleic Acids Res.* **16**, 10,881–10,890.
76. Chen, L.-Y., Leu, W.-M., Wang, K.-T., and Lee, Y.-H. W. (1992) Copper transfer and activation of the *Streptomyces* apotyrosinase are mediated through a complex formation between apotyrosinase and its *trans*-activator MelC1. *J. Biol. Chem.* **267**, 20,100–20,107.
77. Leu, W.-M., Chen, L.-Y., Liaw, L.-L., and Lee, Y.-H. W. (1992) Secretion of the *Streptomyces* tyrosinase is mediated through its *trans*-activator protein MelC1. *J. Biol. Chem.* **267**, 20,108–20,113.
78. Chen, L.-Y., Chen, M.-Y., Leu, W.-M., Tsai, T.-Y., and Lee, Y.-H. W. (1993) Mutational studies of *Streptomyces* tyrosinase *trans*-activator MelC1. *J. Biol. Chem.* **268**, 18,710–18,716.
79. Taguchi, S., Ogawa, T., Endo, T., and Momose, H. (1998) Identification of a structural gene encoding a metallothionein-like domain that includes a putative regulator protein for Streptomyces protease gene expression. *Biosci. Biotechnol. Biochem.* **62**, 2476–2479.
80. Hamer, D. H. (1986) Metallothionein. *Annu. Rev. Biochem.* **55**, 913–951.
81. Wunderli-Ye, H. and Solioz, M. (1999) Copper homeostasis in *Enterococcus hirae*. *Adv. Exp. Med. Biol.* **448**, 255–264.
82. Rensing, C., Fan, B., Sharma, R., Mitra, B., and Rosen, B. (2000) CopA: An *Escherichia coli* Cu(I)-translocating P-type ATPase. *Proc. Natl. Acad. Sci. USA* **97**, 652–656.
83. Solioz, M. and Vulpe, C. (2000) CPx-type ATPases: a class of P-type ATPases that pump heavy metals. *TIBS* **21**, 237–241.
84. Wimmer, R., Herrmann, T., Solioz, M., and Wüthrich, K. (1999) NMR structure and metal interactions of the CopZ copper chaperone. *J. Biol. Chem.* **274**, 22,597–22,603.
85. Odermatt, A., Suter, H., Krapf, R., and Solioz, M. (1993) Primary structure of two P-type ATPases involved in copper homeostasis in Enterococcus hirae. *J. Biol. Chem.* **268**, 12,775–12,779.
86. Odermatt, A. and Solioz, M. (1995) Two *trans*-acting metalloregulatory proteins controlling expression of the copper-ATPases of *Enterococcus hirae*. *J. Biol. Chem.* **270**, 4349–4354.
87. Glerum, D. M., Shtanko, A., and Tzagoloff, A. (1996) Characterization of COX17, a yeast gene involved in copper metabolism and assembly of cytochrome oxidase. *J. Biol. Chem.* **271**, 14,504–14,509.

32

Molecular Hardware of Copper Homeostasis in *Enterococcus hirae*

Reinhard Wimmer, Charles T. Dameron, and Marc Solioz

1. INTRODUCTION

In the past, copper transport in bacteria has been considered only in terms of resistance mechanisms to permit survival of the cells in adverse copper-rich environments. Indeed, most of the systems characterized early on are plasmid encoded, as is typical for defense mechanisms of prokaryotes. Recently, similar copper "resistance" systems were also identified in chromosomal locations, giving rise to the concept that bacteria may need systems for copper homeostasis not only in extreme environments but also under normal growth conditions.

The system for copper homeostasis in *Enterococcus hirae* is currently the best understood example of heavy-metal homeostasis. Because *E. hirae* can easily be genetically manipulated, it represents an ideal system for the study of fundamental aspects of the regulation of cytoplasmic copper. It appears that the major components of this system are encoded by the *cop* operon. It is located on the chromosome and consists of four closely spaced genes in the order *cop*Y, *cop*Z, *cop*A, and *cop*B. *Cop*Y and *cop*Z encode regulatory proteins, whereas *cop*A and *cop*B encode P-type ATPases of 727 and 745 amino acids, respectively *(1)*. Figure 1 summarizes the function of these four gene products and they will be discussed in detail in Section 2. All four *cop* gene products can be purified in milligram quantities for direct structural and functional investigations. This allows the study of fundamental aspects of copper homeostasis in vitro.

2. THE COPPER ATPASES: A NEW CLASS OF P-TYPE ATPASES

Copper ATPases are a key element of most, if not all, copper homeostatic mechanisms and have only recently been discovered and are a milestone in the field of trace element research. Following the discovery of the copper-transporting ATPases CopA and CopB in *E. hirae (2)*, highly homologous ATPases were reported from humans as underlying the copper metabolic defects of Menkes *(3,4)* and Wilson's disease *(5)*, respectively. Later, copper ATPases were described from yeast and other organisms and over two dozen putative copper ATPases have been described today *(6,7)*. In fact, highly homologous copper ATPase genes have been found in every genome that has been completely sequenced, suggesting that these enzymes are ubiquitous. Homologous ATPases specific for other transition metals such as cadmium and zinc have also been discovered *(8,9)*.

From: Handbook of Copper Pharmacology and Toxicology
Edited by: E. J. Massaro © Humana Press Inc., Totowa, NJ

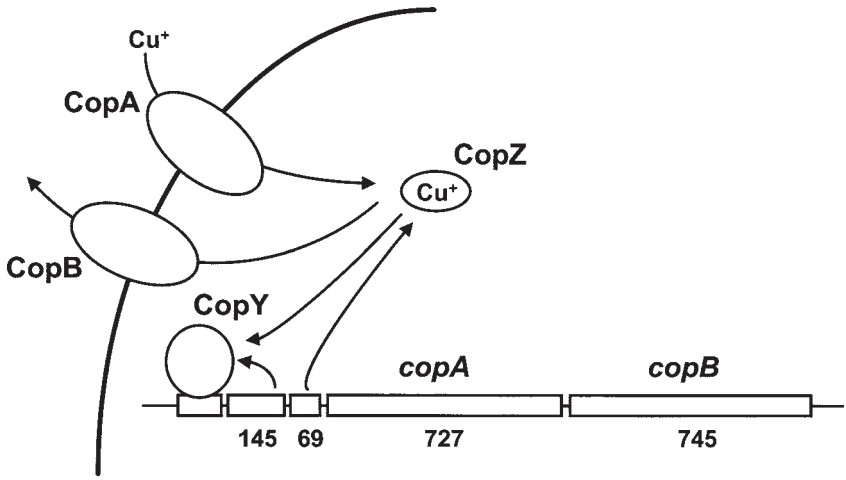

Fig. 1. Schematic drawing of the *cop* operon and model of copper homeostasis in *E. hirae*. Copper(I) is taken up by CopA under copper-limiting conditions. Inside the cell, CopZ complexes copper(I) to safely deliver it to the CopY repressor, which regulates expression of the *cop* operon. If intracellular copper is excessive, CopZ delivers copper to CopB for secretion.

2.1. CPx-Type ATPases

The structure and function of copper ATPases has become one of the focal points of research on copper homeostasis. Copper ATPases differ significantly in their primary structure, membrane topology, and evolutionary relationship from the previously known P-type ATPases, such as the Ca^{2+}-ATPases or the Na^+K^+-ATPases (Fig. 2). They thus form a distinct subclass that has been called P_1-type ATPases *(6)* or CPx-type ATPases based on the conserved intramembranous motif CPC or CPH *(7)*. Bacterial cadmium ATPases, silver ATPases, and the *Escherichia coli* zinc ATPase are close relatives of the copper ATPases and these heavy-metal ATPases are also members of the CPx-type ATPase subclass *(10–12)*. CPx-type ATPases are highly conserved from bacteria to man and must have arisen very early in evolution, probably before the division of prokaryotes and eukaryotes *(13)*. Figure 3 shows a phylogenetic tree of representative members of the CPx-type heavy metal and the P-type non-heavy-metal ATPase families.

2.1.1. The E. hirae CopA ATPase

CopA of *E. hirae* exhibits 43% sequence identity with the human Menkes and Wilson ATPases; in the transduction domain, sequence identity between these enzymes is even 92% *(15)*. This suggests that CopA is a representative model of a copper ATPase. Based on indirect evidence, CopA appears to function in copper uptake. Cells disrupted in *cop*A cease to grow in media in which the copper has been complexed with 8-hydroxyquinoline or *o*-phenanthroline. This growth inhibition could be overcome by adding copper to the growth media. Interestingly, null mutants in copA could grow in the presence of 5 μ*M* $AgNO_3$, conditions that fully inhibit the growth of wild-type cells. Thus, the CopA ATPase provides a route for the entry of copper, but also silver into the cell *(1)*. Silver transport by CopA is probably fortuitous, as silver has no known biological role. The transport of Ag(I) by CopA would indicate that Cu(I) rather than Cu(II) is transported by CopA.

CopA could be expressed in *E. coli* and purified to homogeneity by Ni–NTA affinity chromatography by means of an added histidine tag. Figure 4 shows the single-step purification of CopA from *E. coli* extracts on a Ni–NTA agarose column, eluted with an imidazole gradient. Purified CopA was active and had a pH optimum of 6.3 and a K_m for ATP of 0.2 m*M*. The enzyme formed an acylphosphate intermediate, which is a hallmark of P- and CPx-type ATPases *(16)*. This purified

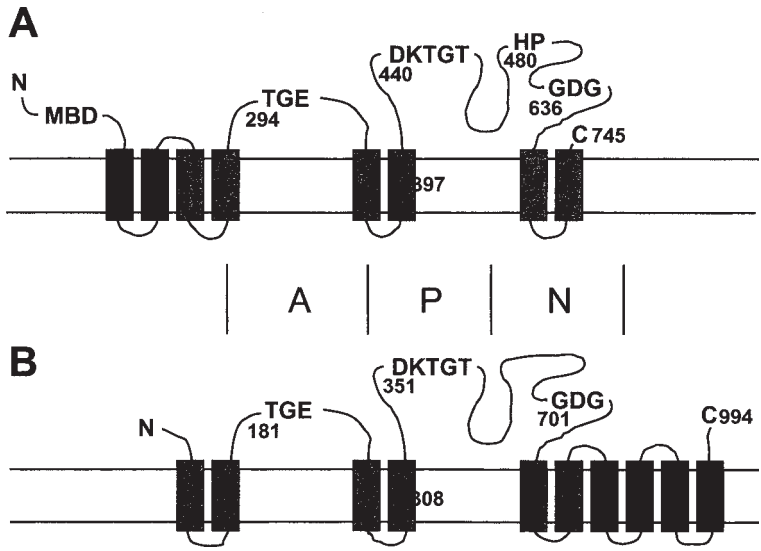

Fig. 2. Comparison of the membrane topology of a CPx-type ATPase and a P-type ATPase. Shown are CopB **(A)** of *E. hirae* and the Ca^{2+}-ATPase of sarcoplasmic reticulum **(B)**. Helices common to both type of ATPases are in black and helices unique to one type of ATPase are in gray. Key sequence motifs are indicated in the one-letter amino acid code and the numbers denote the position of residues in the sequence. In the center of the figure, the approximate locations of the three cytoplasmic domains A, P, and N are indicated. MBD, metal-binding domain containing repeat metal-binding sites; TGE, conserved site in transduction domain **A**; CPx, putative copper-binding site; DKTGT, phosphorylation site in domain P; HP, motif of unknown function, probably in domain N; GDG, nucleotide-binding site residues in domain N.

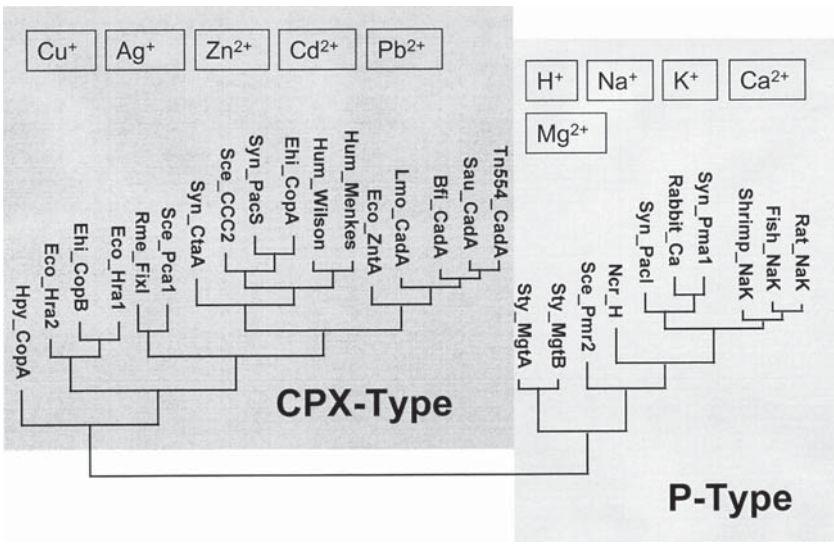

Fig. 3. Phylogram of the CPX-type ATPases with a selected sample of P-type ATPases. Divergence was scored by the Jukes–Cantor method *(50)*. Relationships between distant branches are not reliable.

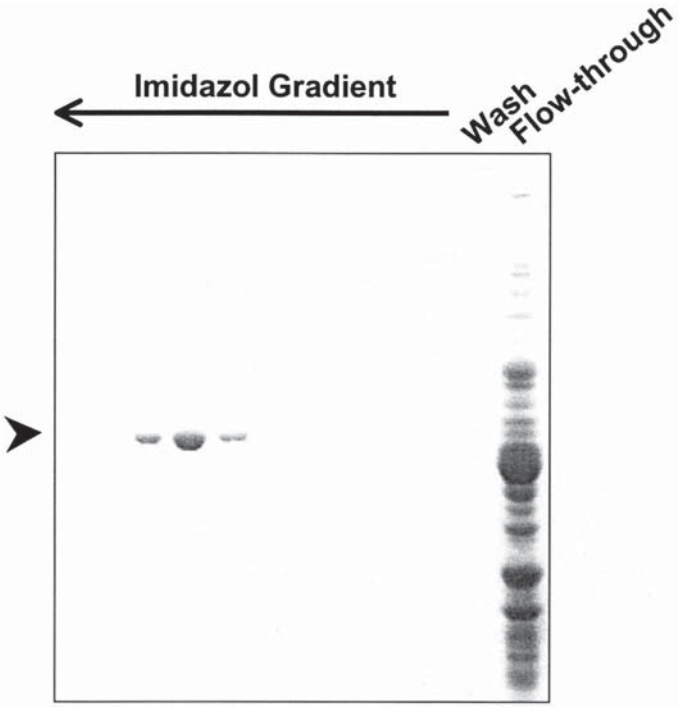

Fig. 4. Purification of CopA. Extract from *E. coli* expressing CopA endowed with a 6xhis tag was bound to a Ni–NTA agarose column and eluted with an imidazole gradient. Fractions were analyzed on a 10% polyacrylamide gel, stained with Coomassie blue. The arrowhead shows the position of purified CopA.

preparation of CopA can now serve to analyze mechanistic aspects of copper transport and to characterize structure–function relationships.

2.1.2. The E. hirae CopB ATPase

CopB differs from CopA and Menkes/Wilson-type copper ATPases mainly at the N-terminus. Instead of a CxxC metal-binding motif, CopB features a histidine-rich N-terminus similar to the one observed in the zinc ATPase of *E. coli (9)*. Wild-type cells of *E. hirae* can grow in the presence of up to 6 m*M* $CuSO_4$. The CopB ATPase was found to be required for this copper-resistant growth. Null mutation of *copB* rendered the cells sensitive to copper, whereas null mutation of *cop*A had no significant effect on the copper tolerance. This suggested that the CopB ATPase is a copper-export ATPase, extruding excess copper from the cytoplasm and thus conferring copper resistance. Using $^{64}Cu^+$ and $^{110m}Ag^+$, CopB was shown to catalyze ATP-driven accumulation of copper(I) and silver(I) in native membrane vesicles. Uptake of copper by these vesicles would correspond to copper extrusion in whole cells. Use of null mutants in either *cop*A, *cop*B, or *cop*A and *cop*B allowed one to clearly assign the observed transport to the activity of the CopB ATPase. Copper transport exhibited an apparent K_m for Cu^+ of 1 μ*M* and a V_{max} of 0.07 nmol/min/mg of membrane protein. $^{110m}Ag^+$ was transported with similar affinity and rate *(17)*. However, because Cu^+ and Ag^+ were not free in solution but complexed to Tris-buffer and dithiothreitol under the experimental conditions, the K_m values must be considered as relative only. The results with membrane vesicles were further supported by $^{110m}Ag^+$ extrusion from whole cells loaded with this isotope. Again, transport depended on the presence of functional CopB *(18)*. Vanadate showed an interesting biphasic inhibition of ATP-driven copper and silver transport: Maximal inhibition of Cu^+ transport was observed at 40 μ*M* VO_4^{3-} and of

Ag^+ transport at 60 μ*M* VO_4^{3-}. Higher concentrations relieved the inhibition of transport. This behavior is unexplained at present, but may relate to the complex chemistry of vanadate involving many oxidation states *(19)*.

For the purification of CopB for further functional analysis and crystallization attempts, a strain for the overproduction of the protein was engineered. Y1 is a repressor-deficient strain that overexpresses CopA and CopB about 50-fold *(20)*. CopB could be extracted from Y1 membranes with dodecyl-β-D-maltoside and purified by Ni–NTA chromatography by means of the endogenous metal-binding capacity of CopB. This single-step purification removed the majority of all contaminating proteins. Final purification was achieved by anion-exchange chromatography on Mono Q Sepharose *(21,22)*.

When CopB was reconstituted into Asolectin proteoliposomes by the method of Apell et al. *(23)*, a threefold increase in ATPase activity was observed. Fifty to eighty percent of this activity could be inhibited by vanadate. Reconstituted CopB was shown to form an acylphosphate intermediate, and thus to exhibit active turnover *(22)*. Using this model system, it was possible to analyze the significance of individual amino acid residues for their functional involvement in catalysis. The Menkes disease mutation C1000R, which changes the conserved CPC motif in membrane helix 6, was mimicked in CopB with the C396S mutation. This mutant CopB ATPase was unable to restore copper resistance in a CopB knockout strain in vivo. The purified C396S ATPase still formed an enzyme–phosphate intermediate, but had no detectable ATPase activity. The Wilson's disease mutation H1069Q, which is the single most frequent mutation in Europe, was introduced into CopB as H480Q. This mutant CopB similarly failed to restore copper resistance in a CopB knockout strain. Purified H480Q CopB formed an acylphosphate intermediate and retained significant ATPase activity *(24)*. These findings show that S396 and H480 of CopB are key residues for ATPase function, which suggests similar roles for S1000 and H1069 in the Menkes and Wilson ATPase, respectively. The results also suggested that these mutations do not directly affect the site of ATP binding and phosphorylation.

3. THE CopY REPRESSOR

The two copper ATPases of *E. hirae* are induced by ambient copper. Induction of the genes is lowest in standard growth media (copper content = 10 μ*M*). If the media copper is increased, an up to 50-fold induction is observed at 2 m*M* extracellular copper. Full induction is also obtained by 5 μ*M* Ag^+ or 5 μ*M* Cd^{2+}. The induction by silver and cadmium is, in all likelihood, fortuitous, because it does not confer resistance to these highly toxic metal ions. Because CopA serves in copper uptake and CopB in its extrusion, this coinduction of CopA and CopB by high and low copper seems puzzling at first. However, it may be a safety precaution: If the cells would express, under copper-limiting conditions, only the import ATPase, they would become highly vulnerable to copper poisoning in case of a sudden increase in ambient copper.

The regulatory gene, *cop*Y, upstream of the genes encoding the CopA and CopB ATPases, was cloned by chromosome walking. *CopY* encodes a repressor protein of 145 amino acids *(20)*. As shown in Fig. 5A, the N-terminal half of CopY exhibits around 30% sequence identity to the bacterial repressors of β-lactamases, MecI, PenI, and BlaI *(25–27)*. In the best studied of these, PenI, this N-terminal portion appears to be the domain that recognizes the operator *(28)*. At position 31, there is a diglutamine motif in CopY. This motif is also found in the phage 434 and lambda Cro repressors at a similar position. By X-ray crystallography, it could be shown that the diglutamine motif of these phage repressors interact with the ACA motif in the DNA with an extraordinarily tight fit. Because the CopY DNA-binding sites feature ACA motifs, it appeared likely that they interact with the QQ motif in CopY (Fig. 5B). Although there is no significant sequence homology between the phage repressors and CopY, they appeared to be a good model.

Because both, the 434 and the Cro repressor are dimeric, the aggregation state of CopY in solution was investigated. It could be shown by crosslinking as well as by size-exclusion chromatography that

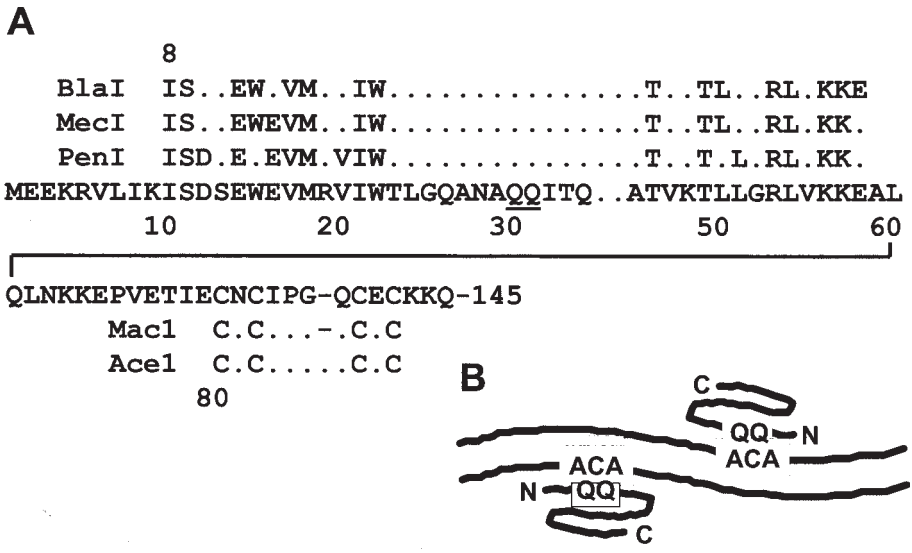

Fig. 5. Structural features of the CopY repressor. **(A)** The N-terminal part of CopY exhibits sequence homology to the β-lactamase repressors of MecI, PenI, and BlaI, whereas the C-terminal portion features cysteine residues that are probably involved in copper binding. **(B)** Schematic drawing of the putative interaction of the QQ motif of CopY with the ACA triplet in the promoter.

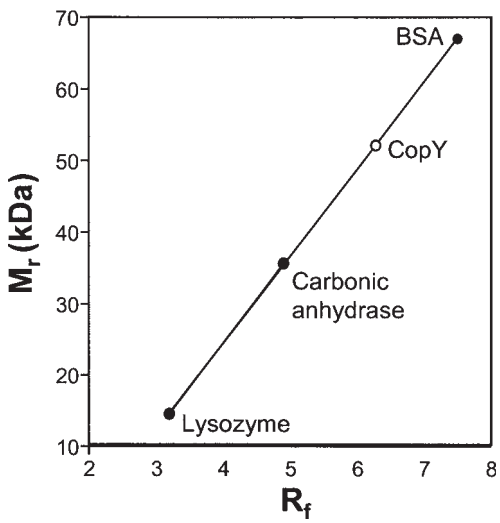

Fig. 6. Seizing of CopY by gel permeation chromatography. R_f values of the indicated standard proteins and of purified CopY were determined on a TSK-100 column.

CopY is a dimer in solution (Fig. 6). By DNaseI fingerprinting and by band-shift assays, it was shown that CopY interacts at two discrete sites on the promoter, featuring an inverted repeat *(29)*. Presumably, each one CopY dimer bound to each of the sites. The two CopY binding sites also featured two ACA triplets each, suggesting that each CopY monomer interacts with an ACA sequence. A possible interaction of CopY with ACA was investigated by site-directed mutagenesis of the promoter. It could be shown that the affinity of CopY for binding sites mutated from ACA to

TCA was strongly reduced. When both CopY binding sites of the inverted repeat were mutated ACA to TCA, the operator became hyperinducible by low copper concentrations *(30)*.

In the C-terminal half of CopY, there are multiple cysteine residues, arranged as $CXCX_4CXC$. The consensus motif $CXCX_{4\text{-}5}CXC$ is also found in the three yeast-copper-responsive transcriptional activators, ACE1, AMT1, and MAC1 *(31-33)* and appears to be the copper-binding site of the repressor.

Disruption of the *E. hirae cop*Y gene results in constitutive overexpression of the *cop* operon in vivo *(20)*. Binding of CopY to an inverted repeat sequence upstream of the *cop*Y gene has been demonstrated in vitro. Thus, CopY appears to be a copper-responsive repressor protein with an N-terminal DNA-binding domain and a C-terminal copper-binding domain.

CopY was overexpressed in *E. coli* and purified to near homogeneity. The interaction of the purified repressor with the promoter region was shown in band-shift assays as follows: DNA fragments of 530 base pairs encompassing the putative promoter region were incubated with purified repressor protein. The formation of DNA–protein complexes was visualized by the change in electrophoretic mobility of the radioactively labeled DNA band on polyacrylamide gels. Increasing concentrations of CopY lead to a shift of the DNA band. This shift occurred in two steps, suggesting that two monomers or two multimers of the repressor interact with the promoter sequence. Competition experiments with either cold promoter DNA or DNA carrying the promoter of the Na^+H^+-antiporter gene of *E. hirae* clearly demonstrate that CopY binding to the *cop* promoter is specific *(29)*.

Thus, the combined evidence of CopY binding to promoter DNA in vitro and the observed hyperinducibility of promoter mutations in the ACA triplets in vivo points to the following mechanism of regulation: If intracellular copper is in the physiological range, CopY is bound to the promoter and transcription of the *cop* operon is turned off. If cytoplasmic copper is increased, CopY is released from the promoter and the expression of the *cop* genes is turned on. But how does CopY sense the cytoplasmic copper level? The answer to this question came from the study of the CopZ chaperone, discussed next.

4. THE CopZ COPPER CHAPERONE

It has recently been discovered that the intracellular delivery of copper to copper-utilizing enzymes requires the action of specialized proteins, the so-called chaperones *(34)*. In *E. hirae*, the 69-amino-acid protein CopZ fulfills this role. CopZ-like copper chaperones have also been described in humans (HAH1), *C. elegans* (CUC-1), and yeast (ATX1) *(35-37)*. The conserved domains feature a universal CxxC metal-binding motif and exhibit sequence similarity over a region of 50–60 amino acids (Fig. 7). Interestingly, the N-termini of heavy-metal-binding proteins, such as copper ATPases, cadmium ATPases, and mercuric reductases also contain one to six copies of the conserved copper chaperone sequence *(7,38,39)*. Figure 8 schematically shows the occurrence of CopZ-like building blocks in a number of enzymes involved in heavy-metal metabolism. Clearly, there has been the evolution of a heavy-metal-binding motif that can function either as an isolated unit as in CopZ or as a component of a larger heavy-metal-binding protein. These CopZ-like building blocks in the copper ATPases have been shown to bind copper ions *(40–42)*. However, whether these copper-binding sites function as an integral part of enzyme catalysis or whether they fulfill a more accessory role in scavenging metal ions or regulating enzyme activity remains to be shown.

4.1. Intracellular Copper Routing

CopZ is so far the only chaperone for which copper transfer has been shown directly in vitro. Purified Zn(II)CopY binds to a synthetic *cop* promoter fragment in vitro (Fig. 9). CopZ was shown to specifically deliver copper(I) to Zn(II)CopY, thereby releasing CopY from the DNA. It could also been shown by luminescence spectroscopy that two copper(I) were thereby quantitatively transferred from Cu(I)CopZ to Zn(II)CopY, with displacement of the zinc(II) and transfer of copper from a nonluminescent exposed binding site in CopZ to a luminescent solvent-shielded binding site in

```
                                        *  *
   CopZ  ~~~~~~~~~~ ~MKQEFSVKG MSCNHCVARI EEAVGRI.SG VKKVKVQLKK EKAVVKFDEA
   HAH1  ~~~~~~~~~~ MPKHEFSVD. MTCGGCAEAV SRVLNKL..G GVKYDIDLPN KKVCIE...S
   ATX1  ~~~~~~~MAE IKHYQFNVV. MTCSGCSGAV NKVLTKLEPD VSKIDISLEK QLVDVY...T
 .CUC-1  ~~~~~~~~~~ ~MTQYVFEMG MTCNGCANAA RKVLGKLGED KIKIDDINVE TKKITVTTDL
 Menkes  ~~~~MDPSMG VNSVTISVEG MTCNSCVWTI EQQIGKV.NG VHHIKVSLEE KNATIIYDPK
   MerP  ~~~VAPVWAA TQTVTLAVPG MTCAACPITV KKALSKV.EG VSKVDVGFEK REAVVTFDDT
   CCC2  ~~~~~~~~~~ MREVILAVHG MTCSACTNTI NTQLRAL.KG VTKCDISLVT NECQVTYDNE
   CopA  ~~~~~~MATN TKMETFVITG MTCANCSARI EKELNEQ.PG VMSATVNLAT EKASVKYTDT
   CadA  MSEQKVKLME EEMNVYRVQG FTCANCAGKF EKNVKKI.PG VQDAKVNFGA SKIDVYGNAS
   MerA  ~~~~~~~~~~ ~~MTHLKITG MTCDSCAAHV KEALEKV.PG VQSALVSYPK GTAQLAIVPG
```

Fig. 7. Alignment of the conserved domain of CopZ with related metal binding motifs. EMBL/GenBank accession numbers are given in parentheses. CopZ, copper chaperone of *E. hirae* (Z46807); HAH1, human copper chaperone (U70660); ATX1, yeast copper chaperone (L35270); CUC-1, *C. elegans* copper chaperone (AB017201); Menkes, copper-binding motif of human Menkes ATPase (L06133); MerP, periplasmic mercury-binding protein (P04129); CCC2, copper-binding motif of yeast CCC2 copper ATPase (L36317); CopA, copper-binding motif of *E. hirae* CopA copper ATPase (L13292); CadA, cadmium-binding motif of *Staphylococcus aureus* cadmium ATPase (J04551); MerA, mercury-binding motif of mercuric reductase (A00406). The asterisks denote the universally conserved cysteine residues.

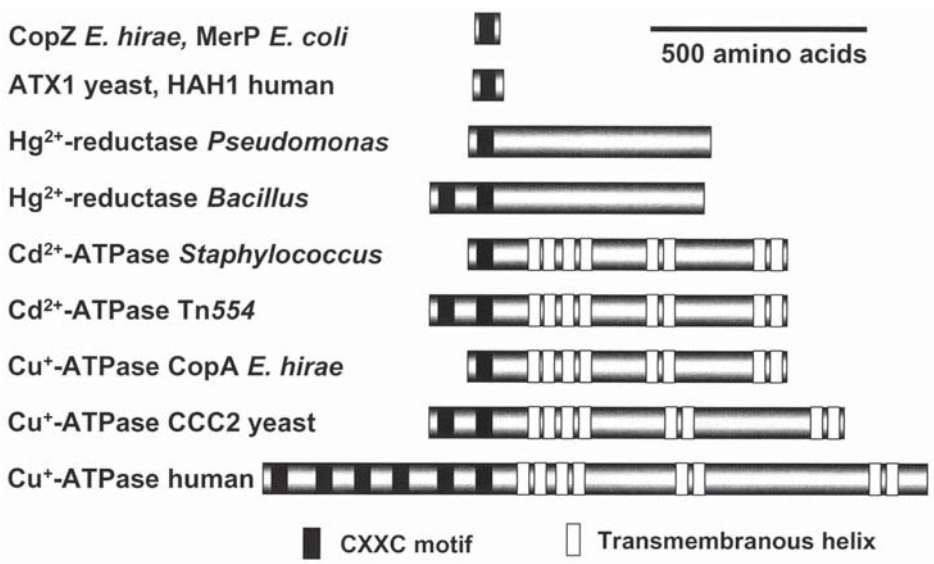

Fig. 8. Schematic representation of the occurrence of CopZ-like motifs in various proteins. The polypeptide chains are drawn to scale as boxes. Transmembranous helices are indicated by open rectangles and CopZ-like building blocks by filled rectangles.

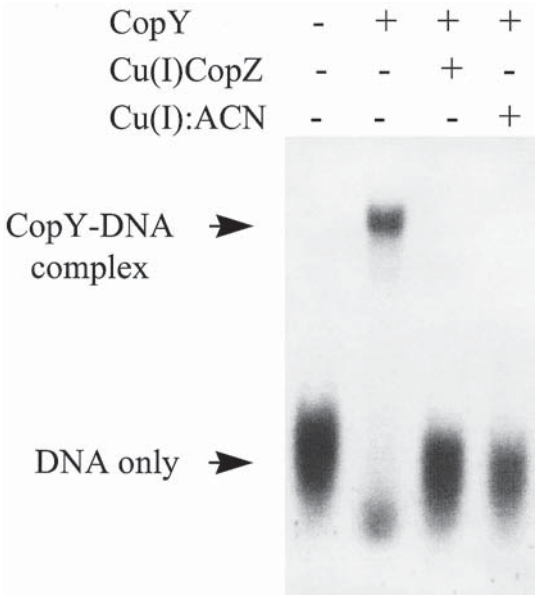

Fig. 9. Effect of Cu(I)CopZ on the CopY–DNA interaction. Native CopY retarded a ^{32}P-labeled oligonucleotide promoter fragment in the band-shift assay. Cu(I)CopZ abolished binding of CopY to the promoter, but not Cu(I)MNKr4. The artificial copper(I) complex Cu(I)acetonitrile could also donate copper to CopY.

CopY *(43)*. These findings were further supported by quantitative gel filtration chromatography, paired with metal analysis.

4.2. Solution Structure of CopZ

To further study the chaperoning function by CopZ, its three-dimensional structure was determined. Universally ^{15}N-labeled CopZ was overexpressed in *E. coli* and purified to homogeneity. By nuclear magnetic resonance (NMR) spectroscopy, the solution structures of *apo*-CopZ and Cu(I)CopZ were derived *(44)*. The structure of *apo*-CopZ was very well defined: the root mean square deviation (r.m.s.d.) of the backbone heavy atoms within the secondary structure elements was 0.32 Å. The bundle of the 20 best conformers is shown in Fig. 10. The amino acid chain in CopZ adopts a βαββαβ fold. The β-strands form an antiparallel β-sheet that is strongly twisted. The two α-helices are packed against the β-sheet. They enclose an angle of about 45°. Figure 11 shows a ribbon drawing of the CopZ molecule. The two copper-binding residues Cys-11 and Cys-14 are located in the loop that connects the first β-strand with the first α-helix.

The charged side chains on the surface of the protein are distributed very unevenly, so that large negatively and positively charged patches exist on the protein surface. The global fold is essentially identical to that of the mercury-binding protein MerP *(45)*, mbd4, the fourth metal-binding domain of the Menkes copper-transporting ATPase *(39)*, Atx1, the yeast analogon to CopZ *(46)*, and Hah1, the human analogon to both CopZ and Atx-1 *(47)*. A detailed comparison of the structure of CopZ with those of mbd4 and MerP shows that the structures are nearly identical except for the metal-binding loop, where the CxxC motif is located. The relative conformations of Cys-11 and Cys-14 in CopZ are such that metal binding by both of them requires structural rearrangement (*see* Fig. 12). This is clearly not the case in mbd4, which can accommodate Ag(I) apparently without any changes in structure. In MerP, only the loop between β_1 and α_1 is rearranging upon Hg(II)-binding whereas in CopZ, it seems that the first α-helix is taking part in the required rearrangement. This difference in behavior might be the result of the presence of two prolines flanking the metal-binding loop in MerP and may be preventing

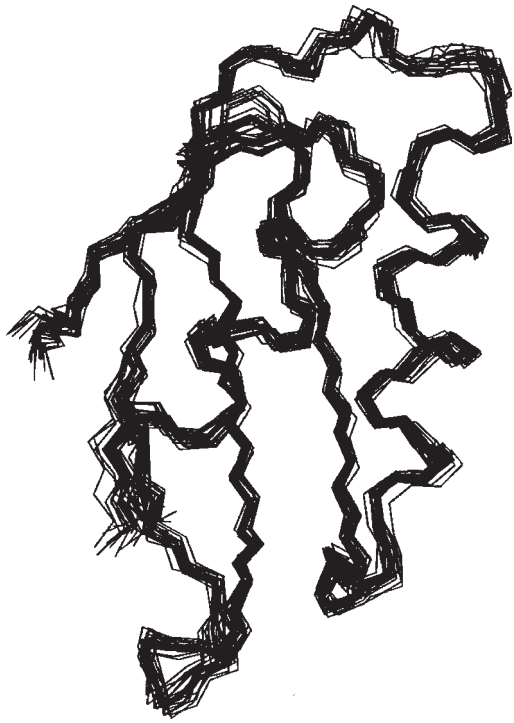

Fig. 10. *apo*-CopZ conformers. Bundle of 20 conformers with the lowest residual target function. The orientation of the molecule is the same as in Fig. 11.

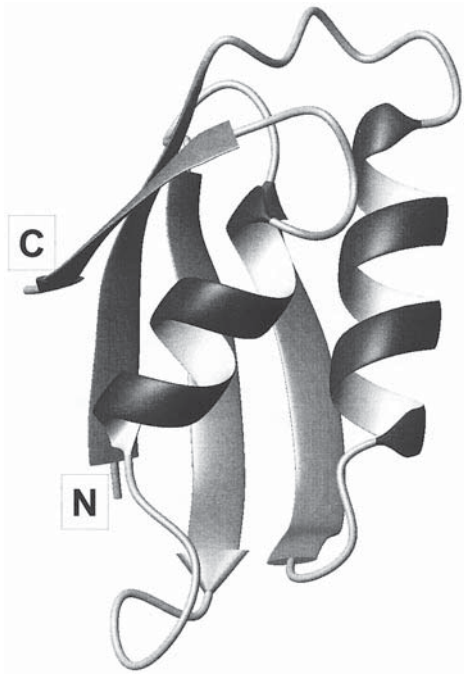

Fig. 11. Ribbon diagram of *apo*-CopZ. *apo*-CopZ with the lowest residual target function is shown, illustrating the secondary structure elements: α_1 (14–24), α_2 (51–59), β_1 (2–7), β_2 (28–34), β_3 (39–44), and β_4 (64–67).

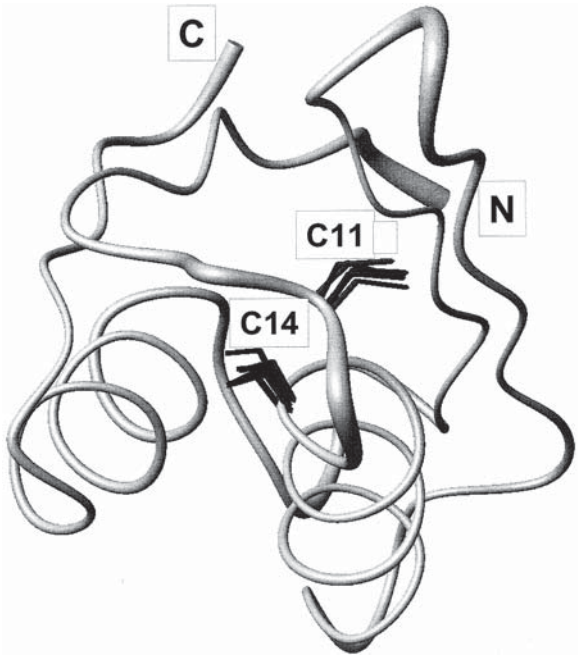

Fig. 12. Copper-binding residues of CopZ. The six best conformers of CopZ are represented by the mean of the backbone coordinates and by a superposition of the two copper-binding cysteine side-chain arrangements in the six conformers.

structural changes of a larger part of the protein, whereas no prolines are present in CopZ. A detailed structural comparison between Atx1 and MerP and mbd4, respectively, can be found in ref. *47*.

4.3. Structural Changes of CopZ upon Interaction with Cu(I)

CopZ undergoes significant changes upon interaction with copper(I). Whereas in *apo*-CopZ, all but a few ^{1}H-NMR signals were observable, the signals of residues 11–21 were missing in the NMR spectra of Cu(I)CopZ. Some weak signals were visible, but because of missing NOEs, they could not be assigned unambiguously. Paramagnetic ions [e.g., Cu(II)], could cause a disappearance of the NMR signals in their vicinity, but electron paramagnetic resonance (EPR) measurements showed that no Cu(II) was contained in the sample. Hence, the disappearance of the signals was ascribed to conformational exchange between two or—presumably—more conformations. This coincides with the findings made with Cu(I)Atx1 *(47)* in the crystal form. Studies of Cu(I)Atx1 in solution revealed a similar behavior only when the protein concentration exceeded 2 m*M*; otherwise, a well-defined binding site could be observed *(48)*.

A comparison of the backbone ^{15}N, H^{N}, and H^{α} chemical shifts revealed that apart from the metal-binding loop and the first helix, no structural changes occurred upon Cu(I) binding (*see* Fig. 13). This was corroborated by careful examination of the NOESY spectra of Cu(I)CopZ and comparing them to the NOESY spectra of *apo*-CopZ. Essentially the same NOEs could be found in both spectra and a structure calculation on Cu(I)CopZ yielded an identical structure to that of CopZ—except for the part of the protein, where no signals could be observed. X-ray absorption studies suggested a mixture of 75% diagonally coordinated/25% triagonally coordinated copper for Cu(I)-CopZ, with all ligands being sulfur atoms *(49)*. The origin of the third contributing ligand in addition to Cys-11 and Cys-14 remained unknown. NMR data showed, clearly, that neither of the additional sulfur atoms in CopZ

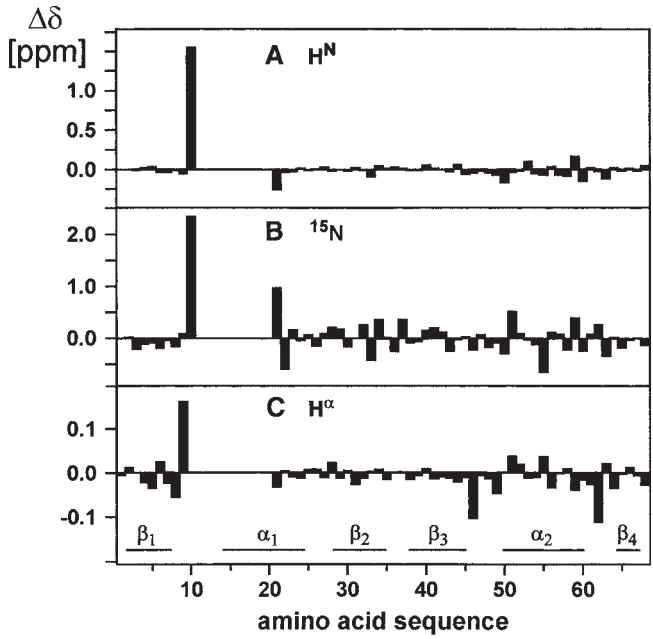

Fig. 13. Structural differences between *apo*- and Cu-CopZ. Differences between corresponding backbone chemical shifts in *apo*-CopZ and Cu(I)-CopZ plotted versus the sequence. Amide protons $\Delta\delta(H^N)$ **(a)**, amide nitrogens $\Delta\delta\ ^{15}N$) **(b)**, α-protons $\Delta\delta(H^\alpha)$ **(c)** in the case of glycines the pair of H^α lines with the greatest difference was chosen, where $\Delta\delta=\delta$(*apo*-CopZ) – δ(Cu(I)-CopZ). (Reprinted with permission from ref. *44*.)

takes part in copper binding. The SH^γ of Cys-55 can be observed in the NMR spectra of both *apo*- and Cu(I)CopZ. The H^α and C^α of Met-9 does not show a significant difference in chemical shift between *apo*- and Cu(I)CopZ.

Determination of NMR relaxation times finally explained the origin of the third ligand. As can be seen from Fig. 14, the longitudinal relaxation time T_1 increased upon copper binding whereas the transverse relaxation time T_2 decreased. This is indicative of a decreased molecular tumbling, which in the experimental setup used can only be explained by aggregation—presumably dimerization. These findings were corroborated by light-scattering measurements on a different set of samples. Thus, the third ligand for copper binding comes most likely from a different CopZ molecule. It is, however, possible, that under biological conditions, a small thiol-containing molecule like glutathione or cysteine plays the role as a third ligand.

4.4. Comparison of the CopZ with Other Metal Chaperones

The structures of metal chaperones homologous to CopZ have also been investigated with bound metal ligands. Although the structures and functions of these proteins seem to be very similar, a different behavior upon ligand binding was observed. Table 1 gives an overview over the data reported so far. In general, copper is bound by three sulfur ligands, one of which has a longer distance to the copper ion than the other two. The stoichiometry of copper:protein has been reported to be 1:1 for CopZ *(43)* and for Hah1 *(47)*, but 0.6–0.8 for Atx1 *(50)*. A well-defined structure of the metal-binding site was obtained only for Hah1 *(47)* and Atx1 in solution at concentrations below 2 m*M* *(48)*. CopZ *(44)* and Atx 1 in the crystal *(47)* exhibited disordered metal-binding sites.

The structure of Cu(I)Hah1, however, would suggest a stoichiometry copper:protein 1:2 rather than 1:1 found experimentally. CopZ, too, showed aggregation—presumably dimerization—upon interaction with copper. Unlike in X-ray crystallography, the Cu ion cannot be observed directly by

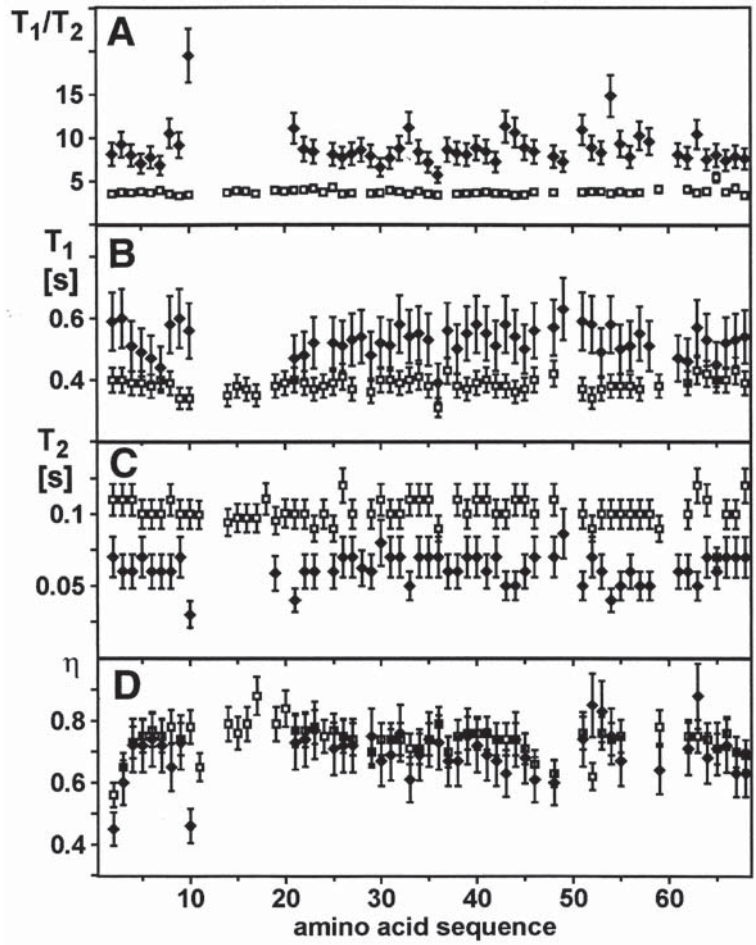

Fig. 14. NMR relaxation times for *apo*- and Cu-CopZ. Relaxation times and steady-state $^{15}N\{^1H\}$ NOEs measured for the backbone amide nitrogen atoms of *apo*-CopZ (❐) and Cu(I)-CopZ (♦). **(A)** T_1/T_2 recorded at a ^{15}N frequency of 50.7 MHz; **(B)** longitudinal relaxation time T_1; **(C)** transverse relaxation time T_2; **(D)** $^{15}N\{^1H\}$-NOEs recorded at a ^{15}N frequency of 60.8 MHz. For Cu(I)-CopZ no measurements were obtained for the residues 11–20 (*see* text). (Reprinted with permission from ref. *44*.)

solution NMR. Therefore, nothing definite about the number of copper ions in the CopZ dimers can be said. Cu–Cu scatter peaks in Cu(I)mbd2, however, suggest a copper-binding site with at least two copper ions for this protein domain, which would fit a dimeric state with a 1:1 stoichiometry, but no structural information for mbd2 is available.

Solutions of Cu(I)Atx1 in concentrations higher than 2 m*M* exhibited a loss of NMR signals from the metal-binding loop and a part of the following helix *(47)* similar to what was found for Cu(I)CopZ. The formation of precipitate was reported under these conditions, but the aggregation state of the protein remained uncharacterized. In the case of CopZ, the NMR signals of the metal-binding loop and the first two turns of the following helix disappeared; in Cu(I)Atx1 at high concentrations, only the NMR signals of the metal-binding loop and two residues of the first helix turn vanish.

For both the Cu(I)Hahl crystals and the Cu(I)CopZ solution, it has been stated that the observed aggregation/dimerization could be an artifact introduced by the non-physiological sample conditions.

Table 1
Overview of Structural Work Reported on CopZ and Similar Metal Chaperones

Protein/ organism	*Natural ligand*	*Ligand*[a]	*No. of ligands*	*Defined binding site*[b]	*Aggregation / dimerization*	*Ref.*
CopZ	Cu(I)	*apo*		Yes	No	*44*
E. hirae		Cu(I)	3	No	Yes	*44*
		Ag(I)	2	No	Yes	Wimmer and Solioz, unpublished
Hah1 human	Cu(I)	Cu(I)	3	Yes	Yes	*47*
		Hg(II)	3	Yes	Yes	*47*
		Cd(II)	4	Yes	Yes	*47*
Atx1	Cu(I)	*apo ox.*		Yes	No	*48*
S. cerevisiae		Cu(I)	3	No[c]	No[c]	*46*
						50
		Hg(II)	2	Yes[d]	No	*1*
						46
mbd4[e] human	Cu(I)	*apo*		Yes	No	*39*
		Ag(I)	2	Yes	No	*39*
mbd2[e,f] human	Cu(I)	Ag(I)	2			*51*
		Cu(I)	3			*52*
MerP	Hg(II)	*apo*		Yes	No	*45*
Shigella flexineri		*apo ox.*		Yes	No	*53*
		Hg(II)	2	Yes	No	*45*

[a]*apo* denotes the reduced form of the protein without ligand, *apo ox.* denotes the oxidized form of the protein without ligand (i.e., the two binding cysteines form a disulfide bridge).

[b]"Defined" denotes that the metal-binding site is not completely disordered, no classification of r.m.s.d. or resolution is intended.

[c]The authors suggest that no well-ordered metal-binding site was observed because of partial copper-ion loss from the crystal.

[d]The authors mention, however, that at protein concentrations higher than 2 m*M*, the binding site can no longer be defined because of the loss of NMR signals in that region and aggregation in the form of a precipitate.

[e]mbd2 and mbd4 are the second and fourth, respectively, metal-binding domains from the Menkes copper-transporting ATPase. They are thus not occurring as independent protein molecules.

[f]No structure was determined for mbd2, but the ligand binding interactions were investigated by extended X-ray absorption fine structure (EXAFS).

5. CONCLUSION

Nature has chosen copper as a cofactor for more than 30 enzymes because of its apparently ideal redox properties. On the other hand, free-copper ions are toxic to cells by initiating the formation of radicals, which can oxidize proteins, nucleic acids, and lipids. Thus, the control of cellular copper levels is crucial for proper cell function. Only in recent years have genes directly involved in copper homeostasis been cloned. This led to the identification of novel copper pumps and carriers in bacteria, yeast, and humans. Today, copper homeostasis is a research area of intense interest and work in this field has recently uncovered several surprising new concepts—and more are likely to emerge. Study of the *E. hirae* model system has significantly contributed to the current understanding of copper homeostasis.

ACKNOWLEDGMENTS

We thank Kurt Wüthrich for valuable discussions on the CopZ structure. Some of the work described here was supported by grant no. 32-56716.99 of the Swiss National Foundation and by a grant from the Novartis Foundation to M.S., grant no. J1559-GEN from the Austrian Science Fund

(FWF) and grant no. 3392.1 from the Commission for Technological Innovation (KTI) to R.W., and grants from the Australian Research Council to C.T.D.

REFERENCES

1. Odermatt, A., Suter, H., Krapf, R., and Solioz, M. (1993) Primary structure of two P-type ATPases involved in copper homeostasis in *Enterococcus hirae*. *J. Biol. Chem.* **268**, 12,775–12,779.
2. Odermatt, A., Suter, H., Krapf, R., and Solioz, M. (1992) An ATPase operon involved in copper resistance by *Enterococcus hirae*. *Ann. NY Acad. Sci.* **671**, 484–486.
3. Vulpe, C., Levinson, B., Whitney, S., Packman, S., and Gitschier, J. (1993) Isolation of a candidate gene for Menkes disease and evidence that it encodes a copper-transporting ATPase. *Nature Genet.* **3**, 7–13.
4. Mercer, J. F. B., Livingston, J., Hall, B., Paynter, J. A., Begy, C., Chandrasekharappa, S., et al. (1993) Isolation of a partial candidate gene for Menkes disease by positional cloning. *Nature Genet.* **3**, 20–25.
5. Bull, P. C., Thomas, G. R., Rommens, J. M., Forbes, J. R., and Cox, D. W. (1993) The Wilson disease gene is a putative copper transporting P-type ATPase similar to the Menkes gene. *Nature Genet.* **5**, 327–337.
6. Lutsenko, S. and Kaplan, J. H. (1995) Organization of P-type ATPases: significance of structural diversity. *Biochemistry* **34**, 15,607–15,613.
7. Solioz, M. and Vulpe, C. (1996) CPx-type ATPases: a class of P-type ATPases that pump heavy metals. *Trends Biochem. Sci.* **21**, 237–241.
8. Silver, S. and Ji, G. (1994) Newer systems for bacterial resistances to toxic heavy metals. *Environ. Health Perspect.* **102(Suppl. 3)**, 107–113.
9. Rensing, C., Mitra, B., and Rosen, B. P. (1997) The *zntA* gene of *Escherichia coli* encodes a Zn(II)-translocating P-type ATPase. *Proc. Natl. Acad. Sci. USA* **94**, 14,326–14,331.
10. Nucifora, G., Chu, L., Misra, T. K., and Silver, S. (1989) Cadmium resistance from *Staphylococcus aureus* plasmid pI258 *cad*A gene results from a cadmium-efflux ATPase. *Proc. Natl. Acad. Sci. USA* **86**, 3544–3548.
11. Gupta, A., Matsui, K., Lo, J. F., and Silver, S. (1999) Molecular basis for resistance to silver cations in *Salmonella*. *Nat. Med.* **5**, 183–188.
12. Beard, S. J., Hashim, R., Membrillo-Hernandez, J., Hughes, M. N., and Poole, R. K. (1997) Zinc(II) tolerance in *Escherichia coli* K-12: evidence that the zntA gene (o732) encodes a cation transport ATPase. *Mol. Microbiol.* **25**, 883–891.
13. Solioz, M. (2001) Bacterial copper transport, in *Microbial Transport Systems* (Winkelmann, G., ed.), Wiley, Weinheim, pp. 361–376.
14. Swofford, D. L., and Olson, P. D. (1990) Phylogeny reconstruction, in *Molecular Systematics* (Hillis, D. M. and Moritz, C., eds.), Sinauer Associates, Sunderland, MA, pp. 21–132.
15. Solioz, M., Odermatt, A., and Krapf, R. (1994) Copper pumping ATPases: common concepts in bacteria and man. *FEBS Lett.* **346**, 44–47.
16. Wunderli-Ye, H. and Solioz, M. (2001) Purification and functional analysis of the copper ATPase CopA of *Enterococcus hirae*. *Biochem. Biophys. Res. Commun.* **280**, 713–719.
17. Solioz, M. and Odermatt, A. (1995) Copper and silver transport by CopB-ATPase in membrane vesicles of *Enterococcus hirae*. *J. Biol. Chem.* **270**, 9217–9221.
18. Odermatt, A., Krapf, R., and Solioz, M. (1994) Induction of the putative copper ATPases, CopA and CopB, of *Enterococcus hirae* by Ag^+ and Cu^{2+}, and Ag^+ extrusion by CopB. *Biochem. Biophys. Res. Commun.* **202**, 44–48.
19. Pope, M. T. and Dale, B. W. (1968) Isopoly-vanadates, -niobates, and -tantalates. *Rev. Chem. Soc.* **22**, 527–545.
20. Odermatt, A. and Solioz, M. (1995) Two *trans*-acting metalloregulatory proteins controlling expression of the copper-ATPases of *Enterococcus hirae*. *J. Biol. Chem.* **270**, 4349–4354.
21. Duda, P., Strausak, D., and Solioz, M. (1996) The *Enterococcus hirae* copper ATPases: structure, function and regulation, in *Therapeutic Uses of Trace Elements* (Nève, J., Chappuis, P., and Lamand, M., eds.), Plenum, New York, pp. 421–428.
22. Wyler-Duda, P. and Solioz, M. (1996) Phosphoenzyme formation by purified, reconstituted copper ATPase of *Enterococcus hirae*. *FEBS Lett.* **399**, 143–146.
23. Apell, H.-J. and Solioz, M. (1990) Electrogenic transport by the *Enterococcus hirae* ATPase. *Biochim. Biophys. Acta* **1017**, 221–228.
24. Bissig, K.-D., Wunderli-Ye, H., Duda, P., and Solioz, M. (2001) Structure–function analysis of purified *Enterococcus hirae* CopB copper ATPase: effect of Menkes/Wilson disease mutation homologues. *Biochem. J.*, **375**, 217–223.
25. Suzuki, E., Kuwahara Arai, K., Richardson, J. F., and Hiramatsu, K. (1993) Distribution of mec regulator genes in methicillin-resistant Staphylococcus clinical strains. *Antimicrob. Agents Chemother.* **37**, 1219–1226.
26. Himeno, T., Imanaka, T., and Aiba, S. (1986) Nucleotide sequence of the penicillinase repressor gene penI of *Bacillus licheniformis* and regulation of *penP* and *penI* by the repressor. *J. Bacteriol.* **168**, 1128–1132.
27. Hackbarth, C. J. and Chambers, H. F. (1993) *bla*I and *bla*R1 regulate β-lactamase and PBP 2a production in methicillin-resistant *Staphylococcus aureus*. *Antimicrob. Agents Chemother.* **37**, 1144–1149.
28. Wittman, V. and Wong, H. C. (1988) Regulation of the penicillinase genes of *Bacillus licheniformis*: interaction of the *pen* repressor with its operators. *J. Bacteriol.* **170**, 3206–3212.
29. Strausak, D. and Solioz, M. (1997) CopY is a copper-inducible repressor of the *Enterococcus hirae* copper ATPases. *J. Biol. Chem.* **272**, 8932-8936.

30. Wunderli-Ye, H. and Solioz, M. (1999) Effects of promoter mutations on the *in vivo* regulation of the *cop* operon of *Enterococcus hirae* by copper(I) and copper(II). *Biochem. Biophys. Res. Commun.* **259**, 443–449.
31. Dobi, A., Dameron, C. T., Hu, S., Hamer, D., and Winge, D. R. (1995) Distinct regions of Cu(I)•ACE1 contact two spatially resolved DNA major groove sites. *J. Biol. Chem.* **270**, 10,171–10,178.
32. Zhou, P. B. and Thiele, D. J. (1991) Isolation of a metal-activated transcription factor gene from *Candida glabrata* by complementation in *Saccharomyces cerevisiae*. *Proc. Natl. Acad. Sci. USA* **88**, 6112–6116.
33. Jungmann, J., Reins, H. A., Lee, J. W., Romeo, A., Hassett, R., Kosman, D., et al. (1993) MAC1, a nuclear regulatory protein related to Cu-dependent transcription factors is involved in Cu/Fe utilization and stress resistance in yeast. *EMBO J.* **12**, 5051–5056.
34. Harrison, M. D., Jones, C. E., Solioz, M., and Dameron, C. T. (2000) Intracellular copper routing: the role of copper chaperones. *Trends Biochem. Sci.* **25**, 29–32.
35. Klomp, L. W., Lin, S. J., Yuan, D. S., Klausner, R. D., Culotta, V. C., and Gitlin, J. D. (1997) Identification and functional expression of HAH1, a novel human gene involved in copper homeostasis. *J. Biol. Chem.* **272**, 9221–9226.
36. Wakabayashi, T., Nakamura, N., Sambongi, Y., Wada, Y., Oka, T., and Futai, M. (1998) Identification of the copper chaperone, CUC-1, in *Caenorhabditis elegans*: tissue specific coexpression with the copper transporting ATPase, CUA-1. *FEBS Lett.* **440**, 141–146.
37. Lin, S. J. and Culotta, V. C. (1995) The ATX1 gene of *Saccharomyces cerevisiae* encodes a small metal homeostasis factor that protects cells against reactive oxygen toxicity. *Proc. Natl. Acad. Sci. USA* **92**, 3784–3788.
38. Bull, P. C. and Cox, D. W. (1994) Wilson disease and Menkes disease: new handles on heavy-metal transport. *Trends Genet.* **10**, 246–252.
39. Gitschier, J., Moffat, B., Reilly, D., Wood, W. I., and Fairbrother, W. J. (1998) Solution structure of the fourth metal-binding domain from the Menkes copper-transporting ATPase. *Nat. Struct. Biol.* **5**, 47–54.
40. Lutsenko, S., Petrukhin, K., Cooper, M. J., Gilliam, C. T., and Kaplan, J. H. (1997) N-terminal domains of human copper-transporting adenosine triphosphatases (the Wilson's and Menkes disease proteins) bind copper selectively *in vivo* and *in vitro* with stoichiometry of one copper per metal-binding repeat. *J. Biol. Chem.* **272**, 18,939-18,944.
41. Forbes, J. R., Hsi, G., and Cox, D. W. (1999) Role of the copper-binding domain in the copper transport function of ATP7B, the P-type ATPase defective in wilson disease. *J. Biol. Chem.* **274**, 12,408–12,413.
42. Voskoboinik, I., Strausak, D., Greenough, M., Brooks, H., Petris, M. J., Smith, S., et al. (1999) Functional analysis of the N-terminal CXXC metal-binding motifs in the human menkes copper-transporting P-type ATPase expressed in cultured mammalian cells. *J. Biol. Chem.* **274**, 22,008–22,012.
43. Cobine, P., Wickramasinghe, W. A., Harrison, M. D., Weber, T., Solioz, M., and Dameron, C. T. (1999) The *Enterococcus hirae* copper chaperone CopZ delivers copper(I) to the CopY repressor. *FEBS Lett.* **445**, 27–30.
44. Wimmer, R., Herrmann, T., Solioz, M., and Wüthrich, K. (1999) NMR structure and metal interactions of the CopZ copper chaperone. *J. Biol. Chem.* **274**, 22,597–22,603.
45. Steele, R. A. and Opella, S. J. (1997) Structures of the reduced and mercury-bound forms of MerP, the periplasmic protein from the bacterial mercury detoxification system. *Biochemistry* **36**, 6885–6895.
46. Rosenzweig, A. C., Huffman, D. L., Hou, M. Y., Wernimont, A. K., Pufahl, R. A., and O'Halloran, T. V. (1999) Crystal structure of the Atx1 metallochaperone protein at 1.02 Å resolution. *Structure* **7**, 605–617.
47. Wernimont, A. K., Huffman, D. L., Lamb, A. L., O'Halloran, T. V., and Rosenzweig, A. C. (2000) Structural basis for copper transfer by the metallochaperone for the Menkes/Wilson disease proteins. *Nat. Struct. Biol.* **7**, 766–771.
48. Arnesano, F., Banci, L., Bertini, I., Huffman, D. L., and O'Halloran, T. V. (2001) Solution structure of the Cu(I) and apo forms of the yeast metallochaperone, Atx1. *Biochemistry* **40**, 1528–1539.
49. Cobine, P., George, G. N., Wickramasinghe, W. A., Solioz, M., and Dameron, C. T. (2002) Coordination environments in the CopZ copper chaperone and its target, the CopY repressor. *Biochemistry*, in press.
50. Pufahl, R. A., Singer, C. P., Peariso, K. L., Lin, S., Schmidt, P. J., Fahrni, C. J., et al. (1997) Metal ion chaperone function of the soluble Cu(I) receptor Atx1. *Science* **278**, 853–856.
51. Harrison, M. D., Meier, S., and Dameron, C. T. (1999) Characterisation of copper-binding to the second sub-domain of the Menkes protein ATPase (MNKr2). *Biochim. Biophys. Acta* **1453**, 254–260.
52. Cobine, P., Harrison, M. D., and Dameron, C. T. (1999) Copper-binding properties of the N-terminus of the Menkes protein. *Adv. Exp. Med. Biol.* **448**, 153–164.
53. Qian, H., Sahlman, L., Eriksson, P. O., Hambraeus, C., Edlund, U., and Sethson, I. (1998) NMR solution structure of the oxidized form of MerP, a mercuric ion binding protein involved in bacterial mercuric ion resistance. *Biochemistry* **37**, 9316–9322.

33
Copper Homeostasis in Plants

Helena Mira, Vicente Sancenón, and Lola Peñarrubia

1. INTRODUCTION

Optimal plant growth and development depend on the appropriate supply of mineral nutrients, but, because of their sessile nature, plants must face wide variations in the environmental availability of these nutrients. In the case of copper, the needs generally vary from 5 to 20 μg/g dry tissue, whereas copper ionic concentrations found in soils range from 10^{-4} to 10^{-9} *M*, which largely surpass and underlie, respectively, plant requirements. The response of plant growth rate to metal concentration defines dose-response curves that can be divided in deficiency, adequate, and toxic zones. Deficiency, often caused by high-production agricultural systems, has been traditionally solved by the addition of chemical or organic fertilizers. Regarding toxicity, even higher copper levels than those indicated can be reached in some areas because of geological causes or human practices, including the excessive use of fertilizers or saline watering that result in soil pollution *(1)*.

At the physiological level, flowering is the most affected process, although copper defects generate as well-whitered stems and leaves. To the contrary, copper excess reduces root and shoot vegetative growth and diminishes the final size of mature leaves, which can also exhibit necrotic lesions and chlorotic symptoms in certain species *(2)*.

Different ecotypes from plant species can be classified as sensitive or tolerant to a certain metal, depending on the characteristics of their growth response curves *(3)*, thus indicating that metal sensitivity or tolerance in plants are controlled by a relatively low number of genes. Metal tolerance can either be constitutive or inducible by acclimation, as a part of the adaptive response after plant pretreatment with moderate metal concentrations. In general, tolerance in plants is not conferred by metal-extruding mechanisms through ionic pumps as it occurs in bacteria, instead, it is mainly based on metal chelation and storage processes that prevent its deleterious effects *(3,4)*.

Therefore, unraveling the homeostatic strategies used by plants to withstand toxic copper levels will permit the improvement of those species destined to agriculture or to phytoremediation, a technique that utilizes tolerant plants to extract mineral excess and recover polluted soils *(4)*.

2. BIOCHEMISTRY OF COPPER IN PLANTS

2.1. Copper Essentiality

Indeed, a wide variety of plant proteins make use of the Cu(I)/Cu(II) pair redox properties, accounting for the essentiality of this metal. Some of the plant proteins that coordinate copper ions

From: Handbook of Copper Pharmacology and Toxicology
Edited by: E. J. Massaro © Humana Press Inc., Totowa, NJ

Table 1
Plant Copper Proteins

Protein	*Location*	*Function*
Phenol oxidase Laccase Diamino oxidase Ascorbate oxidase	Extracellular Apoplastic	Oxidation of organic molecules
Cytochrome-*c* oxidase	Mitochondrial inner membrane	O_2 reduction
Plastocyanin	Thylakoid membrane	Electronic transport
Polyphenol oxidase	Chloroplast	Pigment synthesis
Cu/Zn-SOD	Chloroplast Cytosol	ROIs[a] detoxification
ETR1	Plasma membrane	Ethylene receptor

[a]Reactive oxigen intermediates.

function as oxidases and they are either located at the chloroplast or at the extracellular space (Table 1). For instance, apoplastic laccase and diamino oxidases are associated to cell walls and xylem lignification *(5,6)* and ascorbate oxidase is involved in cell-wall reorganization processes that occur during cell expansion at the initial stages of fruit development *(7,8)*. Moreover, copper participates in the plant hormone ethylene signaling pathway, because the copper ion acts as a cofactor in the *Arabidopsis thaliana* ethylene receptor ETR1, providing a chemical environment where the metal binds the gaseous hormone with unusual stability *(9)*.

2.2. Copper Phytotoxicity

2.2.1. Oxidative Stress and Cellular Damage

Despite being necessary, high copper levels induce oxidative stress that leads to accelerated plant senescence processes. The copper-catalyzed Haber–Weiss reaction takes place primarily at the chloroplast in plant cells *(10)* and results in the oxidative attack of chlorophylls, proteins, and thylakoid lipids, mainly affecting electronic transport at the level of photosystem II *(11,12)*. In this sense, oxidative modifications that make ribulose-1,5-bisphosphate carboxylase/oxygenase prone to degradation have been described as one of the first detectable symptoms after copper treatment *(13)*.

Among the earliest plant physiological responses observed after copper exposure, there is also a K^+ efflux from roots. This leakage has been interpreted as a symptom of the oxidative damage of membrane polyunsaturated fatty acids *(14)*. Lipid peroxidation at the plasma membrane occurs, as well, in other processes such as natural senescence or after pathogen attack, where it becomes associated to an increase in lipoxygenase (LOX) activity. Nevertheless, no correlation has been found between lipid peroxidation and LOX activity during copper exposure; therefore, it has been suggested that the reaction could be directly initiated by copper ions *(15)* or indirectly mediated by free-radical production *(14)*.

2.2.2. Defense Against Oxidative Stress: Antioxidant and Repair Systems

Because of their extra photoelectronic transport chain, plants are specially prepared to deal with oxidative stress-induced processes through a battery of both enzymatic and nonenzymatic mechanisms. Effectively, plants are enriched in antioxidant molecules such as ascorbic acid, glutathione, α-tocopherol, and carotenoids. Moreover, different enzymes, including catalases, peroxidases, and superoxide dismutases, protect plant cells against oxidative damage *(16)*.

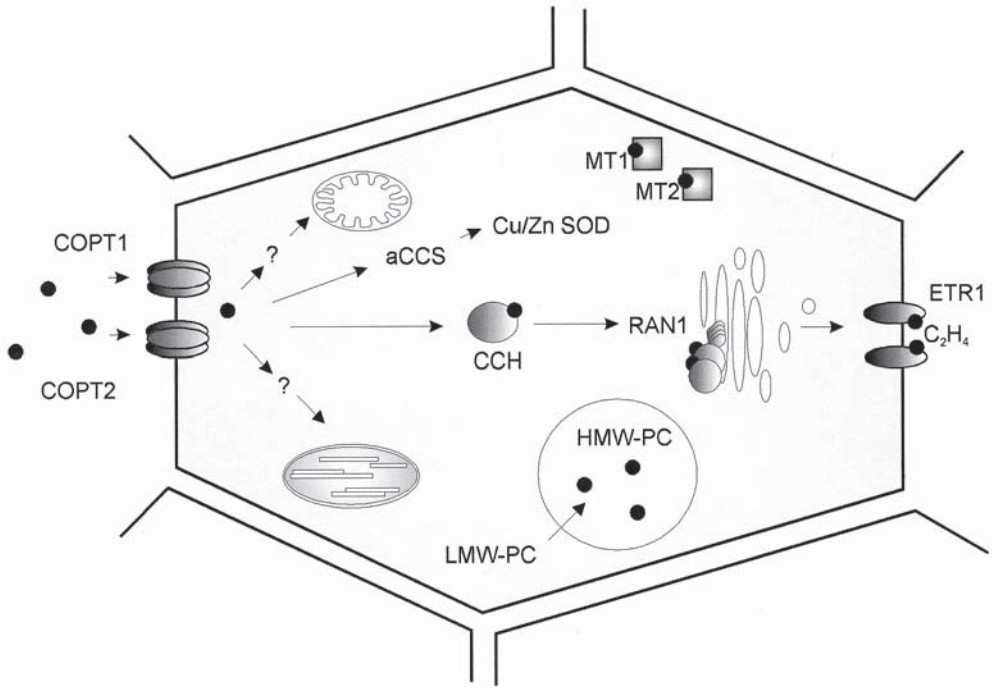

Fig. 1. Plant cell copper homeostasis scheme. Model based on the components identified in *Arabidopsis thaliana*. Copper uptake is performed by the plasma membrane transporters COPT1 and COPT2. Once inside the cell, different metallochaperones bind and distribute specifically copper to the cytosolic Cu/Zn-SOD (aCCS) and to the secretory pathway (CCH). Other uncovered chaperones (?) may deliver copper to mitochondria and chloroplasts. RAN1 is a post-Golgi vesicle transporter that accepts copper from CCH and mediates its incorporation to copper-requiring proteins at the endomembrane system, such as the ethylene receptor ETR1. The copper excess is chelated in the cytosol by metallothioneins (MT1 and MT2) and/or sequestered as low-molecular-weight phytochelatin complexes (LMW-PC) and subsequently stored in the vacuole as high-molecular-weight phytochelatin complexes (HMW-PC).

On the other hand, injured cell structures that escape antioxidative barriers have to be repaired to efficiently protect cells. Recent studies have shown that proteins involved in lipid metabolism accumulate in copper-treated Arabidopsis plants and their absence results in enhanced copper sensitivity *(4)*. In addition, copper tolerance in certain ecotypes has been related to a decrease in the susceptibility of the cell membrane to copper-induced oxidative damage *(17,18)*. Moreover, posttranslational modified metallothionein 1 (MT1) accumulates after copper exposure. It has been suggested that MT1 becomes prenylated and directed to the membrane in order to participate in copper scavenging and, therefore, increase the efficiency of the repair mechanisms *(19)*. Once again, these observations point to the maintenance of plasma membrane integrity as an important resistance mechanism against copper toxicity.

3. PLANT CELL HOMEOSTATIC COPPER NETWORKS

Emerging data suggest that copper homeostasis in plants could follow similar pathways to those described in the yeast *Saccharomyces cerevisiae*. Some of the putative components of the plant homeostatic copper network are shown in Fig. 1.

3.1. Chelation Systems

To diminish free-copper levels and, therefore, to reduce its phytotoxicity, plants have developed both extracellular and intracellular sequestration systems based on organic acids and thiol-rich polypeptides, respectively. For instance, copper exposure provokes the extracellular release of citrate in Arabidopsis. This organic acid is highly effective as a metal chelator and its extrusion does not result in plasma membrane depolarization, maybe because of the above-mentioned use of K^+ as a counterion *(14)*.

Two types of thiol-rich polypeptides have been shown to participate as intracellular sequestration systems:

1. Metallothioneins (MTs), small cysteine-rich proteins, with homologs in other organisms such as yeast and mammals *(20,21)*.
2. Phytochelatins (PCs), enzymatically synthesized glutathione-derived peptides *(3,22)*.

Although direct copper binding to metallothioneins has not been demonstrated in plants yet, there are at least two copper-regulated *MT* gene families in Arabidopsis (Fig. 1) whose function as copper chelators is mainly accepted based on functional complementation of the yeast mutant *Δcup1 (20)*. The pattern of *MT* expression differs depending on the member of the family, but they accumulate in leaf trichomes, suggesting a detoxification mechanism similar to the secretory strategy used by halophyte plants that extrude salts *(23)*. To date, no cis metalloregulatory elements, such as the metal-responsive element (MRE) sequences from yeast, nor other regulatory elements, have been found in the promoters of these genes *(21)*. On the other hand, Arabidopsis plants transformed with a chimeric construct, based on a reporter gene under the control of the yeast metallothionein *CUP1* promoter, do not respond to copper exposure *(24)*. This result suggests that plants possess a copper-sensor/regulatory system different from the one operating in yeast.

The second intracellular copper-chelator system formed by phytochelatins is specific for plants and some fungi such as *Schizosaccharomyces pombe*. PCs, also known as type-3 metallothioneins, have the primary structure $(\gamma\text{-Glu-Cys})_{2\text{-}11}$-Gly. Based on the *S. pombe* pathway, Rauser *(3)* has proposed a model in which a phytochelatin synthase would synthesize low-molecular-weight PCs (LMW-PCs) that, after binding metals in the cytosol, would cross the tonoplast helped by an ATPase pump. Once inside the vacuole, high-molecular-weight PC (HMW-PCs) complexes, which are stronger and more stable chelators, would be formed and stored (Fig. 1). A family of phytochelatin synthases have been recently isolated in Arabidopsis *(25)*. However, the role of PCs in plant copper homeostasis remains still controversial *(26,27)*.

3.2. Copper Transporters in Plant Cells

Although mostly unsolved, plant copper-uptake mechanisms are specially important in the understanding of copper homeostasis because metal tolerance could be controlled at the absorption level *(4)*. On the other hand, copper accumulation at intracellular compartments are also membrane-asso ciated transport processes that could play an important role in metal tolerance and deserve further characterization.

3.2.1. Plasma Membrane Transporters

As mineral nutrients, metal ions are acquired by vascular plants at the root surface and are subsequently distributed to distinct tissues through xylem. To reach cuproproteins, copper ions must cross the plasma membrane of different cell types and organela membranes. To date, there are little available data on the mechanisms operating on copper uptake from soils. Up to 98% of Cu(II) is mainly sequestered by rhizosphere or apoplast organic ligands, making copper poorly accessible to plant cells *(1)*.

Table 2
Heavy Metal Transporters in *Arabidopsis thaliana*

Family	*Features*[a]		*Members*	*Metal specificity*	*PL*[b]	*Putative function*	*Refs.*
ZIP	Length: 308–476 aa		ZIP1	Zn	Pm	Inducible Zn uptake from soils	*33*
	8 TMDs		ZIP2	Zn, Cu?, Cd?	Pm	Cu uptake?	*33*
	Intracellular His-rich variable domain		ZIP3	Zn	Pm	Inducible Zn uptake from soils	*33*
			ZIP4	Zn?	Chl	Zn import into chloroplast?	*33*
			IRT1	Fe(II), Mn, Zn	Pm	Inducible Fe uptake from soils	*34, 35*
Nramp	Conserved hydrophobic core with 10–12 TMDs	Class I	AtNramp1	Fe, Mn, Cd	Pl	Fe compartimentation	*36, 37*
	Nonconserved N- and C-domains	Class II	AtNramp2	Fe?	Pm?	Fe efflux?	*37*
	Intracellular transport signature		AtNramp3	Fe, Mn, Cd	Pm	Inducible Fe uptake from soils	*36*
	Assymetric charge distribution (Extracellular glycosilated loop)		AtNramp4	Fe, Mn, Cd	Pm	Fe uptake	*36*
	Exclusive hydrophilic C-domain	New	EIN2	?	?	Ethylene transduction	*38*
CTR	3 TMDs						
	(N-terminal metal binding motif)		COPT1	Cu	Pm	Cu uptake	*39*
			COPT2	Cu	Pm	Cu uptake	

[a]TMD: transmembrane domain; aa: amino acids. Features in parentheses are not fully conserved.
[b]Possible localization. Pm: plasma membrane; Pl: plastid; Chl: chloroplast.

Copper is thought to be incorporated in two steps, where Cu(II) would first be reduced to Cu(I) through the action of a Cu(II)-chelate reductase activity and Cu(I) would subsequently be captured by plant roots in a transporter-mediated process. This mechanism is operative for iron uptake in dicotyledons *(28)* and compelling data suggest that the same strategy could be utilized as well for copper uptake. Effectively, copper deficiency has been shown to induce Fe(III)-chelate reductase activity, which reduces both Fe(III) and Cu(II), in roots of pea seedlings *(29)*. In addition, Arabidopsis *frd1* mutants, which carry a recessive mutation in the *FRO2* gene, encoding an Fe(III)-chelate reductase *(30)*, lose the ability to reduce Cu(II) chelates *(31)*.

However, some other authors defend that this strategy is not functional in plants. In this sense, it has been reported that Cu(II) but not Cu(I) was efficiently absorbed by maize roots *(32)*. Moreover, copper accumulation was not reduced in Arabidopsis *frd1* plants grown on plates *(31)*, suggesting that copper reduction is not essential for the uptake of this metal.

Regarding copper transport across the plasma membrane, three families of heavy-metal transporters have been identified so far (*see* Table 2):

1. The ZIP (ZRT/IRT-related protein) family defines a group of transition metal transporters with broad specificity.
2. The Nramp (natural resistance-associated macrophage protein) family is also a group of heavy-metal transporters with wide spectrum.
3. The CTR (copper transporters) family is integrated by homologs from the yeast high-affinity plasma membrane copper transporters.

The first Arabidopsis ZIP members (ZIP1, ZIP2, and ZIP3) were isolated by their ability to transport zinc, but not iron, in yeast cells *(33)*. Interestingly, metal-uptake competition experiments indicate that ZIP2 seems to prefer Cu and Cd over other transition metals. A fourth member, ZIP4, was identified by sequence homology, although no metal-transport competence has been detected in yeast. However, the fact that it contains a putative chloroplast target signal suggests a role in metal transport to this compartment in plant cells *(33)*.

In a screen for plant cDNAs that encoded for iron transporters, Eide et al. *(34)* identified the Arabidopsis *IRT1* gene by functional complementation of yeast iron-uptake mutants. Later, IRT1 was also shown to transport Mn and Zn, but not Cu (35). IRT1 is thought to be an Fe(II) transporter that takes up Fe from soil in a manner that is coupled to the Fe(III)-chelate reductase *(1)*.

In higher plants, 10 Nramp-related genes have been identified to date *(36–38,40,41)*. Attending to sequence comparison analyses, they are divided into two major classes (*see* Table 2). Members from the two subgroups have been demonstrated to transport Fe, Mn, and Cd in yeast cells *(36,37)*. It has been suggested that distinct members of the family perform their function at different subcellular compartments and tissues *(37)*. Therefore, all of these transporters would act coordinately to regulate the pool of cytoplasmic metals in the whole plant.

Ethylene insensitive 2 (EIN2) represents a special Arabidopsis member of this Nramp group, involved in the ethylene transduction pathway *(42)*. Ethylene is a plant hormone that influences many aspects of plant growth and development, some of them with outstanding economical impact on agriculture, which traditionally made this gaseous hormone a main focus of attention in plant biology *(43)*. Mechanisms of ethylene action are being elucidated thanks to molecular genetic approaches using the ethylene-evoked triple-response phenotype of Arabidopsis seedlings *(44)*. *EIN2* encodes a protein with a hydrophobic Nramp-like amino terminal domain and an interesting exclusive hydrophilic carboxy terminal domain involved in the expression of genes that respond to oxidative stress and hormones such as jasmonates and ethylene, therefore integrating several important plant signal transduction pathways *(38)*. The EIN2 Nramp-like domain is evolutionary distant from the two other groups of plant Nramp genes *(36)*. In fact, neither EIN2 nor truncated versions of the protein displayed metal-transporting capacity when expressed in heterologous systems *(38)*. In contrast, the

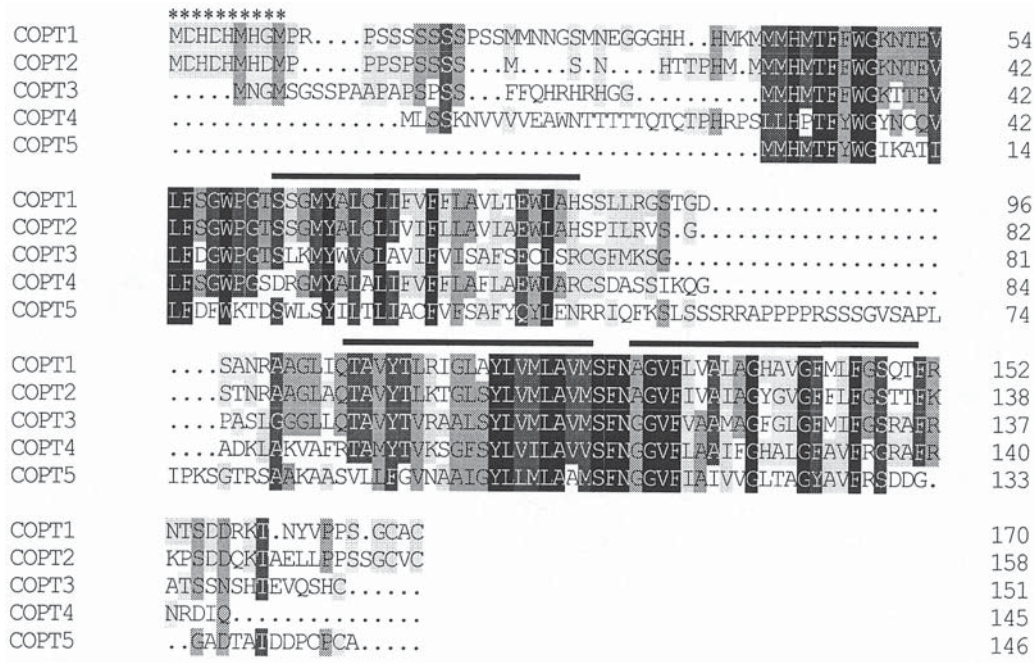

Fig. 2. Sequence comparison of the five members family of Arabidopsis copper transporters (COPT) belonging to the CTR family. At the upper part, bold lines indicate predicted transmembrane domains (TMD) and asterisks display the position of a putative copper-binding motif in COPT1 and COPT2.

Nramp-like domain is necessary for regulating the EIN2 carboxy-terminal domain hormone responses. Thus, the EIN2 Nramp domain has been suggested to be involved in sensing divalent metal ions, rather than transporting them across membranes. Concomitantly, the EIN2 carboxy-terminal domain would transduce the signal to downstream elements, maybe interacting with components of other hormone transduction cascades. If true, a metal ion is predicted to act as a second messenger in the ethylene signaling pathway *(38)*.

Finally, members of a widespread family of eukaryotic CTR transporters have been identified in yeast, worms, flies, mammals, and plants. All of the members belonging to this family contain three predicted transmembrane segments and some of them posses an N-terminal putative metal-binding domain (Fig. 2). The Arabidopsis *COPT1* gene was originally identified by its ability to suppress the phenotype of yeast mutants defective in high-affinity copper uptake *(39)*. *COPT1* encodes a polypeptide of 170 amino acids with 49% similarity to its yeast counterpart *CTR1 (1)*. The 44 amino-terminal residues of COPT1 are enriched in methionine and histidine residues and display similarity with bacterial copper binding motifs *(44)*. This COPT1 amino terminal domain is predicted to face the extracytoplasmic region *(1)*, suggesting copper binding previous to its transport across plasma membrane. Complementation experiments with truncated forms of the protein indicate that the COPT1 amino-terminal domain is necessary for high-affinity copper uptake in yeast (Mira and Peñarrubia, unpublished results).

Sequence analysis of the complete Arabidopsis genome *(45)* reveals a five-member family of *CTR*-related genes, temptatively named *COPT1–5* (Fig. 2 and Table 2). The hydrophobicity profiles of the predicted proteins is in accordance with the three transmembrane spanning domains (TMD) postulated for the CTR family. The alignment of the polypeptides reveals that whereas the TMDs are

highly conserved within the COPT family, the amino- and carboxy-terminal protein regions are variable in sequence and length. COPT2 is closely related to COPT1 (72% identity) and also has a histidine and methionine-rich amino-terminal box, whereas COPT3–5 are more distantly related to COPT1 and do not posses any recognizable copper binding motif (Fig. 2).

Although Northern blot showed that *COPT1* mRNA was undetectable in roots *(39)*, semiquantitative reverse transcription–polymerase chain reaction (RT-PCR) data indicate that *COPT1* is indeed expressed in these nutrient-uptake organs. *COPT2* is also capable of rescuing yeast high-affinity copper-uptake mutants and expressed in roots. Both *COPT1* and *COPT2* mRNA levels are downregulated by copper treatment in leaves, suggesting a role of these genes in copper transport in plants (Sancenón and Peñarrubia, unpublished results).

Although we have tried to summarize disperse data available about metal transporters, further phenotypic characterization of genetically modified plants that silence or overexpress these genes turn out to be essential for assessing the role of the three transporter families in plant copper homeostasis.

3.2.2. The Transport at the Endomembrane System

The *RAN1* (Responsive to Antagonist 1) gene from *Arabidopsis thaliana* has been recently cloned and it encodes a homolog of P-type ATPases from yeast (Ccc2) and humans (Menkes and Wilson proteins) located at post-Golgi vesicles (Fig. 1). RAN1 presents two putative copper-binding boxes of the GMTCXXC type and complements the deficiency in copper transport to the secretory pathway of the yeast mutant *Δccc2 (46)*. However, RAN1 lacks the leucine repeats taht act as signals for the copper-mediated traffic of the protein between Golgi and plasma membranes in the human homolog *(46,47)*. It would be interesting to check RAN1 subcellular localization under different copper status and its tissue distribution during development in order to gain further insight into its specific functionality in plants.

This copper homeostasis-related gene was isolated in a screen for plants with an unusual response to the ethylene antagonist *trans*-cyclooctene *(46)*, further underscoring the critical role of metals in the ethylene signaling pathway. Among the members of this pathway, perception takes place through a small family of receptors. One of these receptors, ETR1, has been shown to form disulfide-linked homodimers *(48)* that require a Cu atom for high-affinity ethylene binding *(9)* (Fig. 1). *ETR1* encodes a polypeptide resembling the sensor module of the two-component regulatory systems widely used by different living organisms. However, ETR1 combines the sensor domain for hormone binding and a membrane-localized regulatory histidine kinase signaling domain (reviewed in ref. *49*). Ethylene-depleted receptors act as negative regulators of the transduction pathway. Upon hormone-binding, the receptor is inactivated and the resulting phenotypic effects are known as the ethylene response. Thus, mutations in the hormone binding domain provoke dominant insensitivity to ethylene because the receptor cannot be inactivated, whereas disruptions in the signaling domain originate a constitutive ethylene response *(50,51)*.

Two types of *RAN1* defective plants have been described. In the first group (composed of *ran1-1* and *ran1-2*), the mutations cause a slight impairment in the receptor structure in such a way that modifies the response to the ethylene antagonist *trans*-cyclooctene. Interestingly, no other phenotypic effects have been observed *(46)*. There is no molecular explanation for this behavior yet, because the mechanisms of the *trans*-cyclooctene action and the receptor structure still remain unsolved. The second class is composed of *ran1* loss-of-function plants and include *ran1-3*, a strong allele mutated in a glycine residue conserved within the rest of homologs *(52)*, *ran1–4*, caused by a transfer-DNA insertion *(53)* and the transgenic CaMV *35S::RAN1* plants that cause cosupression of *RAN1 (46)*. All of these plants appear to have a constitutive ethylene response showing a phenotype similar to the mutants with multiple disruption of ethylene receptors *(51)*. It has been suggested that this fact would indicate the requirement of RAN1 to pump copper into the post-Golgi compartment where it would be added to ethylene aporeceptors as they move toward the plasma membrane. In RAN1-defective

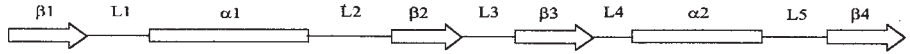

N-domain

```
                          MXCXXC      R   K                                          K   K
Homo          ---MPKHEFSVDMTCGGCAEAVSRVLNKLGG--VKYD-IDLPNKKVCIESEHSMDTLLATLKKTGKTVSYLGLE  68
Canis         ---MPKHEFSVDMTCEGCSNAVSRVLNKLGG--VEFD-IDLPNKKVCINSEHSVDILLETLEKTGKAVSYLGPK  68
Ovis          ---MPKHEFSVDMTCEGCSNAVTRVLNKLGG--VQFD-IDLPNKKVCINSEHSVDTLLETLGKTGKAVSYLGPK  68
Rattus        ---MPKHEFSVDMTCGGCAEAVSRVLNKLGG--VEFN-IDLPNKKVCIESEHSSDILLATLNKTGKAVSYLGPK  68
Mus           ---MPKHEFSVDMTCEGCAEAVSRVLNKLGG--VEFN-IDLPNKKVCIDSEHSSDTLLATLNKTGKAVSYLGPK  68
Caenorhabditis---MTQYVFEMGMTCNGCANAARKVLGKLGEDKIKIDDINVETKKITVTTDLPASDVLEALKKTGKEI---KQLQ 68
Saccharomyces MAEIKHYQFNVVMTCSGCSGAVNKVLTKLEPDVSKID-ISLEKQLVDVYTTLPYDFILEKIKKTGKEVRSGKQL  73
Arabidopsis   --MAQTVVLKVGMSCQGCVGAVNRVLGKMEG-VESFD-IDIKEQKVTVKGNVEPEAVFQTVSKTGKKTSYWPVE  70
                        . *.* **  *  .** *.         * .  . . .        .   . ****
```

C-domain

```
Arabidopsis   AEAEPKAEADPKVETVTETKTEAETKTEAKVDAKADVEPKAAEAETKPSQV                    121
```


Hello-motif

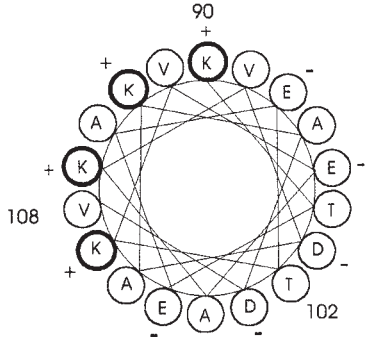

Fig. 3. Sequence comparison of Atx1-like metallochaperones from different species: *Homo sapiens, Canis familiaris, Ovis aries, Rattus norvegicus, Mus musculus, Caenorhabditis elegans, Saccharomyces cerevisiae*, and *Arabidopsis thaliana*. In the upper part, the predicted secondary structure for the *Saccharomyces* chaperone is indicated. β-Sheets are represented by arrows, α-helices are indicated by rectangles, and loops are indicated by lines. In the bottom part, asterisks show identical amino acids and dots indicate conservative substitutions. A schematic representation of the α-helix conformation predicted for the central part of the C-domain (from residue 90 to 108) denominated Hello motif.

plants, the absence of copper delivery to the secretory pathway would avoid metal incorporation to cuproproteins passing through the endomembrane system, including ethylene receptors. These anomalous receptors would cause the permanent activation of the ethylene signaling pathway and the observed constitutive response. Moreover, ethylene-independent effects, such as a rosette-lethal phenotype originated by a defect in cell expansion, have also been observed in the *ran1–3* mutant under an ethylene-insensitive background *(52)*. This phenotype could be caused by the absence of the metal in other copper-requiring enzymes that incorporate this cofactor in a post-Golgi compartment by a RAN1-dependent mechanism. In this sense, it would be interesting to check the activity of apoplastic cuproenzymes, such as laccase, diamino oxidase, and ascorbate oxidase, in these mutants. Furthermore, genetic analysis and the response of the *ran1–3* to ethylene inhibitors indicate that, in addition to forming completely functional ethylene-binding sites, copper is also required for the receptor signaling function *(52)*. The molecular meaning of this observation will require the structural characterization of the ethylene receptor, as well as the reorganizations that take place upon hormone binding. These studies will open new perspectives into the knowledge of how copper influences ethylene action and, to a greater extent, they are promoting a growing and preponderant interest of plant biologists about how plant cells deal with copper.

3.3. Cytosolic Distribution

According to the *Saccharomyces* model, it is conceivable that a small family of cytosolic metallochaperones could also operate in plants (Fig. 1). In this sense, cDNA sequences with homology to yeast *CCS*, which code for putative chaperones that deliver copper to the Cu/Zn-SOD (superoxide dismutase) cytosolic isoform, have been found in the databases from both Arabidopsis (GenBank accession no. AF179371) and tomato (GenBank accession no. AF117707). Tomato CCS, obtained as recombinant protein, has already been structurally characterized *(54)*.

On the other hand, no information is available about how plants transport copper to their organela (Fig. 1). With regard to the yeast chaperone Cox17, which drives copper to the mitochondrial cytochrome oxidase, no plant homologs have been found yet in spite of the fact that the Arabidopsis genome has been already released *(45)* and sequencing programs are in progress for other higher plants. Moreover, plant-specific organelae (i.e., the chloroplasts) should have their own mechanism to guarantee copper delivery to cuproproteins such as plastocyanin and the plastidic isoform of the Cu/Zn-SOD. In these cases, new approaches would be necessary to uncover these plant exclusive processes.

Special attention will be paid next to the copper routing toward the secretory pathway, because the corresponding Arabidopsis copper chaperone has been the first metallochaperone described in plants and our main focus of interest over the past several years.

3.3.1. The Copper Chaperone CCH

The cDNA clone encoding a homolog of the yeast *ATX1 (55)* was identified in the Arabidopsis expressed sequence tag collection and named *CCH* for copper chaperone *(56)* (Fig. 1). Although CCH has an amino-terminal part (N-domain) that exhibits a 36% identity to Atx1, it also has an extra carboxy-terminal region (C-domain) composed of 48 amino acids that is absent in all other nonplant homologs identified to date (Fig. 3).

When compared to the rest of Atx1-like proteins, the CCH N-domain presents two conserved regions. The first region includes the copper-binding motif MXCXXC located at the L1 connection within the structural module βαββαβ, characteristic of both metallochaperones and copper ATPases *(57,58)* (Fig. 3). The cysteines in the Atx1 MT**C**SG**C** box for copper binding are conserved in the CCH-MS**C**QG**C** box**.** However, threonine is replaced by serine, a conservative substitution, in the Arabidopsis motif (Fig. 3). The second region is composed of basic residues where the conservation of the Arabidopsis lysine necessary for the antioxidant role of the Atx1 and its human homolog Hah1

is noticeable *(59,60)* (Fig. 3). In Atx1, these basic residues are at the protein surface and probably participate in electrostatic interactions with acidic residues in the cytosolic exposed surface of Ccc2 *(57,61)*.

3.3.1.1. Characterization of the Plant-Exclusive CCH C-Domain

The CCH C-domain has an unusual amino acid composition with no significant identity with any other sequences in the databases. It is composed of 44% charged residues alternating with noncharged ones, mostly prolines, alanines and hydrophobic-β-branched amino acids, generating a singular (i, $i + 1$) periodicity. Secondary-structure predictions indicate that the central part of this domain could be arranged as an α-helix with a spatial distribution of basic amino acids on one side and acidic amino acids on the other (Fig. 3). This central part has been named Hello motif for helix with lateral opposite charge. From the structural point of view, circular-dicroism (CD) spectroscopy data indicate that the C-domain could adopt an α-helical conformation in the presence of trifluorethanol, but an extended conformation is acquired in aqueous solution, which is further stabilized by lowering the temperature or in the presence of submicellar concentrations of sodium dodecyl sulfate (SDS). The extended conformation that we refer to here could be obtained as a result of the contribution of two or more different types of secondary structures, like type-II polyproline helix and/or antiparallel β-sheet *(62)*. Although this complex structural behavior deserves further characterization, it could reflect the conformational flexibility of the C-domain in response to environmental changes.

In order to know whether the presence of this extra domain is a common feature in plants, two homologs from soybean and rice have been sequenced and shown to contain C-terminal regions with similar sizes and amino acid composition (Mira and Peñarrubia, unpublished results). To gain insight into the evolutionary appearance of the plant extra C-domains, it would be of interest to check its presence in other orthologs from different photosynthetic eukaryotes.

As a first attempt to address the role that the C-domains accomplishes in plant metallochaperones, functional studies were performed in yeast. Our results have shown that the CCH N-terminal domain retains the Atx1-like properties (e.g., the antioxidant function and the delivery of copper to the Ccc2 transporter in the secretory pathway) *(55,59,60)*, indicating that these properties are not affected by the C-terminal part *(62)*. As postulated for other multimodular proteins, the extra C-domain could have been added "in line" *(63)*, a kind of module addition that would allow the structure of the N-terminal part of the protein to remain virtually identical. Moreover, by comparison with the Atx1 structure, recently determined by X-ray, no major structural reorganizations would be expected to take place at the C-domain of the CCH protein upon copper binding to the N-terminal part *(57)*. As a consequence, this kind of assembly would explain the lack of interference with the original intracellular function played by this metallochaperone in single-cell organisms, while probably allowing a novel or more complex role related to pluricellularity in plants, as suggested for other extra domains *(64)*. Nevertheless, because direct interaction between CCH and RAN1 has not been demonstrated yet, a role of this extra domain in protein–protein recognition cannot be discarded. However, Ccc2 and the Arabidopsis homolog RAN1 do not seem to differ enough to justify the existence of the extra CCH C-domain to interact with RAN1 *(46)*.

3.3.1.2. Expression and Localization of CCH

The soybean *CCH* homolog was initially isolated by a search for upregulated genes during leaf senescence *(65)* and Arabidopsis *CCH* mRNA is induced during natural and ozone-accelerated leaf senescence *(56,66)*. These facts indicate that *CCH* can be classified as a senescence-associated gene (SAG), a group of diverse genes that are mainly involved in nutrient salvage from decaying organs *(67)*.

Leaf senescence involves an orderly loss of structures and metabolic functions characterized by macromolecule degradation and mobilization of the resulting nutrients to other parts of the plant *(68,69)*. Metal ions released after metalloproteins break down are recycled from senescing leaves to growing organs *(70–73)*. During these processes, the vascular system, in particular phloem, plays a

key role in the translocation of resources. As detected in Western blots from Arabidopsis phloem exudates, CCH belongs to the pool of soluble polypeptides found in these transport tissues *(74)*, suggesting its requirement for copper remobilization from decaying organs to demanding reproductive structures. In this context, an Arabidopsis metallothionein mRNA has been located to the vascular bundle *(23)*. However, metallothioneins presumably act as chelators that are upregulated by copper *(20)*. In contrast, *CCH* expression is specifically repressed by copper, and, at least in yeast, the CCH protein has the ability to bind and deliver copper to a specific target *(56,62)*, thus indicating that the functions of metallothioneins and CCH are, in fact, different. Moreover, because CCH and its homologs exhibit antioxidant properties *(55,59,62)*, it cannot be discarded that CCH could participate in avoiding the damage of the vascular system produced by oxidant toxic molecules originated during senescence and in keeping these structures functional for the progressive dismantling of decaying organs.

Immunolocalization experiments show that, despite its housekeeping character, CCH is specially abundant in specific phloem elements of green leaves and stems and that, during senescence, CCH levels increase and extend to surrounding cells *(74)*. Perhaps, the high levels of CCH in the phloem are necessary to compete with other molecules for copper and to guarantee its delivery to the secretory pathway, mediating the loading of extracellular copper-requiring proteins along the way from senescent tissues to developing organs. Specially remarkable is the fact that CCH is mainly located at specific phloem cells named sieve elements. These cells suffer a selective degradation of internal structures during differentiation that results in the lost of their competence for transcription, translation and protein maturation, which makes them dependent on associated companion cells for much of their metabolic functions *(75,76)*. Thus, CCH, after being synthesized in companion cells, must cross to the sieve elements through the cell-connecting structures called plasmodesmata. In this sense, CCH is the first metallochaperone shown to be transported from cell to cell, and it is tempting to speculate that the exclusive CCH C-domain of unknown function could be involved in this plant-exclusive transport process.

ACKNOWLEDGMENTS

H.M. and V.S. are recipients of long-term predoctoral fellowships from Conselleria d´Educació i Ciència and from Ministerio de Educación y Cultura, respectively. This work was supported by grants from Plan Nacional I+D (BIO99-1201-C02-02) and from Conselleria de Cultura, Educació i Ciència Generalitat Valenciana (GV98-3-82).

REFERENCES

1. Fox, T. C. and Guerinot, M. L. (1998) Molecular biology of cation transport in plants. *Annu. Rev. Plant Physiol. Plant Mol. Biol.* **49**, 669–696.
2. Märschner, H. (ed.) (1995) *Mineral Nutrition of Higher Plants*, Academic, San Diego, CA.
3. Rauser, W. E. (1995) Phytochelatins and related peptides. *Plant Physiol.* **109**, 1141–1149.
4. Salt, D. E., Smith, R. D., and Raskin, I. (1998) Phytoremediation. *Annu. Rev. Plant Physiol. Plant Mol. Biol.* **49**, 643–668.
5. Bao, W., O'Malley, D., Whetten, R., and Sederoff, R. (1993) A laccase associated with lignification in loblolly pine xylem. *Science* **260**, 672–674.
6. Moller, S. G. and McPherson, M. J. (1998) Developmental expression and biochemical analysis of the *Arabidopsis atao1* gene encoding an H_2O_2-generating diamine oxidase. *Plant J.* **13**, 781–791.
7. Moser, O. and Kanellis, A. K. (1994) Ascorbate oxidase of *Cucumis melo* L. var. reticulatus: purification, characterization and antibody production. *J. Exp. Bot.* **275**, 717–724.
8. Diallinas, G., Pateraki, I., Sanmartin, M., Scossa, A., Stilianou, E., Panopoulos, N. J., et al. (1997) Melon ascorbate oxidase: cloning of a multigene family, induction during fruit development and repression by wounding. *Plant Mol. Biol.* **34**, 759–770.
9. Rodriguez, F. I., Esch, J. J., Hall, A. E., Binder, B.M., Schaller, G. E., and Bleecker, A. B. (1999) A copper cofactor for the ethylene receptor ETR1 from Arabidopsis. *Science* **283**, 996–998.
10. Sandmann, G. and Böger, P. (1980) Copper-mediated lipid peroxidation processes in photosynthetic membranes. *Plant Physiol.* **66**, 797–800.

11. Schöder, W. P., Arellano, J. B., Bittner, T., Baron, M., Eckert, H.-J., and Reuger, G. (1994) Flash-induced absorption spectroscopy studies of copper interaction with photosystem II in higher plants. *J. Biol. Chem.* **30**, 32,865–32,870.
12. Yruela, I., Pueyo, J. J., Alonso, P. J., and Picorel, R. (1996) Photoinhibition of photosystem II from higher plants: effect of copper inhibition. *J. Biol. Chem.* **271**, 27,408–27,415.
13. Mehta, R. A., Fawcett, T. W., Porath, D., and Mattoo, A.K. (1992) Oxidative stress causes rapid membrane translocation and *in vivo* degradation of ribulose-1,5-bisphosphate carboxylase/oxygenase. *J. Biol. Chem.* **267**, 2810–2816.
14. Murphy, A., Eisinger, W. R., Shaff, J. E., Kochian, L. V., and Taiz, L. (1999) Early copper-induced leakage of K^+ from Arabidopsis seedlings is mediated by ion channels and coupled to citrate efflux. *Plant Physiol.* **121**, 1375–1382.
15. Weckx, J. and Clijsters, H. (1996) Oxidative damage and defense mechanisms in primary leaves of *Phaseolus vulgaris* as a result of root assimilation of toxic amounts of copper. *Physiol. Plant.* **96**, 506–512.
16. Inzé, D. and van Montagu, M. (1995) Oxidative stress in plants. *Curr. Opin. Biotech.* **6**, 153–158.
17. De Vos, C. H. R., Vooijs, R., Schat, H., and Ernst, W. H. O. (1989) Copper-induced damage to the permeability barrier in roots of *Silene cucubalus*. *J. Plant Physiol.* **135**, 164–169.
18. Strange, J. and Macnair, M. (1991) Evidence for a role for the cell membrane in copper tolerance of *Mimulus guttatus* Fischer ex DC. *New Phytol.* **119**, 383–388.
19. Murphy, A., Zhou, J., Goldsbrough, P. B., and Taiz, L. (1997) Purification and immunological identification of metallothioneins 1 and 2 from *Arabidopsis thaliana*. *Plant Physiol.* **113**, 1293–1301.
20. Zhou, J. and Goldsbrough, P. B. (1994) Functional homologs of fungal metallothionein genes from Arabidopsis. *Plant Cell* **6**, 875–884.
21. Zhou, J. and Goldsbrough, P. B. (1995) Structure, organization and expression of the metallothionein gene family in *Arabidopsis*. *Mol. Gen. Genet.* **248**, 318–328.
22. Rauser, W. E. (1990) Phytochelatins. *Annu. Rev. Biochem.* **59**, 61–86.
23. García-Hernández, M., Murphy, A., and Taiz, L. (1998) Metallothioneins 1 and 2 have distinct but overlapping expression patterns in Arabidopsis. *Plant Physiol.* **118**, 387–397.
24. Mett, V. L., Lochhead, L. P., and Reynolds, H. S. (1993) Copper-controllable gene expression system for whole plants. *Proc. Natl. Acad. Sci. USA* **90**, 4567–4571.
25. Clemens, S., Kim, E., Neumann, D., and Schroeder, J. (1999) Tolerance to toxic metals by a gene family of phytochelatin sythases from plants and yeast. *EMBO J.* **12**, 3325–3333.
26. Howden, R., Goldsbrough, P. B., Andersen, C. R., and Cobbett C. S. (1995) Cadmium-sensitive, cad1 mutants of *Arabidopsis thaliana* are phytochelatin deficient. *Plant Physiol.* **107**, 1059–1066.
27. Xiang, C. and Oliver, D. J. (1998) Glutathione metabolic genes coordinately respond to heavy metals and jasmonic acid in Arabidopsis. *Plant Cell* **10**, 1539–1550.
28. Mori, S. (1999) Iron acquisition by plants. *Curr. Opin. Plant Biol.* **2**, 250–253.
29. Welch R. M., Norvell W. A., Schaefer S. C., Shaff J. E., and Kochian L. V. (1993) Induction of iron(III) and copper(II) reduction in pea (*Pisum sativum* L.) roots by Fe and Cu status: does the root-cell plasmalemma Fe(III)-chelate reductase perform a general role in regulating cation uptake? *Planta* **190**, 555–561.
30. Robinson N. J., Procter C. M., Connolly E. L., and Guerinot M. L. (1999) A ferric-chelate reductase for iron uptake from soils. *Nature* **397**, 694–697.
31. Yi, Y. and Guerinot, M. L. (1996) Genetic evidence that induction of root Fe(III) chelate reductase is necessary for iron uptake under iron deficiency. *Plant J.* **10**, 835–844.
32. Bell, P. F., Chaney, R. L., and Angle, J. S. (1991) Determination of copper activity required by maize using chelator-buffered nutrient solutions. *Soil Sci. Soc. Am. J.* **55**, 7824–7828.
33. Grotz, N., Fox, T., Connolly, E., Park, W., Guerinot, M. L., and Eide, D. (1998) Identification of a family of zinc transporter genes from *Arabidopsis* that respond to zinc deficiency. *Proc. Natl. Acad. Sci. USA* **95**, 7220–7224.
34. Eide, D., Broderius, M., Fett, J., and Guerinot, M. L. (1996) A novel iron-regulated metal transporter from plants identified by functional expression in yeast. *Proc. Natl. Acad. Sci. USA* **93**, 5624–5628.
35. Korshunova, Y. O., Eide, D., Clark, W. G., Guerinot, M. L., and Pakrasi, H. B. (1999) The IRT1 protein from *Arabidopsis thaliana* is a metal transporter with a broad substrate range. *Plant Mol. Biol.* **40**, 37–44.
36. Thomine, S., Wang, R., Ward, J. M., Crawford, N. M., and Schroeder, J. I. (2000) Cadmium and iron transport by members of a plant metal transporter family in *Arabidopsis* with homology to *Nramp* genes. *Proc. Natl. Acad. Sci. USA* **97**, 4991–4996.
37. Curie, C., Alonso, J. M., Le Jean, M., Ecker, J. R., and Briat, J. F. (2000) Involvement of NRAMP1 from *Arabidopsis thaliana* in iron transport. *Biochem. J.* **347**, 749–755.
38. Alonso, J. M., Hirayama, T., Roamn, G., Nourizadeh, S., and Ecker, J. R. (1999) EIN2, a bifunctional transducer of ethylene and stress response in *Arabidopsis*. *Science* **284**, 2148–2152.
39. Kampfenkel, K., Kushinr, S., Babychuk, E., Inzé, D., and Van Montagu, M. (1995) Molecular characterization of a putative *Arabidopsis thaliana* copper transporter and its yeast homologue. *J. Biol. Chem.* **270**, 28,479–28,486.
40. Belouchi, A., Cellier, M., Kwan, T., Saini, H. S., Leroux, G., and Gros, P. (1995) The macrophage-specific membrane protein Nramp controlling natural resistance to infections in mice has homologues expressed in the root system of plants. *Plant Mol. Biol.* **29**, 1181–1196.
41. Belouchi, A., Kwan, T., and Gros, P. (1997) Cloning and characterization of the OsNramp family from *Oryza sativa*, a new family of membrane proteins possibly implicated in the transport of metal ions. *Plant Mol. Biol.* **33**, 1085–1092.

42. Guzman, P. and Ecker, J. R. (1990) Exploiting the triple response of Arabidopsis to identify ethylene-related mutants. *Plant Cell* **2**, 513–523.
43. Abeles, F. B., Morgan, P. W., and Saltveit, M. E., Jr. (eds.) (1992) *Ethylene in Plant Biology*, 2nd ed, Academic, San Diego, CA.
44. Ecker, J. R. (1995) The ethylene signal transduction pathway in plants. *Science* **268**, 667–675.
45. The Arabidopsis Genome Initiative (2000) Analysis of the genome sequence of the flowering plant *Arabidopsis thaliana*. *Nature* **408**, 796–815.
46. Hirayama, T., Kieber, J. J., Hirayama, N., Kogan, M., Guzman, P., Nourizadeh, S., et al. (1999) RESPONSIVE-TO-ANTAGONIST1, a Menkes/Wilson disease-related copper transporter, is required for ethylene signaling in Arabidopsis. *Cell* **97**, 383–393.
47. Petris, M. J., Camarakis, J., Greenough, M., LaFontaine, S., and Mercer, J. F. B. (1998) A C-terminal di-leucine is required for localization of the Menkes protein in the trans-Golgi network. *Hum. Mol. Genet*. **7**, 2063–2071.
48. Schaller, G., Ladd, A., Lanahan, M., Spanbauer, J., and Bleecker, A. (1995). The ethylene response mediator ETR1 from Arabidopsis forms a disulfide linked dimer. *J. Biol. Chem*. **270**, 12,526–12,530.
49. Stepanova, A. N. and Ecker, J. R. (2000) Ethylene signaling: from mutants to molecules. *Curr. Op. Plant Biol*. **3**, 353–360.
50. Chang, C., Kwok, S. F., Bleecker, A. B., and Meyerowitz, E.M. (1993) Arabidopsis ethylene-response gene ETR1: similarity of product to two-component regulators. *Science* **262**, 539–544.
51. Hua, J. and Meyerowitz, E. M. (1998) Ethylene responses are negatively regulated by a receptor gene family in *Arabidopsis thaliana*. *Cell* **94**, 261–271.
52. Woeste, K. E. and Kieber, J. J. (2000) A strong loss-of function mutation in *RAN1* results in constitutive activation of the ethylene response pathway as well as a rosette-lethal phenotype. *Plant Cell* **12**, 443–455.
53. Himelblau, E. and Amasino, R. M. (2000) Delivering copper within plant cells. *Curr. Opin. Plant Biol*. **3**, 205–210.
54. Zhu, H., Shipp, E., Sanchez, R. J., Liba, A., Stine, J. E., Hart, P. J., Gralla, E. B., et al. (2000) Cobalt(2+) binding to human and tomato copper chaperone for superoxide dismutase: implications for the metal ion transfer mechanism. *Biochemistry* **39**, 5413–5421.
55. Lin, S. J. and Culotta, V. C. (1995) The *ATX1* gene of *Saccharomyces cerevisiae* encodes a small metal homeostasis factor that protects cells against reactive oxygen toxicity. *Proc. Natl. Acad. Sci. USA* **92**, 3784–3788.
56. Himelblau, E., Mira, H., Lin, S.-J., Culotta, V. C., Peñarrubia, L., and Amasino, R. M. (1998). Identification of a functional homolog of the yeast copper homeostasis gene *ATX1* from Arabidopsis. *Plant Physiol*. **117**, 1227–1234.
57. Rosenzweig, A. C., Huffman, D. L., Hou, M. Y., Wernimont, A. K., Pufahl, R. A., and O'Halloran, T. V. (1999) Crystal structure of the Atx1 metallochaperone protein at 1.02 Å resolution. *Structure* **7**, 605–617.
58. Gitschier, J., Moffat, B., Reilly, D., Wood, W. I., and Fairbrother, W. J. (1998) Solution structure of the fourth metal-binding domain from the Menkes copper-transporting ATPase. *Nature Struct. Biol*. **5**, 47–54.
59. Portnoy, M. E., Rosenzweig, A. C., Rae, T., Huffman, D. L., O'Halloran, T. V., and Culotta, V. C. (1999) Structure–function analyses of the ATX1 metallochaperone. *J. Biol. Chem*. **274**, 15,041–15,045.
60. Hung, I. H., Casareno, R. L. B., Labesse, G., Mathews, F. S., and Gitlin, J. D. (1998) HAH1 is a copper-binding protein with distinct amino acid residues mediating copper homeostasis and antioxidant defense. *J. Biol. Chem*. **273**, 1749–1754.
61. Arnesano, F., Banci, L., Bertini, I., Cantini, F., Cioffi-Baffoni, S., Huffman, D. L., and O'Halloran, T. V. (2001) Characterization of the binding interface between the copper chaperone Atx1 and the first cytosolic domain of Ccc2 ATPase. *J. Biol. Chem*. **276**, 41,365–41,376.
62. Mira, H., Vilar, M., Pérez-Payá, E., and Peñarrubia, L. (2001) Functional and conformational properties of the exclusive C-domain from the Arabidopsis copper chaperone CCH, *Biochem. J*. **357**, 545–549.
63. Baron, M., Norman, D. G., and Campbell, I. D. (1991) Protein modules. *Trends Biochem. Sci*. **16**, 13–17.
64. Copley, R. R., Schultz, J., Ponting, C. P., and Bork, P. (1999) Protein families in multicellular organisms. *Curr. Opin. Struct. Biol*. **9**, 408–415.
65. Crowell, D. and Amasino, R. M. (1991) Induction of specific mRNAs in cultured soybean cells during cytokinin or auxin starvation. *Plant Physiol*. **95**, 711–715.
66. Miller, J. D., Arteca, R. N., and Pell, E. J. (1999) Senescence-associated gene expression during ozone-induced leaf senescence in Arabidopsis. *Plant Physiol*. **120**, 1015–1024.
67. Gan, S. and Amasino, R. M. (1997) Making sense of senescence. Molecular genetic regulation and manipulation of leaf senescence. *Plant Physiol*. **113**, 313–319.
68. Weaver, L. M., Himelblau, E., and Amasino, R. M. (1997) Leaf senescence: gene expression and regulation, in *Genetic Engineering* (Setlow, J. K., ed.), Plenum, New York, Vol. 19, pp. 215–234.
69. Bleecker, A. B. (1998) The evolutionary basis of leaf senescence: method to the madness? *Curr. Opin. Plant Biol*. **1**, 73–78.
70. Mauk, C. S. and Nooden, L. D. (1992) Regulation of mineral redistribution in pod-bearing soybean explants. *J. Exp. Bot*. **43**, 1429–1440.
71. Drossopoulos, J. B., Bouranis, D. L., and Bairaktari, B. D. (1994) Patterns of mineral nutrient fluctuations in soybean leaves in relation to their position. *J. Plant Nutr*. **17**, 1017–1035.
72. Drossopoulos, J. B., Kouchaji, G. G., and Bouranis, D. L. (1996) Seasonal dynamics of mineral nutrients by walnut tree reproductive organs. *J. Plant Nutr*. **19**, 421–434.
73. Hocking, P. J. (1994) Dry-matter production, mineral nutrient concentrations, and nutrient distribution and redistribution in irrigated spring wheat. *J. Plant Nutr*. **17**, 1289–1308.

74. Mira, H., Martinez-Garcia, F., and Peñarrubia, L. (2001) Evidence for the plant-specific intercellular transport of the Arabidopsis copper chaperone CCH. *Plant J*. **25**, 1–9.
75. Oparka, K. J. and Turgeon, R. (1999) Sieve elements and companion cells—traffic control centers of the phloem. *Plant Cell* **11**, 739–750.
76. Thompson, G. A. and Schultz, A. (1999) Macromolecular trafficking in the phloem. *Trends Plant Sci*. **4**, 354–360.

34

The Role of Copper Ions in Regulating Methane Monooxygenases in Methanotrophs

J. Colin Murrell, Graham Stafford, and Ian R. McDonald

1. INTRODUCTION TO METHANOTROPHS

Methanotrophs are a unique group of Gram-negative methane-oxidizing bacteria that grow aerobically on methane as their sole carbon and energy source *(1)*. Some methanotrophs can also be grown on methanol; however, they are generally considered to be obligate in their requirement for one-carbon compounds and cannot be grown on other multicarbon substrates. Since 1970, they have received considerable attention from microbiologists and industrialists because they can be exploited in biotransformations and bioremediation processes *(2)*. For example, they can be used to convert propylene to propylene oxide and they can degrade the groundwater pollutant trichloroethylene. They are also used in the production of single-cell protein from methane, a relatively inexpensive feedstock. In addition to their commercial potential, methanotrophs also play a key role in the cycling of methane in the natural environment because they oxidize much of the methane produced in anaerobic sediments such as wetlands, peat bogs, and paddy fields, thereby mitigating release of methane to the atmosphere and reducing global warming. It is also now clear that some methanotrophs in aerobic soils can oxidize atmospheric concentrations of methane (e.g., 1–2 ppm), thereby further reducing global warming as a result of methane. Methane-oxidizing bacteria can be enriched for and isolated from a wide variety of environments, including freshwater, sediments, soils, seawater, peat bogs, tundra, paddy fields, and hot springs.

The methanotrophs form a physiologically and phylogenetically coherent group of bacteria. They can be divided into two groups based on a number of distinct morphological and physiological characteristics. Type I methanotrophs, which include the genera *Methylococcus, Methylomicrobium, Methylobacter, Methylosphaera, Methylocaldum*, and *Methylomonas*, are γ-proteobacteria that possess bundles of unusual intracytoplasmic membranes found throughout the cell. They are bacteria that possess predominantly 16-carbon fatty acids in their membranes and fix formaldehyde, a central intermediate in the methane oxidation pathway, into cell biomass using the ribulose monophosphate cycle. Type-II methanotrophs, which include the genera *Methylosinus*, *Methylocystis*, and *Methylocella* are α-proteobacteria that have their membranes arranged around the periphery of the cell, contain predominantly 18-carbon fatty acids in their membranes and fix carbon at the level of formaldehyde via the serine cycle.

From: Handbook of Copper Pharmacology and Toxicology
Edited by: E. J. Massaro © Humana Press Inc., Totowa, NJ

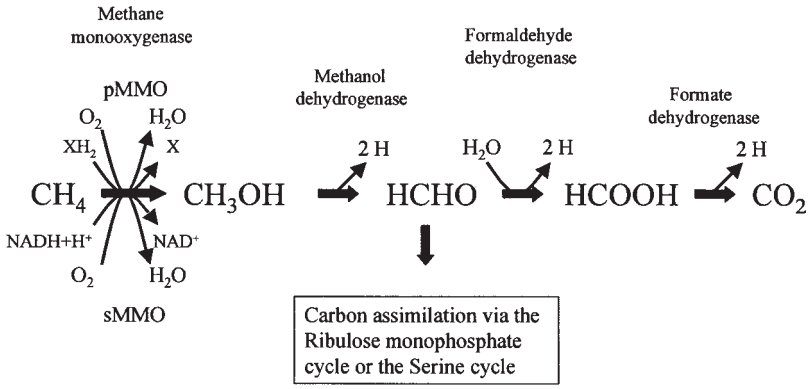

Fig. 1. Pathway of methane oxidation in methane-oxidizing bacteria. The two forms of methane monooxygenase, pMMO and sMMO, use different electron donors. NADH transfers electrons to the sMMO, but the electron donor for pMMO is not yet known. 2H represents reducing equivalents generated. Carbon is assimilated at the level of formaldehyde and proceeds via the ribulose monophosphate cycle (type-I methanotrophs) or serine cycle (type-II methanotrophs).

2. METHANE OXIDATION PATHWAY

The pathway for bacterial methane oxidation is shown in Fig. 1. Methane is oxidized by methanotrophs to CO_2 via the intermediates methanol, formaldehyde, and formate. Approximately 50% of the formaldehyde arising from the oxidation of methane is assimilated into cell carbon and the remainder is oxidized to CO_2 and lost from the cell *(3)*. The dissimilatory reactions, from formaldehyde to CO_2, generate reducing power for biosynthesis and for the initial methane-oxidation step. Recently, it has been shown that methanotrophs also have a tetrahydromethanopterin-based C1 metabolism that provides a further route for the dissimilation of formaldehyde. Therefore there are several routes for the removal of the toxic intermediate formaldehyde within the cell. The first and key enzyme in the methane-oxidation pathway is methane monooxygenase (MMO). There are two distinct types of MMO enzymes: a soluble, cytoplasmic enzyme complex (sMMO) and a membrane-bound particulate enzyme system (pMMO). The following sections will outline the properties of these two distinct enzyme systems.

3. BIOCHEMISTRY OF SOLUBLE METHANE MONOOXYGENASE

It was thought until recently that sMMO was only found in methanotrophs of the genera *Methylosinus*, *Methylocystis*, and *Methylococcus*. However, sMMO has subsequently been characterized in some *Methylomonas (4)* and *Methylomicrobium (5)* species. However, not all methanotrophs contain this enzyme and it is not expressed in, for example, M*ethylocaldum* and *Methylobacter* species. sMMO is only expressed when the copper-to-biomass ratio of the culture is low (i.e., under "low-copper" growth conditions). There is also evidence that copper can inhibit the activity of the sMMO reductase component *(6)*. The sMMO enzyme has an extremely broad substrate specificity, co-oxidizing a wide range of alkanes, alkenes, substituted aliphatic compounds, and even aromatic compounds such as naphthalene, making it an extremely attractive enzyme for biotransformation processes and bioremediation *(2)*.

The first sMMO enzymes to be examined in detail were those from the type-I methanotroph *Methylococcus capsulatus* (Bath) and the type-II methanotroph *Methylosinus trichosporium* OB3b *(7–9)*. They are probably now the most well characterized of these enzymes. sMMO is a member of a family of nonheme iron-containing enzyme complex consisting of three components: hydroxylase,

Table 1
Some Members of the Family of Nonheme Binuclear Iron-Containing Oxygenases

Oxygenase	*Microorganism*
Methane monooxygenase (sMMO)	*Methylosinus trichosporium*
Methane monooxygenase (sMMO)	*Methylococcus capsulatus*
Methane monooxygenase (sMMO)	*Methylocystis* sp. Strain M
Methane monooxygenase (sMMO)	*Methylomonas* sp. KSWIII
Alkene monooxygenase	*Nocardia corallina*
Isoprene monooxygenase	*Rhodococcus* sp. AD45
Alkene monooxygenase	*Xanthobacter* sp. Py2
Benzene monooxygenase	*Pseudomonas aeruginosa*
Toluene-*o*-xylene monooxygenase	*Pseudomonas stutzeri*
Toluene-3-monooxygenase	*Ralstonia pickettii*
Phenol hydroxylase	*Ralstonia* sp. E2
Catechol dioxygenase	*Pseudomonas putida*
Toluene-4-monooxygenase	*Pseudomonas mendocina*
Dimethyl sulfide oxygenase	*Acinetobacter* sp.
Alkane hydroxylase	*Pseudomonas oleovorans*

protein B, and protein C. The hydroxylase component (also known as protein A) has three subunits, α, β, and γ, of approx 60, 45, and 20 kDa, respectively, which are arranged in an $\alpha_2\beta_2\gamma_2$ configuration. The α-subunit contains a nonheme bis-μ-hydroxo-bridged binuclear iron center at the active site of the enzyme, where methanol is formed from methane and oxygen. The crystal structure of hydroxylase components from *M. capsulatus* (Bath) and *M. trichosporium* OB3b have been reported *(10,11)*. The di-iron center of the hydroxylase resides below the "floor" of two canyon regions formed by its α- and β-subunits. Like some other multicomponent oxygenases such as phenol hydroxylase and toluene monooxygenase, sMMO contains a small regulatory or coupling protein, protein B, the activity and stability of which appears to be controlled by proteolysis at its amino terminus *(12)*. The structures of protein B from *M. capsulatus* (Bath) and *M. trichosporium* OB3b have been determined by nuclear magnetic resonance (NMR), and provide insights into its interaction with the hydroxylase *(13,14)*. Protein B at low concentrations converts the hydroxylase from an oxidase to a hydroxylase and stabilizes intermediates needed for oxygen activation. Higher, saturating amounts of protein B dramatically increases the rates of formation of intermediates and improves catalysis of methane to methanol by sMMO. The third component, called protein C, is a 39-kDa NADH-dependent [2Fe–2S]- and FAD-containing reductase, which accepts electrons from $NADH_2$ and transfers them to the di-iron site of the hydroxylase. sMMO is a member of the family of nonheme binuclear iron proteins that includes hemerythrin, ribonucleotide reductase, and purple acid phosphatase and that, together with several other oxygenases, appears to form a subclass of C–H activating oxygenases. Some representatives of this family of di-iron proteins are given in Table 1.

4. MOLECULAR BIOLOGY AND GENETICS OF SMMO

The genes encoding sMMO have been cloned and sequenced from several methanotrophs, including *M. capsulatus* (Bath) (type I) and the type-II representatives *Methylocystis* strain M and *M. trichosporium* OB3b. sMMO genes are clustered on the chromosome of all methanotrophs studied to date. *mmoX*, *mmoY*, and *mmoZ* are the genes that encode the α, β, and γ subunits of the hydroxylase, respectively; *mmoB* and *mmoC* code for protein B and protein C, respectively. An open reading frame *orfY* with a coding capacity of 12 kDa separates *mmoY* and *mmoZ* in all methanotrophs exam-

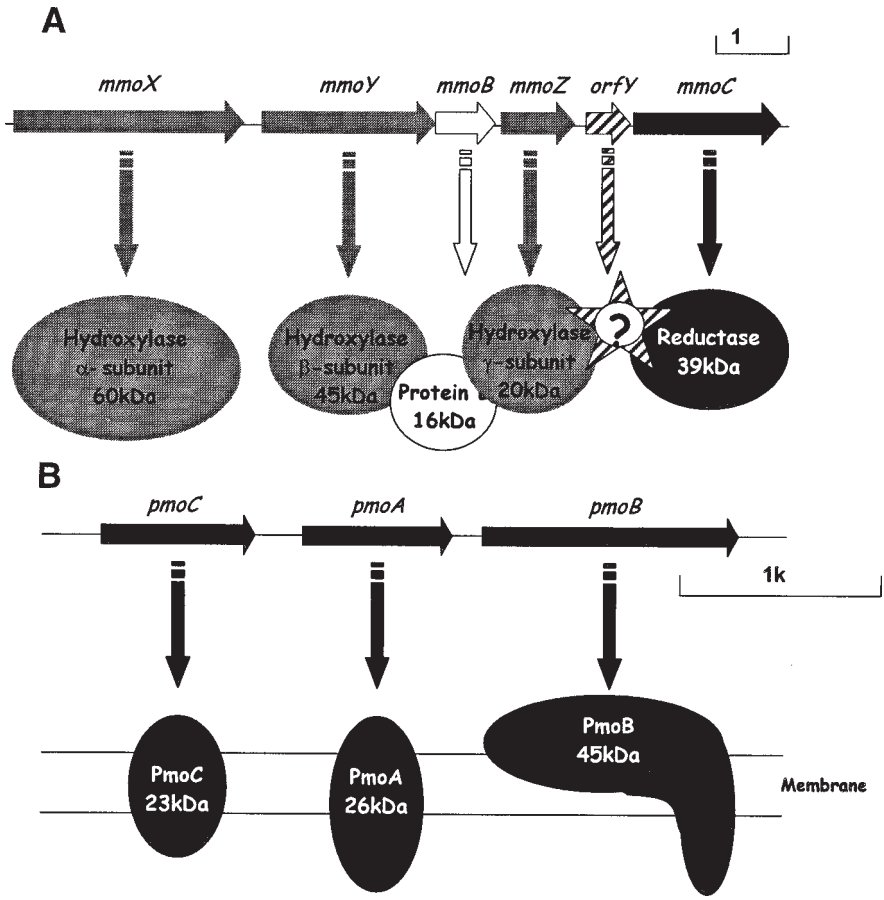

Fig. 2. Organization of the sMMO and pMMO gene clusters in methanotrophs.

ined to date *(15)* (Fig. 2). The exact function of this ORF is unknown and attempts to delete this gene from the cluster to examine effects on methane oxidation have proved unsuccessful. In addition, *orfY* has been expressed as a glutathione-*S*-transferase fusion polypeptide, purified by affinity chromatography and polypeptides raised to this polypeptide in order to probe cell-free extracts of *M. capsulatus* Bath grown under a variety of different growth conditions, including in high- and low-copper media (*see* Section 5.). However, no crossreactivity was observed with this antibody and polypeptides from *M. capsulatus* Bath and, therefore, the function of orfY (if any) remains to be elucidated (Murrell, et al., unpublished) (*see* Section 10.).

As might be expected for such a unique enzyme system, sMMO genes are highly conserved in all methanotrophs examined, with sequence identities of 55–95% and 47–96% being observed between the corresponding DNA and amino acid sequences, respectively. Upstream (5') of the sMMO gene cluster of *M. trichosporium* OB3b lie genes encoding the chaperones Hsp60 and Hsp10 (interestingly they are also found 3' of the corresponding sMMO gene cluster in *Methylococcus*) and it is tempting to speculate that they may be involved in assembly of the sMMO enzyme complex, although there is no proof for this yet. Directly upstream of the chaperone genes lies a homolog of the *acoR* gene from *Ralstonia eutrophus* (*16*; Murrell et al., unpublished). This is a member of the *nifA* family of transcriptional activators. These are absolutely required for activation of transcription from sigma 54-type promoters *(17)* and it is possible that this gene product is involved in positive regulation of the sMMO gene cluster.

5. HETEROLOGOUS AND HOMOLOGOUS EXPRESSION OF SMMO AND THE ROLE OF COPPER IONS

The genes *mmoB* and *mmoC,* encoding the coupling protein, protein B, and the reductase component (protein C), have been expressed in *Escherichia coli* using a T7 polymerase expression system to yield active protein B and protein C *(18)*. This has allowed site-directed mutagenesis experiments on protein B. Protein B in *Methylococcus* is subject to N-terminal cleavage between residues Met-12 and Gly-13, which results in the inactivation of this "effector/regulatory" polypeptide. Substitution of Gly-13 with Gln-13 by site-specific mutagenesis in a recombinant protein B dramatically stabilized the activity of this protein *(12)*. However, our attempts to express the hydroxylase genes in *E. coli* have proved unsuccessful *(18)*.

Active recombinant sMMO from *M. trichosporium* OB3b has been expressed in *Pseudomonas putida* F1, *Agrobacterium tumefaciens*, and *Rhizobium meliloti (19)*. However, when recombinant strains were assayed by following the conversion of propylene to propylene oxide (the standard MMO assay), very low sMMO activity was obtained (*19*; Murrell et al., unpublished). Expression experiments with *E. coli* demonstrated that recombinant *M. trichosporium* OB3b sMMO hydroxylase polypeptides were expressed, albeit at low levels; however, the hydroxylase was inactive, suggesting that it was not assembled correctly in *E. coli* (Lloyd and Murrell, unpublished).

We have demonstrated heterologous expression of sMMO from *M. trichosporium* OB3b using the methanotrophs *Methylomicrobium album* BG8 and *Methylocystis parvus* OBBP. Neither of these strains possesses sMMO. They were thought to be potentially better hosts for expression studies because they are more closely related to *M. trichosporium* and may contain the necessary proteins for the correct assembly and/or insertion of the di-iron center into the hydroxylase of sMMO. Expression was achieved by conjugating a broad-host-range plasmid containing the native promoter and sMMO gene cluster from *M. trichosporium* OB3b into *M. parvus* OBBP and *M. album* BG8. Strains OBBP and BG8, when harbouring this plasmid, expressed active sMMO. *Methylomicrobium album* BG8 constitutively expressed pMMO when grown at both high and low copper-to-biomass ratios; however, transcription of the recombinant sMMO genes was only observed under growth conditions of low copper-to-biomass ratios (*see* Section 8.). Therefore, either this heterologous host contains a regulatory system for sMMO or the regulatory polypeptide(s) necessary for sMMO expression is contained on this plasmid *(20)*.

In a recent breakthrough, homologous expression of the sMMO gene cluster from *M. trichosporium* OB3b has been achieved using an sMMO-minus mutant of this organism. Although it is very difficult to obtain mutants of methanotrophs by conventional mutagenesis procedures, marker-exchange mutagenesis has been used to generate a mutant *M. trichosporium* OB3b with a kanamycin cassette inserted into the chromosomal gene *mmoX (21)*. This mutant strain exhibits a sMMO-minus, pMMO-positive phenotype. Complementation of the sMMO-minus phenotype was achieved by conjugating into this mutant the broad-host-range recombinant plasmid pVK100Sc, which contains the native promoter and sMMO operon from *M. trichosporium* OB3b. The sMMO-minus mutant containing pVK100Sc displayed a sMMO-positive phenotype. In wild-type *M. trichosporium* OB3b, copper-ion concentrations greater than about 0.25 μ*M* repress expression of sMMO genes. The stable maintenance of pVK100Sc in the sMMO-minus mutant resulted in expression of sMMO in this recombinant strain at copper concentrations of 7.5 μ*M*. (Normally, in the wild-type organism, concentrations of around 0.25–1 μ*M* copper ions will repress the expression of sMMO.) However, active sMMO was only detected in cell-free extracts from this strain when grown with 7.5 μ*M* copper ions after the addition of an excess of purified sMMO reductase component, because the reductase is inhibited by copper ions in vitro. This expression of sMMO at elevated copper concentrations may have been the result of an increased copy number of sMMO genes carried on pVK100Sc. To date, this is the only report of expression of recombinant sMMO at specific activities that are at least as high as in the wild-type organism. Indeed, under low-copper growth conditions, the specific activity

of sMMO in the recombinant *M. trichosporium* was approximately three times higher than in the wild-type organism *(22)*. This now allows the possibility for carrying out site-directed mutagenesis and structure–function studies on the hydroxylase of sMMO and we are currently investigating the effects of mutating key residues in the α-subunit of the hydroxylase.

6. BIOCHEMISTRY OF PARTICULATE METHANE MONOOXYGENASE, A COPPER-CONTAINING MEMBRANE-ASSOCIATED ENZYME COMPLEX

Until recently, the dogma was that all methanotrophs possess the membrane-bound or particulate methane monooxygenase (pMMO). The only exception to this may be an acidophilic methanotroph, strain K, recently named *Methylocella*, isolated from northern wetland peat. This *Methylocella* species is a member of the α-subclass of Proteobacteria and most closely related to *Beijerinckia indica (23)*. This strain has been shown to contain sMMO similar to those of type-II methanotrophs but does not appear to contain pMMO (Dedysh and Semrau, personal communication.). The pMMO in methanotrophs is expressed under growth conditions where the copper-to-biomass ratio is high (greater than 1 μ*M*). Removing all trace amounts of copper ions from the growth medium results in poor growth of methanotrophs which do not possess sMMO, such as *M. album* BG8 or *M. parvus* OBBP.

Unlike sMMO, the membrane-bound enzyme pMMO has a relatively narrow substrate specificity, oxidizing alkanes and alkenes of up to five carbons in length. It does not oxidize longer alkanes or alkenes nor does it oxidize aromatic compounds such as naphthalene. However, it can still be useful for bioremediation *(24)*. Partial purification of pMMO was first achieved by solubilizing the enzyme from membranes of *M. capsulatus* Bath using dodecyl maltoside *(25)*. Subsequent studies by several groups have concentrated on the pMMO from this organism, although the pMMO from *M. trichosporium* has also been investigated *(26)* and its properties appear to be similar to those of the pMMO from *Methylococcus.*

The pMMO from *M. capsulatus* Bath consists of three subunits of approx 45, 27, and 23 kDa in a stoichiometry of 1:1:1. The 45- and 27-kDa subunits probably constitute the active site as they can be labeled by the suicide substrate acetylene *(27)*. Active pMMO contains 2 iron atoms and approx 15 copper atoms per mole, both of which are probably involved in catalysis. Duroquinol and $NADH_2$ can be used as artificial reductants for pMMO, but the physiological reductant is not known; potential candidates could include cytochromes-$b_{559/569}$, -*c*, or -c_{553}. The exact nature of the copper in pMMO is not known, but it has been suggested that trinuclear copper clusters are involved in catalysis *(26)*. In addition to copper ions associated with the active-site polypeptides of pMMO, small copper-binding compounds (CBC) of 1.218 and 0.779 kDa are also associated with pMMO. High concentrations of these CBCs can be isolated from the culture medium when *M. trichosporium* OB3b and *M. capsulatus* Bath are expressing pMMO under "copper-starved" growth conditions (i.e., when the majority of free-copper ions had been removed by the organism from the growth medium) *(27,29)*. These CBCs have a high affinity for copper ions and appear to bind a large proportion of the copper associated with the membrane fractions in cells expressing pMMO. Studies assessing the bioavailability of copper to *M. trichosporium* OB3b in different soil matrices suggest the CBCs may play a role in the environment *(30)*. Although their exact function is not known, they could be important for sequestering copper ions, stabilizing pMMO, or maintaining the appropriate redox state of the enzyme *(29)*. Interestingly, sMMO-constitutive mutant of *M. trichosporium* OB3b *(19,41)*, believed to be defective in copper uptake, constitutively produce but cannot reinternalize these CBCs *(29)*. However, experiments showed that functional copper-containing terminal oxidases still persist in these mutants, suggesting that this means of copper uptake is a pMMO-specific or secondary system *(29)*.

7. MOLECULAR BIOLOGY OF PMMO

In the chromosome of *M. capsulatus* Bath, there are two virtually identical copies of the genes encoding pMMO (*pmoCAB*) (13 bp changes over 3183 bp of *pmoCAB*) (Fig. 2). In addition, a third,

separate copy of *pmoC* has also been identified in the chromosome of *M. capsulatus*. Lidstrom and colleagues have constructed chromosomal insertion mutants in all seven *pmo* genes in *M. capsulatus* Bath. With the exception of the lone third copy of *pmoC,* for which no null mutants could be obtained, all other mutants grew on methane, indicating that both sets of genes were probably functionally equivalent. Copy 1 mutants showed about two-thirds of the wild-type methane oxidation activity, whereas copy 2 mutants had about one-third of the activity of the wild-type strain. No double null mutants defective in both copies of *pmoCAB* were obtained, which suggests that the cells require pMMO for normal growth *(31)*. Copy-specific analysis of *pmo* transcripts has revealed that copy 2 predominates at 5 μ*M* copper, but at higher concentrations (50 μ*M*), expression of copy 1 reaches the same levels as copy 2 *(32)*. Interestingly, low levels of *pmo*-specific transcripts were detected under all conditions tested.

This rather unusual type of gene duplication with *pmoCAB* has also been observed with the genes encoding the analogous enzyme ammonia monooxygenase (*amoCAB*) in ammonia-oxidizing bacteria *(33)*. Comparison of *pmo* and *amo* gene sequences suggests that pMMO and AMO could be evolutionarily related *(34,35)*. The *pmo* gene clusters have also been sequenced from the type-II methanotrophs *M. trichosporium* OB3b and *Methylocystis* sp. strain M *(36)*. These methanotrophs also have two copies of *pmoCAB* and there is a high degree of similarity (80–94%) at the derived amino-acid sequence level with pMMO polypeptides from different methanotrophs, again perhaps not surprising in bacteria that rely solely on methane as a carbon and energy source.

PmoC and PmoA are predicted to be highly hydrophobic and consist mainly of putative transmembrane-spanning helices, whereas PmoB only has two putative transmembrane regions. It has only been possible to clone these *pmo* gene clusters on overlapping DNA fragments because parts of these genes appear to be toxic to the *E. coli* host and, therefore, expression of pMMO in heterologous hosts may be difficult, if not impossible. We are currently expressing *pmoA* gene/glutathione-*S*-transferase fusions in *E. coli* in order to raise antibody to pMMO for immunogold-labeling experiments designed to localize pMMO on the membranes of methanotrophs (Murrell et al., unpublished).

8. REGULATION OF MMO EXPRESSION BY A UNIQUE "COPPER SWITCH"

In the type-I methanotroph *M. capsulatus* Bath and the type-II methanotroph *M. trichosporium* OB3b, which possess both pMMO and sMMO, a novel metabolic switch mediated by copper ions occurs. When cells are essentially starved for copper, and the copper-to-biomass ratio of the cell is low, sMMO is expressed. These experiments are best done in a chemostat culture where it is possible to exert fine control over the availability of nutrients and maintain steady-state growth conditions. Cells grown under excess copper (i.e., with a high copper-to-biomass ratio) express pMMO and there is no detectable sMMO expression *(37–39)*. It is interesting that no other metal ion effects this metabolic switch and this is exclusively copper-regulated gene expression.

Although it has been difficult to isolate good intact mRNA from methanotrophs, Northern blotting and primer extension analysis experiments with *M. capsulatus* Bath have shown that the six ORFs of the sMMO gene cluster are organized as an operon. Under low-copper growth conditions, three transcripts have been identified, one of which is probably the full-length 5.5-kb transcript encoding the entire sMMO operon. The only putative promoter identified was one with rather weak identity to *E. coli* –35, –10 consensus sequences located 5' of *mmoX* and the only primer extension product obtained was 37 bp upstream of the *mmoX* start codon. These transcripts were not detected 15 min after the addition of $CuSO_4$ to steady-state chemostat cultures of *M. capsulatus* Bath expressing sMMO *(38)*.

Similar experiments with *M. trichosporium* OB3b have also shown that transcription of the sMMO cluster is switched off within 10 min of the addition of 50 μ*M* $CuSO_4$. Three major sMMO transcripts were identified, corresponding to (a) *mmoX,* (b) *mmoY*, *mmoB*, and *mmoZ*, and (c) *mmoY*, *mmoB*, *mmoZ*, *orfY*, and *mmoC*. An unstable full-length transcript of 5.5 kb was also observed *(39)*. Primer extension analysis has shown that transcription of *mmoX* is directed from a σ^{54}-like promoter immediately upstream of its transcription start site. –12, –24 consensus sequences are also present in the

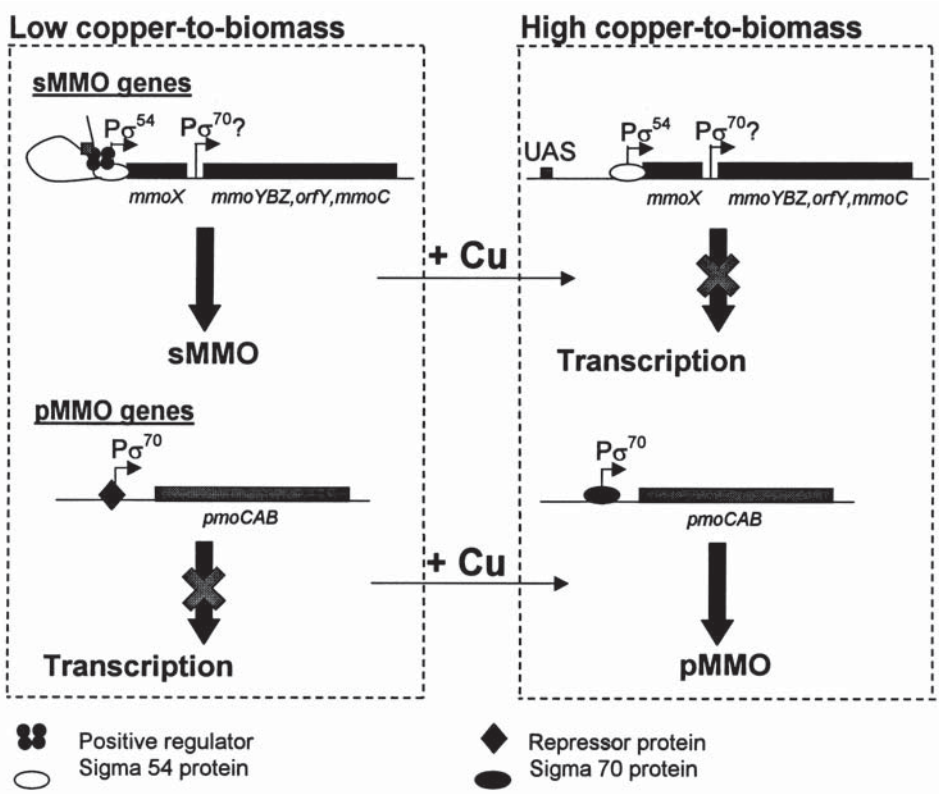

Fig. 3. Hypothetical model for regulation of sMMO and pMMO genes in *M. trichosporium* OB3b. In cells growing under low copper-to-biomass ratios, a positive regulator binds to an upstream activating sequence (UAS) and directly interacts with the sigma 54 protein bound at $P\sigma^{54}$. This directs the formation of an open complex and transcription of the sMMO genes occurs. At the same time, transcription of the pMMO genes from $P\sigma^{70}$ is repressed by an unknown repressor. On the addition of copper sMMO gene transcription becomes deactivated and pMMO gene transcription is derepressed.

same regions upstream of *mmoX* in the gene cluster of *Methylocystis* sp. strain M *(15)* and *Methylomonas* sp. KSWIII *(4)*. The –24 region and the distance between the conserved motifs match the consensus sequence exactly, and only the last base pair of the –12 region differs in two of the three gene sequences; however, this is the most variable position in the consensus sequence. Transcription is initiated approx 110 to 150 bp upstream of the start codon of *mmoX*, and there is no similarity among the three sequences in this region until the 5' end of the *mmoX* gene, except for the Shine–Dalgarno sequence immediately upstream of *mmoX*. A second transcript initiating between mmoX and mmoY has been observed for *M. trichosporium* OB3b, upstream of which putative –35, –10 sequences of σ^{70} promoters have been identified. Concomitant with the loss of sMMO activity and repression of sMMO transcription during the copper switch experiment was the appearance of *pmo* transcripts of 4.0 and 1.2 kb.

Similar transcript analysis has been carried out with *pmo* gene clusters from the type-II methanotrophs *M. trichosporium* OB3b and *Methylocystis* sp. strain M. In these methanotrophs, *pmoCAB* clusters are probably transcribed from a single transcriptional start site located 300 bp upstream of *pmoC*, initiating at a putative σ^{70} promoter that is negatively regulated under low-copper conditions, when these bacteria are expressing sMMO (*36*, Murrell et al., unpublished).

The exact mechanism for the reciprocal regulation of the sMMO and pMMO gene clusters by copper ions is not clear at present. Cu^{2+} could mediate transcription of sMMO gene promoters via a regulatory protein that binds Cu^{2+} and is then able to bind to operator regions on the promoter, thereby interfering with RNA polymerase binding or shielding promoter sequences (i.e., the classic repressor model). An alternative model is that sMMO gene expression is subject to positive control, with Cu^{2+} binding to and thereby inactivating an "activator protein." There is more evidence for the second model because of the presence of a σ^{54} promoter upstream of *mmoX* in three genera of methanotrophs that contain sMMO, because all known σ^{54} promoters rely on activator proteins for the formation of a transcription-competent open complex *(16,40)*. We are currently cloning the *rpoN* from *M. trichosporium* OB3b in order to mutate this gene and then examine the effects on sMMO expression in this methanotroph (Stafford and Murrell, unpublished).

Activation of *pmo* genes in *M. trichosporium* OB3b probably involves a copper-binding activator protein. However, an alternative hypothesis is that *pmo* genes could be subject to negative control in the absence of copper ions. A hypothetical model summarizing one possible mechanism for copper-dependent transcriptional regulation of MMO genes is outlined in Fig. 3.

9. FUTURE STUDIES

A considerable amount is now known about the physiology, biochemistry, and molecular biology of methane oxidation systems in bacteria. Recently, several new methanotrophs have been isolated from more extreme environments (e.g., acidic and alkaline environments, high pH, and also environments where there are extremes of temperature). It will be interesting to learn how the physiology of these new isolates allows them to grow under harsher conditions in these environments. A number of unanswered questions remain concerning the MMO systems in methanotrophs. For example, why are there duplicate copies of pMMO genes and are they differentially regulated in response to environmental changes? What is the exact nature of the pMMO in terms of its molecular structure and copper/iron centers? How is it assembled in the membranes of methanotrophs? How is the sMMO di-iron center inserted into the active-site pocket of this enzyme and what accessory genes and chaperonins are required for its assembly? Another area for further study is the regulation of expression of MMO enzymes by copper ions. At present, virtually nothing is known about the uptake of metal ions into methanotrophs and how they sequester and distribute metal ions. The transcriptional machinery that controls MMO expression is also not fully understood yet and it will be intriguing to learn the exact molecular mechanisms by which copper ions exert their effect. The genome sequence of *M. capsulatus* Bath is nearing completion and this information, coupled with proteomics and transcriptomics technology, should rapidly advance our current understanding of the unique copper switch in methanotrophs.

10. NOTE ADDED IN PROOF

Merkx and Lippard have recently expressed orfY as a fusion protein in *Escherichia coli* and their experiments show that this protein, designated MMOD, is a component of the sMMO system. They discuss the possible functions of MMOD in a recent paper (*see* ref. *42*).

REFERENCES

1. Hanson, R. S. and Hanson, T. E. (1996) Methanotrophic bacteria. *Microbiol. Rev.* **60**, 439–471.
2. Sullivan, J. P., Dickinson, D., and Chase, H. A. (1998) Methanotrophs, *Methylosinus trichosporium* OB3b, sMMO, and their application to bioremediation. *Crit. Rev. Microbiol.* **24**, 335–373.
3. Anthony, C. (1982) *The Biochemistry of Methylotrophs*, Academic, New York.
4. Shigematsu, T., Hanada, S., Eguchi, M., Kamagata, T., and Kurane, R. (1999) Soluble methane monooxygenase gene clusters from trichloroethylene-degrading *Methylomonas* sp. strains and detection of methanotrophs during in situ bioremediation. *Appl. Environ. Microbiol.* **65**, 5198–5206.
5. Fuse, H., Ohta, M., Takimura, O., Murakami, K., Inoue, H., Yamaoka, Y., et al. (1998) Oxidation of trichloroethylene and dimethyl sulfide by a marine *Methylomicrobium* strain containing soluble methane monooxygenase. *Biosci. Biotechnol. Biochem.* **62**, 1925–1931.

6. Green, J., Prior S. D., and Dalton H. (1985) Copper ions as inhibitors of protein C of soluble methane monooxygenase in *Methylococcus capsulatus* (Bath). *Eur. J. Biochem.* **153**, 137–144.
7. Lipscomb, J. D. (1994) Biochemistry of the soluble methane monooxygenase. *Ann. Rev. Microbiol.* **48**, 371–399.
8. Gassner, G. T. and Lippard, S. J. (1999) Component interactions in the soluble methane monooxygenase system from *Methylococcus capsulatus* (Bath). *Biochemistry* **38**, 12,768–12,785.
9. Lee, S. J. and Lipscomb, J. D. (1999) Oxygen activation catalyzed by methane monooxygenase hydroxylase component: Proton delivery during the O–O bond cleavage steps. *Biochemistry* **38**, 4423–4432.
10. Rosenzweig, A. C., Frederick C. A., Lippard S. J., and Nordlund P. (1993) Crystal structure of a bacterial non-haem iron hydroxylase that catalyses the biological oxidation of methane. *Nature* **366**, 537–543.
11. Elango, N., Radhakrishnan, R., Froland, W. A., Wallar, B. J., Earhart, C. A., Lipscomb, J. D., et al. (1997) Crystal structure of the hydroxylase component of methane monooxygenase from *Methylosinus trichosporium* OB3b. *Protein Sci.* **6**, 556–568.
12. Lloyd, J. S., Bhambra A., Murrell J. C., and Dalton, H. (1997) Inactivation of the regulatory protein B of soluble methane monooxygenase from *Methylococcus capsulatus* (Bath) by proteolysis can be overcome by a Gly to Gln modification. *Eur. J. Biochem.* **248**, 72–79.
13. Walters, K. J., Gassner, G. T., Lippard, J. S., and Wagner, G. (1999) Structure of the soluble methane monooxygenase regulatory protein B. *Proc. Natl. Acad. Sci. USA* **96**, 7877–7882.
14. Chang S. L., Wallar B. J., Lipscomb J. D., and Mayo K. H. (1999) Solution structure of component B from methane monooxygenase derived through heteronuclear NMR and molecular modelling. *Biochemistry 38*, 5799–5812.
15. McDonald, I. R., Uchiyama, H., Kambe, S., Yagi, O., and Murrell, J. C. (1997) The soluble methane monooxygenase gene cluster of the trichloroethylene-degrading methanotroph *Methylocystis* sp. strain. *Appl. Environ. Microbiol.* **63**, 1898–1904.
16. Krüger, N. and Steinbüchel, A. (1992) Identification of *acoR*, a regulatory gene for the expression of genes essential for acetoin catabolism in *Alcaligenes eutrophus* HI6. *J. Bacteriol.* **174**, 4391–4400.
17. Buck, M. Gallegos, M., Studholme, D. J., Guo, Y., and Gralla, J. D. (2000) The bacterial enhancer-dependent σ^{54} (σ^{N}) transcription factor. *J. Bacteriol.* **182**, 4129–4136.
18. West, C. A., Salmond, G. P. C., Dalton, H., and Murrell, J. C. (1992) Functional expression in *Escherichia coli* of proteins B and C from methane monooxygenase of *Methylococcus capsulatus* (Bath). *J. Gen. Microbiol.* **138**, 1301–1307.
19. Jahng, D., Kim, C. S., Hanson, R. S., and Wood, T. K. (1996) Optimization of trichloroethlyene degradation using soluble methane monooxygenase of *Methylosinus trichosporium* OB3b expressed in recombinant bacteria. *Biotechnol. Bioengineering* **51**, 349–359.
20. Lloyd, J. S., De Marco, P., Dalton, H., and Murrell, J. C. (1999) Heterologous expression of soluble methane monooxygenase genes in methanotrophs containing only particulate methane monooxygenase. *Arch. Microbiol.* **171**, 364–370.
21. Martin, H. and Murrell, J. C. (1995) Methane monooxygenase mutants of *Methylosinus trichosporium* OB3b constructed by marker-exchange mutagenesis. *FEMS Microbiol. Lett.* **127**, 243–248.
22. Lloyd, J. S., Finch, R., Dalton, H., and Murrell, J. C. (1999) Homologous expression of soluble methane monooxygenase genes in *Methylosinus trichosporium* OB3b. *Microbiology* **145**, 461–470.
23. Dedysh, S. N., Liesack, W., Khmelenina, V. N., Suzina, N. E., Trotsenko, Y. A., Semrau, J. D., et al. (2000) *Methylocella palustris* gen. nov., sp. nov., a new methane-oxidizing acidophilic bacterium from peat bogs, representing a novel subtype of serine-pathway methanotrophs. *Int. J. Syst. Evolut. Microbiol.* **50,** 955–969.
24. DiSpirito, A. A., Gulledge, J., Murrell, J. C., Shiemke, A. K., Lidstrom, M. E., Foster, A., et al. (1992) Trichloroethylene oxidation by the membrane-associated methane monooxygenase in type I, type II and type X methanotrophs. *Biodegradation* **2**, 151–164.
25. Smith, D. D. S and Dalton, H. (1989) Solubilisation of methane monooxygenase from *Methylococcus capsulatus* (Bath). Eur. J. Biochem. **182,** 667–671.
26. Takeguchi M., Miyakawa K., and Okura I. (1998) Purification and properties of particulate methane monooxygenase from *Methylosinus trichosporium* OB3b. *J. Mol. Catal. A: Chem.* **132**, 145–153.
27. Zahn, J. A. and DiSpirito, A. A. (1996) Membrane-associated methane monooxygenase from *Methylococcus capsulatus* (Bath). *J. Bacteriol.* **178**, 1018–1029.
28. Chan, S. I., Nguyen, H.-H. T., Shiemke, A. K., and Lidstrom, M. E. (1993) Biochemical and biophysical studies towards characterization of the membrane-associated methane monooxygenase, in *Microbial Growth on C1 Compounds* (Murrell, J. C. and Kelly, D. P., eds.), Intercept, Andover, UK, pp. 97–107.
29. DiSpitito, A. A., Zahn, J. A., Graham, D. W., Kim, H. J., Larive, C. K., Cox, C. D., and Taylor, A. (1998) Copper-binding compounds from *Methylosinus trichosporium* OB3b. *J. Bacteriol.* **180**, 3606–3613.
30. Morton J. D., Hayes, K. F., and Semrau, J. D. (2000) Bioavailability of chelated and soil-adsorbed copper to *Methylosinus trichosporium* OB3b. *Environ. Sci. Technol.* **34**, 4917–4922.
31. Stolyar, S., Costello, A. M., Peebles, T. L., and Lidstrom, M. E. (1999) Role of multiple gene copies in particulate methane monooxygenase activity in the methane-oxidizing bacterium *Methylococcus capsulatus* Bath. *Microbiology* **145**, 1235–1244.
32. Stolyar, S., Franke, M., and Lidstrom, M. E. (2001) Expression of individual copies of *Methylococcus capsulatus* Bath particulate methane monooxygenase genes. *J. Bacteriol.* **183**, 1810–1812.
33. Sayavedra-Soto, L. A. Hommes, N. G., Alzerreca, J. J., Arp, D. J., Norton, J. M., and Klotz M. G. (1996) Induction of

ammonia monooxygenase and hydroxylamine oxidoreductase mRNAs by ammonium in *Nitrosomonas europaea*. *Mol. Microbiol*. **20**, 541–548.
34. Holmes, A. J., Costello, A., Lidstrom, M. E., and Murrell, J. C. (1995) Evidence that particulate methane monooxygenase and ammonia monooxygenase may be evolutionarily related. *FEMS Microbiol. Lett.* **132**, 203–208.
35. Klotz, M. G. and Norton, J. M. (1998) Multiple copies of ammonia monooxygenase (*amo*) operons have evolved under biased AT/GC mutational pressure in ammonia-oxidizing autotrophic bacteria. *FEMS Microbiol. Lett.* **168**, 303–311.
36. Gilbert, B., McDonald, I. R., Finch, R., Stafford, G. P., Nielsen, A. K., and Murrell, J. C. (2000) Molecular analysis of the *pmo* (particulate methane monooxygenase) operons from two type II methanotrophs. *Appl. Environ. Microbiol*. **66**, 966–975.
37. Stanley, S. H., Prior, S. D., Leak, D. J., and Dalton, H. (1983) Copper stress underlies the fundamental change in intracellular location of methane monooxygenase in methane-oxidising organisms: studies in batch and continuous cultures. *Biotech. Lett.* **5**, 487–492.
38. Nielsen, A. K., Gerdes, K., Degn, H., and Murrell, J. C. (1996) Regulation of bacterial methane oxidation: transcription of the soluble methane monooxygenase operon of *Methylococcus capsulatus* (Bath) is repressed by copper ions. *Microbiology* **142**, 1289–1296.
39. Nielsen, A. K., Gerdes, K., and Murrell, J. C. (1997) Copper-dependent reciprocal transcriptional regulation of methane monooxygenase genes in *Methylococcus capsulatus* and *Methylosinus trichosporium*. *Mol. Microbiol*. **25**, 399–409.
40. Wösten, M. M. S. M. (1998) Eubacterial sigma-factors. *FEMS Microbiol. Rev.* **22**, 127–150.
41. Fitch, M.W., Graham, D.W., Arnold, R.G., Agarwal, S.K., Phelps, P., Speitel, G. E. Jr and Georgiou, G.(1993) Phenotypic characterization of copper-resistant mutants of *Methylosinus trichosporium* OB3b. *Appl. Environ. Microbiol.*, **59**, 2771-2776.
42. Merkx, M. and Lippard, S. J. (2002) Why OrfY. Characterization of MMOD, a long overlooked component of the soluble methane monooxygenase from Methylococcus capsulatus (Bath). *J. Biol. Chem.* **277**, 5858–5865.

35

Regulatory Responses to Copper Ions in Fungi

Simon Labbé, Jude Beaudoin, Daniel R. Bellemare, and Benoit Pelletier

1. INTRODUCTION

Because of their property to promptly gain and lose electrons, copper (Cu) ions serve as catalytic centers of numerous proteins involved in a variety of enzymatic processes *(1,2)*. Despite this essential role, Cu ions, when present in excess, can have detrimental effects because of their proclivity to engage in chemical reactions or by competing with other metal ions for enzyme-active sites *(3–5)*. Therefore, specialized pathways have evolved for the signaling, transport, trafficking, and sequestration of Cu ions within cells to keep the delicate balance between essential and toxic levels *(6–9)*. The importance of maintaining an exquisite Cu equilibrium is underscored by the existence of human inherited disorders of Cu homeostasis (Menkes and Wilson's diseases) and numerous forms of anemia linked to Cu deficiency (e.g., microcytic hypochromic anemia) *(10,11)*. In Menkes disease, the export of Cu in extrahepatic tissues is defective, thereby rendering many Cu-dependent enzymes nonfunctional, which results in deleterious clinical manifestations *(12,13)*. In Wilson's disease, Cu is not incorporated into key proteins in the liver, and the transport of Cu from the liver to the bile or alternative route is defective, thereby causing severe hepatotoxicity as well as brain and kidney toxicity *(12)*. As to anemia, it has been shown that iron (Fe) mobilization relies on the high-affinity Cu-uptake system because of the involvement of essential Cu-containing protein(s) in Fe uptake *(10)*. Over the past few years, positional cloning and molecular genetics have culminated in the isolation of cDNAs corresponding to Menkes (*MNK*) *(14–16)* and Wilson's (*WND*) *(17,18)* disease genes. The mammalian gene involved in the development of microcytic hypochromic anemia (*Heph*) has also been found *(19)*. These findings have given molecular biologists the information needed to identify yeast orthologs to these human disease-related proteins. Studies of yeast genes have uncovered additional yet unidentified loci encoding new components that function in Cu transport and other transition-metal-ion homeostatic pathways *(6,8,9,20,21)*. In this chapter, we focus on recent advances that have been made with respect to molecular mechanisms of Cu transport, Cu detoxification, and regulatory response to Cu ions using the best features of two yeasts, *Saccharomyces cerevisiae* and *Schizosaccharomyces pombe*.*

*In this chapter, we used the nomenclature for *Saccharomyces cerevisiae* and *Schizosaccharomyces pombe* genes and proteins. *S. cerevisiae* wild-type genes are capitalized and italicized (e.g., *CTR1*). *S. pombe* wild-type genes are in regular text, italicized, with a superscripted "+" at the end (e.g., *cuf1*$^{+}$). *S. cerevisiae* and *S. pombe* protein nomenclature is the same and is indicated with a capital letter at the beginning followed by regular letters (e.g., Ctr1, Cuf1).

From: Handbook of Copper Pharmacology and Toxicology
Edited by: E. J. Massaro © Humana Press Inc., Totowa, NJ

2. BUDDING YEAST AS A MODEL ORGANISM FOR EUKARYOTIC CELLS

2.1. Copper Acquisition

2.1.1. High-Affinity Cu-Ion Transport

Studies in bakers' yeast *Saccharomyces cerevisiae* have led to the identification of many components of the high-affinity Cu-transport pathway (Fig. 1). When grown under Cu-starvation conditions, following reduction of Cu^{2+} to Cu^{1+} by Fre plasma membrane Cu^{2+}/Fe^{3+} ion reductases *(22–27)*, Cu ions are transported into yeast cells by two separate high-affinity plasma membrane-transport proteins, Ctr1 *(28,29)* and Ctr3 *(30,31)*. The first high-affinity Cu transporter, denoted Ctr1, was identified using a genetic approach to identify proteins involved in Fe acquisition *(29,32)*. This finding that Fe mobilization relies on the high-affinity Cu-transport system is explained largely by the involvement of a Cu-containing oxidase, Fet3, in Fe uptake *(20,33)*. Therefore, *ctr1Δ* mutants (in which the *CTR3* gene is silent) are defective in the transport of both Cu and Fe, whereas *fet3Δ* mutants are defective only in Fe acquisition. Furthermore, *ctr1Δ* mutants display other phenotypes linked to Cu deficiency, including the inability to grow on respiratory carbon sources (owing to the lack of Cu incorporation into cytochrome-*c* oxidase, which is essential for respiration), impaired superoxide dismutase (SOD) activity (owing to lack of Cu incorporation into Cu,Zn-Sod1), and poor cellular growth under conditions of Cu scarcity *(28,29)*. Importantly, all of these phenotypes can be corrected by the addition of exogenous Cu ranging from 40 to 100 μ*M*, which largely exceeds the K_m of the high-affinity uptake system *(28)*. The *CTR1* open reading frame (ORF) encodes a protein of 406 amino acids harboring 2 (possibly three) potential membrane-spanning regions *(29)*. Its action in Cu uptake at the plasma membrane is highly specific for Cu over other metal ions with an apparent K_m of 1–4 μ*M* Cu *(29)*. The amino terminus of Ctr1 harbors eight copies of the sequence Met-X_2-Met-X-Met, a putative extracellular Cu-binding motif found also in other proteins that participate in Cu transport *(7,8,34,35)*. Furthermore, at the cell surface, the Ctr1 protein is modified, being glycosylated *(28)*. Moreover, the active form of Ctr1 assembles as dimeric or multimeric complexes with itself *(28)*. In response to Cu repletion, Ctr1 is regulated at multiple levels. In addition to the regulation at the level of gene transcription (*see* Section 2.1.4.), at least two other modes of regulation are known to occur at the protein level for Ctr1. When cells are exposed to Cu concentrations between 0.1 to 1.0 μ*M*, the Ctr1 protein undergoes endocytosis *(36)*. In response to Cu concentrations of 10 μ*M* or more, the Ctr1 is specifically degraded *(36)*. This proteolysis is independent of that internalization by endocytosis of Ctr1. In fact, cells defective in Ctr1 endocytosis because of mutations in the general endocytosis system (*end3* or *end4*) or in general vacuolar hydrolysis (*pep4*) are still able to trigger Ctr1 degradation in response to elevated (>10 μ*M*) Cu concentrations *(36)*. Relatively little is understood about the molecular details of how Ctr1 undergoes two forms of posttranslational regulation as a function of changing environmental Cu levels.

Because of its ability to suppress all phenotypes linked with an inactivated *CTR1* gene, the *CTR3*-encoded high-affinity Cu-transport protein was isolated as a dominant extragenic suppressor *(30)*. In several commonly used *S. cerevisiae* laboratory strains, *CTR3* gene expression is inactivated by the presence of a Ty2 transposable element *(30)*. When present, the transposon lies between the TATA box and the start sites for transcription, extinguishing *CTR3* gene expression. Interestingly, *S. cerevisiae* strains that express both transporters (Ctr1 and Ctr3) exhibit a clear growth advantage under Cu-starvation conditions as compared to strains expressing only either *CTR1* or *CTR3 (30)*. Although the Ctr3 protein supports high-affinity Cu transport in a manner similar to Ctr1, its primary structure is distinct. Ctr3 is a 241-amino-acid cysteine-rich integral plasma membrane protein. Furthermore, Ctr3 is predicted to possess three transmembrane domains, an extracellular hydrophilic amino-terminus, and a cytosolic tail *(31)*. Among the 11 cysteine residues found throughout the Cu-transport protein, Cys-16 within the amino-terminal portion, Cys-48 and Cys-51 within the first trans-

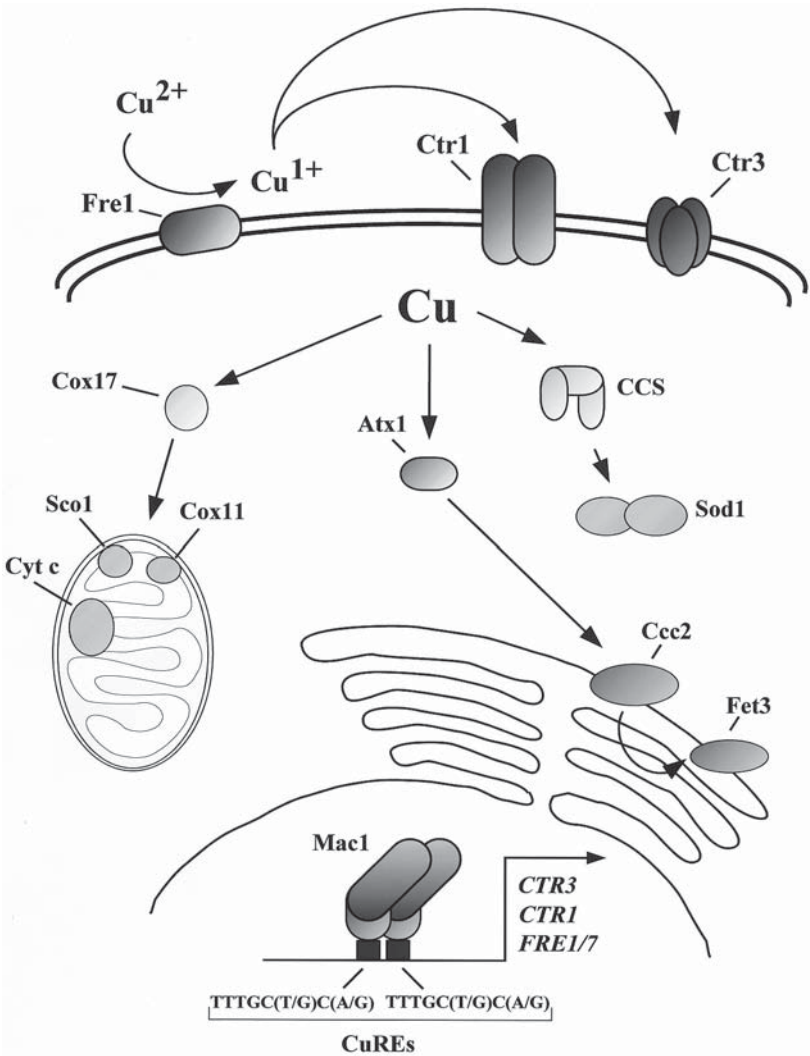

Fig. 1. Identified components for Cu transport in *S. cerevisiae*. When cells are grown during Cu scarcity, cell surface Fe^{3+}/Cu^{2+} reductases (e.g. Fre1) reduce Cu^{2+} to Cu^{1+} prior to uptake. Once reduced, Cu^{1+} is transported by two high-affinity Cu permeases, Ctr1 (existing as a dimer or multimer at the plasma membrane) and Ctr3 (existing as a trimer at the plasma membrane). Within the cell, Cu is mobilized by specific chaperones. Atx1 carries Cu to Ccc2 in a post-Golgi vesicle in which Cu is docked to Fet3. CCS delivers Cu to cytosolic Cu, Zn Sod1. Cox17 shuttles Cu to cytochrome-*c* oxidase, with the assistance of Sco1 and Cox11. In response to Cu-starvation conditions, the nuclear transcription factor Mac1 binds as a dimer to and activates the expression of high-affinity Cu-uptake genes including *CTR1*, *CTR3*, and *FRE1/7*, whereas in response to Cu-replete conditions, Mac1 is rapidly released from the Cu-response elements (CuREs).

membrane domain, and Cys-199 found into the third transmembrane domain are necessary for Cu acquisition *(31)*. Furthermore, these cysteine residues, except Cys-199, are also critical for proper assembly of three Ctr3 molecules as trimer, which is the competent form of the transporter at the plasma membrane *(31)*. Importantly, the carboxy-terminal region of Ctr3 from residues 40–233 represents a module, which is highly conserved among all eukaryotic cell-surface Cu transporters that have been identified so far, except for the *S. cerevisiae* Ctr1 *(8,31,37)*. Although both *CTR1* and *CTR3* genes are regulated at transcriptional level by cellular Cu status (*see* Section 2.1.4.), Ctr3,

unlike Ctr1, is not regulated at the protein level either by endocytosis or degradation in the presence of high Cu concentrations *(31)*. Currently, there is no information suggesting a functional interdependence between the two high-affinity Cu transporters, Ctr1 and Ctr3, at the cell surface.

2.1.2. Cu Chaperones

Once inside the cell, free-Cu ions are virtually undetectable *(38)*. Under Cu-limiting conditions, Cu ions are transiently associated to small Cu-binding proteins, denoted Cu chaperones, which possess the ability to distribute the transition metal as a cofactor to intracellular destinations *(39–42)*. To date, three distinct Cu chaperones Atx1 *(43–45)*, CCS (also termed Lys7) *(46)*, and Cox17 *(47,48)* have been identified and found to be involved in different Cu delivery pathways. Atx1 carries Cu from the cytosol to the secretory pathway by specifically docking with Ccc2 *(45,49–51)*, which is the MNK/WND disease yeast homologue protein *(52)*. Subsequently, Ccc2 donates the bound Cu received from Atx1 to the Cu-dependent ferroxidase Fet3 *(33)*. Once Cu loaded, Fet3 initiates translocation in concert with another component, called Ftr1, which is an Fe permease *(53)*. This Fet3/Ftr1 complex proceeds through the secretory system to the plasma membrane. At the cell surface, Fet3 can convert Fe^{2+} to Fe^{3+} in a Cu-dependent oxidation reaction and then allows the transport of these Fe^{3+} ions across the membrane with the combined action of Ftr1 *(53)*. Therefore, Fe mobilization relies on the high-affinity Cu-uptake system. Although preliminary results in mammalian cells support this intimate connection between both high-affinity Fe and Cu transport systems, the molecular mechanisms are poorly characterized *(54,55)*. Interestingly, it has been shown that *GEF1 (56)*, encoding a putative voltage-regulated chloride channel, is required for Cu loading of Fet3 by Ccc2 within the secretory apparatus *(57,58)*. Gef1 would provide a counterbalancing charge effect that facilitates Cu transfer to the trans-Golgi network. Interestingly, other proteins were isolated from different organisms, including human (HAH1 or ATOX1) *(43,59)*, mouse (mAtx1) *(60)*, rat (rAtox1) *(61)*, dog (Atox1) *(62)*, sheep (SAH) *(63)*, *Caenorhabditis elegans* (Cuc1) *(64)*, and *Arabidopsis thaliana* (CCH) *(65,66)* that would possess orthologous function as the *S. cerevisiae* Atx1 chaperone. Studies have provided insights into the mechanisms by which Atx1 carries Cu to Ccc2 *(50,51,67)*. Structural characterization has shown that the metal-binding motif, MXCXXC, can bind one Cu atom. This motif forms a secondary structure, called "open-faced β-sandwich," which prevents facile release of Cu yet allowing Cu exchange with a specific protein *(38,41,68)*. Based on in vitro and two-hybrid results demonstrating a direct interaction between Atx1 and its partner Ccc2, it has been proposed that Cu transfer occurs through the formation and decay of a series of two- and three- coordinate Cu ligand bonds in which Cys and ionized amino acids are involved *(40,41,51)*. Although it is still unknown how the Atx1 metallochaperone acquires its Cu, it is plausible that Atx1 interacts with components of the high-affinity Cu-uptake machinery at the cell surface.

Another Cu chaperone, CCS, is able to directly activate cytosolic apo-Sod1 under Cu-limiting conditions, which is consistent with the notion that CCS delivers Cu to Sod1 in the metal-transfer process *(69,70)*. CCS possesses three distinct domains, whereas only a single domain forms the Atx1 and Cox17 Cu chaperones. Although Domain I displays a strong similarity to Atx1, its substitution with Atx1 does not confer the ability to the carboxyl-terminal CCS-Domain II/III region to deliver Cu to Sod1 with an overall efficiency similar to that observed for the full-length CCS *(70)*. It has been proposed that the first domain would serve during the process of Cu acquisition from a yet to be identified donor *(41)*. Furthermore, this domain would be implicated to hold Cu with Domain III through cysteine–thiolate bonds. Domain II bears a striking percentage of homology to its target (Sod1). Furthermore, it has been shown that this domain interacts with Sod1 to form either a heterodimeric or heterotetrameric complex *(71,72)*. This complex formation between the two proteins is necessary to allow Cu to be released from CCS and inserted into Sod1 *(73,74)*. The carboxyl-terminal 30 amino acids of CCS (Domain III) is critical for activating the Sod1 enzyme because of its essential role in the release of Cu from the chaperone *(70,75)*. Interestingly, human and mouse homologs of the yeast CCS chaperone have been identified *(46,76)*. Importantly, it has been demonstrated that mice lacking the *CCS* gene show dramatic reductions in scavenging toxic reactive oxygen

species, thereby corroborating with the notion that CCS is required for intracellular Cu delivering to Sod1 enzyme for making it active *(76)*.

The Cox17 Cu chaperone shuttles between the cytosol and the intermitochondrial membrane space, where it provides Cu to cytochrome-*c* oxidase, which is the multisubunit terminal enzyme in the respiration chain *(47,48)*. Like the yeast Atx1 and CCS Cu chaperones for which homologs have been identified in humans, a human homolog of Cox17 has been found by functional complementation of a yeast *cox17Δ* null mutant *(77,78)*. In yeast, genetic evidence suggests that at least two intermediates, Cox11 and Sco1, are also required at the assembly site for the insertion of Cu from Cox17 into the cytochrome-*c* oxidase *(79–81)*. Although Cox17 is a very small protein of similar size to Atx1, they share no homology at the amino-acid sequence level. Of the seven cysteine residues found in Cox17, only mutations in three of these residues affect the ability of the protein to bind Cu *(82)*. Indeed, these three cysteine residues (Cys_{23}-Cys_{24}-X-Cys_{26}) form a Cu-binding motif and have been shown to coordinate three Cu ions with another residue that has yet to be identified *(82)*. Interestingly, the Cu clusters of Cox17 are similar to those in the Cu metalloregulatory transcription factor Ace1 and the MT Cup1 in being pH stable and luminescent *(83)*. Although Cu-metallated Cox17 exhibits reminiscent biophysical properties to CuAce1 and CuCup1, the susceptibility of its Cu clusters to ligand-exchange reactions is much higher. Cox17 is detected as a dimer in the cytosol, whereas the protein is found as a tetramer when isolated from mitochondria *(83)*. This differential oligomeric assembly of Cox17 may play a role in its ability to translocate from the cytosol to the mitochondrial intermembrane space. Clearly, the mechanism by which a chaperone delivers Cu ions appears to be associated, in part, with the nature of the target protein and its intracellular location.

2.1.3. Low-Affinity Cu-Ion Uptake

Under conditions of Cu sufficiency, a low-affinity Cu uptake system is active *(29,84)*. Although this latter system exhibits an apparent K_m of 30–40 μ*M* Cu, the specific components involved in such activity remain to be clarified *(6)*. Fet4 *(85,86)*, Ctr2 *(87)*, and Smf *(88,89)* proteins have been reported to contribute in Cu-ion transport with low-affinity across the plasma membrane. Although these transmembrane proteins may play a role in Cu uptake, the loci encoding these proteins are not expressed according to Cu need *(90)*. Recently, the Fet4 protein has been studied with more details with respect to Cu transport *(91)*. In fact, low-affinity Fe-uptake mediated by Fet4 is competitively inhibited by Cu ions, suggesting that Cu may represent an additional substrate for this low-affinity Fe transporter. Moreover, the level of Cu transport in *ctr1Δ TY2::ctr3 fet4Δ* cells is severely reduced *(91)*. Metal-ion-uptake kinetic measurements revealed that Fet4 supports Cu uptake with an apparent K_m value of 35 μ*M* Cu *(91)*. Furthermore, the Cu taken into the cell by Fet4 requires Cu reduction by the cell-surface metalloreductases Fre1 and Fre2, which are multimembrane-spanning NADPH- and FAD-binding proteins able to solubilize Fe^{3+} and Cu^{2+} to ferrous iron (Fe^{2+}) and cuprous copper (Cu^{1+}), respectively *(26)*. It is thought that such reduction prior to uptake renders ferric and cupric ions from the environment more bioavailable for the transporters at the cell surface *(92)*. Although Fet4 appears to transport Cu with low affinity, one caveat to these results is the fact that Fet4 was overexpressed for most of the experiments performed; thus, the involvement of the endogenous protein in Cu uptake may be different. The *CTR2* gene from *S. cerevisiae* was isolated based on homology to a putative plant Cu transporter gene, denoted *COPT1 (87)*. Sequence comparison analyses revealed that Ctr2 shares sequence similarities to other cell-surface Cu transporters such as Ctr1 and Ctr3 from *S. cerevisiae (8)*, Ctr4 and Ctr5 from *S. pombe (37,93)*, and hCtr1 from human *(94–97)*, thereby suggesting a role for Ctr2 in Cu acquisition. Moreover, overexpression of Ctr2 in yeast is linked with an increased sensitivity to Cu toxicity. Conversely, an *S. cerevisiae ctr2Δ* strain is more resistant when Cu is in excess of physiological requirements *(87)*. Whether Ctr2 is involved in Cu accumulation is still unclear. As structurally related Cu transporters do exist from different organisms, the elucidation of the Ctr2 function should provide additional information on how Cu is mobilized. Recently, based on indirect observations, Smf proteins have been considered to participate in Cu uptake *(88)*. In *S.*

cerevisiae, these proteins that belong to the Nramp transporter family is composed of three members: Smf1, Smf2, and Smf3 *(98)*. When cells are starved for manganese, Smf1 is localized at the plasma membrane, whereas Smf2 is detected to intracellular vesicles. Under manganese-replete conditions, both proteins move to the vacuole *(98)*. Importantly, Cu ions, unlike manganese ions, are unable to trigger such trafficking of Smf1 and Smf2. Interestingly, Smf3 is found to the vacuole membrane *(98)*. Furthermore, only Fe can negatively regulate Smf3 at the protein level, whereas no other metal ions including manganese, copper, and zinc are capable of such regulation. Although Smf proteins can potentially recognize numerous metal ions, their biological specificity may come from their regulation, which would minimize their contribution in Cu transport.

2.1.4. Transcriptional Regulation of the High-Affinity Cu-Ion-Transport Genes

A hallmark of the genes-encoding components of the high-affinity Cu-uptake machinery including *CTR1*, *CTR3*, and *FRE1/7* is the fact that they are transcriptionally expressed according to Cu need *(8)*. The transcription of *CTR1*, *CTR3*, and *FRE1/7* is induced under Cu-starvation conditions, whereas inactivation of the expression of these genes occurs under Cu-replete conditions *(27,99,100)*. This regulation is mediated by cis-acting promoter elements, denoted CuREs (Cu-response elements) with the consensus sequence 5'-TTTGC(T/G)C(A/G)-3' *(27,99)*. The presence of two copies of CuRE in each of the *CTR1*, *CTR3*, and *FRE1/7* promoters is necessary for Cu repression and Cu-starvation activation of gene expression *(27,99,101)*. The CuREs are arranged as either inverted or direct repeats *(27,99)*. Furthermore, the center-to-center distances between CuREs observed for each promoter predict that they lie on opposite faces of the DNA *(99)*. The transcription factor for regulating the expression of genes-encoding components involved in Cu transport through the CuREs is Mac1 *(102)*. The *MAC1* gene was initially discovered as a dominant allele, called $MAC1^{up1}$, that fosters robust expression of the high-affinity Cu-uptake genes even in the presence of elevated Cu concentrations *(99,101,102)*. As would be expected, *mac1Δ* cells display a number of phenotypes linked to defective Cu transport, including poor growth on low Cu medium, inability to grow on nonfermentable carbon sources, and a deficient Cu,Zn-Sod1 activity with a concomitant sensitivity to redox cycling drugs, which can all be biochemically ascribed to Cu insufficiency because exogenous Cu restores the normal phenotype *(100,102)*. Mac1 is a 417-amino-acid protein harboring several basic residues within its amino-terminal region (1–201), whereas its carboxyl-terminal region encompassing amino acids 202–417 exhibits more overall acidic residues *(103–105)*. Precisely, the Mac1 amino-terminal 159 residues constitute the DNA-binding domain of the protein *(106)*. Within this domain, the first 40 residues of Mac1 exhibit a strong homology to the minor groove DNA-binding domain found in the Ace1 and Amt1 Cu metalloregulatory transcription factors that activate *MT* gene expression, but very little homology outside of this region *(102,107,108)*. The carboxyl-terminal region of Mac1 harbors two Cys-rich repeats, denoted REP-I (also identified as C1) and REP-II (also identified as C2) *(103,109)*. The REP-I motif, Cys_{264}-X-Cys_{266}-X_4-Cys_{271}-X-Cys_{273}-X_2-Cys_{276}-X_2-His_{279}, is essential for Cu-sensing because substitutions created in either all or individual conserved Cys and His exhibit elevated and unregulated Cu transporter gene expression *(100,109,110)*. Regarding the REP-II motif, Cys_{322}-X-Cys_{324}-X_4-Cys_{329}-X-Cys_{331}-X_2-Cys_{334}-X_2-His_{337}, its partial or complete disruption alters Mac1 ability of trans-activating target gene expression *(103,109,110)*. Based on immunofluorescence studies, the Mac1 protein harbors two potential nuclear localization signals *(105)*. The first one resides in a region between residues 70 and 287, and the second one was found in the carboxyl-terminal 128 amino acids of Mac1, which contain the REP-II motif. Currently, it is unclear how these nuclear localization signals function. Under low-Cu conditions, it is known that Mac1 binds to CuREs as a dimer *(101,105)* by making contacts in both major [with 5'-GC(T/C)C(A/G)-3' sequence] and minor (with 5'-TTT-3' sequence) grooves *(104)*. Interestingly, it has been shown that Cu^{1+} ions can bind directly to Mac1 *(111)*. Under elevated Cu concentrations, Mac1 is released from the CuREs in vivo *(99)* and it is suggested that the presence of Cu ions trigger intramolecular conformational changes to inactivate the Mac1 transactivation domain *(105,111)*. Furthermore, at Cu concentrations

above 10 μ*M*, the Mac1 protein is degraded, therefore ensuring a complete deactivation of the Cu-transport machinery under conditions of Cu excess *(109)*.

2.2 Copper Detoxification

Yeast genes-encoding proteins that function to prevent the accumulation of Cu to toxic levels into cells are transcriptionally regulated by Cu in the opposite direction from the high-affinity Cu-uptake genes. The transcription of *CUP1*- and *CRS5*-encoded MTs and *SOD1*-encoded Cu,Zn-Sod1 are induced in response to Cu excess (>10 μ*M*) *(90,112,113)*. MTs are known to counteract metal cytotoxicity by sequestering avidly the excess of Cu *(7)*. Regarding Sod1, the enzyme prevents Cu-mediated damages by competing for the surplus of metal ions, thereby acting as a buffer for Cu *(114)*. Increased synthesis of these three proteins in response to Cu are controlled at the transcriptional level by the Ace1 Cu metalloregulatory transcription factor (MRTF) (also denoted Cup2) *(115–117)*. Furthermore, the promoter element necessary for Cu-inducible transcription of the *CUP1*, *CRS5*, and *SOD1* genes is denoted either MRE (metal-regulatory element) or UAS_{Cu} (Cu-responsive upstream activation sequence) and is composed of the consensus sequence, 5'-HTHNNGCTGD-3' (D = A, G or T; H = A, C or T; N = any residue), whereas the GCTG is termed the core sequence, and the region 5' to the core is called the T-rich element *(108,118,119)*. The *CUP1* promoter harbors five MREs and is strongly induced in response to Cu, whereas the *CRS5* and *SOD1* promoters contain a single MRE and are only modestly induced by Ace1 *(7,120)*. The core sequence 5'-GCTG-3' of the MRE is recognized by Ace1 in the major groove, whereas the AT-rich 5' region is contacted in the minor groove *(118)*. Although the Ace1 Cu MRTF was found to bind DNA as a monomer, it has been shown that the protein possesses a bipartite DNA-binding domain, explaining its ability to make contacts with both the minor and major grooves *(108)*. The first subdomain (residues 1–40) of the DNA-binding domain of Ace1 was found to bind a single Zn^{2+} atom through the Cys_{11}, Cys_{14}, Cys_{23}, and His_{25} residues *(121)*. Interestingly, at the carboxyl-terminal side of this amino-terminal 40-residue segment, called the Zn module, a motif denoted (K/R)GRP was identified for AT-rich minor-groove interaction *(118)*. The second subdomain of the DNA-binding domain (residues 41–110), named Cu-regulatory domain *(108)*, harbors nine Cys residues found as follows: one Cys-X_2-Cys motif, three Cys-X-Cys motifs, and a single Cys residue. All of these Cys residues are necessary for Cu response, except for the last Cys_{105} *(108)*. The arrangement of the Cys residues is predicted to coordinate four Cu^{1+} atoms through cysteine sulfur bonds *(122)*. Upon Cu activation, Ace1 undergoes a conformational change due to the formation of a tetra-Cu cluster within the amino terminal Cu-regulatory domain via critical cysteinyl thiolates to make an active detoxifying factor *(7,108,123)*. This enables the cupro-Ace1 protein to interact with the MRES to rapidly foster transactivation of target gene expression via its carboxyl-terminal domain, which is highly negatively charged *(124)*. The discovery of the *C. glabrata ACE1* gene ortholog, called *AMT1*, has also contributed to validate a number of properties predicted for Ace1 with regard to Cu sensing *(125)*. Although at the level of the Amt1 primary structure some differences exist with Ace1, the Zn module and the Cu-regulatory domain in the amino-terminal region of both proteins are highly conserved *(126,127)*.

3. *SCHIZOSACCHAROMYCES POMBE* AS AN ALTERNATIVE MODEL SYSTEM

3.1. Copper Uptake

3.1.1. "The Other Yeast"

Although use of *S. cerevisiae* has rapidly advanced the field of metal-ion metabolism, this organism has some limitations as a model system. One of them is the difficulty in expressing higher eukaryote cDNAs. Furthermore, once the protein is expressed, to ensure its physiological integrity and function within the cell *(128)*. For instance, recently, a human gene for Cu uptake, *hCTR1*, has been isolated and expressed in bakers' yeast cells *(95,97)*. Although this cDNA shows sequence

similarity to yeast *CTR1* and *CTR3*, the complementation of respiratory incompetence in bakers' yeast cells harboring *ctr1Δ ctr3Δ* mutations by *hCTR1* was only partial. Therefore, based on this and other observations, we decided to develop an alternative model system, the fission yeast *Schizosaccharomyces pombe*, that will complement and add to ongoing work on Cu transport, trafficking, and sequestration in *S. cerevisiae (8,37)*. Like *S. cerevisiae*, *S. pombe* has proved to be a tractable eukaryotic organism amenable to genetic analysis *(129,130)*. There are a number of features of *S. pombe* that make the organism an especially attractive one. For example, because *S. pombe* cells normally exist in the haploid state, recessive mutations can be isolated *(131)*. The fission yeast is a rod-shaped cell that divides by septation and medial cleavage in a manner more similar to higher eukaryotes than *S. cerevisiae (132)*. Several other reasons explain the growing popularity to exploit the fission yeast as a model organism. *S. pombe* has been favored because cells have well-organized and morphologically defined organelles (e.g., distinct Golgi complexes, vacuoles which are similar to the lysosome of mammalian cells, etc.) *(128)*. Moreover, posttranslational modifications such as isoprenylation and the addition of terminal galactose in glycoproteins that occur in *S. pombe* are more similar to mammalian cells than those of *S. cerevisiae (128)*. This latter observation may become important with regard to the intracellular targeting of proteins, maturation processes, and functional activation. Although there is a large evolutionary gap between *S. pombe* and *S. cerevisiae*, almost as large as that separating them both from animals, in general, *S. pombe* genes and proteins are more similar to mammalian cells than is *S. cerevisiae (128)*. For the study of the roles and mechanisms of action of genes critical for trace-metal-ion homeostasis, *S. pombe* represents an attractive model organism because the fission yeast exhibits a low level of Cu resistance, presumably as a consequence of lack of "typical" MT *(133,134)*. In *S. pombe*, the only known molecules for sequestering excess metal ions are the phytochelatins *(135,136)*. Furthermore, these short glutathione-related peptides appear to bind Cd predominantly *(137,138)*. Therefore, much like the Chinese hamster cell line *(139)* and the Baby hamster kidney cell line *(140)* in which *MT* genes are not expressed, *S pombe* represents an attractive system for studying metal-ion transport because there is no interference from MTs *(141,142)*, which considerably simplifies analysis. In *S. pombe*, three components involved in the high-affinity Fe-uptake system have been identified *(143,144)*. Frp1, which shares amino-acid sequence similarity with the Fre1 reductase from *S. cerevisiae*, is required at the cell surface of the fission yeast to reduce Fe^{3+} *(144,145)*. Once reduced, Fe^{2+} is taken up by a permease/oxidase complex, called Fip1/Fio1 *(143)*, and transported into the cell, as occurs with the Fet3/Ftr1 complex in *S. cerevisiae (53)*. Although Fio1 is similar to Fet3, by itself Fio1 cannot replace Fet3 in a *S. cerevisiae fet3Δ* mutant strain, thereby indicating that some molecular differences exist for high-affinity Fe uptake between the two species of yeast *(9,143)*.

3.1.2. Cu-Transporter Machinery

Several studies suggest that the high-affinity Cu uptake into eukaryotic cells requires reduction of Cu^{2+} to Cu^{1+} by cell-surface metalloreductases *(26,146–148)*. So far, analysis of genomic DNA sequences from the *S. pombe* Genome project has revealed two open reading frames (*SPBC1683.09C*, denoted *frp1*$^+$, and *SPBC947.05C*) related to cell-surface Fre reductases found in *S. cerevisiae*. Although the *frp1*$^+$-encoded reductase can reduce Fe^{3+} to Fe^{2+}, its role in the metabolism of other metal ions (e.g., Cu) is unknown. Regarding the second ORF, *SPBC947.05C*, its potential role in Fe^{3+}/Cu^{2+} reductase activity is still uncharacterized. As mentioned previously, Cu uptake in *S. pombe* is tightly regulated in response to the availability of Cu in the growth medium (Fig. 2). When cells are grown during Cu scarcity, the nutritional Cu-sensing transcription factor Cuf1 (*see* Section 3.1.3.) fosters the activation of Cu uptake genes, including the *ctr4*$^+$-encoded permease and the *ctr5*$^+$-encoded cotransporter that acts as a partner with Ctr4 for Cu transport at the cell surface *(37,93)*. Conversely, when Cu ions reach the physiological requirements for normal growth, there is an inactivation of Cu-uptake gene transcription. Ctr4 is a 289-amino-acid protein with 5 repeats of the putative Cu-binding Met-X_2-Met-X-Met motif at the amino-terminus. This latter motif is predicted by

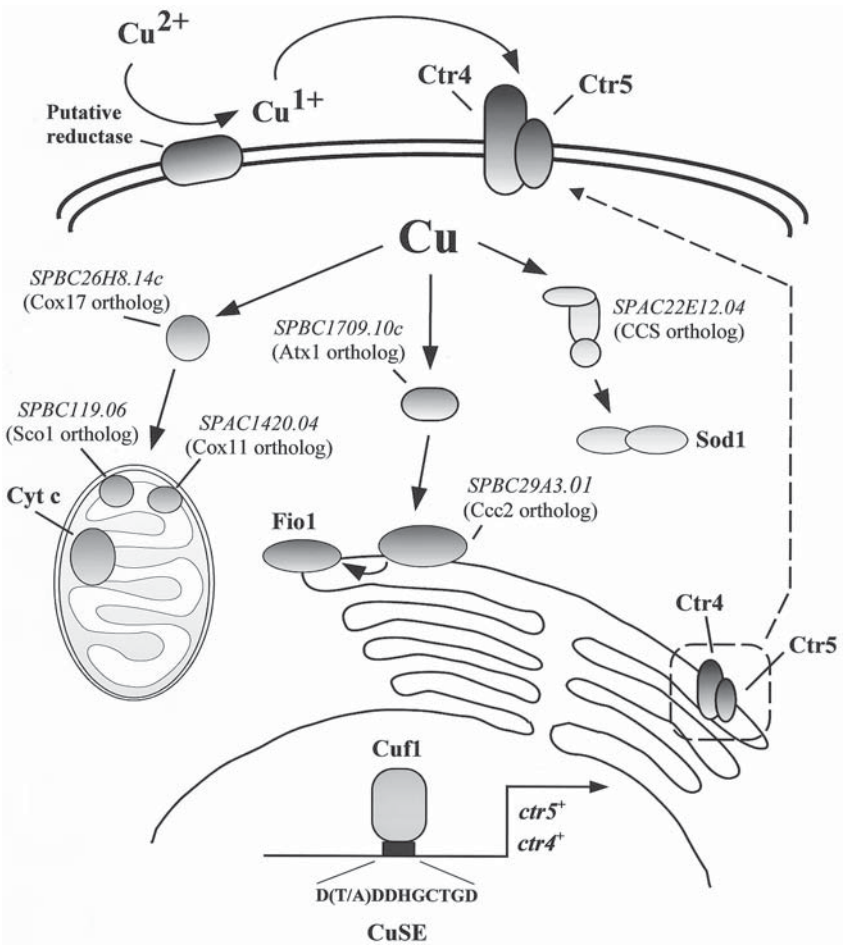

Fig. 2. A model for Cu homeostasis in *S. pombe*. Prior to uptake, Cu^{2+} is reduced to Cu^{1+} by a putative extracellular reductase. The Ctr4–Ctr5 high-affinity Cu-transport complex mediates the passage of Cu ions across the plasma membrane. Furthermore, this physical association between both Ctr4 and Ctr5 must occur for maturation and colocalization to the cell surface. As in Fig. 1, the *S. pombe SPBC1709.10C*, *SPAC22E12.04*, and *SPBC26H8.14C* genes encode putative chaperones orthologous to *S. cerevisiae* Atx1, CCS, and Cox17, respectively. At the transcriptional level, the nuclear protein Cuf1 directly binds the copper-signaling element (CuSE) under conditions of low Cu to activate expression of $ctr4^+$ and $ctr5^+$ genes, whereas elevated Cu concentrations negatively regulate Cuf1.

topological analysis to reside extracellularly *(37)*. Interestingly, this Met-rich motif is also found two times in the human Ctr1 protein and eight times in the *S. cerevisiae* Ctr1 protein *(8)*. Likewise in these proteins, the Met motif is present at the amino-terminus and it is thought to be involved in the capture of extracellular Cu as part of the uptake mechanism. Interestingly, the carboxyl-terminal residues 111–248 of the *S. pombe* Ctr4 exhibit strong homology to the *S. cerevisiae* Ctr3 Cu transporter, especially with respect to several residues within the predicted transmembrane domains *(37)*. Therefore, based on sequence homology, it appears that the *S. pombe* Ctr4 protein displays properties of both Ctr1 and Ctr3, which are the two high-affinity Cu transporters in bakers' yeast that are functionally redundant, but structurally distinct. Perhaps the *S. pombe* Ctr4 is the product of a gene, which was issued from a biological event in which *CTR1* and *CTR3* were fused into a single open reading frame. Using a fully functional Ctr4–GFP fusion protein, the transporter was localized

to the plasma membrane *(37)*. As would be expected, chromosomal disruption of the *ctr4*$^+$ gene renders *S. pombe* cells respiratory deficient because of the lack of Cu as a cofactor for the cytochrome-*c* oxidase enzyme *(37)*. Surprisingly, the Ctr4 protein from *S. pombe* was unable to complement the respiratory defect in *S. cerevisiae ctr1Δ ctr3Δ* cells, unless a specific component of the Cu-transport machinery from *S. pombe*, denoted Ctr5, was provided *(93)*. In fact, the Ctr5 protein, which is an integral membrane protein, was isolated as an indispensable partner for proper localization and function of *S. pombe* Ctr4 when expressed either in *S. cerevisiae* or *S. pombe* cells *(93)*. Ctr5 is a 173-amino-acid protein harboring two putative Cu-binding Met-X_2-Met-X-Met motifs in its amino-terminal region similar to those found in the Ctr4 (five times), *S. cerevisiae* Ctr1 (eight times), and human Ctr1 (two times) *(8,93)*.

Furthermore, like Ctr4 and human Ctr1, the Ctr5 predicted multimembrane-spanning region is homologous to *S. cerevisiae* Ctr3 *(93)*. Elegant biochemical and genetic experiments revealed that Ctr4 and Ctr5 form an heteromeric complex at the cell surface *(93)*. Furthermore, this association between Ctr4 and Ctr5 appears to be critical for protein maturation and secretion of the heteroprotein complex to the plasma membrane *(93)*. Within this complex, the exact function of each protein is unclear. This aspect certainly consists of an exciting area for future investigation. Once inside fission yeast cells, Cu ions are presumably taken by putative Cu chaperones, yet uncharacterized at the molecular level. The open reading frame *SPBC1709.10C* encodes a putative Atx1 ortholog in *S. pombe*. The protein from fission yeast exhibits 57% identity to the *S. cerevisiae* Atx1. Furthermore, the Cu-binding MXCXXC motif is conserved between the two proteins, consistent with a role in Cu delivery within the cell for the fission yeast protein. Based on the *S. pombe* Genome database, *SPAC22E12.04* encodes a putative ortholog of *S. cerevisiae* CCS. Although this putative ortholog bears 30% identity and 47% similarity to its bakers' yeast counterpart, notable differences exist between the two molecules. For instance, the amino-terminal Domain I of the *S. pombe* CCS ortholog lacks the Cu-binding MXCXXC motif. Instead, the protein harbors an extra domain at the carboxyl terminus that contains a series of cysteine residues, which are arranged in Cys–Cys configurations in a manner similar to MTs. Although the exact role of this extra domain in the *S. pombe* CCS ortholog is unknown, one would expect that it may serve as a Cu-binding site for cytoplasmic Cu prior to transfer into Sod1. This example of molecular difference between the *S. pombe* and *S. cerevisiae* CCS chaperones suggests that, although similar in function, these proteins may have mechanistic distinctions. The Cox17 Cu chaperone from *S. cerevisiae*, which delivers Cu to mitochondria for cytochrome-*c* oxidase assembly and function, has a related protein in *S. pombe* encoded by *SPBC26H8.14C*. The Cox17 ortholog in *S. pombe* exhibits a slightly more overall homology to human Cox17 (56% identity) than to bakers' yeast Cox17 (47% identity). Interestingly, the *S. pombe SPBC119.06* and *SPAC1420.04* genes encode proteins that exhibit a strong sequence similarity to *S. cerevisiae* Sco1 and Cox11, respectively. It is likely that these *S. pombe* components function in the mitochondrial Cu-delivery pathway. Based on these observations, it is important to note that the high degree of structural similarity among the budding yeast, fission yeast, and human components involved in Cu transport suggests that different carriers with specific Cu-binding motifs for metal-ion delivery are well conserved through evolution.

3.1.3. Nutritional Cu-Sensing Transcription Factor Cuf1

The *cuf1*$^+$ gene encodes a nuclear protein that occupies a central role in the *S. pombe* high-affinity Cu transport system *(37)*. Indeed, we have shown previously that the deletion of the *cuf1*$^+$ gene (*cuf1Δ*) gives at least three phenotypes associated with Cu starvation in yeast cells: inability to use respiratory carbon sources (owing to lack of Cu incorporation into cytochrome-*c* oxidase), impaired superoxide dismutase activity (owing to lack of Cu incorporation into Cu,Zn-Sod1), and failure in Fe accumulation (owing to lack of Cu incorporation into multi-Cu oxidase Fio1) *(37)*. Because these phenotypes are specifically corrected by the addition of exogenous Cu to the medium, this is consistent with *cuf1Δ* strains being defective in the expression of genes required for high-affinity Cu trans-

port. Furthermore, the observation that, in *S. pombe*, the high-affinity Cu transporters Ctr4 and Ctr5 mRNA levels are dependent on the Cuf1 protein implies a role for trans-activation of Cu transport genes by Cuf1 *(37,93)*. Although the Cuf1 protein is required for *S. pombe* high-affinity Cu transport, Cuf1 shows at its amino-terminus a strong homology (amino acid residues 1-61) to the amino-terminal 63 and 62 amino acids of the *S. cerevisiae* Ace1 and *C. glabrata* Amt1 class of Cu-detoxifying transcription factors and much less similarity to Mac1, its functional ortholog *(37)*. Consistently, we have demonstrated that Cuf1 acts through a closely related MRE-like element to regulate expression of fission yeast genes-encoding components of the Cu-transport machinery *(149)*. The carboxyl-terminal region of Cuf1 contains one cysteine-rich motif Cys_{328}-X-Cys_{330}-X_3-Cys_{334}-X-Cys_{336}-X_2-Cys_{339}-X_2-His_{342}, which is absent in Ace1/Amt1 but found duplicated in both Mac1 and Grisea of *Podospora anserina (37,102,150,151)*. Whether this motif at the carboxyl-terminus of Cuf1 constitutes by itself the Cu-sensing domain remains to be elucidated. The transcriptional control of Cu-transport gene expression in *S. pombe* by the regulator Cuf1 occurs through a specific cis-acting element termed copper-signaling element (CuSE) *(149)*. The sequence 5'-D(T/A)DDHGCTGD-3' (D = A, G or T; H = A, C or T) referred to as CuSE is found in multiple copies on the $ctr4^+$ and $ctr5^+$ promoters and is necessary for appropriate repression and induction of gene transcription in response to Cu and Cu starvation, respectively *(149)*. Although the overall magnitude of the response to Cu is optimal with the presence of multiple elements, the presence of only one element is sufficient to confer regulation in response to Cu changes. The CuSE is strikingly similar in sequence to the MRE, which is defined by the consensus sequence 5'-HTHNNGCTGD-3' (D = A, G or T; H = A, C or T; N = any residue) *(118)*. When a consensus MRE from *S. cerevisiae* is introduced into *S. pombe*, transcription is induced by copper deprivation in a Cuf1-dependent manner, similar to regulation by Mac1, the nuclear sensor for regulating the expression of genes-encoding components involved in copper transport in *S. cerevisiae*. Consistently, when the $cuf1^+$-encoded transcription factor of *S. pombe* is expressed into *S. cerevisiae* in which the *ACE1* gene was deleted (*ace1Δ*), the *CUP1*-encoded MT gene is regulated in opposite direction in response to copper, being induced under copper-starvation conditions *(149)*. This upregulation is just opposite to what is normally seen in the wild-type *S. cerevisiae* strain, whereas Cu deprivation inactivates *CUP1*, whereas elevated Cu concentrations strongly activates expression of *CUP1* through Ace1. Using a $cuf1^+$*-GFP* fusion allele *(37)* and a $cuf1^+$*-FLAG2* epitope-tagged allele *(149)*, which both retain wild-type function, we observed that the presence of Cu ions has little if any effect on the stability of the steady-state levels of the Cuf1 protein. This observation suggests that Cu ions modulate the activity of Cuf1 at a posttranslational level, perhaps by promoting conformational changes that would negatively regulate its DNA-binding function, therefore resulting in the inactivation of the expression of the Cu-uptake genes. Using a *S. cerevisiae* yeast system for expression of heterologous proteins in which the endogenous *ACE1* gene was knocked out, we determined that the Cuf1 protein interacts directly with CuSE *(149)*. Furthermore, no CuSE–Cuf1-dependent complex was observed when extract preparations were derived from cells grown in the presence of Cu prior to extract preparation. Conversely, a specific interaction between CuSE and Cuf1 was seen when extract preparations were obtained from cells grown under conditions of low Cu availability, suggesting an occupancy of the CuSEs in cells deprived of Cu by Cuf1 *(149)*.

3.2. Relationship Between Copper and Iron

3.2.1. Cuf1 Oppositely Regulates Cu and Fe Metabolic Genes

In *S. pombe*, the Fio1 protein is a Cu-dependent Fe oxidase required for high-affinity Fe transport that acts in concert with the Fe permease Fip1 at the cell surface *(143)*. Because of this requirement for Cu as a cofactor for the function of Fio1, Fe transport and mobilization rely on the high-affinity Cu-uptake system. In the *S. pombe* genome, $fio1^+$ and $fip1^+$ genes share a common promoter, but are divergently transcribed *(37,143)*. Previous results suggest that $fio1^+$ and $fip1^+$ gene expression is regulated by Fe availability through a putative Fe-sensing transcription factor *(143)*. Recently, we

have also demonstrated that an additional level of transcriptional control takes place to regulate Fe-transport gene expression *(37)*. Although Cuf1 activates the high-affinity Cu uptake gene expression under Cu starvation conditions, under these same conditions Cuf1 directly represses expression of genes encoding components of the Fe transport machinery. This Cu-dependent homeostatic control of *frp1*$^+$, *fio1*$^+$, and *fip1*$^+$ gene expression by Cuf1 occurs by direct binding of this latter transcription factor to repeated cis-acting elements found in multiple copies in both *frp1*$^+$ promoter and the *fio1*$^+$–*fip1*$^+$ intergenic promoter regions *(37)* (Beaudoin and Labbé, unpublished data). Importantly, this regulated Cu-starvation-mediated repression of the Fe-responsive genes is also observed in bakers' yeast *S. cerevisiae*, where the *FET3* gene is repressed when cells are starved for Cu and activated during Cu repletion *(37)*. Moreover, this downregulation of Fet3 gene expression under conditions of Cu starvation requires a functional *MAC1* gene. Indeed, *mac1Δ* cells exhibit elevated expression of Fe-uptake genes *(37)*. On the other hand, isogenic cells with the *MAC1*^{up1} allele, which encodes a Cu-insensitive Mac1 protein that is constitutively bound to the promoter elements *(99)*, exhibit a very low level of expression of *FET3*, consistent with the notion that Mac1^{up1} represses expression of Fe-uptake genes *(37)*. Clearly, the regulation of Fe-transport genes by nutritional Cu-sensing transcription factors is a useful means for yeast cells to prevent futile expression of the Fe-transport systems under conditions of Cu starvation.

4. SUMMARY AND PERSPECTIVE

Copper is an indispensable trace element required for the activity of a number of enzymes, which are required in processes as fundamental as respiration and Fe metabolism in eukaryotes. Because of its redox chemistry, Cu must be controlled by precise regulatory mechanisms to ensure its delivery to Cu-requiring proteins while preventing its accumulation to toxic levels. Although the discovery of Cu permease genes through the characterization of yeast mutants defective in Fe transport has established the link between Cu availability and Fe mobilization, it is crucial to gain a better understanding of the underlying mechanisms of additional Cu biochemical pathways in living systems. Key mechanistic aspects of Cu metabolism that comprise metal-ion-activated cellular sensing, assembling, recycling, and compartmentalization systems remain to be uncover. By combining the best features of two model systems like *Saccharomyces cerevisiae* and *Schizosaccharomyces pombe*, current and future studies should provide a better understanding on the roles and mechanisms of action of important Cu homeostasis proteins common to all eukaryotes.

ACKNOWLEDGMENTS

The authors wish to thank Sadri Znaidi for comments on this manuscript. The work in our laboratory on Cu homeostasis is supported by the Medical Research Council of Canada grant no. MOP-42406 (to S.L.). Infrastructure equipment for conducting our investigation on Cu was obtained through the Canada Foundation for Innovation grant no. NOF-3754 (to S.L.). S.L. is a New Investigator Scholar from the Canadian Institutes of Health Research.

REFERENCES

1. Andrews, N. C. (2001) Mining copper transport genes. *Proc. Natl. Acad. Sci. USA* **98,** 6543–6545.
2. Peña, M. M. O., Lee, J., and Thiele, D. J. (1999) A delicate balance: homeostatic control of copper uptake and distribution. *J. Nutr.* **129,** 1251–1260.
3. Lippard, S. J. (1999) Free copper ions in the cell? *Science* **284,** 748–749.
4. Predki, P. F. and Sarkar, B (1992) Effect of replacement of "zinc finger" zinc on estrogen receptor DNA interactions. *J. Biol. Chem.* **267,** 5842–5846.
5. Santoro, N. and Thiele, D. J. (1997) Oxidative stress responses in the yeast *Saccharomyces cerevisiae*, in *Yeast Stress Response* (Hohmann, S. and Mager, W. H., eds.), Chapman & Hall/Landes, R. G. Biosciences, London, pp. 165–205.
6. Eide, D. J. (1998) The molecular biology of metal ion transport in *Saccharomyces cerevisiae*. *Annu. Rev. Nutr.* **18,** 441–469.
7. Koch, K. A., Peña, M. M. O., and Thiele, D. J. (1997) Copper-binding motifs in catalysis, transport, detoxification and signaling. *Chem. Biol.* **4,** 549-560.

8. Labbé, S. and Thiele, D. J. (1999) Pipes and wiring: the regulation of copper uptake and distribution in yeast. *Trends Microbiol.* **7,** 500–505.
9. Radisky, D. and Kaplan, J. (1999) Regulation of transition metal transport across the yeast plasma membrane. *J. Biol. Chem.* **274,** 4481–4484.
10. Andrews, N. C., Fleming, M. D., and Gunshin, H. (1999) Iron transport across biologic membranes. *Nutr. Rev.* **57,** 114–123.
11. Camakaris, J., Voskoboinik, I., and Mercer, J. F. (1999) Molecular mechanisms of copper homeostasis. *Biochem. Biophys. Res. Commun.* **261,** 225–232.
12. DiDonato, M. and Sarkar, B. (1997) Copper transport and its alterations in Menkes and Wilson diseases. *Biochim. Biophys. Acta* **1360,** 3–16.
13. Mercer, J. F. (2001) The molecular basis of copper-transport diseases. *Trends Mol. Med.* **7,** 64–69.
14. Chelly, J., Tumer, Z., Tonnesen, T., Petterson, A., Ishikawa-Brush, Y., Tommerup, N., et al. (1993) Isolation of a candidate gene for Menkes disease that encodes a potential heavy metal binding protein. *Nature Genet.* **3,** 14–19.
15. Mercer, J. F., Livingston, J., Hall, B., Paynter, J. A., Begy, C., Chandrasekharappa, S., et al. (1993) Isolation of a partial candidate gene for Menkes disease by positional cloning. *Nature Genet.* **3,** 20–25.
16. Vulpe, C., Levinson, B., Whitney, S., Packman, S., and Gitschier, J. (1993) Isolation of a candidate gene for Menkes disease and evidence that it encodes a copper-transporting ATPase. *Nature Genet.* **3,** 7–13.
17. Bull, P. C., Thomas, G. R., Rommens, J. M., Forbes, J. R., and Cox, D. W. (1993) The Wilson disease gene is a putative copper transporting P-type ATPase similar to the Menkes gene. *Nature Genet.* **5,** 327–337.
18. Tanzi, R. E., Petrukhin, K., Chernov, I., Pellequer, J. L., Wasco, W., Ross, B., et al. (1993) The Wilson disease gene is a copper transporting ATPase with homology to the Menkes disease gene. *Nature Genet.* **5,** 344-350.
19. Vulpe, C. D., Kuo, Y. M., Murphy, T. L., Cowley, L., Askwith, C., Libina, N., et al. (1999) Hephaestin, a ceruloplasmin homologue implicated in intestinal iron transport, is defective in the *sla* mouse. *Nature Genet.* **21,** 195–199.
20. Askwith, C. and Kaplan, J. (1998) Iron and copper transport in yeast and its relevance to human disease. *Trends Biochem. Sci.* **23,** 135–138.
21. Dancis, A. (1998) Genetic analysis of iron uptake in the yeast *Saccharomyces cerevisiae*. *J. Pediatr.* **132,** S24–S29.
22. Dancis, A., Klausner, R. D., Hinnebusch, A. G., and Barriocanal, J. G. (1990) Genetic evidence that ferric reductase is required for iron uptake in *Saccharomyces cerevisiae*. *Mol. Cell. Biol.* **10,** 2294–2301.
23. Dancis, A., Roman, D. G., Anderson, G. J., Hinnebusch, A. G., and Klausner, R. D. (1992) Ferric reductase of *Saccharomyces cerevisiae*: molecular characterization, role in iron uptake, and transcriptional control by iron. *Proc. Natl. Acad. Sci. USA* **89,** 3869–3873.
24. Georgatsou, E. and Alexandraki, D. (1994) Two distinctly regulated genes are required for ferric reduction, the first step of iron uptake in *Saccharomyces cerevisiae*. *Mol. Cell. Biol.* **14,** 3065–3073.
25. Georgatsou, E., Mavrogiannis, L. A., Fragiadakis, G. S., and Alexandraki, D. (1997) The yeast Fre1p/Fre2p cupric reductases facilitate copper uptake and are regulated by the copper-modulated Mac1p activator. *J. Biol. Chem.* **272,** 13,786–13,792.
26. Hassett, R. and Kosman, D. J. (1995) Evidence for Cu(II) reduction as a component of copper uptake by *Saccharomyces cerevisiae*. *J. Biol. Chem.* **270,** 128–134.
27. Martins, L. J., Jensen, L. T., Simons, J. R., Keller, G. L., and Winge, D. R. (1998) Metalloregulation of *FRE1* and *FRE2* homologs in *Saccharomyces cerevisiae*. *J. Biol. Chem.* **273,** 23,716–23,721.
28. Dancis, A., Haile, D., Yuan, D. S., and Klausner, R. D. (1994) The *Saccharomyces cerevisiae* copper transport protein (Ctr1p). Biochemical characterization, regulation by copper, and physiologic role in copper uptake. *J. Biol. Chem.* **269,** 25,660–25,667.
29. Dancis, A., Yuan, D. S., Haile, D., Askwith, C., Elde, D., Moehle, C., et al. (1994) Molecular characterization of a copper transport protein in *S. cerevisiae*: an unexpected role for copper in iron transport. *Cell* **76,** 393–402.
30. Knight, S. A., Labbé, S., Kwon, L. F., Kosman, D. J., and Thiele, D. J. (1996) A widespread transposable element masks expression of a yeast copper transport gene. *Genes Dev.* **10,** 1917–1929.
31. Peña, M. M. O., Puig, S., and Thiele, D. J. (2000) Characterization of the *Saccharomyces cerevisiae* high-affinity copper transporter Ctr3. *J. Biol. Chem.* **275,** 33,244–33,251.
32. Klausner, R. D. and Dancis, A. (1994) A genetic approach to elucidating eukaryotic iron metabolism. *FEBS Lett.* **355,** 109–113.
33. Askwith, C., Eide, D., Van Ho, A., Bernard, P. S., Li, L., Davis-Kaplan, S., et al. (1994) The FET3 gene of *S. cerevisiae* encodes a multicopper oxidase required for ferrous iron uptake. *Cell* **76,** 403–410.
34. Cha, J. S. and Cooksey, D. A. (1991) Copper resistance in *Pseudomonas syringae* mediated by periplasmic and outer membrane proteins. *Proc. Natl. Acad. Sci. USA* **88,** 8915–8919.
35. Odermatt, A., Suter, H., Krapf, R., and Solioz, M. (1993) Primary structure of two P-type ATPases involved in copper homeostasis in *Enterococcus hirae*. *J. Biol. Chem.* **268,** 12,775–12,779.
36. Ooi, C. E., Rabinovich, E., Dancis, A., Bonifacino, J. S., and Klausner, R. D. (1996) Copper-dependent degradation of the *Saccharomyces cerevisiae* plasma membrane copper transporter Ctr1p in the apparent absence of endocytosis. *EMBO J.* **15,** 3515–3523.
37. Labbé, S., Peña, M. M. O., Fernandes, A. R., and Thiele, D. J. (1999) A copper-sensing transcription factor regulates iron uptake genes in *Schizosaccharomyces pombe*. *J. Biol. Chem.* **274,** 36,252–36,260.
38. Rae, T. D., Schmidt, P. J., Pufahl, R. A., Culotta, V. C., and O'Halloran, T. V. (1999) Undetectable intracellular free copper: the requirement of a copper chaperone for superoxide dismutase. *Science* **284,** 805-808.
39. Harrison, M. D., Jones, C. E., Solioz, M., and Dameron, C. T. (2000) Intracellular copper routing: the role of copper chaperones. *Trends Biochem. Sci.* **25,** 29–32.

40. Huffman, D. L. and O'Halloran, T. V. (2001) Function, structure, and mechanism of intracellular copper trafficking proteins. *Annu. Rev. Biochem.* **70,** 677–701.
41. O'Halloran, T. V. and Culotta, V. C. (2000) Metallochaperones, an intracellular shuttle service for metal ions. *J. Biol. Chem.* **275,** 25,057–25,060.
42. Valentine, J. S. and Gralla, E. B. (1997) Delivering copper inside yeast and human cells. *Science* **278,** 817–818.
43. Klomp, L. W., Lin, S. J., Yuan, D. S., Klausner, R. D., Culotta, V. C., and Gitlin, J. D. (1997) Identification and functional expression of HAH1, a novel human gene involved in copper homeostasis. *J. Biol. Chem.* **272,** 9221–9226.
44. Lin, S. J. and Culotta, V. C. (1995) The *ATX1* gene of *Saccharomyces cerevisiae* encodes a small metal homeostasis factor that protects cells against reactive oxygen toxicity. *Proc. Natl. Acad. Sci. USA* **92,** 3784–3788.
45. Lin, S. J., Pufahl, R. A., Dancis, A., O'Halloran, T. V., and Culotta, V. C. (1997) A role for *the Saccharomyces cerevisiae ATX1* gene in copper trafficking and iron transport. *J. Biol. Chem.* **272,** 9215–9220.
46. Culotta, V. C., Klomp, L. W., Strain, J., Casareno, R. L., Krems, B., and Gitlin, J. D. (1997) The copper chaperone for superoxide dismutase. *J. Biol. Chem.* **272,** 23,469–23,472.
47. Beers, J., Glerum, M. D., and Tzagoloff, A. (1997) Purification, characterization, and localization of yeast Cox17p, a mitochondrial copper shuttle. *J. Biol. Chem.* **272,** 33,191–33,196.
48. Glerum, D. M., Shtanko, A., and Tzagoloff, A. (1996) Characterization of *COX17*, a yeast gene involved in copper metabolism and assembly of cytochrome oxidase. *J. Biol. Chem.* **271,** 14,504–14,509.
49. Huffman, D. L. and O'Halloran, T. V. (2000) Energetics of copper trafficking between the Atx1 metallochaperone and the intracellular copper transporter, Ccc2. *J. Biol. Chem.* **275,** 18,611–18,614.
50. Portnoy, M. E., Rosenzweig, A. C., Rae, T., Huffman, D. L., O'Halloran, T. V., and Culotta, V. C. (1999) Structure-function analyses of the ATX1 metallochaperone. *J. Biol. Chem.* **274,** 15,041–15,045.
51. Pufahl, R. A., Singer, C. P., Peariso, K. L., Lin, S. J., Schmidt, P. J., Fahrni, C. J., et al. (1997) Metal ion chaperone function of the soluble Cu(I) receptor Atx1. *Science* **278,** 853–856.
52. Yuan, D. S., Stearman, R., Dancis, A., Dunn, T., Beeler, T., and Klausner, R. D. (1995) The Menkes/Wilson disease gene homologue in yeast provides copper to a ceruloplasmin-like oxidase required for iron uptake. *Proc. Natl. Acad. Sci. USA* **92,** 2632–2636.
53. Stearman, R., Yuan, D. S., Yamaguchi-Iwai, Y., Klausner, R. D., and Dancis, A. (1996) A permease–oxidase complex involved in high-affinity iron uptake in yeast. *Science* **271,** 1552–1557.
54. Winzerling, J. J. and Law, J. H. (1997) Comparative nutrition of iron and copper. *Annu. Rev. Nutr.* **17,** 501–526.
55. Yu, J. and Wessling-Resnick, M (1998) Influence of copper depletion on iron uptake mediated by SFT, a stimulator of Fe transport. *J. Biol. Chem.* **273,** 6909–6915.
56. Greene, J. R., Brown, N. H., DiDomenico, B. J., Kaplan, J., and Eide, D. J. (1993) The *GEF1* gene of *Saccharomyces cerevisiae* encodes an integral membrane protein; mutations in which have effects on respiration and iron-limited growth. *Mol. Gen. Genet.* **241,** 542–553.
57. Davis-Kaplan, S. R., Askwith, C., Bengtzen, A. C., Radisky, D., and Kaplan, J. (1998) Chloride is an allosteric effector of copper assembly for the yeast multicopper oxidase Fet3p: an unexpected role for intracellular chloride channels. *Proc. Natl. Acad. Sci. USA* **95,** 13,641–13,645.
58. Gaxiola, R. A., Yuan, D. S., Klausner, R. D., and Fink, G. R. (1998) The yeast CLC chloride channel functions in cation homeostasis. *Proc. Natl. Acad. Sci. USA* **95,** 4046–4050.
59. Hung, I. H., Casareno, R. L., Labesse, G., Mathews, F. S., and Gitlin, J. D. (1998) HAH1 is a copper-binding protein with distinct amino acid residues mediating copper homeostasis and antioxidant defense. *J. Biol. Chem.* **273,** 1749–1754.
60. Nishihara, E., Furuyama, T., Yamashita, S., and Mori, N. (1998) Expression of copper trafficking genes in the mouse brain. *Mol. Neurosci.* **9,** 3259–3263.
61. Naeve, G. S., Vana, A. M., Eggold, J. R., Kelner, G. S., Maki, R., Desouza, E. B., et al. (1999) Expression profile of the copper homeostasis gene, rAtox1, in the rat brain. *Neuroscience* **93,** 1179–1187.
62. Nanji, M. S. and Cox, D. W. (1999) The copper chaperone Atox1 in canine copper toxicosis in Bedlington terriers. *Genomics* **62,** 108–112.
63. Lockhart, P. J. and Mercer, J. F. (2000) Identification of the copper chaperone SAH in Ovis aries: expression analysis and in vitro interaction of SAH with ATP7B. *Biochim. Biophys. Acta* **1490,** 11–20.
64. Wakabayashi, T., Nakamura, N., Sambongi, Y., Wada, Y., Oka, T., and Futai, M. (1998) Identification of the copper chaperone, CUC-1, in *Caenorhabditis elegans*: tissue specific co-expression with the copper transporting ATPase, CUA-1. *FEBS Lett.* **440,** 141–146.
65. Himelblau, E., Mira, H., Lin, S. J., Culotta, V. C., Peñarrubia, L., and Amasino, R. M. (1998) Identification of a functional homolog of the yeast copper homeostasis gene *ATX1* from *Arabidopsis*. *Plant Physiol.* **117,** 1227–1234.
66. Mira, H., Martinez-Garcia, F., and Peñarrubia, L. (2001) Evidence for the plant-specific intercellular transport of the *Arabidopsis* copper chaperone CCH. *Plant J.* **25,** 521–528.
67. Arnesano, F., Banci, L., Bertini, I., Huffman, D. L., and O'Halloran, T. V. (2001) Solution structure of the Cu(I) and apo forms of the yeast metallochaperone. Atx1. *Biochemistry* **40,** 1528–1539.
68. Rosenzweig, A. C., Huffman, D. L., Hou, M. Y., Wernimont, A. K., Pufahl, R. A., and O'Halloran, T. V. (1999) Crystal structure of the Atx1 metallochaperone protein at 1.02 A resolution. *Struct. Fold Des.* **7,** 605-617.
69. Schmidt, P. J., Kunst, C., and Culotta, V. C. (2000) Copper activation of SOD1 *in vivo*: role for protein–protein interactions with the CCS metallochaperone. *J. Biol. Chem.* **275,** 33,771–33,776.
70. Schmidt, P. J., Rae, T. D., Pufahl, R. A., Hamma, T., Strain, J., O'Halloran, T. V., et al. (1999) Multiple protein domains contribute to the action of the copper chaperone for superoxide dismutase. *J. Biol. Chem.* **274,** 23,719–23,725.

71. Lamb, A. L., Torres, A. S., O'Halloran, T. V., and Rosenzweig, A. C. (2000) Heterodimer formation between superoxide dismutase and its copper chaperone. *Biochemistry* **39,** 14,720–14,727.
72. Lamb, A. L., Wernimont, A. K., Pufahl, R. A., Culotta, V. C., O'Halloran, T. V., and Rosenzweig, A. C. (1999) Crystal structure of the copper chaperone for superoxide dismutase. *Nat. Struct. Biol.* **6,** 724-729.
73. Casareno, R. L., Waggoner, D., and Gitlin, J. D. (1998) The copper chaperone CCS directly interacts with copper/zinc superoxide dismutase. *J. Biol. Chem.* **273,** 23,625–23,628.
74. Rae, T. D., Torres, A. S., Pufahl, R. A., and O'Halloran, T. V. (2001) Mechanism of Cu,Zn-superoxide dismutase activation by the human metallochaperone hCCS. *J. Biol. Chem.* **276,** 5166–5176.
75. Zhu, H., Shipp, E., Sanchez, R. J., Liba, A., Stine, J. E., Hart, P. J., et al. (2000) Cobalt(2+) binding to human and tomato copper chaperone for superoxide dismutase: implications for the metal ion transfer mechanism. *Biochemistry* **39,** 5413–5421.
76. Wong, P. C., Waggoner, D., Subramaniam, J. R., Tessarollo, L., Bartnikas, T. B., Culotta, V. C., et al. (2000) Copper chaperone for superoxide dismutase is essential to activate mammalian Cu/Zn superoxide dismutase. *Proc. Natl. Acad. Sci. USA* **97,** 2886–2891.
77. Amaravadi, R., Glerum M. D., and Tzagoloff, A. (1997) Isolation of a cDNA encoding the human homolog of COX17, a yeast gene essential for mitochondrial copper recruitment. *Hum. Genet.* **99,** 329–333.
78. Punter, F. A., Adams, D. L., and Glerum, M. D. (2000) Characterization and localization of human *COX17*, a gene involved in mitochondrial copper transport. *Hum. Genet.* **107,** 69–74.
79. Dickinson, E. K., Adams, D. L., Schon, E. A., and Glerum, M. D. (2000) A Human *SCO2* mutation helps define the role of Sco1p in the cytochrome oxidase assembly pathway. *J. Biol. Chem.* **275,** 26,780–26,785.
80. Hiser, L., Di Valentin, M., Hamer, A. G., and Hosler, J. P. (2000) Cox11p is required for stable formation of the Cu(B) and magnesium centers of cytochrome c oxidase. *J. Biol. Chem.* **275,** 619–623.
81. Rentzsch, A., Krummeck-Weiss, G., Hofer, A., Bartuschka, A., Ostermann, K., and Rodel, G. (1999) Mitochondrial copper metabolism in yeast: mutational analysis of Sco1p involved in the biogenesis of cytochrome c oxidase. *Curr. Genet.* **35,** 103–108.
82. Heaton, D., Nittis, T., Srinivasan, C., and Winge, D. R. (2000) Mutational analysis of the mitochondrial copper metallochaperone Cox17. *J. Biol. Chem.* **275,** 37,582–37,587.
83. Heaton, D. N., George, G. N., Garrison, G., and Winge D. R. (2001) The mitochondrial copper metallochaperone Cox17 exists as an oligomeric, polycopper complex. *Biochemistry* **40,** 743–751.
84. Lin, C. M., Crawford, B. F., and Kosman, D. J. (1993) Distribution of ^{64}Cu in *Saccharomyces cerevisiae*: cellular locale and metabolism. *J. Gen. Microbiol.* **139,** 1605–1615.
85. Dix, D., Bridgham, J., Broderius, M., and Eide, D. (1997) Characterization of the Fet4 protein of yeast. Evidence for a direct role in the transport of iron. *J. Biol. Chem.* **272,** 11,770–11,777.
86. Dix, D. R., Bridgham, J. T., Broderius, M. A., Byersdorfer, C. A., and Eide, D. J. (1994) The *FET4* gene encodes the low affinity Fe(II) transport protein of *Saccharomyces cerevisiae*. *J. Biol. Chem.* **269,** 26,092–26,099.
87. Kampfenkel, K., Kushnir, S., Babiychuk, E., Inze, D., and Van Montagu, M. (1995) Molecular characterization of a putative *Arabidopsis thaliana* copper transporter and its yeast homologue. *J. Biol. Chem.* **270,** 28,479–28,486.
88. Cohen, A., Nelson, H., and Nelson, N. (2000) The family of SMF metal-ion transporters in yeast cells. *J. Biol. Chem.* **275,** 33,388–33,394.
89. Nelson, N. (1999) Metal ion transporters and homeostasis. *EMBO J.* **18,** 4361–4371.
90. Gross, C., Kelleher, M., Iyer, V. R., Brown, P. O., and Winge, D. R. (2000) Identification of the copper regulon in *Saccharomyces cerevisiae* by DNA microarrays. *J. Biol. Chem.* **275,** 32,310–32,316.
91. Hassett, R., Dix, D. R., Eide, D. J., and Kosman, D. J. (2000) The Fe(II) permease Fet4p functions as a low-affinity copper transporter and supports normal copper trafficking in *Saccharomyces cerevisiae*. *Biochem. J.* **351(Pt. 2)**, 477–484.
92. Askwith, C., de Silva, D. M., and Kaplan, J. (1996) Molecular biology of iron acquisition in *Saccharomyces cerevisiae*. *Mol. Microbiol.* **20,** 27–34.
93. Zhou, H. and Thiele, D. J. (2001) Identification of a novel high-affinity copper transport complex in the fission yeast *Schizosaccharomyces pombe*. *J. Biol. Chem.* **276,** 20,529–20,535.
94. Kuo, Y. M., Zhou, B., Cosco, D., and Gitschier, J. (2001) The copper transporter CTR1 provides an essential function in mammalian embryonic development. *Proc. Natl. Acad. Sci. USA* **98,** 6836–6841.
95. Lee, J., Prohaska, J. R., Dagenais, S. L., Glover, T. W., and Thiele, D. J. (2000) Isolation of a murine copper transporter gene, tissue specific expression and functional complementation of a yeast copper transport mutant. *Gene* **254,** 87–96.
96. Lee, J., Prohaska, J. R., and Thiele, D. J. (2001) Essential role for mammalian copper transporter Ctr1 in copper homeostasis and embryonic development. *Proc. Natl. Acad. Sci. USA* **98,** 6842–6847.
97. Zhou, B. and Gitschier, J. (1997) *hCTR1*: a human gene for copper uptake identified by complementation in yeast. *Proc. Natl. Acad. Sci. USA* **94,** 7481–7486.
98. Portnoy, M. E., Liu, X. F., and Culotta, V. C. (2000) *Saccharomyces cerevisiae* expresses three functionally distinct homologues of the Nramp family of metal transporters. *Mol. Cell. Biol.* **20,** 7893–7902.
99. Labbé, S., Zhu, Z., and Thiele, D. J. (1997) Copper-specific transcriptional repression of yeast genes encoding critical components in the copper transport pathway. *J. Biol. Chem.* **272,** 15,951–15,958.
100. Yamaguchi-Iwai, Y., Serpe, M., Haile, D., Yang, W., Kosman, D. J., Klausner, R. D., et al. (1997) Homeostatic regulation of copper uptake in yeast via direct binding of MAC1 protein to upstream regulatory sequences of *FRE1* and *CTR1*. *J. Biol. Chem.* **272,** 17,711–17,718.

101. Joshi, A., Serpe, M., and Kosman, D. J. (1999) Evidence for $(Mac1p)_2$.DNA ternary complex formation in Mac1p-dependent transactivation at the *CTR1* promoter. *J. Biol. Chem.* **274,** 218–226.
102. Jungmann, J., Reins, H. A., Lee, J., Romeo, A., Hassett, R., Kosman, D., et al. (1993) MAC1, a nuclear regulatory protein related to Cu-dependent transcription factors is involved in Cu/Fe utilization and stress resistance in yeast. *EMBO J.* **12,** 5051–5056.
103. Graden, J. A. and Winge, D. R. (1997) Copper-mediated repression of the activation domain in the yeast Mac1p transcription factor. *Proc. Natl. Acad. Sci. USA* **94,** 5550–5555.
104. Jamison McDaniels, C. P., Jensen, L. T., Srinivasan, C., Winge, D. R., and Tullius, T. D. (1999) The yeast transcription factor Mac1 binds to DNA in a modular fashion. *J. Biol. Chem.* **274,** 26,962–26,967.
105. Serpe, M., Joshi, A., and Kosman, D. J. (1999) Structure–function analysis of the protein-binding domains of Mac1p, a copper-dependent transcriptional activator of copper uptake in *Saccharomyces cerevisiae*. *J. Biol. Chem.* **274,** 29,211–29,219.
106. Jensen, L. T., Posewitz, M. C., Srinivasan, C., and Winge, D. R. (1998) Mapping of the DNA binding domain of the copper-responsive transcription factor Mac1 from *Saccharomyces cerevisiae*. *J. Biol. Chem.* **273,** 23,805–23,811.
107. Turner, R. B., Smith, D. L., Zawrotny, M. E., Summers, M. F., Posewitz, M. C., and Winge, D. R. (1998) Solution structure of a zinc domain conserved in yeast copper-regulated transcription factors. *Nat. Struct. Biol.* **5,** 551–555.
108. Winge, D. R. (1998) Copper-regulatory domain involved in gene expression. *Prog. Nucleic Acid Res. Mol. Biol.* **58,** 165–195.
109. Zhu, Z., Labbé, S., Peña, M. M. O., and Thiele, D. J. (1998) Copper differentially regulates the activity and degradation of yeast Mac1 transcription factor. *J. Biol. Chem.* **273,** 1277–1280.
110. Keller, G., Gross, C., Kelleher, M., and Winge, D. R. (2000) Functional independence of the two cysteine-rich activation domains in the yeast Mac1 transcription factor. *J. Biol. Chem.* **275,** 29,193–29,199.
111. Jensen, L. T. and Winge, D. R. (1998) Identification of a copper-induced intramolecular interaction in the transcription factor Mac1 from *Saccharomyces cerevisiae*. *EMBO J.* **17,** 5400–5408.
112. Culotta, V. C., Howard, W. R., and Liu, X. F. (1994) *CRS5* encodes a metallothionein-like protein in *Saccharomyces cerevisiae*. *J. Biol. Chem.* **269,** 25,295–25,302.
113. Gralla, E. B., Thiele, D. J., Silar, P., and Valentine, J. S. (1991) ACE1, a copper-dependent transcription factor, activates expression of the yeast copper, zinc superoxide dismutase gene. *Proc. Natl. Acad. Sci. USA* **88,** 8558–8562.
114. Culotta, V. C., Joh, H. D., Lin, S. J., Slekar, K. H., and Strain J. (1995) A physiological role for *Saccharomyces cerevisiae* copper/zinc superoxide dismutase in copper buffering. *J. Biol. Chem.* **270,** 29991–29997.
115. Buchman, C., Skroch, P., Welch, J., Fogel, S., and Karin, M. (1989) The *CUP2* gene product, regulator of yeast metallothionein expression, is a copper-activated DNA-binding protein. *Mol. Cell. Biol.* **9,** 4091–4095.
116. Fürst, P., Hu, S., Hackett, R., and Hamer, D. (1988) Copper activates metallothionein gene transcription by altering the conformation of a specific DNA binding protein. *Cell* **55,** 705–717.
117. Thiele, D. J. (1988) ACE1 regulates expression of the *Saccharomyces cerevisiae* metallothionein gene. *Mol. Cell. Biol.* **8,** 2745–2752.
118. Koch, K. A. and Thiele, D. J. (1996) Autoactivation by a *Candida glabrata* copper metalloregulatory transcription factor requires critical minor groove interactions. *Mol. Cell. Biol.* **16,** 724–734.
119. Zhu, Z. and Thiele, D. J. (1996) A specialized nucleosome modulates transcription factor access to a *C. glabrata* metal responsive promoter. *Cell* **87,** 459–470.
120. Jensen, L. T., Howard, W. R., Strain, J. J., Winge, D. R., and Culotta, V. C. (1996) Enhanced effectiveness of copper ion buffering by CUP1 metallothionein compared with CRS5 metallothionein in *Saccharomyces cerevisiae*. *J. Biol. Chem.* **271,** 18,514–18,519.
121. Farrell, R. A., Thorvaldsen, J. L., and Winge, D. R. (1996) Identification of the Zn(II) site in the copper-responsive yeast transcription factor, AMT1: a conserved Zn module. *Biochemistry* **35,** 1571–1580.
122. Graden, J. A., Posewitz, M. C., Simon, J. R., George, G. N., Pickering, I. J., and Winge, D. R. (1996) Presence of a copper(I)–thiolate regulatory domain in the copper-activated transcription factor Amt1. *Biochemistry* **35,** 14,583–14,589.
123. Imbert, J., Culotta, V., Fürst, P., Gedamu, L., and Hamer, D. (1990) Regulation of metallothionein gene transcription by metals. *Adv. Inorg. Biochem.* **8,** 139–164.
124. Hu, S., Fürst, P., and Hamer, D. (1990) The DNA and Cu binding functions of ACE1 are interdigitated within a single domain. *New Biol.* **2,** 544–555.
125. Zhou, P. B. and Thiele, D. J. (1991) Isolation of a metal-activated transcription factor gene from *Candida glabrata* by complementation in *Saccharomyces cerevisiae*. *Proc. Natl. Acad. Sci. USA* **88,** 6112–6116.
126. Winge, D. R. (1999) Copper-regulatory domain involved in gene expression. *Adv. Exp. Med. Biol.* **448,** 237–246.
127. Zhou, P. and Thiele, D. J. (1993) Copper and gene regulation in yeast. *Biofactors* **4,** 105–115.
128. Giga-Hama, Y. (1997) Fission yeast *Schizosaccharomyces pombe*: an attractive host for heterologous protein production, in *Foreign Gene Expression in Fission Yeast Schizosaccharomyces pombe* (Giga-Hama, Y. and Kumagai, H. eds.), Springer-Verlag, New York, pp. 3–29.
129. Forsburg, S. L. (1999) The best yeast? *Trends Genet.* **15,** 340–344.
130. Hayles, J. and Nurse, P. (1992) Genetics of the fission yeast *Schizosaccharomyces pombe*. *Annu. Rev. Genet.* **26,** 373–402.
131. Shiozaki, K. and Russell, P. (1997) Expression, purification and analyses of cell-cycle regulatory proteins in *S. pombe*, in *Foreign Gene Expression in Fission Yeast Schizosaccharomyces pombe* (Giga-Hama, Y. and Kumagai, H. eds.), Springer-Verlag, New York, pp. 133–148.

132. Chang, F. and Nurse, P. (1996) How fission yeast fission in the middle. *Cell* **84,** 191–194.
133. Cherian, G. M. and Chan, H. M. (1993) Biological functions of metallothionein—a review, in *Metallothionein III: Biological Roles and Medical Implications* (Suzuki, K. T., Imura, N., and Kimura, M., eds.), Birkhauser, Basel, pp. 87–109.
134. Perego, P., Jimenez, G., and Howell, S. B. (1996) Isolation and characterization of a cisplatin-resistant strain of *Schizosaccharomyces pombe*. *Mol. Pharmacol.* **50,** 1080–1086.
135. Clemens, S., Kim, E. J., Neumann, D., and Schroeder, J. I. (1999) Tolerance to toxic metals by a gene family of phytochelatin synthases from plants and yeast. *EMBO J.* **18,** 3325–3333.
136. Hayashi, Y. and Winge, D. R. (1992) Properties of cadmium: $(\gamma\text{-Glu-Cys})_n$ Gly complexes in fission yeast, in *Metallothioneins* (Stillman, M. J., Shaw, F. C., III, and Suzuki, K. T., eds.), VCH, New York, pp. 212–229.
137. Rauser, W. E. (1993) Gamma-glutamylcysteinyl isopeptides: structure, synthesis and metal-binding complexes, in *Metallothionein III: Biological Roles and Medical Implications* (Suzuki, K. T., Imura, N., and Kimura, M., eds.), Birkhauser, Basel, pp. 201–217.
138. Rauser, W. E. (1995) Phytochelatins and related peptides. Structure, biosynthesis, and function. *Plant Physiol.* **109,** 1141–1149.
139. Camakaris, J., Petris, M. J., Bailey, L., Shen, P., Lockhart, P., Glover, T. W., et al. (1995) Gene amplification of the Menkes (*MNK*; *ATP7A*) P-type ATPase gene of CHO cells is associated with copper resistance and enhanced copper efflux. *Hum. Mol. Genet.* **4,** 2117–2123.
140. Palmiter, R. D. and Findley, S. D. (1995) Cloning and functional characterization of a mammalian zinc transporter that confers resistance to zinc. *EMBO J.* **14,** 639–649.
141. Palmiter, R. D. (1998) The elusive function of metallothioneins. *Proc. Natl. Acad. Sci. USA* **95,** 8428–8430.
142. Peña, M. M. O., Koch, K. A., and Thiele, D. J. (1998) Dynamic regulation of copper uptake and detoxification genes in *Saccharomyces cerevisiae*. *Mol. Cell. Biol.* **18,** 2514–2523.
143. Askwith, C. and Kaplan, J. (1997) An oxidase-permease-based iron transport system in *Schizosaccharomyces pombe* and its expression in *Saccharomyces cerevisiae*. *J. Biol. Chem.* **272,** 401–405.
144. Roman, D. G., Dancis, A., Anderson, G. J., and Klausner, R. D. (1993) The fission yeast ferric reductase gene *frp1*$^+$ is required for ferric iron uptake and encodes a protein that is homologous to the gp91-phox subunit of the human NADPH phagocyte oxidoreductase. *Mol. Cell. Biol.* **13,** 4342–4350.
145. Anderson, G. J., Dancis, A., Roman, D. G., and Klausner, R. D. (1994) Ferric iron reduction and iron uptake in eucaryotes: studies with the yeasts *Saccharomyces cerevisiae* and *Schizosaccharomyces pombe*. *Adv. Exp. Med. Biol.* **356,** 81–89.
146. Anderson, G. J., Lesuisse, E., Dancis, A., Roman, D. G., Labbé, P., and Klausner, R. D. (1992) Ferric iron reduction and iron assimilation in *Saccharomyces cerevisiae*. *J. Inorg. Biochem.* **47,** 249–255.
147. Finegold, A. A., Shatwell, K. P., Segal, A. W., Klausner, R. D., and Dancis, A. (1996) Intramembrane bis-heme motif for transmembrane electron transport conserved in a yeast iron reductase and the human NADPH oxidase. *J. Biol. Chem.* **271,** 31,021–31,024.
148. Lesuisse, E., Casteras-Simon, M., and Labbé, P. (1996) Evidence for the *Saccharomyces cerevisiae* ferrireductase system being a multicomponent electron transport chain. *J. Biol. Chem.* **271,** 13,578–13,583.
149. Beaudoin, J. and Labbé, S. (2001) The fission yeast copper-sensing transcription factor Cuf1 regulates the copper transporter gene expression through an Ace1/Amt1-like recognition sequence. *J. Biol. Chem.* **276,** 15,472–15,480.
150. Borghouts, C. and Osiewacz, H. D. (1998) GRISEA, a copper-modulated transcription factor from *Podospora anserina* involved in senescence and morphogenesis, is an ortholog of MAC1 in *Saccharomyces cerevisiae*. *Mol. Gen. Genet.* **260,** 492–502.
151. Osiewacz, H. D. and Nuber, U. (1996) GRISEA, a putative copper-activated transcription factor from *Podospora anserina* involved in differentiation and senescence. *Mol. Gen. Genet.* **252,** 115–124.

Index

B

C

D

G

Handbook of Copper Pharmacology and Toxicology

Edited by

Edward J. Massaro

The National Health and Environmental Effects Research Laboratory, Research Triangle Park, NC

Although copper is an essential trace element necessary for the survival of organisms ranging from bacteria to mammals, it is also highly toxic and must be absorbed by the body in precisely orchestrated biological processes. In *Handbook of Copper Pharmacology and Toxicology,* Edward J. Massaro and a panel of leading biomedical researchers and clinical practitioners review, in-depth, the status of our current knowledge concerning the biochemistry of copper in general, and its role in health and disease in particular. Drawing on the wealth of new information emerging from the molecular biology revolution, these experts survey the most important research areas of copper pharmacology and toxicology, including copper proteins and transport, copper toxicity and therapeutics, and copper metabolism and homeostasis. They also discuss the molecular pathogenesis of copper in a variety of metabolic diseases—Menkes and Wilson's diseases and occipital horn syndrome—as well as the role of copper in Parkinson's disease, prion disease, familial amyotrophic lateral sclerosis (ALS), and Alzheimer's disease. The elucidation of the precise mechanisms of copper trafficking, metabolism, and homeostasis will be of considerable importance in understanding the pathophysiology and treatment of such diseases.

Comprehensive and timely, the *Handbook of Copper Pharmacology and Toxicology* authoritatively provides researchers with all the up-to-date information needed to work productively in copper biology today.

Features

- **Up-to-date, in-depth review of the wealth of new research findings on copper biology**
- **Discussion of the molecular pathogenesis of diseases of copper metabolism**
- **New insights into the role of copper in ALS, Parkinson's, and Alzheimer's disease**
- **Review of the mechanisms of copper trafficking, metabolism, and homeostasis**

Contents

ISBN 0-89603-943-9

9 0 0 0 0

9 780896 039438

Handbook of Copper Pharmacology and Toxicology
ISBN: 0-89603-943-9

humanapress.com